2013

Effects of the late Permian mass extinction on chondrichthyan palaeobiodiversity and distribution patterns

Koot, Martha Beatrijs

http://hdl.handle.net/10026.1/1584

http://dx.doi.org/10.24382/4666
University of Plymouth

EFFECTS OF THE LATE PERMIAN MASS EXTINCTION ON CHONDRICHTHYAN PALAEOBIODIVERSITY AND DISTRIBUTION PATTERNS

by

MARTHA BEATRIJS KOOT

A thesis submitted to Plymouth University

in partial fulfillment for the degree of

DOCTOR OF PHILOSOPHY

School of Geography, Earth and Environmental Sciences

Faculty of Science and Technology

In collaboration with the

Geological Museum, Natural History Museum of Denmark

University of Copenhagen

February 2013

DISCLAIMER

(in compliance with the International Code of Zoological Nomenclature – Article 8.2)

This thesis is not issued for purposes of zoological nomenclature. New taxa appearing in this work have been/will be officially erected in the following articles:

KOOT, M. B., CUNY, G., TINTORI, A. and TWITCHETT, R. J. 2013. A new diverse shark fauna from the Wordian (middle Permian) Khuff Formation in the interior Haushi-Huqf area, Sultanate of Oman. *Palaeontology*, **56**, 303–343.

KOOT, M. B., CUNY, G., ORCHARD, M. J., RICHOZ, S., HART, M. B. and TWITCHETT, R. J. submitted. New hybodontiform and neoselachian sharks from the Lower Triassic of Oman. *Journal of Systematic Palaeontology*.

ABSTRACT

MARTHA BEATRIJS KOOT

EFFECTS OF THE LATE PERMIAN MASS EXTINCTION ON CHONDRICHTHYAN PALAEOBIODIVERSITY AND DISTRIBUTION PATTERNS

The Late Permian mass extinction occurring at 252.6 ± 0.2 Ma is the most severe Phanerozoic extinction event and was preceded and followed by additional disturbances. Patterns and processes of extinction and recovery of marine vertebrates have been little studied compared to marine invertebrates. This project focuses on Chondrichthyes, which, together with other marine fish, appeared to have been relatively unaffected by the extinction, while most of their supporting ecosystem collapsed. This study explores the authenticity of extinction among chondrichthyans and possible explanations for the observed patterns, because extinction severities on the taxonomic and ecological levels may be decoupled or the quality of the fossil record may be variable. The presented analyses are based on a newly compiled database that supercedes older compilations. It is supplemented by material obtained from numerous localities globally, which includes newly described taxa. Hence, this study attempts to be the most up-to-date and comprehensive analysis of patterns and trends in chondrichthyan diversity and distribution that is currently available.

The data demonstrate that, despite some variability in the Permian–Triassic chondrichthyan fossil record, the Lopingian record is shown to be of adequate completeness and, furthermore, range-through genus diversity is not significantly correlated with the number of taxonomic occurrences. Genus diversity declined from the mid-Guadalupian following an increasing extinction rate, which intensified throughout the Lopingian and thus supports a combined overall extinction as a result of the end-Guadalupian and Late Permian events. Furthermore, global distribution of chondrichthyan diversity shifted away from tropical regions and particularly the Boreal Sea gained in diversity, tracking extinction and recovery in marine benthic invertebrates in both time and space. No significant dependence of extinction on taxonomic structure or palaeoecological traits exists, which suggests proportional losses, except during the end-Smithian crisis. Also, a significant size decrease is absent among Permian/Triassic boundary-crossing taxa, suggesting selective loss of large-sized chondrichthyans rather than adaptive size decrease. Ultimately, the Hybodontiformes, Neoselachii, Xenacanthiformes and Holocephali are identified as the survivors, which possessed a varying combination of characteristics such as moderate body-size, adaptation to brackish/freshwater environments, benthic or generalist littoral (clutching) feeding behaviour, and a wide palaeogeographic range.

"Cartilaginous fishes must be considered to be one of evolution's success stories"

– Compagno 1990 –

CONTENTS

LIST OF FIGURES

LIST OF TABLES

ACKNOWLEDGEMENTS

First and foremost, I would like to thank my supervisors: Dr Gilles Cuny for inspiring me through his passion for fossil sharks, for insightful discussions, constructive comments and continuously positive attitude and support; Prof. Malcolm Hart for his supervision, (field) assistance, advice and constructive criticism; and Prof. Richard Twitchett for his academic input and access to samples and unpublished field data.

Thanks are due to Dr Mike Orchard, Prof. Charles Henderson, Prof. Andrea Tintori, Prof. Lucia Angiolini and Dr Haruka Yamagishi for their kindness shown in providing access to their personal research collections and sample data; Dr Benoit Beauchamp for his assistance in obtaining missing sample data; and Nikita Jacobsen, Peter Krauss and Kate Zubin-Stathopoulos for technical assistance during my collection visits. I also thank Dr Zerina Johanson for providing assistance in accessing the collections of the Natural History Museum.

Further thanks are due to Dr Alan Pradel for his assistance and being a good friend in the field in East Greenland. In relation to fieldwork in Oman, I am greatly indebted to Dr Michaela Bernecker, Dr Oliver Weidlich, Prof. Aymon Baud, Dr Sylvain Richoz, Prof. Leopold Krystyn and Dr Barbara Seuß. For being an extraordinary host and providing essential field assistance in Japan, I am very grateful to Prof. Tatsuo Oji, and thanks are also due to Dr Seiji Kadowaki and the remaining staff (Tomomi Suzuki, Masumi Nozaki, Hidekazu Yoshida and others) at the Nagoya University Museum for making my stay in Japan so enjoyable.

I would like to acknowledge Sten Jakobsen, Prof. Svend Stouge and Dr A. Ivanov for technical and specialist assistance while visiting the Geological Museum in Copenhagen, and particularly also Dr Jan Adolfssen and Plamen Andreev for technical assistance and insightful discussions, but especially for being good friends. The same is true for Dr John-Paul Hodnett and particularly Carlo Romano, whose co-operative spirit is truly a pleasure.

At Plymouth University, I would like to thank the academic, administrative and technical staff of the Department of Geology for their kindness and assistance over the past four and a half years (Dr Mark Anderson, Dr Sarah Boulton, Dr Stephen Grimes, Dr Helen Hughes, Dr Luke Mander, Dr Kevin Page and others). Special thanks are also due to Prof. Jim Griffiths, Chris Mushens and Debbie Petherick for their kindness, support and encouragement. I further thank the Graduate School staff (Prof. Mick Fuller, Dr Cristina Rivas, Ann Treeby, Sarah Kearns and Julia Crocker). I am much indebted to Andy Arnold for his technical assistance, flexibility, and for being a good friend. I also owe thanks to Dr Roy Moate and Peter Bond of the Plymouth Electron Microscopy Centre.

Finally, my warmest thanks go to my parents, Henk and Ineke Koot, my brother, Maarten Koot, and my husband, Robert Hall, whose continuous support and encouragement was of vital importance to me. I also thank my friends here, at home and elsewhere, Barbara Seuß, Lotte Schouten, Hayley Manners, Andy Leighton, Nikita Jacobsen, Luis Felipe Opazo Mella, Chinwendu Elenwa, Emhemed Alfandi and others, for help, support and dragging me out into the sunshine from time to time.

This research was funded by personal grants from VSBfonds (Utrecht), Prins Bernhard Cultuurfonds (Amsterdam), Stichting Dr. Hendrik Muller Vaderlandsch Fonds (The Hague) and Stichting Fonds Dr. Catharine van Tussenbroek (Utrecht). Additional financial support was received from SYNTHESYS for access to DK-TAF and from the Palaeontological Association in the form of the Sylvester-Bradley Award for fieldwork in Oman and travel grants in support of conference attendance. A FY2010 JSPS Postdoctoral Fellowship (short-term) for North American and European Researchers (2 months) was received from the Japan Society for the Promotion of Science (JSPS; PE10520) and, lastly, financial support was obtained from two grants from the Danish Natural Science Research Council Framework to Dr Gilles Cuny, entitled “Fossil sharks from Greenland and the great Permo-Triassic mass extinction” (09-065757FNU and 09-065946FNU).

AUTHOR'S DECLARATION

At no time during the registration for the degree of Doctor of Philosophy has the author been registered for any other University award without prior agreement of the Graduate Committee.

This study was financed with the aid of personal grants from VSBfonds, Prins Bernhard Cultuurfonds, Stichting Dr. Hendrik Muller Vaderlandsch Fonds, Stichting Fonds Dr. Catharine van Tussenbroek, SYNTHESYS, the Palaeontological Association and the Japan Society for the Promotion of Science (JSPS), and carried out in collaboration with the Geological Museum, Natural History Museum of Denmark, University of Copenhagen.

A programme of advanced study was undertaken, which included an EDIT (European Distributed Institute of Taxonomy) course entitled "Elasmobranch teeth enameloid microstructure as a taxonomic criterion", Scanning Electron Microscopy training and a postgraduate course on laboratory-based teaching methods and practice.

Relevant scientific seminars and conferences were regularly attended at which work was often presented; external institutions were visited for consultation purposes and a couple of papers were prepared for publication.

Publications:

KOOT, M.B. 2012. Permian–Triassic chondrichthyans from the Oman Mountains. *The Palaeontological Association Newsletter* **79**, 75–78.

KOOT, M. B., CUNY, G., TINTORI, A. and TWITCHETT, R. J. 2013. A new diverse shark fauna from the Wordian (middle Permian) Khuff Formation in the interior Haushi-Huqf area, Sultanate of Oman. *Palaeontology*, **56**, 303–343.

KOOT, M. B., CUNY, G., ORCHARD, M. J., RICHOZ, S., HART, M. B. and TWITCHETT, R .J. submitted. New hybodontiform and neoselachian sharks from the Lower Triassic of Oman. *Journal of Systematic Palaeontology*.

Presentations and Conferences attended:

International Conference on the Geology of the Arabian Plate and the Oman Mountains, Muscat, Oman (Jan 2012, poster)

55th Annual Meeting Palaeontological Association, Plymouth, UK (Dec 2011, poster)

7th Postgraduate Society short conference, Plymouth, UK (Nov 2011, poster)

2nd Centre for Research in Earth Sciences conference, Plymouth, UK (Nov 2011, poster)

71st Annual Meeting Society of Vertebrate Paleontology, Las Vegas, USA (Nov 2011, poster)

59th Meeting Symposium of Vertebrate Palaeontology and Comparative Anatomy, Lyme Regis, UK (Sep 2011, oral presentation)

54th Annual Meeting Palaeontological Association, Ghent, Belgium (Dec 2010, poster)

Field workshop as part of IGCP 572: Recovery of ecosystems after the P–Tr mass extinction, GUtech, Muscat, Oman (Feb 2010)

53rd Annual Meeting Palaeontological Association, Birmingham, UK (Dec 2009)

69th Annual Meeting Society of Vertebrate Paleontology, Bristol, UK (Sep 2009, poster)

9th North American Paleontological Convention, Cincinnati, Ohio, USA (Jun 2009, poster)

Progressive Palaeontology, Birmingham, UK (May 2009, poster)

52nd Annual Meeting Palaeontological Association, Glasgow, UK (Dec 2008)

External Contacts: Dr Gilles Cuny

Word count of main body of thesis: 78,698 words

Signed Martha Koot

Date 15 February 2013

1 INTRODUCTION

1.1 RESEARCH FRAMEWORK

The Permian/Triassic (P/Tr) boundary marks a time of major upheaval in the natural world. The mass extinction occurring just before the boundary at 252.6 ± 0.2 Ma (Mundil *et al.* 2004) is the most severe Phanerozoic extinction event (Erwin 1994; Benton 1995; Benton and Twitchett 2003). Although preceded and followed by additional disturbances, the main event has received particular attention in the literature with the focus on possible extinction mechanisms and the description and correlation of boundary sections. Patterns and processes of extinction and recovery of marine invertebrates and terrestrial vertebrates are frequently studied, but those of marine vertebrates comparatively less so. This project focuses on Chondrichthyes, which are predominantly marine fish and one of the top predators. According to some authors, chondrichthyans, and fish in general, appear to have been relatively unaffected by the Late Permian extinction (Schaeffer 1973; Thomson 1977; Patterson and Smith 1987), while most of their supporting ecosystem collapsed. This observation seems to gain support from a radiation of fish families in the fossil record across the P/Tr boundary (Benton 1998). The two main explanations originally offered for chondrichthyan survival state that a pelagic lifestyle protected them from benthic anoxia (Hallam and Wignall 1997) or that it is an artefact of the variable quality of the fossil record (Benton 1998). Other factors that potentially enhanced survival include a change in exploited food sources or reduced body size. The latter is often referred to as the 'Lilliput effect' (see Twitchett 2006) and its implications and expression in a number of invertebrate groups has been described in detail (Twitchett 2007a). It has also been recorded in the chondrichthyan form genus *Listracanthus* (Mutter and Neuman 2009), suggesting that a size decrease may have affected the entire class. Furthermore, it may suggest that if chondrichthyans did not suffer taxonomically from

the Late Permian mass extinction, they may indeed have been significantly affected on an ecological level, because extinction severities on both levels may be decoupled (Droser *et al.* 2000; McGhee *et al.* 2004, 2013).

Around the time of the extinction, Palaeozoic sharks were largely replaced by hybodonts and modern sharks (Neoselachii), but the forcing mechanism is not fully understood. The first major radiation of neoselachians occurred in the Late Triassic (Cuny and Benton 1999), but the earliest unequivocal occurrence of neoselachian teeth is recorded from the Early Triassic (Thies 1982). A number of finds from the Middle Devonian (Turner and Young 1987), the Carboniferous (Gunnell 1933; Duffin and Ward 1983), and the Early Permian (Duffin and Ward 1983; Ivanov 2005), suggest that the Late Permian extinction may not have been responsible for the appearance of modern chondrichthyans, but may at least have influenced their evolutionary trajectory.

1.1.1 Aims and objectives

Following from the above, the overall aim of this project is to understand the extinction, survivorship and diversification of chondrichthyans through the Late Permian mass extinction event. The following objectives were formulated to attain this aim:

- compiling current knowledge of Permian–Triassic chondrichthyans;
- augmenting the chondrichthyan fossil record from key locations and time intervals;
- tracking the appearance of neoselachians in the fossil record;
- compiling current knowledge of Permian–Triassic chondrichthyan phylogeny;
- assessing the completeness of the chondrichthyan fossil record to determine whether the apparent survival is genuine;
- reconstructing taxonomic diversity and global distribution of chondrichthyans through the Permian–Triassic;
- compiling evidence of changes in chondrichthyan palaeoecology and mode of life in order to assess the paradoxical survival of chondrichthyans, if verified.

1.2 BACKGROUND

1.2.1 EXTINCTION AND RECOVERY STUDIES

Patterns in diversification and extinction of marine life are generated from databases of the fossil record, which vary in the level of stratigraphic and taxonomic detail. They are often limited to first and last occurrences of taxa (Alroy 2008) as well as family and genus divisions. Databases at a lower taxonomic level are likely to be less complete (Benton 1995), because biological species are difficult to distinguish from the fossil record and because of the reduced likelihood that representatives of all species have been preserved (Benton and Twitchett 2003).

A number of family level compilations (Sepkoski 1982, 1992; Benton 1993) preceded the most recently published global compendium of fossil marine animal genera (invertebrate and vertebrate) to the stratigraphic level of substage (Sepkoski 2002), although the Paleobiology Database is becoming a comprehensive global resource. Sepkoski's (2002) compendium is still frequently used in current diversity assessment and extinction studies (e.g., Friedman and Sallan 2012), but its drawbacks include the fact that it only records first and last stratigraphic occurrences, it lacks information on higher taxonomic assignment of genera, and its incomplete coverage of currently available literature. The chondrichthyan data were used as a basis here and subsequently updated using specialist literature, including collective works (e.g., Zangerl 1981; Cappetta 1987, 2012; Stahl 1999; Yamagishi 2006; Ginter *et al.* 2010). Further details will be available in the expected work by Maisey (in prep.).

Extinction and recovery studies can be approached in a number of ways, such as that in which extinction magnitude is expressed (see Benton 1995 for a discussion). Also, recovery studies may be aimed at individual regions, clades or ecologies, or focus on broader patterns. Survival and recovery patterns are influenced by the fact that most mass extinction events are spread out over a million or more years, multi-causal, and predominantly the result of repeated environmental perturbations (Kauffman and Harries 1996). This leaves intervals of partial environmental

normalisation, which allow enhanced survival, adaptation, and innovation. Effective survival mechanisms, which are more diverse than just ecological generalism and opportunism, are indicated by characteristic stratigraphic occurrence patterns and have variable contributions to post-extinction radiations (Kauffman and Harries 1996). The definitions of these mechanisms are not without criticism. Lazarus taxa, for example, are likely to have retracted to a core area of their original habitat during the crisis, rather than emigrated to a refugium outside their normal geographical range ('refugia taxa'; Twitchett 2001a, 2006).

Extinction and recovery studies and associated diversity analyses are complex topics requiring careful consideration. Smith (1994) suggested that all taxon-based studies of macroevolutionary patterns are flawed, because it is impossible to determine whether each taxon is monophyletic or whether taxa are equivalent. Benton (1995) added that the termination of a taxon is difficult to identify, unless it was geologically instantaneous. It has also been stressed by Twitchett (2006) that extinction magnitude is overestimated by literally counting the number of taxa lost from the fossil record, and that phylogenetic studies and (semi-)quantitative palaeoecological analyses are key elements (based on studies by Jeffery 2001; Droser *et al.* 2000; and McGhee *et al.* 2004). Furthermore, elements used to assess diversity (e.g., dominance, evenness, etc.) may be affected by preservation, taphonomy, and the scale of the study (Twitchett 2006). Sampling methods can also introduce bias (e.g., Lloyd and Friedman 2013). Those of greatest importance are facies and latitudinal biases, which are respectively based on possible facies dependence of taxa (Twitchett 2006; and references therein) and habitat restriction of taxa (e.g., Allison and Briggs 1993). An added element to latitudinal bias may be differential response patterns of low or high latitude faunas (e.g., Barrera and Keller 1994; Twitchett and Barras 2004). Alroy (2008) further noted the potential influence of taxonomic biases on long-term diversity trends, showing (based on marine invertebrates) that diversity decrease is directly followed by low extinction rates and also that a peak in extinction rate is followed by a similar peak in origination rate, which accelerated recovery from mass extinctions and restricted diversity

fluctuations during the Phanerozoic. Any major events therefore force ecological and taxonomic restructuring (Alroy 2008).

1.2.2 Permian–Triassic (bio)stratigraphy

The Permian and Triassic span an interval of ~100 million years (299–201 Ma; Table 1.1). The Global Boundary Stratotype Section and Point (GSSP) of the P/Tr boundary is at Meishan, Zhejiang Province, China (31.0798°N 119.7058°E; Yin *et al.* 2001). The boundary level is the base of Bed 27c in the Meishan D Section. The correlation event selected for this boundary is the First Appearance Datum (FAD) of the conodont species *Hindeodus parvus*, which replaced the ammonoid *Otoceras woodwardi* as the boundary marker (Yin *et al.* 2001; Nicoll *et al.* 2002).

Global correlation of Permian/Triassic boundary strata based on key index fossils, such as conodonts and ammonoids, has been attempted by a number of authors (e.g., Yin *et al.* 2001), and a recent global correlation of biostratigraphic zonations including both groups was compiled by Gradstein *et al.* (2012). Metcalfe and Isozaki (2009) correlated conodont zones to a robustly constrained Late Permian and Early Triassic timescale (Figure 1.1).

The age of the P/Tr boundary cannot be dated directly, but has previously been approximated using ash layers (Mundil *et al.* 2001, 2004) and most recently as 252.17 ± 0.06 (Shen *et al.* 2011). For use in this study, recent ages of internationally recognised stage boundaries and biotic crises surrounding the P/Tr boundary have been compiled (Table 1.1), as has an overview of regional stratigraphies correlated to the internationally recognised stratigraphy (International Commission on Stratigraphy; Rohde 2005; Figure 1.2).

1.2.3 Permian–Triassic palaeogeography

The supercontinent Pangaea formed towards the end of the Palaeozoic after a series of continental collisions that started in the Devonian (Scotese 2003). It was largely

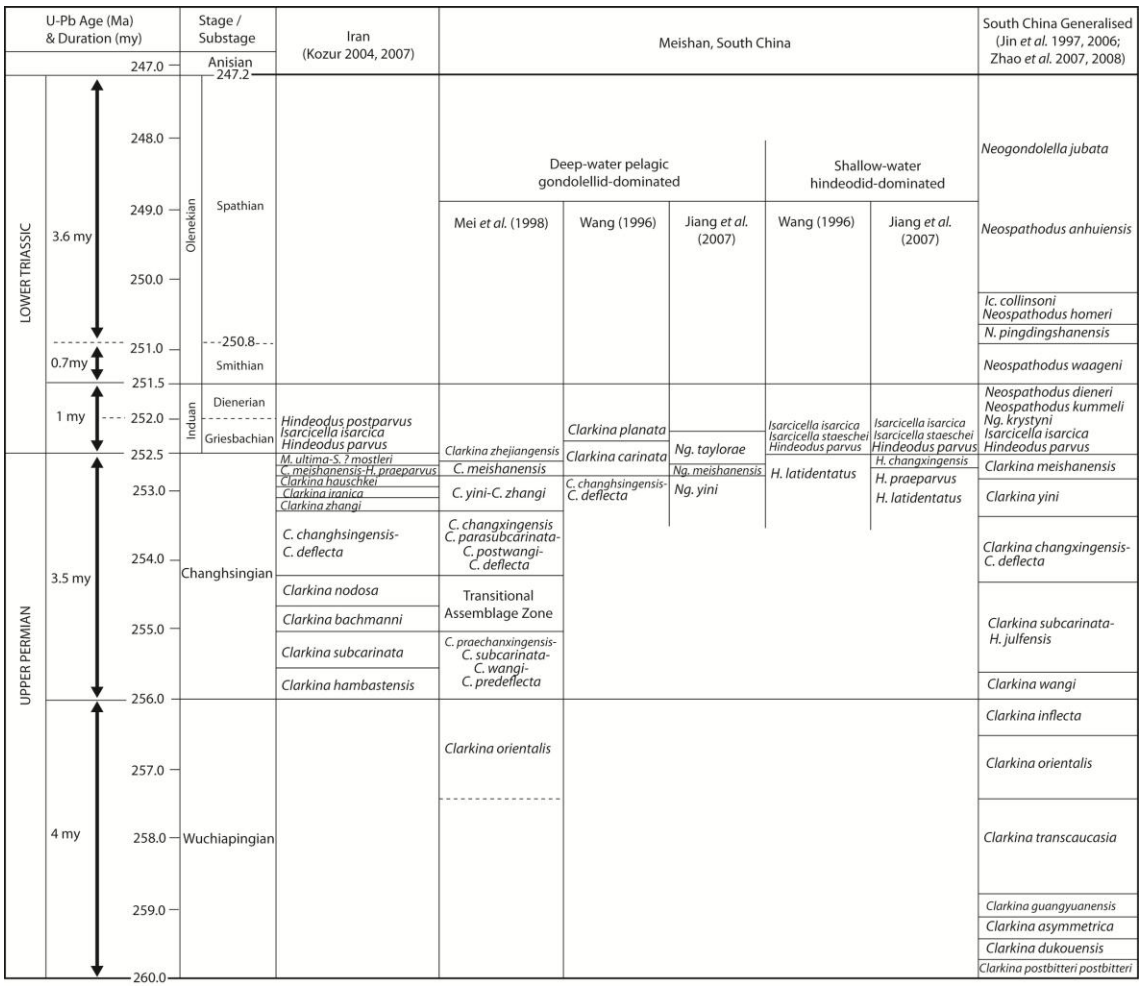

Figure 1.1 – Late Permian and Early Triassic timescale and correlated conodont biochronologies (redrawn from Metcalfe and Isozaki 2009, based on data from references therein). For updated ages, see Table 1.1.

complete by the Early Permian (Scotese 2008). A few small continents remained isolated off the eastern Pangaean margin, comprising Cimmeria (most of the present-day Middle East, Tibet, and Southeast Asia) and Cathaysia (North and South China; Scotese 2003), which did not collide with the supercontinent until the Late Triassic (Scotese 2003, 2008). Western Pangaea remained intact throughout most of the Permian–Triassic interval, but started to break up at around 200 Ma (Scotese 2008). Global key P/Tr boundary sections preserve sequences from shallow marine continental shelves, which were more extensive around smaller continents compared to the generally narrow fringe around Pangaea (Figure 1.3).

Table 1.1 – Compilation of age determinations in the Permian–Triassic interval. Ages used in this study marked in bold. ICS = International Commission on Stratigraphy.

(Sub)stage / time marker	**Age lower boundary (Ma) / Duration (Myr)**	**Reference**	**Remarks**
Hettangian (Jurassic)	**201.3** ± 0.2	Gradstein *et al.* 2012	
Rhaetian	~**208.5**	ICS	
Norian	~**228**	ICS	
Carnian	~**235**	ICS	
Ladinian	**240.6**	see below	
	242.0	Mundil *et al.* 2010	
	~242	ICS	
min. duration Anisian	6.6 +0.7/-0.9	Ovtcharova *et al.* 2006	
Anisian	**247.2** ± 0.1	Lehrmann *et al.* 2006; Mundil *et al.* 2010; ICS	
est. duration Spathian	~3	Ovtcharova *et al.* 2006	
Spathian (Olenekian)	**250.5**	see below	
max. duration Smithian	0.7 ± 0.6	Galfetti *et al.* 2007; see also Song *et al.* 2011	
Smithian (Olenekian)	**251.2**	Mundil *et al.* 2010; ICS; and see below	
max. duration Induan	1.4 ± 0.4	Galfetti *et al.* 2007; see also Song *et al.* 2011	
Dienerian (Induan)	**251.7**	inferred from Song *et al.* 2011	
Griesbachian (Induan)	**252.2** ± 0.5	ICS	
	> 252.10 ± 0.06	Shen *et al.* 2011	ash layer (bed 28) at Meishan
	252.17 ± 0.06	Shen *et al.* 2011	interpolated
duration late Changhsingian extinction interval	$\leq$ 0.2 ± 0.1	Shen *et al.* 2011	
main pulse of late Changhsingian extinction	**252.6** ± 0.2	Mundil *et al.* 2004	
	> 252.28 ± 0.08	Shen *et al.* 2011	ash layer (bed 25) at Meishan
Changhsingian	**254.2** ± 0.1	Gradstein *et al.* 2012	
	254.14	Shen *et al.* 2011	interpolated
Wuchiapingian	**259.9** ± 0.4	Gradstein *et al.* 2012	same age for end-Guadalupian extinction (Mundil *et al.* 2004)
Capitanian	**265.1** ± 0.4	Gradstein *et al.* 2012	
Wordian	**268.8** ± 0.5	Gradstein *et al.* 2012	
Roadian	**272.3** ± 0.5	Gradstein *et al.* 2012	
Kungurian	**279.3** ± 0.6	Gradstein *et al.* 2012	
Artinskian	**290.1** ± 0.1	Gradstein *et al.* 2012	
Sakmarian	**295.5** ± 0.4	Gradstein *et al.* 2012	
Asselian	**298.9** ± 0.2	Gradstein *et al.* 2012	

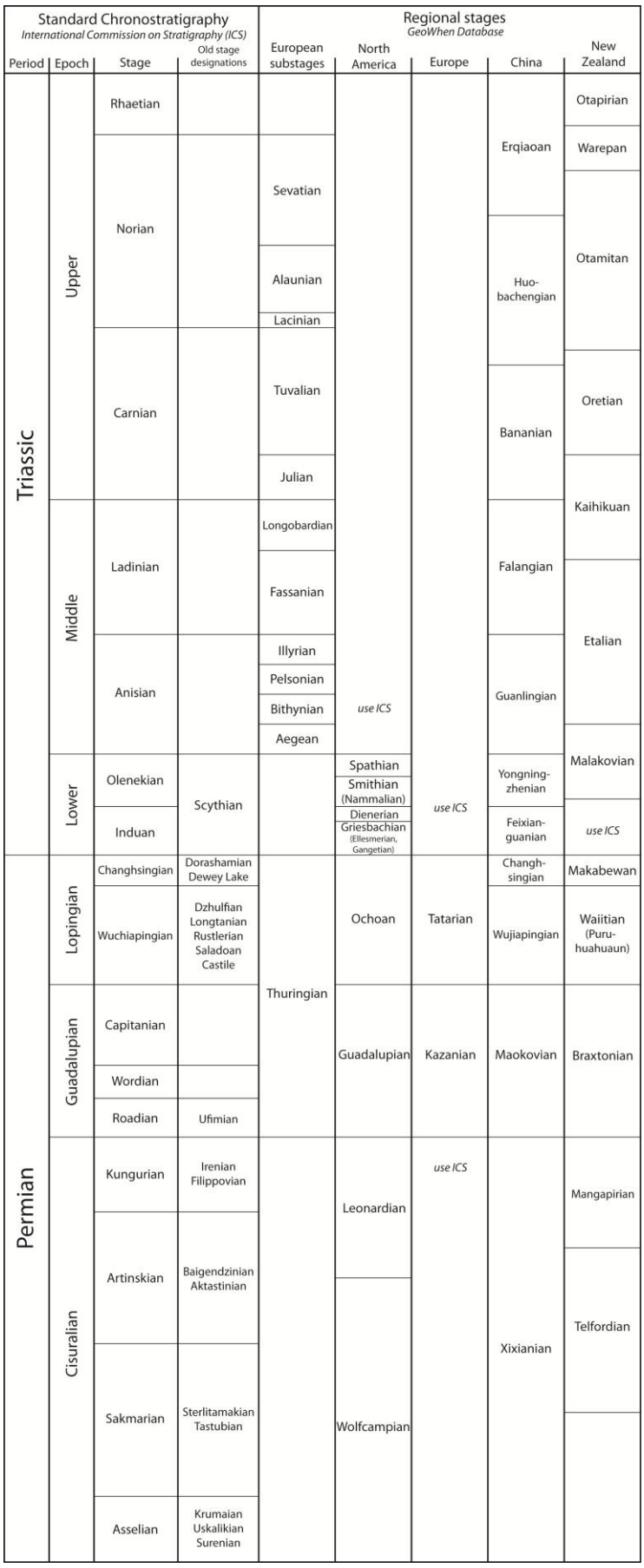

Figure 1.2 – Standard chronostratigraphy correlated with disused stage designations and regional chronostratigraphy.

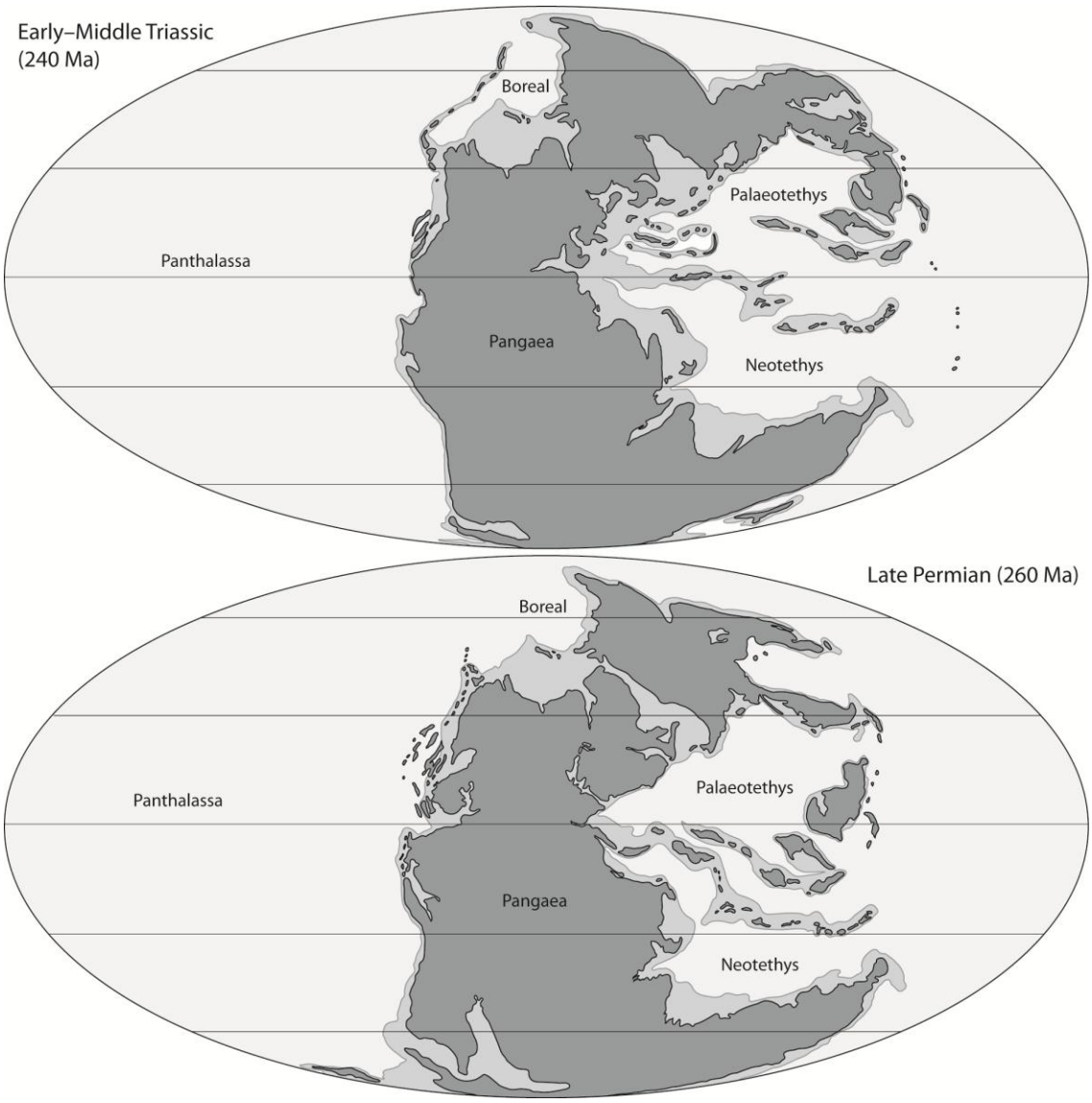

Figure 1.3 – Mollewide plate tectonic maps of the Late Permian and Early–Middle Triassic (redrawn from Blakey 2012).

1.3 Late Permian mass extinction and related biotic crises

1.3.1 Extinction severity

The Late Permian event is one of the 'big five' mass extinctions of all time and is ranked first in both ecological and taxonomic severity (McGhee *et al.* 2004). It was a particularly severe faunal disruption with a mean familial extinction rate of 48.6% for marine organisms (including invertebrates and vertebrates; Benton 1995) and extinction rates of 82% and ~90% for marine genera and species, respectively (Erwin

2006a; Chen and Benton 2012). It marks the changeover from dominance of the Palaeozoic evolutionary fauna—constituted mainly by epifaunal, sessile, filter-feeding organisms—to the Modern evolutionary fauna, of which fish are one of the main components (Sepkoski 1984; Erwin 1993). The two faunas suffered differential impact of marine family extinction rates: 79% for the Palaeozoic fauna and only 27% for the Modern fauna (Sepkoski 1984). The loss of the Palaeozoic groups caused many biological communities to collapse and pre-extinction levels of community complexity were not restored until the Middle Triassic (within 10 Myr), whereas it took much longer (~100 Myr) for global biodiversity at family level to be re-established (Benton and Twitchett 2003).

1.3.2 SEQUENCE OF EVENTS

The Late Permian mass extinction was synchronous globally (Metcalfe and Isozaki 2009 and references therein) and was the more intense of two distinct Permian extinction pulses (Benton 1995). The first, end-Guadalupian extinction pulse marks a major decline in biodiversity at both the family and genus level (Jin *et al.* 1994; Stanley and Yang 1994; Isozaki *et al.* 2004) and is currently estimated to have occurred at *c.* 260 Ma (Mundil *et al.* 2004; He *et al.* 2007). This extinction was previously thought to have affected low-latitude (Tethyan) faunas, while leaving Boreal faunas untouched (Jin *et al.* 1994). However, a negative shift in $\delta^{13}C_{carb}$ has been observed across the Guadalupian/Lopingian boundary in Japanese (mid-Panthalassan) deposits in direct association with an end-Guadalupian diversity decrease (e.g. Ota and Isozaki 2006; Isozaki *et al.* 2007a, b). This shift has also been demonstrated in the GSSP in South China (Isozaki *et al.* 2007a; see Jin *et al.* 2006), in Texas (USA), Spitsbergen (Isozaki *et al.* 2007a), Croatia (Isozaki *et al.* 2011), Greece, and Hungary (Wignall *et al.* 2012) by chemostratigraphical correlations, suggesting that this event was global.

The second, late Changhsingian extinction pulse occured just before the P/Tr boundary (Yin *et al.* 2001; Metcalfe *et al.* 2001) at the base of Bed 25 in the Meishan

type section (Jin *et al.* 2000) and is dated at 252.6 ± 0.2 Ma (Mundil *et al.* 2004). The majority of taxonomic loss (78% of marine invertebrate genera) was concentrated around this extinction horizon (Clapham *et al.* 2009), showing that it was an abrupt, rather than gradual event (Jin *et al.* 2000; Rampino and Adler 1998). The occasional observation of a 'tail' is considered evidence of backward smearing of the extinction peak due to less abundant species being preserved less frequently, better known as the Signor-Lipps effect (Erwin 2006a, b). This effect may be caused by inadequate sampling before the extinction boundary (Benton 1995) but may be considerably enhanced by marine regression (Erwin 1993). First and last occurrences tend to cluster at sequence boundaries and transgressive flooding surfaces, illustrating that palaeobiological patterns (including stepwise or gradual mass extinction) may partly be an artefact of facies control and sequence architecture (Holland 1995).

The true severity of the end-Guadalupian event and its role as a precursor to the late Changhsingian event is still poorly known (Metcalfe and Isozaki 2009). Recent analysis of the marine invertebrate fossil record indicates the absence of a peak in extinction rates and gradual diversity decline from the Wordian to the end of the Permian, driven by a reduction in origination rates that was most intense during the Capitanian and Wuchiapingian (Clapham *et al.* 2009). Nevertheless, a period of radiation and recovery during the Lopingian has been observed among a number of major groups, including reef systems (Weidlich 2002). The patterns of disappearance among marine biota during the late Changhsingian extinction interval are complex, comprising groups that suffered drastically during the end-Guadalupian crisis, others continuing and diversifying up to the late Changhsingian extinction, and groups that remained relatively unaffected by both (Hallam and Wignall 1997; see Section 8.5.3.2 for discussion on extinction selectivity).

The post-extinction interval was characterised by low faunal diversity, cosmopolitanism, numerous benthic Lazarus taxa (Erwin 2006a), and the absence of reefs (Weidlich 2002), coals, and biogenic cherts (Hallam and Wignall 1997). A distinct lag in the recovery of biota after the extinction, in combination with characteristic

sedimentary features in all facies types, signify continued harsh conditions (low oxygen and reduced food supply) during the earliest Triassic (e.g., Metcalfe and Isozaki 2009). Nevertheless, recovery and diversification into vacant ecospace is suggested by higher levels of origination in the Early Triassic (Benton 1995). Further biotic crises are identified in the pelagic fossil record at the end-Griesbachian, end-Smithian and end-Spathian (i.e., ammonoids, conodonts; see Brayard *et al.* 2009a; Stanley 2009). In benthic communities, some evidence of end-Griesbachian extinction is observed (e.g., Twitchett *et al.* 2004) and evidence of the end-Smithian event is observed as a weak pause in diversification (decline in origination rates rather than extinction; Song *et al.* 2011; see also Sun *et al.* 2012). This suggests that Early Triassic faunas were radiating between times of crisis, but that groups with generally high origination rates (such as ammonoids and conodonts) provide the best record of these recovery intervals (Song *et al.* 2011).

1.3.3 Causal mechanisms

The end-Guadalupian and late Changhsingian extinctions have both been linked to environmental degradation caused by the eruption of large flood basalts in the Emeishan igneous province and western Siberia, respectively (Clapham and Payne 2011), for which post-collisional stresses associated with the assembly of Pangaea may have been responsible (Scotese 2008). A complex interrelation of events during the Late Permian, however, has prevented a general consensus on a single cause or even a multiple cause model for the mass extinction (Erwin 2006b). Comprehensive reviews of potential causes consider extraterrestrial impact, volcanism, palaeogeography, sea level regression, and oceanic anoxia (Hallam and Wignall 1999; Erwin 2006a; Payne and Clapham 2012).

Mass volcanism-induced global warming is often deemed the most probable trigger because of its suddenness and magnitude (e.g., Benton and Twitchett 2003; Kidder and Worsley 2004; Twitchett 2007b; Isozaki 2009; Metcalfe and Isozaki 2009). Oceanic

anoxia is believed to have ensued, either through decreased oxygen solubility and consequent eutrophication (Meyer and Kump 2008), or through oceanic stratification (Kidder and Worsley 2004). This anoxic interval has been associated with toxic sulfide levels in oceanic water, contributing to the extinction severity (Kump *et al.* 2005; see also Payne and Clapham 2012; Bottjer 2012). Stratification may have been caused by a slowing down of oceanic circulation due to a reduced Equator to pole temperature gradient (Kidder and Worsley 2004), resulting in reduced primary productivity (Hotinski *et al.* 2001). The subsequent reduction in food supply to the higher food chain is described as a 'key proximate cause' of the extinction (Twitchett 2006) and remained low for several hundred thousand years. Although the extent and duration of anoxic conditions is generally deemed to have greatly impacted on the recovery of benthic ecosystems in the Early Triassic (e.g., Twitchett *et al.* 2004), the onset of anoxia was diachronous (Wignall and Twitchett 2002a), causing some synchroneity problems with the main phase of the extinction (Brookfield *et al.* 2003).

The end-Smithian crisis correlates with a global perturbation of the carbon cycle (Galfetti *et al.* 2007; Payne *et al.* 2004) and coincides with the ultimate peak of anoxia in several Tethyan outer platforms (Galfetti *et al.* 2007; see also Ovtcharova *et al.* 2006) and a thermal maximum (Sun *et al.* 2012). These events were likely triggered by a volcanic pulse, distinct from the main eruptive phase (Ovtcharova *et al.* 2006).

1.3.4 GEOCHEMICAL RECORDS

The end-Guadalupian crisis was directly preceded by 3–4 million years of heightened productivity (Isozaki *et al.* 2007b), referred to as the "Kamura event" (Isozaki *et al.* 2007a), which was of increasing intensity (Musashi *et al.* 2010) and was recorded by high positive values of $\delta^{13}C_{carb}$ (+5‰ or more). Increased carbon burial resulted in climatic cooling, causing fusulinids, bivalves, rugose corals and other taxa adapted to warm conditions to perish. Gradual diversity decrease is consistent with habitat area reduction resulting from climatic cooling or the spread of deep-water anoxia (Clapham

et al. 2009). A negative shift (-4‰ $\delta^{13}C_{carb}$) across the Guadalupian/Lopingian boundary recorded the return of warm conditions in the Wuchiapingian, allowing new faunas to radiate (Isozaki *et al.* 2007a). It is considered to be the start of long-term $\delta^{13}C_{carb}$ fluctuations that lasted from the Capitanian through to the Anisian, and which characterised the transition from the late Palaeozoic icehouse to the Mesozoic-Paleogene greenhouse world (Isozaki *et al.* 2007b).

The end-Guadalupian negative shift in $\delta^{13}C$ was relatively minor compared to the late Changhsingian shift (observed in carbonate and organic carbon; Erwin 2006a), both of which were coincident with the respective extinction pulses (Jin *et al.* 2000). The major excursion has been suggested as an auxiliary marker of the P/Tr boundary in the absence of fossils (Yin *et al.* 2001). Both shifts were global phenomena caused by an input of light carbon to ocean and atmosphere, resulting in increased CO_2 levels (Erwin 2006a), and may have originated from a variety of sources, including volcanic methane release, reduced photosynthesis, or increased weathering (Benton and Twitchett 2003; Kidder and Worsley 2004; Erwin 2006a). Furthermore, a direct relationship may exist between continued disruption of the carbon cycle and delayed biotic recovery during the Early Triassic (Payne *et al.* 2004). The $\delta^{18}O_{carb}$ signature also shows a major negative shift in the late Changhsingian (Holser 1989, 1991; Kearsey *et al.* 2009), which reached its lowest point in the earliest Triassic (Hallam and Wignall 1997) and indicates a global temperature increase (e.g., Kidder and Worsley 2004; Sun *et al.* 2012; see also Twitchett 2007c).

1.3.5 Patterns and processes of extinction and recovery

Rates of extinction have been in a constant state of flux through time (Benton 1995), but were extraordinarily severe during the Late Permian (Hallam and Wignall 1997). Pelagic groups were relatively unaffected, which is opposite to most extinction events (McKinney 1985), whereas benthic groups suffered severely, illustrating the complex disappearance pattern among marine biota (Hallam and Wignall 1997). Benthic

holdover taxa were typically adapted to dysaerobic environments, except for gastropods and certain bivalves, and the record of the planktonic community suggests that the shallow water environment was also unfavourable for a prolonged period of time due to eutrophic and low-oxygen conditions (Hallam and Wignall 1997). A significant surface water productivity loss, and thus a reduced food supply, meant a collapse of the higher tiers of the food web, causing a non-specialised feeding strategy to be identified as a key trait to enhance survival (Twitchett 2006). A wide geographic range was a further key trait (Twitchett 2006), because cosmopolitanism increases the likelihood of species occupying potential refugia (Lazarus taxa; Erwin 1993). Erwin (2006a) proposed that extinction and survival patterns may be largely driven by ecology, association with reefs, or physiology. The latter was suggested by Knoll *et al.* (1996, 2007), who stated that organisms with an active circulation and a high metabolic rate (including vertebrates) are much better buffered against changes in environmental chemistry, which is illustrated by lower extinction rates of these organisms during both Permian extinction pulses (Knoll *et al.* 2007). The idea that marine (top) predators such as chondrichthyans hardly suffered during the extinction event (e.g, Schaeffer 1973; Patterson and Smith 1987) is made plausible by the fact that nektonic organisms living in the pelagic realm may have been better adapted to, or successfully avoided anoxic bottom waters. Nevertheless, it remains unclear how they were seemingly insensitive to the disappearance of their food source.

The apparent enhanced survival of fish may have been the result of a misinterpretation of the fossil record (Schaeffer 1973), although similarities with the conodont fossil record, for example, have indicated that the phenomenon may be genuine (Hallam and Wignall 1997). The quality of the fossil record in the earliest Triassic is deemed poor compared to the Late Permian or Middle Triassic, although not for Chondrichthyes (Twitchett 2001b), which could profoundly influence the observed biological signals.

Late Permian faunal communities were diverse and ecologically complex, and biogeographical provinces were well-developed (Benton and Twitchett 2003). In

contrast, earliest Triassic ecosystems were relatively vacant (Erwin 1993) and cosmopolitan, opportunistic faunas were common (Erwin 1993; Benton and Twitchett 2003). No phyla or classes are known to have originated in the post-extinction diversification (Erwin *et al.* 1987) and no major morphological innovations occured (Erwin 1993), because diversification proceeded from a wide range of adaptive zones, representing a variety of body plans (Erwin *et al.* 1987). Such innovations further strongly depend on the supporting ecosystem (Erwin 2006b), which was unfavourable at the time.

Primary productivity decline is widely associated with stunted growth in marine organisms (Lilliput effect) and is typical of biomass redistribution within a taxon, which results in reduced body size, but an increase in species abundance (Twitchett 2006). This enhances preservation and taxa that show no apparent size change are, therefore, likely to display a fossilisation gap after the extinction horizon (Twitchett 2001a). The continuation of the chondrichthyan fossil record through the immediate aftermath may, therefore, be a preliminary indicator of the Lilliput effect.

1.4 CHONDRICHTHYES

1.4.1 EVOLUTION AND TAXONOMIC GROUPS

The Chondrichthyes consist of the true sharks and their relatives, the skates, rays, and chimaeras. They are an ancient and very successful group that survived four major mass extinctions and today form an integral part of nearly all oceanic food chains, comprising over 970 species (Long 2010). Chondrichthyans originated at least 435 million years ago and are among the earliest known jawed fishes (Gnathostomata; Long 2010). They appear to have been closely allied to the acanthodians (Figure 1.4), but fossil evidence further reveals similarities to jawless thelodonts (Agnatha) and a potentially close relationship with placoderms (Long 2010).

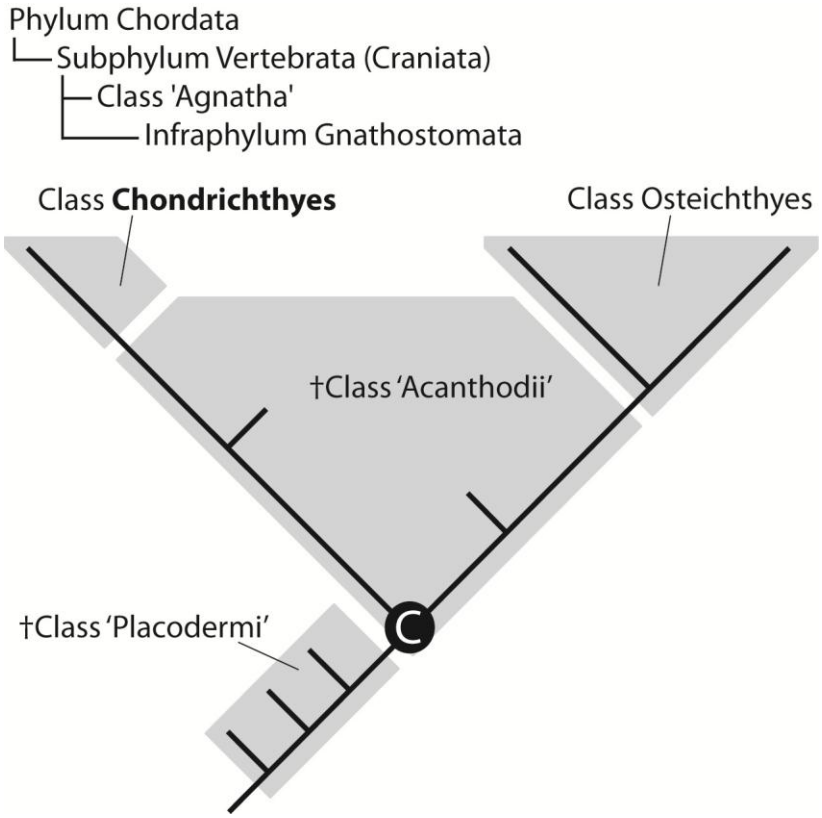

Figure 1.4 – Higher taxonomic relationships among fishes (Benton 2005) and gnathostome phylogeny (redrawn from Ahlberg 2009). Paraphyletic groups provided in parentheses, whereas other groups are monophyletic. 'C' marks the gnathostome crown-group node, hence the 'Placodermi' form the stem-group.

The first unequivocal chondrichthyans are known from denticles (scales) dating back to the early Silurian (e.g., Sansom *et al.* 2000), although chondrichthyan-like denticles are also known from the Ordovician (Sansom *et al.* 1996, 2012; see also Long 2010). Due to the absence of associated teeth in the fossil record (Sansom *et al.* 1996; Williams 2001), it has been postulated that these early lineages lacked teeth or jaws altogether (Long 1995, 2010), but from their systematic position, it is most probable that their teeth were indistinguishable from the dermal denticles (Cuny, pers. comm 2013). Silurian chondrichthyans may have been microphagous filter feeders (Williams 2001).

Characteristic chondrichthyan teeth are first recovered from the Lower Devonian (e.g., Mader 1986; see also Botella 2006). Chondrichthyans rapidly achieved cosmopolitanism in the Middle Devonian and many distinct groups of sharks with characteristic tooth types had evolved towards the end of this epoch, including the

Phoebodontiformes and Xenacanthiformes (Long 2010), the latter of which persisted into the Triassic (Benton 2005). The earliest diverse assemblage from a single formation is from the Middle Devonian Aztec Siltstone of Antarctica (at least five taxa; Long and Young 1995). Symmoriiformes, which possessed unusual features such as the spine-brush complex (Maisey 2009), and Cladoselachiformes arose in the Late Devonian (Long 2010), which appear to have initially retained worn teeth in the jaw rather than shed them (Williams 2001).

Chondrichthyans underwent another major radiation in the Early Carboniferous, following the Late Devonian extinction of the armoured Placodermi and other major fish groups (Long 2010). Because of the broad morphological variety that resulted, the Late Mississippian (~320 Ma) is known as 'the golden age of sharks' (Parker 2008). The Holocephali (chimaeras and rabbitfishes), characterised by the upper jaw fused to the braincase, first appeared at the start of the Carboniferous and diverged from mainstream Devonian lineages (Long 2010). They include the Helodontiformes, Cochliodontiformes, Menaspiformes and Chimaeriformes. Other Carboniferous–Permian groups include the cladodont Ctenacanthiformes and the euchondrocephalian Orodontiformes, Eugeneodontiformes (spiral-like dentition), Petalodontiformes (typically imbricated teeth; Long 2010) and Iniopterygia (Stahl 1999). However, the highly specialised Iniopterygia may potentially be placed in an even more basal position (Pradel *et al.* 2010).

The euselachian (true sharks) Hybodontiformes originated in the Late Devonian (Ginter *et al.* 2010), but were particularly prominent in the early half of the Mesozoic (Long 2010). They were a very diverse group with marine and freshwater representatives and variable tooth morphologies, indicating the utilisation of a wide range of food sources (Benton 2005). The origin of the Neoselachii (modern sharks) remains unresolved at present, but has been traced back to the Early Triassic (Thies 1982) and potentially the early Permian (Ivanov 2005). Their many derived characters suggest a more adaptable feeding system (Benton 2005). The neoselachian

Batomorphii (skates and flattened rays) did not appear until the Early Jurassic (Long 2010).

Phylogenetic relationships between the chondrichthyan clades remain ambiguous, especially in the Palaeozoic forms. For example, the Eugeneodontiformes and Petalodontiformes were traditionally classified with the elasmobranchs (e.g., Zangerl 1981; Cappetta 1987, 2012), but are now placed with the euchondrocephalans because of their tendency to cluster with this group due to their many chimaerid characteristics (see e.g., Lund and Grogan 1997; Grogan and Lund 2008; Ginter *et al.* 2010).

1.4.2 MORPHOLOGY

Chondrichthyans developed a very successful and efficient physiology early in their evolution, which has changed relatively little since that time (Long 2010). Their basic physical characteristics include an internal skeleton, jaws with teeth, skin covered with dermal denticles and, frequently, one or more dorsal fin spines. The skeleton is not ossified, but composed of globular calcified cartilage forming the braincase, jaws, gill arches, vertebrae and fin supports. Skeletal elements are strengthened by calcified tesserae where necessary, while keeping weight at a minimum (Long 2010). Although chondrichthyans only retained a few bony tissues, they once had the potential to develop bone, but lost the trait in the course of their evolution (Coates *et al.* 2002). The cartilaginous condition is thus considered to be highly specialised, enabling more efficient function (Long 2010) and allowing body size to keep increasing throughout life, although the rate of growth declines with age, lower temperatures and food scarcity (Parker 2008).

The simple jaws consist of primary upper and lower cartilages (Meckel's cartilage and palatoquadrate; Long 2010). The teeth are organised in multiple rows that continuously grow and move forward, replacing damaged or shed teeth (polyphyodont; Long 2010). In modern sharks, the shedding rate is relatively rapid (weeks or months)

but is specific to species or conditions (Parker 2008). The teeth lack true roots and are not anchored in the jaw cartilage. Instead, the tooth bases are anchored by connective tissue fibers in the mucosa that covers the jaw cartilage (Cappetta 2012). In general, teeth are composed of a trabecular dentine base and an orthodentine crown covered with a thin layer of enameloid (Long 2010; Figure 1.5). Apart from attack, defence and copulation, teeth are predominantly used for feeding and their shape, therefore, reflects diet (Parker 2008).

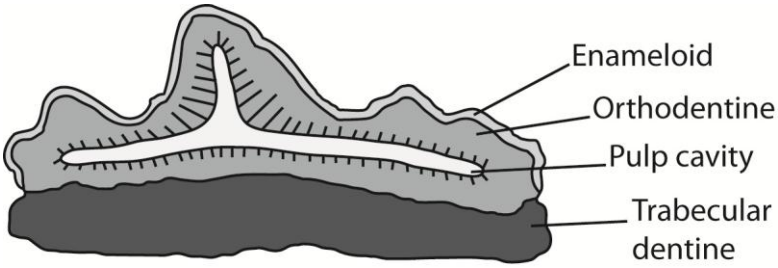

Figure 1.5 – General composition of chondrichthyan teeth (in cross-section).

The integument is covered by dermal denticles (squamation), which are the most primitive type of vertebrate dermal skeleton (Reif 1982a). Denticles were classically considered homologous to teeth of gnathostome vertebrates (Reif 1985), but teeth have since been shown to have a separate origin (Johanson and Smith 2003). Each individual denticle is composed of a basal plate of trabecular dentine anchored in the skin and a dentine crown with a pulp cavity in the centre (Reif 1980a; Parker 2008) and an enameloid outer layer (Reif 1973a). They are shed and replaced in ways similar to teeth, and although their average functional life is unknown (Reif 1982b), replacement is continuous. Denticle size is negatively allometrically scaled to body size (Reif 1985) and their morphology can be simple blade-like or complex, but is generally subject to regional, ontogenetic, and interspecific variation (Reif 1985; Parker 2008; Long 2010). Silurian denticles were non-growing, but were shed and replaced by larger ones, until true growing scales evolved by the end of the Early Devonian (Long 2010). Most denticles are of the placoid (simple and non-growing) type (defined by Reif 1973b),

occurring in all Euselachii, but the ctenacanthid type (growing or non-growing) also occurred during the Palaeozoic–Middle Triassic. The hybodontid type (growing or non-growing, often with a high pointed cusp) did not appear until the Late Triassic or Jurassic (Figure 1.6; Reif 1978a; Cappetta 1987, 2012).

Morphogenetic study of the squamation, detailing distribution of denticle types in different body regions and during individual growth stages is close to impossible in fossil material (Reif 1985). The evolutionary origin and primary function of the squamation is unknown (Reif 1985), but the autecology of chondrichthyans can, to an extent, be inferred from it (Reif 1982b, 1985). For example, specific morphologies have been linked to resistance to abrasion (knob-shaped), protection against ectoparasites (spine-shaped), accommodation of photophores (peculiar shape with open spaces), and drag reduction (overlapping with flat, ridged crowns; Derycke-Khatir *et al.* 2005; see also Reif 1982b, 1985; Reif and Dinkelacker 1982; Parker 2008). Fast swimming sharks also generally have smaller and lighter scales (Raschi and Elsom 1986).

A fin spine positioned anterior to each dorsal fin is a primitive chondrichthyan feature, which may have been used for fin support and defence (Parker 2008; see also Brett and Walker 2002), or as a mating attribute (in highly modified form; Long 2010). They are very strongly modified products of the integument (Reif 1985).

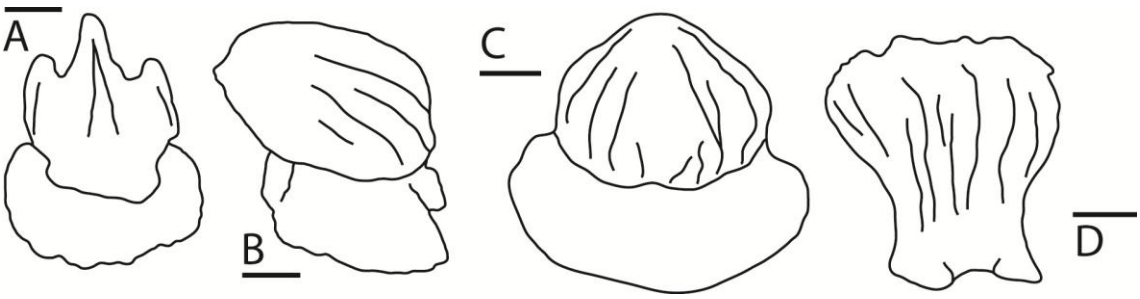

Figure 1.6 – Denticle types as differentiated by Reif (1978a): A–B, placoid type; C, hybodontid type; D, ctenacanthid type. A–B redrawn from Reif and Goto (1979), C–D from Reif (1978a). Scale: A–B = 0.1 mm, C = 0.5 mm, D = 0.2 mm.

1.4.3 FOSSIL RECORD

Chondrichthyans are cartilaginous fishes and because superficial mineralised layers only strengthen certain parts of the skeleton (e.g., cranium, vertebrae; Klug 2010), body fossils are rarely preserved and only under exceptional conditions, whereas highly mineralised hard parts, such as teeth, dermal denticles and fin spines are readily preserved, although usually as disarticulated specimens. The enameloid outer layer enhances their resistance to decay, which is particularly true for neoselachian triple-layered dental enameloid (Klug 2010). The chemical composition of enameloid (fluorohydroxylapatite) is also resistant to diagenetic alteration. Chondrichthyan evolution is, therefore, principally inferred from these elements, starting with Early Silurian denticles and Early Devonian teeth and fin spines, which became readily preserved globally from the Middle Devonian onwards (Long 2010). Teeth and denticles occur in abundance in individual chondrichthyans and because they are replaced throughout life, they are a common component in the fossil record. Fin spines are comparatively rarely recovered, because a maximum of two spines occur in each individual and are not replaced.

In the absence of articulated body fossils, the dentition shows the most characteristic morphological features that may be used for taxonomic purposes. Tooth shape is not constant, but despite possible problems caused by heterodonty (see Applegate 1965; Compagno 1970), different states of consistent features can be used reliably to determine affinity. In comparison, the squamation is of very low taxonomic significance, even in recent sharks, due to extensive ontogenetic and regional variability (Reif 1985). It has been suggested, however, that they may be used instead, as form species, for stratigraphic purposes (Reif 1985; see also Johns 1996; Johns *et al.* 1997).

Both phalacanthous and anacanthous sharks occurred during the Palaeozoic and Mesozoic and phalacanthous taxa could possess either two or a single dorsal fin spine (Maisey 2010). Fin spine morphology is usually characteristic and allows determination of broad affinities, although form taxa also exist among fin spines (known only from isolated remains). It is often difficult or impossible to distinguish between fin spines in

many aspects of their morphology, which has been shown in Mesozoic hybodonts and even in modern genera (Maisey 2010). It is exceptional for fin spine ornamentation to define a single genus (Maisey 2010), meaning that certain morphologies may have ranged across otherwise well-differentiated taxa. Fossil fin spine taxonomy can thus never be fully resolved unless they are recovered in direct association with skeletal remains.

1.4.4 ECOLOGY

Chondrichthyans inhabit a large variety of habitats, ranging from rivers and nearshore reefs to the open ocean, but are mainly marine fish and occur throughout the oceans, from surface waters to abyssal plains (Long 2010). Preferred habitat affects evolutionary trajectories, as is illustrated by the Xenacanthiformes (Devonian–Triassic). Their predominantly freshwater ecology, in combination with their tolerance of low oxygen conditions, may explain why they were little affected by the Late Permian extinction (Cuny 2002). Some chondrichthyans are tachymetabolic, maintaining higher body temperatures than ambient seawater (Long 2010), yet overall chondrichthyan species richness and level of activity generally decreases from tropical to Boreal regions (Parker 2008).

Ecological groups distinguished among extant chondrichthyans have been correlated to potential niches that may have also been occupied by fossil groups, including pelagic or near-shore hunters and demersal or meso- to bathypelagic chondrichthyans (Reif 1985; Compagno 1990). Chondrichthyan movements are dictated by their prey, resulting in seasonal migration and sometimes ontogenetic migration (Parker 2008). They range from top predators to filter feeders and direct evidence of their diet may be recorded in well-preserved body fossils (Long 2010).

Chondrichthyans may be distinguished from other fish based on the display of complex mating behaviour and rituals, but predominantly on reproduction by internal fertilisation (Long 2010). The male possesses intromittent organs called claspers,

which are attached to the pelvic fins and are inserted into the cloaca of the female (Long 2010). Reproduction of most chondrichthyans follows the K-strategy, of which internal fertilisation is a characteristic element, and further involves a non-territorial and solitary lifestyle, few offspring, slow maturation, and infrequent reproduction (Parker 2008). The K-strategy slows the responsiveness of the chondrichthyan community to environmental changes (Parker 2008), suggesting an increased extinction risk. However, this risk has been shown to be significantly lower for oviparity (egg-laying; García *et al.* 2008), which appears to have been the primitive reproductive style in chondrichthyans (Compagno 1990), suggesting potential resistance to extinction. Among extant groups, oviparity is still observed in holocephalans and many Carcharhiniformes, Orectolobiformes and Rajiformes, whereas viviparity (live birth) most commonly occurs among extant elasmobranchs (Schultze and Soler-Gijón 2004).

1.5 CHONDRICHTHYAN DENTITION

1.5.1 MORPHOLOGICAL VARIATION

Heterodonty is typical of many selachian dentitions and either monognathic heterodonty (different dental morphologies within one jaw) or dignathic heterodonty (different dental morphologies in the upper and lower jaws), or a combination of both may occur (Applegate 1965; Cappetta 1987). Gradient and disjunct monognathic heterodonty respectively signify gradual change and large dissimilarity between adjacent teeth (Applegate 1965). Further variety is caused by ontogenetic heterodonty (smaller, narrower, and sharper in juveniles) or gynandric heterodonty (sexual dimorphism) (Compagno 1970). Therefore, if recovered in a disarticulated state, teeth of different morphologies may not be recognised as belonging to the same dentition and assigned to different species, which partly explains the large number of known fossil species. Crown morphology is particularly adaptable and tooth crown variability largely results from specialisation towards the exploitation of different food sources.

Conversely, however, exploitation of the same food source may result in the development of similar tooth morphologies. Convergence (and parallelism) can, therefore, also lead to taxonomic misinterpretation.

The broad spectrum of Palaeozoic dental variability can be explained by a number of specialisations besides heterodonty, including (see Section 1.5.2 for terminology used): tooth enhancement; increased number of cusps associated with transverse expansion of the base; reduced main:lateral cusp ratio; reduced cusp height; spacing devices on base and/or crown to facilitate migration of successive members of a tooth family; and fusion (Zangerl 1981). Similarly, characteristically Mesozoic features include: anterior teeth sharper and narrower than lateral teeth (see Figure 1.7); upper teeth wider than lower teeth and with a rearward slanted cusp, rather than straight; and serrations (if present) larger on upper teeth than on lower teeth (Cappetta 1987). It should be noted, however, that these are generalisations and divergent dental patterns occur.

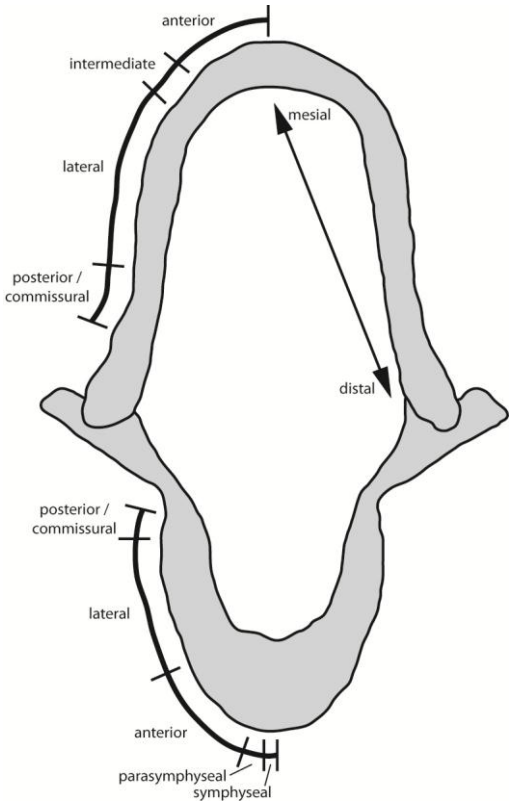

Figure 1.7 – Generalised chondrichthyan dental pattern (variable patterns occur), illustrated on an articulated set of gaping jaws in anterior view (modified from Applegate 1965 based on Cappetta 2012).

1.5.2 DENTAL PATTERN AND TOOTH TYPES

The great complexity of the chondrichthyan dental pattern is described using a widely accepted terminology. For example, the chondrichthyan dentition is divided into segments generally typified by a specific dental type (Figure 1.7). Symphyseal refers to unpaired teeth astride the symphysis and parasymphyseal refers to paired teeth beside the symphysis (both are generally lower jaw only, but variation occurs; Cappetta 2012). Anterior teeth are well-developed with a high, sharp crown, whereas intermediate teeth (upper jaw only) are reduced. Lateral teeth gradually decrease in size and possess a straight (lower jaw) or rearward slanted cusp (upper jaw), leading to reduced posterior teeth (Cappetta 1987, 2012). This pattern does not apply to durophagous chondrichthyans (see e.g., Stahl 1999). Further morphological terminology exists to describe detailed coronal and basal features (Figure 1.8).

Widely recognised chondrichthyan tooth types include a number of elasmobranch (cladodont, symmorid, diplodont), euselachian (hybodont, protacrodont), and euchondrocephalan (orodont, petalodont) types (Figure 1.9). But in cases where crown morphology is taxonomically insufficiently informative, basal morphology is more reliable (Klug 2010). Four different structural stages of root vascularisation and disposition of the foramina were first distinguished by Casier (1947a, b, c; see also Cappetta 1987), which may reflect the attained evolutionary level (Figure 1.10).

Anaulacorhizy is characterised by a flat lower face of the base, which lacks grooves, but shows seemingly randomly located pores. The stage comprises three types: hybodontoid (basal face subperpendicular to crown axis); notidanoid (basal face subparallel to crown axis due to labio-lingual root compression), and presquatinoid (advanced type approaching the polyaulacorhize stage; also known as ‘pseudopolyaulacorhize’). The latter type is characterised by basally open nutritive grooves, restricted to a labial depression, and horizontally aligned to numerous foramina on the lingual basal face (Klug *et al.* 2009). All synechodontiform taxa possessed this vascularisation pattern, even if it was not always distinctly developed in all tooth positions (Klug 2010).

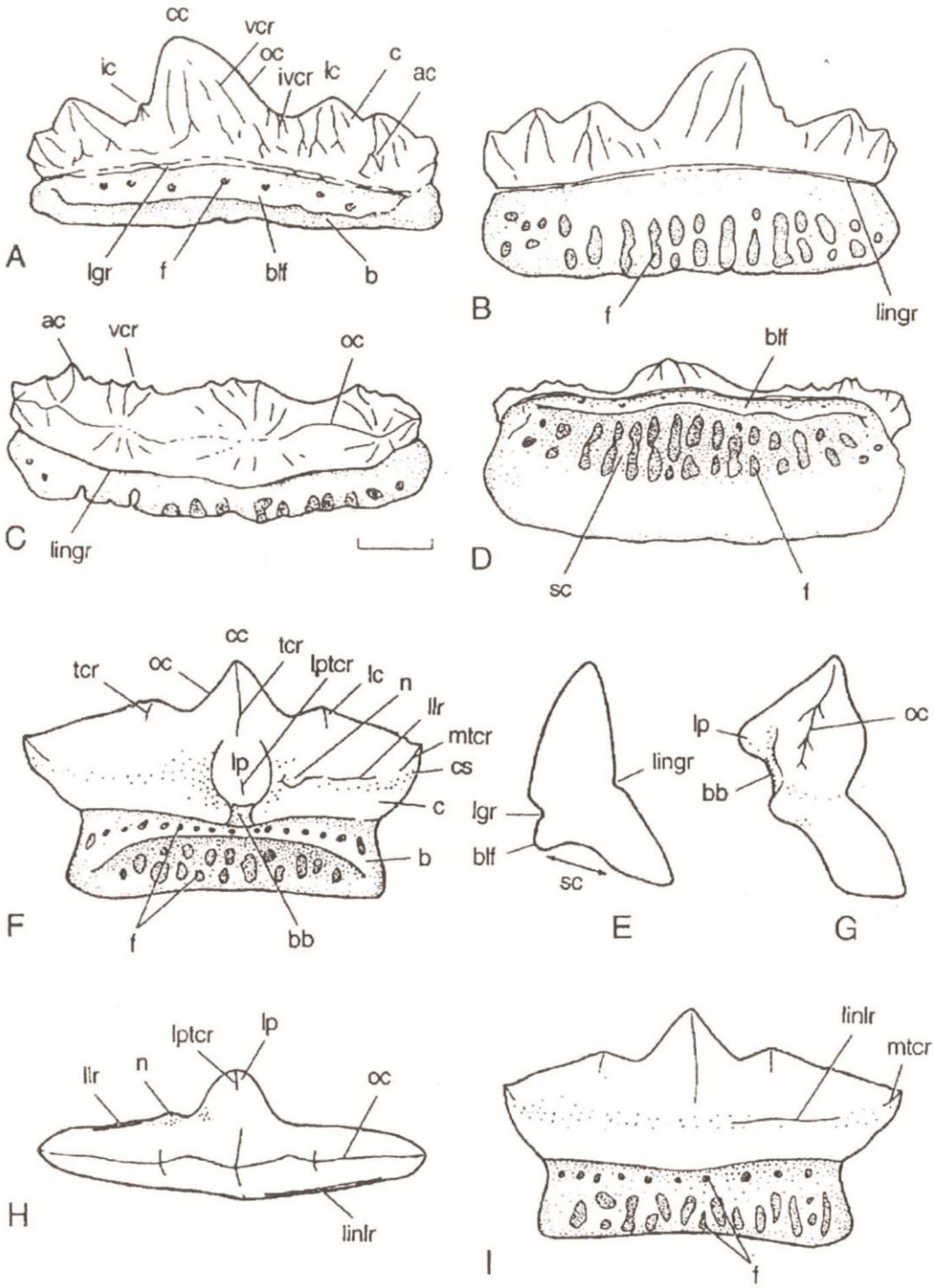

Figure 1.8 – Dental morphological terminology (euselachian; scale = 1 mm). A–E, *Sphenacanthus carbonarius* tooth: A, labial; B, lingual; C, apical; D, and basal views; E, transverse outline. F–I, *Lissodus* tooth*:* F, labial; G, lateral; H, apical; I, and lingual views. Abbreviations: ac, accessory cusp; blf, basolabial flange; b, base; bb, basal buttress; c, crown; cc, central cusp; cs, crown shoulder; r, foramen; ic, intermediate cusp; ivcr, intermediate vertical crest; Ic, lateral cusp; Igr, labial groove; lingr, lingual groove; linlr, lingual longitudinal ridge; llr, labial longitudinal ridge; lp, labial peg; lptcr, transverse crest of labial peg; mtcr, marginal transverse crest; n, node; oc, occlusal crest (referred to here as longitudinal crest); sc, sulcus; tcr, transverse crest; vcr, vertical crest (reproduced from Soler-Gijón 1997a, fig. 3).

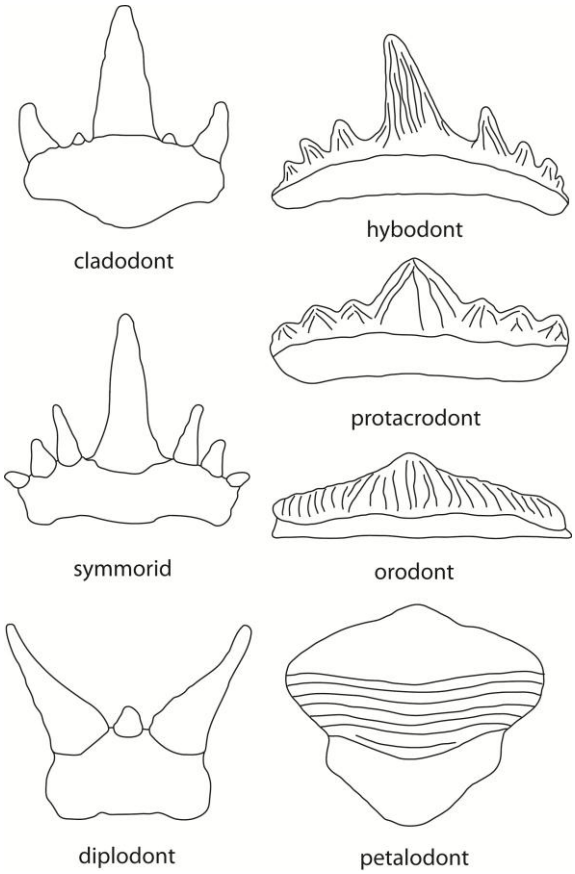

Figure 1.9 – Basic chondrichthyan crown types (compiled and redrawn from Turner and Miller 2005, fig. 8; Ginter *et al.* 2010, figs. 5, 9). The symmorid design occurs among cladodonts and is thus a subcategory.

Hemiaulacorhizy first appeared in the Anachronistidae (Carboniferous; see Ginter *et al.* 2010). The lower basal face is approximately perpendicular to the crown axis and has a central hollow where the central foramen opens. Holaulacorhizy appeared in the Jurassic. The vascular canal is completely open and forms a groove that divides the lateral sides of the base. Polyaulacorhizy only occurs among batoids and is characterised by transverse enlargement of the base. Its basal face displays numerous grooves, separated by parallel laminae. Many small foramina within the grooves have replaced the central foramen.

Holocephalian tooth plates are thought to be compound structures that evolved by fusion of separate teeth, which is supported by morphological evidence (except in chimaeroids), such as regular indentations at the sides of the crown in some taxa (Stahl 1999). In some cochliodonts, fusion may have been limited to the bases of teeth

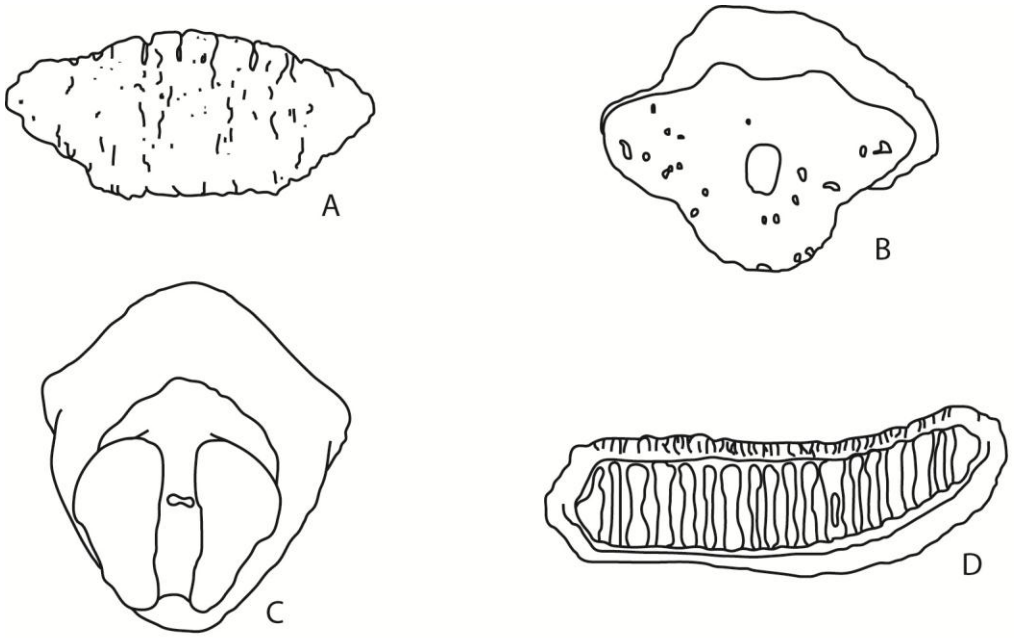

Figure 1.10 – Root vascularisation types: A, anaulacorhize; B, hemiaulacorhize; C, holaulacorhize; D, polyaulacorhize (redrawn from Cappetta 1987, fig. 21).

within a family and this likely delayed or prevented the shedding of these teeth (Stahl 1999). The general evolutionary pattern thus comprises a decrease in the number of teeth in a family, an enlargement in size and the tendency to adhere (Stahl 1999).

1.5.3 HISTOLOGY

1.5.3.1 INTRODUCTION

Enameloid (coronoin) is a well-mineralised hard tissue composed of hydroxylapatite ($Ca_5(PO_4)_3(OH)_x$) that displays 3.0–3.5% hydroxyl substitution with fluoride (fluorohydroxylapatite; Sasagawa 2002) and forms the surface layer of chondrichthyan teeth. It is an analogue to mammalian ectodermal enamel rather than a precursor (Sasagawa 2002) and is similarly functional in processing food. As a result of polyphyodonty, all odontogenetic stages can be observed in a buccolingual histological section of the jaw (Sasagawa 2002). The biomineralisation mechanism employed in enameloid development is distinct, because of the involvement of the mesenchym

(Sasagawa 2002; Gillis and Donoghue 2007). Enamel is a monotypic tissue with incremental growth lines, whereas enameloid is bitypic and mineralisation lacks a discrete front (Smith 1992, 1995). Enameloid may in fact be classified as a specialised form of dentine, because of the major contribution of odontoblasts to the organic matrix deposition and the similarity of the enameloid surface to the dentine-enamel surface in mammals (Sasagawa 2002). Elasmobranch enameloid is distinct from enameloid in bony fish and pleromin in holocephalans based on a number of characteristic features (see Sasagawa 2002).

1.5.3.2 PHYLOGENETIC MICROSTRUCTURAL VARIABILITY

A generalised morphological description of euselachian and neoselachian dental microstructure, based on a phylogenetically systematic Scanning Electron Microscopy (SEM) survey of tooth microstructure in fossil chondrichthyans (see Gillis and Donoghue 2007), shows that euselachians are equipped with multicuspid teeth that are commonly used for clutching and grasping. These are covered by a monolayer consisting of single crystallite enameloid (SCE; Figure 1.11), which is composed of randomly oriented single crystallites that are elongate (0.5–1 µm in length) or (sub)rounded. It is not further microstructurally differentiated and may be hypermineralised to such an extent that no individual hydroxylapatite crystallites can be seen (Gillis and Donoghue 2007).

Neoselachian teeth are commonly used for cutting and gouging. Neoselachian morphology is derived and a rapid and complex microstructural re-organisation around the start of their radiation resulted in a triple-layering of the enameloid (Gillis and Donoghue 2007). Starting from the outer enameloid surface (OES), the following layer differentiation can be observed: shiny layer enameloid (SLE); parallel-fibred enameloid (PFE); and tangle-fibred enameloid (TFE; Figure 1.11; see also Figure 1.12).

SLE is a tissue consisting of randomly oriented single crystallites with no fibre bundles. The individual hydroxylapatite crystals are generally not discernible in PFE,

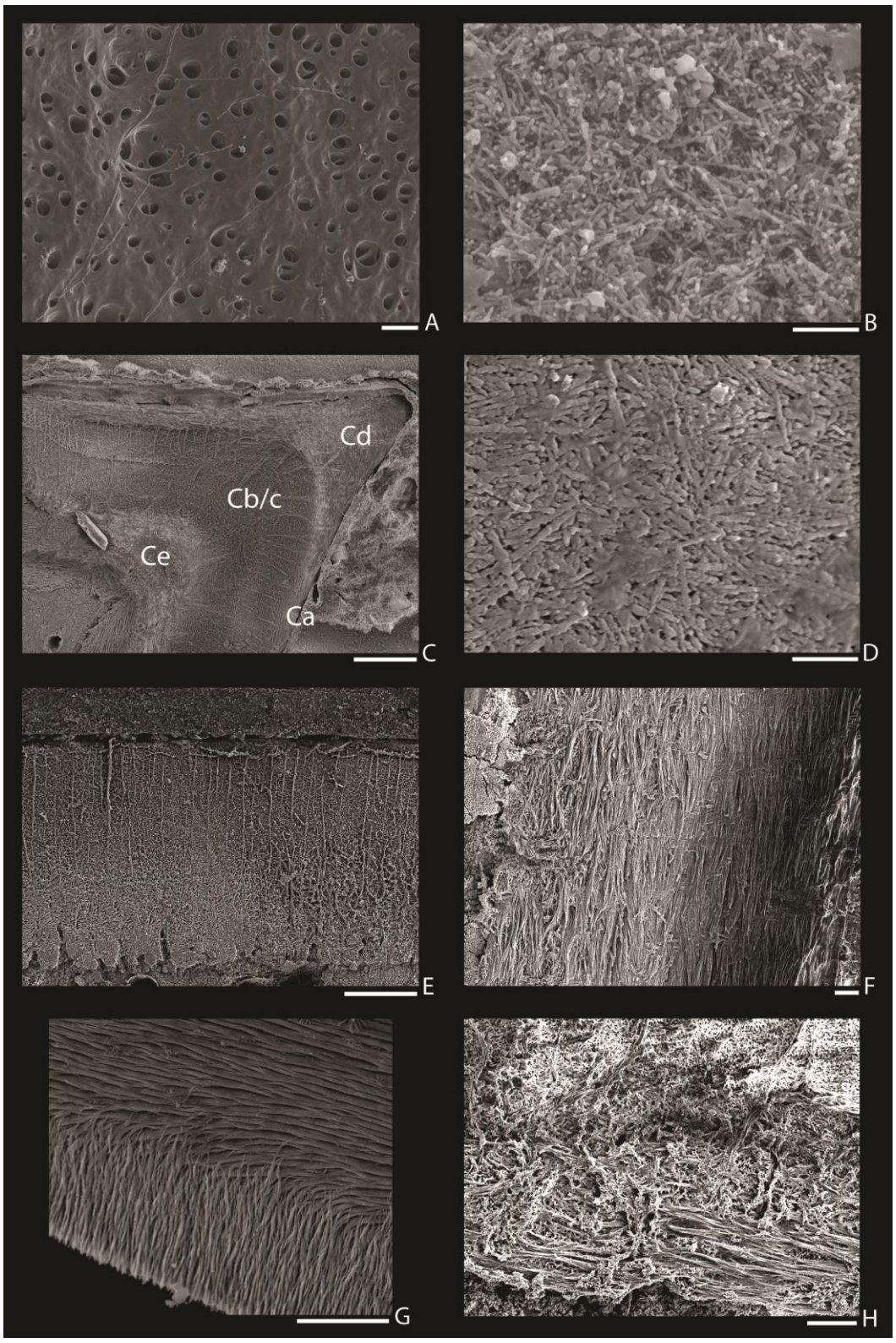

Figure 1.11 – Scanning Electron Microscopy survey of dental tissues: A, dentine; B, single crystallite enameloid; C, triple-layered enameloid, with dental tissues individually magnified: shiny layer enameloid (Ca) in D; parallel fibred enameloid (PFE; and tangle-fibred enameloid in the lower half) in transverse section (Cb) in E; PFE in longitudinal section (Cc) in F; PFE in surface view (Cd) in G, which diverges from normal orientation near the cutting edge; and tangle-fibred enameloid in transverse section (Ce) in H. Scale bars represent: A, F, H = 20 μm; B, D = 1 μm; C, E = 100 μm; and G = 40 μm.

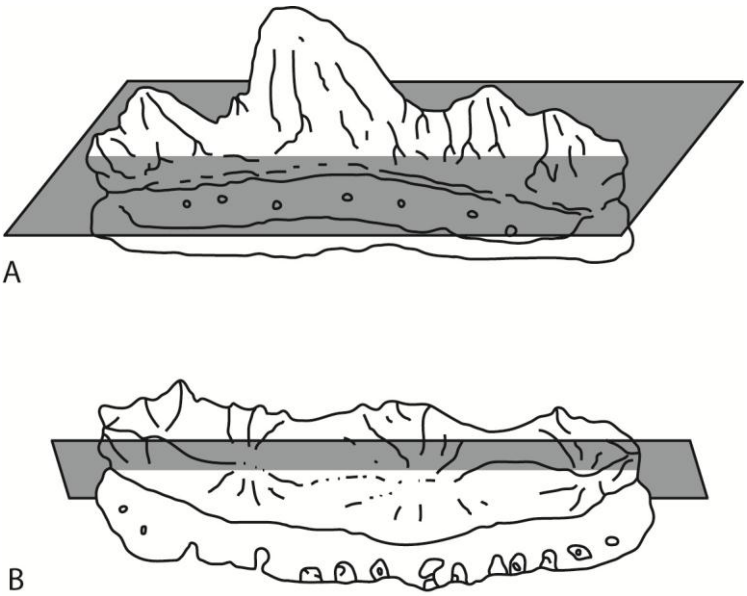

Figure 1.12 – Sections of a tooth: A, transverse; B, longitudinal.

but are fused into two types of fibre bundles. The spatial orientation of these bundle types is here believed to be incorrectly described (interchanged) by Gillis and Donoghue (2007; confirmed by Cuny, pers. comm. 2010): the description by Reif (1973a) is, therefore, followed. The first bundle type consists of longitudinal fibres 2–3μm in diameter, which are arranged parallel to each other, are oriented parallel to the OES, and run in a longitudinal direction. Radial bundles are oriented normal (perpendicular) to the OES and, because they do not show up in longitudinal sections, they may actually be straight ribbon-like septa rather than cylindrical bundles (Fosse *et al.* 1974). PFE tissue morphology has been demonstrated to prevent crack propagation and to enhance tensile strength (Preuschoft *et al.* 1974).

The individual hydroxylapatite crystals are also not discernible in TFE, but here they are organised into interweaving fibre bundles 2–3μm in diameter and oriented parallel to the OES. This morphology gives teeth resistance to compressive force (Preuschoft *et al.* 1974). This layer is underlain by dentine, the transition to which is referred to as the enameloid-dentine junction (EDJ). The junction is extremely irregular and intricate (Sasagawa 2002) and odontoblast cell process canals (dentine tubules) extend across it (Gillis and Donoghue 2007). Dentine is a distinct tissue, because of its high porosity

and its characteristic microstructure (Gillis and Donoghue 2007), but it also consists of much smaller crystals than enameloid (Sasagawa 2002).

1.5.3.3 ENAMELOID DEVELOPMENTAL EVOLUTION

Chondrichthyan tooth enameloid is believed to be a homologous character, involving the presence of an SCE monolayer in the most basal taxa, and indeed, the tissue has been traced back to the earliest known teeth from the Lower Devonian (Botella *et al.* 2009a). Gillis and Donoghue (2007) also observed the presence of an SCE surface layer in several basal elasmobranchs. Early microstructural differentiation may have resulted in double-layered enameloid in certain Hybodontiformes (e.g., *Acrodus*, *Polyacrodus*), comprising a compact outer SCE layer and an inner SCE layer with some parallel bundles perpendicular to the EDJ (Cuny *et al.* 2001). Triple-layered enameloid was acquired later along the neoselachian stem, but the fully differentiated microstructure was present in at least the last common ancestor of all crown group Selachimorpha (Gillis and Donoghue 2007). The Batomorphii are devoid of triple-layered enameloid.

Neoselachian microstructure differentiation is likely a pre-adaptation (exaptation; Gould and Vrba 1982) that facilitated the innovation of novel and complex feeding strategies (Thies and Reif 1985) by enhancing tooth integrity (Gillis and Donoghue 2007). In conjunction with an increase in prey abundance and diversity, it resulted in a major neoselachian radiation during the Jurassic and Cretaceous (Thies and Reif 1985).

1.5.4 MICROWEAR

The rate at which teeth are shed and replaced in chondrichthyans is variable, but is generally rapid. In extant sharks, for example, replacement occurs in a matter of weeks (Cappetta 2012). Advanced tooth wear is, therefore, not commonly observed, but extensive tooth wear is often very severe, with the potential removal of entire cusps.

Wear facets on fossil teeth have been linked to durophagy (e.g., Duffin and Ward 1983; Underwood 2002). More extensive wear facets are frequently observed in bradyodonts (holocephalans), due to the crushing and grinding of hard-shelled prey combined with slower tooth replacement (Zangerl 1981). Holocephalan tooth plates are only shed infrequently or retained and enlarged through life, so the degree of functional wear in these teeth is often greater and may result in depressions in the occlusal surfaces (Stahl 1999, see also fig. 21). Also, tooth corrosion from regurgitation of gastric residue masses (containing a high concentration of hydrochloric acid) may have enhanced dental wear (Zangerl 1981).

In conclusion, the understanding of the Permian–Triassic, the Late Permian mass extinction and related biotic crises, as well as of chondrichthyan taxonomy and morphology developed in the previous based on the treatise of background information, will aid in interpreting the data presented in this study.

2 METHODOLOGY

2.1 MATERIALS

The material used in this study consists of chondrichthyan remains from Permian and Triassic deposits. These include mineralised hard parts, such as isolated dental remains, dermal denticles and fin spines, which are generally the best preserved. Even though all types of isolated remains are used in this study, most importance is assigned to teeth, because of their higher taxonomic potential.

2.1.1 INSTITUTIONAL COLLECTIONS

Fossil collections from natural history museums and geological surveys are a powerful tool in obtaining comprehensive occurrence data on Permian and Triassic chondrichthyans. Data was obtained from three institutions, of which two collections were studied first hand. The first is the Geologisk Museum (Geological Museum; GM) in Copenhagen, Denmark, which is part of Statens Naturhistoriske Museum (the Natural History Museum of Denmark) and attached to the University of Copenhagen. The collection here is curated by Dr G. Cuny. The second intitution is the Palaeontology Department at the Natural History Museum (NHM) in London, United Kingdom, where the collection is curated by Dr Z. Johanson. The third and last collection at the Geologische Bundesanstalt (Geological Survey of Austria; GSA) in Vienna was not visited in person, but a collection list was obtained from the curator, Dr I. Zorn.

Occurrence and age data of the Permian–Triassic chondrichthyan remains registered in the collections have been compiled in individual collection lists (not included here). Publications exist on many of the listed occurrences and these have been integrated into a global database (Appendix A2.1; see Section 2.6.1). Although the collections contain greater detail of faunas recovered locally, these unpublished

(non peer-reviewed) occurrences have not been integrated into the database due to often insufficient labelling information and potentially unreliable identifications. Further study is required to confidently identify all specimens in these collections and compare them to the published record before the occurrence data can be used. This was not possible as part of this study due to time restrictions, which is why the collections were solely used to become familiar with the general diversity and preservation of Permian–Triassic chondrichthyan remains.

2.1.2 PRE-EXISTING SAMPLE RESIDUES

Chondrichthyan microfossil material was obtained by picking through research collections of sample residues remaining from conodont research. Conodont residues are an appropriate source of material because they are obtained with the same processing methods. Three collections were examined in total (Table 2.1). Two of these, belonging to Dr M.J. Orchard of the Geological Survey of Canada (GSC) in Vancouver and also to Prof. C.M. Henderson of the University of Calgary (UC), Canada, yielded fossil remains from Oman, India, Indonesia, China, Iran, Spitsbergen, Canada (including the Canadian Arctic) and the western USA. The third collection was loaned by Prof. A. Tintori of the University of Milan (MPUM) in Italy, consisting solely of material from the Haushi-Huqf area in Oman. In all cases, the residues were obtained using acetic acid digestion and the conodonts and other fossil animal groups were recovered for taxonomic and stratigraphic purposes by the collection owners. The stratigraphical and locality information for these samples is provided in Appendix A1.1, as well as information pertaining to sample size and fossil content.

Table 2.1 – Summary of material obtained from conodont residue collections.

GSC collection	Oman, India, Indonesia, China, Iran, Spitsbergen, Canada (incl. Canadian Arctic), western USA	70 samples	453 specimens
UC collection	Oman, Canadian Arctic	19 samples (+9 barren)	193 specimens
MPUM collection	Haushi-Huqf area, Oman	54 samples	2200+ specimens

2.1.3 HAND SAMPLES

Rock samples were obtained from the research collection of Dr R.J. Twitchett, which were collected from the western USA, Japan, and Spitsbergen. These were processed using acid digestion (see Section 2.3.2) and picked in order to recover any chondrichthyan remains contained within.

2.1.4 FIELDWORK

In addition to the data from existing collections, attempts were made to collect new material and generate novel occurrence data from Permian and Triassic outcrops worldwide. Field collection was undertaken on four occasions, in East Greenland, Oman (twice) and Japan. Upon completion of acid digestion of the limestone/dolomite samples (see Section 2.3.2), the obtained residues were picked for chondrichthyan remains.

In East Greenland, material was collected from the localities of Kap Stosch, Traill Ø, and Schuchert Dal in August 2009 (see Section 5.2). The sampled formations include the Ravnefjeld Formation, Schuchert Dal Formation and Wordie Creek Formation, which are of Wuchiapingian, Changhsingian and Griesbachian–Dienerian age, respectively, and provide a complete record through the late Permian extinction event and the immediate post-extinction phase. Different types of samples were collected, including individual fossils, fossil-bearing hand samples (including concretions and nodules), coprolites, and 27 limestone blocks for acid digestion (Appendix A1.7; GR collection). It was not possible to process all samples, due to time restrictions and as the result of the high clastic content of the samples.

In Oman, 12 localities were sampled in February–March 2010 and February 2011. Material was collected from Wadi Alwa, Wadi Sahtan, Wadi Aday, the Saiq Plateau, Wadi Wasit, Al Buday'ah, Wadi Maqam, Wadi Shuy'ab, Bu Fasiqah, Qarari Block, the Bridge and Aseelah (see Section 3.2). A total number of 107 samples were collected, amounting to 170 kg. The samples all consisted of limestone blocks for acid digestion

and covered an age range from the Guadalupian (Wordian) to the Lower Triassic (Spathian, Olenekian) (Appendix A1.5; OM collection). It was not possible to process all samples, due to time restrictions and as a result of dolomitisation of the samples.

In Japan, the sampling effort in April 2011 focused on the outcrop at Kamura, Takachiho, Miyazaki Prefecture, Kyūshū (see Section 4.2). The section here is extensive (135 m condensed section), comprising the Iwato, Mitai and Kamura formations and providing an age range from the Wordian in the middle Permian through to the Norian in the Upper Triassic. Limestone blocks for acid digestion were again collected (a total of 59 samples, amounting to 130 kg) but the Changhsingian was not sampled due to dolomitisation of the limestone deposits (Appendix A1.6; JP collection).

2.2 FIELD METHODS

Limestone beds were preferentially sampled because limestone samples allow processing in a controlled environment in the laboratory and respond well to acid digestion. A sample size of at least one and preferentially 3–5 kg was recommended by experienced researchers (R.J. Twitchett pers. comm. 2010; C.M. Henderson pers. comm. 2010). Taking into account practical considerations with regard to transport and the large number of samples, a minimum of 1 kg was collected per sample. Larger samples were collected in some instances, depending on the stratigraphic importance of the sample or if the bed was known to yield chondrichthyan remains. In most cases, the stratigraphic position of the samples was noted on a pre-existing detailed log of the studied section with the greatest possible accuracy (provided and referenced in Sections 3.2 and 4.2, reflecting the same boundary definitions as in the source publication). The exact position could be determined if those who logged the section were present or if height markers could be distinguished in the field. This was true for Wadi Sahtan, Wadi Aday, basal section and parts of the middle and top section on the Saiq Plateau, Wadi Wasit, Al Buday'ah, Wadi Maqam, Wadi Shuy'ab, and Kamura. If

time allowed and more detail was required, the stratigraphy of the section was logged at a bed-by-bed scale (10s of centimetres to metres). This was carried out at Wadi Alwa, the P/Tr boundary section on the Saiq Plateau, and Bu Fasiqah. No logs are available for the Qarari block, the “Bridge” or Aseelah, but these are very restricted sections. Sections in East Greenland were logged by Dr R.J. Twitchett. Samples were either collected from every distinct horizon (visibly or known to be fossiliferous) or at regular intervals (every 2-5 m at Wadi Alwa; every 20m at the basal Saiq Plateau; variable at Wadi Wasit: every 2–20 m at section and every 25 cm at block; every 2 m at Kamura). The nature of the fieldwork in Oman in 2010 (IGCP 572 field workshop) imposed time restrictions and placed a limit on the number of samples that could be taken. All samples were bagged and carefully labelled. The position of sampled localities and often also individual samples were recorded with GPS using WGS84 as the reference coordinate system.

2.2.1 Lithological identification

Field identification of the lithology of collected samples was recorded, but regarded as preliminary. Additional notes were taken while processing in the laboratory, for example with regard to colour variation, degree of dolomitisation and clastic content. Samples that yielded chondrichthyan remains were also examined by Dr K. Page (Plymouth University) for accurate limestone classification and identification of fossil content, as confirmation of previously recorded data, and for interpretation of depositional environment.

2.3 Laboratory methods

2.3.1 Sample curation

In the laboratory, the samples were prepared for processing by first cleaning them under running water with a nylon toothbrush to remove any plant growth or adhering

sediment. A representative portion of the sample was separated from the bulk either by using a geological hammer or a diamond-lined circular saw, left to dry, labelled and stored. These fragments were minimally 1-2 cm thick and 100 g in weight, large enough for use in lithological identification. Before the samples were processed further, the dry mass was recorded.

2.3.2 Sample processing

Each sample was chemically processed by acid digestion to extract the fossil content. Limestone can be broken down using two different standard extraction techniques, one of which uses buffered acetic acid (Jeppsson *et al.* 1999) and one that uses buffered formic acid (Jeppsson and Anehus 1995). Acid digestion as an extraction technique is proven to be safe for phosphatic fossil remains, provided that the solution is adequately buffered (Jeppsson *et al.* 1985; Jeppsson and Anehus 1995) and that the freed residue is removed within 24 hours and rinsed thoroughly before leaving it to dry (G. Cuny pers. comm. 2010). This is to prevent etching of the fossils by the acid, which is especially important when using formic acid, because it is more aggressive than acetic acid. Acetic acid is more difficult to rinse out of the residue and 24 hours under running water was recommended (G. Cuny pers. comm. 2010) to avoid crystal formation inside the specimens causing them to disintegrate, but practical restrictions in the laboratory (no dedicated permanent workspace) prevented this to be applied. Instead, the residue was thoroughly rinsed and dried in filter paper, which extracted much of the moisture when drying and crystal formation was only observed on the outer rim of the filter paper. Subsequent study showed that conodonts and fish remains were successfully extracted this way, even from residues that had not been removed every 24 hours, which was the case in the hand samples from the western USA and some from Japan, processed with acetic acid (see Appendix 1.1). In handling the chemicals used for acid digestion, all applicable Control of Substances Hazardous to Health (COSHH) procedures were observed to ensure health and safety of all. This included sufficient ventilation in the work area, the use of a lab coat, latex gloves, safety goggles, and a

fume cupboard of adequate specifications. All solutions were mixed and stored in bulk in a separate container to limit handling of pure acid and to facilitate control over concentration levels. The acid solutions were kept in closed containers (with a lid) to keep evaporation to a minimum, both for safety reasons and to maintain concentration levels. Adequate size containers were selected that allowed only sufficient acid to be added to sustain the reaction for 24 hours and to ensure that the samples were fully submerged, limiting the volume of reactive acid in use at any one time. Finally, samples were usually placed in a metal or plastic colander to facilitate temporary removal from the container while the residue was removed and the solution changed, in order to limit contact with the acid solution.

2.3.2.1 BUFFERED ACETIC ACID TECHNIQUE

Two different methodologies were used for obtaining the required acid solution: mixing the raw materials or re-using part of the spent solution after a processing cycle. The methodology using raw materials was only used to start the processing when spent acid was not available. Both methodologies, taken from the published techique (Jeppsson *et al.* 1999), were first tested by mixing a trial solution. This was done to ensure that the solutions conformed to the recommended guidelines and were safe for the phosphatic remains, for which the acceptable ranges are: pH 3.6–3.8 and 6–8 % (Jeppsson *et al.* 1999).

A trial solution of 100 ml was made up of 93 ml (deionised) water and 7 ml glacial acetic acid ($C_2H_4O_2$ / CH_3COOH) for a 7% solution, which has proven to be an efficient concentration both in terms of dissolution time and equipment (Jeppsson *et al.* 1999). The resulting pH after this step was 2.2, but was raised to 3.6 by adding 3.0 g calcium acetate ($Ca(C_2H_3O_2)_2$), which acts as a buffer, while stirring vigorously. The density of the resulting solution was 1.026 g/ml. The ratios between components of the solution that were determined from the trial were then scaled up to the volumes required for processing.

The mixing of a new solution using spent acid (acetate soup) as a buffer was also tested by a trial solution. The method was based on the recommendations of Jeppsson *et al.* (1985) and Orchard and Irwin (1994), which are very similar. The followed procedure involves mixing a solution using 60% water, 7% glacial acetic acid, and 33% acetate soup. First, about 80% of the required volume of water was poured into a plastic container, to which the appropriate volume of acetate soup and acetic acid was added. Finally, the rest of the water was added. The solution was vigorously mixed between each step. With a composition of acetate soup around pH 4.4 and a density of 1.054 g/ml, the resulting trial solution had a composition of pH 3.7 and a density of 1.028 g/ml, which is very close to the composition of the original trial solution (mixed from raw materials) and within the safe range.

During the initial stages of processing, large volumes were added to the samples (in theory enough to dissolve the entire sample) and the pH and density of the solution were monitored (by means of a calibrated pH meter and a hydrometer) to record the gradual changes in the composition of the solution while dissolution progressed. The pH and [Ca^{2+}] both increase, as H^+ and Ca^{2+} ions are respectively used and freed in the reaction, which influences the reactivity of the solution. The solution was also stirred regularly to prevent density layering, which lowers optimal dissolution rate. Active processing is indicated by CO_2 (g) release, which was monitored and in case the gas release slowed or stopped, Jeppsson *et al.* (1999) recommended the following appropriate measures:

a. if pH >5 and density ≈1.045 g/cm^3 then the acid is spent and needs changing.
b. if pH <4.5 and density >1.045 g/cm^3 then the solution needs to be diluted to 7%. In order to find the appropriate density they refer to an empirical relation, which they illustrate.
c. if pH <4.5 and density ≈1.022-1.030 g/cm^3 then the solution is correct.

In practice, gas release and sample mass decrease slowed down significantly when the pH reached ~4.5 and the density approached 1.050 g/ml, in which case the acid

was considered spent and changed. Once experience with the method was gained, the methodology was shifted towards the use of smaller volumes and only the pH was monitored. For each sample, an estimated appropriate volume for the first 24 hours of processing was added, after which the pH of the solution was interpreted, which indicates whether all the acid is spent and any dissolution potential remains, and the solution removed. The volume of newly mixed acid was then adjusted for the next 24-hour interval.

Initially, removal of the spent acid was achieved by siphoning off the liquid, as was recommended by Jeppsson *et al.* (1999). In time it was decided to move away from this and to simply remove the sample from the container and pour the solution out. In both methods, the spent acid was guided through a 63 µm sieve suspended above the receiving container to catch any residue and the container was then rinsed out with water, which was also poured through the sieve. Extra water was added to the residue to wash it and to remove clay particles until the flow became rapid. Subsequently, the sieve was rinsed out into filter paper, which was left to drain. This process was repeated daily until the sample was completely dissolved. The residue was then oven-dried at 30–40 °C for at least 24 hours.

Lithology dictates the rate of dissolution. Dolomite is not dissolved by acetic acid. The dissolution rate is slowed if the carbonate content is low and also if the argillaceous content is high (Jeppsson *et al.* 1999). Dissolution of argillaceous samples normally ceases around pH 4.0 rather than the pH of 5.0 that was mentioned in Jeppsson *et al.* (1999). In these cases, the buffered formic acid technique was preferentially used.

2.3.2.2 BUFFERED FORMIC ACID TECHNIQUE

The buffered formic acid technique has two advantages over the buffered acetic acid technique, because it breaks down dolomite and is a more rapid process (Jeppsson and Anehus 1995). However, formic acid is more hazardous and more expensive. Only

one methodology was used in this process. Re-using the spent acid is not recommended, because Mg^{2+} is added to the solution in addition to Ca^{2+} during dolomite dissolution, lowering the buffering capacity of the spent acid (Jeppsson and Anehus 1995).

Jeppsson and Anehus (1995) recommend using a solution of a concentration well below 15.9%. A concentration near 10.6% is satisfactory. They empirically derived that 1 L of the formic acid solution dissolves 95 g dolomite, which equates to 11 ml solution per 1 g. They provide a recommended recipe for a hypothetical sample of 1000 g, which works out as a 9.6% solution with ~18 g/L calcium carbonate and ~1 g/L calcium phosphate, but this was adjusted slightly to compensate for the different concentration of formic acid available from the supplier. The solution for 1 g sample was mixed using ~1.294 ml 90% formic acid, 10.776 ml water, 0.220 g calcium carbonate, and 0.013 g calcium phosphate and multiplied according to the mass of the sample. The starting pH of the solution was 2.2–2.3.

During the initial stages of using this technique, a volume of acid solution was mixed that was, in theory, sufficient to dissolve the full weight of the sample. Progress was observed by gas release and monitoring of the pH, which gradually increased, and the solution was stirred regularly to avoid density layering. In later stages, however, an adjusted technique of only using a volume required to sustain dissolution for 24 hours was used in order to maintain optimal dissolution rates at all times. The residue was removed every 24 hours as described for the acetic acid technique until the sample was completely dissolved and adequately rinsed each time before being dried.

2.3.2.3 Further processing

After the residue was dried, it was sieved into different size fractions using stacked sieves with 500, 250, 125, and 63 µm mesh. These sieves were cleaned before use with a double ended nylon sieve brush. The resulting size fractions were transferred into labelled glass tubes and stored until the residues could be picked. Further

processing techniques such as magnetic separation, density separation with sodium polytungstate and electrostatic picking were not required because of limited sample size in most instances. Picking was done using a Kyowa low power binocular microscope and a horse hair paintbrush. All specimens were stored in small, transparent plastic boxes, or on microslides (kept in place with diluted glue from a glue pen). These are kept at Plymouth University or in the permanent collections in which they have been deposited.

2.3.3 Scanning Electron Microscopy (SEM)

Representative specimens of each taxon identified in this project have been imaged using Scanning Electron Microscopy (SEM) under high vacuum. Metal stubs were prepared by adhering double-sided sticky tape to the surface, after which specimens were mounted onto it with a brush and occasionally positioned using wet manipulation. A suitable arrangement and orientation of the specimens is required to allow for rotation and tilting in the SEM, so that there is always a clear line of sight. A drawing of the arrangement was always made, to allow easy recognition and navigation (Figure 2.1). These drawings are kept together with their respective stubs either at Plymouth University or in the permanent collections where they were deposited. After the stubs were thoroughly dried, they were coated in gold or a gold-palladium alloy for a minimum of 90 seconds and a maximum of 2–3 minutes (the author was unaware of the technique using target coating thickness in Å). For microstructure study, a sufficient coating was normally acquired within ~100 seconds, but a longer coating time was allowed for moist, larger, and more complex teeth (~140 seconds). Removal of the specimens from the stubs, if needed, was achieved with acetone.

Electron charging was rarely encountered following the stub preparation methods described here. The effects of charging can be serious, because it obscures features, especially if they are microstructural, or thermally damage the specimens and the specimens can retain the electron charge for some time. Precautions were taken in some instances to prevent it, including the use of carbon discs and ensuring sufficient

contact between the disc and the specimen, as well as extra coating. For regular imaging, uncoated specimens can be placed in the SEM under a low vacuum without charging becoming a major problem, but this was only rarely used.

Four aspects of each specimen were imaged: apical, lingual, labial, and lateral (mesial or distal). The latter three aspects were accessed by tilting the stage to 60°. Sufficient time was taken to obtain a sharp image displaying all the important features before acquiring an image. Focusing was done at a magnification of at least twice that of the desired image. Specimens were positioned in such a way that problems with depth of field were avoided whenever possible, so that every aspect was in focus. Images were taken at a high resolution (up to 600 dpi if possible) and saved in an uncompressed format (.tif). All images were subsequently processed in Adobe Photoshop to remove the background and compiled in Adobe Illustrator to create plates that facilitate review and comparison of the specimens.

In total, three scanning electron microscopes were used at different institutes. At the Geological Museum, Natural History Museum of Denmark in Copenhagen, a FEI Inspect was used mainly for imaging. At the Zoological Museum, Natural History Museum of Denmark in Copenhagen, a JEOL JSM-6335F Field Emission Scanning Electron Microscope was used for microstructural study. Finally, a JEOL JSM-7001F Field Emission Scanning Electron Microscope was used at the Plymouth Electron Microscopy Centre for additional imaging and microstructural study.

2.3.4 Histological study

Histological study (see Section 1.5.3) is the only effective method to establish taxonomical affinity, and to recognise primitive neoselachian sharks and track their appearance in the fossil record (Reif 1973a; Cuny *et al.* 2001). In order to study enameloid microstructure of isolated teeth—also carried out using SEM under high vacuum—acid etching was required to remove the outer surface layer (to create a relief) and reveal the inner structure. In triple-layered enameloid (TLE), the enameloid layer at the base of the cusp is generally thin to the extent that some features (tangle-bundled

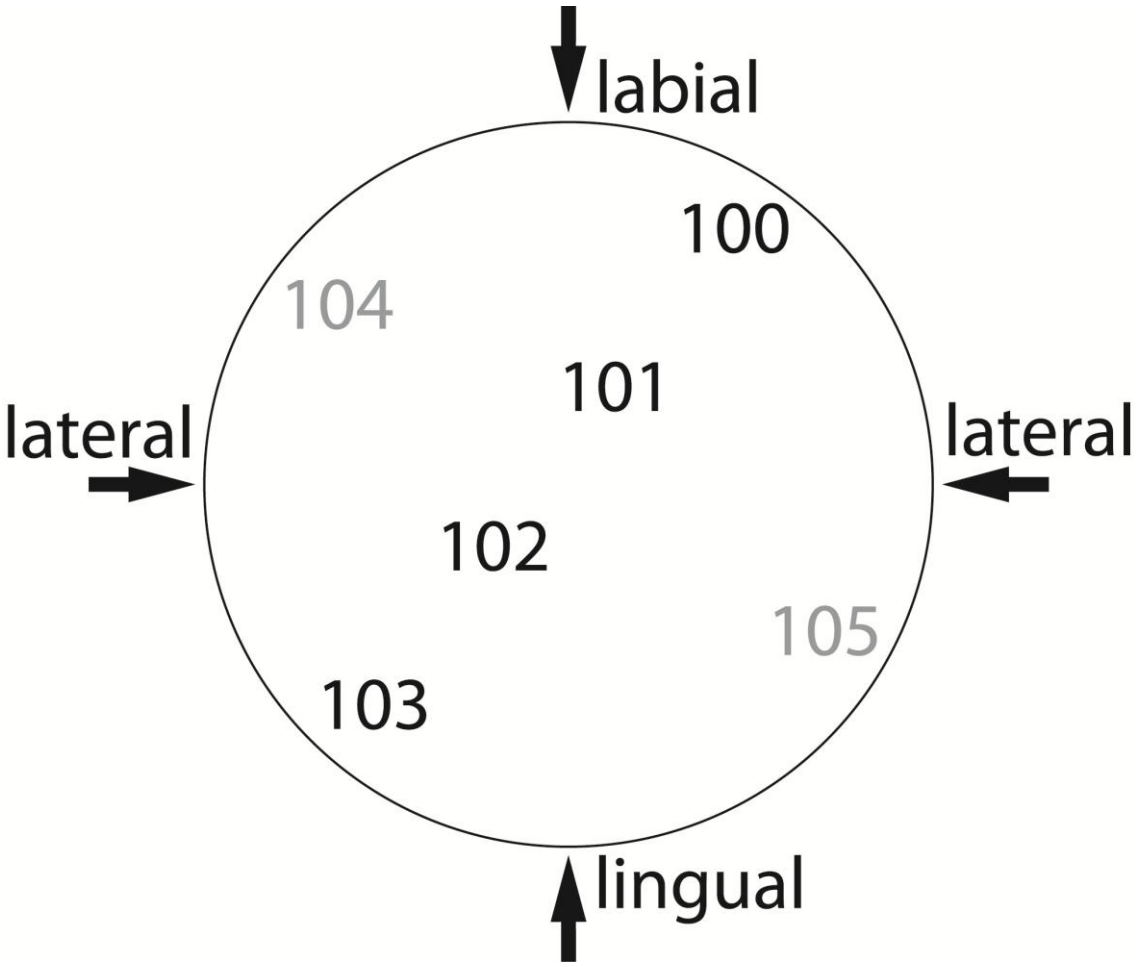

Figure 2.1 – Typical diagram illustrating from an apical viewpoint the arrangement and orientation of specimens on a stub for use in SEM study, to allow easy recognition and navigation. A clear line of sight is ensured from all aspects. The 100–105 arrangement is possible with low cusped teeth and a tilt of 60°, because the specimens are less likely to block line of sight than if the teeth are higher cusped or the used tilt is the maximum possible 90°, in which case 104 and 105 are not mounted.

enameloid; TBE) may be lost entirely (Cuny and Risnes 2005; Guinot and Cappetta 2011) and in primitive neoselachians, it is generally poorly developed (e.g., Cuny and Risnes 2005). Derived features are best developed and, therefore, best observed near the cusp apices in primitive neoselachian teeth. Specimens were preferentially selected that allowed surface study along the length of a complete (main) cusp and also showed a natural fracture, revealing the nature of the entire thickness of the enameloid layer. Fractures, however, even if artificially made, do not allow any real control over the plane of the section, which can severely inhibit accurate interpretation of the orientation of the crystallites or any bundles. This control is restored by making a section.

For sectioning, the tooth was stabilised by embedding it in resin, which was poured into a mould treated with vaseline. The transparent epoxy resin was mixed in the correct ratio of resin to hardener (e.g., 15:2 or 25:3), according to the supplier's instructions. The specimen needed to be fully immersed in the resin in order to prevent breakage due to vibrations when the specimen is sectioned. This often required a 2-step hardening process, because the specimen will normally sink to the bottom and be exposed on one side. The surface of the hardened resin from the first step was cleaned using a surfactant to ensure that the second layer of resin would adhere. The hardening process is exothermic, so air bubbles will normally be expelled. The resin set within ~24 hours and any excess resin was discarded once set. Care was taken to orient the specimen in the resin so that a suitable section was available for study. A longitudinal section is useful for observing the thickness of the enameloid layer along the length axis of the tooth. However, the bundles and other microstructural details are best observed in a transverse section.

Obtaining the section was a difficult process because of the small size of Permian and Triassic shark teeth. Normally it would be possible to polish the sample down until a section of the tooth is exposed, but an actual section was made instead using specialist equipment (diamond-lined microtome). Once the section was acquired by cutting, additional polishing was required to remove any striations left by the cutting blade. Polishing was done wet and in a circular motion. Coarser sandpaper (P600) was used first, after which a finer grade (P1200) was used to complete the process. Progress was monitored under a binocular microscope. The section was then ready to be acid etched.

2.3.4.1 ACID ETCHING

The specimens were dried before starting the etching process. Moisture will cause dilution of the acid around the specimen and results in uneven or a lesser degree of etching. The specimens needed to be submerged in the acid, which is relatively easily

achieved using a pair of tweezers when handling resin blocks. However, handling small, isolated teeth this way has an increased risk of destroying the specimens (by either chemical or mechanical means). These were instead mounted on a metal stub with double-sided sticky tape and the stub was then etched as a whole. This method was tested beforehand and did not influence the outward appearance of the teeth under the SEM. There is a small risk that specimens become detached while the stub is submerged, but this only occurred when using carbon discs and if there was a fragile contact between the disc and the specimen, but never when using sticky tape.

The etching agent used was ~3.7% hydrochloric acid. Sections were exposed for a maximum of 1 second, while complete teeth about 1–3 mm in size were safely etched for 5–10 seconds. To prevent any possible contamination, specimens were rinsed in demineralised water immediately after for 10 minutes. The specimens were dried for ~24 hours in a clean environment. If etching proved to be insufficient or deeper layers needed to be exposed, additional etching was carried out. This was generally the case with more robust specimens or more recent teeth, because triple-layered enameloid is ~10% thicker than single crystallite enameloid. If a gold(-palladium) coating was present, additional etching time (5 seconds) was added for its removal, but this may leave patches untouched if the teeth are complex. In some cases, therefore, the coating was removed manually beforehand using acetone, which does not etch the teeth.

2.3.5 Mechanical preparation

In case acid digestion was not a suitable option for preparation of the sample, for example because the lithology was unresponsive but relatively large (1–2 cm) fossil remains could be observed, the sample was prepared mechanically by means of a pressure-regulated air pen. Extreme care was taken to avoid direct contact with the specimen, which was strengthened with diluted glue against breakage caused by vibrations, allowing the lithified sediment to chip away. The method was stopped if it

was suspected that further processing would cause irreparable damage to the specimen.

2.4 Descriptive methods, systematics and phylogeny

Detailed description of all morphological features of the isolated chondrichthyan material was required for accurate identification. Physical reference material held in the collection of the Natural History Museum of Denmark in Copenhagen and the Natural History Museum in London was examined, including type material mostly relating to taxa recovered from Greenland. Further type material examined belongs to the new genera and species named as part of this project (appropriately deposited in permanent collections associated with the institutes with which the collection owners are affiliated). It was ensured that the naming of these taxa followed the stipulations in the International Code of Zoological Nomenclature (ICZN). The following key features were included in the descriptions: completeness, general dimensions and size ratios between cusps (Figure 2.2), general tooth form and type, crown form and features, root features, and vascularisation type. The descriptive terminology used was based on the standard reference work for each group. These standard works are Zangerl (1981) and Ginter *et al.* (2010) for Palaeozoic elasmobranchs and some euchondrocephalan groups; Cappetta (1987) for Mesozoic elasmobranchs; and Stahl (1999) for holocephalan euchondrocephalans.

The systematic classification used in this study for all genera that occur in the Permian and/or the Triassic is based in principle on the systematics used by Ginter *et al.* (2010), but follows recent revisions (see Appendix A3.1, A3.2 and notes Figure 7.1).

The phylogeny presented in Ginter *et al.* (2010) for early chondrichthyans and based on a compilation by Ginter (2004) is followed here, because it is the most parsimonious explanation for observed morphological evolutionary trends offered at this time, compared to two hypotheses presented by Lund and Grogan (1997, 2004; most recently presented by Grogan *et al.* 2012) and Coates and Sequeira (2001),

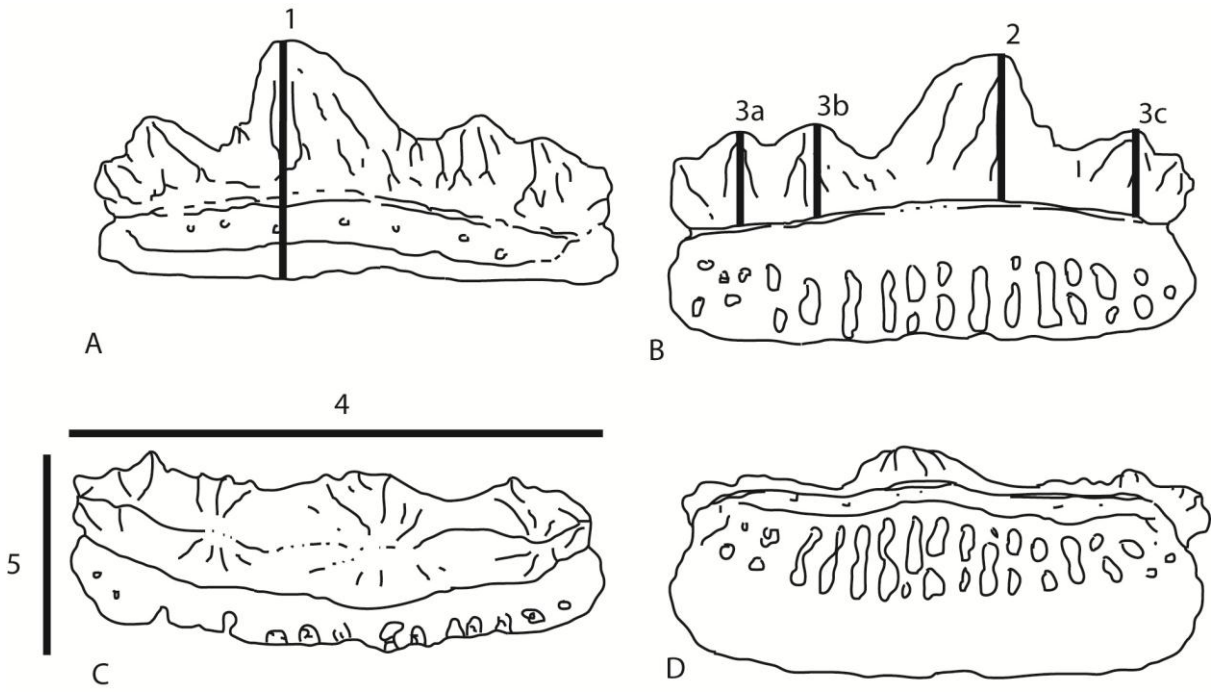

Figure 2.2 – Measurements taken to establish tooth dimensions and cusp ratios: 1, maximal apico-basal height; 2, height main cusp; 3a-c (etc.), height lateral cusps; 4, maximal mesio-distal length; 5, maximal labio-lingual width. A, labial view; B, lingual view; C, apical view; D, basal view.

respectively, the last of which excludes dental characteristics. Ginter *et al.* (2010) explain how the identification of early chondrichthyan remains at ordinal and lower taxonomic levels has been relatively stable for the last 30 years, but that the accepted relationships between orders and the general phylogeny of the Chondrichthyes has not. This is why the older works of Cappetta (1987) and Stahl (1999) are used as a basic systematic framework only and more recent phylogenetic analyses for certain groups (e.g., Klug 2010) are followed. The selected phylogeny is illustrated in Figure 7.1. The use of open nomenclature is based on the recommendations made by Bengtson (1988) and the microstructural terminology follows Cuny *et al.* (2001).

2.5 BIOSTRATIGRAPHY

Conodonts were recovered in conjunction with chondrichthyan remains for the purpose of dating samples accurately and to allow correlation with other localities either within the same basin or worldwide. Well-established conodont biochronologies (e.g.,

Orchard and Tozer 1997, Mei and Henderson 2001, Kozur 2003, Henderson 2005, Metcalfe and Isozaki 2009, Orchard 2010) were used for correlation purposes. The conodont material picked from the sample residues was sent to Dr M.J. Orchard from the Geological Survey of Canada in Vancouver for identification but these data are not yet available.

2.6 Analysis of the fossil record

2.6.1 Database of taxonomic occurrences

A database of Permian–Triassic elasmobranch and euchondrocephalan occurrences has been compiled from peer-reviewed literature (Appendix A2.1). It has been constructed using the most current collective works of chondrichthyan fossil material available (Stahl 1999; Ginter *et al.* 2010; Cappetta 2012), supported by older and more general reference works and online databases (Zangerl 1981; Cappetta 1987; Yamagishi 2006; the Paleobiology Database; the Bibliography of Fossil Vertebrates Online; Shark-References). In addition, over 270 individual publications have been reviewed in order to extract detailed information on the type of remains, dimensions of the specimens, precise location of recovery, (bio)stratigraphy, age, and on any changes in identification and taxonomical position (references provided within the database, Appendix A2.1). The database cannot be considered to comprise all chondrichthyan material ever reported in literature, because of the sheer volume of published work and difficulty in obtaining some publications, but it contains all currently valid taxa and is sufficiently comprehensive to show relevant trends. It is further supplemented by the newly discovered material described in this study.

Each taxon reported in an individual locality constitutes a taxonomic occurrence in the database (following Kriwet *et al.* 2009), and occurrences are organised according to taxonomic position (Appendix A3.1). The main body of the database comprises most types of fossil remains, such as (partial) body fossils, isolated teeth and fin/cephalic spines, which vary in taxonomic resolution (e.g., fin spines are less diagnostic than

teeth). It excludes occurrences based on isolated dermal denticles, which have been listed separately, because of their low taxonomic significance (see Section 1.4.3). All database analyses (see Chapters 7 and 8 for results) also exclude occurrences solely based on isolated denticles.

2.6.2 Data inventory of occurrences

The quality of the chondrichthyan fossil record has been assessed in a variety of ways. The first is global occurrence distribution (see Chapter 7, Figure 7.3), which is a representation of the number of distinct taxonomic occurrences per country. These data are inherently exaggerated, because description of deposits that preserve a more diverse fauna will amplify the sampling intensity recorded from that locality. However, because increased sampling effort is positively correlated to the number of recovered taxa (until sampling is exhaustive, see Benton 1998; Jamniczky *et al.* 2008), it does not require compensation.

A data inventory has been compiled to assess sampling intensity in relative time intervals (see Chapter 7, Figure 7.8). The employed method, derived from Kriwet *et al.* (2009), involves the creation of a data matrix containing occurrence counts per stage and separate columns for occurrences that have been resolved to epoch level only (see Appendix A2.3.7). The stage-level data are considered separately, excluding lesser resolved data, but all occurrences have been included in the evaluation of epoch-level data. A greater number of occurrences tend to accumulate in stages of longer duration, so the correlation between occurrences and interval duration has been tested (see Section 2.6.3). In case of a positive correlation, and therefore dependence on stage duration, it may be considered to correct for disproportionate interval-length and divide the occurrence counts by the duration of their respective intervals. This is not applied here, however, to avoid the risk of introducing standardisation errors.

2.6.3 Proxy dependence (Spearman's rho)

In order to test for dependence of diversity (see Section 2.6.6) on sampling proxies and interval-length or similar comparisons, Spearman's rank correlation coefficient (Spearman's rho) has been calculated. This is a non-parametric measure of statistical dependence between two variables and assesses how well the relationship can be described using a monotonic (linear) function. The data was first ranked from either the lowest or highest value, which was chosen as appropriate in each case, but kept the same for both sets of data. In case of identical values, the arithmetic mean of the ranks concerned was assigned to each.

For a sample of size n, the raw scores X_i,Y_i were converted into ranks x_i, y_i. Rho (ρ, also expressed as r_S) is defined as the Pearson's product-moment correlation coefficient (Pearson's r), but for ranked variables:

$$\rho = \frac{\sum_i (x_i - \bar{x})(y_i - \bar{y})}{\sqrt{\sum_i (x_i - \bar{x})^2 \sum_i (y_i - \bar{y})^2}}$$

Significance was determined using the Spearman's rank correlation coefficient critical values table (significant if ρ exceeded critical value).

2.6.4 Simple linear regression

Simple linear regression has been applied to various data using Excel to find the best-fit trendline, which is based on the expression: $Y = bX + a$. Significance of the correlation coefficient (R^2) was tested by calculating Student's *t* using the expression: $t = R\sqrt{\frac{n-2}{1-R^2}}$; and using the *t* distribution to find the critical *t* at a significance level α(2) of 0.05 and using the degrees of freedom, expressed as: $df = n - 2$. The null hypothesis of no relationship ($R^2 = 0$) was rejected if the *t* statistic exceeded the critical *t*. The *p*-value of the correlation could be calculated by interpolation using the Student's *t* distribution.

2.6.5 PHYLOGENETIC QUALITY ASSESSMENT

The phylogeny of Permian and Triassic chondrichthyan genera compiled here (see Chapter 7, Figure 7.1) has been combined with stratigraphic range data (Appendix A2.3.8, A2.3.9), using the First Appearance Datum (FAD) of individual taxa as minimum node dates (see Benton 2001), in order to assess completeness of the fossil record. This has been done via three methods. The first concept is the Simple Completeness Metric (SCM; Benton 1987). In its simplest form, this metric assesses the ratio of observed fossil ranges (FR) to the total number of ranges per time interval, thus including intervening stages (IS; as observed in Lazarus taxa; Figure 2.3). Once a stratigraphy is linked to a phylogeny, ghost ranges (GR) are also included in this total, which represent ranges of inferred existence despite lack of recovery from the fossil record. Ultimately, SCM is calculated as:

$$SCM\ (\%) = (\Sigma FR)/(\Sigma FR+\Sigma IS+\Sigma GR)*100$$

The second method is the Relative Completeness Index (RCI), which uses the ratio of cladistically implied gap (ghost ranges) to the known record to assess the "phylogenetic fit" of a cladogram to stratigraphy (Benton and Storrs 1994; Benton *et al.* 2000). RCI is calculated as:

$$RCI\ (\%) = (1-\Sigma MIG/\Sigma SRL)*100$$

with ΣMIG (Minimum Implied Gap) being the sum of durations of ghost ranges in the cladogram (Myr), whereas ΣSRL (Simple Range Length) is the sum of durations of known fossil ranges (including intervening stages) in the cladogram (Myr).

RCI values were calculated for two phylogenetic trees resulting from different branching methods applied to the chondrichthyan phylogeny (in which unresolved polytomies have been retained), which constitutes the third concept and is an alternative and more rigorous method of assessing the fit of phylogenies to the fossil record. The first branching method, referred to as the Conventional Branching Method (CBM) by Guinot *et al.* (2012, fig. 2), is widely used and assumes that "sister groups originate from a common ancestor from which they subsequently diverge, thus implying a coeval origination age for the two lineages" (Guinot *et al.* 2012, p.3). Any time gap

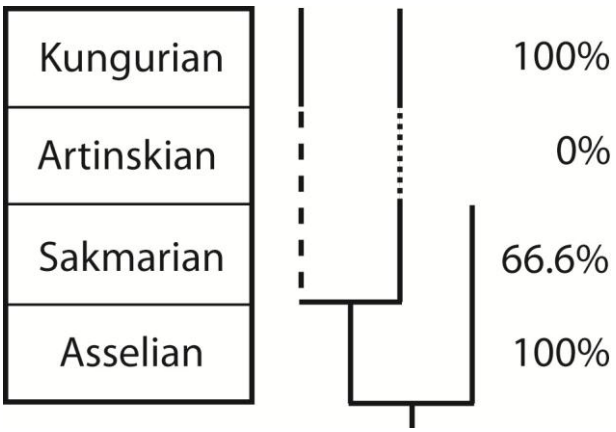

Figure 2.3 – Illustration of the Simple Completeness Metric (Benton 1987), which is calculated using observed fossil ranges (solid line), intervening stages (stippled line), ghost ranges (dashed line).

between the first occurrences of two sister taxa is, therefore, solved by adding a ghost range. Conversely, the Direct Descendence Branching Method (DDBM) considers that "the divergence age of a lineage can be younger than the first occurrence date of its sister group and that the former can be descending directly from the latter" (Guinot *et al.* 2012, p.3). The number of ghost ranges is, therefore, not artifically increased, especially in groups with a poorly resolved phylogeny. From both branching methods, diversity curves can be inferred, which are interpreted to respectively overestimate (CBM) and underestimate (DDBM) genus richness and hence define the Genuine Diversity Domain (GDD). If plotted with standing diversity, the difference between the latter and GDD is indicative of the completeness of the fossil record.

2.6.6 TAXONOMIC DIVERSITY ESTIMATES

Taxon richness is usually calculated on the basis of four main components defined by Foote (2000). These comprise taxa that are confined to an interval (singleton taxa; N_{FL}), that cross the lower boundary and disappear (N_{bL}), that appear and cross the upper boundary (N_{Ft}), and that cross both boundaries (N_{bt}) (Figure 2.4). N_{bt} is here distinguished into two categories, those taxa that are recovered from the fossil record (r) and Lazarus taxa (z), so $N_{bt} = N_{bt(r)} + N_{bt(z)}$. Different richness counts based on

various combinations of these components respond differently to biases (Fröbisch 2008; see Foote and Miller 2007, table 7.4), but total diversity is calculated as:

$$N_{TOT} = N_{FL} + N_{bL} + N_{Ft} + N_{bt}.$$

In order to assess genus and species diversity, two individual data matrices were created that record occurrences per time interval (Appendix A2.4.1, A2.3.4, respectively). The genus diversity matrix is organised per order, each of which consists of a list of named genera, and a cumulative entry for genera in open nomenclature, as well as a cumulative entry for Lazarus occurrences of named genera. Each named genus occurring in a time interval was counted as one unit, whether it concerned a fossil or a Lazarus occurrence. For genera in open nomenclature, the count was limited to one unit per interval, unless it was clear that unnamed genera existed in different taxonomic categories, in which case genera were counted as one unit per taxonomic category. The number of boundary crossers were counted from named genera only as one unit per genus per boundary crossed (this criterion is met if the genus occurs in any interval preceding or following the boundary).

The species diversity matrix was constructed in a similar way, but here the cumulative number of species per genus was recorded for each time interval. Separate entries were created for named species and species left in open nomenclature.

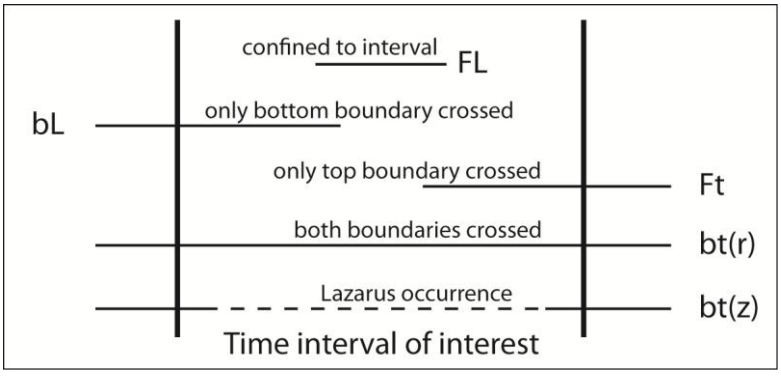

Figure 2.4 – Five fundamental classes of taxa present during a stratigraphic interval, depending on whether they cross the bottom (b) or top (t) interval boundary and whether they have a first (F) or last (L) occurrence within the interval, as well as whether they have been recovered from the fossil record (r) or whether it represents a Lazarus occurrence (z) (modified from Foote 2000).

Occurrences of species in open nomenclature were treated as separate species, unless they originated from the same country (or region in the case of large countries), in which case they were counted as one species to avoid overestimation of species richness. The number of boundary crossers was not counted due to the limited chronological range of many species.

Although they have been recorded as counts in the data matrices, genus and species occurrences that could not be resolved to stage level but to epoch level only have, in principle, been excluded from the analyses. Genera that are solely based on epoch level age determinations and also represent singleton occurrences (*Donguzodus*, *Gansuselache*, *Tiaraju*, *Sinohelicoprion*, *Syntomodus*), have been excluded from the total generic richness count (and any further analyses). However, if indeed they are known from preceding or following epochs, the first or last stage of the epoch, respectively, has been counted as a Lazarus occurrence and the epoch boundary has been considered as crossed.

A family diversity matrix was created based on the genus diversity matrix, grouping genera according to their family assignment and summarising their occurrence data. Only named families, or unnamed but well-defined families (e.g., the unnamed monogeneric family that comprises *Lissodus*), were included in the matrix.

Heterogeneity in the sampling intensity between different time intervals may influence the measured diversity (Kriwet *et al.* 2009). The relationship between sampling intensity and diversity is non-linear (see Benton 1998; Jamnicsky *et al.* 2008) and cannot be compensated for by extrapolation. Instead, sample-standardised diversity may be obtained using subsampling by simple rarefaction (e.g., Kriwet *et al.* 2009), but this method has been criticised for returning an unfair representation of diversity (Alroy 2010a). Rarefaction is not commonly used by vertebrate researchers, because the generally small sample sizes may cause flat diversity curves and type II errors (Lloyd and Friedman 2013). Although the need for sampling correction is currently virtually agreed as opposed to using raw data, appropriate standardising techniques are still a matter of debate (Benton 2009; Alroy 2010b; see also Alroy

2010c). Most recently, shareholder quorum subsampling has been proposed as a better means for assessing diversity (Alroy 2010b), but this method produces greatly biased results for literature-based data, which poses difficulties in calculation of the required single-publication occurrence correction factor (e.g., Lloyd and Friedman 2013). In this study, the heterogeneity in sampling intensity has been assessed by means of a data inventory (Section 2.6.2), but the measured diversity has been left uncorrected to accurately reflect the fossil record, despite its problems, and to avoid the potential introduction of any artificial diversity estimates.

2.6.7 Standing diversity, origination and extinction

In addition to the calculation of taxon richness, one further diversity assessment has been performed based on named genera only (thus excluding genera in open nomenclature and therefore the entire order Phoebodontiformes?). The calculation of estimated mean standing diversity (EMSD), which reflects the average number of taxa at any given time within an interval (Fröbisch 2008), has been defined by Foote (2000) as:

$$EMSD = (N_{bL} + N_{Ft} + 2N_{bt})/2$$

This can be re-written as $EMSD = 0.5N_{bL} + 0.5N_{Ft} + N_{bt}$. Genera occurring in intervals preceding and following the interval of interest were thus assigned one unit, but those displaying their first or last occurrence in the interval only half a unit. This reduces the importance of time intervals recording first and last occurrences because it cannot be assumed that these occurrences are tied directly to the boundaries. Singleton genera were excluded, which is believed to be a control for taphonomic bias such as the Lagerstätten effect (e.g., Lu *et al.* 2006), although others argue the necessity of singleton inclusion (Fitzgerald and Carlson 2006). To accommodate the latter view, singletons were left included in the taxonomic diversity estimate. EMSD avoids underestimation of taxonomic rates (resulting from solely excluding singletons) and artifically high diversity that may be caused by a high turnover rate (Fröbisch 2008).

In the calculation of origination and extinction rates and related diversity estimates, the following expressions have been used. The definitions follow Foote and Miller (2007).

Per-taxon origination rate (per Myr): $P_{O/myr} = (N_{FL} + N_{Ft})/N_{TOT}/\Delta t$

Per-taxon extinction rate (per Myr): $P_{E/myr} = (N_{FL} + N_{bL})/N_{TOT}/\Delta t$

(defined as r_O and r_E, respectively, in Sepkoski 1978)

with:

Number of originations (N_o in Foote 2000): $N_F = N_{FL} + N_{Ft}$

Proportional originations: $P_O = N_F/N_{TOT}$

Number of extinctions (N_e in Foote 2000): $N_L = N_{FL} + N_{bL}$

Proportional extinctions: $P_E = N_L/N_{TOT}$

Duration of each respective interval: Δt

(Sepkoski 1978; Foote 2000; Foote and Miller 2007)

Estimate of overall change in the faunal composition:

Diversification rate (per Myr): $P_D = P_{O/myr} - P_{E/myr}$

Turnover rate (per Myr): $P_T = P_{O/myr} + P_{E/myr}$

(Sepkoski 1978; Lasker 1978; see Kriwet *et al.* 2009, supporting information)

Van Valen metric (excluding singletons)

Origination: $(N_{Ft})/[(N_{bL} + N_{Ft} + 2N_{bt})/2]/\Delta t$

Extinction: $(N_{bL})/[(N_{bL} + N_{Ft} + 2N_{bt})/2]/\Delta t$

(Van Valen 1984; Foote 2000)

Note that $EMSD = (N_{bL} + N_{Ft} + 2N_{bt})/2 = (N_b + N_t)/2$ with:

Lower boundary crossers: $N_b = N_{bL} + N_{bt}$

Upper boundary crossers: $N_t = N_{Ft} + N_{bt}$

(Foote 2000; Foote and Miller 2007)

Per-capita origination rate (per Lmy): $p = -ln(N_{bt}/N_t)/\Delta t$

$= -ln[N_{bt}/(N_{Ft} + N_{bt})]/\Delta t$

Per-capita extinction rate (per Lmy): $q = -ln(N_{bt}/N_b)/\Delta t$

$= -ln[N_{bt}/(N_{bL} + N_{bt})]/\Delta t$

with N_b and N_t as above and lineage-per-million-years (Lmy)

Note: these rates cannot be calculated for intervals with N_{bt}, N_{Ft}, and/or N_{bL} values of zero.

(Foote 2000; Foote and Miller 2007)

Originations and extinctions are usually plotted at interval boundaries, which involves the assumption that all taxa lived throughout each interval in which they occur, but the extent to which turnover is continuous, as opposed to being clustered at boundaries, is still an open question (Foote and Miller 2007). Hence, originations and extinctions are here plotted mid-interval, to avoid forcing originations and extinctions to the boundaries.

2.6.8 Palaeoecological assessment of taxa

For the assessment of palaeoecological aspects such as salinity tolerance, ecomorphotype and feeding habit, the genus richness matrix incorporating Lazarus occurrences was used. Different states for each life-history trait were assigned to each named genus (Appendix A2.4.10).

Salinity tolerance for each genus has either been taken directly from published data (references cited in Appendix A2.4.10) or has been assessed here based on recovery data compiled in the literary database (Appendix A2.1). Ecomorphotypes have been assigned based on comparisons made with the fossil record by Compagno (1990) or approximated here based on published interpretations of the postcranial morphology, body size, dental morphology, and general palaeoenvironment from which the genera have been recovered. Feeding habits have been assigned based on interpretations of

dental morphology taken from literature or assessed using the morphological characteristics listed in Table 2.2.

Table 2.2 – Trophic groups and associated dental morphology (adapted from Cappetta 1987).

Trophic group		
Dental (sub)type	Dental morphology	Remarks
Durophagous		
Crushing	low cusped to flat teeth with bulging crown and smooth or puckered/pitted surface	narrowly imbricated dentition
Grinding	low cusped to flat teeth, which are enlarged and often of polygonal outline, with high crown and ridged surface	very narrowly imbricated dentition
Microtrophic/-phagous		
Filter feeding		exceedingly small and numerous teeth
Macrophagous		
Clutching/grasping /piercing	highly cusped teeth with numerous lateral cusplets that lack cutting edges but possess folds on the labial and lingual faces	little differentiated, largely homodont dentition
Cutting *sensu stricto*	highly cusped teeth, but wider and flatter teeth labio-lingually, with sharp cutting edges, often serrated and rearward slanted main cusp	monognathic and dignathic homodonty
Cutting-clutching	high and narrowly cusped teeth in one jaw, yet the opposite jaw possesses teeth that are wider and flatter in labio-lingual direction	strong dignathic heterodonty
Tearing	narrowly cusped teeth anteriorly and little enlarged teeth laterally, with distinct cutting edges and often one to several pairs of small lateral cusplets	
Clutching-grinding	cuspidate anterior teeth (clutching type) and flat and wide lateral teeth (grinding type)	no true representatives in the Permian–Triassic, although *Asteracanthus* and *Homalodontus* may resemble this type
General notes		
The presence of a labial buttress, as is observed in *Lissodus*, *Cooleyella* and certain eugeneodontiforms, enhances their effectiveness as a bottom feeder because it provides additional structural support to the labial peg (Duffin 1985).		
Cristae increase the surface area of the crown in order to improve its grasping ability (Johnson 2003).		

2.6.9 SELECTIVITY OF EXTINCTION (CHI-SQUARED TEST)

In order to assess the dependence of taxon fate or diversity per (sub)stage (variable A) among chondrichthyans on taxonomic structure or palaeoecological/-geographical factors (variable B) during times of mass exinction, a Pearson's chi-squared test for independence has been conducted in each case. It is used to determine whether there is a significant relationship between the two categorical variables and returns the probability of observing a χ^2 sample statistic as extreme as the test statistic by chance under the assumption of independence. The method has been successfully applied to study echinoid extinction selectivity (Smith and Jeffery 1998; Jeffery 2001).

The test requires null (H_0) and alternative (H_a) hypotheses, formulated as:

H_0: Variable A and variable B are independent;

H_a: Variable A and variable B are not independent.

Taxon fate is qualified as extinction or survival, whereas appropriate qualifying categories are used for each of the palaeobiological factors (salinity tolerance, ecomorphotype, feeding habit), and palaeogeographical factors (palaeobasin, palaeolatitude). It should be noted that, if support is found for the alternative hypothesis, it does not necessarily identify a causal relationship (i.e., driving mechanism).

In the calculations, the following expressions and definitions have been used.

The degrees of freedom are defined as: $dF = (r - 1) * (c - 1)$

where r (row) is the number of levels for one categorical variable (A), and c (column) is the number of levels for the other categorical variable (B).

Expected frequency counts are calculated separately for each row-column combination using: $E_{r,c} = (n_r * n_c)/n_{tot}$

where n_r is the total number of sample observations (genera) at level r of variable A; n_c is the total number of sample observations (genera) at level c of variable B; and n_{tot} is the total sample size (number of genera).

The χ^2 test statistic is defined as: $\chi 2 = \Sigma[(O_{r,c} - E_{r,c})^2/E_{r,c}]$

where $O_{r,c}$ represents the observed frequency counts for each row-column combination. The *p*-value is the probability of observing a sample statistic between 0 and the test statistic (critical value), and is associated with the test statistic using the degrees of freedom in the χ^2 distribution. The significance level (α) was set at 0.05. If the *p*-value falls below the significance level, the null hypothesis must be rejected and the existence of a relationship is concluded.

2.6.10 Dimensional analysis (Mann-Whitney *U* test)

In order to assess tooth and overall body size, as many general measurements of taxa per locality (i.e., one set of measurements per occurrence) as possible have been collected from literature (Appendix A2.2). Published comparative body length estimates based on dental material have also been included. These measurements have then been grouped together per (sub)stage and/or per epoch, regardless of taxonomic position. The temporal resolution per studied aspect is based on the number of available measurements and the resolution required to observe meaningful patterns.

Despite potential biases caused by size heterogeneity (e.g., symphyseal teeth may be larger or smaller than those in more lateral positions), measurements of teeth from all positions in the jaw have been grouped together to ensure the availability of a sufficiently large dataset. The majority of measurements were obtained as sets of two or more per occurrence, but they often comprised minimum and maximum dimensions, as well as variable combinations and incomplete records of dental aspects, precluding the possibility of calculating tooth volume. Eugeneodontiform tooth size was included, but whorl data excluded.

In an effort to remove dimensional bias introduced by the potential temporary absence of large taxa during an extinction interval due to their lower preservation potential (see Twitchett 2007a), the measurements of Permian/Triassic boundary crossing genera were studied separately. From among this group, *Protacrodus*, *Helicampodus*, *Orthacanthus*, *Xenacanthus*, and *Caseodus* were excluded due to the

fact that size data was either entirely lacking, or lacking from either the Permian or Triassic record, the latter of which would cause a skewed distribution showing incomplete patterns. This means that ultimately size data from *'Polyacrodus'*, *Acrodus*, *Palaeobates*, *Omanoselache*, Genus S, 'pre-Jurassic *Synechodus*' and *Fadenia* have been included in this analysis. Only tooth size could be analysed, due to insufficient data on body length.

Many natural phenomena can be approximately described by a normal distribution and box and whisker plots can usually be used to visualise this kind of dimensional data. Box plots do not make any assumptions about the underlying statistical distribution; they are non-parametric. However, the 5-number summaries will be equally spaced if based on normally distributed data. Their use was considered unsuitable for the data used in this study, however, because of the low number of data points in many time intervals. Instead, the data points were plotted individually per time interval.

In order to determine significance of difference between size data for neighbouring time intervals, the Mann-Whitney *U* test was carried out using the PAST software package (v. 1.90). This is a non-parametric significance test used to determine whether two samples of independent observations tend to have different values. It is based on null (H_0) and alternative (H_a) hypotheses, formulated as:

H_0: The distributions of both groups are equal;

H_a: The distributions of both groups are not equal.

The null hypothesis means that there is a symmetry between groups with respect to the probability of random drawing of a larger observation. Under the alternative hypothesis, the probability of an observation from one group exceeding an observation from the other group is not equal to 0.5. The test was carried out in a pairwise manner, testing two neighbouring time intervals in each case and the *p*-value returned by PAST was recorded. The significance level (α) was set at 0.05. If the *p*-value falls below the significance level, the null hypothesis must be rejected and unequal distributions of both groups is concluded.

3 CHONDRICHTHYAN RECORDS FROM NEOTETHYS

3.1 INTRODUCTION

This chapter describes new chondrichthyan records from the Permian–Triassic (shallow) marine continental margins of Pangaea and the Cimmerian Blocks delineating Neotethys, positioned in the eastern part of the southern hemisphere. The new records are based on material from numerous localities in Oman, as well as single localities in Iran, India, and Timor (Figure 3.1). The occurrences are summarised in Table 3.5 and the systematic palaeontology is provided in Appendix A3.2.

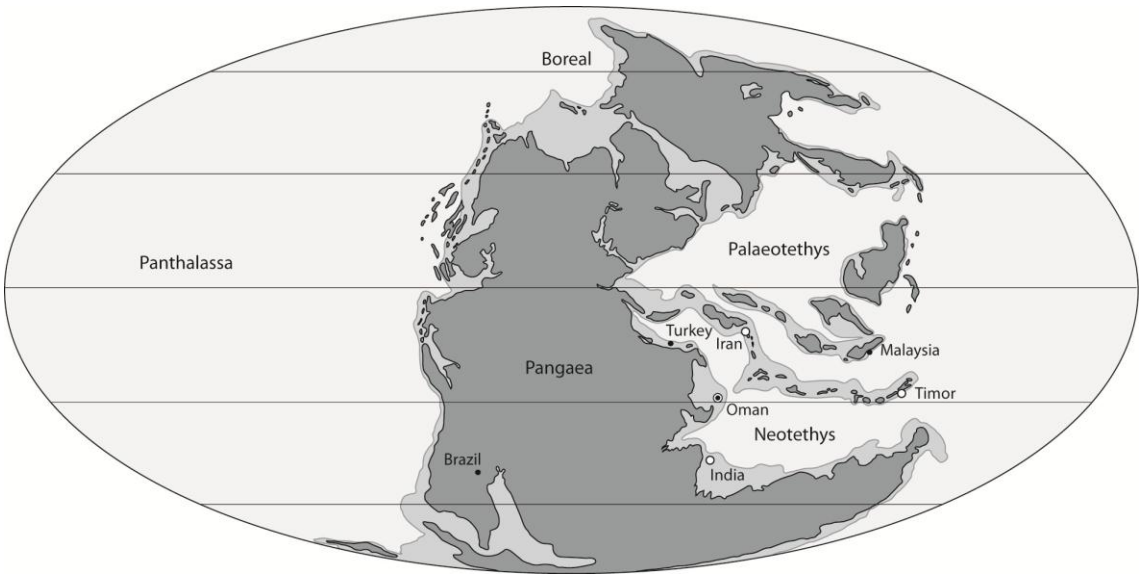

Figure 3.1 – Mollewide plate tectonic map for the Late Permian (260 Ma; modified from Blakey 2012). Circled dots represent localities from which material was directly obtained through fieldwork, whereas open dots represent localities from which material was indirectly obtained. Solid dots represent localities mentioned in the text.

3.2 OMAN

3.2.1 GEOLOGICAL SETTING

The geology of the Sultanate of Oman has been of interest to researchers for a number of decades and the first comprehensive study of the regional geology of the Oman Mountains was made by Glennie *et al.* (1974). This and more recent studies have revealed that there are many localities with Permian–Triassic (P–Tr) outcrops, including boundary sections. The fossil chondrichthyans of these localities have, however, barely been studied. Tintori (1998) and Angiolini *et al.* (2003a) revealed that the Wordian limestones of Oman may be rich in well-preserved chondrichthyan remains and Schultze *et al.* (2008) reported the presence of xenacanth sharks in the Artinskian Gharif Formation in the Al Huqf area. The current study provides the first detailed analysis of Permian and Triassic chondrichthyans of Oman.

The Sultanate of Oman is situated on the southeastern margin of the Arabian Peninsula. P–Tr deposits from a range of depositional environments are readily exposed throughout the region, forming part of the autochthonous Hajar Super-Group, the Hawasina Allochthonous Unit, and the Batain Nappes (Figure 3.2). Glennie *et al.*'s (1974) geological overview of the Oman Mountains has since been updated by Glennie (2005) and the stratigraphy of the Batain Nappes was last revised by Hauser *et al.* (2002).

The autochthonous Hajar Super-Group represents a cyclic shallow marine carbonate sequence that formed on the Arabian Platform between the Guadalupian and the Late Cretaceous (Rabu *et al.* 1990; Richoz *et al.* 2005). Deposition of this sequence started along the Neotethyan continental margin following a thermal subsidence induced Wordian transgression that covered most of Oman (Rabu *et al.* 1990; Angiolini *et al.* 2003a; Richoz *et al.* 2005). It is mainly composed of fossiliferous limestones and dolomites (Glennie 2005), which unconformably overlie pre-Permian basement strata. They are exposed in the Oman Mountains in the northern regions of Oman, such as

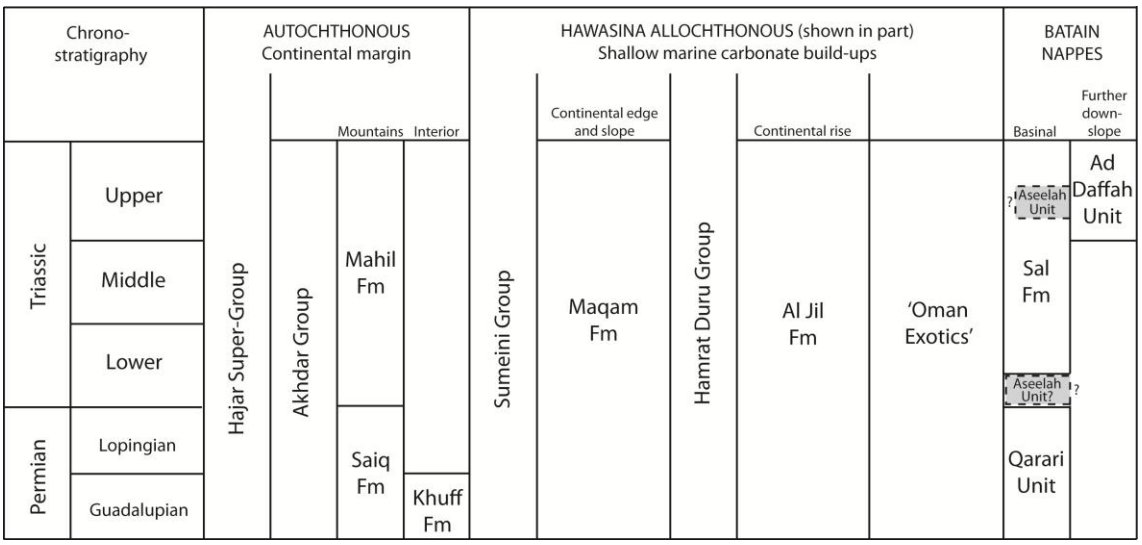

Figure 3.2 – Correlation of Permian–Triassic rock units of Oman (authochthonous and Hawasina allochthonous based on Glennie *et al.* 1974 and Glennie 2005; Batain Nappes based on Hauser *et al.* 2002). The exact time of formation of the Aseelah Unit remains uncertain.

the Jabel Al Akhdar region (Wadi Sahtan, Saiq Plateau), which is virtually unaffected by metamorphism or compressional deformation (Glennie *et al.* 1974), as well as in the Saih Hatat (Wadi Aday) and the interior Haushi-Huqf area along the eastern coast (Haushi Cliff, Saiwan, and Jabel Gharif) (Figure 3.3).

The allochthonous deposits, consisting of nappes, autochthonous olistoliths and true exotics of Permian and Triassic age, cover an extensive area throughout the Oman Mountains. They were formed in depositional settings ranging from the proximal continental edge and slope to more distal basinal environments. The Sumeini Group crops out at Wadi Maqam and Wadi Shuy'ab. The Oman Exotics are observed in the Ba'id area (Wadi Alwa) and at Jabel Safra. The Hamrat Duru Group is exposed at Wadi Wasit (Ba'id), Al Buday'ah, and Rustaq (Figure 3.3).

The Batain Nappes are limited to the northeastern coastal region and, among others, contain a number of olistoliths from the Qarari and Aseelah Units, which are largely covered by recent sand and gravel deposits (Hauser *et al.* 2002). The area was mapped in detail by Shackleton *et al.* (1990). Light to dark grey nodular micritic lime mudstones make up the most common lithofacies of the Qarari Unit, interpreted as hemipelagic deposits originating from an open sea shelf and shelf slope. The Aseelah

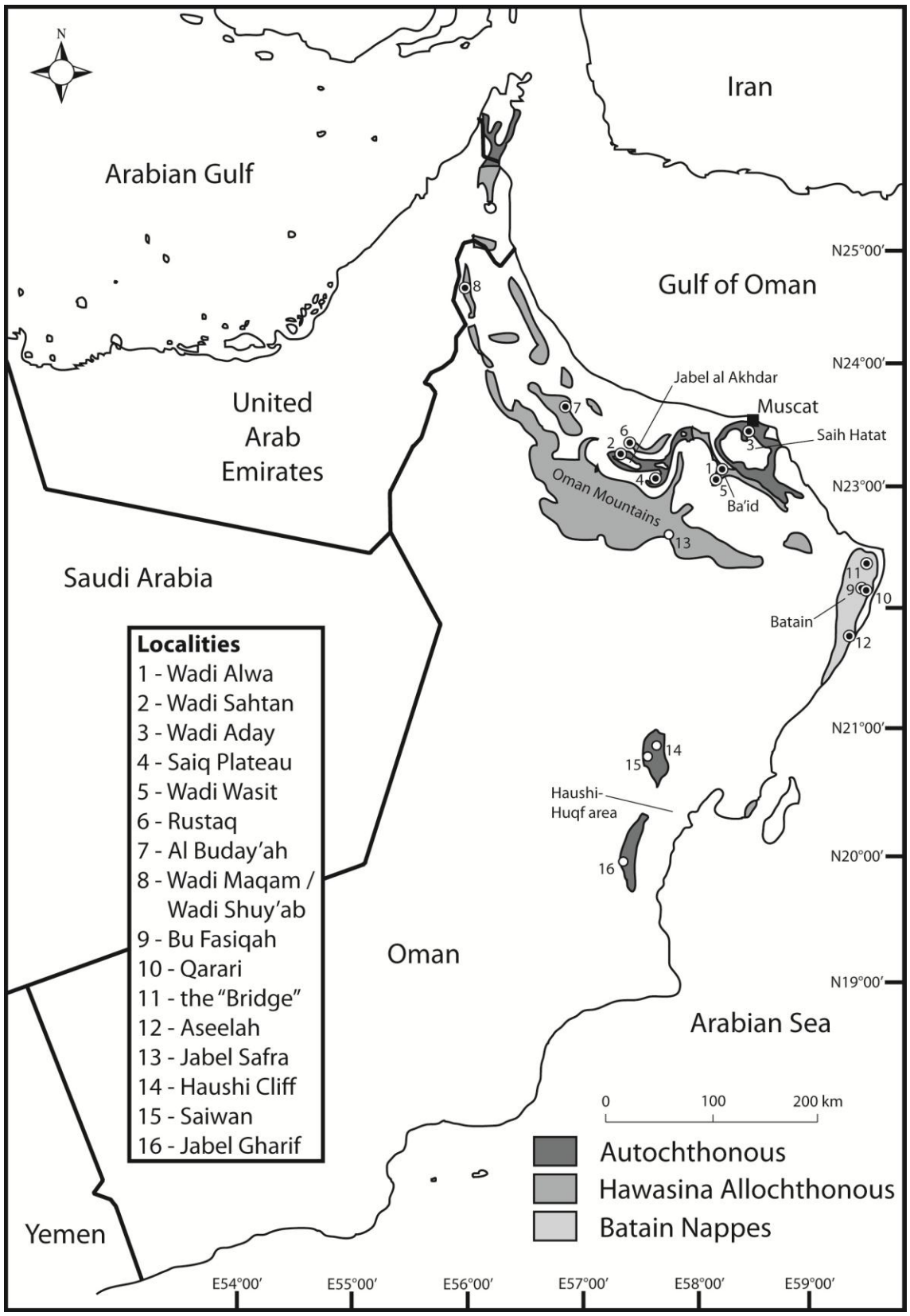

Figure 3.3 – Geological map of Oman showing sampled localities (redrawn from Glennie 2005). Material from these localities was either directly obtained through fieldwork (solid dots), or indirectly obtained (open dots). Locality names are provided in anglicised spelling, following general practice over the last few decades, which are accepted, although they do not necessarily correspond to local usage (e.g., traffic sign boards). "Wadi" is an Arabic term traditionally referring to a valley or an ephemeral riverbed.

Unit is a poorly sorted, clast-supported deposit, consisting of boulders derived from Permian lagoonal and reef limestones and open marine shelf carbonates in a matrix of sandy calcarenites or coarse white sandstones (Hauser *et al.* 2000, 2002). Localities in the Batain area include Bu Fasiqah, the Qarari block, the “Bridge”, and the blocks and section at Aseelah (Figure 3.3).

A summary of the allochthonous geology of Oman is shown in Figure 3.4. The Hawasina Allochthonous Unit is derived from part of Neotethys referred to as the Hawasina Basin (Figure 3.5), which started opening during the Guadalupian and was obducted onto the Arabian margin during the latest Cretaceous (Pillevuit *et al.* 1997). It is composed of a succession of ‘slices’ of sedimentary sequences faulted into an accretionary wedge, most of which were originally deposited as deep-water turbidites on the continental rise and abyssal plain to the northeast of the Arabian continental shelf (Glennie 2005). Among those are the exotics, which are interpreted as “derived from structural highs on the thinned (stretched) continental crust of the Arabian shield” (Pillevuit *et al.* 1997, 211).

There are two types of exotic deposits. The first of these are true exotics, defined as

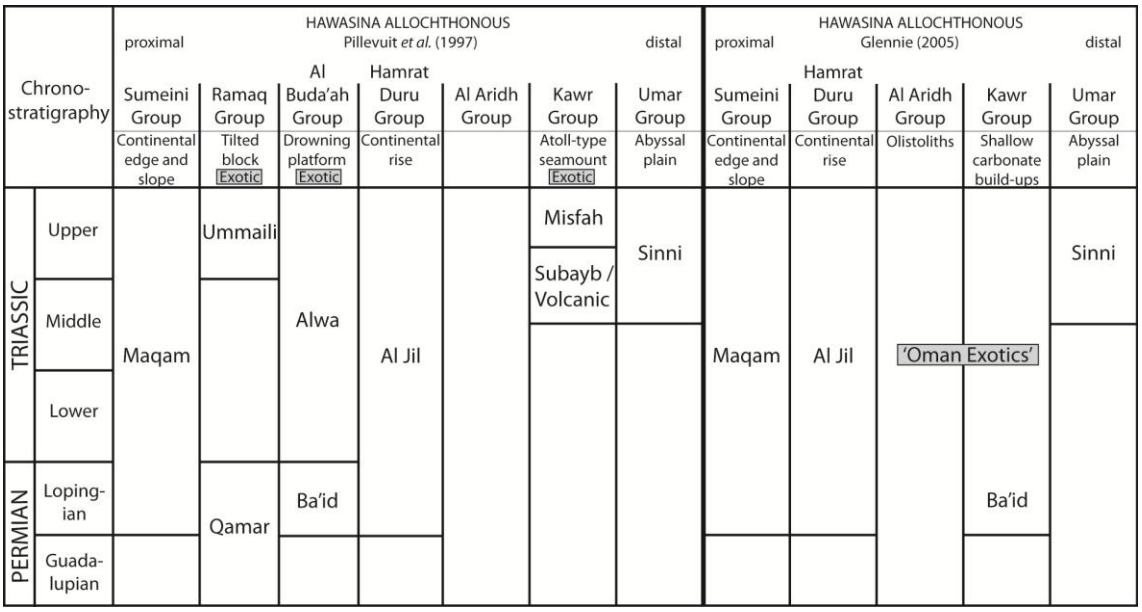

Figure 3.4 – Stratigraphic subdivisions (formations) of the Permian–Triassic Hawasina Allochthonous Unit exposed in the Oman Mountains and their relative palinspastic positions, reflecting schemes proposed by Pillevuit *et al.* (1997) and Glennie (2005).

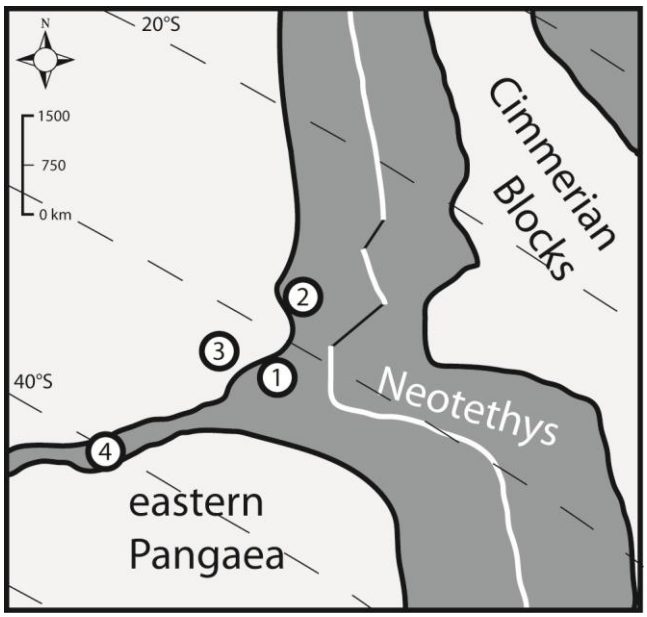

Figure 3.5 – Reconstruction of the Neotethyan realm off the Arabian Platform during the Guadalupian, separated from the Palaeotethys by the Cimmerian Blocks (cf. Figure 3.1). Individual basins include: 1, Batain Basin; 2, Hamrat Duru (Hawasina) Basin; 3, interior Oman Basin; 4, Karoo Rift Basin (modified from Immenhauser *et al.* 2000 and Hauser *et al.* 2002). Scale is approximate. Palaeolatitudes indicated.

tectonic units bounded by shear surfaces, which have been transported *en masse* by thrusting. In Oman, these exotics are often shallow-water platform limestone blocks hundreds of metres to sometimes a few kilometres in size, that are under- and overlain by deep-water sediments, and foreign to their surroundings in terms of facies, palaeoenvironment or both (Pillevuit *et al.* 1997). Olistoliths are of the second type, which are defined as foreign to under- and overlying rocks in terms of matrix, but they still maintain a depositional contact between them and usually have a common palaeogeographic origin. Pillevuit *et al.* (1997) state that olistoliths in the Hawasina sediments are limestone blocks of a few centimetres to 100 m in size that are derived from the true exotics and represent ‘rockfall-deposits’ resulting from tectonic events. These re-deposited blocks mostly represent Permian platform limestones, whereas Triassic Hallstatt-type limestones (similar to the Hallstatt limestone observed in Austria) are relatively rare.

The outlined model for the evolution of the Oman margin was first proposed by Glennie *et al.* (1974), based on previous research and their own observations, and has

been followed by many authors since then (see references in Pillevuit *et al.* 1997). Nevertheless, the large number of different depositional environments represented in the Hawasina Allochthonous Unit has led to slightly different interpretations of its stratigraphic subdivisions and their relative palinspastic position (e.g., Pillevuit *et al.* 1997; Glennie 2005; Figure 3.4).

Pillevuit *et al.* (1997) attributed the exotics to the Ramaq, Al Buda'ah, and Kawr groups (they did not discuss the Al Aridh Group as part of the exotics), which mainly comprise true exotics. The Ramaq Group exotic crops out in the United Arab Emirates and is interpreted as a tilted block of the proximal Oman margin (Pillevuit *et al.* 1997). The palaeogeographically adjacent Al Buda'ah Group is part of a complex tectono-stratigraphic assemblage in the Ba'id area, but displays a sequence characteristic of a drowning platform close to the Oman margin. The more distal Kawr Group is interpreted as a Mesozoic atoll-type seamount and is exposed mainly along the southern flank of the Jabel al Akhdar, thrust onto either the Al Aridh or the Hamrat Duru Group in different areas. Olistoliths, derived from these true exotics, may occur throughout the Hawasina sediments (Pillevuit *et al.* 1997).

In his review of the Hawasina Allochthonous Unit, Glennie (2005) hoped to incorporate the best elements of all existing interpretations, describing the 'Oman Exotics' as comprising two types of deposits: those of Guadalupian to Lopingian age and those of Middle to Late Triassic age (although he noted that many are impossible to date due to recrystallisation). His interpretation of the true exotics of the Kawr Group is that they are representative of reefoid, shallow marine carbonate build-ups that formed on top of deeper marine basaltic substrates (Glennie *et al.* 1974). In contrast, the exotics of the Al Aridh Group are interpreted as fossiliferous shallow-marine limestone olistoliths of boulder to kilometre size that slid down a submarine slope to be re-deposited in deep-water sediments that may be younger (Glennie 2005). He suggested that the olistoliths formed on the eastern, shallow marine margin of the deep-water Hawasina Basin, where the sediments of the Hamrat Duru Group are believed to have been deposited (Glennie 2005; Figure 3.5), and which were

subsequently re-deposited as a result of large-scale tectonic reorganisation during the Late Triassic (Immenhauser *et al.* 2000).

3.2.2 PERMIAN SECTIONS

3.2.2.1 HAUSHI-HUQF AREA

Geological setting

The Haushi-Huqf area contains a number of sections distributed over the localities Haushi Cliff, Saiwan, and Jabel Gharif (Figure 3.6). Upper Palaeozoic rocks are well-exposed on the western side of the Huqf Massif (Angiolini *et al.* 1998). They show two consecutive mega-sequences: the Haushi Group and the Akhdar Group, each recording a major transgressive event (Figure 3.7). The first event was controlled by the last phase of the Gondwanan deglaciation and the second by the opening of Neotethys (Angiolini *et al.* 1998). The younger of the two mega-sequences, the Akhdar Group, comprises the fluvial Gharif Formation, which is conformably overlain by the marine sandstones, marls and bioclastic limestones of the Khuff Formation. The base of the Khuff Formation is currently placed at the first occurrence of marine bioclasts in the sandstones (L. Angiolini, pers. comm. 2011) and the formation contains a rich invertebrate fauna of brachiopods, conodonts, crinoids, bryozoans, cephalopods, gastropods, bivalves, ostracods, and foraminifera (Angiolini and Bucher 1999), as well as vertebrate remains comprising chondrichthyans, actinopterygians and coelacanths (Angiolini *et al.* 2003a). A composite log of the Khuff Formation in the Haushi-Huqf area, based on five sections, was published in Angiolini and Bucher (1999), indicating that it reaches a maximum thickness of 30–40 m. Based on that study, and a more recent synthesis by Angiolini *et al.* (2003a), an updated summary log showing the samples analysed in this study has been produced (Figure 3.8).

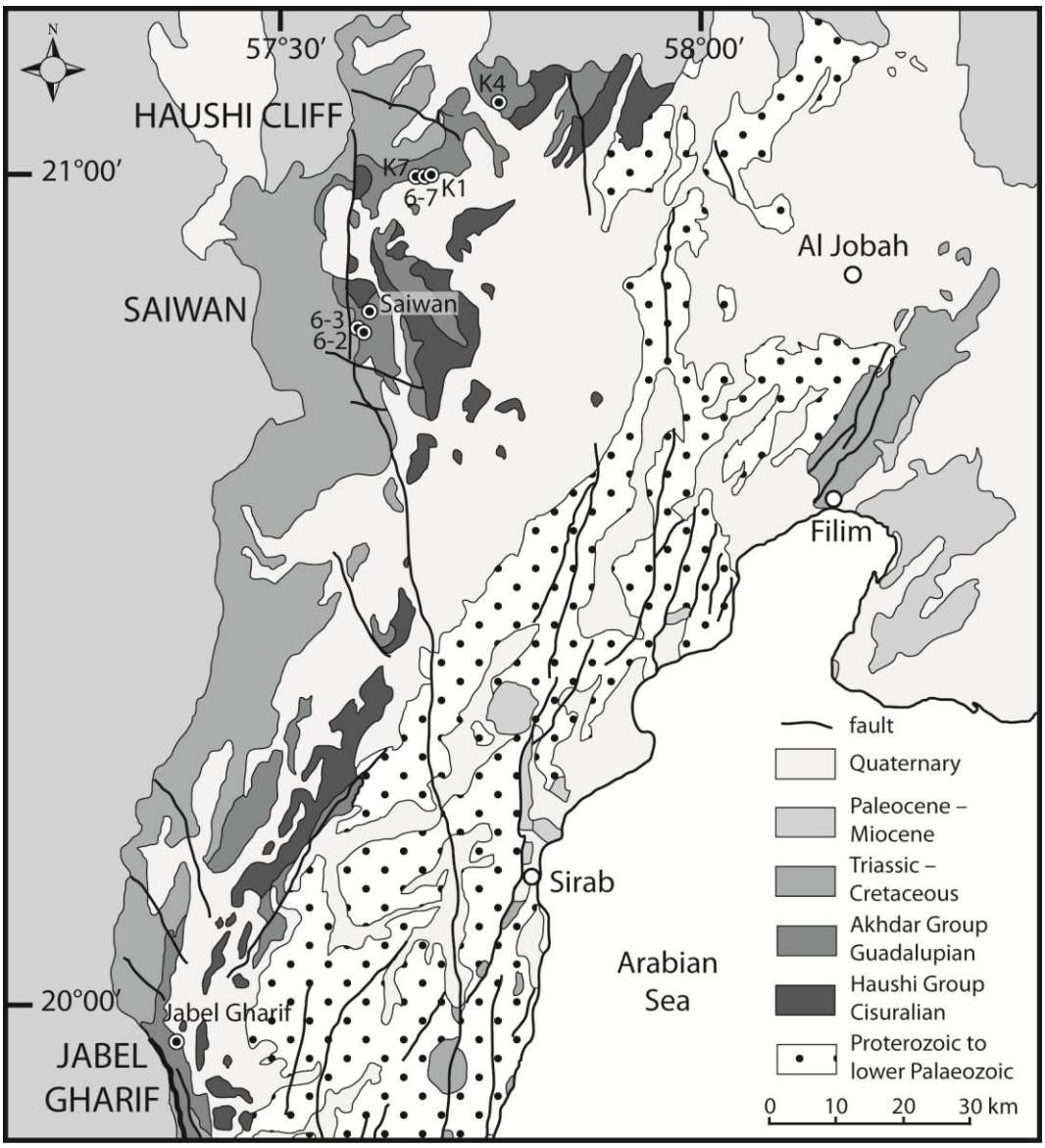

Figure 3.6 – Geological map of the Haushi-Huqf area, showing sampled sections from the Khuff Formation (modified from Angiolini *et al.* 2003a).

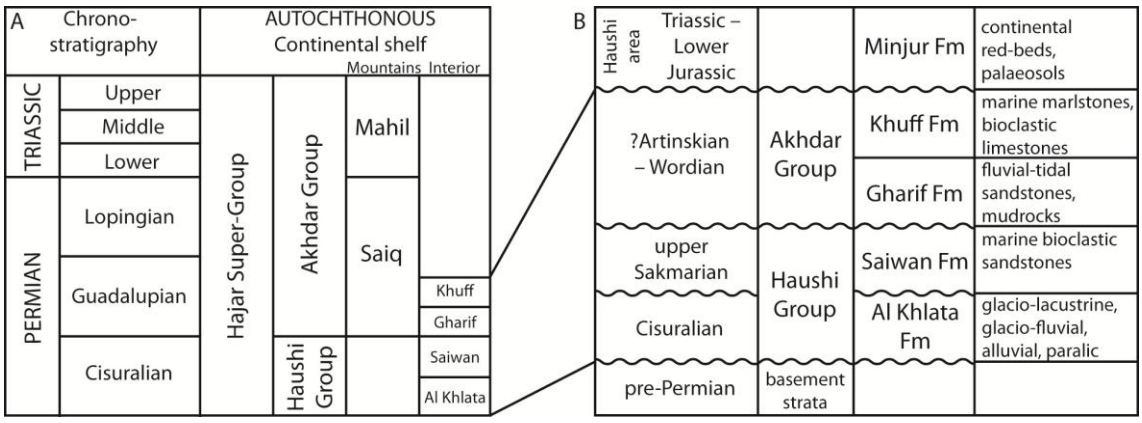

Figure 3.7 – A, Correlation of Permian–Triassic autochthonous rock units of Oman (based on Glennie *et al.* 1974; Glennie 2005). B, Depositional succession of rock units in the Haushi-Huqf area of Oman (based on data from Angiolini *et al.* 2003a).

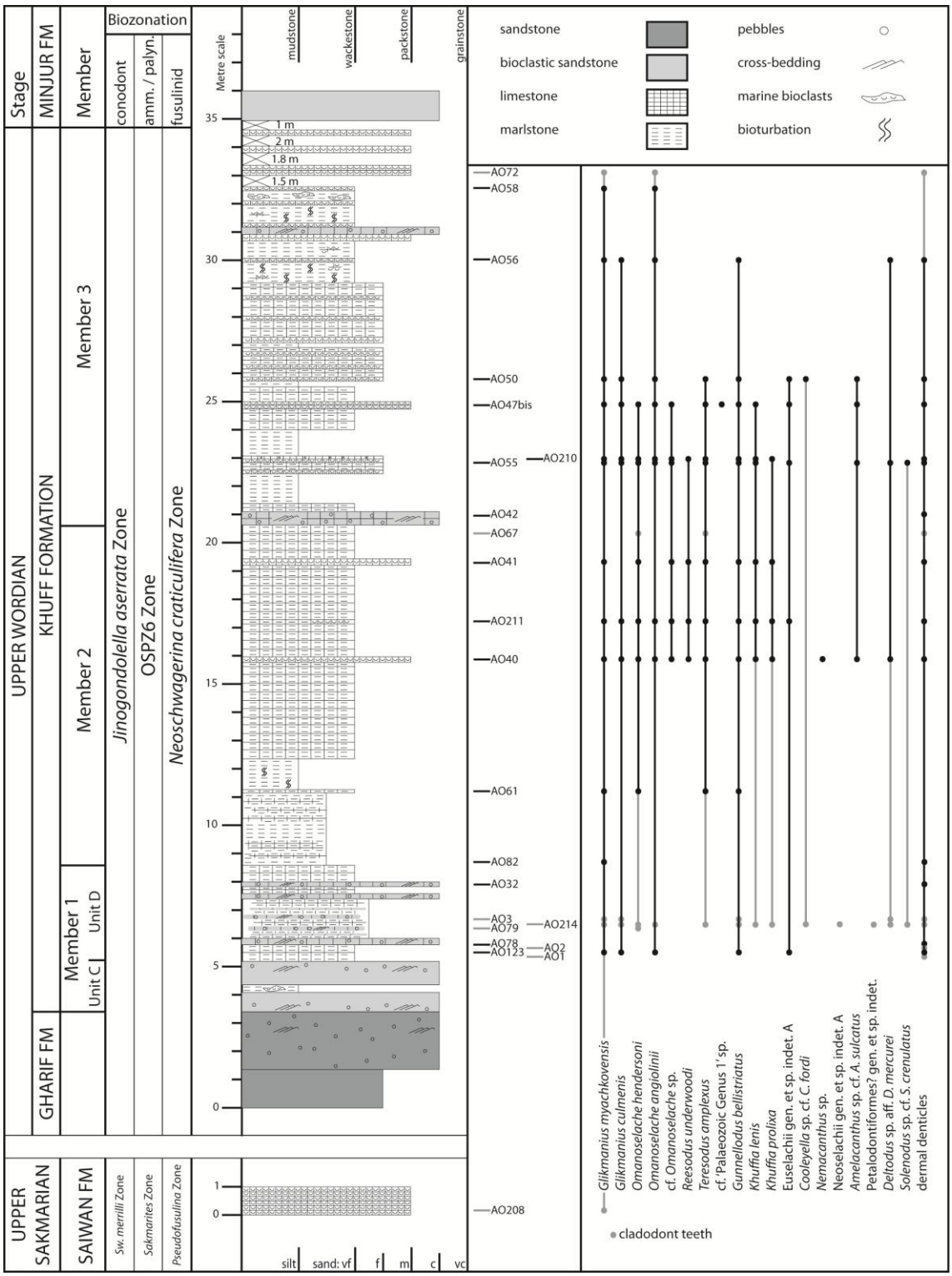

Figure 3.8 – Stratigraphy, sample heights and chondrichthyan occurrence data for the Haushi-Huqf area (MPUM collection; see Section 2.1.2). Composite log of the Khuff Formation modified from Angiolini and Bucher (1999) to reflect changes in member boundaries, and of a section of the Saiwan Formation at Jabel Gharif, based on data in Angiolini *et al.* (2003b). Conodont and Sakmarian ammonoid and fusulinid biozonations from Henderson (2005); Wordian palynological standard OSPZ Arabian biozonation from Jan *et al.* (2009); Wordian Tethyan fusulinid biozonation from Kotlyar and Pronina (1995) as correlated by Angiolini *et al.* (1998). The positions of samples are either exact (black bars) or approximate (grey bars).

Depositional setting. The Khuff Formation represents a shallow carbonate platform deposited on the outer shelf of the Arabian Platform, which faced the Madagascar Embayment in the spreading Neotethys (Angiolini *et al.* 1998), with a NE/SW oriented coastline (Angiolini *et al.* 2003a). The Khuff Formation is currently subdivided into three members (Figure 3.8). Member 1 records a rapid regional transgression and the onset of carbonate shelf sedimentation and consists of two units: Unit C is interpreted as a tidal sand-flat or barrier-beach in a lagoonal or bay environment, whereas Unit D consists of inner- to outer-shelf sediments from above storm wave base (Angiolini *et al.* 2003a). Member 2 records outer-shelf conditions below storm wave base, and the formation of regular distal tempestites (Angiolini *et al.* 2003a). Member 3 contains frequent, more proximal bioclastic tempestites, indicating deposition around storm wave base, with a siliciclastic influx towards the top indicating shallowing towards the lower shoreface (Angiolini and Bucher 1999; Angiolini *et al.* 2003a). Since the study by Angiolini and Bucher (1999), the upper boundaries of members 2 and 3 have been extended upward, the latter to the top of the formation and incorporating a former 'Member 4' that is no longer distinguished (Angiolini *et al.* 2003a; L. Angiolini, pers. comm. 2011).

Extremely rich fossiliferous levels are common throughout the formation, but particularly frequent in Member 1 and the lower part of Member 3 (Angiolini *et al.* 2003a). The brachiopod fauna contains Tethyan genera, indicating a warm/sub-tropical climate (Angiolini *et al.* 1998), as well as endemic, Gondwanan and cosmopolitan genera (Angiolini and Bucher 1999), suggesting that the depositional setting of the Khuff Formation was open to outside influence. The conodont association confirms the shallow marine setting (Angiolini *et al.* 2003a). Fish remains have been recovered throughout the formation, mostly from shallow water shell beds (Angiolini *et al.* 2003a) re-deposited as storm layers (tempestites).

Age. An upper Wordian age (Guadalupian, Permian) has been assigned to the Khuff Formation, based on brachiopod and conodont faunas (Angiolini *et al.* 1998). The

fauna in Member 1 is interpreted as Wordian, based on Roadian–Wordian brachiopods and Wordian–Capitanian conodonts (Angiolini *et al.* 2003a, but also see Shen *et al.* 2009 and Mei and Henderson 2001, respectively). Higher in the succession, some brachiopod differentiation occurs whereas the conodont assemblage remains unaltered, but a Wordian age is still valid for Member 2 and Member 3 (Angiolini *et al.* 2003a). The Khuff Formation can be correlated to the lower part of the Saiq Formation, cropping out in the Oman Mountains (Angiolini *et al.* 2003a; see also Koehrer *et al.* 2010), and to formations further afield, such as the Amb Formation of the Salt Range in Pakistan and the Rat Buri Limestone of South Thailand (Angiolini *et al.* 2003a; see also Mei and Henderson 2001).

Material

The material from the Haushi-Huqf area (residue; Appendix A1.4) consists of chondrichthyan teeth, dermal denticles and fin spines. The majority derives from the Wordian Khuff Formation and was recovered from sections K1 (very near to section 5 of Angiolini *et al.* 1998 starting at N 21°00’37’’ E 57°40’03’’), K3 (exact position unknown), K4 (N 21°02'30'' E 57°42'00''), K5 (exact position unknown) and K7 (N 21°00'35'' E 57°39'27''), located in the Haushi uplift area, and from a section in the Saiwan area (N 20°51'43'' E 57°36'10''). A small amount of material derives from a section of the Sakmarian Saiwan Formation in the Jabel Gharif area (N 19°57'01'' E 57°21'38''). A total of 46 small samples (3–5 kg) were collected by Prof. A. Tintori and Prof. L. Angiolini (University of Milan), and in addition, four bulk rock samples were collected by Prof. A. Tintori for vertebrate purposes and comprise 10–15kg samples from four bioclastic limestone beds, all of which were processed at the University of Milan. Some of the material was reported as part of the vertebrate fauna found by Angiolini *et al.* (2003a) through their detailed sampling of the Khuff Formation, but was not figured or described in detail.

The stratigraphic positions of the samples have been indicated on the composite log (Figure 3.8), but this information was not recorded for all samples, which is why 27

samples that yielded shark remains are omitted. Of the four large samples, AO40 from K1 represents the upper part of a storm layer very rich in brachiopods shells, whereas AO55, AO47bis and AO50 were taken from K4. The lower part of this section consists of bioclastic calcarenites/calcirudites (storm concentration of allochthonous fossils), interbedded with marly limestones, and the upper part consists of shell beds from more proximal settings (L. Angiolini, pers. comm. 2011). Over 2100 specimens were recovered from the four large samples alone, enabling a detailed reconstruction of the composition of the Wordian shark community in the Haushi-Huqf region. Specimens from the smaller samples have only been used in the systematic part of this study if they represent taxa that do not occur in the large samples. For the remainder of the study, they have been used to complete the range data for the most common taxa. All specimens are deposited in the Palaeontological Museum of the University of Milan (MPUM10880–MPUM10953 and MPUM11002–MPUM11058; see Appendix A1.4).

Additional material was sampled in the Haushi Cliff area and at two sections in the Saiwan area: 6-2 at N 20°52'26" E 57°35'15"; 6-3 at N 20°52'38" E 57°34'60"; and 6-7 at N 21°00'37" E 57°39'36" (C. Henderson, pers. comm. 2010). The samples were collected by Prof. C.M. Henderson from the University of Calgary, Alberta, Canada, and were initially intended for conodont research. Each of these samples is estimated to have been a maximum of 5 kg. The samples were collected from gently dipping beds along sub-horizontal sections, each within a different wadi, and their stratigraphic position was recorded as a horizontal distance from the base of the formation (A. Baud, pers. comm. 2011, 2012; Figure 3.9). Due to the absence of more detailed stratigraphic data or dip measurements, precise correlation with sections K1 and K4 is not possible (A. Baud, pers. comm. 2011). The formation is not very thick, however, and based on a general uniformity in the conodont and vertebrate assemblages (Angiolini *et al.* 2003a), the material is assumed to be closely time-equivalent. All material is deposited in the palaeontological collections of the University of Calgary (UC20231–UC20385; see Appendix A1.3).

Section	Sample number	Horiz. distance (m)	Section	Sample number	Horiz. distance (m)
6-2	965-7 965-6 965-10 965-9 965-3	108 50.1 3.3 3.0 1.5	6-7	965-4 965-5 965-2 965-11 965-1	25.1 19.5-20 6.0 5.7 4.5
6-3	965-8	4.5			

Figure 3.9 – Stratigraphic position of samples from Haushi Cliff and Saiwan (UC collection) per sample location, which are sub-horizontal sections.

Results

The recovered fauna consists mainly of ctenacanthiform and hybodontiform taxa, identified as *Glikmanius* cf. *myachkovensis*, *Glikmanius culmenis*, *Omanoselache hendersoni*, *Omanoselache angiolinii*, cf. *Omanoselache* sp., *Reesodus underwoodi*, *Teresodus amplexus*, *Gunnellodus bellistriatus*, *Khuffia lenis*, *Khuffia prolixa* and Euselachii indet. sp. Additional specimens include rare teeth of the lonchidiid? cf. 'Palaeozoic Genus 1' sp., of the neoselachian *Cooleyella* sp. cf. *C. fordi* and a further indeterminate neoselachian, of an indeterminate petalodont?, and of the holocephalan *Deltodus* sp. aff. *D. mercurei* and *Solenodus* sp. cf. *S. crenulatus*. Fin spines add a further two taxa, *Nemacanthus* sp. and *Amelacanthus* sp. cf. *A. sulcatus*, which have neoselachian affinities and, therefore, an unclear relationship to the recovered teeth. Nine dermal denticle morphotypes are recognised (Table 3.1).

Taphonomy and palaeoecology of the Khuff Formation fauna. The Wordian Khuff Formation fauna is well-established, with a total of 15 chondrichthyan genera containing 19 species recorded from the MPUM and UC sample collections (Figure 3.8, Figure 3.10). The material is abundant, diverse and, even though fragmentation occurs due to the fragility of the material, a large number of specimens are in pristine condition. There is no evidence that any specimens have been reworked from significantly older

Table 3.1 – Distribution and interpretation of dermal denticles per morphotype (MPUM collection). Refer to Appendix A3.2 for detailed discussion and images of all morphotypes. X = presence.

Sample Morphotype	AO40	AO55	AO47bis	AO50	Interpretation
1	X	X	X	X	ctenacanth
2	X	X	X	X	hybodont
3				X	indet.
4	X	X	X	X	hybodont
5	X		X	X	hybodont
6	X	X	X	X	hybodont
7	X			X	symmoriiform?
8	X	X	X	X	hybodont
9	X				hybodont

strata, and the differences in colour recorded by specimens within the same sample are attributed to factors such as fungal or bacterial activity and the degree and timing of permineralisation, rather than differences in thermal alteration (cf. Tway *et al*. 1986). The recovered teeth are small, usually not exceeding a few millimetres in size. An ontogenetic bias is rejected, because if these teeth did stem from juveniles, a larger proportion of cusped teeth would be expected rather than the crushing dentitions that are common in this fauna. Instead, the small size and abundance of the material is interpreted as being the result of depositional processes. The four largest samples are

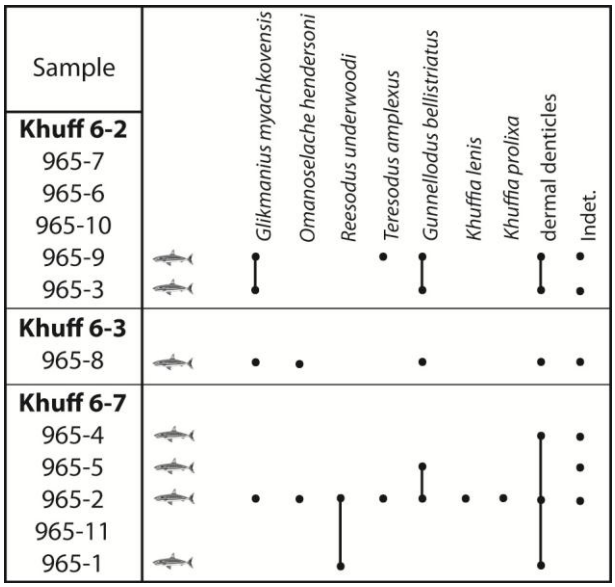

Figure 3.10 – Stratigraphical elasmobranch occurrence data per taxon and range information per section (UC collection). Sections are represented in numerical order, no stratigraphical correlation is intended.

interpreted as storm winnowed tempestites, where shallow water debris was transported basinward and redeposited according to settling velocity, resulting in a size-selected, concentrated assemblage (cf. Dattilo *et al.* 2008).

Because the relative stratigraphical positions of the MPUM collection samples are better known than those of the UC collection, the remaining discussion mostly focuses on the MPUM data (Figure 3.8). The collection illustrates the importance of sample size, because the small samples (3–5 kg) record a maximum of ten genera (AO214 is an unusually rich sample compared to the remaining samples, which reach a maximum of 6–7) but an average richness of three, whereas the four large (10-15 kg) samples yield a maximum of nine genera and an average of eight. Furthermore, due to these differences in sample size and clear evidence that smaller samples normally record fewer taxa, only the four largest samples from the MPUM collection have been analysed palaeoecologically (refer to Appendix A1.4.2 for numeric data).

When pooled together, these four samples are dominated by ctenacanthiform and hybodontiform taxa, in almost equal relative abundance when assessed by numbers of specimens (Figure 3.11A). Individual samples, however, are dominated by either ctenacanthiforms or hybodontiforms (Figure 3.11B). The dominance of the groups across all samples is significantly different from an equal distribution of both groups ($p = 0.0016$; Appendix A1.4.3). Samples dominated by hybodontiforms are coarser grained (Figure 3.8), which suggests a possible taphonomic bias. Alternatively, if grain size reflects depositional setting, then the differences may be recording real habitat preferences: the highly cusped teeth of ctenacanthiforms such as *Glikmanius* indicate a more pelagic lifestyle, and so might be expected to be more common in distal, finer grained lithologies, whereas the crushing dentitions of hybodontiforms might be expected to occur more frequently in coarser beds (in terms of both clastics and bioclastics) from more proximal depositional settings.

An attempt at reassessing this potential bias using the four most abundant smaller samples, of which AO41 is from a coarse bed and AO210, AO211 and AO214 are from finer grained beds, shows that all these samples are dominated by hybodonts (92%,

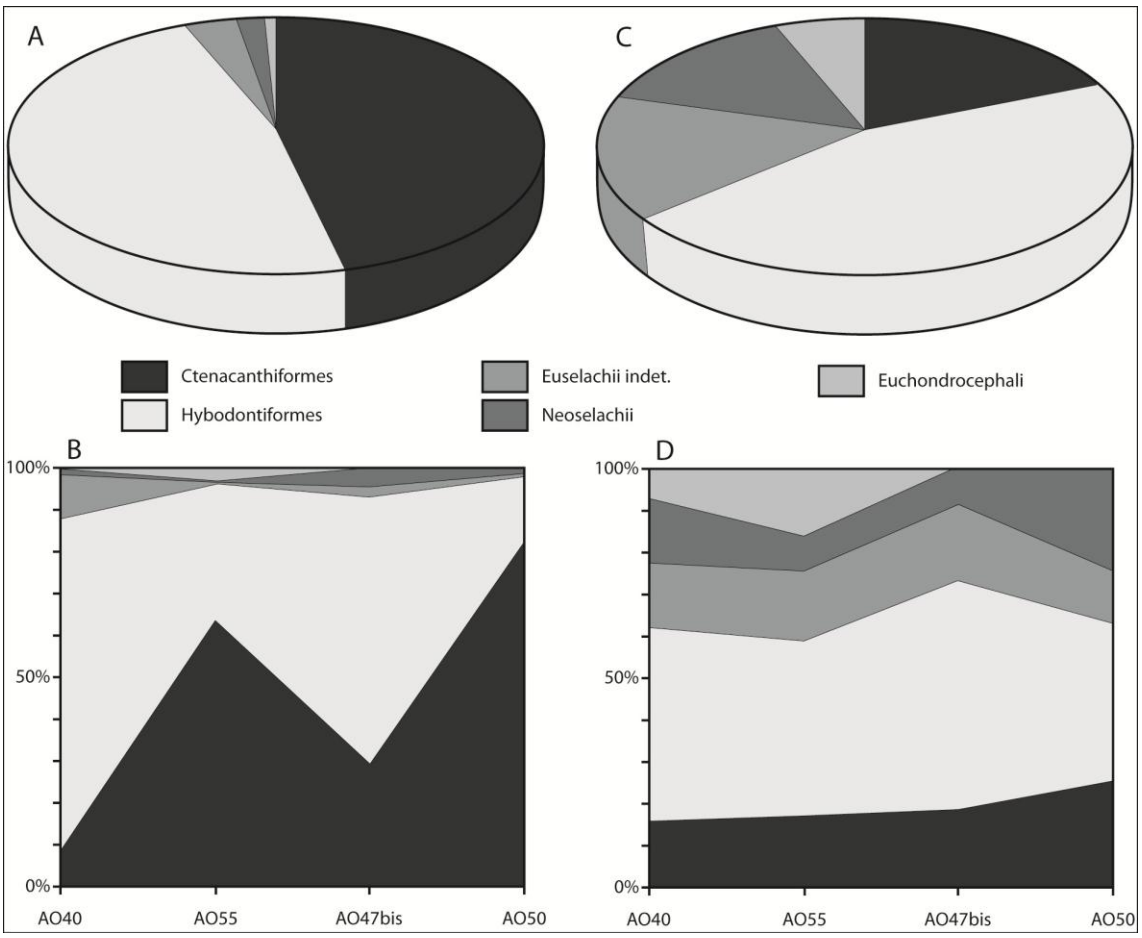

Figure 3.11 – Relative abundances of of chondrichthyan groups from the Wordian Khuff Formation (MPUM collection). A, Overall relative abundance of major groups using numbers of specimens. B, Relative abundance of major groups per sample using numbers of specimens. C, Overall relative abundance of major groups using numbers of genera. D, Relative abundance of major groups per sample using numbers of genera. Samples in B and D are ordered stratigraphically (Figure 3.8).

92%, 96%, and 62%, respectively; Appendix A1.4.4). Sample AO41 has the same lithology as AO40, and so similar observations are expected. AO214 and, to some extent AO210, are cross-bedded and contain pebbles, suggesting more transportation and therefore a higher expected frequency of hybodonts. AO211 is the most fine-grained lithology, and compared to AO55 and AO50, a domination of hybodonts is perhaps unexpected. There are currently no clear indications of more frequent hybodont domination in Member 3 compared to Member 2, which might be expected from the depositional setting, but the two members are not equally sampled and the only large sample from Member 2 is coarse-grained.

In terms of relative diversity, based on the number of genera assigned to each group, the hybodontiforms dominate each of the large samples (Figure 3.11C, D). The euchondrocephalians are represented by the fewest number of specimens and have the lowest generic diversity (Figure 3.11). They were only rarely present in the smaller (3–5 kg) samples (Figure 3.8).

By using the complete suite of samples, the ranges of the most common taxa within the Khuff Formation can be determined. Both ctenacanthiforms and hybodontiforms are recorded from the base of Unit D of Member 1 through to the uppermost part of Member 3 (Figure 3.8). Ctenacanthiforms range even further downward, because they are also recorded from the Sakmarian Saiwan Formation at Jabel Gharif. An even older occurrence in the region is suggested by the recovery of cladodont teeth from the lowermost bed (60 cm) of the Saiwan Formation in the Saiwan area (upper Sakmarian, Cisuralian; Angiolini *et al.* 2003b).

3.2.2.2 QARARI BLOCK

The type locality of the Qarari Limestone is at Jabel Qarari on the Batain Plain, in the vicinity of Wadi Qarihah (Shackleton *et al.* 1990), and many outcrops of the same deposit have been observed at other localities in the Batain area. One of these is the sampled block at N 22°19'01" E 59°43'10" (Figure 3.3), which is a large olistolith protruding from an extensive sand cover. Approximately 50 m of the typical Qarari grey nodular lime mudstone are exposed, which is underlain by a bed of fusulinid limestone and a few metres of pink reefal limestones cropping out on the western face. The fusulinid limestone is typical of a shallow water, tropical facies and the reefal limestone contains crinoids, brachiopods and bivalves, which are also typical of shallow waters (A. Baud, pers. comm. 2010; Shackleton *et al.* 1990). It is believed that the reefal limestone was redeposited in a deeper basinal setting (open sea shelf) where the lime mudstone was formed, and both lithologies were then redeposited as a giant olistolith during the Cretaceous (A. Baud, pers. comm. 2010). The Qarari Limestone typically

ranges from Cisuralian to Lopingian in age (Shackleton *et al.* 1990), but the age of this outcrop has been established as Guadalupian–Lopingian, based on conodonts identified by H. Kozur (A. Baud, pers. comm. 2010).

Two samples (bulk, cumulative mass 3.8 kg; Appendix A1.1) were collected from the deposit. One was collected from the base of the nodular lime mudstone, which proved unfossiliferous, and one from the pink reefal limestone, which revealed the presence of fishes and sharks in the depositional environment based on the recovery of an actinopterygian tooth and chondrichthyan tooth fragments identified as *Stethacanthulus* sp. cf. *S. decorus*.

3.2.2.3 THE "BRIDGE"

An olistolith of a few metres in size protrudes from an extensive gravel cover at N 22°26'35" E 59°46'01" in the north of the Batain Plain (Figure 3.3). Conodont identification has indicated a mid-Wuchiapingian (Lopingian) age for this outcrop (A. Baud and L. Krystyn, pers. comm. 2010). The block is composed of white and red bioclastic mudstone/wackestone associated with framestone. The fossil content comprises coral, crinoids, gastropods and bryozoa, which is typical of the reef association described by Shackleton *et al.* (1990). Numerous ammonoids and foraminifera are also recognised, which suggests a more open marine environment and therefore that some transportation of bioclastic debris of a shallow marine origin may have been involved.

Two samples (bulk, cumulative mass 9.1 kg; Appendix A1.1) were collected, which yielded actinopterygian teeth and twelve chondrichthyan specimens, which have been identified as isolated tooth cusps of *Stethacanthulus* sp. cf. *S. decorus* (Appendix A1.5).

3.2.2.4 ASEELAH (ASILAH)

This outcrop is located at N 21°56'37" E 59°36'32", about 3 km southwest of Aseelah along the eastern coast of the Batain Plain (Figure 3.3). It consists of a number of giant

olistoliths of nodular micritic lime mudstone typical of the Qarari limestone, protruding from the sand cover on the north side of the track, and deposits of the Aseelah Unit exposed on the south side of the track. The Aseelah Unit here measures about 35 m in thickness in a continuous section, consisting mainly of clast-supported sandy limestone conglomerate. Five to 10 m thick bedded channels of sandy calcareous conglomerate occur at the base, consisting of reworked shallow marine Permian limestone boulders, followed by 20 m of 0.5–3 m thick cross-bedded, coarse-grained white sandstone beds with calcareous matrix (Hauser *et al.* 2000, 2002). The boulders are bioclastic wackestones, packstones and grainstones, typical of lagoonal and reef limestones as well as shelf sediments, some of which contain corals and brachiopods (Hauser *et al.* 2002). The calcarenitic matrix of the conglomerate comprises skeletal packstone and crinoidal grainstone (Hauser *et al.* 2002), which contains ammonoids. Early diagenetic weathering surfaces in the sandstones allow identification of a transgressive-regressive sequence (Hauser *et al.* 2000), which may suggest a Guadalupian–Lopingian lowstand (A. Baud, pers. comm. 2010), which fits with the Cisuralian–Lopingian age of the conglomeratic boulders (Hauser *et al.* 2000). Two samples (bulk, cumulative mass 4.1 kg; Appendix A1.1) were collected from the bedded channel deposits. One recrystallised chondrichthyan tooth(?) was recovered (Appendix A1.5). The specimen may represent a monocuspid crown of a tooth, but it is fragmentary and substantially recrystallised, and therefore remains indeterminate.

3.2.3 PERMIAN/TRIASSIC BOUNDARY SECTIONS

3.2.3.1 WADI SAHTAN

This section of considerable thickness is exposed in the Wadi Sahtan valley at N 23°20'31" E 57°18'44" in the northwestern region of the autochthonous Jabel Al Akhdar region in the Oman Mountains (Figure 3.3). The section is accessible on both sides of the wadi. The sequence was deposited on the inner part of the Arabian carbonate platform and is typical of a shallow marine setting (Richoz *et al.* 2005). It comprises the

Saiq and Mahil formations (Akhdar Group), which show a number of transgressive/regressive cycles (Richoz 2006). The Saiq Formation here is a high energy carbonate unit (wackestone/packstone) and is succeeded by the Mahil Formation, comprising thin-bedded dolomites representative of intra- and supratidal environments (Richoz *et al.* 2005). The log (Figure 3.12) is a composite of multiple sections at the same location and includes both the Permian/Triassic boundary and the late Changhsingian extinction event. The P/Tr boundary is marked by a possible emergent hardground, indicating interrupted sedimentation (Richoz *et al.* 2005). Extensive dolomitisation has caused the loss of age diagnostic fossils, and so the age determination is mainly based on $\delta^{13}C$ and $\delta^{18}O$ isotopic signals (Richoz *et al.* 2005; Richoz 2006). Seven samples (bulk, cumulative mass 8.9 kg; Appendix A1.1) were collected, spanning the Wuchiapingian? to the uppermost Smithian. The sample height of 100219-D is an approximation because of partial inaccessibility. The sample residues proved to be largely unfossiliferous and no chondrichthyan remains were recovered.

3.2.3.2 WADI ADAY

This outcrop is about 3 km on the main road south out of Muscat, in the Saih Hatat (Figure 3.3). There are multiple sections, but the sampled interval is located at N 23°34'05" E 58°31'33". Autochthonous deposits of the Saiq and Mahil Formations are exposed, including the Permian/Triassic boundary interval, but deposits here have been faulted and metamorphosed (Weidlich and Bernecker 2003). The total outcrop ranges from the Guadalupian to the Late Triassic, but only the Changhsingian–Middle Triassic interval is shown in Figure 3.13, which comprises siliciclastics and mostly dolomitised carbonates. The biostratigraphy is primarily based on foraminifera, such as *Colaniella minima* for the Changhsingian and *Pilamminella* sp. for the Early Triassic, as well as fusulinids and ostracods, but the stratigraphic control is very poor in comparison to the basal part of the Saiq Formation and dating of the Permian/Triassic boundary is

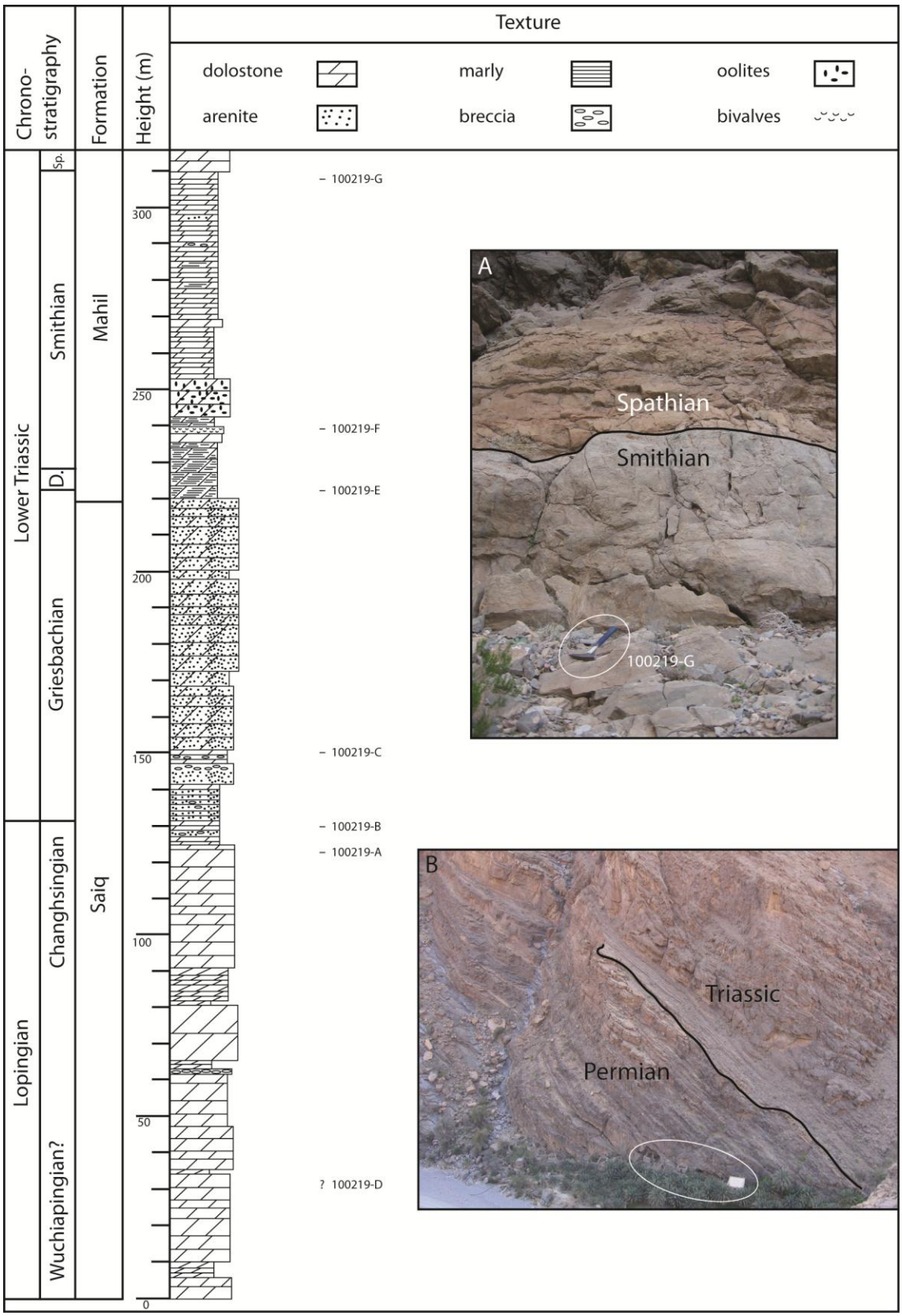

Figure 3.12 – Composite stratigraphic log of the section at Wadi Sahtan. Sampled beds are indicated. Redrawn from Richoz (2006). A, Smithian–Spathian boundary on the eastern side of the wadi, with geological hammer for scale. B, View of the western face of the wadi outcrop, with small houses for scale.

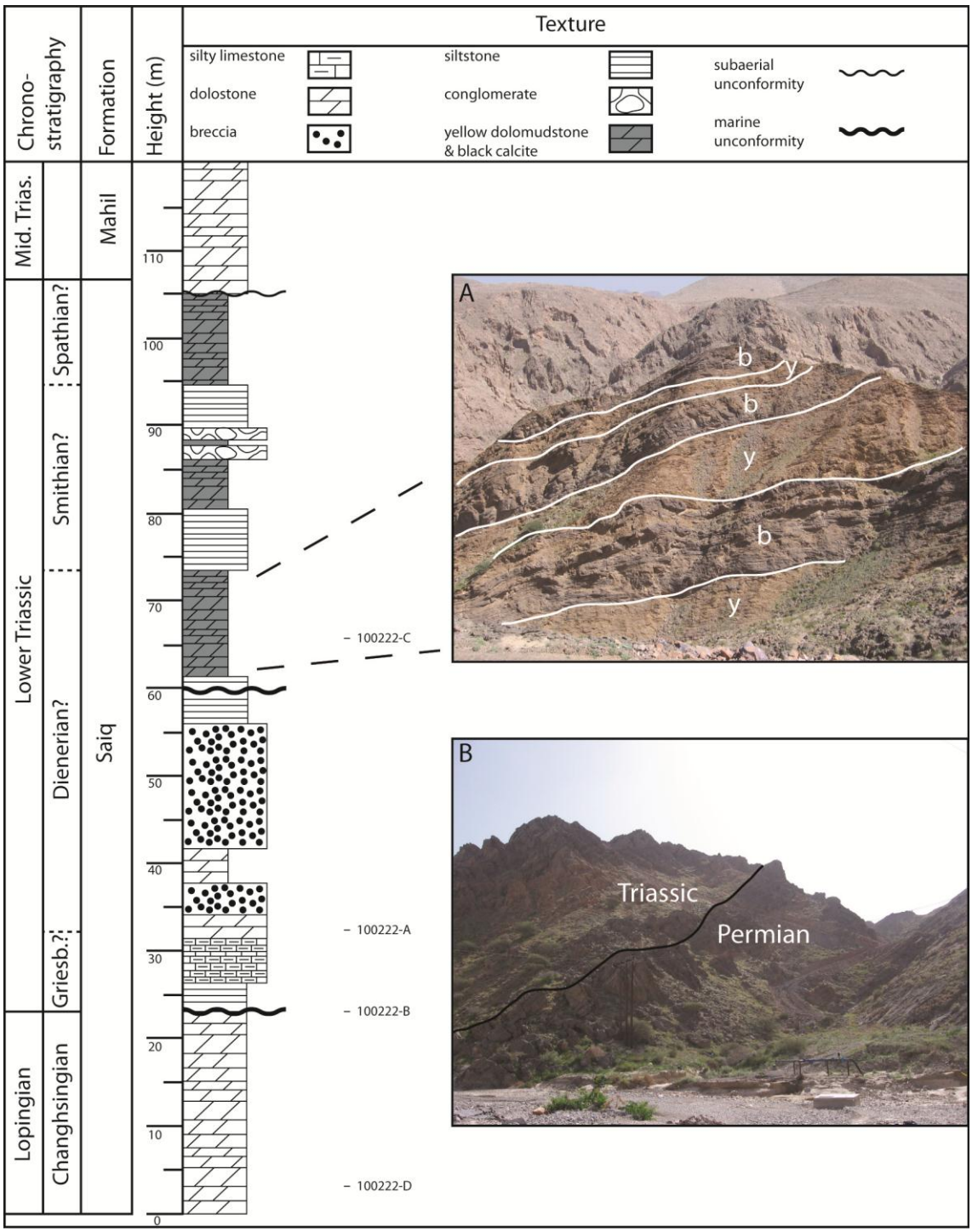

Figure 3.13 – Composite stratigraphic log of the section at Wadi Aday. Sampled beds are indicated. Modified from Weidlich and Bernecker (2007, 2011). A, Lower Triassic yellow silty dolomudstones (y) with bioturbated recrystallised black-calcite limestone beds (b), as viewed towards the north (scale suggested by correlation to log). B, Outcrop locality as viewed towards the east.

particularly difficult due to the absence of conodonts and ammonoids (Weidlich and Bernecker 2011). Substage boundaries in the Lower Triassic were inferred from

correlation with similar facies in the Jabel al Akhdar region, but remain preliminary (Weidlich and Bernecker 2011).

The depositional environment changed from a shallow marine environment with sea water undersaturated in terms of carbonate in the Lopingian, to a siliciclastic-dominated environment in the Early Triassic (Richoz *et al.* 2010; O. Weidlich and M. Bernecker, pers. comm. 2010). The presence of hardgrounds indicate repeated breaks in deposition and tectonic activity in the area resulted in brecciated and conglomeratic beds (Richoz *et al.* 2010). The sequence formed on the rim of the Arabian Platform, which is believed to have experienced a delayed biotic recovery from the late Permian mass extinction compared to inner platform sequences, based on reduced carbonate production (Weidlich and Bernecker 2007; Richoz *et al.* 2010).

Four samples (bulk, cumulative mass 4.1 kg; Appendix A1.1) were collected from Changhsingian to Dienerian? dolomitic beds (Figure 3.13). Even though the top of the P/Tr hardground (100222-B) and the first Triassic bioclastic bed (100222-A) proved to be fossiliferous after processing in terms of crinoids, gastropods and some conodonts, no chondrichthyan remains were recovered.

3.2.3.3 SAIQ PLATEAU

Geological setting

A detailed sampling effort through the Permian/Triassic boundary was undertaken on the Saiq Plateau in the Jabel Akhdar region of the Oman Mountains (Figure 3.3). The Permian and Triassic deposits of the Saiq Plateau comprise the Saiq and Mahil formations (Figure 3.14). The Saiq Formation is >600 m thick (Koehrer *et al.* 2010) and comprises basal conglomerates, bioclastic limestones, coral boundstones and dolostones (Angiolini *et al.* 2003; Figure 3.15). The basal part was deposited in a transgressive, shallow-marine environment and unconformably overlies pre-Permian basement strata (Glennie 2005). The Saiq Formation is overlain by the >500 m thick Mahil Formation, which spans the entire Triassic (Koehrer *et al.* 2010), and is

composed of secondary dolomitised limestones representative of a more restricted environment (Glennie *et al.* 1974). Deposition here is typical of the inner carbonate platform and started in the Wordian with the onset of the Middle Permian transgression (Richoz *et al.* 2005). A basal layer of siliciclastics is overlain by 120 m of shallow water fossiliferous limestones (Koehrer *et al.* 2010). From the upper Wordian, later stage dolomitisation affects the rest of the sequence of shallow water carbonates (Richoz *et al.* 2005; Koehrer *et al.* 2010).

Samples were collected from five localities spread across the plateau (Figure 3.14), which overlap slightly and therefore provide a continuous record from the Wordian through to the Induan. Wordian limestone deposits have been sampled at locality CH (N 23°04’30” E 57°39’45”; C. Henderson, pers. comm. 2010), and at section A, with the base at N 23°04’17” E 57°41’53” and the top at N 23°04’27” E 57°42’14” (Koehrer *et al.* 2010). Wordian–Capitanian deposits have been sampled at section B, which starts at N 23°05’07” E 57°42’25” (Koehrer *et al.* 2010), shows the chert marker (see Figure 3.15)

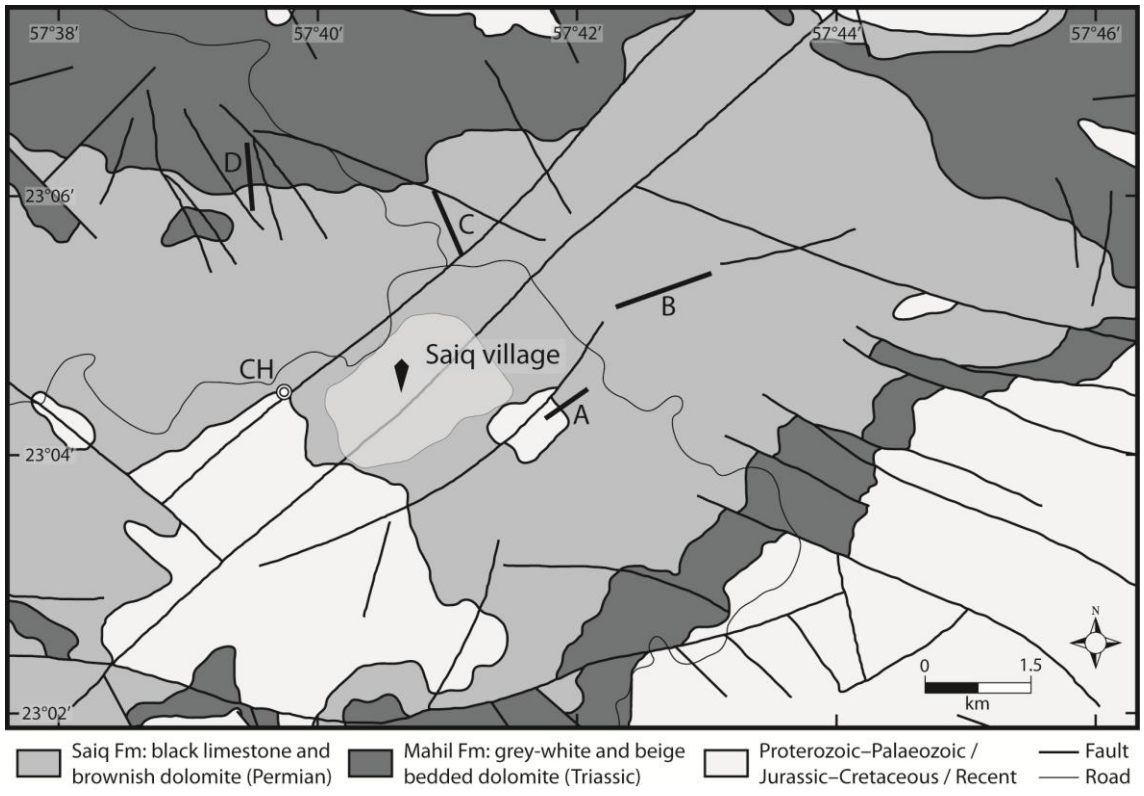

Figure 3.14 – Geological map of the Saiq Plateau (modified from Koehrer *et al.* 2010), showing sections A–D of Koehrer *et al.* (2010) and location CH, which have been sampled in part (see text).

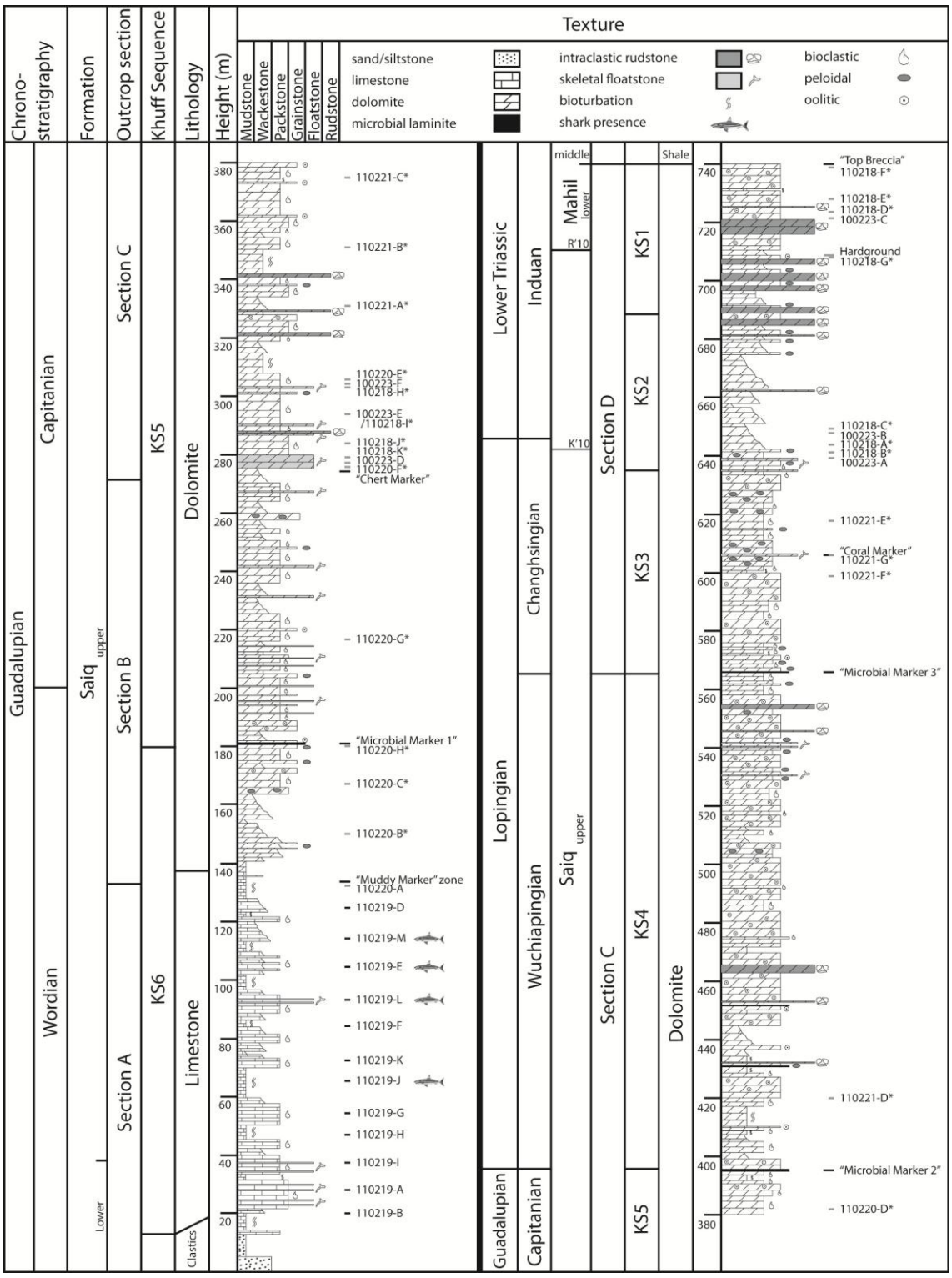

Figure 3.15 – Composite stratigraphic log of the sections on the Saiq Plateau. Sampled beds are indicated (in black if position accurate, in grey if approximate, samples marked with an asterisk remain unprocessed). Modified from Koehrer *et al.* (2010) and Richoz *et al.* (2010). Note: the Saiq/Mahil boundary is placed differently by the two sources. Both are shown on the "Formation" column (K'10 and R'10, respectively), but the interpretation of Richoz *et al.* (2010), based on stable isotopes, is followed in the formation assignment of the samples.

at N 23°05’11” E 57°42’36” and ends at N 23°05’20” E 57°42’49” (these two sets of coordinates are based on own readings, because the longitude of the top of section B quoted in Koehrer *et al.* 2010, fig. 2 is somewhat more easterly than observed in the field and the same longitude in their fig. 7 is believed to be a typographical error because it indicates a position some distance to the west and is identical to the longitude quoted for the base of section D). Capitanian–Wuchiapingian deposits have been sampled at section C, which is exposed on two consecutive hill sides. The bottom half of section C starts at N 23°05’29” E 57°41’13” and ends at N 23°05’41” E 57°41’12” (these are again corrected from the coordinates quoted in Koehrer *et al.* 2010, which place the base of the section slightly too far to the northeast and too high up in the section, and the top of the section some distance to the south-southwest). The top half of section C has not been sampled due to time restrictions. Changhsingian–Induan deposits have been sampled at equivalent sections to section D of Koehrer *et al.* (2010), namely in a quarry between N 23°06'00" E 57°39'52" and N 23°06'06" E 57°40'03" and at road-side cuts to the southeast (towards section C; samples 110221-E–G, see Appendix A1.1 for specific coordinates).

Seven samples (residue; Appendix A1.1) were collected from the Wordian at locality CH by C.H. Henderson (University of Calgary; UC collection; Table 3.2. A total of 44 samples (bulk, cumulative mass 50 kg; Appendix A1.1) were collected from the remaining sections (Figure 3.15 and Figure 3.16). Age diagnostic fossils are no longer preserved in the dolomitised parts of the sequence (Richoz *et al.* 2005), which is why the basal part of the Saiq Formation, Wordian strata of the *Neoschwagerina schuberti* Zone (e.g., Weidlich and Bernecker 2011), was sampled at the highest resolution.

Results

Chondrichthyan remains, comprising 15 isolated and mostly fragmented teeth and 26 dermal denticles, were recovered from locality CH (Table 3.2) and from four beds at section A within a 50 m thick sequence of the basal limestone of the Saiq Formation (110219-E, J, L, M; Figure 3.15). All specimens are of Wordian age. The teeth belong

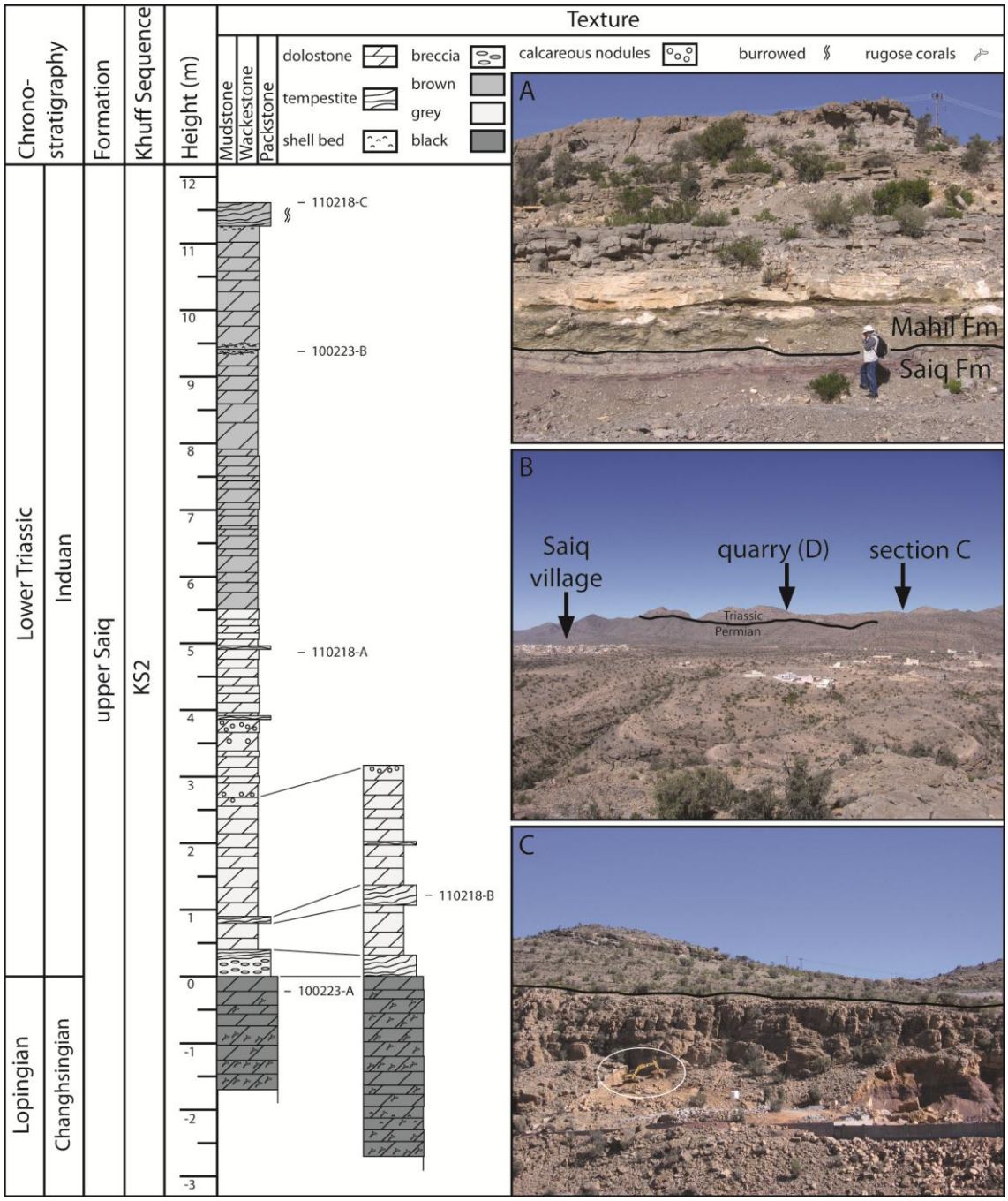

Figure 3.16 – Composite stratigraphic log of the Permian/Triassic boundary on the Saiq Plateau. Due to a fault, two different sequences exist at the logged section. Sampled beds are indicated. A, Saiq/Mahil Formation boundary. B, View towards the northwest from the summit of section A across the Saiq Plateau. C, Section A with digger for scale and the black line indicates an exposed hardground (height equal to sample 110219-I).

to the ctenacanth *Glikmanius* cf. *myachkovensis* Lebedev, 2001, based on cusp fragments only, and to the hybodont genus *Omanoselache*. The latter is represented by the cuspidate *Omanoselache angiolinii* Koot, Cuny, Tintori and Twitchett, 2013 and

the massive cf. *Omanoselache* sp. Actinopterygian fish are present in the Wordian (110219-G) and in the lower Induan (100223-B), but no Early Triassic chondrichthyans were recorded. No other samples have yielded vertebrate remains, but 25 of the available samples remain unprocessed due to time restrictions (see Figure 3.15; Appendix A1.1).

Table 3.2 – Stratigraphic position of samples at locality CH (UC collection).

Sample number	Saiq (height in m)	Fossil content
969-12	40	barren
969-6	22.7	dermal denticles
969-5	19.7	chondrichthyan teeth, dermal denticles
969-4	18.7	chondrichthyan teeth
969-3	18.5	barren
969-2	5.0	barren
969-1	0.5	barren

3.2.3.4 WADI WASIT

Geological setting

Wadi Wasit is located over 50 km south of Muscat in the Ba'id tectonic window, between 5–10 km southwest of Wadi Alwa and about 2 km northeast of Ba'id village (Figure 3.3). The Ba'id geology and the outcrops at Wadi Wasit were described by Blendinger (1988). The Wadi Wasit outcrop is observed at multiple sites in a small area, including isolated blocks and relatively extensive sections (Figure 3.17). Sample 100224-L was collected at N 23°6'33" E 58°20'24", whereas the sampled section (second column) was located at N 23°6'49" E 58°20'55" and the block (third column) at N 23°5'48" E 58°20'02". This block has been described in detail by Krystyn *et al.* (2003) and the invertebrate fauna has been discussed by Twitchett *et al.* (2004) and Wheeley and Twitchett (2005). It occurs in Dienerian slope breccia and is composed of reefal limestone derived from the carbonate platform margin (Krystyn *et al.* 2003; Richoz 2006). This breccia is incorporated in a Guadalupian volcano-sedimentary series composed of multiple levels of pillow lava and overlain by Lower Triassic platy limestones (Pillevuit *et al.* 1997).

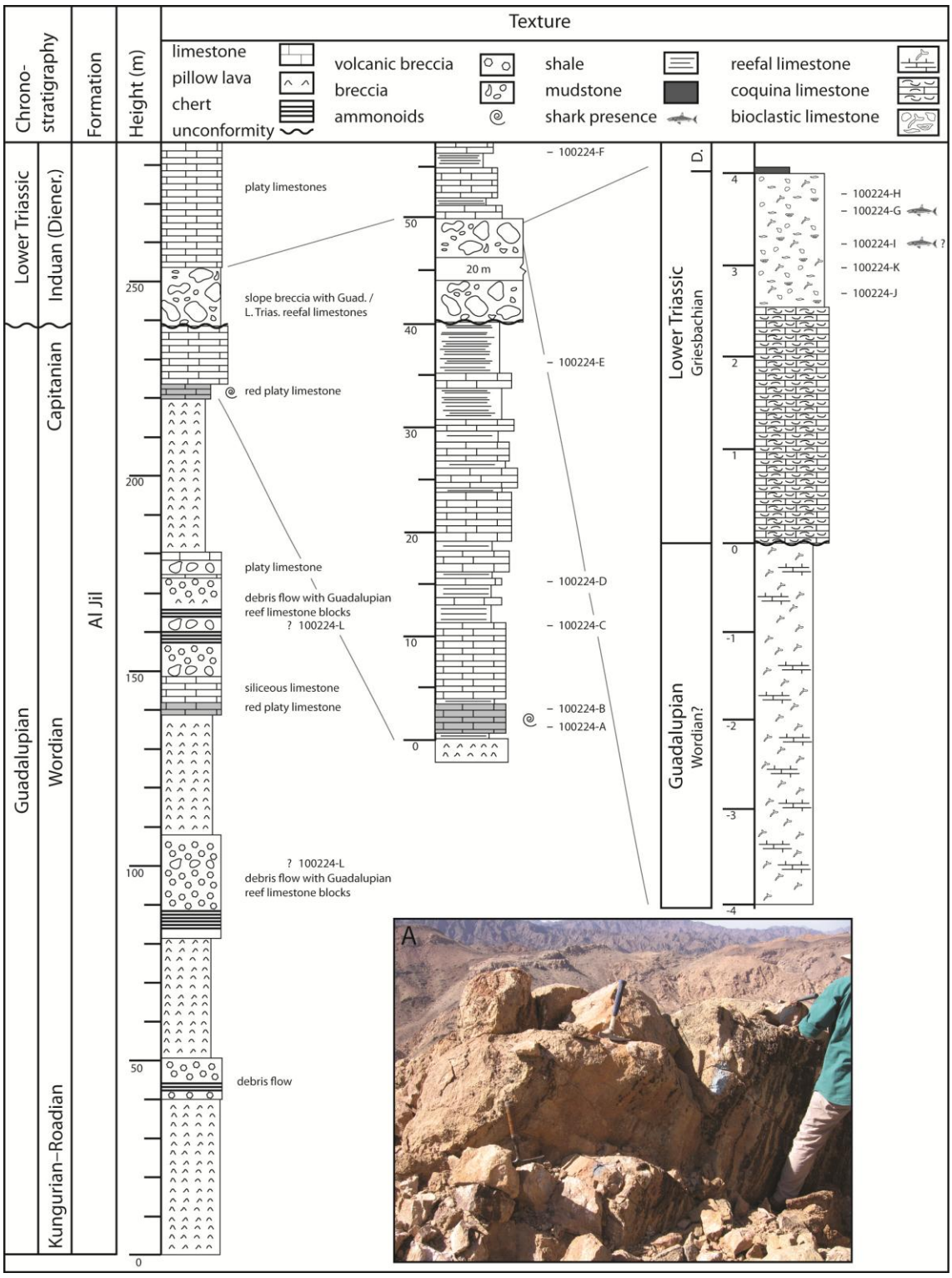

Figure 3.17 – Composite stratigraphic log of the section and block at Wadi Wasit. Sampled beds are indicated. Redrawn from Krystyn *et al.* (2003); Richoz (2006). A, Griesbachian top section of the block as viewed towards the north, with hammers for scale.

The exposed strata belong to the Al Jil Formation of the Hamrat Duru Group, which was deposited in relatively deep waters at the continental rise (Glennie *et al.* 1974;

Glennie 2005; Pillevuit *et al.* 1997), inferred from frequent debris flows in the sequence (Pillevuit *et al.* 1997) and the deposition of ammonoid-rich red limestone during the Capitanian (Krystyn *et al.* 2003; Richoz 2006), indicative of pelagic conditions (see Tozer and Calon 1990). The lithostratigraphy of the block comprises Guadalupian (Wordian?) reefal limestone and Griesbachian coquina and bioclastic limestones, with a significant hiatus in between. A comparable hiatus is present in the exposed section, which causes the entire Lopingian to be missing at Wadi Wasit, which may be attributable to a sea-level lowstand around the Permian/Triassic boundary (Hauser *et al.* 2002). The Wadi Wasit deposit is therefore not a complete boundary section, and similar hiatuses have also been observed in Rustaq (Section 3.2.3.5) and Wadi Alwa (Section 3.2.4.2). Twelve samples were collected (bulk, cumulative mass 19 kg; Appendix A1.1; Figure 3.17), ranging in age from Wordian? through to Capitanian (it is unknown which of two debris flows sample 100224-L originates from due to time restrictions in the field), and Griesbachian through to Dienerian.

Results

One fragment of a chondrichthyan tooth (100224-G) and one possible recrystallised chondrichthyan tooth (100224-I) were recovered from Griesbachian deposits (Figure 3.17; Appendix A1.5). The morphological features of the tooth fragment fit with the diagnostic characters of Genus P sp. P but the assignment is made with some uncertainty, due to the limited and fragmentary nature of the material. It would represent the oldest record of this genus and species, which is best known from the Smithian–Spathian of Jabel Safra and Wadi Alwa (Figure 3.22; Appendix A3.2). The remaining specimen is reminiscent of a multicuspid tooth, but fragmentary and substantially recrystallised, and therefore indeterminate.

Further chondrichthyan material from Wadi Wasit was described by Yamagishi (2006), which was obtained from two samples collected by R.J. Twitchett from the Griesbachian bioclastic limestone in the block at about 3.5 m. The material comprises

five complete and fragmented teeth, originally assigned to *Lissodus* sp.1, and seven dermal denticles. The teeth are referred to *Omanoselache* sp. H (Appendix A3.2), and represent the oldest occurrence of the species, which is best known from the Spathian of Oman (Jabel Safra, Figure 3.22).

3.2.3.5 RUSTAQ

The Al Jil Fm at Rustaq, formerly known as the Rustaq Formation and located at N 23°24'41" E 57°24'34" (C. Henderson, pers. comm. 2010) in the Oman Mountains (Figure 3.3), is a tectonically isolated slab with pillow basalts and green tuffites at the base (Figure 3.18). Overlying this is a partly dolomitised, condensed red argillaceous carbonate sequence (pelagic Hallstatt-type cephalopod limestone), of Wordian, Guadalupian age (e.g., Pillevuit *et al.* 1997; Henderson and Mei 2003; Richoz *et al.* 2005). The palaeoenvironmental setting of the Permian deposits has been interpreted as an atoll within the Hawasina deep-sea basin (Pillevuit *et al.* 1997), but Richoz *et al.* (2005) state that some features indicate a submarine high or seamount on the basinal margin, which is in agreement with Immenhauser *et al.* (2000), who describe them as fault-block highs. The Guadalupian succession is followed by a hiatus and is overlain by Lower Triassic deposits comprising a thin sequence of grey shales and a thick deposit of oolitic calciturbidites with shale interbeds (Richoz *et al.* 2005). Sample 621-2 (residue; Appendix A1.1; UC collection) was obtained at Rustaq by C.M. Henderson (University of Calgary) from an unknown lithology and height within the section. However, the sample yielded one chondrichthyan tooth fragment (Appendix A1.3), which is of a morphology reminiscent of Genus P. An Early Triassic (Olenekian) age is therefore suspected, based on the results from Jabel Safra and Wadi Alwa described in Sections 3.2.4.1 and 3.2.4.2, but this must remain highly speculative.

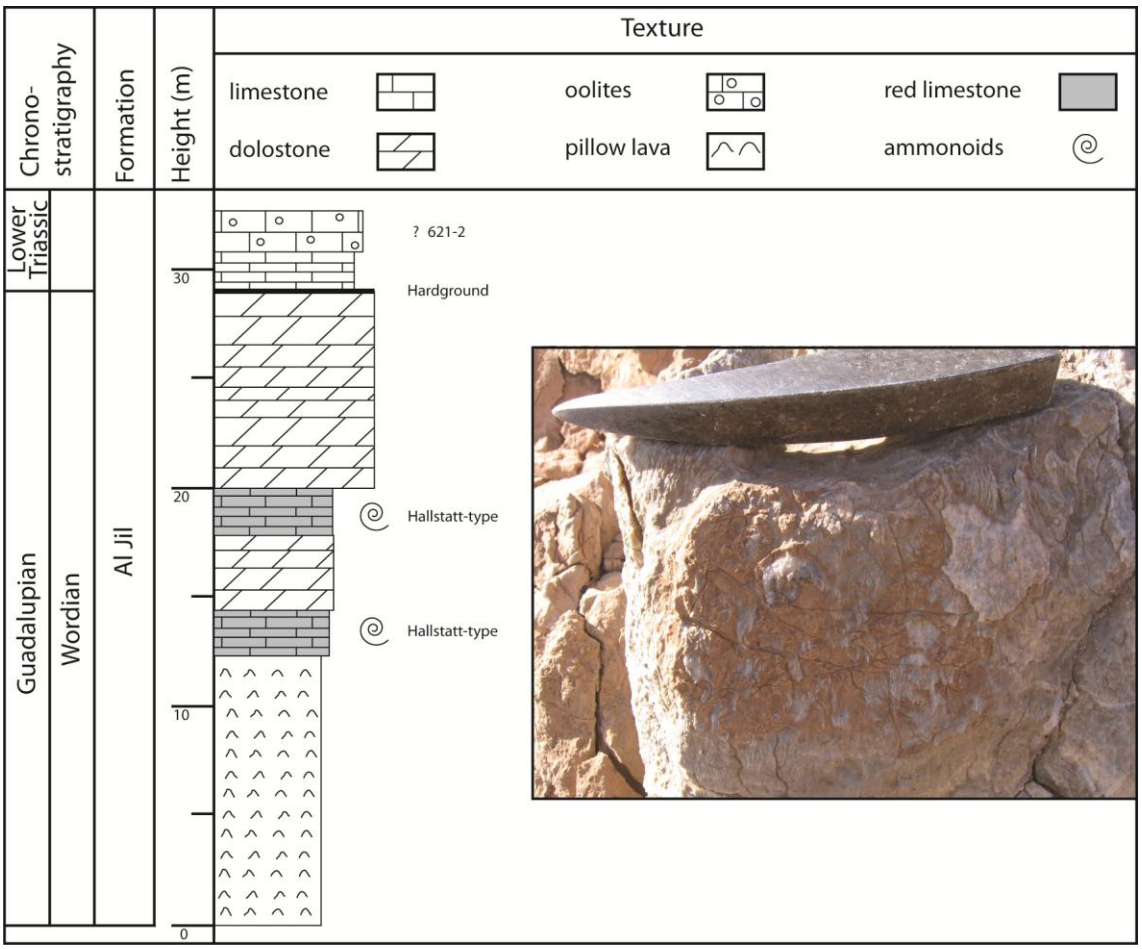

Figure 3.18 – Stratigraphic log of section 1 at Rustaq. Suspected sample height is indicated. Redrawn from Richoz *et al.* (2005). The inset shows Smithian Hallstatt-type limestone from Wadi Alwa, which is widely observed in Oman, with the head of a hammer for scale.

3.2.3.6 AL BUDAY'AH

This exposure is located at N 23°44'37" E 56°54'15" near Buday'ah on the northern margin of the Oman Mountains (Figure 3.3). The log of the section (Figure 3.19) is a composite of three outcrops within about 250 m of each other. The sequence is overturned, but at the base of the unit are Guadalupian pillow lavas, which are overlain by Wuchiapingian pelagic cephalopod-rich lime mudstones and radiolarites (Richoz *et al.* 2010). These are followed by Changhsingian dark grey siliceous shales and light-coloured calcareous shales, after which the Induan is represented by yellow marly shales (fissile marls), and platy as well as marly limestones. The top of the section consists of Smithian papery, laminated limestones and olive shales.

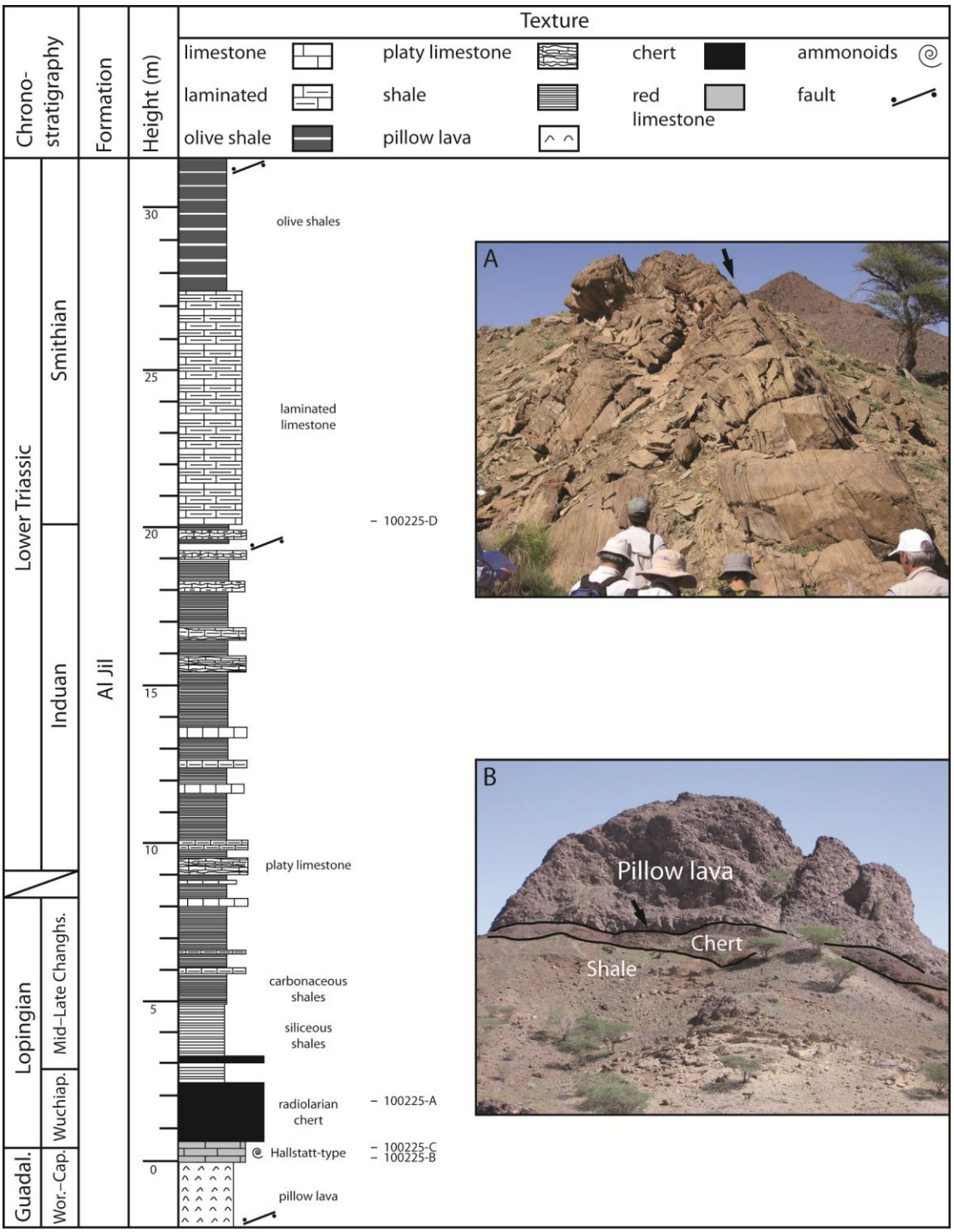

Figure 3.19 – Composite stratigraphic log of the section at Al Buday'ah. Sampled beds are indicated. Redrawn from Richoz *et al.* (2010) and Baud *et al.* (2012). A, Smithian laminated limestone as viewed towards the north, younging to the left (west), with the base of the unit and sampling height indicated by arrow. B, Overturned base of the section as viewed towards the northeast, Hallstatt-type limestone not visible because of erosion but sampling location is indicated by an arrow (chert layer generally two metres in thickness).

The Al Buday'ah section is the most distal deposit of the Hamrat Duru Group successions discussed in this study (see Baud *et al.* 2012; i.e., Wadi Wasit, see Section 3.2.3.4, and Rustaq, see Section 3.2.3.5). The fact that it is a deep depositional sequence is indicated by the red pelagic limestones and the absence of shallow water debris, which makes it an unusual representative of the Al Jil Formation (Richoz *et al.* 2010). Four samples were obtained (bulk, cumulative mass 7.5 kg; Appendix A1.1; Figure 3.19). The Changhsingian–Induan part of the section was not sampled due to a sparsity of conodonts, which is also true for much of the Smithian (C.M. Henderson, pers. comm. 2010), and therefore the low potential for vertebrate fossil remains. No chondrichthyan remains were recovered.

3.2.3.7 WADI MAQAM & WADI SHUY'AB

Geological setting

The Maqam Formation of the Sumeini Group is exposed in two neighbouring valleys in the northwestern part of the Oman Mountains, near the border with the United Arab Emirates (Figure 3.3). The most extensive outcrop is located in Wadi Maqam at N 24°46'30" E 55°51'44" and a second is located in Wadi Shuy'ab at N 24°46'54" E 55°52'27". The deposit is considered part of the Hawasina Allochthonous Unit and is typical of a carbonate platform slope deposit (Figure 3.20). The upper part of the Guadalupian sequence comprises fossiliferous limestones indicative of the outer shelf, whereas the Lopingian dolostones were formed in a deeper marine environment (Richoz *et al.* 2010). Smithian sediments were deposited at the base of the slope, where carbonate-rich submarine fans developed (Richoz *et al.* 2010). There is much chert formation in the Changhsingian strata as a result of biogenic silica production (Richoz *et al.* 2010), but this ceases in the middle Changhsingian, 6 m below the extinction horizon and 9 m below the Permian/Triassic boundary (S. Richoz, pers. comm. 2012). Some of the Changhsingian stratigraphy is missing below the Permian/Triassic boundary due to a hiatus (A. Baud, pers. comm. 2010), but all

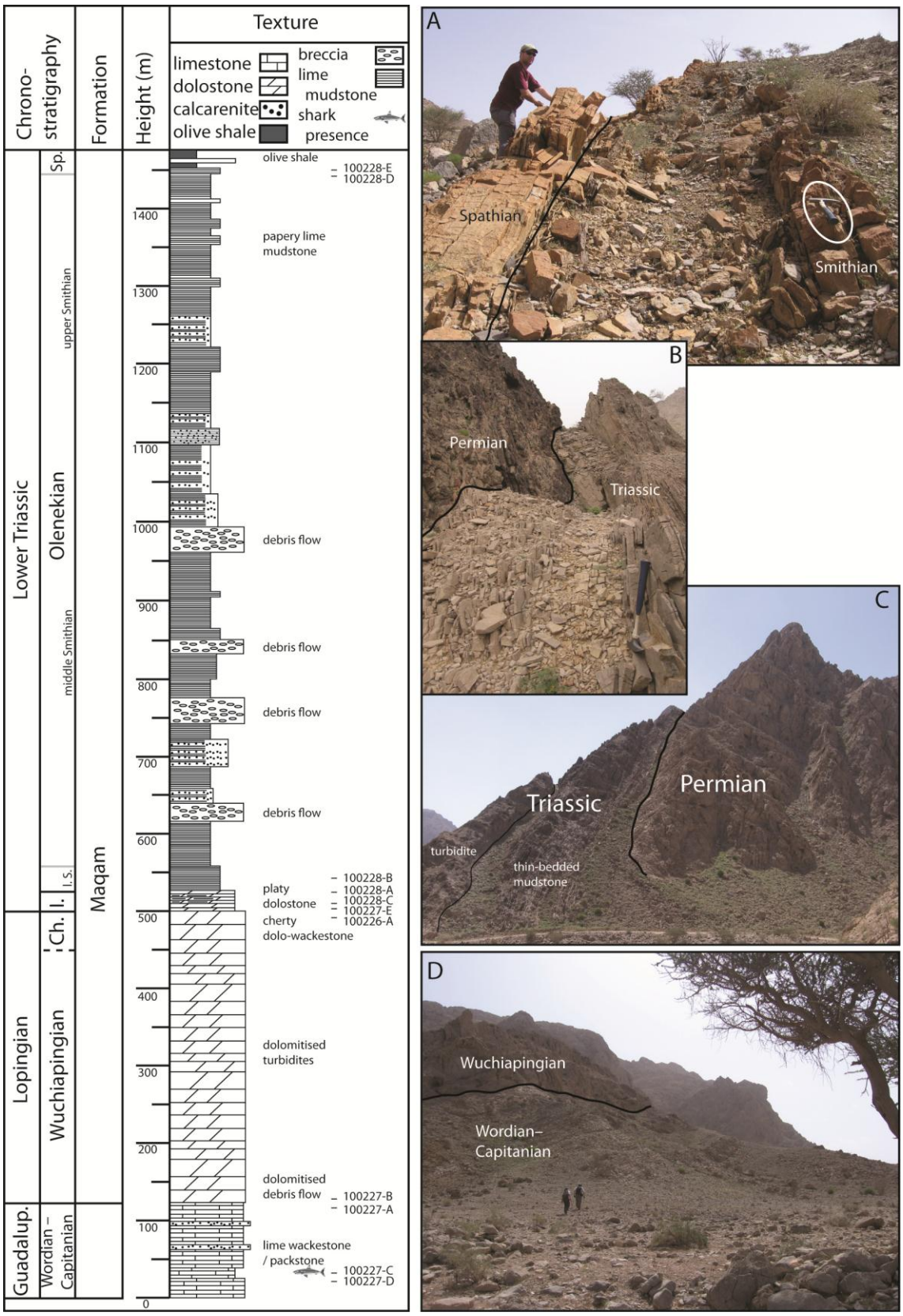

Figure 3.20 – Composite stratigraphic log of sections at Wadi Maqam (WM) and Wadi Shuy'ab (WS) with sampled beds. Redrawn from Richoz (2006). A, Sm/Sp boundary in WS, view to southwest; hammer at 100228-D. B, P/Tr boundary section in WM, view to north; hammer at 100227-E. C, P/Tr boundary in WM, view to south; road for scale. D, G/L boundary in WM, view to southeast; people for scale.

conodont zones have been observed in the sequence, which means that its duration was short (S. Richoz, pers. comm. 2012). Due to instability of the Lopingian slope deposits, the record of the P/Tr boundary is highly variable in the area (Richoz *et al.* 2010). Most of the upper Permian part of the sequence is dolomitised, which has obliterated much of the bedding structures (C.M. Henderson, pers. comm. 2010) and this continues into the lowermost part of the Lower Triassic at some sites (the Induan is locally represented by either finely laminated (papery) lime mudstone or platy dolostone).

Eleven samples (bulk, cumulative mass 18.1 kg; Appendix A1.1) were collected from the Maqam Formation (Figure 3.20), spanning an age range from the Wordian to the earliest Spathian. Most of the Wuchiapingian was not sampled due to the dolomitisation.

Results

One chondrichthyan tooth was recovered from Wordian outer shelf deposits (Appendix A1.5). The age determination is based on ammonoids, ostracods, and conodonts, but the sample concerned was taken 2 m below the bed from which the conodont *Hindeodus wordensis* was recovered (see Richoz *et al.* 2010). The shark tooth cusp fragment has been identified as belonging to *Stethacanthulus* sp. cf. *S. decorus* (Appendix A3.2).

3.2.3.8 BU FASIQAH

The outcrop is located at N 22°18'13" E 59°40'33", roughly 6 km northwest of Bu Fasiqah on the Batain Plain (Figure 3.3). It is not a complete boundary section, but contains a number of different deposits belonging to the Permian Qarari Unit, the Aseelah Unit, the Triassic Sal Formation. The Qarari and Aseelah limestone deposits are referred to as units rather than formations, due to the absence of well-defined formational boundaries (see Hauser *et al.* 2002). Thrust contacts are common in this

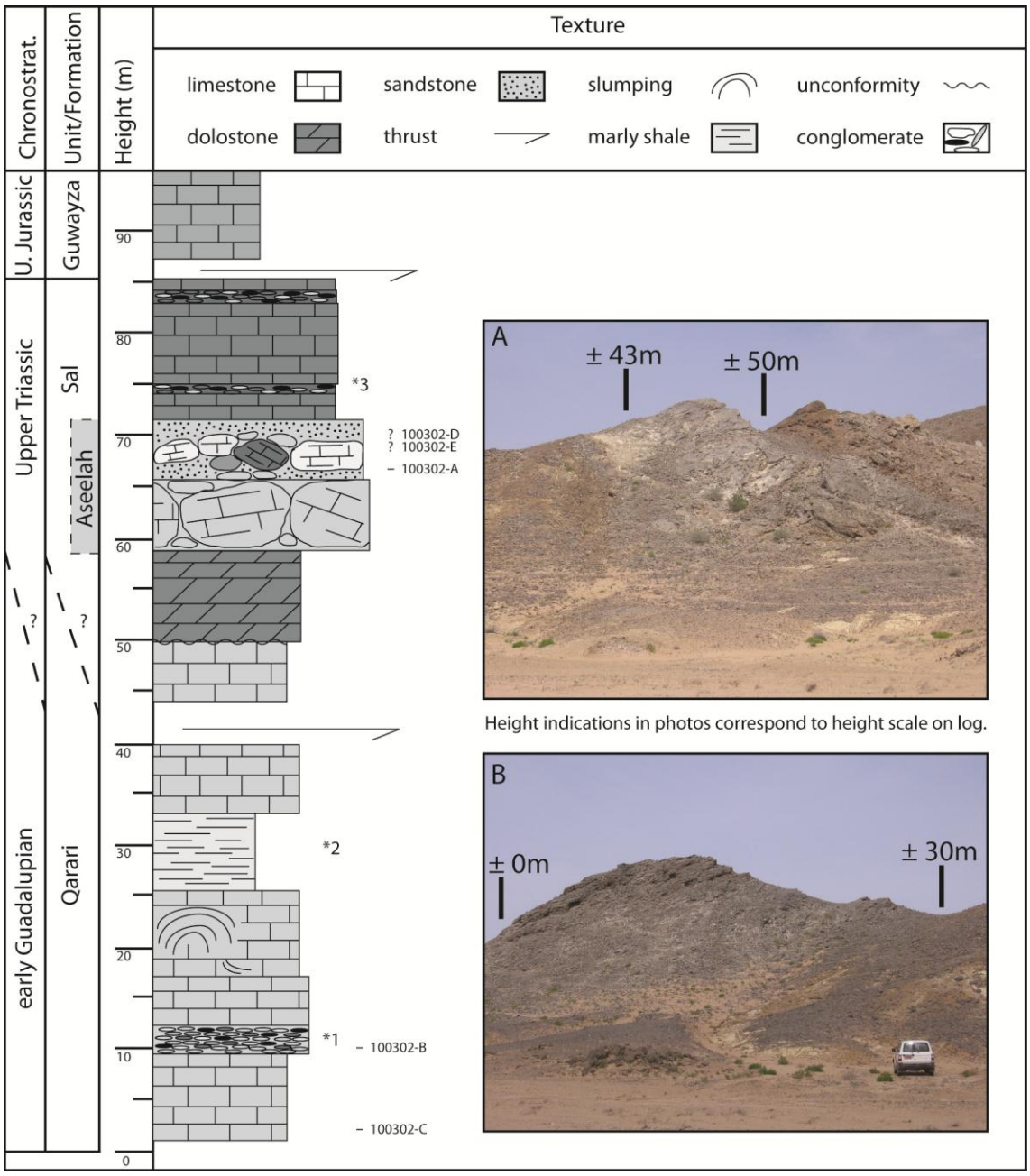

Figure 3.21 – Stratigraphic log of the section at Bu Fasiqah. Sampled beds are indicated. Redrawn from Hauser *et al.* (2002). Heights marked with an asterisk indicate the recovery of: 1, an early Guadalupian ammonoid, brachiopod, and conodont fauna; 2, a Roadian ammonoid fauna; and 3, an early Norian conodont fauna. A, Middle part of the section (±33–60 m) viewed towards the north, same scale as B. B, Basal part of the section (±0–30 m) viewed towards the north, 4WD car for scale.

exposure. A detailed log was published by Hauser *et al.* (2002; Figure 3.21). The section is overturned (see Hauser *et al.* 2000, fig. 2), but starts with nodular Qarari lime mudstone of early Guadalupian age, which contains intra-formational breccia and calcirudite horizons, as well as yellowish inter-beds of marly shales (Hauser *et al.*

2002). The occurrence of slumping and ripple structures, in combination with the recovered biota, suggests deposition in a hemipelagic environment, typical of an open marine shelf and slope (Hauser *et al.* 2002). These deposits are overlain by reddish-brown dolomite that is of uncertain age and formational affinity, but which may belong to the Upper Triassic Sal Formation, which is typically characterised by calcarenite (Hauser *et al.* 2002). The Aseelah Unit is intercalated between the dolomite and the calcarenite, but is considerably older. It consists of poorly sorted, polymict clast-supported carbonate conglomerate, composed of fossiliferous boulders and recrystallised limestone blocks, grading into a sandy matrix-supported conglomerate (Hauser *et al.* 2000). The boulders contain corals, gastropods, bivalves, crinoids and fusulinids. The fusulinids belong to the genus *Neoschwagerina*, which indicates a Cisuralian or Guadalupian age (A. Baud, pers. comm. 2010). The boulders are derived from lagoonal, reef and open-marine shelf environments (Hauser *et al.* 2000), suggesting a debris flow as the origin of the Aseelah Unit (Hauser *et al.* 2002). Five samples (bulk, cumulative mass 9.2 kg; Appendix A1.1) were collected from the Bu Fasiqah section (Figure 3.21). The lime mudstone from the Qarari Unit proved unfossiliferous. Only the boulders within the conglomerates were sampled, which yielded crinoids, bivalves, and conodonts, but no chondrichthyan remains were recovered.

3.2.4 Triassic sections

3.2.4.1 Jabel Safra

Geological setting

Jabel Safra is located about 150 km southwest of Muscat (Figure 3.3). At this locality, Olenekian metre-sized blocks occur in the Upper Jurassic Guwayza Formation of the Hamrat Duru Group, which are of the Hallstatt-type limestone facies—generally interpreted as deep seamount deposits with very low sedimentation rates (Tozer and Calon 1990). They occur in a belt of about 3 km in length and are restricted to a

stratigraphic thickness of under 50 metres (Tozer and Calon 1990). The samples utilised in this study originate from blocks located at N 22°43'23" E 57°48'29" (A. Baud pers. comm. 2011), which are interpeted by Tozer and Calon (1990) as Spathian olistoliths that originated from the east of the main Hawasina depocentre, which suggests a seamount or a carbonate plateau as the most likely source. This fits with the Al Aridh Group of Glennie (2005) and with the Kawr Group of Pillevuit *et al.* (1997). The facies recorded in the blocks is not known from any (par)autochthonous units in the area (A. Baud pers. comm. 2011).

The sampled blocks are block 1, occurring at UTM EA 807127, block 3, occurring at UTM EA 839125 (Tozer and Calon 1990) and block C85314 consisting of a single ammonoid in matrix (Orchard 1995). Block 1 is 2 m wide and has a stratigraphic thickness of 1 m (Tozer and Calon 1990). It was sampled 30 cm from the topographic base (sample number 104A) and within 10 cm of the topographic top (104B/C) (Orchard 1995). Block 3 is 2–5 m wide and has a stratigraphic thickness of 3.5 m. It is well-stratified and composed of mottled red and grey limestone (Tozer and Calon 1990). It was sampled at three levels: 35 cm below the topographic top (103A), about 1.5 m below the topographic top (103B) and at the topographic base (103C) (Orchard 1995). The sample from block C85314 consists of all the matrix encasing the ammonoid (Orchard 1995). Because the samples originate from metre-sized olistoliths, no specific within-block stratigraphic order or any real stratigraphic separation of the samples can be assumed (M. J. Orchard, pers. comm. 2010).

Material

The material (residue; Appendix A1.2) consists of elasmobranch teeth, dermal denticles and fin spines. The samples from which the material originates (Appendix A1.1) were mostly collected by E. T. Tozer on a reconaissance trip with T. Calon to both Jabel Safra and Wadi Alwa in 1984 for ammonoid study (samples with ‘84 TE’) (see Tozer and Calon 1990) and on later fieldtrips in 1991 and 1992 (samples with ‘91 OF’ and ‘92 OF’, respectively). Block C85314 was collected by C. W. Lee and T. Calon

on the same trip in 1984. The samples were later donated to, and processed by, M. J. Orchard for conodont study (published in part in Orchard 1994, 1995). No stratigraphic logs were presented by Tozer and Calon (1990) due to the nature of the trip and the limited nature of the exposures, but accurate descriptions of the blocks and their lithology was nevertheless provided. For correlative purposes, a simple composite log has been reconstructed here using ammonoid and conodont biostratigraphic data from Tozer and Calon (1990), Orchard (1995) and M. J. Orchard (pers. comm. 2009–2010), on which the stratigraphic position of the samples, including those from Wadi Alwa, is indicated (Figure 3.22). Sample mass is estimated to have been a maximum of 500 g each, but the samples have proven to be very fossiliferous and a total of 274 ichthyoliths have been recovered, of which 188 teeth and spine fragments have been identified. All specimens are deposited in the Organic Materials Collections, Earth Sciences Sector of the Geological Survey of Canada (GSC135614–GSC135889; Appendix A1.2).

Results

The recovered fauna contains a small number of pre-existing taxa, but is mainly composed of new hybodont and neoselachian taxa. Based on the major component of dental remains, they are identified as *Omanoselache* sp. H, an indeterminate euselachian, Genus S sp. T, Genus S sp. A and Genus P sp. P. Spine fragments are identified as: cf. *Amelacanthus* sp. Twelve dermal denticle morphotypes are recognised (Table 3.3).

3.2.4.2 WADI ALWA

Geological setting

Wadi Alwa is located about 50 km south of Muscat, in the Ba'id tectonic window (Figure 3.3). The Ba'id block itself is several kilometres in size and comprises a Permian–Cretaceous succession (Richoz 2006 and references therein). It contains

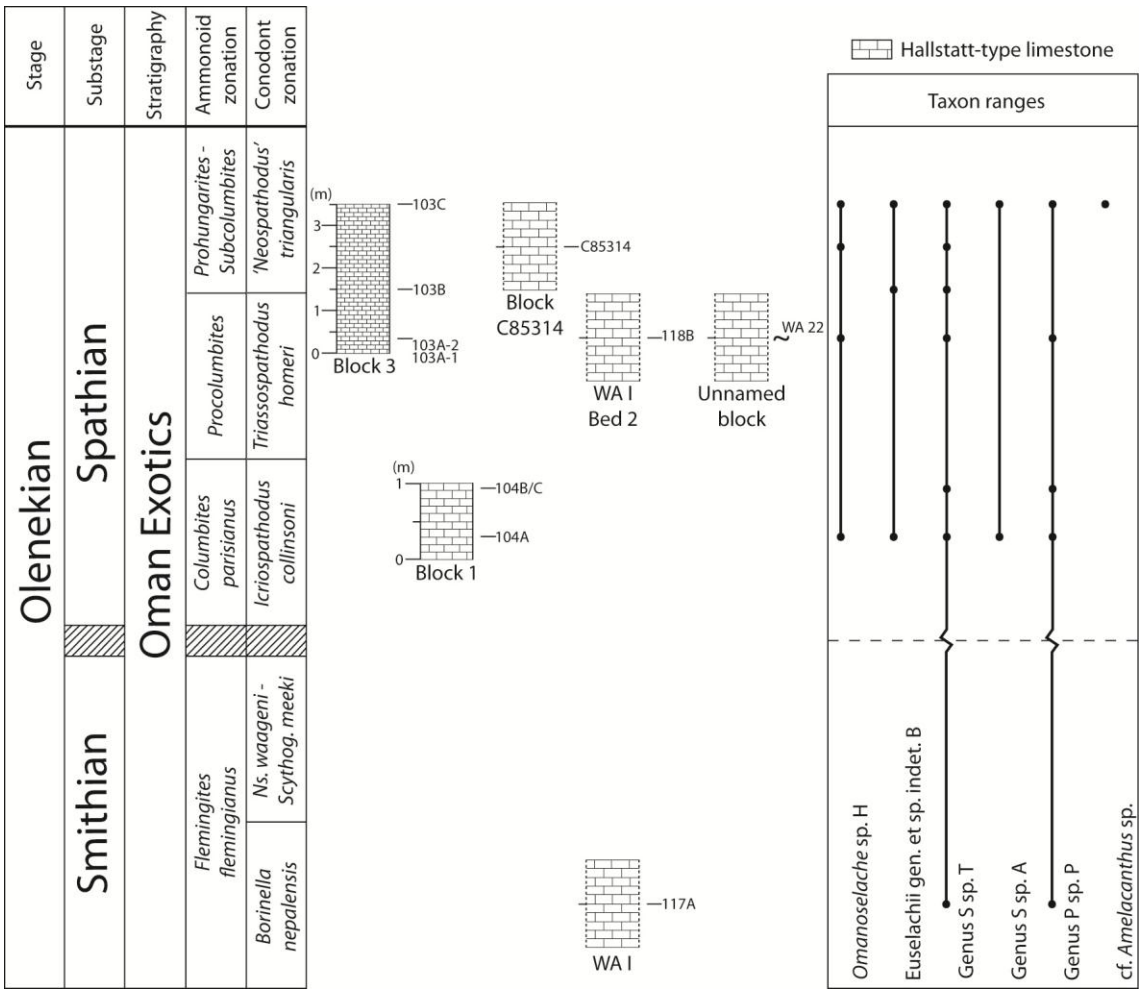

Figure 3.22 – Ranges of recovered taxa and (bio)stratigraphical correlation of sampled limestone blocks/beds in Jabel Safra and Wadi Alwa, based on data from Orchard (1995); Tozer and Calon (1990); and M. J. Orchard (pers. comm. 2010). North American ammonoid zonation based on Kozur (2003) and Tethyan conodont zonation modified from Kozur (2003), based on recommendations by M. J. Orchard (pers. comm. 2010). Zones plotted as equal duration due to absence of data in source publication. Partial omissions in the columns and taxon ranges (hashed fields and zig-zag lines, respectively) are due to a lack of data points during that interval. Dashed lines in the lithology indicate unknown bed thickness. The height of sample WA 22 is approximate, based on a similar conodont content to sample 103A.

blocks of decimetres to several metres (up to about 100 m) in size, which were recorded at this locality by Tozer and Calon (1990). They described the presence of grey Permian limestone but also blocks from the Triassic (Smithian and Spathian, Anisian, and Norian). The Lower and Middle Triassic are represented by the commonly red Hallstatt-type limestone facies and the Upper Triassic by an Ammonitico Rosso-like limestone, both of which are characteristic of the Tethyan realm (Tozer and Calon

Table 3.3 – Classification and interpretation of denticles per morphotype. Refer to Appendix A3.2 for detailed discussion and images of all morphotypes.

Morphotype	Pedicle type	Interpretation
10	Fluted truncate	Hybodont / synechodontiform? (pectoral fin)
11	Fluted truncate	Hybodont / synechodontiform? (dorsal caudal fin margin)
12	Fluted truncate	Hybodont
13	Fluted truncate	Hybodont
14	Fluted truncate	Hybodont?
15	Fluted truncate	Hybodont?
16	Plain truncate	?
17	Plain truncate	?
18	Plain truncate	?
19	Simple tetrahedroid	Synechodontiform
20	Expanded, stretched, keeled tetrahedroid	Synechodontiform
21	Simple tetrahedroid	Synechodontiform

1990). The lithology of the largest block, referred to as Wadi Alwa I, is identical to that of the olistoliths of Jabel Safra (Tozer and Calon 1990). However, the fauna at Wadi Alwa is less well-preserved and the conodonts have much higher CAI values than those from Jabel Safra (M. J. Orchard, pers. comm. 2010). Glennie (2005) places the blocks in the Kawr Group, but Pillevuit *et al.* (1997) named an entirely separate group to accommodate the assemblage (Al Buda'ah Group). The latter is followed in Richoz (2006). The age determinations of Tozer and Calon (1990) and Orchard (1995) indicate that all samples are from the Smithian and Spathian and are, therefore, correlative to the lower member of the Alwa Formation (Dienerian–Lower Carnian; Richoz 2006). The member is representative of pelagic limestones deposited on a distal, drowned platform (Woods and Baud 2008). Wadi Alwa I is shown as section WB in Pillevuit *et al.* (1997, fig. 8), which is very near section 6 of Richoz (2006) located at N 23°10'49" E 58°23'71". In the vicinity and to the south of Wadi Alwa I is section 4 of Pillevuit *et al.* (1997) and Richoz (2006). It contains older sediments of the Alwa Formation and was previously measured in detail at N 23°10'03" E 58°23'35" (Richoz 2006; Woods and Baud 2008). It is measured again here (Figure 3.23) and the P/Tr boundary, marking the transition from the Ba'id Formation to the lower member of the Alwa Formation, is

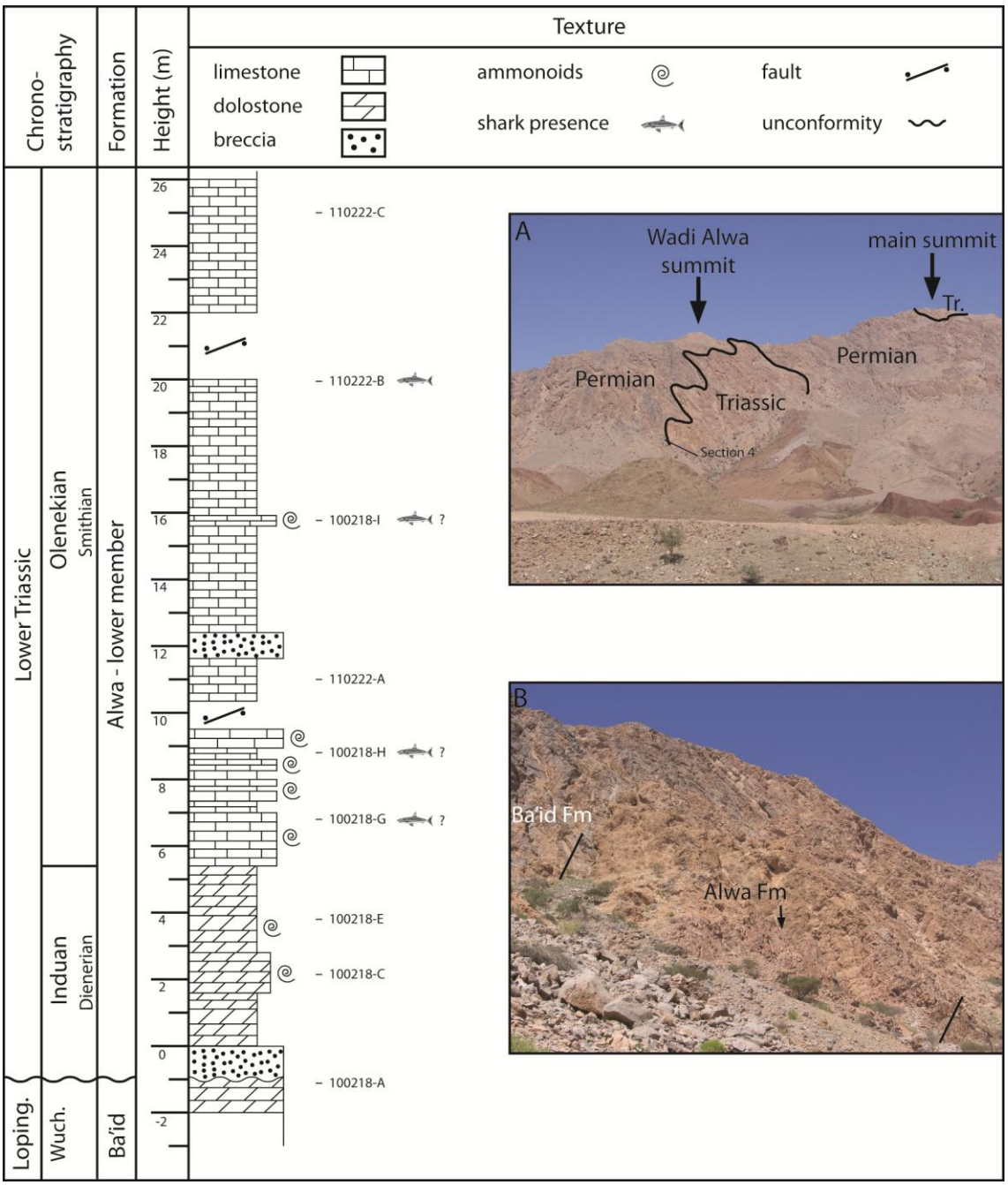

Figure 3.23 – Stratigraphic log of section 4 at Wadi Alwa. Sampled beds are indicated. A, The Ba'id Block with Wadi Alwa in the foreground, as viewed towards the north-northwest, showing the sampled section. The main summit is 1351 m above sea level (Pillevuit *et al.* 1997). B, The sampled section, viewed towards the north, the extent of which (28 m) is indicated by the parallel lines and the bedding plane is indicated by the arrow.

located at N 23°10'06" E 58°23'31". It shows a significant hiatus, which makes that Wadi Alwa is not a complete boundary section.

Material

The samples utilised (residue; Appendix A1.1) are of the Hallstatt-type limestone facies and derive from the Triassic block Wadi Alwa I, which has a maximum dimension of 100 m and shows a stratigraphic thickness of 25 m (Tozer and Calon 1990), and a second block from an unknown location at Wadi Alwa (Figure 3.22). Further samples (bulk, cumulative mass 16 kg; Appendix A1.1) were taken from section 4 (Figure 3.23) and other local deposits. The samples from Wadi Alwa I are 117A from unknown height and 118B from the middle of three ammonoid beds (Bed 2) in a small 25 m bluff near the southern extremity of the block (Tozer and Calon 1990). Sample WA 22 is from the remaining block. From section 4, nine samples were collected from Wuchiapingian (Woods and Baud 2008), Dienerian(?) and Smithian deposits. An additional sample was taken from an outcrop to the (south)east of section 4, which belongs to the Triassic(?) Matbat Formation, consisting of calcareous and siliciclastic turbidites, and two further samples were obtained *ex situ* in the wadi at the foot of the mountain.

Results

One chondrichthyan tooth (sample 100222-B), 14 recrystallised chondrichthyan teeth(?) and two dermal denticles? were obtained from Smithian deposits (Figure 3.23; Appendix A1.5). The tooth has been identified as cf. Genus S. The remaining specimens are reminiscent of multicuspid teeth and highly cusped denticles, but fragmentary and substantially recrystallised, and therefore indeterminate.

3.3 IRAN

3.3.1 GEOLOGICAL SETTING

Iran contains deposits that originated from Palaeotethys and Neotethys, because it formed part of the Cimmerian Blocks during the Permian and Triassic (Figure 3.5; and compare Figure 3.1). The pre-Upper Triassic part of the Neotethyan deposits in Iran is

equivalent to the Hamrat Duru Group of Oman (Figure 3.2), because this sequence formed immediately northeast of the Hawasina basin (in the “Crush Zone Basin” of Glennie 2005). The deposits consist of basaltic lavas and exotic limestone (see Section 3.2.1 for discussion of exotics) exposed in the Sirjan-Sanandaj Province and Central Iran Province (e.g., Transcaucasian region) of Iran (Glennie 2005).

3.3.2 MATERIAL

Four samples (residue; Appendix A1.1) were collected from Lopingian deposits in Iran by an unknown collector. One sample originated from the Changhsingian *Paratirolites* Beds of the Ali Bashi Formation, which also contain *Neogondolella* and *Hindeodus*, at Kuh-e-Ali Bashi, near Dzjulfa in the Transcaucasian region, northwestern Iran (Orchard *et al.* 1994). A sedimentary log of a comparable section at Zal, also located near Dzjulfa in the Transcaucasian region, shown in Richoz (2006, fig. 6.4) and known to be rich in fish remains (H.W. Kozur, pers. comm. 2012), depicts the *Paratirolites* Beds as grey nodular limestone with marly interbeds, occurring at the very end of the Changhsingian. This stage is believed to be completely represented here (L. Krystyn in Richoz, 1006), suggesting a latest Changhsingian age for the sampled deposit. The remaining three samples likely also originated from the Ali Bashi Formation at this locality, but no further information is available on the stratigraphic height from which they were obtained. It is suggested that sample KZK 10 is of late Wuchiapingian(?) age, KZK 34G of late Changhsingian age, and KZM 21 of late Wuchiapiangian age (L. Krystyn, pers. comm. 2012). All samples yielded chondrichthyan remains, but unfortunately, the specimen recovered from Kuh-e-Ali Bashi was lost and is not considered in this study other than as an indicator of shark presence.

3.3.3 RESULTS

From the Iranian samples, eight chondrichthyan specimens were recovered. Among these were three identifiable teeth originating from upper Wuchiapingian(?) deposits,

which are assigned to Genus S sp. T. The remaining specimens included a dermal denticle, three indeterminable synechodontiform teeth, and the unidentified lost tooth. Other specimens include nine indeterminable remains, eight of which are likely of chondrichthyan affinity, and an actinopterygian tooth. This provides evidence of identifiable synechodontiform presence in the late Wuchiapingian and of as yet not further unidentified shark presence in the late Changhsingian.

3.4 India

Lower and Middle Triassic marine strata from the Tethyan realm are exposed at a number of localities near Spiti, India. Exposures comprise bioclastic limestones and mudstones of the Tamba Kurkur Formation, ranging in age from the Induan (Griesbachian) to the Anisian, overlain by the shales and marly limestone of the Ladinian Hanse Formation (Atudorei 1998). The basal Griesbachian *Otoceras* beds consist of pyrite-rich limestone with phosphatic and iron-oxide nodules (Bucher *et al.* 1997). Their age has been determined based on ammonoids and conodonts (e.g., Orchard and Krystyn 1998). One sample (residue; Appendix A1.1) was collected by L. Krystyn (University of Vienna) from the lowermost bed (GU-1) of the *Otoceras* beds at Guling, Spiti (Orchard and Krystyn 1998, fig.2). This yielded one incomplete chondrichthyan tooth, which has been identified as *Omanoselache* sp. A.

3.5 Timor

One sample (residue; Appendix A1.1) was collected from Triassic deposits in Timor by W. Weitschat (University of Hamburg). No confirmed stratigraphic information is available for this sample, but it is believed that it may have come from a condensed/mixed Hallstatt-type limestone block of Anisian–Norian age or even outside this age bracket (M.J. Orchard, pers. comm. 2012). Three fragments of chondrichthyan teeth were recovered from this sample, one of which is identified as Genus S sp. A.

There is good reason to believe that the sample derives from the same locality from which Yamagishi (2006) described chondrichthyan teeth, extracted from samples also obtained by W. Weitschat in the River Bihati region, near Bouwn in Timor. These were recovered from Tethyan red, pelagic Hallstatt-type limestone of Smithian–Spathian age from an exotic block in an accretionary complex belt. The described taxa include *Polyacrodus* sp. 1, *Polyacrodus* sp. 2, and *'Synechodus'* sp. 1 (Yamagishi 2006). The Timor specimen of *Polyacrodus* sp. 2 displays all the characteristics of a posterior tooth of *Omanoselache* sp. H and is therefore reassigned to this taxon, which may further involve reassignment of the Anisian specimen from Bukit Kalong, Kedah, Malaysia that was also assigned to *Polyacrodus* sp. 2 (Yamagishi 2006). The morphology of the *'Synechodus'* sp. 1 specimens described and figured by Yamagishi (2006) is identical to Genus S sp. A and is therefore re-assigned to this taxon. This excludes the specimen figured in plate 9 E–F of Yamagishi (2006), which is instead re-assigned to *Omanoselache* sp. H as a lateral tooth.

3.6 DISCUSSION

3.6.1 SYSTEMATIC CONSIDERATIONS

3.6.1.1 HYBODONTIFORMES

Based on jaws, braincase and postcranial skeletal features, the split between the Hybodontiformes and Neoselachii has been placed tentatively in the Late Devonian (Coates and Gess 2007; Figure 3.24). In turn, the youngest base of the stratigraphic range of the Hybodontiformes as a monophyletic order has been established as Viséan (Mississippian) in age, based on *Onychoselache* Dick, 1978 (Coates and Gess 2007), and the earliest node-date of the Hybodontoidea is Kasimovian–Gzhelian (Pennsylvanian) in age, based on *Hamiltonichthys* Maisey, 1989 (Maisey 1989). The next series of branching events spans the Permian/Triassic boundary (although this may be an artefact of fossil record incompleteness; Coates and Gess 2007), which

means that the hybodont genera described from the Guadalupian in this study are well-positioned within the Hybodontiformes. They are based solely on isolated teeth, but Coates and Gess (2007) suggested that these may be used as a bona fide ichthyolithic signal of hybodontiform distribution. Because of the less porous vascularisation system and the primitive (unresorbed; see Underwood and Cumbaa 2010) attachment of the base to the crown, which causes the base to be recovered with the crown in virtually every instant and is in contrast to the basal features observed in Mesozoic crown group hybodontoids, it is considered that the Guadalupian hybodonts from Oman should be attributed to the stem Hybodontiformes (i.e., Hybodontiformes excluding the Hybodontoidea). *Omanoselache* is a prime example of this hypothesis, because it carries the same basal characteristic forward into its Olenekian representatives from Oman. Furthermore, the tooth bases are also still present in isolated teeth of *'Polyacrodus' contrarius* (Johns *et al.* 1997) and *'P.' bucheri* (Cuny *et al.* 2001), strengthening the affinity between these taxa and *Omanoselache*. Although it is not believed that *Omanoselache* belongs to the Homalodontidae (based on the absence of

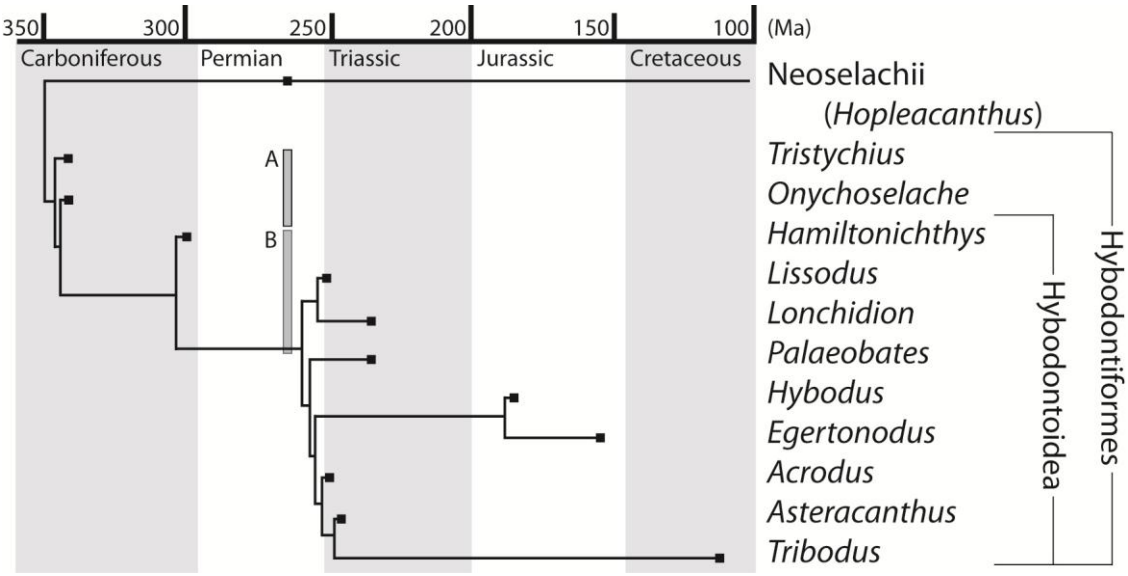

Figure 3.24 – Phylogeny plotted against geological timescale showing youngest dates for divergences in the hybodontiform evolutionary radiation (black squares mark earliest occurrence of taxon; *Hybodus* requires correcting based on its Lower–Upper Triassic and potentially Permian record). Redrawn from Coates and Gess (2007; see references therein). Shaded boxes suggest positions of the Wordian hybodonts from Oman in the phylogeny: in the Hybodontiformes either exclusive (A) or inclusive (B) of the Hybodontoidea. Position A is considered appropriate as a result of basal characteristics.

monocuspid mesial teeth), the taxonomic position of which is also unclear (Mutter *et al.* 2007a), there may be a close relationship between the groups.

3.6.1.2 SYNECHODONTIFORMES

The material described here as Genus S displays a characteristically synechodontiform tooth morphology and has been demonstrated to be very close to *Synechodus* in outward appearance. However, it is placed as a sister genus to *Synechodus* to accommodate primarily the primitive microstructure and the strong basal arching. *Synechodus* originated in the early Permian (Ivanov 2005) and ranges into the Paleocene (Duffin and Ward 1993). Guinot and Cappetta (2011) noted differing enameloid microstructures among species of *Synechodus* and interpreted the strong variability as typical for a genus with a long stratigraphic range and expected many more novel enameloid features to be discovered among the large number of species (20) assigned to the genus. However, Klug (2010) believes that several Permian to Triassic forms have been placed in *Synechodus* whilst their affinities are actually unclear. In addition, tooth crown morphology is considered to be a problematic character, because feeding adaptations have caused similar tooth morphologies to convergently develop in different neoselachian lineages (see references in Klug 2010), which led her to unofficially erect 'pre-Jurassic *Synechodus*'. Andreev and Cuny (2012) subsequently discussed the pre-Jurassic evolution of neoselachians in detail, demonstrating that the oldest record of well-defined TLE (see Section 1.5.3 for discussion of microstructural terminology) is currently known from the late Carnian (*'Synechodus' multinodosus* Johns, Barnes and Orchard, 1997) and questioning the assignment of certain species to *Synechodus* (or even to the Synechodontiformes) based on their primitive microstructural state (*'S.' incrementum* Johns, Barnes and Orchard, 1997 and *'S.' rhaeticus* Duffin, 1982; see Cuny and Risnes 2005). They highlighted the dominance of enameloid microstructures consisting mainly of SCE and of poorly structured PBE during the Early and Middle Triassic, with increased structure

and complexity appearing during the Middle–Late Triassic (Andreev and Cuny 2012). The material described in this study is attributed to the first stage in TLE evolution that they propose, which involves “development of subparallel to parallel crystalline bundles, probably by modification of the SCE retained only as a thin superficial SLE layer” (Andreev and Cuny 2012, p. 264). Histological study of the oldest known synechodontiform, *‘Synechodus’ antiquus* Ivanov, 2005, which is yet to be carried out, could shed more light on the earliest stages of this proposed developmental framework.

In summary, because tooth crown morphology is problematic, whereas polyaulacorhize vascularisation is a synapomorphic character supporting the monophyly of the Synechodontiformes (Klug 2010), the latter is followed here as the unifying characteristic of the order. Furthermore, in agreement with the synthesis of Andreev and Cuny (2012), enameloid microstructure is expected to be a powerful tool in resolving the internal systematic organisation of the Synechodontiformes.

3.6.2 PERMIAN

3.6.2.1 KHUFF FAUNA

Compositional correlations

Isolated hybodont teeth occur abundantly in Upper Palaeozoic and Mesozoic rocks (Rees and Underwood 2002) and provide evidence that the hybodonts were one of the most successful chondrichthyan lineages (Rees 2008). The Wordian Khuff fauna, as well as a Cisuralian fauna from Texas described by Johnson (1981), show that hybodonts were a well-established element of marine faunas throughout the Permian and abundant in certain areas. A potential clue to their success is that the variety of tooth shapes found in hybodont families (Rees 2008) indicates the utilisation of a number of different food sources. Most revisions to the Hybodontiformes have, until now, focused on the Mesozoic (e.g., *Hybodus*, *Polyacrodus*) and new genera have been erected to reflect current taxonomic views. The Palaeozoic material is in need of a similar review.

The composition of the Khuff fauna is comparable to the hybodont-dominated Guadalupian–Lopingian shark assemblages of the Ural Mountains, reviewed by Ivanov (2005), and also strengthens his proposal of a late Palaeozoic (Cisuralian) origin for synechodontiform sharks. Upper Carboniferous–Guadalupian deposits in the Ural Mountains and other localitions in northern Russia have yielded a number of groups that are also (tentatively) represented in the Khuff fauna. These include the Symmoriiformes, with e.g., *Stethacanthus* from the Asselian, (Ivanov 1999) and from the Wordian–Capitanian (Minikh 1999; referred by Ivanov, pers. comm. 2012); the Ctenacanthiformes, with *Heslerodus* from the Gzhelian–Asselian boundary (Ivanov 1999) and *Glikmanius* from the Artinskian (Kozlov 2000) and from the Wordian–Capitanian (Minikh and Minikh 1996, Malysheva *et al.* 2000; all referred to *Glikmanius* by Ivanov 2000 and Ginter *et al.* 2005); the Anachronistidae, with *Cooleyella* from the Sakmarian–Artinskian and Roadian (Ivanov 2000, 2011); and rare Petalodontiformes such as *Permopetalodus* from the Artinskian (Kozlov 2000). Compositional similarities also exist with other Guadalupian chondrichthyan faunas. One is the fauna from the Akasaka Formation at Akasaka, Japan, which contains *Glikmanius occidentalis*, indeterminate cladodont teeth and '*Lissodus*' sp. (Yamagishi and Fujimoto 2011), and another is the fauna from the Pustula Member, Middle Phosphoria Formation, Wyoming, USA, which contains *Glikmanius occidentalis* and other ctenacanthiforms, *Arctacanthus* and euchondrocephalians (eugeneodontiforms and a petalodontiform; Branson 1933). Ivanov *et al.* (2007, 2011) mentioned the presence of Guadalupian phoebodontiforms, symmoriiforms, and *Cooleyella* Gunnell, 1933, as well as ctenacanth, hybodont and neoselachian dermal denticles, in the Guadalupe and Apache Mountains of western Texas. Xenacanthids are common in assemblages of western Europe and North America (Ivanov 2005), such as the very rich upper Pennsylvanian fauna from Nebraska, USA studied by Ossian (1974), which contains *Glikmanius myachkovensis* Lebedev, 2001 (see Ginter *et al.* 2005) and other ctenacanths, xenacanths, protacrodonts, hybodonts, as well as euchondrocephalans such as orodontiforms, eugeneodontiforms, petalodontiforms, and holocephalans such

as *Deltodus* Morris and Roberts, 1862. It therefore also has many elements in common with the Wordian fauna from Oman, but the Khuff fauna lacks xenacanthids, although their presence has been recorded from the underlying Cisuralian (Artinskian) Gharif Formation in the same location in Oman (Schultze *et al.* 2008). From Wuchiapingian deposits, exposed in the Abadeh-Shahreza belt in southwestern Iran, a fragmentary petalodontiform tooth (Golshani and Janvier 1974) assigned to *Megactenopetalus* (Ossian 1976; Hansen 1978) and a polyacrodontid(?) tooth similar to *'Polyacrodus' lapalomensis* Johnson, 1981 (Hampe *et al.* 2011) have been reported, drawing general parallels with the Khuff fauna. The Iranian deposits derive from the northern (outer) shelf of Neotethys and therefore stem from the same palaeogeographic area as the Khuff Formation.

Stratigraphic and palaeogeographic implications

Although the presence of Permian sharks in Oman was mentioned previously in the literature (Tintori 1998; Angiolini *et al.* 2003*a*; Schultze *et al.* 2008), this study represents the first detailed faunal description, and the occurrence of this fauna in the Wordian Khuff Formation requires adjustments to the stratigraphic ranges and geographical distributions of the previously described taxa that have been recognised (Table 3.4). The suggested adjustments to 'Palaeozoic Genus 1' of Rees and Underwood (2002) should remain provisional until the teeth described in this study are definitively assigned to the aforementioned genus. Palaeogeographically, this study represents the first record from the western fringe of Neotethys for all taxa. *Cooleyella* is the only genus with a previous record from the southern hemisphere (Gondwanan) part of Pangaea, i.e. from Brazil (see Figure 3.1), a location that has also yielded Carboniferous and Cisuralian (Artinskian) *Sphenacanthus* fin spines (e.g., Chahud *et al.* 2010), and its occurrence in Oman shows that *Cooleyella* was present in almost all major provinces and approached global distribution.

Stratigraphically, this study represents the first record from the Wordian for all taxa, although *Glikmanius* was already known from this age by means of *G. occidentalis*. All

but one of the previously described taxa are restricted to the Palaeozoic and, except for *Cooleyella*, their occurrence in the Wordian Khuff fauna represents their youngest record (Table 3.4; Figure 3.25). Only *Nemacanthus* was previously restricted to the Mesozoic and its identification here requires a downward range extension leading to its oldest occurrence and the only record from the Palaeozoic so far.

The Permian fossil record and extinction of sharks

The unusually large number of new taxa in the Khuff fauna may be explained by the small size of the remains and the fact that Permian fossil sharks of this region have not been studied before. That a newly sampled location should yield numerous new taxa is a reflection of the general patchiness of the fossil record and, moreover, an excellent indication that both the region and stratigraphic interval in question are undersampled (cf. Tarver *et al*. 2007). This is corroborated by phylogenetic analyses, which hint that a significant part of early hybodont evolution is unknown, because a series of closely

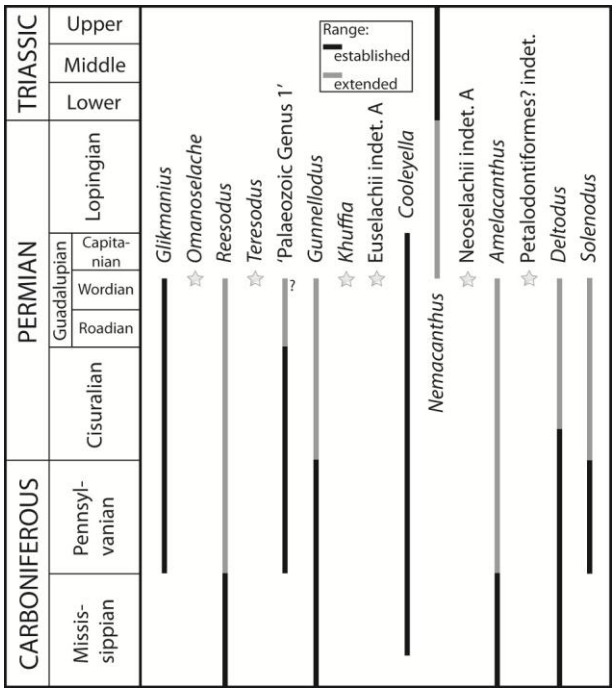

Figure 3.25 – Stratigraphic ranges of all genera recovered in the upper Wordian Khuff fauna. Established ranges based on data in Table 3.4 and range extentions based on data listed under Haushi-Huqf area in Table 3.5. The star symbol represents new records.

Table 3.4 – Global records of pre-existing taxa recognised in the Khuff fauna.

Taxon	Age	Location	Remains	References
Glikmanius	Pennsylvanian –Wordian (Guad.)	USA, Russia, Ukraine, Japan?	Teeth	Ginter *et al.* 2005, 2010; Lebedev 2001
G. myachkovensis	Pennsylvanian	USA, Russia, Ukraine	Teeth	Ginter *et al.* 2005, 2010
Reesodus	Mississippian	England, Russia	Teeth	Rees and Underwood 2002 (as 'Palaeozoic Genus 2')
'Palaeozoic Genus 1'	Pennsylvanian –Cisuralian	Spain, Germany, USA	Teeth	Rees and Underwood 2002
Gunnellodus	Mississippian–Pennsylvanian	USA, Russia?	'Teeth'	Hoffman and Hageman 2011
Cooleyella	Viséan (Miss.) –Capitanian (Guad.)	England, Belgium, Brazil, USA, Russia	Teeth	Ivanov 2011
C. fordi	Viséan (Miss.) –Artinskian (Cis.)	England, Belgium, Russia	Teeth	Ivanov 2011
Nemacanthus	Lower Triassic –Rhaetian (Upp. Triassic)	England, Greenland, Spitsbergen, USA	Fin spines	Cappetta 1987
Amelacanthus	Wordian	Russia	Fin spine(s)	Chabakov 1927 (doubtful; see Appendix A2.1)
	Mississippian	Britain	Fin spines	Maisey 1982a
Deltodus	Tournaisian (Miss.)–Cisuralian	Britain, Belgium, France, Russia, the USA and Thailand?	Teeth	Stahl 1999
Solenodus	Pennsylvanian	Russia	Teeth	Stahl 1999

spaced branching events span the Permian/Triassic boundary (Coates and Gess 2007). It further correlates with a similar gap in the availability of sedimentary formations in the late Palaeozoic, at least in North America (Peters 2006). These observations support the hypothesis of Twitchett (2001) that a relatively poor chondrichthyan fossil record in the Guadalupian and Lopingian is masking the true diversity of shark faunas at that time, leading to inaccurate views on extinction patterns among sharks. Indeed, there are relatively few published studies of Guadalupian and Lopingian chondrichthyan faunas. The Paleobiology Database [accessed December 2011], for example, records 57 Cisuralian collections, but only 21 Guadalupian collections and 27 Lopingian collections. The average richness of these Permian localities is only 1–2 genera, with a

maximum of five genera recorded in the most diverse Cisuralian collection (Ivanov 2005), eight in the Guadalupian (Branson 1933) and four in the Lopingian (Wang *et al.* 2007). With a total of 15 genera recognised, the Khuff fauna is not only the most diverse Guadalupian chondrichthyan fauna recorded to date, it is also the most diverse fauna known from the entire Permian.

The Khuff fauna significantly enhances the Guadalupian fossil record of chondrichthyans and also changes our understanding of their diversity prior to the extinction events of the late Guadalupian and late Changhsingian. The upward range extensions of six chondrichthyan genera into the upper Wordian demonstrates that extinction of these Palaeozoic taxa was not a gradual process spanning ca. 50 million years from the end of the Mississippian to the end of the Cisuralian, but must have been much more abrupt. The upward range extensions also imply more gaps in the Pennsylvanian, Cisuralian and lower Guadalupian fossil record of sharks than has hitherto been appreciated.

Whether the ultimate extinction of most of the taxa in the Khuff fauna can be tied directly to either of the major biotic crises of the Permian remains to be determined, and requires further improvements in our understanding of Guadalupian and Lopingian shark faunas worldwide. The occurrence of *Nemacanthus* in the Khuff fauna, however, demonstrates for the first time that this genus survived both major extinction events of the Permian. The same is true for *Omanoselache* and potentially also *Amelacanthus*, as has become clear from Lower Triassic material from Oman and other regional localities (see Section 3.6.2).

3.6.2.2 LOCAL AND REGIONAL OCCURRENCES

The fauna recovered from the Wordian deposits on the Saiq Plateau is not of the same abundance and diversity as the fauna described from the Khuff Formation (Section 3.2.2.1), but the taxa that were recovered (*Glikmanius* and *Omanoselache*) confirm the general composition of the Wordian palaeocommunity on the Arabian Platform and widen its geographical range. Both localities indicate its established

presence on the inner platform. The recovery of *Stethacanthulus* at the Qarari block (Guadalupian–Lopingian; Section 3.2.2.2) and the “Bridge” on the Batain Plain (Wuchiapingian; Section 3.2.2.3), as well as at Wadi Maqam in the Sumeini area (Wordian; Section 3.2.3.7), expands the environmental range of the cladodontomorphi from its established presence on the inner platform to include more pelagic environments, although there may have been some input of outer shelf debris in the Wadi Maqam deposit. The absence of hybodonts from these more distal deposits may indicate a habitat preference, but the limited amount of material available provides insufficient evidence.

Based on the specimens from the “Bridge”, the known chronological range of *Stethacanthulus*, which previously reached up into the Sakmarian (Ginter *et al.* 2010), is extended into the Wuchiapingian. This occurrence represents its youngest record and the only confirmed record from the Lopingian. It also indicates that *Stethacanthulus* survived the end-Guadalupian extinction event.

The small number of specimens of Genus S from the Lopingian (late Wuchiapingian?) of Iran represent the oldest occurrence of a genus that is better known from the Olenekian of Oman and Timor (see Section 3.6.2), indicating that the genus originated in the Palaeozoic and therefore survived the late Permian mass extinction.

3.6.3 TRIASSIC

3.6.3.1 OMAN FAUNA

Taphonomy and palaeoecology of the Lower Triassic fauna

The Lower Triassic shark fauna from the Sultanate of Oman described in this study comprises five genera and six species. The material originated from three different localities and was recovered from Induan–Olenekian deposits. Wadi Wasit and Wadi Alwa yielded Griesbachian and Smithian–Spathian material, respectively. The majority of the material, however, was obtained from Jabel Safra and is Spathian in age.

Regardless of any differences in age, the composition of the recovered faunas at each locality is very similar. Fewer taxa were recognised from Wadi Alwa and Wadi Wasit, because of a lower quality of fossil preservation and the limited amount of material available, respectively. The average size of the samples was 500 g or less, which does not generally consitute a large enough sample size for accurate assessment of the vertebrate microfossil content of a deposit. The number of samples was also limited, with seven from Jabel Safra, 13 from Wadi Alwa, and seven from Wadi Wasit. The analysis performed by Jamniczky *et al.* (2008) suggests that this does not constitute exhaustive sampling; this is also suggested by the lower average richness recorded for all samples compared to the maximum number of genera recorded from a single sample. In Jabel Safra, the average generic richness is three, whereas the maximum number of genera is five. In Wadi Alwa, the average richness is 1.5 compared to a maximum of 2 genera. In Wadi Wasit, both the average and maximum are limited to one. For the entire Lower Triassic fauna from Oman, the average generic richness is two.

The size of the recovered teeth generally does not exceed 2 mm in mesio-distal dimension, which is very small. This may suggest a small body size, assuming that a relationship with tooth size exists (see Fischer 2008). Twitchett (2007) noted that depressed body size is commonly observed in marine invertebrate animals for the duration of the Early Triassic, although is most dramatic during the earliest Induan. Some evidence for reduced body size in chondrichthyans during the Induan exists, such as the distinct size increase recorded in *Listracanthus* across the Induan/Olenekian boundary in western Canada (Mutter and Neuman 2009). Birkenmajer and Jerzmańska (1979) also noted a much smaller size in Induan (lower? Dienerian) specimens compared to the Olenekian (Spathian), even within the same species (e.g., *Acrodus spitzbergensis*), based on material from Spitsbergen and following on Stensiö (1921). Very few teeth are available from the Induan of Oman (Griesbachian of Wadi Wasit) and many are fragmented, which is why no such trends can be identified here. Limited data, based on posterior teeth of *Omanoselache*, further

show that the general dimensions are very similar in the Griesbachian and Spathian: 1.16 mm versus 0.82–1.26 mm mesiodistally and 160–260 µm versus 150–190 µm labio-lingually, respectively.

The main chondrichthyan groups represented in this material are hybodonts and neoselachians. During the Olenekian, the Neoselachii are the dominant group overall with regard to relative abundance (89%, as opposed to 8% for the hybodonts; Figure 3.26A; see Appendix A1.2.3 for numeric data), as well as with regard to generic richness (three genera, as opposed to one hybodont genus; Figure 3.26B). The most primitive neoselachian order, the Synechodontiformes, constitutes the largest proportion of neoselachian taxa in the fauna. During the Induan, however, the Neoselachii appear subordinate to hybodonts with regard to relative abundance (17%, as opposed to 83% for the hybodonts; Figure 3.26C), and equal with regard to generic richness (one genus each; Figure 3.26D). It must be noted that the Induan data is

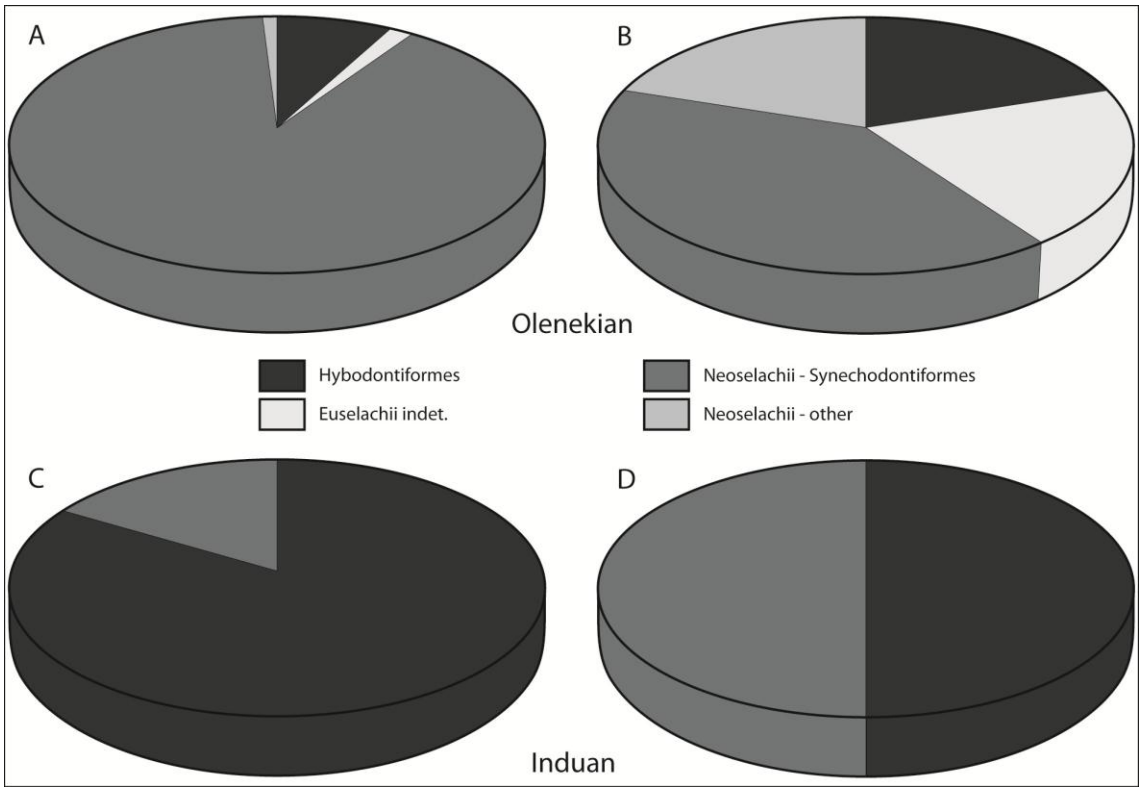

Figure 3.26 – Relative abundances of chondrichthyan groups from the Lower Triassic of Oman. A, C, Overall relative abundance of major groups using numbers of specimens. B, D, Overall relative abundance of major groups using numbers of genera.

based on two samples from the same locality, yielding a total of six specimens, and may therefore not accurately represent the fauna. If the Olenekian and Induan data are pooled together, the Neoselachii remain the dominant group during the Early Triassic. The Neoselachii experienced a dramatic radiation from the Upper Triassic onwards, which potentially spread from western Europe, whereas the more conservative Triassic shark communities were dominated by hybodonts (Cuny and Benton 1999). Indeed, Lower Triassic faunas worldwide are dominated by hybodont taxa such as *Acrodus*, *Homalodontus*, *Hybodus*, *Lissodus*, *Paleobates* and *'Polyacrodus'* (Broom 1909; Stensiö 1921; Teixeira 1956; Sahni and Chhabra 1976; Birkenmajer and Jerzmańska 1979; Thomson 1982; Bendix-Almgreen *et al.* 1988; Goto 1994; Kato *et al.* 1995; Goto *et al.* 1996, 2010; Minikh 2001; Wang *et al.* 2001, 2007; Dorka 2003; Bender and Hancox 2004; Błażejowski 2004; Yamagishi 2004, 2006, 2009; Mutter *et al.* 2007a; Romano and Brinkmann 2010) as well as eugeneodontiform taxa (Nielsen 1952; Obruchev 1965; Zhang 1976; Mutter and Neuman 2008). The Olenekian (Lower Triassic) Oman fauna is therefore unusual in the sense that neoselachians are the dominant taxon so early on in the Triassic (but see also Section 4.4). The only published records of Lower Triassic neoselachian dental remains to date are of a *'Synechodus'*? tooth from the Induan of Turkey (Thies 1982) and *'Synechodus'* teeth from the Olenekian of northern Siberia, Russia (Ivanov and Klets 2007), but the presence of PBE was also shown in *'Synechodus'* sp. 1 from the Spathian of Timor (Yamagishi 2006). This means that the fauna from Oman is the second record of neoselachian teeth from the Induan and is the most extensive record of neoselachians in the Lower Triassic.

The hybodonts and neoselachians described here are similar in gross morphology, which is in accordance with Andreev and Cuny's (2012) hypothesis on the timing of development of novel microstructural patterns. This morphological similarity makes it difficult to distinguish between the respective groups based on outward features alone and histological study of the enameloid layer was required to establish their precise affinities. This study, therefore, also significantly adds to our knowledge on the early

stages of neoselachian evolution. Furthermore, it raises the question whether Early Triassic hybodont teeth from other parts of the world are not indeed primitive neoselachians.

Palaeogeographic and stratigraphic implications.

Except for *Omanoselache* and potentially also *Amelacanthus*, which were previously recognised from the Wordian Khuff Formation (Section 3.2.2.1), as well as Genus S, recognised from the Wuchiapingian of Iran (Section 3.3), the recovery of the remaining genera from Lower Triassic deposits at Jabel Safra, Wadi Alwa, and Wadi Wasit signifies their first record from Oman. It is also their first occurrence in western Neotethys (the southeastern part of the Pangaean continental margin). Palaeogeographically, the closest record of another synechodontiform is from Turkey (Thies 1982; see Figure 3.1).

Genus S and Genus P either belong to the Palaeospinacidae or are closely related, and so their presence is not unexpected, because palaeospinacids may have originated in the early Permian (Ivanov 2005; see Klug 2010) and ranged into the Paleocene (Duffin and Ward 1993; Figure 3.27). The range extension for *Amelacanthus*, known from the lower Carboniferous (Maisey 1982a) and the Guadalupian (Section 3.2.2.1), must remain tentative based on the uncertain generic assignment. An upwards range extension is required for *Omanoselache* and Genus S and so they become the first taxa known from dental remains recovered from the Neotethyan Basin to have survived the late Permian mass extinction, in addition to *Nemacanthus*, a genus known from fin spines (Section 3.2.2.1).

The Triassic fossil record and the extinction and recovery of sharks.

The Paleobiology Database [accessed February 2013] records 33 Early Triassic chondrichthyan collections (Induan: 10; Olenekian: 20; Early Triassic: 3) with an average richness per locality of 2–3 genera and a maximum of six genera recorded in western Canada (Mutter and Neuman 2008a). The Early Triassic shark fauna from

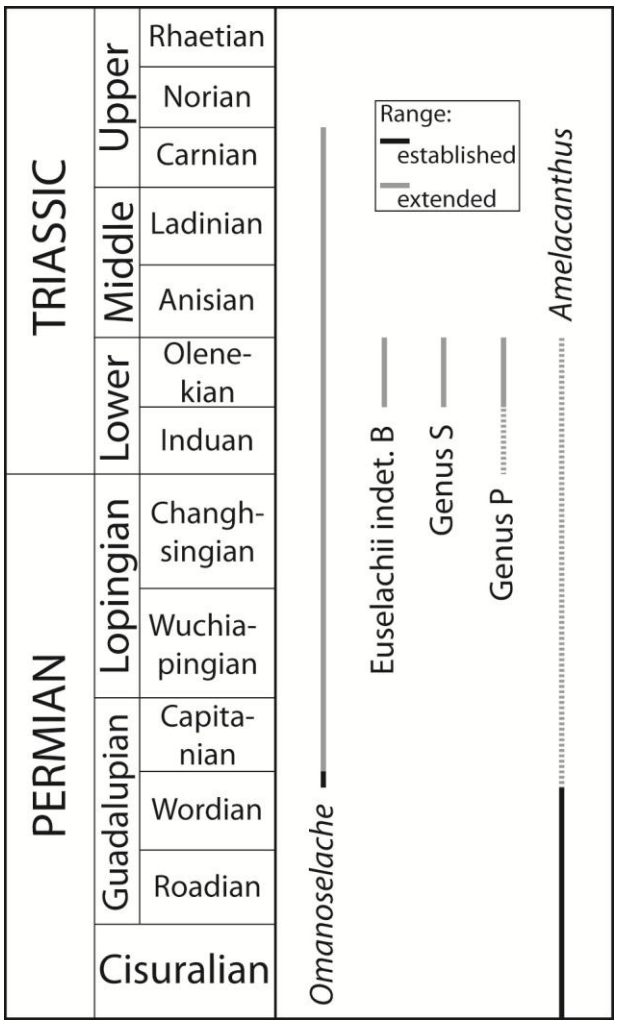

Figure 3.27 – Stratigraphic ranges of all genera recovered in Lower Triassic deposits of Oman. Established ranges based on data from Figure 3.25 and range extensions based on data in Table 3.5. Dashed lines indicate tentative range extensions.

Oman, comprising five genera and an average generic richness of two, therefore lies within the nominal range. Comparing the Early Triassic fauna further with the Permian fauna from Oman provides insight into possible extinction and recovery patterns that occurred during the latest Palaeozoic on the Arabian Platform.

First is the almost complete turnover of taxa that occurred as a result of either or both the end-Guadalupian crisis (*c*. 260 Ma; Isozaki *et al.* 2007) and the late Changhsingian extinction (252.6±0.2 Ma (U–Pb); Mundil *et al.* 2004). Cladodonts were still present after the end-Guadalupian event, but the only taxon present in both the Permian and Early Triassic Oman faunas is *Omanoselache*—although potentially also *Amelacanthus*—, which survived both events even if represented by a different species.

Genus S suvived the later event and *Nemacanthus* also survived both events, but, respectively, are presently not known to occur in the Permian of Oman or to re-occur in the Triassic of Oman.

Second is the apparent rate of re-establishment in the region. If it is assumed that the extinction of all taxa took place at the end-Changhsingian event (which can currently only reasonably be assumed for *Stethacanthulus*), a chondrichthyan community occurred within 0.4–0.9 Myr after the main extinction (Griesbachian; Table 1.1) and had re-established some diversity by 1.4–5.4 Myr after the main event (Olenekian; Table 1.1). If indeed the majority of taxa disappeared as a result of the end-Guadalupian crisis, it adds 8 Myr to the recovery time (end-Capitanian 260.4 Ma; International Commission on Stratigraphy, accessed August 2012). Regardless of the recovery time involved, the Early Triassic was still much less diverse (constituting about 30%) than the Wordian pre-extinction fauna, which consisted of 15 genera.

Last is the unexpected shift in dominance of hybodonts during the Permian to that of (primitive) neoselachians in the Early Triassic, well before the widely recognised radiation of the Neoselachii at the end of the Triassic (Cuny and Benton 1999). In direct comparison of the Wordian Khuff and Early Triassic faunas from Oman, facies differences may have some influence on this pattern, because the faunas respectively originate from shallow limestones deposited around (storm) wave base and pelagic limestones (see Table 3.5 and Figure 3.29). In a general sense, however, the palaeoenvironment that is applicable to the Lower Triassic of Oman and many of the hybodont-dominated faunas recorded from other areas globally (e.g., Stensiö 1921; Birkenmajer and Jerzmańska 1979; Bendix-Almgreen *et al.* 1988; Wang *et al.* 2001; Błażejowski 2004; Mutter *et al.* 2007a; Romano and Brinkmann 2010), is typical of a relatively shallow marine environment near the continental margin. More detailed facies analyses of localities globally are required to determine whether there are any underlying distribution trends.

3.6.3.2 REGIONAL OCCURRENCES AND WIDER IMPLICATIONS

The suspected occurrence of Genus P in the Griesbachian at Wadi Wasit, if validated, would represent the earliest recorded Triassic occurrence of a synechodontiform neoselachian, closely followed by the *'Synechodus'*(?) tooth from the Dienerian of Turkey (Thies 1982). Genus S is shown to be present throughout the Olenekian of Oman, but is also recognised from Triassic deposits of Timor (Spathian, *'Synechodus'* sp. 1 of Yamagishi 2006; and this study), expanding the palaeogeographic range of the genus. *Omanoselache*'s survival of the Late Permian extinction is confirmed and its palaeogeographical distribution is widened by new appearances in the Lower Triassic of India (this study) and Timor (Yamagishi 2006), even though it is represented by different species in the Mesozoic. Continued occurrence in later Triassic epochs and a possible palaeogeographic radiation pattern becomes apparent from the referral of a number of previously recorded occurrences to *Omanoselache*, ranging from the Lower Triassic of Russia (Yamagishi 2006, 2009) to the Middle–Late Triassic of China (Chen *et al.* 2007a), the USA (Cuny *et al.* 2001), and Canada (Johns *et al.* 1997). Overall, the genus is represented by seven species. Iran, Oman, India, and Timor were connected since the Guadalupian by a widening pelagic (open marine) seaway, formed by the Cimmerian microcontinents off the Pangaean margin and allowing unrestricted faunal exchange, which was shown by the occurrence of conspecific ammonoids (Blendinger *et al.* 1992, fig. 4; compare Figure 3.1 and Figure 3.5). One reason for the success of *Omanoselache* may be its wide environmental range, because it has been recovered from depositional environments spanning from the inner carbonate platform (Haushi-Huqf area) to the pelagic realm (Jabel Safra; Figure 3.29).

3.6.4 SYNTHESIS

An overview of the results from the described localities in this chapter, including all newly examined material as well as reassigned material, is shown in Table 3.5 and Figure 3.28, providing an overview of new and revised shark occurrences in Neotethys.

The majority of the material belongs to two comprehensive sets of material from the Haushi-Huqf area in central eastern Oman (MPUM collection and UC collection) and from Jabel Safra and Wadi Alwa in the Oman Mountains (GSC collection). They

Table 3.5 – Overview of all new or revised shark occurrences in Neotethys during the Permian and Triassic. Entries marked with an asterisk indicates a tentative re-assignment. Includes facies data for occurrences in Oman: ME = Madagascar Embayment; HB = Hamrat Duru (Hawasina) Basin.

Taxon	Age	Location	Facies
Stethacanthulus sp. cf. *S. decorus* (Ivanov, 1999)	Guadalupian–Lopingian	Oman, Batain Plain (Qarari)	ME – platform margin
	Wuchiapingian	Oman, Batain Plain ("Bridge")	ME – platform margin
	Wordian	Oman, Sumeini area	HB – slope
Glikmanius culmenis Koot, Cuny, Tintori and Twitchett, 2013	Wordian	Oman, Haushi-Huqf region	ME – rim basin
Glikmanius cf. *myachkovensis* Lebedev, 2001	Wordian	Oman, Haushi-Huqf region	ME – rim basin
	Wordian	Oman, Saiq Plateau	HB – rim basin
	Sakmarian	Oman, Haushi-Huqf region	ME – rim basin
Omanoselache contrarius (Johns, Barnes and Orchard, 1997)	Ladinian–Carnian	Canada, BC (Johns *et al.* 1997)	
	Anisian–Carnian	China, Guizhou province (Chen *et al.* 2007a)	
Omanoselache bucheri (Cuny, Rieppel and Sander, 2001)	Anisian	USA, Nevada (Cuny *et al.* 2001)	
Omanoselache sp. H	Anisian*	Malaysia, Kedah (Yamagishi 2006)	
	Olenekian (Spathian)	Oman, Jabel Safra	HB – basinal seamount
	Olenekian (Spathian)	Timor, Bouwn (Yamagishi 2006)	
	Griesbachian	Oman, Wadi Wasit (Yamagishi 2006)	HB – platform margin
Omanoselache sp. A	Olenekian (Smithian)	Russia, South Primorye (Yamagishi 2006, 2009)	
	Griesbachian	India, Spiti	
Omanoselache hendersoni	Wordian	Oman, Haushi-Huqf region	ME – rim basin
Omanoselache angiolinii	Wordian	Oman, Haushi-Huqf region	ME – rim basin
	Wordian	Oman, Saiq Plateau	HB – rim basin
cf. *Omanoselache* sp.	Wordian	Oman, Haushi-Huqf region	ME – rim basin
	Wordian	Oman, Saiq Plateau	HB – rim basin

Reesodus underwoodi	Wordian	Oman, Haushi-Huqf region	ME – rim basin
Teresodus amplexus	Wordian	Oman, Haushi-Huqf region	ME – rim basin
cf. 'Palaeozoic Genus 1' sp.	Wordian	Oman, Haushi-Huqf region	ME – rim basin
Gunnellodus bellistriatus (Gunnell, 1933)	Wordian	Oman, Haushi-Huqf region	ME – rim basin
Khuffia lenis	Wordian	Oman, Haushi-Huqf region	ME – rim basin
Khuffia prolixa	Wordian	Oman, Haushi-Huqf region	ME – rim basin
Euselachii gen. et sp. indet. A	Wordian	Oman, Haushi-Huqf region	ME – rim basin
Euselachii gen. et sp. indet. B	Olenekian (Spathian)	Oman, Jabel Safra	HB – basinal seamount
Cooleyella sp. cf. *C. fordi* (Duffin and Ward, 1983)	Wordian	Oman, Haushi-Huqf region	ME – rim basin
Genus S sp. T	Olenekian (Smithian–Spathian)	Oman, Jabel Safra & Wadi Alwa	HB – basinal seamount
	Lopingian (Wuchiapingian?)	Iran, Zal?	
Genus S sp. A	Olenekian (Spathian)	Oman, Jabel Safra	HB – basinal seamount
	Triassic	Timor	
	Olenekian (Spathian)	Timor, Bouwn (Yamagishi 2006)	
cf. Genus S sp.	Olenekian (Smithian)	Oman, Wadi Alwa	HB – basinal seamount
Nemacanthus sp.	Wordian	Oman, Haushi-Huqf region	ME – rim basin
Genus P sp. P	Olenekian (Smithian–Spathian)	Oman, Jabel Safra & Wadi Alwa	HB – basinal seamount
cf. Genus P sp. P	Griesbachian	Oman, Wadi Wasit	HB – platform margin
Neoselachii gen. et sp. indet. A	Wordian	Oman, Haushi-Huqf region	ME – rim basin
Amelacanthus sp. cf. *A. sulcatus* (Agassiz, 1837)	Wordian	Oman, Haushi-Huqf region	ME – rim basin
cf. *Amelacanthus* sp. Maisey, 1982a	Olenekian (Spathian)	Oman, Jabel Safra	HB – basinal seamount
Eugeneodontiformes? gen. et sp. indet.	Wordian	Oman, Haushi-Huqf region	ME – rim basin
Petalodontiformes? gen. et sp. indet.	Wordian	Oman, Haushi-Huqf region	ME – rim basin
Deltodus sp. aff. *D. mercurei* Newberry, 1876	Wordian	Oman, Haushi-Huqf region	ME – rim basin
Solenodus sp. cf. *S. crenulatus* Trautschold, 1874	Wordian	Oman, Haushi-Huqf region	ME – rim basin

provide the necessary taxonomic framework to accurately place the material from other localities in Oman and other regions in Neotethys. An overview of the Late Triassic Arabian (Oman) margin and the distribution of sampled localities is shown in Figure 3.29, illustrating the respective depositional environments.

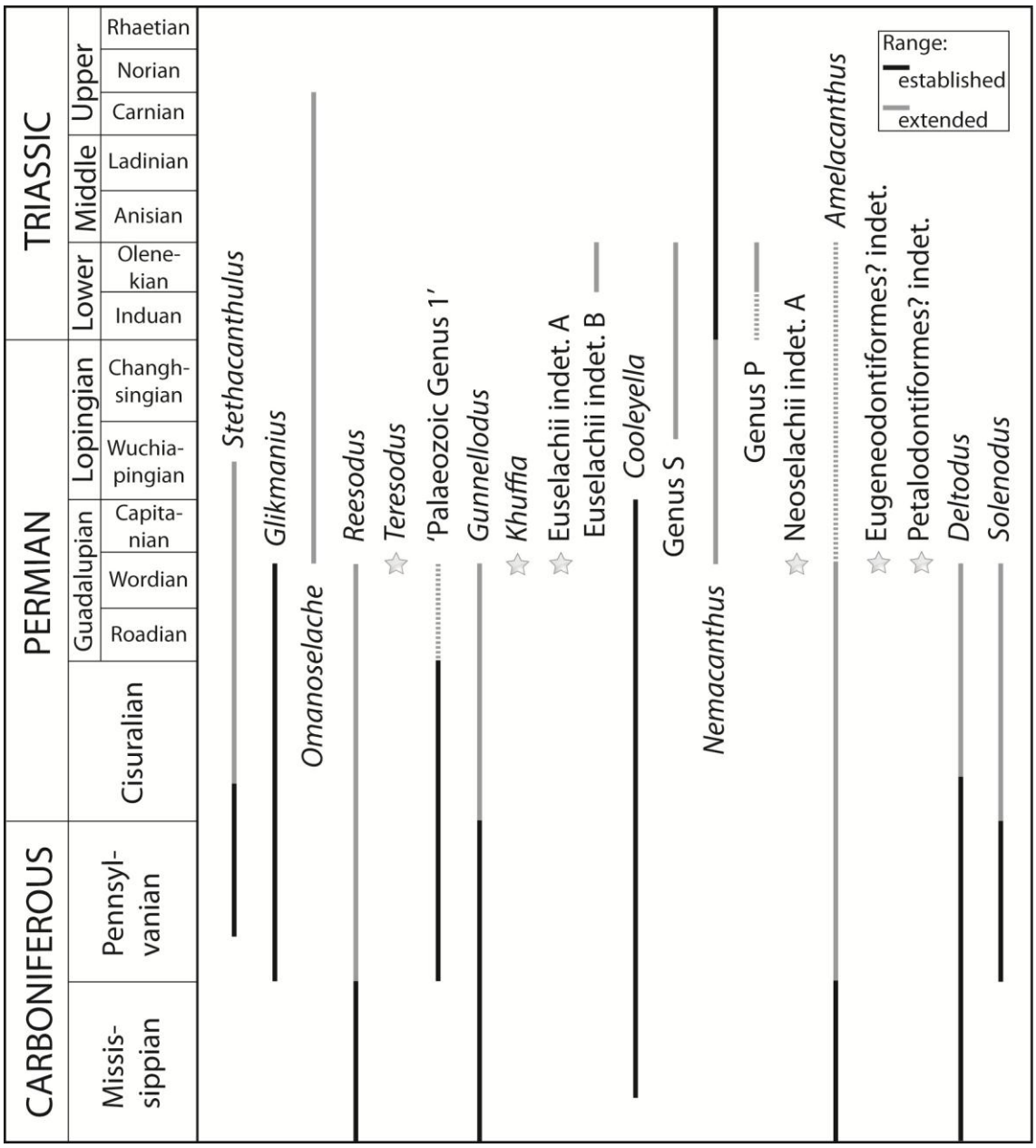

Figure 3.28 – Global ranges of all genera recovered in Neotethys. Established ranges based on data in Table 3.4 and range extensions based on data in Table 3.5. The star symbol represents new records; dashed lines represent tentative ranges.

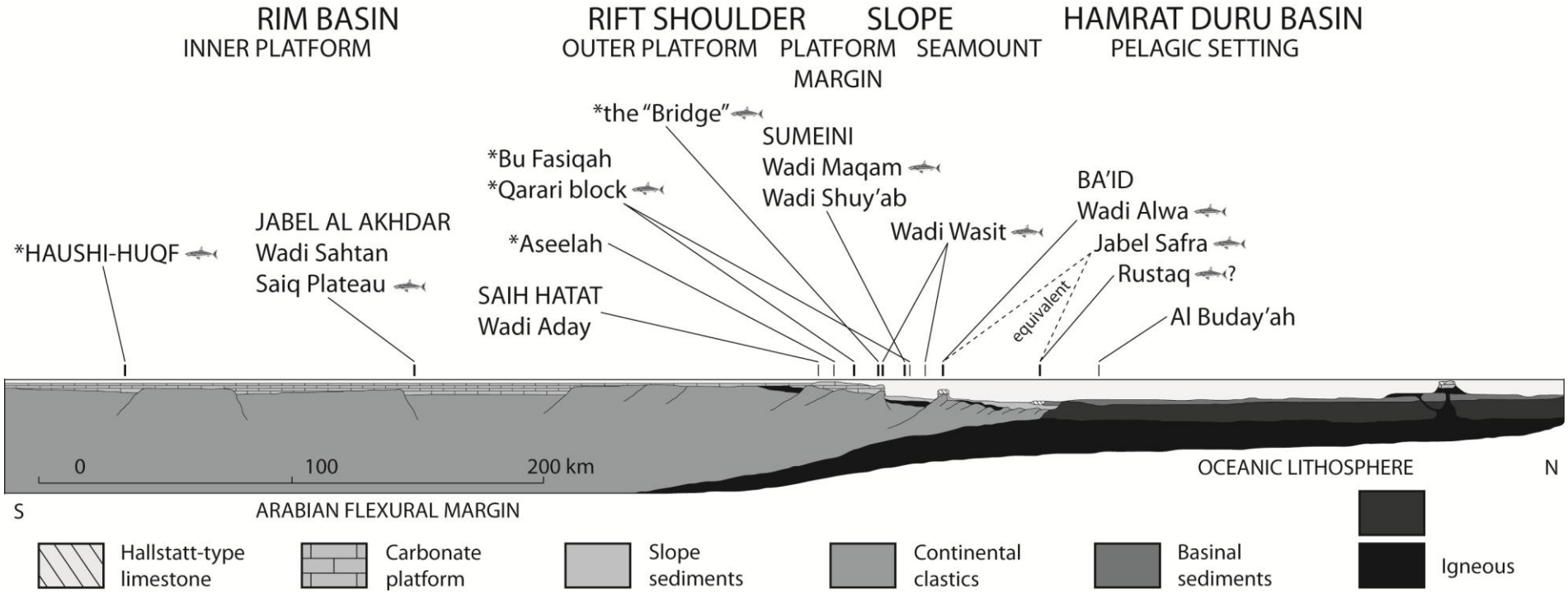

Figure 3.29 – Cross-section of the Neotethyan Arabian (Oman) margin during the Late Triassic, facing the spreading Neotethys and the Cimmerian Blocks (Iran). Redrawn from Pillevuit *et al.* (1997); Richoz *et al.* (2010); Baud *et al.* (2012); modified based on S. Richoz, pers. comm. (2012). The palaeogeographical position of sampled localities on the margin is indicated. Localities originally positioned in the Interior Oman Basin (Haushi-Huqf) and the Batain Basin (marked with asterisk) originate from the margin facing the Madagascar Embayment, but are shown here in their correlative position for comparative purposes. The exact position of Jabel Safra is unknown, but is deemed equivalent to seamount deposits such as Wadi Alwa and Rustaq.

Recovery data from samples collected from the Lopingian–Induan of Oman is shown in Table 3.6. A total number of 38 samples was collected, although processing of ten of those has not been possible (time restrictions). Of the available Lopingian samples, six were barren and five were productive. Two among the productive samples yielded shark remains (Wuchiapingian; both from the “Bridge”). Of the available Induan samples, eight were barren and nine were productive in terms of biogenic remains (vertebrate and invertebrate). One among the productive samples yielded actinopterygian remains (Griesbachian) and one yielded conclusive shark remains (Griesbachian). General biogenic productivity in the Lopingian–Induan has been observed across the entire margin (inner platform: Wadi Sahtan, Saiq Plateau; platform margin: Wadi Aday, the “Bridge”, Wadi Wasit; slope: Wadi Maqam; and basinal seamount: Wadi Alwa. Bony fish presence was recorded from the Induan of the inner margin, whereas sharks appear to only have occurred on the platform margin throughout the Lopingian–Induan interval. Some facies control may therefore be of influence on the recovery of chondrichthyans from this interval.

Statistical tests have been run to determine whether the recovery of fish (vertebrate) remains increases with increased sampling effort (Appendix A1.5.2). These showed that:

- the total number of productive samples has a strong positive relationship with the total number of samples collected ($r^2 = 0.8792$), which is significant;
- the total number of barren samples has a weak positive relationship with the total number of samples collected ($r^2 = 0.2645$), which is not significant;
- the total number of vertebrate-bearing samples has a weak positive relationship with the total number of samples collected ($r^2 = 0.1818$), which is not significant.

Testing for significance of these relationships was done using $p = 0.05$ and a one-tailed t-test, assuming that either a positive relationship or no relationship at all can ever exist between the total number of samples collected and the number of barren or productive samples found among them. These results are based on a small number of samples, which means that only a few extra samples can have a large impact on the calculated

Table 3.6 – Samples collected from Lopingian–Induan deposits in Oman and their yield (see Appendix A1.1, 1.5 for further details).

Locality	Age	Number of samples	Yield
Wadi Alwa	Dienerian	2	productive
	Wuchiapingian	1	barren
Wadi Sahtan	Griesbachian	2	barren
	Changhsingian	2	productive? and barren
	Wuchiapingian	1	barren
Wadi Aday	Dienerian?	1	barren
	Griesbachian	1	productive
	Changhsingian	2	productive and barren
Saiq Plateau	Dienerian?	1	barren
		1	not yet processed
	Griesbachian	1	productive (e.g., Actinopterygii)
		4	not yet processed / picked
	Changhsingian	1	productive
		3	not yet processed
	Wuchiapingian	1	not yet processed
Wadi Wasit	Dienerian	1	barren
	Griesbachian	4	productive
	Griesbachian	1	productive (e.g., Chondrichthyes)
Wadi Maqam	Dienerian	1	barren
	Griesbachian	2	barren
	Changhsingian	1	productive
	Wuchiapingian?	1	barren
Al Buday'ah	Wuchiapingian	1	not processed (chert)
The "Bridge"	Wuchiapingian	2	productive (e.g., Chondrichthyes)

relationships. At this point, however, even though it is weak, the relationship between the total number of samples and vertebrate-bearing samples is positive, which suggests that further study of the chondrichthyan record in Oman deposits may still lead to improved insight into the extinction and recovery patterns in the shark community on the Arabian Platform.

The results presented in this chapter provide evidence of a well-established pre-extinction fauna on the Arabian Platform and highlight the patchiness and relatively poor sampling of the Guadalupian shark fossil record. The upward extension of the stratigraphic ranges of many taxa indicates that extinction of these taxa must have been more abrupt than hitherto supposed. The recovered fauna from Oman significantly enhances the Guadalupian chondrichthyan fossil record and also changes

our understanding of chondrichthyan biodiversity patterns prior to the major mass extinction events of the Permian.

The Early Triassic chondrichthyan faunas from Oman and India are described for the first time, although the small sample size means that the sampling effort cannot be considered as exhaustive as for the Wordian. The occurrence of chondrichthyans after the Late Permian extinction has been recorded as early as the Griesbachian and a community had re-established itself by the Olenekian. This study represents the most extensive record of neoselachian teeth in the Early Triassic. Also, in contrast to the hybodont-dominated faunas described to date, neoselachians were the dominant taxon in the vicinity of the Arabian Platform at this time.

4 CHONDRICHTHYAN RECORDS FROM MID-PANTHALASSA AND EASTERN PALAEOTETHYS

4.1 INTRODUCTION

This chapter describes new chondrichthyan records from the Permian–Triassic mid-Panthalassan seamounts and shallow marine margins of the Yangtze microcontinent in the eastern Palaeotethys, positioned in the palaeoequatorial region. The new records are based on material from localities in Japan and China (Figure 4.1). The occurrences are summarised in Table 4.1 and the systematic palaeontology is provided in Appendix A3.2.

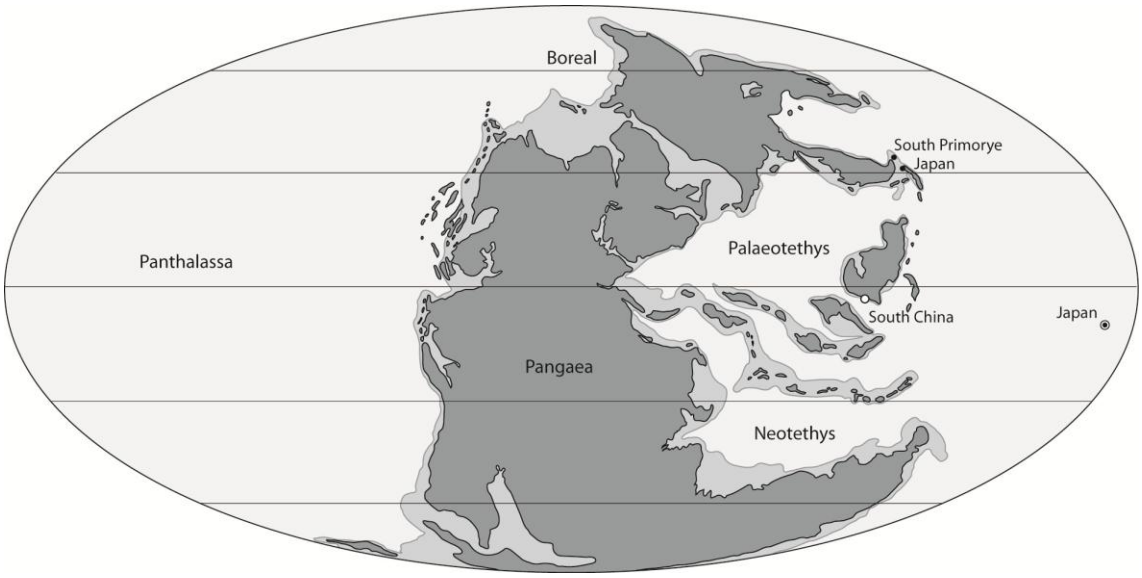

Figure 4.1 – Mollewide plate tectonic map of the Late Permian (260 Ma; modified from Blakey 2012). Circled dots represent localities from which material was directly obtained through fieldwork, whereas open dots represent localities from which material was indirectly obtained. Solid dots represent localities mentioned in the text.

4.2 JAPAN

4.2.1 RATIONALE

Many chondrichthyan remains have been described from Japan since the first reports dating from the early 1900s (e.g., Yabe 1902, 1903). Goto (1972) presented the first summary of the Japanese chondrichthyan record and observed that the bulk of the fossil remains consist of isolated teeth, mostly from marine or brackish-water strata. Publications are often dedicated to single teeth or dentition fragments, although more comprehensive faunal studies are starting to become available (Goto *et al.* 1988; Yamagishi 2004; Yamagishi and Fujimoto 2011). The Japanese elasmobranch record currently ranges from the Carboniferous (Goto 2000) through to the Cenozoic, with the abundance of known fossil remains increasing towards the Recent (Goto *et al.* 1996a). The complete overview of the P–Tr Japanese fossil record presented herein (Appendix A2.1) is based on the most recent summaries available (Goto 2000 for the Palaeozoic; Goto *et al.* 1996a for the Mesozoic), as well as more recent publications (e.g., Yamagishi 2004; Yamagishi and Fujimoto 2011). Figure 4.2 illustrates Permian and Triassic localities containing shark-bearing strata.

Denticles have previously been recovered from the Wordian, Olenekian, Anisian, and from a single horizon in a deposit of Ladinian–Carnian age (Goto 1975, 1994a; Reif and Goto 1979; Yamagishi 2004, 2006). Teeth are more frequently recorded, with 14 records from the Cisuralian (Asselian, Sakmarian/Artinskian, Kungurian, and unspecified), representing the Ctenacanthiformes, Hybodontiformes, Eugeneodontiformes, Petalodontiformes, and Cochliodontiformes (Yabe 1903; Goto 1975; 1984; 1994a; Goto and Okura 2004; Goto *et al.* 1988; Yamagishi 2006). Five chondrichthyan records are known from the Guadalupian (Capitanian and unspecified), comprising ctenacanth and hybodont teeth (Yamagishi 2006; Yamagishi and Fujimoto 2011) and a potentially neoselachian tooth (e.g., Goto 1994a). The five known records from the Lopingian (Wuchiapiangian, Changhsingian) include occurrences of cladodont

teeth (Yamagishi 2006), as well as of Xenacanthiformes, Eugeneodontiformes, and Petalodontiformes (Araki 1980; Goto 1994a; Goto *et al.* 1996b, 2000). The Triassic record is dominated by reports of hybodont teeth (16 records) from the Olenekian, Anisian, and Carnian (Goto 1994a; Goto *et al.* 1991, 2010; Kato *et al.* 1995; Yabumoto and Uyeno 2001; Yamagishi 2004, 2006), with single records of a synechodontiform (neoselachian) and a potential chimaeriform (holocephalan) from the Anisian and indeterminable teeth from the Norian (Yamagishi 2004, 2006).

Fewer records from the Guadalupian (five), Lopingian (five), and Lower Triassic (six), compared to the Cisuralian (14) and Middle Triassic (12), as well as a lower diversity in the Triassic compared to the Permian (six versus 13 genera, respectively, although either or both of these may be underestimated because some material remains unidentified to generic level) may indicate the effects of the end-Guadalupian crisis and late Changhsingian extinction event or may be biased due to the focus of sampling efforts. This study was designed to attempt to close some of these gaps.

The main studied section, at Kamura (Figure 4.2, loc. 16), was selected because it records an extensive chronological range (Wordian–Norian, including the P/Tr boundary), which maximised the potential for reconstructing a complete record through the P–Tr time interval. The Changhsingian–Norian part was previously sampled by Yamagishi (2006) at a variable resolution of 0.5–4.5 m with a sample size of only *c.* 300 g and elasmobranch remains were recovered from the Olenekian (Smithian), the Anisian, and the Carnian–Norian. Yamagishi (2004, 2006) showed that the Kamura section yielded fewer shark remains than a section at Taho (Figure 4.2, loc. 14), which highlighted the necessity for a more detailed sampling effort. Despite the lower yield, Kamura was preferred over Taho, because the stratigraphy is generally less complete at Taho, entirely lacking exposure of Wordian–Wuchiapingian, Smithian, and Ladinian strata (see Musashi *et al.* 2001, fig. 2). Some additional material from Gobanga-dake (Figure 4.2, loc. 17) was also available for study.

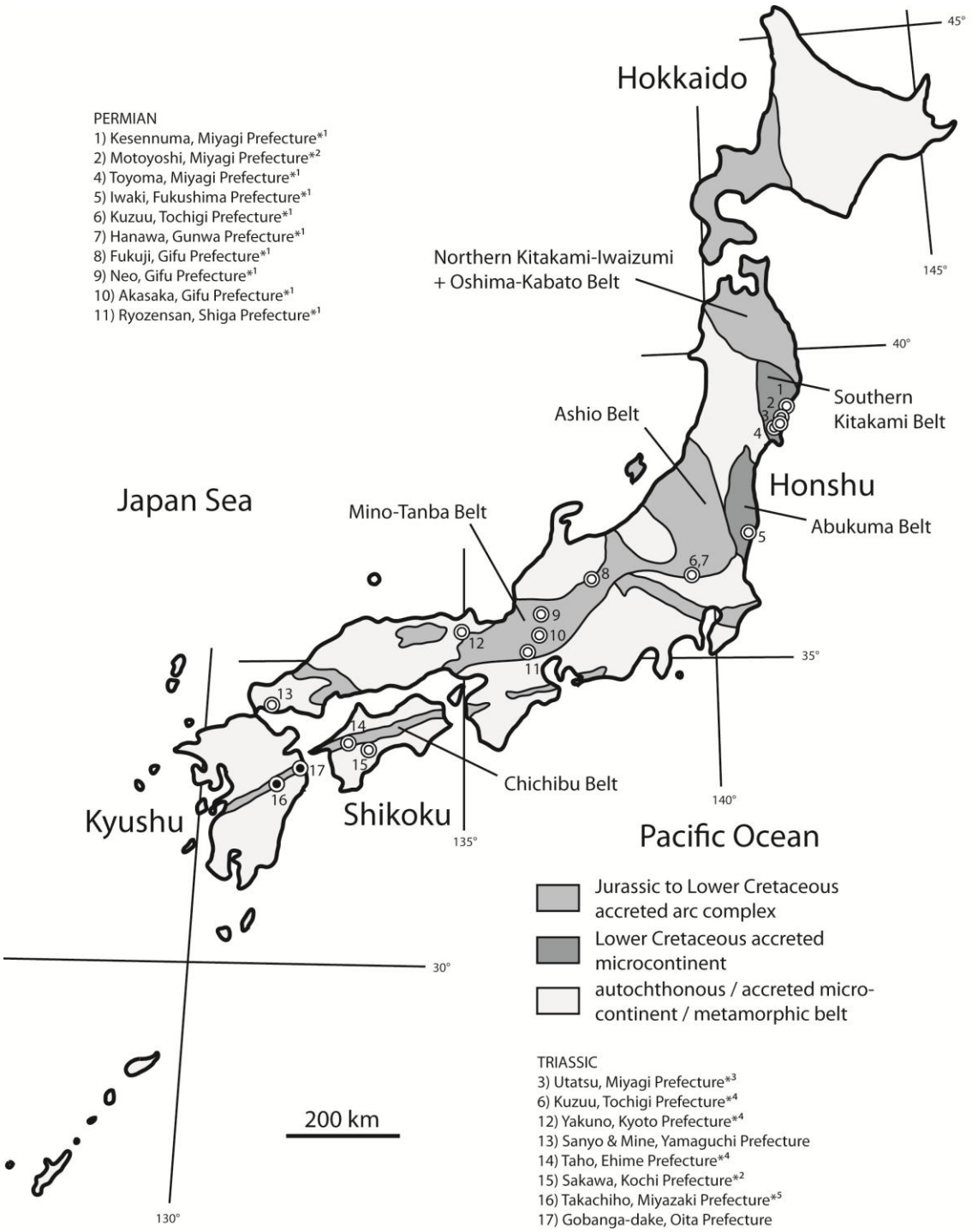

Figure 4.2 – Geological map of Japan (redrawn from Goto 1994a; modified after Isozaki *et al.* 1990 and Barnes 2003), showing the main Permian and Triassic elasmobranch-bearing localities (positions based on: *1, Goto 1994a; *2, Yamagishi 2006; *3, Kato *et al.* 1995; *4, Goto *et al.* 1996a; *5, Ota and Isozaki 2006). See Sasaki (2003) for the exact position of localities 1–4). Localities 13 and 15 are from the Sangun and Shimanto metamorphic belts, respectively (Isozaki *et al.* 1990). Material was directly obtained from locality 16 (solid dot) through fieldwork.

4.2.2 GEOLOGICAL SETTING

The geology of Japan is complex, due to its position in the convergence zone of four crustal plates, where subduction of oceanic plates beneath continental plates occurs (Kimura *et al.* 1991). The Japanese orogenic belts, therefore, contain a large number of accreted oceanic-derived deposits, including seamount fragments, oceanic reef limestone and pelagic sedimentary rocks, which primarily constituted the upper layers of the subducting crust (Isozaki *et al.* 1990). Clastic autochthonous deposits are mainly positioned along the northern coastline of Japan and derive from the same source as, and are age correlative to, deposits on the coast of South Primorye, on the opposite side of the Japanese Sea, some of which are shark-bearing (Shigeta *et al.* 2009). They formed in the same position on the Eurasian continental margin until the Japanese Islands became a separate entity around 19–15 million years ago (Barnes 2003).

Accretion in the Japanese Archipelago was an episodic process, resulting in the creation of accretionary complexes of different ages (Kimura *et al.* 1991). Deposits accreted during the Middle–Late Jurassic coincide with a northward collision of island arcs, oceanic rises and seamounts with the Asian continent (Isozaki *et al.* 1990). Numerous Permian and Triassic exposures yielding shark remains are exposed in the Mino-Tanba and Ashio Belts (e.g., Akasaka; Yamagishi and Fujimoto 2011), which were accreted during the Middle Jurassic–Early Cretaceous (Figure 4.2). Further exposures are known from the allochthonous Southern Kitakami and Abukuma Belts (e.g., Motoyoshi; Goto *et al.* 2000), which derived from a microcontinental fragment that collided and accreted to northeast Japan in the Early Cretaceous (Isozaki *et al.* 1990). The accretionary complex of main importance to this study is the Jurassic Chichibu Belt (Northern Chichibu and Sanbosan Belts), because both sampled localities, including the Kamura section near Takachiho (Figure 4.2, loc. 16), are positioned within it.

The lithology observed in the Chichibu Belt is that of allochthonous palaeo-atoll limestone (e.g., Isozaki and Ota 2001). Large blocks of palaeo-atoll limestone that formed on top of mid-oceanic seamounts between the Late Carboniferous and the Late

Triassic, have been incorporated into the Upper Permian and Jurassic accretionary complexes (Isozaki 2009). These limestones are predominantly shallow-marine, bioclastic packstones or wackestones and lack coarse-grained (>clay) terrigenous clastics (Isozaki 2009; the current study confirms a minor input of fine-grained clastics, potentially of aeolian dust). They yield a typical shallow marine Tethyan fauna suggestive of tropical to sub-tropical warm waters (Isozaki 2009), which is corroborated by palaeomagnetic data suggesting a position in the equatorial Panthalassa (at a latitude of 12° S, Figure 4.1) during the Middle Permian to the Early Triassic (Kirschvink and Isozaki 2007).

Kamura

The strata in the Kamura area (Sanbosan Belt) are exposed in two neighbouring mountain valleys located in Takachiho-chō, Nishiusuki-gun, Miyazaki-ken (Prefecture), on the southern island of Kyūshū. The strata in the area strike ENE–WSW and dip almost vertically (80° northward; Ota and Isozaki 2006). The limestones, dolomitised in places, are subdivided into the Iwato (Guadalupian), Mitai (Lopingian) and Kamura (Lower–Upper Triassic) formations, which can be observed in multiple localities near the villages of Saraito, Kamura, Shioniouso and Hijirikawa (Figure 4.3). The Saraito section is located at N 32°45'25" E 131°20'50" (Section 1), the Hijirikawa section at N 32°45'04" E 131°19'52" (Section 2), the Shioinouso Guadalupian/Lopingian boundary (GLB) section at N 32°45'12" E 131°20'10" (Section 3), the base of the Shioinouso Permian/Triassic boundary (PTB) section (section B of Sano and Nakashima 1997, Horacek *et al.* 2009) at N 32°45'17" E 131°20'19", and the remainder of the Shioinouso PTB section (section D of Sano and Nakashima 1997, Horacek *et al.* 2009) at N 32°45'17" E 131°20'18" (Section 4).

The deposits have been studied many times over the last five decades in terms of biostratigraphy (Kambe 1963; Kanmera and Nakazawa 1973; Watanabe *et al.* 1979; Koike 1996; Isozaki 2006), petrography (Sano and Nakashima 1997; Payne *et al.* 2007) and carbon isotopes (Musashi *et al.* 2001, 2006; Horacek *et al.* 2009). The

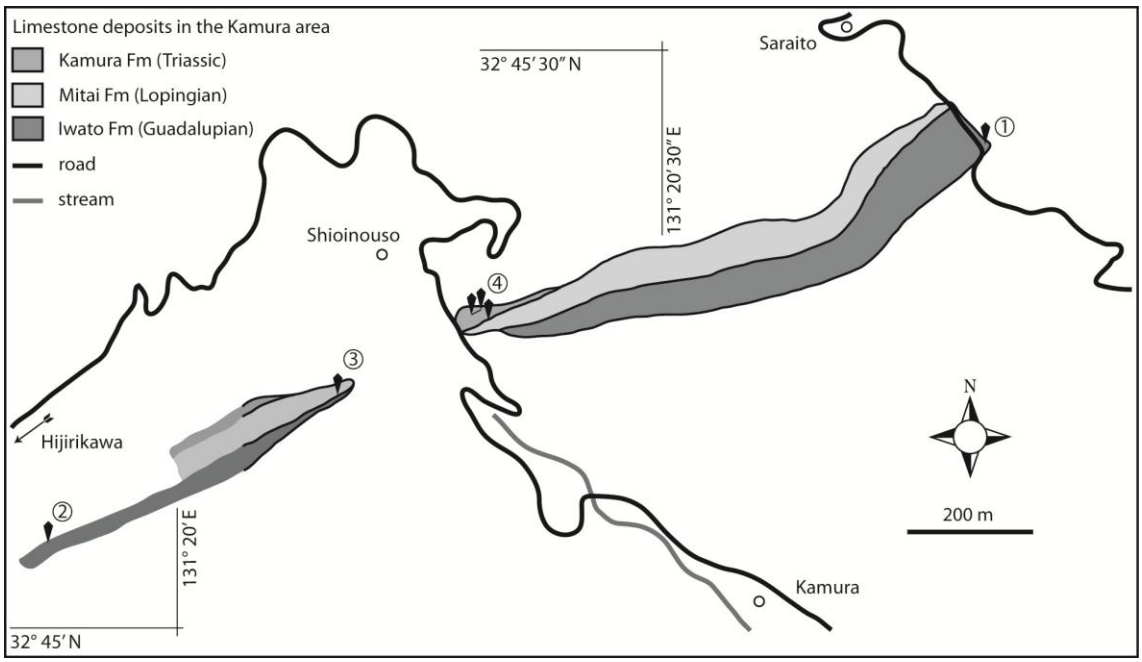

Figure 4.3 – Geological map of the Permian–Triassic limestones exposed in the Kamura area, Miyazaki Prefecture, Kyūshū (modified from Ota and Isozaki 2006; Horacek *et al.* 2009). Sections are individually marked and numbered in order of the age of exposed strata: 1. Saraito (Wordian–Capitanian); 2. Hijirikawa (Capitanian); 3. Shioinouso (Capitanian–Wuchiapingian); 4. Shioinouso (Changhsingian–Norian).

Guadalupian/Lopingian boundary at Kamura has received particular attention in recent years and the faunal and isotopic changes across the boundary have been studied in detail (Ota and Isozaki 2000, 2006; Isozaki and Ota 2001; Ota *et al.* 2002). The extinction event occurring at the boundary has been termed the “Kamura event” by Isozaki *et al.* (2007a, see also 2007b).

The maximum stratigraphic thickness of the Permian–Triassic limestones is estimated at 135 m (Isozaki *et al.* 2007a): the Guadalupian Iwato Formation is ca. 70 m; the Lopingian Mitai Formation is ca. 30 m (Isozaki *et al.* 2007b); and the condensed Triassic Kamura Formation is ca. 38 m thick (Horacek *et al.* 2009; Figure 4.4; Figure 4.5). The Permian part of the sequence consists of dark grey to black limestone (Iwato Formation) as well as white to light grey dolomitic limestone (Mitai Formation; Isozaki *et al.* 2007a). Both formations are composed of bioclastic limestone (wackestone, packstone and lime mudstone) typical of an open marine subtidal facies (Isozaki *et al.* 2007a; Payne *et al.* 2007) and the Guadalupian yields a characteristic

Tethyan shallow marine fauna, including fusulinids, other foraminifera, large bivalves (Alatoconchidae; Isozaki 2006), gastropods, brachiopods, rugose corals and calcareous algae (Isozaki *et al.* 2007a, b). Fusulinids are the most abundant index fossil in these formations and form the basis of the biostratigraphical framework (Ota and Isozaki 2006; see Figure 4.4).

The basal member of the Kamura Formation is composed of black lime mudstone, which is followed by (light) grey bivalve packstone (coquinite) and in turn by skeletal wackestone with a diverse shallow marine fauna. The upper part consists of siliceous limestone with radiolaria and thin-shelled bivalves (Ota and Isozaki 2006; Horacek *et al.* 2009). These strata have been interpreted as a deepening upward succession with increasing biodiversity reflecting the recovery in the post-extinction interval (Sano and Nakashima 1997). The biostratigraphical framework of this formation is based on abundant conodonts (Watanabe *et al.* 1979; Koike 1996; see Figure 4.4), but the deposits also contain ammonoids (Kambe 1963).

Gobanga-dake

The Gobanga-dake locality comprises a poorly exposed block near a mountain of the same name. It is situated within the Chichibu Belt, in the coastal region of Kyūshū towards the northeast from Kamura (Figure 4.2). The block is located at approximately N 33°03'10" E 131°48'16", in the vicinity of Yato, Tsukumi-shi, Ōita-ken (Prefecture). It exposes limestone strata from the Gobangadake Formation, which is of presumed Early Triassic age (R.J. Twitchett, pers. comm. 2012) and has been discussed as such in literature (e.g., Nakazawa 1971). However, no orientation or (definitive bio)stratigraphic data is available (R.J. Twitchett, pers. comm. 2012).

4.2.3 Material

A total number of 59 samples (bulk, cumulative mass 139.4 kg; Appendix A1.1) were collected in the field from the Kamura section (Figure 4.4), covering all the stages from

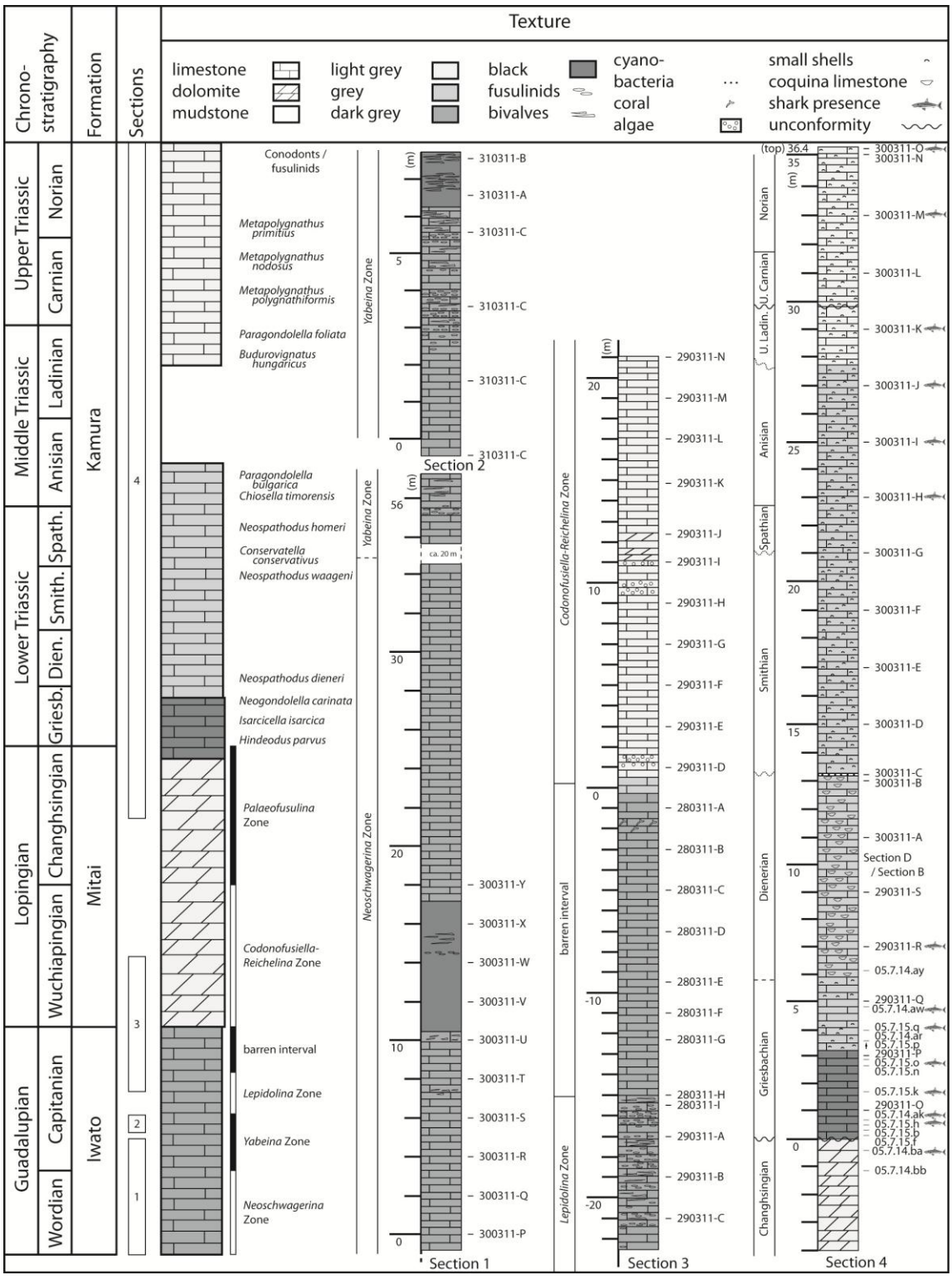

Figure 4.4 – Composite log of the Permian–Triassic limestone strata exposed in the Kamura area. General log modified from Isozaki (2009), based on Horacek *et al.* (2009). Individual sections: 1, Saraito (Isozaki *et al.* 2007b); 2, Hijirikawa (Isozaki *et al.* 2007b); 3, Shioinouso GLB (modified from Isozaki *et al.* 2007a, including scale); 4, Shioinouso PTB (modified from Horacek *et al.* 2009). Notes: relative position of the Iwato/Mitai Fm boundary and the G/L boundary is unresolved (see Isozaki *et al.* 2007a). Some missing time in Section 4 is suspected based on the absence of, or rapid change in, conodont faunas (dashed unconformities; Horacek *et al.* 2009). Grey = approx. sample height; arrow = ex situ, from greater height.

Figure 4.5 – Representative photographs of the different sections and deposits at Kamura. A, Base of Section 1 near Saraito, with exposure continuing around the bend along the road to the right, as viewed towards the northwest. B, Section 2 on the road to Hijirikawa, as viewed towards the southwest. C, G/L boundary at Section 3 near Shioinouso, as viewed towards the west and with hammer for scale. D, Section 3, as viewed towards the northeast and with tape measure perpendicular to bedding plane, marking true thickness. E, Base of the coquina limestone at Section 4 (B) near Shioinouso, as viewed towards the north and with tape measure for scale.

the Wordian through to the Norian, except the dolomitised Changhsingian. The sampled interval includes the Anisian–Carnian, which is the interval from which shark

remains were previously recorded in this area (Yamagishi 2006). The collected samples were 0.9–3.9 kg in mass with an average of 2.2 kg.

A further 16 samples (bulk, cumulative mass 6.9 kg; Appendix A1.1) were collected by R.J. Twitchett (Plymouth University) in 2005 from both the Kamura and Gobanga-dake localities. The two samples from the Gobanga-dake block are of presumed Early Triassic age, whereas of the samples taken at Kamura, two samples originated from the top of the Mitai Formation and are therefore of late Changhsingian age, and the remaining 12 samples originated from the base of the Kamura Formation and are therefore of Induan age. The samples are plotted on the stratigraphic log (Figure 4.4) at approximate heights because how the sections from which they originate compare to the measured section 4 is unknown. Nevertheless, they are concentrated in a restricted time interval around the Permian/Triassic boundary and provide a significant amount of new data for this interval. Two samples were recovered *ex situ*: 05.7.15.b was believed to originate from a horizon in the basal Kamura Formation, which was confirmed by the recovery of one element of *Hindeodus parvus*; and 05.7.15.p was believed to originate from an unknown height above the recovery height of 3.45 m (no conodonts were available to narrow this position).

4.2.4 RESULTS

Both samples from Gobanga-dake proved to be entirely unfossiliferous after processing. However, in association with conodonts, actinopterygian teeth, and bivalve shell fragments, 83 specimens of chondrichthyan remains were recovered from the Kamura Formation at Section 4 near Shioinouso (Shioniouso PTB), including both the lower section B and upper section D (Figure 4.3), covering an age range from the Dienerian to the Norian (Early–Late Triassic; Figure 4.4). In addition, 43 specimens were recovered from the unspecified sections (Twitchett samples) in the Shioinouso PTB area, which are of Changhsingian and Induan (Griesbachian) age. The material consists of teeth, dermal denticles and (cephalic?) spines. The condition of the

recovered material is not optimal, first of all because of the low yield of the formation, which was already shown by Yamagishi (2006), as well as the fragmentary preservation of many specimens. The teeth have been identified as Cladodontomorphi? gen. et sp. indet. from the Anisian and the Norian, cf. *Hybodus* sp. from the Induan (Griesbachian), *Acrodus spitzbergensis* Hulke, 1873 from the Induan (Griesbachian) and Anisian–Ladinian, *Omanoselache* sp. cf. *O.* sp. H from the Induan (Griesbachian and Dienerian), Hybodontiformes gen. et sp. indet. from the Anisian, Euselachii gen. et sp. indet. C from the Anisian, Synechodontiformes gen. et sp. indet. from the Ladinian, and Neoselachii gen. et sp. indet. B from the Norian. Denticles were recovered from the Changhsingian, Induan, and also from the Anisian–Ladinian. All the spines have been interpreted as possible frontal clasper denticles belonging to a taxon identified as aff. *Arctacanthus exiguus* Yamagishi, 2004, recovered from the Induan (Griesbachian) and Anisian–Ladinian, although two Induan specimens have been tentatively assigned to aff. *Arctacanthus*? sp.

4.2.5 Discussion

Substantial diversity was recognised in the fauna at Kamura, including hybodonts and neoselachians, as well as a potential cladodont(?) and holocephalan (chimaeriform?). Only hybodonts were previously recognised by Yamagishi (2006; *Hybodus* sp. 2 and *Polyacrodus* sp. 4), and so this study represents a significant addition to the known diversity (Figure 4.6; Appendix A1.6). Aff. *Arctacanthus* accounts for 46% and 43% of the total number of specimens recovered in the Lower and Middle Triassic, respectively, but is absent in the Upper Triassic (Figure 4.6A, C, E). Hybodonts follow a similar pattern, with 46% and 30% in the Lower and Middle Triassic, respectively, and are also absent in the Upper Triassic. Following the absence of Neoselachii in the Lower Triassic, it is predominantly this group that fills the vacant space, increasing its share from 9% in the Middle Triassic to 92% in the Upper Triassic. The Cladodontimorpha? also occur from the Middle Triassic onwards. The generic richness of all three faunal

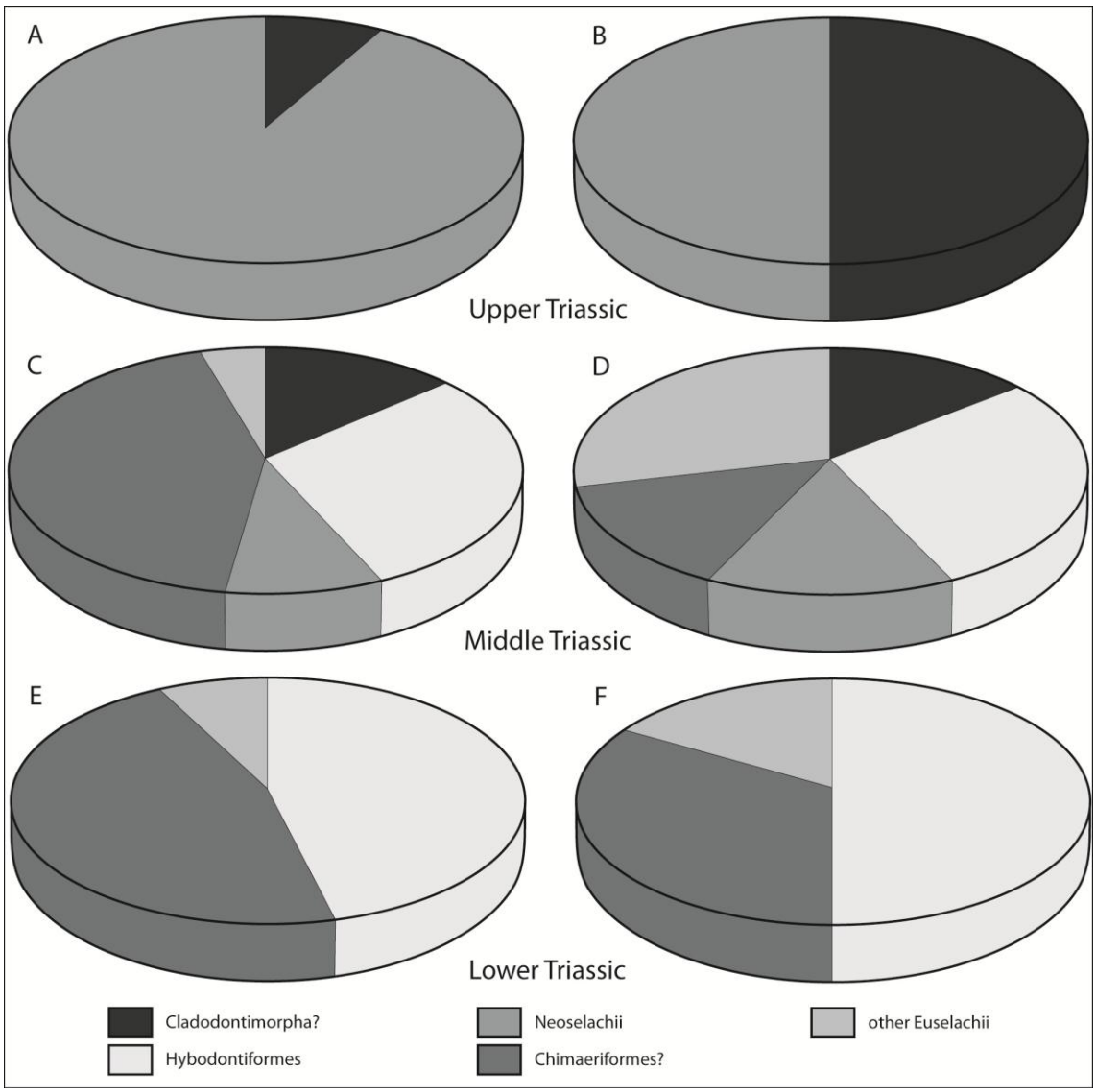

Figure 4.6 – Relative abundances of chondrichthyan groups from the Triassic of Kamura, Japan, based on material recovered in this study. A, C, E, Overall relative abundance of major groups using numbers of specimens. B, D, F, Overall relative abundance of major groups using numbers of genera.

segments follow a similar pattern to that of the number of recovered specimens (Figure 4.6B, D, F), although the share of aff. *Arctacanthus* is reduced in the Middle Triassic (14%) and the balance between the Neoselachii and Cladodontimorpha? is equalised in the Upper Triassic. The Upper Triassic data is based on only two samples, however, so it may not be an accurate representation of the fauna. In fact, some margin of error must be assumed in all the quoted values, due to the high level of fragmentation in the material.

Polyacrodus sp. 4 of Yamagishi (2006) appears similar to *Omanoselache* sp. cf. *O.* sp. H and Hybodontiformes indet. from this study. They may well be proven to belong to the same genus if more and better preserved material can be recovered. Likewise, cf. *Hybodus* sp. is similar to *Hybodus* sp. 2 of Yamagishi (2006). The fauna from Kamura further shares many compositional elements with the fauna recorded at Taho, which consists of hybodonts (*Acrodus*, *Hybodus*, *Lissodus*, and *Polyacrodus*), a neoselachian (*'Synechodus'*), and a chimaeriform(?) (*Arctacanthus*), recovered from the Olenekian–Anisian (Goto 1994a; Yamagishi 2004, 2006; Goto *et al.* 2010).

No shark remains had previously been recovered from the Permian of Kamura, as is also the case at Taho (Yamagishi 2004, 2006). In this study, however, three dermal denticles were recovered from the latest Changhsingian at Kamura. Currently, these represent the only Permian remains to have been recovered from the Chichibu Belt, whereas numerous records are known from the Mino-Tanba and Ashio Belts, in which mid-Panthalassan seamount limestone is also exposed (Figure 4.2). This may be the result of poor preservation or lack of input due to the type of depositional environment in which the rock units of the Chichibu Belt were formed. Undersampling of the strata, and especially of Lopingian deposits, may also be of influence, but the complete barren nature of virtually all Permian samples after processing suggests strongly that increased sampling effort in strata up to mid-Wuchiapingian age will not yield additional results.

The new data from Kamura extend the known chronological range of aff. *Arctacanthus exiguus* Yamagishi, 2004 from the Anisian to include the Ladinian and the Induan (Griesbachian?; Figure 4.9). It also represents the first known Griesbachian records of *Hybodus* (if confirmed) and *Acrodus* globally. The Induan and Ladinian strata of Japan have been shown to be shark-bearing for the first time. All previously described records of shark remains from the Lower Triassic of Japan were of Olenekian hybodonts (see Kato *et al.* 1995; Yamagishi 2004, 2006; Goto *et al.* 2010; seamounts and accreted microcontinent), which makes the Induan records of cf. *Hybodus*, *Acrodus*, *Omanoselache*, and aff. *Arctacanthus* the oldest known sharks

from the Triassic of Japan and increases the diversity in this Early Triassic shark community. In combination with the dermal denticles from the latest Changhsingian, it also indicates an earlier re-establishment of sharks in the vicinity of the mid-Panthalassan seamounts after the Late Permian mass extinction than suggested previously.

4.3 CHINA

4.3.1 GEOLOGICAL SETTING

At Guandao, Guizhou Province in southern China, an extensive section of approximately 750 m in stratigraphic thickness provides continuous exposure of Lopingian (Changhsingian) to Upper Triassic (Carnian) strata without significant unconformities (Lehrmann *et al.* 2005). These strata are components of the "Great Bank of Guizhou", exposed in the Nanpanjiang Basin (Orchard *et al.* 2007). They were deposited on the proximal slope adjacent to an isolated carbonate platform, which was positioned in a deep marine embayment on the southern margin of the South China plate and located at a latitude of approximately 12° N at the start of the Middle Triassic (Orchard *et al.* 2007). Lehrmann *et al.* (2005) give a detailed description of the Guandao section, stating that the typical deposits are deep marine, pelagic carbonates with abundant conodonts (Figure 4.7). They describe how the basal Wujiaping Formation was deposited on the southern margin of the Yangtze Platform, prior to a significant sea level rise, and contains a rich shallow marine benthic fauna consisting of brachiopods, molluscs, echinoderms, bryozoa and foraminifera. The overlying Dalong Formation contains radiolaria and ammonoids and was deposited during the drowning of the area that gave rise to the isolation of the platform (water depth of platform margin roughly 30 m based on palaeobathymetry; refer to Lehrmann 1999, fig. 1 for a palaeogeographic reconstruction). The Luolou Formation (Induan–Olenekian) and Xinyuan Formation (Anisian) are dominated by hemipelagic lime mudstone, allodapic

lime packstone and grainstone, submarine debris-flow breccia beds and shale interbeds (Lehrmann *et al.* 2005). The Induan and lower Olenekian (Smithian) sequence is characterised by a very low skeletal grain count, whereas the upper Olenekian, overlying two thick dolomitised breccia beds (Spathian), contains bivalves, crinoids, cephalopods, brachiopods, ostracods, and foraminifera, and has been interpreted as the start of biotic recovery after the late Permian extinction event (Lehrmann *et al.* 2005; Payne *et al.* 2006). The Olenekian–Anisian boundary beds were sampled in detail by Orchard *et al.* (2007; Figure 4.7, high-resolution inset). The facies in this sequence of the lower Guandao section are primarily skeletal packstone with pelagic lime mudstone interbeds and sporadic ash horizons. The limestones represent carbonate turbidites and debris flow breccias that originated from the platform (Orchard *et al.* 2007) and the ash horizons have been used to date the Olenekian/Anisian boundary to 247.2 Ma (U–Pb; Lehrmann *et al.* 2006). The allochthonous shallow-water grains contained within the turbidites were found to show a distinct and rapid increase in diversity and abundance of fossils occurrring across the Olenekian/Anisian boundary, which reflects the evolution of biologically diverse reef margins on the platform (Payne *et al.* 2006a, b) and is further believed to be another characteristic element of biotic recovery after the late Permian mass extiction (Payne *et al.* 2006b). Recently, however, a study by Goudemand *et al.* (2012) repositioned the boundary interval within the section to occur between samples O40 and O41 (Figure 4.7, dashed shaded area), a conclusion that is followed here.

4.3.2 MATERIAL

Sampled beds are indicated on the stratigraphic log in Figure 4.7. The O coded samples were collected by a research group lead by M.J. Orchard (Geological Survey of Canada, Vancouver) and D. Lehrmann (Trinity University, Texas). The GDL coded samples were collected by D. Lehrmann, and the GQC coded samples by J. Wei (Guizhou Bureau of Geology, Guiyang). The samples (residue; Appendix A1.1) were

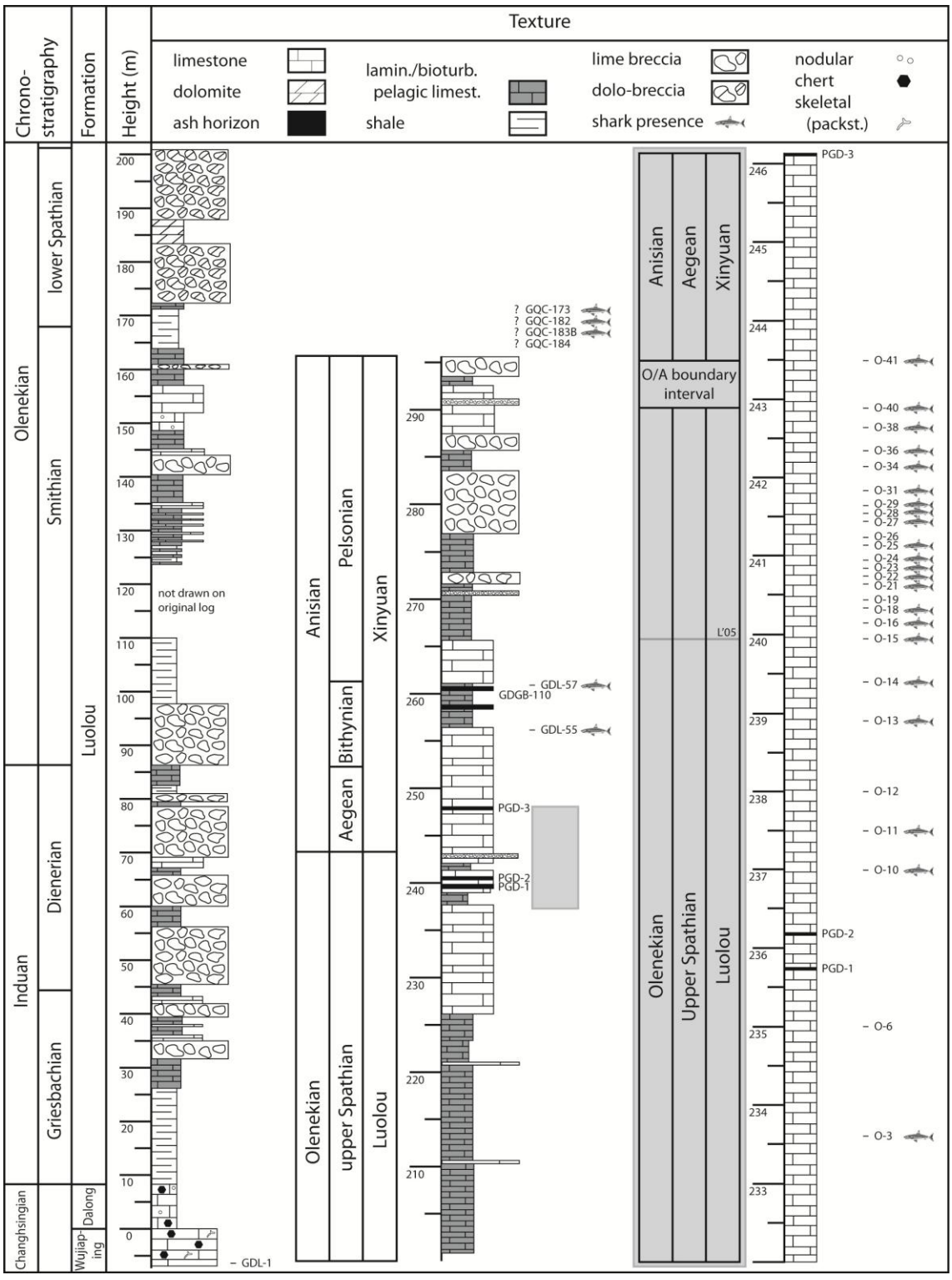

Figure 4.7 – Composite log of the Permian–Triassic limestones of the Lower Guandao section, Guizhou Province, southern China (redrawn from Lehrmann *et al.* 2005). Inset (in grey) shows detail of the Olenekian/Anisian boundary, redrawn from Orchard *et al.* (2007), who re-measured the entire section, but only re-published this part. The lithology is a simplified representation, described as skeletal packstone with pelagic lime mudstone interbeds (Orchard *et al.* 2007). A recent study repositioned the O/A boundary to a new interval based on conodonts (Goudemand *et al.* 2012; original boundary position marked as L'05). Samples coded GQC are Anisian in age but lack detailed stratigraphic information from the collector.

obtained from Changhsingian, uppermost Olenekian (Spathian) and lower Anisian deposits.

One further sample (residue; Appendix A1.1) of Changhsingian age and yielding chondrichthyan remains was collected by M.J. Orchard from a different locality in China. It originates from the upper part of the Changhsing Formation at the Meishan section in Zhejiang Province, southern China (see Orchard *et al.* 1994). This section has been studied in detail and has been ratified as the GSSP of the Permian/Triassic boundary (Yin *et al.* 2001). The formation consists of graded beds of organic-rich calcarenite, marly micrite, and radiolarian chert, representing slope-to-basinal facies (Wignall and Hallam 1993; see also Jin *et al.* 2000).

4.3.3 Results

One indeterminate elasmobranch tooth cusp was recovered from the Changhsingian of the Meishan section. This tooth fragment from the Changhsing Formation belongs to a chondrichthyan fauna that was described from this section by Liu and Chang (1963); Liu and Wang (1994); and Wang *et al.* (2007a). Identified taxa include: the edestid *Helicampodus changhsingensis*; *Meishanselache liui* and *Changxingselache wangi* of unknown elasmobranch affinities; the acrodontid *Sinacrodus donglingensis*; as well as an indeterminate ctenacanthid, hybodontid, and neoselachian. *H. changhsingensis* represents the only chondrichthyan macrofossil teeth known from these strata. All other taxa are based on microfossil remains, consisting of 1–4 dermal denticles per taxon. The fragment recovered in this study therefore represents the first known microfossil tooth fragment.

In total, 61 chondrichthyan teeth and tooth fragments were recovered from the samples collected from the Lower Guandao section. Their age is latest Olenekian (late Spathian) to early Anisian. The preservation of the material is poor. There is a high degree of fragmentation of the specimens, which is unlikely to have been caused by transportation down the slope, suggested by the turbiditic nature of the limestones (see

Lehrmann *et al.* 2005; Orchard *et al.* 2007), but by microfracturing of the samples or processing, indicated by the sharp nature of the fracture surfaces. In addition, black colouration of the specimens is suggestive of thermal alteration, permineralisation or staining (Tway *et al.* 1986). The teeth have been identified as *Omanoselache* sp. cf. *O.* sp. H, *Omanoselache* sp. A, *Omanoselache* sp. cf. *O.* sp. A, cf. *Palidiplospinax* sp., Genus S sp. cf. Genus S sp. T, Genus S sp. A, *'Synechodus'* sp. (pre-Jurassic), and cf. Genus P.

The recovered fauna consists almost entirely of hybodonts and neoselachians, except for a couple of indeterminate elasmobranch remains. The Neoselachii, and more specifically the Synechodontiformes, are the dominant element in the Olenekian, constituting 74% of the total number of specimens (Figure 4.8C; Appendix A1.2.5) and 71% of the generic richness (Figure 4.8D). The contributors to these shares are a tentatively identified palaeospinacid genus and four sycheodontiform taxa of unidentified familial affinities. The Hybodontiformes contribute one genus to total faunal diversity, constituting 14% of generic richness, but represent as much as 22% of specimen abundance. Conversely, hybodonts are the dominant group in the Anisian with 64% of the total number of specimens. The synechodontiforms have been reduced to a share of 36% (Figure 4.8A). Regardless of hybodont domination in specimen abundance, however, the Synechodontiformes contribute two thirds of the total generic richness, whereas the Hybodontiformes account for one third (Figure 4.8B).

This study represents the first detailed record of sharks from the Guandao section and the newly discovered material necessitates important range extensions (Figure 4.9). First of all, *Palidiplospinax* was previously restricted to the Lower Jurassic of Europe (Klug and Kriwet 2008), so the extension of its range down to the Middle Triassic (Anisian) and to include China may be significant, but because this is based on a single fragmented specimen, it must be regarded with caution. The ranges of Genus S and Genus P, which were established in Chapter 3 as late Wuchiapingian–Olenekian and Induan–Olenekian, respectively, are extended upwards to include the Anisian. The wider implications of the occurrence of *'Synechodus'* (pre-Jurassic) in China cannot be

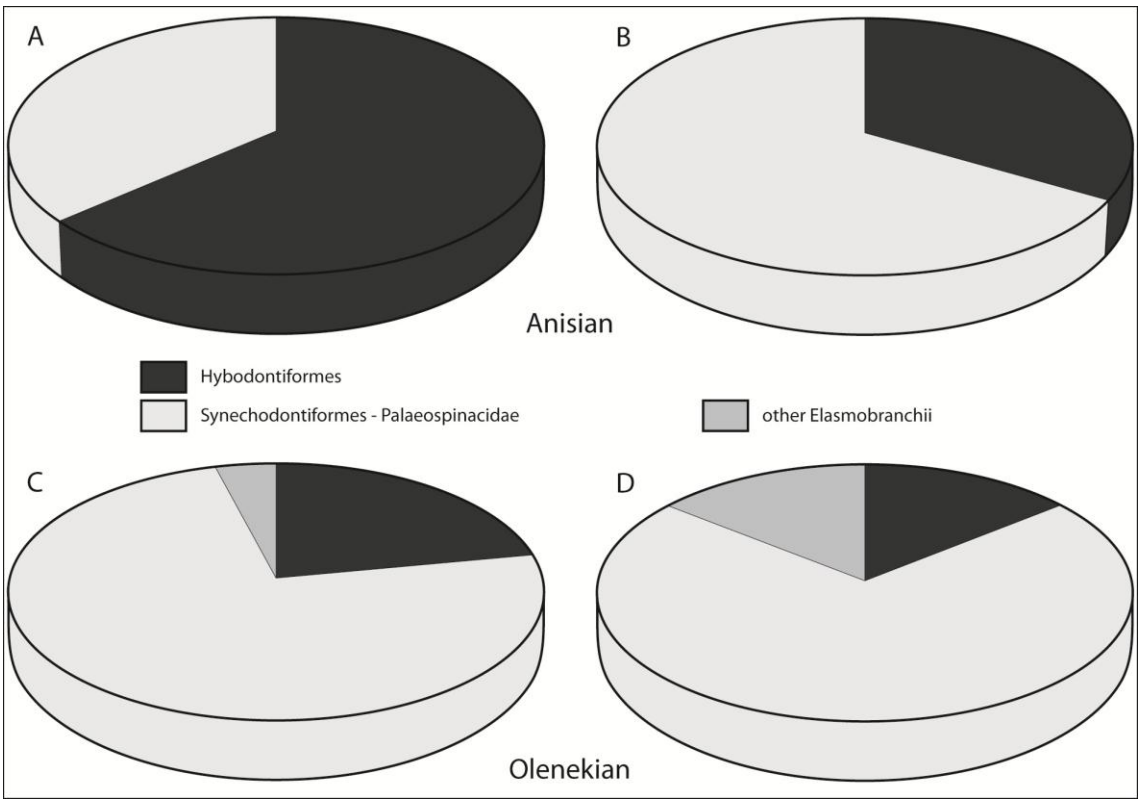

Figure 4.8 – Relative abundances of chondrichthyan groups from the Triassic of Guandao, China, based on material recovered in this study. A, C, Overall relative abundance of major groups using numbers of specimens. B, D, Overall relative abundance of major groups using numbers of genera.

assessed, because any Palaeozoic and Triassic occurrences attributed to this undefined group bear an as yet uncertain relationship to Jurassic–Cenozoic *Synechodus* (see Klug 2010). The Chinese specimen falls well within the range of the group, but signifies an extension of its palaeogeographic distribution to include the eastern Palaeotethys.

4.4 Discussion

An overview of the results from the described localities in this chapter is shown in Table 4.1, providing an overview of new shark occurrences in the mid-Panthalassa and eastern Palaeotethys. The significance of these new discoveries in terms of chronological ranges is shown in Figure 4.9.

Table 4.1 – Overview of all new shark occurrences in the mid-Panthalassa and eastern Palaeotethys during the Permian and Triassic.

Taxon	Age	Location
Cladodontomorphi? gen. et sp. indet.	Anisian, Norian	Japan, Kamura
cf. *Hybodus* sp.	Induan (Griesbachian?)	Japan, Kamura
Acrodus spitzbergensis Hulke, 1873	Induan (Griesbachian?), Anisian–Ladinian	Japan, Kamura
Omanoselache sp. cf. *O.* sp. H	Olenekian (Spathian)–Anisian	China, Guandao
	Induan (Griesbachian?, Dienerian)	Japan, Kamura
Omanoselache sp. A	Anisian	China, Guandao
Omanoselache sp. cf. *O.* sp. A	Olenekian (Spathian)–Anisian	China, Guandao
Hybodontiformes gen. et sp. indet.	Anisian	Japan, Kamura
Euselachii gen. et sp. indet. C	Anisian	Japan, Kamura
cf. *Palidiplospinax* sp.	Anisian	China, Guandao
Genus S sp. cf. Genus S sp. T	Olenekian (Spathian)–Anisian	China, Guandao
Genus S sp. A	Olenekian (Spathian)–Anisian	China, Guandao
'Synechodus' sp. (pre-Jurassic)	Olenekian (Spathian)–Anisian	China, Guandao
cf. Genus P	Olenekian (Spathian)–Anisian	China, Guandao
Synechodontiformes gen. et sp. indet.	Ladinian	Japan, Kamura
Neoselachii gen. et sp. indet. B	Norian	Japan, Kamura
aff. *Arctacanthus exiguus* Yamagishi, 2004	Induan (Griesbachian?), Anisian–Ladinian	Japan, Kamura
aff. *Arctacanthus*? sp.	Induan (Griesbachian?)	Japan, Kamura

It is generally believed that the Cladodontomorphi became extinct during the late Permian mass extinction, but there are a few reports from Triassic deposits that imply their survival: *Acronemus tuberculatus* (Bassani, 1886) from the Middle Triassic (Anisian?) Grenzbitumenzone at Monte San Giorgio, Kt. Tessin, Switzerland (Rieppel 1982), and *Pyknothylacanthus spathianus* Mutter and Rieber, 2005 from the Lower Triassic (Olenekian, lower Spathian) of Bear Lake County, Idaho, USA (Mutter and Rieber 2005). Both of these ctenacanthoid reports are based on fin spines only. In the case of *Acronemus* Rieppel, 1982, the associated teeth conversely indicated a

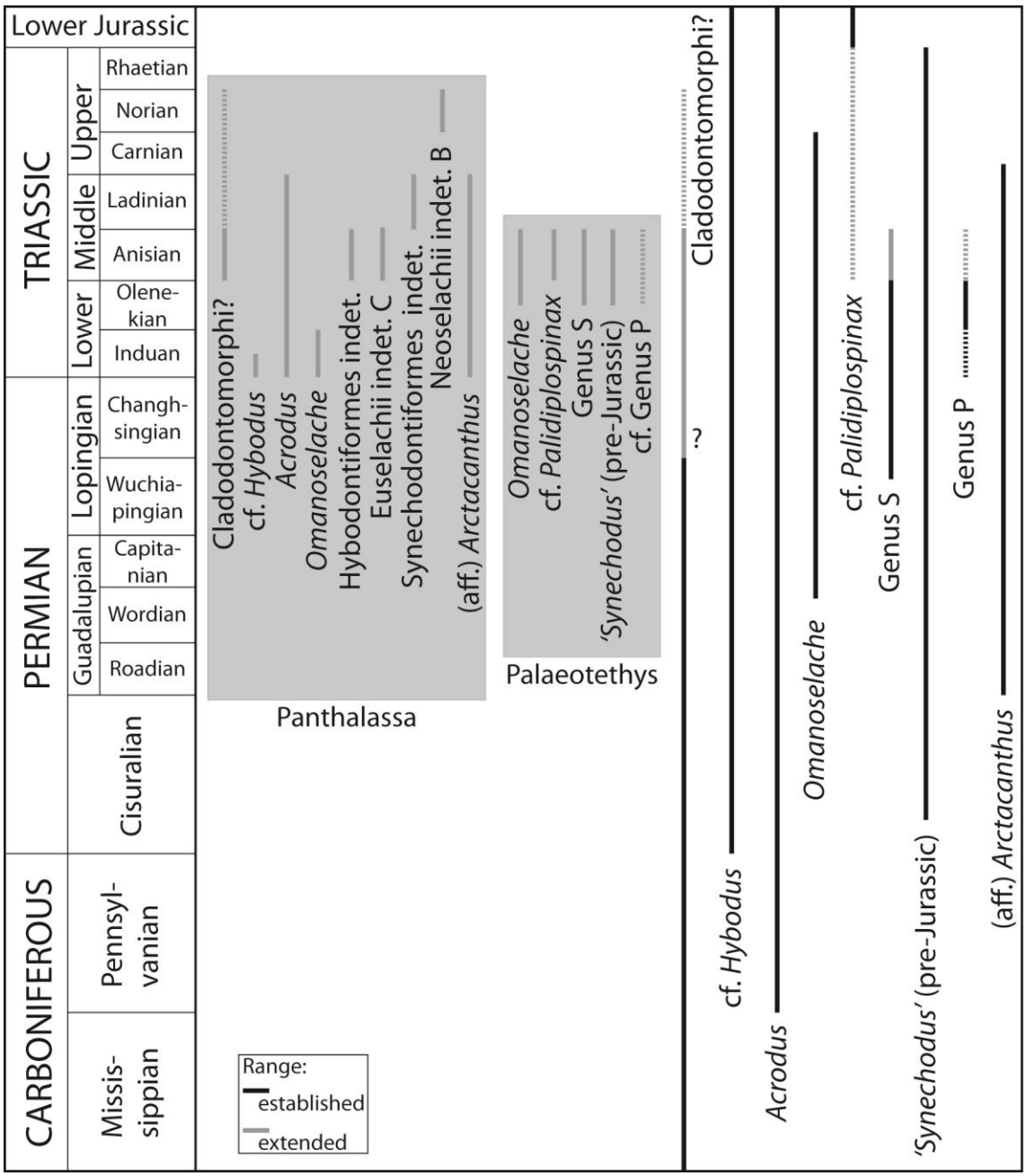

Figure 4.9 – Ranges of all genera recovered in mid-Panthalassa and eastern Palaeotethys, as well as global data showing established and extended ranges. Established ranges based on data in Figure 3.28 and from references quoted in Appendix A3.2. Range extentions based on data in Table 4.1. Dashed lines represent tentative ranges.

hybodont affinity, being *Acrodus*-like, but always lacking lateral cusplets, possessing a transverse crest, and distinct arching in anterior teeth (Rieppel 1982). The identification has, therefore, remained tentative and recently Maisey (2011) has presented conclusive evidence against a ctenacanthoid interpretation. This leaves the cladodont affinity of *Pyknothylacanthus* and the Japanese cladodont? teeth questionable,

although ctenacanths are well-represented in Permian deposits of Japan (e.g., Goto 2000; Yamagishi 2006; Yamagishi and Fujimoto 2011, see also Ginter *et al.* 2005).

Hybodonts are a well-established element of both Permian and Triassic faunas globally, as is also the case in the studied localities in Japan and China. *Hybodus* is a widely distributed taxon known from the start of the Permian through to the Cretaceous (although its Permian record is still uncertain) and has previously been recorded from the Triassic of Japan on a number of occasions (Goto *et al.* 1991; Kato *et al.* 1995; Yamagishi 2004, 2006). The genus *Acrodus* may have originated in the Carboniferous (its Palaeozoic record is still uncertain) and persisted into the Cretaceous, although the species recognised from Japan, *A. spitzbergensis* Hulke, 1873, only ranged from the Lower to the Middle Triassic. The distribution of this species is currently largely restricted to the northern hemisphere, with records from western USA and Spitsbergen (e.g., Birkenmajer and Jerzmańska 1979; Cuny *et al.* 2001), but extends just south of the Equator as recorded in seamount limestone of Japan (Yamagishi 2004). The chronological range of *Omanoselache* was established in Chapter 3 (Wordian, Guadalupian–Carnian, Upper Triassic) and is here corroborated by the material recovered from Japan and China. Furthermore, material described by Chen *et al.* (2007a) was referred to the genus in this study (see Section 3.6), and the specimens from Guandao confirm this interpretation. The occurrence of *Omanoselache* in Japan expands its known palaeogeographical range.

Neoselachians appear to be the dominant element in the Olenekian–Anisian Chinese shark fauna, as opposed to hybodont domination in the Lower and Middle Triassic faunas of Japan. An increasing importance of the neoselachians can be observed in Japan from the Middle Triassic onwards. This trend compares well to typical Triassic shark faunas, which are generally hybodont-dominated until the radiation of the Neoselachii in the Late Triassic (Cuny and Benton 1999). Nevertheless, there appear to be at least local areas where neoselachians dominated, as illustrated by the Chinese fauna and as was also observed in Oman (see Section 3.2.4.1). The predominant neoselachian genera in the Chinese fauna, Genus S and Genus P, were

established from material recovered from the Triassic of Oman and although Genus S was subsequently recovered from Iran and Timor (Chapter 3), both taxa remained restricted to the Neotethyan Basin. Following the study of the Guandao section, the geographical distribution of both genera is extended to include the eastern equatorial Palaeotethys Basin, although the extension of Genus P must remain tentative.

Euchondrocephalans are underrepresented in the Triassic of Japan, with a single holocephalan, compared to the occurrence of multiple eugeneodontiform and petalodontiform taxa in Permian deposits. *Arctacanthus* was first established based on Permian specimens from East Greenland and the western USA (Nielsen 1932; Branson 1933), and has previously also been recognised (including as aff. *Arctacanthus*) from the Middle–Upper Triassic (Anisian–Carnian) of Japan and China (Yamagishi 2004; Chen *et al.* 2007a), which means that no changes to established ranges are required. The dimensions of the specimens recovered here (about 1 mm mesio-distally, 3 mm antero-posteriorly, and 3 mm in height) are very similar to those of previously published Triassic material, which is about ten times smaller than the Permian representatives (25–30 mm), as also remarked by Yamagishi (2004) and Chen *et al.* (2007a).

5 CHONDRICHTHYAN RECORDS FROM THE BOREAL SEA AND EASTERN PANTHALASSA

5.1 INTRODUCTION

This chapter describes new chondrichthyan records from the Permian–Triassic shallow marine continental margins of northern and northeastern Pangaea in the Boreal Sea and eastern Panthalassa, respectively. The new records are based on material from localities in East Greenland, Spitsbergen, Canada (Ellesmere Island, British Columbia), and the southwestern USA (Figure 5.1). The occurrences are summarised in Table 5.2 and the systematic palaeontology of all taxa is provided in Appendix A3.2.

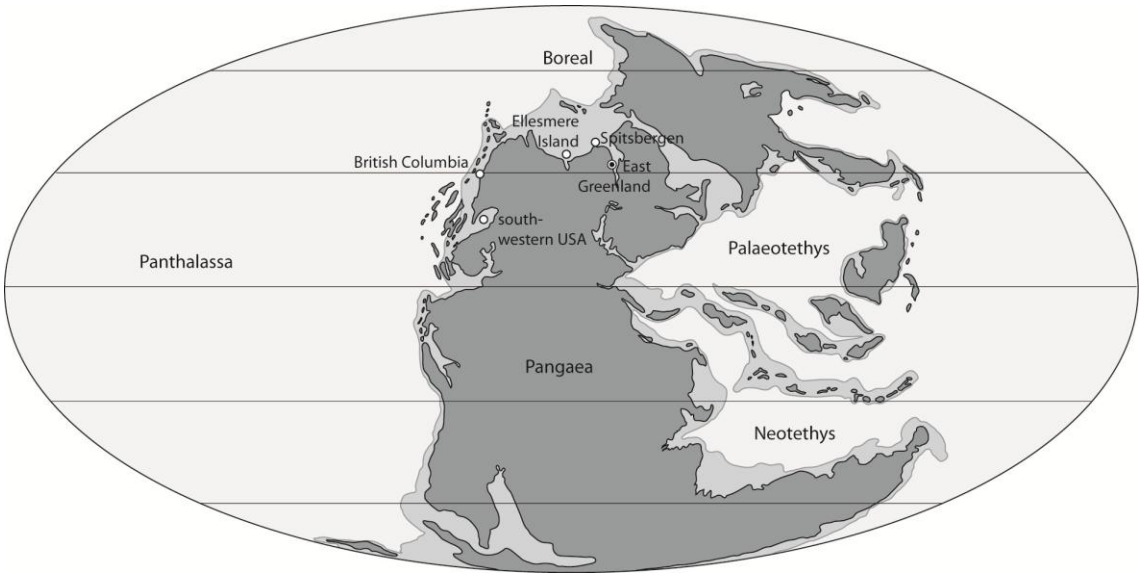

Figure 5.1 – Mollewide plate tectonic map of the Late Permian (260 Ma; modified from Blakey 2012). Circled dots represent localities from which material was directly obtained through fieldwork, whereas open dots represent localities from which material was indirectly obtained.

5.2 EAST GREENLAND

5.2.1 GEOLOGICAL SETTING

The formation of East Greenland in the Palaeozoic is marked by the Caledonian Orogeny, which resulted in a roughly 1300 km long north-south oriented fold belt, after which Greenland became part of the supercontinent Pangaea (Henriksen 2008). The East Greenland Basin was among the shallow seas and narrow straits that existed at the time (Henriksen 2008). Palaeozoic and early Mesozoic sediments were deposited in the N–S oriented basin that is up to 100 km wide and 400 km long (Birkelund and Perch-Nielsen 1976). The successions record the sedimentary response to changes in palaeoclimate and basin-forming processes after the Caledonian Orogeny (Stemmerik 2000) at a palaeolatitude of approximately 35° N (Scholle *et al.* 1993). The East Greenland Basin encompasses typical rift basins, including the Jameson Land Basin in the south (Birkelund and Perch-Nielsen 1976; Figure 5.2). Continental sandstones were deposited through to the Cisuralian, after which increased subsidence during the Guadalupian marked the start of marine sedimentation, as the sea transgressed from the north (Henriksen 2008). The resulting deposits (over 900 m thick) include marine reefal limestones, black shales, and evaporites (e.g., gypsum and halite), and have been largely unaffected by later deformation or metamorphism (Henriksen 2008). A well-preserved and common Lopingian and Induan fish fauna is recorded (e.g., Nielsen 1932, 1935, 1936, 1952; Stensiö 1932, 1961; Bendix-Almgreen 1976, 1993). In the Early Triassic, the deposition of continental sandstones resumed (Henriksen 2008).

Lithostratigraphy

Guadalupian–Lopingian sediments are represented by the Foldvik Creek Group (Figure 5.3). The fluvio-marine conglomerates of the Huledal Formation reflect a shallow inland braidplain fed by alluvial fans, which slowly changed to a wide, very shallow, protected marine bay dominated by fluviatile deposits (Surlyk *et al.* 1986). The shallow marine carbonates and evaporites of the Karstryggen Formation represent the

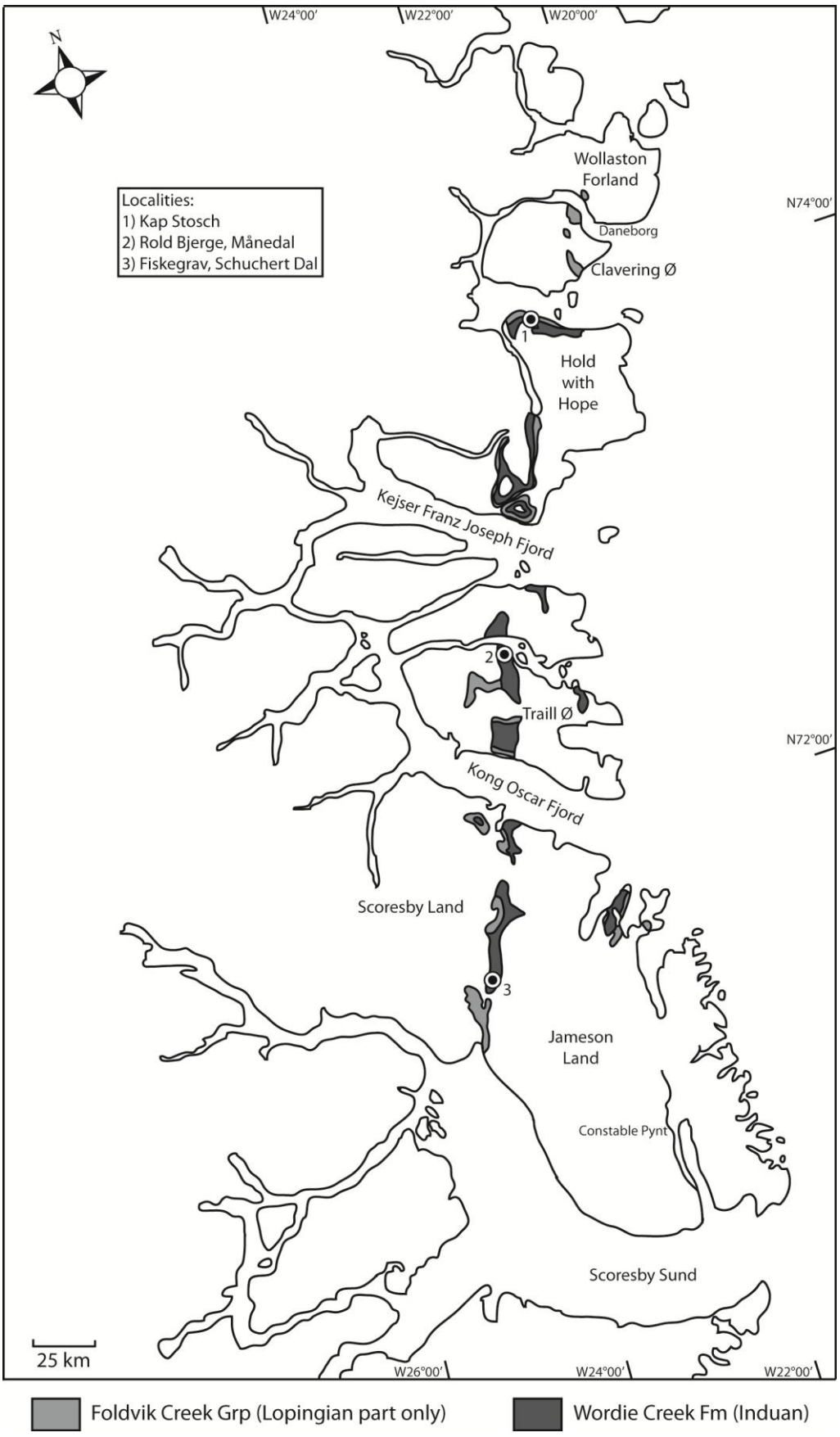

Figure 5.2 – Geological map of central East Greenland showing Lopingian and Induan exposures and sampling localities (modified from the Geological map of Greenland, segment 12, see Henriksen *et al.* 2009 and Bjerager *et al.* 2006).

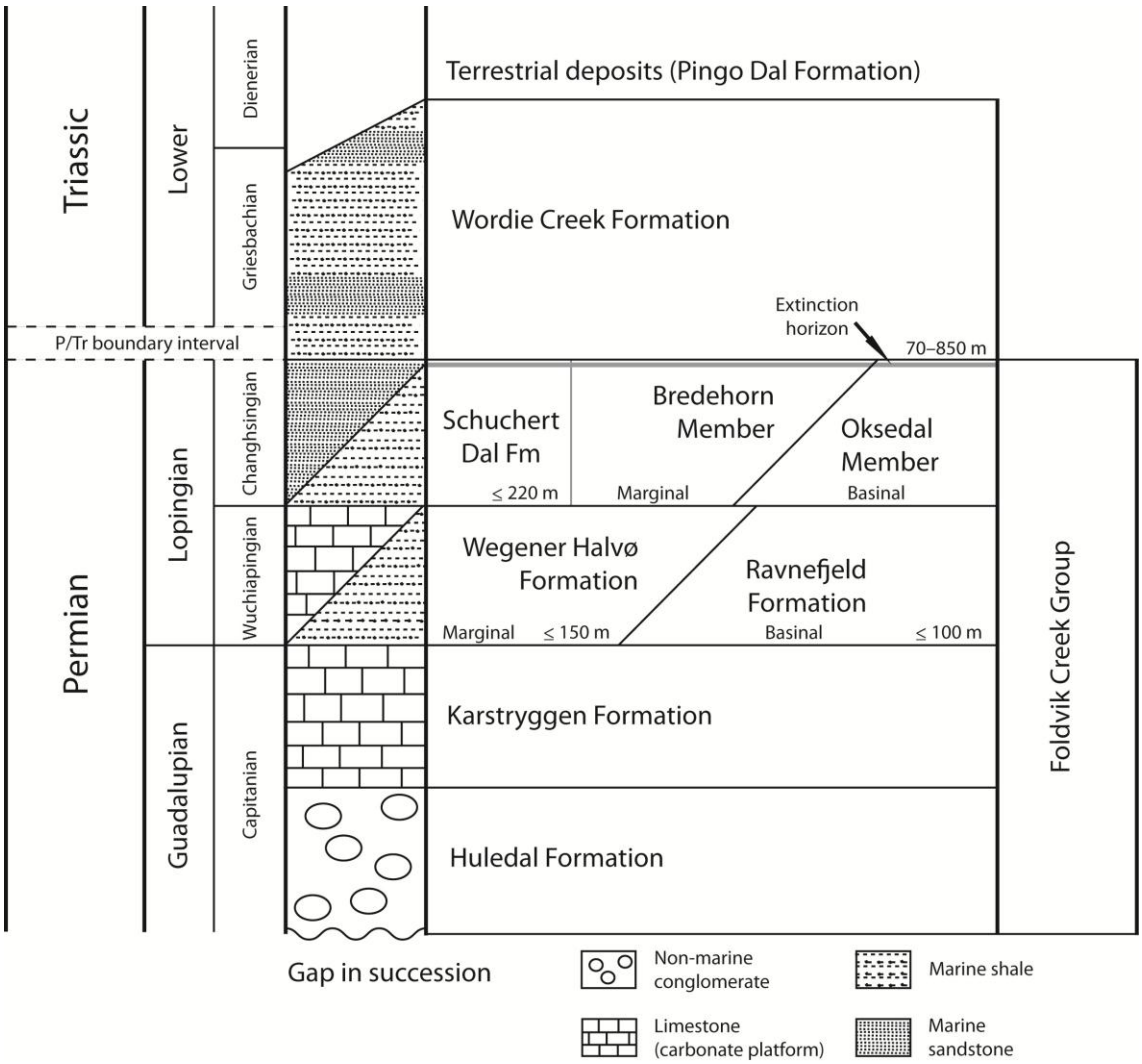

Figure 5.3 – Lithostratigraphy of the East Greenland Basin (based on data presented in Surlyk *et al.* 1986; Stemmerik 2000; Stemmerik *et al.* 2001; Bjerager *et al.* 2006; Henriksen 2008; and Nielsen *et al.* 2010). Position of extinction horizon based on Twitchett *et al.* (2001).

first fully marine deposits (Surlyk *et al.* 1986; Stemmerik *et al.* 2001). A sea level rise in the Lopingian resulted in the deposition of basinal black laminated shales (Ravnefjeld Formation) and marine carbonates along basin margins and over structural highs (Wegener Halvø Formation; Surlyk *et al.* 1986; Piasecki and Stemmerik 1991; Stemmerik *et al.* 2001). Limestone beds in the Ravnefjeld Formation were formerly known as the *Posidonia* Shale and the *Martinia* Beds (Rasmussen *et al.* 1990). These deposits are overlain by the light grey bioturbated shales and siltstones of the Schuchert Dal Formation, followed by the Lower Triassic Wordie Creek Formation (Surlyk *et al.* 1986; Nielsen *et al.* 2010).

There was a change in depositional conditions between the Schuchert Dal and Wordie Creek formations, indicated by the well-oxygenated upper Oksedal Member and the contrasting anoxia of the lower Wordie Creek Formation (Wignall and Twitchett 2002b; Nielsen and Shen 2004; Fenton *et al.* 2007; Nielsen *et al.* 2010). The formational contact is believed to be discontinuous throughout the basin by some authors (e.g., Seidler 2000), whereas others believe some sections are continuous, at least in southern regions such as Schuchert Dal (e.g., Perch-Nielsen *et al.* 1972; Surlyk *et al.* 1986; Twitchett *et al.* 2001; Wignall and Twitchett 2002b; Bjerager *et al.* 2006). The Schuchert Dal Formation may indeed be largely missing at Hold with Hope, due to the greater subsidence in the western, down-tilted part of the basin (e.g., Surlyk *et al.* 1986). The incised submarine channel fills in the upper Schuchert Dal Formation and at the base of the Wordie Creek Formation occurring in the Schuchert Dal area are interpreted as the result of the basin subsidence during a period of sea level rise (Wignall and Twitchett 2002b).

Biostratigraphy

A palynostratigraphy (Balme 1979; Piasecki 1984) and ammonoid zonation (Bjerager *et al.* 2006) have been constructed for the East Greenland Basin, and conodonts have also been recovered (Sweet 1976; see also Stemmerik *et al.* 2001). Ammonoids, conodonts and $\delta^{13}C$ isotopic data, as well as palynology and invertebrate data, show that the Late Permian extinction horizon occurs in the uppermost Schuchert Dal Formation, prior to the P/Tr boundary (Twitchett *et al.* 2001; Wignall and Twitchett 2002b; Bjerager *et al.* 2006; Figure 5.3), as is the case globally (e.g., Yin *et al.* 2001). The First Appearance Datum (FAD) of *Hindeodus parvus* has been placed in the lower Wordie Creek Formation, at the boundary of the *Hypophiceras triviale* (Changhsingian) and *Hypophiceras martini* (Griesbachian) zones (Bjerager *et al.* 2006). According to Bjerager *et al.* (2009), these two zones can probably be correlated with the *Otoceras concavum* Zone of Arctic Canada and northeast Siberia, because fragmented *Otoceras* sp. has been recovered from Hold with Hope. Twitchett *et al.* (2001) suspect that the

FAD of *H. parvus* may still be placed somewhat lower down in the Wordie Creek Formation, predominantly based on a sampling gap, but also the recovery of poorly preserved *Hindeodus* sp. elements in association with the bivalve *Claraia* in western Jameson Land, which does not usually occur in the pre-*parvus* interval. The Wuchiapingian Ravnefjeld and Wegener Halvø formations are definitively assigned to the *Cyclolobus kullingi* Zone, but the Changhsingian age of the Schuchert Dal Formation relies mostly on palynological data (see Stemmerik *et al.* 2001), because its assignment to the *Paramexicoceras/Changhsingoceras* Zone is merely based on the tentative identification of *Changhsingoceras*? from the Traill Ø sub-basin (Bjerager *et al.* 2006).

5.2.2 Material

The material comprises 54 samples (bulk and hand samples; Appendix A1.1) originating from Wuchiapingian–Griesbachian strata at three localities (Figure 5.2): Kap Stosch on the northern coast of Hold with Hope at N 74°01'12" W 21°30'00" (Figure 5.4); Rold Bjerge in Månedal, northern Traill Ø at N 72°47'06" W 23°12'36" (Figure 5.5); and Fiskegrav in Schuchert Dal, western Jameson Land at N 71°32'25" W 24°19'59" (Figure 5.6). The lithology of these samples consists predominantly of limestones, cemented silt/sandstones, and clay/siltstones.

5.2.3 Results

In total, 27 samples were collected from Kap Stosch (Figure 5.4), as well as seven samples from Traill Ø (Figure 5.5), and 20 from Fiskegrav (Figure 5.6). The samples labelled with '09.8.' were collected by R.J. Twitchett (Plymouth University). In Kap Stosch, four of the samples originated from the Wuchiapingian Ravnefjeld Formation, 12 from the Changhsingian Schuchert Dal Formation, and 11 from the Griesbachian Wordie Creek Formation. In Traill Ø, three samples originated from the Wuchiapingian Ravnefjeld Formation and four samples from the lowermost Griesbachian Wordie

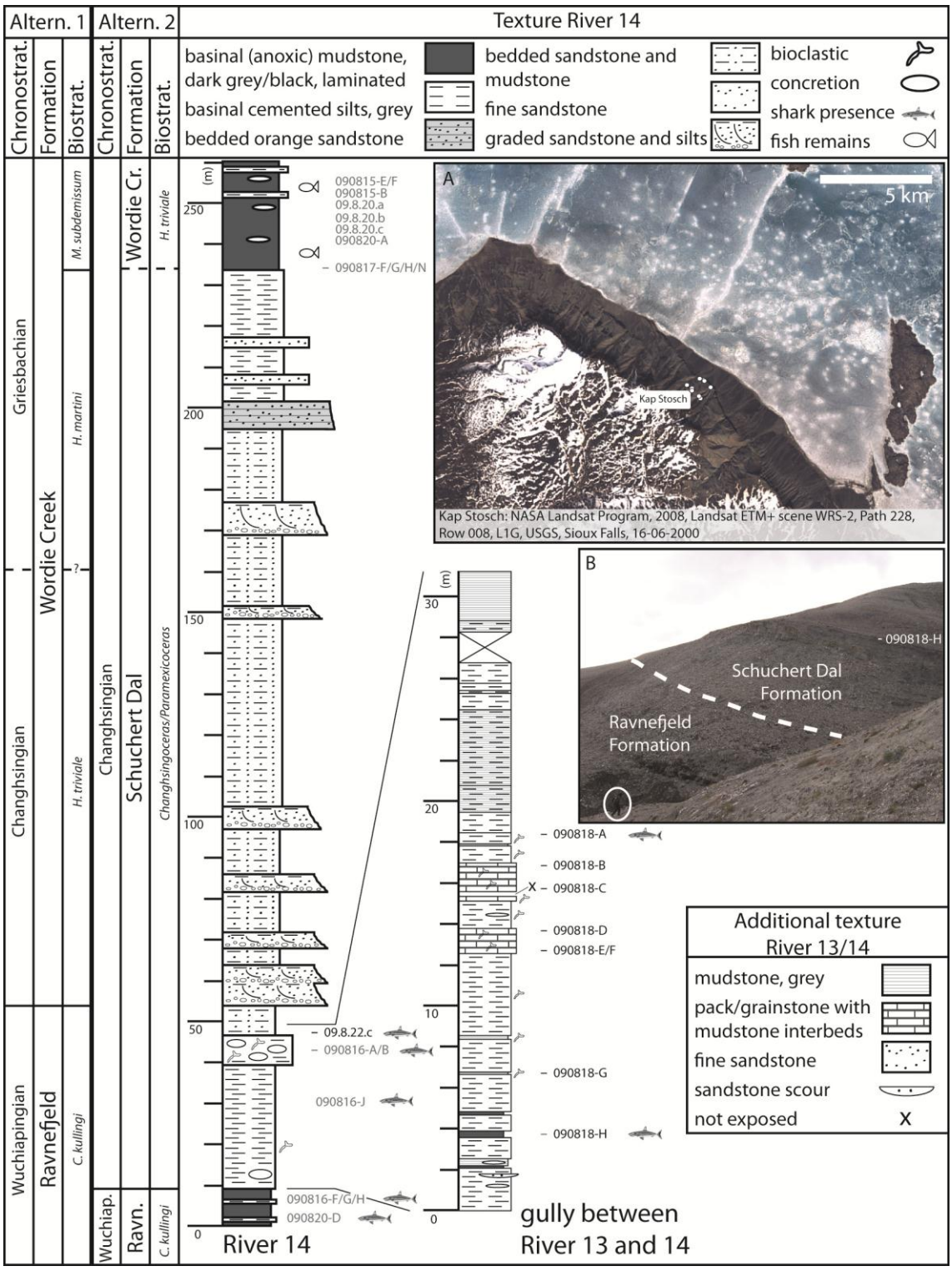

Figure 5.4 – Stratigraphic log of Kap Stosch on Hold with Hope, East Greenland (Twitchett, unpub. data). Sampling heights are indicated: black sample numbers are *in situ*, grey are *ex situ*; grey height markers are approximate, absent markers signify best approximation. The stratigraphy is disputed, hence two alternative schemes are provided: (1) Bjerager *et al.* (2009); and (2) Twitchett, unpub. data. Sample ages follow alternative 2. A, Satellite image (Global Land Cover Facility) of sampled localities (white circles). B, View to the southeast of slope between rivers 13 and 14 containing the transition from the Ravnefjeld Formation to the Schuchert Dal Formation (alternative 2). A person (circled) provides the scale.

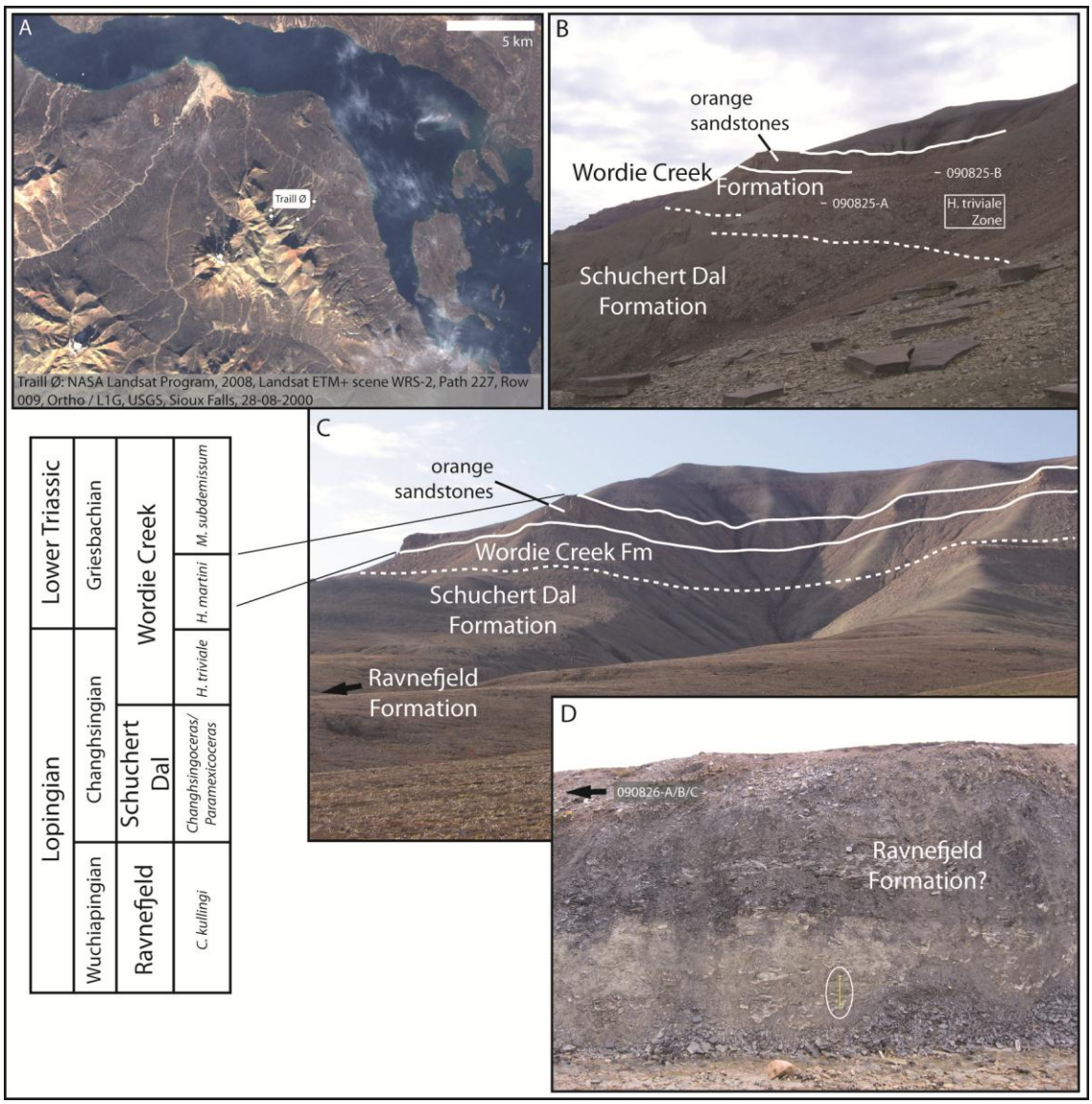

Figure 5.5 – Geographic position and general stratigraphy of Rold Bjerge in Månedal on Traill Ø, East Greenland. A, Satellite image (Global Land Cover Facility) of sampled localities (white circles). B, View to the southeast of slope showing the position of the thick sandstone bed in the lower Wordie Creek Formation. Slabs in foreground are approximately 50 cm across. C, Wide view to the southeast showing outcrop of general stratigraphy (based on Bjerager *et al.* 2009). Hills in the background reach maximally 600–650 m above camera-level. D, View to the southeast of thinly bedded anoxic black shales in low-lying easternmost locality (N 72°46'55.1" W 23°09'48.8"). Scale provided by one metre ruler (circled).

Creek Formation. In Schuchert Dal, three samples were collected from the Changhsingian Schuchert Dal Formation (*ex situ*). From the Wordie Creek Formation, five originated from the Changhsingian sequence and 12 from the Griesbachian sequence.

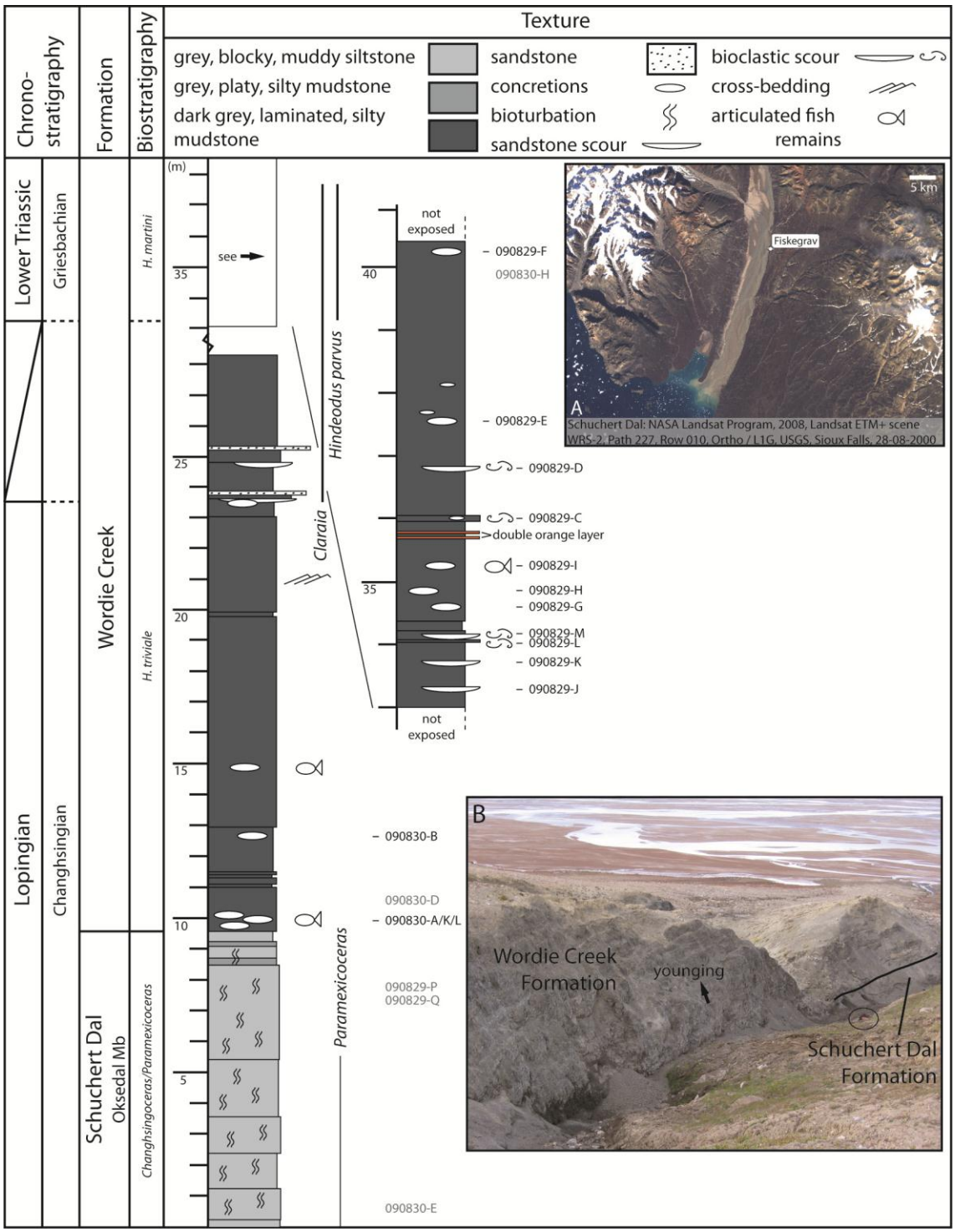

Figure 5.6 – Stratigraphic log of Fiskegrav in the Schuchert Dal area, East Greenland (redrawn from Twitchett *et al.* 2001; Fenton *et al.* 2006). Inset: updated top section, based on Twitchett, unpub. data. Sampling heights are indicated (samples collected *ex situ* marked in grey). A, Satellite image (Global Land Cover Facility) of sampled localities (white circles). B, View of the lower part of the section towards the southwest, with backpack for scale (circled).

Attempts at processing five samples (090818-B/C/D/E/F) from Kap Stosch using the buffered formic acid technique showed that the high siliciclastic content of the samples from East Greenland increases the amount of time required for digestion (from days/weeks to weeks/months). Time restrictions therefore steered the focus away from dissolution, which means that no results from these attempts are available. Hand samples from Kap Stosch, however, revealed chondrichthyan remains in nine samples from the Wuchiapingian–Changhsingian. These specimens were partially encased in matrix, but generally sufficiently exposed to observe the morphological characteristics required for identification.

In three samples of Wuchiapingian–Changhsingian age, remains of indeterminate spines were observed (Appendix A3.2). In five additional samples of the same age, numerous teeth of *Fadenia crenulata* Nielsen, 1932 were identified, which signifies the first confirmed occurrence of this genus in the Changhsingian. One sample (09.8.22.c) was mechanically prepared to further expose a tooth encased in matrix, using an air pen. The specimen could not be completely exposed, however, due to its brittle nature and preparation was stopped to avoid irreparable damage to this unique specimen. Its precise affinities remain indeterminate, but the morphology suggests an eugeneodontiform chondrichthyan (Appendix A3.2). The presence of tubercles on the labial projections and the inward curvature of the projections flanking the main cusp have not previously been recorded in the literature and suggest that it is an undescribed taxon. The new chondrichthyan occurrences described here are discussed in relationship to previous records in Section 5.6.

5.3 SPITSBERGEN

5.3.1 GEOLOGICAL SETTING

In the Svalbard Archipelago (Spitsbergen), positioned on the Barents Sea continental shelf, Triassic strata consisting of frequent siltstones and sandstones are well-exposed

Figure 5.7 – Locality map of Spitsbergen: Vendomdalen (1) and Lusitaniadalen (2); modified from Nabbefeld *et al.* (2010).

and conformably overlie Permian strata (Cox and Smith 1973). The Lower–Middle Sassendalen Group is entirely marine, whereas the Middle–Upper Triassic Kapp Toscana Group is predominantly non-marine, with the exception of the marine, vertebrate-bearing Tschermakfjellet and De Geerdalen formations (Cox and Smith 1973). These formations generally represent a west to east prograding delta front succession (Hounslow *et al.* 2007). The region around both studied sections (Figure 5.7) lies in the northeastern part of the Central Tertiary Basin of southern Spitsbergen (Ny Friesland Block; Hounslow *et al.* 2007).

5.3.2 VENDOMDALEN

In Vendomdalen, central Spitsbergen, the Tschermakfjellet Formation consists of grey shales with thin, cross-laminated, sandstone beds in the upper part, which grade into sandstones of the De Geerdalen Formation (including the Isfjorden Member), while coarsening upwards (Hounslow *et al.* 2007). One sample from Dalsnuten section (N 78°11′52″ E 17°23′46″) in Vendomdalen was examined (residue; Appendix A1.1),

collected by M. Hounslow (Lancaster University) from the Carnian (Upper Triassic). It yielded one indeterminate tooth-like specimen that is not chondrichthyan in origin.

5.3.3 LUSITANIADALEN

In Lusitaniadalen, central Spitsbergen, a Changhsingian–Induan exposure was measured by Nabbefeld *et al.* (2010), including the upper part of the Kapp Starostin Formation and the Deltadalen Member of the Vikinghøgda Formation (Figure 5.8). This section (N 78°17′54.8″ E 16°43′59.3″) comprises three main lithofacies, with well-bioturbated, glauconite-rich sandstones in the lower part. The middle part consists of laminated, dark grey mudstones, deposited in deep water under anoxic conditions, with infrequent thin sandstone beds and tabular carbonate-rich concretions. The upper part comprises grey siltstones with fine sandstone interbeds with returning bioturbation (Nabbefeld *et al.* 2010). Two samples (bulk, cumulative mass 520 g; Appendix A1.1) were collected by R.J. Twitchett (Plymouth University; Figure 5.8), one of which from the tabular carbonate-rich concretionary levels, bearing fragments of marine fish of uppermost Changhsingian (Lopingian) age. The other is of a clay/siltstone bonebed of the same age. This latter lithology proved unresponsive to processing, resulting in the recovery of only one actinopterygian tooth. The presence of chondrichthyan remains could not be determined. The concretionary sample, however, yielded numerous tooth fragments, which have been identified as *Palaeobates* sp., a hybodont genus that is known from the Induan (Dienerian) and Olenekian (Smithian–Spathian) of Sassendalen, Isfjorden and Hornsund, Spitsbergen, including from the Vikinghøgda Formation (Stensiö 1921; Romano and Brinkmann 2010).

The exact position of the base of the Vikinghøgda Formation is unclear, because of the absence of a marker bed, as is the precise position of the Permian/Triassic boundary in this section. Despite previous correlation of the boundary with the base of the Vikinghøgda Formation (see Mørk *et al.* 1999), recent magnetostratigraphic evidence places it about 12 m above the base (Hounslow *et al.* 2008), which is

consistent with global evidence and the onset of marine ecosystem collapse, which which has been placed at 16.32 m in the section (Nabbefeld *et al.* 2010), and thus confirms the uppermost Changhsingian age of the samples.

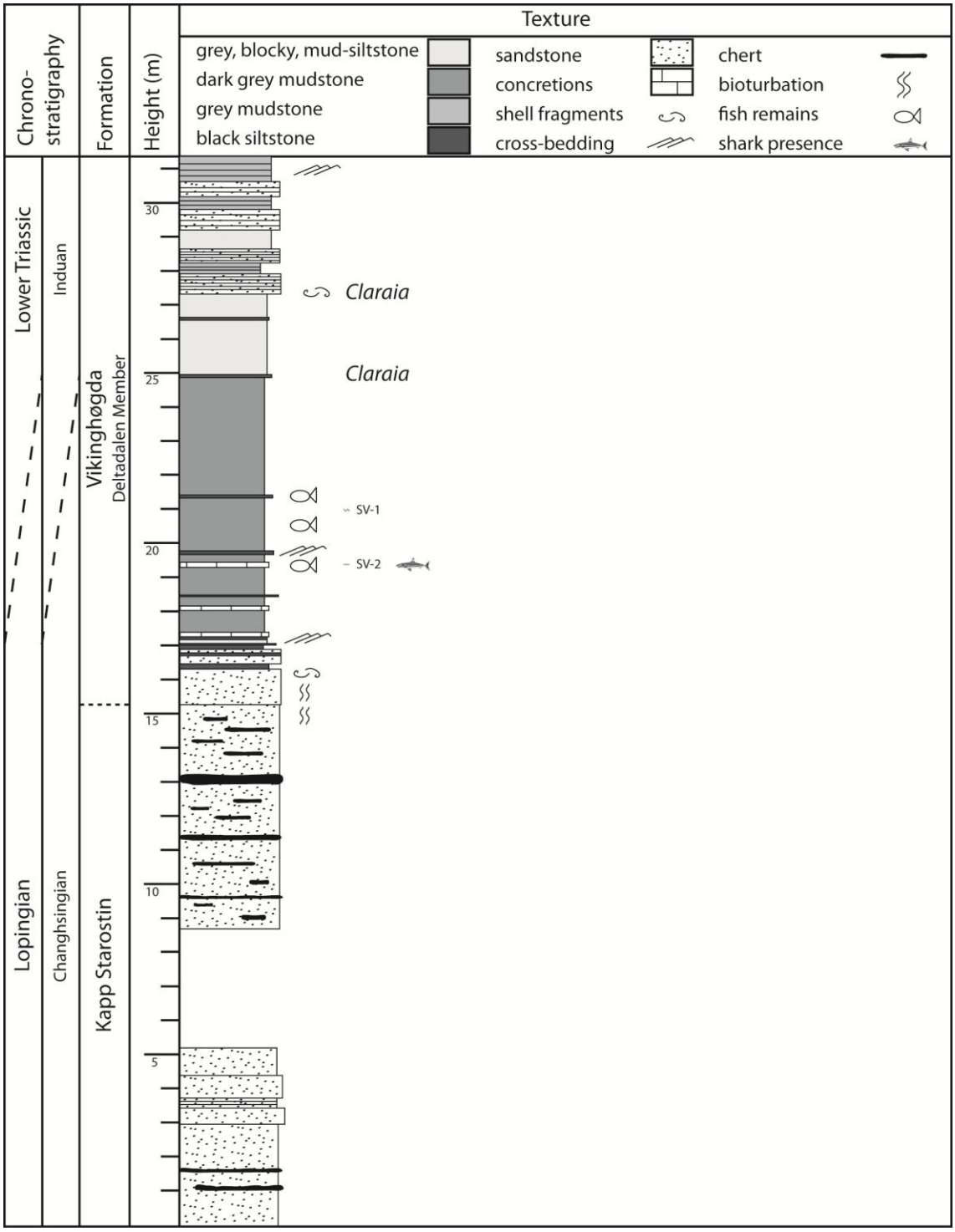

Figure 5.8 – Stratigraphic log of Lusitaniadalen, central Spitsbergen (redrawn from Nabbefeld *et al.* 2010). Approximate sampling heights are indicated.

5.4 CANADA

5.4.1 BRITISH COLUMBIA

Multiple chondrichthyan records are known from British Columbia and Alberta in western Canada. Sharks recorded from the Permian comprise solely the eugeneodontiform genus *Helicoprion* from the Cisuralian (e.g., Logan and McGugan 1968). Eugeneodontiforms ranged into the Early Triassic in this area, during which time they were represented by three genera: *Caseodus*, *Fadenia*, and *Paredestus* (Mutter and Neuman 2008). *Listracanthus* denticles are also known from the Lower Triassic (Mutter and Neuman 2009), as well as the hybodontiform genus *Homalodontus* (Mutter *et al.* 2007a, 2008a). The Hybodontiformes were represented in the Middle–Late Triassic by *'Polyacrodus'* (reassigned to *Omanoselache* in this study) and *Acrodus* (Johns *et al.* 1997). *'Synechodus'*, a neoselachian genus, also occurred in the Middle–Late Triassic (Johns *et al.* 1997).

Orchard and Zonneveld (2009) studied sections in the Kakwa area (including Wapiti Lake) of the Canadian Rocky Mountains, British Columbia, Canada, where Lower–Middle Triassic deposits are exposed. One of their samples (residue; Appendix A1.1) was obtained from Cirque C at Ganoid Ridge, located to the southeast of Wapiti Lake. It was collected from talus blocks from the Vega Member of the Sulphur Mountain Formation. The Vega Member is Olenekian in age and is composed of interlaminated silty shale and siltstone at the base, grading upwards to interlaminated siltstone and very fine-grained sandstone (Orchard and Zonneveld 2009). The sample is of suggested Smithian age, based on conodonts (Orchard and Zonneveld 2009). Although chondrichthyan remains were previously recovered from the Olenekian at Ganoid Ridge, including hybodonts (Mutter *et al.* 2007a, 2008a) and eugeneodontiforms (Mutter and Neuman 2008), the sample studied here only yielded one fish element, which remains unidentified and is potentially actinopterygian in origin.

5.4.2 Ellesmere Island

Geological setting

The Sverdrup Basin is a major late Palaeozoic depocentre that was initiated following an Early Carboniferous rifting phase and which underwent subsidence from the Middle Permian onwards (Stephenson *et al.* 1987; Harrison 1995). It formed a deep-water trough fully connected with Panthalassa to the west (Beauchamp *et al.* 2001) that never experienced subaerial exposure, but condensed intervals or hiatuses may be present (Grasby and Beauchamp 2008). Grasby and Beauchamp (2008) showed that a continuous Permian–Triassic succession is present in the basin centre, whereas Late Permian strata are missing on the basin margin, where a significant latest Permian unconformity occurs (Figure 5.9). The Sverdrup Basin currently forms a 1200 km long, 400 km wide, and 12 km thick deposit underlying the Canadian Arctic islands, one of which is Ellesmere Island.

Material

Samples from Ellesmere Island were collected by C.M. Henderson in 1979 as part of an MSc thesis project and reported in Henderson (1988). The eight samples utilised here (residue; Appendix A1.1) originate from a number of localities and formations spread across the northern part of the island (Figure 5.9). Two samples were collected from brachiopod-rich sandstones of the Roadian Assistance Formation (Figure 5.10) on Hamilton Peninsula, located at N 80°03'11" W 81°45'42". Glauconitic and fossiliferous sandstones of the Wordian Trold Fiord Formation were sampled twice in the same location on Hamilton Peninsula, twice at Henrietta Nesmith, located at N 81°50'26" W 72°10'59", and once at McKinley Bay, located at N 81°10'05" W 79°14'17". One further sample was collected from Middle–Upper Triassic shale and siltstones of the Blaa Mountain Formation on Blaa Mountain, located at N 80°33'19" W 86°15'21". The age determination of the Guadalupian strata was aided by the recovery of index fossils from the Trold Fiord Formation, such as brachiopods, conodonts, ammonoids, and palynomorphs (e.g., Henderson and Mei 2000). The sampled Roadian–Wordian strata

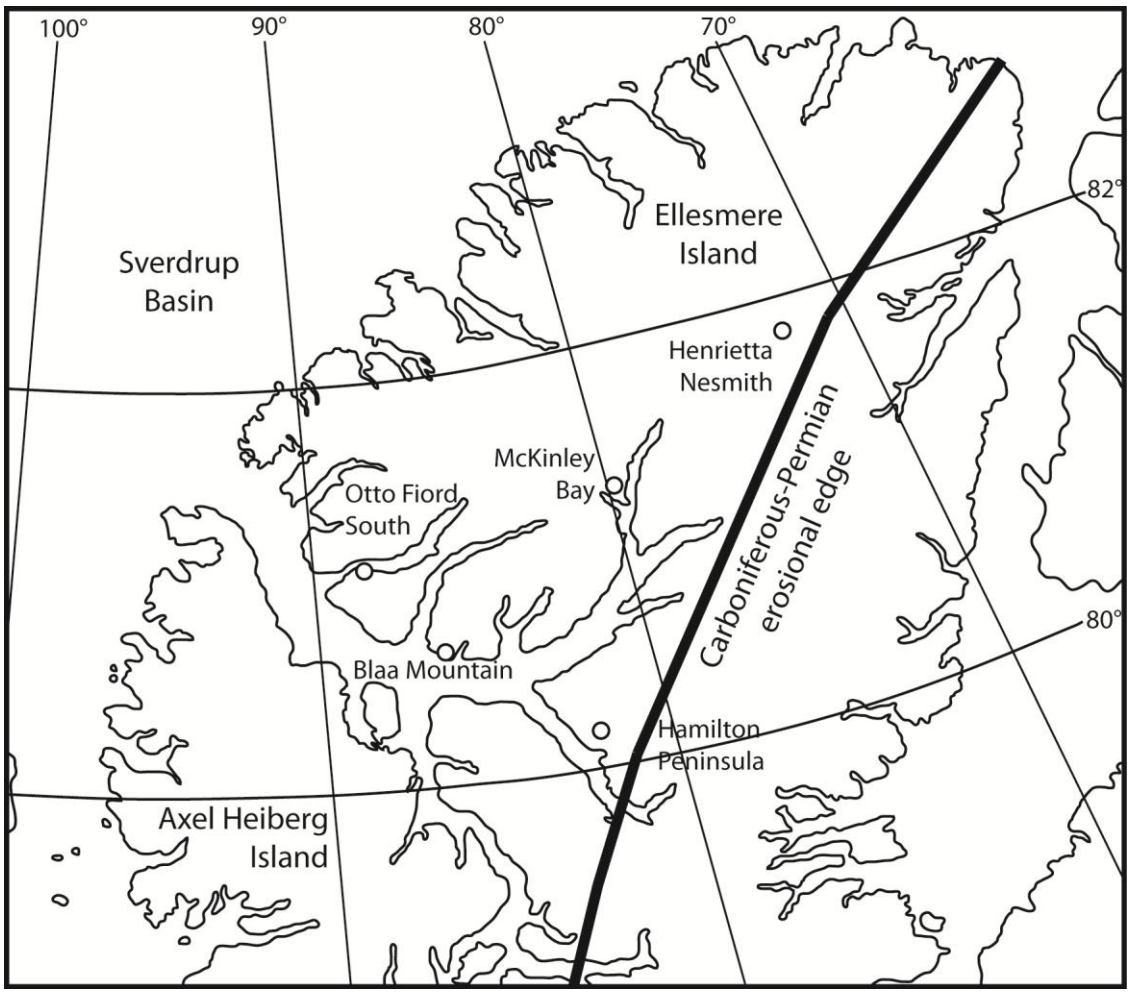

Figure 5.9 – Map of northern Ellesmere Island with sampled localities (modified from Orchard 2008), showing the outline of the Sverdrup Basin (erosional edge; based on Grasby and Beauchamp 2008).

are representative of a mid-shelf depositional environment, whereas the Middle–Upper Triassic bed is representative of a deep shelf (B. Beauchamp, pers. comm. 2012; Figure 5.10).

Triassic deposits on Ellesmere Island have been extensively sampled by Orchard (2008). One sample (residue; Appendix A1.1) from this set is studied here. It originated from the Confederation Point Member in the Blind Fiord Formation, exposed at Otto Fiord South. It has been assigned to the *Bukkenites strigatus* ammonoid Zone, which correlates to a late Griesbachian (Induan) age, and is also dominated by members of the *Neogondolella carinata* group, including *Ng. planata* and *Ng. nevadensis* (Orchard 2008). The Blind Fiord Formation is typically composed of shales and siltstones, deposited in the basin centre (deep shelf; Figure 5.10).

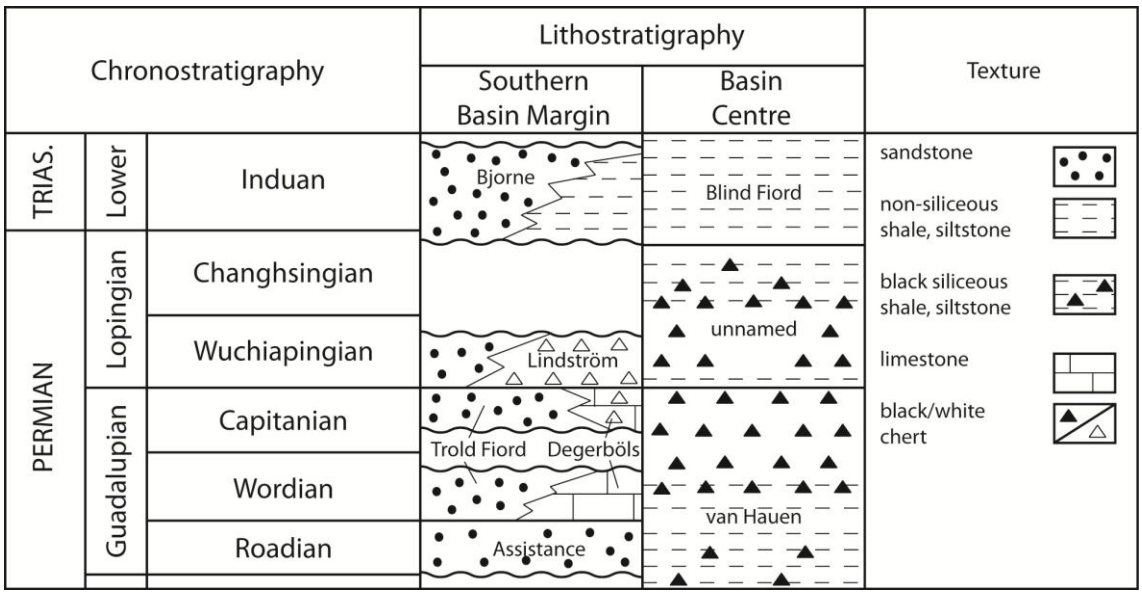

Figure 5.10 – Lithostratigraphic relationships between formations from the southern basin margin to the basin centre in the Sverdrup Basin (adapted from Grasby and Beauchamp 2008).

Results

The Guadalupian samples yielded a total of 17 chondrichthyan specimens, most of which remain unidentified because of the fragmentary nature of the specimens. Nevertheless, the Roadian material from the Hamilton Peninsula comprises two elasmobranch dermal denticles, distinguished as morphotypes 22 and 23 (Appendix A3.2). The Wordian samples from the Hamilton Peninsula yielded three unidentifiable elasmobranch tooth fragments. One further unidentifiable elasmobranch tooth fragment was recovered from the Wordian of McKinley Bay. Eleven specimens were recovered from the Wordian at Henrietta Nesmith, comprising not only unidentifiable elasmobranch tooth fragments, but also a tooth fragment of potential homalodont affinities and dermal denticles distinguished as morphotype 24. Most importantly, however, those same samples yielded three tooth fragments of *Adamantina* Bendix-Almgreen, 1993 (Appendix A3.2), which is rare in the Boreal region. This study represents the first record of this genus from the Canadian Arctic, as well as its first record from the Guadalupian.

Three chondrichthyan tooth fragments were recovered from the Griesbachian at Otto Fiord South, which have been identified as *Caseodus* sp. cf. *C. varidentis* Mutter and

Neuman, 2008 and *Homalodontus* sp. cf. *H. aplopagus* (Mutter, De Blanger and Neuman, 2007). These taxa were previously only known from Olenekian deposits of western Canada (Mutter *et al.* 2007a; Mutter and Neuman 2008), and so these new specimens represent the oldest record for both genera and extend their distributional range to the Boreal region.

The Middle–Late Triassic sample from Blaa Mountain yielded two chondrichthyan tooth fragments, which have been identified as elasmobranch tooth cusps. One of these may have hybodont affinities. These new chondrichthyan occurrences are discussed in relationship to previous records in Section 5.6.

5.5 SOUTHWESTERN USA

5.5.1 INTRODUCTION

An overview of fishes from North America is provided by Wilson and Bruner (2004). It shows that the most important fossil fish assemblages, including chondrichthyans, occur in the Lower Triassic marine deposits of the Wapiti Lake area, western Canada (e.g., Schaeffer and Mangus 1976; Mutter *et al.* 2007a, Mutter and Neuman 2008), in the Middle–Upper Triassic of the Peace River area, western Canada (e.g., Johns *et al.* 1997), as well as in the Upper Triassic freshwater deposits of the Newark Supergroup in the eastern USA (e.g., Bryant 1934) and the Dockum and Chinle groups in the western interior USA (e.g., Huber *et al.* 1993). However, this study shows the increasing importance of the chondrichthyan fauna recovered from a large shallow marine embayment on the western Pangaean continental margin, exposed in the southwestern USA.

5.5.2 GEOLOGICAL SETTING

Exposures of marine Permian–Triassic strata can be found at numerous localities in the southwestern USA. These strata were deposited in eastern Panthalassa, in an

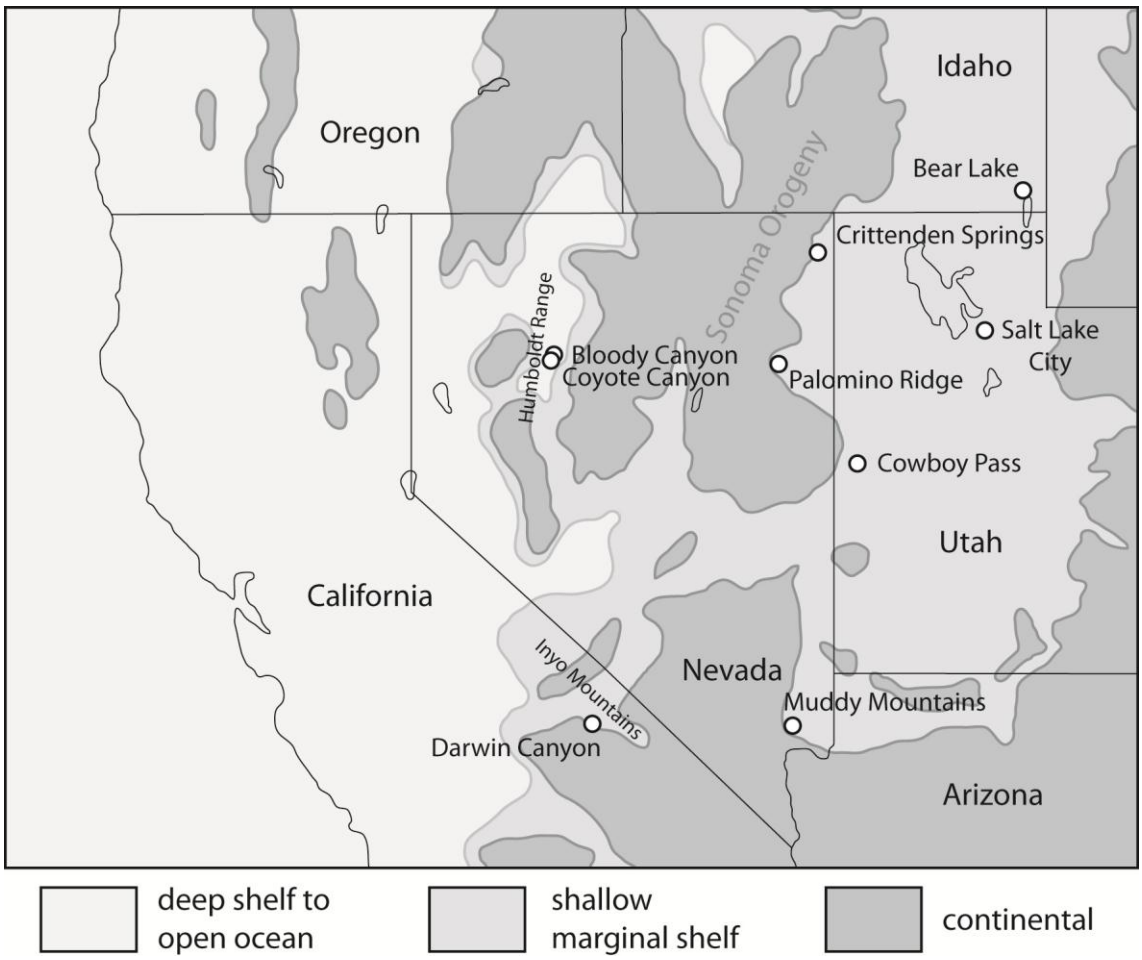

Figure 5.11 – Geographic position of localities in the southwestern USA (open circles) overlain on the Early Triassic (245 Ma) palaeogeographic marginal shelf environment (after Blakey 2012; also Alvarez and O'Connor 2002 and Fraiser and Bottjer 2007).

embayment in the northwestern margin of Pangaea (Figure 5.1). The depositional environment during the Early Triassic in this region is interpreted as a marine passive margin characterised by a broad shallow epicontinental shelf (Marzolf 1993; Figure 5.11). A global eustatic sea-level rise occurred around the Permian/Triassic boundary (e.g., Hallam and Wignall 1999) and some palaeontological evidence indicates that the Lopingian may not be missing throughout the southwestern USA (Alvarez and O'Connor 2002), despite previous suggestions of a significant gap in the sedimentary record as a result of emergence (see Schubert and Bottjer 1995)

Samples were obtained from localities in Nevada, Idaho, Utah, and California, and are Guadalupian/Lopingian?, Induan?, Olenekian (Smithian–Spathian) and Anisian in age. Different lithostratigraphic schemes are used in areas across the region

(Figure 5.12). The sampled localities in southeastern Idaho, northeastern Nevada, and northern and western Utah (Figure 5.11) are outcrops of the Thaynes Formation. The Prida Formation of the Star Peak Group is exposed in localities in north-central Nevada, the Moenkopi Formation in southern Nevada, and the Union Wash Formation in east-central California. In virtually all cases, insufficently detailed data are available to construct individual locality maps and stratigraphic logs showing sampled beds, but generally representative maps and logs of most areas are shown in Guex *et al.* (2010; Cowboy Pass; Hot Springs, Paris Canyon and Hammond Creek at Bear Lake; Bloody and Coyote Canyon; and close to Darwin Canyon) and Pruss *et al.* (2005; Muddy Mountains). A detailed log for Palomino Ridge is shown in Jacobsen *et al.* (2011).

The Thaynes Formation is subdivided into four facies belts (Carr 1981; Carr and Paull 1983). These belts include: (1) a basinal anoxic facies, consisting of dark grey to

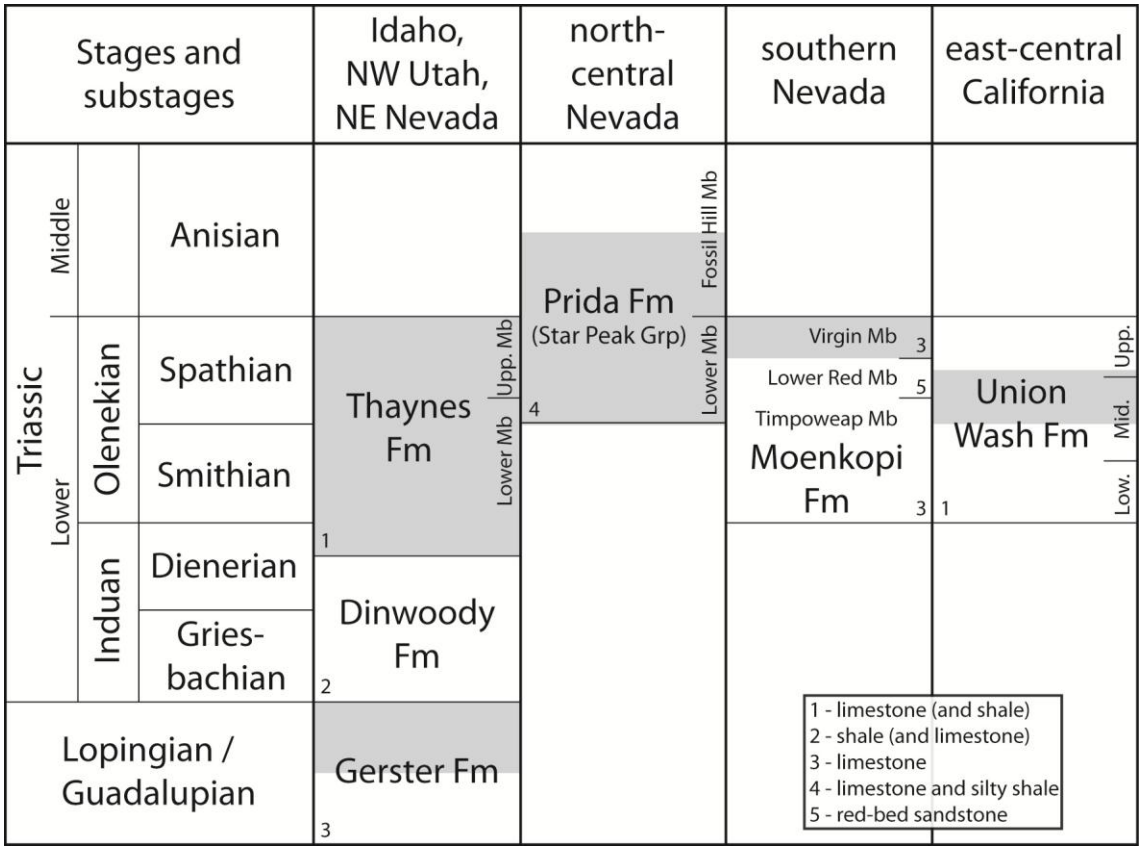

Figure 5.12 – Stratigraphy of Permian–Middle Triassic strata in the southwestern USA (compiled from Bucher 1992; Alvarez and O'Connor 2002; Fraiser and Bottjer 2004, 2007; Pruss *et al.* 2005). Only relevant stratigraphy is shown. Sampled intervals are highlighted in grey.

black silty lime mudstones, siltstones and shales; (2) a normal open marine shelf facies, mainly characterised by dark grey to brown ammonoid-rich wackestone (deposited at or just below wave base) and light grey bioclastic grainstone (above wave base); (3) an inner shelf facies, composed of mainly mudstone and silty limestone (shallow subtidal and intertidal environment); and (4) a red bed facies (Carr 1981; Carr and Paull 1983; see also Schubert and Bottjer 1995). The inner shelf facies characterises the Spathian upper member of the Thaynes Formation, deposited in Idaho and Utah (Newman 1974; see also Fraiser and Bottjer 2007; Figure 5.12).

The Star Peak Group, exposed in and towards the (south)east of the northern Humboldt Range (Figure 5.11), ranges from the Spathian to the Carnian, and is generally characterised by carbonate deposition (Sander *et al.* 1994). Here, an eastward transgression began around the Spathian/Anisian boundary, culminating in the mid–late Anisian (Bucher 1992). The Prida Formation, comprising an unnamed lower member overlain by the Fossil Hill Member (Figure 5.12), crops out in the western part of the Star Peak Basin. Deposits of the lower member are medium-grey to dark, thin-bedded micritic limestones (Goudemand *et al.* 2012), whereas the Fossil Hill Member consists of mainly thin-bedded black micritic limestones and silty shales (Bucher 1992), that were deposited below wave base and in a typically anoxic environment (Sander *et al.* 1994). The Anisian Fossil Hill Member of the correlative Favret Formation, exposed in the southern Tobin Range (Bucher 1992) and on the western slope of the Augusta Mountains, is already known to yield a rich chondrichthyan fauna (Rieppel *et al.* 1996; Cuny *et al.* 2001). It is characterised by thick-bedded, grey, shallow-water limestone (Sander *et al.* 1994) and has been interpreted as characteristic of a setting near the coast (Rieppel *et al.* 1996).

On the Colorado Plateau in the southern Nevada region, the Moenkopi Formation is Smithian–Spathian in age and consists of three members (Figure 5.12). The lower Timpoweap Member, composed of slightly fossiliferous Smithian limestone, is overlain by the unfossiliferous Spathian Lower Red Member (Alvarez and O'Connor 2002). The upper Virgin Member, however, consists of fossiliferous limestone (Alvarez and

O'Connor 2002). The Timpoweap Member is primarily a marginal marine deposit (Schubert and Bottjer 1995), whereas the Lower Red Member is non-marine in origin, and the Virgin Member was deposited in a normal marine subtidal shelf environment as the result of a marine incursion (Marzolf 1993; Schubert and Bottjer 1995; Pruss *et al.* 2005).

The Union Wash Formation is Smithian–Spathian in age (Figure 5.12) and is composed of micritic limestones and calcareous shales, deposited along the outer edge of the continental margin (Woods *et al.* 2007; Figure 5.11). The middle and upper members formed in a basinal slope setting (Stone *et al.* 1991). In the Darwin Canyon area, the upper member of the formation has been interpreted to have been deposited in an outer shelf to slope environment (Stone *et al.* 1991; Woods 1998; see also Woods *et al.* 2007).

5.5.3 Material

A total of 24 samples (residue and bulk) from the southwestern USA were studied (Appendix A1.1; Table 5.1).

5.5.4 Results

Of the 24 studied samples, 13 yielded chondrichthyan remains. The Guadalupian(/Lopingian?), Induan? and Anisian did not yield any chondrichthyan remains. Instead, all taxa have been recognised from the Olenekian. In total, 70 specimens have been recovered, which include non-elasmobranch remains, chondrichthyan denticles, possible spine fragments, unidentifiable tooth fragments and 22 identifiable teeth (Appendix A1.2). The identified taxa comprise *Omanoselache* sp. cf. *O.* sp. H and cf. *Omanoselache* sp. indet., as well as cf. *Hybodus* sp., Genus S sp. T, and *'Synechodus'* sp. (pre-Jurassic; Appendix A3.2), all of which have been recognised from the Spathian. Genus S sp. T was also observed in the Smithian of northern Utah (Figure 5.13). These results indicate a widespread hybodont presence in

the southwestern USA basin during Olenekian times, with *Omanoselache* tentatively recorded in three of the four studied formations. Also, the

Table 5.1 – Overview of sample data collected from the southwestern USA.

Location	**Stratigraphy**	**Age**	**#**	**Code**
Crittenden Springs, NE Nevada	Thaynes Fm	Smithian	1	W
Salt Lake City, N Utah	Thaynes Fm	Smithian	1	W
Georgetown, Paris Canyon & Hot Springs, near Bear Lake, SE Idaho	Thaynes Fm	Smithian–Spathian	3	W
Collector: W. Weitschat (University of Hamburg) Notes: The age of these samples has been determined on the basis of their conodont content (see Orchard and Zonneveld 2009; Orchard, pers. comm. 2010).				
Hammond Creek, near Bear Lake, SE Idaho	Thaynes Fm	Spathian	3	o-… 91-OF
Collector: E.T. Tozer (Geological Survey of Canada) Notes: The samples were collected as ammonoid blocks, from which the matrix was extracted and processed by M.J. Orchard (Geological Survey of Canada).				
Palomino Ridge, N Nevada	Thaynes Fm	Smithian	1	00.10.
	Thaynes Fm	Induan?	2	00.10.
	upper Gerster Fm	Guadalupian (Lopingian?)	2	00.10.
	upper Gerster Fm	Guadalupian	2	00.10.
Collector: R.J. Twitchett (Plymouth University) Notes: The exact ages of these strata are currently still a matter of debate (R.J. Twitchett, pers. comm. 2012). Their relative stratigraphic position is illustrated in Jacobsen *et al.* (2011, fig. 2).				
Hot Springs and Hammond Creek, near Bear Lake, SE Idaho	Thaynes Fm	Spathian	2	CNA
Collector: E.S. Carter (Portland State University) Notes: The Hot Springs sample was collected at N 42°07'25" W 111°14'31", and the Hammond Creek sample at approximately N 42°15’31” W 111°25’05” (Carter, pers. comm. 2012).				

Cowboy Pass, Confusion Range, Millard County, W Utah	Thaynes Fm	Spathian	1	CP
Collector: V. Atudorei (University of New Mexico) Notes: Ammonoids are known from the Smithian–Spathian boundary interval at this locality (Smithian, Brayard *et al.* 2009b; Spathian, Guex *et al.* 2010). See Guex *et al.* (2010, fig. 7) for the section from which the sample originates, which is largely composed of limestones deposited in a shallow water setting with frequent emersion levels.				
Coyote Canyon, Humboldt Range, Pershing County, north-central Nevada	Fossil Hill Mb, Prida Fm	early Anisian	1	COY
Collector: M.J. Orchard (Geological Survey of Canada) Notes: The sample was collected very close to the Olenekian/Anisian boundary (Orchard, pers. comm. 2012).				
Humboldt Range, Pershing County, north-central Nevada	Prida Fm	Spathian	2	HB
Collector: H. Bucher (University of Zürich) Notes: At least one of the samples originated from just south of Bloody Canyon (mentioned in Orchard 1994).				
Nevada?	*Haugi* Zone?	Spathian	1	c-176319
Collector: H. Bucher (University of Zürich)? Notes: The GSC locality, indicated by the sample code, is potentially incorrect and the collector is uncertain (Orchard, pers. comm. 2012).				
northern Muddy Mountains, S Nevada	Virgin Mb, Moenkopi Fm	Spathian	1	02.9.
Collector: R.J. Twitchett (Plymouth University) Notes: -				
Darwin Canyon, Inyo Mountains, east-central California	Union Wash Fm	early Spathian	1	DC
Collector: M.J. Orchard (Geological Survey of Canada) Notes: This section is known to cross the Smithian/Spathian boundary (Orchard, pers. comm. 2012).				

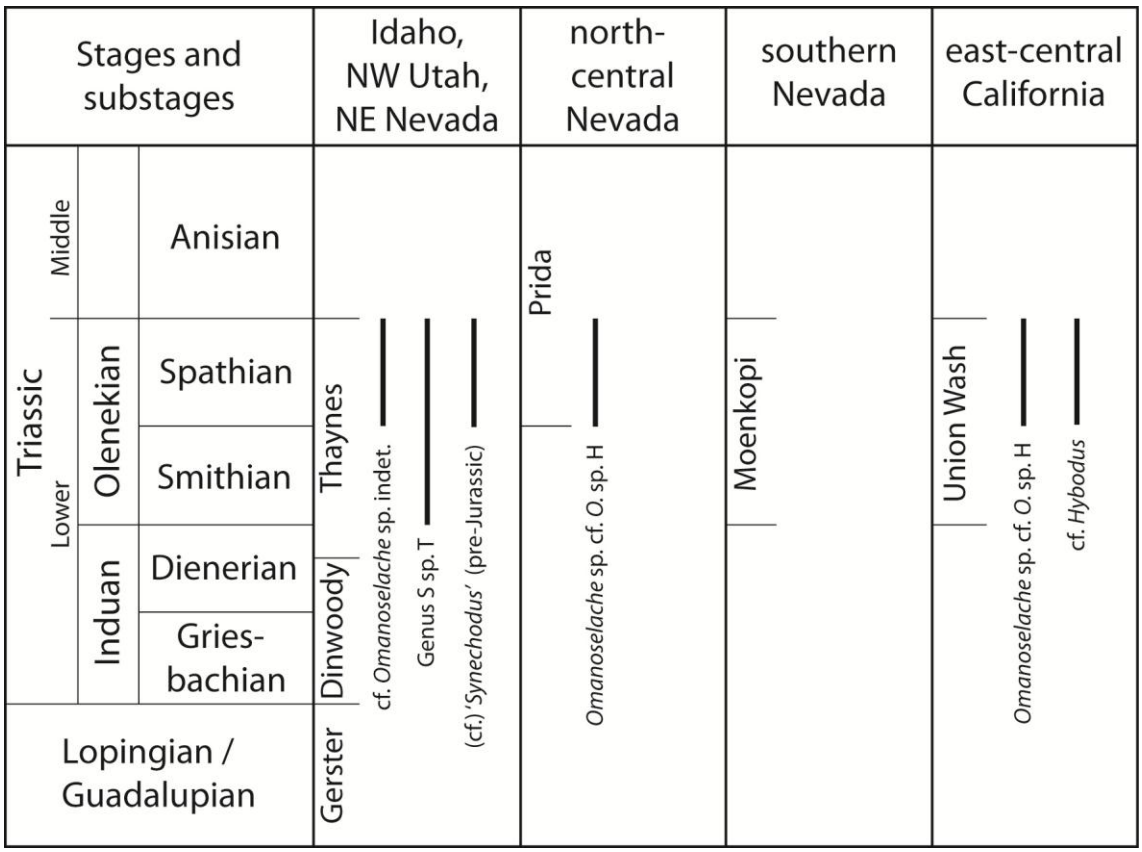

Figure 5.13 – Ranges of all taxa recovered in the southwestern USA, alongside Permian–Middle Triassic stratigraphy. No shark remains were recovered from southern Nevada in this study.

presence of the Synechodontiformes in the Thaynes Formation has been demonstrated (see also Section 5.6). Lastly, chondrichthyan presence in the Prida and Union Wash formations has been recorded for the first time.

5.6 DISCUSSION

The results from the described localities in this chapter are shown in Table 5.2, providing an overview of new shark occurrences in the Boreal Sea and eastern Panthalassa. The significance of these new discoveries in terms of chronological ranges is shown in Figure 5.14.

Table 5.2 – Overview of new Permian–Triassic shark occurrences in the Boreal Sea and eastern Panthalassa.

Taxon	Age	Location
Adamantina sp.	Wordian	Canadian Arctic, Ellesmere Island
Palaeobates sp.	uppermost Changhsingian	Spitsbergen, Lusitaniadalen
Omanoselache sp. cf. *O.* sp. H	Spathian	Southwestern USA, California, Darwin Canyon
Omanoselache sp. cf. *O.* sp. H	Spathian	Southwestern USA, Nevada, Bloody Canyon
cf. *Omanoselache* sp. indet.	Spathian	Southwestern USA, Idaho, Bear Lake
cf. *Hybodus* sp.	Spathian	Southwestern USA, California, Darwin Canyon
Homalodontus sp. cf. *H. aplopagus*	Griesbachian	Canadian Arctic, Ellesmere Island
Genus S sp. T	Spathian	Southwestern USA, Idaho, Bear Lake
	Smithian	Southwestern USA, Utah, Salt Lake City
'Synechodus' sp. (pre-Jurassic)	Spathian	Southwestern USA, Idaho, Bear Lake
cf. *'Synechodus'* sp. (pre-Jurassic)	Spathian	Western USA, Utah, Cowboy Pass
Caseodus sp. cf. *C. varidentis*	Griesbachian	Canadian Arctic, Ellesmere Island
Fadenia crenulata	Wuchiapingian?–Changhsingian	E-Greenland, Kap Stosch
Eugeneodontiformes indet.	Changhsingian	E-Greenland, Kap Stosch
Indeterminate spines	Lopingian	E-Greenland, Kap Stosch

East Greenland

The presence of the Eugeneodontiformes in the East Greenland Basin has been well-documented, with *Fadenia* and *Erikodus* known from the Wuchiapingian of Kap Stosch (Nielsen 1932) and Gauss Halvø (Bendix-Almgreen 1988), and *Sarcoprion* from the Wuchiapingian of Kap Stosch (Nielsen 1952). *Parahelicampodus* is the sole representative of the order in the Mesozoic, being known from the Induan (Griesbachian) of Kap Stosch (Nielsen 1952). This was the first record of an eugeneodontiform after the Permian/Triassic boundary and the first indication that they survived the late Permian mass extinction. This was later confirmed by finds of *Helicampodus* from Lower Triassic deposits in Azerbaijan (e.g., Induan; Rushentzev and Sarycheva 1955; Obruchev 1965; see also Golshani and Janvier 1974) and China

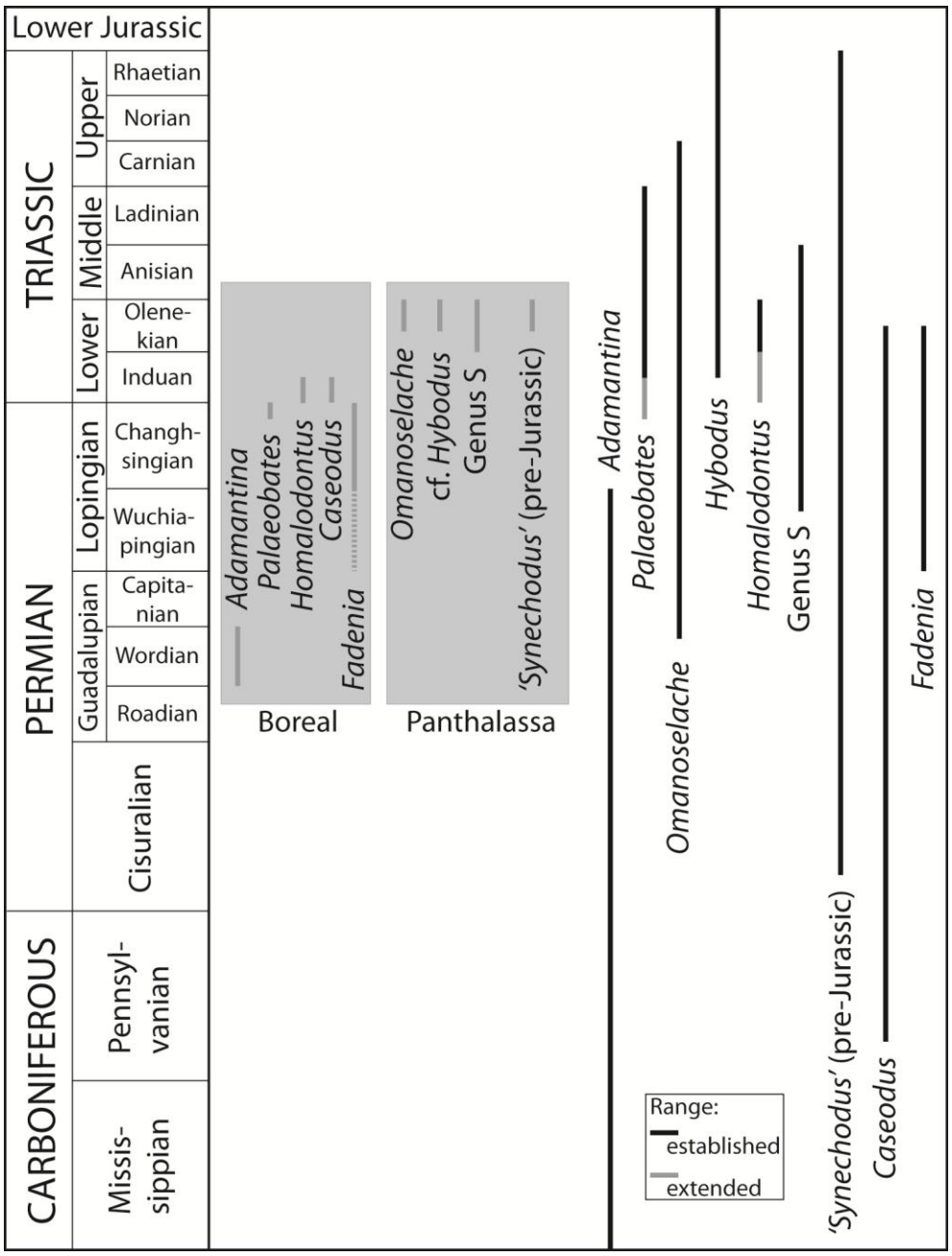

Figure 5.14 – Local (shaded) and global ranges of all genera recovered in the Boreal Sea and eastern Panthalassa. Established ranges based on data in Figure 4.9 and from references quoted in Appendix A3.2. Range extensions based on data in Table 5.2.

(Zhang 1976), and the recovery of a diverse eugeneodontiform fauna in Canada (Olenekian; Mutter and Neuman 2008; see below for further discussion). The material from Greenland described in the current study is in agreement with the reported presence of *Fadenia* in the Lopingian deposits of East Greenland, although it provides the first confirmed occurrence of the genus in the Changhsingian, and has shown the

potential for an even greater eugeneodontiform diversity in the region during the latest Permian.

Other shark orders co-existed with the eugeneodontiforms in East Greenland during the Permian. The only record from a freshwater deposit at Mesters Vig (Profilbjerg Member, Mesters Vig Formation of Asselian–Artinskian age) comprises a single *Xenacanthus* spine (Bendix-Almgreen 1976). From marine strata, cladodont occurrences include *Cladodus* sp. from the Artinskian? 'Upper Marine Group' of Amdrup Land, northeastern Greenland (Bendix-Almgreen 1975, 1976; these teeth may be referable to *Glikmanius occidentalis*, based on a close similarity to contemporary specimens from Wyoming, USA, described by Branson 1916), as well as "*Cladodus*"? sp. and *Adamantina benedictae* from the Wuchiapingian Ravnefjeld Formation of Kap Stosch (Nielsen 1932; Bendix-Almgreen 1993, 1994). Hybodont presence in the Induan Wordie Creek Formation has been established based on the recovery of *Hybodus*? sp. at Gauss Halvø and *'Polyacrodus' claveringensis* at Clavering Ø (e.g., Stensiö 1932; Bendix-Almgreen *et al.* 1988). The only neoselachian records are *Nemacanthus* fin spines known from the Induan Wordie Creek Formation of Kap Stosch (Stensiö 1932). Records of petalodonts include teeth of *Janassa kochi* and *J. unguicula* from the Wuchiapingian Ravnefjeld Formation of Kap Stosch and Gauss Halvø (e.g., Nielsen 1932; Bendix-Almgreen 1976; Bendix-Almgreen *et al.* 1988). '*Helodus*' is the sole representative of helodonts from the Artinskian? 'Upper Marine Group' of Amdrup Land, northern Greenland (Bendix-Almgreen 1975, 1976). Finally, potential cephalic spines of otherwise uncertain affinities described as *Arctacanthus uncinatus*, have been recovered from the Wuchiapingian Ravnefjeld Formation of Clavering Ø and Kap Stosch (Nielsen 1932).

Spitsbergen

Spitsbergen has yielded numerous chondrichthyan remains in previous years, which were first described in detail by Stensiö (1918, 1921), followed by Birkenmajer and Jerzmańska (1979), Błażejowski (2004), and Romano and Brinkmann (2010). These

records show that a diverse, hybodont-dominated chondrichthyan fauna occurred in the area during the Early Triassic, based on records of *Hybodus*, *Acrodus*, *'Polyacrodus'*, *Palaeobates*, and *Lissodus*. Later occurrences remain tentative, with *Acrodus* from the Middle? Triassic and *'Polyacrodus'* from the Upper? Triassic (Stensiö 1921). The only record of neoselachians in Spitsbergen comprises *Nemacanthus* fin spines from the Olenekian (Lower Triassic; Stensiö 1921). Indeterminate eugeneodontiform remains have also been recovered from the Induan (Lower Triassic; Birkenmajer and Jerzmańska 1979), but eugeneodontiform presence has been more confidently established in the Permian, based on *Helicoprion* from the Cisuralian (Siedlecki 1970). The occurrence of *Palaeobates* in the upper Changhsingian of Spitsbergen recorded here represents its oldest known occurrence and its only record from the Permian. *Palaeobates* occurs here in the immediate recovery phase after the late Changhsingian marine ecosystem collapse.

Canadian Arctic

Nassichuk (1971) noted that vertebrate remains in Permian deposits of the Canadian Arctic Archipelago are rare, and prior to this study, no records were known from the Triassic. It is very likely that problems with accessibility are at least partly responsible for the rarity of published accounts of chondrichthyans from this region. Previous reports of Permian chondrichthyans comprise a symmoriiform fin spine identified as *"Physonemus"* (*Stethacanthus*-like spines of as yet unknown affinity, but its ornamentation precludes inclusion with *Stethacanthus*, *Falcatus* or *Damocles*, see Maisey 1983, 2009; Lund 1985, 1986) from the Roadian Assistance Formation on Grinnell Peninsula, Melville Island, and an indeterminate tooth from the Wordian–Capitanian Trold Fiord Formation on Melville Island (Nassichuk 1971). Guadalupian records of *Helicoprion* are known from the Roadian Van Hauen Formation, exposed at Blind Fiord, Ellesmere Island (Nassichuk and Spinosa 1970), which is the basinal equivalent of the Assistance Formation, from which further specimens have been recovered on the Sabine Peninsula, Melville Island (Nassichuk 1971). Consequently,

the current study of material from Ellesmere Island, in which *Adamantina* (Wordian), *Homalodontus* (Griesbachian), and *Caseodus* (Griesbachian) have been identified, represents a significant addition to the knowledge of sharks in the Canadian Arctic Archipelago and an increase in known diversity. It further represents the first record of chondrichthyans from Triassic strata in the Sverdrup Basin. It expands the geographical range of the genus *Adamantina* in the Permian Boreal region and fills a temporal gap, having previously only been recorded from the Lopingian of East Greenland and the Cisuralian of northern Russia (Bendix-Almgreen 1993; Ivanov 1999, 2005).

The eugeneodontiform *Caseodus* and the hybodontiform (homalodontid) *Homalodontus*, here recovered from the Lower Triassic (Griesbachian) of the Canadian Arctic, were previously recognised from the Olenekian of the Wapiti Lake area in British Columbia (e.g., Mutter *et al.* 2007a, 2008a; Mutter and Neuman 2008). These new records represent the oldest Triassic occurrence for *Caseodus* and the oldest overall occurrence for *Homalodontus*, and the first from the Boreal region for both genera.

Southwestern USA

Although none were recovered from Permian strata in this study, numerous records of chondrichthyans from the Permian of the southwestern USA exist. These records include ctenacanths *Glikmanius*, *Heslerodus*, *Saivodus*, *Neosaivodus*, *Kaibabvenator*, and *Nanoskalme* from the Cisuralian Kaibab Formation, Arizona (Hodnett *et al.* 2012). Further recoveries from the Kaibab Formation in Arizona include a *Hybodus* fin spine (Hussakof 1943), the petalodonts *Janassa* (Hussakof 1943) and *Megactenopetalus* (David 1944; Ossian 1976), the cochliodonts *Psephodus* and *Deltodus* (Hussakof 1943; McKee 1982), as well as the neoselachian *Cooleyella* (Thompson 1995; Hodnett *et al.* 2012). Three genera have also been recognised from the Cisuralian of Nevada: *Heslerodus* (Case 1973; see also Ivanov 1999 and Maisey 2010), *Deltodus* (McKee 1982) and *Cooleyella* (Duffin and Ward 1983). The Eugeneodontiformes are represented by *Helicoprion* from the Roadian Phosphoria Formation, exposed in

Bingham and Bear Lake counties, Idaho (e.g., Hay 1907; Dunkle and Williams 1948; Bendix-Almgreen 1966), and from the Cisuralian of Nevada and California (Wheeler 1939; Larson and Scott 1951).

Reports of chondrichthyans from the Lower Triassic are limited to a ctenacanth fin spine (*Pyknothylacanthus*; Mutter and Rieber 2005; see also Section 4.4), *Nemacanthus* fin spines from Idaho (Evans 1904), two *'Polyacrodus'* teeth associated with denticles from the Early Triassic (Spathian, Olenekian) of the Thaynes Formation at Bear Lake, Idaho (Yamagishi 2006), and denticles from the Spathian Virgin Limestone Member at Hurricane, southwestern Utah (Yamagishi 2006).

Hybodontids, such as *Hybodus* and *'Polyacrodus'*, have been reported from the Middle Triassic (Anisian) Star Peak Group of Nevada (Wemple 1906; Rieppel *et al.* 1996; Cuny *et al.* 2001) and the Upper Triassic of California (Wemple 1906; Jordan 1907; Bryant 1914). Of these, *'Polyacrodus' bucheri* from Nevada has since been reassigned to the Homalodontidae (Mutter *et al.* 2007a, 2008a) and has been incorporated into *Omanoselache* in this study (*O. bucheri* comb. nov.; Appendix A3.2). *Lissodus* has been recovered in association with the neoselachian *Rhomaleodus* from the Upper Triassic (Norian) Jungo Terrane of Nevada (Sosson and Martin 1985; Andreev and Cuny 2012). Reports of neoselachians remain scarce and are otherwise limited to *Mucrovenator*, a synechodontiform (Klug 2010), reported from the Middle Triassic (Anisian) Star Peak Group of Nevada (Cuny *et al.* 2001) and another synechodontiform (originally described as *'Palaeospinax'*?) from the same deposit (Rieppel *et al.* 1996), which is probably also referable to *Mucrovenator* (Cuny, pers. comm. 2012).

The material described in this study, recovered solely from Olenekian deposits, is among the oldest Mesozoic records from the southwestern USA. It significantly improves our knowledge of Lower Triassic chondrichthyans in the basin, adding to the known diversity and expanding the geographical range of Spathian hybodonts, as well as recording the occurrence of neoselachians in the Lower Triassic (Smithian–Spathian) for the first time. The only contemporaneous hybodont is *Homalodontus* from the

Wapiti Lake area in western Canada (e.g., Mutter *et al.* 2007a, 2008a), but the genus is of uncertain affinities and not closely related to the Hybodontidae. The present study records the second occurrence of hybodonts from the Thaynes Formation, as well as their first occurrence from both the Prida Formation and the Union Wash Formation. It documents the first record of neoselachians from the Thaynes Formation, and only the second reported occurrence from Triassic strata exposed in the southwestern USA.

If the relative position of the studied formations is compared to their respective palaeoenvironmental settings during the Olenekian, a general deepening trend towards the west becomes apparent, which is consistent with the position of the shelf margin (Figure 5.11). From east to west, the Thaynes Formation has been interpreted as typical of the inner shelf in the Spathian (see Fraiser and Bottjer 2007), although the environment may have been deeper (normal open marine outer shelf facies) during a more extensive Smithian transgression pulse (see Schubert and Bottjer 1995). The dark, thin-bedded limestones of the Prida Formation of the late Spathian and Anisian are indicative of anoxic sediments deposited below wave base (Sander *et al.* 1994; Goudemand *et al.* 2012). Finally, the Olenekian Union Wash Formation has been interpreted as typical of deposition in an outer shelf to slope environment (Stone *et al.* 1991; Woods 1998; see also Woods *et al.* 2007). *Omanoselache* is the only genus that is (tentatively) present in all three studied formations across the basin, suggesting a cosmopolitan life habit, whereas the neoselachian taxa currently appear to be concentrated in shallower settings.

The scarcity of Triassic neoselachian records from the southwestern USA is poorly understood. Cuny and Benton (1999) noted the contrast between the general rarity of neoselachians in North American Upper Triassic deposits and their abundance in the Upper Triassic of western Europe. They postulated that in Canadian deposits (see Johns *et al.* 1997), a deeper marine setting is the most likely cause for the low neoselachian diversity, whereas in the western interior USA (see Huber *et al.* 1993), a more freshwater environment results in a more conservative shark fauna and absence of neoselachians (Cuny and Benton 1999). In contrast, the Thaynes Formation in the

southwestern USA was, at least during the Spathian, deposited in an inner shelf (shallow subtidal or intertidal) environment (see Schubert and Bottjer 1995 and Fraiser and Bottjer 2007), which should, in theory, have been suitable for neoselachians. Yet, only one record of a fin spine was previously known (*Nemacanthus*, Evans 1904), and only two records of teeth from later Triassic formations (*Mucrovenator*, Cuny *et al.* 2001; *Rhomaleodus*, Sosson and Martin 1985). The research focus (of e.g., mass extinction studies) may have been directed away from these strata due to the previously suggested absence of a large proportion of Permian–Triassic stratigraphy (Alvarez and O'Connor 2002). This study documents neoselachian teeth recovered from the Olenekian Thaynes Formation for the first time at five locations in Idaho and Utah, and thus significantly improves the known fossil record. It provides evidence that some of the globally most common and well-established neoselachian forms (the synechodontiforms Genus S and '*Synechodus'* (pre-Jurassic) did inhabit this eastern Panthalassan basin.

6 ORIGIN AND EARLY EVOLUTION OF THE NEOSELACHII

6.1 INTRODUCTION

This chapter describes current knowledge on the evolution of early modern sharks, including those of Palaeozoic age and uncertain affinities, as well as their dental adaptations. A complete overview of the Palaeozoic and early Mesozoic (Triassic) neoselachian fossil record is provided, based on the available literature (see also Appendix A2.1) and complemented by the new contributions described in this study (Chapters 3–5), of which the significance is discussed.

6.2 THE DEFINITION OF NEOSELACHIANS

6.2.1 MORPHOLOGICAL CHARACTERISTICS AND ASSOCIATED PHYLOGENETIC POSITION

Due to insufficiently detailed knowledge of the fossil record at the time with which to create a phylogeny, Schaeffer (1967) recognised “successive levels of elasmobranch organisation”. The Palaeozoic “cladodont level” constituted the most primitive level of sharks, after which elasmobranch evolution was differentiated into the mostly Mesozoic “hybodont level” and the significantly different “modern level” of sharks and batomorphs, which was then only based on extant and post-Triassic Mesozoic groups (Schaeffer 1967; Ginter *et al.* 2010). Schaeffer’s (1967) representation of the different organisational levels within a hypothetical phylogeny (Figure 6.1) shows diversification within levels and the assumption that each level arose from within the preceding level, reflecting major adaptation in a closely integrated complex, such as feeding mechanism (Schaeffer 1967). According to his assessment of “modern level” taxa, the adaptations involved in the transition from the “hybodont level” (i.e., the characteristic features of neoselachians), comprised improved feeding and locomotor mechanisms.

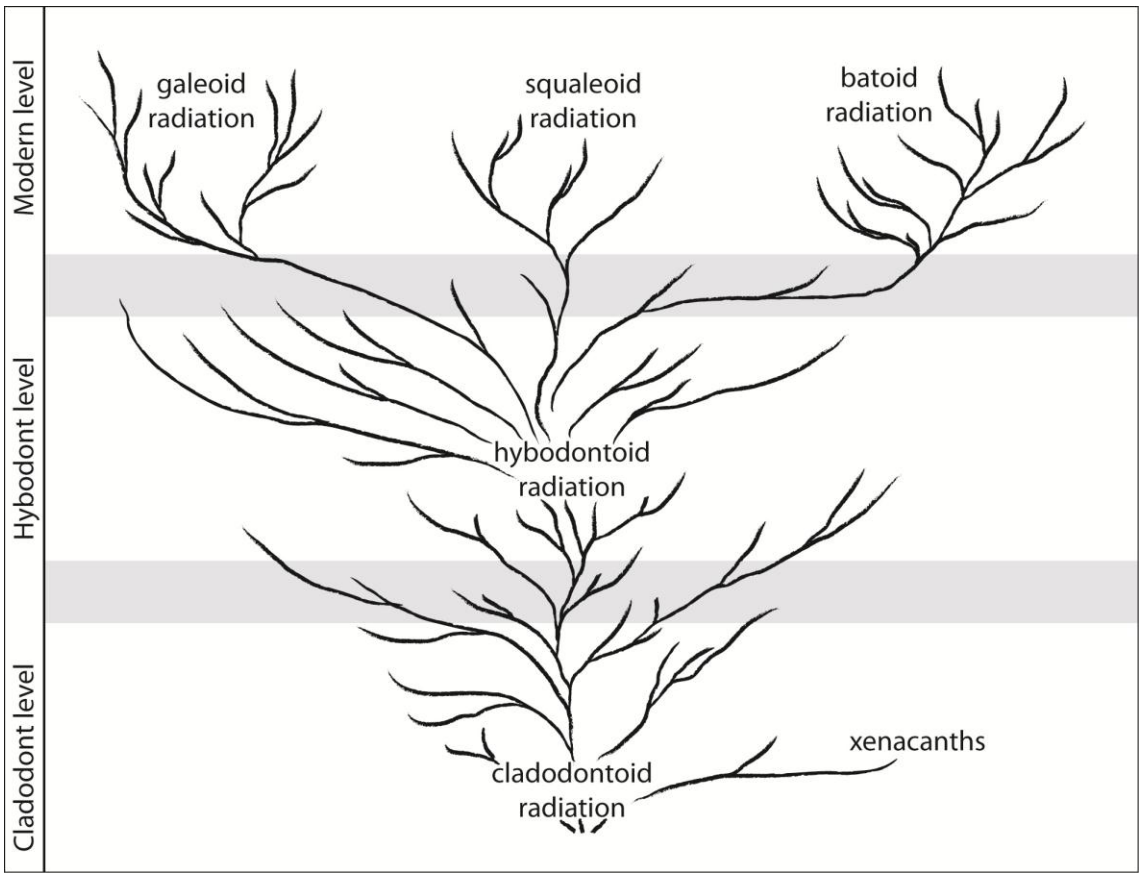

Figure 6.1 – Hypothetical phylogeny through the successive elasmobranch organisational levels, with transitional phases indicated in grey (modified from Schaeffer 1967).

These include greater mobility of the jaws and probably bite force, allowing increased effectiveness in cutting and shearing as a method of feeding, as well as versatility or non-selectivity in food source.

Although accepting the gradational concept, Maisey (1975) moved away from the hybodont-modern level relationship. Instead, he proposed that hybodonts were not ancestral to any extant sharks and that the latter originated from ctenacanth ancestors. This hypothesis was cautiously accepted by Compagno (1977), who conceptually defined the term “neoselachians”, first used informally by Compagno (1973) to refer to “modern level” sharks, based on cladistic analysis and numerous primitive and derived characters proposed to describe the ancestral neoselachian morphotype (Compagno 1977, pp. 304, 305). The neoselachians were proposed to comprise living sharks and rays and certain Mesozoic sharks, including palaeospinacids, and potentially also orthacodonts and anacoracids (Compagno 1977). Later authors accepted the general

outline of the group, but redefined typical neoselachian characters as “a long pelvic metapterygium, only a few mixipterygial cartilages, calcified vertebrae with notochordal constriction, and modern tooth and dermal denticle structures (Shirai 1996, p.10, and references therein). Subsequently, renewed attempts at summarising adaptive neoselachian traits have become more specific with the increasing complexity of phylogenetic analyses (e.g., Maisey *et al.* 2004; Klug *et al.* 2009; and references therein), but despite these, the morphological description of the group remains varied and complex (Klug *et al.* 2009).

Young (1982) and Maisey (1982b) returned to a hybodont-neoselachian relationship and placed the neoselachians as a sister group to Mesozoic and Palaeozoic hybodonts (*Hybodus*, *Tristychius*, and *Onychoselache*). This hypothesis required an earlier origin for neoselachians than was apparent from the fossil record at the time. The earliest known members of the hybodont clade were Early Carboniferous in age, whereas the earliest neoselachian was known from the Early Triassic (Thies 1982). Hybodont monophyly is currently anchored to at least the Viséan based on *Onychoselache* (Coates and Gess 2007).

Over the last 30 years, however, more Palaeozoic neoselachians have been described and some earlier discoveries have been reassigned, largely resolving the temporal discrepancy and even suggesting an Early Devonian origin of the neoselachian clade. More recent analyses have corroborated the proposed phylogenetic position (e.g., Maisey 1989; Coates and Gess 2007) and place the split between the Hybodontiformes and Neoselachii tentatively in the Late Devonian based on skeletal features. *Hopleacanthus* from the Roadian of Germany (Schaumberg 1982) is the oldest commonly accepted member of the neoselachian stem group (Coates and Gess 2007). However, these analyses are mainly focused on the inter-relationships of the hybodonts (Figure 6.2A). Phylogenies for inter-relationships of neoselachians often focus on extant sharks (e.g., Shirai 1996; Maisey *et al.* 2004), with limited comment on the most likely position of the fossil representatives.

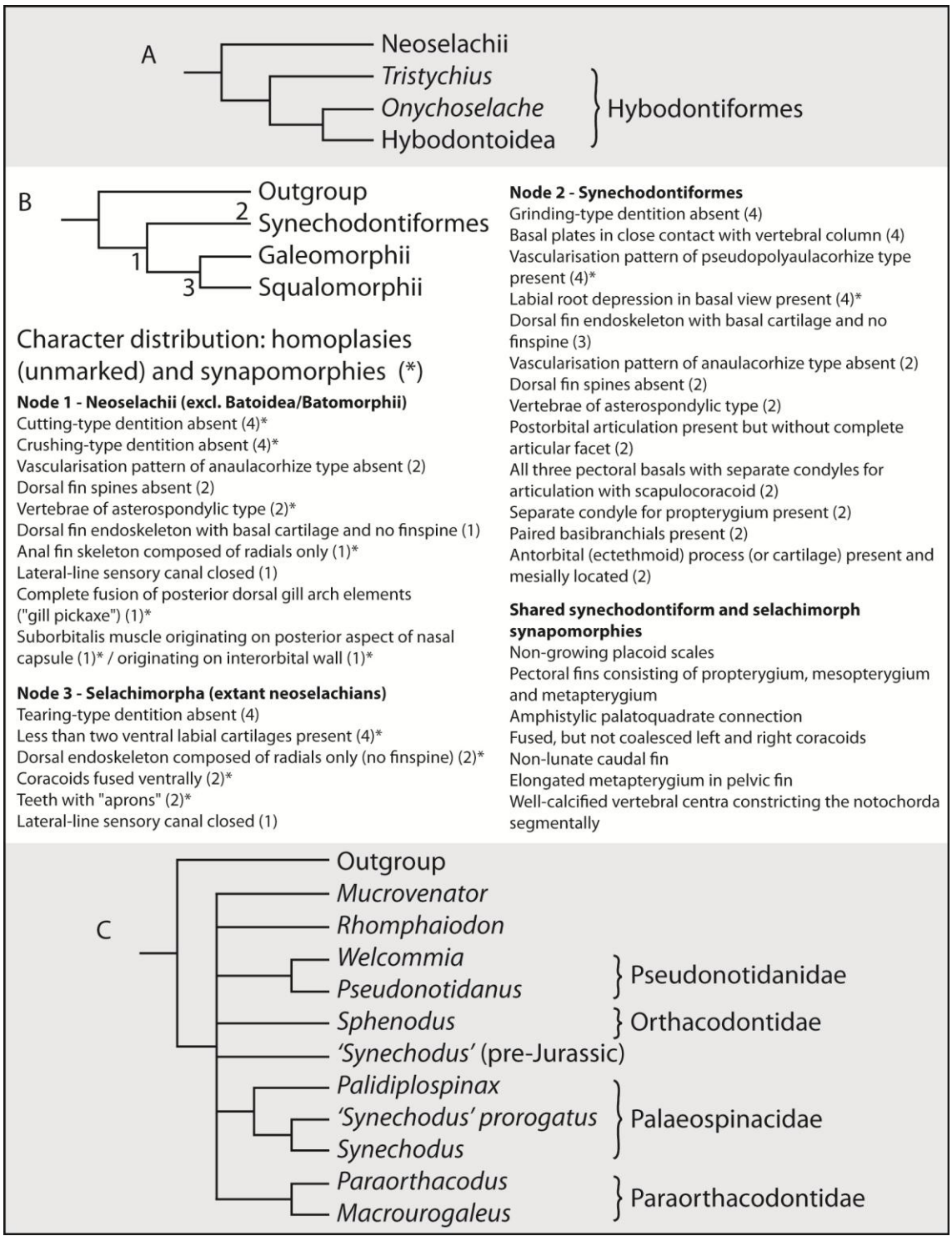

Figure 6.2 – Hypothetical phylogenetic relationships among: A, Hybodontiformes (simplified from Maisey 1989; Coates and Gess 2007), B, Neoselachii (simplified from Klug 2010; character numbers signify number of times represented across two analyses, each with two optimisation techniques), and C, Synechodontiformes (Klug 2010; based on dental and skeletal characters; relevant taxa included are marked with an asterisk in Table 6.2).

Klug (2010) performed a full cladistic analysis of neoselachians, resolving the position of the Synechodontiformes within the clade (Figure 6.2B, C). She excluded batomorphs, because of two possible crown-group configurations based on morphological data (position within Squalomorphii as Batoidea) and molecular data (position as sister group of Squalomorphii and Galeomorphii as Batomorphii). Klug's (2010) analysis supported monophyly of the Neoselachii (at node 1 in Figure 6.2B), which has been established beyond dispute based on morphological and molecular data. Monophyly was concluded from every analytical technique used, although based on a variable set of supporting homoplasies and synapomorphies, among which two supporting dental synapomorphies were consistently found (marked with 4 under Figure 6.2B, node 1; Klug 2010).

The analysis further supported monophyly of of the Synechodontiformes and extant neoselachians (at nodes 2–3 in Figure 6.2B), with a number of homoplasies and synapomorphies. The Synechodontiformes were placed within the Neoselachii as a sister clade to the extant sharks, and represent stem-group Selachimorpha (Klug 2010). A number of shared synapomorphies were found between the synechodontiforms and crown-group neoselachians (Figure 6.2B; Klug 2010, p. 45), consolidating the rightful position of Synechodontiformes within the neoselachian clade, which has been readily accepted (Maisey 2012). This position is strengthened by the presence of a reduced number of labial cartilages in comparison with hybodonts, which form the sister group of the Neoselachii (Klug 2010). The main argument against monophyly of the Synechodontiformes centres on the presence or absence of pseudopolyaulacorhize vascularisation of the tooth base and the morphology of the tooth crown (see Maisey *et al.* 2004). Klug (2010) pointed out that all assigned taxa characteristically possess pseudopolyaulacorhize vascularisation, even if it is not always distinctly developed. Maisey (2012) insists, however, that synechodontiform relationships are still controversial and the characters supporting monophyly of the group remain to be verified.

Despite their proposed monophyly as a clade (Figure 6.2B, node 2), the inter-relationships of synechodontiform taxa remain largely unresolved. Four monophyletic clades could be identified, which have been ranked as separate families (Klug 2010; Figure 6.2C). Unresolved taxa are ranked as family *incertae sedis* (Klug 2010). The high degree of polytomy is due to the scarcity of skeletal remains, resulting in gaps in morphological information (Klug 2010; see also Section 6.2.2). Sampling bias may still conceal much of the palaeogeographical distribution of early neoselachians (as also shown by this study), highlighting the limitations of the fossil record in constructing phylogenies (Maisey 2012).

In summary, since its first use by Compagno (1973), the term “neoselachians” has become widely used and now refers to “all the groups of extant sharks and rays, their fossil representatives, and a few fossil genera of otherwise uncertain affinities” (Ginter *et al.* 2010, p. 102). Although cladistic analysis of neoselachian groups has progressed significantly, a phylogeny incorporating the oldest currently suspected/accepted representatives of the Neoselachii in the Palaeozoic (Devonian–Permian): the Mcmurdodontidae, Anachronistidae and neoselachians of unknown affinities (e.g., *Hopleacanthus* and *Vallisia*?; Table 6.2), does not yet exist and is beyond the scope of this study.

6.2.2 Cladistic limitations resulting from the fossil record

Maisey *et al.* (2004) stressed the phylogenetic ambiguity that is inherent to cladistic analyses based on dental characters alone. Teeth are commonly used for taxonomic purposes because of the morphological variation that they display (Klug *et al.* 2009) and for preservational reasons, but they can be problematic because of intraspecific, sexual, and ontogenetic heterodonty, and the close link between morphology and feeding habits, leading to convergent adaptation in different lineages (Klug *et al.* 2009; Klug 2010). In fossil neoselachians, and especially in those without extant representatives, these variations are still not fully understood (e.g., Klug and Kriwet

2008; Klug *et al.* 2009). Only the combination of extant and fossil taxa (both isolated teeth and body fossils) in phylogenetic analyses "enables the establishment of useful characters including dental features that are useful for systematic purposes and inferring evolutionary traits in neoselachians" (Klug 2010, p. 38). Despite the low taxonomic resolution provided by dental crown morphology, however, basal features are taxonomically and systematically still very important (Klug 2010).

Skeletal remains of sharks are infrequently recovered from the fossil record because of their cartilaginous nature and, indeed, no body fossils of neoselachians have yet been recovered from either the Palaeozoic or the Triassic, with the exception of partial body fossils of *Hopleacanthus* from the Roadian of Germany (Schaumberg 1982; Table 6.2). In comparison, neoselachian fin spines have been recovered more frequently, with the oldest occurrences recognised from the same Roadian body fossils (Schaumberg 1982), the Wordian of Oman (Section 3.2.2.1), and the Wordian–Capitanian of Wyoming, USA (Branson 1933). In addition, they have been recovered on several occasions from the Lower and Upper Triassic (Table 6.2), such as *Nemacanthus*, a form genus known only from isolated fin spines, but which may be closely related to *Palidiplospinax* (Maisey *et al.* 2004). *Palidiplospinax* is the only palaeospinacid known to display the plesiomorphic condition of possessing two dorsal fin spines of neoselachian structure and appearance (a shiny, enameloid covered crown and lacking posterior denticles; Maisey *et al.* 2004; Klug *et al.* 2009). Fin spines are usually found as disarticulated remains throughout the Palaeozoic and Triassic, and so they cannot alone be used to identify any associated teeth as being neoselachian.

Unique morphological features are required to identify early neoselachian dental remains, especially as teeth are the most important components of the fossil record in the absence of skeletal remains (Klug *et al.* 2009). No single set of dental characteristics unifies all Palaeozoic neoselachian taxa (see also Andreev and Cuny 2012). Instead, the assignment of these remains to the Neoselachii is often based on similarities with characters present in extant sharks (see Section 6.3 for details). Gross

tooth morphology of early synechodontiforms is very similar to that of the Hybodontiformes and the teeth of these orders did not begin to diverge significantly until the Middle Triassic (see Andreev and Cuny 2012; and also Section 6.2.3). For this reason, enameloid microstructure is increasingly used to distinguish between these taxa.

6.2.3 Evolution of complex enameloid microstructure

The more complex microstructural pattern of the surficial enameloid layer of neoselachian teeth compared to those of other chondrichthyans has proven to be a relatively stable feature in neoselachian phylogeny (Klug *et al.* 2009). Reif (1973a) proposed the presence of triple-layered enameloid (TLE) as a diagnostic feature of the Neoselachii, consisting of (in an outward direction) tangle-bundled enameloid (TBE), parallel-bundled enameloid (PBE), and shiny layer enameloid (SLE) composed of single crystallites (see Section 1.5.3). The Synechodontiformes are the most primitive shark order in which TLE has been observed (Guinot and Cappetta 2011), but it is not always fully developed in all representatives. Cuny and Risnes (2005) recognised a difference in the degree of crystallite arrangement in the PBE between Triassic and post-Triassic forms (weaker development of radial bundles in Triassic synechodontiforms). Andreev and Cuny (2012) subsequently proposed, based on published records and newly described taxa, that the plesiomorphic single crystallite enameloid (SCE) still dominated during the Early and Middle Triassic, in conjunction with poorly structured PBE (thus double-layered enameloid). This is illustrated by a *'Synechodus'* (pre-Jurassic) tooth from the Induan of Turkey, in which the TBE is absent (Thies 1982). Enameloid apparently increased in structural complexity during the Middle to Late Triassic, until well-defined TLE first appears in the late Carnian (Andreev and Cuny 2012), in *'Synechodus'* (pre-Jurassic) *multinodosus* from British Columbia, Canada (Johns *et al.* 1997).

This developmental sequence corroborates earlier suggestions that the presence of a PBE layer should be considered an aut/synapomorphy of the Neoselachii (see Cuny and Benton 1999, Klug 2010, and references therein) and not fully developed triple-layered enameloid as proposed by Reif (1973a). It is currently the only known diagnostic trait of the group on a microstructural level, although there are a few considerations, such as the secondary loss of the PBE layer in lateral teeth of *Heterodontus* (see Cuny and Benton 1999, and references therein). The same was previously assumed for batomorphs (see Cuny and Benton 1999), but it is currently considered to be most parsimonious to have been primitively lost in this group (see Maisey *et al.* 2004, and references therein; Rees and Cuny 2007; Botella *et al.* 2009b; Andreev and Cuny 2012). If batomorphs never developed a full TLE, the PBE layer thus becomes an autapomorphy of the Selachimorpha (Cuny, pers. comm. 2012), including their stem-group (Synechodontiformes). The Early/Middle Triassic development of poorly structured PBE corresponds to the absence of PBE in Palaeozoic genera that otherwise conform to a neoselachian design (see Sections 6.3.1 and 6.3.2). Enameloid microstructure is a powerful tool in establishing neoselachian affinity if only isolated dental remains are available, but neither TLE, nor PBE can be used as exclusive criteria to characterise all taxa that are considered to be neoselachian (Ginter *et al.* 2010).

6.3 EARLY NEOSELACHIANS IN THE FOSSIL RECORD

In this section, all the Palaeozoic–Upper Triassic records of shark remains of (suspected) neoselachian affinity are discussed, providing an overview of the current state of knowledge on early neoselachian morphology and dental microstructure.

6.3.1 DEVONIAN–CARBONIFEROUS

The oldest suspected representative of the Neoselachii is *Mcmurdodus* White, 1968, which is the only genus in the family Mcmurdodontidae and has been recovered from the Lower–Middle Devonian of Australia (Emsian–Eifelian; Turner and Young 1987) and Antarctica (Givetian; White 1968). The teeth resemble those of recent hexanchiform sharks in a number of features, such as extreme labio-lingual compression (Ginter *et al.* 2010). Also, Burrow *et al.* (2008) considered the morphology and basal vascularisation comparable to modern echinorhinid sharks, and proposed that *Mcmurdodus* may represent the stem-group of either modern group, although this is considered doubtful by Andreev and Cuny (2012). Turner and Young (1987) observed a shiny layer covering the teeth, which they interpreted as enameloid. Burrow *et al.* (2008) identified the presence of a parallel-bundled enameloid, but their evidence remains questionable (Andreev and Cuny 2012).

Two teeth from the Famennian (Upper Devonian) of Dinant, Belgium have been ascribed to *Vallisia*? (Derycke-Khatir 2005). According to Ginter *et al.* (2010), they resemble the typical Late Triassic representatives of the genus in terms of crown morphology, but differ significantly in basal morphology. Any resemblance is, therefore, likely due to convergence and they should be removed from the genus (Ginter *et al.* 2010).

In the Carboniferous, the Neoselachii are represented by three genera from the family Anachronistidae: *Cooleyella* Gunnell, 1933, *Ginteria* Duffin and Ivanov, 2008, and an unnamed new genus (Ivanov 2010). *Cooleyella* occurs throughout the Carboniferous (Mississippian and Pennsylvanian) and has been recovered from western Europe (England, Duffin and Ward 1983; Belgium, Ivanov and Derycke 2005), Russia (Ivanov 1999, 2011), the USA (Gunnell 1933; subtype 058 of Tway and Zidek 1982; Ivanov 2011), and Brazil (Duffin *et al.* 1996). Its neoselachian affinities were first proposed by Duffin and Ward (1983), based on tooth morphological characteristics such as a conical main cusp flanked by lateral blades, a medial vascular pit, a basal buttress supporting the labial flange, and hemiaulacorhize vascularisation. These

features are present in extant sharks (particularly Squatiniformes and Orectolobiformes) but are absent in cladodonts, xenacanths and hybodonts (Duffin and Ward 1983, table 1). An enameloid layer was initially believed to be absent (Duffin and Ward 1983), but its presence and single crystallite nature were established by Ivanov and Cuny (2000). Chen *et al.* (2007a) reported the weak development of irregular bundles arranged perpendicularly to the enameloid surface and suggested a potentially close relationship with the Batomorphii.

Ginteria has a slightly more restricted range and distribution than *Cooleyella*, having been recovered from the Viséan–Serpukhovian of western Europe (England, Duffin and Ivanov 2008; Belgium, Ivanov and Derycke 2005) and Russia (Duffin and Ivanov 2008). It has an anachronistid tooth base (Ginter *et al.* 2010), which suggests a neoselachian affinity, and possesses an enameloid layer (Duffin and Ivanov 2008). An unnamed new anachronistid genus has recently been established by Ivanov (2010), based on material from the Serpukhovian of Russia (Ivanov 2011), but a detailed description and microstructural study is not yet available.

The genus *Amelacanthus* was erected by Maisey (1982a) to accommodate four species of isolated fin spines recovered from the Lower Carboniferous of England and Northern Ireland (Agassiz 1837; Davis 1883; Woodward 1891). A fifth species was recognised from the Pennsylvanian of Nebraska, USA (Maisey 1983). Maisey's (1982a) treatise of *Eunemacanthus* fin spines comprised five species, of which three were retained, from the Carboniferous of the USA, United Kingdom and Russia (see references therein). Both genera possess features such as a thick enameloid layer and a concave posterior wall, which suggest a neoselachian affinity (Maisey 1982a). *Nemacanthus* and *'Palaeospinax'* (now *Palidiplospinax*; see Duffin and Ward 1993, Klug and Kriwet 2008), fossil genera that may also be closely allied to modern sharks (Maisey 1977), possess fin spines that are similar in gross morphology (Maisey 1982a), as do recent squaloids and heterodontids (Maisey 1982a). Morphological comparisons have shown that there are no close relationships with the Hybodontiformes (Maisey

1978, 1982a), Symmoriiformes (Ginter *et al.* 2010), or the Ctenacanthiformes (Maisey 1982a).

6.3.2 PERMIAN

Teeth of *Cooleyella* (Anachronistidae) have been recovered from the Cisuralian–Guadalupian of Russia (Ivanov 2000, 2005, 2011), the USA (Duffin and Ward 1983), and the Wordian of Oman (Section 3.2.2.1). There are presently no records for the Lopingian or younger strata, which suggests that *Cooleyella* did not survive the end-Guadalupian extinction.

Hopleacanthus from the lower Guadalupian (Roadian) of Germany (Schaumberg 1982; Brandt 1997) is the only record of skeletal remains from the Palaeozoic or the Triassic that have been identified as neoselachian with relative certainty. The genus was defined on partial body fossils with articulated teeth and fin spines. Its neoselachian affinity was initially based on the smooth, enameloid-covered dorsal fin spines lacking denticles on the posterolateral margins, the calcification of anterior notochordal sheath segments, and the denticles possessing a simple pulp cavity and single basal canal (Maisey 1984a; Maisey *et al.* 2004). In addition, it lacks calcified ribs and cephalic spines in male individuals, which is in contrast to typical hybodontiform morphology (Ginter *et al.* 2010). Schaumberg (1982) dismissed a close relationship to *'Palaeospinax'* of Maisey (1977; now *Palidiplospinax* and *Synechodus*, see Duffin and Ward 1993), based on the absence of a lingual basal torus. However, the basal vascularisation of the teeth has not been fully assessed (Schaumberg 1982; Ginter *et al.* 2010). Studies of the enameloid miscrostructure were initially not carried out due to the limited nature of the material (Schaumberg 1982), but later study of an isolated tooth has shown the absence of TLE (Cuny, pers. comm. 2012).

Indeterminate neoselachian teeth have been recovered in association with *Cooleyella* from the Wordian of Oman (Section 3.2.2.1). These teeth show a close affinity to the Anachronistidae based on dental characteristics such as well-developed

lateral blades, labial flange with tubercle situated underneath, central vascular pit (see Duffin and Ward 1983), and the presence of a simple SCE (Appendix A3.2). However, they have been excluded here from the Anachronistidae based on differences in vascularisation and the weak development of some of the aforementioned features, and are interpreted as representing a lineage ancestral to the anachronistids (see Appendix A3.2).

Amelacanthus has also been recovered from the Wordian of Oman (Section 3.2.2.1), which represents its youngest and only known Permian occurrence (see Section 6.3.3). It was recovered in association with *Nemacanthus* fin spines, which represent the oldest and only Palaeozoic record of this genus. This suggests that *Nemacanthus* survived both the end-Guadalupian and late Changhsingian extinction events, although that is based on the assumption that the Wordian and Triassic remains (see Section 6.3.3) belong to the same taxon and are not an example of shared morphological characteristics.

A fin spine fragment of *Eunemacanthus* was recovered from the Wordian of Wyoming, USA (Branson 1916) and represents its only Permian and last Palaeozoic record, although Maisey (1982a) has reservations concerning the generic assignment as a result of it being crushed. Also, an indeterminate fin spine from the Guadalupian (Wordian–Capitanian) of Wyoming, USA was assigned to *Ctenacanthus* by Branson (1933) as the new species *C. mutabilis*. It was later removed from the genus by Maisey (1984b), who commented on its similarity to *Nemacanthus* and, therefore, its potential neoselachian origin.

'Pre-Jurassic *Synechodus*' is an artificial group of poorly known Permian and Triassic synechodontiforms that were previously ascribed to *Synechodus* (Klug 2010). As yet, it remains uncertain whether it represents a single taxon and its true affinity to *Synechodus* remains unresolved. Although commonly assigned to the Palaeospinacidae based on dental characteristics (e.g., Ivanov 2005; Ginter *et al.* 2010), this Palaeozoic record should be listed as family *incertae sedis* (Klug 2010), but otherwise has a rightful place within the monophyletic Synechodontiformes

(Figure 6.2C). Key dental features were identified by Klug (2010), but Andreev and Cuny (2012) considered these to be too limited and presented a modified list of characters common to all occurrences of *Synechodus* (including the Permian–Triassic fossil record). However, they note that only a full revision of the genus can establish whether these are accurate for the pre-Jurassic records. The characters include:

- not well-separated crown cusps;
- crown base overhanging crown-root junction;
- basolabial concavity in the base;
- pseudopolyaulacorhize vascularisation (occasionally transitional to anaulacorhize);
- clutching-type dentition;
- posteriorly decreasing tooth height;
- shiny-layered enameloid (SLE); and
- derived PBE with thick radial bundles (*sensu* Guinot and Cappetta 2011).

'Synechodus' (pre-Jurassic) has been recovered from the Cisuralian (Sakmarian–Artinskian) of Russia (Ivanov 2005), which is the oldest known representative of the Synechodontiformes. The enameloid microstructure of these teeth still remains to be studied. The Russian record is evidence that the poorly defined lineage, and therefore the Synechodontiformes, originated in the Permian and survived both the end-Guadalupian and late Changhsingian extinction events, leading on to a wider palaeogeographical distribution during the Triassic (Section 6.3.3).

Further synechodontiform presence in the Permian is demonstrated by the recovery of Genus S from the Lopingian (Wuchiapingian) of Iran (Section 3.3). This genus is believed to be closely allied to *'Synechodus'* (pre-Jurassic; Appendix A3.2) and its neoselachian affinity is well-documented based on microstructural data (see Section 6.3.3), although the microstructure of the Iranian material itself could not been studied due to the limited nature of the material. Based on this Iranian record and its known occurrences in the Triassic (Section 6.3.3), Genus S must have survived the late Changhsingian extinction event.

Finally, a tooth described as “Hexanchidae gen. indet.” was recovered from the Guadalupian (Capitanian) of Japan, as reported by Goto (1994a) and subsequently illustrated by Goto (2002). A brief description of the tooth is provided in Ginter *et al.* (2010), who also comment on its poor preservation and partial encasement in matrix, which prevents an adequate assessment of its relationship to the Neoselachii.

6.3.3 TRIASSIC

Genus S is the only neoselachian genus confidently known to have crossed the Permian/Triassic boundary. The survival of *‘Synechodus’* (pre-Jurassic), *Amelacanthus* and *Nemacanthus* remains tentative. None of the neoselachian genera that were well-established during the Palaeozoic have been recorded from the Triassic. Nevertheless, primitive morphological characteristics are still present in rare Triassic specimens, such as an unnamed tooth recovered from the Ladinian–Carnian of South China (Chen *et al.* 2007a). Its shape and basal vascularisation is unlike hybodont tooth morphology and may suggest a neoselachian affinity (Chen *et al.* 2007a). Despite clear differences with *Cooleyella* in terms of coronal and basal characteristics, they share a well-developed median lingual basal protrusion and vascular canal (Chen *et al.* 2007a). Chen *et al.* (2007a) dismissed a synechodontiform affinity based on the supposed absence of a V-shaped base in sharks of this group, but Klug and Kriwet (2008) described a U- to V-shaped base in *Palidiplospinax*. The smooth crown surface is comparable to *P. occultidens*, whereas the presence of lateral cusplets matches the description of *P. enniskilleni* (Klug and Kriwet 2008). The unroofed nature of the vascular canal is similar to the exposed canals of *Palidiplospinax*, but its vascularisation is near-hemiaulacorhize (Chen *et al.* 2007a), whereas that of *Palidiplospinax* is pseudopolyaulacorhize (Klug and Kriwet 2008).

Another specimen that shows a morphology more commonly observed in the Palaeozoic is a spine fragment recovered from the Spathian (Olenekian) of Oman (Section 3.2.4.1), tentatively identified as *Amelacanthus*. If confirmed, it would

represent the only Mesozoic record of the genus and provide evidence that it crossed the Permian/Triassic boundary, surviving both the end-Guadalupian and late Changhsingian extinction events (again under the assumption that it is not the result of convergent morphological characteristics).

The Early and Middle Triassic neoselachian fauna is dominated by synechodontiform taxa, such as *'Synechodus'* (pre-Jurassic), Genus S, Genus P, *Mucrovenator*, and *Nemacanthus*. From the Middle Triassic onwards, other neoselachians (of uncertain affinities) such as *Rhomaleodus* begin to occur and this group diversify in the Late Triassic. These new Middle Triassic appearances are apparently coincident with the development of derived PBE (highly structured parallel and radial bundles), which has been observed in both the Synechodontiformes and the neoselachians of uncertain taxonomic position, including the stem-neoselachian *Pseudocetorhinus* (see Andreev and Cuny 2012).

Nemacanthus fin spines have been recovered from the Lower Triassic of Spitsbergen (Stensiö 1921), Greenland (Stensiö 1932), and Idaho, USA (Evans 1904) and from the Middle Triassic (Anisian–Ladinian) of Germany (Scheinpflug 1984). Middle Triassic remains from Switzerland have been reassigned to *Acronemus* (see below). *Nemacanthus* further occurs throughout the Upper Triassic of Europe: i.e., England (Agassiz 1837, Woodward 1891, Storrs 1994); Belgium (Duffin *et al.* 1983); France (Cuny and Ramboer 1991, Cuny 1995a); Germany (Schmidt 1928); Luxemburg (Duffin 1993b, Delsate 1995, Godefroit *et al.* 1998) and Poland (Sulej *et al.* 2010). *Nemacanthus* is normally placed with the Synechodontiformes and is considered closely allied to *'Palaeospinax'* (*Palidiplospinax*), but differs in ornamentation and the lesser vertical extent of the trunk inner layer, which suggests that it may be a less advanced form (Maisey 1977). Klug and Kriwet (2008) commented that the anterior enameloid rib barely extends, if at all, on to the lateral faces, in contrast to typical fin spines of *Palidiplospinax*. The fin spines of *Nemacanthus* have never been recovered in articulation with skeletal and dental remains, but a number of authors have speculated on the most likely dentition (see Maisey 1977 and references therein). A

close relationship with *Rhomphaiodon* (*"Hybodus"*) *minor* has been suggested (Cuny *et al.* 1998; Cuny and Risnes 2005), which caused Klug and Kriwet (2008) to exclude *Nemacanthus* from the Palaeospinacidae. The Wordian fauna from Oman that yielded *Nemacanthus* is, however, entirely lacking in synechodontiform sharks and the only neoselachian present is *Cooleyella*. The phylogenetic position of *Nemacanthus* may need to be reconsidered and/or its morphology was perhaps shared by multiple taxa. Also, fin spines have only been observed in *Palidiplospinax* and *Pseudonotidanus* (Klug and Kriwet 2008; Klug 2010; see Figure 6.2), whereas they are believed to have been secondarily lost in all other synechodontiforms (Klug 2010).

The oldest known occurrence of neoselachian dental remains in the Triassic (i.e., after the late Changhsingian extinction event) is a specimen from the Griesbachian (Induan) of Oman, tentatively identified as Genus P (Section 3.2.3.4). This genus is definitely present in the Olenekian of Oman (Section 3.2.4) and possibly around the Olenekian/Anisian boundary in China (Section 4.3). Genus P is newly described in this study and its neoselachian affinity has been determined from the transitional anaulacorhize to pseudopolyaulacorhize basal vascularisation, and, most confidently, from the presence of PBE, although poorly structured and made up entirely of individually identifiable crystallites (Appendix A3.2).

Genus S is also recognised from the Olenekian of Oman (Section 3.2.4) and from around the Olenekian/Anisian boundary in China (Section 4.3). This genus is more widely distributed than Genus P, as it also occurs in Olenekian deposits of Timor (Section 3.5; Yamagishi 2006) and of Idaho and Utah, USA (Section 5.5). It shares crown and basal morphological characteristics with the Synechodontiformes, and the Palaeospinacidae in particular, but its neoselachian affinity is most clearly evidenced by the presence of pseudopolyaulacorhize vascularisation and primitively structured PBE. The bundles are better developed than in Genus P, being more densely packed (especially near the cusp apices) and individual single crystallites can less often be recognised, but radial bundles appear absent (Appendix A3.2).

The microstructure of Genus P and Genus S agrees with the step-by-step acquisition of TLE and, in particular, the gradual development of PBE, proposed by Andreev and Cuny (2012). Their pattern conforms to the initial developmental stage, formulated as “development of subparallel to parallel crystalline bundles, probably by modification of the SCE retained only as a thin superficial SLE layer” (Andreev and Cuny 2012, p. 264). Furthermore, Genus P appears to fit the first of three outlined substages, comprising loosely packed subparallel bundles composed of single crystallites, whereas Genus S fits the second substage, namely the change of individual bundle crystallites into elongated crystalline bundles, combined with increased compaction and order of bundle organisation. Limited but unmistakeable evidence of PBE in the first substage was provided by Thies (1982) from the Dienerian of Turkey and this single tooth represents the earliest unequivocal neoselachian occurrence. Genus P and Genus S provide an extensive record of the Early Triassic early development of bundled enameloid microstructure and demonstrate progression into the second substage by at least the Olenekian for the first time. Thies (1982) further inferred that the development of crystallite bundling was initiated during the (late) Palaeozoic, which was followed by Andreev and Cuny (2012) despite the lack of verification from the fossil record. No Palaeozoic synechodontiform records have yet been studied in terms of microstructure, including the earliest known teeth, i.e., *‘Synechodus’* (pre-Jurassic) from the Cisuralian of Russia (Ivanov 2005; Section 6.3.2). Nevertheless, the presence of Genus S in Wuchiapingian strata of Iran (Section 3.3) provides indirect evidence of crystallite bundling (see Section 6.3.2).

Teeth that are presently identified as *‘Synechodus’* (pre-Jurassic) occur throughout the Triassic. The oldest is from the Dienerian (Induan) of Turkey (Thies 1982) mentioned above. Cuny *et al.* (2001) noted a considerable similarity with *Mucrovenator* from the Anisian of Nevada, USA, but could not establish this with certainty due to the missing base in the Turkish specimen. Kriwet *et al.* (2009) considered the tooth as *Mucrovenator* in their analysis, although data presented by Andreev and Cuny (2012) suggest that the PBE is not equally derived (no radial bundles observed in the Turkish

specimen versus presence in *Mucrovenator*). *'Synechodus'* (pre-Jurassic) is further recorded from the Olenekian of Idaho and Utah, USA (Spathian; Section 5.5), Siberian Russia (Ivanov and Klets 2007), and from around the Olenekian/Anisian boundary in China (Section 4.3). Middle Triassic records are known from Siberian Russia (Ivanov and Klets 2007), Nevada, USA (Rieppel *et al.* 1996; although this material may be referrable to *Mucrovenator*, Cuny, pers. comm. 2012), Japan (Yamagishi 2004, 2006), Bulgaria (Andreev and Cuny 2012), and British Columbia, Canada (Johns *et al.* 1997). Upper Triassic occurrences are known from British Columbia, Canada (Johns *et al.* 1997) and from western Europe (England, Duffin 1998a; Belgium, Delsate and Lepage 1991, 1993; France, see Cuny *et al.* 1998, Cuny and Benton 1999). The Belgian occurrence of *'Synechodus' rhaeticus* was treated as *Paraorthacodus* in the analysis of Kriwet *et al.* (2009), but the species does not appear in Klug *et al.*'s (2009) revision of that genus. *'Synechodus' rhaeticus* was erected from fin spines recovered from the Rhaetian of England (Duffin 1982a) and associated teeth were later referred to the same genus (Duffin 1998a), but not based on an articulated skeleton. If fin spines were secondarily lost in all synechodontiformes apart from *Palidiplospinax* and *Pseudonotidanus* (Klug 2010), then this assignment is somewhat uncertain.

The enameloid microstructure of a number of the *'Synechodus'* (pre-Jurassic) dental records has been investigated. Yamagishi (2006), for example, reported SCE and PBE in *'Synechodus' triangulus* from Japan, whereas Andreev and Cuny (2012) observed SCE and highly structured PBE with parallel and radial bundles in specimens from Bulgaria. *'Synechodus' volaticus* from the Ladinian–Carnian of Canada possesses SCE and PBE, and TBE was assumed to be present but was not observed (likely due to preparation; Johns *et al.* 1997). *'Synechodus' multinodosus* from the Carnian of Canada (Johns *et al.* 1997) possesses the first well-defined record of TLE (Andreev and Cuny 2012). The claimed presence of TLE in *'Synechodus' incrementum* by Johns *et al.* (1997; Norian of Canada) has been shown to be a misinterpretation of a diagenetic structure and the microstructural type has been reinterpreted as similar to hybodont enameloid histology (Andreev and Cuny 2012), although Klug (2010) showed

that the species fits well within the Synechodontiformes based on morphological characteristics. Finally, studies on teeth of *'Synechodus' rhaeticus* from the Rhaetian of England revealed the presence of poorly structured PBE, apparently without radial bundles (Cuny and Benton 1999; Cuny and Risnes 2005). The presence of SLE could not be established, and a structure only somewhat reminiscent of TBE was observed (Cuny and Risnes 2005), causing Andreev and Cuny (2012) to regard the presence of TLE as doubtful at best.

Mucrovenator and *Rhomphaiodon* are the only two taxa from the Triassic that are of confirmed synechodontiform affinity following cladistic analysis (see Klug 2010). They have respectively been recovered from the Anisian of Nevada, USA (Cuny *et al.* 2001) and from the Upper Triassic of western Europe (England, Belgium, France, Germany, Luxemburg; e.g., Duffin 1993a and see references in Cuny and Benton 1999). The neoselachian taxa of uncertain affinity comprise *Rhomaleodus* from the Anisian of Bulgaria (Andreev and Cuny 2012), and a number of taxa from the Upper Triassic: *Grozonodon* from France (Norian; Cuny *et al.* 1998), *Huenichthys* from Germany (Rhaetian; Reif 1977), and *Duffinselache* from England (Rhaetian; Duffin 1998a; Andreev and Cuny 2012). All have been assigned to the Neoselachii based on enameloid microstructure, which is also true for *Reifia* from the Anisian of Poland (Liszkowski 1993) and the Carnian of Germany (Duffin 1980a), and for *Pseudocetorhinus* from the Rhaetian of western Europe (England, Belgium, Luxemburg, France; see references in Cuny and Benton 1999), but *Reifia* records an additional suite of external morphological characteristics shared with modern sharks (Duffin 1980a). *Pseudocetorhinus* was tentatively placed with the Neoselachii based on its resemblance to the Cetorhinidae (basking sharks) and classified in the same family (Duffin 1998b). The teeth were later demonstrated to possess TLE (Cuny 1998, see also Cuny and Benton 1999), confirming their neoselachian affinity, but Andreev and Cuny (2012) prefer to remove the genus from the Cetorhinidae based on morphological discrepancies and a long implied ghost lineage, and to place it among the rest of the stem neoselachians. The enameloid microstructure of these genera has been

Table 6.1 – Summary of character distribution among Triassic neoselachian taxa.

Developmental stage	Taxa
primitive PBE devoid of radial bundles	*'Synechodus'* (pre-Jurassic; in Thies 1982), *'Synechodus' volaticus*, *'S.' rhaeticus*, *Rhomaleodus*, *Reifia*, *Duffinselache*
derived PBE with highly structured parallel and radial bundles	*Hueneichthys*, *Pseudocetorhinus*, *Grozonodon*, *Rhomphaiodon*, *'Synechodus'* (pre-Jurassic; excl. species mentioned elsewhere)
derived PBE with radial bundles, but TBE absent	*Mucrovenator*
well-defined TLE	*'Synechodus' multinodosus*, *Rhomphaiodon*, *Grozonodon*, *Pseudocetorhinus*

discussed in detail by Cuny and Benton (1999) and Andreev and Cuny (2012) and is only briefly summarised here (Table 6.1).

Acronemus is a genus erected by Rieppel (1982) to unite fin spines and teeth recovered from the Middle Triassic (Anisian–Ladinian) of Switzerland, initially described as *Nemacanthus tuberculatus* and *Acrodus bicarinatus*, respectively. A recent analysis of a chondrocranium by Maisey (2011) disproved the ctenacanth relationship suggested by Rieppel (1982) and showed that both hybodontiform and neoselachian characteristics are present. This ambiguity over the position of *Acronemus* within the Euselachii currently remains unresolved and the genus, therefore, cannot confidently be considered as part of the neoselachian lineage.

Vallisia from the Rhaetian of England (Duffin 1982b) and Belgium (Duffin *et al.* 1983), *Doratodus* from the Anisian–Ladinian of France (Sauvage 1883) and Norian of Germany (Schmid 1861; Seilacher 1943), and *Pseudodalatias* from the Ladinian of Spain (Botella *et al.* 2009b) and Upper Triassic (Norian–Rhaetian) of western Europe (e.g., Sykes 1971, 1974) are of presumed neoselachian affinity based on dental morphological characteristics, but are currently left without definitive assignment, because microstructural study has revealed simple SCE and the absence of any bundling (Cuny and Benton 1999). The SCE in *Vallisia* and *Doratodus* is made up of randomly oriented crystallites, whereas *Pseudodalatias* possesses a highly structured SCE with an inner layer of crystallites oriented perpendicular to the crown surface and

an outer layer of crystallites aligned parallel to the outer surface (Botella *et al.* 2009b; Andreev and Cuny 2012).

Raineria is known from a rostrum from the Rhaetian of Austria (Osswald 1928) and has been considered to be a neoselachian shark based on similarities with more derived neoselachian families from the Cretaceous, although these are believed to be the result of convergence (Cuny and Benton 1999). Furthermore, a number of single teeth with an assumed close relationship to the Neoselachii have been documented from the Middle and Upper Triassic of Japan (Section 4.2) and from the Middle Triassic of China (Section 4.3), including cf. *Palidiplospinax* from the Anisian of China, which may represent an ancestral form. Their histology has not been examined, however, due to the limited nature of the available material, leaving their neoselachian affinity yet to be confirmed.

6.4 Distribution, extinction and radiation

6.4.1 Global distribution

If all current interpretations of the fossil record are correct, the neoselachian lineage originated in the Devonian in the southern hemisphere (Australia and Antarctica; Figure 6.3), where *Mcmurdodus* has been recovered. Subsequently, numerous occurrences of predominantly anachronistid taxa have been recorded from the northern hemisphere during the Early Carboniferous (Mississippian) in what is now western Europe (Palaeotethys and Uralian Strait). *Cooleyella* is the most successful neoselachian genus in the Palaeozoic, having originated in western Europe and Russia (Early Carboniferous), and later expanded southwards to North and South America (Late Carboniferous, Pennsylvanian). The genus reached southern Tethys by the Guadalupian, after which it seems to have disappeared, signifying the end of the Anachronistidae. The most successful early neoselachian group, the Synechodontiformes, originated in Russia at the start of the Permian, but remained

Figure 6.3 – Global distribution maps of (suspected) Neoselachii during the Early Devonian–Late Triassic (modified from Blakey 2012).

rare with only one further occurrence in the Lopingian of Iran, potentially indicating slow expansion. From the Early Triassic, however, abundant occurrences are recorded from southern Tethys and North America. The group also reached the western Panthalassan continental margin (China, Japan). Previously, not much was known of Early Triassic synechodontiform diversity, but the recognition of Genus S and Genus P has increased our knowledge significantly. From the Middle Triassic onwards, the Neoselachii started diversifying in western Europe. Other Late Triassic records of Synechodontiformes are only known from the Boreal region of North America, but no

neoselachian occurrences are currently recorded from outside western Europe during the Rhaetian.

6.4.2 Triassic/Jurassic extinction and radiation

The first major radiation and subsequent diversification of neoselachians is generally assumed to have occurred during the Rhaetian, when a eustatic transgression created extensive shallow epicontinental seas over most of western Europe (Cuny and Benton 1999), but the current analysis suggests an earlier radiation at the Early/Middle Triassic boundary (Figure 6.4). An analysis carried out by Maisey *et al.* (2004) suggested the Early Jurassic (ca. Toarcian) as the critical period in early neoselachian evolution. Kriwet *et al.* (2009) pointed out that these opposing hypotheses result from discrepancies in taxonomic and phylogenetic interpretations, respectively. The raw data show a diversity peak in the Late Triassic (in agreement with the interpretations of Cuny and Benton 1999), and a distinct decline in the earliest Jurassic (Kriwet *et al.* 2009, fig. 2). However, following sampling standardisation based on pooled taxonomic occurrences, the pattern of genus richness appears to be low and relatively constant during the Late Triassic and earliest Jurassic, with a steep rise in the diversification rate in the Toarcian (ca. 180 Myr ago; Kriwet *et al.* 2009, fig. 3).

Following this new analysis, Kriwet *et al.* (2009) consider the majority of Palaeozoic and Triassic neoselachian sharks to be short-lived and highly specialised groups that became extinct before the beginning of the Jurassic, with the Synechodontiformes being the only neoselachian group known to cross the Triassic/Jurassic boundary. Maisey (2012) also places emphasis on the importance of extinction among sharks at the end of the Triassic as a major influence on the shaping of neoselachian evolutionary history. Kriwet *et al.* (2009) further considered that Early Jurassic neoselachian diversification and radiation was opportunistic (as indicated by diversity trends), and the high diversification rate potentially the result of small body size, a short lifespan, and oviparity, “enabling faster ecological reorganisations and innovations in

body plans for adapting to changing environmental conditions" (Kriwet *et al.* 2009, p. 945).

6.5 SUMMARY

An overview of all known records of neoselachians from the Palaeozoic and early Mesozoic (Triassic) are shown in Table 6.2, based on data from the literature and the new discoveries described in this study (Chapters 3–5). The reconstructed stratigraphical ranges (Figure 6.4) show that the Mcmurdodontidae (group A) are the earliest suspected neoselachians and that the Anachronistidae (group B) are the dominant Palaeozoic neoselachians. The Synechodontiformes (group C) originated in the Palaeozoic and persisted into (and beyond) the Jurassic, surviving all three extinction events (end-Guadalupian, late Changhsingian, and Late Triassic). The taxa in group D possess bundled enameloid, which confirms their neoselachian relationship, but are of otherwise uncertain affinity. The taxa in group E are of doubtful neoselachian affinity based on ambiguous skeletal characteristics, (un)structured SCE, or indefinite dental characteristics.

The summary of enameloid microstructure shows the first confirmed appearances of poorly structured PBE, derived PBE, and well-defined TLE. The continued persistence of poorly structured bundled enameloid after the first appearance of derived bundled enameloid is shown, as well as its potential downward range before its first recognition (to the earliest known synechodontiforms), although this remains to be confirmed by microstructural study.

The new discoveries of neoselachian remains described in this study are of significance. First of all, they highlight an important new region where neoselachians occurred (Oman, western Neotethys) and expand our knowledge of the known neoselachian stratigraphic range and diversity in certain areas (China, Japan, and the USA). They further increase known neoselachian diversity during the Wordian (from one to five taxa) and the Early Triassic (from two to 4–5 taxa). The specimens from Iran

Table 6.2 – Palaeozoic and early Mesozoic neoselachian taxa recovered globally. For full details, refer to Appendix A2.1. Entries marked with an asterisk are taxa represented in the phylogenetic analysis of Klug (2010; Figure 6.2C). Entries marked in grey are of ambiguous affinity.

Age	Taxon	Location	Remains	Reference
Rhaetian (Tr)	*Raineria*	Austria	rostrum	Osswald 1928
	Vallisia	England, Belgium	teeth	Duffin 1982b; Duffin *et al.* 1983
	Pseudodalatias	England, Belgium, France	teeth	Appendix A2.1
	Pseudocetorhinus	England, Belgium, France, Luxemburg	teeth	Appendix A2.1
	Duffinselache	England, Belgium	teeth	Duffin 1998a; Delsate 1993
	Huenichthys	Germany	tooth	Reif 1977
	*Rhomphaiodon**	England, Belgium, France, Germany, Luxemburg	teeth	Appendix A2.1
	'Synechodus' (pre-Jurassic)*	England, Belgium, France	teeth, fin spines	Appendix A2.1
	Nemacanthus	England, Belgium, France, Germany, Luxemburg	fin spines	Appendix A2.1
Norian (Tr)	gen. indet.	Japan, Kamura	tooth	Section 4.2
	Pseudodalatias	Italy	teeth	Tintori 1980
	Doratodus	Germany	teeth	Schmid 1861; Seilacher 1943
	Grozonodon	France	teeth	Cuny *et al.* 1998
	*Rhomphaiodon**	France, Germany	teeth	Appendix A2.1
	'Synechodus' (pre-Jurassic)*	Canada, BC	teeth	Johns *et al.* 1997
	Nemacanthus	France, Luxemburg	fin spines	Appendix A2.1
Carnian (Tr)	*Reifia*	Germany	teeth	Duffin 1980a
	'Synechodus' (pre-Jurassic)*	Canada, BC	teeth	Johns *et al.* 1997
	Nemacanthus	Poland, Woźniki	fin spines	Sulej *et al.* 2010
Ladinian–Carnian (Tr)	gen. indet. (Neoselachii?)	China, Guanling	tooth	Chen *et al.* 2007a
Ladinian (Tr)	*Pseudodalatias*	Spain	teeth	Botella *et al.* 2009b
	gen. indet. (Palaeosp.)	Japan, Kamura	tooth	Section 4.2
	'Synechodus' (pre-Jurassic)*	Canada, BC	teeth	Johns *et al.* 1997
Anisian–Ladinian (Tr)	*Nemacanthus*	Germany	fin spines	Scheinpflug 1984

	Doratodus	France	teeth	Sauvage 1883
	Acronemus	Switzerland, Italy	teeth, fin spines, braincase	Rieppel 1982
Anisian (Tr)	*Reifia*	Poland	teeth	Liszkowski 1993
	Rhomaleodus	Bulgaria, Vidin Province	teeth	Andreev and Cuny 2012
	cf. *Palidiplospinax*	China, Guandao	tooth	Section 4.3
	*Mucrovenator**	USA, Nevada	teeth	Cuny *et al.* 2001
	'Synechodus' (pre-Jurassic) *	USA, Nevada	teeth	Rieppel *et al.* 1996
		Japan, Ehime Prefecture	teeth	Yamagishi 2004
		Bulgaria, Vidin Province	teeth	Andreev and Cuny 2012
Olenekian–Anisian (Tr)	cf. Genus P	China, Guandao	teeth	Section 4.3
	Genus S	China, Guandao	teeth	Section 4.3
	'Synechodus' (pre-Jurassic)	China, Guandao	teeth	Section 4.3
		Russia, Siberia	teeth	Ivanov and Klets 2007
Olenekian (Tr)	Genus P	Oman, Jabel Safra & Wadi Alwa	teeth	Section 3.2.4.1; 3.2.4.2
	Genus S	Oman, Timor, USA (Idaho & Utah)	teeth	Section 3.2.4.1; 3.2.4.2; 3.5; 5.5
	(cf.) '*Synechodus'* (pre-Jurassic)	USA, Idaho & Utah	teeth	Section 5.5
	cf. *Amelacanthus*	Oman, Jabel Safra	fin spines	Section 3.2.4.1
Induan–Olenekian (Tr)	*Nemacanthus*	Spitsbergen	fin spines	Stensiö 1921
		Greenland	fin spines	Stensiö 1932
		USA, Idaho	fin spines	Evans 1904
Dienerian (Induan, Tr)	*'Synechodus'* (pre-Jurassic)	Turkey, Kocaeli Peninsula	tooth	Thies 1982
Griesbachian (Induan, Tr)	cf. Genus P	Oman, Wadi Wasit	tooth	Section 3.2.3.4
Wuchiapingian? (P)	Genus S	Iran, Zal?	teeth	Section 3.3
Capitanian (P)	gen. indet. (Hexanch.)	Japan, Fukushima Prefecture	tooth	Goto 1994a
	Cooleyella	USA, Texas	teeth	Ivanov, Nestell and Nestell 2011
Wordian–Capitanian (P)	gen. indet. *mutabilis*	USA, Wyoming	fin spine	Branson 1933
Wordian (P)	*Nemacanthus*	Oman, Haushi-Huqf region	fin spines	Section 3.2.2.1
	Amelacanthus	Oman, Haushi-Huqf region	fin spines	Section 3.2.2.1
	gen. indet.	Oman, Haushi-Huqf region	teeth	Section 3.2.2.1

	Cooleyella	Oman, Haushi-Huqf region	teeth	Section 3.2.2.1
Roadian (P)	*Hopleacanthus*	Germany, Hessen	partial body fossils	Schaumberg 1982
	Cooleyella	Russia, Tatarstan, Kirov & Vladimirovka	teeth	Ivanov 2011
Kungurian (P)	*Cooleyella*	USA, Nevada	teeth	Duffin and Ward 1983
Sakmarian–Artinskian (P)	*'Synechodus'* (pre-Jurassic)*	Russia, Urals	teeth	Ivanov 2005
Asselian–Artinskian (P)	*Cooleyella*	Russia, Urals	teeth	Ivanov 2000, 2005, 2011
Gzhelian (C)	*Cooleyella*	USA, Ohio	teeth	Ivanov 2011
		USA, Nebraska	teeth	Tway and Zidek 1982 (sbt. 058)
Kasimovian (C)	*Cooleyella*	USA, Kansas & Ohio	teeth	Ivanov 2011
		USA, Missouri	teeth	Gunnell 1933
Moscovian (C)	*Cooleyella*	Russia, Timan	teeth	Ivanov 1999, 2011
Bashkirian/ Moscovian (C)	*Cooleyella*	Brazil, Amazon Basin	teeth	Duffin, Richter and Neis 1996
Pennsylvanian (upper C)	*Amelacanthus*	USA, Nebraska	fin spines	Maisey 1983
Serpukhovian (C)	gen. nov. (Anachr.)	Russia, Moscow syneclise	teeth	Ivanov 2010, 2011
Viséan–Serpukhovian (C)	*Ginteria*	Russia, Moscow syneclise	teeth	Duffin and Ivanov 2008
	Cooleyella	Russia, Moscow syneclise	teeth	Ivanov 1999, 2011
Viséan (C)	*Ginteria*	Belgium, Royseux	teeth	Ivanov and Derycke 2005
		England, Derbyshire	teeth	Duffin and Ivanov 2008
	Cooleyella	Russia, Polar Urals	teeth	Ivanov 1999, 2011
		Belgium	teeth	Ivanov and Derycke 2005
		England, Derbyshire	teeth	Duffin and Ward 1983
Mississippian (lower C)	*Amelacanthus*	England, Northern Ireland	fin spines	Agassiz 1837; Davis 1883; Woodward 1891
Famennian (D)	*Vallisia?*	Belgium, Dinant	teeth	Derycke-Khatir 2005
Givetian (D)	*Mcmurdodus*	Antarctica	teeth	White 1968
Emsian–Eifelian (D)	*Mcmurdodus*	Australia, Queensland	teeth	Turner and Young 1987

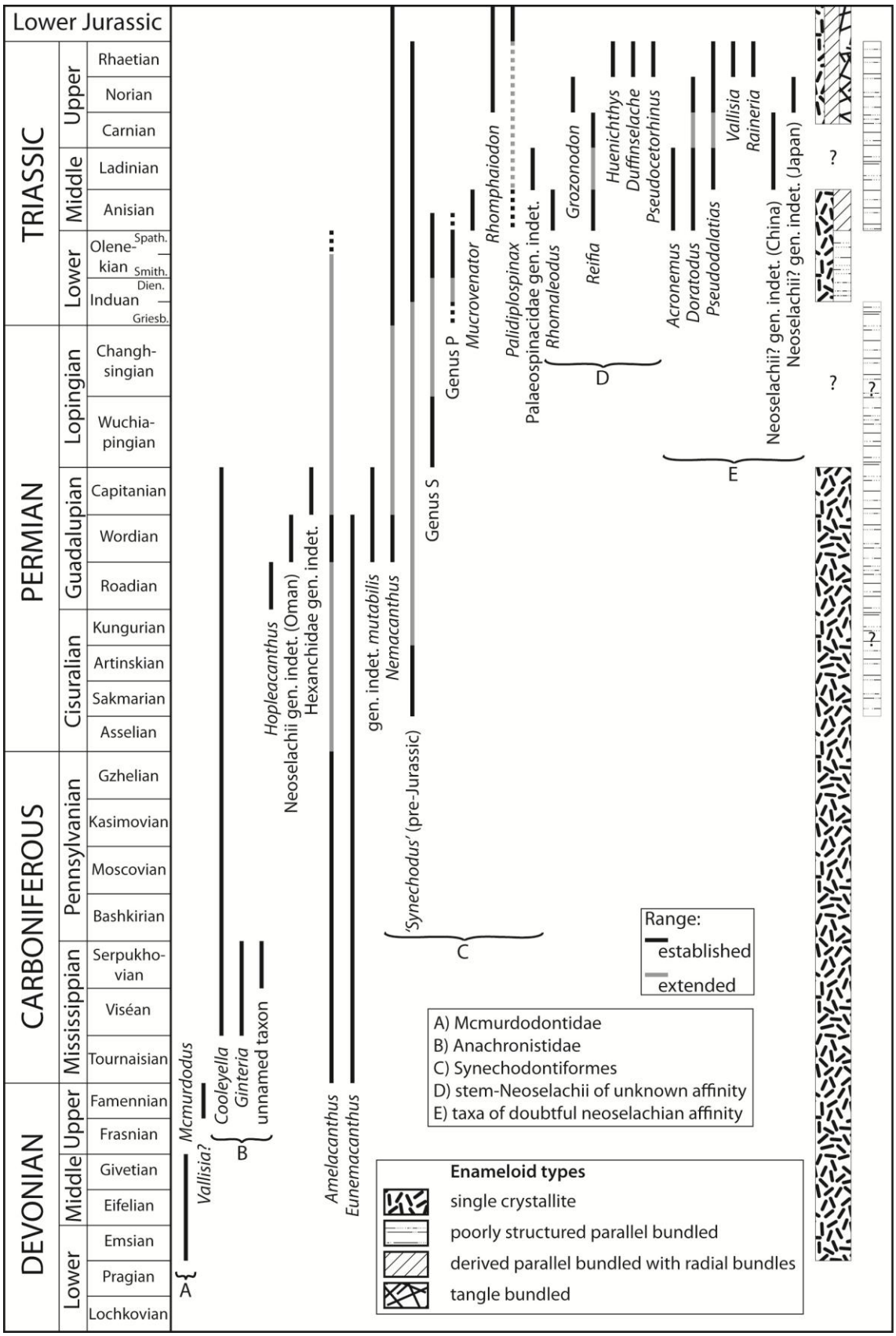

Figure 6.4 – Palaeozoic and early Mesozoic stratigraphic ranges of neoselachian genera recovered globally (based on references quoted in Table 6.2 and Appendix A2.1). The predominant enameloid microstructure during any given time period is indicated (which does not necessarily apply to all taxa), including the (potential) full extent of primitive bundling.

provide the first confirmation of neoselachians (synechodontiforms) during the Lopingian (partially filling a temporal gap), and the recognition of a fragmented specimen from the Griesbachian of Oman represents the earliest neoselachian occurrence in the Triassic. The recognition of Genus S from the Wuchiapingian and the Olenekian–Anisian, of *Nemacanthus* from the Wordian, and potentially *Amelacanthus* from the Olenekian, increases the number of taxa that cross the Permian/Triassic boundary from one (although 'pre-Jurassic *Synechodus*' has not been established as a single taxon) to 3 or 4. The specimens from the Olenekian of Oman, the USA, and China further represent the largest proportion of dental records during that time, complementing the few teeth described from Russia (Ivanov and Klets 2007). Microstructural observations made on the Oman specimens represent the only Olenekian histological study to date, and is the most comprehensive study on this primitive state of crystallite bundling, clearly documenting the extent of bundling and identifying the specific areas of the crown where bundling occurs (see Appendix A3.2).

7 GLOBAL CHONDRICHTHYAN PHYLOGENY AND FOSSIL RECORD

7.1 INTRODUCTION

The most severe bias in the study of ancient diversity patterns results from the heterogeneous quality of the fossil record, which is strongly correlated to sample size (Kriwet *et al.* 2009). Therefore, an assessment of the chondrichthyan fossil record is provided in this chapter, based on a database of Permian–Triassic elasmobranch and euchondrocephalan occurrences that has been newly compiled from literature and material described in this study (Appendix A2.1, with references provided therein).

7.2 HYPOTHETICAL PHYLOGENY

A phylogeny of Permian and Triassic chondrichthyan genera has been compiled based on published cladograms of large-scale relationships and of individual groups (Figure 7.1). This informal supertree has been constructed in the traditional manner of taxonomic substitution using hierarchically nested source trees comprising primarily unique taxa (see Sanderson *et al.* 1998; Bininda-Emonds 2004). Essentially, this means that source trees, each representing a single clade and comprising taxa found on only one source tree, were grafted together. This traditional method is, currently, still in use, despite the drawback that it cannot readily account for conflicting estimates of phylogeny (Bininda-Emonds 2004). Because only one tree can be grafted onto the supertree for a given group, a subjective decision about the best phylogenetic estimate for that group must be made. In the absence of a cladistic hypothesis for specific groups, source trees have been constructed based on their internal systematic relationships, assuming monophyly (see Appendix A3.1). The presented hypothetical phylogeny is based entirely on morphological characteristics but the generation of a complete supertree from comprehensive cladistic analysis has not yet been possible as

Figure 7.1 – ► Hypothetical phylogeny of Permian and Triassic chondrichthyan genera compiled from individual cladograms. Main chondrichthyan framework based on the scenario supported by Ginter *et al.* (2010), complemented by more detailed cladistic analyses of the Xenacanthimorpha (Hampe 1995; Soler-Gijón 1997, 2000; Hampe and Ivanov 2007), Ctenacanthiformes (Hodnett *et al.* 2012), other Cladodontomorphi (Coates and Sequeira 2001; Pradel *et al.* 2011), Eugeneodontiformes (Zangerl 1981), Holocephali (Stahl 1999; *contra* Lund and Grogan 1997), Hybodontoidea (Coates and Gess 2007; Rees 2008; *contra* Maisey 1989), and Neoselachii (Klug 2010).

Notes to Figure 7.1:

1 – taxa marked with an asterisk are positioned based on their systematic classification, assuming monophyly of families (see text), which unavoidably often results in polytomies.
2 – the Jalodontidae have been ejected from the Phoebodontiformes, but may derive from early representatives of the order, and a close relationship with the Xenacanthimorpha has been suggested (Ivanov *et al.* 2012).
3 – the Xenacanthiformes, Phoebodontiformes, and Ctenacanthiformes have been ejected from the Euselachii, in which only the Hybodontiformes and Neoselachii remain as monophyletic sister groups (Lane 2010).
4 – following cladistic analysis performed by Hampe and Ivanov (2007) certain genera were ejected from the Xenacanthiformes and placed in the Bransonelliformes, which is recognised as a primitive sister group to the previous, and together they form the Xenacanthimorpha.
5 – many forms that were initially placed in the Ctenacanthiformes due to a misidentification have now been placed in the Phoebodontiformes, which shows close affinity with the Xenacanthiformes (Ginter *et al.* 2002).
6 – the Stethacanthidae have been included in the Symmoriidae to form a monophyletic group, based on the recognition of sexual dimorphism (Maisey 2009).
7 – the Eugeneodontiformes and Petalodontiformes have previously also been classified with the Elasmobranchii, but are positioned here with the Euchondrocephali (as in Ginter *et al.* 2010) because of their tendency to cluster with this group based on their many chimaerid characteristics.
8 – the placement of the Orodontiformes remains tentative. A recent analysis by Grogan and Lund (2008) indicated that the group should be placed in a clade with the Petalodontiformes, which is supposed to also include the Helodontiformes, which is traditionally placed within the Holocephali. This is, however, not followed by Ginter *et al.* (2010).
9 – a recent analysis (Klug 2010) indicates that the Synechodontiformes should be placed within the Neoselachii as a monophyletic sister group of the Galeomorphii and Squalomorphii.
10 – *Wodnika* is here excluded from the Hybodontidae, contrary to its usual systematic classification, based on diverging tooth morphology (Cuny, pers. comm. 2012) and its absence in the most recent family cladogram (Rees 2008). Hampe (2012) classified the genus with the Sphenacanthidae.
11 – *Nemacanthus* has been ejected from the Palaeospinacidae by Klug and Kriwet (2008).
12 – *Grozonodon* is here positioned near *Rhomphaiodon* and *Mucrovenator* based on great morphological similarity (Cuny *et al.* 1998; Cuny, pers. comm. 2012).
13 – *Pseudocetorhinus* has been ejected from the Cetorhinidae, Lamniformes and positioned as a stem neoselachian by Andreev and Cuny (2012). 'Hexanchidae' refers to an unusual tooth from the Guadalupian of Japan (Goto 1994a).

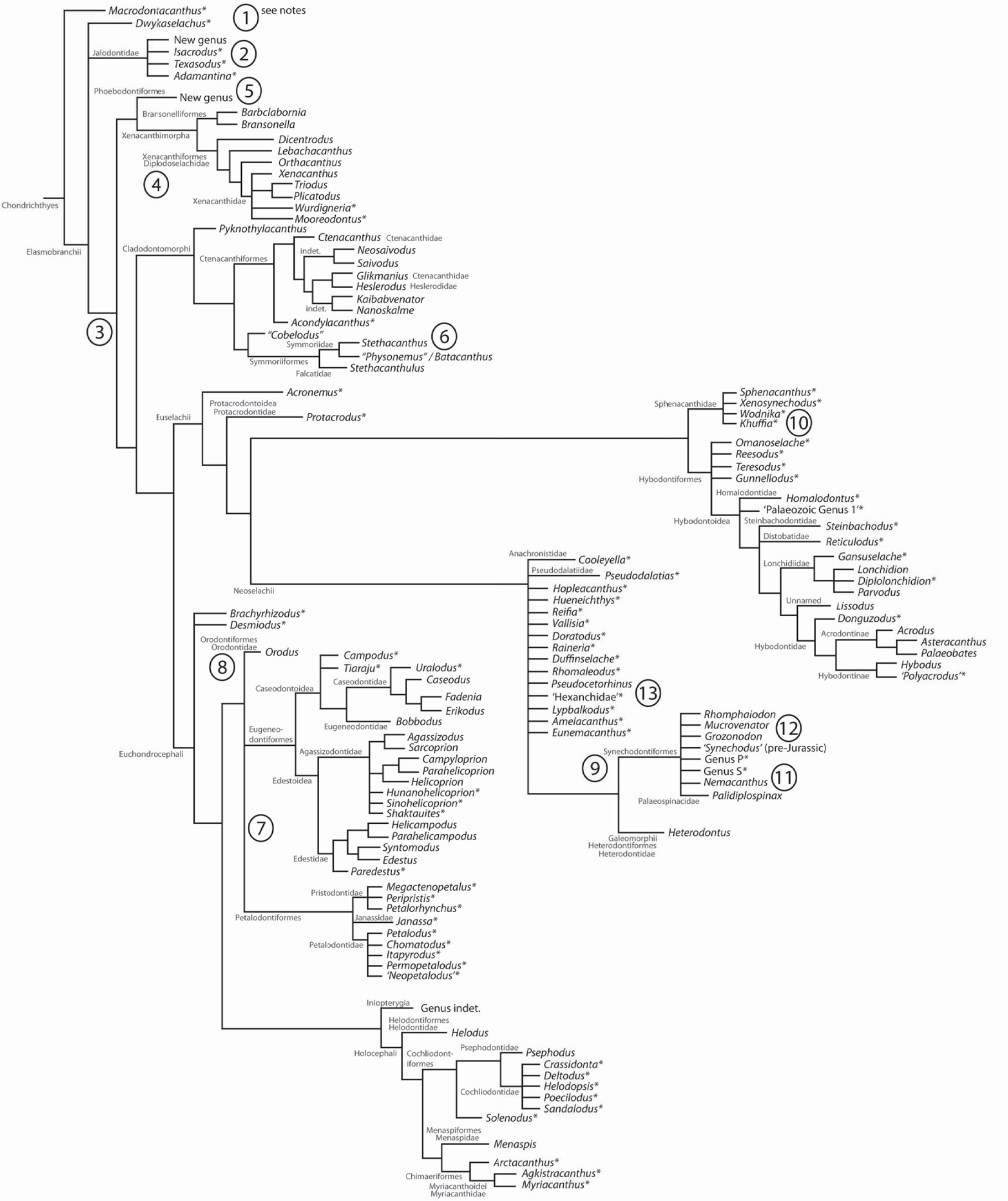
Macrodontacanthus*
Dwykaselachus*
1
see notes
Jalodontidae
New genus
Isacrodus*
Texasodus*
2
Adamantina*
Phoebodontiformes
New genus
5
Bransonelliformes
Barbclabornia
Bransonella
Xenacanthimorpha
Dicentrodus
Lebachacanthus
Xenacanthiformes
Diplodoselachidae
Orthacanthus
Xenacanthus
4
Triodus
Chondrichthyes
Xenacanthidae
Plicatodus
Wurdigneria*
Mooreodontus*
Pyknothylacanthus
Ctenacanthus
Ctenacanthidae
Elasmobranchii
Cladodontomorphi
indet.
Neosaivodus
Saivodus
Ctenacanthiformes
Glikmanius
Ctenacanthidae
Heslerodus
Heslerodidae
Kaibabvenator
indet.
Nanoskalme
Acondylacanthus*
3
"Cobelodus"
Symmoriidae
Stethacanthus
6
"Physonemus" / Batacanthus
Symmoriiformes
Stethacanthulus
Falcatidae
Acronemus*
Protacrodontoidea
Protacrodontidae
Euselachii
Protacrodus*
Sphenacanthidae
Sphenacanthus*
Xenosynechodus*
Wodnika*
Khuffia*
10
Omanoselache*
Reesodus*
Teresodus*
Hybodontiformes
Gunnellodus*
Homalodontidae
Homalodontus*
'Palaeozoic Genus 1'*
Hybodontoidea
Steinbachodontidae
Steinbachodus*
Distobatidae
Reticulodus*
Anachronistidae
Cooleyella*
Lonchidiidae
Gansuselache*
Pseudodalatiidae
Pseudodalatias*
Lonchidion
Diplolonchidion*
Hopleacanthus*
Parvodus
Hueneichthys*
Unnamed
Lissodus
Reifia*
Donguzodus*
Vallisia*
Acrodontinae
Acrodus
Doratodus*
Asteracanthus
Raineria*
Palaeobates
Hybodontidae
Duffinselache*
Hybodus
Rhomaleodus*
'Polyacrodus'*
Hybodontinae
Pseudocetorhinus
13
'Hexanchidae'*
Lypbalkodus*
Amelacanthus*
Eunemacanthus*
Rhomphaiodon
Mucrovenator
12
Grozonodon
'Synechodus' (pre-Jurassic)
Synechodontiformes
Genus P*
9
Genus S*
Nemacanthus
11
Palidiplospinax
Palaeospinacidae
Heterodontus
Galeomorphii
Heterodontiformes
Heterodontidae
Neoselachii
Brachyrhizodus*
Desmiodus*
Orodontiformes
Orodontidae
Orodus
8
Campodus*
Tiaraju*
Uralodus*
Caseodontoidea
Caseodontidae
Caseodus
Fadenia
Erikodus
Eugeneodontidae
Bobbodus
Eugeneo-
dontiformes
Agassizodus
Sarcoprion
Euchondrocephali
Agassizodontidae
Campyloprion
Parahelicoprion
Edestoidea
Helicoprion
Hunanohelicoprion*
Sinohelicoprion*
Shaktauites*
7
Helicampodus
Parahelicampodus
Syntomodus
Edestidae
Edestus
Paredestus*
Pristodontidae
Megactenopetalus*
Peripristis*
Petalorhynchus*
Petalodontiformes
Janassidae
Janassa*
Petalodus*
Petalodontidae
Chomatodus*
Itapyrodus*
Permopetalodus*
'Neopetalodus'*
Iniopterygia
Genus indet.
Helodontiformes
Helodontidae
Helodus
Holocephali
Cochliodont-
iformes
Psephodontidae
Psephodus
Crassidonta*
Deltodus*
Cochliodontidae
Helodopsis*
Poecilodus*
Sandalodus*
Solenodus*
Menaspiformes
Menaspidae
Menaspis
Arctacanthus*
Chimaeriformes
Agkistracanthus*
Myriacanthoidei
Myriacanthidae
Myriacanthus*

the result of a number of difficulties. These difficulties are primarily caused by unstable relationships within, and between, early groups (xenacanths, cladoselachians, ctenacanths, stethacanthids), which, therefore, fail to provide clear evidence of how these clades are linked to other stem-groups (Janvier 1996; Coates and Sequeira 2001; see also Coates and Gess 2007). In addition, numerous taxa occur in the late Palaeozoic and early Mesozoic that display combinations of hybodontiform and neoselachian characteristics (Maisey 2011). As a result, the chondrichthyans—and elasmobranchs in particular—comprise many groups with poorly resolved phylogenies (including numerous polytomies; Guinot *et al.* 2012). Maisey (2011) highlights the fact that more articulated remains need to be recovered, particularly from the Permian–Triassic, in order to improve our understanding of chondrichthyan morphology and so resolve the as yet uncertain phylogenetic relationships of numerous taxa.

Middle–Upper Triassic taxa such as *Vallisia* and *Doratodus* may be ancestral to the Batomorphii, which fit on the neoselachian branch as a probable sister group of Squalomorphii and Galeomorphii (Klug 2010). Despite neoselachian dental morphological characteristics, both genera are characterised by simple SCE and the absence of any bundling (Cuny and Benton 1999), which corresponds to the primitive absence of a PBE layer in batomorphs (see Maisey *et al.* 2004). A similar relationship was also suggested for the Palaeozoic anachronistid *Cooleyella* (Chen *et al.* 2007a).

7.3 Assessment of the fossil record

7.3.1 Global sampling effort

The description of fossil fishes in scientific literature started in the early 1800s with works by De Blainville (1818) and Bonaparte (1832–1841). However, the greatest impact was made by Agassiz (1833–1843), who assessed the known fossil fish record and introduced the first chondrichthyan taxonomic framework based on remains from England, France, Germany and the present-day Czech Republic. Many of the genera

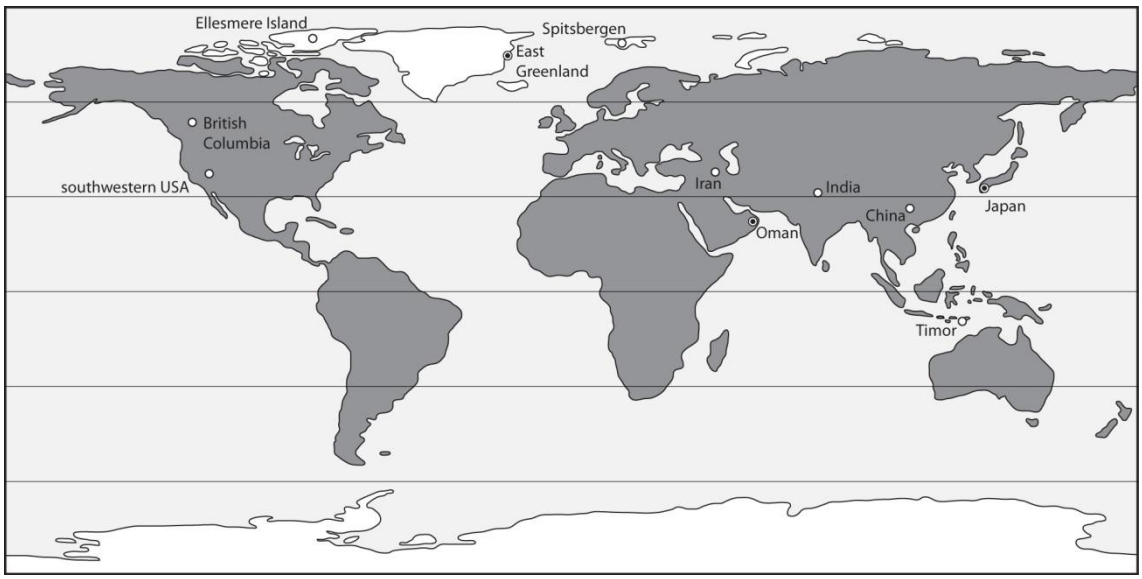

Figure 7.2 – Modern-day geographic map (redrawn from Blakey 2012) showing the position of localities relevant to this study and which have been sampled directly (filled dots) or from which specimens were indirectly obtained (open dots).

and species that he introduced are still valid today. Hundreds of occurrences of fossil chondrichthyans published since then have greatly improved our knowledge of the global record. This study describes remains from 11 locations globally (Figure 7.2) and although all countries of origin were already known to yield shark remains, new productive localities are identified. A global summary of yielding localities shows that chondrichthyan remains have been recovered on each continent from both the Permian and Triassic, although most Permian records come from North America and most Triassic records from Europe (Figure 7.3). Many regions, globally, still require further and more detailed exploration, which is best illustrated by the chondrichthyan record of Oman. Until now, it was based on rare and mostly non-descriptive reports focused on single localities (Tintori 1998; Angiolini *et al.* 2003a; Yamagishi 2006; Schultze *et al.* 2008). This study employs a more integrative approach in providing a detailed faunal overview based on over 40 occurrences from Oman (Figure 7.3; each taxon reported in an individual locality constitutes a taxonomic occurrence, see Section 2.6.1) and presenting a regional interpretation of palaeogeographical and palaeoenvironmental distribution, as well as diversity and domination patterns, related to the Late Permian

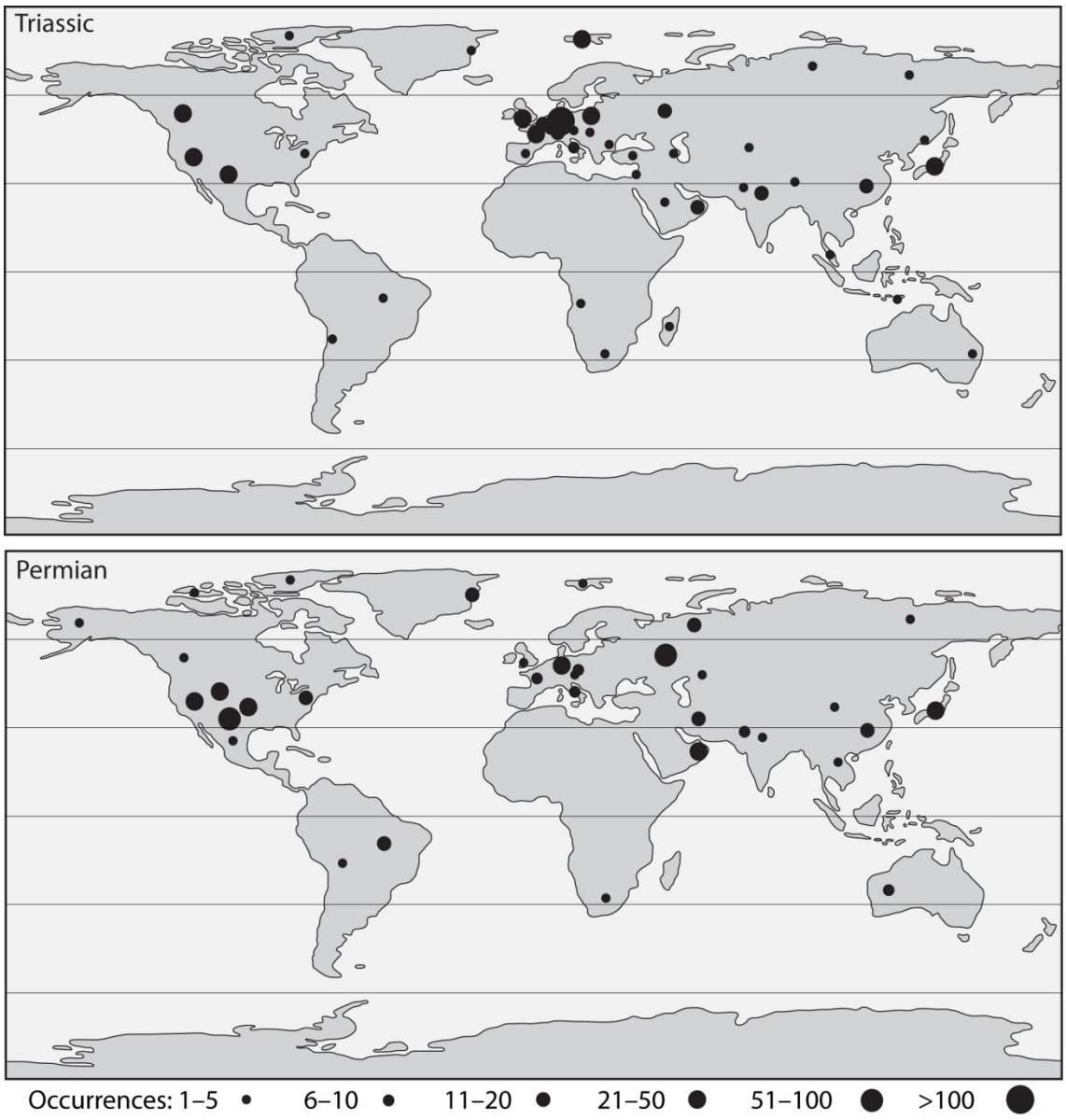

Figure 7.3 – Modern-day geographic map (redrawn from Blakey 2012) showing the global chondrichthyan occurrence distribution per country (or per region in Canada, the USA, Russia, China, and Australia) for both the Permian and Triassic, based on published records (Appendix A2.3.1).

mass extinction. An increasingly regional and global approach to taxonomy and faunal interpretations will aid a comprehensive reconstruction of the global chondrichthyan record.

Global occurrence distribution (Figure 7.3; Appendix A2.3.1; the number of distinct taxonomic occurrences per country, see Section 2.6.2) shows that there is a distinct difference between the northern and southern hemisphere, with 96% of occurrences having been recorded from the northern hemisphere. Focal points are Europe (48.6%

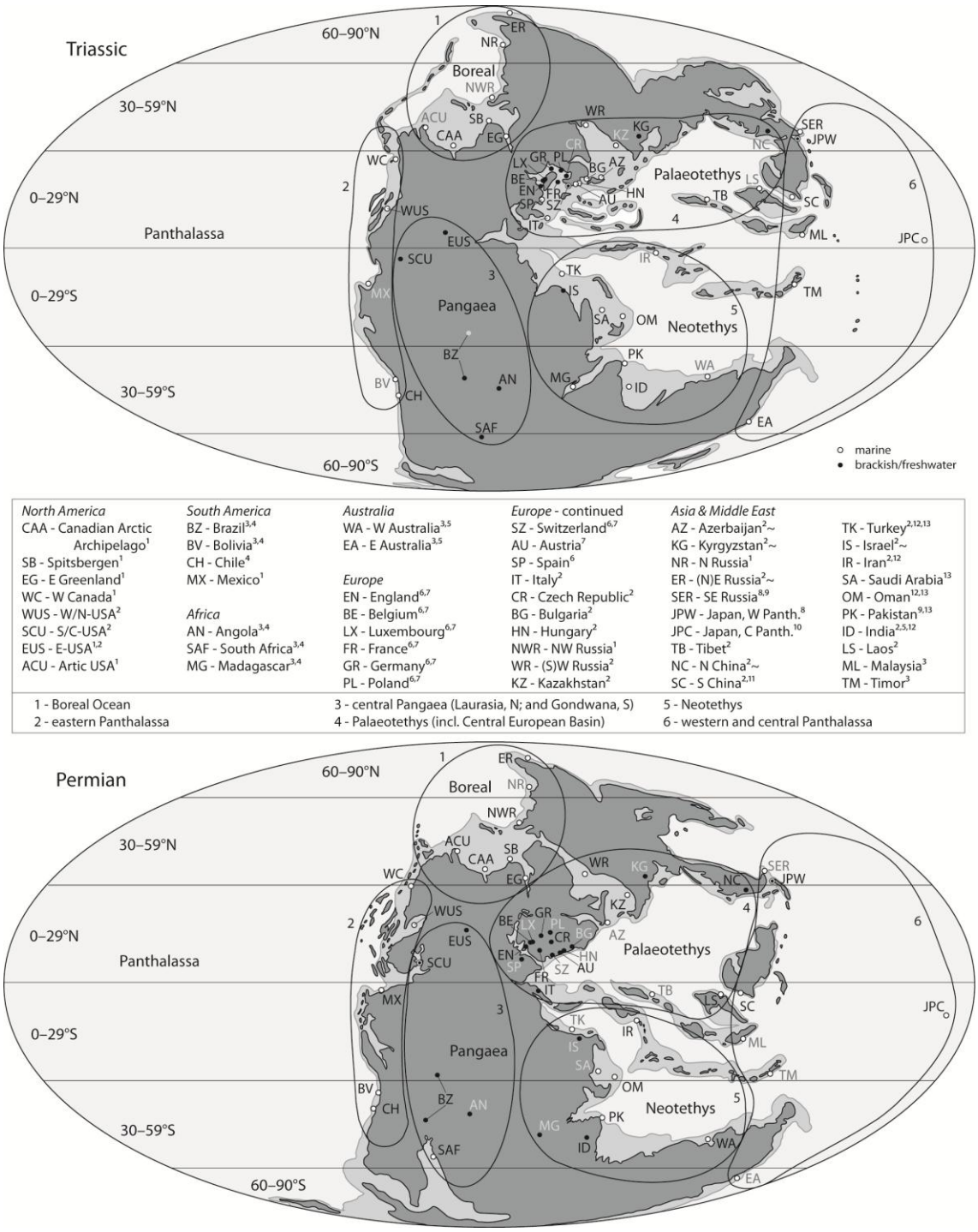

Figure 7.4 – Late Permian (260 Ma) and Early–Middle Triassic (240 Ma) palaeogeographic maps (redrawn from Blakey 2012) showing the position of countries from which Permian–Triassic chondrichthyan remains have been reported. The position of some countries is approximate (indicated by ~ in legend). No material is known from countries shown in grey during that time interval. Generalised basinal positions are outlined. Key to references in superscript: 1, Cocks and Torsvik 2011; 2, Blakey 2012; 3, Scotese 2003; 4, Mutter *et al.* 2007b; 5, Brookfield *et al.* 2003; 6, Fischer *et al.* 2012; 7, Diedrich *et al.* 2009a, b; 8, Yamagishi 2006; 9, Shigeta *et al.* 2009; 10, Isozaki 2009; 11, Lehrmann 1999; 12, Richoz 2006; 13, Jan *et al.* 2009.

of the total), especially in the west, and the USA (25.7%), with the largest concentration in southern and western areas. More localities were situated in the southern hemisphere in Triassic times and especially in the Permian (Figure 7.4), which means that the percentages of occurrences recorded from the northern hemisphere during these time intervals are smaller: 89% in the Triassic and 81% in the Permian (Appendix A2.3.2). In order to understand southern shark faunas better, there is further potential in South America, Africa, the Middle East (as was shown in Oman), Madagascar, Pakistan, India, and Australia, as well as in the region of Indo-China and Indonesia, which record sediments deposited in western and southern Neotethys, as well as in southeastern Panthalassa.

A regional overview of the number of published works reporting new material, therefore excluding papers referring to previously described remains (amounting to a total of 485 publications; Appendix A2.3.3), again shows that the sampling effort is primarily focused on the northern hemisphere (Figure 7.5). This may be explained by the fact that the northern continents have been studied for the largest number of years (Figure 7.6) and there is a significant positive correlation between years of study and the current total number of publications (Table 7.1). Another feature of note is that the rate of exploration appears highest in Asia and the Middle East since the 1940s, compared to relatively constant rates elsewhere (Figure 7.6).

7.3.2 Sampled intervals

The samples used in this study range in age from the late Sakmarian in the Cisuralian to the Norian in the Late Triassic (Figure 7.7). The only intervening stages lacking samples are the Artinskian and Kungurian. The sampled range thus covers the end-Guadalupian crisis and the late Changhsingian extinction event, as well as the subsequent recovery in the Triassic. Globally, no chrondrichthyan material was recovered from the Capitanian and Carnian (Figure 7.7, summary column), but within each region, the chondrichthyan ranges are much more patchy.

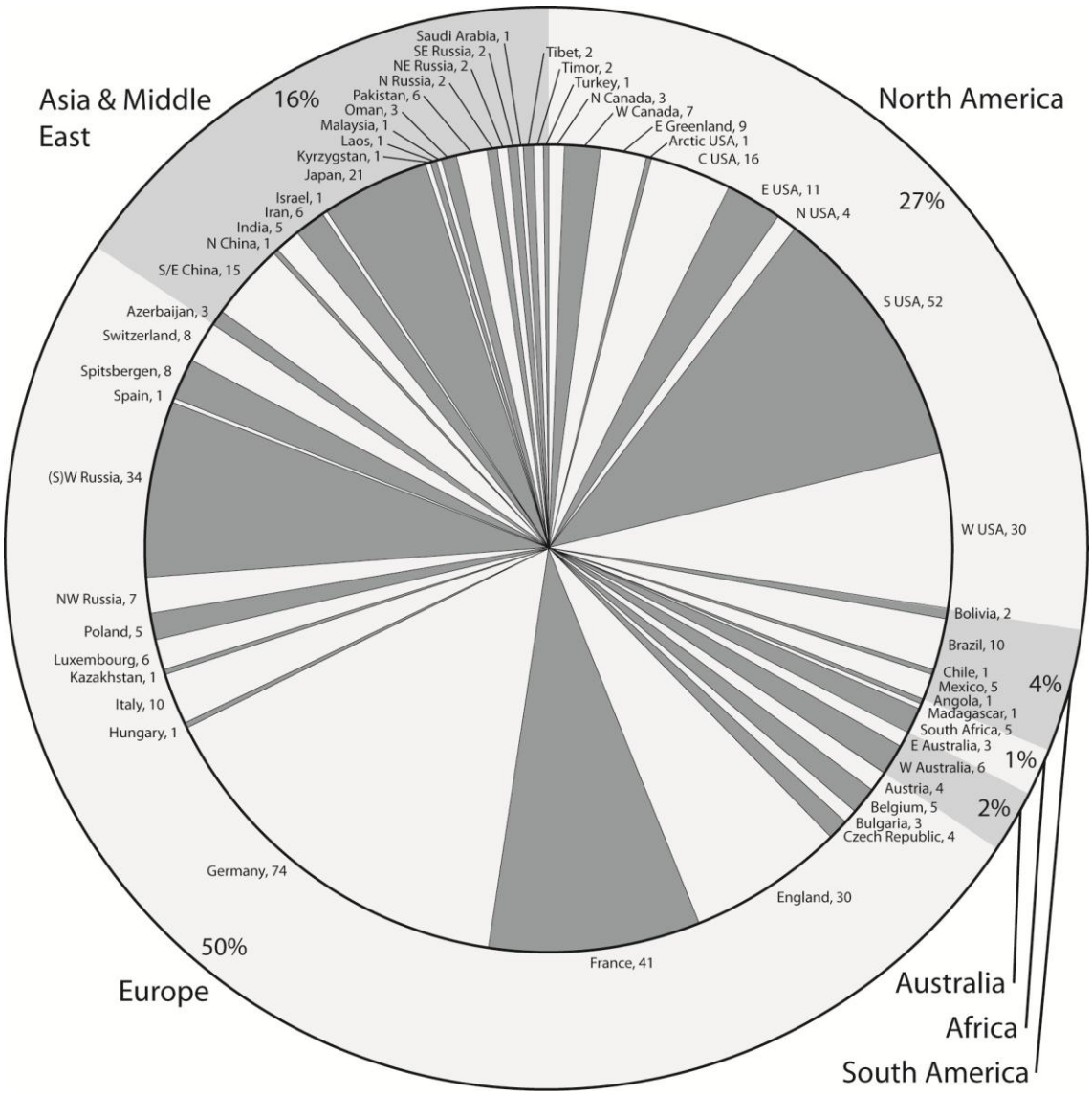

Figure 7.5 – Number of publications per country/region describing new material. Includes contributions made by this study.

The best coverage is available from Oman and Japan. Oman is the only country that provides regional data before each crisis, after each extinction event, in the immediate post-Permian recovery and the later recovery. Japan would have allowed similar observations, but the Permian sediments in the sampled sections appeared to be entirely barren. It should also be noted that some of the samples collected in Oman (from each interval within the Wordian–Smithian range) and East Greenland (from each interval within the Wuchiapingian–Griesbachian range) have not been processed as a result of time constraints (Section 2.1.4; Appendix A1.1).

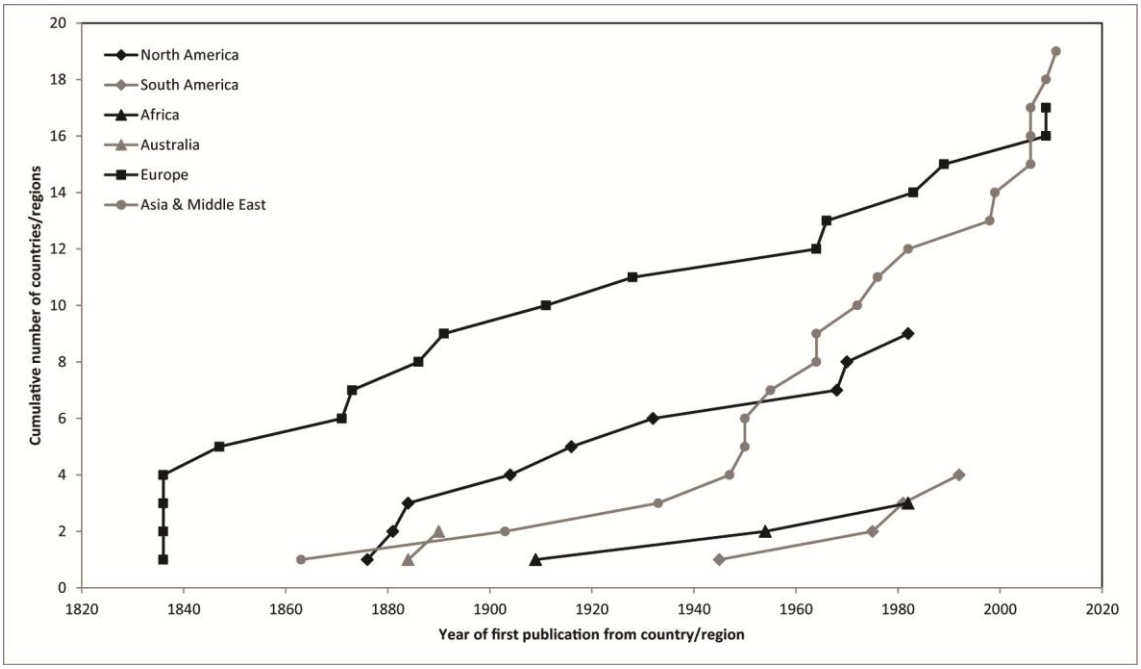

Figure 7.6 – Cumulative count of countries/regions per continent since the year chondrichthyan material was first published from them, illustrating the years of study on each continent and the rate of exploration.

Table 7.1 – Correlation between year of first publication (i.e., years of study) for a country/region and the number of publications from that country/region until the recent. One asterisk indicates a significant correlation at p(2)<0.05 and two a significant correlation at p(2)<0.01 (Appendix A2.3.3).

Correlation	**Spearman's ρ**
Years of study vs. number of publications	0.70** (n = 54)

7.3.3 QUALITY OF THE FOSSIL RECORD

7.3.3.1 DATA INVENTORY

An inventory of occurrence data and raw diversity of Permian and Triassic chondrichthyans (Figure 7.8A, B; Appendix A2.3.5; see also Section 2.6.2), based on the database compiled here, show that counts of taxonomic occurrences are variable throughout the Permian and Triassic. Fewest occurrences are known from the Changhsingian, closely followed by the Induan, whereas the Rhaetian is best sampled, followed by the Anisian–Ladinian interval. However, a significant positive relationship exists between the occurrence data and interval duration (Figure 7.9A, Table 7.2), which means that the observed patterns are not a true representation of sampling effort,

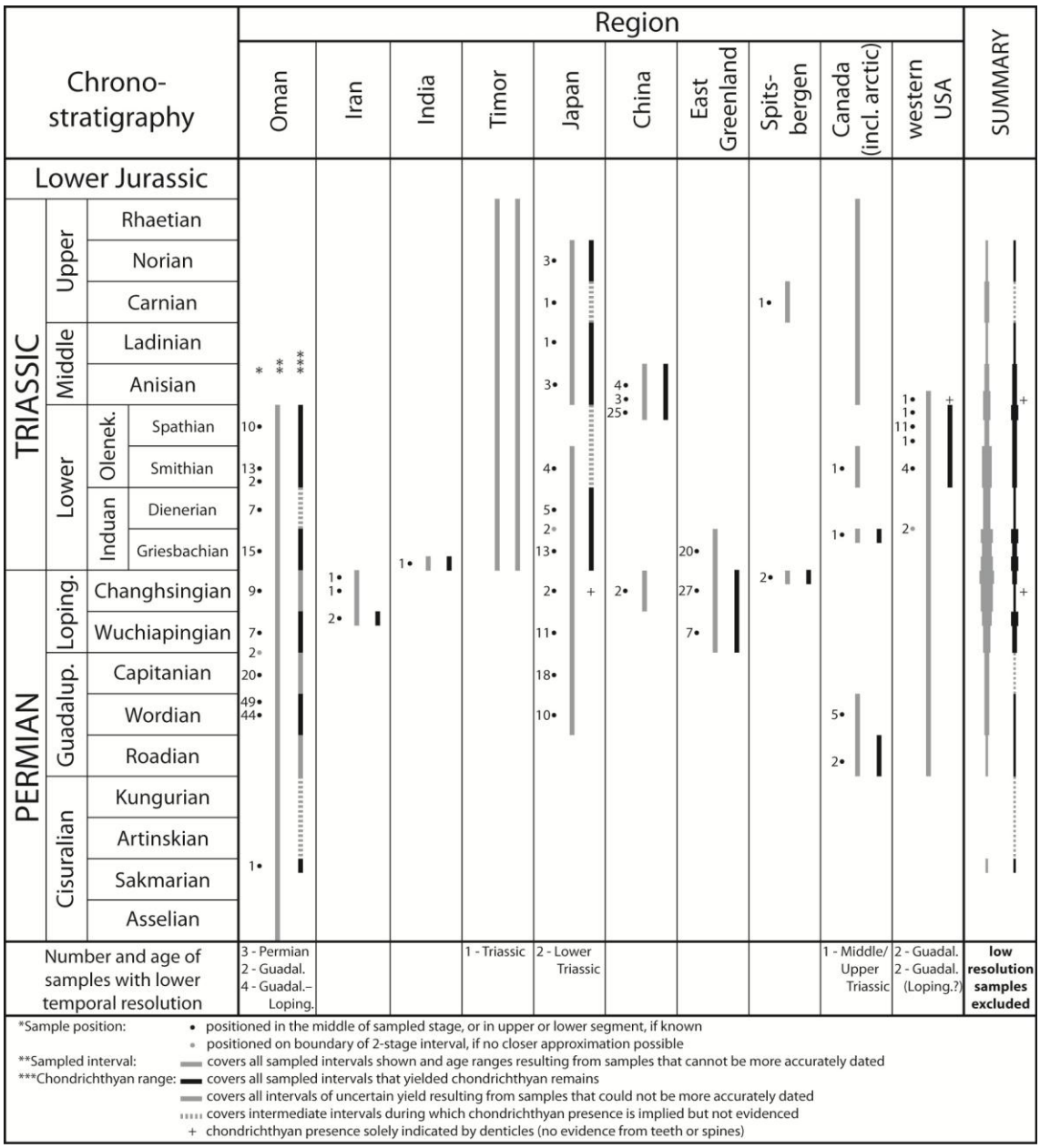

Figure 7.7 – Region and age range of samples used in this study only and the presence of chondrichthyan material obtained from these samples. Includes per-stage regional summary, representing cumulative counts of regions that were sampled or yielded material from a stage (thus irrespective of absolute numbers of samples or specimens recovered) in order to show more frequently sampled and more frequently productive stages, respectively.

but a consequence of artificial bin lengths. One clear outlier is the Norian, from which an unusually low number of occurrences are known, despite its long duration. Also, there is a general trend of better sampling in younger strata, which has previously been observed in analyses on different eras (e.g., Kriwet *et al.* 2009), but it is weak and not significant (Figure 7.8A).

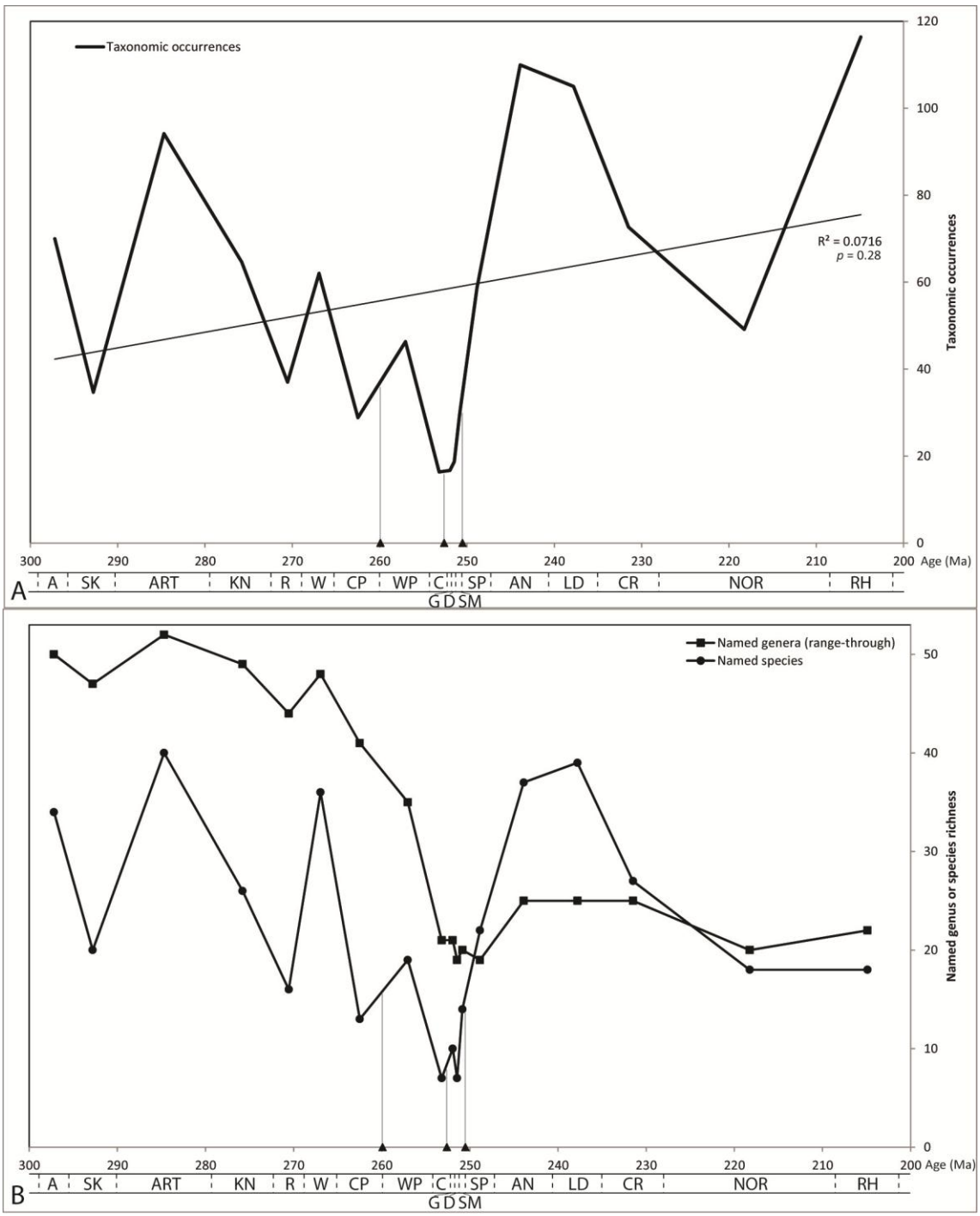

Figure 7.8 – Data inventory of Permian and Triassic chondrichthyans. A, Taxonomic occurrence counts resolved to individual (sub)stages. B, Named genus (fossil and Lazarus) and species counts per (sub)stage. Major biotic crises and extinction events are denoted on the X-axis in age order (triangles): end-Guadalupian crisis, Late Permian extinction, and end-Smithian crisis. Stage abbreviations: A = Asselian, SK = Sakmarian, ART = Artinskian, KN = Kungurian, R = Roadian, W = Wordian, CP = Capitanian, WP = Wuchiapingian, C = Changhsingian, G = Griesbachian, D = Dienerian, SM = Smithian, SP = Spathian, AN = Anisian, LD = Ladinian, CR = Carnian, NOR = Norian, RH = Rhaetian (applies to figures throughout Chapters 7 and 8).

Recorded species diversity closely matches the occurrence pattern, except in the Rhaetian (Figure 7.8B), and a strong positive correlation exists (Figure 7.9B, Table 7.2). Lazarus occurrences have not been counted at species level, but even so, it suggests that species are short-lived and localised. Recorded range-through genus diversity (see Section 8.2.2) also shows a similar trend to the taxonomic occurrence counts, but much less erratic (Figure 7.8B). This diversity curve is not significantly correlated to the taxonomic occurrence counts (Figure 7.9B, Table 7.2), whereas the fossil genus diversity (excluding Lazarus occurrences; see Section 8.2.2) does show a significant positive correlation (Figure 7.9B, Table 7.2). The lower variability in the genus richness curve suggests taxonomic issues at species level and therefore supports further analysis to be carried out at genus level. Geometric morphometric techniques in tooth analysis have been shown to allow differentiation between fossil shark species and may be applied in future for taxonomic purposes (Whitenack and Gottfried 2010).

Division of the overall taxonomic occurrence count into basins reveals the respective productivity in strata originating from these basins, which are related to accessibility, research focus, preservation of relevant strata and chondrichthyan abundance (Figure 7.10A). It highlights, for example, the importance of Palaeotethys (see Figure 7.4) as the major component in the Middle and Late Triassic occurrence peaks, which are predominantly the result of the intensive sampling of strata deposited in the Muschelkalk Basin and the Rhaetian Sea, respectively. Similarly, occurrences recorded from central Pangaea (south-central USA) mainly determine the mid-Cisuralian record (Figure 7.10A, B, C). The Boreal, C/W-Panthalassan and E-Panthalassan basins are of high relative importance during the Early Triassic (Figure 7.10C).

Table 7.2 – Correlation data for taxonomic occurrences. One asterisk indicates a significant correlation at p(2)<0.05 and two a significant correlation at p(2)<0.01 (Appendix A2.3.6).

Correlation of taxonomic occurrences	**Spearman's ρ**
vs. interval duration	0.70** (n = 18)
vs. named, fossil species richness	0.83** (n = 18)
vs. named, fossil genus richness	0.49* (n = 18)
vs. named, range-through genus richness	0.35 (n = 18)

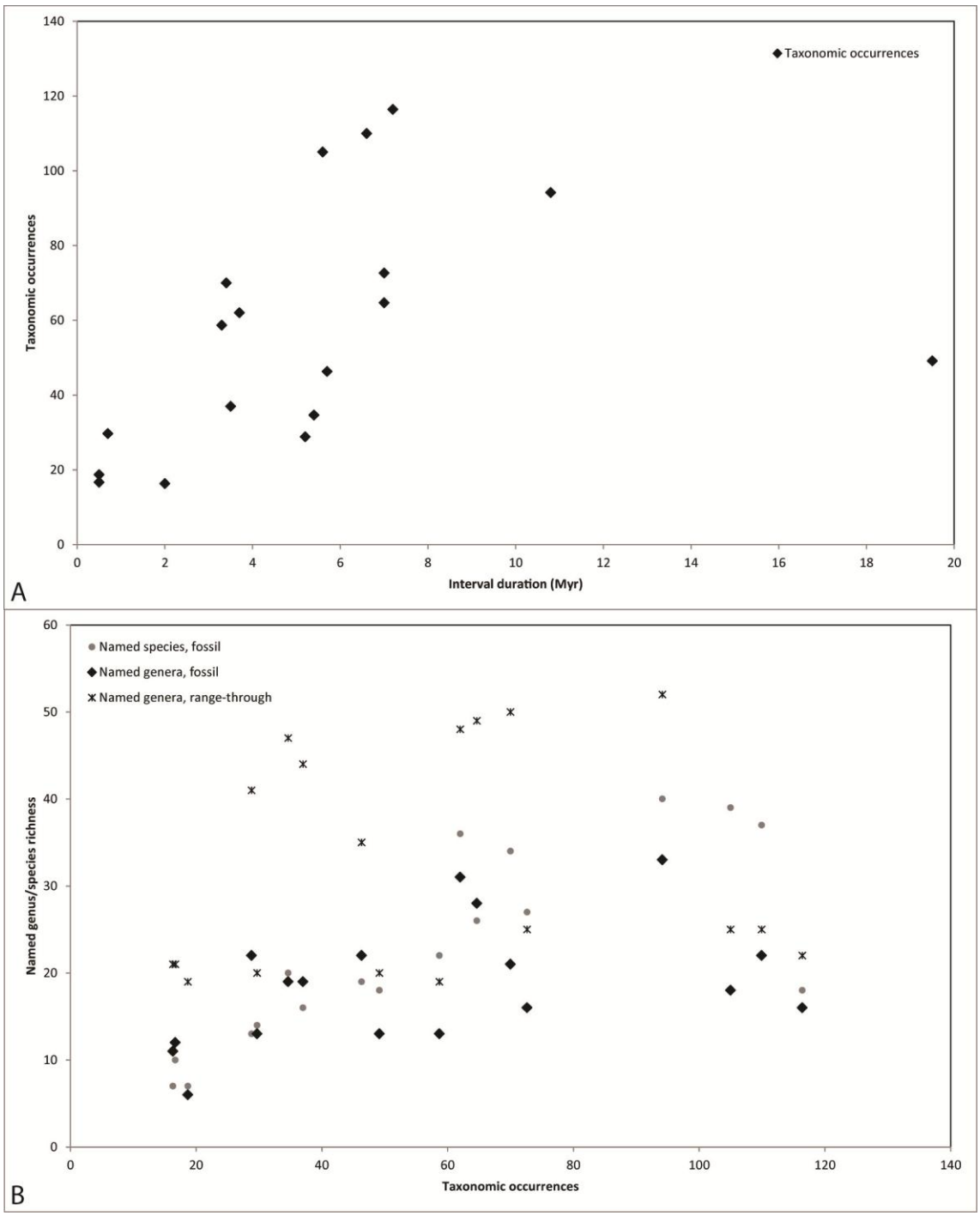

Figure 7.9 – Taxonomic occurrence data for all (sub)stages. A, Taxonomic occurrences against interval duration. B, Species and genus richness based on fossil evidence and also including Lazarus occurrences, against taxonomic occurrences. Correlation data are provided in Table 7.2.

7.3.3.2 PHYLOGENETIC DIVERSITY ESTIMATES

The compilation of stratigraphic ranges of Permian–Triassic chondrichthyan genera has yielded data on the number of known fossil ranges per (sub)stage, as well as

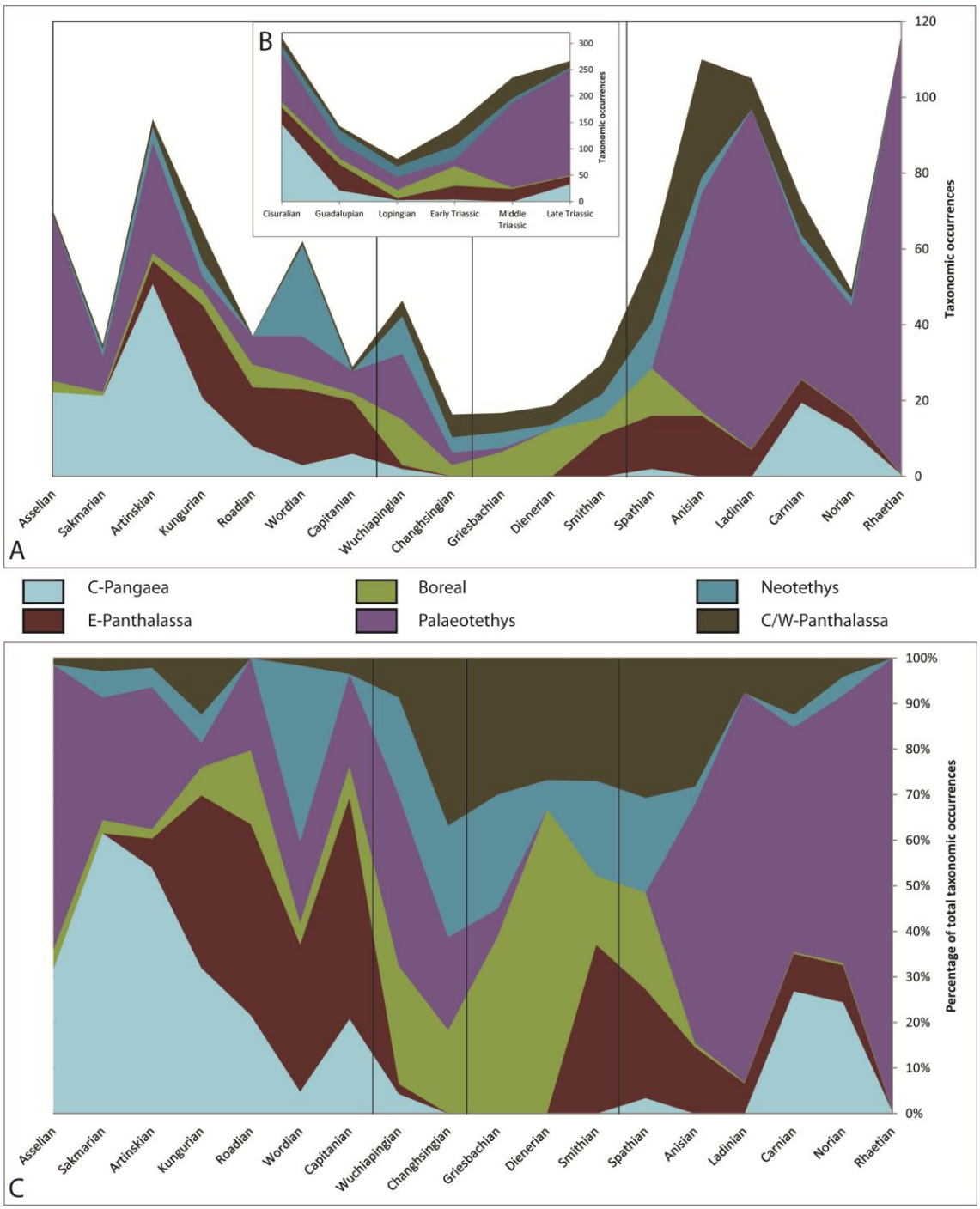

Figure 7.10 – A, Taxonomic occurrences per basin per (sub)stage. B, Taxonomic occurrences per basin per epoch. C, Proportion of taxonomic occurrences per basin per (sub)stage. Major biotic crises and extinction events are marked (vertical lines) in age order: end-Guadalupian crisis, Late Permian extinction, and end-Smithian crisis.

intervening stages (Figure 7.11A). At the genus-level, the fossil record appears to be inadequate only during the Asselian and Sakmarian, the Roadian and, again, during the Dienerian. Conversely, the Permian fossil record appears to be most complete

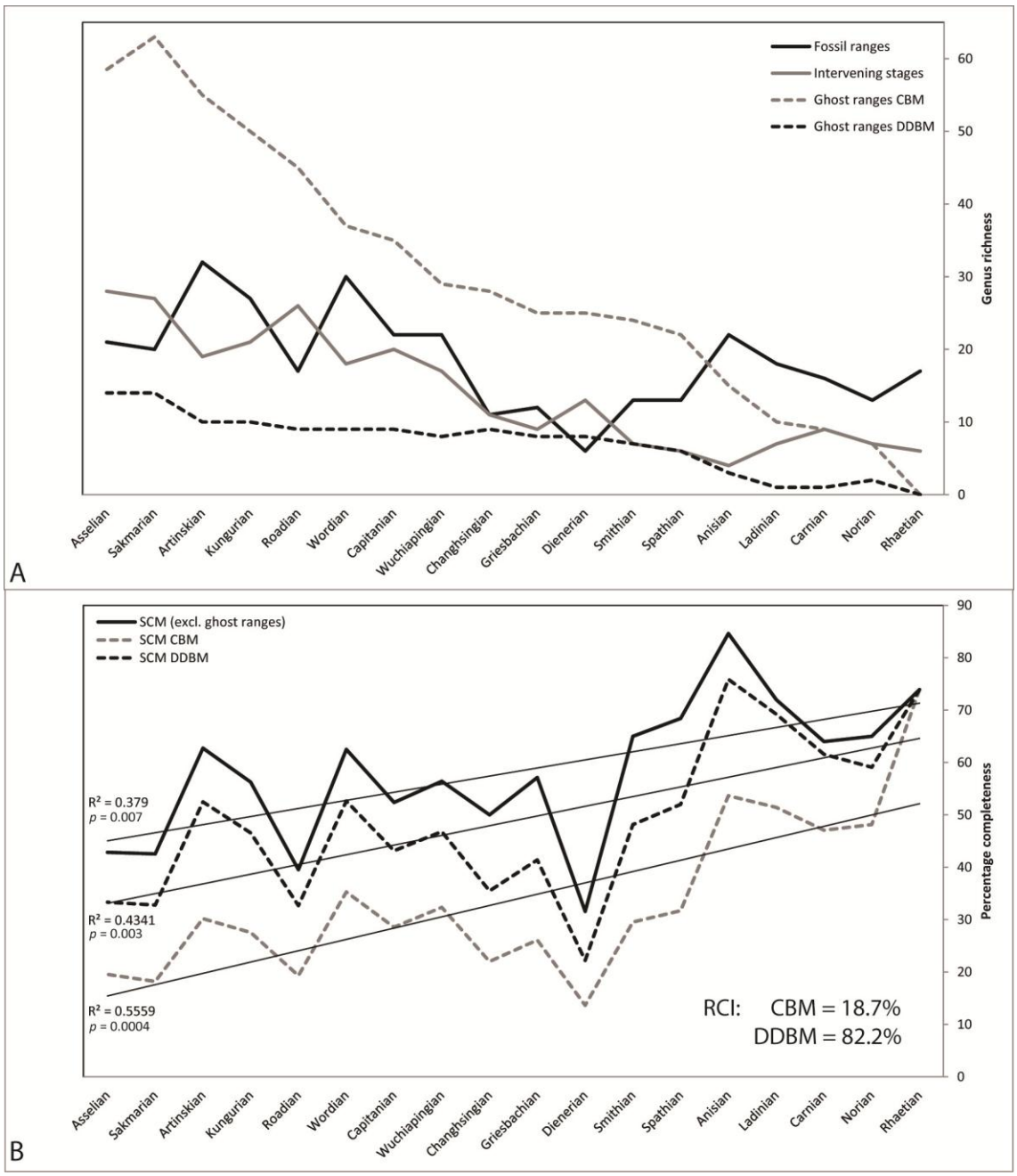

Figure 7.11 – Completeness of the fossil record of Permian and Triassic chondrichthyans. A, Counts of known fossil ranges, intervening stages, and ghost ranges resulting from the CBM and the DDBM per (sub)stage. B, Results of the SCM (in %) for completeness excluding ghost ranges, and completeness including ghost ranges resulting from the CBM and the DDBM per (sub)stage. Includes results of the RCI calculated for both the CBM and DDBM.

during the Artinskian and Wordian, when the proportion of intervening stages is low. The Triassic fossil record, apart from the Induan, is more complete than the Permian, with a consistently lower proportion of intervening stages versus fossil ranges. The most complete stage of the entire Permian–Triassic interval is the Anisian.

Linking the stratigraphy to the phylogeny of the same genera (Figure 7.1), to which both the Conventional Branching Method (CBM) and Direct Descendence Branching Method (DDBM; see Guinot *et al.* 2012) have been applied, also yields two interpretations (an overestimate and underestimate, respectively) of the number of ghost ranges per (sub)stage (Appendix A2.3.8–A2.3.10; see Section 2.6.5). Completeness of the fossil record based on these data has been assessed by application of the Simple Completeness Metric (SCM; Benton 1987; Figure 7.11B). The results show that there is large variability in completeness of the fossil record. Our knowledge of the Permian fossil record is particularly good in the Artinskian and Wordian, from which time intervals the number of known fossil ranges significantly exceeds the number of intervening stages, in contrast to the fossil record of the Roadian. The Griesbachian has a slightly better fossil record compared to the Changhsingian, whereas it is virtually equal to or worse than the Wuchiapingian fossil record and the Dienerian record is comparatively extremely poor. This, therefore, only partially agrees with the suggested enhanced earliest Triassic chondrichthyan fossil record compared to the Lopingian, based on family-level data (Twitchett 2001b), whereas a new compilation of family-level data shows no evidence of an enhanced fossil record in the earliest Triassic (Figure 7.12).

From the Olenekian onwards, completeness gradually improves (Figure 7.11B). Completeness data further suggest that the Middle and Upper Triassic fossil record is consistently better known than that of the Permian–Early Triassic. Significantly positive overall trends are observed in all three completeness estimates. A decline is apparent in both counts of ghost ranges per time interval (Figure 7.11A), although much less drastic in the DDBM as compared to the CBM, suggesting again that there is a gradual increase in our knowledge of the fossil record towards the Recent. This pattern is a stratocladistic methodological consequence (see e.g., Huelsenbeck and Rannala 2000) of the exclusion of Jurassic genera, which may have diverged in the Triassic. The absence of their ghost ranges hence artifically improve the Triassic fossil record. The influence of excluding Jurassic taxa is deemed minimal, however, because the

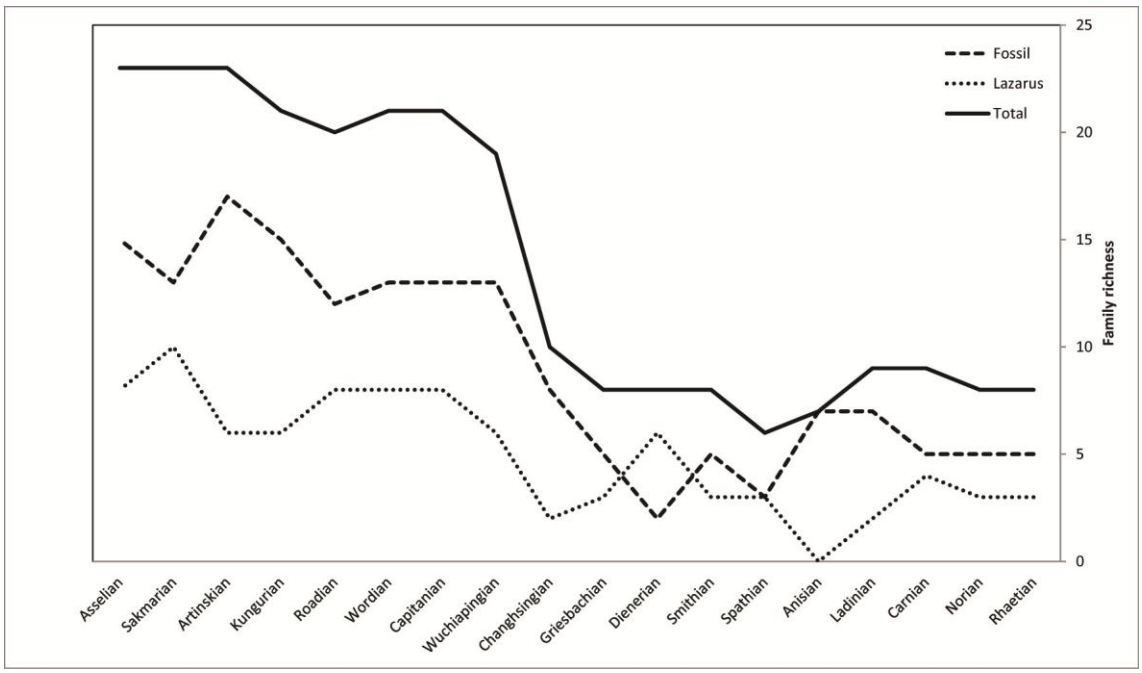

Figure 7.12 – Family diversity of Permian and Triassic chondrichthyans. A, Counts of named fossil families, Lazarus occurrences of named families, and cumulative counts of named families per (sub)stage.

diversification of Jurassic neoselachian groups occurred predominantly in the Early Jurassic (Kriwet *et al.* 2009).

The Relative Completeness Index (RCI), calculated for both of the phylogenetic trees resulting from the respective branching methods, illustrates the large overall difference between the fit of the phylogenies to the stratigraphy. When using the DDBM, 82.2% of the phylogeny matches the observed fossil record, whereas using the CBM, only 18.7% matches. The mean RCI of 63.17% for the Chondrichthyes recorded by Benton *et al.* (1999), based on the analysis of seven cladograms, lies well within the potential range of completeness shown here.

Total diversity estimates resulting from the CBM and DDBM define the boundaries of the Genuine Diversity Domain (GDD; Figure 7.13A), as outlined by Guinot *et al.* (2012). By respectively overestimating and underestimating diversity, it outlines the maximum boundaries between which true diversity should be found. The gap between standing diversity and the GDD is a reflection of the completeness of the fossil record. Both raw standing diversity (based on known fossil ranges and intervening stages) and Estimated Mean Standing Diversity (EMSD; see Section 8.2.3 for detailed discussion)

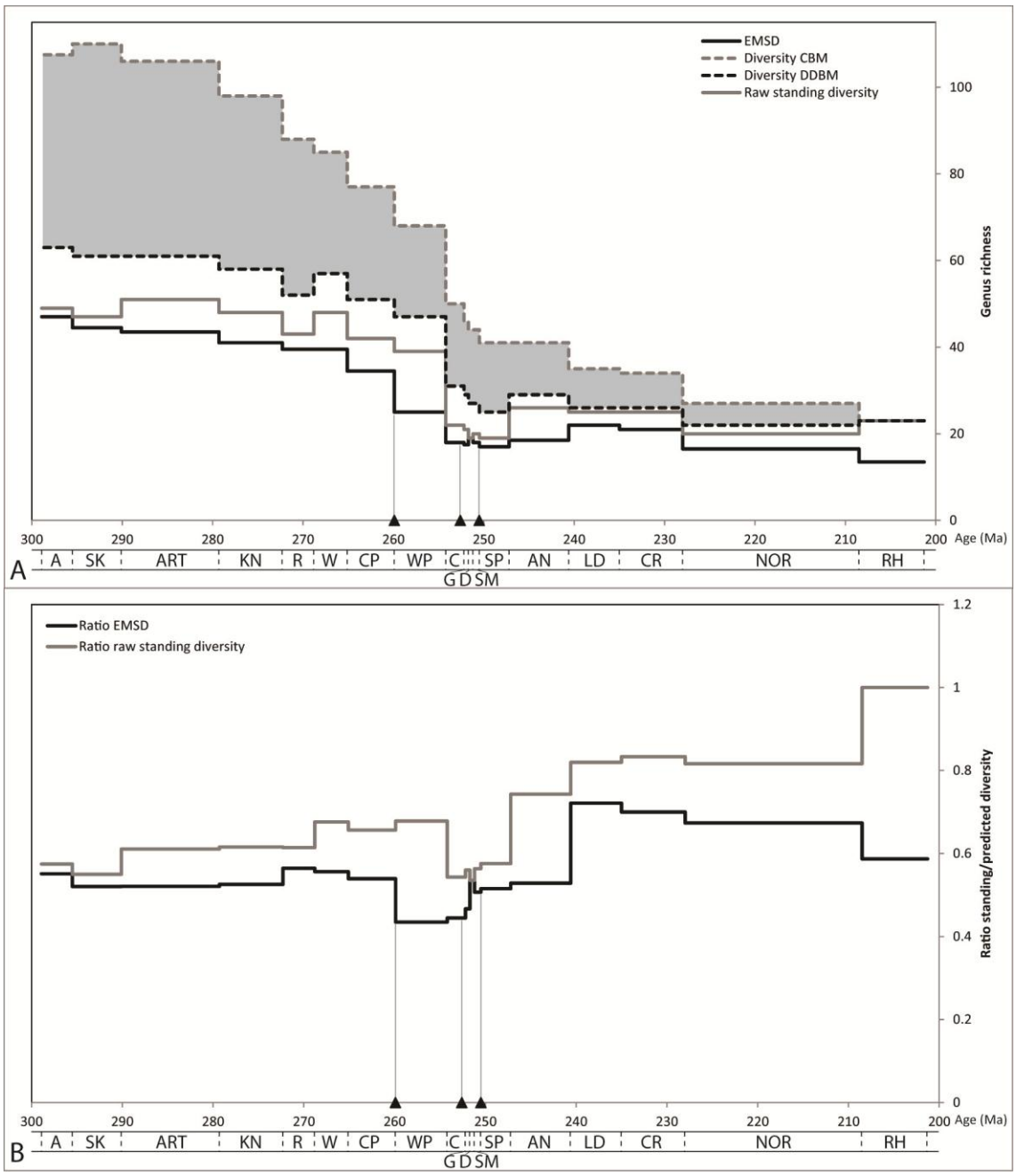

Figure 7.13 – A, Total diversity estimates, based on the fossil record of Permian and Triassic chondrichthyans: EMSD, raw standing diversity, and total diversity based on the CBM and the DDBM against time. Grey shaded area defines the GDD. B, Ratio of standing diversity to predicted diversity (mean GDD value) using EMSD and raw standing diversity. Major biotic crises and extinction events are denoted on the X-axis in age order (triangles): end-Guadalupian crisis, Late Permian extinction, and end-Smithian crisis.

have been included here. The data show a large difference between diversity estimates resulting from the CBM and DDBM in the Permian, leaving great uncertainty in true diversity (Figure 7.13A). All diversity estimates nevertheless show a gradual decline,

with a reduction of the largest magnitude observed across the Wuchiapingian/Changhsingian boundary. Triassic diversity estimates lie closer together, suggesting a more complete fossil record. This is demonstrated by the gap between standing diversity and the GDD, which is consistently large throughout the Permian up until the mid-Lopingian. The gap lessens during the Early Triassic and especially from the end of the Spathian onwards. The ratio of standing diversity to the mean predicted diversity (average of CBM and DDBM diversity estimates) shows a reduction in completeness around the Permian/Triassic boundary, followed by a gradual increase in the Triassic (Figure 7.13B). EMSD diverges again from the GDD in the Rhaetian, which is due to the exclusion of the large number of singleton taxa in this time interval (see Section 2.6.7). A direct comparison with the analyses of Guinot *et al.* (2012) is not possible here, because their work focused only on Mesozoic taxa. There is agreement, however, with regard to the general stability of genus diversity through the Triassic.

7.4 DISCUSSION

7.4.1 GENERAL OBSERVATIONS ON THE FOSSIL RECORD

Observations on the chondrichthyan fossil record have shown that the majority of records originate from the northern hemisphere: around 80–90% in the Permian and Triassic and over 95% in the Recent configuration (Figure 7.3). Relative sampling effort and productivity in strata may not only be related to accessibility, research focus, and preservation of relevant strata, but also to chondrichthyan presence and abundance. Hence, the pooling of taxonomic occurrences into palaeobasinal regions has revealed the relative importance of these areas through time, allowing fluctuations in chondrichthyan presence and/or sampling to be identified (Figure 7.10). The genus diversity of the chondrichthyan community is inherently similarly distributed (see Section 8.4.3).

Occurrence data are variable throughout the Permian and Triassic (sub)stages with fewest occurrences in the Changhsingian and the Induan, whereas the Rhaetian and the Anisian–Ladinian interval are the best sampled (Figure 7.8). However, this is shown to be predominantly a reflection of (sub)stage length by means of a significant positive correlation, although the Norian does not conform to this pattern (Figure 7.9A, Table 7.2). Also, fossil genus diversity significantly correlates with taxonomic occurrence counts, which means that a sampling bias exists in these data (Table 7.2), but ranging this diversity through (including Lazarus occurrences) removes this correlation, which suggests that it is an unbiased representation of diversity with regard to occurrence data. Species-level and family-level data are not used in further analyses, because of instability of the diversity signal and the exclusion of a large part of the dataset, respectively.

Twitchett (2001b) suggested the presence of a preservational bias in the Induan based on family-level data in Cappetta *et al.* (1993), which was considered unique among all marine groups. Enhanced preservation relative to the Late Permian was offered as the explanation for apparent chondrichthyan survival through the mass extinction and an apparent radiation in fish families in the earliest Triassic (Twitchett 2001b). Sun *et al.* (2012) reiterated the exceptional quality of the Early Triassic fossil fish record, attributing this to widespread anoxia. This interpretation of the fossil record is not fully supported by the data presented here. No Early Triassic radiation in chondrichthyan families is observed (Figure 7.12) and both family and genus-level data show that, during the Lopingian and Early Triassic, Lazarus occurrences only exceed fossil taxa in the Dienerian, showing that it is a particularly poorly sampled interval and/or that preservation was reduced (Figure 7.11A, Figure 7.12). Significantly enhanced preservation in the recovery phase is not observed until the Smithian. However, the Griesbachian does have a slightly better fossil record compared to the Changhsingian (Figure 7.11A), which is also consistently evident from phylogenetically assessed completeness (SCI; Figure 7.11B). Completeness assessed through

standing diversity and GDD shows inconsistent and occasionally opposing patterns (Figure 7.13B).

It has been reported in literature that long-term trends of better sampling in more recent strata may be observed (e.g., Kriwet *et al.* 2009). The data presented here only show a weak and non-significant trend of better sampling in younger strata (Figure 7.8A). The data suggest, however, that sampling becomes more exhaustive through the Permian–Triassic and that our understanding of interrelationships among more recent genera is better. The number of Lazarus occurrences in most of the Triassic are much lower than in the Permian and show a large difference with the number of genera observed in the fossil record (Figure 7.11A). Furthermore, completeness data indicate an overall positive trend, with the Smithian–Rhaetian being consistently better known than the Asselian–Dienerian (Figure 7.11B). This is potentially aided by the development of triple layered enameloid, which enhances preservation potential (Klug 2010). Finally, an increasingly better fit of the phylogeny to stratigraphy is observed, with a narrowing GDD range throughout the Permian–Triassic interval (Figure 7.13A), as well as a gradually increasing ratio of observed standing diversity to mean predicted diversity (Figure 7.13B).

7.4.2 Features of the chondrichthyan fossil record

7.4.2.1 Roadian fossil gap and its context

For chondrichthyans, the Cisuralian was an epoch characterised by high abundance (as suggested by the large number of taxonomic occurrences; Figure 7.8). Nevertheless, the data suggest a limited understanding of chondrichthyan phylogeny at this time (Figure 7.13A). The Asselian–Sakmarian fossil record is inadequate, with Lazarus occurrences exceeding the known fossil record (Figure 7.11A) and reduced completeness in the early Cisuralian (Figure 7.11B).

Following a period of high completeness in the late Cisuralian (Figure 7.11B), the Roadian fossil record is characterised by a peak in Lazarus taxa, exceeding the

number of known fossil taxa (Figure 7.11A) and hence very low levels of completeness (Figure 7.11B). This is accompanied by a significant drop in taxonomic occurrences (Figure 7.8), which is predominantly explained by the reduced number of occurrences from north-central Pangaean localities, and to a lesser extent by central and western Panthalassan and Neotethyan localities (Figure 7.10). It may be considered, therefore, that the predominant cause for this temporary gap in the fossil record should be sought in the terrestrial geological record. Strikingly, the Roadian is often discussed in relation to a global hiatus in the tetrapod fossil record, “Olson’s Gap”, which covers the majority of the stage due to its 2.6 Myr duration (Benton 2012). The existence of this gap has been challenged (Benton 2012 and references therein) and it has been interpreted instead as an extinction pulse, characterised by an extended period of low diversity and the loss of two-thirds of global terrestrial vertebrates (Sahney and Benton 2008). The data presented here suggests that this extinction event potentially also affected freshwater chondrichthyans (but see Section 8.3.2).

A large proportion of the following Wordian peak in taxonomic occurrences and observed fossil ranges (Figure 7.8A; Figure 7.11A) is the result of the contribution of Neotethyan occurrences to the total (Figure 7.10A), for which the Khuff fauna from Oman, described in this study (Section 3.2.2.1), is largely responsible. It comprises 15 genera, including three singleton taxa. EMSD shows no peak, however, nor does diversity estimated using the CBM, but raw standing diversity and the DDBM diversity estimate do show a temporary increase (Figure 7.13A). Following the CBM, the fauna creates four ghost ranges among the Hybodontiformes (*Khuffia*, *Omanoselache*, *Teresodus* and *Reesodus*), whereas one ghost range among the Neoselachii is partially filled (*Nemacanthus*; Appendix A2.3.8). Following the DDBM, however, no ghost ranges are created and ‘Palaeozoic Genus 1’ partially fills the ghost range of its sister taxon, *Homalodontus*, although this is an uncertain relationship resulting from a polytomy (Appendix A2.3.9). Overall, the Wordian fossil record stands out for its high completeness (Figure 7.11B).

7.4.2.2 CAPITANIAN/WUCHIAPINGIAN BOUNDARY

The transition from the Capitanian to the Wuchiapingian is characterised by an overall increase in the number of taxonomic occurrences (Figure 7.8), which is attributable to the Boreal, Palaeotethys and Neotethys oceans (Figure 7.10). Conversely, a large decrease in occurrences from the eastern Panthalassan region occurs across the Capitanian/Wuchiapingian boundary (Figure 7.10). The fossil record is shown to be adequate and of generally consistent completeness across the boundary (Figure 7.11B; except for a potential drop in the ratio of EMSD against predicted diversity, Figure 7.13B), providing evidence that the observed trends are not artefacts.

7.4.2.3 LOPINGIAN–MIDDLE TRIASSIC

Phylogenetically assessed diversity estimates suggest a significant drop in diversity in the Changhsingian compared to the Wuchiapingian, but no events occurring across the Permian/Triassic boundary (Figure 7.13A). The number of taxonomic occurrences also declined from the Wuchiapingian to the Changhsingian, resulting in a minimum for the entire Permian–Triassic interval, which was maintained in the Griesbachian (Figure 7.8). However, completeness of the Lopingian fossil record is average for the Permian and fairly stable (Figure 7.11B), despite the suggestion of slightly reduced completeness in the Changhsingian and potentially also the Wuchiapingian by the ratio of standing diversity against the mean GDD (Figure 7.13B). There is, therefore, no evidence to suggest that low occurrence numbers are responsible for the observed diversity low.

Occurrence counts suggest that the Boreal Sea was of great importance throughout the Lopingian–Induan interval and both Neotethys and central and western Panthalassa gained in importance over the Permian/Triassic boundary (Figure 7.10). In contrast, the number of occurrences from Palaeotethys declined and no Changhsingian–Dienerian occurrences were recorded from eastern Panthalassa and central Pangaea (Figure 7.10). Occurrences were again recorded from eastern

Panthalassa from the Smithian onwards, synchronous with a decline in occurrences in the Boreal area (Figure 7.10). The number of taxonomic occurrences rises again through the Dienerian–Anisian, with an increased rate during the Olenekian (Figure 7.8), which may reflect a rapid increase in chondrichthyan abundance over the Early Triassic. Completeness of the Anisian fossil record is extremely good (Figure 7.11B), which is explained by the narrow GDD range (Figure 7.13A) and the low number of Lazarus occurrences compared to observed fossil taxa (Figure 7.11A). In conclusion, having developed an understanding of the mechanics of the chondrichthyan fossil record and its shortcomings, this will aid in identifying actual and artificial patterns in diversity estimates, which may, therefore, be assessed at their rightful value.

8 GLOBAL CHONDRICHTHYAN PALAEOGEOGRAPHICAL DISTRIBUTION, DIVERSIFICATION TRAJECTORIES AND LIFE-HISTORY TRAITS

8.1 INTRODUCTION

In this chapter, global patterns of chondrichthyan diversity, palaeoecology and distribution are presented and discussed, based on a newly compiled database (Appendix A2.1). Previous diversity analyses were primarily based on reference works that are now superceded by new data (including Zangerl 1981, Cappetta 1987, Cappetta *et al.* 1993; Stahl 1999; Sepkoski 2002; see Section 8.5.2), and so this attempts to be the most up-to-date and comprehensive analysis of patterns and trends in chondrichthyan diversity and distribution that is currently available.

8.2 DIVERSIFICATION TRAJECTORIES

8.2.1 INTRODUCTION

Chondrichthyes underwent a series of radiations since their apparent origination in the early Silurian (e.g., Sansom *et al.* 2000) or even the Middle–Upper Ordovician (Sansom *et al.* 1996, 2012), including a diversity increase during the Devonian culminating in a primary radiation peak in the Carboniferous, followed by a secondary peak during the Jurassic and Cretaceous (Compagno 1990). Friedman and Sallan (2012) summarised current knowledge on the effects of the Late Permian extinction event on fossil fish, which remains ambiguous and subjective (e.g., Janvier 1996; Blieck 2011). It is suspected that a relatively poor understanding of the Permian fossil fish record, which is based primarily on body fossils from exceptionally preserved deposits, compared to the well-documented Triassic fossil record based on teeth, is the main reason that recent fish studies in relation to the Late Permian event focus on recovery without attempting to establish whether fish were in fact subject to extinction

(Foote and Sepkoski 1999; Friedman and Sallan 2012). This study confirms that the Permian record is poorly understood but shows, however, that rich pockets of Permian microvertebrate remains do indeed exist (e.g., Oman) from which many previously unknown taxa may still be recognised. Little evidence has hitherto been found for major taxonomic shifts in the fish fauna associated with the Late Permian extinction, nor has a striking decline in richness been apparent (Janvier 1996; Blieck 2011; Friedman and Sallan 2012). From a compositional point of view, however, most of the major Palaeozoic chondrichthyan taxa went extinct around the time of the Permian/Triassic boundary (the last edestoids, ctenacanths and xenacanths died out in the Triassic) and the Triassic community was primarily composed of persistent hybodont, neoselachian and chimaeroid populations (Compagno 1990; Janvier 1996). This section evaluates chondrichthyan diversity and faunal composition in order to reveal patterns based on the current fossil record.

8.2.2 Taxonomic (genus) diversity estimates

The individual elements (N_{FL}, N_{bL}, N_{Ft}, N_{bt}) that amount to an assessment of total genus diversity (N_{TOT}; see Section 2.6.6) show that the majority of genera in both the Permian and Triassic have been assigned a distinctive genus name, although the number (and proportion) of taxa left in open nomenclature tends to increase when generic richness is high (Figure 8.1A). The number of genera observed in the fossil record ($N_{bt(r)}$) tends to exceed the number of Lazarus occurrences ($N_{bt(z)}$) throughout the Permian–Triassic interval, except for the Asselian–Sakmarian, the Roadian and the Dienerian, whereas the lowest proportion of Lazarus occcurrences is observed in the Artinskian, Wordian and the post-Induan Triassic record (particularly the Anisian).

The correlation data of genus diversity with interval duration (Table 8.1) clearly show that richness counts solely based on fossil material are significantly correlated to the duration of time bins and are not an accurate reflection of temporal diversity patterns.

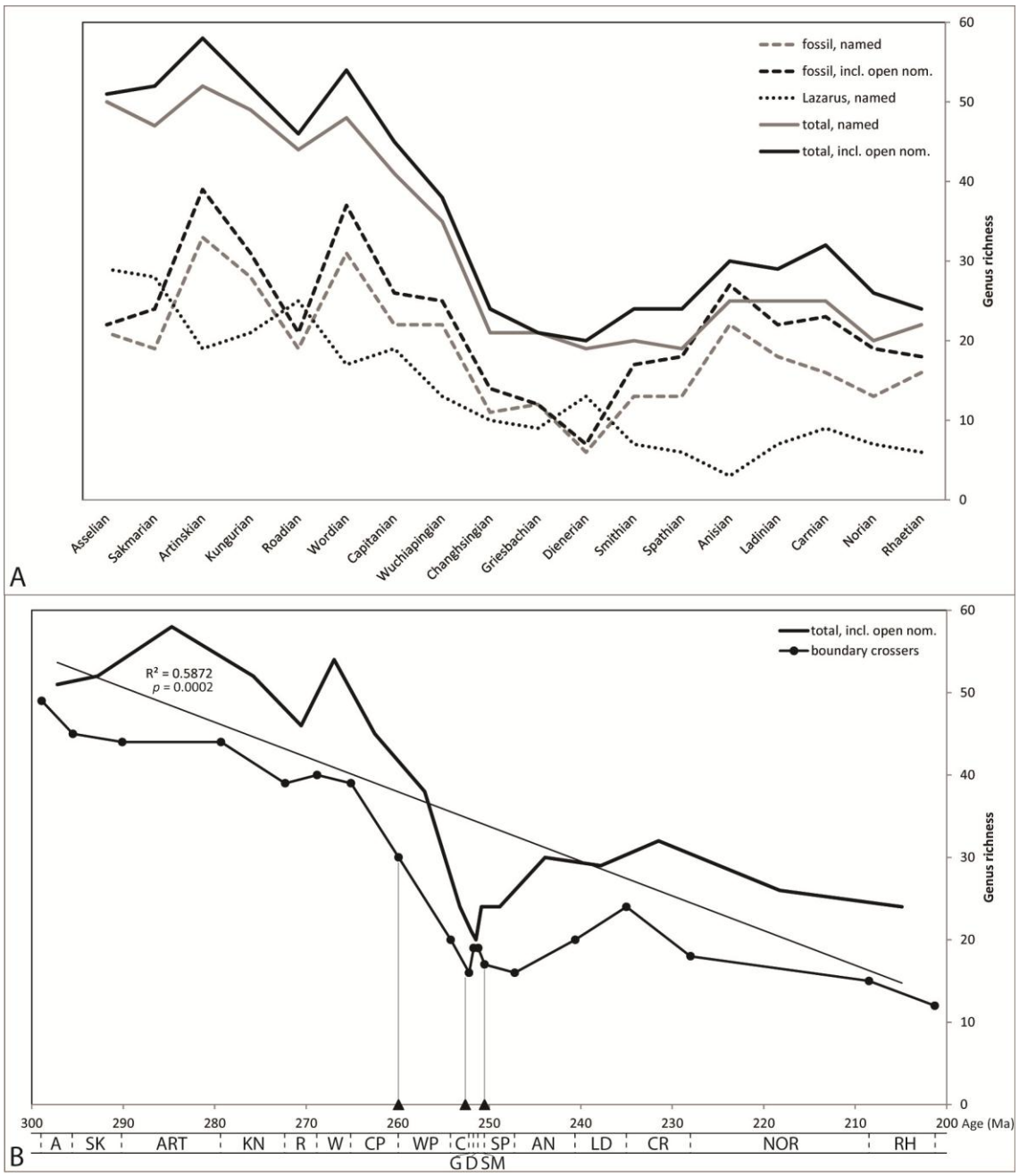

Figure 8.1 – Genus diversity of Permian and Triassic chondrichthyans. A, Counts of named fossil genera, all fossil genera (including those in open nomenclature), Lazarus occurrences of named genera, and range-through data of named genera, and all genera per (sub)stage. B, Range-through data of all genera (plotted at mid-interval), and counts of boundary crossing genera (plotted at interval boundaries) against time. Major biotic crises and extinction events are denoted on the X-axis in age order (triangles): end-Guadalupian crisis, Late Permian extinction, and end-Smithian crisis.

Range-through data, however, incorporating Lazarus occurrences, are not significantly correlated with interval duration and may therefore be biologically interpreted.

Table 8.1 – Correlation data for genus diversity vs. interval duration. One asterisk indicates a significant correlation at p(2)<0.05 and two a significant correlation at p(2)<0.01 (Appendix A2.4.4).

Correlation of interval duration	**Spearman's ρ**
vs. fossil, named genus richness	0.51* (n = 18)
vs. fossil genus richness (incl. open nomenclature)	0.61** (n = 18)
vs. Lazarus, named genus richness	-0.10 (n = 18)
vs. range-through, named genus richness	0.37 (n = 18)
vs. range-through genus richness (incl. open nomenclature)	0.45 (n = 18)

The rapidity at which change in genus diversity takes place is more accurately reflected when plotted against time (Figure 8.1B). It shows a significant decreasing trend through the Permian and Triassic, but is punctuated by events. The genus diversity curve broadly follows the number of genera crossing the stage boundaries, except for a drop in the Roadian, which appears to be due to a reduced quality of the fossil record (Figure 8.1A). A reduction is apparent in both curves surrounding the Late Permian mass extinction, extending from the Wuchiapingian–Anisian for genus diversity and from the Capitanian/Wuchiapingian boundary to the Anisian/Ladinian boundary for boundary crossing taxa (Figure 8.1B). It thus shows a clear effect of the end-Guadalupian crisis, with continued pressure of the subsequent Late Permian mass extinction. The lowest number of boundary crossing taxa associated with the Permian decline occurs at the Permian/Triassic boundary, hence the lowest genus diversity is observed in the Griesbachian–Dienerian. The number of boundary crossers increased briefly during the Induan and early Olenekian, which seemingly resulted in a small diversity increase, but the end-Smithian crisis led to a further decline in boundary crossing taxa and diversity temporarily ceased to increase in the Spathian (see Ovtcharova *et al.* 2006; Song *et al.* 2011). Although greater genus diversity is again recorded from the Anisian, it remained around half the richness recorded during the Cisuralian and middle Guadalupian, and the overall declining trend resumed.

The compositional overview of genus diversity (Figure 8.2A) clearly shows the transition of a diverse chondrichthyan population consisting of seven well-established groups in the Permian to a community dominated by two groups in roughly equal

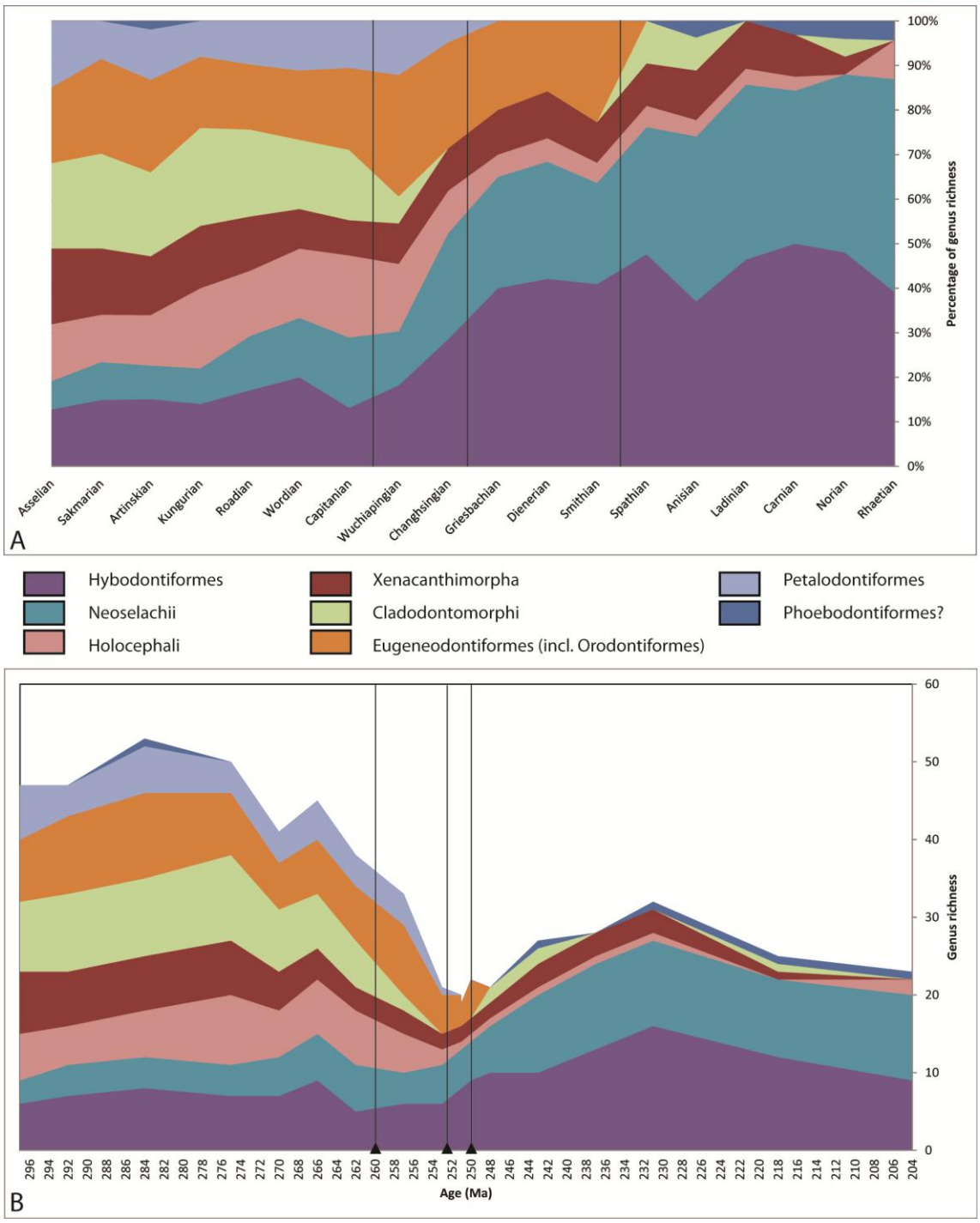

Figure 8.2 – A, Proportion of genus diversity per order or higher taxonomic classification per (sub)stage. B, Genus diversity per order or higher taxonomic classification against time. Major biotic crises and extinction events are denoted on the X-axis in age order (triangles and vertical lines): end-Guadalupian crisis, Late Permian extinction, and end-Smithian crisis.

proportion in the Triassic, with the remaining four groups of minor significance. The Permian community is mainly dominated by the Cladodontomorphi (Symmoriiformes and predominantly Ctenacanthiformes) and Eugeneodontiformes. The orodontiform

component consists of one genus in the Cisuralian, which is included with the eugeneodontiforms for ease of reference and because of the difficulties in distinguishing between isolated teeth of both groups (see Ginter *et al.* 2010). The dominant groups are closely followed in diversity by the Xenacanthimorpha (predominantly Xenacanthiformes and in the Cisuralian also Bransonelliformes) and Petalodontiformes. The Holocephali were a diverse group, consisting mainly of the Cochliodontiformes, but also comprising representatives of the Helodontiformes, Menaspiformes, and potentially the Chimaeriformes (*Arctacanthus*). The Hybodontiformes were subordinate to all groups, as were the Neoselachii, which had the smallest share of the population at the start of the Permian.

Conversely, the Triassic community is dominated by the Hybodontiformes and the Neoselachii, with all synechodontiform genera present by the Griesbachian, and both groups continued to gain importance throughout the period. Most of the Triassic holocephalan record is based on the questionable assignment of *Arctacanthus* to the superorder, but is confirmed based on dental records and fin spines from two chimaeriform genera recovered from the Rhaetian (*Agkistracanthus*, *Myriacanthus*). The Xenacanthiformes were continuously present, until their demise at the end of the Triassic. The remaining two groups, the Phoebodontiformes? and Cladodontomorphi, are based on questionable taxonomic assignments in most cases, and specifically the cladodonts lack clear confirmation from the dental record.

The rapidity of genus diversity change becomes apparent if plotted against time (Figure 8.2B). It clearly shows the overal diversity decline in the Roadian as a result of the reduced quality of the fossil record and the subsequent peak in the Wordian, as well as the P/Tr bottleneck (i.e., a sudden decrease in population density with a resulting decrease in diversity). The different components of the community, however, did not contribute equally to the observed diversity changes, including the late Permian extinction event.

The genus diversity per order shows that the Wordian diversity peak is mainly attributable to the Hybodontiformes (Figure 8.3). Other groups such as the

Eugeneodontiformes and Petalodontiformes show a minor increase, but these are relatively insignificant. Of the total of nine genera occurring in this stage, five (including three singleton genera) were only observed in the Khuff fauna described in this study, highlighting the biased record and the potential that the microfossil record may still hold for the Permian. The Roadian diversity low, caused by a preservational bias, appears to be caused mainly by a reduction in the richness of the Holocephali and the Eugeneodontiformes and, to a minor extent, the Cladodontomorphi.

Diversity of the Hybodontiformes remained fairly stable throughout the Cisuralian–Guadalupian, but declined somewhat in the Capitanian and remained low up until the Permian/Triassic boundary. The Neoselachii suffered slightly in the Wuchiapingian, following the end-Guadalupian crisis, and diversification appears to have been halted briefly around the end-Smithian crisis, but neither the Neoselachii nor the Hybodontiformes show any reduction in diversity as a result of the Late Permian mass extinction and, instead, follow a pattern of stable or increasing diversity. Underwood (2006) placed the origination of clearly defined neoselachians in the Early Triassic, which Friedman and Sallan (2012), therefore, identified as the onset of neoselachian elasmobranch radiation. Cisuralian occurrences of *'Synechodus'* (pre-Jurassic) in the Russian Ural Mountains (Ivanov 2005), however, as well as the occurrence of *Nemacanthus* in the Wordian of Oman and Genus S in the Wuchiapingian of Iran (this study), suggests that definite neoselachians originated much earlier. Also, these data suggest that neoselachian diversity remained stable throughout the Early Triassic (mainly comprising the Synechodontiformes) and showed distinct diversification leading up to the Anisian. The Neoselachii subsequently retained their level of diversity throughout the remainder of the Triassic, whereas the Hybodontiformes reached their highest diversity in the Carnian, but gradually declined thereafter (Figure 8.3).

The Xenacanthiformes crossed the Permian/Triassic boundary without being severely affected. They declined over the course of the Guadalupian, but reached a new equilibrium that persisted until the Carnian, with a minor yet stable reduction in

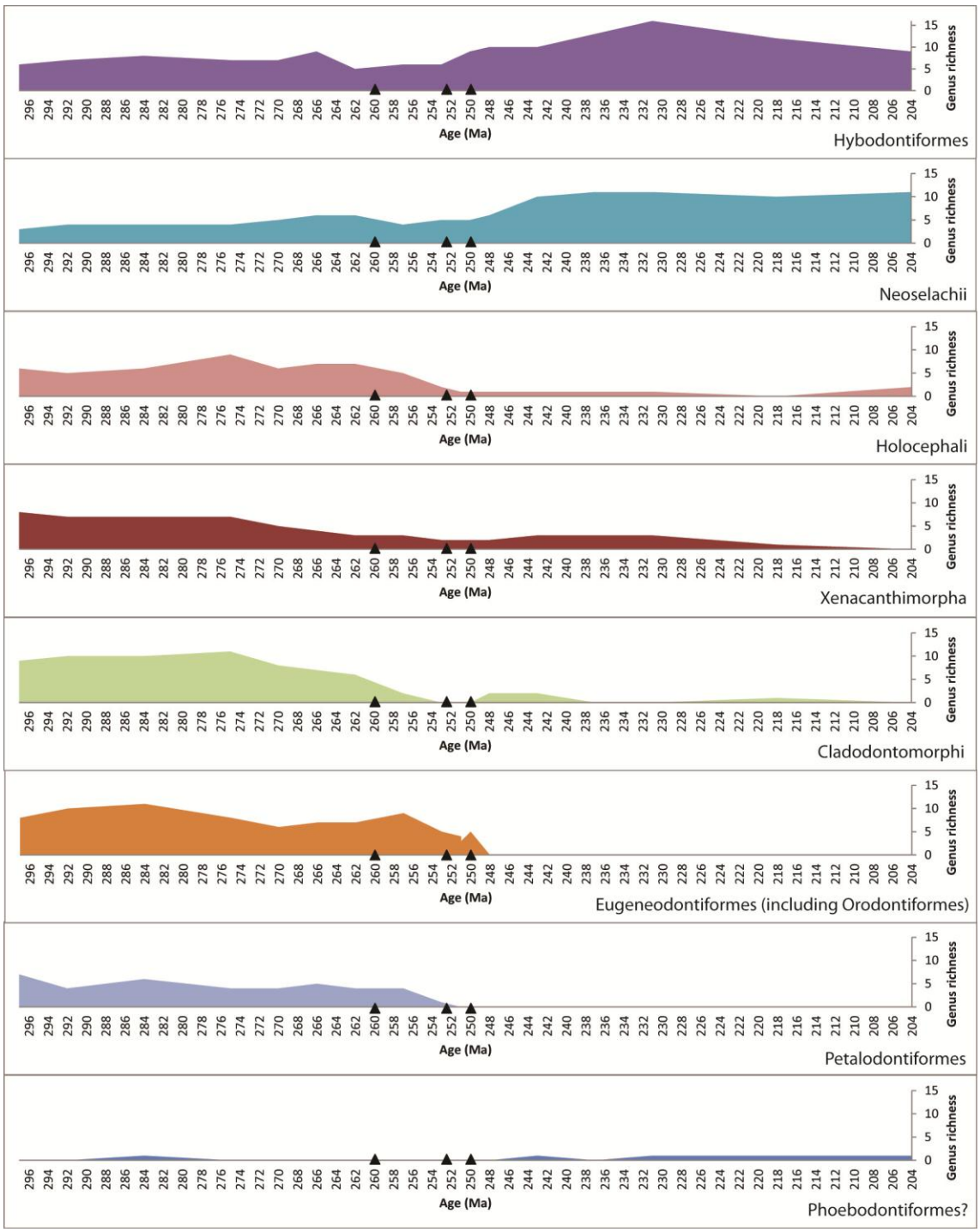

Figure 8.3 – Genus diversity separated per order or higher taxonomic classification, against time. Major biotic crises and extinction events are denoted on the X-axis in age order (triangles): end-Guadalupian crisis, Late Permian extinction, and end-Smithian crisis.

richness during the Changsingian–Olenekian, but then gradually declined and went extinct in the Norian.

The Cladodontiformes were in decline from the end of the Cisuralian onwards, although a more rapid reduction in diversity appears to have been brought on by the

end-Guadalupian crisis. The group appears to have gradually 'petered out', resulting in apparent extinction during the late Permian mass extinction, although there is some evidence to suggest that a few representatives may have persisted into the Spathian and Anisian, or even into the Norian (see Section 4.2.4).

The only groups that appear to have suffered directly from the late Permian extinction are the Holocephali, Eugeneodontiformes and the Petalodontiformes, which all declined rapidly from the Wuchiapingian onwards. However, their individual response to the extinction was different. The Petalodontiformes went extinct in the Griesbachian, whereas the Holocephali merely experienced their lowest diversity in the earliest Triassic and persisted at the same level of richness. They temporarily disappeared from the fossil record in the Norian, but re-appeared more diverse than before in the Rhaetian. The composition of this group confirms the absence of any non-chimaeroid holocephalans from Triassic strata, as was observed by Friedman and Sallan (2012; based on data in Cappetta *et al.* 1993; Stahl 1999; and Sepkoski 2002). The Eugeneodontiformes experienced their lowest diversity during the Dienerian, but rapidly started to diversify again until they abruptly went extinct in the Spathian, potentially as a result of the end-Smithian crisis. They are, therefore, the only group to display the typical pattern for 'holdover taxa' (see Urbanek 1993).

The role of the Phoebodontiformes? is not clear. Teeth that resemble representatives of this Palaeozoic (Devonian–Carboniferous) order occur intermittently in the fossil record and appear to have reached some stability in the Late Triassic, but the lineage went extinct at the close of the period.

The proportion extinction of total diversity and relative extinction levels of higher taxonomic groups have been studied across all Lopingian boundaries (Capitanian/Wuchiapingian = CWB; Wuchiapingian/Changhsingian = WCB; Changhsingian/Griesbachian = CGB; comprising the end-Guadalupian crisis and Late Permian mass extinction) and the Smithian/Spathian boundary (SSB; comprising the end-Smithian crisis; Figure 8.4). It shows that among genera included in the major taxonomic groups, the largest extinction took place across the WCB, whereas the

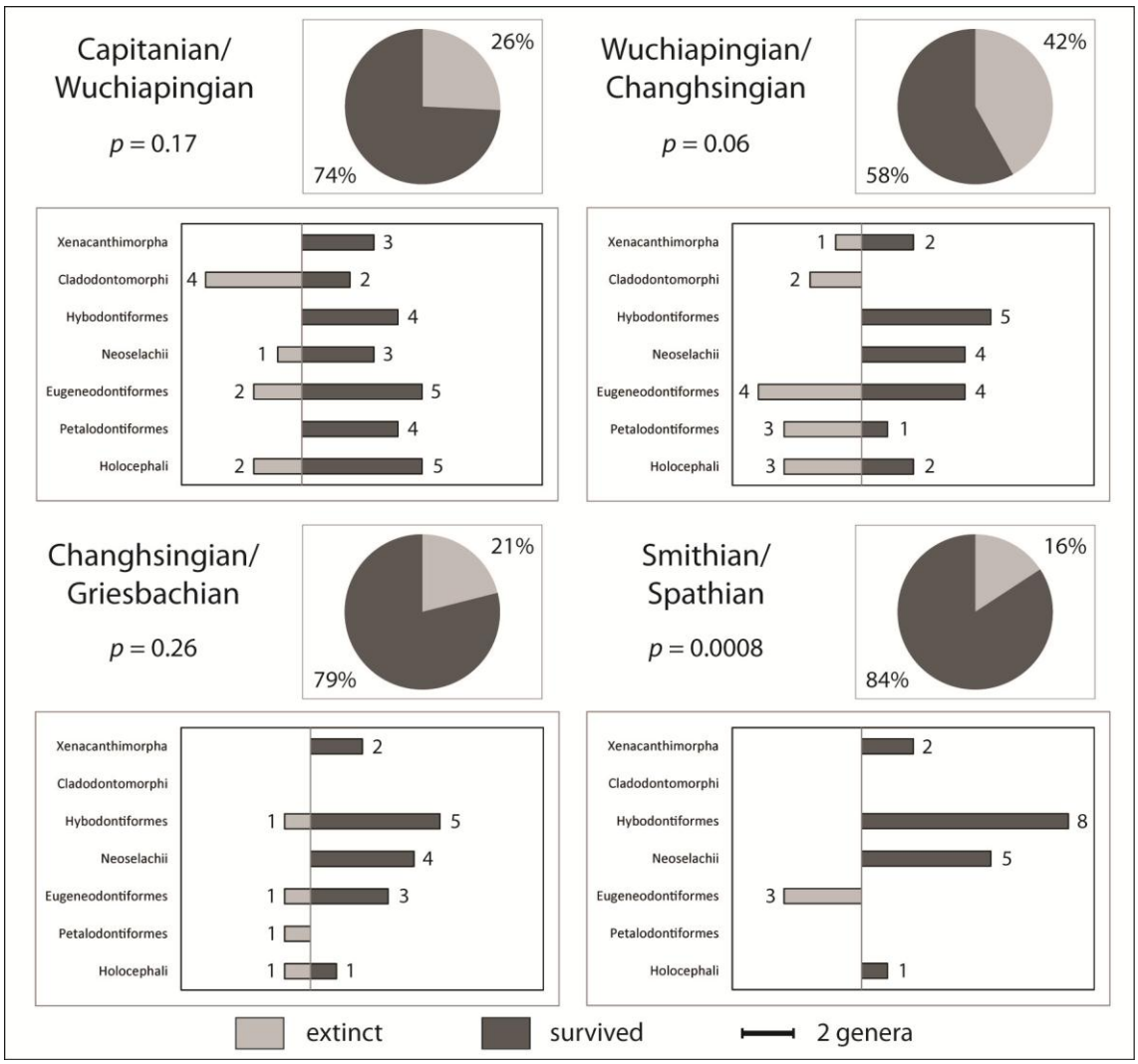

Figure 8.4 – Extinctions as proportions of total diversity (pie charts) and relative extinction levels partitioned according to higher taxonomic groups (bar charts) across relevant boundaries surrounding the Late Permian mass extinction. *P* represents the significance level found with a chi-squared test for independence (based on range-through data for named genera only; Appendix A2.4.5).

smallest proportion of extinction is observed across the SSB. Furthermore, extinction selectivity among higher taxonomic groups is significant across the SSB (extinction recorded solely among the Eugeneodontiformes) and a strong correlation exists across the WCB. However, extinction was only weakly correlated with taxonomic structure across the CWB and independent across the CGB.

8.2.3 STANDING DIVERSITY, ORIGINATION AND EXTINCTION

Permian–Triassic chondrichthyan Estimated Mean Standing Diversity (EMSD) shows the highest diversity at the start of the Cisuralian, at which time the environment supported about 45 chondrichthyan genera (Figure 8.5A). A gradual decline is apparent, however, the onset of which may have already occurred in the final stages of the Carboniferous. However, the decline grows much steeper in the Capitanian, potentially as a result of the end-Guadalupian biotic crisis and subsequently of environmental changes leading up to the Late Permian extinction. Over the Permian/Triassic boundary, only a minor drop in EMSD is observed. A short-lived peak occurs in the Dienerian, but another decline results in an even lower EMSD in the Spathian than in the Griesbachian. The accuracy of these temporal patterns are supported by the absence of a significant correlation between EMSD and interval duration (Table 8.2).

In a stable population, the diversification rate and turnover rates are expected to remain at the same level through time. For diversification, this level is zero, where origination equals extinction with no net effect on diversity. Turnover is always likely to be positive, but is expected to be low if there are no significant environmental changes. These patterns are observed through the Asselian–Roadian and also through the Spathian–Rhaetian, although more fluctuations are observed in the latter interval (Figure 8.5A). During the Wordian–Changhsingian, however, diversification and turnover show an increasingly divergent trend, which can be entirely attributed to an increasing extinction rate (Figure 8.5B). The extinction rate peaks in either the Changshingian or Griesbachian, depending on the calculation method used, but essentially it is the culmination of a trend that began in the Wordian and shows no sudden increase as a result of the Late Permian mass extinction. There is no argument about the very sudden and very large Griesbachian peak in origination rate, however, resulting in synchronous peaks in both diversification and turnover rate. Origination then declined equally rapidly in the Dienerian, resulting in the lowest turnover rate of the entire Permian–Triassic interval and a rapidly declining diversification rate, but the

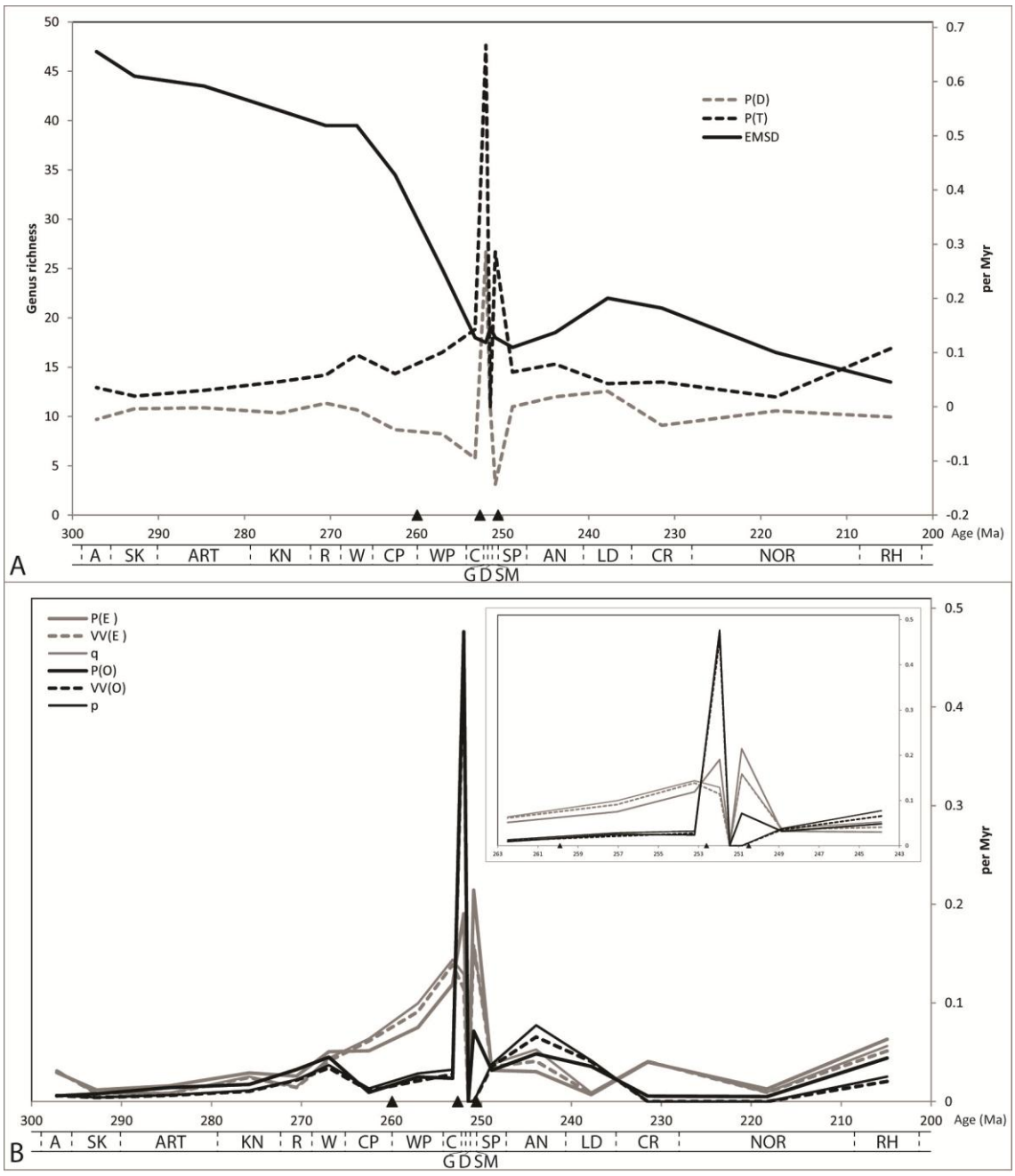

Figure 8.5 – Diversity estimates of Permian and Triassic chondrichthyans. A, Estimated mean standing diversity, and diversification and turnover rates. B, Per-taxon origination and extinction rates, Van Valen origination and extinction metrics, and per-capita origination and extinction rates. Major biotic crises and extinction events are denoted on the X-axis in age order (triangles): end-Guadalupian crisis, Late Permian extinction, and end-Smithian crisis.

latter reached its lowest point in the Smithian, when the extinction rate peaked once more, which may be linked to the end-Smithian crisis.

Sepkoski's (2002) data suggested that the Induan was an interval of intense turnover among fishes, which Friedman and Sallan (2012) deemed potentially indicative of

Table 8.2 – Correlation data for EMSD. One asterisk indicates a significant correlation at p(2)<0.05 and two a significant correlation at p(2)<0.01 (Appendix A2.4.4).

Correlation of interval duration	Spearman's ρ
vs. EMSD	0.08 (n = 18)

turbulent post-extinction recovery, but cautioned that this observation was based on a very low genus count (six). In this study, high turnover rates are confirmed for the Griesbachian and Smithian, based on an average total of 18 genera (EMSD). The poor quality of the Dienerian fossil record precludes any definitive interpretation of the low turnover rate in this interval.

The Spathian saw a return to 'normal' levels, although origination remained higher than extinction for the duration of the Middle Triassic, whereas the situation was reversed in the Carnian. This potentially indicates some influence of the Carnian pluvial event (see Preto *et al.* 2010), which marks a global episode of increased rainfall and the most distinctive climate change of the Triassic, but no specific effects on the marine realm have yet been identified. Finally, there is some evidence to suggest that the extinction rate entered another slowly increasing trend in the Rhaetian, which may be a precursor of the end-Triassic mass extinction (see Hautmann 2001; Hallam 2002).

In order to determine the underlying patterns of the overall observed EMSD, the EMSD of each order or higher taxonomic group has been calculated separately (Figure 8.6A, B, excluding the Phoebodontiformes?, see Section 2.6.7). It shows similar patterns to those observed in generic richness (Figure 8.2A, B), but displays smoother trends and excludes 'noise' caused by singleton genera and those in open nomenclature. A transition can still be observed from a diverse community of seven well-established groups to a community consisting of six groups, but with very uneven distribution and dominated by the Hybodontiformes and Neoselachii. The Cladodontomorphi remain the most important component of EMSD in the Cisuralian, whereas the Neoselachii had the smallest share. Hybodonts and neoselachians gained

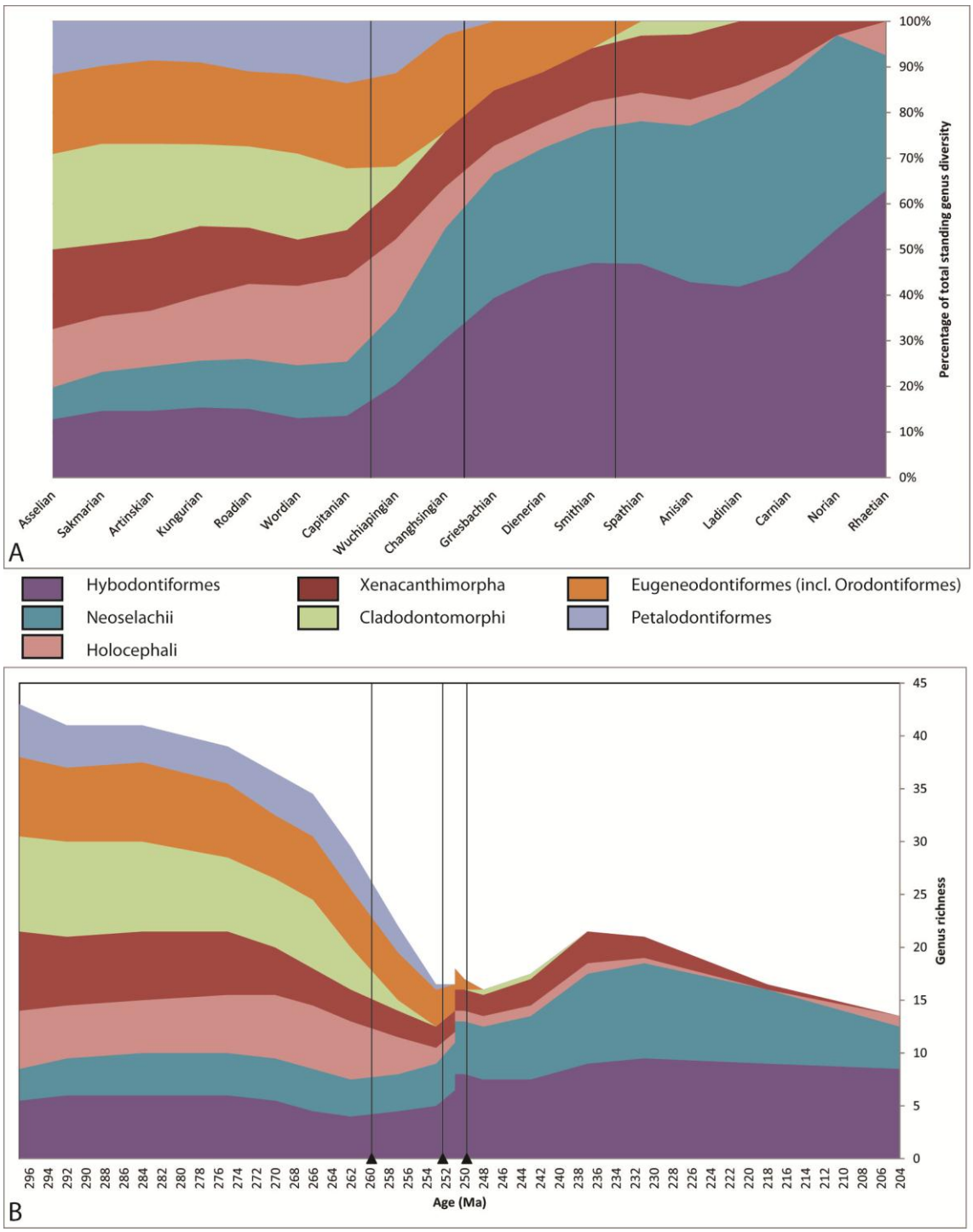

Figure 8.6 – A, Proportion of estimated mean standing diversity per order or higher taxonomic classification per (sub)stage. B, Estimated mean standing diversity per order or higher taxonomic classification against time. Major biotic crises and extinction events are denoted on the X-axis in age order (triangles and vertical lines): end-Guadalupian crisis, Late Permian extinction, and end-Smithian crisis.

in relative importance from the Capitanian onwards, with the decline of the Cladodontomorphi, the Holocephali and the Petalodontiformes.

If plotted against time, the decline in total chondrichthyan EMSD throughout the Permian–Triassic becomes particularly apparent, as does the lack of any contribution to the decline by the Hybodontiformes or the Neoselachii, which appear unaffected. Especially low levels of EMSD occur during the Changhsingian–Anisian (Figure 8.6B). The Ladinian and Carnian, however, again show elevated overall EMSD, resulting from a small increase in the Hybodontiformes and a relatively large radiation in the Neoselachii. Subsequently, EMSD shows renewed decline during the Norian and Rhaetian, most of which appears to be due to a loss of the Neoselachii.

A sudden increase in cumulative EMSD occurs across the Griesbachian/Dienerian boundary (Figure 8.6B), for which the Hybodontiformes are predominantly responsible (Figure 8.7). The Neoselachii also display a sudden diversity increase, but to a smaller extent. The hybodontiform EMSD remains largely stable from the Carnian onwards, whereas neoselachian EMSD gradually declines, which is in direct contrast to the patterns observed in genus richness (Figure 8.3). The remaining groups display comparable patterns to those observed in genus richness, including the Eugeneodontiformes, in which a sudden decline across the Griesbachian/Dienerian boundary is apparent.

Origination and extinction rates per order show that the various groups experienced similar turnover from the Asselian through to the Roadian (Figure 8.8A, B). In the Wordian, only the Hybodontiformes show a peak in origination and extinction rates, which are predominantly linked to the Khuff fauna, recording both first and last occurrences of longer-ranging taxa, as well as singletons. An elevated extinction rate among hybodonts is again observed in the Changhsingian, but it remains low in the remaining time intervals. The group’s origination rate, however, shows the highest peak of any group in the Griesbachian, which, combined with zero extinction, causes the most rapid diversification observed immediately following the Late Permian mass extinction. The Neoselachii show similar behaviour with a synchronous peak in origination rate. Although this peak is lower, combined with zero extinction, the net effect is still one of significant diversification. An elevated neoselachian origination rate

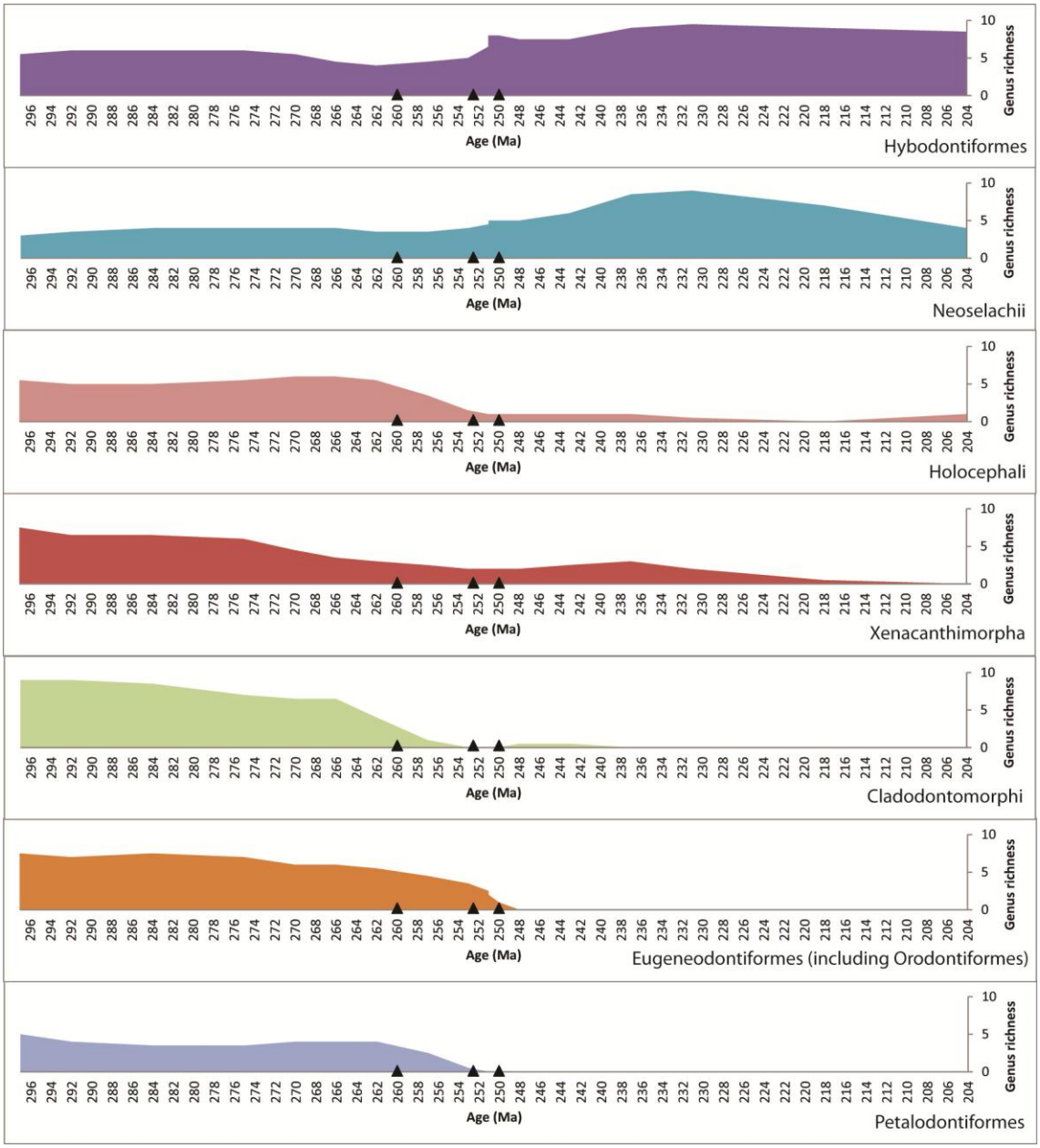

Figure 8.7 – Estimated mean standing diversity separated per order or higher taxonomic classification, against time. Major biotic crises and extinction events are denoted on the X-axis in age order (triangles): end-Guadalupian crisis, Late Permian extinction, and end-Smithian crisis.

over the Spathian–Ladinian is the dominant factor behind the diversity increase that was already recognised from Figure 8.6B.

The Eugeneodontiformes show a higher origination rate in the Wuchiapingian and peaks of origination in the Griesbachian and Smithian. However, these peaks were accompanied by even higher rates in extinction, causing drastic swings in turnover rate and ultimately the disappearance of the group. The Cladodontomorphi show an

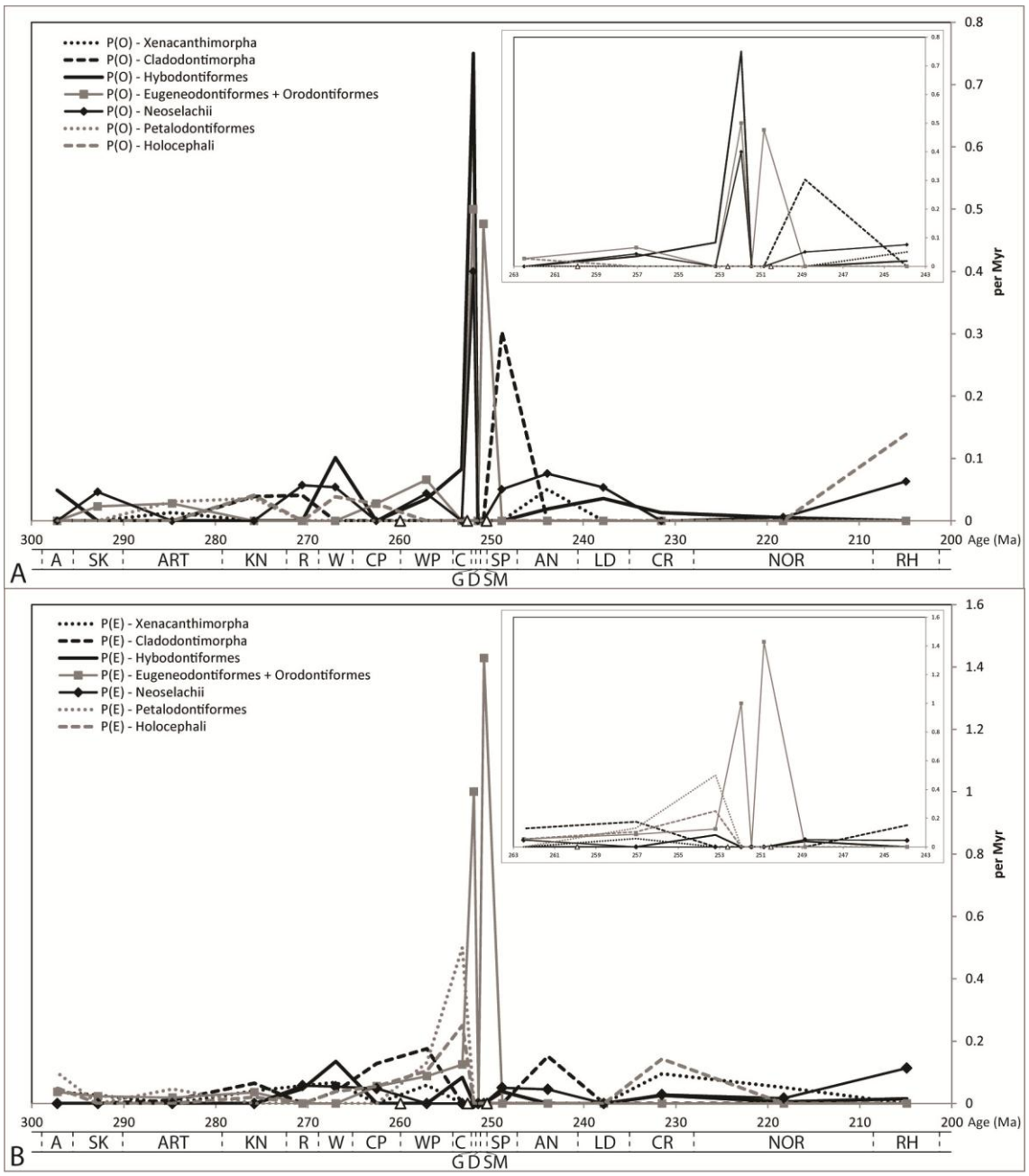

Figure 8.8 – Diversity estimates of Permian and Triassic chondrichthyans per order or higher taxonomic classification. A, Per-taxon origination rates. B, Per-taxon extinction rates. Major biotic crises and extinction events are denoted on the X-axis in age order (open triangles): end-Guadalupian crisis, Late Permian extinction, and end-Smithian crisis.

elevated extinction rate over the Capitanian and Wuchiapingian, leading to the group's apparent disappearance in the Changhsingian. As stated previously, their re-appearance in the Spathian is solely based on dorsal fin spines (*Pyknothylacanthus*) and lacks confirmation from the dental fossil record.

Elevated extinction rates are observed in the Petalodontiformes and the Holocephali in the Wuchiapingian and especially the Changhsingian. The higher rate is observed among the Petalodontiformes, however, which may be related to the extinction of this group at the close of the Permian, whereas the Holocephali persisted with low diversity and did not diversify again until the Rhaetian. Noticeably absent among the origination and extinction peaks surrounding the Permian/Triassic boundary are the Xenacanthimorpha, which illustrates once more the stability of this group through any of the extinctions or biotic crises of the Permian and Triassic.

8.3 Evolutionary life-history traits and environmental adaptability

8.3.1 Introduction

A total genus diversity curve alone cannot reveal the true dynamics of a population and, therefore, the contribution of different taxonomic groups to particular diversity fluctuations has been assessed. Another aspect of the underlying compositional cause and response driving these diversity fluctuations that needs to be addressed, however, is palaeoecology. In order to create a better understanding of the palaeoecological changes in the chondrichthyan population throughout the Permian–Triassic interval, and specifically in relation to the Late Permian mass extinction and other times of biotic crisis, a number of life-history traits are studied here. These traits comprise salinity tolerance, ecomorphotype, feeding habit and body size (definitions in Section 2.6.8).

8.3.2 Salinity tolerance

Chondrichthyans are believed to have been primarily a marine group from the onset, never reaching a level of diversity in freshwater that would rival their success in the world's oceans (Zangerl 1981; Compagno 1990). Friedman and Sallan (2012) postulated that marine selectivity played a part in the differential effects of the Late

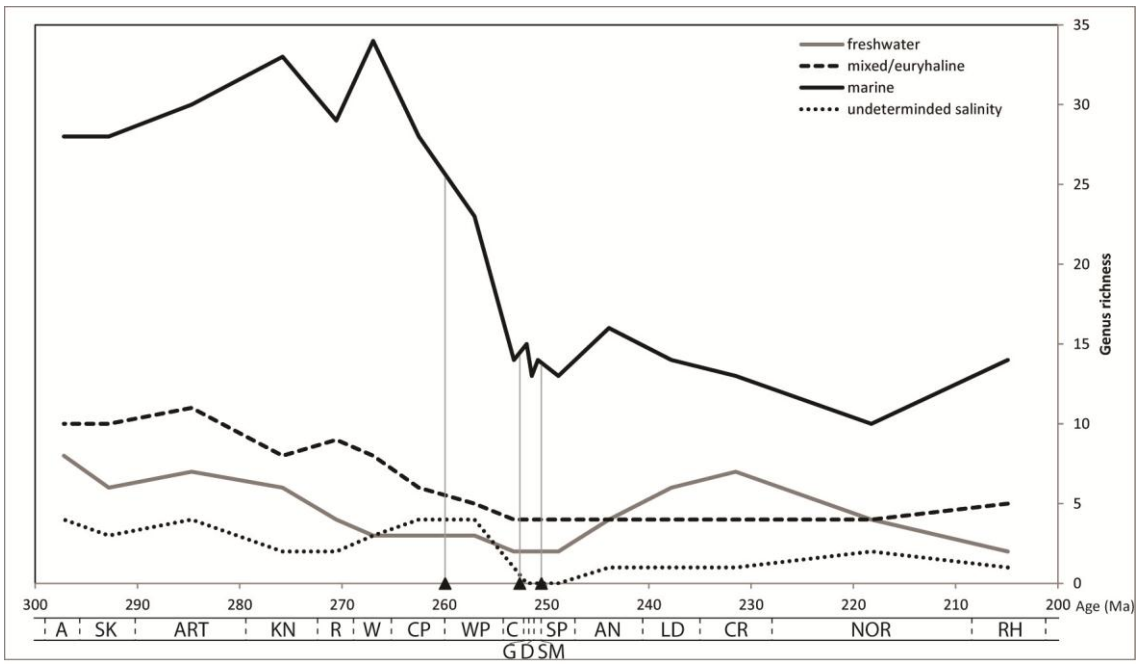

Figure 8.9 – Genus diversity of Permian and Triassic chondrichthyans according to salinity tolerance. Counts of named fossil genera (marine, freshwater, mixed/euryhaline and undetermined salinity) against time. Major biotic crises and extinction events are denoted on the X-axis in age order (triangles): end-Guadalupian crisis, Late Permian extinction, and end-Smithian crisis.

Permian extinction event on chondrichthyan taxa, based on the fact that the vast majority of Palaeozoic holocephalans and all Symmoriiformes were lost, all of which were marine lineages, in contrast to unaffected elasmobranchs that were of euryhaline or freshwater ecology.

At first glance, genus richness counts based on salinity tolerance confirm this theory of marine selectivity (Figure 8.9). The apparent trends show that the Permian chondrichthyan population was dominated by marine genera, whereas there was a more even distribution across marine and freshwater genera over most of the Triassic. The suddenness and extent of the reduced genus richness observed in the Roadian is entirely explained by the marine component (or preservation of the central/western panthalassan and neotethyan marine fossil record, see Section 7.4.2.1), which returns to expected diversity levels in the Wordian based on the increasing Cisuralian trend. From the Wordian through to the Changhsingian, marine genus diversity shows a steep and continuous decline. Diversity fluctuates throughout the Early Triassic, with declines

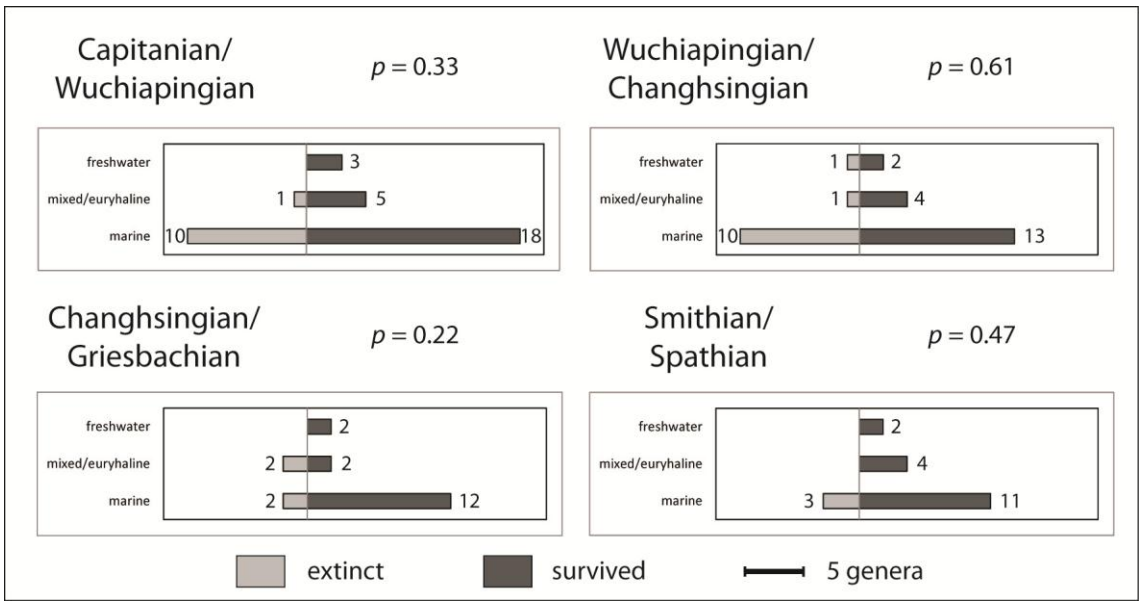

Figure 8.10 – Relative extinction levels partitioned according to salinity tolerance across relevant boundaries surrounding the Late Permian mass extinction. *P* represents the significance level found with a chi-squared test for independence (based on range-through data for named genera only; Appendix A2.4.12).

to equal richness levels in the Dienerian and Spathian, but the lowest overall diversity was recorded in the Norian. The freshwater and euryhaline components each show a gradual diversity decline throughout the Permian. In both cases, however, diversity stabilises from the Changhsingian onwards. The freshwater component again diversified significantly throughout the Middle Triassic and Carnian, returning to similar levels as observed in the Cisuralian.

The relative extinction levels among the salinity components confirm that the largest extinction, but also survival, took place among marine genera across all Lopingian boundaries and the SSB (Figure 8.10). The extinction is greatest across the CWB and WCB, associated with the end-Guadalupian crisis and the time period preceding the Late Permian mass extinction. The CGB, directly associated with the latter extinction, however, shows a relatively small number of genera becoming extinct. The strongest correlation between taxon fate and salinity tolerance is observed across the CGB, but no significant extinction selectivity is observed across any of the four boundaries,

disproving the suggestion of preferential loss of marine taxa and pointing towards proportionate levels of extinction.

8.3.3 ECOMORPHOTYPE

Ecomorphotypes, broad adaptive types that are also referred to as 'habitus' (Zangerl 1981), are "particular groupings of taxa that may or may not be phyletically related by similar morphology, habitat and behaviour" (Compagno 1990, p. 53). Compagno (1990) listed and discussed in detail the ecomorphotypes that exist among extant chondrichthyans, providing clear examples from the fossil record, which have been extrapolated here in generalised form to all known Permian–Triassic fossil genera (Figure 8.11). He also remarked that reproductive modes are not strongly correlated with ecomorphotypes, but it has been shown that extinction risk is significantly lower for oviparity than for other reproduction modes (García *et al.* 2008). Because oviparity appears to have been the primitive reproductive style in chondrichthyans (Compagno 1990), this may be a reason why some chondrichthyan lineages were adapted against extinction. Lastly, Compagno (1990) noted much repetition in morphological form and function in chondrichthyans, which illustrates their high success rate in recolonising ecological niches after marine extinctions and biotic crises, despite competition from other marine vertebrates. Lineages that display convergent evolution, or homoplasy, through extinctions are generally referred to as Elvis taxa (Erwin and Droser 1993; see

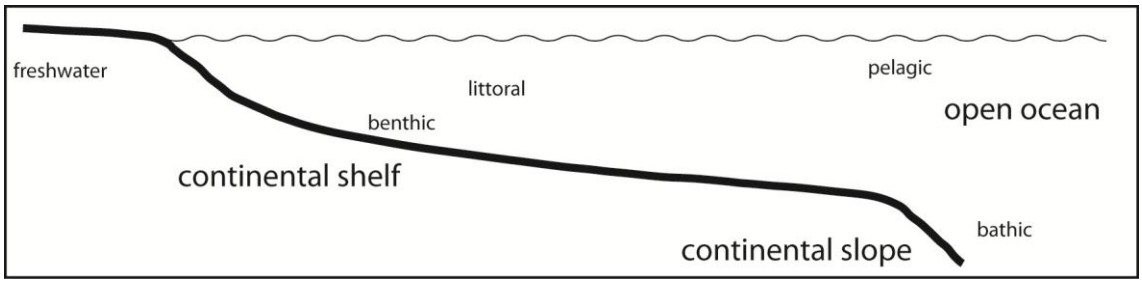

Figure 8.11 – Generalised ecomorphotypes and habitat occupation recognised among extant chondrichthyans and extrapolated to fossil taxa (adapted from Compagno 1990; see Appendix A2.4.10 for taxon assigments to each generalised ecomorphotype).

also Hallam and Wignall 1997). Based on the diversification trajectories described in Section 8.2.2, most of this adaptive evolution is expected to have taken place among the hybodonts and the neoselachians.

The ecomorphotypes have been grouped into freshwater, littoral (marine), benthic, pelagic and bathic types in order to determine patterns in each generalised habitat (Figure 8.11). This ecological partitioning of chondrichthyans over the Permian and Triassic shows that the benthic types comprise the largest genus diversity, followed by the pelagic, littoral marine and freshwater types, and that the bathic types comprise particularly low diversity (Figure 8.12). The bathic types generally display a stable presence, but temporarily disappear from the fossil record from the Changhsingian through to the Smithian, potentially highlighting vacancy of this habitus or reduced abundance preventing them from being recorded in the fossil record (see Twitchett 2001a). The freshwater types declined from the Artinskian through to the Changhsingian, after which they remained stable during the Early Triassic and started diversifying again from the Anisian onwards. The littoral marine types declined from the end of the Cisuralian, but show a steeper reduction in diversity across the Guadalupian/Lopingian boundary, which may result from the effects of the end-Guadalupian crisis. The littoral habitus reached its lowest diversity in the Changhsingian, rebounded somewhat during the Early Triassic, and subsequently diversified rapidly across the Early/Middle Triassic boundary to a higher level of diversity than observed in the Permian. The pelagic types show a variable pattern with diversity reducing and increasing several times over the course of the Permian. The largest declines are apparent from the Roadian and Changhsingian fossil record. Pelagic diversity remained unstable during the Early Triassic, and generally in decline. It stabilised from the Spathian through to the Anisian, but apparently dropped to zero in the Ladinian. The absence of the group from the known fossil record was only temporary, however, and it reappeared in the Rhaetian. The benthic types apparently show the most drastic decline in the second half of the Permian, following on a Wordian diversity high. Benthic types remained stable during the Early Triassic,

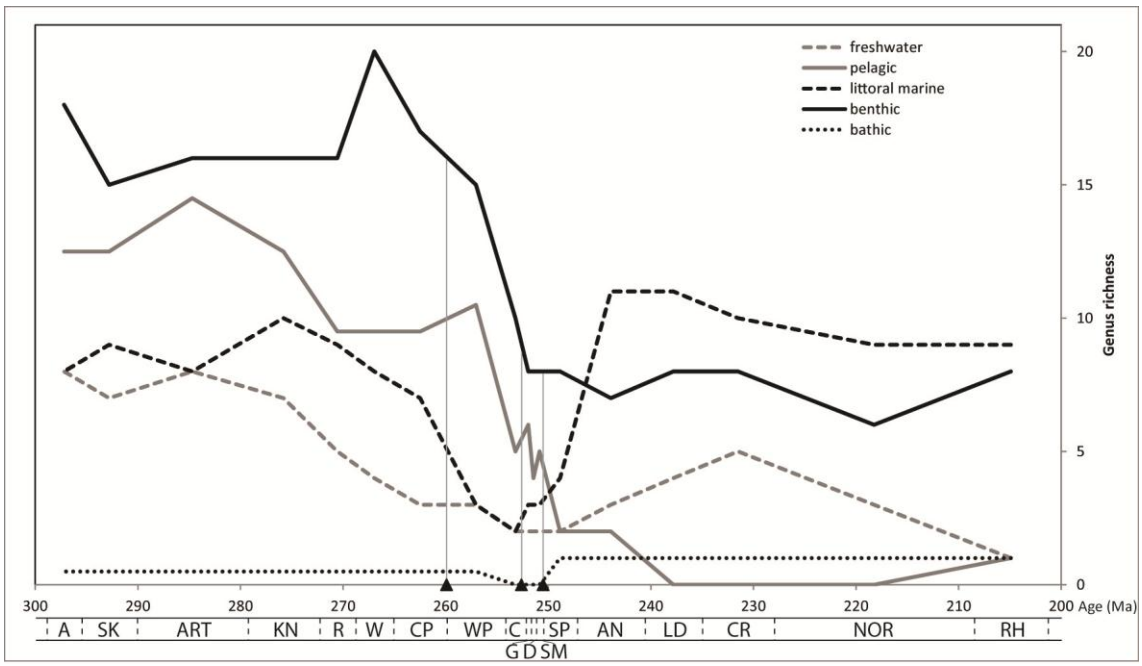

Figure 8.12 – Genus diversity of Permian and Triassic chondrichthyans according to generalised ecomorphotype. Counts of named fossil genera (benthic, pelagic, littoral marine, freshwater, and bathic) against time. Major biotic crises and extinction events are denoted on the X-axis in age order (triangles): end-Guadalupian crisis, Late Permian extinction, and end-Smithian crisis.

however, with relatively minor fluctuations throughout the Middle and Late Triassic epochs.

Relative extinction levels among generalised ecomorphotypes show consistent extinction among the pelagic and benthic habitus throughout the Lopingian, and particularly across the WCB (Figure 8.13A). However, extinction is shown to be independent of ecomorphotype across these boundaries. Extinction selectivity among ecomorphotypes is significant across the SSB and is limited to the pelagic habitus. All genera becoming extinct belong to the Eugeneodontiformes and the pelagic habitus partly reflects the behaviour typical of holdover taxa, as displayed by the order (see Section 8.2.2).

Closer investigation of the conspicuous diversification trend among marine littoral genera during the Smithian–Anisian shows that the largest proportion diversification of total diversity is observed across the Spathian/Anisian boundary, which can predominantly be explained by an increase in genus richness in the littoral marine

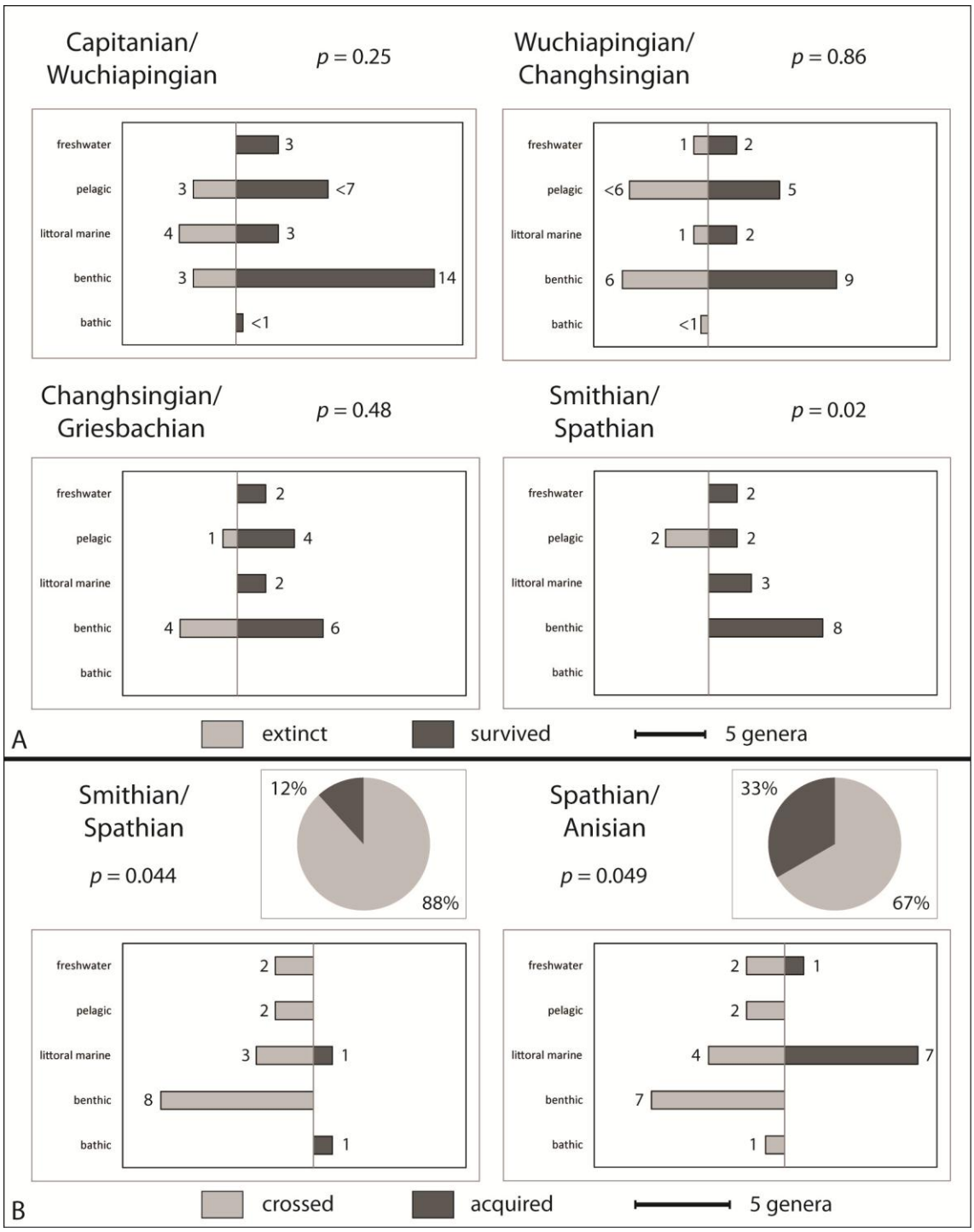

Figure 8.13 – A, Relative extinction levels partitioned according to general ecomorphotype across relevant boundaries surrounding the Late Permian mass extinction. B, Diversification as proportions of total diversity (pie charts) and relative diversification levels partitioned according to general ecomorphotype (bar charts) across relevant boundaries surrounding the end-Smithian crisis. *P* represents the significance level found with a chi-squared test for independence (based on range-through data for named genera only; Appendix A2.4.14).

habitus (Figure 8.13B). Furthermore, survival and diversification are observed to be significantly correlated with, and thus dependent on ecomorphotype across both Olenekian boundaries. It suggests that the littoral habitus may have provided the most opportunity for adaptive radiation after the environmental effects of the Late Permian extinction and end-Smithian crisis were lifted.

8.3.4 Feeding habit

The Chondrichthyes are entirely predatory and able to feed on a large variety of prey ranging from plankton and invertebrates to large marine animals (Compagno 1990) by employing a range of feeding habits (see Cappetta 1987). This facilitates the evolution of representatives at all ecological levels (see Section 8.3.3). Regardless of specific feeding habit or occupied niche, chondrichthyans generally constitute the dominant group, which places them near the top of the food web (Compagno 1990). Compagno (1990) further postulated that sharks are highly opportunistic and, therefore, very competitive with other marine vertebrates, resulting in their radiation synchronous with the rise of marine tetrapods and the Osteichthyes, which presented a potential food source. A more recent perspective on these interactive dynamics can be taken from Friedman and Sallan (2012, fig. 2).

Rare opportunities may allow the analysis of articulated (post)cranial anatomy to determine jaw suspension or position of the mouth (e.g., Maisey 1980), or even gut content analysis (e.g., Brett and Walker 2002), which assist in determining feeding habit. However, as is also the case with extant chondrichthyans, tooth function and thus feeding types in fossil taxa are usually determined on the basis of isolated dental morphology without any biomechanical testing (Whitenack *et al.* 2011). The relationship between tooth morphology and feeding habit is still uncertain, with clear patterns yet to be established (Whitenack and Motta 2010). Nevertheless, the ancestral mode of predation in fossil chondrichthyans is believed to be bite-feeding and has been

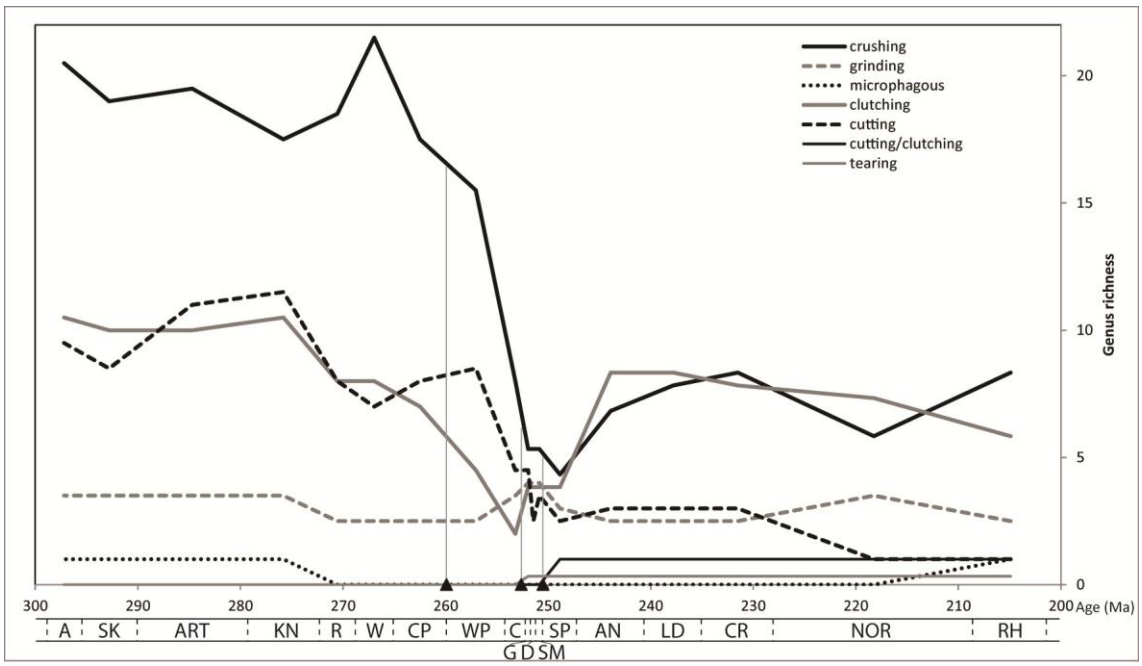

Figure 8.14 – Genus diversity of Permian and Triassic chondrichthyans according to feeding habit. Counts of named fossil genera (crushing, clutching, cutting, grinding, microphagous, cutting/clutching, and tearing) against time. Major biotic crises and extinction events are denoted on the X-axis in age order (triangles): end-Guadalupian crisis, Late Permian extinction, and end-Smithian crisis.

retained in most lineages (Wilga *et al.* 2007), although a number of different feeding types co-evolved (Table 2.2).

Genus richness counts based on feeding habit show that microphagous (filter-feeding) chondrichthyans are of very low diversity in the Permian–Triassic fossil record and are only known from the Cisuralian and Rhaetian (Figure 8.14). Among the macrophagous dental types, novel feeding techniques and unique combinations were developed in the Triassic. For example, tearing is only employed by some *Hybodus* species occurring in the Triassic (Cappetta 1987). The generalised Triassic range of tearing dentitions shown at genus level must, therefore, be regarded as tentative. The cutting-clutching subtype is also of relatively low diversity, and only occurs from the Spathian onwards. Among the more generally employed feeding habits, the genus diversity of chondrichthyans with cutting dentitions shows a fluctuating pattern through the Permian, with elevated diversity in the Artinskian–Kungurian and the Wuchiapingian. From the Wuchiapingian onwards, however, cutting diversity enters a

period of rapid decline, culminating in the Dienerian. It shows a minor increase in the Smithian, but declines to the previous level in the Spathian, after which it remains stable throughout the Anisian–Carnian, but is reduced to its lowest observed diversity in the rest of the Late Triassic. Clutching-type chondrichthyans show a slow diversity decrease across the entire Permian–Triassic, save for an increasingly rapid decline over the Capitanian–Changhsingian. Clutching diversity shows some recovery in the Griesbachian and remains stable throughout the remainder of the Early Triassic. Across the Early/Middle Triassic boundary, it experienced the most rapid radiation of all dental types, regaining diversity levels previously observed in the Guadalupian and equalling crushing-type dentitions. Surprisingly, any adaptive advantages expected from the gradual development of triple-layered enameloid (Chapter 6), are not evident from these results.

The two identified durophagous dental types show drastically different behaviour. In the Permian, crushing-type dentitions are the most diverse of all known types, despite being in gradual decline, except for a minor rise in the Roadian and a prominent peak in the Wordian. From the Wuchiapingian to the Changhsingian, however, there is a sudden and rapid drop in diversity, the most severe decline that is observed and which may be linked to the Late Permian mass extinction. Some stability is regained over the course of the Early Triassic, with another minor decline across the Smithian/Spathian boundary, which may be linked to the end-Smithian crisis. A slow radiation is observed through the Anisian–Carnian, followed by yet another drop in the Norian. Chondrichthyans with grinding-type dentitions display stable genus richness over the entire Permian–Triassic interval. Interestingly, genera that employ this feeding habit actually show a minor diversity increase across the Changhsingian–Early Triassic interval, displaying typical behaviour of opportunistic disaster taxa (Kauffman and Harries 1996; see also Hallam and Wignall 1997).

Friedman and Sallan (2012) postulated a selective loss of durophagous lineages as a result of the Late Permian mass extinction, based on the loss of many Palaeozoic euchondrocephalan groups, such as petalodonts, cochliodonts, menaspids, and

helodonts (see Stahl 1999 and Ginter *et al.* 2010). These groups predominantly possess crushing dentitions (the Petalodontiformes also include some genera with cutting dentitions), which, indeed, display a dramatic decline in the run-up to the extinction event (Figure 8.14). The severity of their decline, although not its sudden nature, may be directly linked to their high initial diversity, because they were not the only group to suffer a reduction in diversity. In relative terms, clutching and cutting dentitions suffered a similar decline, although the reduction of the clutching-type appears more gradual. In summary, the chondrichthyan groups employing these dental types were apparently reduced to a new carrying capacity, whereas the carrying capacity of the grinding feeding habit was increased. Friedman and Sallan (2012) noted that the vast majority of Palaeozoic holocephalan lineages fed upon known invertebrate victims of the extinction (bivalves, other molluscs and crustaceans; Hallam and Wignall 1997; Stahl 1999), which is indeed likely to have driven their demise. Relative extinction levels confirm that the largest number of genera was lost from among the crushing-type chondrichthyans across all Lopingian boundaries (Figure 8.15A). However, extinction proved independent of feeding habit, suggesting proportional losses and no selective loss of durophagous lineages. Of all studied boundaries, the weakest correlation exists between extinction and feeding habit across the SSB.

With regard to the previously mentioned Lower/Middle Triassic radiation observed among crushing and clutching dentitions, the data show that a large proportion of Anisian genera were new, as opposed to those that crossed the Spathian/Anisian boundary (Figure 8.15B). Relative diversification levels also show the domination of crushing and clutching dentitions among these new genera, yet diversification proved independent of feeding habit.

One remarkable dental feature that has been highlighted in this study and is worth noting again here is the frequent absence of the tooth base in isolated teeth of Mesozoic crown group hybodontoids, as opposed to teeth of their Palaeozoic ancestors, from which both base and crown are normally recovered together (Section

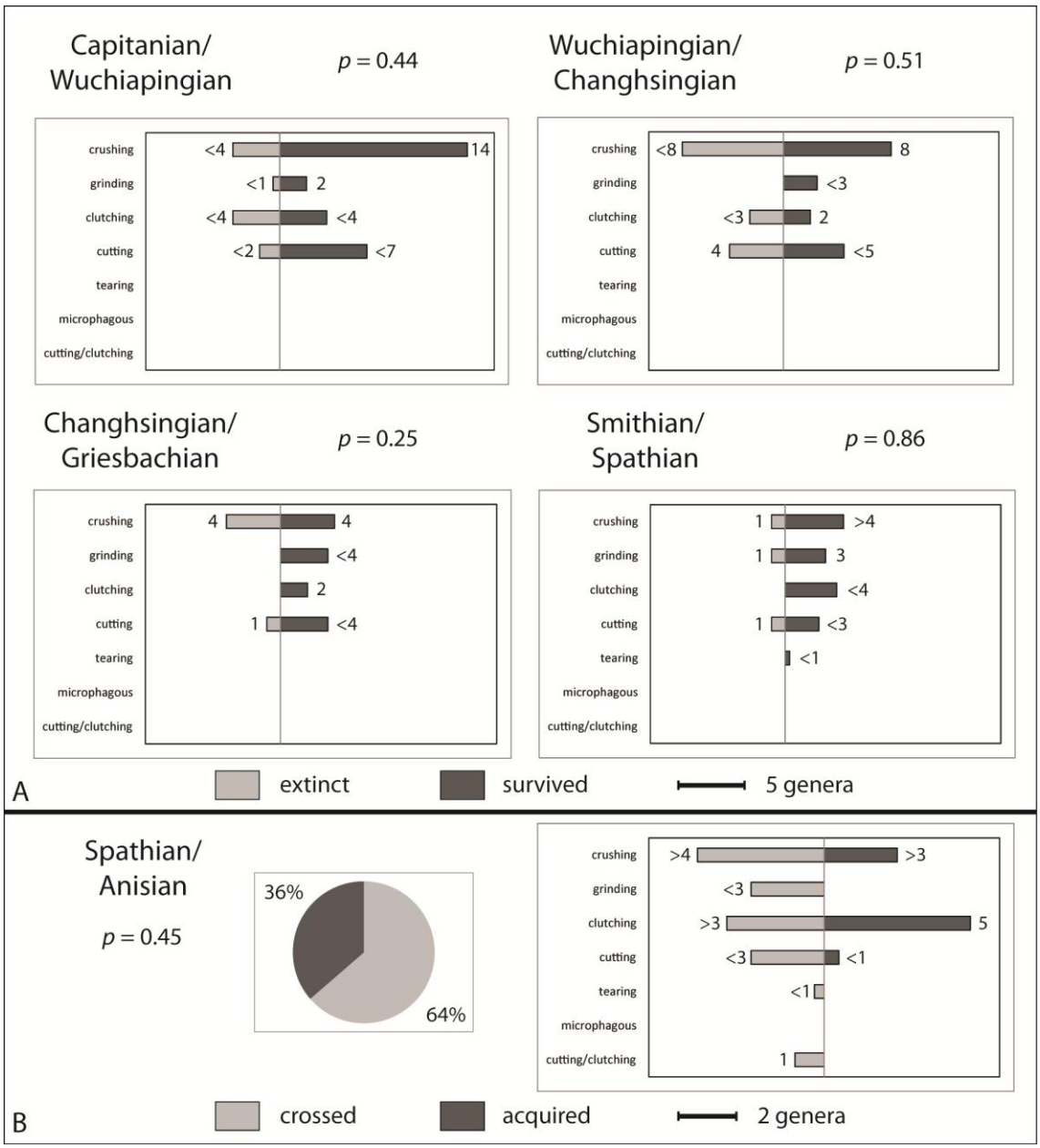

Figure 8.15 – A, Relative extinction levels partitioned according to feeding habit across relevant boundaries surrounding the Late Permian mass extinction. B, Diversification as proportions of total diversity (pie charts) and relative diversification levels partitioned according to feeding habit (bar charts) across the Spathian/Anisian boundary. *P* represents the significance level found with a chi-squared test for independence (based on range-through data for named genera only; Appendix A2.4.16).

3.6.1.1; Appendix A3.2). Williams (2001) noted that all cladodonts may have displayed tooth retention, as in many other Palaeozoic and Mesozoic chondrichthyans (eugeneodontids, petalodonts, iniopterygians, desmiodontids, cochliodonts, and myriacanthoids), generally displayed in the form of tooth whorls or compound teeth. He presents tooth retention as a conservational technique, facilitating resorption of the

mineral matter. It is therefore suggested that food scarcity as a result of the Late Permian mass extinction may have selected for adaptive conservational techniques in the hybodont population. Therefore, rather than the shedding of entire teeth, as occurred in the Permian, the crown/base contact was resorbed during tooth dehiscence (see Underwood and Cumbaa 2010), resulting in the shedding of only the tooth crown in the Triassic.

8.3.5 TOOTH AND BODY SIZE

Published estimates of body size are predominantly based on partial body fossils and also on extrapolations of dental dimensions, derived from ratios observed in articulated or otherwise directly associated remains (e.g., Richter 2005; Fischer 2008; Lebedev 2009; Hodnett *et al.* 2012). However, caution is advised in carrying out such extrapolations, because the relationship between tooth size and complete body size is still largely unknown due to the sparsity of body fossils (see Mutter and Neuman 2009).

Giant superpredatory sharks of 6 metres or more in length occurred during the Carboniferous (Compagno 1990), some of which persisted into the Permian (e.g., Hodnett *et al.* 2012), but entered into gradual decline from the end of the Cisuralian onwards (e.g., the Eugeneodontiformes; see Figure 8.3). This suggests that a general reduction in body size may have already occurred over the course of the Permian, which is a pattern that is also observed in the invertebrate record (Twitchett 2007a). Furthermore, *Arctacanthus* (cephalic) spines have been used as an example of reduced size in the Triassic compared to the Permian (Appendix A3.2; Chen *et al.* 2007a). Some specific evidence of size reduction as a result of the Late Permian mass extinction among chondrichthyans was obtained from dermal denticle size analysis in the form genus *Listracanthus* from the Lower Triassic strata of western Canada (Mutter and Neuman 2009).

In benthic marine invertebrates, a reduction in body size immediately following the Late Permian extinction has been observed (the Lilliput effect; e.g., Twitchett 2007a).

The Lilliput effect is a temporary, significant size decrease of surviving taxa in the immediate aftermath of an extinction event (Urbanek 1993), i.e., in the *parvus* and *isarcica* zones of the earliest Induan (Twitchett 2007a), although it was shown that body size remained depressed in most groups for the duration of the Early Triassic (e.g., Twitchett 2007a). This size reduction has been associated with reduced primary productivity, and interpreted as a possible survival mechanism (Twitchett 2001a). Gut content analysis in Palaeozoic chondrichthyans has indicated size partitioning of food resources (Brett and Walker 2002), which suggests that if smaller body size in prey is the result of stressed environments, smaller predators have an advantage due to lower sustainability requirements, potentially driving a reduction in the size of sharks. Especially in times of scarcity, cannibalistic behaviour (the occurrence of which has been shown by, e.g., Brett and Walker 2002 and Soler-Gijón 1995) may have sustained some larger sized sharks, but this strategy may have been of limited duration with continued stress on the environment.

Unfortunately, the resolution and abundance of the early Induan fish record is not as good as the ammonoid or conodont record, and is insufficient to facilitate a large-scale size analysis to determine whether the Lilliput effect occurred in chondrichthyans. Instead, this study focuses on dimensions of fossil material resolved to (sub)stage and epoch level, obtained from the global record, allowing analysis of general size patterns in the chondrichthyan community through the entire Permian–Triassic interval.

Any observed reduction in the size of chondrichthyan remains (Chen *et al.* 2007a; Mutter and Neuman 2009) has been considered to be of uncertain significance, based on the potentially variable dimensions in a single taxon, the frequently unknown size of ancestors pre-dating the extinction event (Friedman and Sallan 2012), and potentially also oversampling of stressed environments in recovery intervals, which can affect recorded averages (McGowan *et al.* 2009). To avoid some of these effects, particular attention will be drawn here to those taxa that cross the Permian/Triassic boundary and from which pre- and post-extinction measurements are available. In addition, this may correct for an apparent size reduction resulting from the temporary absence of large

taxa during an extinction interval due to their differential preservation potential, as was noted by Twitchett (2007a).

Trends emerging from the three different dimensional dental aspects (height, length, and width) show some similarity, because they are inherently related (Figure 8.16A, B, C). The Roadian and Capitanian are based on a low number of measurements for all aspects (0–1 measurements), whereas dimensions from the Spathian–Ladinian are best documented. Tooth length is based on the largest number of measurements (height: n = 237, length: n = 463, width: n = 230) and is therefore expected to yield the most reliable pattern. The largest mean tooth size is recorded from the Cisuralian and the overall trend through the Permian is one of decreasing size (Figure 8.16). The smallest tooth sizes from the Permian–Triassic interval occur in the Early Triassic. Not all substages show equally reduced dimensions, however, as there is some evidence to suggest that larger tooth sizes occurred in the Smithian with a renewed decline in the Spathian (Figure 8.16), although this is not significant (Table 8.3). Somewhat larger sizes, although fluctuating, are again observed in the Middle and Late Triassic, but generally remain smaller than sizes recorded from the Permian. Statistical testing revealed that significant size differences exist in tooth length between epochs during the Cisuralian–Middle Triassic interval, including across the Permian/Triassic boundary, which is supported by tooth width (Table 8.3).

Dorsal fin spines are rarely recovered intact and the available data on fin spine height from the Permian–Triassic show an erratic pattern, which is probably the result of low counts even if resolution is reduced to epoch-level only (Figure 8.17A). Instead, overall body size data show a clear divide between the Permian and Triassic (Figure 8.17B), which is significant (Table 8.4) and indicates that chondrichthyans were, on average, two metres longer before the Late Permian mass extinction. No decreasing trend becomes apparent from the Permian data, as was the case in tooth size data, with comparable mean sizes in the Cisuralian and Lopingian, whereas the Guadalupian data show greater body length. The Triassic data show a similar pattern

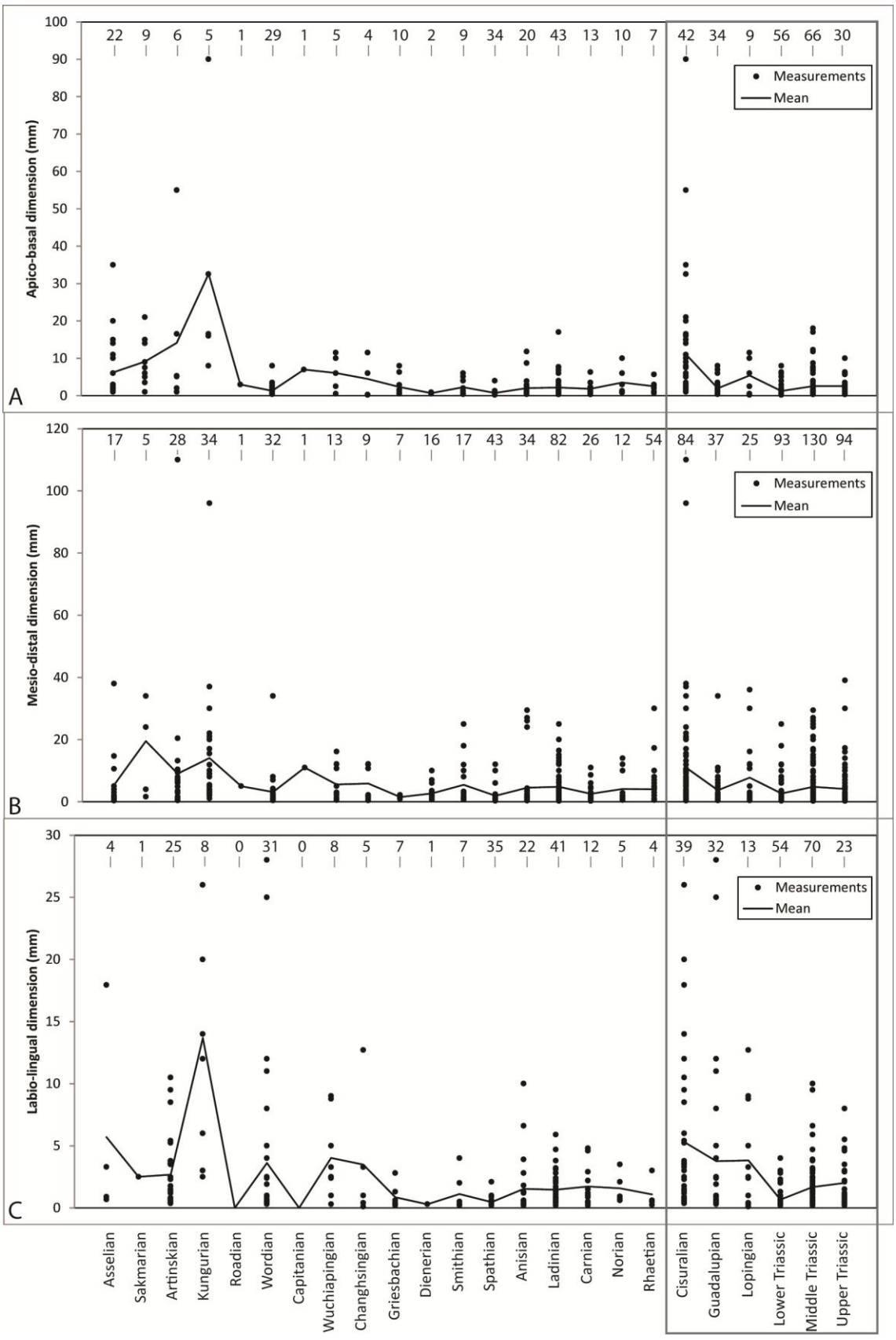

Figure 8.16 – Tooth size patterns among Permian and Triassic chondrichthyans: A, height; B, length; and C, width per (sub)stage (Appendix A2.2). Epoch data are a summary of all (sub)stage data and measurements from occurrences resolved to epoch-level only. Numbers of measurements are indicated.

Table 8.3 – Pairwise Mann–Whitney U significance tests of differences in the median of chondrichthyan dental dimensions.

Paired (sub)stages/epochs		Tooth height	Tooth length	Tooth width
Asselian	Sakmarian	0.08	0.055	-
Sakmarian	Artinskian	0.81	0.07	-
Artinskian	Kungurian	0.14	**0.005**	**<0.001**
Kungurian	Roadian	-	-	-
Roadian	Wordian	-	-	-
Wordian	Capitanian	-	-	-
Capitanian	Wuchiapingian	-	-	-
Wuchiapingian	Changhsingian	0.54	0.62	0.51
Changhsingian	Griesbachian	0.83	0.31	0.52
Griesbachian	Dienerian	0.45	0.84	-
Dienerian	Smithian	0.64	0.44	-
Smithian	Spathian	0.06	0.10	0.51
Spathian	Anisian	**0.03**	0.84	0.17
Anisian	Ladinian	0.19	**0.01**	**0.02**
Ladinian	Carnian	0.53	**0.048**	0.96
Carnian	Norian	0.50	0.85	0.96
Norian	Rhaetian	1	**0.03**	0.22
Cisuralian	Guadalupian	**<0.001**	**<0.001**	**0.04**
Guadalupian	Lopingian	0.26	**0.04**	0.29
Lopingian	Lower Triassic	0.08	**<0.001**	**0.001**
Lower Triassic	Middle Triassic	**0.001**	**0.002**	**<0.001**
Middle Triassic	Upper Triassic	0.07	0.34	0.57

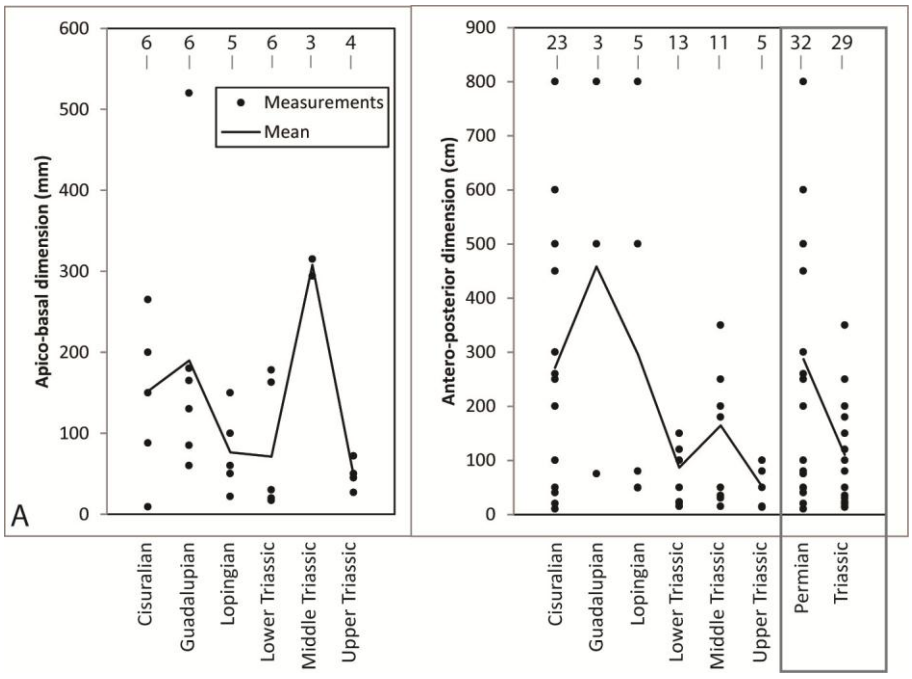

Figure 8.17 – Size patterns among Permian and Triassic chondrichthyans: A, dorsal fin spine height; and B, overall body length per epoch (same legend as for A; Appendix A2.2). Period data are a summary of all epoch-level data and measurements from occurrences resolved to period-level only. Numbers of measurements are indicated.

Table 8.4 – Pairwise Mann–Whitney U significance tests of differences in the median of chondrichthyan fin spine and body dimensions.

Paired (sub)stages/epochs		**Spine height**	**Body length**
Cisuralian	Guadalupian	0.81	0.28
Guadalupian	Lopingian	0.10	0.55
Lopingian	Lower Triassic	0.52	0.73
Lower Triassic	Middle Triassic	**0.03**	0.09
Middle Triassic	Upper Triassic	0.052	0.09
Permian	Triassic	-	**0.01**

to the Permian, with reduced sizes in the Early and Late Triassic compared to the Middle Triassic, although at lower mean sizes.

In order to remove noise from the size data caused by taxa going extinct or disappearing temporarily across the Permian/Triassic boundary, boundary crossing taxa that are represented by tooth size data in both the Permian and Triassic are reviewed separately (Figure 8.18A, B, C; height n = 155; length n = 351; width n = 193). The overall pattern emerging from these data is one of fluctuating but generally increasing size over the course of the Permian and Triassic. The Early Triassic is characterised by a size reduction, although it is not significantly different from the Lopingian (Table 8.5). However, Lower Triassic sizes are consistently and significantly different from the Middle Triassic across all dental aspects. From the Anisian onwards, a gradual size increase is generally observed, with tooth sizes actually exceeding those that were recorded from the Permian. In summary, the Lilliput effect cannot be established due to the low resolution of the data, but a general reduction in tooth size for the duration of the Early Triassic as a result of the Late Permian extinction has been established, in concordance with the pattern recorded in marine invertebrates (e.g., Twitchett 2007a).

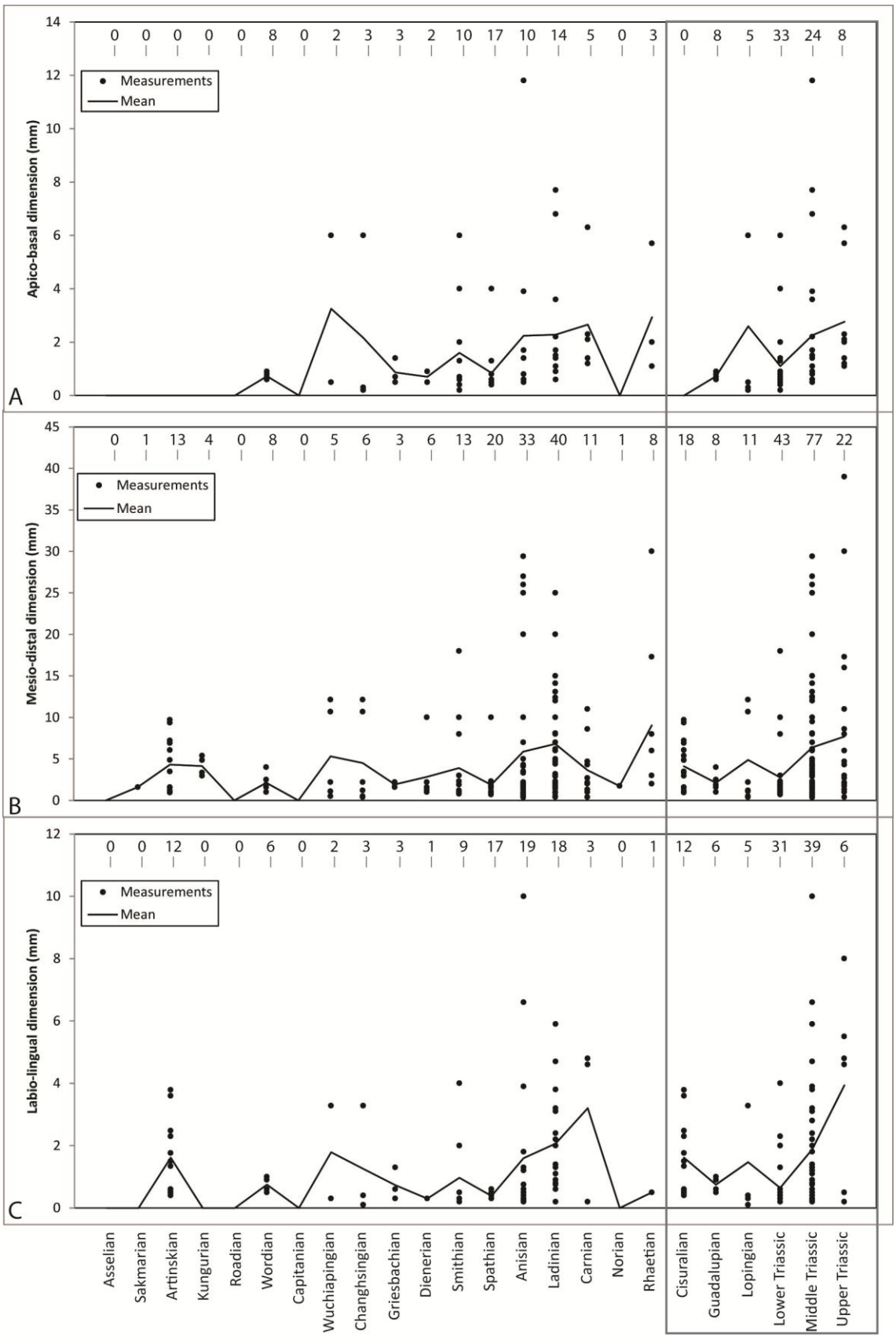

Figure 8.18 – Tooth size patterns among Permian/Triassic boundary crossing chondrichthyan genera: A, height; B, length; and C, width per (sub)stage (Appendix A2.2). Epoch data are a summary of all (sub)stage data and measurements from occurrences resolved to epoch-level only. Numbers of measurements are indicated.

Table 8.5 – Pairwise Mann–Whitney U significance tests of differences in the median of chondrichthyan dental dimensions for boundary crossing genera.

Paired (sub)stages/epochs		Tooth height	Tooth length	Tooth width
Asselian	Sakmarian	-	-	-
Sakmarian	Artinskian	-	-	-
Artinskian	Kungurian	-	0.95	-
Kungurian	Roadian	-	-	-
Roadian	Wordian	-	-	-
Wordian	Capitanian	-	-	-
Capitanian	Wuchiapingian	-	-	-
Wuchiapingian	Changhsingian	0.56	0.78	1
Changhsingian	Griesbachian	0.66	1	1
Griesbachian	Dienerian	1	0.52	-
Dienerian	Smithian	0.91	1	-
Smithian	Spathian	0.44	0.42	0.32
Spathian	Anisian	**0.04**	0.25	0.36
Anisian	Ladinian	0.14	**0.047**	**0.02**
Ladinian	Carnian	0.35	0.15	0.55
Carnian	Norian	-	-	-
Norian	Rhaetian	-	-	-
Cisuralian	Guadalupian	-	0.25	0.26
Guadalupian	Lopingian	0.61	0.97	0.65
Lopingian	Lower Triassic	0.93	0.64	0.85
Lower Triassic	Middle Triassic	**0.003**	**0.005**	**0.002**
Middle Triassic	Upper Triassic	0.11	0.48	0.19

8.4 PALAEOGEOGRAPHICAL DISTRIBUTION

8.4.1 INTRODUCTION

Data gathered from the modern-day chondrichthyan community suggest that species diversity on continental and insular shelves, comprising the majority of all species, is highest in tropical regions and lowest in high latitudes (Compagno 1990) and many other organisms follow the same latitudinal diversity gradient (e.g., Jablonski *et al.* 2006). Furthermore, lower species diversity may be observed in larger genera that are mobile and have a global distributional range, which enables more rapid gene flow and panmixia (Compagno 1990). It is these less diverse groups that are, therefore, expected to be more likely victims of a mass extinction such as the Late Permian event. It has been demonstrated in the marine fossil record that geographic range is the most consistently significant predictor of extinction risk (Payne and Finnegan 2007). The distributional aspects of the Permian–Triassic chondrichthyan population will be

explored in this section to examine global patterns and temporal variability, as well as diversity fluctuations in individual basins, especially in relation to times of biotic crises and potential refugia (see Twitchett 2006 for a discussion).

The distributional analyses presented here are based on the grouping of localities into six global oceanic basins and other palaeogeographic areas that existed in Permian–Triassic times (see Figure 7.4), comprising east Panthalassa, the epicontinental basins of central Pangaea, the Boreal Sea, Palaeotethys, Neotethys, and central and west Panthalassa. Lazarus occurrences are excluded from these analyses, because they cannot be linked to a specific region. Furthermore, freshwater genera are excluded from the palaeolatitudinal analyses, because they are not as free to migrate in response to environmental changes as marine or euryhaline genera.

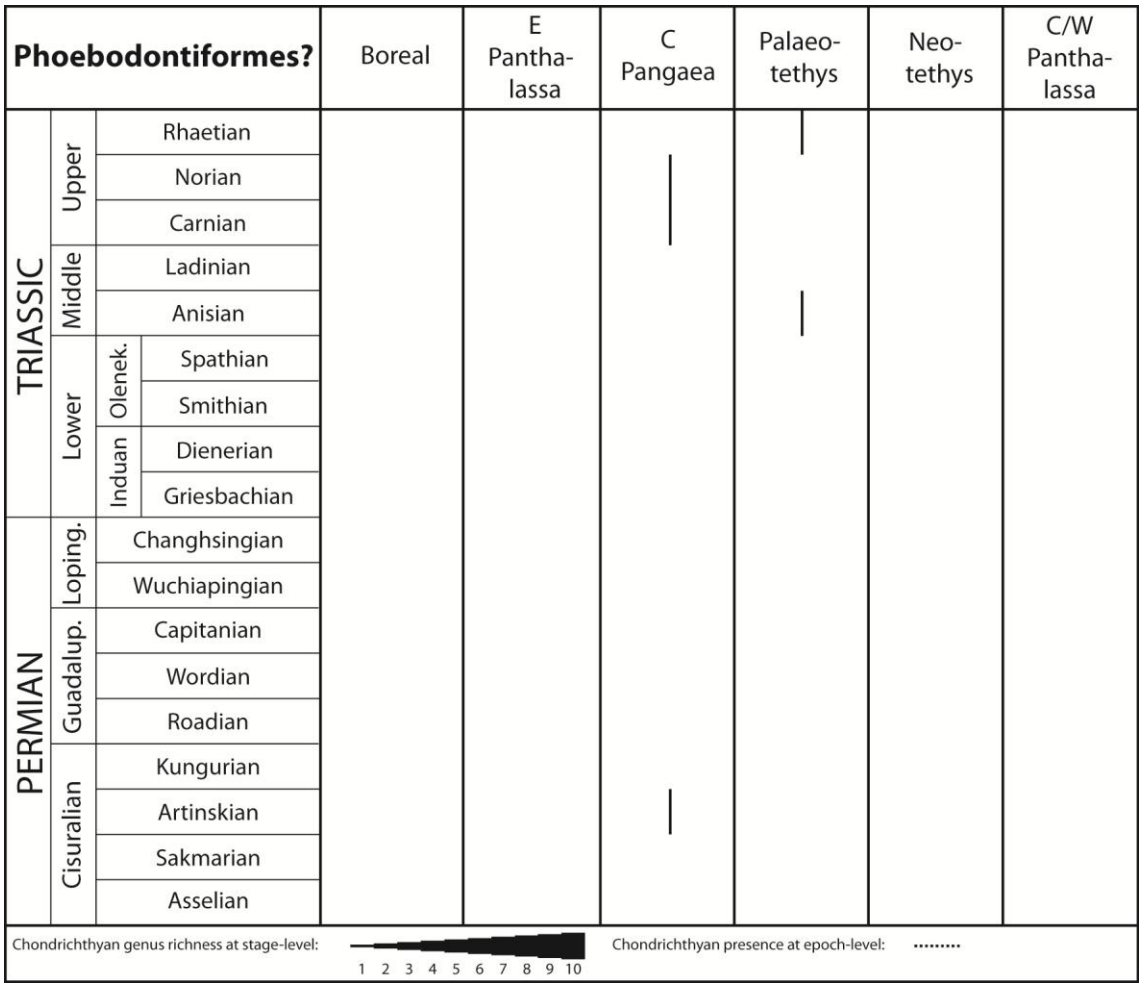

Figure 8.19 – Stratigraphy showing phoebodontiform? genus richness per basin/region.

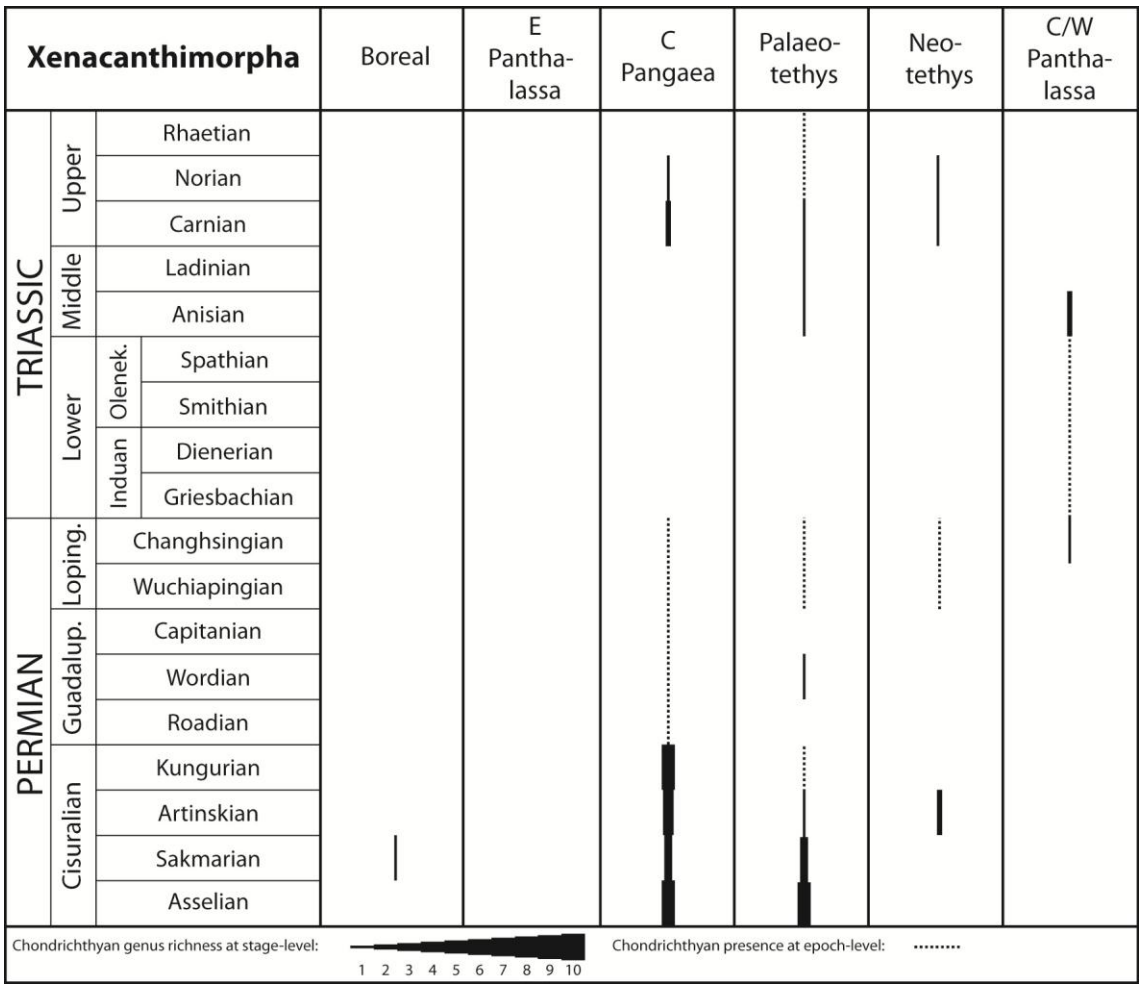

Figure 8.20 – Stratigraphy showing xenacanthimorph genus richness per basin/region.

8.4.2 Distribution of individual taxonomic groups

The Phoebodontiformes? show very intermittent and very limited distribution, being restricted to Palaeotethys and the freshwater deposits of central Pangaea, and are never represented by more than one genus at any time during the Permian and Triassic (Figure 8.19). Comparatively, the Xenacanthimorpha were widely distributed in the Cisuralian, with representatives in four of the six major areas and their highest diversity in central Pangaea and Palaeotethys at this time (Figure 8.20), both of which comprised predominantly freshwater localities. Most xenacanth genera were apparently endemic (see Johnson 2003), which is common among freshwater taxa, but the group also remained common in marine habitats (see Schultze 2009). Xenacanthimorphs gradually declined in Palaeotethys from the start of the Permian, but disappeared

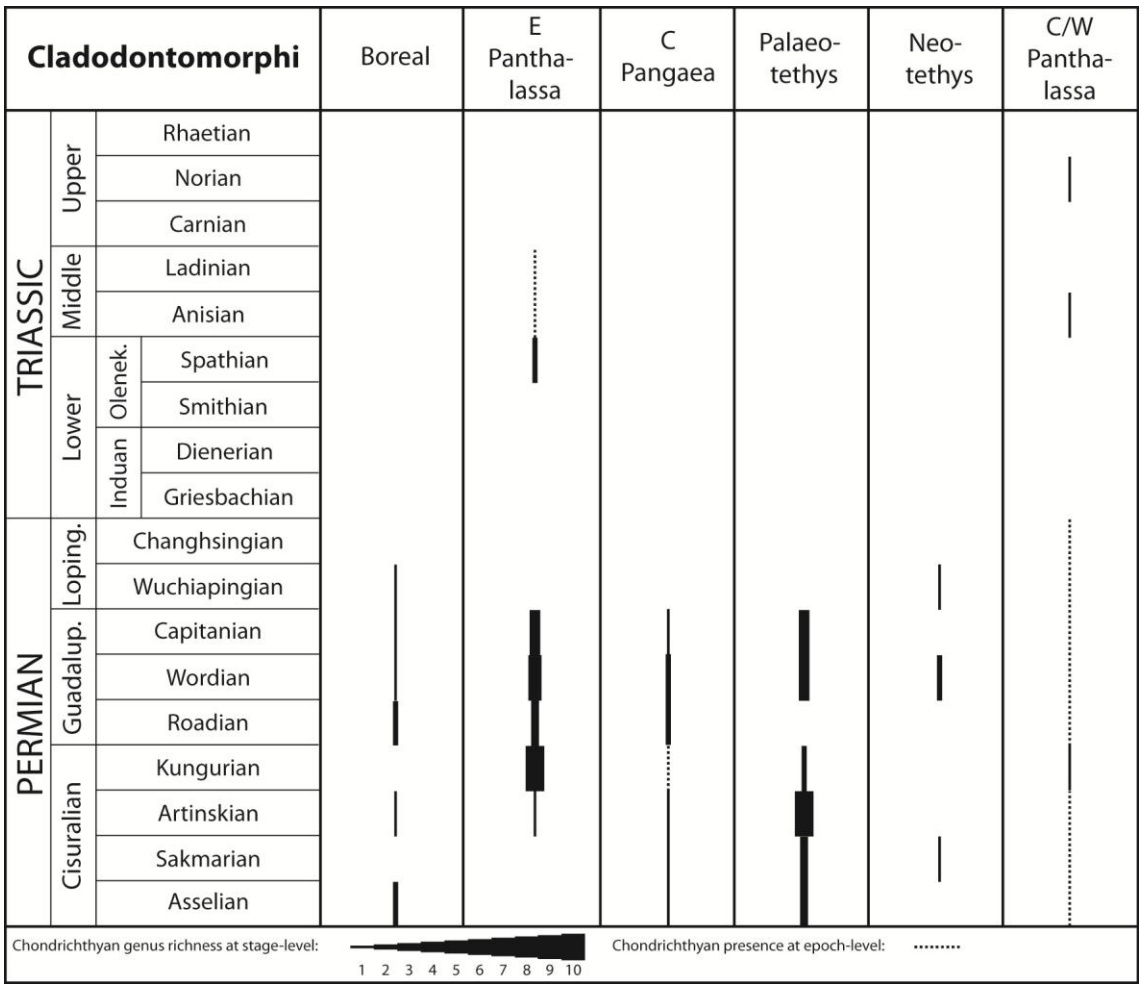

Figure 8.21 – Stratigraphy showing cladodontomorph genus richness per basin/region.

suddenly from central Pangaea at the end of the Cisuralian (Figure 8.20). Their presence in central and western Panthalassa is only recorded from Changhsingian–Anisian freshwater deposits, a time at which they are not known from any of the other areas globally.

The Cladodontomorphi were most diverse in the marine eastern Panthalassa and Palaeotethys during the Cisuralian–Guadalupian (Figure 8.21). Both areas show opposite trends, however, with an overall decline in Palaeotethys over the course of the Cisuralian, supporting the notion that cladodont (ctenacanth) diversity and distribution declined in the Permian compared to the Carboniferous (Hodnett *et al.* 2012). Cladodonts first occurred in eastern Panthalassa in the Artinskian, however, and subsequently experienced a rapid diversity increase in the Kungurian (one to seven genera; Figure 8.21). Although they regained their Cisuralian diversity levels in

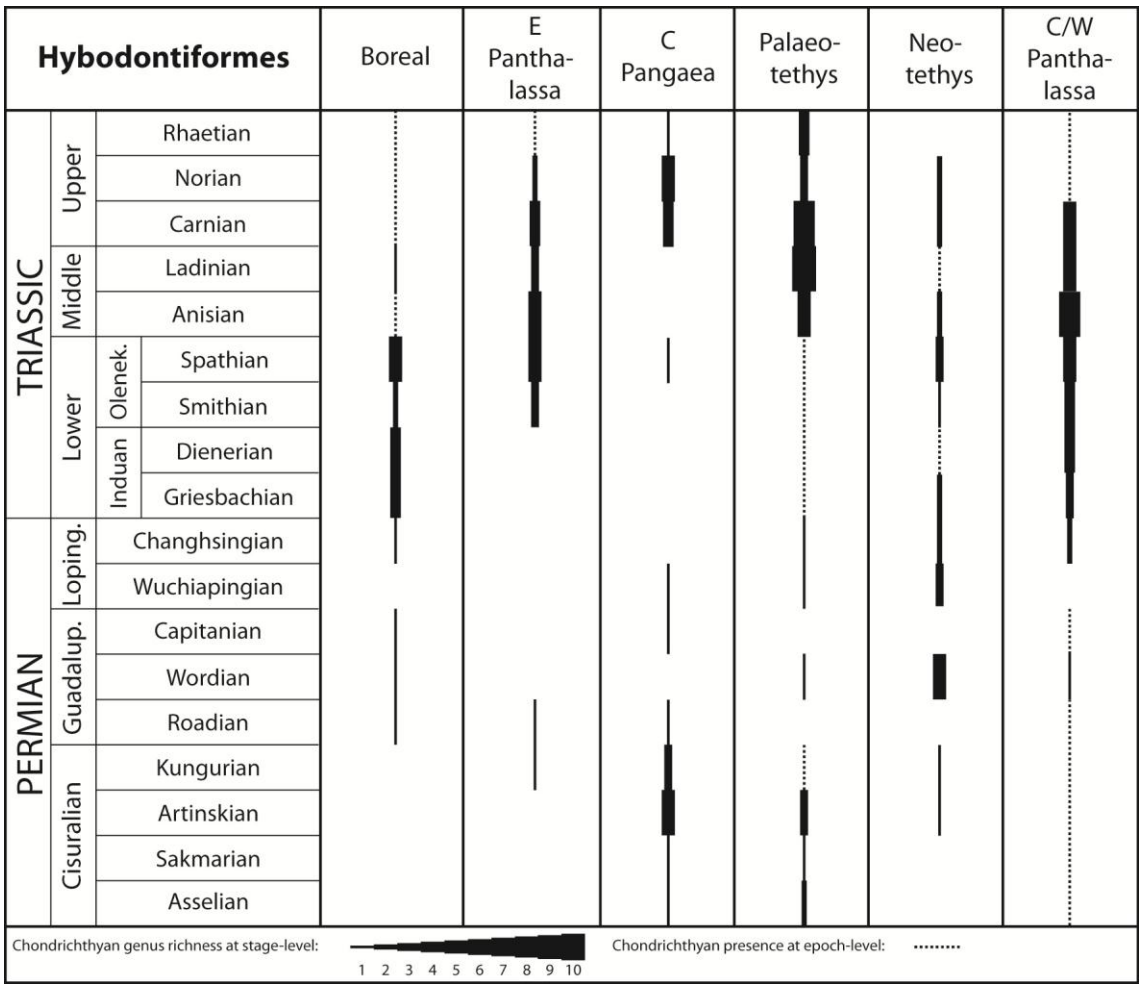

Figure 8.22 – Stratigraphy showing hybodontiform genus richness per basin/region.

Palaeotethys in the Wordian and Capitanian and were globally distributed, the end-Guadalupian crisis appears to have affected them severely, suggested by their sudden disappearance in most areas. Very low diversity is observed in the Lopingian in the Boreal Sea, Neotethys and western Panthalassa. All Triassic occurrences of the group are equivocal (see Section 8.2.2) and provide no clear indication that cladodonts survived the Late Permian mass extinction.

The Hybodontiformes were globally distributed in both the Permian and Triassic and in both freshwater and marine habitats, illustrating their high success rate (Figure 8.22). This is also reflected in the high diversity of the group, especially after the Permian/Triassic boundary. In the immediate aftermath of the Late Permian mass extinction (Griesbachian–Dienerian), they were most diverse in the Boreal Sea and central and western Panthalassa, followed by western Neotethys (Figure 8.22).

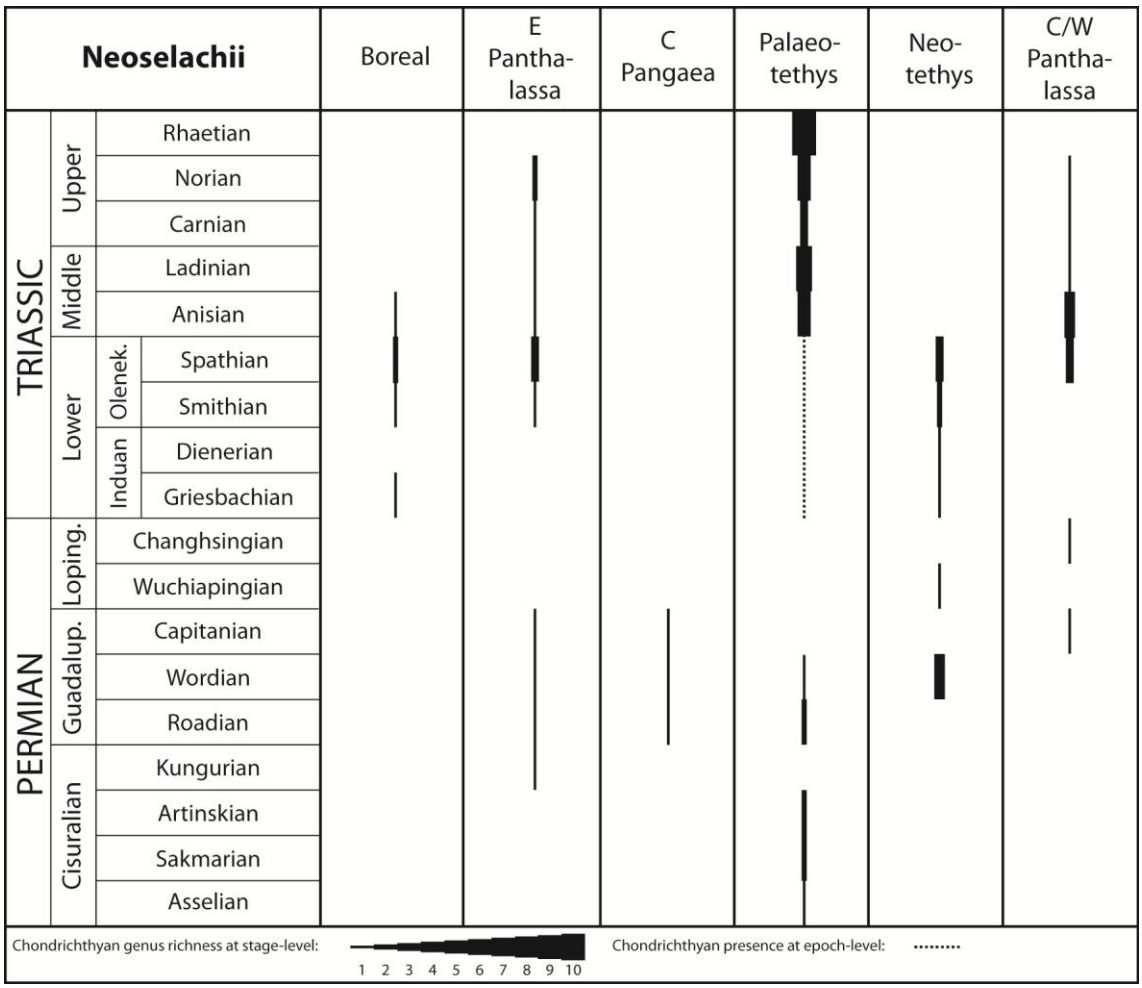

Figure 8.23 – Stratigraphy showing neoselachian genus richness per basin/region.

Subsequently, increasing diversity is also recorded in eastern Panthalassa from the Smithian. Hybodontiforms appear to have been most successful in Palaeotethys in the Middle Triassic, but this may be related to the intense sampling of this epoch in Europe.

The Neoselachii were present in all areas globally during the Permian, except for the Boreal Sea (Figure 8.23), albeit generally at low diversity. The short-lived Wordian diversity peak in Neotethys is related to the Khuff fauna described in this study (Figure 8.23). The only known Lopingian representatives of the group occur in Neotethys and western Panthalassa, whereas the Boreal Sea and Neotethys represent their known distributional range in the Griesbachian. Diversity increased slightly globally in the Smithian–Spathian, but the highest level of neoselachian diversity is observed in Palaeotethys from the Middle Triassic onwards.

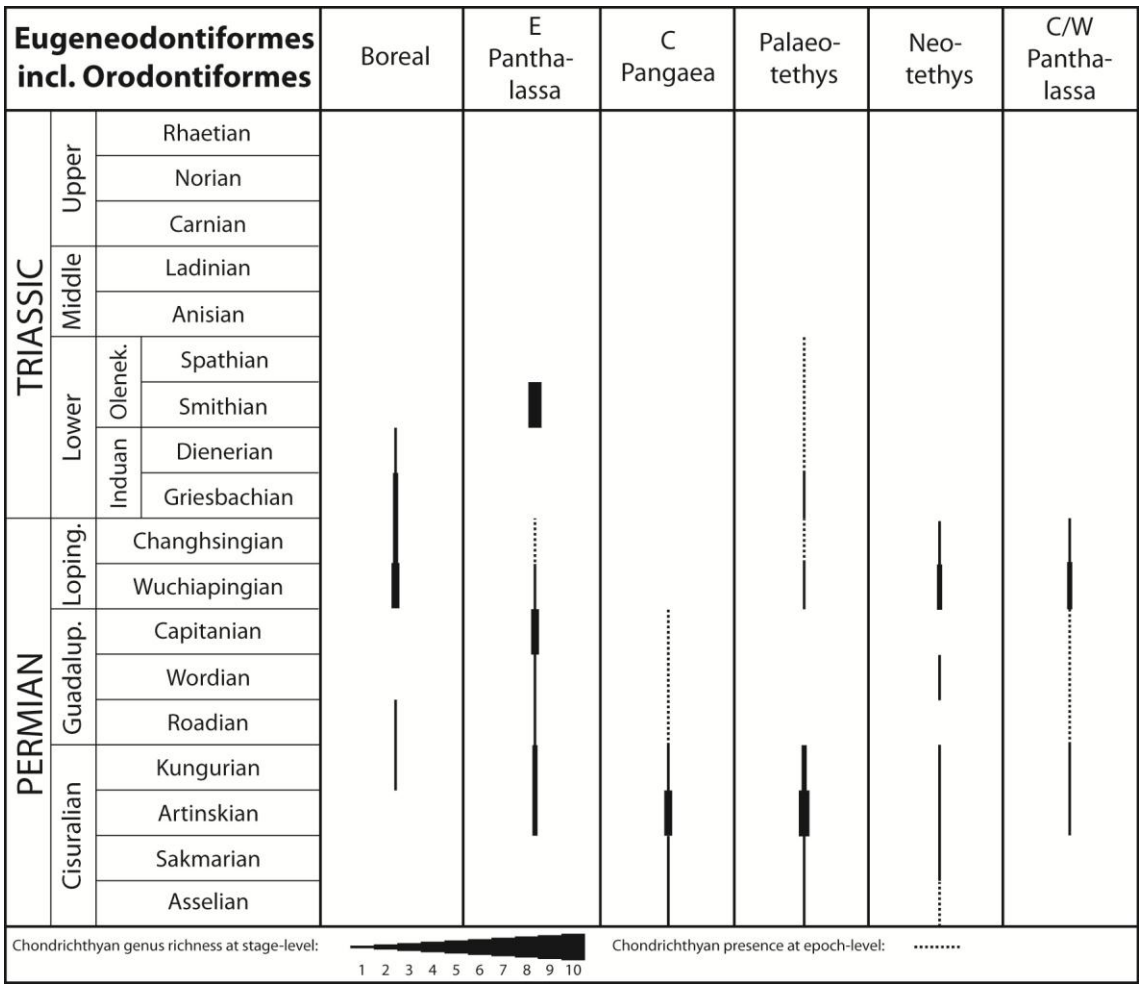

Figure 8.24 – Stratigraphy showing eugeneodontiform (incl. orodontiform) genus richness per basin/region.

The Eugeneodontiformes (including one Cisuralian orodontiform genus) were never diverse, but still ranged into all major global areas, including central Panthalassa; a consequence of their mobile pelagic lifestyle (Figure 8.24). In most areas their last occurrences are either Wuchiapingian or Changhsingian in age, but they nevertheless survived the Late Permian mass extinction (e.g., Mutter and Neuman 2008). The data suggest that they retreated to northern regions (Figure 8.24). The group subsequently re-appeared in northeastern Panthalassa in the Smithian, but then suddenly disappeared, potentially as a result of the end-Smithian crisis.

The Petalodontiformes were similarly distributed in all global areas during the Permian, but were usually represented by only one genus in each region at any time (Figure 8.25). They appear to have been most diverse during the Artinskian and Kungurian. Prior to the Late Permian mass extinction, they were still widely recorded in

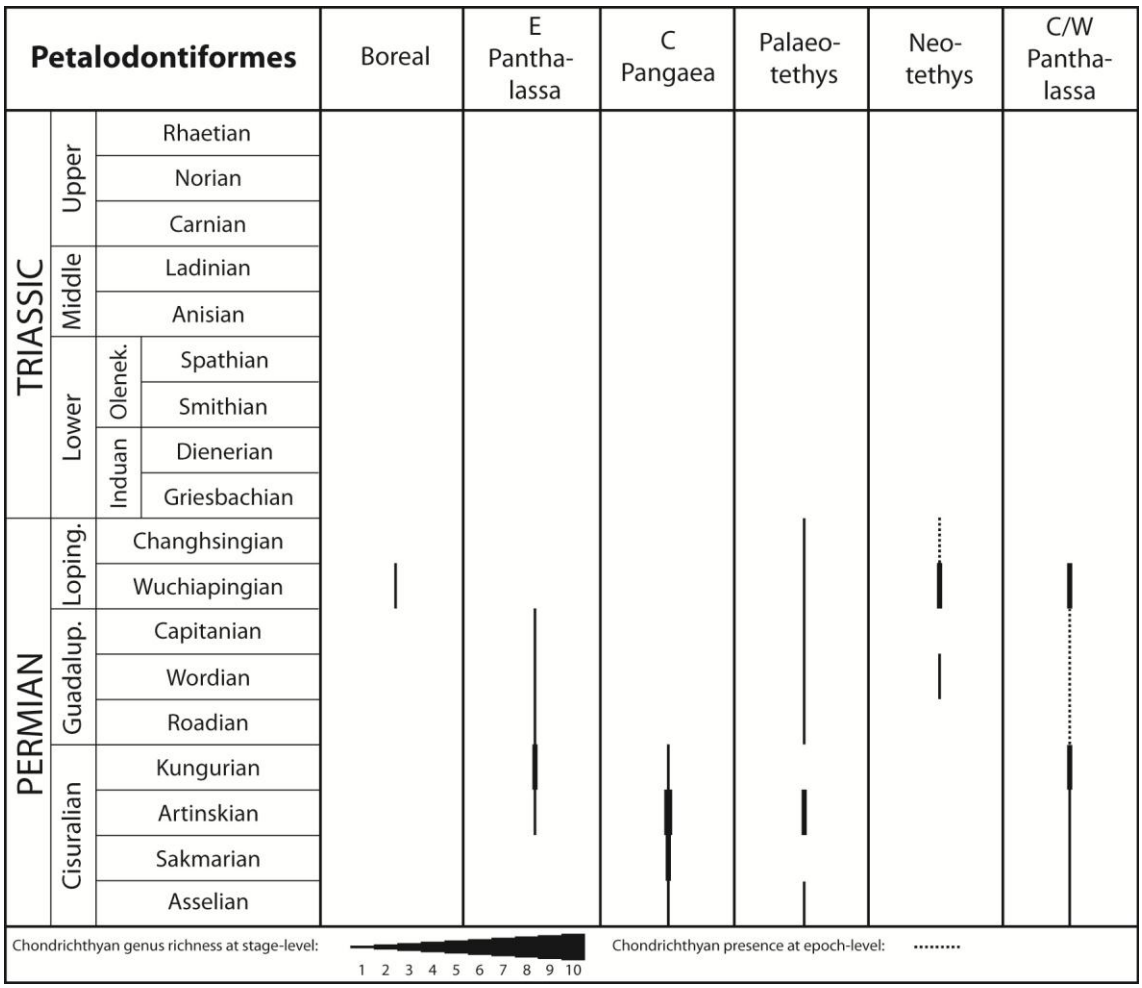

Figure 8.25 – Stratigraphy showing petalodontiform genus richness per basin/region.

the Wuchiapingian in Palaeotethys, the neighbouring Boreal Sea and western Neotethys, as well as in the remote central Panthalassa. In the Changhsingian, however, the only records are from Palaeotethys, and no petalodontiform genera survived into the Triassic.

The Holocephali were most diverse in eastern Panthalassa during the Kungurian–Capitanian (Figure 8.26). Their sudden disappearance across the Guadalupian/Lopingian boundary may have been the result of the end-Guadalupian crisis. Holocephalans ranged into all major areas, including the remote central Panthalassa. For most of the Triassic, holocephalan occurrences have only been recorded from central and western Panthalassa, following their disappearance from the Boreal Sea, Palaeotethys and Neotethys during or at the end of the Lopingian, until their re-appearance in Palaeotethys in the Rhaetian.

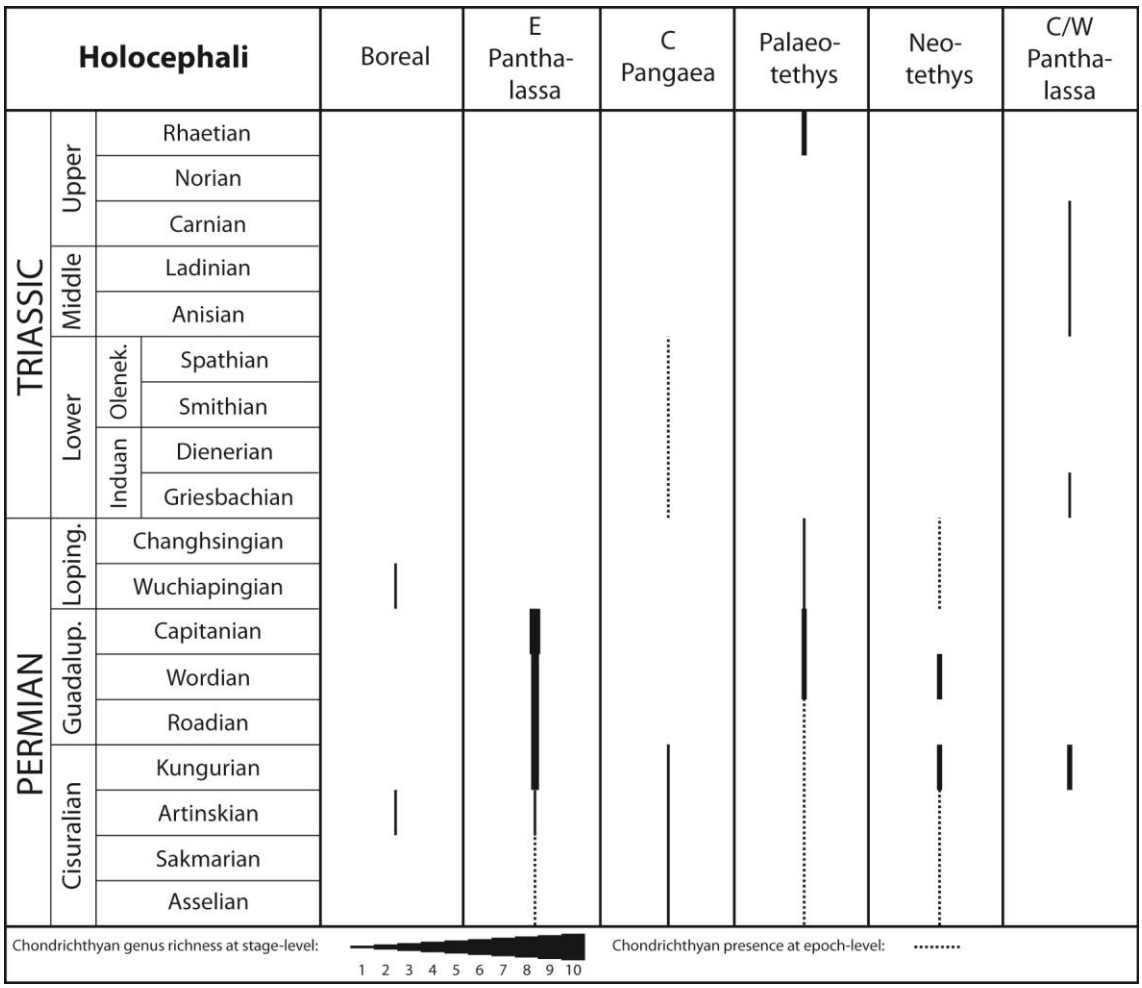

Figure 8.26 – Stratigraphy showing holocephalan genus richness per basin/region.

8.4.3 Global chondrichthyan distribution

Proportions of global genus diversity per basin or region show that central Pangaea and Palaeotethys comprised most chondrichthyan diversity at the start of the Permian, with lower diversity in the Boreal Sea, Neotethys, and central and western Panthalassa (Figure 8.27). The focal point then shifted to eastern Panthalassa during the Guadalupian. The Boreal Sea also displays a gradual proportional increase at this time, which peaked at around 50% of global diversity in the Griesbachian–Dienerian, following a reduction in importance of the Palaeotethys. Central and western Panthalassa displays a similar increase in importance to around 40% in the Dienerian. The largest proportion of Olenekian diversity was located in eastern Panthalassa, but

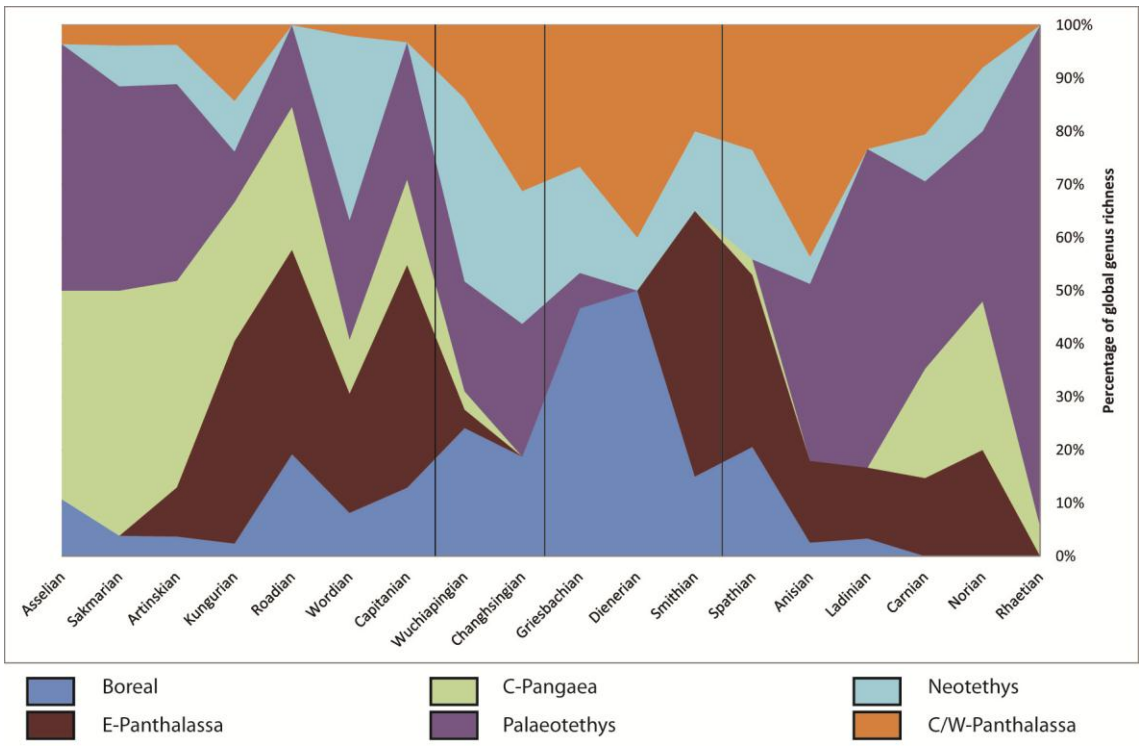

Figure 8.27 – Proportion of genus diversity per palaeobasin or region per (sub)stage. Major biotic crises and extinction events are marked (vertical lines) in age order: end-Guadalupian crisis, Late Permian extinction, and end-Smithian crisis.

the Palaeotethys regained its importance in the Middle Triassic and retained it for the remainder of the Triassic.

Genus richness is significantly correlated to palaeogeographic region, suggesting differential diversity fluctuations during the (sub)stages surrounding the Late Permian mass extinction (Figure 8.28A). Despite this, a generally decreasing trend through time is apparent as well as the disappearance of highly diverse areas. Eastern Panthalassa lost the most diversity across the CWB, whereas the Boreal Sea and Neotethys gained in diversity. The Wuchiapingian–Griesbachian data further suggest that tropical regions in the vicinity of Pangaea primarily experienced diversity loss. Instead, chondrichthyans were best represented in regions at higher palaeolatitudes (Boreal Sea, Neotethys) and in more remote locations (at a large distance from Pangaea; central Panthalassa) at this time.

Genus richness is also significantly correlated to palaeogeographic region during the time interval comprising the end-Smithian crisis and subsequent Anisian radiation

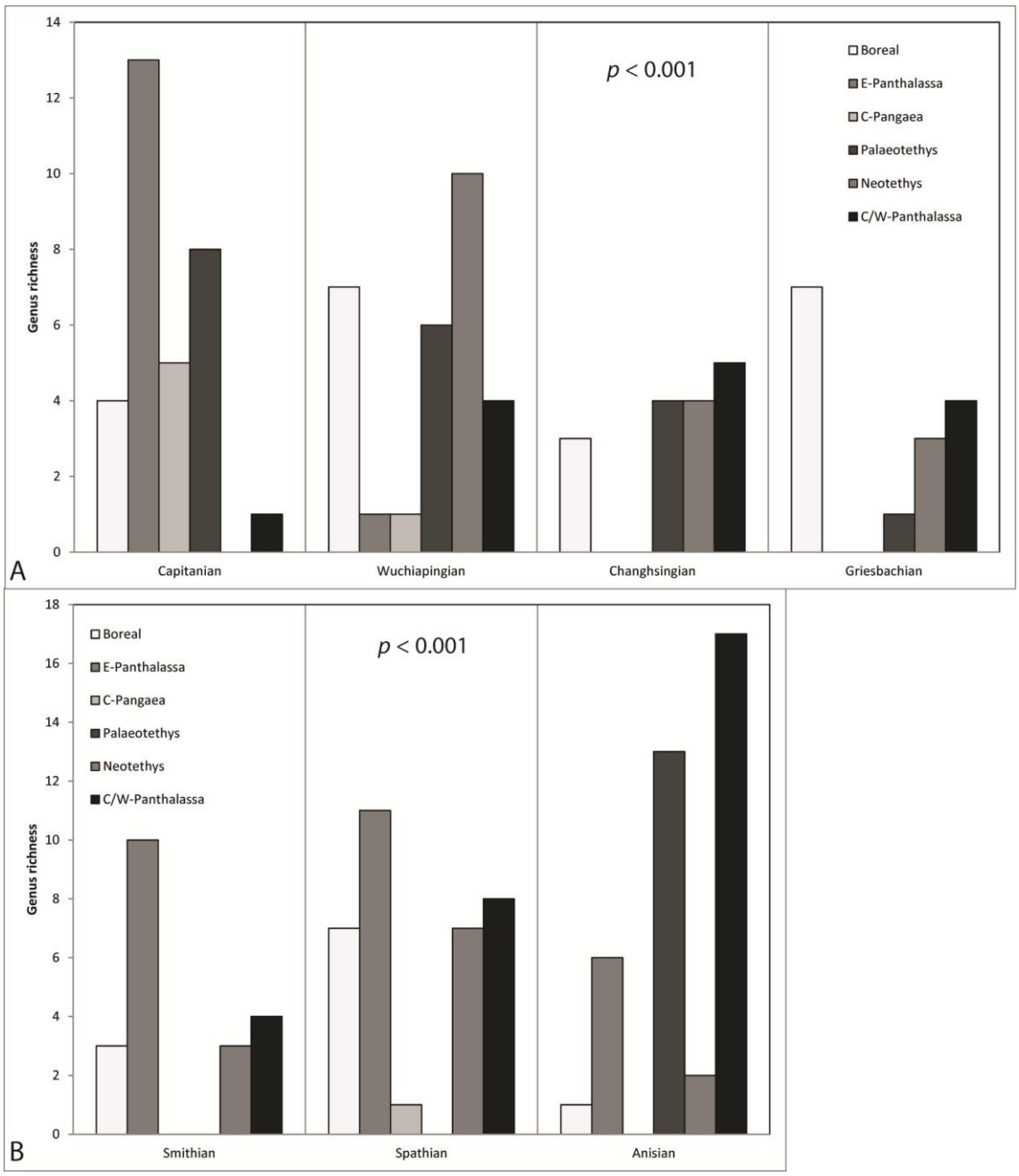

Figure 8.28 – A, Genus richness levels partitioned according to palaeobasin/region for (sub)stages surrounding the Late Permian mass extinction and B, surrounding the end-Smithian crisis and Anisian radiation. *P* represents the significance level found with a chi-squared test for independence (based on fossil genera incl. open nomenclature; Appendix A2.4.19).

(Figure 8.28B). Eastern Panthalassa was highly diverse in the Smithian–Spathian, but in the Anisian the greatest diversity is observed in the Palaeotethys and central and western Panthalassa. In the latter area, this followed a gradual increase, whereas an apparent rapid radiation took place in Palaeotethys. Diversity became reduced in all other areas.

Proportions of global genus diversity per palaeolatitudinal zone show that the largest proportion is known from the northern hemisphere, and particularly from 0°N–60°N throughout the Permian–Triassic (Figure 8.29). The Permo–Carboniferous southern hemisphere glaciation came to an end in the Sakmarian, causing a climatic cooling on the northern hemisphere (Korte *et al.* 2005), which may have caused a (temporary) increase in genus richness on the southern hemisphere. Around the Late Permian mass extinction there was a prominent decrease in the proportion of the 0°N–30°N zone, resulting in an increase in the 31°N–60°N and 0°S–30°S zones, most probably because of the harsh hot-house climatic conditions that characterised the Lopingian and likely persisted during the Early Triassic (Preto *et al.* 2010). The overall Triassic climate was characterised by a non-zonal pattern, with a strong global monsoon system that predominantly affected Tethys (Preto *et al.* 2010). This may have influenced that, from the Smithian onwards, the importance of the 31°N–60°N zone decreased and the 0°N–30°N zone became the most important for global diversity. This

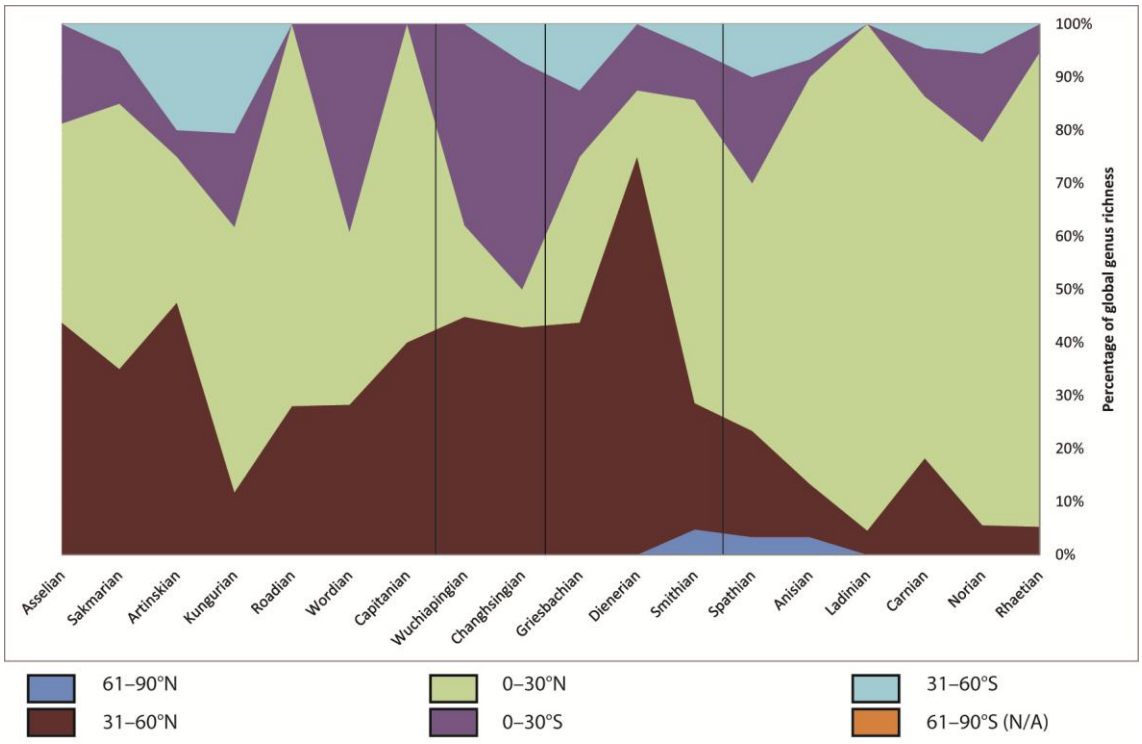

Figure 8.29 – Proportion of genus diversity per palaeolatitudinal zone per (sub)stage. Major biotic crises and extinction events are marked (vertical lines) in age order: end-Guadalupian crisis, Late Permian extinction, and end-Smithian crisis.

high diversity in the 0°N–30°N zone persisted throughout the remainder of the Triassic, during which the Middle Triassic was characterised locally by humid episodes and the late Carnian and Norian seem to have been climatically stable, whereas the end-Triassic extinction event is associated with climatic warming and increased rainfall (Preto *et al.* 2010).

The drastic reduction in diversity in the 0°N–30°N zone over the course of the Capitanian–Changhsingian can also be observed in the absolute levels of genus diversity per palaeolatitudinal zone (Figure 8.30A). In contrast, the 31°N–60°N zone retains much of its diversity and the 0°S–30°S zone attains much higher diversity levels. Genus richness is significantly correlated to palaeolatitudinal zone, suggesting differential diversity fluctuations in palaeolatitudinal zones during the (sub)stages surrounding the Late Permian mass extinction. Genus richness is independent of palaeolatitudinal zone during the Smithian–Anisian, suggesting proportional fluctuations in genus diversity among palaeolatitudinal zones (Figure 8.30B). The 0°N–30°N zone remains the dominant zone throughout the interval with a genus richness about eight times as high or more than is recorded from other zones in the Anisian.

The proportions of global genus diversity per hemisphere shows the increased importance of the southern hemisphere following the start of the extinctions across the CWB, but a rebound throughout the Griesbachian–Anisian, with the exception of the Spathian, following the end-Smithian crisis (Figure 8.31A). Grouping of palaeolatitudinal zones shows that the proportion of tropical zones of global diversity gradually declined from 60% in the Capitanian to around 40% in the Griesbachian (and potentially around 25% in the Dienerian, but this may be influenced by the poor quality of the fossil record from this substage), suggesting that tropical regions were more severely affected during the end-Guadalupian and Late Permian extinction events (Figure 8.31B). Subsequently, the proportion of genus diversity located in tropical regions increased again in the Smithian–Anisian.

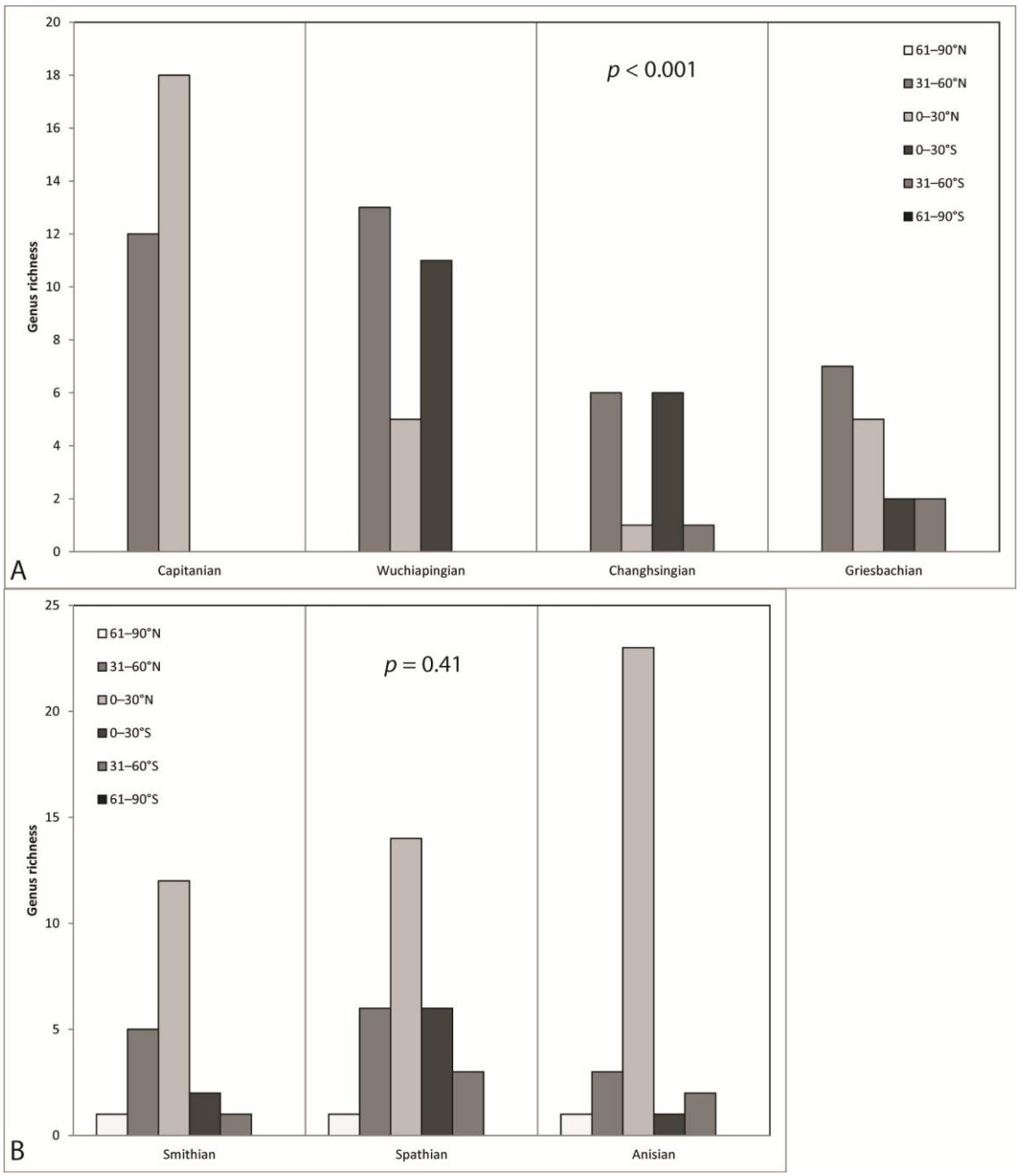

Figure 8.30 – A, Genus richness levels partitioned according to palaeolatitudinal zone for (sub)stages surrounding the Late Permian mass extinction and B, surrounding the end-Smithian crisis and Anisian radiation. *P* represents the significance level found with a chi-squared test for independence (based on fossil genera incl. open nomenclature, excl. freshwater genera; Appendix A2.4.21).

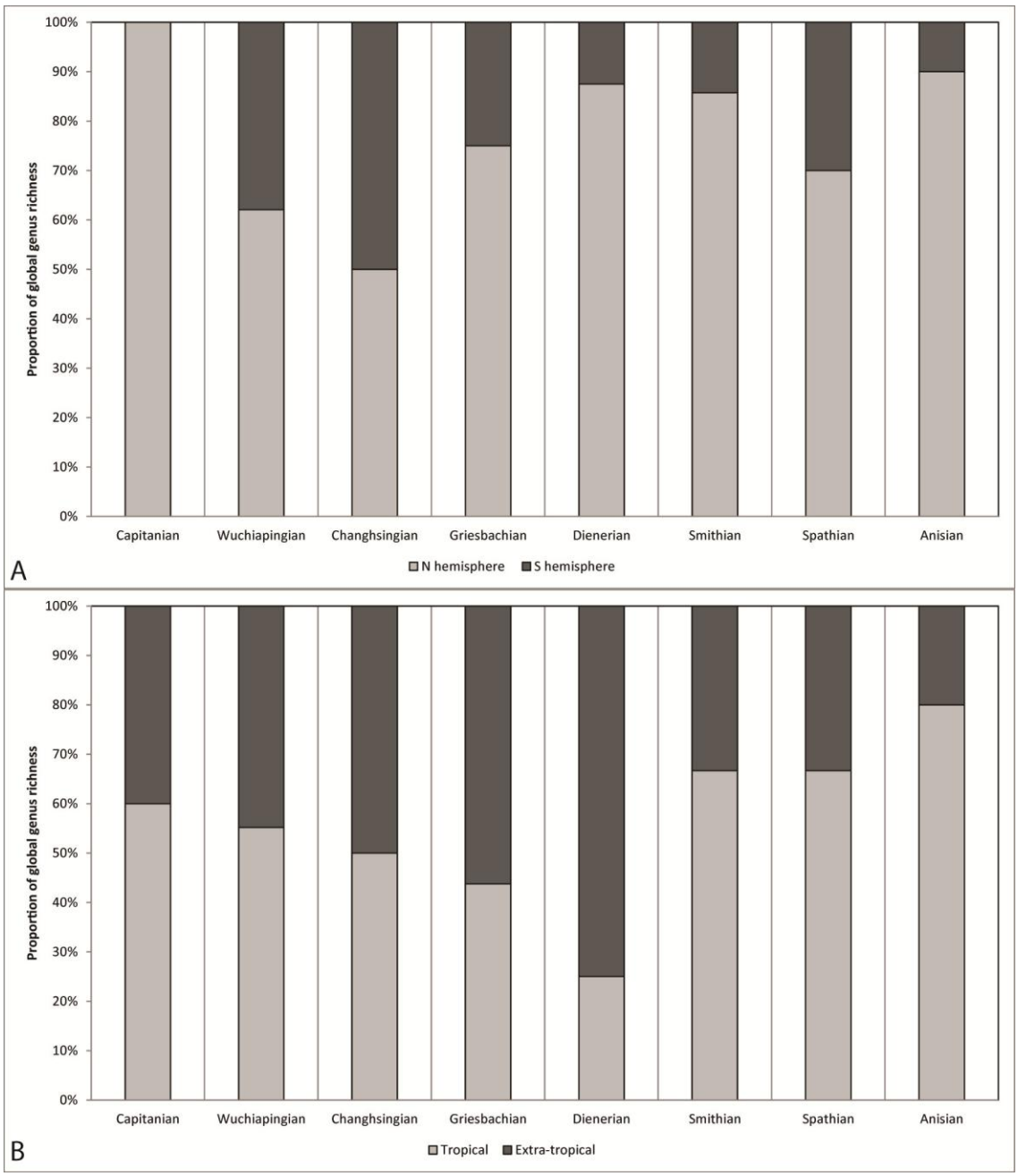

Figure 8.31 – Proportions of total diversity for A, the northern and southern hemispheres and B, tropical (30°N–30°S) and extra-tropical zones.

8.5 SYNTHESIS AND DISCUSSION

8.5.1 EVENTS IN CHONDRICHTHYAN DIVERSITY

8.5.1.1 CISURALIAN–GUADALUPIAN

The Cisuralian was an epoch characterised by high chondrichthyan diversity (Figure 8.1) and high standing diversity (Figure 8.5A), with low and stable origination

and extinction rates, and therefore similar diversification and turnover rates (Figure 8.5A, B). Furthermore, chondrichthyans were diverse, comprising seven well-established groups (Figure 8.2, Figure 8.6), that had a combined global distribution with representatives in all major basins (Figure 8.19–Figure 8.26).

The Roadian is characterised by a significant decline in genus diversity. The Holocephali and the Eugeneodontiformes, and to a minor extent also the Cladodontomorphi, show a decline in genus richness at this time, but other groups appear largely unaffected (Figure 8.3). This means that the decline is only detected in the marine component (Figure 8.9), but in both benthic and pelagic groups (Figure 8.12), and a decline of varying degree is observed in all feeding types, except among crushing dentitions (Figure 8.14). These Roadian patterns can be attributed to a reduction in the quality of the fossil record (see Section 7.3.3.2), an interpretation that is supported by the fact that the number of boundary crossers is virtually unaffected (Figure 8.1B). Furthermore, neither general EMSD, nor the standing diversity of any of the aforementioned groups show signs of temporarily enhanced diversity decline and turnover rate is unaffected (Figure 8.5A, Figure 8.7), which is evidence against a true extinction event. Minor peaks in origination and extinction in the Wordian (Figure 8.5B) and the peak in genus diversity (Figure 8.1A) are the result of the contribution of Neotethys to the total (Figure 8.27) and can be largely explained by the Khuff fauna from Oman (see Section 7.4.2.1).

8.5.1.2 END-GUADALUPIAN CRISIS

Genus diversity shows an overall decline (Figure 8.1), to which the Cladodontomorphi are the major contributors, although their decline was gradual and had already begun at the end of the Cisuralian (Figure 8.2, Figure 8.3). A minor decline is also observed in the Neoselachii and Holocephali, whereas all other groups show no change (Figure 8.3), despite identical extinction and survival levels between the Holocephali and Eugeneodontiformes (Figure 8.4). Standing diversity also began to decline more

steeply (Figure 8.5A), as a result of the increasing extinction rate (Figure 8.5B) and a decline in the number of boundary crossers (Figure 8.1B). This decline involved all groups, except for the Hybodontiformes and Neoselachii (Figure 8.6, Figure 8.7). The decline in genus richness primarily resulted from losses amongst the marine and euryhaline components (Figure 8.9), affecting the benthic and littoral marine groups (Figure 8.12). Crushing and clutching dentitions were particularly affected (Figure 8.14). Distributional patterns show that eastern Panthalassa lost most of its diversity across the Capitanian/Wuchiapingian boundary, whereas Neotethys and also the Boreal Sea and central and western Panthalassa gained (Figure 8.28A).

8.5.1.3 Late Permian mass extinction

Genus diversity declined steeply throughout the Lopingian. The decline had begun in the Wordian and intensified in the Changhsingian (Figure 8.1A) following an increase in extinction rate (Figure 8.5B). The decline continued into the Dienerian at a somewhat reduced rate (Figure 8.1B). Standing diversity shows a similar pattern to absolute genus richness, but suggests that the declining trend was apparent from the earliest Permian and gradually gained in intensity (Figure 8.5A), which is a pattern reflected in the number of boundary crossing taxa (Figure 8.1B).

Different chondrichthyan groups were far from equally affected by the Late Permian extinction, with the Hybodontiformes and Neoselachii surviving the event without showing any decline in genus richness and standing diversity (Figure 8.3, Figure 8.7). The Holocephali and Xenacanthimorpha started to decline earlier in the Permian and continued their decline over the course of the Lopingian. Although both groups survived into the Triassic, the holocephalans record an elevated extinction rate in the Wuchiapingian and Changhsingian (Figure 8.8B). The Cladodontomophi became (temporarily?) extinct without any steep decline, whereas the previously stable diversity of the Petalodontiformes started to decline in the Wuchiapingian (Figure 8.3, Figure 8.7; see also Figure 8.4). Hence, the petalodonts did not cross the Permian/Triassic

boundary, following the highest extinction rate of any group at the time (Figure 8.8B). The Eugeneodontiformes continued into the Early Triassic, following a minor decline during the Lopingian (Figure 8.3, Figure 8.7).

Further selectivity is evidenced by most of the diversity decline being explained by the marine component (Figure 8.9). All ecomorphotypes were in decline at the time of the mass extinction, with bathic types disappearing entirely (Figure 8.12), which may be attributed to deep water anoxia. Freshwater and littoral marine taxa showed a relatively gradual decrease, and pelagic and benthic genera respectively showed an abrupt and intensified reduction in the Changhsingian (Figure 8.12). Crushing, cutting and clutching dentitions followed similar trends, but the largest decline is apparent among those employing crushing dentitions (all holocephalans and many petalodonts; Figure 8.14). A significant size decrease is recorded across the Permian/Triassic boundary in two of the three tooth dimensions at epoch-level for all genera (Figure 8.16; Table 8.3), as well as a significant decrease in body length at period-level (Figure 8.17; Table 8.4), but this decrease is not significant at any level for those genera that continue into the Triassic (Figure 8.18; Table 8.5). This suggests the selective loss of large-sized chondrichthyans as a result of the Late Permian mass extinction, but it negates the suggestion of a decrease in size as an adaptation for survival, unless this occurred on a much shorter time scale.

The distribution of genus richness throughout the Wuchiapingian–Griesbachian interval shows a decrease in all basins/regions, except for an increase in the Boreal Sea across the Permian/Triassic boundary (Figure 8.28A). The palaeolatitudinal distribution throughout the same interval suggests that the tropical regions primarily experienced diversity loss (Figure 8.31B). Instead, chondrichthyans were best represented in regions at higher (northern) palaeolatitudes at this time (Figure 8.30A).

8.5.1.4 EARLY TRIASSIC RADIATION AND END-SMITHIAN CRISIS

Following the Late Permian mass extinction, genus diversity continues to decline somewhat through the Induan, with the first increase apparent in the Smithian, followed by a brief stabilisation in the Spathian (Figure 8.1A). EMSD already increases again briefly in the Dienerian, but then also declines through to the Spathian (Figure 8.5A). This Spathian stagnation interrupts an increase that peaks in the Anisian–Ladinian, which suggests that it may be linked to the end-Smithian crisis. Both turnover and diversification rates peaked in the Griesbachian (Figure 8.5A), resulting from extremely high origination rates (Figure 8.5B). Origination and extinction dropped to zero in the Dienerian (Figure 8.5B), which may be partly related to the incompleteness of the fossil record (see Section 7.3.3.2), and the extinction rate rose again in the Smithian (Figure 8.5B), providing further evidence for a possible crisis at the end of this stage.

The Boreal Sea was of primary importance in the Induan, with other dispersion centres in the Neotethys and central and western Panthalassa (Figure 8.27). Eastern Panthalassa rapidly regained high diversity in the Smithian, synchronous with a decline in diversity in the Boreal Sea (Figure 8.27, Figure 8.28B). The Eugeneodontiformes were primarily responsible for the Smithian diversity high in eastern Panthalassa (Figure 8.24), but the Hybodontiformes and Neoselachii also re-appeared (Figure 8.22, Figure 8.23) and remained in the area after the eugeneodontiforms rapidly went extinct across the Smithian/Spathian boundary (Figure 8.3, Figure 8.7). Because the extinction peak at this time is entirely explained by the disappearance of the Eugeneodontiformes (Figure 8.8B), they are identified as the sole victims of the end-Smithian crisis. The Hybodontiformes were the primary contributors to the Early Triassic diversification (Figure 8.8A). They were spread across a number of regions, especially in the Boreal Sea during the Griesbachian (Figure 8.22), which resulted in a sudden increase in their standing diversity in the Dienerian (Figure 8.7).

The marine component remained at the greatest level of diversity through the Griesbachian–Smithian (Figure 8.9) and the same is true for benthic and pelagic communities (Figure 8.12), whereas crushing, grinding, cutting and clutching dentitions

all show relatively similar richness (Figure 8.14). Tooth size generally remained low throughout the Early Triassic, but shows a somewhat increased mean in the Smithian (Figure 8.16), which is not significant (Table 8.3) but may be related to the temporary prominence of the eugeneodontiforms.

8.5.1.5 MIDDLE–UPPER TRIASSIC RADIATION

The Ladinian and the Carnian record the highest genus diversity and EMSD of the Triassic, respectively, following a rapid increase across the Spathian/Anisian boundary (Figure 8.1B, Figure 8.5A) and high origination rates in the Anisian (Figure 8.5B). The Neoselachii display an enhanced origination rate through the Spathian–Ladinian (Figure 8.8A), making them primarily responsible for the genus diversity peak (Figure 8.3), whereas the Hybodontiformes show a later increase in origination rate (Figure 8.8A). Distribution of genus richness indicates that this radiation primarily took place in the Palaeotethys and in central Panthalassa (Figure 8.27; Figure 8.28B), whereas diversity decreased in all other areas (Figure 8.28B).

In the Anisian, increased genus diversity is recorded in the marine realm, but also in freshwater environments (Figure 8.9), the latter of which is driven by an elevated origination rate among the Xenacanthimorpha (Figure 8.8A). A minor radiation took place among freshwater ecomorphotypes and, because benthic radiation was delayed until the Ladinian, the majority of the Anisian radiation took place among littoral marine ecomorphotypes (Figure 8.12). Hence, taxa employing crushing and clutching dentitions displayed a significant radiation of similar magnitude (Figure 8.14). An increase in tooth and body size is also detected (Figure 8.16–Figure 8.18), which is significant among various dental aspects on both (sub)stage and epoch-level across the Lower/Middle Triassic boundary and within the Middle Triassic (Table 8.3, Table 8.5), but is not significant for body length (Table 8.4).

8.5.2 New insights into diversity patterns

A number of publications over recent decades have included estimates of fish and chondrichthyan diversity, based on the most recent compilations of the time. Early studies, such as Thomson (1977), based on data compiled in Romer (1966) and Harland *et al.* (1967), noted that there was little evidence for a Late Permian extinction among fishes in general. This view has been reiterated in subsequent studies (e.g., Hallam and Wignall 1997; Benton 1998; Friedman and Sallan 2012), based on more recent compilations (Benton 1993, including Cappetta *et al.* 1993; Sepkoski 2002). The fish record, or vertebrate record as a whole has, however, long been considered poor and inadequate (Thomson 1977; Benton 1998). Individual studies of chondrichthyan diversity dynamics have traditionally shown a decline from maximum diversity in the Carboniferous, and that diversity halved over the course of the Permian, reaching a minimum in the Early Triassic (Pitrat 1973; Thomson 1977; Benton 1998). This pattern is confirmed by the data presented here (Figure 8.1A, Figure 8.5A). General disagreement has focused on the reality of accelerated decline in the Late Permian and a radiation of fish families in the earliest Triassic. The latter has previously been attributed to a preservational bias (Twitchett 2001b), but this bias is shown to be inaccurate (see Section 7.4.1). High turnover rate at this time was suggested by Sepkoski's (2002) data (see Friedman and Sallan 2012) and this is confirmed, as is an enhanced diversification rate (Figure 8.5A), the effects of which can be detected on genus level (Figure 8.5A) but not family level (Figure 7.12).

The question of accelerated decline is more complex. It should be stressed that the continuation of chondrichthyans relied on a relatively small number of groups that persisted unaffected (although only temporarily in one case), whereas a large number of Palaeozoic groups disappeared either gradually or abruptly (Figure 8.32). It has been suggested that patterns of extinction may be much more rapid than can be observed from the fossil record, based on the notion of backsmearing of extinctions by incomplete sampling and, therefore, the high probability of offsets between extinction and last appearance of one or more stages (Foote 2007). The nature of the Late

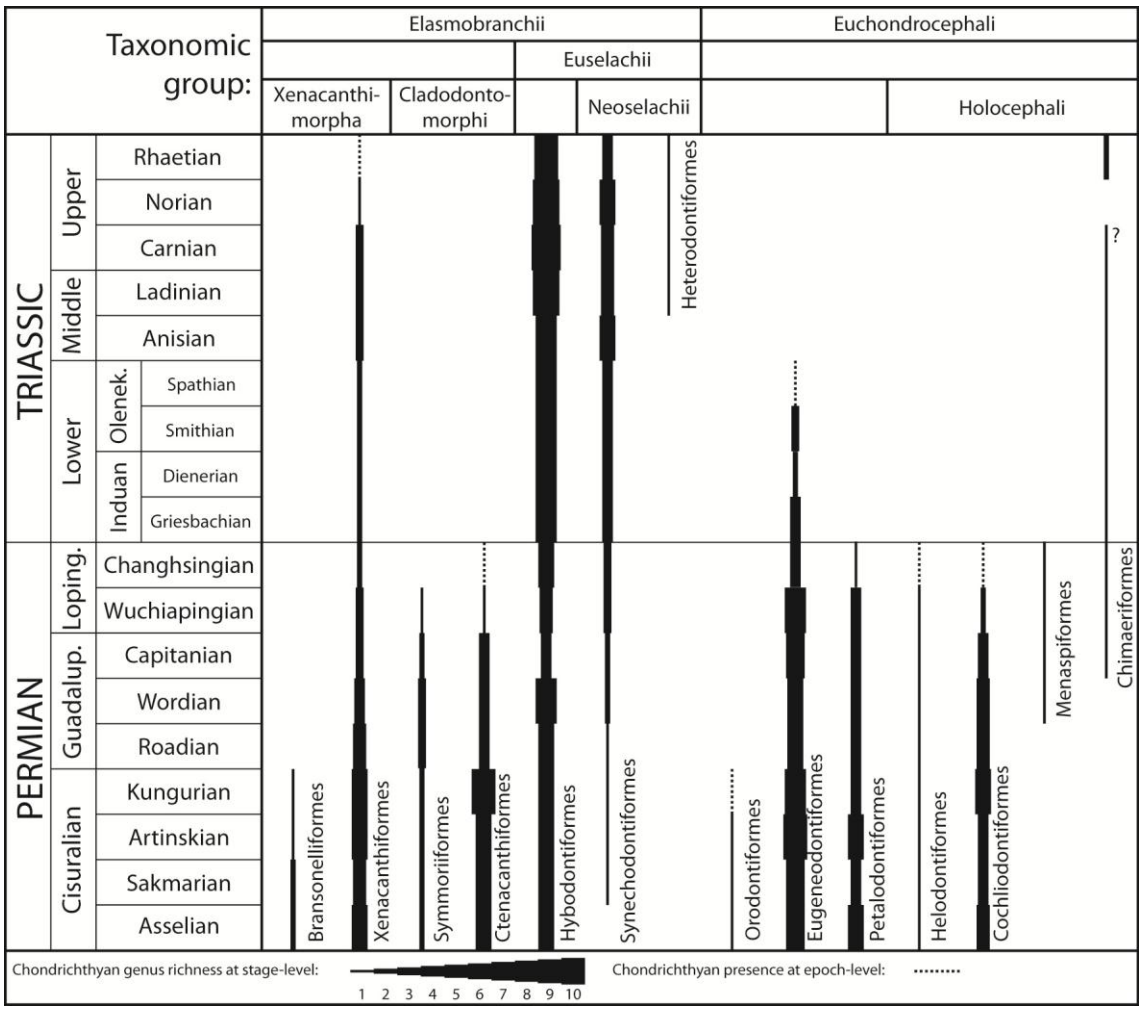

Figure 8.32 – Stratigraphy showing genus richness based on named genera per defined order for the Permian–Triassic. The Phoebodontiformes? are not included due to the absence of named genera. Pre-Rhaetian presence of the Chimaeriformes in the Permian and Triassic is uncertain (based on tentative assignment of *Arctacanthus*).

Permian fossil record has been deemed particularly poor, characterised by an exceedingly high number of Lazarus taxa (Twitchett 2007b) and completeness of the fossil record (using the SCM) was shown to decline dramatically at the end-Guadalupian and the P/Tr boundary (Twitchett 2001a). Some evidence exists of poor sampling close to the Permian/Triassic boundary (few occurrences; Figure 7.8) and completeness of the Permian fossil record is generally lower compared to the Triassic (Figure 7.11B), but completeness estimates close to the boundary are largely unaffected. Also, a poor fossil record is expected to affect all taxa in similar ways, but

the extinction or survival patterns observed among chondrichthyan groups display very different trends.

Further selectivity has been noted among adaptations to environmental factors and other life-history traits. Marine selectivity of the Late Permian mass extinction among chondrichthyans was advocated by Pitrat (1973) and this hypothesis is currently still considered to be accurate (Friedman and Sallan 2012). Similarly, a selective loss of durophagous lineages is believed to have occurred (Friedman and Sallan 2012). This study confirms that the majority of the chondrichthyan diversity decline is explained by the marine component and shows that euryhaline taxa were largely unaffected. However, the extinction is actually shown to be independent of salinity tolerance (Figure 8.10) and, therefore, does not support the notion of selective loss. This study further confirms that benthic taxa suffered the largest number of losses (Figure 8.13A), as did those employing crushing dentitions (Figure 8.15A), but demonstrates that pelagic lineages were also affected (Figure 8.13A). The evidence supports the views of Hallam and Wignall (1997), who thought the apparent immunity of pelagic taxa to be unlikely. However, extinction is also shown to be independent of ecomorphotype and feeding habit (Figure 8.13A; Figure 8.15A), disproving selective loss of durophagous lineages. Finally, the data indicate that the largest losses among the ecological groups highlighted above commenced in the mid-Guadalupian, but intensified from the Wuchiapingian onwards and continued into the Griesbachian (Figure 8.9, Figure 8.12, Figure 8.14), thus confirming that the majority of the decline occurred during the Late Permian mass extinction, which was a question left open by Friedman and Sallan (2012). Similar questions with regard to extinction intensity and selectivity among chondrichthyans as discussed here are also being assessed by others, but using a different analytical approach (Clayton *et al.* 2008; Ciampaglio *et al.* 2009; Clayton and Ciampaglio 2011), which may independently confirm the trends observed here.

8.5.3 PALAEOECOLOGICAL AND PALAEOENVIRONMENTAL LINKS

8.5.3.1 PREDATOR-PREY RELATIONSHIPS

Chondrichthyans fed on a wide variety of food sources ranging from plankton and invertebrates to large marine animals (Compagno 1990), as evidenced by dental morphology and analyses of gut contents, coprolites, or trace fossils (e.g., bite marks; see Kowalewski 2002). A durophagous diet could consist of benthic organisms such as bivalves, gastropods and other molluscs, as well as crustaceans, brachiopods and echinoderms such as crinoids (Stahl 1999; Brett and Walker 2002). Other food sources comprised fish and pelagic invertebrate prey, such as swimming crustaceans, cephalopods (e.g., ammonoids and nautiloids) and conodont animals (see Blieck *et al.* 2010), and also chondrichthyans (cannibalism as well as scavenging; Hansen and Mapes 1990; Soler-Gijón 1995; Brett and Walker 2002). The Late Permian mass extinction caused devastation among major marine groups, including those that formed part of the chondrichthyan diet, causing Hallam and Wignall (1997) to stress the low probability that chondrichthyans survived without their supporting invertebrate food chain. Comparison of events in the chondrichthyan community in relation to the Late Permian mass extinction with those in other marine groups, especially those outlined above, enables the identification of putative palaeoecological links.

Pitrat (1973) noted the similarity between the diversity patterns of marine chondrichthyans and invertebrates and Compagno (1990) further stated that chondrichthyans have tracked diversity fluctuations in other marine and freshwater organisms throughout their existence. This may indicate predator dependence on prey evolution and abundance or also the effects of vertebrate predation on the evolution of invertebrates (see Sallan *et al.* 2011). Due to the limited available evidence, however, trophic relationships and predator identity are notoriously difficult to infer from the fossil record, which leads to frequent dismissal of the role of predation in macroevolution in favour of competition and abiotic factors (Sallan *et al.* 2011). Also, the general vertebrate model suggests that postcranial morphological divergence, based on habitat

preference, precedes cranial (dental) morphological change based on trophic adaptations (Streelman and Danley 2003; Sallan and Friedman 2012). This may cause a delayed view of chondrichthyan radiation following the Late Permian mass extinction, because the Early Triassic record is predominantly based on isolated teeth. However, this model has recently been challenged on the basis of actinopterygian morphological diversification (Sallan and Friedman 2012).

8.5.3.2 PERMIAN EXTINCTION EVENTS AND FAUNAL SELECTIVITY

Yamagishi (2006) suggested the existence of a palaeoecological link between chondrichthyans and benthic fauna, based on evidence from trace fossils, proposing the dependence of the timing and distribution of the Triassic chondrichthyan radiation on marine invertebrate recovery. However, no specific links to the benthic fauna have yet been proposed with regard to the Permian chondrichthyan diversity decline and extinction.

Invertebrate groups responded in different ways to Late Permian environmental changes. This varies between largely unresponsive and being severely reduced in diversity, which often lead to extinction (e.g., Twitchett 2007b). A typical pattern is one of gradual decline through the Permian, particularly during the latter half, which was then followed by the disappearance of the last remaining taxa in the Changhsingian (Twitchett 2007b). High levels of extinction occurred among Palaeozoic marine communities dominated by epifaunal suspension feeders, such as articulate brachiopods, crinoids, blastoids, tabulate and rugose corals, and stenolaemate bryozoans, whereas modern shallow marine clades such as bivalve and gastropod molluscs, arthropods, and nautiloid cephalopods fared much better (Erwin *et al.* 2002). Even so, significant extinction selectivity has been identified even within these broad groups (Erwin *et al.* 2002).

Dramatic losses in diversity are recorded during the end-Guadalupian crisis (Twitchett 2007b). Erwin *et al.* (2002) describe how blastoid echinoderms went extinct,

as well as most tabulate and rugose corals, the last of which disappeared in the Changhsingian, whereas crinoids and fusulinids marginally survived. Tethyan benthic groups such as corals, fusulinids, and bryozoans, underwent a significant decline and dominant elements of brachiopod faunas disappeared, but diversity remained essentially the same among ammonoids and conodonts despite some turnover, and non-fusulinid foraminifera, bivalves, and gastropods failed to display any distinctive changes (Erwin *et al.* 2002).

Twitchett (2007b) suggested that this 'event' was largely due to sea level fall across the southern USA (Texas) at the end of the Guadalupian and was not a true extinction. This specific facies change is not recognised here in the chondrichthyan fossil record, but a gradual decline in occurrences from this region is observed through the Artinskian–Changhsingian (Figure 7.10A) synchronous with a decline in genus richness (Figure 8.27; Appendix A2.4.18). Furthermore, it is now considered to be a discrete and global episode (Erwin *et al.* 2002; see also Isozaki *et al.* 2007a, b, 2011; Wignall *et al.* 2012).

Suggested causes for the extinction patterns described above include longer-term Permian changes in the marine realm, such as a rise in global temperature and/or a decrease in atmospheric oxygen levels (see Twitchett 2007b), with particular importance assigned to extreme global warming, driving organisms with low oxygen-limited thermal tolerance, such as vertebrates, to vacate the palaeotropics (Sun *et al.* 2012). Physiological selectivity has thus been identified as the main driving factor behind survivorship through both the end-Guadalupian crisis and Late Permian mass extinction, causing them to be classed as similar events of different magnitude (Knoll *et al.* 2007; Clapham and Payne 2011; Payne and Clapham 2012).

Selective loss among marine invertebrates combined with the differential impact of abiotic factors on specific habitats are likely to have driven differential chondrichthyan diversity decline and extinction and have affected their distribution. The trends in marine invertebrates described here match the gradual rise in chondrichthyan extinction rate from the early Permian, becoming increasingly intense from the mid-

Guadalupian onwards, which is a pattern reflected in standing diversity and the number of taxa crossing stage boundaries, and which is predominantly explained by the marine component. In terms of specific ecomorphotypes, the gradual decrease in freshwater and littoral marine taxa may be related to increasing oceanic temperature, whereas the abrupt and intensified Changhsingian reduction of the benthic and pelagic (and bathic) types may be explained by reduced oxygen levels and ultimately the onset of deep and shallow water marine anoxia.

8.5.3.3 EXTINCTION AND RECOVERY AMONG MAJOR MARINE BENTHIC GROUPS

In South China and other areas globally, benthic groups such as brachiopods, gastropods and bivalves show drastic extinction in the late Changhsingian, with prolonged low diversity through the Griesbachian–Smithian and a slow rate of recovery in the Spathian, followed by a positive shift from the start of the Anisian (Chen and Benton 2012; Sun *et al.* 2012; see also Wheeley and Twitchett 2005; Twitchett 2007b). Bivalves also showed great diversity loss during the end-Smithian crisis (see Sun *et al.* 2012). Abrupt size-selective extinction at the species level and within-lineage anagenetic size change occurred among gastropods across the Permian/Triassic boundary and Early Triassic individuals remained unusually small afterwards (Payne 2005). These microgastropods behaved as repopulation-interval opportunists (Fraiser and Bottjer 2004) and have been shown to recover relatively quickly in the early Griesbachian Neotethys in the regional absence of benthic anoxia (Wheeley and Twitchett 2005). The distribution of microgastropod-dominated shell-beds indicates that the recovery patterns were regionally variable with proliferation in low palaeolatitudes but absence in the Boreal Sea (Fraiser *et al.* 2005). The microgastropod biofacies had largely disappeared by the Spathian (Fraiser *et al.* 2005), with larger individuals gradually returning in the Middle Triassic (Payne 2005).

Selective extinction during the Late Permian event affected echinoderms, with some evidence of preferential survival of deposit-feeders (Twitchett and Oji 2005). High

levels of diversity in the Early Triassic, recorded from very shallow, oxygenated, low palaeolatitude environments, remain uncertain due to potential bias in the fossil record and taxonomic problems, which means that the earliest radiation of some echinoderm groups is currently known to have occurred in latest Spathian and Anisian, whereas other groups did not recover significantly until later in the Triassic (Twitchett and Oji 2005).

8.5.3.4 EXTINCTION AND RECOVERY AMONG MAJOR MARINE PELAGIC GROUPS

Ammonoids showed a slight diversity increase from the end-Carboniferous onward, culminating in the Guadalupian, but subsequently experienced two successive phases of severe extinction (end-Guadalupian and late Changhsingian), with a minor increase during the intermediate Wuchiapingian (Brayard *et al.* 2009b). By taxonomic measures, ammonoid recovery is considered rapid with evidence suggesting early diversification in the late Changhsingian (McGowan and Smith 2007) and pre-extinction levels regained by the Dienerian (McGowan 2005) or the Smithian coincident with the emergence of a latitudinal gradient (Brayard *et al.* 2009b). The end-Smithian crisis subsequently caused a renewed decline (see Sun *et al.* 2012). Morphological recovery showed a slower rate more akin to the revival of other marine invertebrate fauna during the Spathian–Anisian and in a globally synchronous manner (McGowan 2004, 2005).

Orchard (2007) showed that conodonts displayed a gradual diversity decline through the Changhsingian–late Griesbachian with extinction near the Permian/Triassic boundary and in the late Griesbachian. His findings further suggest an initial diversification phase during the Dienerian with a subsequent marked radiation in the early–middle Smithian, followed by a major extinction in the late Smithian. Significant renewed radiation in the early Spathian may have preceded the general recovery of marine benthic groups and was followed by gradual turnover and decline in the late Spathian–early Anisian (Orchard 2007; see also Sun *et al.* 2012).

8.5.3.5 TIMING AND REGIONAL VARIABILITY OF RECOVERY PATTERNS

Mass extinctions cause an apparent collapse of ecospace that requires rebuilding during recovery (Erwin 2001). Indeed, palaeoecological indicators suggest that benthic shallow marine communities were restructured during the Early Triassic, with decoupled taxonomic and ecologic recovery from the Late Permian mass extinction, which was furthermore geographically varied and asynchronous (Fraiser and Bottjer 2005). Widespread bottom water anoxia/dysoxia occurred in marine settings throughout the P/Tr boundary interval, following a rapid onset in the latest Permian (Wignall and Twitchett 2002a) as a result of weakened ocean circulation due to persistent global warming (see Sano *et al.* 2012). The oxygen minimum zone, therefore, at times extended into shallow environments and the photic zone (Grice *et al.* 2005). The immediate response following the Late Permian mass extinction is typical of any such event, with low-diversity assemblages dominated by widespread, eurytopic species, but a unique long-term recovery response is associated with the Late Permian event (Erwin 1998). The best documented Early Triassic recovery faunas from low palaeolatitudes (western USA and Europe) were affected by marine anoxia in the immediate aftermath and show a lack of recovery throughout the Griesbachian (Recovery stage 1; Twitchett *et al.* 2004). In the absence of anoxia, however, as was the case for the duration of the Griesbachian in shallow marine environments throughout Neotethys (Wignall and Twitchett 2002a; Twitchett *et al.* 2004), recovery was much faster and allowed the establishment of benthic communities typical of Recovery stage 3 and with a level of ecological complexity (comprising bivalves, gastropods, articulate brachiopods, crinoids, echinoids and ostracods) that was not recorded in eastern Panthalassa or western Palaeotethys until the Spathian (Twitchett *et al.* 2004).

It has been shown that the re-establishment of tiering above and below the substrate provides a measure of post-extinction biotic recovery (Twitchett 1999; Zonneveld 2011). Benthic oxygen restrictions were lifted in the late Induan, allowing deeper burrowing suspension feeders to re-appear, and subsequently also burrowing crustaceans

(*Thalassinoides*; Twitchett and Barras 2004; Twitchett 2007b). However, whereas small trace fossils of this kind already appear in the late Induan in the Boreal Sea, they are still only rarely observed in low (tropical) palaeolatitudes in the Spathian, suggesting a slower rate of recovery in the latter regions (Twitchett and Barras 2004; Twitchett 2007b). Early Induan benthic communities are thus characteristically low diversity assemblages of small-sized animals, comprising bivalves, inarticulate brachiopods and rare microgastropods (Twitchett 2007b), which may be considered pioneering opportunists (e.g., Fraiser and Bottjer 2004). Fairly diverse Induan communities consisting of small-sized nekton of fish and ammonoids have been recorded from mid- to high palaeolatitude regions (Boreal Sea and Neotethys; Twitchett 2007b), again indicating a much faster ecological recovery rate in these areas.

The presence of diverse and locally abundant Griesbachian trace fossil assemblages in high palaeolatitudes, which record the activities of a wide variety of marine invertebrates (including *Thalassinoides*), are interpreted to have been of vital importance in survival and post-extinction recolonisation (Zonneveld *et al.* 2010). Nevertheless, an unexpectedly diverse and complex ichnofauna of late Griesbachian age was recently discovered in western Palaeotethys (tropical shelf sediments; including *Thalassinoides*), which is similar in diversity to those known from the Boreal Realm (Hofmann *et al.* 2011). It suggests that recovery of trace fossil producers was not necessarily latitudinally restricted and that advanced recovery stages were reached much earlier than the Spathian, but in order to explain the overall delay of benthic recovery until the Spathian, it implies a succession of global ecological crises in post-Griesbachian times (Hofmann *et al.* 2011).

Advanced recovery of marine ecosystems, subsequent to re-establishment of benthic invertebrates, occurred in a palaeogeographically asynchronous manner, starting in the Boreal Sea and Neotethys in the Induan, and showing signs of recovery at lower palaeolatitudes (eastern Panthalassa and western Palaeotethys) in the Spathian–Anisian. This is a pattern also reflected in the chondrichthyan fossil record. Based on the patterns of recovery of well-preserved shallow marine Early Triassic

faunas (see Twitchett *et al.* 2004) and chondrichthyan distribution patterns (Figure 8.28A, B), the establishment of diverse chondrichthyan communities corresponds to recovery stages in the following manner: stage 2 in eastern Panthalassa; stage 4 in western Palaeotethys; and stage 3 in western Neotethys. This suggests that, on average, the recovery of a relatively diverse invertebrate fauna with higher tier organisms (crinoids) and infaunal crustaceans was required to sustain sharks and their relatives, but it is also likely that these conditions needed to persist for a period of time to allow higher tiers of the food web to establish, which would explain the prolonged absence of chondrichthyans from the western Palaeotethys. In central Panthalassa, photic zone oceanic anoxia occurred at the end of the Permian (Sano *et al.* 2012), which is considered to be the trigger of extinction among radiolarians (Kiessling and Danelian 2011; Sano *et al.* 2012). In this location, anoxia persisted into the Induan but relaxed episodically, allowing radiolarian recovery blooms, which implies that central Panthalassa was characterised by more hospitable conditions compared to the Tethyan oceans and Pangean marginal seas (Sano *et al.* 2012). This may explain the moderate diversification of chondrichthyans in this area in the Griesbachian (Figure 8.28A).

Sun *et al.* (2012) observed the general absence of fish from equatorial regions, especially during the late Griesbachian and Smithian, despite being more common at higher latitudes, which they attribute to their relatively low oxygen-limited thermal tolerance in relation to elevated oceanic temperatures. They state that a decrease in tolerance is likely to occur in larger sized organisms and juveniles, promoting a fossil record dominated by small individuals in the worst affected areas. The most evident link is between the Late Smithian Thermal Maximum (LSTM) and the end-Smithian crisis, causing major decline among, e.g., bivalves, conodonts and ammonoids (Sun *et al.* 2012 and references therein). The estimated temperature curve and the diversity patterns of the pelagic component throughout the Changhsingian–Smithian illustrate a potentially close link with large-sized pelagic fish such as the Eugeneodontiformes, the only holdover group among the chondrichthyans. Eugeneodontiforms suffered through

the Changsingian–Dienerian and across the Smithian/Spathian boundary, synchronous with significant temperature increase and thermal maxima, as well as extinction among conodonts and ammonoids (see Sun *et al.* 2012, fig. 3; Stanley 2009). The link further explains the selective loss of larger taxa that is observed across the Permian/Triassic boundary (see Section 8.5.1.3).

The above discussion outlines that, in summary, recovery patterns in chondrichthyans most closely match those observed in the benthic realm, which is likely to be partly due to the sheer size of the chondrichthyan benthic community that it supports relative to other ecomorphotypes. Nevertheless, a close relationship is also observed between extinction and recovery patterns in pelagic chondrichthyan (holdover) taxa and other pelagic animals. These patterns illustrate that chondrichthyans behaved like other marine groups and suffered great losses of large-sized pelagic and benthic indivuals, whereas those living in shallower environments (littoral marine and freshwater) fared better. However, significantly selective loss is only recorded during the end-Smithian crisis in terms of taxonomic structure and ecomorphotype, despite a strong correlation between extinction and taxonomic structure across the Wuchiapingian/Changhsingian boundary. Chondrichthyan distribution in the extinction aftermath largely tracked recovery in marine benthic invertebrates in both time and space, which initially took place primarily in higher palaeolatitudes. Ultimately, it is the Hybodontiformes, Neoselachii, Xenacanthiformes and Holocephali that survived, which possessed a varying combination of characteristics such as moderate body-size, adaptation to brackish/freshwater environments, benthic or generalist littoral (clutching) feeding behaviour, and a wide palaeogeographic range. Whether these properties specifically applied to the Holocephali during the Permian/Triassic boundary interval, however, is currently more an assumption than knowledge taken from the fossil record, because so few holocephalans are known from around this time.

9 CONCLUSIONS

The overall aim of this project was to understand the extinction, survivorship and diversification of Chondrichthyes through the Late Permian mass extinction event. This has been achieved by following the objectives formulated in Section 1.1.1, which are individually discussed in the following.

Current knowledge of Permian–Triassic chondrichthyans has been presented in a newly compiled database (Appendix A2.1). It has been constructed using the most current collective works on chondrichthyan fossil material available (Stahl 1999; Ginter *et al.* 2010; Cappetta 2012), supported by older and more general reference works and online databases (Zangerl 1981; Cappetta 1987; Yamagishi 2006; the Paleobiology Database; the Bibliography of Fossil Vertebrates Online; Shark-References). In addition, more detailed information has been extracted from over 270 individual peer-reviewed publications. Previous diversity analyses were primarily based on compilations that are now superceded by new data (including Cappetta *et al.* 1993; Sepkoski 2002). The new database contains all currently valid taxa and is supplemented by newly discovered material described in this study. Hence, this study attempts to be the most up-to-date and comprehensive analysis of patterns and trends in chondrichthyan diversity and distribution that is currently available.

The chondrichthyan fossil record has been augmented by newly discovered material obtained through fieldwork on Permian–Triassic sections in Oman, Japan and East Greenland, as well as specimens from pre-existing (but undescribed) collections from Oman, Iran, India, Timor, China, Spitsbergen, western Canada and the southwestern USA (Chapters 3–5). New genera and species have been described from the Permian and Triassic of Oman (Appendix A3.2), which is a country from which previously only few brief mentions of chondrichthyan-yielding strata existed, but is here shown to hold

abundant and diverse assemblages, which have been described in detail. Furthermore, genera have newly been recorded from regions in which they were not previously known to occur (e.g., *Adamantina* from the Canadian Arctic; Section 5.4.2).

A detailed summary of the neoselachian lineage has been compiled, including current advances on the evolutionary development of enameloid microstructural features in chondrichthyan teeth (Chapter 6). The presence of primitive neoselachians in the Permian has been strengthened based on the recovery of anachronistid remains from the Wordian of Oman (Chapter 3) and synechodontiform material from the Wuchiapingian of Iran (Chapter 4). Furthermore, microstructural study of neoselachian specimens from the Olenekian of Oman supports the step-by-step acquisition of triple-layered enameloid and the gradual development of parallel bundled enameloid, as proposed by Andreev and Cuny (2012). This study provides an extensive record of the Early Triassic early development of bundled enameloid microstructure and demonstrates developmental progression of individual bundle crystallites into elongated crystalline bundles, combined with increased compaction and order of bundle organisation by the Olenekian for the first time. It further provides indirect evidence in support of the initiation of crystallite bundling during the (late) Palaeozoic.

A comprehensive phylogeny of Permian and Triassic chondrichthyan genera has been compiled based on published cladograms of large-scale relationships and of individual groups (Chapter 7). This informal supertree has been constructed in the traditional manner of taxonomic substitution using hierarchically nested source trees comprising primarily unique taxa. In the absence of a cladistic hypothesis for specific groups, source trees have been constructed based on their internal systematic relationships, assuming monophyly. The presented hypothetical phylogeny is based entirely on morphological characteristics but the generation of a complete supertree from comprehensive cladistic analysis has not yet been possible as the result of a number of difficulties, including unstable relationships within, and between, early groups as well

as the observed mixture of hybodontiform and neoselachian characteristics in numerous late Palaeozoic and early Mesozoic taxa. This cannot be resolved until more articulated remains are recovered from the Permian–Triassic that aid to improve our understanding of phylogenetic relationships.

Assessment of the completeness of the Permian–Triassic chondrichthyan fossil record has shown that fossil genus diversity significantly correlates with taxonomic occurrence counts but that this correlation is absent in range-through data, which suggests that it is an unbiased representation of diversity with regard to occurrence data (Chapter 7). The Roadian fossil record is characterised by very low levels of completeness, accompanied by a significant drop in taxonomic occurrences. Furthermore, the Dienerian is shown to be a particularly poorly sampled interval and/or preservation may have been reduced. The Wordian fossil record stands out for its high completeness, but a large proportion of the peak in taxonomic occurrences and observed fossil ranges is the result of the contribution by the Khuff fauna from Oman. The completeness of the Lopingian fossil record is average for the Permian and fairly stable, whereas completeness of the Anisian fossil record is extremely good. Overall, the data presented here show a weak and non-significant trend of better sampling in younger strata (increasing number of known occurrences), but they do suggest that sampling becomes more exhaustive through the Permian–Triassic (fewer Lazarus occurrences) and that our understanding of interrelationships among more recent genera is better (positive completeness trend).

Reconstruction of the taxonomic diversity of chondrichthyans through the Permian–Triassic has shown that genus diversity started to decline from the Wordian following an increasing extinction rate and both intensified in tandem throughout the Lopingian (Chapter 8). Standing diversity suggests that the declining trend was apparent from the earliest Permian and gained in intensity in the Capitanian, which is reflected in the number of boundary crossing taxa. These data support a combined overall extinction

as a result of the end-Guadalupian and Late Permian extinction events. Extinction has further been shown to be strongly (but not significantly) correlated with taxonomic structure across the Wuchiapingian/Changhsingian boundary, at which time also phylogenetic diversity estimates suggest a significant drop in diversity. The Hybodontiformes and Neoselachii survived the events without being affected in terms of genus richness or standing diversity. The Holocephali and Xenacanthimorpha started to decline earlier in the Permian and continued their decline over the course of the Lopingian. Both groups survived into the Triassic, but holocephalans record an elevated extinction rate in the Lopingian. The Cladodontomorphi gradually became (temporarily?) extinct, whereas diversity of the Petalodontiformes was stable until their sudden decline in the Changhsingian, suffering the highest extinction rate of any group at the time, which resulted in their extinction. The Eugeneodontiformes held over into the Early Triassic, following a minor decline over the second half of the Lopingian. Strongly significant extinction selectivity has been shown across the Smithian/Spathian boundary, with extinction observed solely among the Eugeneodontiformes, which subsequently disappeared entirely.

Evidence has been presented suggesting a change in global distribution of chondrichthyan diversity as a result of the Permian extinction and the contemporary environmental changes. All basins suffered overall diversity loss, except for the Boreal Sea, which gained across both the Capitanian/Wuchiapingian and Permian/Triassic boundaries. The palaeolatitudinal distribution suggests that the tropical regions primarily experienced diversity loss through the Capitanian–Dienerian. Furthermore, chondrichthyans were best represented in regions at higher northern palaeolatitudes or on the southern hemisphere at this time.

An assessment of chondrichthyan palaeoecology and mode of life has shown that the largest number of extinct genera has been identified among marine groups at the time of the Permian (mass) extinctions (Chapter 8). All ecomorphotypes declined, with benthic and pelagic groups losing the largest number of genera and respectively

showing an intensified and abrupt reduction in the Changhsingian. In terms of feeding habit, those employing crushing dentitions suffered the largest diversity loss. However, no significant selectivity for any of these palaeoecological traits has been demonstrated, suggesting proportionate losses, except for a significantly selective loss of pelagic taxa as a result of the end-Smithian crisis. A significant size decrease is recorded across the Permian/Triassic boundary in two of the three tooth dimensions at epoch-level for all genera, as well as a significant decrease in body length at period-level, but this decrease is not significant at any level for those genera that continue into the Triassic, which show a significant size increase across the Early/Middle Triassic boundary instead. This suggests the selective loss of large-sized chondrichthyans as a result of the Late Permian mass extinction and negates the suggestion of a decrease in size as an adaptation for survival, unless this occurred on a much shorter time scale.

Ultimately, it has been shown that chondrichthyan distribution in the extinction aftermath largely tracked recovery in marine benthic invertebrates in both time and space, which initially took place primarily in higher palaeolatitudes. The Hybodontiformes, Neoselachii, Xenacanthiformes and Holocephali are the surviving groups, which possessed a varying combination of characteristics such as moderate body-size, adaptation to brackish/freshwater environments, benthic or generalist littoral (clutching) feeding behaviour, and a wide palaeogeographic range. Whether these properties specifically applied to the Holocephali during the Permian/Triassic boundary interval, however, is currently more an assumption than knowledge taken from the fossil record, because so few holocephalans are known from around this time.

APPENDIX 1 COLLECTION AND SAMPLE DATA

A1.1. SAMPLE DATABASE (STARTS NEXT PAGE)

Sample entries are provided in batches of three pages, providing data on sampling location, lithostratigraphy, biostratigraphy, as well as processing and curation. Any shading is explained in the last batch of entries.

All terms are as they appear in published literature and as used here in text, figures and collection listings for the relevant samples.

Bold entries in conodont biostratigraphy are directly relevant to the official names of conodont zones. All taxonomic names are as they appear in the relevant publications.

Sample	Location	Section	GPS coordinates	Lithostratigraphy	Age (provisional)	Height (m)	Lithology (field)
GSC collection - Oman							
c-177651 84 TE 103A-1	Jabel Safra (150km SW of Muscat), Oman	Block 103, Block 3 (Tozer & Calon, 1990)	UTM EA 839125 (GSC locality C-177651)	Oman Exotics, Hawasina Allochthonous (in Guwayza Fm)	Spathian	0.35m below topographic top	3.5m thick, 2-5m wide, mottled red and grey well-stratified limestone olistolith
c-177652 84 TE 103A-2	Jabel Safra (150km SW of Muscat), Oman	Block 103, Block 3 (Tozer & Calon, 1990)	UTM EA 839125 (GSC locality C-177652)	Oman Exotics, Hawasina Allochthonous (in Guwayza Fm)	Spathian	0.35m below topographic top	3.5m thick, 2-5m wide, mottled red and grey well-stratified limestone olistolith
c-177673 84 TE 103B	Jabel Safra (150km SW of Muscat), Oman	Block 103, Block 3 (Tozer & Calon, 1990)	UTM EA 839125 (GSC locality C-177673)	Oman Exotics, Hawasina Allochthonous (in Guwayza Fm)	Spathian	~1.5m below topographic top	3.5m thick, 2-5m wide, mottled red and grey well-stratified limestone olistolith
c-177674 84 TE 103C	Jabel Safra (150km SW of Muscat), Oman	Block 103, Block 3 (Tozer & Calon, 1990)	UTM EA 839125 (GSC locality C-177674)	Oman Exotics, Hawasina Allochthonous (in Guwayza Fm)	Spathian	topographic base	3.5m thick, 2-5m wide, mottled red and grey well-stratified limestone olistolith
c-177653 84 TE 104A	Jabel Safra (150km SW of Muscat), Oman	Block 104, Block 1 (Tozer & Calon, 1990)	UTM EA 807127 (GSC locality C-177653)	Oman Exotics, Hawasina Allochthonous (in Guwayza Fm)	Spathian	0.30m above topographic base	1.0m thick, 2m wide olistolith
c-177654 84 TE 104 B/C	Jabel Safra (150km SW of Muscat), Oman	Block 104, Block 1 (Tozer & Calon, 1990)	UTM EA 807127 (GSC locality C-177654)	Oman Exotics, Hawasina Allochthonous (in Guwayza Fm)	Spathian	within 0.10m of topographic top	1.0m thick, 2m wide olistolith
c-117658 84 TE 117A-1	Wadi Alwa (50km south of Muscat), Oman			Alwa Fm, Oman Exotics, Hawasina Allochthonous	Smithian (early)		Hallstatt-type talus block
c-117659 84 TE 117A-2	Wadi Alwa (50km south of Muscat), Oman	probably same as 117A-1		Alwa Fm, Oman Exotics, Hawasina Allochthonous	Smithian (early)		Hallstatt-type talus block
o-177663 84 TE c.85314	Jabel Safra (150km SW of Muscat), Oman	Ammonoid block, Calon & Lee, collection British Museum	GSC locality C-177663	Oman Exotics, Hawasina Allochthonous (in Guwayza Fm)	Spathian		limestone block
c-202251 91OF-TE-118B	Wadi Alwa (50km south of Muscat), Oman	Wadi Alwa I, Bed 2 (Tozer & Calon, 1990)		Alwa Fm, Oman Exotics, Hawasina Allochthonous	Spathian		Hallstatt-type limestone
92 OF WA 22	Wadi Alwa, Oman			Alwa Fm, Oman Exotics, Hawasina Allochthonous	Spathian		Hallstatt-type talus block?
GSC collection - global							
c-302286 95-OF GU-1	Guling, Spiti, Himalaya, India			Tamba Kurkur Fm, Tethyan Himalaya	Griesbachian		
30/09/2003	Timor				Anisian–Norian?		condensed/mixed Hallstatt-type limestone
88 OF CHXD-5	China	Meishan		upper Changhsing Fm	Changhsingian		
05 OF O-3	Nanpanjiang basin, Guizhou Province, China	Lower Guandao, Great Bank of Guizhou		Luolou Fm	Olenekian (Spathian, upper)	233.7m (from base)	skeletal packstone with pelagic lime mudstone interbeds; bed thickness: 1-20 cm
05 OF O-6	Nanpanjiang basin, Guizhou Province, China	Lower Guandao, Great Bank of Guizhou		Luolou Fm	Olenekian (Spathian, upper)	235.0m (from base)	skeletal packstone with pelagic lime mudstone interbeds; bed thickness: 1-20 cm

Lithology (lab)	Facies	Checked Lithology / Facies	Biostratigraphy (provisional)	Conod. present	Conodont biostratigraphy	Ammonoid biostratigraphy	Remarks
			II - Procolumbites beds (N-Am. amm.)		*Necspathodus abruptus* , *Ns. symmetricus* , *Ns. homeri* , *Ns. brochus*		Orchard 1995
			II - Procolumbites beds (N-Am. amm.)		*Necspathodus abruptus* , *Ns. symmetricus* , *Ns. homeri* , *Ns. brochus*		Orchard 1995
			III - Prohungarites / subcolombites beds (N-Am. amm.)		*Necspathodus abruptus* , *Ns. symmetricus* , *Ns. homeri* , *Ns. brochus* , *Ns. curtatus*		Orchard 1995
			III - Prohungarites / subcolombites beds (N-Am. amm.)		*Necspathodus abruptus* , *Ns. symmetricus* , *Ns. brochus* , *Ns. triangularis*		Orchard 1995
			I - Columbites beds (N-Am. amm.)		*Ichicspathodus collinsoni* , *Necspathodus crassatus* , *Ns. brevissimus* , *Ns. pusillus* , *Ns. abruptus* , *Ns. symmetricus* , *Ns. homeri*		Orchard 1995
			I - Columbites beds (N-Am. amm.)		*Ichicspathodus collinsoni* , *Necspathodus crassatus* , *Ns. brevissimus* , *Ns. pusillus* , *Ns. abruptus* , *Ns. symmetricus* , *Ns. homeri*		Orchard 1995
			III - Prohungarites / subcolombites beds (N-Am. amm.)		*Necspathodus abruptus* , *Ns. symmetricus* , *Ns. homeri* , *Ns. brochus* , *Ns. curtatus* , *Ns. triangularis*		Orchard 1995
			II - Procolumbites beds (N-Am. amm.)		*Necspathodus abruptus* , *Ns. symmetricus* , *Ns. homeri*		Orchard 1995
					Conodont content similar to 103A		
					Hindeodus typicalis , *H. praeparvus* , ***H. parvus*** , *H.* sp. indet., *Necgondolella carinata* , ***N. meishanensis*** , *N. nassichuki* , *N. orchardi* , *N. planata* , *N. taylorae* δβ , *N. tulongensis* δγ , *N. zhejiangensis*	*Otoceras woodwardi* / *O. boreale* (Him. amm.), *O. boreale* (Arc. amm.)	Orchard & Krystyn, 1998
							Orchard *et al.* 2004
	deeper marine proximal slope to a carbonate platform				*Necspathodus triangularis* , *Triassospathodus* ex. gr. *homeri* , New genus A		Orchard *et al.* 2007
	deeper marine proximal slope to a carbonate platform				*Cornudina* sp., *Necspathodus spathi* , *Triassospathodus brochus*		Orchard *et al.* 2007

Processing technique	Total weight (g)	Saved weight (g)	Diss. weight (g)	Status	Notes	Productive	All residue	>500 µm	500–250 µm	250–125 µm	<125 µm	<63 µm	Specimen numbers
													1–35
													36–45
													46–60
													61–132
													133–226
													227–239
													240–245
													246
													247–257
													258–269
													270–274
													450
													451–454
													362
													363
													364–365

05 OF O-10	Nanpanjiang basin, Guizhou Province, China	Lower Guandao, Great Bank of Guizhou		Luolou Fm	Olenekian (Spathian, upper)	237.0m (from base)	skeletal packstone with pelagic lime mudstone interbeds; bed thickness: 1-20 cm
05 OF O-11	Nanpanjiang basin, Guizhou Province, China	Lower Guandao, Great Bank of Guizhou		Luolou Fm	Olenekian (Spathian, upper)	237.5m (from base)	skeletal packstone with pelagic lime mudstone interbeds; bed thickness: 1-20 cm
05 OF O-12	Nanpanjiang basin, Guizhou Province, China	Lower Guandao, Great Bank of Guizhou		Luolou Fm	Olenekian (Spathian, upper)	238.0m (from base)	skeletal packstone with pelagic lime mudstone interbeds; bed thickness: 1-20 cm
05 OF O-13	Nanpanjiang basin, Guizhou Province, China	Lower Guandao, Great Bank of Guizhou		Luolou Fm	Olenekian (Spathian, upper)	238.9m (from base)	skeletal packstone with pelagic lime mudstone interbeds; bed thickness: 1-20 cm
05 OF O-14	Nanpanjiang basin, Guizhou Province, China	Lower Guandao, Great Bank of Guizhou		Luolou Fm	Olenekian (Spathian, upper)	239.4m (from base)	skeletal packstone with pelagic lime mudstone interbeds; bed thickness: 1-20 cm
05 OF O-15	Nanpanjiang basin, Guizhou Province, China	Lower Guandao, Great Bank of Guizhou		Luolou Fm	Olenekian (Spathian, upper)	239.9m (from base)	skeletal packstone with pelagic lime mudstone interbeds; bed thickness: 1-20 cm
05 OF O-16	Nanpanjiang basin, Guizhou Province, China	Lower Guandao, Great Bank of Guizhou		Luolou Fm	Olenekian (Spathian, upper)	240.2m (from base)	skeletal packstone with pelagic lime mudstone interbeds; bed thickness: 1-20 cm
05 OF O-18	Nanpanjiang basin, Guizhou Province, China	Lower Guandao, Great Bank of Guizhou		Luolou Fm	Olenekian (Spathian, upper)	240.35m (from base)	skeletal packstone with pelagic lime mudstone interbeds; bed thickness: 1-20 cm
05 OF O-19	Nanpanjiang basin, Guizhou Province, China	Lower Guandao, Great Bank of Guizhou		Luolou Fm	Olenekian (Spathian, upper)	240.45m (from base)	skeletal packstone with pelagic lime mudstone interbeds; bed thickness: 1-20 cm
05 OF O-21	Nanpanjiang basin, Guizhou Province, China	Lower Guandao, Great Bank of Guizhou		Luolou Fm	Olenekian (Spathian, upper)	240.7m (from base)	skeletal packstone with pelagic lime mudstone interbeds; bed thickness: 1-20 cm
05 OF O-22	Nanpanjiang basin, Guizhou Province, China	Lower Guandao, Great Bank of Guizhou		Luolou Fm	Olenekian (Spathian, upper)	240.75m (from base)	skeletal packstone with pelagic lime mudstone interbeds; bed thickness: 1-20 cm
05 OF O-23	Nanpanjiang basin, Guizhou Province, China	Lower Guandao, Great Bank of Guizhou		Luolou Fm	Olenekian (Spathian, upper)	240.8m (from base)	skeletal packstone with pelagic lime mudstone interbeds; bed thickness: 1-20 cm
05 OF O-24	Nanpanjiang basin, Guizhou Province, China	Lower Guandao, Great Bank of Guizhou		Luolou Fm	Olenekian (Spathian, upper)	240.9m (from base)	skeletal packstone with pelagic lime mudstone interbeds; bed thickness: 1-20 cm

	deeper marine proximal slope to a carbonate platform				*Triassospathodus* ex. gr. *homeri*, New genus A		Orchard *et al.* 2007
	deeper marine proximal slope to a carbonate platform				*Cornudina* sp., *Cratognathus* sp. A, *Gladigondolella carinata*, *Triassospathodus* ex. gr. *homeri*, New genus A		Orchard *et al.* 2007
	deeper marine proximal slope to a carbonate platform				*Cratognathus* sp. A, *Gladigondolella carinata*, *Triassospathodus* ex. gr. *homeri*		Orchard *et al.* 2007
	deeper marine proximal slope to a carbonate platform				*Cornudina* sp., *Cratognathus* sp. A, *Cratognathus* sp. B, *Necspathodus spathi*, *Triassospathodus* ex. gr. *homeri*, New genus A		Orchard *et al.* 2007
	deeper marine proximal slope to a carbonate platform				*Cratognathus* sp. A, *Necspathodus triangularis*, *Ns. spathi*, *Triassospathodus brochus*, *Tr.* ex. gr. *homeri*, New genus A		Orchard *et al.* 2007
	deeper marine proximal slope to a carbonate platform				*Chiosella gondolelloides*, *Ch. timorensis*, *Cratognathus* sp. A, *Cratognathus* sp. B, *Gladigondolella carinata*, *Necspathodus spathi*, *Triassospathodus* ex. gr. *homeri*		Orchard *et al.* 2007
	deeper marine proximal slope to a carbonate platform				*Chiosella gondolelloides*, *Cratognathus* sp. A, *Gladigondolella carinata*, *Necspathodus spathi*, *Triassospathodus* ex. gr. *homeri*		Orchard *et al.* 2007
	deeper marine proximal slope to a carbonate platform				*Chiosella timorensis*, *Cratognathus* sp. A, *Cratognathus* sp. B, *Necspathodus spathi*, *Triassospathodus* ex. gr. *homeri*		Orchard *et al.* 2007
	deeper marine proximal slope to a carbonate platform				*Chiosella timorensis*, *Cratognathus* sp. A, *Cratognathus* sp. B, *Necspathodus spathi*, *Triassospathodus* ex. gr. *homeri*		Orchard *et al.* 2007
	deeper marine proximal slope to a carbonate platform				*Chiosella gondolelloides*, *Ch. timorensis*, *Cratognathus* sp. A, *Cratognathus* sp. B, *Gladigondolella carinata*, *Necspathodus spathi*, *Triassospathodus* ex. gr. *homeri*, New genus A		Orchard *et al.* 2007
	deeper marine proximal slope to a carbonate platform				*Chiosella gondolelloides*, *Ch. timorensis*, *Cratognathus* sp. A, *Cratognathus* sp. B, *Gladigondolella carinata*, *Triassospathodus* ex. gr. *homeri*, New genus A		Orchard *et al.* 2007
	deeper marine proximal slope to a carbonate platform				*Chiosella gondolelloides*, *Cratognathus* sp. A, *Cratognathus* sp. B, *Gladigondolella carinata*, *Necspathodus spathi*, *Triassospathodus* ex. gr. *homeri*, New genus A		Orchard *et al.* 2007
	deeper marine proximal slope to a carbonate platform				*Chiosella gondolelloides*, *Cratognathus* sp. A, *Gladigondolella carinata*, *Triassospathodus* ex. gr. *homeri*, New genus A		Orchard *et al.* 2007

													366–368
													369–371
													372
													373–374
													375–378
													379–384
													385–386
													387
													388
													389–390
													391–392
													393–394
													395–396

05 OF O-25	Nanpanjiang basin, Guizhou Province, China	Lower Guandao, Great Bank of Guizhou		Luolou Fm	Olenekian (Spathian, upper)	241.2m (from base)	skeletal packstone with pelagic lime mudstone interbeds; bed thickness: 1-20 cm
05 OF O-26	Nanpanjiang basin, Guizhou Province, China	Lower Guandao, Great Bank of Guizhou		Luolou Fm	Olenekian (Spathian, upper)	241.25m (from base)	skeletal packstone with pelagic lime mudstone interbeds; bed thickness: 1-20 cm
05 OF O-27	Nanpanjiang basin, Guizhou Province, China	Lower Guandao, Great Bank of Guizhou		Luolou Fm	Olenekian (Spathian, upper)	241.45m (from base)	skeletal packstone with pelagic lime mudstone interbeds; bed thickness: 1-20 cm
05 OF O-28	Nanpanjiang basin, Guizhou Province, China	Lower Guandao, Great Bank of Guizhou		Luolou Fm	Olenekian (Spathian, upper)	241.55m (from base)	skeletal packstone with pelagic lime mudstone interbeds; bed thickness: 1-20 cm
05 OF O-29	Nanpanjiang basin, Guizhou Province, China	Lower Guandao, Great Bank of Guizhou		Luolou Fm	Olenekian (Spathian, upper)	241.7m (from base)	skeletal packstone with pelagic lime mudstone interbeds; bed thickness: 1-20 cm
05 OF O-31	Nanpanjiang basin, Guizhou Province, China	Lower Guandao, Great Bank of Guizhou		Luolou Fm	Olenekian (Spathian, upper)	241.8m (from base)	skeletal packstone with pelagic lime mudstone interbeds; bed thickness: 1-20 cm
05 OF O-34	Nanpanjiang basin, Guizhou Province, China	Lower Guandao, Great Bank of Guizhou		Luolou Fm	Olenekian (Spathian, upper)	242.2m (from base)	skeletal packstone with pelagic lime mudstone interbeds; bed thickness: 1-20 cm
05 OF O-36	Nanpanjiang basin, Guizhou Province, China	Lower Guandao, Great Bank of Guizhou		Luolou Fm	Olenekian (Spathian, upper)	242.35m (from base)	skeletal packstone with pelagic lime mudstone interbeds; bed thickness: 1-20 cm
05 OF O-38	Nanpanjiang basin, Guizhou Province, China	Lower Guandao, Great Bank of Guizhou		Luolou Fm	Olenekian (Spathian, upper)	242.65m (from base)	skeletal packstone with pelagic lime mudstone interbeds; bed thickness: 1-20 cm
05 OF O-40	Nanpanjiang basin, Guizhou Province, China	Lower Guandao, Great Bank of Guizhou		Luolou Fm	Olenekian (Spathian, upper)	242.9m (from base)	skeletal packstone with pelagic lime mudstone interbeds; bed thickness: 1-20 cm
05 OF O-41	Nanpanjiang basin, Guizhou Province, China	Lower Guandao, Great Bank of Guizhou		Xinyuan Fm	Anisian, lowermost	243.5m (from base)	skeletal packstone with pelagic lime mudstone interbeds; bed thickness: 1-20 cm
GQC-173	Nanpanjiang basin, Guizhou Province, China	Lower Guandao, Great Bank of Guizhou		Xinyuan Fm	Anisian		
GQC-182	Nanpanjiang basin, Guizhou Province, China	Lower Guandao, Great Bank of Guizhou		Xinyuan Fm	Anisian		
GQC 183B	Nanpanjiang basin, Guizhou Province, China	Lower Guandao, Great Bank of Guizhou		Xinyuan Fm	Anisian		

	deeper marine proximal slope to a carbonate platform				*Chicsella gondolellcides* , *Cratognathus* sp. A, *Gladigondolella carinata* , *Triassospathodus* ex. gr. *homeri* , New genus A		Orchard *et al* 2007
	deeper marine proximal slope to a carbonate platform				*Chicsella gondolellcides* , *Cratognathus* sp. A, *Triassospathodus* ex. gr. *homeri*		Orchard *et al* 2007
	deeper marine proximal slope to a carbonate platform				*Cratognathus* sp. A, *Cratognathus* sp. B, *Gladigondolella carinata* , *Triassospathodus* ex. gr. *homeri*		Orchard *et al* 2007
	deeper marine proximal slope to a carbonate platform				*Cratognathus* sp. A, *Cratognathus* sp. B, *Gladigondolella carinata* , *Necspathodus spathi* , *Triassospathodus* ex. gr. *homeri* , New genus A		Orchard *et al* 2007
	deeper marine proximal slope to a carbonate platform				*Cratognathus* sp. A, *Cratognathus* sp. B, *Necspathodus spathi* , *Triassospathodus* ex. gr. *homeri*		Orchard *et al* 2007
	deeper marine proximal slope to a carbonate platform				*Cratognathus* sp. A, *Cratognathus* sp. B, *Necspathodus spathi* , *Triassospathodus* ex. gr. *homeri*		Orchard *et al* 2007
	deeper marine proximal slope to a carbonate platform				*Cratognathus* sp. A, *Gladigondolella carinata* , *Necspathodus spathi* , *Triassospathodus* ex. gr. *homeri*		Orchard *et al* 2007
	deeper marine proximal slope to a carbonate platform				*Cratognathus* sp. A, *Gladigondolella carinata* , *Necspathodus spathi* , *Triassospathodus* ex. gr. *homeri*		Orchard *et al* 2007
	deeper marine proximal slope to a carbonate platform				*Cratognathus* sp. A, *Gladigondolella carinata* , *Necspathodus spathi* , *Triassospathodus* ex. gr. *homeri*		Orchard *et al* 2007
	deeper marine proximal slope to a carbonate platform				*Chicsella gondolellcides* , *Ch.* n. sp. A, *Cratognathus* sp. A, *Gladigondolella carinata* , *Necspathodus spathi* , *Triassospathodus* ex. gr. *homeri*		Orchard *et al* 2007
	deeper marine proximal slope to a carbonate platform				*Chicsella gondolellcides* , *Ch. timorensis* , *Cratognathus* sp. A, *Cratognathus* sp. B, *Gladigondolella tethydis* , *Triassospathodus* ex. gr. *homeri*		Orchard *et al* 2007
	deeper marine proximal slope to a carbonate platform						
	deeper marine proximal slope to a carbonate platform						
	deeper marine proximal slope to a carbonate platform						

													397–398
													399–400
													401–402
													403–404
													405–407
													408–410
													411–412
													413–417
													418
													419–423
													424
													425
													426–432
													433

GQC 184	Nanpanjiang basin, Guizhou Province, China	Lower Guandao, Great Bank of Guizhou		Xinyuan Fm	Anisian		
c-306527 GDL-1	Nanpanjiang basin, Guizhou Province, China	Lower Guandao, Great Bank of Guizhou		Wujiaping Fm	Changhsingian	-7 m	cherty skeletal lime packstone
c-306561 GDL-55	Nanpanjiang basin, Guizhou Province, China	Lower Guandao, Great Bank of Guizhou		Xinyuan Fm	Anisian, lower	256 m	allodapic lime grainstone/packstone
c-306563 GDL-57	Nanpanjiang basin, Guizhou Province, China	Lower Guandao, Great Bank of Guizhou		Xinyuan Fm	Anisian, lower	261 m	allodapic lime grainstone/packstone
9307 TE-72-119A	Kuh-e-Ali Bashi, NW Iran			Ali Bashi Fm	Changhsingian		
c-306362 02 OF KZK 10	Zal?, NW Iran			Ali Bashi Fm?	Wuchiapingian, late?		
c-306363 02 OF KZK 34G	Zal?, NW Iran			Ali Bashi Fm?	Changhsingian, late		
c-306365 02 OF KZM 21	Zal?, NW Iran			Ali Bashi Fm?	Wuchiapingian, late		
c-307115 04-OF MH-DA-34	Vendomdalen, central Spitsbergen	Dalsnuten		Tschermakfjellet Fm–De Geerdalen Fm (incl. Isfjorden Mb)	Carnian		
c-303560 97 OF WAP-T33	Cirque C, Ganoid Ridge, Wapiti Lake, Kakwa area, BC, Canada			Vega Mb, Sulphur Mountain Fm	Smithian	talus blocks	coarsening upward, with interlaminated silty shale and siltstone at the base grading upwards to interlaminated siltstone and very fine-grained sandstone
o-51663 93 OF TE-5 1663 62-TE 325A (strigatus)	Otto Fiord South, Ellesmere Island, Canadian Arctic			Confederation Point Mb, Blind Fiord Fm	Griesbachian (upper)	80m above base	
c-301214 93 OF W-1	Crittenden Springs, Nevada, USA			Thaynes Fm	Smithian		
c-301221 93 OF W-8	Bear Lake, SE Idaho, USA	Georgetown		Thaynes Fm	Smithian		
c-301224 93 OF W-11	Bear Lake, SE Idaho, USA	Paris Canyon		Thaynes Fm	Spathian		
c-301226 93 OF W-13	Bear Lake, SE Idaho, USA	Hot Springs		Thaynes Fm	Spathian		
c-301227 93 OF W-14	Salt Lake City, Utah, USA			Thaynes Fm	Smithian		
c-202664 92-OF DC10	Darwin Canyon, Inyo Mountains, California, USA			Union Wash Formation	Spathian, early		
o-64675 91-OF	Bear Lake, SE Idaho, USA	Hammond Creek		Thaynes Fm	Spathian		
o-64671 91-OF	Bear Lake, SE Idaho, USA	Hammond Creek		Thaynes Fm	Spathian		
o-64670 91-OF TE 30 3A	Bear Lake, SE Idaho, USA	Hammond Creek		Thaynes Fm	Spathian		
c-176319 (potentially incorrect)	Nevada, USA				Spathian		

	deeper marine proximal slope to a carbonate platform						
	shallow marine proximal slope to a carbonate platform						Lehrmann *et al.* 2005
	deeper marine proximal slope to a carbonate platform						Lehrmann *et al.* 2005
	deeper marine proximal slope to a carbonate platform						Lehrmann *et al.* 2005
					Neogondolella n. sp. A	*Paratirolites* beds	Orchard *et al.* 1994
							Hounslow *et al.* 2007
	heterolithic siltstone and shale-prone facies				*Conservatella conservativa* , *Novispathodus waageni* s. l.		Orchard & Zonneveld 2009
					Borinella megacuspa , *Merrillina peculiaris* , *M.* sp. nov., *Neogondolella carinata* , *Ng. griesbachensis* , *Ng. krystyni* , *Ng. nevadensis* , *Ng. planata* , *Necspathodus cristagalli* , *Ns. dieneri*	*Strigatus* Zone: *Bukkenites strigatus* (Arc. amm.)	Orchard 2008
					Scythogondolella lachrymiformis	*Romunduri* Zone: *Euflemingites romunduri*	Orchard & Zonneveld 2009
					Scythogondolella mosheri ? *Sc. milleri*	*Tardus* zone: *Anawasatchites tardus*	Orchard & Zonneveld 2009
						Columbites beds	
						Columbites beds	
					Scythogondolella mosheri ? *Sc. milleri*	*Tardus* zone: *Anawasatchites tardus*	Orchard & Zonneveld 2009
						Prohungarites beds	
						Procolumbites beds	
						Procolumbites beds	
						Haugi Zone	

													434
													435–442
													443
													444
													N/A
													275–283
													284–285
													286–291
													449
													448
													445–447
													339–341
													337–338
													292–294
													297
													342–348
													298–304
													305–324
													325–328
													329
													335

c-201552 91 OF HB110	Humboldt Range, Pershing County, Nevada, USA			lower member of Prida Fm, Star Peak Grp	Spathian, late		
c-159815 89 OF HB236	south of Bloody Canyon, Humboldt Range, Pershing County, Nevada, USA			lower member of Prida Fm, Star Peak Grp	Spathian		carbonate unit
c-300257 92 OF COY 4	Coyote Canyon, Humboldt Range, Pershing County, Nevada, USA			Fossil Hill Mb, Prida Fm, Star Peak Grp	Anisian, early		
c-306809 02 OF CP-C1-BASE	Cowboy Pass, Confusion Range, Millard County, Utah, USA			Thaynes Fm	Spathian		
c-304703 99-IG CNA-AHC-24	Bear Lake, SE Idaho, USA	Hammond Creek	N 42° 15.51 W 111° 14.52	Thaynes Fm	Spathian		
c-304708 99-IG CNA-HS 4	Bear Lake, SE Idaho, USA	Hot Springs	N 42° 07.42 W 111° 14.52	Thaynes Fm	Spathian		
UC collection - Oman							
621-2	Rustaq, Oman		23 24°40.68"N 57 24°34.19"E	Rustaq Fm			
965-1	Haushi-Huqf area, Oman	Khuff 6-7	UTM 568599 2323415	Khuff Fm	Wordian	4.5	
965-2	Haushi-Huqf area, Oman	Khuff 6-7	UTM 568599 2323415	Khuff Fm	Wordian	6	
965-3	Haushi-Huqf area, Oman	Khuff 6-2	UTM 561110 2308294	Khuff Fm	Wordian	1.5	
965-4	Haushi-Huqf area, Oman	Khuff 6-7	UTM 568599 2323415	Khuff Fm	Wordian	25.1	
965-5	Haushi-Huqf area, Oman	Khuff 6-7	UTM 568599 2323415	Khuff Fm	Wordian	19.5-20	
965-6	Haushi-Huqf area, Oman	Khuff 6-2	UTM 561110 2308294	Khuff Fm	Wordian	50.1	
965-7	Haushi-Huqf area, Oman	Khuff 6-2	UTM 561110 2308294	Khuff Fm	Wordian	108	
965-8	Haushi-Huqf area, Oman	Khuff 6-3	UTM 560665 2308682	Khuff Fm	Wordian	4.5	
965-9	Haushi-Huqf area, Oman	Khuff 6-2	UTM 561110 2308294	Khuff Fm	Wordian	3	
965-10	Haushi-Huqf area, Oman	Khuff 6-2	UTM 561110 2308294	Khuff Fm	Wordian	3.3	

						Haugi Zone	
					Necospathodus ex gr. *homeri*	*Yatesi* beds, upper *Haugi* Zone	Orchard 1994
							Bucher 1992 (for lithostratigraphy only)
						? *Columbites* beds	
						Subcolumbites beds	
						Tenuicolumbites beds	
							height indication may be horizontal distance from base
							height indication may be horizontal distance from base
							height indication may be horizontal distance from base
							height indication may be horizontal distance from base
							height indication may be horizontal distance from base
							height indication may be horizontal distance from base
							height indication may be horizontal distance from base
							height indication may be horizontal distance from base
							height indication may be horizontal distance from base
							height indication may be horizontal distance from base

													336
													330–334
													352–359
													360–361
													349
													350–351
						yes							474
						yes							475
						yes							476-498, 499-562, 563-581
						yes							582-583, 584-585
						yes							586-589, 590
						yes							641-643
						no							
						no							
						yes							591-596, 597-606
						yes							607-626
						no							

965-11	Haushi-Huqf area, Oman	Khuff 6-7	UTM 568599 2323415	Khuff Fm	Wordian	5.7	
965-12	Haushi-Huqf area, Oman			Saiwan Fm	Sakmarian		
969-1	Saiq Plateau, Oman		23 04°30"N 57 39°45"E	lower Saiq Fm, Akhdar Grp	Wordian	0.5	
969-2	Saiq Plateau, Oman		23 04°30"N 57 39°45"E	lower Saiq Fm, Akhdar Grp	Wordian	5	
969-3	Saiq Plateau, Oman		23 04°30"N 57 39°45"E	lower Saiq Fm, Akhdar Grp	Wordian	18.5	
969-4	Saiq Plateau, Oman		23 04°30"N 57 39°45"E	lower Saiq Fm, Akhdar Grp	Wordian	18.7	Brachiopod rich
969-5	Saiq Plateau, Oman		23 04°30"N 57 39°45"E	lower Saiq Fm, Akhdar Grp	Wordian	19.7	
969-6	Saiq Plateau, Oman		23 04°30"N 57 39°45"E	lower Saiq Fm, Akhdar Grp	Wordian	22.7	Calc sponge, Tabulates, Ikaite?
969-12	Saiq Plateau, Oman		23 04°30"N 57 39°45"E	lower Saiq Fm, Akhdar Grp	Wordian	40	with ikaite
UC collection - Canadian Arctic							
CH-F36-79 HP	Hamilton Peninsula, Ellesmere Island, Canadian Arctic		80° 3'11"N 81°45'42"W	Trold Fiord Fm	Wordian		Glauconitic & fossiliferous sandstone
CH-F78-79 HP-Aa coarse	Hamilton Peninsula, Ellesmere Island, Canadian Arctic		80° 3'11"N 81°45'42"W	Assistance Fm	Roadian		Brachiopod-rich sandstone
CH-F79-79 HP MSc samples	Hamilton Peninsula, Ellesmere Island, Canadian Arctic		80° 3'11"N 81°45'42"W	Assistance Fm	Roadian		Brachiopod-rich sandstone
CH-F104-79 MB	McKinley Bay, Ellesmere Island, Canadian Arctic		81°10'5"N 79°14'17"W	Trold Fiord Fm	Wordian		Glauconitic & fossiliferous sandstone
CH-F136-79 HN	Henrietta Nesmith, Ellesmere Island, Canadian Arctic		81°50'26"N 72°10'59"W	Trold Fiord Fm	Wordian		Glauconitic & fossiliferous sandstone
CH-F136-79 HN 2of2	Henrietta Nesmith, Ellesmere Island, Canadian Arctic		81°50'26"N 72°10'59"W	Trold Fiord Fm	Wordian		Glauconitic & fossiliferous sandstone
F-83	Hamilton Peninsula, Ellesmere Island, Canadian Arctic		80° 3'11"N 81°45'42"W	Trold Fiord Fm	Wordian		Glauconitic & fossiliferous sandstone
T2 Blaa	Blaa Mountain, Ellesmere Island, Canadian Arctic		80°33'19"N 86°15'21"W	Blaa Mountain Fm	Mid/Upper Triassic		Shale and siltstone
MPUM collection							
AO1	Haushi-Huqf area, Oman	Haushi K1		Khuff Fm, Member 1	Wordian	6, level 2-3 (Angiolini & Bucher 1999 - composite)	Marly limestone
AO2	Haushi-Huqf area, Oman	Haushi K1		Khuff Fm, Member 1	Wordian	6, level 3-4 (Angiolini & Bucher 1999 - composite)	Marly limestone

							height indication may be horizontal distance from base
	Mid shelf						
	Mid shelf						
	Mid shelf						
	Mid shelf						
	Mid shelf						
	Mid shelf						
	Mid shelf						
	Deep shelf						

						no							
						no							
						no							
						no							
						no							
						yes							627-631
						yes							632-640
						yes							644-647
						no							
													455
													456
													457
													458
													459–461
													462–469
													470–471
													472–473
	3-5 kg					yes	ED						AO1-0001
	3-5 kg					yes	ED						AO2-0001

AO3	Haushi-Huqf area, Oman	Haushi K1		Khuff Fm, Member 1	Wordian	7, level 5-6 (Angiolini & Bucher 1999 - composite)	Marly limestone
AO3bis	Haushi-Huqf area, Oman			Khuff Fm	Wordian		
AO6	Haushi-Huqf area, Oman	Haushi K4		Khuff Fm	Wordian	level 17-18	
AO8	Haushi-Huqf area, Oman			Khuff Fm	Wordian		
AO9	Haushi-Huqf area, Oman			Khuff Fm	Wordian		
AO10	Haushi-Huqf area, Oman			Khuff Fm	Wordian		
AO10bis	Haushi-Huqf area, Oman			Khuff Fm	Wordian		
AO11	Haushi-Huqf area, Oman			Khuff Fm	Wordian		
AO12	Haushi-Huqf area, Oman			Khuff Fm, Member 1	Wordian		
AO15	Haushi-Huqf area, Oman			Khuff Fm	Wordian		
AO16	Haushi-Huqf area, Oman			Khuff Fm	Wordian		
AO17	Haushi-Huqf area, Oman			Khuff Fm	Wordian		
AO18	Haushi-Huqf area, Oman			Khuff Fm	Wordian		
AO19	Haushi-Huqf area, Oman			Khuff Fm	Wordian		
AO22	Haushi-Huqf area, Oman	Haushi K6		Khuff Fm	Wordian		
AO23	Haushi-Huqf area, Oman	Haushi K6		Khuff Fm	Wordian		
AO24	Haushi-Huqf area, Oman	Haushi K6		Khuff Fm	Wordian		
AO25	Haushi-Huqf area, Oman	Haushi K6		Khuff Fm	Wordian		
AO26	Haushi-Huqf area, Oman	Haushi K6		Khuff Fm	Wordian		
AO32	Haushi-Huqf area, Oman	Haushi K1		Khuff Fm, Member 1	Wordian	8, level 7 (Angiolini & Bucher 1999 - composite)	Bio-intraclastic calcareous sandstone
AO33	Haushi-Huqf area, Oman	Haushi K1		Khuff Fm, Member 2	Wordian		
AO34	Haushi-Huqf area, Oman	Haushi K1		Khuff Fm, Member 2	Wordian		
AO35	Haushi-Huqf area, Oman			Khuff Fm	Wordian		
AO36	Haushi-Huqf area, Oman			Khuff Fm	Wordian		
AO37	Haushi-Huqf area, Oman			Khuff Fm	Wordian		

	3-5 kg					yes	ED, ET						AO3-0001
	3-5 kg					yes	ET						AO3bis-0001
	3-5 kg					no							
	3-5 kg					yes	ED, ET						AO8-0001
	3-5 kg					yes	ED						AO9-0001
	3-5 kg					yes	ED, ET						AO10-0001
	3-5 kg					yes	ED, ET						AO10bis-0001
	3-5 kg					yes	ED, ET						AO11-0001
	3-5 kg					yes	ET						AO12-0001
	3-5 kg					yes	ED, ET						AO15-0001
	3-5 kg					yes	ED, ET						AO16-0001
	3-5 kg					yes	ED, ET						AO17-0001
	3-5 kg					no							
	3-5 kg					yes	ED, ET						AO19-0001
	3-5 kg					yes	ED, ET						AO22-0001
	3-5 kg					yes							
	3-5 kg					yes	ED						AO24-0001
	3-5 kg					yes	ED, ET						AO25-0001
	3-5 kg					yes	ED, ET						AO26-0001
	3-5 kg					yes	ED						AO32-0001
	3-5 kg					no							
	3-5 kg					no							
	3-5 kg					no							
	3-5 kg					yes	ED, ET						AO36-0001
	3-5 kg					yes	ED, ET						AO37-0001

AO38	Haushi-Huqf area, Oman			Khuff Fm	Wordian		
AO39	Haushi-Huqf area, Oman			Khuff Fm	Wordian		
AO40	Haushi-Huqf area, Oman	Haushi K1		Khuff Fm, Member 2	Wordian	16, level 13 (Angiolini & Bucher 1999 - composite)	Bioclastic limestone
AO41	Haushi-Huqf area, Oman			Khuff Fm, Member 2	Wordian	20, level 14 (Angiolini & Bucher 1999 - composite)	Bioclastic limestone
AO42	Haushi-Huqf area, Oman	Haushi K1		Khuff Fm, Member 3	Wordian	21-22, level 15 (Angiolini & Bucher 1999 - composite)	Bio-intraclastic calcareous sandstone
AO43	Haushi-Huqf area, Oman			Khuff Fm	Wordian		
AO44	Haushi-Huqf area, Oman			Khuff Fm	Wordian		
AO47	Haushi-Huqf area, Oman			Khuff Fm	Wordian		
AO47bis	Haushi-Huqf area, Oman	Haushi K4		Khuff Fm, Member 3	Wordian	25, level 17 (Angiolini & Bucher 1999 - composite)	Bioclastic limestone
AO48	Haushi-Huqf area, Oman			Khuff Fm	Wordian		
AO50	Haushi-Huqf area, Oman	Haushi K4		Khuff Fm, Member 3	Wordian	26, level 18 (Angiolini & Bucher 1999 - composite)	Bioclastic limestone
AO51	Haushi-Huqf area, Oman			Khuff Fm	Wordian		
AO52	Haushi-Huqf area, Oman			Khuff Fm	Wordian		
AO54	Haushi-Huqf area, Oman			Khuff Fm	Wordian		
AO55	Haushi-Huqf area, Oman	Haushi K4		Khuff Fm, Member 3	Wordian	23, level <16 (Angiolini & Bucher 1999 - composite)	Bioclastic/Marly limestone
AO56	Haushi-Huqf area, Oman	Haushi K5		Khuff Fm, Member 3	Wordian	30-31, level 25 (Angiolini & Bucher 1999 - composite)	Bioclastic limestone
AO58	Haushi-Huqf area, Oman	Haushi K5		Khuff Fm, Member 3	Wordian	33, level 27 (Angiolini & Bucher 1999 - composite)	Bioclastic limestone
AO61	Haushi-Huqf area, Oman	Haushi K3		Khuff Fm, Member 2	Wordian	12, level 11 (Angiolini & Bucher 1999 - composite)	Marly limestone

	3-5 kg					yes	ED, ET						AO38-0001 - AO38-0002
	3-5 kg					no							
	10-15 kg					yes	ED, ET, ES						
	3-5 kg					yes	ED, ET						AO41-0001
	3-5 kg					yes	ED						AO42-0001
	3-5 kg					yes	ET						AO43-0001
	3-5 kg					no							
	3-5 kg					no							
	10-15 kg					yes	ED, ET, ES						
	3-5 kg					yes	ED, ET						AO48-0001
	10-15 kg					yes	ED, ET, ES						
	3-5 kg					yes	ED, ET						AO51-0001
	3-5 kg					yes	ED, ET						AO52-0001
	3-5 kg					yes	ED, ET						AO54-0001
	10-15 kg					yes	ED, ET, ES						AO55-0018
	3-5 kg					yes	ED, ET						AO56-0001
	3-5 kg					yes	ED, ET						AO58-0001
	3-5 kg					yes	ET						AO61-0001

AO67	Haushi-Huqf area, Oman	Haushi K1		Khuff Fm, Member 2 (top)	Wordian		
AO68	Haushi-Huqf area, Oman	Haushi K1		Khuff Fm, Member 2 (top)	Wordian	21, level 14-15 (Angiolini & Bucher 1999 - composite)	Marly limestone
AO72	Haushi-Huqf area, Oman	Haushi K7	21°00'35"N 57°39'27"E	Khuff Fm, Member 3	Wordian	29.27, level 27/28? (Angiolini et al. 2003a - K7)	Bioclastic limestone
AO73	Haushi-Huqf area, Oman	Haushi K7		Khuff Fm, Member 3	Wordian		
AO76bis	Haushi-Huqf area, Oman	Haushi K7		Khuff Fm, Member 3?	Wordian		
AO77	Haushi-Huqf area, Oman	Haushi K7		Khuff Fm, Member 1	Wordian		
AO78	Haushi-Huqf area, Oman	Haushi K7	21°00'35"N 57°39'27"E	Khuff Fm, Member 1	Wordian	(Angiolini et al. 2003a - K7)	
AO79	Haushi-Huqf area, Oman	Haushi K7	21°00'35"N 57°39'27"E	Khuff Fm, Member 1	Wordian	6.18 (Angiolini et al. 2003a - K7)	Limestone
AO80	Haushi-Huqf area, Oman	Haushi K7		Khuff Fm, Member 1	Wordian		
AO82	Haushi-Huqf area, Oman	Haushi K7	21°00'35"N 57°39'27"E	Khuff Fm, Member 1	Wordian	9.36, level >8 (Angiolini et al. 2003a - K7)	Siltite, max. flooding surface
AO86	Haushi-Huqf area, Oman	Loose		Khuff Fm	Wordian		
AO87	Haushi-Huqf area, Oman	Haushi area	(probably not far from the section 7 bis -to the North) in Angiolini et al 1998	Minjur Fm	Lower Jurassic		
AOLTER	Haushi-Huqf area, Oman			Khuff Fm	Wordian		
AO123	Haushi-Huqf area, Oman	Saiwan	20°51'43"N 57°36'10"E	Khuff Fm	Wordian	0.37 (Angiolini et al. 2003a - Saiwan)	Marly limestone
AO202	Haushi-Huqf area, Oman	Jabel Gharif	19°57'01"N 57°21'38"E	top Khuff Fm	Wordian	41.86 (Angiolini et al. 2003a - Jabel Gharif)	Bioclastic limestone
AO204	Haushi-Huqf area, Oman	Jabel Gharif	19°57'01"N 57°21'38"E	top Khuff Fm	Wordian	40.32 (Angiolini et al. 2003a - Jabel Gharif)	Bioclastic limestone
AO205	Haushi-Huqf area, Oman	Jabel Gharif		top Khuff Fm	Wordian	(Angiolini et al. 2003a)	
AO206	Haushi-Huqf area, Oman	Jabel Gharif	19°57'01"N 57°21'38"E	top Khuff Fm	Wordian	40.32 (Angiolini et al. 2003a - Jabel Gharif)	Bioclastic limestone
AO208	Haushi-Huqf area, Oman	Jabel Gharif		probably middle Saiwan Fm	Sakmarian, upper Cisuralian		

	3-5 kg					yes	ED, ET						AO67-0001
	3-5 kg					yes							
	3-5 kg					yes	ET						AO72-0001
	3-5 kg					yes							
	3-5 kg					yes	ED						AO76bis-0001
	3-5 kg					yes							
	3-5 kg					yes	ED						AO78-0001
	3-5 kg					yes	ET						AO79-0001
	3-5 kg					no							
	3-5 kg					yes	ED, ET						AO82-0001
	3-5 kg					yes	ED, ET						AO86-0001
	3-5 kg					yes							AO87-0001 - AO87-0003
	3-5 kg					yes	ED, ET						AOLTER-0001
	3-5 kg					yes	ED, ET						AO123-0001 - AO123-0002
	3-5 kg					yes (see Angiolini et al. 2003a)							
	3-5 kg					yes (see Angiolini et al. 2003a)							
	3-5 kg					yes (see Angiolini et al. 2003a)							
	3-5 kg					yes (see Angiolini et al. 2003a)							
	3-5 kg					yes	ET						AO208-0001

AO210	Haushi-Huqf area, Oman	Haushi K7	21°00'35"N 57°39'27"E	Khuff Fm, Member 3	Wordian	22.18, level 16 (Angiolini et al. 2003a - K7)	Bioclastic limestone
AO211	Haushi-Huqf area, Oman	Haushi K1		Khuff Fm, Member 2	Wordian	18, level 13-14 (Angiolini & Bucher 1999 - composite)	Bioclastic limestone
AO214	Haushi-Huqf area, Oman	Saiwan		Khuff Fm, Member 1	Wordian	7, level 5-6 (Angiolini & Bucher 1999 - composite)	Marly limestone
AO215	Haushi-Huqf area, Oman	Saiwan		Khuff Fm (ex situ)	Wordian		
K7 II LEV	Haushi-Huqf area, Oman			Khuff Fm	Wordian		
Member 2	Haushi-Huqf area, Oman			Khuff Fm	Wordian	(Angiolini et al. 2003a)	
ultimo livello	Haushi-Huqf area, Oman						
OM collection							
100218-A	Wadi Alwa, Bai'd area, Oman	Section 4	N 23.16843 E 58.39202	Ba'id Fm	Wuchiapingian	-1	dolomitic packstone
100218-C	Wadi Alwa, Bai'd area, Oman	Section 4	N 23.16831 E 58.39212	Lower Mb, Alwa Fm	Dienerian	2	dolomitic wackestone
100218-E	Wadi Alwa, Bai'd area, Oman	Section 4	N 23.16845 E 58.39201	Lower Mb, Alwa Fm	Dienerian	4	dolomitic mudstone
100218-G	Wadi Alwa, Bai'd area, Oman	Section 4	N 23.16847 E 58.39197	Lower Mb, Alwa Fm	Smithian	7	wacke/packstone
100218-H	Wadi Alwa, Bai'd area, Oman	Section 4	N 23.16836 E 58.39206	Lower Mb, Alwa Fm	Smithian	9	mudstone
100218-I	Wadi Alwa, Bai'd area, Oman	Section 4	N/A	Lower Mb, Alwa Fm	Smithian	16	wacke/packstone
110222-A	Wadi Alwa, Bai'd area, Oman	Section 4	N/A	Lower Mb, Alwa Fm	Smithian	11	mudstone
110222-B	Wadi Alwa, Bai'd area, Oman	Section 4	N/A	Lower Mb, Alwa Fm	Smithian	20	mudstone
110222-C	Wadi Alwa, Bai'd area, Oman	Section 4	N/A	Lower Mb, Alwa Fm	Smithian	25	mudstone
110222-D	Wadi Alwa, Bai'd area, Oman	SE block	approx. N 23.16516 E 58.3951	Matbat Fm?	Triassic?	N/A	calcareous / siliciclastic turbidite
110222-E	Wadi Alwa, Bai'd area, Oman	Wadi	N 23.1643 E 58.39391	ex situ	Triassic?	N/A	wackestone
110222-F	Wadi Alwa, Bai'd area, Oman	Wadi	N 23.16407 E 58.39365	ex situ	Triassic?	N/A	wackestone
100219-A	Wadi Sahtan, Jabel al Akhdar, Oman		N 23.34188 E 57.31215	Saiq Fm	Changhsingian	123	dolomitic wackestone with coral/crinoids
100219-B	Wadi Sahtan, Jabel al Akhdar, Oman		N 23.34192 E 57.31217	Saiq Fm	Changhsingian	130	black bioclastic dolomite
100219-C	Wadi Sahtan, Jabel al Akhdar, Oman		N 23.33823 E 57.31032	Saiq Fm	Griesbachian	150	dolomudstone
100219-D	Wadi Sahtan, Jabel al Akhdar, Oman		N 23.33808 E 57.31124	Saiq Fm	Wuchiapingian?	+/- 30	foraminiferal-rich dolomite

	carbonate platform		-	no	-		
	pelagic		-	yes	Orchard		
	pelagic		-	no	-		
	pelagic		-	yes	Orchard		
	pelagic	pelagic lime mudstone (micrite), ammonoid	-	yes	Orchard		
	pelagic		-	yes	Orchard		
red Hallstatt, ammonoids	pelagic		-	yes	-		
red Hallstatt, ammonoids?	pelagic	pelagic lime mudstone (micrite), pink Hallstatt	-	yes	Orchard		
red Hallstatt, muddy, ammonoids?	pelagic		-	no	-		
dark red limestone, silicified?			-	N/A	-		
red Hallstatt, ammonoids	pelagic		-	yes	-		
pink limestone, many small ammonoids			-	yes	-		
	shallow marine			no	-		
	tidal flat			no	-		
	shallow marine			no	-		
	high energy shallow marine			no	-		

	3-5 kg					yes	ED, ET						AO210-0001
	3-5 kg					yes	ED, ET						AO211-0001
	3-5 kg					yes	ED, ET						AO214-0001 - AO214-0007
	3-5 kg					yes	ED, ET						AO215-0001
						yes	ES						K7 II LEV-0001
						yes (see Angiolini et al. 2003a)							
						yes	ES						ultimolivello-0001
formic	795.17	195.1	598.94	picked		no		-	-	-	(np)	N/A	-
formic	1384.9	195.06	490.56	picked		yes		GS	CN, GS	-	(np)	N/A	-
formic	1109.8	198.01	558.47	picked		yes		BF?	OS	- (pp)	(np)	N/A	OM1
formic	1341.9	219.83	465.91	picked		yes		ET?, GS, TB	CN, GS	CN	(np)	N/A	OM2–7
formic / acetic	864.51	165.04	517.82 / 180.99	picked / picked		yes / yes		ET?, TB, SF, OS	ET?, ED?, BF, CN, GS, SF, OS	CN	(np)	N/A	OM8–18
formic	1325.3	244.65	476.79	picked		yes		ET?, GS	ET?, CN	CN	(np)	N/A	OM19–20
acetic	1260	105	1155	picked		yes		-	BF, CN	(np)	(np)	N/A	-
acetic	1225	205	1020	picked		yes		ET	BF, CN	(np)	(np)	N/A	OM21–24
acetic	1340	210	1130	picked		yes		ET?	BF	(np)	(np)	N/A	OM25–26
acetic / formic	950	175	~~775~~	processing failed		no		-	N/A	N/A	N/A	N/A	-
acetic	2535	260	2275	picked		yes		CN	-	(np)	(np)	N/A	-
acetic	1880	135	1745	picked		yes		CN	CN (pp)	(np)	(np)	N/A	-
formic	1350.7	253.12	510.47	picked		yes		CR?	- (pp)	- (pp)	(np)	N/A	-
formic	989.06	133.29	578.9	picked		no		-	-	- (pp)	(np)	N/A	-
formic	786.18	108.42	686.44	picked		no		-	-	- (pp)	(np)	N/A	-
formic	1523.9	251.42	568.93	picked		no		-	-	- (pp)	(np)	N/A	-

100219-E	Wadi Sahtan, Jabel al Akhdar, Oman		N 23.34181 E 57.31462	Mahil Fm	Griesbachian	221	stromatolitic dolomite
100219-F	Wadi Sahtan, Jabel al Akhdar, Oman		N 23.34449 E 57.313	Mahil Fm	Smithian	240	Claraia dolomitic tempestite
100219-G	Wadi Sahtan, Jabel al Akhdar, Oman		N 23.34342 E 57.31612	Mahil Fm	Smithian	311	dolomitic tempestite
100222-A	Wadi Aday, Saih Hatat, Oman		N 23.56719 E 58.52773	Saiq Fm	Griesbachian?-Dienerian?	+/- 33	bioclastic dolomitic grainstone
100222-B	Wadi Aday, Saih Hatat, Oman		N 23.5671 E 58.52765	Saiq Fm	Changhsingian	+/- 22	bioclastic dolomitic floatstone
100222-C	Wadi Aday, Saih Hatat, Oman		N 23.56676 E 58.52986	Saiq Fm	Dienerian?	+/- 65	black calcitic, recrystallised dolomitic grainstone
100222-D	Wadi Aday, Saih Hatat, Oman		N 23.56722 E 58.52733	Saiq Fm	Changhsingian	+/- 3	bioclastic dolomitic floatstone
100223-A	Saiq Plateau, Jabel Al Akhdar, Oman	Section 3 (quarry, bottom)	N 23.10004 E 57.66437	Saiq Fm	Changhsingian	+/- 640	?skeletal float dolostone
100223-B	Saiq Plateau, Jabel Al Akhdar, Oman	Section 3 (quarry, bottom)	N 23.10009 E 57.66437	Saiq Fm	Griesbachian	650	bivalve lens wacke/pack dolostone
100223-C	Saiq Plateau, Jabel Al Akhdar, Oman	Section 3 (quarry, top)	N 23.10158 E 57.66741	Mahil Fm	Dienerian?	720	grain dolostone, stromatolites
100223-D	Saiq Plateau, Jabel Al Akhdar, Oman	Section 2 (Alat. Section)	N 23.09102 E 57.6877	Saiq Fm	Capitanian	+/- 280	wacke dolostone, bivalves/gastropods
100223-E	Saiq Plateau, Jabel Al Akhdar, Oman	Section 2 (Alat. Section)	N 23.09202 E 57.68762	Saiq Fm	Capitanian	295	coral bound dolostone
100223-F	Saiq Plateau, Jabel Al Akhdar, Oman	Section 2 (Alat. Section)	N 23.09218 E 57.68743	Saiq Fm	Capitanian	305	?bioclastic pack dolostone
110218-A	Saiq Plateau, Jabel Al Akhdar, Oman	Section 3 (quarry, bottom)		Saiq Fm	Griesbachian	645	wacke/pack dolostone, tempestite
110218-B	Saiq Plateau, Jabel Al Akhdar, Oman	Section 3 (quarry, bottom)		Saiq Fm	Griesbachian	640	pack dolostone, tempestite
110218-C	Saiq Plateau, Jabel Al Akhdar, Oman	Section 3 (quarry, bottom)		Saiq Fm	Griesbachian	650	wacke/pack dolostone, laminated tempestite
110218-D	Saiq Plateau, Jabel Al Akhdar, Oman	Section 3 (quarry, top)		Mahil Fm	Dienerian?	725	coquina pack dolostone
110218-E	Saiq Plateau, Jabel Al Akhdar, Oman	Section 3 (quarry, top)		Mahil Fm	Smithian	730	coquina pack dolostone
110218-F	Saiq Plateau, Jabel Al Akhdar, Oman	Section 3 (quarry, top)		Mahil Fm	Smithian	740	?oolitic grain dolostone
110218-G	Saiq Plateau, Jabel Al Akhdar, Oman	Section 3 (quarry, top)		Saiq Fm	Griesbachian	710	?oolitic grain dolostone
110218-H	Saiq Plateau, Jabel Al Akhdar, Oman	Section 2 (Alat. Section)		Saiq Fm	Capitanian	303	skeletal float dolostone, Alatoconchida
110218-I	Saiq Plateau, Jabel Al Akhdar, Oman	Section 2 (Alat. Section)		Saiq Fm	Capitanian	295	coral bound dolostone, Syringafora
110218-J	Saiq Plateau, Jabel Al Akhdar, Oman	Section 2 (Alat. Section)		Saiq Fm	Capitanian	285	bioclastic packstone, crinoids
110218-K	Saiq Plateau, Jabel Al Akhdar, Oman	Section 2 (Alat. Section)		Saiq Fm	Capitanian	280	skeletal float dolostone, pyritic, bivalves/crinoids
110219-A	Saiq Plateau, Jabel Al Akhdar, Oman	Section A (opposite quarry)		Saiq Fm	Wordian	27	rugose coral lime packstone
110219-B	Saiq Plateau, Jabel Al Akhdar, Oman	Section A (opposite quarry)		Saiq Fm	Wordian	20	shelly lime wackestone
110219-C/D	Saiq Plateau, Jabel Al Akhdar, Oman	Section A (blue markers)		Saiq Fm	Wordian	124	lime wackestone

	peritidal			no	-		
	peritidal			no	-		
	peritidal			no	-		
	shallow water			yes	Orchard		
	shallow marine			no	-		
	shallow water (4–6 m), lagoonal?			no	-		
	shallow marine			no	-		
	shallow marine			no	-		
	shallow marine			yes	Orchard		
	shallow marine			no	-		
	shallow marine			no	-		
	shallow marine			no	-		
	shallow marine			no	-		
	shallow marine						
	shallow marine						
	shallow marine						
	shallow marine						
	shallow marine						
	shallow marine						
	shallow marine						
	shallow marine						
	shallow marine						
	shallow marine						
	shallow marine						
black/dark grey muddy limestone, large corals	shallow marine			no	-		
grey coarse limestone	shallow marine			no	-		
dark grey limestone	shallow marine			no	-		

formic	1795.9	203.94	557.74	picked		no		-	-	- (pp)	(np)	N/A	-
formic	1272.4	186.71	634.03	picked		yes		GS?	-	- (pp)	(np)	N/A	-
formic	1205.5	166.91	625.15	picked		no		-	-	- (pp)	(np)	N/A	-
formic	1115.3	117.06	506.46	picked		yes		GS, CR, FM?	GS, CN, FM?	- (pp)	(np)	N/A	-
formic	984.24	142.35	499.2	picked		yes		CR	CR	- (pp)	(np)	N/A	-
formic	976.18	110.88	532.5	picked		no		-	-	- (pp)	(np)	N/A	-
formic	1052.3	110.8	529.51	picked		no		-	-	- (pp)	(np)	N/A	-
formic	1737	149.02	563.43	picked		yes		CR	CR	- (pp)	(np)	N/A	-
formic	1393.7	110.55	526.75 / 756.4	picked / picked		yes		CR, BF, BV?	CR, CN	-	(np)	N/A	OM27
formic	2270+	102.3	571.09	picked		no		-	-	- (pp)	(np)	N/A	-
formic	2346.9	119.39	534.59	picked		yes		CR	-	-	(np)	N/A	-
formic	1209.6	102.42	573.9	picked		yes		CR	CR	-	(np)	N/A	-
formic	1232	127	587.44	picked		no		-	-	- (pp)	(np)	N/A	-
				processed									
				processed									
				processed									
				not yet processed									
				not yet processed									
				processed									
				not yet processed									
				not yet processed									
				not yet processed									
				not yet processed									
				not yet processed									
acetic	2210	250	1960	picked		yes		BV	BV	(np)	(np)	N/A	-
acetic	1180	140	1040	picked		no		-	-	(np)	(np)	N/A	-
acetic	890	180	710	picked		no		-	-	(np)	(np)	N/A	-

110219-E	Saiq Plateau, Jabel Al Akhdar, Oman	Section A (blue markers)		Saiq Fm	Wordian	104	bioclastic lime packstone, bivalves/gastropods
110219-F	Saiq Plateau, Jabel Al Akhdar, Oman	Section A (blue markers)		Saiq Fm	Wordian	83	lime wackestone, bivalves/gastropods
110219-G	Saiq Plateau, Jabel Al Akhdar, Oman	Section A (blue markers)		Saiq Fm	Wordian	56	bioclastic lime packstone, crinoids
110219-H	Saiq Plateau, Jabel Al Akhdar, Oman	Section A (blue markers)		Saiq Fm	Wordian	47	bioclastic lime packstone, crinoids
110219-I	Saiq Plateau, Jabel Al Akhdar, Oman	Section A (blue markers)		Saiq Fm	Wordian	38	skeletal lime floatstone, rugose corals
110219-J	Saiq Plateau, Jabel Al Akhdar, Oman	Section A (blue markers)		Saiq Fm	Wordian	66	burrowed lime mudstone
110219-K	Saiq Plateau, Jabel Al Akhdar, Oman	Section A (blue markers)		Saiq Fm	Wordian	73	bioclastic lime packstone
110219-L	Saiq Plateau, Jabel Al Akhdar, Oman	Section A (blue markers)		Saiq Fm	Wordian	93	bioclastic lime packstone
110219-M	Saiq Plateau, Jabel Al Akhdar, Oman	Section A (blue markers)		Saiq Fm	Wordian	116	lime wackestone
110220-A	Saiq Plateau, Jabel Al Akhdar, Oman	Section B (off-road section)		Saiq Fm	Wordian	+/- 133	burrowed lime mudstone
110220-B	Saiq Plateau, Jabel Al Akhdar, Oman	Section B (off-road section)		Saiq Fm	Wordian	+/- 150	wacke dolostone
110220-C	Saiq Plateau, Jabel Al Akhdar, Oman	Section B (off-road section)		Saiq Fm	Wordian	+/- 168	bioclastic dolowackestone
110220-D	Saiq Plateau, Jabel Al Akhdar, Oman	Section B (off-road section)		Saiq Fm	Capitanian	+/- 382	?bioclastic pack dolostone
110220-E	Saiq Plateau, Jabel Al Akhdar, Oman	Section B (off-road section)		Saiq Fm	Capitanian	+/- 307	bioclastic pack dolostone, rugose corals/gastropods/bivalves
110220-F	Saiq Plateau, Jabel Al Akhdar, Oman	Section B (off-road section)		Saiq Fm	Capitanian	+/- 277	skeletal float dolostone, bryozoa/shells/crinoids?/rugose corals?
110220-G	Saiq Plateau, Jabel Al Akhdar, Oman	Section B (off-road section)		Saiq Fm	Capitanian	+/- 218	bioclastic pack dolostone, gastropods
110220-H	Saiq Plateau, Jabel Al Akhdar, Oman	Section B (off-road section)		Saiq Fm	Wordian	+/- 180	bioclastic pack dolostone, shelly
110221-A	Saiq Plateau, Jabel Al Akhdar, Oman	Section C/2 (Alat. Section)		Saiq Fm	Capitanian	+/- 330	wacke dolostone, gastropods/forams
110221-B	Saiq Plateau, Jabel Al Akhdar, Oman	Section C/2 (Alat. Section)		Saiq Fm	Capitanian	+/- 350	bioclastic pack dolostone, dense forams/shelly
110221-C	Saiq Plateau, Jabel Al Akhdar, Oman	Section C/2 (Alat. Section)		Saiq Fm	Capitanian	+/- 375	bioclastic pack dolostone, dense forams/shelly
110221-D	Saiq Plateau, Jabel Al Akhdar, Oman	Section C/2 (Alat. Section)		Saiq Fm	Wuchiapingian	+/- 420	white shelly pack dolostone
110221-E	Saiq Plateau, Jabel Al Akhdar, Oman	Road section (between C&3)		Saiq Fm	Changhsingian	+/- 618	bioclastic pack dolostone, bivalves/gastropods/rugose corals
110221-F	Saiq Plateau, Jabel Al Akhdar, Oman	Road section (between C&3)		Saiq Fm	Changhsingian	+/- 599	oolitic grain dolostone

dark grey limestone, small shells/gastropods	shallow marine	dark grey wacke/packstone (sparse/packed biomicrite), bivalves?/forams?		no	-		
dark grey/black limestone	shallow marine			no	-		
dark grey (/black) limestone, packstone (shells?)	shallow marine	packstone (biomicrite), fine shells/crinoids		no	-		
dark grey limestone, coarse, crinoids?	shallow marine			no	-		
dark grey limestone, corals, shelly	shallow marine			no	-		
dark grey limestone, muddy	shallow marine	wackestone (fossiliferous micrite), shelly		no	-		
dark grey limestone	shallow marine			no	-		
dark grey limestone	shallow marine	dark grey wackestone (fossiliferous biomicrite), shelly/crinoids?		yes	Orchard		
dark grey limestone, very muddy	shallow marine	dark grey wackestone (sparse micrite)		no	-		
dark grey limestone	shallow marine			no	-		
	shallow marine						
	shallow marine						
	shallow marine						
	shallow marine						
	shallow marine						
	shallow marine						
	shallow marine						
	shallow marine						
	shallow marine						
	shallow marine						
	shallow marine						
	shallow marine						
	shallow marine						
	shallow marine						

acetic	870	130	740	picked		yes		ET, VB	ET, BF, VB	-	(np)	N/A	OM28–41
acetic	810	110	700	picked		no		-	-	(np)	(np)	N/A	-
acetic	1270	150	1120	picked		yes		ED	BF	(np)	(np)	N/A	OM42–44
acetic	1030	130	900	picked		no		-	-	(np)	(np)	N/A	-
acetic	980	150	830	picked		yes		OS?	-	(np)	(np)	N/A	-
acetic	1005	115	890	picked		yes		OS, ET, BF, ED	BF	(np)	(np)	N/A	OM45–47
acetic	930	80	850	picked		no		-	-	(np)	(np)	N/A	-
acetic	1140	200	940	picked		yes		ET, ED, VB	ET, ED, BF, CN	(np)	(np)	N/A	OM48–65
acetic	1300	200	1100	picked		yes		ET, ED, VB, OS?	ET, ED, BF, OS	(np)	(np)	N/A	OM66–84
acetic	1310	60	1250	picked		no		-	-	(np)	(np)	N/A	-
				not yet processed									
				not yet processed									
				not yet processed									
				not yet processed									
				not yet processed									
				not yet processed									
				not yet processed									
				not yet processed									
				not yet processed									
				not yet processed									
				not yet processed									
				not yet processed									
				not yet processed									
				not yet processed									

110221-G	Saiq Plateau, Jabel Al Akhdar, Oman	Road section (between C&3)		Saiq Fm	Changhsingian	+/- 606	skeletal float dolostone, corals
100224-A	Wadi Wasit, Ba'id area, Oman	section	N 23.11373 E 58.3485	Al Jil Fm	Capitanian	1.5	red platy lime wackestone with ammonoids
100224-B	Wadi Wasit, Ba'id area, Oman	section	N 23.11373 E 58.3485	Al Jil Fm	Capitanian	3	red platy lime wackestone with ammonoids
100224-C	Wadi Wasit, Ba'id area, Oman	section	N 23.11367 E 58.34858	Al Jil Fm	Capitanian	11	turbiditic platy lime packstone
100224-D	Wadi Wasit, Ba'id area, Oman	section	N 23.11368 E 58.34856	Al Jil Fm	Capitanian	15	turbiditic platy lime packstone
100224-E	Wadi Wasit, Ba'id area, Oman	section	N 23.11359 E 58.34861	Al Jil Fm	Capitanian	35	red shale
100224-F	Wadi Wasit, Ba'id area, Oman	section	N 23.11342 E 58.34908	Al Jil Fm	Dienerian	56	platy limestone
100224-G	Wadi Wasit, Ba'id area, Oman	block	N 23.09658 E 58.33387	Al Jil Fm	Griesbachian	3.7	bioclastic (grain/pack) limestone
100224-H	Wadi Wasit, Ba'id area, Oman	block	N 23.09656 E 58.33388	Al Jil Fm	Griesbachian	4	bioclastic (grain/pack) limestone
100224-I	Wadi Wasit, Ba'id area, Oman	block	N 23.09656 E 58.33393	Al Jil Fm	Griesbachian	3.2	bioclastic (grain/pack) limestone
100224-J	Wadi Wasit, Ba'id area, Oman	block	N 23.09656 E 58.3339	Al Jil Fm	Griesbachian	2.6	bioclastic (grain/pack) limestone
100224-K	Wadi Wasit, Ba'id area, Oman	block	N 23.09656 E 58.33389	Al Jil Fm	Griesbachian	3	bioclastic (grain/pack) limestone
100224-L	Wadi Wasit, Ba'id area, Oman	section	N 23.10922 E 58.34005	Al Jil Fm	Wordian?	100 / 160?	reefal limestone, badly preserved fossils
100226-A	Wadi Maqam, Sumeini, Oman		N 24.77311 E 55.86832	Maqam Fm	Changhsingian		limestone with bryozoa
100227-A	Wadi Maqam, Sumeini, Oman		N 24.76871 E 55.86553	Maqam Fm	Capitanian		limestone
100227-B	Wadi Maqam, Sumeini, Oman		N 24.76862 E 55.86575	Maqam Fm	Wuchiapingian?		dolostone
100227-C	Wadi Maqam, Sumeini, Oman		N 24.7682 E 55.86509	Maqam Fm	Wordian		lime grainstone (channel / debris flow)
100227-D	Wadi Maqam, Sumeini, Oman		N 24.7683 E 55.86499	Maqam Fm	Wordian		lime mudstone
100227-E	Wadi Maqam, Sumeini, Oman		N 24.76873 E 55.8705	Maqam Fm	Griesbachian		platy limestone
100228-A	Wadi Maqam, Sumeini, Oman		N 24.77254 E 55.86908	Maqam Fm	Dienerian		papery lime wackestone
100228-B	Wadi Maqam, Sumeini, Oman		N 24.773 E 55.86898	Maqam Fm	Smithian		vermicular / platy limestone
100228-C	Wadi Maqam, Sumeini, Oman		N 24.77313 E 55.86814	Maqam Fm	Griesbachian		platy limestone
100228-D	Wadi Shuy'ab, Sumeini, Oman		N 24.78155 E 55.87426	Maqam Fm	Smithian		orange marly limestone
100228-E	Wadi Shuy'ab, Sumeini, Oman		N 24.78174 E 55.87419	Maqam Fm	Spathian		orange marly limestone
100225-A	Al Buday'ah, Oman		N 23.74484 E 56.9051	Al Jil Fm	Wuchiapingian	2	radiolarian chert

	shallow marine						
	pelagic			yes	Orchard		
	pelagic			yes	Orchard		
	deep water, continental rise			yes	Orchard		
	deep water, continental rise			yes	Orchard		
	deep water, continental rise			yes	Orchard		
	deep water, continental rise			no	-		
	shallow water reef, continental margin	bioclastic packstone (biomicrite), shelly/crinoids	*Clarkina carinata*	yes	Orchard		
	shallow water reef, continental margin		*Clarkina carinata*	yes	Orchard		
	shallow water reef, continental margin		*Isarcicella isarcica*	yes	Orchard		
	shallow water reef, continental margin		*Isarcicella isarcica*	yes	Orchard		
	shallow water reef, continental margin		*Isarcicella isarcica*	yes	Orchard		
	shallow water reef, continental margin			no	-		
	deep marine			yes	Orchard		
	outer shelf			no	-		
	deep marine			no	-		
	outer shelf, shallow water debris	grainstone (biosparite), tabulate coral/shelly/forams/crinoids/bryozoa, well-fragmented, shallow water		yes	Orchard		
	outer shelf			no	-		
	basal continental slope			no	-		
	basal continental slope			no	-		
	basal continental slope			no	-		
	basal continental slope			no	-		
	basal continental slope			no	-		
	basal continental slope			no	-		
	distal marine		-	N/A	-		

				not yet processed									
formic	2220.1	182.48	534.61	picked		yes		-	CN, CR	CN (pp)	(np)	N/A	-
formic	1396.7	121.87	563.16	picked		yes		CN, OS	CN, OS, CR	CN (pp)	(np)	N/A	-
formic	1198.4	114.63	515.09	picked		yes		-	CN, GS, CR	CN (pp)	(np)	N/A	-
formic	1586.9	116.6	505.65	picked		yes		-	CN	CN (pp)	(np)	N/A	-
formic	2390+	132.48	655.9	picked		yes		-	CN	CN (pp)	(np)	N/A	-
formic	2900+	154.38	538.21	picked		no		-	-	- (pp)	(np)	N/A	-
formic	1044.9	69.1	503.5	picked		yes		BV, AM?	ET, CN, GS, OS	CN (pp)	(np)	N/A	OM85-86
formic	2074.3	91.22	633.96	picked		yes		GS	CN, OS	CN (pp)	(np)	N/A	-
formic	495.18	49.65	444.02	picked		yes		ET?, EC, GS, CN	GS, CN	CN (pp)	(np)	N/A	OM87
formic	694.15	170	524.13	picked		yes		GS, BV, EC, AM?	GS, BV, EC, CN, OS?	CN (pp)	(np)	N/A	-
formic	1303.3	84.7	511.17	picked		yes		BV, GS	BV?, GS, OS, CN	CN (pp)	(np)	N/A	-
formic	1611.1	191.64	513.96	picked		yes		BV?, GS?	CN?	CN? (pp)	(np)	N/A	OM88
formic	1582.1	93.06	537.92	picked		yes		OS	OS, CN	- (pp)	(np)	N/A	-
formic	1886.3	72.33	526.83	picked		yes		-	OS?	- (pp)	(np)	N/A	-
formic	1293.1	95.95	564.9	picked		no		-	-	-	(np)	N/A	-
formic	784.24	129	627.06	picked		yes		ET, BR/CL, OS, BV	BR/CL, OS, CN	OS (pp)	(np)	N/A	OM89
formic	1780.7	135.43	552.83	picked		yes		OS	OS	- (pp)	(np)	N/A	-
formic	1992.1	152.46	516.04	picked		no		-	-	- (pp)	(np)	N/A	-
formic	2090.2	169.5	555.02	picked		no		-	-	- (pp)	(np)	N/A	-
formic	1645.7	128.19	549.75	picked		no		N/A	-	- (pp)	(np)	N/A	-
formic	1297.6	110.73	532.36	picked		no		-	-	- (pp)	(np)	N/A	-
formic	1912.2	151.11	518.34	picked		no		-	-	- (pp)	(np)	N/A	-
formic	1874.4	52.85	523.8	picked		no		-	-	- (pp)	(np)	N/A	-
				not processed		N/A		N/A	N/A	N/A	N/A	N/A	-

100225-B	Al Buday'ah, Oman		N 23.7461 E 56.9064	Al Jil Fm	Capitanian - Wuchiapingian	0.5	red Hallstatt lime mudstone
100225-C	Al Buday'ah, Oman		N 23.746 E 56.90643	Al Jil Fm	Capitanian - Wuchiapingian	0.5	red Hallstatt lime mudstone
100225-D	Al Buday'ah, Oman		N 23.74056 E 56.90607	Al Jil Fm	Smithian	25?	papery laminated limestone
100302-A	Bu Fasiqah, Batain Plain, Oman		N 22.30373 E 59.67572	Aseelah Unit	Permian	65	white brecciated wackel/packstone with crinoids and bivalves in sandstone matrix
100302-B	Bu Fasiqah, Batain Plain, Oman		N 22.30349 E 59.67542	Qarari Unit	Guadalupian	10	brown brecciated clast-supported limestone conglomerate with crinoids
100302-C	Bu Fasiqah, Batain Plain, Oman		N 22.3036 E 59.67486	Qarari Unit	Guadalupian	2	grey microbial lime mudstone with white venation
100302-D	Bu Fasiqah, Batain Plain, Oman		-	Aseelah Unit	Permian	ex situ	fusulinid-rich brecciated limestone
100302-E	Bu Fasiqah, Batain Plain, Oman		-	Aseelah Unit	Permian	ex situ	brecciated limestone
100302-F	Qarari Block, Batain Plain, Oman		N 22.31724 E 59.71928	Qarari Unit	Guadalupian–Lopingian	N/A	pink reefal limestone
100302-G	Qarari Block, Batain Plain, Oman		N 22.31729 E 59.71959	Qarari Unit	Guadalupian–Lopingian	near base	nodular lime mudstone
100302-H	The Bridge, Batain Plain, Oman		N 22.44292 E 59.76681	Qarari Unit	Wuchiapingian	ex situ	
110223-A	The Bridge, Batain Plain, Oman			Qarari Unit	Wuchiapingian		
100303-A	Aseelah, Batain Plain, Oman		N 21.94309 E 59.61071	Aseelah Unit	Guadalupian – Lopingian?	within 10 m from base	coarse-grained sandy limestone
100303-B	Aseelah, Batain Plain, Oman		N 21.94365 E 59.61218	Aseelah Unit	Guadalupian – Lopingian?	within 10 m from base	crinoid packstone cement of sandy limestone
JP collection							
300311-O	Kamura, Miyazaki Prefecture, Japan	ShioinousoPT (D)	between N32,75467 E131,33824 and N32,75469 E131,33842	Kamura Fm	Norian	36.4	radiolaria bivalve mudstone?
300311-N	Kamura, Miyazaki Prefecture, Japan	ShioinousoPT (D)	between N32,75467 E131,33824 and N32,75469 E131,33842	Kamura Fm	Norian	35	radiolaria bivalve mudstone?
300311-M	Kamura, Miyazaki Prefecture, Japan	ShioinousoPT (D)	between N32,75467 E131,33824 and N32,75469 E131,33842	Kamura Fm	Norian	33	radiolaria bivalve mudstone?

	pelagic		-	yes	Orchard		
	pelagic		-	yes	Orchard		
	distal marine		-	no			
				no	-		
				yes	Orchard		
				no	-		
				no	-		
				no	-		
	shallow marine		-	yes	Orchard		
	hemipelagic, open sea shelf (slope)		-	no	-		
white / red bioclastic mudstone/wackestone and framestone	reef / pelagic	pale yellow packstone (packed micrite), ammonoids/forams/bryozoa/crinoids/ostracods?, pelagic with reefal debris	-	yes	Orchard		
white / red bioclastic mudstone/wackestone and framestone	reef / pelagic		-	yes	-		
				yes	Orchard		
				yes	Orchard		
light/dark grey limestone	tropical, shallow water, mid-oceanic seamount		*Metapolygnathus nodosus* , *N. primitius*	yes	Orchard		top section
light/dark grey limestone	tropical, shallow water, mid-oceanic seamount		*Metapolygnathus nodosus* , *N. primitius*	yes	Orchard		
light grey limestone	tropical, shallow water, mid-oceanic seamount		*Metapolygnathus nodosus* , *N. primitius*	yes	Orchard		

formic	2133.4	155.61	583.28	partly processed, picked		yes		OS, CN	OS, CN	- (pp)	(np)	N/A	-
formic	1376	105.34	511.65	partly processed, picked		yes		-	CN	- (pp)	(np)	N/A	-
formic	2310+	172.5	535.97	picked		no		-	-	- (pp)	(np)	N/A	
formic	2330+	80.3	647.38	picked		yes		CR	CR	- (pp)	(np)	N/A	-
formic	1362.2	53.31	545.12	picked		yes		CR, CN	CR, CN	CN	(np)	N/A	-
formic	2260+	110.02	545.34	picked		no		-	-	-	(np)	N/A	-
formic	1579.8	69.85	520.02	picked		yes		BV	-	- (pp)	(np)	N/A	-
formic	1653.4	76.89	512.53	picked		yes		CR	CR	- (pp)	(np)	N/A	-
formic / acetic	2400+	115.01	687.15 / 1600+	picked / picked		yes		BV, CR, ET	CN, BF, ET	- (pp)	(np)	N/A	OM90, 98–100
formic	1319.7	89.31	524.59	picked		no		-	-	-	(np)	N/A	-
formic / acetic	1435.5	98.78	536,76 / 740	picked / picked		yes		CR, CL, GS, ET	CR, CN, ET	CN	(np)	N/A	OM91–96
acetic	7705	0	7705	picked		yes		CR, BV, CN, ET	CR, BV, CN, BF, ET	(np)	(np)	N/A	OM101–110
formic	2136.6	106.64	502.76	picked		yes		BV	CN, GS	CN (pp)	(np)	N/A	-
formic	1934.5	60.66	521.4	picked		yes		CL/BR, CR, BV	CN	- (pp)	(np)	N/A	OM97
acetic	1570	70	1500	picked		yes		BF	BF, CN	BF, CN (pp)	(np)	N/A	JP95
acetic	1800	100	1700	picked		yes		BF	BF, CN	CN (pp)	(np)	N/A	-
acetic	3100	150	2950	picked		yes		BF?, CN	BF/ET, CN	CN (pp)	(np)	N/A	JP82–94

300311-L	Kamura, Miyazaki Prefecture, Japan	ShioinousoPT (D)	between N32,75467 E131,33824 and N32,75469 E131,33842	Kamura Fm	Carnian	31	radiolaria bivalve mudstone?
300311-K	Kamura, Miyazaki Prefecture, Japan	ShioinousoPT (D)	between N32,75467 E131,33824 and N32,75469 E131,33842	Kamura Fm	Ladinian	29	radiolaria bivalve mudstone?
300311-J	Kamura, Miyazaki Prefecture, Japan	ShioinousoPT (D)	between N32,75467 E131,33824 and N32,75469 E131,33842	Kamura Fm	Anisian	27	bivalve packstone?
300311-I	Kamura, Miyazaki Prefecture, Japan	ShioinousoPT (D)	between N32,75467 E131,33824 and N32,75469 E131,33842	Kamura Fm	Anisian	25	bivalve packstone?
300311-H	Kamura, Miyazaki Prefecture, Japan	ShioinousoPT (D)	between N32,75467 E131,33824 and N32,75469 E131,33842	Kamura Fm	Anisian	23	molluscan wackestone/packstone?
300311-G	Kamura, Miyazaki Prefecture, Japan	ShioinousoPT (D)	between N32,75467 E131,33824 and N32,75469 E131,33842	Kamura Fm	Smithian	21	molluscan wackestone
300311-F	Kamura, Miyazaki Prefecture, Japan	ShioinousoPT (D)	between N32,75467 E131,33824 and N32,75469 E131,33842	Kamura Fm	Smithian	19	molluscan wackestone
300311-E	Kamura, Miyazaki Prefecture, Japan	ShioinousoPT (D)	between N32,75467 E131,33824 and N32,75469 E131,33842	Kamura Fm	Smithian	17	molluscan wackestone
300311-D	Kamura, Miyazaki Prefecture, Japan	ShioinousoPT (D)	between N32,75467 E131,33824 and N32,75469 E131,33842	Kamura Fm	Smithian	15	molluscan wackestone
300311-C	Kamura, Miyazaki Prefecture, Japan	ShioinousoPT (D)	between N32,75467 E131,33824 and N32,75469 E131,33842	Kamura Fm	Dienerian	13.2-13.3	filamentous cyanobacteria grainstone
300311-B	Kamura, Miyazaki Prefecture, Japan	ShioinousoPT (D)	between N32,75467 E131,33824 and N32,75469 E131,33842	Kamura Fm	Dienerian	13	coquinite

light grey limestone	tropical, shallow water, mid-oceanic seamount		*Metapolygnathus polygnathiformis* , *M. nodosus* , *M. primitius*	no	-		
dark grey limestone	tropical, shallow water, mid-oceanic seamount		*Budurovignathus hungaricus* , *Paragondolella foliata*	yes	Orchard		
dark grey limestone	tropical, shallow water, mid-oceanic seamount		*Paragondolella bulgarica*	yes	Orchard		
dark grey limestone	tropical, shallow water, mid-oceanic seamount		*Chiosella timorensis*	yes	Orchard		
light grey limestone	tropical, shallow water, mid-oceanic seamount		*Chiosella timorensis*	yes	Orchard		
light grey limestone	tropical, shallow water, mid-oceanic seamount		*Necospathodus homeri* ?, *Triassospathodus symmetricus*	yes	Orchard		
light grey limestone	tropical, shallow water, mid-oceanic seamount		*Necospathodus homeri* ?	yes	Orchard		
light grey limestone	tropical, shallow water, mid-oceanic seamount		*Conservatella conservativus* , *Necospathodus waageni*	yes	Orchard		
light grey limestone	tropical, shallow water, mid-oceanic seamount		barren interval	yes	Orchard		
light grey limestone	tropical, shallow water, mid-oceanic seamount		barren interval	yes	Orchard		
light grey coquinite	tropical, shallow water, mid-oceanic seamount		barren interval	yes	-		

acetic	2650	100	2550	picked		no		-	-	(np)	(np)	N/A	-
acetic	2550	160	2390	picked		yes		BF, ET?	BF, CN	CN (pp)	(np)	N/A	JP72–81
acetic	2670	140	2530	picked		yes		BF, ET, ES, CN	BF, ES, CN	CN (pp)	(np)	N/A	JP39–71
acetic	2020	100	1920	picked		yes		BF, ES, ED	BF, ET, ED, CN	BF, CN (pp)	(np)	N/A	JP9–38
acetic	3070	250	2820	picked		yes		-	CN	(np)	(np)	N/A	JP8
acetic	2875	100	2775	picked		yes		-	CN	CN (pp)	(np)	N/A	-
acetic	2700	130	2570	picked		yes		CN	CN	(np)	(np)	N/A	-
acetic	1730	50	1680	picked		yes		SF	CN	CN (pp)	(np)	N/A	-
acetic	2580	160	2420	picked		yes		-	CN	(np)	(np)	N/A	-
acetic	1055	50	1005	picked		yes		CN	BF?, CN	(np)	(np)	N/A	-
acetic	3400	100	3300	picked		yes		-	CN	(np)	(np)	N/A	-

300311-A	Kamura, Miyazaki Prefecture, Japan	ShioinousoPT (D)	between N32,75467 E131,33824 and N32,75469 E131,33842	Kamura Fm	Dienerian	11	coquinite
290311-S	Kamura, Miyazaki Prefecture, Japan	ShioinousoPT (B)	N32,75459 E131,33855	Kamura Fm	Dienerian	9	coquinite
290311-R	Kamura, Miyazaki Prefecture, Japan	ShioinousoPT (B)	N32,75459 E131,33855	Kamura Fm	Dienerian	7	coquinite
290311-Q	Kamura, Miyazaki Prefecture, Japan	ShioinousoPT (B)	N32,75459 E131,33855	Kamura Fm	Griesbachian	5	grey limestone, small shelly fauna
290311-P	Kamura, Miyazaki Prefecture, Japan	ShioinousoPT (B)	N32,75459 E131,33855	Kamura Fm	Griesbachian	3	black limestone
290311-O	Kamura, Miyazaki Prefecture, Japan	ShioinousoPT (B)	N32,75459 E131,33855	Kamura Fm	Griesbachian	1	black limestone
290311-N	Kamura, Miyazaki Prefecture, Japan	ShioinousoGL	N32,75335 E131,33607	Mitai Fm	Wuchiapingian	21	light/dark grey limestone
290311-M	Kamura, Miyazaki Prefecture, Japan	ShioinousoGL	N32,75335 E131,33607	Mitai Fm	Wuchiapingian	19	light grey algal limestone (part dolomitised)
290311-L	Kamura, Miyazaki Prefecture, Japan	ShioinousoGL	N32,75335 E131,33607	Mitai Fm	Wuchiapingian	17	light grey algal limestone (part dolomitised)
290311-K	Kamura, Miyazaki Prefecture, Japan	ShioinousoGL	N32,75335 E131,33607	Mitai Fm	Wuchiapingian	14.8	light/dark grey limestone
290311-J	Kamura, Miyazaki Prefecture, Japan	ShioinousoGL	N32,75335 E131,33607	Mitai Fm	Wuchiapingian	12.4	white dolomite
290311-I	Kamura, Miyazaki Prefecture, Japan	ShioinousoGL	N32,75335 E131,33607	Mitai Fm	Wuchiapingian	11	light/dark grey limestone
290311-H	Kamura, Miyazaki Prefecture, Japan	ShioinousoGL	N32,75335 E131,33607	Mitai Fm	Wuchiapingian	9	light grey algal limestone (part dolomitised)
290311-G	Kamura, Miyazaki Prefecture, Japan	ShioinousoGL	N32,75335 E131,33607	Mitai Fm	Wuchiapingian	7	light/dark grey limestone
290311-F	Kamura, Miyazaki Prefecture, Japan	ShioinousoGL	N32,75335 E131,33607	Mitai Fm	Wuchiapingian	5	light/dark grey limestone (part dolomitised)
290311-E	Kamura, Miyazaki Prefecture, Japan	ShioinousoGL	N32,75335 E131,33607	Mitai Fm	Wuchiapingian	3	light/dark grey limestone
290311-D	Kamura, Miyazaki Prefecture, Japan	ShioinousoGL	N32,75335 E131,33607	Mitai Fm	Wuchiapingian	1	light/dark grey limestone
280311-A	Kamura, Miyazaki Prefecture, Japan	ShioinousoGL	N32,75335 E131,33607	Iwato Fm	Capitanian	-1	black limestone
280311-B	Kamura, Miyazaki Prefecture, Japan	ShioinousoGL	N32,75335 E131,33607	Iwato Fm	Capitanian	-3	black limestone
280311-C	Kamura, Miyazaki Prefecture, Japan	ShioinousoGL	N32,75335 E131,33607	Iwato Fm	Capitanian	-5	black limestone
280311-D	Kamura, Miyazaki Prefecture, Japan	ShioinousoGL	N32,75335 E131,33607	Iwato Fm	Capitanian	-7	black limestone
280311-E	Kamura, Miyazaki Prefecture, Japan	ShioinousoGL	N32,75335 E131,33607	Iwato Fm	Capitanian	-9.5	black limestone
280311-F	Kamura, Miyazaki Prefecture, Japan	ShioinousoGL	N32,75335 E131,33607	Iwato Fm	Capitanian	-11	black limestone

light grey coquinite	tropical, shallow water, mid-oceanic seamount		barren interval	no	-		
light grey coquinite	tropical, shallow water, mid-oceanic seamount		*Necospathodus dieneri*	yes	-		
light grey coquinite	tropical, shallow water, mid-oceanic seamount		*Necospathodus dieneri*	yes	Orchard		
light grey limestone, small shells and gastropods	tropical, shallow water, mid-oceanic seamount		barren interval	no	-		
dark grey limestone	tropical, shallow water, mid-oceanic seamount		barren interval	yes	-		
dark grey/black limestone, oily	tropical, shallow water, mid-oceanic seamount		*Hindeodus parvus* , *Isarcicella isarcica* , *Necgondolella carinata*	no	-		PTB at 0m
light grey limestone, grainy	tropical, shallow water, mid-oceanic seamount		*Codonofusiella - Reichelina* zone	no	-		SW
light/dark grey limestone (part dolomite?)	tropical, shallow water, mid-oceanic seamount		*Codonofusiella - Reichelina* zone	no	-		SW
light/dark grey limestone, some shimmering (part dolomite?)	tropical, shallow water, mid-oceanic seamount		*Codonofusiella - Reichelina* zone	no	-		SW
light grey limestone with black patches, oolitic?	tropical, shallow water, mid-oceanic seamount		*Codonofusiella - Reichelina* zone	no	-		SW
white/light grey dolostone? Some shimmering, dark grey patches	tropical, shallow water, mid-oceanic seamount		*Codonofusiella - Reichelina* zone	no	-		SW
light grey limestone, grainy	tropical, shallow water, mid-oceanic seamount		*Codonofusiella - Reichelina* zone	no	-		SW
dark grey limestone, patchy/flecky black, shiny (part dolomitised)	tropical, shallow water, mid-oceanic seamount		*Codonofusiella - Reichelina* zone	no	-		SW
light/dark grey limestone	tropical, shallow water, mid-oceanic seamount		*Codonofusiella - Reichelina* zone	no	-		SW
light grey limestone, patchy/flecky dark grey, shiny (part dolomitised)	tropical, shallow water, mid-oceanic seamount		*Codonofusiella - Reichelina* zone	no	-		SW
dark grey/black limestone, oolitic?	tropical, shallow water, mid-oceanic seamount		*Codonofusiella - Reichelina* zone	no	-		SW
dark grey limestone	tropical, shallow water, mid-oceanic seamount		*Codonofusiella - Reichelina* zone	no	-		SW
black limestone	tropical, shallow water, mid-oceanic seamount		barren interval	no	-		SW, GLB at 0m
black limestone	tropical, shallow water, mid-oceanic seamount		barren interval	no	-		SW
dark grey limestone	tropical, shallow water, mid-oceanic seamount		barren interval	no	-		SW
dark grey limestone	tropical, shallow water, mid-oceanic seamount		barren interval	no	-		SW
black limestone	tropical, shallow water, mid-oceanic seamount		barren interval	no	-		SW
black limestone	tropical, shallow water, mid-oceanic seamount		barren interval	no	-		NE

acetic	1720	130	1590	picked		no		-	-	(np)	(np)	N/A	-
acetic	1560	150	1410	picked		yes		-	CN	(np)	(np)	N/A	-
acetic	3590	180	3410	picked		yes		ET	ET?, CN	(np)	(np)	N/A	JP2-7
acetic	1300	100	1200	picked		no		-	- (pp)	(np)	(np)	N/A	-
acetic	1970	90	1880	picked		yes		-	CN	(np)	(np)	N/A	-
acetic	2250	100	2150	picked		no		-	-	(np)	(np)	N/A	-
acetic	2495	195	2300	picked		no		-	-	(np)	(np)	N/A	-
acetic	2175	200	1975	picked		no		-	-	(np)	(np)	N/A	-
acetic	2625	210	2415	picked		no		-	- (pp)	(np)	(np)	N/A	-
acetic	3170	140	3030	picked		no		- (pp)	- (pp)	(np)	(np)	N/A	-
acetic	1925	145	1780	picked		no		-	- (pp)	(np)	(np)	N/A	-
acetic	2625	135	2490	picked		no		- (pp)	- (pp)	(np)	(np)	N/A	-
acetic	3410	180	3230	picked		no		-	-	(np)	(np)	N/A	-
acetic	1495	110	1385	picked		no		-	-	(np)	(np)	N/A	-
acetic	2985	225	2760	picked		no		-	- (pp)	(np)	(np)	N/A	-
acetic	2335	155	2180	picked		no		-	-	(np)	(np)	N/A	-
acetic	3410	325	3085	picked		no		-	-	(np)	(np)	N/A	-
acetic	2965	160	2805	picked		no		-	-	(np)	(np)	N/A	-
acetic	3140	170	2970	picked		no		-	-	(np)	(np)	N/A	-
acetic	2210	125	2085	picked		no		-	-	(np)	(np)	N/A	-
acetic	2480	110	2370	picked		no		-	-	(np)	(np)	N/A	-
acetic	3085	160	2925	picked		no		-	-	(np)	(np)	N/A	-
acetic	2900	125	2775	picked		no		-	-	(np)	(np)	N/A	-

280311-G	Kamura, Miyazaki Prefecture, Japan	ShioinousoGL	N32,75335 E131,33607	Iwato Fm	Capitanian	-12.3	black limestone
280311-H	Kamura, Miyazaki Prefecture, Japan	ShioinousoGL	N32,75335 E131,33607	Iwato Fm	Capitanian	-15	black limestone
280311-I	Kamura, Miyazaki Prefecture, Japan	ShioinousoGL	N32,75335 E131,33607	Iwato Fm	Capitanian	-15.5	black limestone
290311-A	Kamura, Miyazaki Prefecture, Japan	ShioinousoGL	N32,75335 E131,33607	Iwato Fm	Capitanian	-17	black limestone
290311-B	Kamura, Miyazaki Prefecture, Japan	ShioinousoGL	N32,75335 E131,33607	Iwato Fm	Capitanian	-19	black limestone
290311-C	Kamura, Miyazaki Prefecture, Japan	ShioinousoGL	N32,75335 E131,33607	Iwato Fm	Capitanian	-21	black limestone
310311-B	Kamura, Miyazaki Prefecture, Japan	Hijirikawa	N32,75122 E131,3311	Iwato Fm	Capitanian	2	black/grey mudstone, bivalves?
310311-A	Kamura, Miyazaki Prefecture, Japan	Hijirikawa	N32,75122 E131,3311	Iwato Fm	Capitanian	1	black mudstone
310311-C	Kamura, Miyazaki Prefecture, Japan	Hijirikawa	N32,75122 E131,3311	Iwato Fm	Capitanian	0	black mudstone, fusulinids and bivalves
310311-D	Kamura, Miyazaki Prefecture, Japan	Hijirikawa	N32,75122 E131,3311	Iwato Fm	Capitanian	-2	dark grey limestone, fusulinids
310311-E	Kamura, Miyazaki Prefecture, Japan	Hijirikawa	N32,75122 E131,3311	Iwato Fm	Capitanian	-4	dark grey limestone
310311-F	Kamura, Miyazaki Prefecture, Japan	Hijirikawa	N32,75122 E131,3311	Iwato Fm	Capitanian	-6	dark grey limestone
300311-Y	Kamura, Miyazaki Prefecture, Japan	Saraito	N32,75686 E131,34731	Iwato Fm	Wordian	18	dark grey / black? limestone
300311-X	Kamura, Miyazaki Prefecture, Japan	Saraito	N32,75686 E131,34731	Iwato Fm	Wordian	16	dark grey / black? limestone
300311-W	Kamura, Miyazaki Prefecture, Japan	Saraito	N32,75686 E131,34731	Iwato Fm	Wordian	14	dark grey limestone
300311-V	Kamura, Miyazaki Prefecture, Japan	Saraito	N32,75686 E131,34731	Iwato Fm	Wordian	12	dark grey limestone
300311-U	Kamura, Miyazaki Prefecture, Japan	Saraito	N32,75686 E131,34731	Iwato Fm	Wordian	10	dark grey limestone
300311-T	Kamura, Miyazaki Prefecture, Japan	Saraito	N32,75686 E131,34731	Iwato Fm	Wordian	8	dark grey limestone (weathered)
300311-S	Kamura, Miyazaki Prefecture, Japan	Saraito	N32,75686 E131,34731	Iwato Fm	Wordian	6	dark grey limestone
300311-R	Kamura, Miyazaki Prefecture, Japan	Saraito	N32,75686 E131,34731	Iwato Fm	Wordian	4	dark grey limestone
300311-Q	Kamura, Miyazaki Prefecture, Japan	Saraito	N32,75686 E131,34731	Iwato Fm	Wordian	2	dark grey limestone
300311-P	Kamura, Miyazaki Prefecture, Japan	Saraito	N32,75686 E131,34731	Iwato Fm	Wordian	0	dark grey limestone
05.7.13.h	Gobanga-dake, Oita Prefecture, Japan	block	approx. 33°03'10"N 131°48'16"E	Gobangadake Fm	Lower Triassic?		limestone
05.7.13.g	Gobanga-dake, Oita Prefecture, Japan	block	approx. 33°03'10"N 131°48'16"E	Gobangadake Fm	Lower Triassic?		limestone
05.7.14.ak	Kamura, Miyazaki Prefecture, Japan	ShioinousoPT (C/D?)	approx. 32°45'15"N 131°20'20"E	Kamura Fm	Induan (Griesbachian)	0.7 above base	limestone
05.7.14.ar	Kamura, Miyazaki Prefecture, Japan	ShioinousoPT (C/D?)	approx. 32°45'15"N 131°20'20"E	Kamura Fm	Induan (Griesbachian)?	3.55 above base	limestone

black limestone	tropical, shallow water, mid-oceanic seamount		barren interval	no	-		NE
dark grey/black limestone	tropical, shallow water, mid-oceanic seamount		*Lepidolina* zone	no	-		NE
dark grey limestone	tropical, shallow water, mid-oceanic seamount		*Lepidolina* zone	no	-		NE
dark grey/black limestone, large coiled gastropods (2-3 x 1-1.5cm)	tropical, shallow water, mid-oceanic seamount		*Lepidolina* zone	no	-		NE
black mud/limestone, fusulinids	tropical, shallow water, mid-oceanic seamount		*Lepidolina* zone	no	-		NE
dark grey limestone	tropical, shallow water, mid-oceanic seamount		*Lepidolina* zone	no	-		NE, bottom section at -21.2m
dark grey/black limestone	tropical, shallow water, mid-oceanic seamount		*Yabeina* zone	no	-		
dark grey/black mud/limestone	tropical, shallow water, mid-oceanic seamount		*Yabeina* zone	no	-		
dark grey/black limestone	tropical, shallow water, mid-oceanic seamount		*Yabeina* zone	no	-		fusulinid/bivalve boundary
light/dark grey limestone	tropical, shallow water, mid-oceanic seamount		*Yabeina* zone	no	-		
dark grey limestone	tropical, shallow water, mid-oceanic seamount		*Yabeina* zone	no	-		
light/dark grey limestone	tropical, shallow water, mid-oceanic seamount		*Yabeina* zone	no	-		bottom section at -7/-8m
black limestone	tropical, shallow water, mid-oceanic seamount		*Necoschwagerina* zone	no	-		
dark grey/black limestone	tropical, shallow water, mid-oceanic seamount		*Necoschwagerina* zone	no	-		
black limestone	tropical, shallow water, mid-oceanic seamount		*Necoschwagerina* zone	no	-		
dark grey/black limestone	tropical, shallow water, mid-oceanic seamount		*Necoschwagerina* zone	no	-		
light/dark grey limestone, oolitic?	tropical, shallow water, mid-oceanic seamount		*Necoschwagerina* zone	no	-		
light grey limestone	tropical, shallow water, mid-oceanic seamount		*Necoschwagerina* zone	no	-		
dark grey limestone	tropical, shallow water, mid-oceanic seamount		*Necoschwagerina* zone	no	-		
dark grey limestone	tropical, shallow water, mid-oceanic seamount		*Necoschwagerina* zone	no	-		
black limestone	tropical, shallow water, mid-oceanic seamount		*Necoschwagerina* zone	no	-		
dark grey limestone	tropical, shallow water, mid-oceanic seamount		*Necoschwagerina* zone	no	-		
	mid-oceanic seamount			no	-		
	mid-oceanic seamount			no	-		
	mid-oceanic seamount		*Hindeodus parvus* , *Isarcicella isarcica* , *Neogondolella carinata*	yes	N/A		
	mid-oceanic seamount			yes	N/A		

acetic	2615	135	2480	picked		no		-	-	(np)	(np)	N/A	-
acetic	1030	100	930	picked		no		-	-	(np)	(np)	N/A	-
acetic	1860	110	1750	picked		no		-	-	(np)	(np)	N/A	-
acetic	2305	150	2155	picked		yes		GS	-	(np)	(np)	N/A	-
acetic	2600	110	2490	picked		no		-	-	(np)	(np)	N/A	-
acetic	4165	255	3910	picked		no		-	-	(np)	(np)	N/A	-
acetic	2630	100	2530	picked		no		-	-	(np)	(np)	N/A	-
acetic	1970	150	1820	picked		no		-	-	(np)	(np)	N/A	-
acetic	2375	125	2250	picked		no		-	-	(np)	(np)	N/A	-
acetic	2380	140	2240	picked		no		-	- (pp)	(np)	(np)	N/A	-
acetic	2200	110	2090	picked		no		-	-	(np)	(np)	N/A	-
acetic	2105	130	1975	picked		no		-	-	(np)	(np)	N/A	-
acetic	1730	80	1650	picked		no		-	-	(np)	(np)	N/A	-
acetic	1280	120	1160	picked		no		-	-	(np)	(np)	N/A	-
acetic	1750	120	1630	picked		no		-	-	(np)	(np)	N/A	-
acetic	1780	80	1700	picked		no		-	-	(np)	(np)	N/A	-
acetic	2060	100	1960	picked		no		-	- (pp)	(np)	(np)	N/A	-
acetic	2450	100	2350	picked		no		-	-	(np)	(np)	N/A	-
acetic	2550	100	2450	picked		no		-	-	(np)	(np)	N/A	-
acetic	1150	80	1070	picked		no		-	-	(np)	(np)	N/A	-
acetic	2730	120	2610	picked		no		-	-	(np)	(np)	N/A	-
acetic	2120	120	2000	picked		no		?	-	(np)	(np)	N/A	JP1
formic	778.67	0	778.67	picked		no		- (pp)	- (pp)	(np)	(np)	N/A	
acetic	170.89	0	170.89	picked		no		-	-	-	- (pp)	-	
formic	354.95	0	354.95	picked		yes		BF, ET, ES	BF, ED, CN	CN (pp)	(np)	N/A	JP96-105
formic	295.74	0	295.74	picked		yes		BF	BF, CN	(np)	(np)	N/A	

05.7.14.aw	Kamura, Miyazaki Prefecture, Japan	ShioinousoPT (C/D?)	approx. 32°45'15"N 131°20'20"E	Kamura Fm	Induan (Griesbachian)?	4.83 above base	limestone
05.7.14.ay	Kamura, Miyazaki Prefecture, Japan	ShioinousoPT (C/D?)	approx. 32°45'15"N 131°20'20"E	Kamura Fm	Induan (Griesbachian/Dienerian)?	6.15 above base	limestone
05.7.14.ba	Kamura, Miyazaki Prefecture, Japan	ShioinousoPT (C/D?)	approx. 32°45'15"N 131°20'20"E	Mitai Fm	Changhsingian?	0.4 below top	limestone
05.7.14.bb	Kamura, Miyazaki Prefecture, Japan	ShioinousoPT (C/D?)	approx. 32°45'15"N 131°20'20"E	Mitai Fm	Changhsingian?	1.15 below top	limestone
05.7.15.b	Kamura, Miyazaki Prefecture, Japan	Saraito	approx. 32°45'25"N 131°20'50"E	Kamura Fm	Induan (Griesbachian)	basal, *ex situ*	microbial limestone
05.7.15.f	Kamura, Miyazaki Prefecture, Japan	ShioinousoPT	approx. 32°45'15"N 131°20'20"E	Kamura Fm	Induan (Griesbachian)	0.16 above base	limestone
05.7.15.h	Kamura, Miyazaki Prefecture, Japan	ShioinousoPT	approx. 32°45'15"N 131°20'20"E	Kamura Fm	Induan (Griesbachian)	0.45 above base	limestone
05.7.15.k	Kamura, Miyazaki Prefecture, Japan	ShioinousoPT	approx. 32°45'15"N 131°20'20"E	Kamura Fm	Induan (Griesbachian)	1.68 above base	limestone
05.7.15.n	Kamura, Miyazaki Prefecture, Japan	ShioinousoPT	approx. 32°45'15"N 131°20'20"E	Kamura Fm	Induan (Griesbachian)?	2.65 above base	limestone
05.7.15.o	Kamura, Miyazaki Prefecture, Japan	ShioinousoPT	approx. 32°45'15"N 131°20'20"E	Kamura Fm	Induan (Griesbachian)?	2.85 above base	limestone
05.7.15.p	Kamura, Miyazaki Prefecture, Japan	ShioinousoPT	approx. 32°45'15"N 131°20'20"E	Kamura Fm	Induan (Griesbachian/Dienerian)?	*ex situ* , from higher up, recovered at 3.45 above base	limestone
05.7.15.q	Kamura, Miyazaki Prefecture, Japan	ShioinousoPT	approx. 32°45'15"N 131°20'20"E	Kamura Fm	Induan (Griesbachian)?	4.0 above base	limestone
GR collection							
231 (test sample)	Hold with Hope, E Greenland	Kap Stosch, River 8-9			Upper Permian		Lime mudstone
090815-B	Hold with Hope, E Greenland	Kap Stosch, River 13 (E bank)	N74°00'5.2" W021°26'14.2" 339m	Wordie Creek Fm	Griesbachian	ex situ	
090815-E	Hold with Hope, E Greenland	Kap Stosch, River 13 (E bank)	N74°00'3.9" W021°26'12.1" >369m	Wordie Creek Fm	Griesbachian	ex situ	
090815-F	Hold with Hope, E Greenland	Kap Stosch, River 13 (E bank)	N74°00'3.9" W021°26'12.1" >369m	Wordie Creek Fm	Griesbachian	ex situ	shale / sandstone
090816-A	Hold with Hope, E Greenland	Kap Stosch, River 13-14	N74°00'18.1" W021°25'35.1" 207m	Schuchert Dal Fm	Changhsingian	ex situ	
090816-B	Hold with Hope, E Greenland	Kap Stosch, River 13-14	N74°00'18.1" W021°25'35.1" 207m	Schuchert Dal Fm	Changhsingian	ex situ	grey shale
090816-F	Hold with Hope, E Greenland	Kap Stosch, River 13-14	N74°00'07.0" W021°24'45.0" 213m	Ravnefjeld Fm?	Wuchiapingian	ex situ	black shale
090816-G	Hold with Hope, E Greenland	Kap Stosch, River 13-14	N74°00'07.0" W021°24'45.0" 213m	Ravnefjeld Fm?	Wuchiapingian	ex situ	

	mid-oceanic seamount			yes	N/A		
	mid-oceanic seamount			no	-		
	mid-oceanic seamount		*Palaeofusulina* zone	no	-		
	mid-oceanic seamount		*Palaeofusulina* zone	no	-		
	mid-oceanic seamount		*Hindeodus parvus* , *Isarcicella isarcica* , *Necgondolella carinata*	yes	N/A (*H. parvus* ?)		
	mid-oceanic seamount		*Hindeodus parvus* , *Isarcicella isarcica* , *Necgondolella carinata*	yes	Orchard		
	mid-oceanic seamount		*Hindeodus parvus* , *Isarcicella isarcica* , *Necgondolella carinata*	yes	N/A		
	mid-oceanic seamount			no	-		
	mid-oceanic seamount			no	-		
	mid-oceanic seamount			yes	Orchard		
	mid-oceanic seamount			no	-		
	mid-oceanic seamount			yes	N/A		
					N/A		
	shelf						
	basinal						
	basinal						

formic	395.82	0	395.82	picked		yes		BF, ES	BF, CN	(np)	(np)	N/A	JP106
formic	558.28	0	558.28	picked		no		-	-	(np)	(np)	N/A	
formic	128.14	0	128.14	picked		yes		ED	BF, ED	(np)	(np)	N/A	JP107–109
acetic	649.48	0	649.48	picked		no		-	-	(np)	(np)	N/A	
acetic	581.43	0	581.43	picked		yes		-	CN	(np)	(np)	N/A	
acetic	252.9	0	252.9	picked		yes		-	CN, BV, OS?	CN	(np)	(np)	
acetic	389.69	0	389.69	picked		yes		BF, ET	BF, ED, CN	(np)	(np)	N/A	JP110–113
acetic	458.25	0	458.25	picked		yes		BF, ET	BF	(np)	(np)	N/A	JP114–115
acetic	521.59	0	521.59	picked		yes		-	BF	(np)	(np)	N/A	
acetic	273.38	0	273.38	picked		yes		BF, CN, ED	BF, CN, EC, ED	BF, CN (pp)	(np)	(np)	JP116
acetic	253.52	0	253.52	picked		yes?		-	-	OS?	-(pp)	(np)	
acetic	867.61	0	867.61	picked		yes		BF	BF, ET, CN	(np)	(np)	N/A	JP117–118
				picked									
				to be examined									
				to be examined									
				to be examined									
				to be examined									GR2
				to be examined									GR11
				to be examined									GR3a, b
				to be examined									GR4, 5, 10

090816-H	Hold with Hope, E Greenland	Kap Stosch, River 13-14	N74°00'07.0" W021°24'45.0" 213m	Ravnefjeld Fm?	Wuchiapingian	ex situ	
090816-J	Hold with Hope, E Greenland	Kap Stosch, River 13-14	N74°00'16.3" W021°25'17.6" 187m	Ravnefjeld Fm/Schuchert Dal Fm? (below Claraia bed)	Changhsingian	ex situ	
090817-F	Hold with Hope, E Greenland	Kap Stosch, River 13	N74°00'9.0-10.0" W021°26'37.4-38.1" 300-330m	Wordie Creek Fm	Griesbachian	ex situ	
090817-G	Hold with Hope, E Greenland	Kap Stosch, River 13	N74°00'9.0-10.0" W021°26'37.4-38.1" 300-330m	Wordie Creek Fm	Griesbachian	ex situ	
090817-H	Hold with Hope, E Greenland	Kap Stosch, River 13	N74°00'9.0-10.0" W021°26'37.4-38.1" 300-330m	Wordie Creek Fm	Griesbachian	ex situ	
090817-N	Hold with Hope, E Greenland	Kap Stosch, River 13	N74°00'9.0-10.0" W021°26'37.4-38.1" 300-330m	Wordie Creek Fm	Griesbachian	ex situ	
090818-A	Hold with Hope, E Greenland	Kap Stosch, River 13-14	N74°00'18.1" W021°25'35.8" 207m	Schuchert Dal Fm	Changhsingian	ex situ	
090818-B	Hold with Hope, E Greenland	Kap Stosch, River 14 (W tributary)		Ravnefjeld Fm? - Schuchert Dal Fm	Changhsingian		lime
090818-C	Hold with Hope, E Greenland	Kap Stosch, River 14 (W tributary)		Ravnefjeld Fm? - Schuchert Dal Fm	Changhsingian		lime
090818-D	Hold with Hope, E Greenland	Kap Stosch, River 14 (W tributary)		Ravnefjeld Fm? - Schuchert Dal Fm	Changhsingian		lime
090818-E	Hold with Hope, E Greenland	Kap Stosch, River 14 (W tributary)		Ravnefjeld Fm? - Schuchert Dal Fm	Changhsingian		lime
090818-F	Hold with Hope, E Greenland	Kap Stosch, River 14 (W tributary)		Ravnefjeld Fm? - Schuchert Dal Fm	Changhsingian		lime
090818-G	Hold with Hope, E Greenland	Kap Stosch, River 14 (W tributary)		Ravnefjeld Fm? - Schuchert Dal Fm	Changhsingian		lime
090818-H	Hold with Hope, E Greenland	Kap Stosch, River 14 (W tributary)		Ravnefjeld Fm? - Schuchert Dal Fm (transition zone)	Changhsingian	in situ?	lime
090820-A	Hold with Hope, E Greenland	Kap Stosch, River 14	N73°59'53.6" W021°25'34.9" 389m	Wordie Creek Fm	Griesbachian	ex situ	
09.8.20.a	Hold with Hope, E Greenland	Kap Stosch, River 14			Griesbachian		lime
09.8.20.b	Hold with Hope, E Greenland	Kap Stosch, River 14			Griesbachian		lime
09.8.20.c	Hold with Hope, E Greenland	Kap Stosch, River 14			Griesbachian		lime
09.8.22.c	Hold with Hope, E Greenland	Kap Stosch, River 14		Schuchert Dal Fm (base, just above red layers)	Changhsingian		
090820-D	Hold with Hope, E Greenland	Kap Stosch, River 14 (base)	N74°00'7.1" W021°24'43.4" 213m	Ravnefjeld Fm	Wuchiapingian		
090825-A	E Greenland	Traill Ø	N72°46'36.0" W023°14'13.0" 476m	Schuchert Dal Fm - Wordie Creek Fm	Changhsingian		
090825-B	E Greenland	Traill Ø	N72°46'23.2" W023°14'05.2" 550m	Schuchert Dal Fm - Wordie Creek Fm	Changhsingian		lime

				to be examined									GR8
				to be examined									GR12
				to be examined									
				to be examined									
				to be examined									
				to be examined									
				to be examined									GR6, 7
				to be processed									
				to be processed									
				to be processed									
				to be processed									
				to be processed									
				to be processed									
				being processed									
				to be examined									
				to be processed									
				to be processed									
				to be processed									
													GR1
				to be examined									GR9a, b
				to be examined									
				to be processed									

090826-A	E Greenland	Traill Ø, E river	N72°46'55.1" W023°09'48.8" 160m	Ravnefjeld Fm?	Wuchiapingian?		lime
090826-B	E Greenland	Traill Ø, E river	N72°46'55.1" W023°09'48.8" 160m	Ravnefjeld Fm?	Wuchiapingian?		lime
090826-C	E Greenland	Traill Ø, E river	N72°46'55.1" W023°09'48.8" 160m	Ravnefjeld Fm?	Wuchiapingian?		lime
090826-D	E Greenland	Traill Ø, E river	N72°46'20.9" W023°11'22.7" 269m	Schuchert Dal Fm?	Changhsingian	ex situ	
090826-E	E Greenland	Traill Ø, E river	N72°46'20.9" W023°11'22.7" 269m	Schuchert Dal Fm/Wordie Creek Fm?	Changhsingian	ex situ	
090829-C a&b	Schuchert Dal, E Greenland	Fiskegrav	N71°32'1.3" W024°20'4.4" 48m	Wordie Creek Fm	Griesbachian	36	lime
090829-D a&b	Schuchert Dal, E Greenland	Fiskegrav	N71°32'1.3" W024°20'4.4" 48m	Wordie Creek Fm	Griesbachian	36.8	lime
090829-E a-d	Schuchert Dal, E Greenland	Fiskegrav	N71°32'1.3" W024°20'4.4" 48m	Wordie Creek Fm	Griesbachian	37.5	lime
090829-F a&b	Schuchert Dal, E Greenland	Fiskegrav	N71°32'1.3" W024°20'4.4" 48m	Wordie Creek Fm	Griesbachian	40.2	lime
090829-G a&b	Schuchert Dal, E Greenland	Fiskegrav	N71°32'1.3" W024°20'4.4" 48m	Wordie Creek Fm	Griesbachian	34.6	lime
090829-H a&b	Schuchert Dal, E Greenland	Fiskegrav	N71°32'1.3" W024°20'4.4" 48m	Wordie Creek Fm	Griesbachian	34.9	lime
090829-I a&b	Schuchert Dal, E Greenland	Fiskegrav	N71°32'1.3" W024°20'4.4" 48m	Wordie Creek Fm	Griesbachian	35.2	lime
090829-J a&b	Schuchert Dal, E Greenland	Fiskegrav	N71°32'1.3" W024°20'4.4" 48m	Wordie Creek Fm	Griesbachian	33.3	lime
090829-K a&b	Schuchert Dal, E Greenland	Fiskegrav	N71°32'1.3" W024°20'4.4" 48m	Wordie Creek Fm	Griesbachian	33.7	lime
090829-L a&b	Schuchert Dal, E Greenland	Fiskegrav	N71°32'1.3" W024°20'4.4" 48m	Wordie Creek Fm	Griesbachian	34.1	lime
090829-M a&b	Schuchert Dal, E Greenland	Fiskegrav	N71°32'1.3" W024°20'4.4" 48m	Wordie Creek Fm	Griesbachian	34.2	lime
090829-P	Schuchert Dal, E Greenland	Fiskegrav	N71°32'1.0" W024°20'1.6" 43m	Schuchert Dal Fm	Changhsingian	ex situ	
090829-Q	Schuchert Dal, E Greenland	Fiskegrav	N71°32'1.0" W024°20'1.6" 43m	Schuchert Dal Fm	Changhsingian	ex situ	
090830-A a&b	Schuchert Dal, E Greenland	Fiskegrav	N71°32'1.3" W024°20'4.4" 48m	Wordie Creek Fm (basal)	Changhsingian	10	lime
090830-B a-e	Schuchert Dal, E Greenland	Fiskegrav	N71°32'1.3" W024°20'4.4" 48m	Wordie Creek Fm	Changhsingian	12.8	lime
090830-D	Schuchert Dal, E Greenland	Fiskegrav	N71°32'1.3" W024°20'4.4" 48m	Wordie Creek Fm (basal)	Changhsingian	ex situ	
090830-E	Schuchert Dal, E Greenland	Fiskegrav	N71°32'1.6" W024°20'23.6" 32m	Schuchert Dal Fm	Changhsingian	ex situ	
090830-H	Schuchert Dal, E Greenland	Fiskegrav	N71°32'1.6" W024°19'52.3" 57m	Wordie Creek Fm	Griesbachian	ex situ	
090830-K	Schuchert Dal, E Greenland	Fiskegrav	N71°32'1.3" W024°20'4.4" 48m	Wordie Creek Fm (basal)	Changhsingian	10	lime

				to be processed									
				to be processed									
				to be processed									
				to be examined									
				to be examined									
				to be processed									
				to be processed									
				to be processed									
				to be processed									
				to be processed									
				to be processed									
				to be processed									
				to be processed									
				to be processed									
				to be processed									
				to be processed									
				to be examined									
				to be examined									
				to be processed									
				to be processed									
				to be examined									
				to be examined									
				to be examined									
				to be examined									

090830-L	Schuchert Dal, E Greenland	Fiskegrav	N71°32'1.3" W024°20'4.4" 48m	Wordie Creek Fm (basal)	Changhsingian	10	lime
SV collection							
SV-1	Lusitaniadalen, central Spitsbergen		N78°17'54.8" E016°43'59.3"	Deltadalen Mb, Vikinghøgda Fm	Changhsingian, uppermost		carbonate-rich concretion
SV-2	Lusitaniadalen, central Spitsbergen		N78°17'54.8" E016°43'59.3"	Deltadalen Mb, Vikinghøgda Fm	Changhsingian, uppermost		carbonate-rich concretion
US collection							
00.10.9.c	Palomino Ridge, N Nevada, USA			upper Gerster Fm	Guadalupian		
00.10.9.d	Palomino Ridge, N Nevada, USA			upper Gerster Fm	Guadalupian		
00.10.9.e	Palomino Ridge, N Nevada, USA			upper Gerster Fm	Guadalupian (Lopingian?)		
00.10.9.f	Palomino Ridge, N Nevada, USA			upper Gerster Fm	Guadalupian (Lopingian?)		
00.10.9.g	Palomino Ridge, N Nevada, USA			Thaynes Fm	Induan?		
00.10.9.i	Palomino Ridge, N Nevada, USA			Thaynes Fm	Induan?		
00.10.9.j	Palomino Ridge, N Nevada, USA			Thaynes Fm	Smithian		
02.9.9.a	northern Muddy Mountains, S Nevada, USA			Virgin Limestone Mb, Moenkopi Fm	Spathian		
	Legend						
	AM	Ammonoid			chondrichthyan-yielding samples		
	BF	Bony fish			specimen numbers for biogenic remains		
	BR	Bryozoa			specimen numbers for chondrichthyan remains		
	BV	Bivalves					
	CL	Coral					
	CN	Conodonts					
	CR	Crinoids					
	EC	Echinoids					
	EL	Elasmobranchs					
	ED	Elasmobranch denticles					
	ES	Elasmobranch spines					
	ET	Elasmobranch teeth					
	FM	Forams					
	GS	Gastropods					
	OS	Ostracods					
	SC	Spicules					
	SF	Shell fragments					
	SP	Spongy					
	TB	Tubes					
	VB	Vertebrae					
	(pp)	partly picked					
	(np)	not picked					

				no	-		Nabbefeld *et al.* 2010
mudstone					-		Nabbefeld *et al.* 2010
				no	-		
				no	-		
				yes	N/A		
				no	-		
				yes	?		
				yes	Twitchett		
				yes	Twitchett		
				yes	N/A		

				to be examined									
acetic / formic	407.9		minimal	processing failed		yes		CL, FT	N/A	N/A	N/A	N/A	-
acetic	113.83		113.83	picked		yes		ET	ET	(np)	(np)	(np)	SV01
acetic / formic	535.23	0	535.23	picked	NOTE: residue retrieved once processing finished	yes		CL/BR, VB, EC, BV	CL/BR, VB, EC, GS	CL/BR (pp)	(np)	(np)	
acetic	1324.6	0	1324.59	picked	NOTE: residue only retrieved daily in later stage	yes		SC, SF, CL, GS (pp)	SC, BF (pp)	(np)	(np)	(np)	
acetic / formic	282.52	0	282.52	picked	NOTE: residue retrieved once processing finished	yes		CR, SC, SF	CN, SC, GS	(np)	(np)	(np)	
acetic / formic	272.89	0	272.89	picked	NOTE: residue only retrieved daily in later stage	no		-	-	(np)	(np)	(np)	
acetic	125.67	0	125.67	picked	NOTE: residue retrieved once processing finished	yes		CR?, SC, TB, SP	CN, SC, TB, SP	- (pp)	(np)	(np)	
acetic	303.51	0	303.51	picked	NOTE: residue retrieved once processing finished	yes		GS, SF	CN, GS, SF	CN, GS, BV, SF	- (pp)	- (pp)	
acetic	1181.2	0	1181.2	picked	NOTE: residue retrieved once processing finished	yes		CN, GS, SC, SF	GS, EC, SC, SF, VB?	GS, EC, SC, SF	- (pp)	- (pp)	
acetic	900.78	0	900.78	picked	NOTE: residue retrieved once processing finished	yes		CR, EC, GS	CR, EC, GS	CN, GS	(np)	(np)	

A1.2. GEOLOGICAL SURVEY OF CANADA (GSC) COLLECTION

A1.2.1 SAMPLE DATA – OMAN

List of original sample numbers, corresponding GSC localities, and respective sample weights for all samples from Oman.

Sample number	GSC locality	Sample weight
84 TE 103A-1	c-177651	<500
84 TE 103A-2	c-177652	<500
84 TE 103B	c-117673	<500
84 TE 103C	c-117674	<500
84 TE 104A	c-177653	<500
84 TE 104 B/C	c-177654	<500
84 TE 117A-1	c-117658	N/A
84 TE 117A-2	c-117659	N/A
84 TE c.85314	o-177663	<500
91OF-TE-118B	c-202251	<500
92 OF WA 22		N/A

A1.2.2 SAMPLE AND SPECIMENS NUMBERS – OMAN

List of original specimen numbers and corresponding collection numbers for specimens in the GSC collection occurring in samples from Oman.

Sample nr.	Spec. nr	GSC coll. nr	Identification
84 TE 103A-1	1	GSC135614	Genus S sp. T
	2	GSC135615	Genus S sp. T
	3	GSC135616	Genus S sp. T
	4	GSC135617	Genus S sp. T
	5	GSC135618	Genus S sp. T
	6	GSC135619	Genus S sp. T
	7	GSC135620	Genus S sp. T
	8	GSC135621	Genus S sp. T
	9	GSC135622	Genus S sp. T
	10	GSC135623	Genus S sp. T
	11	GSC135624	Genus S sp. T
	12	GSC135625	Genus S sp. T
	13	GSC135626	Genus S sp. T
	14	GSC135627	Genus S sp. T
	15	GSC135628	*Omanoselache* sp. H
	16	GSC135629	Genus P sp. P
	17	GSC135630	Genus P sp. P
	18	GSC135631	Genus P sp. P
	19	GSC135632	Indet. elasmobranch
	20	GSC135633	Genus S sp. T
	21	GSC135634	Genus P sp. P
	22	GSC135635	Indet.
	23	GSC135636	Indet.
	24	GSC135637	Dermal denticle
	25	GSC135638	cf. Genus P sp. P
	26	GSC135639	Indet. elasmobranch
	27	GSC135640	Genus S sp. T
	28	GSC135641	cf. Genus P sp. P
	29	GSC135642	cf. Genus S sp. T
	30	GSC135643	cf. Genus S sp. T
	31	GSC135644	cf. Genus S sp. T

	32	GSC135645	Indet.
	33	GSC135646	Indet.
	34	GSC135647	Genus S sp. T
	35	GSC135648	Bony fish tooth
84 TE 103A-2	36	GSC135649	Genus P sp. P
	37	GSC135650	*Omanoselache* sp. H
	38	GSC135651	Genus S sp. T
	39	GSC135652	cf. Genus S sp. T
	40	GSC135653	cf. Genus S sp. T
	41	GSC135654	cf. Genus S sp. T
	42	GSC135655	*Omanoselache* sp. H
	43	GSC135656	cf. Genus S sp. T
	44	GSC135657	Bony fish jaw fragment
	45	GSC135658	Indet.
84 TE 103B	46	GSC135659	Euselachii gen. et sp. indet.
	47	GSC135660	Genus S sp. T
	48	GSC135661	cf. Genus S sp. T
	49	GSC135662	cf. Genus S sp. T
	50	GSC135663	Genus S sp. T
	51	GSC135664	Genus S sp. T
	52	GSC135665	Indet. elasmobranch
	53	GSC135666	Genus S sp. T
	54	GSC135667	Bony fish jaw fragment
	55	GSC135668	Dermal denticle? / Tooth fragment?
	56	GSC135669	Bony fish tooth fragment
	57	GSC135670	Indet.
	58	GSC135671	Dermal denticle
	59	GSC135672	Bony fish tooth?
	60	GSC135673	Spine? / Bony fish tooth?
84 TE 103C	61	GSC135674	Genus S sp. T
	62	GSC135675	cf. Genus S sp. T
	63	GSC135676	Genus S sp. T
	64	GSC135677	Genus S sp. T
	65	GSC135678	Genus S sp. T
	66	GSC135679	Genus S sp. T
	67	GSC135680	cf. Genus S sp. T
	68	GSC135681	Genus S sp. T
	69	GSC135682	Genus S sp. T
	70	GSC135683	Genus S sp. T
	71	GSC135684	Indet. elasmobranch
	72	GSC135685	Genus S sp. T
	73	GSC135686	Genus S sp. T
	74	GSC135687	Euselachii gen. et sp. indet.
	75	GSC135688	Genus S sp. T
	76	GSC135689	Genus S sp. T
	77	GSC135690	Genus S sp. T
	78	GSC135691	*Omanoselache* sp. H
	79	GSC135692	Genus S sp. T
	80	GSC135693	Genus P sp. P
	81	GSC135694	Genus S sp. T
	82	GSC135695	Genus S sp. T
	83	GSC135696	Genus S sp. T
	84	GSC135697	Genus S sp. T
	85	GSC135698	cf. Genus S sp. T
	86	GSC135699	Genus S sp. T

	87	GSC135700	cf. Genus S sp. T
	88	GSC135701	Genus S sp. T
	89	GSC135702	cf. Genus S sp. T
	90	GSC135703	Genus S sp. T
	91	GSC135704	*Omanoselache* sp. H
	92	GSC135705	Genus S sp.
	93	GSC135706	cf. Genus S sp. T
	94	GSC135707	Genus S sp. T
	95	GSC135708	Genus S sp. T
	96	GSC135709	Genus S sp.
	97	GSC135710	cf. Genus S sp.
	98	GSC135711	Genus S sp. T
	99	GSC135712	cf. Genus S sp. T
	100	GSC135713	Genus S sp. T
	101	GSC135714	Indet. elasmobranch
	102	GSC135715	Genus S sp. T
	103	GSC135716	Bony fish jaw fragment
	104	GSC135717	cf. Genus S sp. T
	105	GSC135718	Indet. elasmobranch
	106	GSC135719	Indet. elasmobranch
	107	GSC135720	Indet. elasmobranch
	108	GSC135721	cf. Genus S sp. T
	109	GSC135722	*Omanoselache* sp. H
	110	GSC135723	cf. Genus P sp. P
	111	GSC135724	Genus S sp.
	112	GSC135725	Genus S sp. T
	113	GSC135726	cf. Genus S sp.
	114	GSC135727	*Omanoselache* sp. H
	115	GSC135728	Synechodontiform?
	116	GSC135729	*Omanoselache* sp. H
	117	GSC135730	Synechodontiform?
	118	GSC135731	Synechodontiform?
	119	GSC135732	Indet. elasmobranch
	120	GSC135733	Indet. elasmobranch
	121	GSC135734	Synechodontiform?
	122	GSC135735	Genus P sp. P
	123	GSC135736	cf. *Amelacanthus* sp.
	124	GSC135737	cf. *Amelacanthus* sp.
	125	GSC135738	Genus S sp. T
	126	GSC135739	Genus S sp. T
	127	GSC135740	Genus S sp. T
	275 (lot)	GSC135741	Dermal denticles
	128	GSC135742	cf. Genus S sp. T
	129	GSC135743	Indet. elasmobranch
	130	GSC135744	Bony fish tooth
	131	GSC135745	Dermal denticle
	132	GSC135746	Indet. elasmobranch
84 TE 104A	133	GSC135747	Indet. elasmobranch
	134	GSC135748	Indet. elasmobranch
	135	GSC135749	cf. Genus S sp. T
	136	GSC135750	Genus S sp. T
	137	GSC135751	Genus P sp. P
	138	GSC135752	Genus P sp. P
	139	GSC135753	Genus S sp.
	140	GSC135754	Genus S sp. T

	141	GSC135755	Genus S sp. T
	142	GSC135756	Genus S sp. T
	143	GSC135757	Genus S sp. T
	144	GSC135758	Genus S sp. T
	145	GSC135759	Genus S sp. T
	146	GSC135760	Genus S sp. T
	147	GSC135761	Genus S sp. T
	148	GSC135762	cf. Genus S sp. T
	149	GSC135763	Bony fish jaw fragment
	150	GSC135764	cf. Genus S sp. T
	151	GSC135765	cf. Genus S sp. T
	152	GSC135766	Genus P sp. P
	153	GSC135767	cf. Genus S sp. T
	154	GSC135768	cf. Genus S sp. T
	155	GSC135769	cf. Genus S sp. T
	156	GSC135770	*Omanoselache* sp. H
	157	GSC135771	Genus S sp. T
	158	GSC135772	Genus S sp. T
	159	GSC135773	cf. Genus S sp. T
	160	GSC135774	Genus S sp. T
	161	GSC135775	cf. Genus S sp. T
	162	GSC135776	Genus S sp. T
	163	GSC135777	cf. Genus S sp. T
	164	GSC135778	Genus S sp. T
	165	GSC135779	Dermal denticle
	166	GSC135780	Genus S sp. T
	167	GSC135781	Genus S sp. T
	168	GSC135782	cf. Genus S sp. T
	169	GSC135783	cf. Genus S sp. T
	170	GSC135784	cf. Genus S sp. T
	171	GSC135785	cf. Genus S sp. T
	172	GSC135786	cf. Genus S sp. T
	173	GSC135787	Genus S sp. T
	174	GSC135788	Genus S sp. T
	175	GSC135789	Genus P sp. P
	176	GSC135790	cf. Genus S sp. T
	177	GSC135791	cf. Genus S sp. T
	178	GSC135792	cf. Genus S sp. T
	179	GSC135793	*Omanoselache* sp. H
	180	GSC135794	Genus P sp. P
	181	GSC135795	Indet. elasmobranch
	182	GSC135796	cf. Genus S sp. T
	183	GSC135797	Indet. elasmobranch
	184	GSC135798	Indet. elasmobranch
	185	GSC135799	Genus P sp. P
	186	GSC135800	cf. Genus S sp. T
	187	GSC135801	cf. Genus S sp. T
	188	GSC135802	cf. Genus S sp. T
	189	GSC135803	cf. Genus S sp. T
	190	GSC135804	cf. Genus S sp. T
	191	GSC135805	cf. Genus S sp. T
	192	GSC135806	cf. Genus S sp. T
	193	GSC135807	cf. Genus S sp. T
	194	GSC135808	Genus S sp. T
	195	GSC135809	Bony fish jaw fragment

	196	GSC135810	Genus S sp. T
	197	GSC135811	Bony fish jaw fragment
	198	GSC135812	Genus S sp. T
	199	GSC135813	Bony fish jaw fragment
	200	GSC135814	Genus S sp. T
	201	GSC135815	*Omanoselache* sp. H
	202	GSC135816	Indet. elasmobranch
	203	GSC135817	Indet. elasmobranch
	276 (lot)	GSC135818	Dermal denticles
	204	GSC135819	Euselachii gen. et sp. indet.
	205	GSC135820	Genus P sp. P
	206	GSC135821	Indet. elasmobranch
	207	GSC135822	Indet. elasmobranch
	208	GSC135823	Indet. elasmobranch
	209	GSC135824	Indet. elasmobranch
	210	GSC135825	Synechodontiform?
	211	GSC135826	Bony fish tooth?
	212	GSC135827	Bony fish tooth?
	213	GSC135828	cf. Genus S sp. T
	214	GSC135829	cf. Genus S sp. T
	215	GSC135830	cf. Genus S sp. T
	216	GSC135831	Indet. elasmobranch
	217	GSC135832	Bony fish jaw fragment
	218	GSC135833	Indet. elasmobranch
	219	GSC135834	cf. Genus S sp. T
	220	GSC135835	Genus S sp. T
	221	GSC135836	Indet. elasmobranch
	222	GSC135837	Bony fish jaw fragment
	223	GSC135838	Indet. elasmobranch
	224	GSC135839	Indet. elasmobranch
	225	GSC135840	cf. Genus P sp. P
	226	GSC135841	cf. Genus S sp. T
84 TE 104 B/C	227	GSC135842	Genus S sp. T
	228	GSC135843	Genus S sp. T
	229	GSC135844	Indet. elasmobranch
	230	GSC135845	Genus S sp. T
	231	GSC135846	Genus S sp. T
	232	GSC135847	Genus S sp. T
	233	GSC135848	Genus S sp. T
	234	GSC135849	Genus P sp. P
	235	GSC135850	Indet. elasmobranch
	236	GSC135851	Indet. elasmobranch
	237	GSC135852	Indet. elasmobranch
	238	GSC135853	Indet. elasmobranch
	239	GSC135854	Indet. elasmobranch
84 TE 117A-1	240	GSC135855	Genus P sp. P
	241	GSC135856	Genus S sp. T
	242	GSC135857	Dermal denticle
	243	GSC135858	Indet. elasmobranch
	244	GSC135859	Indet. elasmobranch
	245	GSC135860	Indet.
84 TE 117A-2	246	GSC135861	Genus P sp. P
84 TE c.85314	247	GSC135862	cf. Genus S sp. T
	248	GSC135863	Genus S sp. T

	249	GSC135864	Genus S sp. T
	250	GSC135865	*Omanoselache* sp. H
	251	GSC135866	Genus S sp. T
	252	GSC135867	Genus S sp. T
	253	GSC135868	Genus S sp. T
	254	GSC135869	*Omanoselache* sp. H
	255	GSC135870	*Omanoselache* sp. H
	256	GSC135871	Bony fish jaw fragment
	257	GSC135872	Bony fish jaw fragment
91OF-TE-118B	258	GSC135873	Indet. elasmobranch
	259	GSC135874	Indet. elasmobranch
	260	GSC135875	Bony fish tooth + jaw fragment
	261	GSC135876	Indet. elasmobranch
	262	GSC135877	Indet. elasmobranch
	263	GSC135878	Bony fish tooth
	264	GSC135879	Bony fish tooth
	265	GSC135880	*Omanoselache* sp. H
	266	GSC135881	Dermal denticle
	267	GSC135882	Indet. elasmobranch
	268	GSC135883	Dermal denticle
	269	GSC135884	Bony fish jaw fragment
92 OF WA 22	270	GSC135885	Synechodontiform?
	271	GSC135886	Genus P sp. P
	272	GSC135887	Genus S sp. T
	273	GSC135888	Indet.
	274	GSC135889	Bony fish tooth

A1.2.3 Abundance data – Oman

Absolute abundances (AA) and relative abundances (RA) for all taxa in the GSC collection occurring in samples from Oman, supplemented by material from the OM collection.

	Omanoselache		**Euselachii indet.**		**Genus S**		**Genus P**		**cf. *Amelacanthus***		**Specimen abundance**	**Genus abundance**
Sample	AA	RA	AA	RA	AA	RA	AA	RA	AA	RA		
Olenekian												
103A-1	1	0.04		0.00	20	0.74	6	0.22		0.00	**27**	3
103A-2	2	0.25		0.00	5	0.63	1	0.13		0.00	**8**	3
103B		0.00	1	0.14	6	0.86		0.00		0.00	**7**	2
103C	5	0.09	1	0.02	45	0.80	3	0.05	2	0.04	**56**	5
104A	3	0.04	1	0.01	56	0.82	8	0.12		0.00	**68**	4
104 B/C		0.00		0.00	6	0.86	1	0.14		0.00	**7**	2
c.85314	3	0.33		0.00	6	0.67		0.00		0.00	**9**	2
117A-1		0.00		0.00	1	0.50	1	0.50		0.00	**2**	2
117A-2		0.00		0.00		0.00	1	1.00		0.00	**1**	1
118B	1	1.00		0.00		0.00		0.00		0.00	**1**	1
WA 22		0.00		0.00	1	0.50	1	0.50		0.00	**2**	2
110222-B		0.00		0.00	1	1.00		0.00		0.00	**1**	1
Totals	**15**	**0.08**	**3**	**0.02**	**147**	**0.78**	**22**	**0.12**	**2**	**0.01**	**189**	N/A
Induan												
100224-G		0.00		0.00		0.00	1	1.00		0.00	**1**	1
01.1.15c	5	1.00		0.00		0.00		0.00		0.00	**5**	1
Totals	**5**	**0.83**	**0**	**0.00**	**0**	**0.00**	**1**	**0.17**	**0**	**0.00**	**6**	N/A

A1.2.4 Sample and specimen numbers – global

List of sample numbers and specimen numbers for specimens in the GSC collection occurring in samples from global localities.

Locality	**Sample nr**	**Spec. nr**	**Identification**
Guling, Spiti, India	95-OF GU-1	450	*Omanoselache* sp. A
Timor	30/09/2003	451	Genus S sp.
		452–453	Indet. elasmobranch tooth
		454	Indet.
Meishan, China	88 OF CHXD-5	362	Indet. elasmobranch tooth cusp
Guandao, China	05 OF O-3	363	Genus S sp. cf. Genus S sp. T?
	05 OF O-6	364–365	Indet. non-elasmobranch
	05 OF O-10	366	*Synechodus* sp. (pre-Jurassic)
		367	Synechodontiform indet.
		368	*Omanoselache* sp. cf. *O.* sp. H
	05 OF O-11	369	Genus S sp. cf. Genus S sp. T?
		370	Genus S sp. A
		371	Genus S sp. cf. Genus S sp. T
	05 OF O-12	372	Indet. non-elasmobranch
	05 OF O-13	373	Genus S sp. cf. Genus S sp. T
		374	*Omanoselache* sp. cf. *O.* sp. A
	05 OF O-14	375	cf. Genus P

		376	Genus S sp. cf. Genus S sp. T
		377	Indet.
		378	Genus S sp. cf. Genus S sp. T
	05 OF O-15	379	Genus S sp. cf. Genus S sp. T
		380	*Omanoselache* sp. A
		381–382	Indet.
		383	cf. *Palidiplospinax* sp.
		384	Synechodontiform indet.
	05 OF O-16	385–386	*Omanoselache* sp. cf. *O.* sp. A
	05 OF O-18	387	*Omanoselache* sp. cf. *O.* sp. A
	05 OF O-19	388	Indet.
	05 OF O-21	389–390	*Omanoselache* sp. cf. *O.* sp. A
	05 OF O-22	391–392	Genus S sp. cf. Genus S sp. T
	05 OF O-23	393	Synechodontiform indet.
		394	cf. Genus P
	05 OF O-24	395	Indet.
		396	cf. *Palidiplospinax* sp.
	05 OF O-25	397–398	Indet. elasmobranch
	05 OF O-26	399	Actinopterygian tooth
		400	Indet.
	05 OF O-27	401	*Omanoselache* sp. cf. *O.* sp. H
		402	Genus S sp. cf. Genus S sp. T
	05 OF O-28	403	Genus S sp. cf. Genus S sp. T
		404	Genus S sp. A
	05 OF O-29	405	*Synechodus* sp. (pre-Jurassic)
		406–407	Genus S sp. cf. Genus S sp. T
	05 OF O-31	408	Genus S sp. cf. Genus S sp. T ?
		409	cf. Genus P
		410	*Synechodus* sp. (pre-Jurassic)
	05 OF O-34	411–412	Genus S sp. cf. Genus S sp. T
	05 OF O-36	413	Genus S sp. A
		414–415	Genus S sp. cf. Genus S sp. T
		416	Indet.
		417	Genus S sp. cf. Genus S sp. T
	05 OF O-38	418	Synechodontiform indet.
	05 OF O-40	419	*Omanoselache* sp. cf. *O.* sp. A
		420	cf. Genus P
		421–422	Genus S sp. cf. Genus S sp. T
		423	*Omanoselache* sp. cf. *O.* sp. A
	05 OF O-41	424	Genus S sp. cf. Genus S sp. T
	GQC-173	425	*Omanoselache* sp. cf. *O.* sp. H
	GQC-182	426	*Omanoselache* sp. cf. *O.* sp. H
		427	cf. Genus P
		428	*Omanoselache* sp. cf. *O.* sp. H
		429	Indet.
		430–432	*Omanoselache* sp. cf. *O.* sp. H
	GQC 183B	433	*Omanoselache* sp. A
	GQC 184	434	Indet.
	c-306527 GDL-1	435–442	Indet. non-elasmobranch
	c-306561 GDL-55	443	Genus S sp. cf. Genus S sp. T
	c-306563 GDL-57	444	Genus S sp. cf. Genus S sp. T
Kuh-e-Ali Bashi,	9307 TE-72-	N/A (one	N/A

Iran	119A	spec., lost)	
Zal?, Iran	c-306362 02 OF KZK 10	275–277	Genus S sp. T
		278	Dermal denticle
		279	Synechodontiform indet.
		280	Indet.
		281	Synechodontiform indet.
		282	Actinopterygian tooth
		283	Indet.
	c-306363 02 OF KZK 34G	284–285	Indet.
	c-306365 02 OF KZM 21	286	Indet. non-elasmobranch
		287	Synechodontiformes indet.?
		288–291	Indet.
Dalsnuten, Spitsbergen	c-307115 O4-OF MH-DA-34	449	Indet. (non-elasmobranch)
British Columbia, Canada	c-303560 97 OF WAP-T33	448	Indet. (Actinopterygian?)
Ellesmere Island, Canadian Arctic	o-51663 93 OF TE-5 1663 62-TE 325A (strigatus)	445–446	*Caseodus* sp. cf. *C. varidentis*
		447	*Homalodontus* sp. cf. *H. aplopagus*
Bear Lake, Idaho, USA	c-301221 93 OF W-8	337–338	Indet. non-elasmobranch
	c-301224 93 OF W-11	292	Genus S sp. T
		293	*Synechodus* sp. (pre-Jurassic)
		294	cf. Genus S sp. T
	c-301226 93 OF W-13	297, 648–649	*Synechodus* sp. (pre-Jurassic)
	o-64675 91-OF	305, 307–308, 310–313, 315–324	Indet. non-elasmobranch
		306, 309, 314	Indet. Elasmobranch
	o-64671 91-OF	325	*Synechodus* sp. (pre-Jurassic)
		326–327	cf. *Omanoselache* sp. indet.
		328	Indet. crown fragments, probably belonging to specimen 325
	o-64670 91-OF TE 30 3A	329	Dermal denticle?
	c-304703 99-IG CNA-AHC-24	349	Indet. non-elasmobranch
	c-304708 99-IG CNA-HS 4	350	Genus S sp. T
		351	Synechodontiform indet. cusp fragment
Crittenden Springs, Nevada, USA	c-301214 93 OF W-1	339–341	Indet. non-elasmobranch?
Salt Lake City, Utah, USA	c-301227 93 OF W-14	342	Indet. non-elasmobranch
		343	Genus S sp. T
		344	Actinopterygian?
		345	Genus S sp. T

		346	Indet.
		347	Indet. elasmobranch
		348	Dermal denticle
Cowboy Pass, Utah, USA	c-306809 02 OF CP-C1-BASE	360	cf. *Synechodus* sp. (pre-Jurassic)
		361	Indet. elasmobranch
Nevada, USA	c-176319	335	Dermal denticle?
Humboldt Range, Nevada, USA	c-201552 91 OF HB110	336	Dermal denticle – morphotype 25
Bloody Canyon	c-159815 89 OF HB236	330	*Omanoselache* sp. cf. *O.* sp. H
		331	Elasmobranch tooth fragment
		332	Indet.
		333	Indet. spine?
		334	Dermal denticle
Coyote Canyon	c-300257 92 OF COY 4	352–353	Dermal denticles – morphotype 25
		354	Elasmobranch spine fragment?
		355	Ctenacanth? dermal denticle?
		356	Dermal denticle – morphotype 25
		357	Ctenacanth? dermal denticle
		358	Elasmobranch crown fragment?
		359	Indet. elasmobranch?
Darwin Canyon, California, USA	c-202664 92-OF DC10	298–299	*Omanoselache* sp. cf. *O.* sp. H
		300–304	cf. *Hybodus* sp.

A1.2.5 ABUNDANCE DATA – CHINA

Absolute abundances (AA) and relative abundances (RA) for all taxa in the GSC collection occurring in samples from China.

	Omanoselache		**cf. *Pali-diplospinax***		**Genus *S***		***Synechodus* (pre-Jurassic)**		**cf. Genus P**		**other Synecho-dontiformes**		**other Elasmo-branchii**		**Spec.men abundance**	**Genus abundance**
Sample	AA	RA	AA	RA	AA	RA	AA	RA	AA	RA	AA	RA	AA	RA		
Olenekian																
O-3		0.00		0.00	1	1.00		0.00		0.00		0.00		0.00	**1**	1
O-10	1	0.33		0.00		0.00	1	0.33		0.00	1	0.33		0.00	**3**	3
O-11		0.00		0.00	3	1.00		0.00		0.00		0.00		0.00	**3**	1
O-13	1	0.50		0.00	1	0.50		0.00		0.00		0.00		0.00	**2**	2
O-14		0.00		0.00	2	0.67		0.00	1	0.33		0.00		0.00	**3**	2
O-15	1	0.25	1	0.25	1	0.25		0.00		0.00	1	0.25		0.00	**4**	4
O-16	2	1.00		0.00		0.00		0.00		0.00		0.00		0.00	**2**	1
O-18	1	1.00		0.00		0.00		0.00		0.00		0.00		0.00	**1**	1
O-21	2	1.00		0.00		0.00		0.00		0.00		0.00		0.00	**2**	1
O-22		0.00		0.00	2	1.00		0.00		0.00		0.00		0.00	**2**	1
O-23		0.00		0.00		0.00		0.00	1	0.50	1	0.50		0.00	**2**	2
O-24		0.00	1	1.00		0.00		0.00		0.00		0.00		0.00	**1**	1
O-25		0.00		0.00		0.00		0.00		0.00		0.00	2	1.00	**2**	1
O-27	1	0.50		0.00	1	0.50		0.00		0.00		0.00		0.00	**2**	2
O-28		0.00		0.00	2	1.00		0.00		0.00		0.00		0.00	**2**	1
O-29		0.00		0.00	2	0.67	1	0.33		0.00		0.00		0.00	**3**	2
O-31		0.00		0.00	1	0.33	1	0.33	1	0.33		0.00		0.00	**3**	3
O-34		0.00		0.00	2	1.00		0.00		0.00		0.00		0.00	**2**	1
O-36		0.00		0.00	4	1.00		0.00		0.00		0.00		0.00	**4**	1
O-38		0.00		0.00		0.00		0.00		0.00	1	1.00		0.00	**1**	1
O-40	2	0.40		0.00	2	0.40		0.00	1	0.20		0.00		0.00	**5**	3
Totals	**11**	**0.22**	**2**	**0.04**	**24**	**0.48**	**3**	**0.06**	**4**	**0.08**	**4**	**0.08**	**2**	**0.04**	**50**	N/A

	Omanoselache		cf. *Pali-diplospinax*		Genus S		*Synechodus* (pre-Jurassic)		cf. Genus P		other Synecho-dontiformes		other Elasmo-branchii		Spec.men abundance	Genus abundance
Sample	AA	RA	AA	RA	AA	RA	AA	RA	AA	RA	AA	RA	AA	RA		
Anisian																
O-41		0.00		0.00	1	1.00		0.00		0.00		0.00		0.00	**1**	1
GQC173	1	1.00		0.00		0.00		0.00		0.00		0.00		0.00	**1**	1
GQC182	5	0.83		0.00		0.00		0.00	1	0.17		0.00		0.00	**6**	2
GQC183B	1	1.00		0.00		0.00		0.00		0.00		0.00		0.00	**1**	1
GDL55		0.00		0.00	1	1.00		0.00		0.00		0.00		0.00	**1**	1
GDL57		0.00		0.00	1	1.00		0.00		0.00		0.00		0.00	**1**	1
Totals	**7**	**0.64**	**0**	**0.00**	**3**	**0.27**	**0**	**0.00**	**1**	**0.09**	**0**	**0.00**	**0**	**0.00**	**11**	N/A

A1.3. UNIVERSITY OF CALGARY (UC) COLLECTION

A1.3.1 SAMPLE AND SPECIMEN NUMBERS – OMAN

List of original sample numbers and specimen numbers with corresponding collection numbers for specimens in the UC collection occurring in samples from Oman.

Sample nr	Spec. nr	UC coll. nr	Identification
621-2	474	UC20230	cf. Genus P
965-1	475	UC20231	*Reesodus underwoodi*
965-2	476	UC20232	*Khuffia prolixa*
	477	UC20233	*Omanoselache hendersoni*
	478	UC20234	*Reesodus underwoodi*
	479	UC20235	*Reesodus underwoodi*
	480	UC20236	indet. elasmobranch
	481	UC20237	indet. elasmobranch
	482	UC20238	helodont?
	483	UC20239	*Glikmanius* cf. *myachkovensis*
	484	UC20240	*Gunnellodus bellistriatus*
	485	UC20241	*Gunnellodus bellistriatus*
	486	UC20242	*Gunnellodus bellistriatus*
	487	UC20243	dermal denticle
	488	UC20244	dermal denticle
	489	UC20245	dermal denticle
	490	UC20246	dermal denticle
	491	UC20247	dermal denticle
	492	UC20248	indet. elasmobranch tooth
	493	UC20249	indet.
	494	UC20250	indet.
	495	UC20251	indet.
	496	UC20252	bony fish tooth
	497	UC20253	bony fish tooth
	498	UC20254	indet. non-elasmobranch?
	499	UC20255	*Omanoselache hendersoni*
	500	UC20256	cf. *Omanoselache hendersoni*
	501	UC20257	*Omanoselache hendersoni*
	502	UC20258	*Teresodus amplexus*
	503	UC20259	*Omanoselache hendersoni*
	504	UC20260	*Teresodus amplexus*
	505	UC20261	*Teresodus amplexus*
	506	UC20262	*Omanoselache hendersoni*
	507	UC20263	*Teresodus amplexus*
	508	UC20264	*Omanoselache hendersoni*
	509	UC20265	*Omanoselache hendersoni*
	510	UC20266	*Teresodus amplexus*
	511	UC20267	*Omanoselache hendersoni*
	512	UC20268	Hybodontiformes indet.
	513	UC20269	*Reesodus underwoodi*
	514	UC20270	*Khuffia lenis*
	515	UC20271	*Omanoselache hendersoni*
	516	UC20272	Eugeneodontiformes?
	517	UC20273	cf. *Omanoselache angiolinii*
	518	UC20274	*Teresodus amplexus*
	519	UC20275	*Omanoselache hendersoni*
	520	UC20276	indet. elasmobranch
	521	UC20277	Hybodontiformes indet.

	522	UC20278	*Omanoselache hendersoni*
	523	UC20279	*Teresodus amplexus*
	524	UC20280	Hybodontiformes indet.
	525	UC20281	*Khuffia lenis*
	526	UC20282	*Omanoselache hendersoni*
	527	UC20283	indet. elasmobranch
	528	UC20284	indet. elasmobranch
	529	UC20285	*Omanoselache hendersoni*
	530	UC20286	*Teresodus amplexus*
	531	UC20287	*Gunnellodus bellistriatus*
	532	UC20288	*Gunnellodus bellistriatus*
	533	UC20289	*Khuffia lenis*
	534	UC20290	*Reesodus underwoodi*
	535	UC20291	cf. *Omanoselache hendersoni*
	536	UC20292	Hybodontiformes indet.
	537	UC20293	Hybodontiformes indet.
	538	UC20294	*Omanoselache hendersoni*
	539	UC20295	indet. elasmobranch
	540	UC20296	indet. elasmobranch
	541	UC20297	*Teresodus amplexus*
	542	UC20298	*Omanoselache hendersoni*
	543	UC20299	*Omanoselache hendersoni*
	544	UC20300	Hybodontiformes indet.
	545	UC20301	*Omanoselache hendersoni*
	546	UC20302	Hybodontiformes indet.
	547	UC20303	*Glikmanius* cf. *myachkovensis*
	548	UC20304	*Glikmanius* indet.
	549	UC20305	*Glikmanius* cf. *myachkovensis*
	550	UC20306	*Teresodus amplexus*
	551	UC20307	indet. elasmobranch
	552	UC20308	indet. elasmobranch
	553	UC20309	indet. elasmobranch
	554	UC20310	Eugeneodontiformes?
	555	UC20311	cf. *Omanoselache hendersoni*
	556	UC20312	indet. elasmobranch
	557	UC20313	indet. elasmobranch
	558	UC20314	indet.
	559	UC20315	indet.
	560	UC20316	indet.
	561	UC20317	cf. *Khuffia lenis*
	562	UC20318	indet.
	563	UC20319	Hybodontiformes indet.
	564	UC20320	cf. *Gunnellodus bellistriatus*
	565	UC20321	*Gunnellodus bellistriatus*
	566	UC20322	dermal denticle
	567	UC20323	*Glikmanius* cf. *myachkovensis*
	568	UC20324	*Reesodus underwoodi*
	569	UC20325	*Khuffia lenis*
	570	UC20326	indet.
	571	UC20327	indet.
	572	UC20328	indet.
	573	UC20329	indet.
	574	UC20330	indet.
	575	UC20331	indet.
	576	UC20332	*Khuffia lenis*

	577	UC20333	indet.
	578	UC20334	indet.
	579	UC20335	indet.
	580	UC20336	*Omanoselache hendersoni*
	581	UC20337	*Omanoselache hendersoni*
965-3	582	UC20338	*Glikmanius* cf. *myachkovensis*
	583	UC20339	indet.
	584	UC20340	indet. elasmobranch
	585	UC20341	*Gunnellodus bellistriatus*
965-4	586	UC20342	bony fish jaw fragment
	587	UC20343	bony fish tooth
	588	UC20344	dermal denticle
	589	UC20345	dermal denticle
	590	UC20346	Hybodontiformes indet.
965-5	641	UC20347	indet. elasmobranch
	642	UC20348	*Gunnellodus bellistriatus*
	643	UC20349	indet.
965-8	591	UC20350	*Glikmanius* indet.
	592	UC20351	*Gunnellodus bellistriatus*
	593	UC20352	dermal denticle
	594	UC20353	dermal denticle
	595	UC20354	indet.
	596	UC20355	indet.
	597	UC20356	*Omanoselache hendersoni*
	598	UC20357	cf. *Omanoselache hendersoni*
	599	UC20358	*Teresodus amplexus*
	600	UC20359	indet.
	601	UC20360	indet. elasmobranch
	602	UC20361	*Glikmanius* cf. *myachkovensis*
	603	UC20362	indet. elasmobranch
	604	UC20363	bony fish jaw fragment
	605	UC20364	indet.
	606	UC20365	indet.
965-9	607	UC20366	*Glikmanius* cf. *myachkovensis*
	608	UC20367	*Teresodus amplexus*
	609	UC20368	*Glikmanius* indet.
	610	UC20369	*Glikmanius* cf. *myachkovensis*
	611	UC20370	dermal denticle?
	612	UC20371	indet. elasmobranch tooth
	613	UC20372	dermal denticle - ctenacanth
	614	UC20373	dermal denticle - ctenacanth
	615	UC20374	dermal denticle
	616	UC20375	dermal denticle
	617	UC20376	dermal denticle
	618	UC20377	dermal denticle
	619	UC20378	dermal denticle
	620	UC20379	dermal denticle?
	621	UC20380	*Gunnellodus bellistriatus*
	622	UC20381	*Glikmanius* indet.
	623	UC20382	*Glikmanius* indet.
	624	UC20383	non-elasmobranch
	625	UC20384	*Gunnellodus bellistriatus*
	626	UC20385	Eugeneodontiformes?
969-4	627	UC20386	indet.
	628	UC20387	dermal denticle

	629	UC20388	dermal denticle
	630	UC20389	indet.
	631	UC20390	indet.
969-5	632	UC20391	cf. *Omanoselache angiolinii*
	633	UC20392	indet. elasmobranch tooth
	634	UC20393	indet. elasmobranch tooth
	635	UC20394	dermal denticle
	636	UC20395	dermal denticle
	637	UC20396	dermal denticle
	638	UC20397	dermal denticle
	639	UC20398	indet.
	640	UC20399	indet.
969-6	644	UC20400	cf. *Omanoselache angiolinii*
	645	UC20401	cf. *Omanoselache angiolinii*
	646	UC20402	indet. elasmobranch
	647	UC20403	indet. elasmobranch

A1.3.2 Sample and specimen data – Canadian Arctic

List of sample numbers and specimen numbers for specimens in the UC collection occurring in samples from the Canadian Arctic.

Sample nr	**Spec. nr**	**Identification**
CH-F36-79 HP	455	Elasmobranch tooth fragment?
CH-F78-79 HP-Aa coarse	456	Dermal denticle – morphotype 22
CH-F79-79 HP MSc samples	457	Dermal denticle – morphotype 23
CH-F104-79 MB	458	Indet. elasmobranch tooth fragment
CH-F136-79 HN	459	Homalodont? tooth fragment
	460	Striated elasmobranch cusp fragment
	461	*Adamantina* sp.
CH-F136-79 HN 2of2	462–463	*Adamantina* sp.
	464–468	Dermal denticles? – morphotype 24
	469	Indet. cusp fragment?
F-83	470	Indet.
	471	Indet. elasmobranch tooth fragment
T2 Blaa	472	Hybodont? main cusp
	473	Indet. elasmobranch tooth cusp?

A1.4. PALAEONTOLOGICAL MUSEUM OF THE UNIVERSITY OF MILAN (MPUM) COLLECTION

A1.4.1 SAMPLE AND SPECIMEN NUMBERS

List of original specimen numbers (with integrated sample numbers) and corresponding collection numbers for the MPUM collection.

Spec. nr	MPUM coll. nr	Type	Identification
AO1-0001	MPUM11002	lot	denticles
AO2-0001	MPUM11003	lot	denticles
AO3-0001	MPUM11004	lot	*Glikmanius* cf. *myachkovensis*, *G. culmenis*, *Gunnellodus bellistriatus*, *Deltodus* aff. *mercurei*, denticles
AO3b-0001	MPUM11005	lot	*Omanoselache hendersoni*
AO8-0001	MPUM11006	lot	*Glikmanius* cf. *myachkovensis*, *Gunnellodus bellistriatus*, denticles
AO9-0001	MPUM11007	lot	denticles
AO10-0001	MPUM11008	lot	*Omanoselache hendersoni*?, denticles
AO10b-0001	MPUM11009	lot	*Glikmanius* cf. *myachkovensis*, *G. culmenis*, *Omanoselache angiolinii*, *Teresodus amplexus*, *Gunnellodus bellistriatus*, denticles
AO11-0001	MPUM11010	lot	*Glikmanius* cf. *myachkovensis*, *Omanoselache hendersoni*, *O. angiolinii*, *Reesodus underwoodi*, *Gunnellodus bellistriatus*, Euselachii gen. et sp. indet., denticles
AO12-0001	MPUM11011	lot	*Gunnellodus bellistriatus*
AO15-0001	MPUM11012	lot	*Gunnellodus bellistriatus*, denticles
AO16-0001	MPUM11013	lot	*Glikmanius* cf. *myachkovensis*, denticles
AO17-0001	MPUM11014	lot	*Glikmanius* cf. *myachkovensis*, *Teresodus amplexus*, *Khuffia prolixa*?, denticles
AO19-0001	MPUM11015	lot	*Glikmanius* cf. *myachkovensis*, *G. culmenis*, *Omanoselache angiolinii*, denticles
AO22-0001	MPUM11016	lot	*Glikmanius* cf. *myachkovensis*, *G. culmenis*, *Omanoselache hendersoni*, denticles
AO24-0001	MPUM11017	lot	denticles
AO25-0001	MPUM11018	lot	*Omanoselache angiolinii*, *Reesodus underwoodi*, *Teresodus amplexus*, *Khuffia lenis*, *K. prolixa*, denticles
AO26-0001	MPUM11019	lot	*Glikmanius* cf. *myachkovensis*, *Omanoselache hendersoni*, *O. angiolinii*, cf. *Omanoselache* sp., *Reesodus underwoodi*, *Teresodus amplexus*, *Khuffia lenis*, *K. prolixa*?, denticles
AO32-0001	MPUM11020	lot	denticles
AO36-0001	MPUM11021	lot	*Glikmanius* cf. *myachkovensis*, *Omanoselache hendersoni*, *O. angiolinii*, *Teresodus amplexus*, *Gunnellodus bellistriatus*, *Khuffia lenis*,

			denticles
AO37-0001	MPUM11022	lot	*Glikmanius* cf. *myachkovensis*, *G. culmenis*, *Omanoselache hendersoni*, *O. angiolinii*, cf. *Omanoselache* sp., *Teresodus amplexus*, *Gunnellodus bellistriatus*, *Khuffia lenis*, denticles
AO38-0001	MPUM11023	lot	*Glikmanius* cf. *myachkovensis*, *G. culmenis*, *Omanoselache hendersoni*, *O. angiolinii*, *Teresodus amplexus*, *Gunnellodus bellistriatus*, *Khuffia lenis*, *K. prolixa*, denticles
AO38-0002	MPUM11024	specimen	Neoselachii gen. et sp. indet. A
AO40-0001	MPUM10880	specimen	*Gunnellodus bellistriatus*
AO40-0002	MPUM10881	specimen	*Khuffia lenis*
AO40-0003	MPUM10882	specimen	*Khuffia lenis*
AO40-0004	MPUM10883	specimen	*Omanoselache hendersoni*
AO40-0005	MPUM10884	specimen	*Omanoselache hendersoni*
AO40-0006	MPUM10885	specimen	*Omanoselache hendersoni*
AO40-0007	MPUM10886	specimen	cf. *Omanoselache* sp.
AO40-0008	MPUM10887	specimen	*Omanoselache angiolinii*
AO40-0009	MPUM10888	specimen	*Teresodus amplexus*
AO40-0010	MPUM10889	specimen	*Teresodus amplexus*
AO40-0011	MPUM10890	specimen	*Teresodus amplexus*
AO40-0012	MPUM10891	specimen	*Reesodus underwoodi*
AO40-0013	MPUM10892	specimen	*Khuffia prolixa*
AO40-0014	MPUM10893	lot	*Glikmanius* cf. *myachkovensis*
AO40-0015	MPUM10894	lot	*Glikmanius culmenis*
AO40-0016	MPUM10895	lot	*Gunnellodus bellistriatus*
AO40-0017	MPUM10896	lot	*Omanoselache hendersoni*
AO40-0018	MPUM10897	lot	cf. *Omanoselache* sp.
AO40-0019	MPUM10898	lot	*Omanoselache angiolinii*
AO40-0020	MPUM10899	lot	*Reesodus underwoodi*
AO40-0021	MPUM10900	lot	*Teresodus amplexus*
AO40-0022	MPUM10901	lot	*Khuffia lenis*
AO40-0023	MPUM10902	lot	*Khuffia prolixa*
AO40-0024	MPUM10903	specimen	*Deltodus* aff. *mercurei*
AO40-0025	MPUM10904	lot	denticles
AO40-0026	MPUM10905	specimen	*Nemacanthus* sp.
AO40-0027	MPUM10906	specimen	*Nemacanthus* sp.
AO40-0028	MPUM10907	specimen	*Amelacanthus* cf. *sulcatus*
AO40-0029	MPUM10908	lot	*Amelacanthus* cf. *sulcatus*
AO41-0001	MPUM11025	lot	*Glikmanius* cf. *myachkovensis*, *Omanoselache hendersoni*, cf. *Omanoselache* sp., *Reesodus underwoodi*, *Teresodus amplexus*, *Gunnellodus bellistriatus*, *Khuffia lenis*, *K. prolixa*, denticles
AO42-0001	MPUM11026	lot	denticles
AO43-0001	MPUM11027	lot	*Glikmanius* cf. *myachkovensis*, *Omanoselache angiolinii*
AO47b-0001	MPUM10926	specimen	*Glikmanius* cf. *myachkovensis*
AO47b-0002	MPUM10927	specimen	*Glikmanius* cf. *myachkovensis*
AO47b-0003	MPUM10928	specimen	*Glikmanius culmenis*
AO47b-0004	MPUM10929	specimen	*Omanoselache angiolinii*
AO47b-0005	MPUM10930	specimen	*Omanoselache angiolinii*

AO47b-0006	MPUM10931	specimen	Euselachii gen. et sp. indet.
AO47b-0007	MPUM10932	specimen	cf. ‘Palaeozoic Genus 1’ sp.
AO47b-0008	MPUM10933	lot	*Glikmanius* cf. *myachkovensis*
AO47b-0009	MPUM10934	lot	*Glikmanius culmenis*
AO47b-0010	MPUM10935	lot	*Gunnellodus bellistriatus*
AO47b-0011	MPUM10936	lot	*Omanoselache hendersoni*
AO47b-0012	MPUM10937	lot	cf. *Omanoselache* sp.
AO47b-0013	MPUM10938	lot	*Omanoselache angiolinii*
AO47b-0014	MPUM10939	lot	*Teresodus amplexus*
AO47b-0015	MPUM10940	specimen	*Khuffia lenis*
AO47b-0016	MPUM10941	lot	Euselachii gen. et sp. indet.
AO47b-0017	MPUM10942	lot	denticles
AO47b-0018	MPUM10943	lot	*Amelacanthus* cf. *sulcatus*
AO48-0001	MPUM11028	lot	*Glikmanius* cf. *myachkovensis*, denticles
AO50-0001	MPUM10944	specimen	denticle
AO50-0002	MPUM10945	specimen	*Cooleyella* cf. *fordi*
AO50-0003	MPUM10946	lot	*Glikmanius* cf. *myachkovensis*
AO50-0004	MPUM10947	lot	*Glikmanius culmenis*
AO50-0005	MPUM10948	lot	*Gunnellodus bellistriatus*
AO50-0006	MPUM10949	lot	*Omanoselache angiolinii*
AO50-0007	MPUM10950	lot	*Teresodus amplexus*
AO50-0008	MPUM10951	specimen	Euselachii gen. et sp. indet.
AO50-0009	MPUM10952	lot	denticles
AO50-0010	MPUM10953	specimen	*Amelacanthus* cf. *sulcatus*
AO51-0001	MPUM11029	lot	*Glikmanius* cf. *myachkovensis*, *Deltodus* aff. *mercurei*, denticles
AO52-0001	MPUM11030	lot	*Glikmanius* cf. *myachkovensis*, *Omanoselache hendersoni*, *Khuffia lenis*, denticles
AO54-0001	MPUM11031	lot	*Glikmanius* cf. *myachkovensis*, *Omanoselache angiolinii*, denticles
AO55-0001	MPUM10909	specimen	*Glikmanius culmenis*
AO55-0002	MPUM10910	specimen	*Glikmanius culmenis*
AO55-0003	MPUM10911	specimen	*Gunnellodus bellistriatus*
AO55-0004	MPUM10912	specimen	*Deltodus* aff. *mercurei*
AO55-0005	MPUM10913	specimen	*Deltodus* aff. *mercurei*
AO55-0006	MPUM10914	lot	*Glikmanius* cf. *myachkovensis*
AO55-0007	MPUM10915	lot	*Glikmanius culmenis*
AO55-0008	MPUM10916	lot	*Gunnellodus bellistriatus*
AO55-0009	MPUM10917	lot	*Omanoselache hendersoni*
AO55-0010	MPUM10918	lot	cf. *Omanoselache* sp.
AO55-0011	MPUM10919	lot	*Omanoselache angiolinii*
AO55-0012	MPUM10920	lot	*Teresodus amplexus*
AO55-0013	MPUM10921	lot	*Khuffia lenis*
AO55-0014	MPUM10922	lot	Euselachii gen. et sp. indet.
AO55-0015	MPUM10923	lot	*Deltodus* aff. *mercurei*
AO55-0016	MPUM10924	lot	denticles
AO55-0017	MPUM10925	lot	*Amelacanthus* cf. *sulcatus*
AO55-0018	MPUM11032	lot	*Solenodus* cf. *crenulatus*
AO56-0001	MPUM11033	lot	*Glikmanius* cf. *myachkovensis*, *G. culmenis*, *Omanoselache angiolinii*, *Gunnellodus bellistriatus*, *Deltodus* aff. *mercurei*, denticles
AO58-0001	MPUM11034	lot	*Glikmanius* cf. *myachkovensis*,

			Omanoselache angiolinii, denticles
AO61-0001	MPUM11035	lot	*Glikmanius* cf. *myachkovensis*, *Omanoselache hendersoni*, *Teresodus amplexus*, *Gunnellodus bellistriatus*
AO67-0001	MPUM11036	lot	*Omanoselache hendersoni*, *Teresodus amplexus*, denticles
AO72-0001	MPUM11037	lot	*Glikmanius* cf. *myachkovensis*, *Omanoselache angiolinii*
AO76b-0001	MPUM11038	lot	denticles
AO78-0001	MPUM11039	lot	denticles
AO79-0001	MPUM11040	lot	*Omanoselache hendersoni*
AO82-0001	MPUM11041	lot	*Glikmanius* cf. *myachkovensis*, denticles
AO86-0001	MPUM11042	lot	*Glikmanius culmenis*, *Omanoselache hendersoni*, *Khuffia lenis*, denticles
AOLTER-0001	MPUM11043	lot	*Glikmanius* cf. *myachkovensis*, *Teresodus amplexus*, *Gunnellodus bellistriatus*, *Khuffia lenis*, denticles
AO123-0001	MPUM11044	lot	*Glikmanius* cf. *myachkovensis*, *G. culmenis*, *Omanoselache angiolinii*, *Gunnellodus bellistriatus*, denticles
AO123-0002	MPUM11045	specimen	Euselachii gen. et sp. indet.
AO208-0001	MPUM11046	lot	*Glikmanius* cf. *myachkovensis*
AO210-0001	MPUM11047	lot	*Glikmanius* cf. *myachkovensis*, *G. culmenis*, *Omanoselache hendersoni*, *O. angiolinii*, cf. *Omanoselache* sp., *Reesodus underwoodi*, *Teresodus amplexus*, *Gunnellodus bellistriatus*, *Khuffia lenis*, *K. prolixa*, denticles
AO211-0001	MPUM11048	lot	*Glikmanius* cf. *myachkovensis*, *G. culmenis*, *Omanoselache hendersoni*, *O. angiolinii*, cf. *Omanoselache* sp., *Reesodus underwoodi*, *Teresodus amplexus*, *Gunnellodus bellistriatus*, *Khuffia lenis*, *K. prolixa*, Euselachii gen. et sp. indet., denticles
AO214-0001	MPUM11049	lot	*Glikmanius* cf. *myachkovensis*, *G. culmenis*, *Omanoselache hendersoni*, *O. angiolinii*, *Teresodus amplexus*, *Gunnellodus bellistriatus*, *Khuffia lenis*, *K. prolixa*, *Deltodus* aff. *mercurei*, denticles
AO214-0002	MPUM11050	specimen	Neoselachii gen. et sp. indet. A
AO214-0003	MPUM11051	specimen	*Gunnellodus bellistriatus*
AO214-0004	MPUM11052	specimen	*Solenodus* cf. *crenulatus*
AO214-0005	MPUM11053	specimen	Petalodontiformes? gen. et sp. indet.
AO214-0006	MPUM11054	specimen	Petalodontiformes? gen. et sp. indet.
AO214-0007	MPUM11055	specimen	*Cooleyella* cf. *fordi*
AO215-0001	MPUM11056	lot	*Glikmanius* cf. *myachkovensis*, *G. culmenis*, *Omanoselache angiolinii*, *Gunnellodus bellistriatus*, denticles
K7 II LEV-0001	MPUM11057	lot	*Nemacanthus* sp.
ultimolivello-0001	MPUM11058	lot	*Amelacanthus* cf. *sulcatus*

A1.4.2 Abundance data – large samples

Absolute abundances (AA) and relative abundances (RA in %) for specimens of all taxa in the MPUM collection.

Sample	AO40		AO55		AO47bis		AO50	
Taxon	AA	RA	AA	RA	AA	RA	AA	RA
Glikmanius cf. *myachkovensis*	65	6.63	420	51.41	56	27.72	108	78.83
Glikmanius culmenis	25	2.55	103	12.61	4	1.98	5	3.65
Omanoselache hendersoni	579	59.02	104	12.73	34	16.83	-	-
Omanoselache angiolinii	35	3.57	28	3.43	21	10.40	5	3.65
cf. *Omanoselache* sp.	5	0.51	4	0.49	5	2.48	-	-
Reesodus underwoodi	6	0.61	-	-	-	-	-	-
Teresodus amplexus	72	7.34	14	1.71	14	6.93	3	2.19
cf. ‘Palaeozoic Genus 1’ sp.	-	-	-	-	1	0.50	-	-
Gunnellodus bellistriatus	76	7.75	112	13.71	53	26.24	13	9.49
Khuffia lenis	76	7.75	2	0.24	1	0.50	-	-
Khuffia prolixa	27	2.75	-	-	-	-	-	-
Euselachii gen. et sp. indet.	-	-	4	0.49	4	1.98	1	0.73
Cooleyella cf. *fordi*	-	-	-	-	-	-	1	0.73
Nemacanthus sp.	2	0.20	-	-	-	-	-	-
Amelacanthus cf. *sulcatus*	12	1.22	3	0.37	9	4.46	1	0.73
Deltodus aff. *mercurei*	1	0.10	20	2.45	-	-	-	-
Solenodus cf. *crenulatus*	-	-	3	0.37	-	-	-	-
Denticles	many	excl.	many	excl.	many	excl.	many	excl.
Total	**981**		**817**		**202**		**137**	

A1.4.3 Statistical testing of dominance

Statistical significance of domination of Ctenacanthiformes (C) or Hybodontiformes (H) in the four large samples of the MPUM collection. Calculated using relative abundances (RA in %), corrected for exclusion of other groups. T-test calculated using an expected RA of 50% (equal distribution).

Sample	Expect. RA	Low RA	Corr. RA		High RA	Corr. RA		Comb-ined RA
AO40	50	9.17	10.43	C	78.80	89.57	H	87.97
AO55	50	32.07	33.38	H	64.01	66.62	C	96.08
AO47bis	50	29.70	31.91	C	63.37	68.09	H	93.07
AO50	50	15.33	15.67	H	82.48	84.33	C	97.81
One-tailed t-test		0.0011	**0.0016**		0.0021	**0.0016**		

A1.4.4 Abundance data – small samples

Absolute abundances (AA) and relative abundances (RA) for specimens from all small samples in the MPUM collection of which stratigraphic data is available. The samples are listed in stratigraphic order.

Sample	Member	Grain size	Ctenacanths		Hybodonts		Total nr of spec.
			AA	RA	AA	RA	
AO72	3	coarse	2	**0.67**	1	0.33	3
AO58	3	fine	1	0.13	7	**0.88**	8
AO56	3	fine	7	**0.78**	2	0.22	9
AO210	3	fine	8	0.08	94	**0.92**	**102**
AO42	3	coarse	N/A	N/A	N/A	N/A	N/A
AO67	2	fine	0	0.00	3	**1.00**	3
AO41	2	coarse	4	0.08	44	**0.92**	**48**
AO211	2	fine	6	0.04	144	**0.96**	**150**
AO61	2	fine	1	0.13	7	**0.88**	8
AO82	2	fine	1	**1.00**	0	0.00	1
AO32	1	coarse	N/A	N/A	N/A	N/A	N/A
AO3	1	fine	7	**0.78**	2	0.22	9
AO214	1	fine	127	0.38	211	**0.62**	**338**
AO79	1	fine	0	0.00	1	**1.00**	1
AO78	1	coarse	N/A	N/A	N/A	N/A	N/A
AO2	1	fine	N/A	N/A	N/A	N/A	N/A
AO123	1	fine	4	**0.67**	2	0.33	6
AO1	1	fine	N/A	N/A	N/A	N/A	N/A

A1.5. OMAN (OM) COLLECTION

A1.5.1 SAMPLE AND SPECIMEN NUMBERS

Locality	Sample nr	Spec. nr	Identification
Wadi Alwa	110218-E	OM1	Bony fish jaw fragment? (recrystallised)
	110218-G	OM2–OM7	Chondrichthyan teeth? (recrystallised)
	110218-H	OM8–OM13	Chondrichthyan teeth? (recrystallised)
		OM14–OM15	Dermal denticles?
		OM16–OM17	Actinopterygian teeth
		OM18	Indet.
	110218-I	OM19–OM20	Chondrichthyan teeth? (recrystallised)
	110222-B	OM21	cf. Genus S
		OM22–OM24	Actinopterygian teeth
	110222-C	OM25	Chondrichthyan tooth? (recrystallised)
		OM26	Actinopterygian tooth
Saiq Plateau	100223-B	OM27 (lot)	Actinopterygian teeth (2)
	110219-E	OM28–29	*Omanoselache angiolinii*
		OM30	Actinopterygian tooth
		OM31–41	Actinopterygian vertebrae
	110219-G	OM42	Actinopterygian plate
		OM43–44	Actinopterygian teeth
	110219-J	OM45	*Glikmanius* cf. *myachkovensis*
		OM46	Actinopterygian plate
		OM47	Actinopterygian tooth
	110219-L	OM48–49	*Glikmanius* cf. *myachkovensis*
		OM50	Indet.
		OM51–60	Dermal denticles
		OM61	Actinopterygian tooth
		OM62–65	Actinopterygian vertebrae
	110219-M	OM66	cf. *Omanoselache* sp.
		OM67	*Omanoselache angiolinii*
		OM68	Indet.
		OM69	*Glikmanius* cf. *myachkovensis*
		OM70	cf. *Omanoselache* sp.
		OM71–80	Dermal denticles
		OM81–83	Actinopterygian teeth
		OM84	Actinopterygian vertebra
Wadi Wasit	100224-G	OM85	cf. Genus P sp. P
		OM86	Indet.
	100224-I	OM87	Chondrichthyan tooth? (recrystallised)
	100224-L	OM88	Indet.
Wadi Maqam	100227-C	OM89	*Stethacanthulus* sp. cf. *S. decorus*
Qarari block	100302-F	OM90	Actinopterygian tooth
		OM98–100	*Stethacanthulus* sp. cf. *S. decorus*
The “Bridge”	100302-H	OM91–95	*Stethacanthulus* sp. cf. *S. decorus*
		OM96	Indet.
	110223-A	OM101–107	*Stethacanthulus* sp. cf. *S. decorus*
		OM108–110	Actinopterygian teeth
Aseelah	100303-B	OM97	Chondrichthyan tooth? (recrystallised)

A1.5.2 PRODUCTIVITY ANALYSIS

Strength of relationship

	Total nr of samples	Barren	Productive	Vertebrate productive	Total prod. (sum)
Wuchiapingian	5	3	0	2	2
Changhsingian	6	2	4	0	4
Griesbachian	11	4	5	2	7
Dienerian	6	4	2	0	2

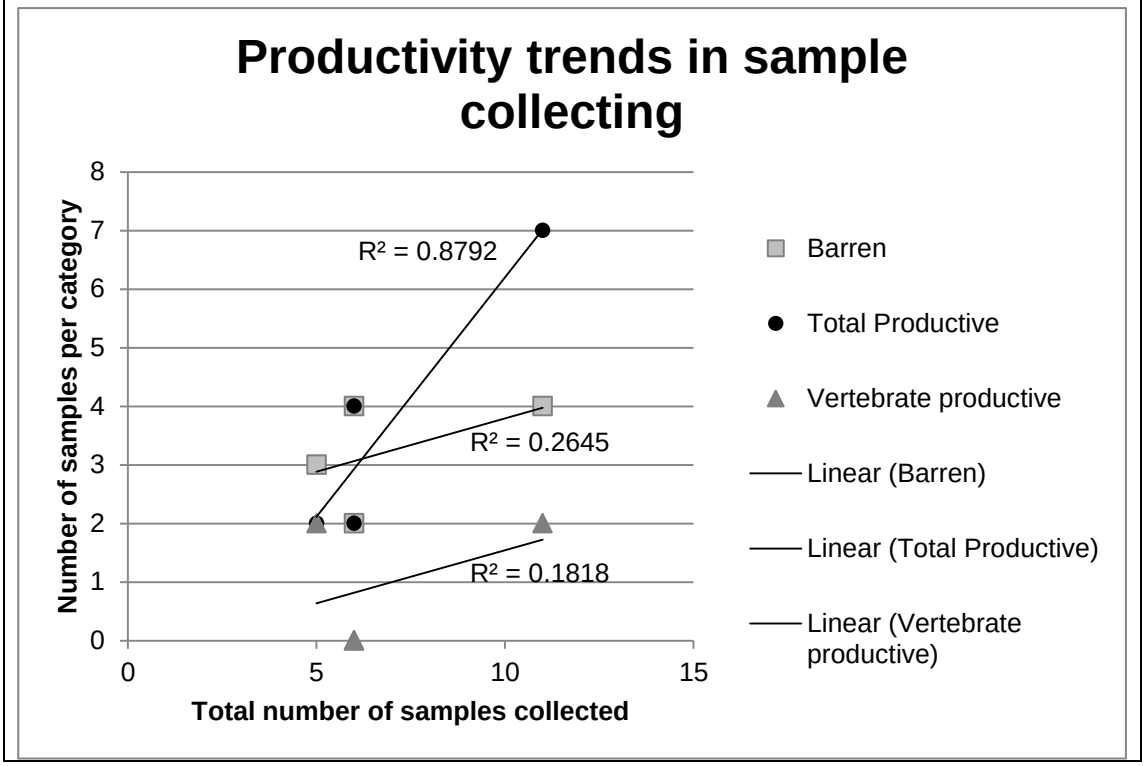

Significance of relationship

Descriptor	Total product.	Barren	Vertebrate product.	Remarks
R^2	0.8792	0.2645	0.1818	correlation coefficient
R	0.9377	0.5143	0.4264	coefficient of determination
α	0.05	0.05	0.05	significance level
n	4	4	4	number of time periods tested
df	2	2	2	degrees of freedom
critical t	4.303	4.303	4.303	2-tailed; assumes that both a a negative as well as a positive correlation are possible
critical t	2.920	2.920	2.920	1-tailed, assumes that there can only be a positive correlation between the number of total and barren/productive samples
t	3.815	0.848	0.667	
t < critical t?	yes p=0.062	yes p=0.486	yes p=0.573	2-tailed; if yes, then null hypothesis of r = 0 (no relationship) cannot be rejected
t < critical t?	no p=0.031	yes p=0.243	yes p=0.287	1-tailed; see above

A1.6. JAPAN (JP) COLLECTION

A1.6.1 SAMPLE AND SPECIMEN NUMBERS

Locality	Sample nr	Spec. nr	Identification
Saraito	300311-P	JP1	Indet.
Shioinouso PTB (B)	290311-R	JP2	*Omanoselache* sp. cf. *O.* sp. H
		JP3–6	Indet.
		JP7	Dermal denticle?
Shioinouso PTB (D)	300311-H	JP8	Elasmobranch tooth cusp
	300311-I	JP9–16	aff. *Arctacanthus exiguus*
		JP17–32	Denticles
		JP33–35	Cladodontomorphi? indet.
		JP36–37	*Acrodus spitzbergensis*
		JP38 (lot)	Actinopterygian teeth
	300311-J	JP39–48	aff. *Arctacanthus exiguus*
		JP49	Hybodontiformes indet.
		JP50	Euselachii indet. C
		JP51–59	*Acrodus spitzbergensis*
		JP60–62	Cladodontomorphi? indet.
		JP63–69	Denticles
		JP70–71	Indet.
	300311-K	JP72	*Acrodus spitzbergensis*
		JP73–76	Synechodontiformes indet.
		JP77	aff. *Arctacanthus exiguus*
		JP78–79	Denticles
		JP80–81	Actinopterygian teeth
	300311-M	JP82–92	Neoselachii indet. B
		JP93–94	Indet.
	300311-O	JP95	Cladodontomorphi? indet.
Shioinouso PTB	05.7.14.ak	JP96	*Omanoselache* sp. cf. *O.* sp. H
		JP97	cf. *Hybodus*
		JP98–100	aff. *Arctacanthus exiguus*
		JP101–105	Denticles
	05.7.14.aw	JP106	aff. *Arctacanthus exiguus*
	05.7.14.ba	JP107–109	Denticles
	05.7.15.h	JP110	aff. *Arctacanthus*? sp.
		JP111	aff. *Arctacanthus*? sp. (tentative)
		JP112–113	Denticles
	05.7.15.k	JP114	*Acrodus spitzbergensis*
		JP115	Indet. elasmobranch tooth
	05.7.15.o	JP116 (lot)	Denticles (21)
	05.7.15.q	JP117–118	cf. *Hybodus*

A1.6.2 Abundance data

Absolute abundances (AA) and relative abundances (RA) for all groups occurring in samples from Japan (JP collection).

Sample	Cladodonti-morpha?		Hybodonti-formes		Neoselachii		Chimaeri-formes?		other Euselachii		Specimen abundance	Genus abundance
	AA	RA	AA	RA	AA	RA	AA	RA	AA	RA		
Upper Triassic												
300311-M		0.00		0.00	11	1.00		0.00		0.00	**11**	1
300311-O	1	1.00		0.00		0.00		0.00		0.00	**1**	1
Totals	**1**	**0.08**	**0**	**0.00**	**11**	**0.92**	**0**	**0.00**	**0**	**0.00**	**12**	N/A
Middle Triassic												
300311-H		0.00		0.00		0.00		0.00	1	1.00	**1**	1
300311-I	3	0.23	2	0.15		0.00	8	0.62		0.00	**13**	3
300311-J	3	0.13	10	0.42		0.00	10	0.42	1	0.04	**24**	5
300311-K		0.00	1	0.17	4	0.67	1	0.17		0.00	**6**	3
Totals	**6**	**0.14**	**13**	**0.30**	**4**	**0.09**	**19**	**0.43**	**2**	**0.05**	**44**	N/A
Lower Triassic												
290311-R		0.00	1	1.00		0.00		0.00		0.00	**1**	1
05.7.14.ak		0.00	2	0.40		0.00	3	0.60		0.00	**5**	3
05.7.14.aw		0.00		0.00		0.00	1	1.00		0.00	**1**	1
05.7.15.h		0.00		0.00		0.00	2	1.00		0.00	**2**	1
05.7.15.k		0.00	1	0.50		0.00		0.00	1	0.50	**2**	2
05.7.15.q		0.00	2	1.00		0.00		0.00		0.00	**2**	1
Totals	**0**	**0.00**	**6**	**0.46**	**0**	**0.00**	**6**	**0.46**	**1**	**0.08**	**13**	N/A

A1.7. East Greenland (GR) collection

A1.7.1 Sample and specimen numbers

Locality	Sample nr	Spec. nr	Identification
Kap Stosch	09.08.22.c	GR1	Eugeneodontiformes? indet.
	090816-A	GR2	*Fadenia crenulata*?
	090816-B	GR11	*Fadenia crenulata*
	090816-F	GR3	*Fadenia crenulata*
	090816-G	GR4–5, GR10	*Fadenia crenulata*
	090816-H	GR8	Gen. et sp. indet.
	090816-J	GR12	Gen. et sp. indet.
	090818-A	GR6–7	*Fadenia crenulata*
	090820-D	GR9	Gen. et sp. indet.

A1.8. Svalbard (SV) collection

A1.8.1 Sample and specimen numbers

Locality	Sample nr	Spec. nr	Identification
Lusitaniadalen	SV-2	SV01	*Palaeobates* sp.

APPENDIX 2 OCCURRENCE AND DIVERSITY DATA

A2.1. CHONDRICHTHYAN OCCURRENCE DATABASE (STARTS NEXT PAGE)

Database entries are provided in batches of three pages, providing data on taxonomy, types of remains, age, location of recovery, stratigraphy and facies, as well as publication information. Entries are provided with a reference number (first column) but this is of no other specific significance. Miscellaneous remains (e.g., dermal denticles) are listed after the skeletal, dental and related records and are marked with 'M'.

Shaded full entries are described in this study, whereas shaded names only are revised here. References provided in grey have not been personally checked by the author. Stage information provided in grey indicates uncertainty with regard to age and in bold indicates an established occurrence range or the more likely age out of a possible range.

All terms are as they appear in published literature and as used here in text, figures and collection listings for the relevant entries.

#	Genus	Species	Junior synonym	Senior synonym	Type of remains	Family	Order	Period	Epoch	Stage
1	New genus	*brodiei* Woodward, 1893					Phoebodontiformes?	Triassic	Upper	Rhaetian (Upper Keuper)
2	gen. indet.	sp. indet.			tooth		Phoebodontiformes?	Triassic	Upper	Carnian, upper middle
3	gen. indet.	sp. indet.					Phoebodontiformes?	Triassic	Upper	Norian, lower
4	gen. indet.	sp. indet.			teeth		Phoebodontiformes?	Triassic	Middle	Anisian
5	gen. indet.	sp. indet.			tooth		Phoebodontiformes?	Permian	Cisuralian	Artinskian, lower
6	*Barbclabornia*	*luedersensis* Berman, 1970			teeth		Bransonelliformes	Permian	Cisuralian	Artinskian
7	*Barbclabornia*	*luedersensis* Berman, 1970			teeth		Bransonelliformes	Permian	Cisuralian	Asselian–Sakmarian
8	*Barbclabornia*	*luedersensis* Berman, 1970			N/A		Bransonelliformes	Permian	Cisuralian	
9	*Barbclabornia*	*luedersensis* Berman, 1970			teeth, palatoquadrate		Bransonelliformes	Permian	Cisuralian	Kungurian
10	*Barbclabornia*	*luedersensis* Berman, 1970			teeth		Bransonelliformes	Permian	Cisuralian	Artinskian
11	*Barbclabornia*	*luedersensis* Berman, 1970			teeth		Bransonelliformes	Permian	Cisuralian	Artinskian
12	*Barbclabornia*	*luedersensis* Berman, 1970			teeth		Bransonelliformes	Permian	Cisuralian	Artinskian
13	*Barbclabornia*	*luedersensis* Berman, 1970			teeth		Bransonelliformes	Permian	Cisuralian	Artinskian
14	*Barbclabornia*	*luedersensis* Berman, 1970			teeth		Bransonelliformes	Permian	Cisuralian	Asselian
15	*Barbclabornia*	*luedersensis* Berman, 1970			teeth		Bransonelliformes	Permian	Cisuralian	Asselian
16	*Barbclabornia*	*luedersensis* Berman, 1970			teeth		Bransonelliformes	Permian	Cisuralian	**Asselian–Sakmarian**
17	*Barbclabornia*	*luedersensis* Berman, 1970			teeth		Bransonelliformes	Permian	Cisuralian	Artinskian
18	*Barbclabornia*	*luedersensis* Berman, 1970			teeth		Bransonelliformes	Permian	Cisuralian	Artinskian
19	*Barbclabornia*	cf. *luedersensis* Berman, 1970			teeth		Bransonelliformes	Permian	Cisuralian	Artinskian
20	*Bransonella*	*nebraskensis* Johnson, 1984			teeth		Bransonelliformes	Permian	Cisuralian	Sakmarian
21	*Dicentrodus*	*belemnoideus* Zidek, 1978			spines	Diplodoselachidae	Xenacanthiformes	Permian	Cisuralian	Kungurian
22	*Dicentrodus*	*ruthenorum* Chabakov, 1928			spines	Diplodoselachidae	Xenacanthiformes	Permian	Guadalupian	Wordian (Kazanian)
23	*Lebachacanthus*	*senckenbergianus* (Fritsch, 1889)			neurocranium	Diplodoselachidae	Xenacanthiformes	Permian	Cisuralian	Asselian, upper
24	*Lebachacanthus*	*senckenbergianus* (Fritsch, 1889)			body, anterior half	Diplodoselachidae	Xenacanthiformes	Permian	Cisuralian	Asselian
25	*Lebachacanthus*	*senckenbergianus* (Fritsch, 1889)				Diplodoselachidae	Xenacanthiformes	Permian	Cisuralian	
26	*Lebachacanthus*	*senckenbergianus* (Fritsch, 1889)			anterior body	Diplodoselachidae	Xenacanthiformes	Permian	Cisuralian	Asselian

Basin/Orogeny	Region	Country	Location	Stratigraphy	Facies
	PT-W	England	Shrewley, Warwickshire		
	PG-C	USA-S	*Placerias* /Downs Quarry, Arizona	Mesa Redondo Mb, Chinle Fm	floodplain
	PG-C	USA-S	Arizona, New Mexico, Texas	Chinle Fm / Dockum Grp	floodplain
Tethys	PT-W	Poland	Upper Silesia and Holy Cross Mountains, SE	Muschelkalk	
	PG-C	USA-S	Brushy Creek, Texas	upper Petrolia Fm	coastal plain
	PG-C	USA-S	Texas	Lueders Fm, Wichita Grp	
	PG-C	USA-C	Oklahoma (E Manitou, NE Frederick, Waurika)		
	PG-C	USA-C	Kirby Quarry, Noble County, north-central Oklahoma	Unit 9, Billings Pool Mb, Wellington Fm	olive shale, terrestrial
	PG-C	USA-C	Lake Frederick site, near Deep Red Creek, Tillman County, southwestern Oklahoma	upper Garber (Sandstone) Fm, upper Sumner Grp	sandstones, mudstone conglomerates, claystones; fluvial and lacustrine environments in a coastal-plain setting
	PG-C	USA-S	Little Moonshine Creek, Texas	upper Lueders Fm, Albany Grp	claystone
	PG-C	USA-S	many localities, Texas	Clyde Fm, Wichita Grp	coastal plain
	PG-C	USA-S	Wolf and Brushy Creeks, Texas	upper Belle Plains Fm, Wichita Grp	coastal plain
	PG-C	USA-S	Rattlesnake Canyon, Texas	upper Admiral Fm, Wichita Grp	coastal plain
	PG-C	USA-S	Archer County, Texas	Archer City Bonebed 3, Archer City Fm, Bowie Grp	lenticular mudstone; abandoned channel
Dunkard Basin (freshwater, but marine influenced; Schultze & Soler-Gijón 2004)	PG-N	USA-E	Franklin Mall	Colvin Limestone, Waynesburg Fm, Dunkard Grp	
Dunkard Basin (freshwater, but marine influenced; Schultze & Soler-Gijón 2004)	PG-N	USA-E	Powhatan Point	Washington Fm, Dunkard Grp	
Dunkard Basin (freshwater, but marine influenced; Schultze & Soler-Gijón 2004)	PG-N	USA-E	Limestone Hill, Wirt County, W Virginia	Nineveh Limestone Mb, Greene Fm	
Dunkard Basin (freshwater, but marine influenced; Schultze & Soler-Gijón 2004)	PG-N	USA-E		Greene Fm (incl. Windy Gap Limestone + Rockport Mb), Dunkard Grp	
	PG-C	USA-S	East Coffee Creek, Texas	lower Arroyo Fm, Clear Fork Grp	floodplain
	PG-C	USA-C	Geary County, Kansas	Funston Limestone, Speiser Shale, Council Grove Grp; Wreford Limestone and Wymore Shale Mb, Matfield Shale, Chase Grp; Wreford Megacyclothem	intertidal to open marine (50 m water depth)
	PG-C	USA-C	Northeast Frederick site, near Deep Red Creek, Tillman County, southwestern Oklahoma	upper Garber (Sandstone) Fm, upper Sumner Grp	sandstones, mudstone conglomerates, claystones; lacustrine environment in a coastal-plain setting
	PT-N	Russia-W	(Arkhangelsk and Vyatka districts, Tataria) European Russia		brachiopod limestone; hemipelagic (shelf)
	PT-W	Germany	Saar-Nahe Basin, SW	Thallichtenberg Fm	
Rotliegend, Lebach Basin	PT-W	Germany	Lebach, Rümmelbach-Gresaubach region, Saar-Nahe Basin	uppermost Lauterecken-Odernheim Fm	Lebacher Toneisenstein-Geoden
	PT-W	Germany	Saar-Nahe Basin, SW		fluvio-lacustrine basin
Rotliegend	PT-W	Germany	Geisberg, near Rockenhausen, Pfälz, W	upper Jeckenbach Fm, Lebach Grp (lower Rotliegend)	grey/black shales

Salinity	Life habit	Biostratigraphy	Reference	Secondary reference	Remarks
			Woodward 1893	Ginter *et al.* 2010; Cappetta 2012	(as *Phoebodus*) may be synonymous with *Keupernus* Seilacher 1948 (Cappetta 2012)
freshwater			Kaye & Padian 1994	Irmis 2005; Parker 2005; Milner *et al.* 2006	(as *Phoebodus*)
freshwater				Milner *et al.* 2006	(as cf. *Phoebodus*)
marine			Liszkowski 1993		(as *Phoebodus*)
freshwater			Johnson 2005a		
freshwater (partly marine)			Berman 1970	Johnson 2003; Hampe & Ivanov 2007	
			Olson 1967; Simpson 1979; Johnson 1979	Johnson 2003; Hampe & Ivanov 2007; Ginter et al. 2010	
freshwater			May & Hall 2002		
freshwater	4.5-5m in length		Zidek *et al.* 2004		
			Johnson 2003	Johnson 1996	
freshwater			Johnson 2003	Johnson 2005b	
freshwater			Johnson 2003	Johnson 2005b	
freshwater			Johnson 2003	Johnson 2005b	
freshwater			Johnson 2012		
			Johnson 2003	Johnson 1992	
			Johnson 2003		
			Johnson 2003		
			Johnson 2003		
freshwater			Johnson 2003	Johnson 2005b	
marine to brackish			Schultze 1985	Schneider & Zajic 1994; Johnson 1992, 2003; Hampe & Ivanov 2007; Johnson & Thayer 2009	(as *Xenacanthus luedersensis*)
freshwater			Zidek *et al.* 2004		(as *Ancodontacanthus*; spines of *Dicentrodus* closely similar to *Lebachacanthus*; Ginter *et al.* 2010)
marine			Chabakov 1927	Khabakov 1926–27, 1939; Ivanov 2000	(as *Ancodontacanthus*; spines of *Dicentrodus* closely similar to *Lebachacanthus*; Ginter *et al.* 2010)
	up to 2.6m in length (Heyler & Poplin 1990)		Fritsch 1889	Heyler & Poplin 1989; Schneider 1996; Ginter *et al.* 2010	
freshwater			Soler-Gijón 1997b		
freshwater			Boy 1976	Hampe 1988b	
freshwater			Heidtke 1982	Hampe 1988b; Heyler & Poplin 1989; Soler-Gijón 1997b	(as *Orthacanthus*)

27	*Lebachacanthus*	*senckenbergianus* (Fritsch, 1889)			body	Diplodoselachidae	Xenacanthiformes	Permian	Cisuralian	
28	*Lebachacanthus*	*senckenbergianus* (Fritsch, 1889)			body	Diplodoselachidae	Xenacanthiformes	Permian	Cisuralian	
29	*Lebachacanthus*	*senckenbergianus* (Fritsch, 1889)				Diplodoselachidae	Xenacanthiformes	Permian	Cisuralian	Asselian–Sakmarian
30	*Lebachacanthus* ?	*americanus* (Hussakof, 1911)			spine	Diplodoselachidae	Xenacanthiformes	Permian	Cisuralian	
31	*Lebachacanthus* ?	*americanus* (Hussakof, 1911)			spines	Diplodoselachidae	Xenacanthiformes	Permian	Cisuralian	Asselian?
32	*Lebachacanthus* ?	*americanus* (Hussakof, 1911)			spines	Diplodoselachidae	Xenacanthiformes	Permian	Cisuralian	Asselian?
33	*Lebachacanthus* ?	*americanus* (Hussakof, 1911)			spines	Diplodoselachidae	Xenacanthiformes	Permian	Cisuralian	Artinskian
34	*Lebachacanthus* ?	*americanus* (Hussakof, 1911)			spines	Diplodoselachidae	Xenacanthiformes	Permian	Cisuralian	Artinskian
35	*Lebachacanthus* ?	*americanus* (Hussakof, 1911)			spines	Diplodoselachidae	Xenacanthiformes	Permian	Cisuralian	Artinskian
36	*Lebachacanthus* ?	*avircostratus* Zidek, 1978			spines	Diplodoselachidae	Xenacanthiformes	Permian	Cisuralian	Kungurian
37	*Orthacanthus*	*compressus* (Newberry, 1856)			teeth	Diplodoselachidae	Xenacanthiformes	Permian	Cisuralian	Sakmarian
38	*Orthacanthus*	*compressus* (Newberry, 1856)			teeth	Diplodoselachidae	Xenacanthiformes	Permian	Cisuralian	Asselian
39	*Orthacanthus*	*?compressus* (Newberry, 1856)			teeth	Diplodoselachidae	Xenacanthiformes	Permian	Cisuralian	Asselian
40	*Orthacanthus*	*?compressus* (Newberry, 1856)			teeth	Diplodoselachidae	Xenacanthiformes	Permian	Cisuralian	Asselian
41	*Orthacanthus*	*?compressus* (Newberry, 1856)			teeth, occipital spines	Diplodoselachidae	Xenacanthiformes	Permian	Cisuralian	Asselian
42	*Orthacanthus*	*kounoviensis* Fritsch, 1889	*buvieri* Heyler & Poplin, 1989		teeth, anterior body, spines	Diplodoselachidae	Xenacanthiformes	Permian	Cisuralian	Asselian
43	*Orthacanthus*	*kounoviensis* Fritsch, 1889	idem		clasper	Diplodoselachidae	Xenacanthiformes	Permian	Cisuralian	Asselian
44	*Orthacanthus*	*commailli* Heyler and Poplin, 1982			neurocranium	Diplodoselachidae	Xenacanthiformes	Permian	Cisuralian	Asselian
45	*Orthacanthus*	*platypternus* (Cope, 1884)			teeth	Diplodoselachidae	Xenacanthiformes	Permian	Cisuralian	Sakmarian–Kungurian
46	*Orthacanthus*	*platypternus* (Cope, 1884)			teeth	Diplodoselachidae	Xenacanthiformes	Permian	Cisuralian	Sakmarian–Kungurian
47	*Orthacanthus*	*platypternus* (Cope, 1884)			teeth	Diplodoselachidae	Xenacanthiformes	Permian	Cisuralian	Kungurian
48	*Orthacanthus*	*platypternus* (Cope, 1884)			teeth	Diplodoselachidae	Xenacanthiformes	Permian	Cisuralian	Kungurian
49	*Orthacanthus*	*platypternus* (Cope, 1884)			teeth	Diplodoselachidae	Xenacanthiformes	Permian	Cisuralian	**Sakmarian–Artinskian**

	PT-W	Germany	Saar-Nahe Basin, SW		
	PT-W	Germany	Saar-Nahe Basin, SW		
	PT-W	Germany	Saar-Nahe Basin, SW	Remigiusberg Fm; Disibodenberg Fm	fluvio-lacustrine basin
	PG-C	USA-S	Texas	Wichita Grp	
	PG-C	USA-S	Little Bitter Creek, Young County, Texas	Moran Fm, Wichita Grp	
	PG-C	USA-S	Cottonwood Creek (headwaters), Archer County, Texas	Moran Fm, Wichita Grp	
	PG-C	USA-S	Former Woodrum Ranch, south of Dundee, Archer County, Texas	Admiral/Belle Plains Fm, Wichita Grp	
	PG-C	USA-S	Daggett Creek, Baylor County, Texas	Belle Plains Fm, Wichita Grp	
	PG-C	USA-S	Little Wichita River below Fulda, Baylor County, Texas	Belle Plains Fm, Wichita Grp	
	PG-C	USA-C	Northeast Frederick site, near Deep Red Creek, Tillman County, southwestern Oklahoma	upper Garber (Sandstone) Fm, upper Sumner Grp	sandstones, mudstone conglomerates, claystones; lacustrine environment in a coastal-plain setting
	PG-C	USA-S	Texas	Archer City Fm, Bowie Grp	
Dunkard Basin (freshwater, but marine influenced; Schultze & Soler-Gijón 2004)	PG-N	USA-E	Franklin Mall, Pennsylvania	Colvin Limestone, Waynesburg Fm, Dunkard Grp	
Dunkard Basin (freshwater, but marine influenced; Schultze & Soler-Gijón 2004)	PG-N	USA-E	west-central Pennsylvania	Dunkard Grp	
	PG-C	USA-S	Archer County, Texas	Archer City Bonebed 3, Archer City Fm, Bowie Grp	lenticular mudstone; abandoned channel
	PG-C	USA-S	Connor Ranch, near Cottonwood Creek, Archer County, Texas	bonebed	floodplain facies
Rotliegend, Autun Basin (Bourbon-l'Archambault Basin)	PT-W	France	Buxières-les-Mines, Allier, Massif Central	Supra-Buxières Mb, Buxières Fm	shale, lacustrine
Rotliegend, Autun Basin	PT-W	France	Buxières-les-Mines, Allier, Massif Central	Supra-Buxières Mb, Buxières Fm	marginal marine (coastal, lagoonal, estuarine)
Rotliegend, Autun Basin	PT-W	France	Buxières-les-Mines, Allier, Massif Central		
Dunkard Basin (freshwater, but marine influenced; Schultze & Soler-Gijón 2004)	PG-N	USA-E	SE Ohio, NW Virginia, SW Pennsylvania		
	PG-C	USA-C	Oklahoma, Kansas		
	PG-C	USA-S	Texas	San Angelo Fm, Pease River Grp	
	PG-C	USA-C	Oklahoma	Chickasha Fm	
Dunkard Basin (freshwater, but marine influenced; Schultze & Soler-Gijón 2004)	PG-N	USA-E		Greene Fm, Dunkard Grp	

			Klausewitz 1986	Hampe 1988b; Soler-Gijón 1997b; Heidtke 1998	
			Klausewitz 1987	Hampe 1988b; Soler-Gijón 1997b; Heidtke 1998	
freshwater			Hampe 1988b	Hampe 1997; Soler-Gijón 1997b	(as *Orthacanthus*)
freshwater			Hussakof 1911	Romer 1942; Ginter *et al.* 2010	(as *Anodontacanthus* ; spines of *Dicentrodus* closely similar to *Lebachacanthus* ; Ginter *et al.* 2010)
			Romer 1942		(as *Anodontacanthus* ; spines of *Dicentrodus* closely similar to *Lebachacanthus* ; Ginter *et al.* 2010)
			Romer 1942		(as *Anodontacanthus* ; spines of *Dicentrodus* closely similar to *Lebachacanthus* ; Ginter *et al.* 2010)
			Romer 1942		(as *Anodontacanthus* ; spines of *Dicentrodus* closely similar to *Lebachacanthus* ; Ginter *et al.* 2010)
			Romer 1942		(as *Anodontacanthus* ; spines of *Dicentrodus* closely similar to *Lebachacanthus* ; Ginter *et al.* 2010)
			Romer 1942		(as *Anodontacanthus* ; spines of *Dicentrodus* closely similar to *Lebachacanthus* ; Ginter *et al.* 2010)
freshwater			Zidek *et al.* 2004		(as *Platyacanthus*)
			Johnson 1992	Ginter *et al.* 2010	
			Johnson 1999	Johnson 2011	
			Ciampaglio 2011 in pers. comm. with Johnson 2012		
freshwater	adult and juvenile		Johnson 2012	Johnson 2011	
freshwater			Sander & Krahl 2007	Johnson 2012	(as xenacanth)
freshwater	about 2m in length		Heyler 1969, 1987; Heyler & Debriette 1986; Poplin & Heyler 1989; Heyler & Poplin 1989, 1990	Steyer & Escuillie 1997; Hampe 1988b; Steyer *et al.* 2000; Ginter *et al.* 2010	
freshwater with marine influence			Schultze & Soler-Gijón 2004		
freshwater			Heyler & Poplin 1982	Heyler & Poplin 1989; Poplin & Heyler 1989	(as *Expleuracanthus*)
	species is assumed juvenile (Zidek 1993; Ginter *et al.* 2010)		Cope 1884	Schneider 1996; Ginter *et al.* 2010	
	species is assumed juvenile (Zidek 1993; Ginter *et al.* 2010)		Cope 1884	Schneider 1996; Ginter *et al.* 2010	
			Olson 1962	Johnson 1992	
			Olson 1965	Johnson 1992	
			Johnson 1999	Johnson 2012	

50	*Orthacanthus*	*platypternus* (Cope, 1884)			teeth	Diplodoselachidae	Xenacanthiformes	Permian	Cisuralian	**Sakmarian–Artinskian**
51	*Orthacanthus*	*platypternus* (Cope, 1884)			N/A	Diplodoselachidae	Xenacanthiformes	Permian	Cisuralian	
52	*Orthacanthus* -like	*platypternus* (Cope, 1884)			teeth	Diplodoselachidae	Xenacanthiformes	Permian	Cisuralian	Kungurian
53	*Orthacanthus*	*platypternus* (Cope, 1884)			chrondrocranium, jaws	Diplodoselachidae	Xenacanthiformes	Permian	Cisuralian	
54	*Orthacanthus*	*platypternus* (Cope, 1884)			teeth	Diplodoselachidae	Xenacanthiformes	Permian	Cisuralian	Artinskian
55	*Orthacanthus*	*platypternus* (Cope, 1884)			teeth	Diplodoselachidae	Xenacanthiformes	Permian	Cisuralian	Artinskian
56	*Orthacanthus*	*platypternus* (Cope, 1884)			teeth	Diplodoselachidae	Xenacanthiformes	Permian	Cisuralian	Artinskian
57	*Orthacanthus*	*platypternus* (Cope, 1884)			teeth, occipital spines, skeletal elements	Diplodoselachidae	Xenacanthiformes	Permian	Cisuralian	
58	*Orthacanthus*	*platypternus* (Cope, 1884)			teeth	Diplodoselachidae	Xenacanthiformes	Permian	Cisuralian	Asselian
59	*Orthacanthus*	*texensis* (Cope, 1888)			teeth	Diplodoselachidae	Xenacanthiformes	Permian	Cisuralian	Artinskian
60	*Orthacanthus*	*texensis* (Cope, 1888)			teeth	Diplodoselachidae	Xenacanthiformes	Permian	Cisuralian	Artinskian
61	*Orthacanthus*	*texensis* (Cope, 1888)			teeth, cranium	Diplodoselachidae	Xenacanthiformes	Permian	Cisuralian	Asselian–Sakmarian
62	*Orthacanthus*	*texensis* (Cope, 1888)			N/A	Diplodoselachidae	Xenacanthiformes	Permian	Cisuralian	
63	*Orthacanthus*	*texensis* (Cope, 1888)			teeth, chondrocrania, jaws	Diplodoselachidae	Xenacanthiformes	Permian	Cisuralian	Artinskian
64	*Orthacanthus*	*texensis* (Cope, 1888)			teeth	Diplodoselachidae	Xenacanthiformes	Permian	Cisuralian	Artinskian
65	*Orthacanthus*	*texensis* (Cope, 1888)			teeth	Diplodoselachidae	Xenacanthiformes	Permian	Cisuralian	Artinskian
66	*Orthacanthus*	*texensis* (Cope, 1888)			teeth	Diplodoselachidae	Xenacanthiformes	Permian	Cisuralian	Kungurian
67	*Orthacanthus* -like	*texensis* (Cope, 1888)			teeth, cranium, jaws	Diplodoselachidae	Xenacanthiformes	Permian	Cisuralian	Kungurian
68	*Orthacanthus*	*texensis* (Cope, 1888)			teeth	Diplodoselachidae	Xenacanthiformes	Permian	Cisuralian	Asselian
69	*Orthacanthus*	*texensis* (Cope, 1888)			teeth	Diplodoselachidae	Xenacanthiformes	Permian	Cisuralian	Sakmarian
70	*Orthacanthus* -like	sp.				Diplodoselachidae	Xenacanthiformes	Permian	Cisuralian	Asselian
71	*Orthacanthus* -like	sp.			occipital spines	Diplodoselachidae	Xenacanthiformes	Permian	Cisuralian	Kungurian
72	*Orthacanthus*	sp.			tooth	Diplodoselachidae	Xenacanthiformes	Permian	Lopingian	Changhsingian
73	*Orthacanthus*	sp.			teeth	Diplodoselachidae	Xenacanthiformes	Triassic	Middle	Anisian

Dunkard Basin (freshwater, but marine influenced; Schultze & Soler-Gijón 2004)	PG-N	USA-E		Greene Fm, Dunkard Grp	
	PG-C	USA-C	Kirby Quarry, Noble County, north-central Oklahoma	Unit 9, Billings Pool Mb, Wellington Fm	olive shale, terrestrial
	PG-C	USA-C	Northeast Frederick and Lake Frederick sites, near Deep Red Creek, Tillman County, southwestern Oklahoma	upper Garber (Sandstone) Fm, upper Sumner Grp	sandstones, mudstone conglomerates, claystones; fluvial and lacustrine environments in a coastal-plain setting
	PG-C	USA-S	Craddoks Ranch, between Seymour and Vernon, Baylor county, Texas	Wichita beds	red clay layers
	PG-C	USA-S	Texas	Arroyo Fm, Clear Fork Grp	river/stream
	PG-C	USA-S	north central Texas	Wichita Grp (upper Nocona Fm, upper Petrolia Fm, Waggoner Ranch Fm)–Clear Fork Grp	
	PG-C	USA-S	Little Moonshine Creek, Texas	upper Lueders Fm, Albany Grp	claystone
	PG-C	USA-S	Baylor County, Texas	Craddock Bonebed	reddish-brown, calcareous mudstone
	PG-C	USA-S	Benson's Pasture, near Olney, Archer/Young County, Texas	Putnam Fm, correlative to upper Archer City Fm, Bowie Grp	
Dunkard Basin (freshwater, but marine influenced; Schultze & Soler-Gijón 2004)	PG-N	USA-E		Greene Fm, Dunkard Grp	
Dunkard Basin (freshwater, but marine influenced; Schultze & Soler-Gijón 2004)	PG-N	USA-E		Greene Fm, Dunkard Grp	
	PG-C	USA-S/C	Texas, Oklahoma, New Mexico, ?Utah		
	PG-C	USA-C	Kirby Quarry, Noble County, north-central Oklahoma	Unit 9, Billings Pool Mb, Wellington Fm	olive shale, terrestrial
	PG-C	USA-S	Texas	Belle Plains Fm, Wichita Grp	lacustrine sandstone and shale
	PG-C	USA-S	north central Texas	Wichita Grp (upper Nocona Fm, upper Petrolia Fm, Waggoner Ranch Fm)	
	PG-C	USA-S	Little Moonshine Creek, Texas	upper Lueders Fm, Albany Grp	claystone
	PG-C	USA-S	Tillman County, Texas	upper Garber Fm	
	PG-C	USA-C	Northeast Frederick and Lake Frederick sites, near Deep Red Creek, Tillman County, southwestern Oklahoma	upper Garber (Sandstone) Fm, upper Sumner Grp	sandstones, mudstone conglomerates, claystones; fluvial and lacustrine environments in a coastal-plain setting
	PG-C	USA-S	Benson's Pasture, near Olney, Archer/Young County, Texas	Putnam Fm, correlative to upper Archer City Fm, Bowie Grp	
	PG-C	USA-C	Geary County, Kansas	Funston Limestone, Speiser Shale, Council Grove Grp; Wreford Limestone and Wymore Shale Mb, Kinney Limestone Mb, Matfield Shale, Chase Grp; Wreford Megacyclothem	intertidal to open marine (50 m water depth)
	PT-W	Italy	Guardia Pisano Basin, Sulcis area, SW Sardinia	Top of lithofacies B	80-90mm thick brownish-grey lacustrine micritic limestone (parautochthonous)
	PG-C	USA-C	Northeast Frederick and Lake Frederick sites, near Deep Red Creek, Tillman County, southwestern Oklahoma	upper Garber (Sandstone) Fm, upper Sumner Grp	sandstones, mudstone conglomerates, claystones; fluvial and lacustrine environments in a coastal-plain setting
	PL-W	Japan	Kanoko, Motoyoshi-cho, Motoyoshi-gun, Miyagi Prefecture, NE Honshu	Senmatsu Fm, South Kitakami Belt	black shale
Tethys	PT-W	Poland	Holy Cross Mountains, SE Poland	Muschelkalk	

			Johnson 1992		
freshwater			May & Hall 2002		
freshwater			Zidek *et al.* 2004		
			Broili 1904	Hotton III 1952; Hampe 1988a	(as *Diacranodus tewensis*)
freshwater			Hotton III 1952	Hampe 1988a	(as *Nenacanthus*)
freshwater			Johnson 1999	Johnson 2005b; Johnson & Thayer 2009; Johnson 2012	
			Johnson 1996		
			Donelan & Johnson 1997		
freshwater			Johnson 2012		
			Johnson 1992		
			Johnson 1999	Johnson 2012	
brackish/freshwater (Johnson 2003)			Cope 1884, 1888; Newberry 1890	Schneider 1996	
freshwater			May & Hall 2002		
freshwater			Hotton III 1952	Hampe 1988b	(as *Nenacanthus*)
freshwater			Johnson 1999	Johnson 2005b; Johnson & Thayer 2009; Johnson 2012	
			Johnson 1996		
freshwater			Simpson 1976, 1979	Zidek *et al.* 2004	(as *O. compressus*)
freshwater	2.0–2.6m in length		Zidek *et al.* 2004		
freshwater			Johnson 2012		
marine to brackish			Schultze 1985	Hampe 1988b; Johnson 1992	(as sp.)
freshwater (lacustrine)			Fischer *et al.* 2010		
freshwater			Zidek *et al.* 2004		
freshwater			Goto *et al.* 1996b	Goto 1996a–c, 1999a, b, 2000; Goto *et al.* 2000	
freshwater/brackish			Liszkowski 1993	Schneider 1996	

74	*Orthacanthus*					Diplodoselachidae	Xenacanthiformes	Triassic	Upper	
75	*Xenacanthus*	*decheni* (Goldfuss, 1847)			teeth	Xenacanthidae	Xenacanthiformes	Permian	Cisuralian	**Asselian**(–Sakmarian)
76	*Xenacanthus*	*decheni* (Goldfuss, 1847)			teeth	Xenacanthidae	Xenacanthiformes	Permian	Cisuralian	Asselian
77	*Xenacanthus*	*humbergensis* Hampe, 1994			teeth	Xenacanthidae	Xenacanthiformes	Permian	Cisuralian	Asselian
78	*Xenacanthus*	*meisenheimensis* Hampe, 1994			teeth	Xenacanthidae	Xenacanthiformes	Permian	Cisuralian	Asselian, lower
79	*Xenacanthus*	*remigiusbergensis* Hampe, 1994			teeth	Xenacanthidae	Xenacanthiformes	Permian	Cisuralian	Asselian–Sakmarian
80	*Xenacanthus*	*oelbergensis* Fritsch, 1890			teeth	Xenacanthidae	Xenacanthiformes	Permian	Cisuralian	Asselian–Sakmarian
81	*Xenacanthus*	*slaughteri* Johnson, 1999			teeth	Xenacanthidae	Xenacanthiformes	Permian	Cisuralian	Artinskian
82	*Xenacanthus*	sp.			teeth	Xenacanthidae	Xenacanthiformes	Permian	Cisuralian	Asselian
83	*Xenacanthus*	sp.			teeth	Xenacanthidae	Xenacanthiformes	Permian	Cisuralian	Asselian, lower
84	*Xenacanthus*					Xenacanthidae	Xenacanthiformes	Triassic	Lower	
85	*Xenacanthus*					Xenacanthidae	Xenacanthiformes	Triassic	Middle	Anisian, late
86	*Xenacanthus*				spine	Xenacanthidae	Xenacanthiformes	Permian	Cisuralian	**Sakmarian**/Artinskian?
87	*Xenacanthus*	sp.			neurocranium	Xenacanthidae	Xenacanthiformes	Permian	Cisuralian	
88	*Xenacanthus*	sp.				Xenacanthidae	Xenacanthiformes	Triassic	Upper	Carnian, upper middle
89	*Xenacanthus*	sp.			teeth	Xenacanthidae	Xenacanthiformes	Triassic	Middle	Ladinian
90	*Xenacanthus*	sp.			fin spine	Xenacanthidae	Xenacanthiformes	Permian	Cisuralian	
91	*Xenacanthus*	sp.			occipital spines	Xenacanthidae	Xenacanthiformes	Permian	Cisuralian	Asselian
92	*Xenacanthus*	sp.			occipital spines	Xenacanthidae	Xenacanthiformes	Permian	Cisuralian	Asselian
93	*Triodus*	*carinatus* (Fritsch, 1890)			teeth, body?	Xenacanthidae	Xenacanthiformes	Permian	Cisuralian	Asselian
94	*Triodus*	*carinatus* (Fritsch, 1890)				Xenacanthidae	Xenacanthiformes	Permian	Cisuralian	Asselian (Lower Rotliegend)
95	*Triodus*				teeth	Xenacanthidae	Xenacanthiformes	Permian	Cisuralian	Asselian
96	*Triodus*	*frossardi* (Gaudry, 1883)			spine	Xenacanthidae	Xenacanthiformes	Permian	Cisuralian	Asselian
97	*Triodus*	? *frossardi* (Gaudry, 1883)			anterior body	Xenacanthidae	Xenacanthiformes	Permian	Cisuralian	Asselian
98	*Triodus*	*kraetschmeri* Hampe, 1989			teeth	Xenacanthidae	Xenacanthiformes	Permian	Cisuralian	Asselian–Artinskian
99	*Triodus*	*obscurus* Hampe, 1989			teeth	Xenacanthidae	Xenacanthiformes	Permian	Cisuralian	Asselian
100	*Triodus*	*palatinus* Hampe, 1989			teeth	Xenacanthidae	Xenacanthiformes	Permian	Cisuralian	Asselian
101	*Triodus*	*palatinus* Hampe, 1989			teeth, body	Xenacanthidae	Xenacanthiformes	Permian	Cisuralian	Asselian
102	*Triodus*	*sessilis* Jordan, 1849			teeth, articulated crania	Xenacanthidae	Xenacanthiformes	Permian	Cisuralian	Asselian
103	*Triodus*	*sessilis* Jordan, 1849			teeth	Xenacanthidae	Xenacanthiformes	Permian	Cisuralian	Sakmarian
104	*Triodus*	*lauterensis* Hampe, 1989			teeth	Xenacanthidae	Xenacanthiformes	Permian	Cisuralian	Asselian
105	*Triodus*	sp.				Xenacanthidae	Xenacanthiformes	Permian	Cisuralian	Asselian

	PT-W	Germany			
	PT-W	Czech Republic	Ruppersdorf (Ruprechtice), Intrasudetic Basin, Bohemia	Ruprechtice Horizon, Olivětín Mb, Broumov Fm	
	PT-W	Czech Republic	Kostialov, Podkrkonose Basin (Krkonoše Piedmont Basin), Boskovice Furrow, Bohemia		
	PT-W	Germany	Saar-Nahe Basin, SW	upper Odernheim SubFm	
	PT-W	Germany	Saar-Nahe Basin, SW	Wahnwegen to Odernheim SubFms	fluvio-lacustrine basin
	PT-W	Germany	Saar-Nahe Basin, SW	Remigiusberg Fm	fluvio-lacustrine basin
	PT-W	Czech Republic	Ruppersdorf (Ruprechtice), Intrasudetic Basin, Bohemia	Ruprechtice Horizon, Olivětín Mb, Broumov Fm	
	PG-C	USA-S	north central Texas	Wichita Grp (upper Nocona Fm, upper Petrolia Fm, Waggoner Ranch Fm)	
	PT-W	Italy	Guardia Pisano Basin, Sulcis area, SW Sardinia	Top of lithofacies B	80-90mm thick brownish-grey lacustrine micritic limestone (parautochthonous)
	PT-W	Italy	Ortu Manu, Perdasdefogu Basin, Sardinia	Rio su Luda Fm	cherty carbonate
	PL-SW	Australia-E	Gosford, Sidney Basin	Narabeen Grp	floodplain
	PL-SW	Australia-E	St. Peters, Sidney Basin	Wianamatta Grp	floodplain/lacustrine
	BOR	Greenland-E	Profilfjeldet, Mesters Vig	Profilbjerg Mb, Mesters Vig Fm	
	PG-C	USA-S	Texas		
	PG-C	USA-S	Arizona, New Mexico, Texas	Chinle Fm / Dockum Grp	floodplain
Tethys	PT-W	Poland	Upper Silesia, SE	Muschelkalk	
	PG-S	Brazil	NE		
	PG-C	USA-S	Archer County, Texas	Archer City Bonebed 3, Archer City Fm, Bowie Grp	lenticular mudstone; abandoned channel
	PG-C	USA-S	Connor Ranch, near Cottonwood Creek, Archer County, Texas	bonebed	floodplain facies
	PT-W	Czech Republic	Intrasudetic Basin, Krkonoše Piedmont Basin, Boskovice Furrow		
	PT-W	Czech Republic	Kostialov, Podkrkonose Basin, Bohemia	Rudnik Horizon, Stara Paka Sandstone Mb, Vrchlabi Fm	
	PT-W	Czech Republic	Kostialov, Podkrkonose Basin, Bohemia		
Rotliegend, Autun Basin	PT-W	France	Massif Central		
Rotliegend, Autun Basin	PT-W	France	Muse		
	PT-W	Germany	Jakobsweiler, Saar-Nahe Basin, SW	Disibodenberg Fm - middle Wadern Fm; Nahe Grp	fluvio-lacustrine basin
	PT-W	Germany	Gundersweiler, Saar-Nahe Basin, SW	Lauterecken–Odernheim Fm, Humberg Bank	fluvio-lacustrine basin
	PT-W	Germany	Saar-Nahe Basin, SW		fluvio-lacustrine basin
	PT-W	Germany	St. Julian, Saar-Nahe Basin, SW	Quirnbach and Lauterecken–Odernheim Fm	fluvio-lacustrine basin
Rotliegend, Lebach Basin	PT-W	Germany	Lebach (Rümmelbach-Gresaubach area?), Saar-Nahe Basin, SW	Meisenheim Fm; upper Jeckenbach and Odernheim SubFms	fluvio-lacustrine basin
	PT-W	Czech Republic	Svitavca, Boskovice Furrow		
	PT-W	Germany	Gimsbach, Saar-Nahe Basin, SW	Remigiusberg Fm	fluvio-lacustrine basin
	PT-W	Italy	Guardia Pisano Basin, Sulcis area, SW Sardinia	Top of lithofacies B	80-90mm thick brownish-grey lacustrine micritic limestone (parautochthonous)

			Schultze & Kriwet 1999	Brinkmann *et al.* 2010	
			Goldfuss 1847	Hampe 1988a; Schneider 1996; Ginter *et al.* 2010	
			Kner 1867	Hampe 1988a; Ginter *et al.* 2010	
			Hampe 1994	Ginter *et al.* 2010; Schneider 1996	
freshwater			Hampe 1988a	Hampe 1994, 1997; Ginter *et al.* 2010	(as *Xenacanthus* sp. ME)
freshwater			Hampe 1994	Hampe 1997	
			Fritsch 1890	Ginter *et al.* 2010	
freshwater			Johnson 1999	Johnson 2005b; Ginter *et al.* 2010	
freshwater (lacustrine)			Fischer *et al.* 2010		
alluvial/lacustrine to freshwater			Freytet *et al.* 2002		
freshwater			Woodward 1890, 1908; Wade 1942	Lopez-Arbarello 2004	(as *Pleuracanthus* ; erroneous? See Brinkmann *et al.* 2010)
freshwater			Woodward 1890, 1908; Wade 1942	Lopez-Arbarello 2004	(as *Pleuracanthus*)
freshwater			Bendix-Almgreen 1976		(as *Pleuracanthus*)
			Schaeffer 1981	Schultze & Soler-Gijón 2004	(similar to *Triodus*)
freshwater				Milner *et al.* 2006	
freshwater/brackish			Liszkowski 1993		(as *Pleuracanthus*)
freshwater				Johnson *et al.* 2002	
freshwater			Johnson 2012		
freshwater			Sander & Krahl 2007	Johnson 2012	(as xenacanth)
			Fritsch 1890	Ginter *et al.* 2010	
			Fritsch 1890	Schneider 1996	
			Kner 1867	Hampe 1988a	(as *Xenacanthus decheni*)
freshwater			Gaudry 1883	Heyler & Debriette 1986; Ginter *et al.* 2010	
freshwater			Soler-Gijón & Hampe 1998	Schultze & Soler-Gijón 2004	
freshwater			Hampe 1989	Schneider 1996; Hampe 1997; Ginter *et al.* 2010	
freshwater			Hampe 1989	Schneider 1996; Ginter *et al.* 2010	
freshwater			Boy 1976	Hampe 1989	(as *Xenacanthus* sp. B)
freshwater			Hampe 1989	Schneider 1996; Hampe 1997; Ginter *et al.* 2010	
freshwater			Jordan 1849	Schneider 1996; Hampe 1989, 1997, 2003; Johnson & Thayer 2009; Ginter *et al.* 2010	
			Schneider 1985	Hampe 1989; Schneider 1996	(as *T.* cf. *sessilis*)
freshwater			Hampe 1989	Schneider 1996	
freshwater (lacustrine)			Fischer *et al.* 2010	Ginter *et al.* 2010	

106	*Tricodus*	sp.			teeth	Xenacanthidae	Xenacanthiformes	Permian	Cisuralian	Asselian, lower
107	*Tricodus*	sp.			teeth, fin spines	Xenacanthidae	Xenacanthiformes	Permian	Cisuralian	Asselian
108	*Tricodus*	sp.				Xenacanthidae	Xenacanthiformes	Permian	Cisuralian	Asselian
109	*Tricodus*	sp.				Xenacanthidae	Xenacanthiformes	Permian	Guadalupian /Lopingian	
110	*Tricodus?*	sp.			teeth	Xenacanthidae	Xenacanthiformes	Permian	Cisuralian	Asselian
111	*Tricodus*	sp.			teeth	Xenacanthidae	Xenacanthiformes	Permian	Cisuralian	Artinskian
112	*Tricodus*	sp.				Xenacanthidae	Xenacanthiformes	Permian	Lopingian	
113	*Plicatodus*	*jordani* Hampe, 1995			body, anterior half, incl. teeth	Xenacanthidae	Xenacanthiformes	Permian	Cisuralian	Asselian
114	*Wurdigneria*	*obliterata* Richter, 2005			teeth	Xenacanthidae	Xenacanthiformes	Permian	Guadalupian	
115	*Wurdigneria ?*	*pricei* (Würdig-Maciel, 1975)			teeth	Xenacanthidae	Xenacanthiformes	Permian	Cisuralian	Kungurian
116	*Wurdigneria ?*	*santosi* (Würdig-Maciel, 1975)			teeth	Xenacanthidae	Xenacanthiformes	Permian	Guadalupian	
117	*Wurdigneria*	sp.			teeth	Xenacanthidae	Xenacanthiformes	Permian	Cisuralian	Artinskian
118	*Maocrecodontus*	*moorei* (Woodward, 1889c)			teeth	Xenacanthidae	Xenacanthiformes	Triassic	Upper	Carnian
119	*Maocrecodontus*	*moorei* (Woodward, 1889c)			teeth	Xenacanthidae	Xenacanthiformes	Triassic	Upper	Carnian, lower
120	*Maocrecodontus*	*moorei* (Woodward, 1889c)			teeth	Xenacanthidae	Xenacanthiformes	Triassic	Upper	Carnian (Norian, lower)
121	*Maocrecodontus*	*moorei* (Woodward, 1889c)			teeth	Xenacanthidae	Xenacanthiformes	Triassic	Upper	Carnian, upper middle
122	*Maocrecodontus*	*moorei* (Woodward, 1889c)			teeth	Xenacanthidae	Xenacanthiformes	Triassic	Upper	Norian, lower
123	*Maocrecodontus*	*moorei* (Woodward, 1889c)			teeth	Xenacanthidae	Xenacanthiformes	Triassic	Upper	Carnian, upper
124	*Maocrecodontus*	*moorei* (Woodward, 1889c)			teeth	Xenacanthidae	Xenacanthiformes	Triassic	Upper	Carnian, upper
125	*Maocrecodontus*	*moorei* (Woodward, 1889c)			teeth	Xenacanthidae	Xenacanthiformes	Triassic	Upper	Carnian, upper
126	*Maocrecodontus*	*parvidens* (Woodward, 1908)			body fossils	Xenacanthidae	Xenacanthiformes	Triassic	Middle	Anisian
127	*Maocrecodontus*	*indicus* (Jain, 1980)			teeth, cranial elements	Xenacanthidae	Xenacanthiformes	Triassic	Upper	Carnian–Norian
128	*Maocrecodontus*	*angaluhensis* Ragonha, 1984 (*nomen dubium*)				Xenacanthidae	Xenacanthiformes	Triassic	Upper	Carnian?
129	*Maocrecodontus*	*camaquensis* Ragonha, 1984 (*nomen dubium*)				Xenacanthidae	Xenacanthiformes	Triassic	Upper	Carnian?
130	*Maocrecodontus*	*ferrazensis* Ragonha, 1984 (*nomen dubium*)				Xenacanthidae	Xenacanthiformes	Triassic	Upper	Carnian?
131	gen. indet.	sp. indet.			teeth	Xenacanthidae	Xenacanthiformes	Permian	Lopingian	
132	gen. indet.	sp. indet.			teeth		Xenacanthiformes?	Permian	Lopingian	

	PT-W	Italy	Ortu Manu, Perdasdefogu Basin, Sardinia	Rio su Luda Fm	cherty carbonate
Rotliegend, Autun Basin (Bourbon-l'Archambault Basin)	PT-W	France	Buxières-les-Mines, Allier, Massif Central	Buxières Fm	lacustrine siltstone
	PG-N	USA-E	Pennsylvania		
	NT-W	India	Bihar		
	PT-W	France	Autun Basin, Massif Central		
	NT-W	Oman	WAFRA-6 oil well, Al Wusta region	Gharif Fm	nearshore to intertidal coastal plain
Damodar Basin	NT-W	India			
	PT-W	Germany	Lebach (Rümmelbach-Gresaubach area?), Saar-Nahe basin, SW	upper Odernheim SubFm	fluvio-lacustrine basin
Paraná Basin	PG-S	Brazil	Tiarajú region, São Gabriel Municipality, Rio Grande do Sul, S	Teresina Fm, Passa Dois Grp	fossiliferous bone bed within loosely consolidated redstone; epeiric (shallow epicontinental) sea
Paraná Basin	PG-S	Brazil	Minas do Leão Municipality, Rio Grande do Sul, S	Irati Fm, Passa Dois Grp	
Paraná Basin	PG-S	Brazil	Dom Pedrito, Rio Grande do Sul, S	Teresina Fm (previously Estrada Nova Fm), Passa Dois Grp	epeiric (shallow epicontinental) sea
	NT-W	Oman	WAFRA-6 oil well, Al Wusta region	Gharif Fm	nearshore to intertidal coastal plain
	PT-W	England	Ruishton, near Taunton, Somersetshire	North Curry Sandstone Mb, Mercia Mudstone Grp	
	PT-W	Germany	near Gaildorf, Baden-Württemberg	upper Gipskeuper	
	PG-C	USA-S	Crosby and Oldham Counties, Texas	Tecovas Fm, Dockum Grp	floodplain/lacustrine
	PG-C	USA-S	*Placerias* /Downs Quarry, Stinking Springs, and Petrified Forest National Park, Arizona	Mesa Redondo Mb and Blue Mesa Bed, Petrified Forest Mb, Chinle Fm	floodplain
	PG-C	USA-S	New Mexico	Chinle Fm / Dockum Grp	floodplain
	PG-C	USA-S	Crosby, Potter, and Randall counties, Texas	Tecovas Mb, Dockum Fm, Chinle Grp	siltstone-dominated, pond/lacustrine
	PG-C	USA-S	*Placerias* / Downs' quarries, Apache County, Arizona	Blue Mesa Mb, Petrified Forest Fm, Chinle Grp	pond/lacustrine
	PG-C	USA-S	Dying Grounds and Crocodile Hill localities, Petrified Forest National Park, Arizona	Blue Mesa Mb, Petrified Forest Fm, Chinle Grp	pond/lacustrine
	PL-SW	Australia-E	St. Peters, New South Wales	Ashfield Shale, Wianamatta Grp, Hawkesbury Series (sandstone)	gradual change from lacustrine to brackish to shallow marine
	NT-W	India	Pranhita-Godavari Valley, Deccan	Maleri Fm	inter-channel floodplain
Paraná Basin	PG-S	Brazil		Corumbataí Fm	
Paraná Basin	PG-S	Brazil		Corumbataí Fm	
Paraná Basin	PG-S	Brazil		Corumbataí Fm	
Paraná Basin	PG-S	Brazil	Rio Grande do Sul State, S	Rio do Rasto Fm	conglomerates intercalated in red mudstones; lacustrine and channel deposits
		Russia-SW?			

alluvial/lacustrine to freshwater			Freytet *et al.* 2002		(as *Bohemiacanthus*)
freshwater	50-100 cm in length		Schneider & Zajic 1994; Steyer & Escuillie 1997	Steyer *et al.* 2000	(as *Bohemiacanthus*)
				Ginter *et al.* 2010	
				Ginter *et al.* 2010	
	40–50 cm in length? Heyler & Poplin 1990		Heyler 1969; Heyler & Debriette 1986	Hampe 1989	(as *Expleuracanthus*)
marine/freshwater			Schultze *et al.* 2008		
			Schneider, pers. comm. in Schultze *et al.* 2008		
freshwater			Schneider 1988	Schneider 1996; Hampe 1989; 1995, 1997; Ginter *et al.* 2010	(as *Xenacanthus plicatus* A)
brackish–freshwater	predatory; cutting and gouging		Richter 2005	Ginter *et al.* 2010	
			Würdig-Maciel 1975	Richter 2005; Ginter *et al.* 2010	(as *Xenacanthus*)
brackish–freshwater?			Würdig-Maciel 1975	Johnson *et al.* 2002; Richter 2005; Ginter *et al.* 2010	(as *Xenacanthus*) tentative assignment to *Plicatodus* by Hampe 1995 is invalid (Ginter et al. 2010)
marine/freshwater			Schultze *et al.* 2008		
			Woodward 1889c	Jain 1980; Johnson 1980; Schneider 1996; Hampe 1997; Johnson *et al.* 2002; Ginter *et al.* 2010; Cappetta 2012	(as *Diplodus* and *Tricodus*)
			Seilacher 1943	Jain 1980; Johnson 1980; Hampe 1997; Johnson *et al.* 2002; Ginter *et al.* 2010; Cappetta 2012	(as *Diplodus* and *Tricodus*)
freshwater			Johnson 1980	Jain 1980; Hampe 1997; Johnson *et al.* 2002; Milner *et al.* 2006; Ginter *et al.* 2010; Capetta 2012	(as *Xenacanthus* and *Tricodus*)
freshwater			Heckert 2004	Irmis 2005; Parker 2005; Milner *et al.* 2006; Ginter *et al.* 2010	
freshwater				Milner *et al.* 2006; Ginter *et al.* 2010	
freshwater			Murry 1982, 1986, 1989	Huber *et al.* 1993	(as *Xenacanthus*)
freshwater			Jacobs & Murry 1980; Murry & Long 1989	Huber *et al.* 1993; Kaye & Padian 1994; Parker 2005	(as *Xenacanthus*)
freshwater			Murry & Long 1989	Huber *et al.* 1993	
freshwater/brackish/marine			Woodward 1908	Jain 1980; Johnson 1980; Schneider 1996; Johnson *et al.* 2002; Ginter *et al.* 2010; Cappetta 2012	(as *"Pleuracanthus"*)
freshwater			Jain *et al.* 1964	Jain 1980; Johnson 1980; Schneider 1996; Hampe 1997; Johnson *et al.* 2002; Chang & Miao 2004; Ginter *et al.* 2010; Capetta 2012	(as *Diplodus* and *Xenacanthus* and *Tricodus*)
			Ragonha 1984	Ginter *et al.* 2010; Cappetta 2012	(as *Xenacanthus*)
			Ragonha 1984	Ginter *et al.* 2010; Cappetta 2012	(as *Xenacanthus*)
			Ragonha 1984	Ginter *et al.* 2010; Cappetta 2012	(as *Xenacanthus*)
freshwater			Würdig-Maciel 1975	Richter & Langer 1998; Johnson *et al.* 2002	
			Olson 1962	Johnson 1980	

133	gen. indet.	sp. indet.			teeth		Xenacanthiformes?	Permian		
134	gen. indet.	sp. indet.					Xenacanthiformes?	Permian	Cisuralian	
135	"*Cobelodus*"	*obliguus* Ivanov, 2005			teeth		*incertae sedis*	Permian	Cisuralian	**Asselian–Artinskian**
136	*Stethacanthus*	cf. *altonensis* (St. John & Worthen, 1875)			teeth	Symmoriidae	Symmoriiformes	Permian	Cisuralian	Asselian
137	*Stethacanthus*	*altonensis* (St. John & Worthen, 1875)			teeth	Symmoriidae	Symmoriiformes	Permian	Guadalupian	Wordian–Capitanian
138	*Stethacanthus*	*grunti* Minikh, 2004			teeth	Symmoriidae	Symmoriiformes	Permian	Guadalupian	Roadian
139	*Stethacanthus*	spp.			teeth	Symmoriidae	Symmoriiformes	Permian	Cisuralian	Kungurian
140	*Stethacanthus*	sp.			tooth	Symmoriidae	Symmoriiformes	Permian	Cisuralian	Artinskian
141	gen. indet.	sp. indet.			teeth	Symmoriidae	Symmoriiformes	Permian	Guadalupian	Roadian
142	"*Physonemus*"	sp.			fin spine		Symmoriiformes	Permian	Guadalupian	Roadian
143	*Batacanthus*	*gigas* Branson 1916			fin spine		Symmoriiformes?	Permian	Guadalupian	Wordian
144	*Stethacanthulus*	*decorus* (Ivanov, 1999)			teeth	Falcatidae	Symmoriiformes	Permian	Cisuralian	**Asselian–Artinskian**
145	*Stethacanthulus*	*decorus* (Ivanov, 1999)			teeth	Falcatidae	Symmoriiformes	Permian	Guadalupian	Roadian
146	*Stethacanthulus*	cf. *decorus* (Ivanov, 1999)			teeth	Falcatidae	Symmoriiformes	Permian	Guadalupian–Lopingian	
147	*Stethacanthulus*	cf. *decorus* (Ivanov, 1999)			teeth	Falcatidae	Symmoriiformes	Permian	Lopingian	Wuchiapingian
148	*Stethacanthulus*	cf. *decorus* (Ivanov, 1999)			tooth	Falcatidae	Symmoriiformes	Permian	Guadalupian	Wordian
149	*Stethacanthulus*	*meccaensis* (Williams, 1985)			teeth	Falcatidae	Symmoriiformes	Permian	Guadalupian	Capitanian
150	*Stethacanthulus*	*meccaensis* (Williams, 1985)			teeth	Falcatidae	Symmoriiformes	Permian	Guadalupian	Wordian–Capitanian
151	*Ctenacanthus*	*kurgaensis* Minikh, 1999			teeth	Ctenacanthidae	Ctenacanthiformes	Permian	Guadalupian	Wordian–Capitanian
152	*Ctenacanthus*	sp.			spine fragment	Ctenacanthidae	Ctenacanthiformes	Permian	Guadalupian	
153	*Ctenacanthus*	sp.				Ctenacanthidae	Ctenacanthiformes	Permian	Guadalupian	**Roadian–Capitanian**
154	*Glikmanius*	*occidentalis* (Leidy, 1859)	*Ctenacanthus amblyuiphias* Cope, 1891; and probably *Cladodus girtyi* Hay, 1900; *Ctenacanthus volgensis* Minikh and Minikh, 1996; *Ctenacanthus artiensis* Kozlov, 2000			Ctenacanthidae	Ctenacanthiformes	Permian	Guadalupian	Wordian

	PG-S	Brazil	Alto Garças, near 'Boa Esperança', Mato Grosso/Goiás State	Passa Dois Grp	
	PG-C	USA-S	Red House Cliffs (eastern face), SE Utah	Organ Rock Shale	redbeds, intertidal environment
	PT-N	Russia-W	Middle and South Urals		marls and nodular, detrital, and reef limestones
	BOR	Russia-NW	Novaya Zemlya, Arkhangelsk district, northern		
East European Platform	PT-N	Russia-W	Pinega River Basin, Arkhangelsk district, northern European Russia		
Vorkuta–Pechora Basin	BOR	Russia-NW	Kozhim River Basin, northern Cis-Urals	Kozhimrudnitskaya Fm, Inta Fm	
	PT-N	Russia-W	East European Platform		
	PT-N	Russia-W	South Urals		marls and detrital limestones
	PG-C	USA-S	Quarry section, Guadelupe Mountains, western Texas	William Ranch Mb, Cutoff Fm	fossiliferous debris flows interbedded with radiolarian-bearing limestone
Sverdrup Basin	BOR	Canada-N	Lyall River, Grinnell Peninsula, Melville Island, Parry Islands, Canadian Arctic Archipelago	Assistance Fm	loosely consolidated grey-green glauconitic sandstone and minor dusky red siltstone bands (southern basin margin)
Phosphoria Basin (see Piper & Link 2002)	PL-E	USA-N	North Fork of Little Wind River and Bull Lake Creek, Wind River Mountains, Lander, Wyoming	Embar Fm (basal Phosphoria Fm) (=Park City Fm)	
	PT-N	Russia-W	Middle and South Urals		marls and nodular, detrital, and reef limestones
	PG-C	USA-S	Quarry section, Guadelupe Mountains, western Texas	William Ranch Mb, Cutoff Fm	fossiliferous debris flows interbedded with radiolarian-bearing limestone
Madagascar Embayment	NT-W	Oman	Qarari block, Batain Plain, NE	Batain Melange	platform margin
Madagascar Embayment	NT-W	Oman	the "Bridge", Batain Plain, NE	Batain Melange	platform margin
Hawasina Basin	NT-W	Oman	Wadi Maqam, Sumeini area, NW	Maqam Fm	continental slope
	PG-C	USA-S	Guadelupe and Apache Mountains, western Texas	Rader Limestone Mb and Lamar Limestone Mb, Bell Canyon Fm	
	PG-C	USA-S	PI section, Guadelupe Mountains, western Texas	Hegler and Pinery Mbs, Bell Canyon Fm	thin limestone intervals interbedded with sandstone and siltstone
	PT-N	Russia-W	Pinega River basin, Arkhangelsk district, northern European Russia		
Paraná Basin	PG-S	Brazil	Dom Pedrito, Rio Grande do Sul, S	Teresina Fm (previously Estrada Nova Fm), Passa Dois Grp	epeiric (shallow epicontinental) sea
Phosphoria Basin (see Piper & Link 2002)	PL-E	USA-N	Wyoming	Meade Peak and Retort Mbs, Phosphoria Fm; lower and upper Mbs, Shedhorn Fm	mudflat and near-shore sands
	PG-C	USA-S/C	New Mexico, Arizona, Indiana, Illinois, Ohio, Colorado		

			Mutter *et al.* 2008b		
marine?			Sumida *et al.* 1999		
marine		*Sph. vulgaris – Par. solidissima* fusulinid zone	Ivanov 2000	Ivanov 2005; Ginter *et al.* 2010	(as *Cochelodus* sp.)
			Ivanov 1999	Ivanov 2000	not described in systematic part
			Minikh 1999	Lozovsky *et al.* 2009	(as *Ctenacanthus rosanovi* sp. nov., re-assigned to *Pinegia* Minikh, 2004 (pre-occupied), re-assigned to *Pinegocaptus* Minikh, 2006, synonymised with *Stethacanthus*; Ivanov 2007, pers. comm. 2012)
			Minikh 2004	Lozovsky *et al.* 2009	(as *Pinegia grunti* (pre-occupied), re-assigned to *Pinegocaptus* Minikh 2006, synonymised with *Stethacanthus*; Ivanov 2007, pers. comm. 2012)
			Minikh *et al.* 2003	Lozovsky *et al.* 2009	(as *Pinegocaptus*)
marine		*Ps. pedissequa – Ps. concavutas* fusulinid zones	Ivanov 2005		(similar to *S. altonensis*)
marine			Ivanov *et al.* 2012		(as Stethacanthidae, but see Maisey 2009)
marine			Nassichuk 1971		(diverse array of morphologies, Maisey 1983, but *Stethacanthus* -like, Maisey 2009; genus synonymised in part with *Stethacanthus* , Ginter *et al.* 2010)
			Branson 1916		(tentatively included in "*Physonemus* ", Maisey 1983; which has in turn been synonymised in part with *Stethacanthus* , Ginter *et al.* 2010)
marine		*Sph. vulgaris – Par. solidissima* fusulinid zone	Ivanov 1999	Ivanov 2000, 2005; Ginter *et al.* 2010	(as *"Ctenaea" decora*)
marine			Ivanov *et al.* 2012		
marine			this study		Sample 100302-F
marine			this study		Samples 100302-H, 110223-A
marine			this study		Sample 100227-C
marine			Ivanov *et al.* 2011		
marine			Ivanov *et al.* 2012		
			Minikh 1999		
brackish–freshwater?			Würdig-Maciel 1975	Richter 2005	
marine			Yochelson & Van Sickle 1968		
				Ginter *et al.* 2010	

155	*Gilkmanius*	*occidentalis* (Leidy, 1859)	idem			Ctenacanthidae	Ctenacanthiformes	Permian	Cisuralian	
156	*Gilkmanius*	*occidentalis* (Leidy, 1859)	idem		fin spines	Ctenacanthidae	Ctenacanthiformes	Permian	Cisuralian	
157	*Gilkmanius*	*occidentalis* (Leidy, 1859)	idem			Ctenacanthidae	Ctenacanthiformes	Permian	Cisuralian	
158	*Gilkmanius*	*occidentalis* (Leidy, 1859)	idem		fin spine	Ctenacanthidae	Ctenacanthiformes	Permian	Guadalupian	**Roadian–Wordian**
159	*Gilkmanius*	*occidentalis* (Leidy, 1859)	idem		teeth	Ctenacanthidae	Ctenacanthiformes	Permian	Guadalupian	**Roadian–Wordian**
160	*Gilkmanius*	*occidentalis* (Leidy, 1859)	idem		teeth	Ctenacanthidae	Ctenacanthiformes	Permian	Guadalupian	Capitanian
161	*Gilkmanius*	*occidentalis* (Leidy, 1859)	idem		fin spine	Ctenacanthidae	Ctenacanthiformes	Permian	Cisuralian	
162	*Gilkmanius*	*occidentalis* (Leidy, 1859)	idem		fin spine	Ctenacanthidae	Ctenacanthiformes	Permian	Cisuralian	
163	*Gilkmanius*	*occidentalis* (Leidy, 1859)	idem		fin spines	Ctenacanthidae	Ctenacanthiformes	Permian	Cisuralian	Asselian?
164	*Gilkmanius*	*occidentalis* (Leidy, 1859)	idem		teeth	Ctenacanthidae	Ctenacanthiformes	Permian	Cisuralian	Artinskian
165	*Gilkmanius*	*occidentalis* (Leidy, 1859)	idem		tooth	Ctenacanthidae	Ctenacanthiformes	Permian	Cisuralian	Kungurian
166	*Gilkmanius*	*occidentalis* (Leidy, 1859)	idem		teeth	Ctenacanthidae	Ctenacanthiformes	Permian	Guadalupian	
167	*Gilkmanius*	*occidentalis* (Leidy, 1859)	idem		teeth	Ctenacanthidae	Ctenacanthiformes	Permian	Cisuralian	Artinskian
168	*Gilkmanius*	*occidentalis* (Leidy, 1859)	idem		teeth	Ctenacanthidae	Ctenacanthiformes	Permian	Guadalupian –Lopingian	**Wordian–Capitanian**
169	*Gilkmanius*	*occidentalis* (Leidy, 1859)	idem		teeth	Ctenacanthidae	Ctenacanthiformes	Permian	Guadalupian –Lopingian	Wordian–Capitanian
170	*Gilkmanius*	*occidentalis* (Leidy, 1859)	idem		teeth	Ctenacanthidae	Ctenacanthiformes	Permian	Guadalupian	Wordian–Capitanian
171	*Gilkmanius*	*occidentalis* (Leidy, 1859)	idem		teeth	Ctenacanthidae	Ctenacanthiformes	Permian	Cisuralian	Kungurian
172	*Gilkmanius*	*occidentalis* (Leidy, 1859)	idem		teeth	Ctenacanthidae	Ctenacanthiformes	Permian	Cisuralian	Kungurian
173	*Gilkmanius*	cf. *occidentalis* (Leidy, 1859)			teeth	Ctenacanthidae	Ctenacanthiformes	Permian	Cisuralian	Artinskian?
174	*Gilkmanius*	*myachkovensis* (Lebedev, 2001)			teeth	Ctenacanthidae	Ctenacanthiformes	Permian	Cisuralian	Kungurian
175	*Gilkmanius*	*myachkovensis* (Lebedev, 2001)			teeth	Ctenacanthidae	Ctenacanthiformes	Permian	Cisuralian	Kungurian
176	*Gilkmanius*	*myachkovensis* (Lebedev, 2001)			teeth	Ctenacanthidae	Ctenacanthiformes	Permian	Cisuralian	Sakmarian
177	*Gilkmanius*	*myachkovensis* (Lebedev, 2001)			teeth	Ctenacanthidae	Ctenacanthiformes	Permian	Guadalupian	Wordian
178	*Gilkmanius*	*myachkovensis* (Lebedev, 2001)			teeth	Ctenacanthidae	Ctenacanthiformes	Permian	Guadalupian	Wordian

	PG-C	USA-C	Pottawatomie County, Kansas	Neva Limestone Mb., Genola Limestone Fm, Council Grove Grp	Poorly consolidated limey mud
	PG-C	USA-C	Pottawatomie County, Kansas	Neva Limestone Mb., Genola Limestone Fm, Council Grove Grp	Poorly consolidated limey mud
	PG-C	USA-C	Wabaunsee County, Kansas	Council Grove Grp	
Phosphoria Basin (see Piper & Link 2002)	PL-E	USA-N	North Fork of Little Wind River and Bull Lake Creek, Wind River Mountains, Lander, Wyoming	Embar Fm (=Park City Fm) / Meade Peak Mb, Phosphoria Fm	
Phosphoria Basin (see Piper & Link 2002)	PL-E	USA-N	North Fork of Little Wind River and Bull Lake Creek, Wind River Mountains, Lander, Wyoming	Embar Fm (=Park City Fm) / Meade Peak Mb, Phosphoria Fm	
Phosphoria Basin (see Piper & Link 2002)	PL-E	USA-N	Dinwoody Creek, Wind River Mountains, Wyoming	Pustula Mb, Middle Phosphoria Fm (=Retort Mb)	Thin phosphate bed
	PG-C	USA-S	Texas	Wichita Grp	redbeds
	PG-C	USA-S	Texas	Wichita Grp	redbeds
	PG-C	USA-S	Little Bitter Creek, Young County, Texas	Moran Fm, Wichita Grp	clays near marine limestones in red beds
	PG-C	USA-S	north central Texas	Wichita Grp (Petrolia Fm, Waggoner Ranch Fm)	coastal plain (mixed marine, freshwater and terrestrial vertebrates)
	PL-C	Japan	Kinshozan, Akasaka-cho, Ohgaki City, Gifu Prefecture, central Honshu	lower Akasaka Limestone	pale orange and dark grey part of grey-white massive limestone
	PL-C	Japan	Kinshozan, Akasaka-cho, Ohgaki City, Gifu Prefecture, central Honshu	middle Akasaka Limestone	bedded, black, coaly limestone, beneath *Colania gifuensis* concentrated bed
	PT-N	Russia-W	Middle and South Urals		
	PT-N	Russia-W	Arkhangelsk and Vyatka districts, Tatarstan, near Kazan	East European Platform	
	PT-N	Russia-W	Telegrafniy Gully, near Pechishchi, Volga region	"Mylnik" Mb	
	BOR	Russia-NW	Vym' River, Komi Republic		
Kaibab Sea	PL-E	USA-W	Kachina Village, Flagstaff, Arizona	lower Fossil Mountain Mb, Kaibab Fm	shallow (15–180m), open marine sea, calcareous/sandy limestones
Kaibab Sea	PL-E	USA-W	SW of Flagstaff, Arizona	Harrisburg Mb, Kaibab Fm	shallow (15–180m), restricted, marine sea, calcareous/sandy limestones
	BOR	Greenland-E	Amdrup Land, NE	'Upper Marine group'	calcareous sandstone
Kaibab Sea	PL-E	USA-W	Kachina Village, Flagstaff, Arizona	lower Fossil Mountain Mb, Kaibab Fm	shallow (15–180m), open marine sea, calcareous/sandy limestones
Kaibab Sea	PL-E	USA-W	SW of Flagstaff, Arizona	Harrisburg Mb, Kaibab Fm	shallow (15–180m), restricted, marine sea, calcareous/sandy limestones
Madagascar Embayment	NT-W	Oman	Jabel Gharif, Haushi-Huqf region, E	Khuff Fm	rim basin
Madagascar Embayment	NT-W	Oman	Haushi Cliff and Saiwan, Haushi-Huqf region, E	Khuff Fm	rim basin
Hawasina Basin	NT-W	Oman	Saiq Plateau, Jabal al Akhdar, Oman Mountains, N	Saiq Fm	rim basin

			Ewell & Everhart 2005		(as *Cladodus*) Location from Everhart, pers. comm. 2010
			Ewell & Everhart 2005		(as *Ctenacanthus* cf. *amblissiphias*) Location from Everhart, pers. comm. 2010
			M. Everhart [http://www.oceansofkansas.com/Leidy1859.html]	Ginter *et al.* 2005; Hodnett *et al.* 2012	
			Branson 1916		(as *Ctenacanthus amblissiphias*)
			Branson 1916	Bendix-Almgreen 1975; Hodnett *et al.* 2012	(as *Cladodus*)
			Branson 1933	Nielsen 1935; Hodnett *et al.* 2012	(as *Cladodus*)
			Cope 1891	Romer 1942	
			Hussakof 1911	Romer 1942	
marine			Romer 1942	Johnson 1981	
marine			Johnson 2008	Hodnett *et al.* 2012	
marine		*Parafusulina* Zone	Goto *et al.* 1988	Goto 1985?, 1994a, b, 1996a–c, 1999a, b, 2000; (Yokoi 1994, 2000? See Yamagishi 2006); Ginter *et al.* 2005	(as " *Cladodus* "?, *Symmorium(?)*)
marine		*Colania amicula - C. gifuensis* Zone	Yamagishi 2006; Yamagishi & Fujimoto 2011		(as " *Cladodus* " sp. (*nomen dubium*))
			Kozlov 2000	Ivanov 2000, 2005; Ginter *et al.* 2005, 2010; Hodnett *et al.* 2012	(as *Ctenacanthus artiensis* sp. nov.)
			Minikh & Minikh 1996	Ivanov 2000, 2005; Ginter *et al.* 2005, 2010	(as *Ctenacanthus volgensis* sp. nov.)
				Minikh & Minikh 1998	
			Malysheva *et al.* 2000	Ivanov 2005; Ginter *et al.* 2005, 2010	(as " *Symmorium* " cf. *occidentalis*)
marine			Hodnett *et al.* 2012		
marine, increasingly saline			Hodnett *et al.* 2012		
marine		*Athyris ambrupi* brachiopod Zone	Bendix-Almgreen 1975	Bendix-Almgreen 1976	(as ' *Cladodus* ' sp.; not officially reassigned, but close to Branson 1916)
marine			Hodnett *et al.* 2012		
marine, increasingly saline			Hodnett *et al.* 2012		
marine		*Sweetognathus merrilli* conodont Zone; *Sakmarites* ammonoid Zone; *Pseudofusulina* fusulinid Zone	this study		Samples AO40, AO55, AO47bis, AO50; and 965-2, 965-3, 965-8, 965-9
marine		*Jinogondolella aserrata* conodont Zone; OSPZ6 palynology Zone; *Neoschwagerina craticulifera* fusulinid Zone	this study		Sample AO208
marine			this study		Samples 110219-J, 110219-L, 110219-M

179	*Gilkmanius*	*culmenis* Koot, Cuny, Tintori and Twitchett, 2013			teeth	Ctenacanthidae	Ctenacanthiformes	Permian	Guadalupian	Wordian
180	*Gilkmanius*				teeth	Ctenacanthidae	Ctenacanthiformes	Permian		
181	*"Cladodus"*?	sp.			tooth	Ctenacanthidae	Ctenacanthiformes	Permian	Lopingian	Wuchiapingian
182	*"Cladodus"*	sp.			tooth	Ctenacanthidae	Ctenacanthiformes	Permian	Cisuralian	
183	*"Cladodus"*	sp.			tooth	Ctenacanthidae	Ctenacanthiformes	Permian	Lopingian	
184	*"Cladodus"*	sp.			teeth	Ctenacanthidae	Ctenacanthiformes	Permian	Cisuralian	Artinskian
185	*"Cladodus"*	sp. 1				Ctenacanthidae	Ctenacanthiformes	Permian	Guadalupian	Wordian (Kazanian)
186	*"Cladodus"*	sp. 2				Ctenacanthidae	Ctenacanthiformes	Permian	Guadalupian	Wordian–Capitanian (Kazanian)
187	*"Cladodus"*	sp. 3				Ctenacanthidae	Ctenacanthiformes	Permian	Cisuralian–Guadalupian	Artinskian–Kungurian, Wordian (Kazanian)
188	*"Cladodus"*	sp.			teeth	Ctenacanthidae	Ctenacanthiformes	Permian	Cisuralian–Guadalupian	Kungurian–Roadian
189	*"Cladodus"*	sp.			tooth	Ctenacanthidae	Ctenacanthiformes	Permian	Cisuralian	Artinskian–Kungurian
190	*"Cladodus"*	sp.			teeth	Ctenacanthidae	Ctenacanthiformes	Permian	Cisuralian	Artinskian–Kungurian
191	*"Cladodus"*	sp.				Ctenacanthidae	Ctenacanthiformes	Permian	Guadalupian	**Roadian–Capitanian**
192	*Heslerodus*	*divergens* (Trautschold, 1879)		*Phoebodus heslerorum* Williams, 1985		Heslerodidae	Ctenacanthiformes	Permian		
193	*Heslerodus*	*divergens* (Trautschold, 1879)		idem	tooth	Heslerodidae	Ctenacanthiformes	Permian	Cisuralian	Sakmarian
194	*Heslerodus*	*divergens* (Trautschold, 1879)		idem	teeth	Heslerodidae	Ctenacanthiformes	Permian	Cisuralian	Kungurian
195	*Heslerodus*	*divergens* (Trautschold, 1879)		idem		Heslerodidae	Ctenacanthiformes	Permian	Cisuralian	Asselian
196	*Heslerodus*	*divergens* (Trautschold, 1879)		idem		Heslerodidae	Ctenacanthiformes	Permian	Cisuralian	Asselian
197	*Heslerodus*	*divergens* (Trautschold, 1879)		idem	teeth	Heslerodidae	Ctenacanthiformes	Permian	Cisuralian	Asselian, Artinskian
198	*Saivodus*	sp.				*incertae sedis*	Ctenacanthiformes	Permian	Cisuralian	Kungurian

Madagascar Embayment	NT-W	Oman	Haushi Cliff and Saiwan, Haushi-Huqf region, E	Khuff Fm	rim basin
	NT-E	Australia-W	Irwin River district, W	Holmwood Shale Fm, Fossil Cliff Mb	
	BOR	Greenland-E	Section F (120 m above sea level), Kap Stosch, Hold with Hope, E	*Productus* (*Martinia*) Limestone (Ravnefjeld Fm), Foldvik Creek Grp	limestones and shales
	PL-C	Japan	Hajikadani, Neo-mura, Motosu-gun, Gifu Prefecture, central Honshu	Funabuseyama Fm, Okumino Grp	limestone
	PL-W	Japan	Motoyoshi, Toyoma-cho, Toyoma-gun, Miyagi Prefecture, NE Honshu	Toyoma Fm	
	PT-N	Russia-W	Pre-Uralian region and Southern Urals		
	PT-N	Russia-W	(Arkhangelsk and Vyatka districts, Tataria) European Russia		brachiopod limestone; hemipelagic (shelf)
	PT-N	Russia-W	(Arkhangelsk and Vyatka districts, Tataria) European Russia		brachiopod and pelecypod limestone; hemipelagic (shelf)
	PT-N	Russia-W	Krasnoufimsk, European Russia		*Helicoprion* marls, basinal; brachiopod limestone, hemipelagic (shelf)
Kaibab Sea	PL-E	USA-W	Grand Canyon, Arizona	Kaibab Fm	
Andes	PL-E	Bolivia	Isla del Sol, Lake Titicaca	Copacabana Fm, Titicaca Grp	
Andes	PL-E	Bolivia	Jacha Khatawi Hill, Yaurichambi, La Paz department	Copacabana Fm, Titicaca Grp (fish horizon 1)	limestone, shallow benthic environment
Phosphoria Basin (see Piper & Link 2002)	PL-E	USA-N	Wyoming	Meade Peak, Retort and Rex Mbs, Phosphoria Fm; lower and upper Mbs, Shedhorn Fm	mudflat and near-shore sands
	PL-E	USA-W	Nevada		
	PG-C	USA-C	Pottawatomie County, Kansas	Speiser Shale, Council Grove Grp; Threemile Limestone Mb, Schroyer Limestone Mb, Wreford Limestone, Chase Grp; Wreford Megacyclothem	open marine (50 m water depth)
Kaibab Sea	PL-E	USA-W	Kachina Village, Flagstaff, Arizona	lower Fossil Mountain Mb, Kaibab Fm	shallow (15–180m), open marine sea, calcareous/sandy limestones
	BOR	Russia-NW	Gulyaevskaya, Pechora Sea, Russia		
	PT-N	Russia-W	Moscow region, Russia		
	PT-N	Russia-W	Middle and South Urals		marls and nodular, detrital, and reef limestones
Kaibab Sea	PL-E	USA-W	Flagstaff, Arizona	lower Fossil Mountain Mb, Kaibab Fm	shallow (15–180m), open marine sea, calcareous/sandy limestones

marine		*Idiognathodella aserrata* conodont Zone; OSPZ6 palynology Zone; *Neoschwagerina craticulifera* fusulinid Zone	this study		Samples AO40, AO55, AO47bis, AO50
			Daymond 1993	Ginter *et al.* 2005; Hodnett *et al.* 2012	(as *Stethacanthus*)
marine			Nielsen 1932	Nielsen 1935; Stensiö 1961; Bendix-Almgreen 1976; Hodnett *et al.* 2012	(true affinities difficult to assess, Hodnett *et al.* 2012)
		Pseudofusulina ambigua Zone	Yamagishi 2006	(as *nomen dubium* ; same as *Gilkmanius occidentalis* ? based on Akasaka)	
			Yamagishi 2006	(as *nomen dubium* ; same as *Gilkmanius occidentalis* ? based on Akasaka)	
			Karpinsky 1899, 1903, 1916	Ivanov 2000	
marine			Chabakov 1927	Khabakov 1926–27, 1939; Ivanov 2000	
marine			Chabakov 1927	Khabakov 1926–27, 1939; Ivanov 2000	
marine			Chabakov 1927		(as *Hybodus/Hypodus* in Krasnopolsky, 1889)
marine			McKee 1982	Hunt *et al.* 2005	
marine			Janvier 1981	Merino-Rodo & Janvier 1986	
marine	durophagous (bryozoa, molluscs, crinoids)	? *Mecostreptognathodus* aff. *sulcoplicatus* conodont zone; *Eoparafusulina* fusulinid zone	Merino-Rodo & Janvier 1986		
marine			Yochelson & Van Sickle 1968		
			Case 1973	Ivanov 1999; Maisey 2010	(as *Phoebodus* sp.)
marine			Schultze 1985	Ginter 2002b; Maisey 2010; Ginter *et al.* 2010; Hodnett *et al.* 2012	(as "*Cladodus*")
marine			Hodnett *et al.* 2012		
			Ivanov 1999	Ginter 2002b; Maisey 2010; Ginter *et al.* 2010; Hodnett *et al.* 2012	(as "*Cladodus*" *divergens*)
			Ivanov 1999	Ginter 2002b; Maisey 2010; Ginter *et al.* 2010; Hodnett *et al.* 2012	(as "*Cladodus*" *divergens*)
marine		*Sph. vulgaris* – *Ps. fecunda*, *Ps. pedissequa*–*Ps. concavutas* ?, and *Par. solidissima* fusulinid zones	Ivanov 2005	Hodnett *et al.* 2012	(as *Heslerodus* sp.)
marine			Hodnett *et al.* 2012		

199	*Necosaivodus*	*flagstaffensis* Hodnett, Elliot, Olson & Wittke, 2012			teeth	*incertae sedis*	Ctenacanthiformes	Permian	Cisuralian	Kungurian
200	*Necosaivodus*	*flagstaffensis* Hodnett, Elliot, Olson & Wittke, 2012			teeth	*incertae sedis*	Ctenacanthiformes	Permian	Cisuralian	Kungurian
201	*Kaibabvenator*	*swiftae* Hodnett, Elliot, Olson & Wittke, 2012			teeth	*incertae sedis*	Ctenacanthiformes	Permian	Cisuralian	Kungurian
202	*Kaibabvenator*	*swiftae* Hodnett, Elliot, Olson & Wittke, 2012			teeth	*incertae sedis*	Ctenacanthiformes	Permian	Cisuralian	Kungurian
203	*Nanoskalme*	*natans* Hodnett, Elliot, Olson & Wittke, 2012			teeth	*incertae sedis*	Ctenacanthiformes	Permian	Cisuralian	Kungurian
204	*Nanoskalme*	*natans* Hodnett, Elliot, Olson & Wittke, 2012			teeth	*incertae sedis*	Ctenacanthiformes	Permian	Cisuralian	Artinskian
205	gen. indet.	sp. indet.			teeth	*incertae sedis*	Ctenacanthiformes?	Permian	Guadalupian	
206	gen. indet.	sp. indet.			teeth	*incertae sedis*	Ctenacanthiformes?	Permian	Cisuralian	Sakmarian–Artinskian
207	*Acondylacanthus?*	*browni* Branson, 1916			fin spine	*incertae sedis*	Ctenacanthiformes	Permian	Guadalupian	Wordian
208	*Acondylacanthus?*	*browni* Branson, 1916			fin spine	*incertae sedis*	Ctenacanthiformes	Permian	Guadalupian	Capitanian
209	*Acondylacanthus?*	*obscuracostatus* Branson, 1916			fin spine	*incertae sedis*	Ctenacanthiformes	Permian	Guadalupian	Wordian
210	gen. indet.	sp. indet.			fin spine	*incertae sedis*	Ctenacanthiformes	Permian	Cisuralian	
211	*Pyknothylacanthus*	*spathianus* Mutter & Rieber, 2005			fin spine, denticles		*incertae sedis*	Triassic	Lower	Olenekian (Spathian, lower)
212	*Pyknothylacanthus?*	*humboldtensis* Davidson, 1919			fin spine fragment		*incertae sedis*	Triassic	Middle	
213	gen. indet.	sp. indet.			partial body		*incertae sedis*	Triassic	Lower	Olenekian
214	gen. indet.	sp. indet.			tooth fragments		*incertae sedis* (Cladodontomorphi?)	Triassic	Middle–Upper	Anisian, Norian
215	*Dwykaselachus*	*oosthuizeni* Oelofsen, 1986			neurocranium		*incertae sedis*	Permian	Cisuralian	Sakmarian–**Artinskian**
216	New genus	sp. indet.			teeth	Jalodontidae	*incertae sedis*	Permian	Guadalupian	Capitanian
217	New genus	sp. indet.			teeth	Jalodontidae		Permian	Guadalupian	Roadian
218	New genus	sp. indet.			teeth	Jalodontidae		Permian	Guadalupian	Wordian–Capitanian
219	*Isacrodus*	*marthae* Ivanov, Nestell & Nestell, 2012			teeth	Jalodontidae	*incertae sedis*	Permian	Guadalupian	Roadian
220	*Texascodus*	*variedentatis* Ivanov, Nestell & Nestell, 2012			teeth	Jalodontidae	*incertae sedis*	Permian	Guadalupian	Wordian–Capitanian
221	*Adamantina*	*benedictae* Bendix-Almgreen, 1993			teeth, denticles	Jalodontidae	*incertae sedis*	Permian	Lopingian	Wuchiapingian
222	*Adamantina*	*benedictae* Bendix-Almgreen, 1993				Jalodontidae	*incertae sedis*	Permian	Guadalupian	**Roadian–Capitanian**
223	*Adamantina*	*foliacea* Ivanov, 1999			teeth	Jalodontidae	*incertae sedis*	Permian	Cisuralian	Asselian
224	*Adamantina*	*foliacea* Ivanov, 1999			teeth	Jalodontidae	*incertae sedis*	Permian	Cisuralian	Artinskian
225	*Adamantina*	*foliacea* Ivanov, 1999			tooth	Jalodontidae	*incertae sedis*	Permian	Guadalupian	Roadian

Kaibab Sea	PL-E	USA-W	Kachina Village, Flagstaff, Arizona	lower Fossil Mountain Mb, Kaibab Fm	shallow (15–180m), open marine sea, calcareous/sandy limestones
Kaibab Sea	PL-E	USA-W	SW of Flagstaff, Arizona	Harrisburg Mb, Kaibab Fm	shallow (15–180m), restricted, marine sea, calcareous/sandy limestones
Kaibab Sea	PL-E	USA-W	Kachina Village, Flagstaff, Arizona	lower Fossil Mountain Mb, Kaibab Fm	shallow (15–180m), open marine sea, calcareous/sandy limestones
Kaibab Sea	PL-E	USA-W	SW of Flagstaff, Arizona	Harrisburg Mb, Kaibab Fm	shallow (15–180m), restricted, marine sea, calcareous/sandy limestones
Kaibab Sea	PL-E	USA-W	Kachina Village, Flagstaff, Arizona	lower Fossil Mountain Mb, Kaibab Fm	shallow (15–180m), open marine sea, calcareous/sandy limestones
	PG-C	USA-S	West Franklin Bend, Baylor County, Texas	middle Waggoner Ranch Fm, Wichita Grp	
	PL-C	Japan	Kinshozan, Akasaka-cho, Ohgaki City, Gifu Prefecture, central Honshu	middle Akasaka Limestone	bedded, black, coaly limestone, beneath *Colania gifuensis* concentrated bed
	PT-N	Russia-SW	Southern Urals, Orenburg and Chelyabinsk districts		
Phosphoria Basin (see Piper & Link 2002)	PL-E	USA-N	North Fork of Little Wind River and Bull Lake Creek, Wind River Mountains, Lander, Wyoming	Embar Fm (basal Phosphoria Fm) (=Park City Fm)	
Phosphoria Basin (see Piper & Link 2002)	PL-E	USA-N	Dinwoody Creek, Wind River Mountains, Wyoming	Pustula Mb, Middle Phosphoria Fm (=Retort Mb)	Thin phosphate bed
Phosphoria Basin (see Piper & Link 2002)	PL-E	USA-N	North Fork of Little Wind River and Bull Lake Creek, Wind River Mountains, Lander, Wyoming	Embar Fm (basal Phosphoria Fm) (=Park City Fm)	
	PG-C	USA-S	Tit Butte locality, Texas		
	PL-E	USA-W	near Hot Springs, Bear Lake, Bear Lake County, SE Idaho	Middle Shale unit, Thaynes Fm	
	PL-E	USA-W	western Humboldt Range, Nevada		
	PL-E	Canada-W	Ganoid Ridge, Wapiti Lake, British Columbia	Vega-Phroso Siltstone Mb, Sulphur Mountain Fm	siltstone, deltaic/shallow continental shelf environment
	PL-C	Japan	Kamura, Takachiho-chō, Nishiusuki-gun, Miyazaki-ken (Prefecture), Kyūshū	Kamura Fm	mid-oceanic seamount
	PG-S	South Africa	Farm Zwartskraal, Prince Albert District, Cape Province	Prince Albert Fm (upper Dwyka shales), Ecca Grp, Karoo Supergrp	
	PG-C	USA-S	Guadelupe Mountains, western Texas	Rader Limestone Mb, Bell Canyon Fm	
	PG-C	USA-S	Quarry section, Guadelupe Mountains, western Texas	William Ranch Mb, Cutoff Fm	fossiliferous debris flows interbedded with radiolarian-bearing limestone
	PG-C	USA-S	PI section, Guadelupe Mountains, western Texas	Hegler and Pinery Mbs, Bell Canyon Fm	thin limestone intervals interbedded with sandstone and siltstone
	PG-C	USA-S	Quarry section, Guadelupe Mountains, western Texas	William Ranch Mb, Cutoff Fm	fossiliferous debris flows interbedded with radiolarian-bearing limestone
	PG-C	USA-S	PI section, Guadelupe Mountains, western Texas	Hegler and Pinery Mbs, Bell Canyon Fm	thin limestone intervals interbedded with sandstone and siltstone
	BOR	Greenland-E	River 14 (335m from Hajbastionen), SE from Kap Stosch, Hold with Hope, E	Upper fish horizon, Ravnefjeld Fm, Foldvik Creek Grp	
	BOR	Russia-NW	Kanin Peninsula		
	BOR	Russia-NW	Polar Urals		marls and nodular, detrital, and reef limestones
	PT-N	Russia-W	Middle and South Urals		marls and nodular, detrital, and reef limestones
	PG-C	USA-S	Quarry section, Guadelupe Mountains, western Texas	William Ranch Mb, Cutoff Fm	fossiliferous debris flows interbedded with radiolarian-bearing limestone

marine			Hodnett *et al.* 2012		
marine, increasingly saline			Hodnett *et al.* 2012		
marine			Hodnett *et al.* 2012		
marine, increasingly saline			Hodnett *et al.* 2012		
marine			Hodnett *et al.* 2012		
			Johnson 2008	Hodnett *et al.* 2012	(as *Glikmanius? occidentalis* posterior? tooth)
marine		*Colania amicula* - *C. gifuensis* Zone	Yamagishi 2006; Yamagishi & Fujimoto 2011		(as cladodont)
			Yankevich & Minikh 1998	Ivanov 2000	(as cladodont)
			Branson 1916		(as *Ctenacanthus*)
			Branson 1933	Nielsen 1935; Maisey 1984b	(as *Ctenacanthus*)
			Branson 1916	Maisey 1984b	(as *Ctenacanthus*)
			Berman 1970	Johnson 1981	
marine		*Columbites parisianus* Zone	Mutter & Rieber 2005	Cappetta 2012	(as Ctenacanthoidea?)
			Davidson 1919	Mutter & Rieber 2005	(as *"Cosmacanthus"*)
marine			Mutter *et al.* 2007a		(as Ctenacanthoidea?)
marine		*Chicsella timorensis* , *Paragondolella bulgarica* – *Metapolygnathus nodosus* , *N. primitius*	this study		Samples 300311-I, 300311-J, 300311-O
marine			Oelofsen 1981, 1986	Murray 2000	
marine			Ivanov *et al.* 2007a	Ivanov *et al.* 2011	
marine			Ivanov *et al.* 2012		
marine			Ivanov *et al.* 2012		
marine			Ivanov *et al.* 2012		
marine			Ivanov *et al.* 2012		
			Bendix-Almgreen 1993, 1994	Ginter *et al.* 2010	(as Guadalupian in Ivanov *et al.* 2012)
			Ivanov & Lebedev 2007	Ivanov *et al.* 2012	
marine		e.g., *Par. solidissima* fusulinid zone	Ivanov 1999	Ivanov 2000, 2005; Ginter *et al.* 2010; Ivanov *et al.* 2012	
marine		e.g., *Par. solidissima* fusulinid zone	Ivanov 1999	Ivanov 2000, 2005; Ginter *et al.* 2010; Ivanov *et al.* 2012	
marine			Ivanov *et al.* 2012		

226	*Adamantina*	sp.			teeth	Jalodontidae	*incertae sedis*	Permian	Cisuralian	Artinskian
227	*Adamantina*	sp.			teeth	Jalodontidae	*incertae sedis* (Elasmobranchii)	Permian	Guadalupian	Wordian
228	'Genus A'	sp.			denticles		*incertae sedis (Elasmobranchii)*	Triassic	Lower	Olenekian (lower Smithian?–Spathian?)
229	'Genus A'?	sp.			partial body		*incertae sedis (Elasmobranchii)*	Triassic	Lower	Olenekian (lower Smithian?–Spathian?)
230	gen. indet.	*keuperinus* Murchison & Strickland, 1840			fin spines, teeth		Hybodontiformes?/ Cladodontiformes?	Triassic	Upper	
231	gen. indet.	*keuperinus* Murchison & Strickland, 1840					Hybodontiformes?/ Cladodontiformes?	Triassic	Upper	
232	*Protacrodus*	sp.			teeth	Protacrodontidae	*incertae sedis*	Triassic	Middle	Anisian
233	*Dionguvodus*	*latus* Minikh, 1996b			tooth	Hybodontidae	Hybodontiformes	Triassic	Middle	
234	*Dionguvodus*	*barchanensis* Minikh, 1996b			tooth	Hybodontidae	Hybodontiformes	Triassic	Middle	
235	*Dionguvodus*	*donatus* Minikh, 1996b			tooth	Hybodontidae	Hybodontiformes	Triassic	Middle	
236	*Hybodus*	*longiconus* Agassiz, 1843			teeth	Hybodontidae	Hybodontiformes	Triassic	Middle	
237	*Hybodus*	*longiconus* Agassiz, 1843			teeth	Hybodontinae	Hybodontiformes	Triassic	Middle	Anisian–Ladinian
238	*Hybodus*	*longiconus* Agassiz, 1843 var. *minor* Jaekel, 1889?			teeth	Hybodontinae	Hybodontiformes	Triassic	Middle	Anisian–Ladinian
239	*Hybodus*	*longiconus* Agassiz, 1843			teeth	Hybodontinae	Hybodontiformes	Triassic	Middle	Anisian, uppermost–Ladinian
240	*Hybodus*	*longiconus* Agassiz, 1843			teeth, fin spine and fragments	Hybodontinae	Hybodontiformes	Triassic	Middle	Ladinian
241	*Hybodus*	*longiconus* Agassiz, 1843			teeth	Hybodontinae	Hybodontiformes	Triassic	Middle	Anisian–Ladinian
242	*Hybodus*	*longiconus* Agassiz, 1843 var. *minor* Jaekel, 1889?			tooth	Hybodontinae	Hybodontiformes	Triassic	Middle	Anisian–Ladinian
243	*Hybodus*	*rajasi* Stensiö, 1921			teeth	Hybodontinae	Hybodontiformes	Triassic	Lower	Olenekian (Spathian)
244	*Hybodus*	*plicatilis* Agassiz, 1843			teeth	Hybodontinae	Hybodontiformes	Triassic	Middle	Anisian–Ladinian
245	*Hybodus*	*plicatilis* Agassiz, 1843			tooth	Hybodontinae	Hybodontiformes	Triassic	Middle	Anisian–Ladinian
246	*Hybodus*	*plicatilis* Agassiz, 1843			tooth	Hybodontinae	Hybodontiformes	Triassic	Middle	Anisian–Ladinian
247	*Hybodus*	*plicatilis* Agassiz, 1843			tooth	Hybodontinae	Hybodontiformes	Triassic	Middle	Anisian–Ladinian
248	*Hybodus*	*plicatilis* Agassiz, 1843			teeth	Hybodontinae	Hybodontiformes	Triassic	Middle	Anisian–Ladinian
249	*Hybodus*	*plicatilis* Agassiz, 1843			tooth	Hybodontinae	Hybodontiformes	Triassic	Middle	Anisian, lower
250	*Hybodus*	*plicatilis* Agassiz, 1843			teeth	Hybodontinae	Hybodontiformes	Triassic	Middle	Anisian–Ladinian
251	*Hybodus*	*plicatilis* Agassiz, 1843			teeth	Hybodontinae	Hybodontiformes	Triassic	Middle	Anisian–Ladinian
252	*Hybodus*	*plicatilis* Agassiz, 1843			teeth	Hybodontinae	Hybodontiformes	Triassic	Lower–Middle	Olenekian–Anisian
253	*Hybodus*	*plicatilis* Agassiz, 1843			teeth	Hybodontinae	Hybodontiformes	Triassic	Middle	
254	*Hybodus*	*plicatilis* Agassiz, 1843			teeth	Hybodontinae	Hybodontiformes	Triassic	Middle	Anisian–Ladinian
255	*Hybodus*	sp. aff. *plicatilis* Agassiz, 1843			teeth	Hybodontinae	Hybodontiformes	Triassic	Middle	
256	*Hybodus*	*angustus* Agassiz, 1843			teeth	Hybodontinae	Hybodontiformes	Triassic	Middle	Anisian–Ladinian
257	*Hybodus*	*angustus* Agassiz, 1843			teeth	Hybodontinae	Hybodontiformes	Triassic	Middle	Anisian
258	*Hybodus*	*multiplicatus* Jaekel, 1889			teeth	Hybodontinae	Hybodontiformes	Triassic	Middle	Anisian, uppermost–Ladinian
259	*Hybodus*	*multiplicatus* Jaekel, 1889			teeth	Hybodontinae	Hybodontiformes	Triassic	Middle	Anisian–Ladinian

	PT-N	Russia-W	Middle and South Urals		marls and nodular, detrital, and reef limestones
Sverdrup Basin	BOR	Canada-N	Henrietta Nesmith, Ellesmere Island, Canadian Arctic Archipelago	Trold Fiord Fm	brachiopod-rich sandstones; mid shelf depositional environment
	PL-E	Canada-W	Ganoid Ridge, Wapiti Lake, British Columbia	Vega-Phroso Siltstone Mb, Sulphur Mountain Fm	siltstone, deltaic/shallow continental shelf environment
	PL-E	Canada-W	Ganoid Ridge, Wapiti Lake, British Columbia	Vega-Phroso Siltstone Mb, Sulphur Mountain Fm	siltstone, deltaic/shallow continental shelf environment
	PT-W	England			
	PT-W	Germany	Gaildorf, Württemberg	Gipskeuper	
Tethys	PT-W	Poland	Holy Cross Mountains, SE	Muschelkalk	
	PT-N	Russia-SW	Donguz, Orenburg, Southern Urals	Donguzskaya Fm	
	PT-N	Russia-SW	Gurievskaya region, North Caspian Basin	Masteksayskogo horizon, Inder Fm	
	PT-N	Russia-SW	Berdyanka, Orenburg	Donguzskaya Fm	
	PT-W	France	Lunéville, NE	Muschelkalk	
	PT-W	France	Lorraine and Chauffontaine	Muschelkalk and Lettenkohle	
Tethys	PT-W	Poland	Upper Silesia and Holy Cross Mountains, SE	Muschelkalk	
Tethys	PT-W	Poland	Upper Silesia and Holy Cross Mountains, SE	Muschelkalk	
N Tethys, western Germanic Basin	PT-W	Germany	Bissendorf, Osnabrücker Bergland, NW	Meißner Fm, upper Muschelkalk	bioclastic rudstone; shallow marine, subtidal
Germanic Basin	PT-W	Germany	oberen Werntal, east of Arnstein, Main-Spessart, south of Würzburg	upper Muschelkalk	
Germanic Basin	PT-W	Germany	oberen Werntal, east of Arnstein, Main-Spessart, south of Würzburg	upper Muschelkalk	
	BOR	Spitsbergen	Mt. Viking, Sassen Bay, Isfjorden	"Grippia niveau", Kaosfjellet Mb, Sticky Keep Fm, Kongressfjellet Subgrp, Sassendalen Grp	
	PT-W	Germany	Täbingen, Württemberg	Muschelkalk	
	PT-W	Germany	Schwenningen, Württemberg	Muschelkalk	
	PT-W	France	Lunéville, NE	Muschelkalk	
	PT-W	Poland	Tarnowitz	Muschelkalk	
	PT-W	France	Lorraine	Muschelkalk and Lettenkohle	
	PT-N	Bulgaria	north of Sofia	Balkanide carbonate	
	PT-W	Luxembourg	Heselbierg Quarry, Moersdorf, E	upper Muschelkalk	dolomites with interbedded blue shaly marls; platform deposits
Tethys	PT-W	Poland	Upper Silesia and Holy Cross Mountains, SE	Muschelkalk	
Medito-Tethyan	NT-W	India	Himalayas		shallow water
	PT-W	Switzerland	S Alps, Monte San Giorgio, Kt. Tessin	Grenzbitumenzone	
Germanic Basin	PT-W	Germany	oberen Werntal, east of Arnstein, Main-Spessart, south of Würzburg	upper Muschelkalk	
west Tethyan	NT-W	Saudi Arabia	Site 1, Ar Rubay'iyah village, east of Buraydah	Jilh Fm	sandstone, shallow marine to offshore environment
	PT-W	France	Lunéville, NE	Muschelkalk	
Tethys	PT-W	Poland	Upper Silesia, SE	Muschelkalk	
Tethys	PT-W	Poland	Upper Silesia and Holy Cross Mountains, SE	Muschelkalk	
Germanic Basin	PT-W	Germany	oberen Werntal, east of Arnstein, Main-Spessart, south of Würzburg	upper Muschelkalk	

marine		*Par. solidissima* fusulinid zone	Ivanov 2005		
marine			this study		Sample CH-F136-79
marine			Mutter *et al.* 2007a		
marine			Schaeffer & Mangus 1976	Mutter *et al.* 2007a; Romano & Brinkmann 2010	(as cf. *Palaeobates*)
			Murchison & Strickland 1840	Seilacher 1948; Rieppel 1981; Romano & Brinkmann 2010	(as *Acrodus (Hybodus)*)
			Seilacher 1943	Seilacher 1948; Rieppel 1981; Romano & Brinkmann 2010	(referred to *Palaeobates*, criticised by Rieppel 1981)
marine			Liszkowski 1993		
marine			Minikh 1996b	Minikh 2001	
marine			Minikh 1996b	Minikh 2001	
marine			Minikh 1996b	Minikh 2001	
			Agassiz 1836		
			Corroy 1928		
marine	clutching		Liszkowski 1993		
marine	clutching		Liszkowski 1993		
marine		*Ceratites compressus* Zone	Diedrich 2009b		see Salamon *et al.* 2003 for biostratigraphic age
marine			Scheinpflug 1984		
marine			Scheinpflug 1984		
marine		*Glenikites pilatiocus – Keyserlingites subrobustus* Zone (ammonoid)	Stensiö 1921	Stensiö 1925; Deecke 1926; Cappetta 1987, 2012	assigned to *H. longiconus* by Corroy 1928; correlates to "Grippia niveau", Vendomdalen Mb, Vikinghøgda Fm (Romano & Brinkmann 2010)
			Agassiz 1836		
	clutching		Agassiz 1836	Cappetta 1987, 2012	
	clutching		Agassiz 1836	Cappetta 1987, 2012	(not mentioned in Rieppel 1981)
			Agassiz 1836		
			Corroy 1928		
			Stefanov 1966, 1977	Vickers-Rich *et al.* 1999; Delsate & Duffin 1999; Brinkmann *et al.* 2010	
marine		*Ceratites nodosus* (ammonoid)	Delsate & Duffin 1999	Delsate 1992, 1993, 1995, 1997	
marine	clutching		Liszkowski 1993		
marine			Sahni & Chhabra 1976		
			Rieppel 1981	Rieppel 1982; Cappetta 1987	(as sp. cf. *plicatilis*; referred by Delsate & Duffin 1999)
marine			Wilczewski 1967; Scheinpflug 1984		
marine			Vickers-Rich *et al.* 1999		
			Agassiz 1836		
marine	clutching		Liszkowski 1993		assigned to *H. plicatilis* by Corroy 1928
marine	clutching		Liszkowski 1993		assigned to *H. plicatilis* by Corroy 1928
marine			Scheinpflug 1984		

260	*Hybodus*	*multiconus* Jaekel, 1889				Hybodontinae	Hybodontiformes	Triassic	Middle	Anisian–Ladinian
261	*Hybodus*	*multiplicatus/multiconus* Jaekel, 1889			tooth fragments	Hybodontinae	Hybodontiformes	Triassic	Middle	Anisian–Ladinian
262	*Hybodus*	*sasseniensis* Stensiö, 1921			teeth	Hybodontinae	Hybodontiformes	Triassic	Lower	Olenekian (Spathian)
263	*Hybodus*	*sasseniensis* Stensiö, 1921			teeth	Hybodontinae	Hybodontiformes	Triassic	Lower	Induan (Dienerian)
264	*Hybodus*	*sasseniensis* Stensiö, 1921			teeth	Hybodontinae	Hybodontiformes	Triassic	Lower	Induan (Dienerian)
265	*Hybodus*	*microdus* Stensiö, 1921			teeth	Hybodontinae	Hybodontiformes	Triassic	Lower	Olenekian (Spathian)
266	*Hybodus*	*microdus* Stensiö, 1921			teeth	Hybodontinae	Hybodontiformes	Triassic	Lower	Induan (Dienerian)
267	*Hybodus*	*microdus* Stensiö, 1921			teeth	Hybodontinae	Hybodontiformes	Triassic	Lower	Induan (Dienerian)
268	*Hybodus*	*nevadensis* Wemple, 1906				Hybodontinae	Hybodontiformes	Triassic	Middle	Ladinian?
269	*Hybodus*	*shastensis* Wemple, 1906				Hybodontinae	Hybodontiformes	Triassic	Upper	
270	*Hybodus*	*shastensis* Wemple, 1906			teeth, fin spine, denticles	Hybodontinae	Hybodontiformes	Triassic	Upper	
271	*Hybodus*	*otschevi* Minikh, 1985			head spines	Hybodontinae	Hybodontiformes	Triassic	Middle	
272	*Hybodus*	*otschevi* Minikh, 1985			head spines	Hybodontinae	Hybodontiformes	Triassic	Middle	
273	*Hybodus*	*otschevi* Minikh, 1985			teeth, fin and cephalic spines	Hybodontinae	Hybodontiformes	Triassic	Lower	
274	*Hybodus*	*spasskiensis* Minikh			teeth, fin and cephalic spines	Hybodontinae	Hybodontiformes	Triassic	Lower	
275	*Hybodus*	*mawimi* Minikh			teeth, fin and cephalic spines	Hybodontinae	Hybodontiformes	Triassic	Lower	
276	*Hybodus*	*karagatshkaensis* Minikh			teeth, fin and cephalic spines	Hybodontinae	Hybodontiformes	Triassic	Lower	
277	*Hybodus*	*zuodengensis* Yang, Wang & Hao 1984			teeth	Hybodontinae	Hybodontiformes	Triassic	Lower	Olenekian (Spathian, lower)
278	*Hybodus*	*jiohi* Yang, Wang & Hao 1984			tooth	Hybodontinae	Hybodontiformes	Triassic	Lower	Olenekian (Spathian, lower)
279	*Hybodus*	sp.				Hybodontinae	Hybodontiformes	Triassic	Lower	Induan (Dienerian)
280	*Hybodus*	sp. 1			tooth	Hybodontinae	Hybodontiformes	Triassic	Middle	Anisian, lower
281	*Hybodus*	sp.			tooth	Hybodontinae	Hybodontiformes	Triassic	Lower	Olenekian (Spathian)
282	*Hybodus*	sp.			teeth	Hybodontinae	Hybodontiformes	Triassic	Lower	**Induan (Dienerian, lower)–Olenekian (Smithian, lower)**

	PT-W	France	Lorraine, E	Muschelkalk	
	PT-W	Luxembourg	Heselbierg Quarry, Moersdorf, E	upper Muschelkalk	dolomites with interbedded blue shaly marls; platform deposits
	BOR	Spitsbergen	Mt. Viking, Sassen Bay, Isfjorden	"Grippia niveau", Kaosfjellet Mb, Sticky Keep Fm, Kongressfjellet Subgrp, Sassendalen Grp	
Boreal	BOR	Spitsbergen	Hyrnefjellet, Hornsund, S	Brevassfjellet *Myalina* Bed, Urnetoppen Mb, Vardebukta Fm, Torell Land Grp	iron-rich, fine-grained conglomerate, concentrated deposit, offshore sand bars
Boreal	BOR	Spitsbergen	Hyrnefjellet Mountain, Hornsund, SW	Brevassfjellet *Myalina* Bed, Urnetoppen Mb, Vardebukta Fm	fine-grained, iron rich conglomerate
	BOR	Spitsbergen	Mt. Viking, Sassen Bay, Isfjorden	"Grippia niveau", Kaosfjellet Mb, Sticky Keep Fm, Kongressfjellet Subgrp, Sassendalen Grp	
Boreal	BOR	Spitsbergen	Hyrnefjellet, Hornsund, S	Brevassfjellet *Myalina* Bed, Urnetoppen Mb, Vardebukta Fm, Torell Land Grp	iron-rich, fine-grained conglomerate, concentrated deposit, offshore sand bars
Boreal	BOR	Spitsbergen	Hyrnefjellet Mountain, Hornsund, SW	Brevassfjellet *Myalina* Bed, Urnetoppen Mb, Vardebukta Fm	fine-grained, iron rich conglomerate
	PL-E	USA-W	Cottonwood Canyon, west Humboldt Range, Nevada		
	PL-E	USA-W	Bear Cove, Shasta County, California		black limestone
	PL-E	USA-W	Bear Cove, Brushy Slope, and "Camp Wemple", Shasta County, California		black limestone
	PT-N	Russia-SW	Donguz, Orenburg Region, Sol' -Iletsk District, South Urals	Donguz Fm	
	PT-N	Russia-SW	near Gmelinka, Volgograd Region, North Caspian (east of European Russia)	Inder Fm	clayey limestones
	PT-N	Russia-SW	Big Bogda Mountain, Caspian Basin		
	PT-N	Russia-SW	Big Bogda Mountain, Caspian Basin		
	PT-N	Russia-SW	Big Bogda Mountain, Caspian Basin		
	PT-N	Russia-SW	Big Bogda Mountain, Caspian Basin		
	PT-E	China-SE	Denggaoling, Zuodeng area, Tiandong County, Guangxi Zhuang region, S	Luolou Fm	open sea environment
	PT-E	China-SE	Denggaoling, Zuodeng area, Tiandong County, Guangxi Zhuang region, S	Luolou Fm	open sea environment
Boreal	BOR	Spitsbergen	Hyrnefjellet Mountain, Hornsund, SW	Brevassfjellet *Myalina* Bed, Urnetoppen Mb, Vardebukta Fm	fine-grained, iron rich conglomerate
	PL-W	Japan	Nukata, Yakuno-cho, Amada-gun, Kyoto Prefecture, central Honshu	Waruishi Fm, Yakuno Grp	black mudstone
	PL-W	Japan	Masuzawa, Utatsu-cho, Miyagi Prefecture, NE Honshu	Osawa Fm, Inai Grp	black slate
	PL-W	Russia-SE	Abrek Bay area, Vladivostok, South Primorye	Zhitkov Fm	ammonoid turbidites

	clutching		Jaekel 1898; Deecke 1926; Schmidt 1928; Seilacher 1943	Cappetta 1987, 2012	assigned to *H. plicatilis* by Corroy 1928
marine			Delsate & Duffin 1999		uncertain as to whether both can be distinguished on specific level; assigned to *H. plicatilis* by Corroy 1928
marine		*Olenikites pilaticus – Keyserlingites subrobustus* Zone (ammonoid)	Stensiö 1918, 1921	Cox & Smith 1973; Birkenmajer & Jerzmańska 1979	(as sp.) / not mentioned in Romano & Brinkmann (2010), but correlates to "Grippia niveau", Vendomdalen Mb, Vikinghøgda Fm
marine		*Proptychites candidus* Zone (ammonoid)	Stensiö 1921; Birkenmajer & Jerzmańska 1979	Romano & Brinkmann 2010	assigned to *H. plicatilis* by Corroy 1928
marine			Błażejowski 2004	Romano & Brinkmann 2010	
marine		*Olenikites pilaticus – Keyserlingites subrobustus* Zone (ammonoid)	Stensiö 1921	Birkenmajer & Jerzmańska 1979	correlates to "Grippia niveau", Vendomdalen Mb, Vikinghøgda Fm (Romano & Brinkmann 2010)
marine		*Proptychites candidus* Zone (ammonoid)	Birkenmajer & Jerzmańska 1979	Romano & Brinkmann 2010	
marine			Błażejowski 2004	Romano & Brinkmann 2010	
marine			Wemple 1906	Cappetta 1987, 2012; Cuny *et al.* 2001	
marine			Wemple 1906	Jordan 1907; Cappetta 1987, 2012	note: different from *Palaeobates shastensis* .
marine			Jordan 1907		
			Minikh 1985, 1996a		
marine			Minikh 1996a		
marine			Auerbach 1871	Minikh 2001	(as *Hybodus*)?
marine			Auerbach 1871	Minikh 1975, 1985, 2001	original description needs checking
marine			Auerbach 1871	Minikh 1975, 1985, 2001	original description needs checking
marine			Auerbach 1871	Minikh 1975, 1985, 2001	original description needs checking
marine		*Necrathodus homeri – N. triangularis* Zone (conodont)	Yang *et al.* 1984	Wang *et al.* 2001; Chang & Miao 2004; Jin 2006; Wang *et al.* 2009	(as *Pachycladina*)
marine		*Necrathodus homeri – N. triangularis* Zone (conodont)	Yang *et al.* 1984	Wang *et al.* 2001; Chang & Miao 2004; Jin 2006; Wang *et al.* 2009	(as *Pseudogondolella*)
marine			Błażejowski 2004	Romano & Brinkmann 2010	
			Goto *et al.* 1991	Goto 1985, 1994a, b, 1996b; Goto & Kuga 1982; Goto *et al.* 1996a, 2010; Chang & Miao 2004	
			Kato *et al.* 1995	Goto *et al.* 2010	
marine		*Clypeoceras spitiense* "bed" – *Clypeoceras timorense* Zone (*Gyronites subdharmus – Anasibirites nevolini* Zone)	Yamagishi 2009	Yamagishi 2006	(as *Hybodus* sp. 2 in Yamagishi 2006)

283	*Hybodus*	sp. 1			teeth	Hybodontinae	Hybodontiformes	Triassic	Middle	Anisian, lower-middle
284	*Hybodus*	sp. 2			teeth	Hybodontinae	Hybodontiformes	Triassic	Lower–Middle	**Olenekian (Smithian–Spathian)–Anisian, lower–upper**
285	*Hybodus*	sp. 2			teeth	Hybodontinae	Hybodontiformes	Triassic	Lower–Upper	**Olenekian (Smithian)–Anisian, middle; Carnian**
286	cf. *Hybodus*	sp.			teeth	Hybodontinae	Hybodontiformes	Triassic	Lower	Induan (Griesbachian?)
287	*Hybodus*	sp. 2			teeth	Hybodontinae	Hybodontiformes	Triassic	Lower	Olenekian (Smithian, upper)
288	*Hybodus* ?	sp.			tooth	Hybodontinae	Hybodontiformes	Triassic	Upper	Carnian
289	cf. *Hybodus*	sp.			teeth	Hybodontinae	Hybodontiformes	Triassic	Lower	Olenekian (Spathian)
290	*Hybodus* ?	sp. indet.				Hybodontinae	Hybodontiformes	Triassic	Lower	Induan
291	*Hybodus* ?	*jepseni* Bryant, 1934			partial bodies, fin spines, teeth	Hybodontinae	Hybodontiformes	Triassic	Upper	Norian, lower
292	*Hybodus*	*jcungi* Liu, 1962			teeth	Hybodontinae	Hybodontiformes	Triassic	Middle	Ladinian, upper
293	*Hybodus*	sp.				Hybodontinae	Hybodontiformes	Triassic	Upper	
294	*Hybodus*	sp.				Hybodontinae	Hybodontiformes	Triassic	Upper	Carnian, lower
295	*Hybodus*	*hexagonus*				Hybodontinae	Hybodontiformes	Triassic	Upper	Carnian, lower
296	*Hybodus*	sp.				Hybodontinae	Hybodontiformes	Triassic	Upper	Carnian, lower
297	*Hybodus*	cf. *tenuis* Agassiz, ...				Hybodontinae	Hybodontiformes	Triassic	Upper	Carnian, lower
298	*Hybodus*	*sublaevis* Agassiz, 1843			teeth	Hybodontinae	Hybodontiformes	Triassic	Upper	
299	*Hybodus*	*sublaevis* Agassiz, 1843			teeth	Hybodontinae	Hybodontiformes	Triassic	Middle	Anisian–Ladinian
300	*Hybodus*	*raricostatus* Agassiz, 1843			teeth	Hybodontinae	Hybodontiformes	Triassic	Middle	Anisian–Ladinian
301	*Hybodus*	*raricostatus* Agassiz, 1843			teeth	Hybodontinae	Hybodontiformes	Triassic	Middle	Anisian
302	*Hybodus*	*raricostatus* Agassiz, 1843			teeth	Hybodontinae	Hybodontiformes	Triassic	Lower–Middle	Olenekian–Anisian
303	*Hybodus*	*non striatus* Winkler, 1880			teeth	Hybodontinae	Hybodontiformes	Triassic	Upper	
304	*Hybodus*	cf. *non striatus* Winkler, 1880			teeth	Hybodontinae	Hybodontiformes	Triassic	Middle	Anisian–Ladinian
305	*Hybodus*	*acanthocyphocrus* Winkler, 1880			fin spines	Hybodontinae	Hybodontiformes	Triassic	Upper	
306	*Hybodus*	*major* Agassiz, 1843			fin spines	Hybodontinae	Hybodontiformes	Triassic	Middle	Anisian–Ladinian
307	*Hybodus*	*major* Agassiz, 1843			fin spines	Hybodontinae	Hybodontiformes	Triassic	Middle	Anisian–Ladinian
308	*Hybodus*	*major* Agassiz, 1843			fin spines	Hybodontinae	Hybodontiformes	Triassic	Middle	Anisian–Ladinian
309	*Hybodus*	*major* Agassiz, 1843			fin spines	Hybodontinae	Hybodontiformes	Triassic	Middle	Anisian–Ladinian
310	*Hybodus*	*falcatus* (Agassiz, 1837)			fin spine	Hybodontinae	Hybodontiformes	Triassic	Middle	Anisian–Ladinian
311	*Hybodus*	*falcatus* (Agassiz, 1837)			fin spine fragments	Hybodontinae	Hybodontiformes	Triassic	Middle	Anisian–Ladinian
312	*Hybodus*	sp.				Hybodontinae	Hybodontiformes	Triassic	Lower–Middle	Olenekian–Anisian
313	*Hybodus*	sp.			fin spines	Hybodontinae	Hybodontiformes	Triassic	Middle	Anisian, lower

	PL-C	Japan	Tahokamigumi, Nishiuwa City (prev. Shirokawa-cho, Higashiuwa-gun), Ehime Prefecture, Shikoku	Taho Fm	biomicritic limestone
	PL-C	Japan	Tahokamigumi, Nishiuwa City (prev. Shirokawa-cho, Higashiuwa-gun), Ehime Prefecture, Shikoku	Taho Fm	biomicritic limestone
	PL-C	Japan	Shioinouso, Takachiho-cho, Miyazaki Prefecture, Kyushu	Kamura Fm	micritic limestone
	PL-C	Japan	Kamura, Takachiho-chō, Nishiusuki-gun, Miyazaki-ken (Prefecture), Kyūshū	Kamura Fm	mid-oceanic seamount
	PL-W	Malaysia	Gua Panjang	unnamed	limestone
	PL-W	Japan	Otogo, Sakawa-cho, Takaoka-gun, Kochi Prefecture, Shikoku	Kochigatani Grp	sandy mudstone
	PL-E	USA-W	Darwin Canyon, Inyo Mountains, California	Union Wash Fm	micritic limestones and calcareous shales; basinal outer shelf to slope environment, below storm wave base
	BOR	Greenland-E	Margrethedal, Gauss Halvø	Wordie Creek Fm	concretions
	PG-N	USA-E	south of North Wales, near Norristown, Pennsylvania	Lockatong Fm, Newark Grp	black shale, estuarine deposition?
	PT-E	China-E	Zhangjiatan (Changchiatan), Yanchang (Yenshang), Shaanxi (Shensi) Province	Changchiatan black shales, upper Tongchuan Fm	black shales
	PT-E	China-S	Lufeng, Yunnan Province		
	PT-W	Italy	Stuores Wald/Bosco di Stuores	San Cassiano Fm	basinal marls, micrites and oolitic-bioclastic calciturbidites
	PT-W	Italy	San Cassiano	San Cassiano Fm	basinal marls, micrites and oolitic-bioclastic calciturbidites
	PT-W	Germany	Steinbach near Schwäbisch Hall, SW	lower Lettenkeuper	brackish/deltaic
	PT-W	Germany	Steinbach near Schwäbisch Hall, SW	lower Lettenkeuper	brackish/deltaic
	PT-W	Germany	Täbingen, near Rottweil, Württemberg	Keuper	breccia
Germanic Basin	PT-W	Germany	oberen Werntal, east of Arnstein, Main-Spessart, south of Würzburg	upper Muschelkalk	
Germanic Basin	PT-W	Germany	oberen Werntal, east of Arnstein, Main-Spessart, south of Würzburg	upper Muschelkalk	
Tethys	PT-W	Poland	Holy Cross Mountains, SE	Muschelkalk	
Medito-Tethyan	NT-W	India	Himalayas		shallow water
	PT-W	Germany	Ipsheim	Gipskeuper	
Germanic Basin	PT-W	Germany	oberen Werntal, east of Arnstein, Main-Spessart, south of Würzburg	upper Muschelkalk	
	PT-W	Germany	Ipsheim	Gipskeuper	
	PT-W	France	Rehainvillers and Harol, NE	Muschelkalk	
	PT-W	Germany	Bayreuth, E	Muschelkalk	
	PT-W	Poland	Breslau, W	Muschelkalk	
Germanic Basin	PT-W	Germany	oberen Werntal, east of Arnstein, Main-Spessart, south of Würzburg	upper Muschelkalk	
	PT-W	France	Lunéville, NE	Muschelkalk	
	PT-W	Germany	Bayreuth, E	Muschelkalk	
Medito-Tethyan	NT-W	India	Himalayas		shallow water
	PL-E	USA-W	Holbrook Quarry, Navajo County, Arizona	Holbrook Mb, Moenkopi Fm	siltstone

		Necogondolella timorensis – Ng. bulgarica Zones	Yamagishi 2004; Yamagishi 2006	Goto *et al.* 2010	
		Neospathodus triangularis / *Ns. homeri – Necogondolella timorensis* Zones	Yamagishi 2004; Yamagishi 2006	Goto *et al.* 2010	(as *Synechodus* sp. in Yamagishi 2004)
marine			Yamagishi 2006		
marine		*Hindeodus parvus* , *Isarcicella isarcica* , *Necogondolella carinata*	this study		Samples 05.7.14.ak, 05.7.15.q
marine		*Neospathodus dieneri* , *N. transcoi*	Yamagishi 2006		
		Otapiria dubia Zone	Yamagishi 2006		(cf. *Paracrthaccodus*)
marine			this study		Sample 92-OF DC10
marine			Bendix-Almgreen et al. 1988		
freshwater (marine influence?)	>13 cm in length		Bryant 1934	Schaeffer & Mangus 1970; Cappetta 1987, 2012; Huber *et al.* 1993	(as *Carinacanthus*) may also be a ctenacanth (Maisey 1975) and is relatively similar to Wodnika (Maisey 1982b)
freshwater (with marine influence?)			Liu 1962	Wang *et al.* 2001, 2009; Chang & Miao 2004; Jin 2006	(former Yenchang Fm)
freshwater				Wang *et al.* 2001	
marine			Bizzarini *et al.* 2001	Bernardi *et al.* 2011	
marine			Broglio Loriga 1967	Bernardi *et al.* 2011	
brackish			Reif 1980b		(as *Hybodonchus*)
brackish			Reif 1980b		
			Agassiz 1836		
marine			Wilczewski 1967	Scheinpflug 1984	
marine			Wilczewski 1967	Scheinpflug 1984	
marine	clutching-crushing		Liszkowski 1993		
marine			Sahni & Chhabra 1976		(correct? normally Jurassic species)
		Estheria	Winkler 1880		(should also be referred to *Polaycodus* ? see Seilacher 1943?)
marine			Wilczewski 1967	Scheinpflug 1984	
			Winkler 1880		
			Agassiz 1836		
			Agassiz 1836		
			Agassiz 1836		
marine			Scheinpflug 1984		
			Agassiz 1836	Cappetta 2012	(as *Leiacanthus*)
			Agassiz 1836	Cappetta 2012	(as *Leiacanthus*)
marine			Sahni & Chhabra 1976		(as *Leiacanthus* sp.)
			Welles 1947	Morales 1987	(as *Leiacanthus* sp.)

314	*Hybodus*	sp.			fin spine	Hybodontinae	Hybodontiformes	Triassic	Middle	Anisian–Ladinian
315	*Hybodus?*	sp.			teeth	Hybodontinae	Hybodontiformes	Triassic	Middle	Anisian, lower middle
316	*Hybodus?*	sp.			teeth	Hybodontinae	Hybodontiformes	Triassic	Lower–Middle	Induan (Scythian)–Anisian
317	*Hybodus*	sp. nov.				Hybodontinae	Hybodontiformes	Triassic	Upper	Rhaetian
318	*Hybodus*	sp.				Hybodontinae	Hybodontiformes	Triassic	Upper	Norian
319	*Hybodus*				teeth	Hybodontinae	Hybodontiformes	Triassic	Upper	Rhaetian
320	*Hybodus*				teeth	Hybodontinae	Hybodontiformes	Triassic	Upper	Rhaetian
321	*Hybodus*				teeth	Hybodontinae	Hybodontiformes	Triassic	Upper	Rhaetian
322	*Hybodus*				teeth	Hybodontinae	Hybodontiformes	Triassic	Upper	Rhaetian
323	*Hybodus*				teeth	Hybodontinae	Hybodontiformes	Triassic	Upper	Rhaetian
324	*Hybodus*				teeth	Hybodontinae	Hybodontiformes	Triassic	Upper	Rhaetian
325	*Hybodus*	sp.				Hybodontinae	Hybodontiformes	Triassic	Upper	Rhaetian
326	*Hybodus*	sp.				Hybodontinae	Hybodontiformes	Triassic	Upper	Rhaetian
327	*Hybodus*	sp.				Hybodontinae	Hybodontiformes	Permian	Cisuralian	Sakmarian
328	*"Hybodus"*	sp.				Hybodontinae	Hybodontiformes	Permian	Cisuralian	Sakmarian
329	*Hybodus*	sp.			teeth	Hybodontinae	Hybodontiformes	Permian	Cisuralian	Artinskian
330	*Hybodus*	sp.			spine	Hybodontinae	Hybodontiformes	Permian	Cisuralian–Guadalupian	Kungurian–Roadian
331	*Hybodus*	sp.			spine	Hybodontinae	Hybodontiformes	Permian	Cisuralian	
332	*"Hybodus"*	*copei* Hay, 1899			fin spine	Hybodontinae	Hybodontiformes	Permian	Cisuralian	Artinskian?
333	*"Hybodus"*	*copei* Hay, 1899			fin spine	Hybodontinae	Hybodontiformes	Permian	Cisuralian	Artinskian
334	*"Hybodus"*	*copei* Hay, 1899			fin spine fragments	Hybodontinae	Hybodontiformes	Permian	Cisuralian	Asselian?
335	*"Hybodus"*	*copei* Hay, 1899			fin spine fragments	Hybodontinae	Hybodontiformes	Permian	Cisuralian	Sakmarian
336	*"Hybodus"*	*copei* Hay, 1899			fin spine fragments	Hybodontinae	Hybodontiformes	Permian	Cisuralian	Artinskian
337	*Hybodus*	sp.			spine fragments	Hybodontinae	Hybodontiformes	Permian	Cisuralian	
338	*Hybodus*	sp.			teeth	Hybodontinae	Hybodontiformes	Permian	Cisuralian	Artinskian
339	*'Polyacrodus'*	*lapalomensis* Johnson, 1981				Hybodontinae	Hybodontiformes	Permian	Cisuralian	Artinskian
340	*Polyacrodus?*	sp.			teeth	Hybodontinae	Hybodontiformes	Permian	Lopingian	**Wuchiapingian–Changhsingian**

Germanic Basin	PT-W	Germany	oberen Werntal, east of Arnstein, Main-Spessart, south of Würzburg	upper Muschelkalk	
	PL-E	USA-W	west slope Augusta Mountains, Pershing County, Nevada	lower Fossil Hill Mb, Favret Fm, Star Peak Grp	litharenite, debris flow deposit, high energy, coastal influence, outer platform
	NT-W	Israel	Makhtesh Ramon (Wadi Raman), Negev Desert, S		marginal belt: shallow marine - near-shore/lagoonal - deltaic
Central European Basin (Rhaetian Sea)	PT-W	Belgium	Sagnette and Unter der Kirchen, Hachy		
	PT-W	France	Saint-Nicolas-de-Port, NE		
Central European Basin (Rhaetian Sea)	PT-W	England	Westbury-on-Severn	basal Westbury Fm	bone bed; shallow marine to nearshore environment / restricted lagoonal to estuarine setting
Central European Basin (Rhaetian Sea)	PT-W	England	Barnstone	basal Westbury Fm	bone bed; shallow marine to nearshore environment / restricted lagoonal to estuarine setting
Central European Basin (Rhaetian Sea)	PT-W	Germany	Hildesheim-Ochtersum	Exter Fm, base contorta beds	bone bed; shallow marine nearshore to deltaic setting
Central European Basin (Rhaetian Sea)	PT-W	Germany	Moseberg	basal Exter Fm	bone bed; shallow marine nearshore to deltaic setting
Central European Basin (Rhaetian Sea)	PT-W	France	Saint-Nicolas-de-Port	basal Grés rhétiens	bone bed; shallow marine nearshore
NW Tethys	PT-W	Switzerland	Schesaplana, canton Grison	Kössen Fm, Austroalpine nappes	tempestites; continental shelf, lagoonal to shallow marine environment with a strong detrital influx
	PT-W	France	Provenchères-sur-Meuse, Haute-Marne		
	PT-W	France	Boisset, Jura		
	PG-C	USA-C	Cowley County, Geary County, Kansas	Havensville Shale Mb, Schroyer Limestone Mb, Wreford Limestone Fm, Chase Grp	intertidal to open marine (50 m water depth)
	PG-C	USA-C	Cowley County, Kansas	Threemile Limestone Mb, Wreford Limestone Fm, Chase Grp	intertidal to open marine (50 m water depth)
	PT-N	Russia-W	Pre-Uralian region and Southern Urals		
Kaibab Sea	PL-E	USA-W	Grand Canyon, Arizona	Kaibab Fm	
	PG-C	USA-S	Texas		
	PG-C	USA-S	Seymour District, Baylor County, Texas	Lueders Fm, Clear Fork Grp?	
	PG-C	USA-S	Military Trail below Kemp Lake dam, Seymour District, Baylor County, Texas	Lueders Fm, Clear Fork Grp	
	PG-C	USA-S	Little Bitter Creek, Young County, Texas	Moran Fm, Wichita Grp	clays near marine limestones in red beds
	PG-C	USA-S	Godwin Creek, Baylor County, Texas	upper Admiral Fm, Wichita Grp	clays near marine limestones in red beds
	PG-C	USA-S	Little Wichita River below Fulda, Baylor County, Texas	Belle Plains Fm, Wichita Grp	clays near marine limestones in red beds
	PG-C	USA-C	Kirby Quarry, Noble County, north-central Oklahoma	Unit 9, Billings Pool Mb, Wellington Fm	olive shale, terrestrial
Dunkard Basin (freshwater, but marine influenced; Schultze & Soler-Gijón 2004)	PG-N	USA-E		Greene Fm, Dunkard Grp	
	PG-C	USA-S	Baylor, Wichita and Archer Counties, north central Texas	Wichita-Albany Grp (upper Belle Plains Fm, Clyde Fm)	
Neo-Tethys	NT-W	Iran	Baghuk Mountain, NW of Abadeh	Hambast Fm	deep/outer shelf, thin to medium bedded limestone

marine			Scheinpflug 1984		
marine	durophagous, crushing	*Meraggarti* Subzone of the *Hyatti* Zone	Cuny *et al.* 2001		
marine–freshwater			Shaw 1947; Brotzen 1955,1956; Werner 1982; Gans 1983	Brinkmann *et al.* 2010	
marine with freshwater influence			Duffin *et al.* 1983	Delsate 1993	
				Delsate 1993	(age see Duffin 1993a)
brackish	pelagic, wide variety of prey		Fischer *et al.* 2012		
brackish	pelagic, wide variety of prey		Fischer *et al.* 2012		
brackish (deltaic)	pelagic, wide variety of prey		Fischer *et al.* 2012		
brackish (deltaic)	pelagic, wide variety of prey		Fischer *et al.* 2012		
brackish	pelagic, wide variety of prey		Fischer *et al.* 2012		
marine	pelagic, wide variety of prey		Fischer *et al.* 2012		
				Cuny 1995a	
				Cuny 1995a	
marine to brackish			Schultze 1985	Johnson 1992	reassigned to *Sphenacanthus* ? See Ginter *et al.* 2010
marine to brackish			Schultze 1985		reassigned to *Sphenacanthus* ? See Ginter *et al.* 2010
			Karpinsky 1899, 1903, 1916	Ivanov 2000	
marine			Hussakof 1943	Hunt *et al.* 2005	
			Berman 1970	Simpson 1974	(reassignable to hybodontoid indet.?)
			Cope 1891	Hay 1899; Romer 1942	
			Hussakof 1911	Romer 1942	(as hybodont)
marine			Romer 1942		(noted as not *Hybodus* , but unknown which)
marine			Romer 1942		(noted as not *Hybodus* , but unknown which)
marine			Romer 1942		(noted as not *Hybodus* , but unknown which)
freshwater			May & Hall 2002		(reassignable to hybodontoid indet.?)
			Johnson 1992		
marine?/freshwater?			Johnson 1981	Ginter *et al.* 2010	
marine			Hampe *et al.* 2011, 2013		(as '*P.* ' cf. *lapalomensis*)

341	*'Polyacrodus'*	*nitchiei* Johnson, 1981				Hybodontinae	Hybodontiformes	Permian	Cisuralian	Artinskian
342	*'Polyacrodus'*	*wichitaensis* Johnson, 1981				Hybodontinae	Hybodontiformes	Permian	Cisuralian	Artinskian
343	*'Polyacrodus'*	*?wichitaensis* Johnson, 1981			teeth	Hybodontinae	Hybodontiformes	Permian	Cisuralian	Artinskian
344	*'Polyacrodus'*	sp.			teeth, fin spines	Hybodontinae	Hybodontiformes	Permian	Lopingian	Changhsingian
345	*'Polyacrodus'*	*jiangxiensis* Wang, Zhu, Jin & Wang, 2007			tooth	Hybodontinae	Hybodontiformes	Permian	Lopingian	Changhsingian
346	*'Polyacrodus'*	*claveringensis* Stensiö, 1932			teeth, fin spines, crania	Hybodontinae	Hybodontiformes	Triassic	Lower	Induan (Griesbachian)
347	*'Polyacrodus'*	*pyramidalis* Stensiö, 1921			teeth	Hybodontinae	Hybodontiformes	Triassic	Upper?	
348	*'Polyacrodus'*	*polycyphus* (Agassiz, 1837)			teeth	Hybodontinae	Hybodontiformes	Triassic	Middle	Anisian–Ladinian
349	*'Polyacrodus'*	*polycyphus* (Agassiz, 1837)			teeth	Hybodontinae	Hybodontiformes	Triassic	Middle	Anisian–Ladinian
350	*'Polyacrodus'*	*polycyphus* (Agassiz, 1837)			teeth	Hybodontinae	Hybodontiformes	Triassic	Middle	Anisian–Ladinian
351	*'Polyacrodus'*	*polycyphus* (Agassiz, 1837)			teeth	Hybodontinae	Hybodontiformes	Triassic	Middle	Ladinian, upper
352	*'Polyacrodus'*	*polycyphus* (Agassiz, 1837)			teeth	Hybodontinae	Hybodontiformes	Triassic	Middle	Ladinian (younger?)
353	*'Polyacrodus'*	*polycyphus* (Agassiz, 1837)			teeth	Hybodontinae	Hybodontiformes?	Triassic	Middle	Anisian–Ladinian
354	*'Polyacrodus'*	*polycyphus* (Agassiz, 1837)			teeth	Hybodontinae	Hybodontiformes?	Triassic	Middle	Ladinian
355	*'Polyacrodus'*	*polycyphus* (Agassiz, 1837)			teeth	Hybodontinae	Hybodontiformes?	Triassic	Middle	Anisian–Ladinian
356	*'Polyacrodus'*	*polycyphus* (Agassiz, 1837)			teeth	Hybodontinae	Hybodontiformes?	Triassic	Middle	Ladinian, upper
357	*'Polyacrodus'*	*polycyphus* (Agassiz, 1837)				Hybodontinae	Hybodontiformes?	Triassic	Upper	Carnian, lower
358	*'Polyacrodus'*	*obracinus* (Quenstedt, 1856)			teeth	Hybodontinae	Hybodontiformes	Triassic	Upper	Rhaetian
359	*'Polyacrodus'*	*obracinus* (Quenstedt, 1856)			teeth	Hybodontinae	Hybodontiformes	Triassic	Upper	Rhaetian
360	*'Polyacrodus'*	*obracinus* (Quenstedt, 1856)				Hybodontinae	Hybodontiformes	Triassic	Upper	Rhaetian
361	*'Polyacrodus'*	*obracinus* (Quenstedt, 1856)			teeth	Hybodontinae	Hybodontiformes	Triassic	Upper	Rhaetian
362	*'Polyacrodus'*	*obracinus* (Quenstedt, 1856)			teeth	Hybodontinae	Hybodontiformes	Triassic	Upper	Rhaetian, lower
363	*'Polyacrodus'*	*obracinus* (Quenstedt, 1856)				Hybodontinae	Hybodontiformes	Triassic	Upper	Rhaetian
364	*'Polyacrodus'*	*obracinus* (Quenstedt, 1856)				Hybodontinae	Hybodontiformes	Triassic	Upper	Rhaetian
365	*'Polyacrodus'*	*cuspidatus* (Agassiz, 1843)			tooth	Hybodontinae	Hybodontiformes	Triassic	Upper	
366	*'Polyacrodus'*	*cuspidatus* (Agassiz, 1843)			teeth	Hybodontinae	Hybodontiformes	Triassic	Upper	
367	*'Polyacrodus'*	*cuspidatus* (Agassiz, 1843)			teeth	Hybodontinae	Hybodontiformes	Triassic	Upper	Rhaetian
368	*'Polyacrodus'*	*krafti* Seilacher, 1943			teeth	Hybodontinae	Hybodontiformes	Triassic	Upper	Carnian
369	*'Polyacrodus'*	*krafti* Seilacher, 1943			teeth	Hybodontinae	Hybodontiformes	Triassic	Middle	Ladinian, upper
370	*'Polyacrodus'*	*krafti* Seilacher, 1943			teeth	Hybodontinae	Hybodontiformes	Triassic	Middle	Ladinian, upper
371	*'Polyacrodus'*	*keuperianus* (Winkler, 1880)			teeth	Hybodontinae	Hybodontiformes	Triassic	Upper	**Carnian**–Norian
372	*'Polyacrodus'*	*keuperianus* (Winkler, 1880)			teeth	Hybodontinae	Hybodontiformes	Triassic	Upper	Carnian
373	*'Polyacrodus'*	*keuperianus* (Winkler, 1880)			teeth	Hybodontinae	Hybodontiformes	Triassic	Middle	Ladinian, upper
374	*'Polyacrodus'*	*keuperianus* (Winkler, 1880)			teeth	Hybodontinae	Hybodontiformes	Triassic	Middle	Ladinian, upper
375	*'Polyacrodus'*	*keuperianus* (Winkler, 1880)			teeth	Hybodontinae	Hybodontiformes	Triassic	Middle	Ladinian, upper
376	*'Polyacrodus'*	*keuperianus* (Winkler, 1880)			teeth	Hybodontinae	Hybodontiformes	Triassic	Middle	Ladinian (younger?)

	PG-C	USA-S	Rattlesnake Canyon, Archer County, Texas	upper Admiral Fm, Wichita-Albany Grp	
	PG-C	USA-S	Baylor, Wichita and Archer Counties, north central Texas	Wichita-Albany Grp (upper Belle Plains Fm, Clyde Fm, low-mid Lueders Fm)	
	PG-C	USA-S	Little Moonshine Creek, Texas	upper Lueders Fm, Albany Grp	claystone
	PT-N	Russia-W			
	PT-E	China-SE	Dongling, Xiushui County, Jiangxi Province	upper Mb, Changxing Fm	
	BOR	Greenland-E	Hird's fox-farm, Clavering Island	Fish Zone II, Wordie Creek Fm	
Boreal	BOR	Spitsbergen	Mt. Bertil, Ekman Bay, Isfjorden	Sticky Keep Fm?	
	PT-W	France	Lunéville, NE	Muschelkalk	
	PT-W	France	Lunéville, Lorraine, NE	Muschelkalk	
	PT-W	France	Mont, Azerailles, and Mortagne, Lorraine	Muschelkalk	
	PT-W	Germany	quarry near Kirchberg an der Jagst, Baden-Württemberg	Lettenkeuper	
	PT-W	Germany	Schumann quarry, near Eschenau, Baden-Württemberg	Hauptsandstein	
Tethys	PT-W	Poland	Upper Silesia and Holy Cross Mountains, SE	Muschelkalk	
N Tethys, western Germanic Basin	PT-W	Germany	Bissendorf, Osnabrücker Bergland, NW	Meißner Fm, upper Muschelkalk	bioclastic rudstone; shallow marine, subtidal
Germanic Basin	PT-W	Germany	oberen Werntal, east of Arnstein, Main-Spessart, south of Würzburg	upper Muschelkalk	
	PT-W	Germany	Neidenfels, near Crailsheim, S	base Hauptsandstein, lower Letterkeuper, lower Keuper	bone bed; estuary
	PT-W	Germany	Steinbach near Schwäbisch Hall, SW	lower Lettenkeuper	brackish/deltaic
	PT-W	Germany	Württemberg		
	PT-W	England	Aust Cliff		
Central European Basin (Rhaetian Sea)	PT-W	Belgium	Sagnette and Unter der Kirchen, Hachy		
Central European Basin (Rhaetian Sea)	PT-W	Belgium	Attert		
	PT-W	Luxembourg	Commune Weyler-la-Tour, Syren	Keuper	
	PT-W	France	Provenchères-sur-Meuse, Haute-Marne		
	PT-W	France	Lons-le-Saunier, Jura		
	PT-W	Germany	Rietheim, near Hall, Württemberg	Keuper	
	PT-W	Germany	Täbingen, near Rottweil, Württemberg	Keuper	breccia
	PT-W	Germany	Kirnberg, near Tübingen, Baden-Württemberg		
	PT-W	Germany	Eibachtal, E of Gaildorf, Baden-Württemberg, SW	Gaildorfer Bank (Dunkle Mergel), Stuttgart Fm, middle Keuper	
	PT-W	Germany	Bopp quarry, near Ilsfeld, Baden-Württemberg	bonebed, base Hauptsandstein	
	PT-W	Germany	quarry near Kirchberg an der Jagst, Baden-Württemberg	Lettenkeuper	
	PT-W	Germany	Würzburg	middle Keuper	
	PT-W	Germany	Eibachtal, E of Gaildorf, Baden-Württemberg, SW	Gaildorfer Bank (Dunkle Mergel), Stuttgart Fm, middle Keuper	
	PT-W	Germany	clay quarry, near Schöningen, lower Saxony	Muschelkalk-Keuper boundary	near-shore / limnic
	PT-W	Germany	clay quarry near Wienerberger, near Schoningen, Lower Saxony	bonebeds	
	PT-W	Germany	"Am Hahnritz" quarries, near Bedheim, Thuringia	Lettenkeuper	
	PT-W	Germany	Schumann quarry, near Eschenau, Baden-Württemberg	Hauptsandstein	

marine?/freshwater?			Johnson 1981	Ginter *et al.* 2010	
marine?/freshwater?			Johnson 1981	Ginter *et al.* 2010	
			Johnson 1996		
			Minikh & Minikh 1981	Ivanov 2000, 2005	
			Wang *et al.* 2007a	Wang *et al.* 2007b	
marine		*Metophiceras subdemissum – Ophiceras commune* Zone (ammonoid)	Stensiö 1932; Nielsen 1936	Bendix-Almgreen 1976; Birkenmajer & Jerzmańska 1979; Cappetta 1987, 2012	
			Stensiö 1921	Cox & Smith 1973; Cappetta 1987, 2012	(cf. *Lissodus angulatus* ?)
			Agassiz 1836	Dorka 2003; Ginter *et al.* 2010; Cappetta 2012	(as *Hybodus*)
			Jaekel 1889	Cappetta 2012	
			Corroy 1928	Cappetta 2012	
			Dorka 2003		
			Dorka 2003		
marine	clutching-crushing		Liszkowski 1993		
marine		*Ceratites compressus* Zone	Diedrich 2009b		see Salamon *et al.* 2003 for biostratigraphic age
marine			Scheinpflug 1984		
brackish	2–2.5 m in length?		Hagdorn & Reif 1988	Böttcher 2010	
brackish			Reif 1980b		
			Quenstedt 1856	Storrs 1994; Cuny & Benton 1999; Dorka 2003	(as *Hybodus obtusus* ; species considered invalid by Dorka 2003 and considered synonymous to *P. cuspidatus* by Böttcher 2010)
				Duffin 1982a, 1998a; Storrs 1994	
marine with freshwater influence			Duffin *et al.* 1983	Delsate 1993	
marine			Duffin & Delsate 1993		
			Godefroit *et al.* 1998	Delsate 1998	
				Cuny 1995a	(as *Hybodus*)
				Cuny 1995a	(as *Hybodus*)
			Agassiz 1836		(as *Hybodus*)
			Agassiz 1836		(as *Hybodus*)
			Dorka 2003		
			Seilacher 1943	Dorka 2003	
			Dorka 2003		
			Dorka 2003		
			Winkler 1880	Dorka 2003	(as *Hybodus*)
			Seilacher 1943	Dorka 2003	(Seilacher 1943 referred the species from *Hybodus*)
freshwater/brackish?			Dorka 2001		
			Dorka 2003		
			Dorka 2003		
			Dorka 2003		

377	cf. *'Polyacrodus'*	*keuperianus* (Winkler, 1880)			teeth	Hybodontinae	Hybodontiformes	Triassic	Middle	Ladinian, upper
378	*'Polyacrodus'*	*keuperianus* (Winkler, 1880)			teeth	Hybodontinae	Hybodontiformes	Triassic	Upper	Carnian
379	*'Polyacrodus'*	*keuperianus* (Winkler, 1880)				Hybodontinae	Hybodontiformes	Triassic	Upper	Carnian, lower
380	*'Polyacrodus'*	*tregovi* Rieppel, Kindlimann & Bucher, 1996			teeth	Hybodontinae	Hybodontiformes	Triassic	Middle	Anisian, lower middle
381	*'Polyacrodus'*	*tregovi* Rieppel, Kindlimann & Bucher, 1996			teeth	Hybodontinae	Hybodontiformes	Triassic	Middle	Anisian, lower middle
382	*'Polyacrodus'*	sp. nov.			teeth	Hybodontinae	Hybodontiformes?	Triassic	Middle	Ladinian
383	*'Polyacrodus'*	sp. 1			teeth	Hybodontinae	Hybodontiformes	Triassic	Upper	Carnian
384	*'Polyacrodus'*	sp.			teeth	Hybodontinae	Hybodontiformes	Triassic	Middle	Anisian, lower-middle
385	*'Polyacrodus'*	sp. 4			teeth	Hybodontinae	Hybodontiformes	Triassic	Middle	Anisian, lower–middle
386	*'Polyacrodus'*?	sp.			tooth	Hybodontinae	Hybodontiformes	Triassic	Middle	Anisian
387	*'Polyacrodus:?'*	sp.			skeletal elements, teeth	Hybodontinae	Hybodontiformes?	Triassic	Lower	Olenekian (lower Smithian?–Spathian?)
388	*'Polyacrodus'*	sp. A			teeth	Hybodontinae	Hybodontiformes?	Triassic	Middle	Anisian, lower middle
389	*'Polyacrodus'*	sp.			teeth	Hybodontinae	Hybodontiformes?	Triassic	Middle	Anisian–Ladinian
390	*'Polyacrodus'*	sp.			teeth	Hybodontinae	Hybodontiformes?	Triassic	Middle	Ladinian, upper
391	*'Polyacrodus'*					Hybodontinae	Hybodontiformes?	Triassic	Upper	Rhaetian
392	*'Polyacrodus'*	sp. 1			teeth	Hybodontinae	Hybodontiformes?	Triassic	Lower	Olenekian (Spathian)
393	*'Polyacrodus'*	sp. 1			teeth	Hybodontinae	Hybodontiformes?	Triassic	Lower	Olenekian (Spathian)
394	*Acrodus* ?	*olsoni* Johnson, 1981			teeth	Acrodontinae	Hybodontiformes	Permian	Cisuralian	Artinskian
395	*Acrodus* ?	cf. *olsoni* Johnson, 1981			teeth	Acrodontinae	Hybodontiformes	Permian	Cisuralian	Kungurian
396	*Acrodus* ?	cf. *olsoni* Johnson, 1981			teeth	Acrodontinae	Hybodontiformes	Permian	Cisuralian	
397	*Acrodus* ?	*sweetiacruensis* Johnson, 1981			teeth	Acrodontinae	Hybodontiformes	Permian	Cisuralian	Artinskian
398	*Acrodus* ?	*sweetiacruensis* Johnson, 1981			teeth	Acrodontinae	Hybodontiformes	Permian	Cisuralian	Kungurian
399	*Acrodus* ?	cf. *sweetiacruensis* Johnson, 1981			teeth	Acrodontinae	Hybodontiformes	Permian	Cisuralian	
400	*Acrodus* ?	sp.			teeth	Acrodontinae	Hybodontiformes	Permian	Cisuralian	Artinskian
401	*Acrodus* ?	sp.			teeth	Acrodontinae	Hybodontiformes	Permian	Cisuralian	Kungurian
402	*Acrodus*	sp.				Acrodontinae	Hybodontiformes	Permian	Cisuralian	

	PT-W	Germany	Neidenfels, near Crailsheim, S	base Hauptsandstein, lower Letterkeuper, lower Keuper	bone bed; estuary
	PT-W	Germany	Goldersbach, near Tübingen	Schilfsandstein (= Stuttgart Fm)	
	PT-W	Germany	Steinbach near Schwäbisch Hall, SW	lower Lettenkeuper	brackish/deltaic
	PL-E	USA-W	west slope Augusta Mountains, Pershing County, Nevada	lower Fossil Hill Mb, Favret Fm, Star Peak Grp	litharenite, debris flow deposit, high energy, coastal influence, outer platform
	PL-E	USA-W	west slope Augusta Mountains, Pershing County, Nevada	lower Fossil Hill Mb, Favret Fm, Star Peak Grp	litharenite, debris flow deposit, high energy, coastal influence, outer platform
Tethys	PT-W	Poland	Upper Silesia and Holy Cross Mountains, SE	Muschelkalk	
	PT-W	Germany	Eibachtal, E of Gaildorf, Baden-Württemberg, SW	Gaildorfer Bank (Dunkle Mergel), Stuttgart Fm, middle Keuper	
	PL-C	Japan	Tahokamigumi, Nishiuwa City (prev. Shirokawa-cho, Higashiuwa-gun), Ehime Prefecture, Shikoku	Taho Fm	biomicritic limestone
	PL-C	Japan	Shioinouso, Takachiho-cho, Miyazaki Prefecture, Kyushu	Kamura Fm	micritic limestone
	PL-W	Japan	Oyugo, Yakuno-cho, Amada-gun, Kyoto Prefecture, central Honshu	Waruishi Fm?, Yakuno Grp	grey sandy mudstone
	PL-E	Canada-W	Ganoid Ridge, Wapiti Lake, British Columbia	Vega-Phroso Siltstone Mb, Sulphur Mountain Fm	siltstone, deltaic/shallow continental shelf environment
	PL-E	USA-W	west slope Augusta Mountains, Pershing County, Nevada	lower Fossil Hill Mb, Favret Fm, Star Peak Grp	litharenite, debris flow deposit, high energy, coastal influence, outer platform
	PT-W	Luxembourg	Heselbierg Quarry, Moersdorf, E	upper Muschelkalk	dolomites with interbedded blue shaly marls; platform deposits
	PT-W	Germany	Neidenfels, near Crailsheim, S	base Hauptsandstein, lower Letterkeuper, lower Keuper	bone bed; estuary
	PT-W	England		Blue Anchor Fm, Mercia Mudstone Grp	
	PL-E	USA-W	Bear Lake, Bear Lake County, SE Idaho	Thaynes Fm	mudstone; shallow subtidal and intertidal environment (inner shelf facies)
	NT-E	Timor	River Bihati region, near Bouwn	exotic	pelagic Hallstatt-type limestone
	PG-C	USA-S	Baylor, Wichita and Archer Counties, north central Texas	Wichita-Albany Grp (upper Belle Plains Fm, Clyde Fm, low-mid Lueders Fm)	
	PG-C	USA-C	Lake Frederick site, near Deep Red Creek, Tillman County, SW Oklahoma	upper Garber (Sandstone) Fm, upper Sumner Grp	sandstones, mudstone conglomerates, claystones; fluvial and lacustrine environments in a coastal-plain setting
	PL-C	Japan	Hajikadani, Neo-mura, Motosu-gun, Gifu Prefecture, central Honshu	Funabuseyama Fm, Okumino Grp	limestone
	PG-C	USA-S	Baylor, Wichita and Archer Counties, north central Texas	Wichita-Albany Grp (upper Belle Plains Fm, Clyde Fm, low-mid Lueders Fm)	
	PG-C	USA-C	Lake Frederick site, near Deep Red Creek, Tillman County, SW Oklahoma	upper Garber (Sandstone) Fm, upper Sumner Grp	sandstones, mudstone conglomerates, claystones; fluvial and lacustrine environments in a coastal-plain setting
	PL-C	Japan	Hajikadani, Neo-mura, Motosu-gun, Gifu Prefecture, central Honshu	Funabuseyama Fm, Okumino Grp	limestone
	PG-C	USA-S	Texas	Clyde Fm, Wichita-Albany Grp	
	PL-C	Japan	Kinshozan, Akasaka-cho, Ohgaki City, Gifu Prefecture, central Honshu	lower Akasaka Limestone	
	PG-C	USA-C	Geary County, Kansas	Neva Limestone Mb., Genola Limestone Fm, Council Grove Grp	Poorly consolidated limey mud

brackish	2–2.5 m in length?		Hagdorn & Reif 1988	Böttcher 2010	
			Dorka 2003		
brackish			Reif 1980b		
marine	durophagous, crushing	*Motaggarti* Subzone of the *Hyatti* Zone	Rieppel *et al.* 1996	Cuny *et al.* 2001	
marine	durophagous, crushing	*Motaggarti* Subzone of the *Hyatti* Zone	Cuny *et al.* 2001	Cappetta 2012	
marine	clutching-crushing		Liszkowski 1993		
			Seilacher 1943	Dorka 2003	(as *P. krafft*)
		Necogondolella timorensis – *Ng. bulgarica* Zones	Yamagishi 2004; Yamagishi 2006	Goto *et al.* 2010	
marine			Yamagishi 2006		
			Yamagishi 2006		
marine			Mutter *et al.* 2007a		
marine	durophagous, crushing	*Motaggarti* Subzone of the *Hyatti* Zone	Rieppel *et al.* 1996	Cuny *et al.* 2001	
marine			Delsate & Duffin 1999		
brackish			Hagdorn & Reif 1988	Böttcher 2010	
			Warrington & Whittaker 1984	Storrs 1994	
marine		*Necsprathodus dieneri* ; *Columbites*	Yamagishi 2006		
marine		*Columbites parisianus* ammonoid Zone (Albanites)	Yamagishi 2006		
marine?/freshwater?			Johnson 1981	Ginter *et al.* 2010	
freshwater			Zidek *et al.* 2004	Ginter *et al.* 2010	(tentative)
		Pseudofusulina ambigua Zone	Yamagishi 2006		
marine?/freshwater?			Johnson 1981	Ginter *et al.* 2010	
freshwater			Zidek *et al.* 2004	Ginter *et al.* 2010	(tentative)
		Pseudofusulina ambigua Zone	Yamagishi 2006		(as *Liscodus*)
marine?/freshwater?			Johnson 1981	Ginter *et al.* 2010	
marine		*Parafusulina* Zone	Goto 1994a	Goto 1994b, 1996a–c, 1999a, b, 2000	
			Ewell & Everhart 2005		

403	*Acrodus*	*gaillardoni* Agassiz, 1837			teeth	Acrodontinae	Hybodontiformes	Triassic	Middle	Anisian–Ladinian
404	*Acrodus*	*gaillardoni* Agassiz, 1837			teeth	Acrodontinae	Hybodontiformes	Triassic	Middle	Anisian–Ladinian
405	*Acrodus*	*gaillardoni* Agassiz, 1837			teeth	Acrodontinae	Hybodontiformes	Triassic	Middle	Anisian–Ladinian
406	*Acrodus*	*gaillardoni* Agassiz, 1837			teeth	Acrodontinae	Hybodontiformes	Triassic	Middle	Anisian–Ladinian
407	*Acrodus*	*gaillardoni* Agassiz, 1837			teeth	Acrodontinae	Hybodontiformes	Triassic	Middle	Anisian–Ladinian
408	*Acrodus*	*gaillardoni* Agassiz, 1837	morphotype *gaillardoni* Agassiz, 1837		teeth	Acrodontinae	Hybodontiformes	Triassic	Middle	Anisian–Ladinian
409	*Acrodus*	*gaillardoni* Agassiz, 1837	morphotype *lateralis* Agassiz, 1837		teeth	Acrodontinae	Hybodontiformes	Triassic	Middle	Anisian–Ladinian
410	*Acrodus*	*gaillardoni* Agassiz, 1837			teeth	Acrodontinae	Hybodontiformes	Triassic	Middle	Anisian–Ladinian
411	*Acrodus*	*gaillardoni* Agassiz, 1837			teeth	Acrodontinae	Hybodontiformes	Triassic	Middle	Ladinian
412	*Acrodus*	*gaillardoni* Agassiz, 1837			teeth	Acrodontinae	Hybodontiformes	Triassic	Middle	Anisian–Ladinian
413	*Acrodus*	*lateralis* Agassiz, 1837			teeth	Acrodontinae	Hybodontiformes	Triassic	Middle	Anisian–Ladinian
414	*Acrodus*	*lateralis* Agassiz, 1837			partial body, articulated dentition, fin spines, head spines	Acrodontinae	Hybodontiformes	Triassic	Middle	Anisian
415	*Acrodus*	*lateralis* Agassiz, 1837			teeth	Acrodontinae	Hybodontiformes	Triassic	Lower	Olenekian (Spathian)
416	*Acrodus*	*lateralis* Agassiz, 1837			teeth	Acrodontinae	Hybodontiformes	Triassic	Middle	Anisian, upper
417	*Acrodus*	*lateralis* Agassiz, 1837				Acrodontinae	Hybodontiformes	Triassic	Middle	Anisian–Ladinian
418	*Acrodus*	*lateralis* Agassiz, 1837				Acrodontinae	Hybodontiformes	Triassic	Middle–Upper	Anisian, Carnian
419	*Acrodus*	*lateralis* Agassiz, 1837			teeth	Acrodontinae	Hybodontiformes	Triassic	Middle	Anisian–Ladinian
420	*Acrodus*	*lateralis* Agassiz, 1837			teeth	Acrodontinae	Hybodontiformes	Triassic	Middle	Anisian
421	*Acrodus*	*lateralis* Agassiz, 1837			teeth	Acrodontinae	Hybodontiformes	Triassic	Middle	Ladinian, upper
422	*Acrodus*	*lateralis* Agassiz, 1837			teeth	Acrodontinae	Hybodontiformes	Triassic	Middle	Ladinian
423	*Acrodus*	*lateralis* Agassiz, 1837			teeth	Acrodontinae	Hybodontiformes	Triassic	Middle	Anisian–Ladinian
424	*Acrodus*	*lateralis* Agassiz, 1837			teeth	Acrodontinae	Hybodontiformes	Triassic	Middle	Ladinian, upper
425	*Acrodus*	*lateralis* Agassiz, 1837				Acrodontinae	Hybodontiformes	Triassic	Upper	Carnian, lower
426	*Acrodus*	cf. *lateralis* Agassiz, 1837			tooth	Acrodontinae	Hybodontiformes	Triassic	Middle	Anisian
427	*Acrodus*	*spitzbergensis* Hulke, 1873				Acrodontinae	Hybodontiformes	Triassic	Lower	Olenekian
428	*Acrodus*	*spitzbergensis* Hulke, 1873				Acrodontinae	Hybodontiformes	Triassic	Middle–Upper	Ladinian–Rhaetian
429	*Acrodus*	*spitzbergensis* Hulke, 1873			teeth	Acrodontinae	Hybodontiformes	Triassic	Lower	Olenekian (Spathian)
430	*Acrodus*	*spitzbergensis* Hulke, 1873				Acrodontinae	Hybodontiformes	Triassic	Lower	Induan (Dienerian)

	PT-W	France	Lunéville, NE	Muschelkalk	
	PT-W	Germany	Bayreuth, E	Muschelkalk	
	PT-W	Germany	Wilhelmshall, near Rottweil, Württemberg	Muschelkalk	
	PT-W	Germany	Kitzingen and Sommershausen, near Würzburg	Muschelkalk	
	PT-W	France	Lorraine	Muschelkalk and Lettenkohle	
	PT-W	Luxembourg	Heselbierg Quarry, Moersdorf, E	upper Muschelkalk	dolomites with interbedded blue shaly marls; platform deposits
	PT-W	Luxembourg	Heselbierg Quarry, Moersdorf, E	upper Muschelkalk	dolomites with interbedded blue shaly marls; platform deposits
Tethys	PT-W	Poland	Upper Silesia and Holy Cross Mountains, SE	Muschelkalk	
N Tethys, western Germanic Basin	PT-W	Germany	Bissendorf, Osnabrücker Bergland, NW	Meißner Fm, upper Muschelkalk	bioclastic rudstone; shallow marine, subtidal
Germanic Basin	PT-W	Germany	oberen Werntal, east of Arnstein, Main-Spessart, south of Würzburg	upper Muschelkalk	
	PT-W	France?	Vosges Mountains	Muschelkalk	
	PT-W	Switzerland	S Alps, Monte San Giorgio, Kt. Tessin	Grenzbitumenzone	
Medito-Tethyan	NT-W	India	Khreuh, near Srinagar, Kashmir Himalayas		shallow water
Medito-Tethyan	NT-W	India	Malla Johar, near Sumna, Lapthal, Kiogar Valley, Kumaun and Garhwal Himalayas	Kalapani Limestone	shallow water
	PT-W	Germany	Thüringen	Muschelkalk	
	PT-N	Bulgaria	north of Sofia	Balkanide carbonate	
Tethys	PT-W	Poland	Upper Silesia and Holy Cross Mountains, SE	Muschelkalk	
	PT-W	Poland	Raciborowice, North-Sudetic Basin, Lower Silesia, SW		limestone
	PT-W	Germany	clay quarry, near Schöningen, lower Saxony	Muschelkalk-Keuper boundary	fully marine
N Tethys, western Germanic Basin	PT-W	Germany	Bissendorf, Osnabrücker Bergland, NW	Meißner Fm, upper Muschelkalk	bioclastic rudstone; shallow marine, subtidal
Germanic Basin	PT-W	Germany	oberen Werntal, east of Arnstein, Main-Spessart, south of Würzburg	upper Muschelkalk	
	PT-W	Germany	Neidenfels, near Crailsheim, S	base Hauptsandstein, lower Letterkeuper, lower Keuper	bone bed; estuary
	PT-W	Germany	Steinbach near Schwäbisch Hall, SW	lower Lettenkeuper	brackish/deltaic
	PT-W	Poland	Raciborowice, North-Sudetic Basin, Lower Silesia, SW		limestone
Boreal	BOR	Spitsbergen	Mt. Saurie (Saurieberget), central	Sticky Keep Fm	
Boreal	BOR	Spitsbergen	Mt. Saurie (Saurieberget), central	Kapp Toscana Fm	
Boreal	BOR	Spitsbergen	Mt. Viking, Sassen Bay + Mt. Tschermak / Congress, Isfjorden	"Grippia–lower saurian niveau", Kaosfjellet Mb, Sticky Keep Fm, Kongressfjellet Subgrp, Sassendalen Grp	
Boreal	BOR	Spitsbergen	Hornsund	Brevassfjellet *Myalina* Bed, Urnetoppen Mb, Vardebukta Fm, Torell Land Grp	iron-rich, fine-grained conglomerate, concentrated deposit, offshore sand bars

			Agassiz, in Gaillardot 1835/Geinitz 1937; Agassiz 1836	Cappetta 1987, 2012; Ginter *et al.* 2010	
			Agassiz 1836		
			Agassiz 1836		
		Ceratites nodosus , *C. semipartites* (ammonoid)	Winkler 1880		
			Corroy 1928		
marine		*Ceratites nodosus* (ammonoid)	Delsate & Duffin 1999	Delsate 1992, 1993, 1995, 1997	
marine		*Ceratites nodosus* (ammonoid)	Delsate & Duffin 1999	Delsate 1992, 1993, 1995, 1997	
marine	durophagous		Liszkowski 1993		
marine		*Ceratites compressus* Zone	Diedrich 2009b		see Salamon *et al.* 2003 for biostratigraphic age
marine			Scheinpflug 1984		
			Agassiz 1836		
			Kuhn 1945	Rieppel 1981, 1982	(as sp.); assigned to *A. gaillardoti* by Corroy 1928; followed by Delsate & Duffin 1999
marine	crushing	*Neogondolella jubata* Zone (conodont)	Sahni & Chhabra 1976		
marine	crushing		Sahni & Chhabra 1976		
			??Stefanov 1966	Sahni & Chhabra 1976	
			Stefanov 1966, 1977	Sahni & Chhabra 1976; Brinkmann *et al.* 2010	
marine	durophagous		Liszkowski 1993		
			Chrząstek & Niedźwiedski 2004		
marine			Dorka 2001		
marine		*Ceratites compressus* Zone	Diedrich 2009b		see Salamon *et al.* 2003 for biostratigraphic age
marine			Scheinpflug 1984		
brackish			Hagdorn & Reif 1988	Böttcher 2010	
brackish			Reif 1980b		
			Chrząstek & Niedźwiedski 2004		
marine			Hulke 1873	Cox & Smith 1973; Birkenmajer & Jerzmańska 1979; Cappetta 1987, 2012	
marine			Hulke 1873	Cox & Smith 1973; Birkenmajer & Jerzmańska 1979; Cappetta 1987, 2012	
marine		*Olenikites pilaticus – Keyserlingites subrobustus* Zone (ammonoid)	Stensiö 1921	Birkenmajer & Jerzmańska 1979; Błażejowski 2004	correlates to "Grippia niveau", Vendomdalen Mb, Vikinghøgda Fm (Romano & Brinkmann 2010)
marine			Stensiö 1918, 1921	Birkenmajer & Jerzmańska 1979; Romano & Brinkmann 2010	

431	*Acrodus*	*spitzbergensis* Hulke, 1873			teeth	Acrodontinae	Hybodontiformes	Triassic	Lower	Induan (Dienerian)
432	*Acrodus*	*spitzbergensis* Hulke, 1873				Acrodontinae	Hybodontiformes	Triassic	Lower	Induan (Dienerian)
433	*Acrodus*	*spitzbergensis* Hulke, 1873			teeth	Acrodontinae	Hybodontiformes	Triassic	Middle	Anisian–Ladinian
434	*Acrodus*	*spitzbergensis* Hulke, 1873			teeth	Acrodontinae	Hybodontiformes	Triassic	Middle	Anisian, lower middle
435	*Acrodus*	*spitzbergensis* Hulke, 1873			teeth	Acrodontinae	Hybodontiformes	Triassic	Middle	Anisian, lower middle
436	*Acrodus*	*spitzbergensis* Hulke, 1873			teeth	Acrodontinae	Hybodontiformes	Triassic	Lower–Middle	Induan (Griesbachian?), Anisian–Ladinian
437	*Acrodus*	cf. *spitzbergensis* Hulke, 1873			teeth	Acrodontinae	Hybodontiformes	Triassic	Lower–Middle	**Olenekian–Anisian, lower–middle**
438	*Acrodus*	cf. *spitzbergensis* Hulke, 1873			tooth	Acrodontinae	Hybodontiformes	Triassic	Middle	Anisian
439	*Acrodus*	cf. *spitzbergensis* Hulke, 1873			tooth	Acrodontinae	Hybodontiformes	Triassic	Upper	Carnian
440	*Acrodus*	*oppenheimeri* Stensiö, 1921			teeth + dermal denticles	Acrodontinae	Hybodontiformes	Triassic	Middle?	
441	*Acrodus*	*scaber* Stensiö, 1921			teeth	Acrodontinae	Hybodontiformes	Triassic	Lower	Olenekian (Spathian)
442	*Acrodus*	*substriatus* (Schmid, 1861)				Acrodontinae	Hybodontiformes	Triassic	Middle	
443	*Acrodus*	cf. *substriatus* (Schmid, 1861)			tooth	Acrodontinae	Hybodontiformes	Triassic	Middle	Anisian–Ladinian
444	*Acrodus*	*substriatus* (Schmid, 1861)			teeth	Acrodontinae	Hybodontiformes	Triassic	Lower–Middle	**Olenekian (Smithian–Spathian)–Anisian, lower**
445	*Acrodus*	*substriatus* (Schmid, 1861)			teeth	Acrodontinae	Hybodontiformes	Triassic	Middle	Anisian, upper
446	*Acrodus*	*substriatus* (Schmid, 1861)			teeth	Acrodontinae	Hybodontiformes	Triassic	Middle	Anisian–Ladinian
447	*Acrodus*	*vermiformis* Stensiö, 1921			teeth	Acrodontinae	Hybodontiformes	Triassic	Lower	Olenekian (Spathian)
448	*Acrodus*	sp.			tooth	Acrodontinae	Hybodontiformes	Triassic	Upper	Carnian
449	*Acrodus* ?	sp. 1			teeth	Acrodontinae	Hybodontiformes	Triassic	Upper	Carnian, upper
450	*Acrodus*	*alexandrae* Wemple, 1906				Acrodontinae	Hybodontiformes	Triassic	Middle	Ladinian?
451	*Acrodus*	*crecodontus* Wemple, 1906				Acrodontinae	Hybodontiformes	Triassic	Middle	Ladinian?
452	*Acrodus*	cf. *crecodontus* Wemple, 1906			teeth	Acrodontinae	Hybodontiformes	Triassic	Middle	Anisian, lower middle
453	*Acrodus*	*cunecocostatus* Cuny, Rieppel & Sander, 2001			teeth	Acrodontinae	Hybodontiformes	Triassic	Middle	Anisian, lower middle
454	*Acrodus*	*cunecocostatus* Cuny, Rieppel & Sander, 2001			teeth	Acrodontinae	Hybodontiformes	Triassic	Middle	Anisian, lower middle

Boreal	BOR	Spitsbergen	Hyrnefjellet, Hornsund, S	Brevassfjellet *Mytilus* Bed, Urnetoppen Mb, Vardebukta Fm, Torell Land Grp	iron-rich, fine-grained conglomerate, concentrated deposit, offshore sand bars
Boreal	BOR	Spitsbergen	Hyrnefjellet Mountain, Hornsund, SW	Brevassfjellet *Mytilus* Bed, Urnetoppen Mb, Vardebukta Fm	fine-grained, iron rich conglomerate
	PT-W	France	Mont-sur-Meurthe and d'Azerailles, Lorraine	Muschelkalk	
	PL-E	USA-W	west slope Augusta Mountains, Pershing County, Nevada	lower Fossil Hill Mb, Favret Fm, Star Peak Grp	litharenite, debris flow deposit, high energy, coastal influence, outer platform
	PL-E	USA-W	west slope Augusta Mountains, Pershing County, Nevada	lower Fossil Hill Mb, Favret Fm, Star Peak Grp	litharenite, debris flow deposit, high energy, coastal influence, outer platform
	PL-C	Japan	Kamura, Takachiho-chō, Nishiusuki-gun, Miyazaki-ken (Prefecture), Kyūshū	Kamura Fm	mid-oceanic seamount
	PL-C	Japan	Tahokamigumi, Nishiuwa City (prev. Shirokawa-cho, Higashiuwa-gun), Ehime Prefecture, Shikoku	Taho Fm	biomicritic limestone
	PL-W	Japan	Oyugo, Yakuno-cho, Amada-gun, Kyoto Prefecture, central Honshu	Waruishi Fm?, Yakuno Grp	grey sandy mudstone
	PL-W	Japan	Heki, Yakuno-cho, Amada-gun, Kyoto Prefecture, central Honshu	Heki Fm, Nabae Grp	conglomerate
Boreal	BOR	Spitsbergen	Mt. Tschermak, Saurie + S of Sassen Bay, Isfjorden	"upper saurian niveau"	
Boreal	BOR	Spitsbergen	Mt. Congress, Isfjorden	"lower saurian niveau", Kaosfjellet Mb, Sticky Keep Fm, Kongressfjellet Subgrp, Sassendalen Grp	
	PT-W	Germany	Jena		
	PT-W	Luxembourg	Heselbierg Quarry, Moersdorf, E	upper Muschelkalk	dolomites with interbedded blue shaly marls; platform deposits
Medito-Tethyan	NT-W	India	Guryul Ravine, Kreuh, Mandakpal, and Pastannah, Kashmir Himalayas		shallow water
Medito-Tethyan	NT-W	India	Niti Pass and Malla Johar, Kumaun and Garhwal Himalayas		shallow water
Tethys	PT-W	Poland	Upper Silesia and Holy Cross Mountains, SE	Muschelkalk	
Boreal	BOR	Spitsbergen	Mt. Viking, Sassen Bay + Mt. Tschermak / Congress, Isfjorden	"Grippia–lower saurian niveau", Kaosfjellet Mb, Sticky Keep Fm, Kongressfjellet Subgrp, Sassendalen Grp	
	PL-W	Japan	Heki, Yakuno-cho, Amada-gun, Kyoto Prefecture, central Honshu	Heki Fm, Nabae Grp	sandstone
	PL-E	Canada-W	Brown Hill, Childerhose Cove, Chowade South, Laurier Pass, and Pardonet Hill, Peace River area, northeastern BC	Ludington, Charlie Lake, and Baldonnel fms	
	PL-E	USA-W	Fisher Canyon, west Humboldt Range, Nevada		
	PL-E	USA-W	Cottonwood Canyon, west Humboldt Range, Nevada		
	PL-E	USA-W	west slope Augusta Mountains, Pershing County, Nevada	lower Fossil Hill Mb, Favret Fm, Star Peak Grp	litharenite, debris flow deposit, high energy, coastal influence, outer platform
	PL-E	USA-W	west slope Augusta Mountains, Pershing County, Nevada	lower Fossil Hill Mb, Favret Fm, Star Peak Grp	litharenite, debris flow deposit, high energy, coastal influence, outer platform
	PL-E	USA-W	west slope Augusta Mountains, Pershing County, Nevada	lower Fossil Hill Mb, Favret Fm, Star Peak Grp	litharenite, debris flow deposit, high energy, coastal influence, outer platform

marine		*Proptychites candidus* Zone (ammonoid)	Birkenmajer & Jerzmańska 1979	Romano & Brinkmann 2010	
marine			Błażejowski 2004	Romano & Brinkmann 2010	
			Corroy 1928		
marine	durophagous, crushing	*Meekoceras gracilitatis* Subzone of the *Hedenstroemia hedenstroemi* Zone	Rieppel *et al.* 1996	Cuny *et al.* 2001	
marine	durophagous, crushing	*Meekoceras gracilitatis* Subzone of the *Hedenstroemia hedenstroemi* Zone	Cuny *et al.* 2001		
marine		*Chiosella timorensis* , *Paragondolella bulgarica* – *Budurovignathus hungaricus* , *Paragondolella foliata*	this study		Samples 300311-I, 300311-J, 300311-K, 05.7.15.k
		Neogondolella timorensis – *Ng. bulgarica* Zones	Yamagishi 2004; Yamagishi 2006	Goto *et al.* 2010	
			Yamagishi 2006		
			Yamagishi 2006		
			Stensiö 1921	Cappetta 1987, 2012	
marine		*Keyserlingites subrobustus* Zone (ammonoid)	Stensiö 1921	Cappetta 1987, 2012	cf. *spitzbergensis* ♦ correlates to "Grippia niveau", Vendomdalen Mb, Vikinghøgda Fm (Romano & Brinkmann 2010)
			Schmid 1861	Cappetta 1987, 2012	
marine			Delsate & Duffin 1999	Delsate 1995, 1997	
marine	crushing	*Necogondolella waageni* , *Necogondolella juhata* zones (conodont)	Sahni & Chhabra 1976		
marine	crushing		Sahni & Chhabra 1976		
marine	durophagous		Liszkowski 1993		
marine		*Olenikites pilaticus* – *Keyserlingites subrobustus* Zone (ammonoid)	Stensiö 1921	Cappetta 1987, 2012	cf. *spitzbergensis* ♦ correlates to "Grippia niveau", Vendomdalen Mb, Vikinghøgda Fm (Romano & Brinkmann 2010)
			Goto *et al.* 1991	Goto 1985, 1994a,b, 1996b; Goto & Kuga 1982; Goto *et al.* 1996a, 2010; Chang & Miao 2004	
marine		*Metapolygnathus nodosus* conodont Zone; *Tropites welleri* ammonoid Zone	Johns *et al.* 1997		
marine			Wemple 1906	Rieppel *et al.* 1996; Cuny *et al.* 2001	
marine			Wemple 1906	Rieppel *et al.* 1996; Cuny *et al.* 2001	
marine	durophagous, crushing	*Meekoceras gracilitatis* Subzone of the *Hedenstroemia hedenstroemi* Zone	Rieppel *et al.* 1996	Cuny *et al.* 2001	
marine	durophagous, crushing	*Meekoceras gracilitatis* Subzone of the *Hedenstroemia hedenstroemi* Zone	Rieppel *et al.* 1996	Cuny *et al.* 2001	(as *A.* cf. *vermicularis* (*vermiformis*))
marine	durophagous, crushing	*Meekoceras gracilitatis* Subzone of the *Hedenstroemia hedenstroemi* Zone	Cuny *et al.* 2001		

455	*Acrodus*	cf. *cuneocostatus* Cuny, Rieppel & Sander, 2001			teeth	Acrodontinae	Hybodontiformes	Triassic	Lower	**Induan (Dienerian, lower)–Olenekian (Smithian, lower)**
456	*Acrodus*	sp. 1			teeth	Acrodontinae	Hybodontiformes	Triassic	Middle	Ladinian, upper
457	*Acrodus*	sp. 2			teeth	Acrodontinae	Hybodontiformes	Triassic	Middle	Ladinian, upper
458	*Acrodus*	sp. 3			teeth	Acrodontinae	Hybodontiformes	Triassic	Middle	Ladinian, upper
459	*Acrodus*	sp.			tooth	Acrodontinae	Hybodontiformes	Triassic	Middle	Anisian
460	*Acrodus*	*braunii* Agassiz, 1839			tooth	Acrodontinae	Hybodontiformes	Triassic	Middle	Anisian
461	*Acrodus*	*georgii* Mutter, 1998b			teeth, jaws, skeletal elements, fin spines, denticles	Acrodontinae	Hybodontiformes	Triassic	Middle	Anisian, upper
462	*Acrodus*	*mutteri* Delsate & Duffin, 1999			teeth	Acrodontinae	Hybodontiformes	Triassic	Middle	Anisian–Ladinian
463	*Acrodus*	sp.			teeth	Acrodontinae	Hybodontiformes	Triassic	Upper	Carnian, lower
464	*Acrodus*	*dunkeri* Auerbach, 1871			teeth	Acrodontinae	Hybodontiformes	Triassic	Lower	
465	*Acrodus*					Acrodontinae	Hybodontiformes	Triassic	Lower	
466	*Acrodus?*	sp.			skull, jaws, teeth	Acrodontinae	Hybodontiformes	Triassic	Lower	
467	*Acrodus*	*microdus* Winkler, 1880			teeth	Acrodontinae	Hybodontiformes	Triassic		
468	*Acrodus*	*wempliae* Jordan, 1907			teeth	Acrodontinae	Hybodontiformes	Triassic	Upper	
469	*Acrodus*	spp.			teeth	Acrodontinae	Hybodontiformes	Triassic	Middle	
470	*Acrodus*	sp.			tooth	Acrodontinae	Hybodontiformes	Triassic	Upper	Carnian, upper middle
471	*Acrodus*	sp.			teeth	Acrodontinae	Hybodontiformes	Triassic	Upper	Norian, lower–middle
472	*Acrodus*	*flemingianus* De Koninck, 1863			teeth	Acrodontinae	Hybodontiformes	Permian/ Triassic?	Lopingian/ **Lower**	
473	*Acrodus*	sp.			teeth	Acrodontinae	Hybodontiformes	Permian/ Triassic?	Lopingian/ **Lower**	
474	*Acrodus*	*jaekeli* Waagen, 1895			teeth	Acrodontinae	Hybodontiformes	Triassic	Lower	Olenekian (Smithian) derived from (Scythian, middle, *Ceratites* Zone)
475	*Acrodus*					Acrodontinae	Hybodontiformes	Triassic	Lower	Induan (Griesbachian)
476	*Acrodus?*	sp.			teeth	Acrodontinae	Hybodontiformes	Permian	Lopingian	**Wuchiapingian–Changhsingian**
477	*Asteracanthus*	*agassizii* (Alberti, 1864)			tooth/teeth?	Acrodontinae	Hybodontiformes	Triassic	Middle	Ladinian, upper
478	*Asteracanthus*	sp. (cf. *reticulatus* Agassiz, 1837; cf. *agassizii* Alberti, 1864)			dissociated dentition	Acrodontinae	Hybodontiformes	Triassic	Middle	
479	*Asteracanthus*	sp.			teeth	Acrodontinae	Hybodontiformes	Triassic	Middle	Ladinian

	PL-W	Russia-SE	Abrek Bay area, Vladivostok, South Primorye	Zhitkov Fm	ammonoid turbidites
	PT-W	Germany	clay quarry, near Schöningen, lower Saxony	Muschelkalk-Keuper boundary	near-shore / limnic
	PT-W	Germany	clay quarry, near Schöningen, lower Saxony	Muschelkalk-Keuper boundary	near-shore / limnic
	PT-W	Germany	clay quarry, near Schöningen, lower Saxony	Muschelkalk-Keuper boundary	near-shore / limnic
	PT-W	Poland	Raciborowice, North-Sudetic Basin, Lower Silesia, SW		limestone
	PT-W	Germany	Zweibrücken, Rheinland-Pfalz	lower Muschelkalk (Udelfangen Fm)	sandstone
	PT-W	Switzerland	Valporina, Cava Tre Fontane, Monte San Giorgio, Kt. Tessin, S Alps	middle Grenzbitumenzone	
	PT-W	Luxembourg	Heselbierg Quarry, Moersdorf, E	upper Muschelkalk	dolomites with interbedded blue shaly marls; platform deposits
	PT-W	Italy	near Sief Pass, near Richthofen Riff, Badia Valley, Bolzano Province, Dolomites region, NE	San Cassiano Fm	basinal marls, micrites and oolitic-bioclastic calciturbidites
	PT-N	Russia-SW	Big Bogda Mountain, Caspian Basin	Bogdinsko Fm	limestone
	BOR	Russia-N	Olenek River, Siberia		
	NT-W	Madagascar	Ambilobe Bay locality, N		nodule
	PT-W	Germany?	Würzburg		
	PL-E	USA-W	Bear Cove and North Fork, Shasta County, California		black limestone
west Tethyan	NT-W	Saudi Arabia	Site 1, Ar Rubay'iyah village, east of Buraydah	Jilh Fm	sandstone, shallow marine to offshore environment
	PG-C	USA-S	*Placerias* /Downs Quarry and Petrified Forest National Park, Arizona	Mesa Redondo Mb and Blue Mesa Mb, Chinle Fm	floodplain
	PG-C	USA-S	Crystal Forest and "Lungfish" localities, Petrified Forest National Park, Arizona	Sonsela and Painted Desert Mbs, Petrified Forest Fm, Chinle Grp	fluvial - crevasse splay/overbank
	NT-W	Pakistan	Salt Range	*Productus* limestone?	
	NT-W	Pakistan	Salt Range	*Productus* limestone?	
	NT-W	Pakistan	Salt Range	Ceratite Beds	
	NT-W	Pakistan	Salt Range, Surghar Range, and Trans-Indus Range	Kathwai Mb, Mianwali Fm	
	NT-W	Iran	Baghuk Mountain, NW of Abadeh	Hambast Fm	deep shelf limestone
	PT-W	Germany	Rottweil, Württemberg	Lettenkohle (Muschelkalk/Keuper boundary)	
	PT-W	Switzerland	S Alps, Monte San Giorgio, Kt. Tessin	Grenzbitumenzone	
Tethys	PT-W	Poland	Upper Silesia and Holy Cross Mountains, SE	Muschelkalk	

marine		*Clypeoceras spitiense* "bed" – *Clypeoceras timorense* Zone (*Gyronites subdharmus – Anasibirites nevolini* Zone)	Yamagishi 2009	Yamagishi 2006	
freshwater/brackish?			Dorka 2001		
freshwater/brackish?			Dorka 2001		
freshwater/brackish?			Dorka 2001		
			Chrząstek & Niedźwiedski 2004		
marine			Agassiz 1836	Woodward 1889a; Böttcher 2010	(not Buntsandstein, see discussion in Böttcher 2010; synonymised with *A. gaillardoti* by Woodward 1889, but considered closer to *A. lateralis* by Böttcher 2010)
	durophagous, 1.8–2.5 m in length		Mutter 1998a	Mutter 1998b	
marine			Delsate & Duffin 1999		
marine			Bernardi *et al.* 2011		
marine			Auerbach 1871	Minikh 2001	
			Obruchev (pers. comm., 1959) in Schaeffer & Mangus 1976	Brinkmann *et al.* 2010	
			Thomson 1982		
			Winkler 1880	Cuny *et al.* 2001	
			Jordan 1907	Cuny *et al.* 2001	
marine			Vickers-Rich *et al.* 1999		
freshwater			Kaye & Padian 1994	Irmis 2005; Parker 2005; Milner *et al.* 2006	
freshwater			Murry & Long 1989	Huber *et al.* 1993	
			De Koninck 1863	Waagen 1895; Brinkmann *et al.* 2010	(Permian age questioned by Waagen 1895)
			De Koninck 1863	Waagen 1895; Brinkmann *et al.* 2010	(Permian age questioned by Waagen 1895)
marine			Waagen 1895	Chang & Miao 2004; Brinkmann *et al.* 2010	
			Kummel & Teichert 1966, 1970	Brinkmann *et al.* 2010	
marine			Hampe *et al.* 2013		
			Alberti 1864	Rieppel 1981	(as *Strophodus* and as *S. (Psammodus) reticulatus* in Agassiz 1937)
			Rieppel 1981	Rieppel 1982; Cappetta 1987, 2012	
marine	durophagous		Liszkowski 1993		

480	*Asteracanthus* , cf.	sp.			tooth	Acrodontinae	Hybodontiformes	Permian	Lopingian	Wuchiapingian
481	*Palaeobates*	*angustissimus* (Agassiz, 1838)			teeth	Acrodontinae	Hybodontiformes	Triassic	Middle	Anisian–Ladinian
482	*Palaeobates*	*angustissimus* (Agassiz, 1838)			teeth	Acrodontinae	Hybodontiformes	Triassic	Middle	Anisian–Ladinian
483	*Palaeobates*	*angustissimus* (Agassiz, 1838)			teeth	Acrodontinae	Hybodontiformes	Triassic	Middle	Anisian–Ladinian
484	*Palaeobates*	*angustissimus* (Agassiz, 1838)			teeth	Acrodontinae	Hybodontiformes	Triassic	Middle	Anisian–Ladinian
485	*Palaeobates*	*angustissimus* (Agassiz, 1838)			teeth + fin spines	Acrodontinae	Hybodontiformes	Triassic	Middle	
486	*Palaeobates*	*angustissimus* (Agassiz, 1838)			teeth	Acrodontinae	Hybodontiformes	Triassic	Middle	Anisian–Ladinian
487	*Palaeobates*	*angustissimus* (Agassiz, 1838)			tooth	Acrodontinae	Hybodontiformes	Triassic	Middle	Anisian
488	*Palaeobates*	cf. *angustissimus* (Agassiz, 1838)			teeth	Acrodontinae	Hybodontiformes	Triassic	Middle	Ladinian, upper
489	*Palaeobates*	*angustissimus* (Agassiz, 1838)			teeth	Acrodontinae	Hybodontiformes	Triassic	Middle	Anisian
490	*Palaeobates*	*angustissimus* (Agassiz, 1838)			teeth, fin spine	Acrodontinae	Hybodontiformes	Triassic	Middle	Ladinian
491	*Palaeobates*	*angustissimus* (Agassiz, 1838)			teeth	Acrodontinae	Hybodontiformes	Triassic	Middle	Anisian–Ladinian
492	*Palaeobates*	sp. nov.			teeth	Acrodontinae	Hybodontiformes	Triassic	Middle	Ladinian
493	*Palaeobates*	sp.			teeth	Acrodontinae	Hybodontiformes	Triassic	Middle	Anisian
494	*Palaeobates*					Acrodontinae	Hybodontiformes	Triassic	Middle	
495	*Palaeobates*	sp.			teeth	Acrodontinae	Hybodontiformes	Triassic	Middle	Anisian, lower middle
496	*Palaeobates*	sp.			teeth	Acrodontinae	Hybodontiformes	Triassic	Middle	Anisian, lower middle
497	*Palaeobates* ?	*shastensis* Bryant, 1914			teeth	Acrodontinae	Hybodontiformes	Triassic	Upper	
498	cf. *Palaeobates*					Acrodontinae	Hybodontiformes	Triassic	Upper	
499	*Palaeobates*					Acrodontinae	Hybodontiformes	Triassic	Upper	Rhaetian
500	*Palaeobates*	*reticulatus* Duffin, 1998a			teeth	Acrodontinae	Hybodontiformes	Triassic	Upper	Rhaetian
501	*Palaeobates*	sp.			teeth	Acrodontinae	Hybodontiformes	Triassic	Upper	Carnian
502	*Palaeobates*					Acrodontinae	Hybodontiformes	Triassic		
503	*Palaeobates*	sp.				Acrodontinae	Hybodontiformes	Triassic	Upper	Carnian, lower
504	*Palaeobates*					Acrodontinae	Hybodontiformes	Triassic		
505	*Palaeobates*	*polaris* Stensiö, 1921			teeth, dermal denticles, skeletal elements	Acrodontinae	Hybodontiformes	Triassic	Lower	Olenekian (Smithian(–Spathian))
506	*Palaeobates*	*polaris* Stensiö, 1921			body fossil, teeth, denticles	Acrodontinae	Hybodontiformes	Triassic	Lower	Olenekian (Smithian, upper)
507	*Palaeobates*	sp.			teeth	Acrodontinae	Hybodontiformes	Triassic	Lower	Olenekian (Spathian)

Neo-Tethys	NT-W	Iran	Baghuk Mountain, NW of Abadeh	Hambast Fm	deep/outer shelf, nodular limestone
	PT-W	Germany	Wilhelmshall, near Rottweil, Württemberg	Muschelkalk	
	PT-W	France	Lunéville, NE	Muschelkalk	
	PT-W	France	Lunéville, Rehainvillers, and Chauffontaine, Lorraine	Muschelkalk and Lettenkohle	
	PT-W	Luxembourg	Heselbierg Quarry, Moersdorf, E	upper Muschelkalk	dolomites with interbedded blue shaly marls; platform deposits
	PT-W	Switzerland	S Alps, Monte San Giorgio, Kt. Tessin	Grenzbitumenzone	
Tethys	PT-W	Poland	Upper Silesia and Holy Cross Mountains, SE	Muschelkalk	
	PT-W	Poland	Raciborowice, North-Sudetic Basin, Lower Silesia, SW		limestone
	PT-W	Germany	clay quarry, near Schöningen, lower Saxony	Muschelkalk-Keuper boundary	
Tethys	PT-W	Poland	Upper Silesia and Holy Cross Mountains, SE	Muschelkalk	
N Tethys, western Germanic Basin	PT-W	Germany	Bissendorf, Osnabrücker Bergland, NW	Meißner Fm, upper Muschelkalk	bioclastic rudstone; shallow marine, subtidal
Germanic Basin	PT-W	Germany	oberen Werntal, east of Arnstein, Main-Spessart, south of Würzburg	upper Muschelkalk	
Tethys	PT-W	Poland	Upper Silesia and Holy Cross Mountains, SE	Muschelkalk	
	PT-W	Poland	Raciborowice, North-Sudetic Basin, Lower Silesia, SW		limestone
	PT-W	Germany			
	PL-E	USA-W	west slope Augusta Mountains, Pershing County, Nevada	lower Fossil Hill Mb, Favret Fm, Star Peak Grp	litharenite, debris flow deposit, high energy, coastal influence, outer platform
	PL-E	USA-W	west slope Augusta Mountains, Pershing County, Nevada	lower Fossil Hill Mb, Favret Fm, Star Peak Grp	litharenite, debris flow deposit, high energy, coastal influence, outer platform
	PL-E	USA-W	Cow Creek, Shasta County, N California	upper Hosselkus Limestone Fm	
	PG-C	USA-S		Dockum Grp	
	PT-W	France	Provenchères-sur-Meuse, Haute-Marne		
	PT-W	England	Holwell Quarry, near Frome, Somerset, SW	Westbury Fm, Penarth Grp	fissure infill
	PT-W	Austria	Judenbach near Mieming, and Kohlergraben in Hinterautal, Mieming and Karwendel mountain ranges, western Northern Calcareous Alps, Tirol	horizon 1a (lower shale series), lower part ("Cardita Beds") of Northalpine Raibl Beds	oncolite and coquina beds intercalated in dark shales; tempestites from inner shelf environment
	PT-W	Italy			
	PT-W	Italy	Stuores Wald/Bosco di Stuores	San Cassiano Fm	basinal marls, micrites and oolitic-bioclastic calciturbidites
	PT-W	Hungary			
	BOR	Spitsbergen	Mt. Stensiö (was Mt. Andersson), Sassendalen, Isfjorden	"fish niveau", Iskletten Mb, Sticky Keep Fm, Kongressfjellet Subgrp, Sassendalen Grp	
	BOR	Spitsbergen	Mt. Stensiö (was Mt. Andersson), Sassendalen, Isfjorden	"fish niveau", upper Lusitaniadalen Mb, Vikinghøgda Fm	moderately deep shelf, towards the east from a deltaic coast
	BOR	Spitsbergen	Mt. Viking, Sassen Bay, Isfjorden	"Grippia niveau", Kaosfjellet Mb, Sticky Keep Fm, Kongressfjellet Subgrp, Sassendalen Grp	

marine			Hampe *et al.* 2011, 2013		(as Helodontiformes? indet.)
			Agassiz 1836	Cappetta 1987, 2012	(as *Strophodus (Psammodus) angustissimus*)
			Agassiz 1836	Cappetta 1987	(as *Strophodus (Psammodus) angustissimus*)
			Corroy 1928	Cappetta 1987, 2012; Romano & Brinkmann 2010	
marine		*Ceratites nodosus* (ammonoid)	Delsate & Duffin 1999	Delsate 1993, 1995, 1997	
			Rieppel 1981	Rieppel 1982; Romano & Brinkmann 2010	
marine	durophagous		Liszkowski 1993	Romano & Brinkmann 2010	
			Chrząstek & Niedźwiedski 2004		
			Dorka 2001		
marine	durophagous		Liszkowski 1993		(as *angustus* Schmid, 1861; referred by Delsate & Duffin 1999)
marine		*Ceratites compressus* Zone	Diedrich 2009b	Romano & Brinkmann 2010	see Salamon *et al.* 2003 for biostratigraphic age
marine			Scheinpflug 1984		
marine	durophagous		Liszkowski 1993		
			Chrząstek & Niedźwiedski 2004		
			Meyer 1849; Seilacher 1943	Cappetta 1987, 2012; Romano & Brinkmann 2010	
marine	durophagous, crushing	*Meraggarti* Subzone of the *Hyatti* Zone	Rieppel *et al.* 1996	Cuny *et al.* 2001; Romano & Brinkmann 2010	(as cf. *P. shastensis*)
marine	durophagous, crushing	*Meraggarti* Subzone of the *Hyatti* Zone	Cuny *et al.* 2001	Romano & Brinkmann 2010, Cappetta 2012	(may belong to *Reticulodus* , Cappetta 2012)
marine			Bryant 1914	Stensiö 1921; Cappetta 1987, 2012; Rieppel *et al.* 1996; Romano & Brinkmann 2010	(as *Strophodus shastensis* , reassignment probable) note: different from *Hybodus shastensis* .
freshwater				Schaeffer & Mangus 1970	
				Cuny 1995a	
marine			Duffin 1998a	Romano & Brinkmann 2010, Cappetta 2012	
marine			Krainer *et al.* 2011		(possibly *P. angustissimus* , but base lacking; sample 1 or 9 is assumed for non-existing sample 10)
			Tommasi 1890	Romano & Brinkmann 2010	
marine			Bizzarini *et al.* 2001	Bernardi *et al.* 2011	
			Jaeckel 1911	Romano & Brinkmann 2010	
marine	1 m in length	*Euflemingites romunderi – Olenikites pilaticus* Zone (ammonoid)	Stensiö 1921	Cox & Smith 1973; Cappetta 1987, 2012; Romano & Brinkmann 2010	(resembles *Acrodus* , Cappetta 1987, 2012) ? correlates to "fish niveau", upper Lusitaniadalen Mb, Vikinghøgda Fm (Romano & Brinkmann 2010)
marine	1 m in length	*Euflemingites romunderi – Wasatchites tardus* Zone (ammonoid)	Romano & Brinkmann 2010		
marine		*Olenikites pilaticus – Keyserlingites subrobustus* Zone (ammonoid)	Stensiö 1921	Cox & Smith 1973; Cappetta 1987, 2012	correlates to "Grippia niveau", Vendomdalen Mb, Vikinghøgda Fm (Romano & Brinkmann 2010)

508	*Palaeobates*	sp.			teeth	Acrodontinae	Hybodontiformes	Triassic	Lower	Induan (Dienerian)
509	*Palaeobates*	sp.			teeth	Acrodontinae	Hybodontiformes	Permian	Lopingian	Changhsingian, uppermost
510	gen. indet.	sp. indet.				Acrodontinae	Hybodontiformes	Triassic	Upper	Carnian, lower
511	*Hybodus*/*Acrodus*				dermal denticles, cephalic + fin spines	Hybodontidae	Hybodontiformes	Triassic	Lower	Olenekian (Spathian)
512	*Hybodus*/*Acrodus*				fin spine fragments	Hybodontidae	Hybodontiformes	Triassic	Middle	
513	gen. indet. 1	sp. indet.			teeth, denticles	Hybodontidae	Hybodontiformes	Triassic	Middle	Anisian (Scythian)
514	gen. indet. 2	sp. indet.			denticles	Hybodontidae	Hybodontiformes	Triassic	Middle–Upper	Ladinian–lower Carnian
515	gen. indet.	sp. indet.			teeth	Hybodontidae	Hybodontiformes	Triassic	Upper	Carnian
516	gen. indet.	sp. indet.			denticles	Hybodontidae	Hybodontiformes	Permian	Guadalupian	Wordian (Murgabian)
517	gen. indet.	sp. indet.				Hybodontidae	Hybodontiformes	Triassic	Upper	Carnian–Norian
518	gen. indet.	sp. indet.				Hybodontidae	Hybodontiformes	Triassic	Upper	Norian
519	gen. indet.	sp. indet.				Hybodontidae	Hybodontiformes	Triassic	Middle	Ladinian, upper
520	gen. indet.	sp. indet.			teeth, denticles	Hybodontidae	Hybodontiformes	Triassic	Lower	Olenekian?
521	gen. indet.	sp. indet.			teeth	Hybodontidae	Hybodontiformes	Triassic	Lower?	
522	gen. indet.	sp. indet.				Hybodontidae	Hybodontiformes	Triassic	Upper	Carnian, lower
523	*Lissodus*	*africanus* (Broom, 1909)			body fossils, incl. teeth, fin spines, and head spines	Unnamed	Hybodontiformes	Triassic	Lower	Scythian
524	*Lissodus*	sp. (cf. *africanus* (Broom, 1909))			teeth, fin spines	Unnamed	Hybodontiformes	Triassic	Lower	Olenekian (Spathian)
525	*Lissodus*	*angulatus* (Stensiö, 1921)			teeth	Unnamed	Hybodontiformes	Triassic	Lower	Olenekian (Spathian)
526	*Lissodus*	*angulatus* (Stensiö, 1921)			tooth	Unnamed	Hybodontiformes	Triassic	Lower	Induan (Griesbachian)
527	*Lissodus*	*angulatus* (Stensiö, 1921)			teeth	Unnamed	Hybodontiformes	Triassic	Lower	Induan (Dienerian)
528	*Lissodus*	*angulatus* (Stensiö, 1921)			teeth	Unnamed	Hybodontiformes	Triassic	Lower	Induan (Dienerian)
529	*Lissodus*	*cassangensis* (Teixeira, 1956)			body fossils, whole, incl. teeth, cephalic spines	Unnamed	Hybodontiformes	Triassic	Lower	Scythian (Spathian?)

Boreal	BOR	Spitsbergen	Hornsund, S	Brevassfjellet *Aviculina* Bed, Urnetoppen Mb, Vardebukta Fm, Torell Land Grp	iron-rich, fine-grained conglomerate, concentrated deposit, offshore sand bars
	BOR	Spitsbergen	Lusitaniadalen	Deltadalen Mb, Vikinghøgda Fm	anoxic, deep water environment
	PT-W	Italy	Forcella Giau, Milieres-Cian Zoppè	San Cassiano Fm	basinal marls, micrites and oolitic-bioclastic calciturbidites
Boreal	BOR	Spitsbergen	Mt. Viking + Marmier, Sassen Bay + Mt. Tschermak / Congress (?), Isfjorden	"Grippia–lower saurian niveau", Kaosfjellet Mb, Sticky Keep Fm, Kongressfjellet Subgrp, Sassendalen Grp	
west Tethyan	NT-W	Saudi Arabia	Site 1, Ar Rubay'iyah village, east of Buraydah	Jilh Fm	sandstone, shallow marine to offshore environment
	PL-C	Japan	Taho, Shirokawa-cho, Higashiuwa-gun, Ehime Prefecture, Shikoku	Taho Fm	grey limestone
	PL-C	Japan	Karasawa, Yamasuge area (Asio Mountains), Kuzuu-cho, Aso-gun, Tochigi Prefecture, central Honshu	Adoyama Fm	laminated limestone
	PL-W	Japan	Sanyo & Mine, Yamagushi Prefecture, S Honshu	Momonoki Fm, Mine Grp	
	PL-C	Japan	Karasawa, Yamasuge area (Asio Mountains), Kuzuu-cho, Aso-gun, Tochigi Prefecture, central Honshu	Nabeyama Fm	black limestone
	PG-C	USA-S	Arizona, New Mexico, Texas	Chinle Fm / Dockum Grp	floodplain
	PT-E	Tibet	Tulong, Nielamu (Nyalam), Xizang	middle Mb, Qulonggongba Fm	
	PT-E	China-SE	Xinpu and Gangwu, Guanling, Guizhou Province	Zhuganpo Mb, Falang Fm	
	PL-E	USA-W	Bear River Range, between Slights and Paris canyons, Bear Lake County, SE Idaho	Thaynes Fm	limestone
La Coipa Basin	PG-S	Chile	La Coipa mine-Quebrada Maranceles area	La Coipa beds	lacustrine
	PT-W	Italy	Forcella Giau, Milieres-Cian Zoppè	San Cassiano Fm	basinal marls, micrites and oolitic-bioclastic calciturbidites
	PG-S	South Africa	Bekker's Kraal, Rouxville district, Orange Free State	Upper Beaufort Series, Karoo Supergroup	sandstone
	PG-S	South Africa	Driefontein (farm), Paul Roux district, Free State Province, northern Karoo Basin	lowermost Burgersdorp Fm, Upper Beaufort Grp, Karoo Supergroup	lacustrine lag deposit, ≤30 cm thick (time averaged)
	BOR	Spitsbergen	Mt Congress, Isfjorden, Isfjorden	"Grippia niveau", Kaosfjellet Mb, Sticky Keep Fm, Kongressfjellet Subgrp, Sassendalen Grp	
	BOR	Spitsbergen		Fish Horizon I (*Posidonomya* Bed)	
Boreal	BOR	Spitsbergen	Hyrnefjellet, Hornsund, S	Brevassfjellet *Aviculina* Bed, Urnetoppen Mb, Vardebukta Fm, Torell Land Grp	iron-rich, fine-grained conglomerate, concentrated deposit, offshore sand bars
Boreal	BOR	Spitsbergen	Hyrnefjellet Mountain, Hornsund, SW	Brevassfjellet *Aviculina* Bed, Urnetoppen Mb, Vardebukta Fm	fine-grained, iron rich conglomerate
	PG-S	Angola	Lutoa, Baixa do Cassange, Congo Basin, N	Cassanga Series, Karoo Supergroup	shallow, marginal freshwater lake

marine		*Proptychites candidus* Zone (ammonoid)	Stensiö 1921	Birkenmajer & Jerzmańska 1979; Romano & Brinkmann 2010; Cappetta 2012	
marine			this study		Sample SV-2
marine				Bernardi *et al.* 2011	(as Palaeobatidae)
marine		*Olenikites pilaticus – Keyserlingites subrobustus* Zone (ammonoid)	Stensiö 1921		
marine			Vickers-Rich *et al.* 1999		
			Goto 1994a	Goto 1994b, 1996b	
			Hayashi 1968; Goto 1975	Reif & Goto 1979; Goto 1985, 1994a, b, 1996b; Goto & Kuga 1982; Goto *et al.* 1996a, 2010; Chang & Miao 2004	
freshwater			Yabumoto & Uyeno 2001	Chang & Miao 2004; Yamagishi 2006	
			Hayashi 1971; Goto 1975	Reif & Goto 1979; Goto 1985, Goto *et al.* 1988	
freshwater			?? Murry 1981	Milner *et al.* 2006	
marine			Dong 1972	Chang & Miao 2004; Jin 2006	
marine			Li & Jin 2003	Jin 2006	
marine			Youngquist 1952		(teeth as probably *Polyacrodus* '; denticles as possibly *Hybodus*/*Acrodus*)
freshwater			Suarez & Bell 1992		potentially of Late Permian age
marine				Bernardi *et al.* 2011	
freshwater	23 cm in length	lower *Cyncognathus* Assemblage Zone - subzone B	Broom 1909	Brough 1931, 1935; Jubb & Gardiner 1975; Duffin 1985, 1989, 1993, 2001; Cappetta 1987, 2012; Gomez Pallerola 1992; Murray 2000; Rees & Underwood, 2002; Bender & Hancox 2004; Lopez-Arbarello 2004; Rubidge 2005; Fischer 2008; Ginter *et al.* 2010	(as *Hybodus* or *Acrodus*)
freshwater		lower *Cyncognathus* Assemblage Zone (CAZ) - Subzone A	Bender & Hancox 2004	Rubidge 2005; Fischer 2008	
marine		*Olenikites pilaticus – Keyserlingites subrobustus* Zone (ammonoid)	Stensiö 1921	Birkenmajer & Jerzmańska 1979; Rees & Underwood 2002; Cappetta 2012	(as *Polyacrodus*) ! correlates to "Grippia niveau", Vendomdalen Mb, Vikinghøgda Fm (Romano & Brinkmann 2010)
marine		? *Otoceras* ! *Ophiceras* Zone (ammonoid)	Stensiö 1921	Duffin 1985, 1989, 1993b, 2001; Gomez Pallerola 1992, Fischer 2008	(as *Polyacrodus*)
marine		*Proptychites candidus* Zone (ammonoid)	Birkenmajer & Jerzmańska 1979	Duffin 1985, 1989, 1993b, 2001; Gomez Pallerola 1992, Fischer 2008; Romano & Brinkmann 2010	(as *Polyacrodus*)
marine			Błażejowski 2004	Fischer 2008; Romano & Brinkmann 2010	
freshwater	>20 cm in length		Teixeira 1954	Teixeira 1956, 1979; Maisey 1982; Maisey 1990; Antunes *et al.* 1990; Murray 2000; Duffin 2001; Rees & Underwood 2002; Lopez-Arbarello 2004; Cappetta 2012	(as *Hybodus* , *H. pusillus* preocc.; cf. *L. africanus* ?)

530	*Lissodus*	*tiandongensis* Wang, Yang, Jin & Wang, 2001			tooth	Unnamed	Hybodontiformes	Triassic	Lower	Olenekian (Spathian, lower)
531	*Lissodus*	*volgensis* Minikh, 2001			teeth	Unnamed	Hybodontiformes	Triassic	Lower	
532	*Lissodus*	*aquilus* Minikh, 1996b			teeth	Unnamed	Hybodontiformes	Triassic	Lower	
533	*Lissodus*	sp.			tooth	Unnamed	Hybodontiformes	Triassic	Lower	Olenekian (Spathian)
534	*Lissodus*	*triaktis* Minikh, 1996b			teeth	Unnamed	Hybodontiformes	Triassic	Lower	
535	*Lissodus*	*triaktis* Minikh, 1996b			teeth	Unnamed	Hybodontiformes	Triassic	Middle	
536	*Lissodus*	*prykaspiensis* Minikh, 1996b			teeth	Unnamed	Hybodontiformes	Triassic	Middle	
537	*Lissodus*	sp. aff. *angulatus* (Stensiö, 1921)			teeth	Unnamed	Hybodontiformes	Triassic	Middle	Anisian
538	*Lissodus*	sp. aff. *africanus* (Broom, 1909)			teeth	Unnamed	Hybodontiformes	Triassic	Middle	Anisian
539	*Lissodus*	*cristatus* Delsate & Duffin, 1999			teeth	Unnamed	Hybodontiformes	Triassic	Middle	Anisian–Ladinian
540	*Lissodus*	cf. *cristatus* Delsate & Duffin, 1999			teeth	Unnamed	Hybodontiformes	Triassic	Lower	**Induan (Dienerian)–Olenekian (Smithian, lower)**
541	*Lissodus*	sp.			tooth	Unnamed	Hybodontiformes	Triassic	Middle	Anisian–Ladinian
542	*Lissodus*	*subhercynicus* Dorka, 2001	type 1		teeth	Unnamed	Hybodontiformes	Triassic	Middle	Ladinian, upper
543	*Lissodus*	*subhercynicus* Dorka, 2001	type 2		teeth	Unnamed	Hybodontiformes	Triassic	Middle	Ladinian, upper
544	*Lissodus*	*subhercynicus* Dorka, 2001	type 3		teeth	Unnamed	Hybodontiformes	Triassic	Middle	Ladinian, upper
545	*Lissodus*	sp.			teeth	Unnamed	Hybodontiformes	Triassic	Middle	Ladinian, upper
546	*Lissodus?*	sp.			tooth	Unnamed	Hybodontiformes	Triassic	Middle	
547	*Lissodus*	*nodosus* (Seilacher, 1943)			teeth	Unnamed	Hybodontiformes	Triassic	Middle	Ladinian
548	*Lissodus*	*nodosus* (Seilacher, 1943)				Unnamed	Hybodontiformes	Triassic	Middle	Ladinian, upper
549	*Lissodus*	*nodosus* (Seilacher, 1943)				Unnamed	Hybodontiformes	Triassic	Middle–Upper	Anisian–Norian
550	*Lissodus*	*nodosus* (Seilacher, 1943)				Unnamed	Hybodontiformes	Triassic	Middle–Upper	Anisian–Norian
551	*Lissodus*	*nodosus* (Seilacher, 1943)				Unnamed	Hybodontiformes	Triassic	Middle–Upper	Anisian–Norian
552	*Lissodus*	*nodosus* (Seilacher, 1943)			teeth	Unnamed	Hybodontiformes	Triassic	Middle	Ladinian, upper
553	*Lissodus*	*nodosus* (Seilacher, 1943)			teeth	Unnamed	Hybodontiformes	Triassic	Middle	Ladinian, upper
554	*Lissodus*	*nodosus* (Seilacher, 1943)	*spinosus* Seilacher, 1943			Unnamed	Hybodontiformes	Triassic	Upper	Carnian–Norian

W? Tethys	PT-E	China-SE	Denggaoling, Zuodeng area, Tiandong County, Guangxi Zhuang region, S	Luolou Fm	open sea environment
	PT-N	Russia-W	Tikhvinskoye locality, near Volga river, Rybinsk district, Yaroslav region, Moscow Syncline	Rybinsk Fm, Vetluzhsky series	
	PT-N	Russia-SW	south shore of Lake Baskunchak, Big Bogda Mountain, Asktrakhan region, Caspian Basin	Garnsky horizon, Yarenian superhorizon, Dinskaya Fm	
	PL-C	Japan	Kamigumi, Taho, Uonashi, Seiyo City, Ehime Prefecture, Shikoku	Taho Fm	
	PT-N	Russia-SW	Volgograd region		
	PT-N	Russia-SW	Donguz, Orenburg, Southern Cis-Urals	Donguzskaya Formation, Donguz suite	
	PT-N	Russia-SW	Caspian Basin and Gurjev region, pre-Urals foredeep	Inderskaja suite	
Tethys	PT-W	Poland	Upper Silesia and Holy Cross Mountains, SE	Muschelkalk	
Tethys	PT-W	Poland	Upper Silesia and Holy Cross Mountains, SE	Muschelkalk	
	PT-W	Luxembourg	Heselbierg Quarry, Moersdorf, E	upper Muschelkalk	dolomites with interbedded blue shaly marls; platform deposits
	PL-W	Russia-SE	Abrek Bay area, Vladivostok, South Primorye	Zhitkov Fm	ammonoid turbidites
	PT-W	Luxembourg	Heselbierg Quarry, Moersdorf, E	upper Muschelkalk	dolomites with interbedded blue shaly marls; platform deposits
	PT-W	Germany	clay quarry, near Schöningen, lower Saxony	Muschelkalk-Keuper boundary	near-shore / limnic
	PT-W	Germany	clay quarry, near Schöningen, lower Saxony	Muschelkalk-Keuper boundary	near-shore / limnic
	PT-W	Germany	clay quarry, near Schöningen, lower Saxony	Muschelkalk-Keuper boundary	near-shore / limnic
	PT-W	Germany	clay quarry, near Schöningen, lower Saxony	Muschelkalk-Keuper boundary	near-shore / limnic
west Tethyan	NT-W	Saudi Arabia	Site 1, Ar Rubay'iyah village, east of Buraydah	Jilh Fm	sandstone, shallow marine to offshore environment
Tethys	PT-W	Poland	Upper Silesia and Holy Cross Mountains, SE	Muschelkalk	
	PT-W	Germany	Heldenmühle, near Crailsheim, S	Vitriolschiefer, lower Lettenkohle, upper Muschelkalk	
	PT-W	Germany	SW	Upper Muschelkalk–Keuper	
	PT-W	Germany	SW	Upper Muschelkalk–Keuper	
	PT-W	Germany	SW	Upper Muschelkalk–Keuper	
	PT-W	Germany	clay quarry, near Schöningen, lower Saxony	Muschelkalk/Keuper boundary	
	PT-W	Germany	Heldenmühle, near Crailsheim, S	Vitriolschiefer, lower Lettenkohle	bone bed
	PT-W	Germany	Württemberg	Keuper	

marine		*Necsprathodus homeri – N. triangularis* Zone (conodont)	Wang *et al.* 2001	Chang & Miao 2004; Jin 2006; Fischer 2008; Wang *et al.* 2009	(as *Polyacrodus*)
marine			Minikh 2001	Prasad *et al.* 2008; Fischer 2008	
marine			Minikh 1996b	Minikh 2001; Prasad *et al.* 2008; Fischer 2008	(cf. *L. angulatus*)
			Goto *et al.* 2010		
marine			Minikh 2001		
marine			Minikh 1996b	Minikh 2001; Prasad *et al.* 2008; Fischer 2008	(cf. *L. africanus*)
marine			Minikh 1996b	Minikh 2001; Prasad *et al.* 2008; Fischer 2008	(cf. *L. minimus*)
freshwater/marine	clutching-crushing		Liszkowski 1993	Duffin 2001; Fischer 2008	
freshwater/marine	clutching-crushing		Liszkowski 1993	Duffin 2001; Fischer 2008	
marine		*Ceratites nodosus* (ammonoid)	Delsate & Duffin 1999	Delsate 1992, 1995, 1997; Rees & Underwood 2002; Fischer 2008, Cappetta 2012	(as sp. and cf. *minimus*)
marine		*Paranorites varians* Zone– *Radiopronites atrekensis* "bed" (*Hedenstroemia hosphorensis – Anasibirites nevolini* Zone)	Yamagishi 2006	Yamagishi 2009	(also as sp. 2)
marine			Delsate & Duffin 1999	Fischer 2008	
freshwater/brackish?			Dorka 2001	Fischer 2008	
freshwater/brackish?			Dorka 2001		
freshwater/brackish?			Dorka 2001		
freshwater/brackish?			Dorka 2001	Fischer 2008	
marine			Vickers-Rich *et al.* 1999		
marine	clutching-crushing		Liszkowski 1993	Duffin 2001; Fischer 2008	
marine	species well below 1 m in length? Böttcher 2010		Thürach 1888	Duffin 1985, 2001	(as *Acrodus* sp.)
			Lang 1910	Duffin 1985, 2001	(as *Acrodus* sp.)
			Oertle 1928	Duffin 1985, 2001	(as *Acrodus lateralis*)
			Reiff 1938	Duffin 1985	(as *Acrodus* sp.)
brackish?-freshwater			Seilacher 1943	Werneburg 1994; Dorka 2001; Seegis 2005; Fischer 2008	
marine			Seilacher 1943	Duffin 1985, 1989, 1993b, 2001; Gomez Pallerola 1992(this entry?); Rees & Underwood 2002; Cappetta 2012	(as *Palaeobates*)
marine			Seilacher 1943	Duffin 1985, 1989, 1993b, 2001; Cappetta 1987; Hampe 1996	(as *Palaeobates spinosus*)

555	*Lissodus*	*nodosus* (Seilacher, 1943)	type 1		teeth	Unnamed	Hybodontiformes	Triassic	Middle	Ladinian, upper
556	*Lissodus*	*nodosus* (Seilacher, 1943)	type 2		teeth	Unnamed	Hybodontiformes	Triassic	Middle	Ladinian, upper
557	*Lissodus*	*nodosus* (Seilacher, 1943)	type 3		teeth	Unnamed	Hybodontiformes	Triassic	Middle	Ladinian, upper
558	*Lissodus*	*nodosus* (Seilacher, 1943)	type 4		teeth	Unnamed	Hybodontiformes	Triassic	Middle	Ladinian, upper
559	*Lissodus*	*nodosus* (Seilacher, 1943)	type 5		teeth	Unnamed	Hybodontiformes	Triassic	Middle	Ladinian, upper
560	*Lissodus*	*nodosus* (Seilacher, 1943)			teeth	Unnamed	Hybodontiformes	Triassic	Middle	Ladinian, upper
561	*Lissodus*	*minimus* (Agassiz, 1839)	*acutus* (Agassiz, 1839)		tooth	Unnamed	Hybodontiformes	Triassic	Middle	Anisian (Scythian)
562	*Lissodus*	*minimus* (Agassiz, 1839)	idem		teeth	Unnamed	Hybodontiformes	Triassic	Middle	Anisian–Ladinian
563	*Lissodus*	*minimus* (Agassiz, 1839)	idem		teeth	Unnamed	Hybodontiformes	Triassic	Middle	Anisian–Ladinian
564	*Lissodus*	*minimus* (Agassiz, 1839)	idem		teeth	Unnamed	Hybodontiformes	Triassic	Middle	Ladinian, upper
565	*Lissodus*	*minimus* (Agassiz, 1839)	idem		teeth	Unnamed	Hybodontiformes	Triassic	Upper	Rhaetian
566	*Lissodus*	*minimus* (Agassiz, 1839)	idem		teeth	Unnamed	Hybodontiformes	Triassic	Upper	Rhaetian
567	*Lissodus*	*minimus* (Agassiz, 1839)	idem			Unnamed	Hybodontiformes	Triassic	Upper	Carnian–Rhaetian
568	*Lissodus*	*minimus* (Agassiz, 1839)	idem			Unnamed	Hybodontiformes	Triassic	Upper	Rhaetian
569	*Lissodus*	*minimus* (Agassiz, 1839)	idem			Unnamed	Hybodontiformes	Triassic	Upper	Carnian–Rhaetian
570	*Lissodus*	*minimus* (Agassiz, 1839)	idem			Unnamed	Hybodontiformes	Triassic	Upper	Carnian–Rhaetian
571	*Lissodus*	*minimus* (Agassiz, 1839)	idem			Unnamed	Hybodontiformes	Triassic	Upper	Carnian–Rhaetian
572	*Lissodus*	*minimus* (Agassiz, 1839)	idem			Unnamed	Hybodontiformes	Triassic	Upper	Carnian–Rhaetian
573	*Lissodus*	*minimus* (Agassiz, 1839)	idem			Unnamed	Hybodontiformes	Triassic	Upper	
574	*Lissodus*	*minimus* (Agassiz, 1839)	idem			Unnamed	Hybodontiformes	Triassic	Upper	Carnian–Rhaetian
575	*Lissodus*	*minimus* (Agassiz, 1839)	idem			Unnamed	Hybodontiformes	Triassic	Upper	Carnian–Rhaetian
576	*Lissodus*	*minimus* (Agassiz, 1839)	idem			Unnamed	Hybodontiformes	Triassic	Upper	Rhaetian
577	*Lissodus*	*minimus* (Agassiz, 1839)	idem			Unnamed	Hybodontiformes	Triassic	Upper	Carnian–Rhaetian
578	*Lissodus*	*minimus* (Agassiz, 1839)	idem			Unnamed	Hybodontiformes	Triassic	Upper	Carnian–Rhaetian
579	*Lissodus*	*minimus* (Agassiz, 1839)	idem			Unnamed	Hybodontiformes	Triassic	Upper	Carnian–Rhaetian
580	*Lissodus*	*minimus* (Agassiz, 1839)	idem			Unnamed	Hybodontiformes	Triassic	Upper	Carnian–Rhaetian
581	*Lissodus*	*minimus* (Agassiz, 1839)	idem			Unnamed	Hybodontiformes	Triassic	Upper	Carnian–Rhaetian
582	*Lissodus*	*minimus* (Agassiz, 1839)	idem			Unnamed	Hybodontiformes	Triassic	Upper	
583	*Lissodus*	*minimus* (Agassiz, 1839)	idem			Unnamed	Hybodontiformes	Triassic	Upper	Carnian–Rhaetian
584	*Lissodus*	*minimus* (Agassiz, 1839)	idem			Unnamed	Hybodontiformes	Triassic	Upper	Carnian–Rhaetian
585	*Lissodus*	*minimus* (Agassiz, 1839)	idem			Unnamed	Hybodontiformes	Triassic	Upper	
586	*Lissodus*	*minimus* (Agassiz, 1839)	idem			Unnamed	Hybodontiformes	Triassic	Upper	
587	*Lissodus*	*minimus* (Agassiz, 1839)	idem			Unnamed	Hybodontiformes	Triassic	Upper	Carnian–Rhaetian
588	*Lissodus*	*minimus* (Agassiz, 1839)	idem			Unnamed	Hybodontiformes	Triassic	Upper	Carnian–Rhaetian
589	*Lissodus*	*minimus* (Agassiz, 1839)	idem			Unnamed	Hybodontiformes	Triassic	Upper	Rhaetian
590	*Lissodus*	*minimus* (Agassiz, 1839)	idem			Unnamed	Hybodontiformes	Triassic	Upper	Carnian–Rhaetian
591	*Lissodus*	*minimus* (Agassiz, 1839)	idem		teeth	Unnamed	Hybodontiformes	Triassic	Upper	Rhaetian
592	*Lissodus*	*minimus* (Agassiz, 1839)	idem			Unnamed	Hybodontiformes	Triassic	Upper	Carnian, lower
593	*Lissodus*	*minimus* (Agassiz, 1839)	idem		teeth	Unnamed	Hybodontiformes	Triassic	Upper	Rhaetian
594	*Lissodus*	*minimus* (Agassiz, 1839)	idem		teeth	Unnamed	Hybodontiformes	Triassic	Upper	Rhaetian

	PT-W	Germany	clay quarry, near Schöningen, lower Saxony	Muschelkalk-Keuper boundary	near-shore / limnic
	PT-W	Germany	clay quarry, near Schöningen, lower Saxony	Muschelkalk-Keuper boundary	near-shore / limnic
	PT-W	Germany	clay quarry, near Schöningen, lower Saxony	Muschelkalk-Keuper boundary	near-shore / limnic
	PT-W	Germany	clay quarry, near Schöningen, lower Saxony	Muschelkalk-Keuper boundary	near-shore / limnic
	PT-W	Germany	clay quarry, near Schöningen, lower Saxony	Muschelkalk-Keuper boundary	near-shore / limnic
	PT-W	Germany	Neidenfels, near Crailsheim, S	base Hauptsandstein, lower Letterkeuper, lower Keuper	bone bed; estuary
	PL-C	Japan	Taho, Shirokawa-cho, Higashiuwa-gun, Ehime Prefecture, Shikoku	Taho Fm	grey limestone
	PT-W	France	Rehainvillers, Mont, Azerailles, and Chauffontaine, Lorraine	Muschelkalk and Lettenkohle	
Germanic Basin	PT-W	Germany	oberen Werntal, east of Arnstein, Main-Spessart, south of Würzburg	upper Muschelkalk	
	PT-W	Germany	Bedheim, S Thuringia	Lettenkohlensandstein, lower Keuper	
	PT-W	England	Aust Cliff, Avon	Westbury Fm, Penarth Grp	
	PT-W	Germany	Täbingen, Württemberg		sandstone
	PT-W	England?			
	PT-W	Germany	Täbingen, Württemberg		sandstone
	PT-W	Germany			
	PT-W	Germany			
	PT-W	Germany	Schwaben		
	PT-W	Germany	Jena		
	PT-W	France			
	PT-W	Germany	(Oberschlesien)		
	PT-W	Germany	Württemberg		
	PT-W	England			
	PT-W	France			
	PT-W	Germany	Würzburg		
	PT-W	Germany			
	PT-W	England			
	PT-W	England			
	PT-W	Germany	Gotha		
	PT-W	Germany	Württemberg		
	PT-W	France	Paris Basin		
	PT-W	Germany			
	PT-W	Germany			
	PT-W	Germany	Thüringen		
	PT-W	England/Germany			
	PT-W	England	Barnstone, Nottinghamshire		
	PT-N	Russia-W	Tatra Mountains		
	PT-W	England	Aust Cliff, Avon	bone bed basal to the Westbury Fm, Penarth Grp	
	PT-W	Germany	Steinbach near Schwäbisch Hall, SW	lower Lettenkeuper	brackish/deltaic
	PT-W	England	Chilcompton, Somerset		
	PT-W	England	Hapsford Bridge, Vallis Vale, near Frome, Somerset, SW	basal clay, Westbury Beds, Penarth Grp	intertidal and very shallow

freshwater/brackish?			Dorka 2001		
freshwater/brackish?			Dorka 2001		
freshwater/brackish?			Dorka 2001		
freshwater/brackish?			Dorka 2001		
freshwater/brackish?			Dorka 2001		
brackish	species well below 1 m in length?		Hagdorn & Reif 1988	Böttcher 2010	
marine			Goto 1994a	Goto 1994b, 1996b; Goto *et al.* 1996a; Chang & Miao 2004; Fischer 2008	(as *Polyacrodus* / *Hybodus*)
			Corroy 1928	Duffin 1985, 2001	(as *Polyacrodus*); reassigned all *Thectodus* spp.
marine			Scheinpflug 1984		(as *Acrodus*)
brackish?-freshwater			Werneburg 1994	Duffin 2001; Fischer 2008	
			Agassiz 1836	Duffin 1985, 2001; Storrs 1994; Rees & Underwood 2002; Cappetta 2012	(as *Acrodus*)
			Agassiz 1836	Duffin 1985, 2001	(as *Acrodus acutus*)
			Portlock 1843	Duffin 1985, 2001	(as *Acrodus*)
			Meyer & Plieninger 1844	Duffin 1985, 2001	(as *Acrodus* , *Thectodus inflatus* , *T. glaber* , *T. crenatus* , and *T. tricuspidatus*)
			Quenstedt 1852	Duffin 1985, 2001	(as *Acrodus*)
			Quenstedt 1858	Duffin 1985, 2001	(as *Acrodus*)
			Rolle 1858	Duffin 1985, 2001	(as *Acrodus*)
			Schmid 1861	Duffin 1985, 2001	(as *Acrodus* , and *A. acutus*)
			Martin 1863	Duffin 2001	(as *Acrodus*)
			Eck 1865	Duffin 1985, 2001	(as *Thectodus tricuspidatus*)
			Endlich 1870	Duffin 1985, 2001	(as *Thectodus inflatus* , *T. glaber* , *T. crenatus* , and *T. tricuspidatus*)
			Etheridge 1871	Duffin 1985, 2001	(as *Acrodus*)
			Henry 1875	Duffin 1985, 2001	(as *Thectodus tricuspidatus*)
			Winkler 1880	Duffin 1985, 2001	(as *Acrodus*)
			Quenstedt 1885	Duffin 1985, 2001	(as *Acrodus*)
			Woodward 1885	Duffin 1985, 2001	(as *Acrodus*)
			Woodward 1889a	Duffin 1985, 2001	(as *Acrodus*)
			Arnthor 1907	Duffin 2001	(as *Acrodus*)
			Engel 1908	Duffin 1985, 2001	(as *Acrodus*)
			Priem 1908	Duffin 1985, 2001	(as *Acrodus*)
			Schmidt 1928	Duffin 2001	(as *Acrodus* , and *A. acutus*)
			Oertle 1928	Duffin 2001	(as *Acrodus*)
			Dreyer 1962	Duffin 1985, 2001; Fischer 2008	(as *Acrodus* , and *A. lateralis*)
			Patterson 1966	Duffin 1985, 2001	(as *Polyacrodus*)
freshwater / marine			Sykes *et al.* 1970	Duffin 1985, 2001	(as *Acrodus*)
			Duffin & Gaździcki 1977	Duffin 1985, 2001	(as *Acrodus*)
freshwater / marine	euryhaline?		Duffin 1978	Duffin 1982a, 1985, 2001; Fischer 2008	(as *Acrodus*)
brackish			Reif 1980b		(as *Polyacrodus*)
marine			Duffin 1980b	Duffin 1985	(as *Acrodus*)
marine		? *Rhaetinolis* Zone	Duffin 1982b		(as *Polyacrodus* / *Hybodus*)

595	*Lissodus*	*minimus* (Agassiz, 1839)	idem		teeth	Unnamed	Hybodontiformes	Triassic	Upper	Rhaetian
596	*Lissodus*	*minimus* (Agassiz, 1839)	idem		teeth	Unnamed	Hybodontiformes	Triassic	Upper	
597	*Lissodus*	*minimus* (Agassiz, 1839)	idem		teeth	Unnamed	Hybodontiformes	Triassic	Upper	Norian
598	*Lissodus*	*minimus* (Agassiz, 1839)	idem		teeth	Unnamed	Hybodontiformes	Triassic	Upper	Rhaetian
599	*Lissodus*	*minimus* (Agassiz, 1839)	idem		teeth	Unnamed	Hybodontiformes	Triassic	Upper	Norian
600	*Lissodus*	*minimus* (Agassiz, 1839)	idem			Unnamed	Hybodontiformes	Triassic	Upper	Rhaetian
601	*Lissodus*	*minimus* (Agassiz, 1839)	idem		teeth	Unnamed	Hybodontiformes	Triassic	Upper	Rhaetian, lower
602	*Lissodus*	*minimus* (Agassiz, 1839)	idem		teeth	Unnamed	Hybodontiformes	Triassic	Upper	Rhaetian
603	*Lissodus*	*minimus* (Agassiz, 1839)	idem		teeth	Unnamed	Hybodontiformes	Triassic	Upper	Rhaetian
604	*Lissodus*	*minimus* (Agassiz, 1839)	idem		teeth	Unnamed	Hybodontiformes	Triassic	Upper	
605	*Lissodus*	*minimus* (Agassiz, 1839)	idem		teeth	Unnamed	Hybodontiformes	Triassic	Upper	Rhaetian
606	*Lissodus*	*minimus* (Agassiz, 1839)	idem		teeth	Unnamed	Hybodontiformes	Triassic	Upper	Rhaetian
607	*Lissodus*	*minimus* (Agassiz, 1839)	idem		teeth	Unnamed	Hybodontiformes	Triassic	Upper	Rhaetian
608	*Lissodus*	*minimus* (Agassiz, 1839)	idem		teeth	Unnamed	Hybodontiformes	Triassic	Upper	Rhaetian
609	*Lissodus*	*minimus* (Agassiz, 1839)	idem		teeth	Unnamed	Hybodontiformes	Triassic	Upper	Rhaetian
610	*Lissodus*	*minimus* (Agassiz, 1839)	idem		teeth	Unnamed	Hybodontiformes	Triassic	Upper	Rhaetian
611	*Lissodus*	*minimus* (Agassiz, 1839)	idem		teeth	Unnamed	Hybodontiformes	Triassic	Upper	
612	*Lissodus*	*duffini* Prasad, Singh, Parmar, Goswami & Sudan, 2008			teeth	Unnamed	Hybodontiformes	Triassic	Upper	Carnian–Norian
613	*Lissodus*	sp.			tooth	Unnamed	Hybodontiformes	Triassic	Upper	Norian
614	*Lissodus*	*lepagei* Duffin, 1993b			teeth	Unnamed	Hybodontiformes	Triassic	Upper	Norian, middle
615	*Lissodus*	*lepagei* Duffin, 1993b			teeth, denticles	Unnamed	Hybodontiformes	Triassic	Upper	Norian, uppermost
616	*Lissodus*	*lepagei* Duffin, 1993b			teeth	Unnamed	Hybodontiformes	Triassic	Upper	Rhaetian
617	*Lissodus*	*lepagei* Duffin, 1993b			teeth	Unnamed	Hybodontiformes	Triassic	Upper	Rhaetian, lower
618	*Lissodus*	sp.			teeth	Unnamed	Hybodontiformes	Triassic	Upper	Norian
619	*Lissodus*	sp.			teeth, spines	Unnamed	Hybodontiformes	Triassic	Upper	(Carnian–)Norian, upper
620	*Lissodus*	sp.				Unnamed	Hybodontiformes	Triassic	Upper	Norian, middle
621	*Lissodus*	sp.			tooth	Unnamed	Hybodontiformes	Triassic	Upper	
622	*Lissodus*	sp.				Unnamed	Hybodontiformes	Triassic	Upper	Carnian–Norian
623	*Lissodus*	sp.			tooth	Unnamed	Hybodontiformes	Triassic	Upper	Rhaetian
624	*Lissodus*	sp.				Unnamed	Hybodontiformes	Triassic	Upper	Norian
625	*Lissodus*	sp.				Unnamed	Hybodontiformes	Triassic	Upper	Rhaetian
626	*Lissodus*					Unnamed	Hybodontiformes	Triassic	Upper	Rhaetian
627	*Lissodus*				teeth	Unnamed	Hybodontiformes	Triassic	Upper	Rhaetian
628	*Lissodus*				teeth	Unnamed	Hybodontiformes	Triassic	Upper	Rhaetian

	PT-W	England	Holwell Quarry, near Frome, Somerset, SW	fissure infill	intertidal and very shallow
	PT-W	France	Lorraine		
	PT-W	France	Saint-Nicolas-de-Port, near Nancy, NE	"Keuper" marls	near-shore shallow marine environment
	PT-W	France	Grozon (quarry), near Poligny, Jura, NE	Marnes de Châlins Fm, Steinmergel Grp	foliated black marl
	PT-W	Luxembourg	Syren, Medernach	Keuper	dolomitic bone beds
	PT-W	Luxembourg	Junglinster and Remich		
	PT-W	Luxembourg	Commune Weyler-la-Tour, Syren	Keuper	
Central European Basin (Rhaetian Sea)	PT-W	Belgium	Habay-la-Vieille, Sagnette, and Unter der Kirchen	Grès de Mortinsart	
Central European Basin (Rhaetian Sea)	PT-W	Belgium	Attert		
	PT-W	France/Luxembourg			
	PT-W	England	SW	Westbury Fm, Penarth Grp	
	PT-W	France	Saint-Germain-les-Arlay, Jura		
	PT-W	France	Provenchères-sur-Meuse, Haute-Marne		
	PT-W	France	Lons-le-Saunier, Jura		
	PT-W	France	Belfort, Territoire de Belfort		
	PT-W	England		Penarth Grp	
	PT-W	England			
	NT-W	India	Tiki Village, Shahdol District, Madhya Pradesh	Tiki Fm, South Rewa Gondwana Basin	
	PT-W	Switzerland	Frick, N	Upper Variegated Marls, Keuper	
	PT-W	Luxembourg	Rinkebierg Hill, Medernach	Steinmergelgruppe, Keuper	dolomitic bone bed
	PT-W	France	Grozon (quarry), near Poligny, Jura, NE	Marnes de Châlins Fm, Steinmergel Grp	green, sandy marl
	PT-W	Luxembourg	Syren	just below Levallois Marls	bone bed
	PT-W	Luxembourg	Commune Weyler-la-Tour, Syren	Keuper	
	PT-W	France	Grande Séolane Klippe, Alpes de Haute Provence		
	PG-C	USA-S	Union County, New Mexico, (Texas, Arizona)	(lower Petrified Forest Mb), Sloan Canyon Fm, Dockum Grp	floodplain/lacustrine
	PG-C	USA-S	*Placerias* Quarry, Romero Spring, near St. Johns, Arizona	upper Owl Rock Mb, Chinle Fm	floodplain
	PL-E	USA-W	Little Poverty Peak, NW Nevada	Sonomia tectonic unit, Golconda Allochthon	
	PG-N	USA-E	North Carolina	Durham subbasin, Deep River Basin	
	PT-W	Poland	Opole area, Silesia		limestone
	PT-W	France	Saint-Nicolas-de-Port (Meurthe and Moselle)		
	PT-W	France	Boisset, Jura		
	PT-W	England		Blue Anchor Fm, Mercia Mudstone Grp	
Central European Basin (Rhaetian Sea)	PT-W	England	Aust Cliff	basal Westbury Fm	bone bed; shallow marine to nearshore environment / restricted lagoonal to estuarine setting
Central European Basin (Rhaetian Sea)	PT-W	England	Westbury-on-Severn	basal Westbury Fm	bone bed; shallow marine to nearshore environment / restricted lagoonal to estuarine setting

marine			Duffin 1985	Duffin 1989, 1993b; Gomez Pallerola 1992 (?); Fraser 1994; Fischer 2008	
			Delsate & Lepage 1991	Duffin 2001	
marine/brackish			Duffin 1993a	Delsate 1993; Sigogneau-Russel & Hahn 1994; Duffin 2001; Fischer 2008	
marine?-brackish			Cuny *et al.* 1998	Duffin 2001; Fischer 2008	
marine?-brackish			Duffin & Delsate 1993	Duffin 2001; Fischer 2008	
			Müller 1964	Delsate 1992, 1995; Duffin 2001	(as *Acrodus*)
			Godefroit *et al.* 1998	Delsate 1998	
marine with freshwater influence			Duffin *et al.* 1983	Delsate 1993	(as *Acrodus*)
marine			Duffin & Delsate 1993		
			Cuny 1993	Duffin 2001	
				Storrs 1994; Duffin 2001	
			Cuny *et al.* 1994	Cuny 1995a; Duffin 2001	
			Cuny 1995b	Cuny 1995a; Cuny et al. 1998; Duffin 2001	
				Cuny 1995a	
				Cuny 1995a	
			Duffin 1999	Duffin 2001	
			Dineley & Metcalf 1999	Duffin 2001	
freshwater			Prasad *et al.* 2008	Fischer 2008	
freshwater			Sander 1992	Sander 1990; Sander & Gee 1989a, b; Sander & Kindlimann 20?? (in prep.); Duffin 2001; Fischer 2008	
			Duffin 1993b	Delsate 1992, 1995; Duffin 1993a, 2001; Cuny 1995a; Cuny et al. 1998; Rees & Underwood 2002; Fischer 2008; Cappetta 2012	
brackish?-freshwater			Cuny *et al.* 1998	Duffin 2001; Fischer 2008	
			Duffin 1993b(?)	Duffin 2001	
			Godefroit *et al.* 1998	Delsate 1998	
			Maury *et al.* 1984	Duffin 2001; Fischer 2008	(as *Polacrodus*)
freshwater			Hunt & Lucas 1989; Huber *et al.* 1993	Hunt & Lucas 1993; Murry & Kirby 2002; Milner *et al.* 2006; Fischer 2008	(as *Lissodus* sp. nov.)
freshwater			Jacobs & Murry 1980	Tannenbaum 1983; Murry 1986; Duffin 2001; Milner *et al.* 2006	
			Sosson & Martin 1985	Duffin 2001	(as *Polacrodus*)
freshwater			Sues *et al.* 2001	Fischer 2008	
			Chrząstek & Niedźwiedski 2004		
				Cuny 1995a	
				Cuny 1995a	
			Warrington & Whittaker 1984	Storrs 1994	
brackish	bottom-dwelling, durophagous		Fischer *et al.* 2012		
brackish	bottom-dwelling, durophagous		Fischer *et al.* 2012		

629	*Lissodus*				teeth	Unnamed	Hybodontiformes	Triassic	Upper	Rhaetian
630	*Lissodus*				teeth	Unnamed	Hybodontiformes	Triassic	Upper	Rhaetian
631	*Lissodus*				teeth	Unnamed	Hybodontiformes	Triassic	Upper	Rhaetian
632	*Lissodus*				teeth	Unnamed	Hybodontiformes	Triassic	Upper	Rhaetian
633	*Lissodus*				teeth	Unnamed	Hybodontiformes	Triassic	Upper	Rhaetian
634	*Lissodus*				teeth	Unnamed	Hybodontiformes	Triassic	Upper	Rhaetian
635	*Lissodus*				teeth	Unnamed	Hybodontiformes	Triassic	Upper	Rhaetian
636	*Lissodus*				teeth	Unnamed	Hybodontiformes	Triassic	Upper	Rhaetian
637	*Lissodus*				teeth	Unnamed	Hybodontiformes	Triassic	Upper	Rhaetian
638	cf. *Lissodus*				fin spines	Unnamed	Hybodontiformes	Triassic	Upper	Norian, upper–Rhaetian
639	*Lissodus* / *Lonchidion*						Hybodontiformes	Triassic	Middle	Anisian–Ladinian
640	*Lonchidion*	*humblei* Murry, 1981			teeth, fin spine fragments, cepalic spine fragment	Lonchidiidae	Hybodontiformes	Triassic	Upper	Carnian, middle/upper
641	*Lonchidion*	*humblei* Murry, 1981			teeth, fin spine fragments, cepalic spine fragment	Lonchidiidae	Hybodontiformes	Triassic	Upper	Norian, lower
642	*Lonchidion*	*humblei* Murry, 1981			teeth / spines	Lonchidiidae	Hybodontiformes	Triassic	Upper	Carnian, upper middle
643	*Lonchidion*	*humblei* Murry, 1981				Lonchidiidae	Hybodontiformes	Triassic	Upper	Carnian, upper middle
644	*Lonchidion*	*humblei* Murry, 1981				Lonchidiidae	Hybodontiformes	Triassic	Upper	Carnian–Norian
645	*Lonchidion*	*humblei* Murry, 1981			teeth	Lonchidiidae	Hybodontiformes	Triassic	Upper	Carnian, upper middle
646	*Lonchidion*	*humblei* Murry, 1981			teeth	Lonchidiidae	Hybodontiformes	Triassic	Upper	Carnian, upper middle
647	*Lonchidion*	*humblei* Murry, 1981			teeth	Lonchidiidae	Hybodontiformes	Triassic	Upper	Norian, upper–Rhaetian
648	*Lonchidion*	sp.				Lonchidiidae	Hybodontiformes	Triassic	Middle	Ladinian?
649	*Lonchidion*	sp. cf. *selachos* Estes, 1964				Lonchidiidae	Hybodontiformes	Triassic	Upper	Carnian
650	*Lonchidion*	*estesi* Prasad, Singh, Parmar, Goswami & Sudan, 2008			teeth	Lonchidiidae	Hybodontiformes	Triassic	Upper	Carnian–Norian
651	*Lonchidion*	*incumbens* Prasad, Singh, Parmar, Goswami & Sudan, 2008			teeth	Lonchidiidae	Hybodontiformes	Triassic	Upper	Carnian–Norian
652	*Lonchidion*	*ferganensis* Fischer, Voigt, Schneider, Buchwitz & Voigt, 2011			teeth, denticles	Lonchidiidae	Hybodontiformes	Triassic	Middle–Upper	**Ladinian–Carnian**
653	*Diplolonchidion*	*murrayi* Heckert, 2004			teeth	Lonchidiidae	Hybodontiformes	Triassic	Upper	Carnian, upper middle

Central European Basin (Rhaetian Sea)	PT-W	England	Barnstone	basal Westbury Fm	bone bed; shallow marine to nearshore environment / restricted lagoonal to estuarine setting
Central European Basin (Rhaetian Sea)	PT-W	Germany	Moseberg	basal Exter Fm	bone bed; shallow marine nearshore to deltaic setting
Central European Basin (Rhaetian Sea)	PT-W	Germany	Kallenberg	basal Exter Fm	bone bed; shallow marine nearshore to deltaic setting
Central European Basin (Rhaetian Sea)	PT-W	Germany	Stuttgart-Degerloch	Exter Fm, uppermost contorta beds	bone bed; shallow marine nearshore to deltaic setting
Central European Basin (Rhaetian Sea)	PT-W	France	Saint-Nicolas-de-Port	basal Grés rhétiens	bone bed; shallow marine nearshore
Central European Basin (Rhaetian Sea)	PT-W	Switzerland	Frenkendorf, canton Baselland		bone bed; shallow marine nearshore environment
Central European Basin (Rhaetian Sea)	PT-W	Switzerland	Balmberg, canton Solothurn		sandstone
NW Tethys	PT-W	Switzerland	Piz Mitgel, canton Grison	Kössen Fm, Austroalpine nappes	tempestites; continental shelf, lagoonal to shallow marine environment with a strong detrital influx
NW Tethys	PT-W	Switzerland	Alplihorn, canton Grison	Kössen Fm, Austroalpine nappes	tempestites; continental shelf, lagoonal to shallow marine environment with a strong detrital influx
	PT-W	Poland	Poręba, Jura Krakowsko-Częstochowska region, SW	Zbąszynek Beds, Keuper	bone breccia, fluvial
	PT-W	France	S	Muschelkalk	
	PG-C	USA-S	near the headwaters of Home Creek, SE Crosby County, Texas	Tecovas Fm, Dockum Grp	shales(silt)/sandstones, floodplain/pond/lacustrine
	PG-C	USA-S	Petrified Forest National Park, Texas, Arizona, New Mexico	lower Petrified Forest Mb, Dockum Grp	floodplain
	PG-C	USA-S	*Placerias* / Downs' quarries, Romero Spring, near St. Johns, Apache County, and the "Dying Grounds" and "Crocodile Hill" localities, Petrified Forest National Park, Arizona	Mesa Redondo Mb and Blue Mesa Bed, Petrified Forest Mb, Chinle Fm	floodplain/pond/lacustrine
	PG-C	USA-S	North Stinking Springs Mountain, near St. Johns, Arizona	Blue Mesa Bed, Petrified Forest Mb, Chinle Fm	floodplain
	PG-C	USA-S	Otis Chalk Trilophosaurus quarry 1, Texas	Chinle Grp	floodplain
	PG-C	USA-S	Kalgary, Texas	Tecovas Fm, Chinle Grp	floodplain
	PG-C	USA-S	Ojo Huelos, New Mexico	Ojo Huelos Mb, San Pedro Arroyo Fm, Chinle Grp	carbonate, floodplain
	PG-C	USA-S	New Mexico	Sloan Canyon Fm	floodplain
	PT-W	Germany	Crailsheim	Muschelkalk	
	PG-N	USA-E	Richmond Basin, Virginia	Turkey Branch Fm	
	NT-W	India	Tiki Village, Shahdol District, Madhya Pradesh	Tiki Fm, South Rewa Gondwana Basin	
	NT-W	India	Tiki Village, Shahdol District, Madhya Pradesh	Tiki Fm, South Rewa Gondwana Basin	
	PT-N	Kyrgyzstan	Urochishche Madygen, west of Batken, county Batken, SW	Madygen Fm	shallow lacustrine mudstones, (sub)littoral
	PG-C	USA-S	Crosby County, Texas	lower Tecovas Fm, Chinle Grp	floodplain

brackish	bottom-dwelling, durophagous		Fischer *et al.* 2012		
brackish (deltaic)	bottom-dwelling, durophagous		Fischer *et al.* 2012		
brackish (deltaic)	bottom-dwelling, durophagous		Fischer *et al.* 2012		
brackish (deltaic)	bottom-dwelling, durophagous		Fischer *et al.* 2012		
brackish	bottom-dwelling, durophagous		Fischer *et al.* 2012		
brackish	bottom-dwelling, durophagous		Fischer *et al.* 2012		
brackish	bottom-dwelling, durophagous		Fischer *et al.* 2012		
marine	bottom-dwelling, durophagous		Fischer *et al.* 2012		
marine	bottom-dwelling, durophagous		Fischer *et al.* 2012		
freshwater			Sulej *et al.* 2012		correlative to Arnstadt and lowermost Exter formations
			Cappetta 1987		
freshwater (fluviatile/lacustrine)			Murry 1981, 1982, 1989	Duffin 1985, 2001; Cappetta 1987, 2012; Huber *et al.* 1993; Rees & Underwood 2002; Milner *et al.* 2006	
freshwater			Jacobs & Murry 1980	Tannenbaum 1983; Murry 1986; Hunt & Lucas 1993; Kaye & Padian 1994; Heckert 2004; Heckert *et al.* 2004; Jenkins & Heckert 2004, Heckert & Jenkins 2005; Irmis 2005; Milner *et al.* 2006; Heckert *et al.* 2007; Fischer 2008	
freshwater			Jacobs & Murry 1980; Murry 1989; Murry & Long 1989	Huber *et al.* 1993; Kaye & Padian 1994; Irmis 2005; Parker 2005; Heckert *et al.* 2007	see also Milner *et al.* 2006
freshwater			Polcyn *et al.* 2002	Irmis 2005; Parker 2005; Heckert *et al.* 2007	see also Milner *et al.* 2006
freshwater			Murry 1989	Heckert *et al.* 2007	tentative; see also Milner *et al.* 2006
freshwater	cutting-crushing		Heckert *et al.* 2007	Milner *et al.* 2006	
freshwater			Heckert *et al.* 2007	Milner *et al.* 2006	
freshwater			Heckert *et al.* 2007		
			Patterson 1966	Rees & Underwood 2002; Cappetta 2012	
freshwater			Johansson 1992	Rees & Underwood 2002	
freshwater			Prasad *et al.* 2008	Fischer 2008	
freshwater			Prasad *et al.* 2008	Fischer 2008	compares well with *Lissodus* sp. (subtype 107), Tway & Zidek 1983
freshwater	juvenile		Fischer *et al.* 2011	Fischer 2008	
freshwater			Heckert 2004	Milner *et al.* 2006; Cappetta 2012	

654	*Parvodus?*	sp.			tooth	Lonchidiidae	Hybodontiformes	Triassic	Middle	Anisian
655	*Gansuselache*	*tungshengi* Wang, Zhang, Zhu, Zhao, 2009			articulated body fossil	Lonchidiidae?	Hybodontiformes	Permian	Lopingian	
656	*Steinbachodus*	*estheriae* Reif, 1980b				Steinbachodontidae	Hybodontiformes	Triassic	Upper	Carnian, lower
657	*Steinbachodus*	*estheriae* Reif, 1980b			teeth	Steinbachodontidae	Hybodontiformes	Triassic	Middle	Ladinian, upper
658	*Steinbachodus*	*estheriae* Reif, 1980b			teeth	Steinbachodontidae	Hybodontiformes	Triassic	Middle	Ladinian, upper
659	*Reticulodus*	*synergus* Murry & Kirby, 2002				Distobatidae	Hybodontiformes	Triassic	Upper	Norian, lower
660	*Reticulodus*	*synergus* Murry & Kirby, 2002				Distobatidae	Hybodontiformes	Triassic	Upper	Norian, lower
661	*Reticulodus*	*synergus* Murry & Kirby, 2002			teeth	Distobatidae	Hybodontiformes	Triassic	Upper	Norian, lower
662	gen. indet.	sp. indet.			tooth	*incertae sedis*	Hybodontiformes	Permian	Cisuralian	Artinskian
663	gen. indet.	sp. indet.			spine	*incertae sedis*	Hybodontiformes	Permian	Cisuralian	Sakmarian
664	gen. indet.	sp. indet.			teeth	*incertae sedis*	Hybodontiformes	Permian	Guadalupian	Capitanian
665	gen. indet.	sp. indet.			spine fragment	*incertae sedis*	Hybodontiformes	Permian	Lopingian	Wuchiapingian?
666	gen. indet.	sp. indet.			spine	*incertae sedis*	Hybodontiformes	Permian	Lopingian	Wuchiapingian?
667	gen. indet.	sp. indet.			spine fragments	*incertae sedis*	Hybodontiformes	Permian	Cisuralian	Artinskian
668	gen. indet.	sp. indet.			spines	*incertae sedis*	Hybodontiformes	Permian	Cisuralian	Kungurian
669	gen. indet.	sp. indet.			spines	*incertae sedis*	Hybodontiformes	Permian	Cisuralian	Kungurian
670	gen. indet.	sp. indet.			spines	*incertae sedis*	Hybodontiformes	Permian	Cisuralian	Kungurian
671	gen. indet.	sp. indet.			fin and cephalic spines	*incertae sedis*	Hybodontiformes	Permian	Cisuralian	Artinskian
672	gen. indet.	sp. indet.			cephalic spines	*incertae sedis*	Hybodontiformes	Permian	Cisuralian	
673	gen. indet.	sp. indet.			teeth	*incertae sedis*	Hybodontiformes	Triassic	Middle	Ladinian, upper
674	gen. indet.	sp. indet.			teeth	*incertae sedis*	Hybodontiformes	Permian	Guadalupian	Roadian
675	*Homalodontus*	*apicopagus* (Mutter, De Blanger, Neuman, 2007)			body, teeth, denticles	Homalodontidae	Hybodontiformes?	Triassic	Lower	Olenekian (lower Smithian)
676	*Homalodontus*	cf. *apicopagus* (Mutter, De Blanger and Neuman, 2007)			tooth	Homalodontidae	*incertae sedis* (Hybodontiformes?)	Triassic	Lower	Induan (Griesbachian, upper)
677	*Homalodontus*	*homalorhizo* (Mutter, De Blanger, Neuman, 2007)			body, teeth, fin spines	Homalodontidae	Hybodontiformes?	Triassic	Lower	Olenekian (Spathian)
678	*Homalodontus*	sp.			partial body fossils, teeth	Homalodontidae	Hybodontiformes?	Triassic	Lower	Olenekian (lower Smithian?–Spathian?)
679	'Palaeozoic Genus 1'	*zidei* (Johnson, 1981)			teeth	*incertae sedis*	Hybodontiformes	Permian	Cisuralian	Artinskian
680	'Palaeozoic Genus 1'	*zidei* (Johnson, 1981)			teeth	*incertae sedis*	Hybodontiformes	Permian	Cisuralian	

	PT-E	China-SE	Yongning, Guanling County, Guizhou Province, SW	Yang Liu Jing Fm	thickbedded grey dolomites and dolomite breccia with gypsum crystals (hypersaline)
	PT-E	China-N	Mazongshan Mountain, Gansu Province, NW	Fangshankou Fm	
	PT-W	Germany	Steinbach near Schwäbisch Hall, SW (and other localities)	lower Lettenkeuper	brackish/deltaic
	PT-W	Germany	clay quarry, near Schöningen, lower Saxony	Muschelkalk-Keuper boundary	near-shore / limnic
	PT-W	Germany	Neidenfels, near Crailsheim, S	base Hauptsandstein, lower Letterkeuper, lower Keuper	bone bed; estuary
	PG-C	USA-S	Texas	Bull Canyon Fm, Dockum Grp	
	PG-C	USA-S	Petrified Forest National Park, Arizona	Sonsela and Petrified Forest Mbs, Chinle Fm	floodplain
	PG-C	USA-S	Goforth locality, head of Landmark Wash, Ward's Terrace, Coconino County, Arizona	upper Owl Rock Fm, Chinle Grp	fluvial/lacustrine / floodplain
	PT-N	Russia-W	Middle and South Urals		marls and nodular, detrital, and reef limestones
	PT-N	Russia-W	South Urals		detrital limestones
	PG-C	USA-S	Guadelupe Mountains, western Texas	Rader Limestone Mb, Bell Canyon Fm	
Paraná Basin	PG-S	Brazil	Posto Queimado, Timbaúva region, São Gabriel municipality, Rio Grande do Sul State, S	Rio do Rasto Fm	conglomerates intercalated in red mudstones; lacustrine and channel deposits
Paraná Basin	PG-S	Brazil	Posto Queimado, Timbaúva region, São Gabriel municipality, Rio Grande do Sul State, S	Morro Pelado Mb, Rio do Rasto Fm	conglomerates intercalated in red mudstones; lacustrine and channel deposits
	PG-C	USA-S	Rattlesnake Canyon, near Lake Kickapoo, Archer County, Texas	upper Admiral Fm, Wichita-Albany Grp	
	PG-C	USA-C	East Manitou site, Tillman County, SW Oklahoma	upper Garber Fm	
	PG-C	USA-C	East Manitou site, Tillman County, SW Oklahoma	upper Garber Fm	
	PG-C	USA-C	Northeast Frederick and Lake Frederick sites, near Deep Red Creek, Tillman County, SW Oklahoma	upper Garber (Sandstone) Fm, upper Sumner Grp	sandstones, mudstone conglomerates, claystones; fluvial and lacustrine environments in a coastal-plain setting
	PG-C	USA-S	Texas	Wichita-Albany Grp	
	PG-C	USA-S	Tit Butte and Lake Kemp localities, Texas		
	PT-W	Germany	clay quarry, near Schöningen, lower Saxony	Muschelkalk-Keuper boundary	
	PG-C	USA-S	Quarry section, Guadelupe Mountains, western Texas	William Ranch Mb, Cutoff Fm	fossiliferous debris flows interbedded with radiolarian-bearing limestone
	PL-E	Canada-W	Ganoid Ridge, Wapiti Lake, British Columbia	Vega-Phroso Siltstone Mb, Sulphur Mountain Fm	siltstone, deltaic/shallow continental shelf environment
Sverdrup Basin	BOR	Canada-N	Otto Fiord South, Ellesmere Island, Canadian Arctic Archipelago	Confederation Point Mb, Blind Fiord Fm	shales and siltstone; deep shelf environment
	PL-E	Canada-W	Ganoid Ridge, Wapiti Lake, British Columbia	Vega-Phroso Siltstone Mb, Sulphur Mountain Fm	siltstone, deltaic/shallow continental shelf environment
	PL-E	Canada-W	Ganoid Ridge, Wapiti Lake, British Columbia	Vega-Phroso Siltstone Mb, Sulphur Mountain Fm	siltstone, deltaic/shallow continental shelf environment
	PG-C	USA-S	Baylor, Wichita and Archer Counties, north central Texas	Wichita-Albany Grp (upper Admiral Fm, upper Belle Plains Fm, Clyde Fm, low-mid Lueders Fm)	
	PG-C	USA-C	Oklahoma, Nebraska, Texas?	upper Admiral–middle Lueders Fms, Wichita-Albany Grp	

marine		*Microcella kockeli* conodont Zone	Chen *et al.* 2007a		
	490 mm in length		Wang *et al.* 2009	Ginter *et al.* 2010	
brackish	80–100 cm in length		Reif 1980b	Duffin 1981; Cappetta 1987, 2012; Rees & Underwood 2002; Böttcher 2010	
freshwater/brackish?			Dorka 2001		
brackish			Hagdorn & Reif 1988	Böttcher 2010	
freshwater			Murry & Kirby 2002	Irmis 2005; Milner *et al.* 2006	
freshwater			Murry 1989; Kirby 1993	Irmis 2005; Parker 2005; Milner et al. 2006	(as *Acrodus* sp.)
freshwater			Murry 1989; Kirby 1989, 1993	Huber *et al.* 1993; Irmis 2005; Parker 2005; Milner et al. 2006; Cappetta 2012	(as new hybodont / *Acrodus* sp.)
marine		*Par. solidissima* fusulinid zone	Ivanov 2005	(resembles *Tristychius*)	
marine		*Ps. moelleri* – *Ps. uralica* fusulinid zones	Ivanov 2005		
marine			Ivanov *et al.* 2011		
freshwater			Richter & Langer 1998	Malabarba *et al.* 2003	
freshwater			Malabarba *et al.* 2003		
marine?/freshwater?			Simpson 1974	Johnson 1981	(as *Hybodus*; reassigned by Zidek *et al.* 2004)
freshwater			Simpson 1974, 1976, 1979; Zidek 1976	May & Hall 2002	(as *Hybodus*; reassigned by Zidek *et al.* 2004)
freshwater			Johnson 1979	Zidek et al. 2004	
freshwater			Zidek *et al.* 2004		
			Johnson 1981	Simpson 1974 (as *Hybodus*)	
			Berman 1970	Johnson 1981	(as cladodont teeth)
			Dorka 2001		
marine			Ivanov *et al.* 2012		Hybodontoidea
marine	1.2–1.5 m in length		Mutter *et al.* 2007a	Mutter *et al.* 2008a; Cappetta 2012	(as *Ivalpitiodus*)
marine		*Eukkenites strigatus* ammonoid Zone; *Neogondolella carinata*, *Ng. planata*, *Ng. nevadensis*	this study		Sample 93 OF TE-5 1663 62-TE 325A
marine		*Necosphathodus homeri*	Mutter *et al.* 2007a	Mutter *et al.* 2008a; Cappetta 2012	(as *Ivalpitiodus*)
marine			Mutter *et al.* 2007a	Mutter *et al.* 2008a	(as *Ivalpitiodus*)
marine?/freshwater?			Johnson 1981	Duffin 1985; Duffin 2001; Rees & Underwood 2002; Ginter et al. 2010	(as *Polyacrodus* / '*Lissodus*')
marine?-brackish			Duffin 2001	Fischer 2008	(as '*Lissodus*')

681	'Palaeozoic Genus 1'	*zideki* (Johnson, 1981)			tooth	*incertae sedis*	Hybodontiformes	Permian	Cisuralian	
682	'Palaeozoic Genus 1'	*zideki* (Johnson, 1981)			teeth	*incertae sedis*	Hybodontiformes	Permian	Cisuralian	Kungurian
683	'Palaeozoic Genus 1'	sp. cf. *zideki* (Johnson, 1981)			teeth	*incertae sedis*	Hybodontiformes	Permian	Cisuralian	Asselian
684	cf. 'Palaeozoic Genus 1'	sp.			tooth	*incertae sedis*	Hybodontiformes	Permian	Guadalupian	Wordian
685	'Palaeozoic Genus 1'	sp.			teeth, denticles, fin spine	*incertae sedis*	Hybodontiformes	Permian	Cisuralian	Asselian?
686	cf. *'Lissodus'*	sp.				*incertae sedis*	Hybodontiformes	Permian	Cisuralian	
687	*'Lissodus'*	sp.			teeth	*incertae sedis*	Hybodontiformes	Permian/ Carboniferous?	Cisuralian?	
688	*'Lissodus'*	*lacustris* Gebhardt, 1988			tooth	*incertae sedis*	Hybodontiformes	Permian?	Cisuralian	
689	*'Lissodus'*	*sardiniensis* Fischer *et al.*, 2010			teeth, denticles, fin spines	*incertae sedis*	Hybodontiformes	Permian	Cisuralian	Asselian
690	*'Lissodus'*	sp.			denticles	*incertae sedis*	Hybodontiformes	Permian	Cisuralian	
691	*'Lissodus'*	sp. cf. *lacustris* Gebhardt, 1988			tooth	*incertae sedis*	Hybodontiformes	Permian	Cisuralian	Asselian
692	cf. *'Lissodus'*	sp.			teeth, cephalic spine, fin spines	*incertae sedis*	Hybodontiformes	Permian	Cisuralian	Asselian
693	*'Lissodus'*	sp.			teeth	*incertae sedis*	Hybodontiformes	Permian	Cisuralian	Asselian
694	*'Lissodus'*-like	sp.			fin spine	*incertae sedis*	Hybodontiformes	Permian	Cisuralian	Asselian
695	*'Lissodus'*	sp.			teeth?	*incertae sedis*	Hybodontiformes	Permian	Cisuralian	Artinskian
696	*'Lissodus'*	sp.			tooth	*incertae sedis*	Hybodontiformes	Permian	Cisuralian	Artinskian
697	*'Lissodus'*	sp.			tooth	*incertae sedis*	Hybodontiformes	Permian	Guadalupian	Roadian
698	*'Lissodus'*	sp.			teeth	*incertae sedis*	Hybodontiformes	Permian	Guadalupian	Wordian–Capitanian
699	*'Lissodus'*	sp.			teeth	*incertae sedis*	Hybodontiformes	Permian	Guadalupian	
700	*'Lissodus'*	*bigibbus* Minikh and Minikh, 1996			teeth	*incertae sedis*	Hybodontiformes	Permian	Lopingian (+ Guadalupian ?)	Wuchiapingian (Capitanian–Changhsingian)
701	*'Lissodus'*	*bigibbus* Minikh and Minikh, 1996			tooth	*incertae sedis*	Hybodontiformes	Permian	Guadalupian –Lopingian	Wordian
702	*'Lissodus'*	*wushuiensis* Wang, Zhu, Jin & Wang, 2007			tooth, denticle	*incertae sedis*	Hybodontiformes	Permian	Lopingian	Changhsingian
703	*'Lissodus'*	*wushuiensis* Wang, Zhu, Jin & Wang, 2007			denticle	*incertae sedis*	Hybodontiformes	Permian	Lopingian	Changhsingian

	PG-C	USA-C	East Manitou site, Tillman County, SW Oklahoma		
	PG-C	USA-C	Lake Frederick site, near Deep Red Creek, Tillman County, SW Oklahoma	upper Garber (Sandstone) Fm, upper Sumner Grp	sandstones, mudstone conglomerates, claystones; fluvial and lacustrine environments in a coastal-plain setting
	PT-W	Germany	Saar-Nahe Basin, SW	Remigiusberg Fm	
Madagascar Embayment	NT-W	Oman	Haushi Cliff, Haushi-Huqf region, E	Khuff Fm	rim basin
	PT-W	Germany	Niedermoschel, Saar-Nahe Basin, SW	Niedermoschel Bank, Jeckenbach Subfm, Meisenheim Fm, Lauterecken–Odernheim Fm (lower Rotliegend)	fluvial-lacustrine
	PG-C	USA-C	Pottawatomie County, Kansas (Everhart, pers. comm.)	Neva Limestone Mb., Genola Limestone Fm, Council Grove Grp	Poorly consolidated limey mud
	PT-W	Austria	eastern Tirol	Laas beds of the western Drauzug	carbonate nodules
	PT-W	Germany	Löbejün, NE Saale Basin	Kieselschiefer-Quarzit-Konglomerat, base of the Halle Fm	
	PT-W	Italy	Guardia Pisano Basin, Sulcis area, SW Sardinia	Top of lithofacies B	80-90mm thick brownish-grey lacustrine micritic limestone (parautochthonous)
	PT-W	Germany	Odenbach, Saar-Nahe Basin	Odenbach-Bank, Lauterecken Fm	
	PT-W	Germany	Grüneberg Borehole 3/76, Grüneberg, E Brandenburg, Brandenburg Basin, N German Basin	Grüneberg Fm	
Rotliegend, Autun Basin (Bourbon-l'Archambault Basin)	PT-W	France	Buxières-les-Mines, Allier, Massif Central	Buxières Fm	lacustrine siltstone
	PT-W	France	Hilaire		
	PT-W	France	Usclas du Bosc	Usclas St. Private Fm	
	PT-N	Russia-W	pre-Urals foredeep and the Urals, European Russia		
	NT-W	Oman	WAFRA-6 oil well, Al Wusta region	Gharif Fm	nearshore to intertidal coastal plain
	BOR	Russia-NW	near Timan region, European Russia		
	BOR	Russia-NW	Vym' River, Komi Republic		
	PL-C	Japan	Kinshozan, Akasaka-cho, Ohgaki City, Gifu Prefecture, central Honshu	middle Akasaka Limestone	bedded, black, coaly limestone, beneath *Colania gifuensis* concentrated bed
	PT-N	Russia-W	pre-Urals foredeep, Tatarstan, near Kazan, Moscow district, Vologda, East European Platform, European Russia		
	PT-N	Russia-W	Isheyevo, Tatarstan		sandy lens
	PT-E	China-SE	Dongling, Xiushui County, Jiangxi Province	upper Mb, Changxing Fm	
	PT-E	China-SE	Tieshikou, Xinfeng County, Jiangxi Province	upper Mb, Changxing Fm	

			Simpson 1979	Johnson 1981	
freshwater			Zidek *et al.* 2004	Fischer 2008	(as '*Lissodus*', '*Polyacrodus*')
freshwater			Boy & Schindler 2000	Fischer 2008	(as '*Lissodus*')
marine(-brackish)		*Hindeodella aserrata* conodont Zone; OSPZ6 palynology Zone; *Neoschwagerina craticulifera* fusulinid Zone	this study	Tintori 1998; Angiolini *et al.* 2003a; Schultze *et al.* 2008; Fischer 2008	(as '*Lissodus*') Sample AO47bis
freshwater	durophagous, benthic detritus feeder		Hampe 1996	Duffin 2001; Rees & Underwood 2002; Krätschmer & Forst 2005; Heidtke 2007; Fischer 2008; Ginter et al. 2010	(as '*Lissodus*' sp. NM)
			Ewell & Everhart 2005		
freshwater			Schneider, in prep.	Blieck *et al.* 1995, 1997; Fischer 2008	
freshwater			Fischer 2005	Fischer 2008	may be reworked from the Carboniferous
freshwater (lacustrine)	durophagous, bottom-dwelling		Fischer *et al.* 2010	Freytet *et al.* 2002; Fischer 2005; Werneburg *et al.* 2007; Ronchi *et al.* 2008; Fischer 2008	
freshwater			Schindler & Poschmann 2001	Fischer 2008	
freshwater			Gaitsch 1995	Fischer 2008	
freshwater			Steyer *et al.* 2000	Kaulfuß 2004; Schultze & Soler-Gijón 2004; Fischer 2008	
freshwater			Fischer 2005	Fischer 2008	
freshwater			Fischer 2005	Fischer 2008	
marine			Ivanov 2000	Ivanov 2005; Fischer 2008	
marine/freshwater			Schultze *et al.* 2008	Fischer 2008	
marine			Ivanov 2000	Ivanov 2005; Fischer 2008	
			Malysheva *et al.* 2000	Ivanov 2005	
marine		*Colania amicula – C. gifuensis* zone	Yamagishi 2006; Yamagishi & Fujimoto 2011		(as Euselachii indet.)
marine			Minikh & Minikh 1996	Ivanov 2000, 2005; Fischer 2008	(resembles more *Lophodus*, Ivanov 2000)
			Minikh & Minikh 1998		
			Wang *et al.* 2007a	Wang *et al.* 2007b	
			Wang *et al.* 2007a	Wang *et al.* 2007b	

704	*Omanoselache*	*contrarius* Johns, Barnes & Orchard, 1997			teeth	*incertae sedis*	Hybodontiformes	Triassic	Middle–Upper	Ladinian, Carnian
705	*Omanoselache*	*contrarius* Johns, Barnes & Orchard, 1997			teeth	*incertae sedis*	Hybodontiformes	Triassic	Middle–Upper	**Ladinian, upper–Carnian, lowermost**
706	*Omanoselache*	*contrarius* Johns, Barnes & Orchard, 1997			tooth	*incertae sedis*	Hybodontiformes	Triassic	Middle	Anisian, uppermost
707	*Omanoselache*	*bucheri* Cuny, Rieppel & Sander, 2001			teeth	*incertae sedis*	Hybodontiformes	Triassic	Middle	Anisian, lower middle
708	*Omanoselache*	*bucheri* Cuny, Rieppel & Sander, 2001			teeth	*incertae sedis*	Hybodontiformes	Triassic	Middle	Anisian, lower middle
709	*Omanoselache*	*hendersoni* Koot, Cuny, Tintori and Twitchett, 2013			teeth	*incertae sedis*	Hybodontiformes	Permian	Guadalupian	Wordian
710	*Omanoselache*	*angiolinii* Koot, Cuny, Tintori and Twitchett, 2013			teeth	*incertae sedis*	Hybodontiformes	Permian	Guadalupian	Wordian
711	*Omanoselache*	*angiolinii* Koot, Cuny, Tintori and Twitchett, 2013			teeth	*incertae sedis*	Hybodontiformes	Permian	Guadalupian	Wordian
712	*Omanoselache*	sp. H			teeth	*incertae sedis*	Hybodontiformes	Triassic	Lower	Olenekian (Spathian)
713	*Omanoselache*	sp. H			teeth	*incertae sedis*	Hybodontiformes	Triassic	Lower	Olenekian (Spathian)
714	*Omanoselache*	sp. H			teeth	*incertae sedis*	Hybodontiformes	Triassic	Lower	Induan (Griesbachian)
715	*Omanoselache*	sp. H			tooth	*incertae sedis*	Hybodontiformes	Triassic	Lower	Olenekian (Spathian)
716	*Omanoselache*	sp. H			tooth	*incertae sedis*	Hybodontiformes	Triassic	Lower	Olenekian (Spathian)

	PL-E	Canada-W	Aylard Creek East, Beattie Hill, Beattie Ledge, Brown Hill, Childerhose Cove, and Toad River, Peace River area, northeastern BC	Liard and Baldonnel fms	
	PT-E	China-SE	Zhuganpo Village, Guanling County, Guizhou Province, SW	Zhuganpo Fm	grey micritic limestone + dolomitic limestone / bioclastic limestone --> shallow to deep (below storm wave-base) water platform
	PT-E	China-SE	Yongning, Guanling County, Guizhou Province, SW	Yang Liu Jing Fm	thickbedded grey dolomites and dolomite breccia with gypsum crystals (hypersaline)
	PL-E	USA-W	west slope Augusta Mountains, Pershing County, Nevada	lower Fossil Hill Mb, Favret Fm, Star Peak Grp	litharenite, debris flow deposit, high energy, coastal influence, outer platform
	PL-E	USA-W	west slope Augusta Mountains, Pershing County, Nevada	lower Fossil Hill Mb, Favret Fm, Star Peak Grp	litharenite, debris flow deposit, high energy, coastal influence, outer platform
Madagascar Embayment	NT-W	Oman	Haushi Cliff and Saiwan, Haushi-Huqf region, E	Khuff Fm	rim basin
Madagascar Embayment	NT-W	Oman	Haushi Cliff and Saiwan, Haushi-Huqf region, E	Khuff Fm	rim basin
Hawasina Basin	NT-W	Oman	Saiq Plateau, Jabal al Akhdar, Oman Mountains, N	Saiq Fm	rim basin
Hawasina Basin	NT-W	Oman	Jabel Safra, Oman Mountains, N	Hallstatt-type limestone olistoliths	basinal seamount
Hawasina Basin	NT-W	Oman	Wadi Alwa, Ba'id, Oman Mountains, N	Alwa Fm	basinal seamount
Hawasina Basin	NT-W	Oman	Wadi Wasit, Ba'id, Oman Mountains	Al Jil Fm	platform margin
	NT-E	Timor	River Bihati region, near Bouwn	exotic	pelagic Hallstatt-type limestone
	NT-E	Timor	River Bihati region, near Bouwn	exotic	pelagic Hallstatt-type limestone

marine		unzoned to *Metapolygnathus nodosus* conodont zones; ? *Macleamoceras macleami* to *Tropites welleri* ammonoid zones	Johns *et al.* 1997	Mutter *et al.* 2007a	(as *'Polyacrodus'*, Homalodontidae?)
marine		*Neogondolella kockeli – Metapolygnathus polygnathiformis* conodont zones	Chen *et al.* 2007a		(as *'Polyacrodus'*, Homalodontidae?)
marine		*Neogondolella kockeli* conodont Zone	Chen *et al.* 2007a		(as *'Polyacrodus'*, Homalodontidae?)
marine	durophagous, crushing	*M. taggarti* Subzone of the *Hyatti* Zone	Rieppel *et al.* 1996	Cuny *et al.* 2001	(as *'Polyacrodus'*, Homalodontidae?)
marine	durophagous, crushing	*M. taggarti* Subzone of the *Hyatti* Zone	Cuny *et al.* 2001	Mutter *et al.* 2007a	(as *'Polyacrodus'*, Homalodontidae?)
marine		*Jinogondolella aserrata* conodont Zone; OSPZ6 palynology Zone; *Neoschwagerina craticulifera* fusulinid Zone	this study	Tintori 1998; Angiolini *et al.* 2003a	(as *'Polyacrodus'*) Samples AO40, AO55, AO47bis; and 965-2, 965-8
marine		*Jinogondolella aserrata* conodont Zone; OSPZ6 palynology Zone; *Neoschwagerina craticulifera* fusulinid Zone	this study		Samples AO40, AO55, AO47bis, AO50; and 965-2
marine			this study		Samples 969-5, 969-6; and 110219-E, 110219-M
marine		*Icriospathodus collinsoni – 'Neospathodus' triangularis* conodont zones; *Columbites parisianus – Prohungarites/Subcolumbites* ammonoid zones	this study		Samples 103A, 103C, 104A
marine		*Triassospathodus homeri – 'Neospathodus' triangularis* conodont zones; *Procolumbites – Prohungarites/Subcolumbites* ammonoid zones	this study		Samples C85314, 118B
marine		*Clarkina carinata* conodont Zone (*Hindeodus sosioensis*)	Yamagishi 2006	this study	(as *Lissodus* sp.1)
marine		*Columbites parisianus* ammonoid Zone (Owenites, Albanites)	Yamagishi 2006	this study	(as *Synechodus* sp.1; in part)
marine		*Columbites parisianus* ammonoid Zone (Albanites)	Yamagishi 2006	this study	(as *Polyacrodus* sp.2)

717	*Dimanocselache*	sp. H		tooth	*incertae sedis*	Hybodontiformes	Triassic	Middle	Anisian, lower–middle
718	*Dimanocselache*	cf. sp. H		teeth	*incertae sedis*	Hybodontiformes	Triassic	Lower	Induan (Griesbachian?–Dienerian)
719	*Dimanocselache*	cf. sp. H		teeth	*incertae sedis*	Hybodontiformes	Triassic	Lower–Middle	Olenekian (Spathian)–Anisian
720	*Dimanocselache*	cf. sp. H		teeth	*incertae sedis*	Hybodontiformes	Triassic	Lower	Olenekian (Spathian, lower)
721	*Dimanocselache*	cf. sp. H		tooth	*incertae sedis*	Hybodontiformes	Triassic	Lower	Olenekian (Spathian)
722	*Dimanocselache*	sp. A		tooth	*incertae sedis*	Hybodontiformes	Triassic	Lower	Induan (Griesbachian, basal)
723	*Dimanocselache*	sp. A		teeth	*incertae sedis*	Hybodontiformes	Triassic	Middle	Anisian
724	*Dimanocselache*	sp. A		teeth	*incertae sedis*	Hybodontiformes	Triassic	Lower	**Induan (Dienerian)–Olenekian (Smithian, lower)**
725	*Dimanocselache*	cf. sp. A		teeth	*incertae sedis*	Hybodontiformes	Triassic	Lower–Middle	Olenekian (Spathian)–Anisian
726	cf. *Dimanocselache*	sp.		teeth	*incertae sedis*	Hybodontiformes	Permian	Guadalupian	Wordian
727	cf. *Dimanocselache*	sp.		teeth	*incertae sedis*	Hybodontiformes	Permian	Guadalupian	Wordian
728	cf. *Dimanocselache*	sp.		teeth	*incertae sedis*	Hybodontiformes	Triassic	Lower	Olenekian (Spathian)

	PL-W	Malaysia	Bukit Kalong, Kedah		limestone
	PL-C	Japan	Kamura, Takachiho-chō, Nishiusuki-gun, Miyazaki-ken (Prefecture), Kyūshū	Kamura Fm	mid-oceanic seamount
	PT-E	China-SE	Guandao, Guizhou Province, S	Luolou and Xinyuan fms	carbonate platform slope
	PL-E	USA-W	Darwin Canyon, Inyo Mountains, California	Union Wash Fm	micritic limestones and calcareous shales; basinal outer shelf to slope environment, below storm wave base
	PL-E	USA-W	south of Bloody Canyon, Humboldt Range, Pershing County, N Nevada	lower member of Prida Fm, Star Peak Grp	micritic limestones; below wave base?
	NT-W	India	Spiti	Tamba Kurkur Fm	nodular limestone
	PT-E	China-SE	Guandao, Guizhou Province, S	Xinyuan Fm	carbonate platform slope
	PL-W	Russia-SE	Abrek Bay area, Vladivostok, South Primorye	Zhitkov Fm	ammonoid turbidites
	PT-E	China-SE	Guandao, Guizhou Province, S	Luolou and Xinyuan fms	carbonate platform slope
Madagascar Embayment	NT-W	Oman	Haushi Cliff, Haushi-Huqf region, E	Khuff Fm	rim basin
Hawasina Basin	NT-W	Oman	Saiq Plateau, Jabal al Akhdar, Oman Mountains, N	Saiq Fm	rim basin
	PL-E	USA-W	Hammond Creek, near Bear Lake, Bear Lake County, SE Idaho	Thaynes Fm	mudstone and silty limestone; shallow subtidal and intertidal environment (inner shelf facies)

marine		*Neogondolella bulgarica* , *Gladigondolella tethydis*	Yamagishi 2006	this study	(as *Polyacrodus* sp.2; tentative)
marine		*Hindeodus parvus* , *Isarcicella isarcica* , *Neogondolella carinata* – *Necospathodus dieneri*	this study		Samples 290311-R, 05.7.14.ak
marine		*Triassospathodus homeri* , *Gladigondolella carinata* –?	this study		Samples O-10, O-27, GQC-173, GQC-182
marine			this study		Sample 92-OF DC10
marine		*Necospathodus homeri* ; *Yatesi* Beds, upper *Haugi* ammonoid Zone	this study		Sample 89 OF HB236
marine		*Otoceras* Beds	this study		Sample 95-OF GU-1
marine		*Chiosella gondolelloides* , *Ch. timorensis* , *Gladigondolella carinata* , *Necospathodus spathi* , *Triassospathodus homeri*	this study		Samples O-15, GQC183B
marine		*Paranorites varians* Zone– *Radiognicnites abrekensis* "bed" (*Hedenstroemia bosphorensis* – *Anasibirites nevolini* Zone)	Yamagishi 2006	Yamagishi 2009; this study	(as *Polyacrodus* sp.1sp. 3)
marine		*Necospathodus spathi* , *Triassospathodus homeri* , *Chiosella gondolelloides* , *Ch. timorensis* , *Gladigondolella carinata*	this study		Samples O-13, O-16, O-18, O-21, O-40
marine		*Hindeogondolella aserrata* conodont Zone; OSPZ6 palynology Zone; *Neoschwagerina craticulifera* fusulinid Zone	this study		Samples AO40, AO55, AO47bis
marine			this study		Sample 110219-M
marine		*Procolumbites* Beds	this study		Sample o-64671 91-OF

729	*Reesodus*	*underwoodi* Koot, Cuny, Tintori and Twitchett, 2013			teeth	*incertae sedis*	Hybodontiformes	Permian	Guadalupian	Wordian
730	*Teresodus*	*amplexus* Koot, Cuny, Tintori and Twitchett, 2013			teeth	*incertae sedis*	Hybodontiformes	Permian	Guadalupian	Wordian
731	gen. indet.	sp. indet.			tooth	*incertae sedis*	Hybodontiformes	Triassic	Middle	Anisian
732	*Gunnellodus*	*bellistriatus* (Gunnell, 1933)	*cameratus* (Gunnell, 1933); sp. (Gunnell, 1933); *trispinosus* (Gunnell, 1933)		teeth?		Hybodontiformes?	Permian	Guadalupian	Wordian
733	new genus?	*keuperinus* Seilacher, 1948			teeth		Hybodontiformes?	Triassic	Upper	
734	*Sphenacanthus*	*sangaulensis* Chahud, Fairchild & Petri, 2010			fin spine	Sphenacanthidae		Permian	Cisuralian	Artinskian
735	*Sphenacanthus*	*carbonarius* (Giebel, 1848)			teeth	Sphenacanthidae		Permian	Cisuralian	**Asselian–Sakmarian**
736	*Wodnika*	*striatula* Münster, 1843			anterior body, fin spine, dentition	Sphenacanthidae		Permian	Guadalupian	Roadian
737	*Wodnika*	*striatula* Münster, 1843			dentition, fin spine	Sphenacanthidae		Permian	Guadalupian	
738	*Wodnika*	*striatula* Münster, 1843				Sphenacanthidae		Permian	Guadalupian	Roadian
739	*Wodnika*	*striatula* Münster, 1843			body fossils	Sphenacanthidae		Permian	Lopingian	Wuchiapingian
740	*Wodnika*	*striatula* Münster, 1843				Sphenacanthidae		Permian	Guadalupian	Roadian
741	*Wodnika*	*borealis* Maisey, 1982a			fin spine	Sphenacanthidae		Permian		
742	*Wodnika*	sp.			teeth, fin spines	Sphenacanthidae		Permian	Guadalupian –Lopingian	**Capitanian, upper–Changhsingian**
743	*Wodnika*	sp.				Sphenacanthidae		Permian	Lopingian	
744	gen. indet.	sp. indet.			fin spine	Sphenacanthidae		Permian	Guadalupian	Wordian–Capitanian
745	*Xenacanthodus*	*egloni* Glikman, 1980			teeth, fin spines, anterior body	Sphenacanthidae		Permian	Guadalupian –Lopingian	Wordian
746	*Xenacanthodus*	*egloni* Glikman, 1980			teeth	Sphenacanthidae		Permian	Guadalupian –Lopingian	Wuchiapingian

Madagascar Embayment	NT-W	Oman	Haushi Cliff, Haushi-Huqf region, E	Khuff Fm	rim basin
Madagascar Embayment	NT-W	Oman	Haushi Cliff and Saiwan, Haushi-Huqf region, E	Khuff Fm	rim basin
	PL-C	Japan	Kamura, Takachiho-chō, Nishiusuki-gun, Miyazaki-ken (Prefecture), Kyūshū	Kamura Fm	mid-oceanic seamount
Madagascar Embayment	NT-W	Oman	Haushi Cliff and Saiwan, Haushi-Huqf region, E	Khuff Fm	rim basin
	PT-W	Germany	Gaildorf, Württemberg	Gipskeuper	
Paraná Basin	PG-S	Brazil	Rio Claro, São Paolo State	Taquaral Mb, Irati Fm, Passa Dois Grp	Bioclasts in a bed of light-grey to grey, fining-upward, cross-laminated conglomeratic sandstone with angular to rounded, abundant granules and rare pebbles of quartz and chert dispersed in a very fine to coarse sandy matrix
Dunkard Basin (freshwater, but marine influenced; Schultze & Soler-Gijón 2004)	PG-N	USA-E		Waynesburg, Washington and Greene Fms, Dunkard Grp	
	PT-W	Germany	Richelsdorf, Hessen	Kupferschiefer	
	PT-W	Germany	Mansfeld	Kupferschiefer	
	PT-W	Germany	Lower Saxony, Thuringia	Kupferschiefer	
	PT-W	Germany	Hüggel Mountain, Hasbergen, Osnabrücker Bergland, NW	Copper Shale Mb (Kupferschiefer Mb), Werra Fm	laminated bituminous black shale marls (fish bed), shallow-water submarine swell zone (coastal)
	PT-W	England	Durham	Marl Slate	
	BOR	USA-ARC	Lisburne Hills, Point Hope Quadrangle, N of Mt. Itsalik, Alaska	Siksikpuk Fm	
	PT-N	Russia-W	East European Platform, Vologda Oblast		
	PT-N	Russia-W	Vyazniki, Vladimir Region, central		alluvial clays and sands
	BOR	Russia-NW	Vym' River, Komi Republic		
	PT-N	Russia-W	Isheyevo, Tatarstan		sandy lens
	PT-N	Russia-W	Tatarstan, near Kazan	East European Platform	

marine		*Lingognodolella aserrata* conodont Zone; OSPZ6 palynology Zone; *Necoschwagerina craticulifera* fusulinid Zone	this study		Sample AO40; and 965-1, 965-2
marine		*Lingognodolella aserrata* conodont Zone; OSPZ6 palynology Zone; *Necoschwagerina craticulifera* fusulinid Zone	this study		Samples AO40, AO55, AO47bis, AO50; and 965-2, 965-9
marine		*Paragondolella bulgarica*	this study		Sample 300311-J
marine		*Lingognodolella aserrata* conodont Zone; OSPZ6 palynology Zone; *Necoschwagerina craticulifera* fusulinid Zone	this study		Samples AO40, AO55, AO47bis, AO50; and 965-2, 965-3, 965-5, 965-8, 965-9
			Seilacher 1948	Ginter *et al.* 2010; Cappetta 2012	(as *Phoebodus*) synonymous to *brodiei* ? Cappetta 2012
mixed marine/freshwater (transgressive lag?)			Chahud *et al.* 2010		
			Johnson 1992		(as *Hybodus alleghenensis* , see Soler-Gijon 1997a)
			Münster 1843	Schaumberg 1977, 1999; Hampe 2012	(as *H. striatula* , *Strophodus arcuatus* , and *Radamas macrocephalus*)
			Weigelt 1930	Schaumberg 1977; Haubold & Schaumberg 1985; Schaumberg 1999	
				Hampe 2012	
marine with freshwater influence	50–80 cm in length		Diedrich 2009a		
				Bell *et al.* 1979; Hampe 2012	
	up to 100 cm in length		Maisey 1982a	Schaumberg 1999; Hampe 2012	(as Sphenacanthidae)
			Minikh & Minikh 1981	Ivanov 2000; Hampe 2012	
freshwater			Sennikov & Golubev 2006		
			Malysheva *et al.* 2000	Ivanov 2000	
			Glikman 1980	Minikh & Minikh 1998; Ivanov 2000, 2005, 2011	
			Minikh & Minikh 1996	Ivanov 2000, 2005	

747	*Khuffia*	*lenis* Koot, Cuny, Tintori and Twitchett, 2013			teeth	Sphenacanthidae	*incertae sedis* (Euselachii)	Permian	Guadalupian	Wordian
748	*Khuffia*	*prolina* Koot, Cuny, Tintori and Twitchett, 2013			teeth	Sphenacanthidae	*incertae sedis* (Euselachii)	Permian	Guadalupian	Wordian
749	gen. indet.	sp. indet. A			teeth		*incertae sedis* (Euselachii)	Permian	Guadalupian	Wordian
750	gen. indet.	sp. indet. B			teeth		*incertae sedis* (Euselachii)	Triassic	Lower	Olenekian (Spathian)
751	gen. indet.	sp. indet. C			tooth		*incertae sedis* (Euselachii)	Triassic	Middle	Anisian
752	gen. indet.	sp. indet.			fin spine fragment		*incertae sedis* (Euselachii)	Permian	Lopingian	Wuchiapingian
753	*Cooleyella*	*lordi* (Duffin & Ward, 1983)			teeth	Anachronistidae		Permian	Cisuralian	**Sakmarian–Artinskian**
754	*Cooleyella*	cf. *lordi* (Duffin and Ward, 1983)			teeth	Anachronistidae		Permian	Guadalupian	Wordian
755	*Cooleyella*	*amazonensis* Duffin, Richter and Neis, 1996			teeth	Anachronistidae		Permian	Guadalupian	Roadian
756	*Cooleyella*	*amazonensis* Duffin, Richter and Neis, 1996			teeth	Anachronistidae		Permian	Guadalupian	Roadian
757	*Cooleyella*	sp.			teeth	Anachronistidae		Permian	Cisuralian	Asselian, Artinskian
758	*Cooleyella*	sp. nov.			teeth	Anachronistidae		Permian	Cisuralian	Kungurian
759	*Cooleyella*	sp. nov.			teeth	Anachronistidae		Permian	Guadalupian	Capitanian
760	*Cooleyella*	sp. nov.			teeth	Anachronistidae		Permian	Guadalupian	Roadian

Madagascar Embayment	NT-W	Oman	Haushi Cliff and Saiwan, Haushi-Huqf region, E	Khuff Fm	rim basin
Madagascar Embayment	NT-W	Oman	Haushi Cliff and Saiwan, Haushi-Huqf region, E	Khuff Fm	rim basin
Madagascar Embayment	NT-W	Oman	Haushi Cliff, Haushi-Huqf region, E	Khuff Fm	rim basin
Hawasina Basin	NT-W	Oman	Jabel Safra, Oman Mountains, N	Hallstatt-type limestone olistoliths	basinal seamount
	PL-C	Japan	Kamura, Takachiho-chō, Nishiusuki-gun, Miyazaki-ken (Prefecture), Kyūshū	Kamura Fm	mid-oceanic seamount
	NT-W	Iran	Baghuk Mountain, NW of Abadeh	Hambast Fm	deep shelf limestone
	PT-N	Russia-W	Middle and South Urals		marls and nodular, detrital, and reef limestones
Madagascar Embayment	NT-W	Oman	Haushi Cliff, Haushi-Huqf region, E	Khuff Fm	rim basin
	PT-N	Russia-W	Tatarstan, Kirov region, and Vladimirovka	East European Platform	
	PG-C	USA-S	Quarry section, Guadelupe Mountains, western Texas	William Ranch Mb, Cutoff Fm	fossiliferous debris flows interbedded with radiolarian-bearing limestone
	PT-N	Russia-W	Middle and South Urals		marls and nodular, detrital, and reef limestones
	PL-E	USA-W	Ward Mountain, White Pine County, Nevada	Arcturus Fm	
	PG-C	USA-S	Guadelupe Mountains, western Texas	Rader Limestone Mb, Bell Canyon Fm	
	PG-C	USA-S	Quarry section, Guadelupe Mountains, western Texas	William Ranch Mb, Cutoff Fm	fossiliferous debris flows interbedded with radiolarian-bearing limestone

marine		*Hindeodella aserrata* conodont Zone; OSPZ6 palynology Zone; *Necoschwagerina craticulifera* fusulinid Zone	this study		Samples AO40, AO55, AO47bis; and 965-2
marine		*Hindeodella aserrata* conodont Zone; OSPZ6 palynology Zone; *Necoschwagerina craticulifera* fusulinid Zone	this study		Sample AO40; and 965-2
marine		*Hindeodella aserrata* conodont Zone; OSPZ6 palynology Zone; *Necoschwagerina craticulifera* fusulinid Zone	this study		Samples AO55, AO47bis, AO50, AO123
marine		*Ioriciospathodus collinsoni – Mecospathodus 'triangularis* conodont zones; *Columbites parisianus – Prohungarites/Subcolumbites* ammonoid zones	this study		Samples 103B, 103C, 104A
marine		*Paragondolella bulgarica*	this study		Sample 300311-J
marine			Hampe *et al.* 2013		
marine		*Ps. urdalensis* and *Par. lutiqini – Ps.juresanensis* fusulinid zones	Ivanov 2005	Ginter *et al.* 2010; Ivanov 2011	(as *Cocleyella* cf. *kordi*)
marine		*Hindeodella aserrata* conodont Zone; OSPZ6 palynology Zone; *Necoschwagerina craticulifera* fusulinid Zone	this study		Samples AO50, AO214
			Ivanov 2011		
marine			Ivanov *et al.* 2012		
marine		*Sph. vulgaris – Sph. fusiformis* and *Par. solidissima* fusulinid zones	Ivanov 2005	Ginter *et al.* 2010	(as *Cocleyella* sp. A); idem those mentioned in Ivanov 2011?
	bottom feeder	probably *Parafusulina* conodont Zone	Duffin & Ward 1983	Ginter et al. 2010; Ivanov 2011	(as *Anachronistes* sp.)
marine			Ivanov *et al.* 2011	Ivanov 2011	
marine			Ivanov *et al.* 2012		

761	*Cooleyella*	*peculiaris* Gunnell, 1933			teeth	Anachronistidae		Permian	Cisuralian–Guadalupian	Kungurian–Roadian
762	*Cooleyella*	sp.			teeth	Anachronistidae		Permian	Cisuralian	Kungurian
763	*Cooleyella*	sp.			tooth	Anachronistidae		Permian	Guadalupian	Wordian–Capitanian
764	*Pseudodalatias*	*barnstonensis* (Sykes, 1971)			teeth	Pseudodalatiidae		Triassic	Upper	Rhaetian
765	*Pseudodalatias*	*barnstonensis* (Sykes, 1971)			teeth	Pseudodalatiidae		Triassic	Upper	Rhaetian
766	*Pseudodalatias*	*barnstonensis* (Sykes, 1971)				Pseudodalatiidae		Triassic	Upper	Rhaetian
767	*Pseudodalatias*	*barnstonensis* (Sykes, 1971)				Pseudodalatiidae		Triassic	Upper	Rhaetian
768	*Pseudodalatias*	*barnstonensis* (Sykes, 1971)			teeth	Pseudodalatiidae		Triassic	Upper	Rhaetian
769	*Pseudodalatias*	*barnstonensis* (Sykes, 1971)				Pseudodalatiidae		Triassic	Upper	Rhaetian
770	*Pseudodalatias*	*barnstonensis* (Sykes, 1971)				Pseudodalatiidae		Triassic	Upper	Rhaetian
771	*Pseudodalatias*	*barnstonensis* (Sykes, 1971)				Pseudodalatiidae		Triassic	Upper	Rhaetian
772	*Pseudodalatias*	*barnstonensis* (Sykes, 1971)				Pseudodalatiidae		Triassic	Upper	Rhaetian
773	*Pseudodalatias*	*barnstonensis* (Sykes, 1971)				Pseudodalatiidae		Triassic	Upper	
774	*Pseudodalatias*	*barnstonensis* (Sykes, 1971)			articulated lower teeth	Pseudodalatiidae		Triassic	Upper	Norian
775	*Pseudodalatias*	*henarejensis* Botella, Plasencia, Marquez-Aliaga, Cuny & Dorka, 2009				Pseudodalatiidae		Triassic	Middle	Ladinian
776	cf. *Palidipleospinax*	sp.			teeth	Palaeospinacidae	Synechodontiformes	Triassic	Middle	Anisian
777	Genus S	sp. T			teeth	*incertae sedis*	Synechodontiformes	Triassic	Lower	Olenekian (Spathian)

Kaibab Sea	PL-E	USA-W	Grand Canyon, Arizona	Fossil Mountain Mb, Kaibab Fm	
Kaibab Sea	PL-E	USA-W	SW of Flagstaff, Arizona	Harrisburg Mb, Kaibab Fm	shallow (15–180m), restricted, marine sea, calcareous/sandy limestones
	PG-C	USA-S	PI section, Guadelupe Mountains, western Texas	Hegler and Pinery Mbs, Bell Canyon Fm	thin limestone intervals interbedded with sandstone and siltstone
	PT-W	England	Barnstone, Nottinghamshire	Westbury Fm, Penarth Grp	bone bed
	PT-W	England	Aust Cliff, Axminster, Blue Anchor Point, Westbury, Penarth, Lavernick, Lincolnshire, Leicestershire, Holwell, SW	Westbury Fm, Penarth Grp	
	PT-W	England	Aust Cliff, Axminster, Blue Anchor Point, Westbury, Penarth, Lavernick, Lincolnshire, Leicestershire, Holwell, SW	Westbury Fm, Penarth Grp	
Central European Basin (Rhaetian Sea)	PT-W	Belgium	Habay-la-Vieille and Sagnette	Grès de Mortinsart	
Central European Basin (Rhaetian Sea)	PT-W	Belgium	Attert		
	PT-W	France	Lons-le-Saunier, Jura		
	PT-W	France	Saint-Germain-les-Arlay, Jura		
	PT-W	France	Boisset, Jura		
	PT-W	France	Lavigny, Jura		
	PT-W	France	SE		
	PT-W	Italy	Cene, Lombardy	Calcare di Zorzino	
	PT-W	Spain	Henarejos, Cuenca Province, Castilian branches, SE Iberian Ranges	Cañete Dolomites and Limestones Fm (Muschelkalk correlative)	limestone
	PT-E	China-SE	Guandao, Guizhou Province, S	Xinyuan Fm	carbonate platform slope
Hawasina Basin	NT-W	Oman	Jabel Safra, Oman Mountains, N	Hallstatt-type limestone olistoliths	basinal seamount

marine			Thompson 1995	Hunt *et al.* 2005	
marine, increasingly saline			Hodnett *et al.* 2012		
marine			Ivanov *et al.* 2012		
			Sykes 1971	Reif 1978b; Duffin 1981; Cappetta 1987, 2012; Duffin & Delsate 1993; Storrs 1994; Botella *et al.* 2009b	(excluded from Neoselachii by Reif 1978b, but based on strict use of triple-layered enameloid to characterise neoselachians, despite some organisation of crystallites)
			Sykes 1974	Duffin 1981, 1982a, b; Duffin & Delsate 1993; Storrs 1994; Cuny & Benton 1999; Botella *et al.* 2009b	
			Duffin 1978; 1980b, 1999	Duffin 1981; Duffin & Delsate 1993; Botella *et al.* 2009b	
marine with freshwater influence			Duffin *et al.* 1983	Delsate 1993; Duffin & Delsate 1993; Cuny & Benton 1999; Botella *et al.* 2009b	
marine			Duffin & Delsate 1993	Delsate 1993; Cuny & Benton 1999; Botella *et al.* 2009b; Capetta 2012	
			Cuny *et al.* 1994, 2000	Cuny 1995a; Cuny & Benton 1999; Botella *et al.* 2009b	
			Cuny *et al.* 1994, 2000	Cuny 1995a; Cuny & Benton 1999; Botella *et al.* 2009b	
			Cuny *et al.* 1994, 2000	Cuny 1995a; Cuny & Benton 1999; Botella *et al.* 2009b	
			Henry 1875	Cuny & Benton 1999; Cappetta 2012	(as *Hemipristis lavignensis* , tentative re-assignment, see Cuny 1998 and Duffin 1981)
			Cappetta, pers. obs.	Cappetta *et al.* 1993	
			Tintori 1980	Duffin *et al.* 1983; Cappetta 1987, 2012; Duffin & Delsate 1993; Cuny & Benton 1999; Botella *et al.* 2009b	
marine	cutting-clutching		Botella *et al.* 2009b	Andreev & Cuny 2012; Cappetta 2012	
marine		*Chiloscyllium gondolellioides* , *Ch. timorensis* , *Gladigondolella carinata* , *Neospathodus spathi* , *Triassospathodus homeri*	this study		Samples O-15, O-24
marine		*Icriospathodus collinsoni – Neospathodus 'triangularis* conodont zones; *Columbites parisianus – Prohungarites/Subcolumbites* ammonoid zones	this study		Samples 103A, 103B, 103C, 104A, 104B/C

778	Genus S	sp. T			teeth	*incertae sedis*	Synechodontiformes	Triassic	Lower	Olenekian (Smithian–Spathian)
779	Genus S	sp. T			teeth	*incertae sedis*	Synechodontiformes	Permian	Lopingian	Wuchiapingian, upper?
780	Genus S	sp. T			teeth	*incertae sedis*	Synechodontiformes	Triassic	Lower	Olenekian (Spathian)
781	Genus S	sp. T			teeth	*incertae sedis*	Synechodontiformes	Triassic	Lower	Olenekian (Smithian)
782	Genus S	cf. sp. T			teeth	*incertae sedis*	Synechodontiformes	Triassic	Lower–Middle	Olenekian (Spathian)–Anisian
783	Genus S	sp. A			teeth	*incertae sedis*	Synechodontiformes	Triassic	Lower	Olenekian (Spathian)
784	Genus S	sp. A			tooth	*incertae sedis*	Synechodontiformes	Triassic		
785	Genus S	sp. A			teeth	*incertae sedis*	Synechodontiformes	Triassic	Lower–Middle	Olenekian (Spathian)–Anisian
786	Genus S	sp. A			teeth	*incertae sedis*	Synechodontiformes	Triassic	Lower	Olenekian (Spathian)
787	cf. Genus S	sp.			tooth	*incertae sedis*	Synechodontiformes	Triassic	Lower	Olenekian (Smithian)
788	*Synechodus* (pre-Jurassic)	*antiquus* Ivanov, 2005			teeth	*incertae sedis*	Synechodontiformes	Permian	Cisuralian	**Sakmarian–Artinskian**
789	*Synechodus* (pre-Jurassic)	sp.				*incertae sedis*	Synechodontiformes	Triassic	Lower	Induan (Dienerian)
790	*Synechodus* (pre-Jurassic)	*rhaeticus* Duffin, 1982a			fin spines / teeth	*incertae sedis*	Synechodontiformes	Triassic	Upper	Rhaetian

Hawasina Basin	NT-W	Oman	Wadi Alwa, Ba'id, Oman Mountains, N	Alwa Fm	basinal seamount
	NT-W	Iran	Zal?, near Djulfa	Ali Bashi Fm?	exotic limestone
	PL-E	USA-W	Paris Canyon and Hot Springs, near Bear Lake, Bear Lake County, SE Idaho	Thaynes Fm	mudstone and silty limestone; shallow subtidal and intertidal environment (inner shelf facies)
	PL-E	USA-W	Salt Lake City, N Utah	Thaynes Fm	??bioclastic grainstone; above wave base (normal open marine outer shelf facies)
	PT-E	China-SE	Guandao, Guizhou Province, S	Luolou and Xinyuan fms	carbonate platform slope
Hawasina Basin	NT-W	Oman	Jabel Safra, Oman Mountains, N	Hallstatt-type limestone olistoliths	basinal seamount
	NT-E	Timor			pelagic Hallstatt-type limestone?
	PT-E	China-SE	Guandao, Guizhou Province, S	Luolou and Xinyuan fms	carbonate platform slope
	NT-E	Timor	River Bihati region, near Bouwn	exotic	pelagic Hallstatt-type limestone
Hawasina Basin	NT-W	Oman	Wadi Alwa, Ba'id, Oman Mountains, N	Alwa Fm	basinal seamount
	PT-N	Russia-W	Middle and South Urals		marls and nodular, detrital, and reef limestones
	NT-W	Turkey	Tepeköy, Kocaeli Peninsula, Anatolia, W		
	PT-W	England	Aust Cliff, Avon and Holwell, near Frome, Somerset	Westbury Fm, Penarth Grp	

marine		*Eoinella nepalensis – Neospathodus 'triangularis* conodont zones; *Flemingites flemingianus – Prohungarites/Subcolumbites* ammonoid zones	this study		Samples C85314, 117A
marine			this study		Sample 02 OF KZK 10
marine		*Columbites – Tenuicolumbites* Beds	this study		Samples 93 OF W-11, 99-IG CNA-HS 4
marine		*Scythogondolella mosheri* / *Sc. milleri* conodont Zone– *Anawasatchites tardus* ammonoid Zone	this study		Sample 93 OF W-14
marine		*Neospathodus triangularis* , *Triassospathodus homeri* , *Gladigondolella carinata* , *Neospathodus spathi* , *Triassospathodus brochus* , *Chiosella gondolelloides* , *Ch. timorensis* , *Gladigondolella tethydis*	this study		Samples O-3, O-11, O-13, O-14, O-15, O-22, O-24?, O-27, O-28, O-29, O-31, O-34, O-36, O-40, O-41, GDL-55, GDL-57
marine		*Ioriospathodus collinsoni – Neospathodus 'triangularis* conodont zones; *Columbites parisianus – Prohungarites/Subcolumbites* ammonoid zones	this study		Samples 103C, 104A
marine			this study		Sample 30/09/2003
marine		*Gladigondolella carinata* , *Triassospathodus homeri* , *Neospathodus spathi*	this study		Samples O-11, O-28, O-36
marine		*Columbites parisianus* ammonoid Zone (Owenites, Albanites)	Yamagishi 2006	this study	(as *Synechodus* sp.1; in part)
marine			this study		Sample 110222-B
marine		*Ps. urdalensis* and *Par. solidissima* fusulinid zones	Ivanov 2000	Ivanov 2005; Ginter *et al.* 2010; Cappetta 2012	(as palaeospinacids)
		cristagalli Zone	Thies 1982	Brinkmann *et al.* 2010	(as *Palaeospinax* ?)
marine	clutching-grinding (showing adaptations towards durophagous, C&B99)		Duffin 1982a, 1998b	Duffin 1982b; Storrs 1994; Cuny & Benton 1999	(as *Palaeospinax* / *Synechodus*)

791	*Synechodus* (pre-Jurassic)	*rhaeticus* Duffin, 1982a			teeth	*incertae sedis*	Synechodontiformes	Triassic	Upper	Rhaetian
792	*Synechodus* (pre-Jurassic)	*rhaeticus* Duffin, 1982a			teeth	*incertae sedis*	Synechodontiformes	Triassic	Upper	Rhaetian
793	*Synechodus* (pre-Jurassic)	*rhaeticus* Duffin, 1982a			teeth	*incertae sedis*	Synechodontiformes	Triassic	Upper	Rhaetian, lower
794	*Synechodus* (pre-Jurassic)	*triangulus* Yamagishi, 2004				*incertae sedis*	Synechodontiformes	Triassic	Middle	Anisian, lower
795	*Synechodus* (pre-Jurassic)	sp.				*incertae sedis*	Synechodontiformes	Triassic	Lower	Olenekian
796	*Synechodus* (pre-Jurassic)	sp. nov.				*incertae sedis*	Synechodontiformes	Triassic	Lower–Middle	**Olenekian–Anisian**
797	*Synechodus* (pre-Jurassic)	*incrementum* Johns, Barnes and Orchard, 1997			teeth	*incertae sedis*	Synechodontiformes	Triassic	Upper	Norian, lower–middle
798	*Synechodus* (pre-Jurassic)	*incrementum* Johns, Barnes and Orchard, 1997			teeth	*incertae sedis*	Synechodontiformes	Triassic	Upper	Norian, uppermost lower
799	*Synechodus* (pre-Jurassic)	*multincodosus* Johns, Barnes and Orchard, 1997			teeth	*incertae sedis*	Synechodontiformes	Triassic	Upper	Carnian, upper
800	*Synechodus* (pre-Jurassic)	cf. *multincodosus* Johns, Barnes and Orchard, 1997			teeth	*incertae sedis*	Synechodontiformes	Triassic	Upper	Carnian, upper

Central European Basin (Rhaetian Sea)	PT-W	Belgium	Habay-la-Vieille	Grès de Mortinsart	
	PT-W	France	Lons-le-Saunier, Jura		
	PT-W	Luxembourg	Commune Weyler-la-Tour, Syren	Keuper	
	PL-C	Japan	Tahokamigumi, Nishiuwa City (prev. Shirokawa-cho, Higashiuwa-gun), Ehime Prefecture, Shikoku	Taho Fm	biomicritic bedded limestone, seamount
	BOR	Russia-NE	Tikhaya River, Kotelniy Island, New Siberian Archipelago, Sakha (Yakutia) Republic, Siberia	Tuor-Yuryakh Fm	
	BOR	Russia-N	Cape of Tsvetkov and Chernokhrebetnaya River, eastern Taimyr Peninsula, Krasnoyarsk area (Kray), Siberia	Pribrezhnaya Fm and Morzhovaya Fm	
	PL-E	Canada-W	Brown Hill, Childerhose Cove, Crying Girl Prairie Creek, and Ne Parle Pas Rapids, Peace River area, northeastern BC	Pardonet Fm	
	PL-E	Canada-W	Moose Lick Creek ridge, Trutch map area, northeastern BC	Charlie Lake, Baldonnel, and Pardonet fms	
	PL-E	Canada-W	Black Bear Ridge, Chowade South, Peace River area, northeastern BC	Ludington Fm and Baldonnel Fm	
	PL-E	Canada-W	Black Bear Ridge, Chowade South, Peace River area, northeastern BC	Ludington Fm and Baldonnel Fm	

	clutching-grinding (showing adaptations towards durophagous, C&B99)		Delsate & Lepage 1991, 1993	Delsate 1993; Cuny & Benton 1999	
	clutching-grinding (showing adaptations towards durophagous, C&B99)		Cuny *et al.* in prep.	Cuny & Benton 1999	
	clutching-grinding (showing adaptations towards durophagous, C&B99)		Godefroit *et al.* 1998	Delsate 1998	
marine		*Neogondolella timorensis* conodont Zone	Yamagishi 2004; Yamagishi 2006	Goto *et al.* 2010	
			Ivanov & Klets 2007		
			Ivanov & Klets 2007		
marine	clutching-grinding (showing adaptations towards durophagous, C&B99)	Upper *Metapolygnathus primitius* to *Epigondolella spiculata* conodont zones; *Stikinoceras kerri II* to *Meschinavatites columbianus* Iaſb ammonoid zones	Johns *et al.* 1997		
marine		*Epigondolella triangularis* conodont Zone; *Juvavites magnus* ammonoid Zone	Johns *et al.* 1999		
marine		*Upper Metapolygnathus nodosus* and *Metapolygnathus communisti* conodont zones; Upper *Tropites welleri* and *Klamathites macrolobatus* ammonoid zones	Johns *et al.* 1997	Johns *et al.* 1999	
marine		*Metapolygnathus communisti* and Upper *Metapolygnathus nodosus* conodont zones; *Klamathites macrolobatus* and *Upper Tropites dilleri* ammonoid zones	Johns *et al.* 1997		

801	*Synechodus* (pre-Jurassic)	*volaticus* Johns, Barnes and Orchard, 1997			teeth	*incertae sedis*	Synechodontiformes	Triassic	Middle–Upper	**Ladinian–Carnian**
802	*Synechodus* (pre-Jurassic)	sp. 1			teeth	*incertae sedis*	Synechodontiformes	Triassic	Middle	Ladinian
803	*Synechodus* (pre-Jurassic)	sp. 2			teeth	*incertae sedis*	Synechodontiformes	Triassic	Middle–Upper	**Ladinian–Carnian**
804	*Synechodus* (pre-Jurassic)	sp.				*incertae sedis*	Synechodontiformes	Triassic	Middle	Anisian
805	*Synechodus* (pre-Jurassic)	sp.			teeth	*incertae sedis*	Synechodontiformes	Triassic	Middle	Anisian–Ladinian
806	*Synechodus* (pre-Jurassic)	sp. indet.			teeth	*incertae sedis*	Synechodontiformes	Triassic	Lower–Middle	Olenekian (Spathian)–Anisian
807	*Synechodus* (pre-Jurassic)	sp. indet.			teeth	*incertae sedis*	Synechodontiformes	Triassic	Lower	Olenekian (Spathian)
808	*Synechodus* (pre-Jurassic)	sp. indet.			teeth	*incertae sedis*	Synechodontiformes	Triassic	Lower	Olenekian (Spathian)
809	*Nemacanthus*	sp.			fin spines	*incertae sedis*	Synechodontiformes	Triassic	Lower	Olenekian (Spathian)
810	*Nemacanthus*	sp.			fin spines	*incertae sedis*	Synechodontiformes	Triassic	Lower	Induan (Griesbachian)
811	*Nemacanthus*	*elegans* Evans, 1904			fin spines	*incertae sedis*	Synechodontiformes	Triassic	Lower	Olenekian (Spathian) derived from biostrat (not Induan?)
812	*Nemacanthus*	sp.			fin spine fragment	*incertae sedis*	Synechodontiformes	Triassic	Middle	Anisian–Ladinian
813	*Nemacanthus*	*monilifer* Agassiz, 1837			fin spines	*incertae sedis*	Synechodontiformes	Triassic	Upper	Rhaetian
814	*Nemacanthus*	*monilifer* Agassiz, 1837			fin spine	*incertae sedis*	Synechodontiformes	Triassic	Upper	Rhaetian
815	*Nemacanthus*	*monilifer* Agassiz, 1837			fin spine	*incertae sedis*	Synechodontiformes	Triassic	Upper	Norian
816	*Nemacanthus*	*monilifer* Agassiz, 1837				*incertae sedis*	Synechodontiformes	Triassic	Upper	Rhaetian
817	*Nemacanthus*	*monilifer* Agassiz, 1837				*incertae sedis*	Synechodontiformes	Triassic	Upper	Rhaetian
818	*Nemacanthus*	*monilifer* Agassiz, 1837			fin spine	*incertae sedis*	Synechodontiformes	Triassic	Upper	
819	*Nemacanthus*	*monilifer* Agassiz, 1837			fin spine	*incertae sedis*	Synechodontiformes	Triassic	Upper	

	PL-E	Canada-W	Aylard Creek East, Beattie Hill, Beattie Ledge, Black Bear Ridge, Brown Hill, Laurier Pass, Peace River area, northeastern BC	Liard Fm, Ludington Fm, and Baldonnel Fm	
	PL-E	Canada-W	Aylard Creek East, Beattie Hill, Beattie Ledge, Toad River, Peace River area, northeastern BC	Liard Fm	
	PL-E	Canada-W	Black Bear Ridge, Brown Hill, Peace River area, northeastern BC	Liard Fm and Baldonnel Fm	
	PT-N	Bulgaria	Bobuk Dol section, near Belogradchik, Vidin Province, NW	Babino Fm, Iskar Carbonate Grp	
Tethys	PT-W	Poland	Upper Silesia and Holy Cross Mountains, SE	Muschelkalk	
	PT-E	China-SE	Guandao, Guizhou Province, S	Luolou and Xinyuan fms	carbonate platform slope
	PL-E	USA-W	Paris Canyon, Hot springs, and Hammond Creek, near Bear Lake, Bear Lake County, SE Idaho	Thaynes Fm	mudstone and silty limestone; shallow subtidal and intertidal environment (inner shelf facies)
	PL-E	USA-W	Cowboy Pass, Confusion Range, Millard County, W Utah	Thaynes Fm	mudstone and silty limestone; shallow subtidal and intertidal environment (inner shelf facies)
	BOR	Spitsbergen	Mt. Viking, Sassen Bay, Isfjorden	"Grippia niveau", Kaosfjellet Mb, Sticky Keep Fm, Kongressfjellet Subgrp, Sassendalen Grp	
	BOR	Greenland-E	Kap Stosch, Hold with Hope	Fish Zone I, Wordie Creek Fm	
	PL-E	USA-W	Paris Canyon, near Bear Lake, west of Paris, Bear Lake County, SE Idaho	Thaynes Fm	
Germanic Basin	PT-W	Germany	oberen Werntal, east of Arnstein, Main-Spessart, south of Würzburg	upper Muschelkalk	
	PT-W	England	Aust Cliff, near Bristol	Westbury Fm, Penarth Grp	
Central European Basin (Rhaetian Sea)	PT-W	Belgium	Habay-la-Vieille and Sagnette	Grès de Mortinsart	
	PT-W	France	Saint-Nicolas-de-Port (Meurthe and Moselle), NE		
	PT-W	France	Provenchères-sur-Meuse, Haute-Marne		
	PT-W	France	Boisset, Jura		
	PT-W	Germany			
	PT-W	England			

marine		? *Macleamnoceras macleanni* to *Klamathites macrolobatus* ammonoid zones; Ladinian (unzoned) to *Metapolygnathus communisti* /Lower *M. primitius* conodont zones	Johns *et al.* 1997		
marine		? *Macleamnoceras macleanni* and *Frankites sutherlandi* ammonoid zones	Johns *et al.* 1997		
marine		*Frankites sutherlandi* to *Klamathites macrolobatus* ammonoid zones; Ladinian (unzoned) to *Metapolygnathus communisti* conodont zones	Johns *et al.* 1997		
		Paragondolella bifurcata Conodont Zone	Andreev & Cuny 2012		
marine	clutching-crushing		Liszkowski 1993		(as *Palaeospinax* (?))
marine		*Triassospathodus homeri* , *Necospathodus spathi*	this study		Samples O-10, O-29, O-31
marine		*Columbites – Procolumbites* Beds	this study		Samples 93 OF W-11, 93 OF W-13, o-64671 91-OF
marine		*Columbites* ? Beds	this study		Sample 02 OF CP-C1-BASE
marine		*Glenikites pilaticus – Keyserlingites subrobustus* Zone (ammonoid)	Stensiö 1921	Cappetta 1987	correlates to "Grippia niveau", Vendomdalen Mb, Vikinghøgda Fm (Romano & Brinkmann 2010)
marine		*Glyptophiceras triviale* (ammonoid)	Stensiö 1932; Nielsen 1936	Nielsen 1935; Bendix-Almgreen 1976; Cappetta 1987	see Birkenmajer & Jerzmańska 1979 for fish zone
marine		*Columbites parisianus* Zone	Evans 1904	Cappetta 1987; Mutter & Rieber 2005; Brinkmann *et al.* 2010	(as *Cosmacanthus*)
marine			Scheinpflug 1984		
			Agassiz 1836	Duffin 1982a, b; Cappetta 1987, 2012	
marine with freshwater influence			Duffin *et al.* 1983	Delsate 1993; Cuny & Benton 1999	
				Delsate 1993; Cuny 1995a; Cuny & Benton 1999	(age, see Duffin 1993a)
				Cuny 1995a	
				Cuny 1995a	
			Schmidt 1928	Cuny & Benton 1999	
			Woodward 1891; Storrs 1994	Cuny & Benton 1999	

820	*Nemacanthus*	*monilifer* Agassiz, 1837			fin spine	*incertae sedis*	Synechodontiformes	Triassic	Upper	Norian
821	*Nemacanthus*	*monilifer* Agassiz, 1837			fin spines	*incertae sedis*	Synechodontiformes	Triassic	Upper	Norian
822	*Nemacanthus*	*monilifer* Agassiz, 1837			fin spine fragments	*incertae sedis*	Synechodontiformes	Triassic	Upper	Rhaetian, lower
823	*Nemacanthus*				fin spine	*incertae sedis*	Synechodontiformes	Triassic	Upper	Norian
824	*Nemacanthus*	sp.			fin spines	*incertae sedis*	Synechodontiformes	Triassic	Upper	Carnian, middle–upper
825	*Nemacanthus*	*granulosus* Münster, ...				*incertae sedis*	Synechodontiformes	Triassic	Upper	Carnian, lower
826	*Nemacanthus*	sp.			fin spine fragments	*incertae sedis*	Synechodontiformes	Permian	Guadalupian	Wordian
827	gen. indet.	sp. indet.			tooth fragments	*incertae sedis*	Synechodontiformes	Triassic	Middle	Ladinian
828	Genus P	sp. P			teeth	*incertae sedis*	Synechodontiformes	Triassic	Lower	Olenekian (Spathian)
829	Genus P	sp. P			teeth	*incertae sedis*	Synechodontiformes	Triassic	Lower	Olenekian (Smithian–Spathian)
830	cf. Genus P	sp. P			tooth fragment	*incertae sedis*	Synechodontiformes	Triassic	Lower	Induan (Griesbachian)
831	cf. Genus P	sp.			teeth	*incertae sedis*	Synechodontiformes	Triassic	Lower–Middle	Olenekian (Spathian)–Anisian
832	*Rhomphaicodon*	*minor* (Agassiz, 1837)			fin spine, teeth	*incertae sedis*	Synechodontiformes	Triassic	Upper	Rhaetian
833	*Rhomphaicodon*	*minor* (Agassiz, 1837)				*incertae sedis*	Synechodontiformes	Triassic	Middle	Ladinian
834	*Rhomphaicodon*	*minor* (Agassiz, 1837)				*incertae sedis*	Synechodontiformes	Triassic	Middle	Ladinian, upper
835	*Rhomphaicodon*	*minor* (Agassiz, 1837)				*incertae sedis*	Synechodontiformes	Triassic	Upper	Rhaetian
836	*Rhomphaicodon*	*minor* (Agassiz, 1837)			teeth	*incertae sedis*	Synechodontiformes	Triassic	Upper	
837	*Rhomphaicodon*	*minor* (Agassiz, 1837)			teeth	*incertae sedis*	Synechodontiformes	Triassic	Upper	Rhaetian
838	*Rhomphaicodon*	*minor* (Agassiz, 1837)			teeth	*incertae sedis*	Synechodontiformes	Triassic	Upper	Rhaetian
839	*Rhomphaicodon*	*minor* (Agassiz, 1837)			teeth	*incertae sedis*	Synechodontiformes	Triassic	Upper	Rhaetian
840	*Rhomphaicodon*	*minor* (Agassiz, 1837)			teeth	*incertae sedis*	Synechodontiformes	Triassic	Upper	Norian

	PT-W	Luxembourg			
	PT-W	Luxembourg	Rinkebierg, Medernach		
	PT-W	Luxembourg	Commune Weyler-la-Tour, Syren	Keuper	
	PT-W	France			
	PT-W	Poland	Woźniki clay-pit, near Częstochowa, S		
	PT-W	Germany	Steinbach near Schwäbisch Hall, SW	lower Lettenkeuper	brackish/deltaic
Madagascar Embayment	NT-W	Oman	Haushi Cliff, Haushi-Huqf region, E	Khuff Fm	rim basin
	PL-C	Japan	Kamura, Takachiho-chō, Nishiusuki-gun, Miyazaki-ken (Prefecture), Kyūshū	Kamura Fm	mid-oceanic seamount
Hawasina Basin	NT-W	Oman	Jabel Safra, Oman Mountains, N	Hallstatt-type limestone olistoliths	basinal seamount
Hawasina Basin	NT-W	Oman	Wadi Alwa, Ba'id, Oman Mountains, N	Alwa Fm	basinal seamount
Hawasina Basin	NT-W	Oman	Wadi Wasit, Ba'id, Oman Mountains, N	Al Jil Fm	platform margin
	PT-E	China-SE	Guandao, Guizhou Province, S	Luolou and Xinyuan fms	carbonate platform slope
	PT-W	England	Purton Passage, near Berkeley, Gloucestershire (spine) / Axmouth, Devon (teeth)	Penarth Grp	bone bed
	PT-W	Germany	N	upper Muschelkalk	
	PT-W	Germany	Bibersfeld, W	Lettenkohlesandstein	
	PT-W	England		Westbury Fm, Penarth Grp	
	PT-W	Germany			
	PT-W	Luxembourg	Junglinster and Remich		
Central European Basin (Rhaetian Sea)	PT-W	Belgium	Sagnette and Unter der Kirchen, Hachy, and Habay-la-Vieille	Grès de Mortinsart	
Central European Basin (Rhaetian Sea)	PT-W	Belgium	Attert		
	PT-W	France	Saint-Nicolas-de-Port, NE		

			Duffin 1993b	Cuny & Benton 1999	
			Delsate 1995	Cuny *et al.* 1998; Cuny & Benton 1999	
			Godefroit *et al.* 1998	Delsate 1998; Cuny & Benton 1999	
			Cuny & Ramboer 1991	Cuny *et al.* 1998	
			Sulej *et al.* 2010		
brackish			Reif 1980b		
marine		*Hindeodella aserrata* conodont Zone; OSPZ6 palynology Zone; *Neoschwagerina craticulifera* fusulinid Zone	this study		Sample AO40
marine		*Eudurovignathus hungaricus* , *Paragondolella foliata*	this study		Sample 300311-K
marine		*Ioriospathodus collinsoni – Neospathodus 'triangularis'* conodont zones; *Columbites parisianus – Prohungarites/Subcolumbites* ammonoid zones	this study		Samples 103A, 103C, 104A, 104B/C
marine		*Eoninella nepalensis – Triassospathodus homeri* conodont zones; *Flemingites flemingianus – Proocelumbites* ammonoid zones	this study		Samples 117A, WA 22
marine		basal *Clarkina carinata* conodont Zone	this study		Sample 100224-G
marine		*Neospathodus triangularis* , *Ns. spathi* , *Triassospathodus brochus* , *Tr. homeri* , *Chiosella gondolelloides* , *Gladigondolella carinata*	this study		Samples O-14, O-23, O-31, O-40, GQC182
			Agassiz 1836	Duffin 1993b; Duffin & Delsate 1993; Storrs 1994; Cuny *et al.* 1998	(as *Hybodus* ; referred by Cuny & Risnes 2005)
			Struckmann 1871	Duffin & Delsate 1993; Duffin 1993b	(as "Hybodus"; referred by Cuny & Risnes 2005)
			Oertle 1928	Duffin & Delsate 1993; Duffin 1993b	(as middle Norian; as "Hybodus"; referred by Cuny & Risnes 2005)
			Woodward 1891	Storrs 1994; Cuny 1998; Cuny & Benton 1999	(as "*Hybodus*" ; referred by Cuny & Risnes 2005)
			Schmidt 1928	Cuny 1998; Cuny & Benton 1999	(as "*Hybodus*" ; referred by Cuny & Risnes 2005)
			Müller 1964	Delsate 1992, 1995	(as "*Hybodus*" ; referred by Cuny & Risnes 2005)
marine with freshwater influence			Duffin *et al.* 1983	Delsate 1993; Duffin & Delsate 1993; Duffin 1993b; Cuny 1998; Cuny *et al.* 1998; Cuny & Benton 1999	(as "*Hybodus*" ; referred by Cuny & Risnes 2005)
marine			Duffin & Delsate 1993		
			Delsate 1993	Cappetta 2012	(as "*Hybodus*" ; referred by Cuny & Risnes 2005; age see Duffin 1993a)

841	*Rhomphaicodon*	*minor* (Agassiz, 1837)				*incertae sedis*	Synechodontiformes	Triassic	Upper	Rhaetian
842	*Rhomphaicodon*	*minor* (Agassiz, 1837)				*incertae sedis*	Synechodontiformes	Triassic	Upper	Rhaetian
843	*Rhomphaicodon*	*minor* (Agassiz, 1837)				*incertae sedis*	Synechodontiformes	Triassic	Upper	Rhaetian
844	*Rhomphaicodon*	*minor* (Agassiz, 1837)				*incertae sedis*	Synechodontiformes	Triassic	Upper	Rhaetian
845	*Rhomphaicodon*	*minor* (Agassiz, 1837)				*incertae sedis*	Synechodontiformes	Triassic	Upper	Rhaetian
846	*Rhomphaicodon*	*minor* (Agassiz, 1837)			teeth	*incertae sedis*	Synechodontiformes	Triassic	Upper	Norian, uppermost
847	*Rhomphaicodon*	*minor* (Agassiz, 1837)			teeth / fin spine	*incertae sedis*	Synechodontiformes	Triassic	Upper	Rhaetian
848	*Rhomphaicodon*	*minor* (Agassiz, 1837)			teeth	*incertae sedis*	Synechodontiformes	Triassic	Upper	Rhaetian
849	*Rhomphaicodon*	*minor* (Agassiz, 1837)			teeth	*incertae sedis*	Synechodontiformes	Triassic	Upper	Norian, middle
850	*Rhomphaicodon*	*minor* (Agassiz, 1837)			teeth	*incertae sedis*	Synechodontiformes	Triassic	Upper	Rhaetian, lower
851	*Rhomphaicodon*	*niccolensis* Duffin, 1993a			teeth	*incertae sedis*	Synechodontiformes	Triassic	Upper	Norian
852	*Rhomphaicodon*	*niccolensis* Duffin, 1993a			teeth	*incertae sedis*	Synechodontiformes	Triassic	Upper	Norian
853	*Groconodon*	*candaui* Cuny, Martin, Rauscher & Mazin, 1998			teeth	*incertae sedis*	Synechodontiformes	Triassic	Upper	Norian, uppermost
854	*Mucrovenator*	*minimus* Cuny, Rieppel & Sander, 2001			teeth	*incertae sedis*	Synechodontiformes	Triassic	Middle	Anisian, lower middle
855	*Mucrovenator?*	sp.			teeth	*incertae sedis*	Synechodontiformes	Triassic	Middle	Anisian, lower middle
856	*Mucrovenator?*	*minimus* Cuny, Rieppel & Sander, 2001			tooth	*incertae sedis*	Synechodontiformes	Triassic	Upper	Norian, lower
857	*Hopleacanthus*	*richelsdorfensis* Schaumberg, 1982			anterior body, fin spine	*incertae sedis*		Permian	Guadalupian	Roadian
858	*Hopleacanthus*	*richelsdorfensis* Schaumberg, 1982			partial body fossils, fin spines	*incertae sedis*		Permian	Guadalupian	Roadian
859	*Hopleacanthus*	*richelsdorfensis* Schaumberg, 1982			teeth, fin spines, skeletal remains	*incertae sedis*		Permian	Guadalupian	Roadian
860	*Hueneichthys*	*costatus* Reif, 1977			tooth	*incertae sedis*		Triassic	Upper	Rhaetian
861	*Reifia*	*minuta* Duffin, 1980a			teeth	*incertae sedis*		Triassic	Upper	Carnian
862	*Reifia*	aff. *minuta* Duffin, 1980a			teeth	*incertae sedis*		Triassic	Middle	Anisian
863	*Vallisia*	*coppi* Duffin, 1982b			teeth	*incertae sedis*		Triassic	Upper	Rhaetian
864	*Vallisia*	*coppi* Duffin, 1982b			teeth	*incertae sedis*		Triassic	Upper	Rhaetian
865	*Vallisia*	*coppi* Duffin, 1982b			teeth	*incertae sedis*		Triassic	Upper	Rhaetian
866	*Dicrotodus*	*tricuspidatus* Schmid, 1861				*incertae sedis*	Hybodontiformes	Triassic	Upper	Carnian
867	*Dicrotodus*	*tricuspidatus* Schmid, 1861				*incertae sedis*	Hybodontiformes	Triassic	Middle	Anisian–Ladinian
868	*Dicrotodus*	*tricuspidatus* Schmid, 1861			teeth	*incertae sedis*	Hybodontiformes	Triassic	Middle	Ladinian, upper

	PT-W	France	Provenchères-sur-Meuse, Haute-Marne		
	PT-W	France	Lons-le-Saunier, Jura		
	PT-W	France	Saint-Germain-les-Arlay, Jura		
	PT-W	France	Boisset, Jura		
	PT-W	France	Belfort, Territoire de Belfort		
	PT-W	France	Grozon (quarry), near Poligny, Jura, NE	Marnes de Châlins Fm	green, sandy marl
	PT-W	England	Aust Quarry (at Manor Farm), near Aust, Gloucestershire		
	PT-W	England	Hapsford Bridge, Vallis Vale, near Frome, Somerset, SW	basal clay, Westbury Beds, Penarth Grp	intertidal and very shallow
	PT-W	Luxembourg	Rinkebierg Hill, Medernach	Steinmergelgruppe, Keuper	dolomitic bone bed
	PT-W	Luxembourg	Commune Weyler-la-Tour, Syren	Keuper	
	PT-W	France	Saint-Nicolas-de-Port, near Nancy, NE	"Keuper" marls	near-shore shallow marine environment
	PT-W	Germany	Halberstadt	Knollenmergel	
	PT-W	France	Grozon (quarry), near Poligny, Jura, NE	Marnes de Châlins Fm	green, sandy marl
	PL-E	USA-W	west slope Augusta Mountains, Pershing County, Nevada	lower Fossil Hill Mb, Favret Fm, Star Peak Grp	litharenite, debris flow deposit, high energy, coastal influence, outer platform
	PL-E	USA-W	west slope Augusta Mountains, Pershing County, Nevada	lower Fossil Hill Mb, Favret Fm, Star Peak Grp	litharenite, debris flow deposit, high energy, coastal influence, outer platform
	PT-W	Austria	south face Feuerkogel, Saltzkammergut	lower Roter Bankkalk	pelagic Hallstatt limestone
	PT-W	Germany	Wolfsberg, Richelsdorf, Hessen	Kupferschiefer	
	PT-W	Germany	Richelsdorf, Hessen	Kupferschiefer	
	PT-W	Germany	Richelsdorf, Hessen	Kupferschiefer	
	PT-W	Germany	Rüdern, Kreis Esslingen/Neckar, near Stuttgart, S	Rhaetic sandstone	
	PT-W	Germany	Eisbach valley, near Gaildorf, S	Dunkle Mergel	marly, coastal border facies
Tethys	PT-W	Poland	Upper Silesia, SE	Muschelkalk	
	PT-W	England	Hapsford Bridge, Vallis Vale, near Frome, Somerset, SW	basal clay, Westbury Beds, Penarth Grp	intertidal and very shallow
	PT-W	England	Holwell Quarry, near Frome, Somerset, SW	fissure infill	intertidal and very shallow
Central European Basin (Rhaetian Sea)	PT-W	Belgium	Unter der Kirchen, Hachy, near Habay-la-Vieille	Grès de Mortinsart	
	PT-W	Germany	Jena, E	lower Keuper, Dunkle Mergel?	
	PT-W	France	Pontpierre, Lorraine, NE	Muschelkalk	
	PT-W	Germany	clay quarry, near Schöningen, lower Saxony	Muschelkalk-Keuper boundary	near-shore / limnic

				Cuny 1995a; Cuny 1998; Cuny & Benton 1999	
				Cuny 1995a; Cuny 1998; Cuny & Benton 1999	
				Cuny 1995a; Cuny 1998; Cuny & Benton 1999	
				Cuny 1995a; Cuny 1998; Cuny & Benton 1999	
				Cuny 1995a; Cuny 1998; Cuny & Benton 1999	
			Cuny *et al.* 1998		(as "*Hybodus*"; referred by Cuny & Risnes 2005)
				Duffin 1982a; Cuny *et al.* 1998	(as "*Hybodus*"; referred by Cuny & Risnes 2005)
marine		? *Rhaetipollis* Zone	Duffin 1982b		(as "*Hybodus*"; referred by Cuny & Risnes 2005)
			Duffin 1993b	Delsate 1992, 1993, 1995; Duffin & Delsate 1993; Cuny 1995a, 1998; Cuny et al. 1998; Cuny & Benton 1999; Dorka 2001	(as "*Hybodus*"; referred by Cuny & Risnes 2005)
			Godefroit *et al.* 1998	Delsate 1998; Cappetta 2012	(as "*Hybodus*"; referred by Cuny & Risnes 2005)
marine			Duffin 1993a	Cuny 1995a; Cuny & Benton 1999; Cappetta 2012	
			Jaekel 1914	Duffin 1993a; Cuny & Benton 1999	tentative
			Cuny *et al.* 1998	Cuny & Benton 1999; Cappetta 2012	initially identified as Hybodus sp. in Cuny 1995a (Cuny, pers. comm. 2012)
marine		*Mclaggarti* Subzone of the *Hyatti* Zone	Cuny *et al.* 2001	Cappetta 2012	
marine		*Mclaggarti* Subzone of the *Hyatti* Zone	Rieppel *et al.* 1996	Cuny *et al.* 2001	(as *Palaeospinax* ?) probably *Mucrovenator*, Cuny, pers. comm. 2012
marine		*Epigondolella spatulata*, *Neogondolella navicula*	Yamagishi 2006		
			Bendix-Almgreen & Malzahn 1969	Schaumberg 1977, 1982	(as *Ctenacanthus* sp. indet)
			Schaumberg 1977	Schaumberg 1982	(as *Ctenacanthus* sp. indet)
	approx. 75 cm in length		Schaumberg 1982	Ginter *et al.* 2010	
			Reif 1977	Cappetta 1987, 2012; Cuny & Benton 1999	
			Duffin 1980a	Cappetta 1987, 2012; Cuny & Benton 1999	not lower Norian in age, see Dorka 2001, Andreev & Cuny 2012
marine			Liszkowski 1993	Andreev & Cuny 2012	
marine		? *Rhaetipollis* Zone	Duffin 1982b	Cappetta 1987, 2012; Storrs 1994; Ginter *et al.* 2010	
marine			Duffin 1982b	Ginter *et al.* 2010	
marine with freshwater influence			Duffin *et al.* 1983	Delsate 1993; Cuny & Benton 1999; Cappetta 2012	
			Schmid 1861	Schmidt 1928; Duffin 1981; Cappetta 1987, 2012; Cuny & Benton 1999	not lower Norian in age, see Dorka 2001, Andreev & Cuny 2012
			Sauvage 1883	Duffin 1981; Cuny & Benton 1999	
freshwater/brackish?			Dorka 2001		

869	*Dicrateodus*	*tricuspidatus* Schmid, 1861			teeth	*incertae sedis*	Hybodontiformes	Triassic	Middle	Ladinian, upper
870	*Dicrateodus*	*tricuspidatus* Schmid, 1861				*incertae sedis*	Hybodontiformes	Triassic	Upper	Carnian, lower
871	*Dicrateodus*	cf. *tricuspidatus* Schmid, 1861			teeth	*incertae sedis*	Hybodontiformes	Triassic	Upper	Carnian
872	*Raineria*	*osswaldi* Cappetta, 1987			rostrum	*incertae sedis*	Hybodontiformes	Triassic	Upper	Rhaetian
873	*Duffinselache*	*holwellensis* (Duffin, 1998a)			teeth	*incertae sedis*	Hybodontiformes	Triassic	Upper	Rhaetian
874	*Duffinselache*	*holwellensis* (Duffin, 1998a)			teeth	*incertae sedis*	Hybodontiformes	Triassic	Upper	Rhaetian
875	*Duffinselache*	*holwellensis* (Duffin, 1998a)			teeth	*incertae sedis*	Hybodontiformes	Triassic	Upper	Rhaetian
876	*Rhomaleodus*	*buduroui* Andreev & Cuny, 2012			teeth	*incertae sedis*		Triassic	Middle	Anisian
877	*Rhomaleodus*	sp.			teeth	*incertae sedis*		Triassic	Upper	Norian
878	*Pseudocetorhinus*	*pickfordi* Duffin, 1998b			teeth		*incertae sedis* (Neoselachii)	Triassic	Upper	Rhaetian
879	*Pseudocetorhinus*	*pickfordi* Duffin, 1998b			teeth		*incertae sedis* (Neoselachii)	Triassic	Upper	Rhaetian
880	*Pseudocetorhinus*	*pickfordi* Duffin, 1998b			teeth		*incertae sedis* (Neoselachii)	Triassic	Upper	Rhaetian, lower
881	*Pseudocetorhinus*	*pickfordi* Duffin, 1998b			teeth		*incertae sedis* (Neoselachii)	Triassic	Upper	Rhaetian
882	*Pseudocetorhinus*	*pickfordi* Duffin, 1998b			teeth		*incertae sedis* (Neoselachii)	Triassic	Upper	Rhaetian
883	*Pseudocetorhinus*	*pickfordi* Duffin, 1998b			teeth		*incertae sedis* (Neoselachii)	Triassic	Upper	Rhaetian
884	*Pseudocetorhinus*	*pickfordi* Duffin, 1998b			teeth		*incertae sedis* (Neoselachii)	Triassic	Upper	Rhaetian
885	Hexanchidae gen. indet.	sp. indet.			tooth	*incertae sedis*		Permian	Guadalupian	Capitanian
886	*Lyptahlkodus*	*gladius* Minikh, 1996b			teeth	*incertae sedis*		Triassic	Lower	
887	*Lyptahlkodus*	*gladius* Minikh, 1996b			teeth	*incertae sedis*		Triassic	Middle	
888	*Amelacanthus*	cf. *sulcatus* (Agassiz, 1837)			fin spine fragments		*incertae sedis* (Neoselachii)	Permian	Guadalupian	Wordian
889	cf. *Amelacanthus*	sp.			fin spine fragments		*incertae sedis* (Neoselachii)	Triassic	Lower	Olenekian (Spathian)
890	*Amelacanthus*	*compressus* Eichwald, 1860			fin spine(s)	*incertae sedis*		Permian	Guadalupian	Wordian (Kazanian)
891	*Eunemacanthus*	*kewtei* Branson, 1916			fin spine	*incertae sedis*		Permian	Guadalupian	Wordian

	PT-W	Germany	Neidenfels, near Crailsheim, S	base Hauptsandstein, lower Letterkeuper, lower Keuper	bone bed; estuary
	PT-W	Germany	Steinbach near Schwäbisch Hall, SW	lower Lettenkeuper	brackish/deltaic
	PT-W	Germany	Gaildorf, Baden-Württemberg, SW	Dunkle Mergel	marly, coastal border facies
	PT-W	Austria	Grubereck, Risserkogel Mountains, Alps	Kössen Limestone	
	PT-W	England	Holwell Quarry, near Frome, Somerset, SW	Westbury Fm, Penarth Grp	fissure infill
	PT-W	England	Chilcompton, Somerset	Cotham Mb (base), Lilstock Fm, Penarth Grp	lagoonal?
Central European Basin (Rhaetian Sea)	PT-W	Belgium	Habay-la-Vieille	Grès de Mortinsart	
	PT-N	Bulgaria	Quarries section, near Belogradchik, Vidin Province, NW	Babino Fm, Iskar Carbonate Grp	
	PL-E	USA-W	Little Poverty Peak, NW Nevada	Sonomia tectonic unit, Golconda Allochthon	
	PT-W	England	Holwell Quarry, near Frome, Somerset, SW	Westbury Fm, Penarth Grp	fissure infill
	PT-W	England	Aust Cliff		
	PT-W	Luxembourg	Commune Weyler-la-Tour, Syren	Keuper	
Central European Basin (Rhaetian Sea)	PT-W	Belgium	Attert		
Central European Basin (Rhaetian Sea)	PT-W	Belgium	Habay-la-Vieille	Grès de Mortinsart	
Central European Basin (Rhaetian Sea)	PT-W	Belgium	Sagnette and Unter der Kirchen, Hachy		
	PT-W	France	Saint-Germain-les-Arlay, Jura		
	PL-W	Japan	Yotsukura, Iwaki City, Fukushima Prefecture, NE Honshu	Kashiwadaira Fm, Takakurayama Grp	black shale
	PT-N	Russia-SW	Don Luke, Don Basin, Volgograd region	Gamsky horizon, Yarensk superhorizon, Lipovskaya Fm	
	PT-N	Russia-SW	Donguz, Southern Urals		
Madagascar Embayment	NT-W	Oman	Haushi Cliff, Haushi-Huqf region, E	Khuff Fm	rim basin
Hawasina Basin	NT-W	Oman	Jabel Safra, Oman Mountains, N	Hallstatt-type limestone olistolith	basinal seamount
	PT-N	Russia-W	European Russia		brachiopod limestone; hemipelagic (shelf)
Phosphoria Basin (see Piper & Link 2002)	PL-E	USA-N	North Fork of Little Wind River and Bull Lake Creek, Wind River Mountains, Lander, Wyoming	Embar Fm (basal Phosphoria Fm) (=Park City Fm)	

brackish			Hagdorn & Reif 1988	Böttcher 2010	
brackish			Reif 1980b		
			Seilacher 1943	Duffin 1980a, 1981; Cuny & Benton 1999	not lower Norian in age, see Dorka 2001, Andreev & Cuny 2012
			Osswald 1928	Duffin 1981; Thies & Reif 1985; Cappetta 1987, 2012; Cuny & Benton 1999	
marine			Duffin 1998a	Andreev & Cuny 2012	(as *'Polyacrodus'*), considered as lateral teeth of *Pseudocetorhinus* by Cappetta 2012
marine			Duffin 1980b, 1998a	Storrs 1994; Andreev & Cuny 2012	(as *'Polyacrodus'*), considered as lateral teeth of *Pseudocetorhinus* by Cappetta 2012
				Delsate 1993; Cuny & Benton 1999; Andreev & Cuny 2012; Cappetta 2012	(as *'Polyacrodus'*), considered as lateral teeth of *Pseudocetorhinus* by Cappetta 2012
		Paragondolella bulgarica Conodont Zone	Andreev & Cuny 2012		
			Sosson & Martin 1985	Andreev & Cuny 2012	(as *Hybodus*)
marine	filter feeder, pelagic		Duffin 1980b, 1998b	Duffin & Delsate 1993; Cuny & Benton 1999; Cappetta 2012	
	filter feeder, pelagic		Cuny & Benton 1999		
	filter feeder, pelagic		Godefroit *et al.* 1998	Delsate 1998; Cuny & Benton 1999; Cappetta 2012	
marine	filter feeder, pelagic		Duffin & Delsate 1993	Cuny & Benton 1999	(as new hybodont genus)
	filter feeder, pelagic		Delsate & Lepage 1991	Cuny & Benton 1999	
marine with freshwater influence	filter feeder, pelagic		Duffin *et al.* 1983	Delsate 1993; Duffin & Delsate 1993; Cappetta 2012	(as *'Polyacrodus'* sp. 2)
	filter feeder, pelagic		Cuny *et al.* 1994	Cuny 1995a, Cuny & Benton 1999; Cappetta 2012	
			Koizumi 1991 (oral presentation)	Goto 1994a, b, 1996a–c, 1999a, b, 2000, 2002; Burrow *et al.* 2008; Ginter *et al.* 2010	
marine			Minikh 1996b	Minikh 2001	(as Squatinactiformes?, Dalatiidae?)
marine			Minikh 1996b	Minikh 2001	(as Squatinactiformes?, Dalatiidae?)
marine		*Hindeodella aserrata* conodont Zone; OSPZ6 palynology Zone; *Necoschwagerina craticulifera* fusulinid Zone	this study		Samples AO40, AO55, AO47bis, AO50
marine		*Necogondolella 'triangularis'* conodont Zone; *Prohungarites/Subcolumbites* ammonoid Zone	this study		Sample 103C
marine			Eichwald 1860	Chabakov 1927	(as *Onchus?*; genus (without naming species) referred by Maisey 1982a
			Branson 1916	Maisey 1982a (as *keyti*)	

892	gen. indet.	sp. indet. A			teeth		*incertae sedis* (Neoselachii)	Permian	Guadalupian	Wordian
893	gen. indet.	sp. indet. B			tooth fragments		*incertae sedis* (Neoselachii)	Triassic	Upper	Norian
894	gen. indet. (Neoselachii?)	*mutabilis* Branson, 1933			fin spine	*incertae sedis*		Permian	Guadalupian	Capitanian
895	gen. indet. (Neoselachii?)	sp. indet.			tooth	*incertae sedis*		Triassic	Middle–Upper	Carnian, lowermost
896	gen. indet. 2	sp. indet.			tooth	*incertae sedis*		Permian	Lopingian	Changhsingian
897	*Heterodontus*	sp.			teeth	Heterodontidae	Heterodontiformes	Triassic	Middle	Ladinian
898	*Acronemus*	*tuberculatus* (Bassani, 1886)			fin spines, teeth, denticles, jaw and skull fragments		*incertae sedis* (Hybodontiformes/Neoselachii)	Triassic	Middle	Anisian–Ladinian
899	*Acronemus*	*tuberculatus* (Bassani, 1886)					*incertae sedis* (Hybodontiformes/Neoselachii)	Triassic	Middle	Anisian–Ladinian
900	*Acronemus*	*tuberculatus* (Bassani, 1886)					*incertae sedis* (Hybodontiformes/Neoselachii)	Triassic	Middle	Anisian–Ladinian
901	*Acronemus*	sp. nov.			teeth		*incertae sedis* (Hybodontiformes/Neoselachii)	Triassic	Middle	Anisian
902	*Acronemus*	*simplex* Meyer, 1851			teeth		*incertae sedis* (Hybodontiformes/Neoselachii)	Triassic	Middle	Ladinian
903	gen indet.	sp. indet.			teeth		*incertae sedis* (Elasmobranchii)	Triassic	Upper	Norian, uppermost upper
904	*Orodus*	*jpeunaensis* Chahud, Fairchild & Petri, 2010			tooth	Orodontidae	Orodontiformes	Permian	Cisuralian	Artinskian
905	*Orodus*	sp.			tooth	Orodontidae	Orodontiformes	Permian	Cisuralian	
906	gen. indet.	*corrugatus* Romer, 1942 (Newberry & Worthen, 1870)			teeth		Eugeneodontiformes?	Permian	Cisuralian	Artinskian
907	gen. indet.	*corrugatus* Romer, 1942 (Newberry & Worthen, 1870)			tooth		Eugeneodontiformes?	Permian	Cisuralian	Sakmarian/Artinskian?
908	*"Caseodus"*	*varidentis* Mutter & Neuman, 2008			neurocranium, jaws, teeth	Caseodontidae	Eugeneodontiformes	Triassic	Lower	Olenekian (Smithian)?
909	*Caseodus*	cf. *varidentis* Mutter and Neuman, 2008			teeth	Caseodontidae	Eugeneodontiformes	Triassic	Lower	Induan (Griesbachian, upper)
910	*Fadenia*	*crenulata* Nielsen, 1932			teeth, denticles	Caseodontidae	Eugeneodontiformes	Permian	Lopingian	Wuchiapingian

Madagascar Embayment	NT-W	Oman	Saiwan, Haushi-Huqf region, E	Khuff Fm	rim basin
	PL-C	Japan	Kamura, Takachiho-chō, Nishiusuki-gun, Miyazaki-ken (Prefecture), Kyūshū	Kamura Fm	mid-oceanic seamount
Phosphoria Basin (see Piper & Link 2002)	PL-E	USA-N	Middle Fork of Popo Agie River, Wind River Mountains, Wyoming	Pustula Mb, Middle Phosphoria Fm (=Retort Mb)	Thin phosphate bed
	PT-E	China-SE	Yongning, Guanling County, Guizhou Province, S	Zhuganpo Fm	grey micritic limestone + dolomitic limestone / bioclastic limestone --> shallow to deep (below storm wave-base) water platform
	PT-E	China-SE	Dongling, Xiushui County, Jiangxi Province	upper Mb, Changxing Fm	
Tethys	PT-W	Poland	Upper Silesia and Holy Cross Mountains, SE	Muschelkalk	
	PT-W	Switzerland	S Alps, Monte San Giorgio, Kt. Tessin	Grenzbitumenzone, Besano Fm	
	PT-W	Italy	S Alps, Besano, Lombardy	Grenzbitumenzone	
	PT-W	Switzerland	S Alps, Monte San Giorgio, Kt. Tessin	Grenzbitumenzone, Besano Fm	
Tethys	PT-W	Poland	Upper Silesia and Holy Cross Mountains, SE	Muschelkalk	
Tethys	PT-W	Poland	Upper Silesia, SE	Muschelkalk	
	PL-E	Canada-W	Moose Lick Creek ridge, Trutch map area, northeastern BC	Charlie Lake, Baldonnel, and Pardonet fms	
Paraná Basin	PG-S	Brazil	Rio Claro, São Paolo State	Taquaral Mb, Irati Fm, Passa Dois Grp	Bioclasts in a bed of light-grey to grey, fining-upward, cross-laminated conglomeratic sandstone with angular to rounded, abundant granules and rare pebbles of quartz and chert dispersed in a very fine to coarse sandy matrix
	PG-C	USA-C	Oklahoma		
	PG-C	USA-S	Rattlesnake Canyon, Archer County, Texas	upper Admiral Fm, Wichita Grp	clays near marine limestones in red beds
	PG-C	USA-S	Texas	middle Lueders Fm	
	PL-E	Canada-W	Ganoid Ridge, Wapiti Lake, near "Fossil Fish Lake", British Columbia, W	Vega-Phroso Siltstone Mb, Sulphur Mountain Fm	siltstone, deltaic/shallow continental shelf environment
Sverdrup Basin	BOR	Canada-N	Otto Fiord South, Ellesmere Island, Canadian Arctic Archipelago	Confederation Point Mb, Blind Fiord Fm	shales and siltstone; deep shelf environment
	BOR	Greenland-E	Section F (120 m above sea level) and River 8–9 and 14, Kap Stosch, Hold with Hope	*Posidonia* Shale Mb (Ravnefjeld Fm), Foldvik Creek Grp	

marine		*Idiognathodella aserrata* conodont Zone; OSPZ6 palynology Zone; *Neoschwagerina craticulifera* fusulinid Zone	this study		Samples AO38, AO214
marine		*Metapolygnathus nodosus* , *M. primitius*	this study		Sample 300311-M
			Branson 1933	Nielsen 1935; Maisey 1984b	(as *Ctenacanthus*), similar to *Nemacanthus* , may be neoselachian
marine		*Metapolygnathus polygnathiformis* conodont Zone	Chen *et al.* 2007a		
			Wang *et al.* 2007a	Wang *et al.* 2007b	
marine	clutching-crushing		Liszkowski 1993		
marine	30-35 cm in length		Rieppel 1982	Maisey 2011; Cappetta 2012	(incorporating *Nemacanthus tuberculatus* and *Acrodus bicarinatus* Bassani, 1886)
marine			Bassani 1886; Alessandri 1910	Rieppel 1982; Cappetta 2012	(as *Acrodus* and *Nemacanthus*)
marine			Woodward 1891	Rieppel 1982	(as *Nemacanthus*)
marine	clutching-crushing		Liszkowski 1993		
marine	clutching-crushing		Liszkowski 1993		
marine		*Epigondolella bidentata* conodont Zone; *Oncomchalcites cordilleranus* ammonoid Zone	Johns *et al.* 1999		
mixed marine/freshwater (transgressive lag?)			Chahud *et al.* 2010		
			Olson 1967	Zidek 1973	(lost, see Zidek 1973)
marine			Romer 1942	Johnson 1981	(as *Orodus* ?)
			Berman 1970	Johnson 1981	(as ? *Orodus*)
marine	1–1.5 m in length		Mutter & Neuman 2008a	Mutter & Neuman 2008b; Ginter *et al.* 2010	(affinities unclear: similarities to *Sarcoprion* and *Fadenia*)
marine		*Bukkenites strigatus* ammonoid Zone; *Neogondolella carinata* , *Ng. planata* , *Ng. nevadensis*	this study		Sample 93 OF TE-5 1663 62-TE 325A
marine			Nielsen 1932, 1952	Nielsen 1935; Stensiö 1961; Bendix-Almgreen 1976; Ginter *et al.* 2010	

911	*Fadenia*	*crenulata* Nielsen, 1932			teeth	Caseodontidae	Eugeneodontiformes	Permian	Lopingian	Wuchiapingian
912	*Fadenia*	*crenulata* Nielsen, 1932			teeth	Caseodontidae	Eugeneodontiformes	Permian	Lopingian	Wuchiapingian?–Changhsingian
913	*Fadenia*	*crenulata* Nielsen, 1932				Caseodontidae	Eugeneodontiformes	Permian	Lopingian	Wuchiapingian
914	*Fadenia*	*crenulata* Nielsen, 1932				Caseodontidae	Eugeneodontiformes	Permian	Lopingian	
915	*Fadenia*	*ureclasmata* Mutter & Neuman, 2008a			anterior body, teeth	Caseodontidae	Eugeneodontiformes	Triassic	Lower	Olenekian (Smithian)?
916	*Fadenia*	sp.			partial body	Caseodontidae	Eugeneodontiformes	Triassic	Lower	Olenekian (Smithian)?
917	*Erikodus*	*groenlandicus* (Nielsen, 1932)			teeth	Caseodontidae	Eugeneodontiformes	Permian	Lopingian	Wuchiapingian
918	*Erikodus*	*groenlandicus* (Nielsen, 1932)			teeth	Caseodontidae	Eugeneodontiformes	Permian	Lopingian	Wuchiapingian
919	*Uralodus*	*zangerli* Kozlov, 2000			teeth	Caseodontidae	Eugeneodontiformes	Permian	Cisuralian	Artinskian
920	gen indet.	sp. indet.			partial bodies	Caseodontidae	Eugeneodontiformes	Triassic	Lower	Olenekian (Smithian)?
921	*Ellobodus*	*schaefferi* Zangerl, 1981			dentition, jaw, cranial elements	Eugeneodontidae	Eugeneodontiformes	Permian	Cisuralian	Asselian
922	*Ellobodus*	*wenesi* Hampe, Hairapetian, Dorka, Witzmann, Akbari & Korn, 2013			tooth	Eugeneodontidae	Eugeneodontiformes	Permian	Lopingian	Wuchiapingian
923	gen. indet.	sp. indet.			tooth	Eugeneodontidae	Eugeneodontiformes	Permian	Lopingian	Wuchiapingian
924	*Campodus*	*agassizianus* De Koninck, 1844				*incertae sedis*	Eugeneodontiformes	Permian	Cisuralian	
925	*Campodus*	cf. *agassizianus* De Koninck, 1844				*incertae sedis*	Eugeneodontiformes	Permian	Cisuralian	Artinskian
926	*Campodus*	*krasnopolskyi* Kozlov, 2000			teeth	*incertae sedis*	Eugeneodontiformes	Permian	Cisuralian	Artinskian
927	*Campodus*	sp.			teeth	*incertae sedis*	Eugeneodontiformes	Permian	Cisuralian	Artinskian
928	*Campodus*	sp.			teeth	*incertae sedis*	Eugeneodontiformes	Permian	Cisuralian	Kungurian
929	*Tiaraju*	*tenuis* Richter, 2007				*incertae sedis*	Eugeneodontiformes	Permian	Guadalupian	
930	*Agassizodus*	*variabilis* (Newberry & Worthen, 1870)				Agassizodontidae	Eugeneodontiformes	Permian	Guadalupian	Capitanian
931	*Agassizodus*	*variabilis* (Newberry & Worthen, 1870)				Agassizodontidae	Eugeneodontiformes	Permian	Cisuralian	
932	*Agassizodus*	sp. indet.			tooth	Agassizodontidae	Eugeneodontiformes	Permian	Guadalupian	Wordian
933	*Campyloprion*	*ivanovi* (Karpinsky, 1922)				Agassizodontidae	Eugeneodontiformes	Permian	Cisuralian	Asselian?
934	*Helicoprion*	sp.			tooth whorl fragment	Agassizodontidae	Eugeneodontiformes	Permian	Cisuralian	Kungurian
935	*Helicoprion*	sp.				Agassizodontidae	Eugeneodontiformes	Permian	Guadalupian	Capitanian
936	*Helicoprion*	sp.				Agassizodontidae	Eugeneodontiformes	Permian	Cisuralian	Artinskian
937	*Helicoprion*	sp.			tooth whorl fragment	Agassizodontidae	Eugeneodontiformes	Permian	Guadalupian	Roadian
938	*Helicoprion*	sp.			tooth whorls	Agassizodontidae	Eugeneodontiformes	Permian	Guadalupian	Kungurian, uppermost–Roadian
939	*Helicoprion*	sp.			tooth whorl and isolated crowns	Agassizodontidae	Eugeneodontiformes	Permian	Guadalupian	Roadian
940	*Helicoprion*	*svalis* Siedlecki, 1970				Agassizodontidae	Eugeneodontiformes	Permian	Cisuralian	Kungurian (Artinskian–Roadian)
941	*Helicoprion*	sp.				Agassizodontidae	Eugeneodontiformes	Permian	Cisuralian	

	BOR	Greenland-E	Margrethedal, Gauss Halvø	*Posidonia* Shale Mb (Ravnefjeld Fm), Foldvik Creek Gp	
E Greenland Basin	BOR	Greenland-E	Kap Stosch, Hold with Hope	Ravnefjeld and Schuchert Dal/Wordie Creek fms	basinal to marginal
	PT-W	England	Durham	Marl Slate, Kupferschiefer	
	PT-W	Germany	Gera	Zechstein	
	PL-E	Canada-W	Ganoid Ridge, Wapiti Lake, near "Fossil Fish Lake", British Columbia, W	Vega-Phroso Siltstone Mb, Sulphur Mountain Fm	siltstone, deltaic/shallow continental shelf environment
	PL-E	Canada-W	Ganoid Ridge, Wapiti Lake, near "Fossil Fish Lake", British Columbia, W	Vega-Phroso Siltstone Mb, Sulphur Mountain Fm	siltstone, deltaic/shallow continental shelf environment
	BOR	Greenland-E	Section F (120 m above sea level) and River 8–9 and 14, Kap Stosch, Hold with Hope	*Posidonia* Shale Mb (Ravnefjeld Fm), Foldvik Creek Grp	
	BOR	Greenland-E	Margrethedal, Gauss Halvø	*Posidonia* Shale Mb (Ravnefjeld Fm), Foldvik Creek Grp	
	PT-N	Russia-W	middle and south Urals		
	PL-E	Canada-W	Ganoid Ridge, Wapiti Lake, near "Fossil Fish Lake", British Columbia, W	Vega-Phroso Siltstone Mb, Sulphur Mountain Fm	siltstone, deltaic/shallow continental shelf environment
	PG-C	USA-C	Tuttle Creek Reservoir, near Manhattan, Pottowatomie County, Kansas	Bennett Shale Mb, Red Eagle Limestone Fm, Council Grove Grp	
	NT-W	Iran	Baghuk Mountain, NW of Abadeh	Hambast Fm	deep shelf limestone
	NT-W	Iran	Baghuk Mountain, NW of Abadeh	Hambast Fm	deep shelf limestone
	PT-N	Russia-W	Krasnoufimsk, Sverdlovsk Oblast		
	PT-N	Russia-W	Krasnoufimsk, European Russia		*Helicoprion* marls; basinal
	PT-N	Russia-W	middle and south Urals		
	PT-N	Russia-W	pre-Uralian region and southern Urals		
	PT-N	Russia-W	pre-Uralian region		
Paraná Basin	PG-S	Brazil	São Gabriel Municipality, Rio Grande do Sul, S	Teresina Fm, Passa Dois Grp	
Phosphoria Basin (see Piper & Link 2002)	PL-E	USA-N	Dinwoody Creek, Wind River Mountains, Wyoming	Pustula Mb, Middle Phosphoria Fm (=Retort Mb)	Thin phosphate bed
	PG-C	USA-C	Pottawatomie County, Kansas (Everhart, pers. comm.)	Neva Limestone Mb., Genola Limestone Fm, Council Grove Grp	Poorly consolidated limey mud
Phosphoria Basin (see Piper & Link 2002)	PL-E	USA-N	North Fork of Little Wind River and Bull Lake Creek, Wind River Mountains, Lander, Wyoming	Embar Fm (basal Phosphoria Fm) (=Park City Fm)	
	PT-N	Russia-W	Ural Mountains	*Omphalotrochus* Beds	
Artinskian	BOR	Russia-NW	Kozhim, Nearpolar Urals		
Phosphoria Basin (see Piper & Link 2002)	PL-E	USA-N	Wyoming	Retort Mb, Phosphoria Fm	mudflat
	PL-E	Canada-W	Dunedin River, British Columbia	Fantasque Fm	
Nward extension of Phosphoria conditions	PL-E	Canada-W	Sundance Canyon, Banff, Rocky Mountains, Alberta	base Ranger Canyon Fm, Ishbel Grp	phosphatic conglomerate; Phosphoria depositional conditions
Sverdrup Basin	BOR	Canada-N	Blind Fiord, Ellesmere Island, Canadian Arctic Archipelago	Van Hauen Fm	black shales (basin centre)
Sverdrup Basin	BOR	Canada-N	St. Arnaud Hills, Sabine Peninsula, Melville Island, Parry Islands, Canadian Arctic Archipelago	Assistance Fm	fine-grained, quartzose sandstone from a concretionary sandstone bed (southern basin margin)
	BOR	Spitsbergen	Bellsund	"Brachiopod cherts" (=Vøringen Mb, Kapp Starostin Fm)	
	NT-W	Iran?			

marine			Bendix-Almgreen *et al.* 1988		
marine		TBC	this study		Samples 090816-F, 090816-G, 090816-A, 090816-B, 090818-A
			Westoll 1941	Schultze 1986; Ginter *et al.* 2010	
			Hrouda & Brandt 2005	Ginter *et al.* 2010	(as *Hybodus mackrothi* Geinitz 1861/62)
marine	1 m in length		Mutter & Neuman 2008a	Ginter *et al.* 2010	
marine			Mutter & Neuman 2008a		
marine			Nielsen 1932, 1952	Nielsen 1935; Stensiö 1961; Bendix-Almgreen 1976; Ginter *et al.* 2010	(as *Agassizodus* and *Copodus* ? sp.)
marine			Bendix-Almgreen *et al.* 1988		
			Kozlov 2000	Ivanov 2000	
marine			Mutter & Neuman 2008a		
			Schultze & West 1996	Ginter *et al.* 2010	
marine			Hampe *et al.* 2013		
marine			Hampe *et al.* 2013		
				Ginter *et al.* 2010	
marine				Chabakov 1927	
			Kozlov 2000	Ivanov 2000	
			Karpinsky 1903	Ivanov 2000	
			Khabakov 1939	Ivanov 2000	
freshwater			Richter 2007	Ginter *et al.* 2010	
			Branson 1933	Nielsen 1935	(as ? *Campodus*)
			Ewell & Everhart 2005		
			Branson 1916		(as *Campodus* sp. indet., but cf. *variabilis*)
			Karpinsky 1922	Teichert 1940; Ginter *et al.* 2010	
			Chuvashov 1989	Ivanov 1999, 2000; Chuvachov 2001; Lebedev 2009	
marine			Dunkle & Van Sickle 1968	Yochelson & Van Sickle 1968; Chorn 1978; Ginter *et al.* 2010	
marine			Bamber *et al.* 1968	Nassichuk 1971, Chorn 1978; Lebedev 2009; Ginter *et al.* 2010	
marine, restricted circulation			Logan & McGugan 1968	Nassichuk 1971; Ginter *et al.* 2010	(may be conspecific with *H. ferrieri*), age revised from Art-Kung using Lexicon of Canadian Geologic Units
marine			Nassichuk & Spinosa 1970; Nassichuk 1971	Lebedev 2009; Ginter *et al.* 2010	
marine			Nassichuk 1971		
			Siedlecki 1970	Bendix-Almgreen 1966?; Lebedev 2009; Ginter *et al.* 2010	age based on correlation by Nakamura *et al.* 1987
			Obruchev 1964	Lebedev 2009; Ginter *et al.* 2010	

942	*Helicoprion*	*davisi* (Woodward, 1886)				Agassizodontidae	Eugeneodontiformes	Permian	Cisuralian	Kungurian (Artinskian)
943	*Helicoprion*	*davisi* (Woodward, 1886)				Agassizodontidae	Eugeneodontiformes	Permian	Cisuralian	Kungurian (Artinskian)
944	*Helicoprion*	cf. *davisi* (Woodward, 1886)				Agassizodontidae	Eugeneodontiformes	Permian	Cisuralian	Artinskian
945	*Helicoprion*	sp.				Agassizodontidae	Eugeneodontiformes	Permian	Cisuralian	Artinskian?
946	*Helicoprion*	*mexicanus* Mülleried, 1945				Agassizodontidae	Eugeneodontiformes	Permian	Cisuralian	Artinskian–Kungurian
947	*Helicoprion*					Agassizodontidae	Eugeneodontiformes	Permian	Cisuralian	Artinskian–Kungurian
948	*Helicoprion*	sp.				Agassizodontidae	Eugeneodontiformes	Permian	Cisuralian	Artinskian–Kungurian
949	*Helicoprion*	*bessonowi* Karpinsky, 1899			tooth whorl	Agassizodontidae	Eugeneodontiformes	Permian	Cisuralian	Artinskian
950	*Helicoprion?*	*bessonowi* Karpinsky, 1899			tooth	Agassizodontidae	Eugeneodontiformes	Permian	Cisuralian	Artinskian
951	*Helicoprion*	*bessonowi* Karpinsky, 1899			tooth whorl fragments	Agassizodontidae	Eugeneodontiformes	Permian	Cisuralian	Artinskian
952	*Helicoprion?*	*bessonowi* Karpinsky, 1899			teeth, denticles	Agassizodontidae	Eugeneodontiformes	Permian	Cisuralian	Artinskian
953	*Helicoprion*	*bessonowi* Karpinsky, 1899			tooth whorl fragment	Agassizodontidae	Eugeneodontiformes	Permian	Cisuralian	Kungurian
954	*Helicoprion*	*ergassaminon* Bendix-Almgreen, 1966			jaw, tooth spiral	Agassizodontidae	Eugeneodontiformes	Permian	Guadalupian	Roadian
955	*Helicoprion*	*ferrieri* Hay, 1907			tooth spiral, part	Agassizodontidae	Eugeneodontiformes	Permian	Guadalupian	Roadian
956	*Helicoprion*	*ferrieri* Hay, 1907			neurocrania, jaws, tooth spirals	Agassizodontidae	Eugeneodontiformes	Permian	Guadalupian	Roadian
957	*Helicoprion*	cf. *ferrieri* Hay, 1907			tooth spiral, part	Agassizodontidae	Eugeneodontiformes	Permian	Guadalupian	Roadian
958	*Helicoprion*	*ferrieri* Hay, 1907			tooth spiral, part	Agassizodontidae	Eugeneodontiformes	Permian	Cisuralian	Asselian–**Artinskian** (Wolfcampian)
959	*Helicoprion*	*nevadensis* Wheeler, 1939				Agassizodontidae	Eugeneodontiformes	Permian	Lopingian	
960	*Helicoprion*	*sierrensis* Wheeler, 1939				Agassizodontidae	Eugeneodontiformes	Permian	Cisuralian	Artinskian?
961	*Helicoprion*	sp.				Agassizodontidae	Eugeneodontiformes	Permian	Lopingian	
962	*Helicoprion*	sp. indet.				Agassizodontidae	Eugeneodontiformes	Permian	Cisuralian	Kungurian
963	*Helicoprion*	sp. indet.			tooth spiral, part	Agassizodontidae	Eugeneodontiformes	Permian	Lopingian	Wuchiapingian
964	*Helicoprion*	*jingmenense* Chen, Cheng & Yin, 2007				Agassizodontidae	Eugeneodontiformes	Permian	Cisuralian / Guadalupian	Artinskian
965	*Helicoprion*	sp. indet.				Agassizodontidae	Eugeneodontiformes	Permian	Cisuralian	Artinskian–Kungurian

	NT-E	Australia-W	Arthur River Valley, Gascoyne River District, Carnarvon Basin, W	*ex situ*	
	NT-E	Australia-W	Minilya River, near Wandagee Homestead, and Coolkilya Flat, near Wandagee Hill, Carnarvon Basin, W	Wandagee Fm	
	NT-W	Iran	Kuhgalu, Zagros Mountains		
	PT-E	Laos	north of Sarvane	Houei Nam Cham limestone	
	PL-E	Mexico	Las Delicias, Coahuila state		
	PL-E	Mexico	Chihuahua	La Casita Fm	
	PL-E	Mexico	Cerro Puntiagudo, San Salvador Patlanoaya, Puebla state	Patlanoaya Fm, Unit IV	calcarous concretion in shale
	PT-N	Russia-W	Divya Gora quarry, Krasnoufimsk District, Sverdlovsk Region, Ural Mountains, European Russia	Arta Beds, Divya Fm	*Helicoprion* marls; basinal
	PT-N	Russia-W	Divya Gora quarry, Krasnoufimsk District, Sverdlovsk Region, Ural Mountains, European Russia	Arta Beds, Divya Fm	
Uralian Strait	PT-N	Kazakhstan	Aktasty River, Aktyubinsk Region, Cisurals		
Uralian Strait	PT-N	Kazakhstan	Aktasty River, Aktyubinsk Region, Cisurals		
	PL-C	Japan	Waterasegawa River, near Hanawa, Azuma-mura, Seta-gun, Gunma Prefecture, central Honshu	Yagihawa Limestone	grey limestone
Phosphoria Basin (see Piper & Link 2002)	PL-E	USA-W	Gay Mine, Fort Hall Reservation, Bingham County, Idaho	Phosphoria Fm	bituminous, phosphatic limestone boulders
Phosphoria Basin (see Piper & Link 2002)	PL-E	USA-W	Montpelier, Bear Lake County, Idaho	Phosphoria Fm	
Phosphoria Basin (see Piper & Link 2002)	PL-E	USA-W	Waterloo Mine, Montpelier Canyon, Montpelier, Bear Lake County, Idaho	Phosphoria Fm	bituminous, phosphatic limestone boulders
Phosphoria Basin (see Piper & Link 2002)	PL-E	USA-W	Waterloo Mine, Montpelier Canyon, Montpelier, Bear Lake County, Idaho	Phosphoria Fm	bituminous, phosphatic limestone boulders
	PG-C	USA-S	Dugout Mountain, Glass Mountains, near Marathon, Texas	Decie Ranch Mb, Skinner Ranch Fm	crinoidal and fusulinid-rich limestone typical of rocky, near-shore environment in shallow, perhaps turbulent water
	PL-E	USA-W	near Upper Rochester, Humboldt Range, Perking and Lander County, NW Nevada	Koipato Volcanics, Rochester trachyte	stratified tuff
	PL-E	USA-W	Frazier Creek, Mohawk Valley, Plumas County, N Sierra Nevada, California	*ex situ*	boulder from glacial moraine
Phosphoria Basin (see Piper & Link 2002)	PL-E	USA-W	Gay Mine, Fort Hall Reservation, Bingham County, Idaho	Phosphoria Fm	
	PL-E	USA-W	China Mountain, near Contact, Nevada		
Phosphoria Basin (see Piper & Link 2002)	PL-E	USA-W	Waterloo Mine, Montpelier Canyon, Montpelier, Bear Lake County, Idaho	Phosphoria Fm	bituminous, phosphatic limestone boulders
	PT-E	China-E	Jingmen County, Hubei Province	Qixia Fm?, Yangsin Series	
	PG-C	USA-S	Williams Ranch, Bone Canyon, Guadalupe Mountains, Culberson County, Texas	Bone Spring Fm	Black lime mudstone beds (deep, stagnant basin)

marine			Woodward 1886	Teichert 1940; Lebedev 2009; Ginter *et al.* 2010	(as *Edestus davisii*)
marine			Teichert 1940	Turner 1993; Lebedev 2009; Ginter *et al.* 2010	
			Douglas 1950	Hampe *et al.* 2013	
			Hoffet 1933	Wheeler 1939; Teichert 1940; Lebedev 2009; Ginter *et al.* 2010	
			Mülleried 1945; Applegate 1989	Derycke-Khatir *et al.* 2005; Lebedev 2009; Ginter *et al.* 2010	
			Bridges & De Ford 1962	Derycke-Khatir *et al.* 2005; Ginter *et al.* 2010	
marine			Sour-Tovar *et al.* 1991, 2000	Derycke-Khatir *et al.* 2005; Lebedev 2009; Ginter *et al.* 2010	
marine			Karpinsky 1899	Karpinsky 1911; Chabakov 1927; Obruchev 1964; Ivanov 2000; Derycke-Khatir *et al.* 2005; Lebedev 2009; Ginter *et al.* 2010	(also as *H. bezsonowi*)
			Karpinsky 1904	Nielsen 1952; Lebedev 2009	(as *Campodus* sp.)
marine	cephalopod and fish feeder		Lebedev 2009		
marine	cephalopod and fish feeder		Lebedev 2009		(teeth as ? *Helicoprion bessonowi* (*Campodus* sp.))
		Fusulina limestone	Yabe 1903	Teichert 1940; Goto 1972, 1975, 1985, 1994a, b, 1996a–c, 1999a, b, 2000; Goto & Kuga 1982; Goto *et al.* 1988; Lebedev 2009; Ginter *et al.* 2010	
marine, restricted circulation			Bendix-Almgreen 1966	Lebedev 2009; Ginter *et al.* 2010	
marine, restricted circulation			Hay 1907, 1909, 1929	Bendix-Almgreen 1966; Lebedev 2009; Ginter *et al.* 2010	(as *Lissoprion*)
marine, restricted circulation			Bendix-Almgreen 1966		
marine, restricted circulation			Bendix-Almgreen 1966		
marine			Kelly & Zangerl 1976	Chorn 1978; Lebedev 2009; Ginter *et al.* 2010	
			Wheeler 1939	Bendix-Almgreen 1966; Lebedev 2009; Ginter *et al.* 2010	(problematic stratigraphy, Artinskian was suggested based on known range of *Helicoprion* in 1939; see also Alvarez & O'Connor 2002)
			Wheeler 1939	Bendix-Almgreen 1966; Lebedev 2009; Ginter *et al.* 2010	(problematic stratigraphy, Artinskian age based on correlations)
marine, restricted circulation			Dunkle & Williams 1948	Bendix-Almgreen 1966	
			Larson & Scott 1951	Bendix-Almgreen 1966	
marine, restricted circulation			Bendix-Almgreen 1966		
			Chen *et al.* 2007b	Lebedev 2009	
			Chorn 1978	Derycke-Khatir *et al.* 2005	

966	*Helicoprion*	sp.			tooth whorl fragment	Agassizodontidae	Eugeneodontiformes	Permian	Lopingian	Wuchiapingian
967	*Helicoprion*	*karpinskii* Obruchev, 1953				Agassizodontidae	Eugeneodontiformes	Permian	Cisuralian	Kungurian
968	*Helicoprion*	sp.			tooth whorl	Agassizodontidae	Eugeneodontiformes	Permian	Cisuralian	Kungurian
969	*Helicoprion*	sp.				Agassizodontidae	Eugeneodontiformes	Permian	Cisuralian	Artinskian
970	*Helicoprion*	sp.				Agassizodontidae	Eugeneodontiformes	Permian	Cisuralian	Artinskian
971	*Parahelicoprion*	*clerci* (Karpinsky, 1916)			tooth whorl	Agassizodontidae	Eugeneodontiformes	Permian	Cisuralian	Artinskian
972	*Parahelicoprion?*	sp.			spine	Agassizodontidae	Eugeneodontiformes	Permian	Cisuralian	Artinskian
973	*Parahelicoprion*	*maricsuarezi* Merino-Rodo & Janvier, 1986			tooth whorl	Agassizodontidae	Eugeneodontiformes	Permian	Cisuralian	Artinskian–Kungurian
974	*Sarcoprion*	*edax* Nielsen, 1952			teeth, denticles, crania	Agassizodontidae	Eugeneodontiformes	Permian	Lopingian	Wuchiapingian
975	*Hunanohelicoprion*	*xiandongensis* Liu 1994				Agassizodontidae	Eugeneodontiformes	Permian	Cisuralian / Guadalupian	Changhsingian
976	*Hunanohelicoprion*	*xiandongensis* Liu 1994				Agassizodontidae	Eugeneodontiformes	Permian	Guadalupian	
977	*Sinohelicoprion*	*macrodontus* Lei, 1983				Agassizodontidae	Eugeneodontiformes	Permian	Lopingian	
978	*Shaktaulites*	*sewyi* Chuvashov, 2001			tooth whorl	Agassizodontidae	Eugeneodontiformes	Permian	Cisuralian	Sakmarian
979	~~*Edestus*~~	~~*minusculus* Hay, 1909~~				~~Edestidae~~	~~Eugeneodontiformes~~	~~Permian~~	~~Cisuralian~~	~~Artinskian~~
980	*Edestus?*	sp.			tooth fragments	Edestidae	Eugeneodontiformes	Permian	Guadalupian	Capitanian
981	*Symcomodus*	*abbreviatus* Obruchev, 1964				Edestidae	Eugeneodontiformes	Permian	Lopingian	
982	*Helicampodus*	*changhsingensis* (Liu & Chang, 1963)				Edestidae	Eugeneodontiformes	Permian	Lopingian	
983	*Helicampodus*	*changhsingensis* (Liu & Chang, 1963)				Edestidae	Eugeneodontiformes	Permian	Lopingian	
984	*Helicampodus*	*kokeni* Branson, 1935				Edestidae	Eugeneodontiformes	Permian	Lopingian	Changhsingian
985	*Helicampodus*	*ealoni* Obruchev, 1965				Edestidae	Eugeneodontiformes	Triassic	Lower	Induan (most likely Griesbachian derived from biostrat)
986	*Helicampodus*	*ealoni* Obruchev, 1965				Edestidae	Eugeneodontiformes	Triassic	Lower	
987	*Helicampodus?*	*gomolangma* (Zhang, 1976)				Edestidae	Eugeneodontiformes	Triassic	Lower	
988	*Helicampodus*	sp.			teeth	Edestidae	Eugeneodontiformes	Permian	Lopingian	Wuchiapingian (–Changhsingian)
989	*Parahelicampodus*	*spaeroki* Nielsen, 1952			fused teeth	Edestidae	Eugeneodontiformes	Triassic	Lower	Induan (Griesbachian)
990	gen. indet.	sp. indet.				Edestidae	Eugeneodontiformes	Triassic	Lower	Induan (Dienerian)

	PL-W	Japan	Kamiya-tsuse, Kesennuma City, Miyagi Prefecture, NE Honshu	Kanokura Fm/Toyoma Fm boundary	sandy shale
	PT-N	Russia-W	middle Urals (Cisurals)		
	BOR	Russia-NW	Timan-Pechora Basin		
	PT-N	Russia-W	southern Urals	Cajgadsinskji horizon	
	PT-N	Russia-W?	south of Osch		
	PT-N	Russia-W	Ural Mountains, European Russia	Arta Beds	*Helicoprion* marls; basinal
	PT-N	Russia-W	pre-Uralian region and southern Urals		
Andes	PL-E	Bolivia	Jacha Khatawi Hill, Yaurichambi, La Paz department	Copacabana Fm, Titicaca Grp (fish horizon 2)	burrowed calcareous red sandstone, sandy intertidal zone?
	BOR	Greenland-E	River 8–9 and 14, Kap Stosch, Hold with Hope	*Posidonia* Shale Mb (Ravnefjeld Fm), Foldvik Creek Grp	
	PT-E	China-SE	Xiandong, Lianyuan, Hunan	Qixia Fm, Yangsin Series	limestone intercalated between black shales
	PT-E	China-SE	Weining, Guizhou Province	Maokou Fm	
	PT-E	China-SE	Maanshan District, Jiahe, Hunan	Dalong Fm	
	PT-N	Russia-SW	Shakh-Tau quarry, near Sterlitamak, Bashkortostan, Cisurals (South Urals)	Sterlitamak Fm	
	~~PT-N~~	~~Russia-W~~	~~Myachkova, Moscow Region~~		
Phosphoria Basin (see Piper & Link 2002)	PL-E	USA-W	Dinwoody Creek, Wind River Mountains, Wyoming	Pustula Mb, Middle Phosphoria Fm (=Retort Mb)	Thin phosphate bed
	BOR	Russia-NE	Echi, Yana River, Yakutia		
	PT-E	China-E	Meishan, Changxing District, Zhejiang province	Changxing Limestone	
	PT-E	China-E	Meishan, Changxing District, Zhejiang province	Changxing Limestone	
	NT-W	Pakistan	Salt Range, Punjab	upper *Productus* limestone, Chiddru Fm	
	PT-N	Azerbaijan	Dorasham area		
	PT-N	Azerbaijan	Dzhul'fa (Julfa), Araks River, Nakhichevan Province		
	PT-E	Tibet	near Qubu, Dingri, Xian (Xizang) County	lower Tulong Grp	
	PL-W	Japan	Toyoma-cho, Toyoma-gun, Miyagi Prefecture, NE Honshu	Toyoma Fm	black shale
	BOR	Greenland-E	E of River 13, Kap Stosch, Hold with Hope	Fish Zone II, Wordie Creek Fm	
Boreal	BOR	Spitsbergen	Hyrnefjellet, Hornsund, S	Brevassfjellet *Aviculina* Bed, Urnetoppen Mb, Vardebukta Fm, Torell Land Grp	iron-rich, fine-grained conglomerate, concentrated deposit, offshore sand bars

			Araki 1980	Goto 1985, 1994a, b, 1996a–c, 1999a, b, 2000; Goto & Kuga 1982; Goto *et al.* 1988; Ginter *et al.* 2010	
			Obruchev 1953	Ivanov 2000; Lebedev 2009	
			Yankevich & Minikh 1998	Ivanov 2000	
			Licharew 1937 in pers. comm. with Wheeler 1939	Wheeler 1939	
			Licharew 1937 in pers. comm. with Wheeler 1939	Wheeler 1939	
marine			Karpinsky 1916	Chabakov 1927; Merino-Rodo & Janvier 1986; Ivanov 2000; Ginter *et al.* 2010	(as *Helicoprion* but also *Parahelicoprion* in Chabakov 1927)
			Khabakov 1939	Ivanov 2000	
marine	pelagic (stranded?)	? *Necostreptognathodus* aff. *sulcoplicatus* conodont zone; *Eoparafusulina* fusulinid zone	Merino-Rodo & Janvier 1986	Derycke-Khatir *et al.* 2005; Ginter *et al.* 2010	
marine			Nielsen 1952	Stensiö 1961; Bendix-Almgreen 1976; Ginter *et al.* 2010	
		Pseudohalorites (ammonoids) beds	Liu 1994	Chen *et al.* 2007b; Lebedev 2009	
			Cheng *et al.* 2004	Chen *et al.* 2007b; Lebedev 2009	
			Lei 1983	Liu & Wang 1994; Chen *et al.* 2007b; Lebedev 2009	(referable to *Helicampodus* ?)
			Chuvashov 2001	Ivanov 2007; Lebedev 2009	
			~~Karpinsky 1899, Hay 1899~~	Ivanov 2005; Ginter *et al.* 2010; Itano *et al.* 2012	(as *E.* cf. *minor*) age corrected as Pennsylvanian by Itano *et al.* 2012
			Branson 1933	Nielsen 1935; Itano *et al.* 2012	likely to belong to *Helicoprion* instead, Itano *et al.* 2012
			Obruchev 1964	Ginter *et al.* 2010	
			Liu & Chang 1963	Wang et al. 2007a; Chen *et al.* 2007b; Lebedev 2009; Ginter et al. 2010	(as e.g., *Sinohelicoprion changwingensis*)
			Liu & Wang 1994	Wang et al. 2007a; Chen *et al.* 2007b; Lebedev 2009	(as e.g., *Sinohelicoprion changwingensis*)
			Koken 1901	Branson 1935; Teichert 1940; Chorn 1978; Liu & Wang, 1994; Ginter *et al.* 2010	
		Claraia beds, *Tompophiceras* - *Paratirolites* beds	Ruzhentzev & Sarycheva 1955	Golshani & Janvier 1974	(as *Helicampodus egloni*)
			Obruchev 1965, 1967	Ginter *et al.* 2010; Brinkmann *et al.* 2010	
marine			Zhang 1976	Zhang 1979; Liu & Wang 1994; Chang & Miao 2004; Jin 2006; Chen *et al.* 2007b; Lebedev 2009; Ginter et al. 2010	(as *Sinohelicoprion*)
			Ueno *et al.* 1979 (oral presentation)	Goto 1985, 1994a, b, 1996a–c, 1999a, b, 2000; Goto & Kuga 1982; Goto et al. 1988	
marine		*Metophiceras subdemissum – Ophiceras commune* Zone (ammonoid)	Nielsen 1936, 1952	Bendix-Almgreen 1976; Birkenmajer & Jerzmańska 1979; Ginter *et al.* 2010	(as Undetermined Edestid genus)
marine		*Proptychites candidus* Zone (ammonoid)	Birkenmajer & Jerzmańska 1979	Romano & Brinkmann 2010	

991	*Paredestus*	*bricircum* Mutter & Neuman, 2008			tooth whorl	Edestidae?	Eugeneodontiformes	Triassic	Lower	Olenekian (Smithian)?
992	gen. indet.	sp. indet.			partial bodies, denticles, tooth		Eugeneodontiformes	Triassic	Lower	Olenekian (Smithian)?
993	gen. indet.	sp. indet.					Eugeneodontiformes	Permian	Cisuralian	Sakmarian
994	gen. indet.	sp. indet.			tooth		Eugeneodontiformes?	Permian	Lopingian	Changhsingian
995	gen. indet.	sp. indet.			tooth fragments		Eugeneodontiformes?	Permian	Guadalupian	Wordian
996	*Janassa*	*angularis* Branson, 1916			tooth	Janassidae	Petalodontiformes	Permian	Guadalupian	Wordian
997	*Janassa*	*angularis* Branson, 1916				Janassidae	Petalodontiformes	Permian	Lopingian	
998	*Janassa*	*bituminosa* (Schlotheim, 1820)				Janassidae	Petalodontiformes	Permian	Guadalupian	
999	*Janassa*	*bituminosa* (Schlotheim, 1820)				Janassidae	Petalodontiformes	Permian	Guadalupian	
1000	*Janassa*	*bituminosa* (Schlotheim, 1820)				Janassidae	Petalodontiformes	Permian	Guadalupian	
1001	*Janassa*	*bituminosa* (Schlotheim, 1820)				Janassidae	Petalodontiformes	Permian	Lopingian	Wuchiapingian
1002	*Janassa*	*bituminosa* (Schlotheim, 1820)				Janassidae	Petalodontiformes	Permian	Lopingian	Wuchiapingian
1003	*Janassa*	*bituminosa* (Schlotheim, 1820)			part body fossil, teeth	Janassidae	Petalodontiformes	Permian	Lopingian	Wuchiapingian
1004	*Janassa*	*bituminosa* (Schlotheim, 1820)			tooth plates	Janassidae	Petalodontiformes	Permian	Guadalupian –Lopingian	Roadian–Wordian (Kazanian), Wuchiapingian (Tatarian)
1005	*Janassa*	*bituminosa* (Schlotheim, 1820)			teeth, body	Janassidae	Petalodontiformes	Permian	Lopingian	Wuchiapingian
1006	*Janassa*	*bituminosa* (Schlotheim, 1820)			body, anterior	Janassidae	Petalodontiformes	Permian	Lopingian	Wuchiapingian
1007	*Janassa*	*empalinus* (Cope, 1883)				Janassidae	Petalodontiformes	Permian		
1008	*Janassa*	*koohi* Nielsen, 1932			teeth	Janassidae	Petalodontiformes	Permian	Lopingian	Wuchiapingian
1009	*Janassa*	*koohi* or *unguicula*				Janassidae	Petalodontiformes	Permian	Lopingian	Wuchiapingian
1010	*Janassa*	*korni* (Weigelt, 1930)				Janassidae	Petalodontiformes	Permian	Guadalupian	
1011	*Janassa*	*korni* (Weigelt, 1930)				Janassidae	Petalodontiformes	Permian	Lopingian	**Vuchiapingian–Changhsingian**
1012	*Janassa*	*strigilina* (Cope, 1881)				Janassidae	Petalodontiformes	Permian		
1013	*Janassa*	*unguicula* (Eastman, 1903)				Janassidae	Petalodontiformes	Permian	Lopingian	Wuchiapingian
1014	*Janassa*	*unguicula* (Eastman, 1903)				Janassidae	Petalodontiformes	Permian	Guadalupian	Capitanian
1015	*Janassa*	*unguicula* (Eastman, 1903)			teeth	Janassidae	Petalodontiformes	Permian	Guadalupian	Wordian
1016	*Janassa*	*unguiformes* (Newberry & Worthen, 1870)			tooth	Janassidae	Petalodontiformes	Permian	Guadalupian	Wordian
1017	*Janassa*	sp.			tooth	Janassidae	Petalodontiformes	Permian	Cisuralian–Guadalupian	Kungurian–Roadian

	PL-E	Canada-W	Ganoid Ridge, Wapiti Lake, near "Fossil Fish Lake", British Columbia, W	Vega-Phroso Siltstone Mb, Sulphur Mountain Fm	siltstone, deltaic/shallow continental shelf environment
	PL-E	Canada-W	Ganoid Ridge, Wapiti Lake, near "Fossil Fish Lake", British Columbia, W	Vega-Phroso Siltstone Mb, Sulphur Mountain Fm	siltstone, deltaic/shallow continental shelf environment
	NT-E	Australia-W	W	Fossil Cliff Mb, Holmwood Shale	
E Greenland Basin	BOR	Greenland-E	Kap Stosch, Hold with Hope	Schuchert Dal/Wordie Creek Fm	marginal
Madagascar Embayment	NT-W	Oman	Haushi Cliff, Haushi-Huqf region, E	Khuff Fm	rim basin
Phosphoria Basin (see Piper & Link 2002)	PL-E	USA-W	North Fork of Little Wind River and Bull Lake Creek, Wind River Mountains, Lander, Wyoming	Embar Fm (basal Phosphoria Fm) (=Park City Fm)	
	NT-W	Pakistan		*Productus* Limestone	
	PT-W	Germany	Richelsdorf and Schmerbach, Thüringen / Mansfeld	Kupferschiefer	
	PT-W	Germany		Kupferschiefer	
	PT-W	England	Durham	Marl Slate	
	PT-W	England	Thickley, South Durham	Marl Slate (correlative to Kupferschiefer)	5-6 ft. thick, layered, soft, yellow, flaggy arenaceous limestone
	PT-W	England	Middridge, South Durham	Marl Slate	
	PT-W	Germany	Hüggel Mountain, Hasbergen, Osnabrücker Bergland, NW	Copper Shale Mb (Kupferschiefer Mb), Werra Fm	laminated bituminous black shale marls (fish bed), shallow-water submarine swell zone (coastal)
	PT-N	Russia-W	(Arkhangelsk and Vyatka districts, Tataria) northern European Russia		pelecypod limestone, hemipelagic (shelf); variegated marl, littoral/lagoon/estuary/delta
	PT-W	Germany	Rossenray	Kupferschiefer	
	PT-W	Germany	Hessen	Kupferschiefer	
	PG-N	USA-E	Illinois		
	BOR	Greenland-E	Section F (120 m above sea level), Kap Stosch, Hold with Hope	*Posidonia* Shale Mb (Ravnefjeld Fm), Foldvik Creek Grp	
	BOR	Greenland-E	Margrethedal, Gauss Halvø	*Posidonia* Shale Mb (Ravnefjeld Fm), Foldvik Creek Gp	
	PT-W	Germany	Mansfeld	Kupferschiefer	
	PT-W	Germany	Eisleben, Sachsen-Anhalt	Kupferschiefer and Zechsteinkalk	
	PG-N	USA-E	Illinois		
	BOR	Greenland-E		*Posidonia* Shale Mb (Ravnefjeld Fm), Foldvik Creek Grp	
Phosphoria Basin (see Piper & Link 2002)	PL-E	USA-W	Little Wind River, Wind River Mountains, Wyoming	Pustula Mb, Middle Phosphoria Fm (=Retort Mb)	Thin phosphate bed
Phosphoria Basin (see Piper & Link 2002)	PL-E	USA-W	North Fork of Little Wind River and Bull Lake Creek, Wind River Mountains, Lander, Wyoming	Embar Fm (basal Phosphoria Fm) (=Park City Fm)	
Phosphoria Basin (see Piper & Link 2002)	PL-E	USA-W	North Fork of Little Wind River and Bull Lake Creek, Wind River Mountains, Lander, Wyoming	Embar Fm (basal Phosphoria Fm) (=Park City Fm)	
Kaibab Sea	PL-E	USA-W	Grand Canyon, Arizona	Kaibab Fm	

marine			Mutter & Neuman 2008a	Ginter *et al.* 2010	
marine	1 m in length		Mutter & Neuman 2008a		
			Fernandino 1992	Turner 1993	
marine		TBC	this study		Sample 09.08.22.c
marine		*Idiognathodella aserrata* conodont Zone; OSPZ6 palynology Zone; *Neoschwagerina craticulifera* fusulinid Zone	this study		Sample 965-2
			Branson 1916	Ginter *et al.* 2010	
				Ginter *et al.* 2010	
			Schlotheim 1820	Weigelt 1930; Schaumberg 1977; Ginter *et al.* 2010	(as *Trilobites*)
			Münster 1839, 1840	Schaumberg 1977	(as *Dictea*)
				Bell *et al.* 1979; Ginter *et al.* 2010	
			Brown 1905		
			Hancock & Howse 1870	Brown 1905; Malzahn 1968	
marine with freshwater influence	benthic bryozoa feeder		Diedrich 2009a		
marine				Chabakov 1927; Khabakov 1926–27, 1939; Ivanov 2000, 2005	
	bottom-dweller		Malzahn 1968	Schaumberg 1977	
			Malzahn 1972		
			Cope 1883	Ginter *et al.* 2010	(as *Thoracocdus*)
marine			Nielsen 1932	Nielsen 1935; Stensiö 1961; Bendix-Almgreen 1976; Ginter *et al.* 2010	
marine			Bendix-Almgreen *et al.* 1988		
			Weigelt 1930	Malzahn 1968; Schaumberg 1977; Ginter *et al.* 2010	(as *Ctenoptychius*)
			Brandt 1996		
			Cope 1881	Ginter *et al.* 2010	
marine				Bendix-Almgreen 1976	
			Branson 1933	Nielsen 1935	
			Branson 1916		
			Branson 1916	Ginter *et al.* 2010	
marine			Hussakof 1943	Hunt *et al.* 2005	

1018	*Janassa*	sp.				Janassidae	Petalodontiformes	Permian	Cisuralian	Kungurian
1019	*Janassa*	sp.			tooth	Janassidae	Petalodontiformes	Permian	Cisuralian	Kungurian
1020	*Janassa*	sp.				Janassidae	Petalodontiformes	Permian	Cisuralian	Sakmarian
1021	*Janassa*	sp.				Janassidae	Petalodontiformes	Permian	Guadalupian	**Roadian–Wordian**
1022	*Janassa*	sp.				Janassidae	Petalodontiformes	Permian	Guadalupian	Capitanian (Kazanian)
1023	*Megactenopetalus*	*kaibabanus* David, 1944			tooth	Pristodontidae	Petalodontiformes	Permian	Cisuralian	Kungurian
1024	*Megactenopetalus*	*kaibabanus* David, 1944			tooth	Pristodontidae	Petalodontiformes	Permian	Lopingian	Wuchiapingian
1025	*Megactenopetalus*	*kaibabanus* David, 1944			tooth	Pristodontidae	Petalodontiformes	Permian	Cisuralian	Kungurian
1026	*Megactenopetalus*	*kaibabanus* David, 1944			tooth	Pristodontidae	Petalodontiformes	Permian	Cisuralian	Kungurian
1027	*Megactenopetalus*	*kaibabanus* David, 1944			tooth	Pristodontidae	Petalodontiformes	Permian	Cisuralian	Kungurian
1028	*Megactenopetalus*	*kaibabanus* David, 1944			tooth, spine	Pristodontidae	Petalodontiformes	Permian	Cisuralian	Artinskian–Kungurian
1029	*Megactenopetalus*	*kaibabanus* David, 1944				Pristodontidae	Petalodontiformes	Permian	Cisuralian	
1030	*Megactenopetalus*	*kaibabanus* David, 1944			symphyseal tooth fragment	Pristodontidae	Petalodontiformes	Permian	Cisuralian	Artinskian–Kungurian
1031	*Megactenopetalus*	*kaibabanus* David, 1944			tooth	Pristodontidae	Petalodontiformes	Permian	Lopingian	Wuchiapingian
1032	*Megactenopetalus*	*kaibabanus* David, 1944			tooth	Pristodontidae	Petalodontiformes	Permian	Guadalupian	
1033	*Peripristis*	*semicircularis* Newberry & Worthen, 1866				Pristodontidae	Petalodontiformes	Permian	Cisuralian	
1034	*Petalorhynchus* ?	sp.				Pristodontidae	Petalodontiformes	Permian	Lopingian	Wuchiapingian
1035	gen. indet.	sp. indet.					Petalodontiformes	Permian	Cisuralian	Asselian, lower
1036	*Petalodus*	sp. A			tooth	Petalodontidae	Petalodontiformes	Permian		
1037	*Petalodus*	sp. B			tooth	Petalodontidae	Petalodontiformes	Permian		
1038	*Petalodus*	sp. C			teeth	Petalodontidae	Petalodontiformes	Permian	Cisuralian	Asselian–Artinskian
1039	*Petalodus*	sp. D			teeth	Petalodontidae	Petalodontiformes	Permian	Cisuralian	Asselian–Artinskian
1040	*Petalodus*	*alleghaniensis* Leidy, 1856				Petalodontidae	Petalodontiformes	Permian	Cisuralian	
1041	*Petalodus*	*acuminatus* (Agassiz, 1838)				Petalodontidae	Petalodontiformes	Permian	Cisuralian	Asselian
1042	*Petalodus*	*ohioensis* (Safford, 1853)				Petalodontidae	Petalodontiformes	Permian	Cisuralian	
1043	*Petalodus*	*ohioensis* (Safford, 1853)				Petalodontidae	Petalodontiformes	Permian	Cisuralian	
1044	*Petalodus*	*ohioensis* (Safford, 1853)			teeth	Petalodontidae	Petalodontiformes	Permian	Cisuralian	Artinskian
1045	*Petalodus*	sp.			tooth	Petalodontidae	Petalodontiformes	Permian	Cisuralian	Asselian–Sakmarian

Kaibab Sea	PL-E	USA-W	near Point Sublime, North Rim, Grand Canyon, Arizona	β Mb, Kaibab Fm	Facies 3 (McKee 1938), fine-grained sandstone (near-shore deposit)
	PL-C	Japan	Yamasuge, Kuzuu-cho, Aso-gun, Tochigi Prefecture, central Honshu	Nabeyama Fm	black limestone
	PG-C	USA-C	Cowley County, Kansas	Speiser Shale, Council Grove Grp; Wreford Limestone, Chase Grp; Wreford Megacyclothem	shallow to open marine (50 m water depth)
Phosphoria Basin (see Piper & Link 2002)	PL-E	USA-N	Wyoming	Meade Peak Mb, Phosphoria Fm; lower Mb, Shedhorn Fm	mudflat and near-shore sands
	PT-N	Russia-W	European Russia		pelecypod limestone; hemipelagic (shelf)
Kaibab Sea	PL-E	USA-W	near Point Sublime, North Rim, Grand Canyon, Arizona	β Mb, Kaibab Fm	Facies 3 (McKee 1938), fine-grained sandstone (near-shore deposit)
	NT-W	Iran	Kuh-e-Hambast, Abadeh region, central (N 30°55' E 53°15')		thin-bedded, grey to brown-red / red, hard limestone
Kaibab Sea	PL-E	USA-W	near Point Sublime, North Rim, Grand Canyon, near Sedona, Arizona	α Mb, Kaibab Fm	
	PG-C	USA-S	Glass Mountains, Texas	Cathedral/Road Canyon Fm?	shallow water, clastic-rich environment
	PG-C	USA-S	near Hachita, Hidalgo County, New Mexico	Glorieta Fm/Concha Fm?	near-shore clastic environment?
	PG-C	USA-S	Santa Cruz County, Arizona	Concha Fm, Naco Grp	
	PG-C	USA-C	Oklahoma		
Andes	PL-E	Bolivia	Jacha Khatawi Hill, Yaurichambi, La Paz department	Copacabana Fm, Titicaca Grp (fish horizon 1)	limestone, shallow benthic environment
	PT-E	China-E	Pahsien, Szechuan	Loping Series	
	PT-E	China-E	Liangshan, Hanchung, southern Shensi (Shaanxi)	Maokou Limestone, Yangsin Series	
	PG-N	USA-E	mid-continent and Appalachian Basin (Indiana, Ohio, Pennsylvania, Kentucky, West Virginia)		
	NT-W	Iran	Kuh-e-Hambast, Abadeh region, central (N 30°55' E 53°15')		thin-bedded, grey to brown-red / red, hard limestone
	PT-W	Italy	Piani di Lanza, Carnic Alps, Paularo, Friuli-Venzia Giulia Region, NE	Formazione inferiore a *Pseudoschwagerina* , basal Rattendorf Group	black limestone (shallow sea, 10–30m depth)
	PG-C	USA-C	S Kansas	Grenola Limestone, Council Grove Grp	
	PG-C	USA-C	Blu Mont Hill, near Manhattan, Riley County, Kansas	Hughes Creek shale	brown shale
	PG-C	USA-C	south of Manhattan, Riley County, Kansas	Florence Limestone, Chase Grp	
	PG-C	USA-C	Payne County, Oklahoma	Americus Limestone, Council Grove Grp	
	PG-C	USA-C	Pottawatomie County, Kansas	Neva Limestone Mb., Genola Limestone Fm, Council Grove Grp	poorly consolidated limey mud
	PL-C	Japan	Fukuji, Kamitakara-mura, Gifu Prefecture, central Honshu	Mizuyagadani Fm	black limestone
	PG-N	USA-E	Pennsylvania, Ohio, Illinois, Nebraska, Missouri		
	PG-C	USA-S/C	Colorado, Arkansas, Kansas, Arizona, Texas		
	PT-N	Russia-W	Dewitschja-Berges, near Krasnoufimsk, pre-Uralian region and southern Urals, European Russia		*Helicoprion* marls; basinal
	PG-C	USA-S	Big Hatchet Mountains, Hidalgo County, SW New Mexico	Horquilla Fm	

brackish			David 1944		
			Goto 1975, 1984	Goto 1985; 1994a, b, 1996a–c, 1999a, b, 2000; Goto & Kuga 1982; Goto *et al.* 1988	(as *Petalorhynchus* (*Petalodus*))
marine			Schultze 1985		
marine			Yochelson & Van Sickle 1968		
marine			Krotov 1903	Chabakov 1927	(as *"Cymatodus"*; considered close to *Helodus*)
brackish			David 1944	Hansen 1978; Hunt *et al.* 2005; Ginter *et al.* 2010	
		Pseudogastrioceras beds	Golshani & Janvier 1974	Hansen 1978; Hunt *et al.* 2005; Ginter *et al.* 2010; Hampe *et al.* 2011, 2013	(as tentative)
			Ossian 1976	Hansen 1978; Hunt *et al.* 2005; Ginter *et al.* 2010; Hodnett *et al.* 2012	
			Ossian 1976	Hansen 1978; Hunt *et al.* 2005; Ginter *et al.* 2010	
			Ossian 1976	Hansen 1978; Hunt *et al.* 2005; Ginter *et al.* 2010	
			Hansen 1978	Hunt *et al.* 2005; Ginter *et al.* 2010	
				Ginter *et al.* 2010	
marine	durophagous (bryozoa, molluscs, crinoids)	? *Mecstreptognathodus* aff. *sulcoplicatus* conodont zone; *Eoparafusulina* fusulinid zone	Merino-Rodo & Janvier 1986	Ginter *et al.* 2010	(as *Megactenopetalus* sp.)
			Young 1950	Liu & Hsieh 1965; Hansen 1978; Ginter *et al.* 2010	(as *Petalodus shinkuoi* n. sp.) *nomen dubium* (Ginter *et al.* 2010)
			Liu & Hsieh 1965	Hansen 1978; Hunt *et al.* 2005	(as *Petalodus* cf. *shinkuoi*)
				Ginter *et al.* 2010	
		Pseudogastrioceras beds	Golshani & Janvier 1974	Hampe *et al.* 2013	
marine			Dalla Vecchia 2000		(resembles *Petalodus*, recovered from same area as *P. ohioensis*)
			Miller & Mann 1958		
			Miller & Mann 1958		
			Miller & Mann 1958		
			Miller & Mann 1958		
			Ewell & Everhart 2005		Location from (Everhart, pers. comm.)
			Okura 1984	Goto 1994a, b, 1996a–c, 1999a, b, 2000; Goto *et al.* 1988; Goto & Okura 2004	(as *P. alleghaniensis*) as undefined Middle Permian occurrence in Ginter *et al.* 2010?
			Hansen 1985	Dalla Vecchia 2000; Ginter *et al.* 2010	
			Hansen 1985	Dalla Vecchia 2000; Ginter *et al.* 2010	
marine			Karpinsky 1899, 1903, 1916	Fredericks, 1915; Chabakov 1927; Romer 1945; Miller & Mann 1958; Ivanov 2000, 2005; Ginter *et al.* 2010	(as *Petalodus* sp.)
			Ivanov *et al.* 2007b		

1046	*Petalodus* ?	sp.			tooth	Petalodontidae	Petalodontiformes	Permian	Cisuralian	Sakmarian–Artinskian
1047	*Petalodus* ?	sp.				Petalodontidae	Petalodontiformes	Permian	Cisuralian	Sakmarian
1048	*Chomatodus* ?	sp.				Petalodontidae	Petalodontiformes	Permian	Cisuralian	
1049	*Itapyrodus*	*punctatus* Silva Santos, 1990				Petalodontidae	Petalodontiformes	Permian		
1050	*Itapyrodus*	*punctatus* Silva Santos, 1990			teeth	Petalodontidae	Petalodontiformes	Permian	Cisuralian	Artinskian
1051	*Permopetalodus*	*fredenii* Kozlov, 2000			teeth	Petalodontidae	Petalodontiformes	Permian	Cisuralian	Artinskian
1052	*'Mecpetalodus'*	sp. 1			teeth?	Petalodontidae	Petalodontiformes	Permian	Cisuralian	Kungurian
1053	*'Mecpetalodus'*	sp. 2			tooth	Petalodontidae	Petalodontiformes	Permian	Cisuralian	Kungurian (Artinskian–Capitanian)
1054	*'Mecpetalodus'*	sp. 3			tooth	Petalodontidae	Petalodontiformes	Permian	Lopingian	Wuchiapingian
1055	gen?	sp?				Petalodontidae	Petalodontiformes	Permian		
1056	gen. indet.	sp. indet.			teeth		Petalodontiformes?	Permian	Guadalupian	Wordian
1057	~~*Brachyhinodus*~~	~~*wichitaensis* Romer, 1942~~			~~tooth~~	~~*incertae sedis*~~		~~Permian~~	~~Cisuralian~~	~~Sakmarian~~
1058	*Desmiodus* ?	sp.				*incertae sedis*		Permian	Cisuralian	Sakmarian
1059	gen. indet.	sp. nov.			tooth whorls	*incertae sedis*		Permian	Cisuralian	Sakmarian
1060	*Helodus*	*subpollitus* Branson, 1916			teeth	Helodontidae	Helodontiformes	Permian	Guadalupian	Wordian
1061	*Helodus*	sp.			tooth	Helodontidae	Helodontiformes	Permian	Guadalupian	Wordian
1062	*Helodus*	sp.				Helodontidae	Helodontiformes	Permian	Guadalupian	**Roadian–Capitanian**
1063	*Helodus*	sp.			teeth	Helodontidae	Helodontiformes	Permian	Cisuralian	**Asselian–Artinskian**
1064	*Helodus*	sp.				Helodontidae	Helodontiformes	Permian	Cisuralian	**Sakmarian–Artinskian**
1065	*Helodus*	sp.			teeth	Helodontidae	Helodontiformes	Permian	Cisuralian	Artinskian
1066	*Helodus*	sp.			teeth	Helodontidae	Helodontiformes	Permian	Cisuralian	Asselian
1067	*Helodus*	sp.			teeth	Helodontidae	Helodontiformes	Permian	Cisuralian	Kungurian
1068	*Helodus*	sp.				Helodontidae	Helodontiformes	Permian	Cisuralian	Sakmarian

	PL-C	Japan	Ryozensan, Inukami-gun, Shiga Prefecture, central Honshu	Ryozensan Limestone	
	PG-C	USA-C	Morris County, Kansas	Speiser Shale, Council Grove Grp; Wreford Limestone, Chase Grp; Wreford Megacyclothem	shallow to open marine (50 m water depth)
	PG-C	USA-C	Pottawatomie County, Kansas (Everhart, pers. comm.)	Neva Limestone Mb., Genola Limestone Fm, Council Grove Grp	Poorly consolidated limey mud
Parnaíba Basin	PG-S	Brazil		Pedra do Fogo Fm	
Paraná Basin	PG-S	Brazil	Rio Claro, São Paolo State	Taquaral Mb, Irati Fm, Passa Dois Grp	Bioclasts in a bed of light-grey to grey, fining-upward, cross-laminated conglomeratic sandstone with angular to rounded, abundant granules and rare pebbles of quartz and chert dispersed in a very fine to coarse sandy matrix (shallow marine, coastal settings)
	PT-N	Russia-W	middle and south Urals		
	PL-C	Japan	Kinshozan, Akasaka-cho, Ohgaki City, Gifu Prefecture, central Honshu	lower Akasaka Limestone	
	PL-C	Japan	Neo-mura, Motosu-gun, Gifu Prefecture, central Honshu	Funabuseyama Fm	grey limestone
	PL-C	Japan	Kinshozan, Akasaka-cho, Ohgaki City, Gifu Prefecture, central Honshu	uppermost Akasaka Limestone	grey limestone
Paraná Basin	PG-S	Brazil	São Paulo State, S	Corumbataí Fm (equivalent of Teresina Fm, Passa Dois Grp)	
Madagascar Embayment	NT-W	Oman	Saiwan, Haushi-Huqf region, E	Khuff Fm	rim basin
	~~PG-C~~	~~USA-S~~	~~Godwin Creek, Baylor County, Texas~~	~~upper Admiral Fm, Wichita Grp~~	~~clays near marine limestones in red beds~~
	PG-C	USA-C	Greenwood County, Kansas	Speiser Shale, Council Grove Grp; Wreford Limestone, Chase Grp; Wreford Megacyclothem	shallow to open marine (50 m water depth)
	PGC	USA-S	Rattlesnake Canyon, Archer County, Texas	upper Nocona Fm	near-shore marine?
Phosphoria Basin (see Piper & Link 2002)	PL-E	USA-N	North Fork of Little Wind River and Bull Lake Creek, Wind River Mountains, Lander, Wyoming	Embar Fm (basal Phosphoria Fm) (=Park City Fm)	
Phosphoria Basin (see Piper & Link 2002)	PL-E	USA-N	North Fork of Little Wind River and Bull Lake Creek, Wind River Mountains, Lander, Wyoming	Embar Fm (basal Phosphoria Fm) (=Park City Fm)	
	PL-E	USA-N	Wyoming	Grandeur and Ervay Mbs, Park City Fm; lower and upper Mbs, Shedhorn Fm	lime sand/mud and near-shore sands
Dunkard Basin (freshwater, but marine influenced; Schultze & Soler-Gijón 2004)	PG-N	USA-E		Waynesburg, Washington and Greene Fms, Dunkard Grp	
	PG-C	USA-S	Rattlesnake Canyon, Archer County, north-central Texas	upper Admiral and upper Belle Plains Fms, Wichita-Albany Grp	
	PG-C	USA-S	Little Moonshine Creek, Texas	upper Lueders Fm, Albany Grp	claystone
	PG-C	USA-S	Archer County, Texas	Archer City Bonebed 3, Archer City Fm, Bowie Grp	lenticular mudstone; abandoned channel
	PG-C	USA-C	Northeast Frederick site, near Deep Red Creek, Tillman County, SW Oklahoma	upper Garber (Sandstone) Fm, upper Sumner Grp	sandstones, mudstone conglomerates, claystones; lacustrine environment in a coastal-plain setting
	PG-C	USA-C	Kansas	Matfield Shale, Chase Grp; Wreford Megacyclothem	intertidal

				Goto 1985, 1994a, b, 1996a–c, 1999a, b, 2000; Goto *et al.* 1988	(as *Serratodus?*)
marine			Schultze 1985	Johnson 1992	(as cf. *Serratodus*)
			Ewell & Everhart 2005		(as *Chomatodus*)
			Silva Santos 1990	Chahud *et al.* 2010	
mixed marine/freshwater (transgressive lag?)			Chahud *et al.* 2010		
			Kozlov 2000	Ivanov 2000	(similar to *Chomatodus*, Ivanov 2000)
		Parafusulina Zone	Ono 1980; Murata 1981	Goto 1985, 1994a, b, 1996a–c, 1999a, b, 2000; Goto & Kuga 1982; Goto *et al.* 1988; (Yokoi 1994, 2000? See Yamagishi 2006)	
		Parafusulina Zone	Murata & Ueno 1979 (oral presentation); Hamada & Itoigawa 1983	Goto 1985, 1994a, b, 1996a–c, 1999a, b, 2000; Goto & Kuga 1982	
marine			Goto 1994a	Goto 1994b, 1996a–c, 1999a, b, 2000	
marine/freshwater ?			Toledo *et al.* 1997	Richter 2005	
marine		*Jinogondolella aserrata* conodont Zone; OSPZ6 palynology Zone; *Necoschwagerina craticulifera* fusulinid Zone	this study		Sample AO214
~~marine~~			~~Romer 1942~~	Stahl 1999; Ginter *et al.* 2010	(deposit re-interpreted as reworked and tooth re-interpreted as Upper Cretaceous, Cappetta 1987)
marine			Schultze 1985	Johnson 1992	(as *Desmiodus*)
freshwater with marine influence			Johnson 2006		
			Branson 1916	Stahl 1999	(potentially older)
			Branson 1916		(as *H. rugosus*; anterior teeth of related form, see Stahl 1999)
marine			Yochelson & Van Sickle 1968		
			Johnson 1992		
			Johnson 1981	Stahl 1999; Johnson 1992, 2006	
			Johnson 1996		
freshwater			Johnson 2012		
freshwater			Zidek *et al.* 2004		
brackish			Schultze 1985	Johnson 1992	

1069	*Helodus*	sp.			tooth	Helodontidae	Helodontiformes	Permian	Cisuralian	Kungurian (Artinskian)
1070	*Helodus*	sp.				Helodontidae	Helodontiformes	Permian	Lopingian	
1071	*'Helodus'*	sp.			teeth	Helodontidae	Helodontiformes	Permian	Cisuralian	Artinskian?
1072	gen. indet.	sp. indet.			teeth	Helodontidae?	Helodontiformes	Permian	Cisuralian	Artinskian–Kungurian
1073	*Psephodus*	*depressus* Waagen, 1879			tooth plate	Psephodontidae	Cochliodontiformes	Permian	Lopingian	
1074	*Psephodus*	*indicus* Waagen, 1879			tooth plates	Psephodontidae	Cochliodontiformes	Permian	Lopingian	
1075	*Psephodus*	sp.			tooth plate	Psephodontidae	Cochliodontiformes	Permian	Guadalupian	Wordian–Capitanian (Kazanian)
1076	*Psephodus*	sp.				Psephodontidae	Cochliodontiformes	Permian	Cisuralian–Guadalupian	Kungurian–Roadian
1077	*Crassidonta*	*stuckenbergi* Branson, 1916			tooth plates	Cochliodontidae	Cochliodontiformes	Permian	Cisuralian	
1078	*Crassidonta*	*stuckenbergi* Branson, 1916			tooth plate	Cochliodontidae	Cochliodontiformes	Permian	Guadalupian	Wordian
1079	*Crassidonta*	sp.				Cochliodontidae	Cochliodontiformes	Permian	Guadalupian	**Wordian–Capitanian**
1080	*Crassidonta*	*subcrenulata* Teichert, 1943			tooth plates	Cochliodontidae	Cochliodontiformes	Permian	Cisuralian	Kungurian (Artinskian)
1081	*Deltodus*	*mercurei* Newberry, 1876			tooth plates	Cochliodontidae	Cochliodontiformes	Permian	Cisuralian	
1082	*Deltodus*	*mercurei* Newberry, 1876			tooth plates	Cochliodontidae	Cochliodontiformes	Permian	Guadalupian	Wordian
1083	*Deltodus*	*mercurei* Newberry, 1876			tooth plates	Cochliodontidae	Cochliodontiformes	Permian	Cisuralian–Guadalupian	Kungurian–Roadian
1084	*Deltodus*	*mercurei* Newberry, 1876			tooth plates	Cochliodontidae	Cochliodontiformes	Permian	Cisuralian–Guadalupian	Kungurian–Roadian
1085	*Deltodus*	aff. *mercurei* Newberry, 1876			tooth plates	Cochliodontidae	Cochliodontiformes	Permian	Guadalupian	Wordian
1086	*Deltodus*	sp.				Cochliodontidae	Cochliodontiformes	Permian	Guadalupian	**Roadian–Capitanian**
1087	*Deltodus*	sp.			tooth plates	Cochliodontidae	Cochliodontiformes	Permian	Cisuralian (lower)	
1088	~~*Deltodus*~~	~~*sp.*~~			~~tooth plates~~	~~Cochliodontidae~~	~~Cochliodontiformes~~	~~Permian~~	~~Cisuralian~~	
1089	*Helodopsis*	*elongata* Waagen, 1879			tooth plates	Cochliodontidae	Cochliodontiformes	Permian	Lopingian	
1090	*Helodopsis*	*abbreviata* Waagen, 1879			tooth plate	Cochliodontidae	Cochliodontiformes	Permian	Cisuralian	
1091	*Poecilodus*	*jonesi* McCoy, 1855			tooth plates	Cochliodontidae	Cochliodontiformes	Permian?	Cisuralian?	
1092	*Poecilodus* ?	*paradoxus* Waagen, 1879			tooth plate	Cochliodontidae?	Cochliodontiformes	Permian		
1093	*Sandalodus*	sp.			tooth plate	Cochliodontidae	Cochliodontiformes	Permian	Cisuralian	Kungurian
1094	gen. indet.	sp. indet.			tooth plate	Cochliodontidae *incertae sedis*	Cochliodontiformes	Permian	Cisuralian	Kungurian

	NT-E	Australia-W	Wandagee Hill, Mungadan Paddock, Wandagee Station, Carnarvon Basin, NW Division, W	Wandagee Fm	
	NT-W	Pakistan		*Productus* Limestone	
	BOR	Greenland-E	Amdrup Land, NE	'Upper Marine group'	calcareous sandstone
Andes	PL-E	Bolivia	Jacha Khatawi Hill, Yaurichambi, La Paz department	Copacabana Fm, Titicaca Grp (fish horizon 1)	limestone, shallow benthic environment
	NT-W	Pakistan	Salt range	*Productus* Limestone	
	NT-W	Pakistan	Kiri and Bilot, Salt range	*Productus* Limestone	
	PT-N	Russia-SW	Pechishchi locality, Pology Gully, Volga River, European Russia	"Podboy" Mb	brachiopod and pelecypod limestone; hemipelagic (shelf) - lagoon
Kaibab Sea	PL-E	USA-W	Grand Canyon, Arizona	Kaibab Fm	
	PT-N	Russia-SW	Samarskaya Luka (Samara Bend), Volga region		
Phosphoria Basin (see Piper & Link 2002)	PL-E	USA-N	North Fork of Little Wind River and Bull Lake Creek, Wind River Mountains, Lander, Wyoming	Embar Fm (basal Phosphoria Fm) (=Park City Fm)	
Phosphoria Basin (see Piper & Link 2002)	PL-E	USA-N	Wyoming	Retort Mb, Phosphoria Fm; lower Mb, Shedhorn Fm	mudflat and near-shore sands
	NT-E	Australia-W	Nalbia Paddock, Wandagee Station, Carnarvon Basin, NW Division, W	Wandagee Fm	
	PG-C	USA-S	Santa Fé, New Mexico		
Phosphoria Basin (see Piper & Link 2002)	PL-E	USA-N	North Fork of Little Wind River and Bull Lake Creek, Wind River Mountains, Lander, Wyoming	Embar Fm (basal Phosphoria Fm) (=Park City Fm)	
Kaibab Sea	PL-E	USA-W	Grand Canyon, Arizona	Kaibab Fm	
Kaibab Sea	PL-E	USA-W	Grand Canyon, Arizona	Kaibab Fm	
Madagascar Embayment	NT-W	Oman	Haushi Cliff and Saiwan, Haushi-Huqf region, E	Khuff Fm	rim basin
Phosphoria Basin (see Piper & Link 2002)	PL-E	USA-N	Wyoming	Meade Peak and Retort Mbs, Phosphoria Fm; lower Mb, Shedhorn Fm	mudflat and near-shore sands
	PL-E	USA-W	Iceberg Canyon, Nevada	Pakoon Fm	
		~~Thailand~~	~~Ban Na Chareon, NE~~		
	NT-W	Pakistan	Khund Ghat and Khoora and Jabi, Salt Range	*Productus* Limestone	
	NT-W	Pakistan	Salt Range, Nilwan	*Productus* Limestone	
	NT-E	Australia-W	near Mount Percy, Kimberly District, W		
	NT-W	Pakistan	Salt Range, Virgal	*Productus* Limestone	
	PL-C	Japan	Kinshozan, Akasaka-cho, Ohgaki City, Gifu Prefecture, central Honshu	lower Akasaka Limestone	
	PL-C	Japan	Kinshozan, Akasaka-cho, Ohgaki City, Gifu Prefecture, central Honshu	lower Akasaka Limestone	pale orange and dark grey part of grey-white massive limestone

marine		*Linoproductus* zone	Teichert 1943		
			Waagen 1879	Stahl 1999	(potentially unrelated)
marine		*Athyris amdrupi* brachiopod Zone	Bendix-Almgreen 1975	Bendix-Almgreen 1976	
marine	crushing, durophagous (bryozoa, molluscs, crinoids)	? *Necostreptognathodus* aff. *sulcoplicatus* conodont zone; *Eoparafusulina* fusulinid zone	Merino-Rodo & Janvier 1986	Stahl 1999	
			Waagen 1879	Stahl 1999	(questionable species)
			Waagen 1879	Stahl 1999; Dalla Vecchia 2000	(as *Petalorhynchus*)
marine/brackish			Krotov 1903, 1904	Chabakov 1927; Minikh & Minikh 1998; Stahl 1999	
marine			Hussakof 1943	Hunt *et al.* 2005	
			Stuckenberg 1905	Teichert 1943; Stahl 1999	
			Branson 1916	Teichert 1943; Stahl 1999	
marine			Yochelson & Van Sickle 1968		
marine		*Calcedispongia* zone	Teichert 1943	Stahl 1999	
			Newberry 1876	Stahl 1999	
			Branson 1916	Stahl 1999	
marine			Hussakof 1943	Hunt *et al.* 2005	(as *D. mercurii*)
marine			McKee 1982	Hunt *et al.* 2005	
marine		*Idiognathodella aserrata* conodont Zone; OSPZ6 palynology Zone; *Neoschwagerina craticulifera* fusulinid Zone	this study		Samples AO40, AO55
marine			Yochelson & Van Sickle 1968		
			McKee 1982		
			~~Ingavat & Janvier 1981~~	Stahl 1999	(deposit re-identified as Upper Carboniferous)
			Waagen 1879	Stahl 1999	
			Waagen 1879	Stahl 1999	
marine			Hardmann 1884	Teichert 1943; Stahl 1999	
			Waagen 1879	Stahl 1999	(species apparently incorrectly referred to genus and even cochliodontids)
marine		*Parafusulina* Zone	Goto 1994a	Goto 1994b, 1996a–c, 1999a, b, 2000; Stahl 1999	(as *Sandalodus* (*Deltodus*); also as Guadalupian)
marine		*Parafusulina* Zone	Goto *et al.* 1988	Goto 1991, 1994a, b, 1996a–c, 1999a, b, 2000; Stahl 1999	(also as Guadalupian)

1095	*Solenodus*	cf. *crenulatus* Trautschold, 1874			tooth plates	*incertae sedis*	Cochliodontiformes	Permian	Guadalupian	Wordian
1096	*Menaspis*	*armata* Ewald, 1848				Menaspidae	Menaspiformes	Permian	Lopingian	Wuchiapingian
1097	*Menaspis*	*armata* Ewald, 1848			body fossil	Menaspidae	Menaspiformes	Permian	Lopingian	Wuchiapingian
1098	*Menaspis*	*armata* Ewald, 1848			lower jaw	Menaspidae	Menaspiformes	Permian	Guadalupian	
1099	*Menaspis*	*armata* Ewald, 1848				Menaspidae	Menaspiformes	Permian	Lopingian	Wuchiapingian
1100	*Menaspis*	*armata* Ewald, 1848				Menaspidae	Menaspiformes	Permian	Lopingian	Wuchiapingian
1101	*Menaspis*	*diversispinus* Minikh and Minikh, 1996				Menaspidae	Menaspiformes	Permian	Guadalupian –Lopingian	Capitanian–Changhsingian
1102	*Menaspis*	*diversispinus* Minikh and Minikh, 1996			tooth plate	Menaspidae	Menaspiformes	Permian	Guadalupian –Lopingian	Wordian
1103	*Arctacanthus*	*uncinatus* Nielsen, 1932			cephalic spines		Chimaeriformes?	Permian	Lopingian	Wuchiapingian
1104	*Arctacanthus*	*wyomingensis* Branson, 1934			cephalic spines		Chimaeriformes?	Permian	Guadalupian	Capitanian
1105	*Arctacanthus*	sp.			cephalic spines		Chimaeriformes?	Permian	Guadalupian	**Capitanian**
1106	*Arctacanthus*				cephalic spines		Chimaeriformes?	Triassic	Lower	
1107	*Arctacanthus*	*exiguus* Yamagishi, 2004			cephalic spines		Chimaeriformes?	Triassic	Middle	Anisian, lower–middle
1108	*Arctacanthus*	*exiguus* Yamagishi, 2004			spines		Chimaeriformes?	Triassic	Lower–Middle	Induan (Griesbachian?), Anisian–Ladinian
1109	*Arctacanthus*	sp.			cephalic spines		Chimaeriformes?	Triassic	Middle–Upper	**Ladinian, uppermost–Carnian, lowermost**
1110	*Arctacanthus* ?	sp.			spines		Chimaeriformes?	Triassic	Lower	Induan (Griesbachian?)
1111	*Agkistracanthus*	*mitgelensis* Duffin & Furrer, 1981			tooth plates and fin spines	Myriacanthidae	Chimaeriformes	Triassic	Upper	Rhaetian
1112	*Agkistracanthus*	*mitgelensis* Duffin & Furrer, 1981			tooth plates	Myriacanthidae	Chimaeriformes	Triassic	Upper	Rhaetian
1113	*Agkistracanthus*	*mitgelensis* Duffin & Furrer, 1981			tooth plates	Myriacanthidae	Chimaeriformes	Triassic	Upper	Rhaetian
1114	*Agkistracanthus*	sp. nov.			fin spine	Myriacanthidae	Chimaeriformes	Triassic	Upper	Rhaetian

Madagascar Embayment	NT-W	Oman	Haushi Cliff and Saiwan, Haushi-Huqf region, E	Khuff Fm	rim basin
	PT-W	Germany	Lonau near Herzberg, Glückaufer Revier, Harz Mountains, and Richelsdorfer Revier, Hesse	Kupferschiefer	
	PT-W	Germany	Eisleben, Saxony	Kupferschiefer	
	PT-W	Germany	Glücksbrunn, Thüringen	Kupferschiefer	
	PT-W	Germany	Mansfeld	Kupferschiefer	
	PT-W	Germany	Richelsdorfer Revier	Kupferschiefer	
	PT-N	Russia-W	Tatarstan, near Kazan		
	PT-N	Russia-W	Isheyevo, Tatarstan		sandy lens
	BOR	Greenland-E	Hird's fox-farm, Clavering Island + Section F (190 m above sea level), Kap Stosch, Hold with Hope	*Martinia* limestone (Ravnefjeld Fm), Foldvik Creek Grp	
Phosphoria Basin (see Piper & Link 2002)	PL-E	USA-N	Dinwoody Creek, Wind River Mountains, Wyoming	Pustula Mb, Middle Phosphoria Fm (=Retort Mb)	Thin phosphate bed
Phosphoria Basin (see Piper & Link 2002)	PL-E	USA-N	Wyoming	Retort Mb, Phosphoria Fm	mudflat
	PG-S	South Africa			
	PL-C	Japan	Tahokamigumi, Nishiuwa City (prev. Shirokawa-cho, Higashiuwa-gun), Ehime Prefecture, Shikoku	Taho Fm	biomicritic bedded limestone, seamount
	PL-C	Japan	Kamura, Takachiho-chō, Nishiusuki-gun, Miyazaki-ken (Prefecture), Kyūshū	Kamura Fm	mid-oceanic seamount
	PT-E	China-SE	Zhuganpo Village, Guanling County, Guizhou Province, SW	Zhuganpo Fm	grey micritic limestone + dolomitic limestone / bioclastic limestone --> shallow to deep (below storm wave-base) water platform
	PL-C	Japan	Kamura, Takachiho-chō, Nishiusuki-gun, Miyazaki-ken (Prefecture), Kyūshū	Kamura Fm	mid-oceanic seamount
	PT-W	Switzerland	Graubünden		
	PT-W	England	Holwell Quarry, near Frome, Somerset, SW	Westbury Fm, Penarth Grp	fissure infill
	PT-W	England	St. Audries Bay, Somerset, SW	Cotham Mb (base), Lilstock Fm, Penarth Grp	
	PT-W	France	S		

marine		*Mesogondolella aserrata* conodont Zone; OSPZ6 palynology Zone; *Neoschwagerina craticulifera* fusulinid Zone	this study		(as holocephalians in Schultze *et al.* 2008) Samples AO55, AO214
			Ewald 1848	Schaumberg 1977; Stahl 1999	
			Giebel 1856; Jaekel 1891	Patterson 1965, 1968; Schaumberg 1977, 1992; Stahl 1999	
			Zittel 1887-1890	Weigelt 1930	(as *Chalcodus permianus*)
			Weigelt 1930	Stahl 1999	
				Schaumberg 1977; Stahl 1999	
			Minikh & Minikh 1996	Ivanov 2007	
			Minikh & Minikh 1998		
marine			Nielsen 1932	Nielsen 1935; Stensiö 1961; Bendix-Almgreen 1976	
			Branson 1933	Branson 1934; Nielsen 1935	(as *Diplognoncodus unoinatus*); Word Fm? (Stensiö 1961)
marine			Yochelson & Van Sickle 1968		
			Bender & Hancox 2003	Durand 2005	
marine		*Mesogondolella timorensis – Mg. bulgarica* Zones	Yamagishi 2004; Yamagishi 2006	Goto *et al.* 2010	
marine		*Hindeodus parvus* , *Isarcicella isarcica* , *Mesogondolella carinata – Eudurovignathus hungaricus* , *Paragondolella foliata* , *P. bulgarica* , *Chiosella timorensis*	this study		(as aff. *Arctacanthus*) Samples 300311-I, 300311-J, 300311-K, 05.7.14.ak, 05.7.14.aw
marine		*Metapolygnathus polygnathiformis* conodont Zone	Chen *et al.* 2007a		(as aff. *Arctacanthus*)
marine		*Hindeodus parvus* , *Isarcicella isarcica* , *Mesogondolella carinata*	this study		(as aff. *Arctacanthus*) Sample 05.7.15.h
			Duffin & Furrer 1981	Stahl 1999	
marine			Duffin & Furrer 1981	Storrs 1994; Duffin 1998a; Stahl 1999	
			Duffin & Furrer 1981	Storrs 1994	
			Cuny (1997, pers. comm. in Stahl 1999)	Stahl 1999	

1115	*Myriacanthus*	*paradoxus* Agassiz, 1836	*Myriacanthus retrorsus* Agassiz, 1837; *Chimaera* (*Ischyodon*) *johnsonii* Agassiz, 1843; *Ischyodus johnsoni* Egerton, 1847; *Prognathodus guentheri* Egerton, 1872		tooth plate	Myriacanthidae	Chimaeriformes	Triassic	Upper	Rhaetian
1116	gen. indet.	sp. indet.					*incertae sedis*	Triassic	Upper	Rhaetian
1117	*Macrodontacanthus*	*kingi* Romer, 1942			fin spine fragment		*incertae sedis*	Permian	Cisuralian	Artinskian
1118	gen. indet.	sp. indet.			tooth		*incertae sedis*	Permian	Lopingian	Changhsingian
M1	*"Petrodus"*	sp.			dermal tooth		*incertae sedis* (Euselachii)	Permian	Cisuralian	Kungurian
M2	*"Petrodus"*				denticles		*incertae sedis* (Euselachii)	Permian	Cisuralian	Sakmarian
M3	gen. indet.	sp. indet.			denticles		*incertae sedis* (Euselachii)	Triassic	Lower–Upper	**Olenekian–Anisian, Carnian**
M4	*Ancistrodus*	*multisectus* Branson, 1933						Permian	Guadalupian	Capitanian
M5	*Ancistrodus*	sp.						Permian	Guadalupian	Capitanian
M6	*Hamatus*	*phosphoriensis* Branson, 1933						Permian	Guadalupian	Capitanian
M7	*Hamatus*	sp.						Permian	Guadalupian	Roadian–Wordian
M8	*Holmesella*	*quadrata*						Permian	Cisuralian	
M9	*Cooperella*	*typicalis* Gunnell, 1933			denticle	Hybodontidae?	Hybodontiformes?	Permian	Cisuralian	Artinskian?
M10	*Cooperella*	*striatula* Gunnell, 1933			denticles	Hybodontidae?	Hybodontiformes?	Permian	Cisuralian–Guadalupian	
M11	*Cooperella*				denticles			Permian	Guadalupian	Capitanian
M12	*Cooperella*				denticles			Permian	Guadalupian	Roadian
M13	*Cooperella*				denticles			Permian	Guadalupian	Wordian–Capitanian
M14	*Kirkella*				denticles			Permian	Guadalupian	Capitanian
M15	*Kirkella*				denticles			Permian	Guadalupian	Roadian
M16	*Kirkella*				denticles			Permian	Guadalupian	Wordian–Capitanian
M17	*Listracanthus*	*pectenatus* Mutter & Neuman, 2006			denticles			Triassic	Lower	Induan (Griesbachian?)–Olenekian (Smithian, lower?)

	PT-W	England	Aust Cliff, Somerset	Westbury Fm, Penarth Grp	
	PT-W	France	Provenchères-sur-Meuse, Haute-Marne		
	PG-C	USA-S	Culbertson Pasture, east of Wichita Falls, Wichita County, Texas	Admiral/Belle Plains Fm?, Wichita Group	clays near marine limestones in red beds
	NT-W	Iran	Baghuk Mountain, NW of Abadeh	Hambast Fm	deep shelf limestone
	PL-C	Japan	Kinshozan, Akasaka-cho, Ohgaki City, Gifu Prefecture, central Honshu	lower Akasaka Limestone	pale orange and dark grey part of grey-white massive limestone
	PT-N	Russia-W	South Urals		marls and nodular and reef limestones
	PL-C	Japan	Tahokamigumi, Nishiuwa City (prev. Shirokawa-cho, Higashiuwa-gun), Ehime Prefecture, Shikoku	Taho Fm	biomicritic limestone
Phosphoria Basin (see Piper & Link 2002)	PL-E	USA-N	Middle Fork of Popo Agie River, Dinwoody Creek, Wind River Mountains, Wyoming	Pustula Mb, Middle Phosphoria Fm (=Retort Mb)	Thin phosphate bed
Phosphoria Basin (see Piper & Link 2002)	PL-E	USA-N	Wyoming	Retort Mb, Phosphoria Fm	mudflat
Phosphoria Basin (see Piper & Link 2002)	PL-E	USA-N	Middle Fork of Popo Agie River, Bull Lake Creek, Dinwoody Creek, Wind River Mountains; Red Creek, Owl Creek Mountains, Wyoming	Pustula Mb, Middle Phosphoria Fm (=Retort Mb)	Thin phosphate bed
Phosphoria Basin (see Piper & Link 2002)	PL-E	USA-N	Wyoming	Meade Peak Mb, Phosphoria Fm	mudflat
	PG-C	USA-C	Pottawatomie County, Kansas (Everhart, pers. comm.)	Neva Limestone Mb., Genola Limestone Fm, Council Grove Grp	Poorly consolidated limey mud
	PL-E	Mexico	San Salvador Patlanoaya, Puebla state	Mb f, Patlanoaya Fm, Mixteco Terrane	Limestones and interbedded siliciclastics (storm reworked shallow carbonate platform)
Kaibab Sea	PL-E	USA-W	Grand Canyon, Arizona	Fossil Mountain Mb, Kaibab Fm	
	PG-C	USA-S	Guadelupe and Apache Mountains, western Texas	Rader Limestone Mb and Lamar Limestone Mb, Bell Canyon Fm	
	PG-C	USA-S	Quarry section, Guadelupe Mountains, western Texas	William Ranch Mb, Cutoff Fm	fossiliferous debris flows interbedded with radiolarian-bearing limestone
	PG-C	USA-S	PI section, Guadelupe Mountains, western Texas	Hegler and Pinery Mbs, Bell Canyon Fm	thin limestone intervals interbedded with sandstone and siltstone
	PG-C	USA-S	Guadelupe and Apache Mountains, western Texas	Rader Limestone Mb and Lamar Limestone Mb, Bell Canyon Fm	
	PG-C	USA-S	Quarry section, Guadelupe Mountains, western Texas	William Ranch Mb, Cutoff Fm	fossiliferous debris flows interbedded with radiolarian-bearing limestone
	PG-C	USA-S	PI section, Guadelupe Mountains, western Texas	Hegler and Pinery Mbs, Bell Canyon Fm	thin limestone intervals interbedded with sandstone and siltstone
	PL-E	Canada-W	Ganoid Ridge, Wapiti Lake, near "Fossil Fish Lake", British Columbia, W	Vega-Phroso Siltstone Mb, Sulphur Mountain Fm	siltstone, deltaic/shallow continental shelf environment

			Duffin 1994	Storrs 1994; Duffin 1998a; Stahl 1999	
				Cuny 1995a	
marine			Romer 1942	Stahl 1999	
marine			Hampe *et al.* 2013		
marine		*Parafusulina* zone	Goto *et al.* 1988	Goto 1994a, b, 1996a–c, 1999a, b, 2000	
marine		*Ps. urdalensis* fusulinid zone	Ivanov 2005		
		Necospathodus triangularis / *Ns. homeri* – *Neogondolella bulgarica* Zones	Yamagishi 2004; Yamagishi 2006		
			Branson 1933	Nielsen 1935	(also as *serratus*)
marine			Yochelson & Van Sickle 1968		
			Branson 1933	Nielsen 1935	
marine			Yochelson & Van Sickle 1968		
			Ewell & Everhart 2005		
marine	fast-swimming (off-shore)	*Skinnerella imlayi* and *Paraskinnerella skinneri* (fusulinids)	Derycke-Khatir *et al.* 2005		
marine			Thompson 1995	Hunt *et al.* 2005	
marine			Ivanov *et al.* 2011		
marine			Ivanov *et al.* 2012		
marine			Ivanov *et al.* 2012		
marine			Ivanov *et al.* 2011		
marine			Ivanov *et al.* 2012		
marine			Ivanov *et al.* 2012		
marine			Schaeffer & Mangus 1976	Mutter & Neuman 2006	(as Chondrichthyes indet.)

M18	*Listracanthus*	*pectenatus* Mutter & Neuman, 2006			denticles			Triassic	Lower	
M19	*Listracanthus*	*pectenatus* Mutter & Neuman, 2006	type I		denticles		*incertae sedis*	Triassic	Lower	Induan (Griesbachian?)–Olenekian (Smithian, lower?)
M20	*Listracanthus*	*pectenatus* Mutter & Neuman, 2006	type II		denticles		*incertae sedis*	Triassic	Lower	Induan (Griesbachian?)–Olenekian (Smithian, lower?)
M21	*Listracanthus*	*pectenatus* Mutter & Neuman, 2006			denticles		*incertae sedis*	Triassic	Lower	Induan (Griesbachian?)–Olenekian (Smithian, lower?)
M22	*Listracanthus*	*pectenatus* Mutter & Neuman, 2006			denticles		*incertae sedis*	Triassic	Lower	
M23	*Listracanthus*	*pectenatus* Mutter & Neuman, 2006			denticles		*incertae sedis*	Triassic	Lower	
M24	*Listracanthus*	sp.			denticles			Permian	Cisuralian	Sakmarian–Artinskian
M25	*Listracanthus*	sp.			denticles			Permian	Lopingian	
M26	*Mcreyella*	*typicalis* Gunnell, 1933			denticles	Hybodontidae?	Hybodontiformes?	Permian	Cisuralian–Guadalupian	
M27	*Mcreyella*	*typicalis* Gunnell, 1933			denticle	Hybodontidae?	Hybodontiformes?	Permian	Cisuralian	Artinskian?
M28	*Mcreyella*	cf. *typicalis*			denticle	Hybodontidae?	Hybodontiformes?	Permian	Cisuralian	Artinskian–Kungurian
M29	*Mcreyella* ?	sp.			denticle	Hybodontidae?	Hybodontiformes?	Permian	Cisuralian	Artinskian–Kungurian
M30	*Mcreyella*				denticles	Hybodontidae?	Hybodontiformes?	Permian	Guadalupian	Capitanian
M31	*Mcreyella*				denticles			Permian	Guadalupian	Roadian
M32	*Mcreyella*				denticles			Permian	Guadalupian	Wordian–Capitanian
M33	gen. indet.	sp. indet. 2			denticle	Hybodontidae	Hybodontiformes	Permian	Cisuralian	Artinskian–Kungurian
M34	*"Stemmatias"*							Permian	Cisuralian	Asselian–Sakmarian
M35	*"Stemmatias"*				denticles			Permian	Cisuralian	Asselian–Artinskian
M36	*Xystrodus*					Hybodontidae	Hybodontiformes			
M37	*Meishanselache*	*liui* Wang, Zhu, Jin & Wang, 2007			denticles		*incertae sedis* (Elasmobranchii)	Permian	Lopingian	Changhsingian
M38	*Changxingselache*	*wangi* Wang, Zhu, Jin & Wang, 2007			denticles		*incertae sedis* (Elasmobranchii)	Permian	Lopingian	Changhsingian
M39	gen. indet. 2	sp. indet.			denticle	Ctenacanthidae	Ctenacanthiformes	Permian	Lopingian	Changhsingian
M40	gen. indet. 2	sp. indet.			denticles		Hybodontiformes	Permian	Lopingian	Changhsingian
M41	gen. indet. 2	sp. indet.			denticles	Hybodontidae	Hybodontiformes	Permian	Lopingian	Changhsingian

	PL-E	Canada-W	Needham Creek, Graham River, Horn Creek, British Columbia	Toad-Grayling Fm	
	PL-E	Canada-W	various Cirques, Ganoid Ridge, Wapiti Lake, near "Fossil Fish Lake", British Columbia, W	Vega-Phroso Siltstone Mb, Sulphur Mountain Fm	siltstone, deltaic/shallow continental shelf environment
	PL-E	Canada-W	various Cirques, Ganoid Ridge, Wapiti Lake, near "Fossil Fish Lake", British Columbia, W	Vega-Phroso Siltstone Mb, Sulphur Mountain Fm	siltstone, deltaic/shallow continental shelf environment
	PL-E	Canada-W		Spray River Group	
	PL-E	Canada-W	Meosin Mountain, British Columbia, W	Sulphur Mountain Fm	
	PL-E	Canada-W	"Massive locality", Banff National Park, W	Sulphur Mountain Fm	
	PT-N	Russia-W	South Urals		marls and nodular, detrital, and reef limestones
	PT-E	China-E	Hubei Province	Dalong Fm	
Kaibab Sea	PL-E	USA-W	Grand Canyon, Arizona	Fossil Mountain Mb, Kaibab Fm	
	PL-E	Mexico	San Salvador Patlanoaya, Puebla state	Mb f, Patlanoaya Fm, Mixteco Terrane	Limestones and interbedded siliciclastics (storm reworked shallow carbonate platform)
	PL-E	Mexico	San Salvador Patlanoaya, Puebla state	unit 28, Mb f, Patlanoaya Fm, Mixteco Terrane	Limestones and interbedded siliciclastics (inner carbonate platform, lower limit photic zone, 50m depth)
	PL-E	Mexico	San Salvador Patlanoaya, Puebla state	unit 28, Mb f, Patlanoaya Fm, Mixteco Terrane	Limestones and interbedded siliciclastics (inner carbonate platform, lower limit photic zone, 50m depth)
	PG-C	USA-S	Guadelupe and Apache Mountains, western Texas	Rader Limestone Mb and Lamar Limestone Mb, Bell Canyon Fm	
	PG-C	USA-S	Quarry section, Guadelupe Mountains, western Texas	William Ranch Mb, Cutoff Fm	fossiliferous debris flows interbedded with radiolarian-bearing limestone
	PG-C	USA-S	PI section, Guadelupe Mountains, western Texas	Hegler and Pinery Mbs, Bell Canyon Fm	thin limestone intervals interbedded with sandstone and siltstone
	PL-E	Mexico	San Salvador Patlanoaya, Puebla state	unit 28, Mb f, Patlanoaya Fm, Mixteco Terrane	Limestones and interbedded siliciclastics (inner carbonate platform, lower limit photic zone, 50m depth)
	PG-C	USA-C	Marshall County, Kansas	Threemile Limestone Mb, Wreford Limestone Fm, Chase Grp	open marine (50 m water depth)
	PT-N	Russia-W	Middle and South Urals		marls and nodular, detrital, and reef limestones
	PT-E	China-E	Meishan section D, Changxing District, Zhejiang Province	lower Meishan Mb, Changxing Fm	
	PT-E	China-E	Meishan section D, Changxing District, Zhejiang Province	Baoqing and Meishan Mbs, Changxing Fm	
	PT-E	China-E	Meishan section D, Changxing District, Zhejiang Province	Baoqing Mb, Changxing Fm	
	PT-E	China-SE	Tieshikou, Xinfeng County, Jiangxi Province	upper Mb, Changxing Fm	
	PT-E	China-E	Meishan sections D & Z, Changxing District, Zhejiang Province	Baoqing and upper Meishan Mbs, Changxing Fm	

marine			Schaeffer & Mangus 1976		
marine			Mutter & Neuman 2006	Mutter & Neuman 2009; Cappetta 2012	
marine			Mutter & Neuman 2006	Mutter & Neuman 2009; Cappetta 2012	
marine			Mutter & Neuman 2006		
marine			Mutter & Neuman 2006		
marine			Mutter & Neuman 2006		
marine		*Ps. urdalensis* and *Par. lutigini* – *Ps.juresanensis* fusulinid zones	Ivanov 2005		(as "*Listracanthus*")
				Chen *et al.* 2007a	
marine			Thompson 1995	Hunt *et al.* 2005	
marine	fast-swimming (off-shore)	*Skinnerella imlayi* and *Paraskinnerella skinneri* (fusulinids)	Derycke-Khatir *et al.* 2005		
marine	fast-swimming (off-shore)		Derycke-Khatir *et al.* 2005		
marine	fast-swimming (off-shore)		Derycke-Khatir *et al.* 2005		
marine			Ivanov *et al.* 2011		
marine			Ivanov *et al.* 2012		
marine			Ivanov *et al.* 2012		
marine			Derycke-Khatir *et al.* 2005		
marine			Schultze 1985		
marine		*Sph. vulgaris* – *Par. solidissima* fusulinid zones	Ivanov 2005		
			Wang *et al.* 2007a	Wang *et al.* 2007b	
			Wang *et al.* 2007a	Wang *et al.* 2007b	
			Wang *et al.* 2007a	Wang *et al.* 2007b	
			Wang *et al.* 2007a	Wang *et al.* 2007b	
			Wang *et al.* 2007a	Wang *et al.* 2007b	

M42	*Sinacrodus*	*donglingensis* Wang, Zhu, Jin & Wang, 2007			denticles	Acrodontidae	Hybodontiformes	Permian	Lopingian	Changhsingian
M43	*Sinacrodus*	*donglingensis* Wang, Zhu, Jin & Wang, 2007			denticles	Acrodontidae	Hybodontiformes	Permian	Lopingian	Changhsingian
M44	*Sinacrodus*	*donglingensis* Wang, Zhu, Jin & Wang, 2007			denticles	Acrodontidae	Hybodontiformes	Permian	Lopingian	Changhsingian
M45	gen. indet. 2	sp. indet.			denticle		*incertae sedis* (Neoselachii)	Permian	Lopingian	Changhsingian
M46	gen. indet. 2	sp. indet.			denticle		*incertae sedis* (Neoselachii)	Permian	Lopingian	Changhsingian
M47	gen. indet. 2	sp. indet.			denticles and spines	Hybodontidae?	Hybodontiformes?	Permian(–Triassic?)	Cisuralian? (–Lower?)	
M48	gen. indet.	sp. indet.			denticles			Permian	Cisuralian	Asselian–Sakmarian
M49	gen. indet.	sp. indet.			tooth			Permian	Cisuralian	Asselian–Sakmarian
M50	gen. indet.	sp. indet.			tooth			Permian	Guadalupian	Wordian–Capitanian
M51	gen. indet.	sp. indet.			denticles			Permian	Lopingian	Wuchiapingian (Dzulfian)
M52	gen. indet.	sp. indet.			dermal denticles			Permian	Lopingian	Wuchiapingian
M53	gen. indet.	sp. indet.			denticles			Triassic	Lower	
M54	gen. indet.	sp. indet.			teeth, fragmented			Triassic	Upper	Norian, middle
M55	gen. indet.	sp. indet.			denticles			Triassic	Middle	Anisian, upper
M56	gen. indet.	sp. indet. (undescribed)			teeth, denticles			Triassic	Lower–Middle	Olenekian (Smithian)–Ladinian, upper
M57	gen. indet.	sp. indet.			denticles			Triassic	Lower	Induan (Dienerian, lower)–Olenekian (Smithian, lower)
M58	gen. indet.	sp. indet.			dermal denticles			Permian	Guadalupian	
M59	gen. indet.	sp. indet.			dermal denticles			Triassic	Lower	Olenekian (Spathian)
M60	gen. indet.	sp. indet.			dermal denticles			Triassic	Lower	Induan (Griesbachian)
M61	gen. indet.	sp. indet.			dermal denticles			Triassic	Middle	Anisian, lower-middle
M62	gen. indet.	sp. indet.			dermal denticles			Triassic	Lower	Olenekian (Smithian, upper)

	PT-E	China-SE	Dongling, Xiushui County, Jiangxi Province	upper Mb, Changxing Fm	
	PT-E	China-SE	Tieshikou, Xinfeng County, Jiangxi Province	upper Mb, Changxing Fm	
	PT-E	China-E	Meishan section, Changxing District, Zhejiang Province	upper Mb, Changxing Fm	
	PT-E	China-E	Meishan section D, Changxing District, Zhejiang Province	Baoqing Mb, Changxing Fm	
	PT-E	China-SE	Tieshikou, Xinfeng County, Jiangxi Province	upper Mb, Changxing Fm	
	PG-S	Zambia		Madumabisa Mudstones, Ecca Grp– *Cistecephalus* Zone, Beaufort Grp (*I– Dicynognathus* Zone, Beaufort Grp)	
	PG-C	USA-C	Cowley County, Morris County, Kay County, Riley County, Geary County, Butler County, Kansas	Havensville Shale Mb, Schroyer Limestone Mb, Wreford Limestone Fm, Chase Grp	shallow to open marine (50 m water depth)
	PG-C	USA-C	Greenwood County, Butler County, Cowley County, Geary County, Kansas	Havensville Shale Mb, Schroyer Limestone Mb, Wreford Limestone Fm, Chase Grp; Speiser Shale Fm, Council Grove Grp	intertidal to open marine (50 m water depth)
Sverdrup Basin	BOR	Canada-N	N of Raglan Range, Melville Island, Parry Islands, Canadian Arctic Archipelago	Trold Fiord Fm? ('Unit B')	calcarous sandstone (southern basin margin)
	PT-W	Greece	Kaki Vigla Bay, Salamis		
Neo-Tethys	NT-W	Iran	Baghuk Mountain, NW of Abadeh	Hambast Fm	deep/outer shelf, red nodular limestone
	PT-W	Greece	Chios		
	PL-C	Japan	Shioinouso, Takachiho-cho, Miyazaki Prefecture, Kyushu	Kamura Fm	micritic limestone
	PL-C	Japan	Shioinouso, Takachiho-cho, Miyazaki Prefecture, Kyushu	Kamura Fm	micritic limestone
	BOR	Spitsbergen	Wallenbergfjellet / Tschermakfjellet / Stensiofjellet / Botneheia / Roslagenfjellet, central	Sassendalen Grp	deltaic to shallow shelf environment
	PL-W	Russia-SE	Abrek Bay area, Vladivostok, South Primorye	upper Lazurnaya Bay Fm–Zhitkov Fm	ammonoid turbidites
	PL-E	USA-W	Palomino Ridge, NE Nevada	Gerster Fm	limestone
	PL-E	USA-W	Hurricane, SW Utah	Virgin Mb, Moenkopi Fm	calcareous sandstone; normal marine subtidal shelf environment
Hawasina Basin	NT-W	Oman	Wadi Wasit, Ba'id, Oman Mountains	Al Jil Fm	platform margin
	PL-E	Malaysia	Bukit Kalong, Kedah		limestone
	PL-E	Malaysia	Gua Panjang	unnamed	limestone

			Wang *et al.* 2007a	Wang *et al.* 2007b	
			Wang *et al.* 2007a	Wang *et al.* 2007b	
			Wang *et al.* 2007a	Wang *et al.* 2007b	
			Wang *et al.* 2007a	Wang *et al.* 2007b	
			Wang *et al.* 2007a	Wang *et al.* 2007b	
freshwater?			Kemp 1975	Murray 2000	
marine			Schultze 1985		
brackish to marine			Schultze 1985		
marine			Nassichuk 1971		
			unpub.	Reif & Goto 1979	
marine			Hampe *et al.* 2011, 2013		XIX morphotypes
			unpub.	Reif & Goto 1979	
marine			Yamagishi 2006		
marine			Yamagishi 2006		
marine		*tardus* , *subrobustus* , *Ptychites* , *tozeri* ammonoid zones; Grippia's lower sauria Zone?	Yamagishi 2006		
marine		*Ambitoides fuliginates* – *Radioprionites abrekensis* Zone (*Gyronites subdharmus* – *Anasibirites nevolini* Zone)	Yamagishi 2009	Yamagishi 2006	
marine			Yamagishi 2006		
marine			Yamagishi 2006		
marine		*Hindeodus scitiensis*	Yamagishi 2006		
marine		*Neogondolella bulgarica* , *Gladigondolella tethydis*	Yamagishi 2006		
marine		*Neospathodus dieneri* , *N. transcoi*	Yamagishi 2006		

M63	gen. indet.	sp. indet.			dermal denticles		*incertae sedis*	Permian	Guadalupian	Wordian
M64	gen. indet.	sp. indet.			dermal denticles		*incertae sedis*	Triassic	Lower	Olenekian (Spathian)
M65	gen. indet.	sp. indet.			dermal denticles		*incertae sedis*	Triassic	Lower	Olenekian (Smithian–Spathian)
M66	gen. indet.	sp. indet.			dermal denticles		*incertae sedis*	Permian	Guadalupian	Roadian–Wordian
M67	gen. indet.	sp. indet.			dermal denticles		*incertae sedis*	Triassic	Lower–Middle	Olenekian (Spathian, upper)–Anisian, lower
M68	gen. indet.	sp. indet.			denticles		Hybodontiformes	Triassic	Middle	
M69	gen. indet.	sp. indet.			denticles		Hybodontiformes	Triassic	Middle	Anisian, lower middle
M70	gen. indet.	sp. indet.			denticles, fin spines			Triassic	Middle	Ladinian, upper
M71	gen. indet.	sp. indet.			denticles			Triassic	Middle	Anisian–Ladinian
M72	gen. indet.	sp. indet.	4 types		denticles			Triassic	Upper	Norian, middle
M73	gen. indet.	sp. indet.			buccopharyngeal denticles		Symmoriiformes	Permian	Guadalupian	Roadian
M74	gen. indet.	sp. indet.			buccopharyngeal denticles		Symmoriiformes	Permian	Guadalupian	Wordian–Capitanian
M75	gen. indet.	sp. indet.			denticles		Ctenacanthiformes	Permian	Guadalupian	Roadian
M76	gen. indet.	sp. indet.			denticles		Ctenacanthiformes	Permian	Guadalupian	Wordian–Capitanian
M77	gen. indet.	sp. indet.			denticles		Orodontiformes	Permian	Guadalupian	Roadian
M78	gen. indet.	sp. indet.			denticles		*incertae sedis* (Euselachii)	Permian	Guadalupian	Roadian
M79	gen. indet.	sp. indet.			denticles		*incertae sedis* (Euselachii)	Permian	Guadalupian	Wordian–Capitanian
	gen. indet.	sp. indet.			dermal denticles		*incertae sedis* (Neoselachii)	Triassic	Upper	Carnian, upper
M80	*Parvidiabolus*	aff. *convexus* Johns, Barnes & Orchard, 1997			denticles		*incertae sedis* (Elasmobranchii)	Triassic	Middle	Anisian, lower middle

Madagascar Embayment	NT-W	Oman	Haushi Cliff and Saiwan, Haushi-Huqf region, E	Khuff Fm	rim basin
Hawasina Basin	NT-W	Oman	Jabel Safra, Oman Mountains, N	Hallstatt-type limestone olistoliths	basinal seamount
Hawasina Basin	NT-W	Oman	Wadi Alwa, Ba'id, Oman Mountains, N	Alwa Fm	basinal seamount
Sverdrup Basin	BOR	Canada-N	Hamilton Peninsula and Henrietta Nesmith, Ellesmere Island, Canadian Arctic Archipelago	Assistance and Trold Fiord fms	sandstones; mid shelf depositional environment
	PL-E	USA-W	e.g., Coyote Canyon, Humboldt Range, Pershing County, N Nevada	lower and Fossil Hill mbs, Prida Fm, Star Peak Grp	micritic limestones; below wave base? / black micritic limestones and silty shales; below wave base and in an anoxic environment
west Tethyan	NT-W	Saudi Arabia	Site 1, Ar Rubay'iyah village, east of Buraydah	Jilh Fm	sandstone, shallow marine to offshore environment
	PL-E	USA-W	west slope Augusta Mountains, Pershing County, Nevada	lower Fossil Hill Mb, Favret Fm, Star Peak Grp	litharenite, debris flow deposit, high energy, coastal influence, outer platform
	PT-W	Germany	clay quarry, near Schöningen, lower Saxony	Muschelkalk-Keuper boundary	
	PT-W	Luxembourg	Heselbierg Quarry, Moersdorf, E	upper Muschelkalk	dolomites with interbedded blue shaly marls; platform deposits
	PT-W	Luxembourg	Rinkebierg Hill, Medernach	Steinmergelgruppe, Keuper	dolomitic bone bed
	PG-C	USA-S	Quarry section, Guadelupe Mountains, western Texas	William Ranch Mb, Cutoff Fm	fossiliferous debris flows interbedded with radiolarian-bearing limestone
	PG-C	USA-S	PI section, Guadelupe Mountains, western Texas	Hegler and Pinery Mbs, Bell Canyon Fm	thin limestone intervals interbedded with sandstone and siltstone
	PG-C	USA-S	Quarry section, Guadelupe Mountains, western Texas	William Ranch Mb, Cutoff Fm	fossiliferous debris flows interbedded with radiolarian-bearing limestone
	PG-C	USA-S	PI section, Guadelupe Mountains, western Texas	Hegler and Pinery Mbs, Bell Canyon Fm	thin limestone intervals interbedded with sandstone and siltstone
	PG-C	USA-S	Quarry section, Guadelupe Mountains, western Texas	William Ranch Mb, Cutoff Fm	fossiliferous debris flows interbedded with radiolarian-bearing limestone
	PG-C	USA-S	Quarry section, Guadelupe Mountains, western Texas	William Ranch Mb, Cutoff Fm	fossiliferous debris flows interbedded with radiolarian-bearing limestone
	PG-C	USA-S	PI section, Guadelupe Mountains, western Texas	Hegler and Pinery Mbs, Bell Canyon Fm	thin limestone intervals interbedded with sandstone and siltstone
Palo Duro Basin	PG-C	USA-S	Rotten Hill, Oldham County, Texas	Tecovas Mb, Dockum Fm, Chinle Grp	siltstone-dominated, fluviodeltaic/marginal lacustrine
	PL-E	USA-W	west slope Augusta Mountains, Pershing County, Nevada	lower Fossil Hill Mb, Favret Fm, Star Peak Grp	litharenite, debris flow deposit, high energy, coastal influence, outer platform

marine		*Hindeodella aserrata* conodont Zone; OSPZ6 palynology Zone; *Neoschwagerina craticulifera* fusulinid Zone	this study		Many samples
marine		*Ictiospathodus collinsoni – Neospathodus triangularis* conodont zones; *Columbites parisianus – Prohungarites/Subcolumbites* ammonoid zones	this study		Many samples
marine		*Eoinella nepalensis – Triassospathodus homeri* conodont zones; *Flemingites flemingianus – Procolumbites* ammonoid zones	this study		Many samples
marine			this study		Samples CH-F78-79, CH-F79-79, CH-F136-79
marine		*Haugi* ammonoid Zone–?	this study		Samples 91 OF HB110, 92 OF COY 4
marine			Vickers-Rich *et al.* 1999		
marine		*Mclaughlini* Subzone of the *Hyatti* Zone	Rieppel *et al.* 1996	Cuny *et al.* 2001	
			Dorka 2001		
marine			Delsate & Duffin 1999		
			Duffin 1993b		
marine			Ivanov *et al.* 2012		
marine			Ivanov *et al.* 2012		
marine			Ivanov *et al.* 2012		
marine			Ivanov *et al.* 2012		
marine			Ivanov *et al.* 2012		
marine			Ivanov *et al.* 2012		
marine			Ivanov *et al.* 2012		
freshwater			Murry 1989	Huber *et al.* 1993	
marine		*Mclaughlini* Subzone of the *Hyatti* Zone	Cuny *et al.* 2001		

M81	*Labascicorona*	sp.			denticles		*incertae sedis* (Elasmobranchii)	Triassic	Middle	Anisian, lower middle
M82	*Complanicorona*	aff. *rugosimargines* Johns, Barnes & Orchard, 1997			denticles		*incertae sedis* (Elasmobranchii)	Triassic	Middle	Anisian, lower middle
M83	*Glabrisubcorona*	sp.			denticles		*incertae sedis* (Elasmobranchii)	Triassic	Upper	Rhaetian
	etc. in Johns *et al.* 1997, 1999, see Cappetta 2012 for an overview									

	PL-E	USA-W	west slope Augusta Mountains, Pershing County, Nevada	lower Fossil Hill Mb, Favret Fm, Star Peak Grp	litharenite, debris flow deposit, high energy, coastal influence, outer platform
	PL-E	USA-W	west slope Augusta Mountains, Pershing County, Nevada	lower Fossil Hill Mb, Favret Fm, Star Peak Grp	litharenite, debris flow deposit, high energy, coastal influence, outer platform
	PL-E	Chile	Quebrada Punta del Viento, Domeyko Basin	Punta del Viento Limestone Fm	limestone, marginal sea

marine		*Metaggarti* Subzone of the *Hyatti* Zone	Cuny *et al.* 2001		
marine		*Metaggarti* Subzone of the *Hyatti* Zone	Cuny *et al.* 2001		
marine		*Epigondolella mosheri* conodont Biozone = " *Paracochloceras amonense* ammonoid Biozone	Sansom 2000		

A2.2. RAW SIZE DATA (STARTS NEXT PAGE)

Shortened database entries (using the same, but only relevant reference numbers as in A2.1) providing data on dimensions of teeth and spines, and also body length (in mm unless otherwise specified). Additional entries have been created (from 1200 onwards) for body length estimates unrelated to specific fossil material.

Shaded full entries are described in this study, whereas shaded names only are revised here. References provided in grey have not been personally checked by the author. Category explanation: apico-bas = apico-basal; mes-dist = mesio-distal; lab-lin = labio-lingual.

All terms are as they appear in published literature and as used here in text, figures and collection listings for the relevant entries.

						apico-bas		mes-dist		lab-lin		spines				
Entry	Genus	Species	Family	Order	Life habit	min	max	min	max	min	max	height	min ant-post	max ant-post	width	Reference
6	*Barbolabrornia*	*luedersensis* Berman, 1970		Bransonelliformes			2									
9	*Barbolabrornia*	*luedersensis* Berman, 1970		Bransonelliformes	4.5-5m in length			2	2.5	2.5	3					
23	*Lebachacanthus*	*senckenbergianus* (Fritsch, 1889)	Diplodoselachidae	Xenacanthiformes	up to 2.6m in length (Heyler & Poplin 1990)											
29	*Lebachacanthus*	*senckenbergianus* (Fritsch, 1889)	Diplodoselachidae	Xenacanthiformes		6	14									
37	*Orthacanthus*	*compressus* (Newberry, 1856)	Diplodoselachidae	Xenacanthiformes		7.5	15									
38	*Orthacanthus*	*compressus* (Newberry, 1856)	Diplodoselachidae	Xenacanthiformes				0.8	3	0.9	3.3					
40	*Orthacanthus*	*?compressus* (Newberry, 1856)	Diplodoselachidae	Xenacanthiformes				0.83	14.69	0.67	17.9					
42	*Orthacanthus*	*kounoviensis* Fritsch, 1889	Diplodoselachidae	Xenacanthiformes	about 2m in length	15	20					265		20		
55	*Orthacanthus*	*platypternus* (Cope, 1884)	Diplodoselachidae	Xenacanthiformes				0.9	13.2	0.8	9.5					
57	*Orthacanthus*	*platypternus* (Cope, 1884)	Diplodoselachidae	Xenacanthiformes								150 (spine estimate)				
58	*Orthacanthus*	*platypternus* (Cope, 1884)	Diplodoselachidae	Xenacanthiformes				2	5							
64	*Orthacanthus*	*texensis* (Cope, 1888)	Diplodoselachidae	Xenacanthiformes				0.9	7.9	0.7	8.5					
67	*Orthacanthus* -like	*texensis* (Cope, 1888)	Diplodoselachidae	Xenacanthiformes	2.0–2.6m in length											
81	*Xenacanthus*	*slaughteri* Johnson, 1999	Xenacanthidae	Xenacanthiformes				0.41	1.09	0.36	0.66					
94	*Triodus*	*carinatus* (Fritsch, 1890)	Xenacanthidae	Xenacanthiformes		1	3									
97	*Triodus*	*? brossardi* (Gaudry, 1883)	Xenacanthidae	Xenacanthiformes		1	1.8	0.7	1.5							
98	*Triodus*	*kraetschmeri* Hampe, 1989	Xenacanthidae	Xenacanthiformes			< 1									
99	*Triodus*	*obscurus* Hampe, 1989	Xenacanthidae	Xenacanthiformes		1	2									
101	*Triodus*	*palatinus* Hampe, 1989	Xenacanthidae	Xenacanthiformes		1	3									
102	*Triodus*	*sessilis* Jordan, 1849	Xenacanthidae	Xenacanthiformes		1	2									
104	*Triodus*	*lauterensis* Hampe, 1989	Xenacanthidae	Xenacanthiformes		1	2.5									
107	*Triodus*	sp.	Xenacanthidae	Xenacanthiformes	50-100 cm in length			1.5	3							
110	*Triodus?*	sp.	Xenacanthidae	Xenacanthiformes	40–50 cm in length? Heyler & Poplin 1990											
113	*Plicatodus*	*jordani* Hampe, 1995	Xenacanthidae	Xenacanthiformes		10	35									
114	*Wurdigneria*	*obliterata* Richter, 2005	Xenacanthidae	Xenacanthiformes			6		6		8					
118	*Mocrecodontus*	*mocrei* (Woodward, 1889)	Xenacanthidae	Xenacanthiformes				1.5	2	1.2	2.2					
119	*Mocrecodontus*	*mocrei* (Woodward, 1889)	Xenacanthidae	Xenacanthiformes				0.65	2.18	1.03	2.91					
122	*Mocrecodontus*	*mocrei* (Woodward, 1889)	Xenacanthidae	Xenacanthiformes					2.8		3.5					
127	*Mocrecodontus*	*indicus* (Jain, 1980)	Xenacanthidae	Xenacanthiformes								50				
142	*"Physonemus"*	sp.		Symmoriiformes								180			24	
143	*Eutacanthus*	*gigas* Branson 1916		Symmoriiformes?			26 (broken)					520 (est)	41	65		
146	*Stethacanthulus*	cf. *decorus* (Ivanov, 1999)	Falcatidae	Symmoriiformes			2.5		2.8		2.4					
147	*Stethacanthulus*	cf. *decorus* (Ivanov, 1999)	Falcatidae	Symmoriiformes			2.5		2.8		2.4					
148	*Stethacanthulus*	cf. *decorus* (Ivanov, 1999)	Falcatidae	Symmoriiformes			2.5		2.8		2.4					
164	*Glikmanius*	*occidentalis* (Leidy, 1859)	Ctenacanthidae	Ctenacanthiformes				1.28	10.15	0.75	5.23					
165	*Glikmanius*	*occidentalis* (Leidy, 1859)	Ctenacanthidae	Ctenacanthiformes			16.5		15.5							
171	*Glikmanius*	*occidentalis* (Leidy, 1859)	Ctenacanthidae	Ctenacanthiformes				4	17							
172	*Glikmanius*	*occidentalis* (Leidy, 1859)	Ctenacanthidae	Ctenacanthiformes				4	17							
174	*Glikmanius*	*myachkovensis* (Lebedev, 2001)	Ctenacanthidae	Ctenacanthiformes				3.5	11.9							
175	*Glikmanius*	*myachkovensis* (Lebedev, 2001)	Ctenacanthidae	Ctenacanthiformes				3.5	11.9							
176	*Glikmanius*	*myachkovensis* (Lebedev, 2001)	Ctenacanthidae	Ctenacanthiformes			3.5		4		2.5					
178	*Glikmanius*	*myachkovensis* (Lebedev, 2001)	Ctenacanthidae	Ctenacanthiformes			3.5		4		2.5					
179	*Glikmanius*	*culmenis* Koot, Cuny, Tintori and Twitchett, 2013	Ctenacanthidae	Ctenacanthiformes		2	8	2	8	1	5					
181	*"Cladodus"?*	sp.	Ctenacanthidae	Ctenacanthiformes			10				9					
194	*Heslerodus*	*divergens* (Trautschold, 1879)	Heslerodidae	Ctenacanthiformes				3	4							

199	*Necosaivodus*	*flagstaffensis* Hodnett, Elliot, Olson & Wittke, 2012	*incertae sedis*	Ctenacanthiformes					17								
200	*Necosaivodus*	*flagstaffensis* Hodnett, Elliot, Olson & Wittke, 2012	*incertae sedis*	Ctenacanthiformes					17								
201	*Xaibatvenator*	*swiftae* Hodnett, Elliot, Olson & Wittke, 2012	*incertae sedis*	Ctenacanthiformes				20	30								
202	*Xaibatvenator*	*swiftae* Hodnett, Elliot, Olson & Wittke, 2012	*incertae sedis*	Ctenacanthiformes				20	30								
203	*Nanoskalme*	*natans* Hodnett, Elliot, Olson & Wittke, 2012	*incertae sedis*	Ctenacanthiformes				2.5	8								
207	*Acondylacanthus?*	*browni* Branson, 1916	*incertae sedis*	Ctenacanthiformes								130	20	27			
209	*Acondylacanthus?*	*obscuracostatus* Branson, 1916	*incertae sedis*	Ctenacanthiformes								165	27	41			
211	*Pyknotylacanthus*	*spathianus* Mutter & Rieber, 2005		*incertae sedis*				0.25	1.3			178		34	16.2		
221	*Adamantina*	*benedictae* Bendix-Almgreen, 1993	Jalodontidae	*incertae sedis*				3	5	2.5	5						
227	*Adamantina*	sp.	Jalodontidae	*incertae sedis* (Elasmobranchii)			1.7		1.3								
233	*Dicrenodus*	*latus* Minikh, 1996	Hybodontidae	Hybodontiformes					2		1.8						
234	*Dicrenodus*	*barchanensis* Minikh, 1996	Hybodontidae	Hybodontiformes					1.1		1.1						
235	*Dicrenodus*	*donatus* Minikh, 1996	Hybodontidae	Hybodontiformes					3		2.5						
240	*Hybodus*	*longiconus* Agassiz, 1843	Hybodontinae	Hybodontiformes	6	17											
241	*Hybodus*	*longiconus* Agassiz, 1843	Hybodontinae	Hybodontiformes					15								
253	*Hybodus*	*plicatilis* Agassiz, 1843	Hybodontinae	Hybodontiformes	7.1	12.3											
254	*Hybodus*	*plicatilis* Agassiz, 1843	Hybodontinae	Hybodontiformes				3	4								
255	*Hybodus*	sp. aff. *plicatilis* Agassiz, 1843	Hybodontinae	Hybodontiformes		18			17								
261	*Hybodus*	*multiplicatus/multiconus* Jaekel, 1889	Hybodontinae	Hybodontiformes	4	7.5		5	16.5								
262	*Hybodus*	*sasseniensis* Stensiö, 1921	Hybodontinae	Hybodontiformes					12								
263	*Hybodus*	*sasseniensis* Stensiö, 1921	Hybodontinae	Hybodontiformes				1	7								
266	*Hybodus*	*microdus* Stensiö, 1921	Hybodontinae	Hybodontiformes				0.6	2.5 (3.5)								
277	*Hybodus*	*zucodengensis* Yang, Wang & Hao 1984	Hybodontinae	Hybodontiformes	1	1.1		1	1.6	0.2	0.6						
278	*Hybodus*	*gohi* Yang, Wang & Hao 1984	Hybodontinae	Hybodontiformes		0.75		1.7	1.8	0.4	0.6						
280	*Hybodus*	sp. 1	Hybodontinae	Hybodontiformes		> 8.7			> 24								
282	*Hybodus*	sp.	Hybodontinae	Hybodontiformes					1								
286	cf. *Hybodus*	sp.	Hybodontinae	Hybodontiformes	0.5	0.6			1.4		0.2						
289	cf. *Hybodus*	sp.	Hybodontinae	Hybodontiformes		0.5		1	1.5		0.3						
291	*Hybodus* ?	*jepseni* Bryant, 1934	Hybodontinae	Hybodontiformes	>13 cm in length							27 (ant) 45 (post)					
299	*Hybodus*	*sublaevis* Agassiz, 1843	Hybodontinae	Hybodontiformes				0.8	1.5								
300	*Hybodus*	*raricostatus* Agassiz, 1843	Hybodontinae	Hybodontiformes				3	7								
304	*Hybodus*	cf. *nonstriatus* Winkler, 1880	Hybodontinae	Hybodontiformes					1								
319	*Hybodus*		Hybodontinae	Hybodontiformes				2	4								
320	*Hybodus*		Hybodontinae	Hybodontiformes				2	4								
321	*Hybodus*		Hybodontinae	Hybodontiformes				2	4								
322	*Hybodus*		Hybodontinae	Hybodontiformes				2	4								
323	*Hybodus*		Hybodontinae	Hybodontiformes				2	4								
324	*Hybodus*		Hybodontinae	Hybodontiformes				2	4								
337	*Hybodus*	sp.	Hybodontinae	Hybodontiformes								3–5.5 (fragm.)					
339	*'Polyacrodus'*	*lapalomensis* Johnson, 1981	Hybodontinae	Hybodontiformes				0.95	3.48	0.4	1.34						
340	*Polyacrodus?*	sp.	Hybodontinae	Hybodontiformes					12.13		3.28						
341	*'Polyacrodus'*	*nitchiei* Johnson, 1981	Hybodontinae	Hybodontiformes				1.17	4.86	0.48	1.5						
342	*'Polyacrodus'*	*wichitaensis* Johnson, 1981	Hybodontinae	Hybodontiformes				1.55	7.22	0.52	1.76						

349	*'Polyacrodus'*	*polycyphus* (Agassiz, 1837)	Hybodontinae	Hybodontiformes				10	25							
351	*'Polyacrodus'*	*polycyphus* (Agassiz, 1837)	Hybodontinae	Hybodontiformes		6.8	7.7	12.4	13.1	3.8	4.7					
352	*'Polyacrodus'*	*polycyphus* (Agassiz, 1837)	Hybodontinae	Hybodontiformes					14.1		5.9					
355	*'Polyacrodus'*	*polycyphus* (Agassiz, 1837)	Hybodontinae	Hybodontiformes?					25							
356	*'Polyacrodus'*	*polycyphus* (Agassiz, 1837)	Hybodontinae	Hybodontiformes?	2–2.5 m in length?				>15							
359	*'Polyacrodus'*	*oknacinus* (Quenstedt, 1856)	Hybodontinae	Hybodontiformes				2	3							
361	*'Polyacrodus'*	*oknacinus* (Quenstedt, 1856)	Hybodontinae	Hybodontiformes					30							
367	*'Polyacrodus'*	*cuspidatus* (Agassiz, 1843)	Hybodontinae	Hybodontiformes			5.7		17.3							
368	*'Polyacrodus'*	*krafti* Seilacher, 1943	Hybodontinae	Hybodontiformes			1.4									
369	*'Polyacrodus'*	*krafti* Seilacher, 1943	Hybodontinae	Hybodontiformes		0.9	0.9	1.8	2.3	0.8	0.9					
370	*'Polyacrodus'*	*krafti* Seilacher, 1943	Hybodontinae	Hybodontiformes		0.6	0.9	1.4	2.9	0.6	0.8					
372	*'Polyacrodus'*	*keuperianus* (Winkler, 1880)	Hybodontinae	Hybodontiformes			6.3		4.3							
376	*'Polyacrodus'*	*keuperianus* (Winkler, 1880)	Hybodontinae	Hybodontiformes			3.6		8.1							
377	cf. *'Polyacrodus'*	*keuperianus* (Winkler, 1880)	Hybodontinae	Hybodontiformes	2–2.5 m in length?				>15							
378	*'Polyacrodus'*	*keuperianus* (Winkler, 1880)	Hybodontinae	Hybodontiformes			2.1		4.7							
383	*'Polyacrodus'*	sp. 1	Hybodontinae	Hybodontiformes			1.2		2.7							
387	*'Polyacrodus?'*	sp.	Hybodontinae	Hybodontiformes?			4		10							
390	*'Polyacrodus'*	sp.	Hybodontinae	Hybodontiformes?					<3							
394	*Acrodus* ?	*oilsoni* Johnson, 1981	Acrodontinae	Hybodontiformes				1.59	9.36	0.59	3.79					
395	*Acrodus* ?	cf. *oilsoni* Johnson, 1981	Acrodontinae	Hybodontiformes				4.85	5.4							
397	*Acrodus* ?	*sweetlacruensis* Johnson, 1981	Acrodontinae	Hybodontiformes				1.53	6.07	0.6	2.48					
398	*Acrodus* ?	*sweetlacruensis* Johnson, 1981	Acrodontinae	Hybodontiformes				2.95	3.36							
400	*Acrodus* ?	sp.	Acrodontinae	Hybodontiformes				6.9	9.7	2.3	3.6					
406	*Acrodus*	*gaillardoti* Agassiz, 1837	Acrodontinae	Hybodontiformes				0.5	2.2							
412	*Acrodus*	*gaillardoti* Agassiz, 1837	Acrodontinae	Hybodontiformes				20								
414	*Acrodus*	*lateralis* Agassiz, 1837	Acrodontinae	Hybodontiformes			11.8	26	27		10	294 / 310-315				
420	*Acrodus*	*lateralis* Agassiz, 1837	Acrodontinae	Hybodontiformes				0.6	0.7	0.2	0.3					
421	*Acrodus*	*lateralis* Agassiz, 1837	Acrodontinae	Hybodontiformes			1.7	4.7	~10	2.4	3.1					
422	*Acrodus*	*lateralis* Agassiz, 1837	Acrodontinae	Hybodontiformes					12							
423	*Acrodus*	*lateralis* Agassiz, 1837	Acrodontinae	Hybodontiformes				5	7							
424	*Acrodus*	*lateralis* Agassiz, 1837	Acrodontinae	Hybodontiformes					6							
426	*Acrodus*	cf. *lateralis* Agassiz, 1837	Acrodontinae	Hybodontiformes					0.4		0.2					
431	*Acrodus*	*spitzbergensis* Hulke, 1873	Acrodontinae	Hybodontiformes				1.3	8 (10-12)							
435	*Acrodus*	*spitzbergensis* Hulke, 1873	Acrodontinae	Hybodontiformes					4.1		1.2					
436	*Acrodus*	*spitzbergensis* Hulke, 1873	Acrodontinae	Hybodontiformes			1.4		2		1.3					
448	*Acrodus*	sp.	Acrodontinae	Hybodontiformes			2.3		8.6		4.6					
449	*Acrodus* ?	sp. 1	Acrodontinae	Hybodontiformes					<2							
454	*Acrodus*	*cunecocostatus* Cuny, Rieppel & Sander, 2001	Acrodontinae	Hybodontiformes					4.3		1.8					
455	*Acrodus*	cf. *cunecocostatus* Cuny, Rieppel & Sander, 2001	Acrodontinae	Hybodontiformes					1							
456	*Acrodus*	sp. 1	Acrodontinae	Hybodontiformes		0.9	1.1	5	6.2	1.4	2					
457	*Acrodus*	sp. 2	Acrodontinae	Hybodontiformes			1.5	1.6	3.2	1.1	2					
458	*Acrodus*	sp. 3	Acrodontinae	Hybodontiformes		1.7	2.2	3.2	4.4	2.2	3.2					
459	*Acrodus*	sp.	Acrodontinae	Hybodontiformes					0.35		0.25					
461	*Acrodus*	*georgii* Mutter, 1998	Acrodontinae	Hybodontiformes	1.8–2.5 m in length	1.7	3.9	3.5	29.4	3.9	6.6	315		30		
462	*Acrodus*	*mutteri* Delsate & Duffin, 1999	Acrodontinae	Hybodontiformes				0.9	1.8	0.75						
466	*Acrodus:?*	sp.	Acrodontinae	Hybodontiformes			2		8		2.3					
467	*Acrodus*	*microdus* Winkler, 1880	Acrodontinae	Hybodontiformes				0.2	1							
469	*Acrodus*	spp.	Acrodontinae	Hybodontiformes				0.9	3.8							
476	*Acrodus:?*	sp.	Acrodontinae	Hybodontiformes			6		10.69							
478	*Asteracanthus*	sp. (cf. *reticulatus* Agassiz, 1837; cf. *agassizii* Alberti, 1864)	Acrodontinae	Hybodontiformes					21		9.5					

480	*Asteracanthus* , cf.	sp.	Acrodontinae	Hybodontiformes					16.11		8.77					
485	*Palaeobates*	*angustissimus* (Agassiz, 1838)	Acrodontinae	Hybodontiformes				9.5	12.5	2.8	3.2					
487	*Palaeobates*	*angustissimus* (Agassiz, 1838)	Acrodontinae	Hybodontiformes					0.85		0.25					
490	*Palaeobates*	*angustissimus* (Agassiz, 1838)	Acrodontinae	Hybodontiformes					8							
491	*Palaeobates*	*angustissimus* (Agassiz, 1838)	Acrodontinae	Hybodontiformes				5	10							
493	*Palaeobates*	sp.	Acrodontinae	Hybodontiformes					0.75		0.3					
497	*Palaeobates* ?	*shastensis* Bryant, 1914	Acrodontinae	Hybodontiformes				16	39	5.5	8					
500	*Palaeobates*	*reticulatus* Duffin, 1998	Acrodontinae	Hybodontiformes		1.1		3	6	0.5						
501	*Palaeobates*	sp.	Acrodontinae	Hybodontiformes					11		4.8					
505	*Palaeobates*	*polaris* Stensiö, 1921	Acrodontinae	Hybodontiformes	1 m in length											
506	*Palaeobates*	*polaris* Stensiö, 1921	Acrodontinae	Hybodontiformes	1 m in length	2	6	3	18	2	4					
509	*Palaeobates*	sp.	Acrodontinae	Hybodontiformes		0.2	0.3	0.4	1.2	0.1	0.4					
523	*Lissodus*	*africanus* (Broom, 1909)	Unnamed	Hybodontiformes	23 cm in length			0.7	1.3							
527	*Lissodus*	*angulatus* (Stensiö, 1921)	Unnamed	Hybodontiformes				1	4 (6-7)							
529	*Lissodus*	*cassangensis* (Teixeira, 1956)	Unnamed	Hybodontiformes	>20 cm in length		<1		<1		<1	30 (ant) 20 (post)				
530	*Lissodus*	*tiandongensis* Wang, Yang, Jin & Wang, 2001	Unnamed	Hybodontiformes		0.6			2.4		0.6					
531	*Lissodus*	*volgensis* Minikh, 2001	Unnamed	Hybodontiformes				0.6	1	0.3	0.7					
532	*Lissodus*	*aquilus* Minikh, 1996	Unnamed	Hybodontiformes				0.8	1.5							
533	*Lissodus*	sp.	Unnamed	Hybodontiformes					6		2.1					
534	*Lissodus*	*triaktis* Minikh, 1996	Unnamed	Hybodontiformes				1	1.8							
535	*Lissodus*	*triaktis* Minikh, 1996	Unnamed	Hybodontiformes				1	1.8							
536	*Lissodus*	*pykaspiensis* Minikh, 1996	Unnamed	Hybodontiformes				1	3							
539	*Lissodus*	*cristatus* Delsate & Duffin, 1999	Unnamed	Hybodontiformes			0.5	0.8	1.8							
540	*Lissodus*	cf. *cristatus* Delsate & Duffin, 1999	Unnamed	Hybodontiformes					1							
542	*Lissodus*	*subhercynicus* Dorka, 2001	Unnamed	Hybodontiformes		0.8	1.5	1.6	3.1	0.8	1.5					
543	*Lissodus*	*subhercynicus* Dorka, 2001	Unnamed	Hybodontiformes		0.6	1.3	1.5	3	0.7	1.4					
544	*Lissodus*	*subhercynicus* Dorka, 2001	Unnamed	Hybodontiformes		0.6	1.3	2	3.8	0.8	1.5					
545	*Lissodus*	sp.	Unnamed	Hybodontiformes		0.5	1.1	1.2	2.5	0.6	1.7					
548	*Lissodus*	*nodosus* (Seilacher, 1943)	Unnamed	Hybodontiformes	species well below 1 m in length? Böttcher 2010			1	5							
553	*Lissodus*	*nodosus* (Seilacher, 1943)	Unnamed	Hybodontiformes				0.6	1.7							
555	*Lissodus*	*nodosus* (Seilacher, 1943)	Unnamed	Hybodontiformes				0.8	2.1	0.4	0.8					
556	*Lissodus*	*nodosus* (Seilacher, 1943)	Unnamed	Hybodontiformes		0.6	1.2	1.8	2.7	0.7	0.9					
557	*Lissodus*	*nodosus* (Seilacher, 1943)	Unnamed	Hybodontiformes		0.5	0.7	1.1	1.4	0.5	0.9					
558	*Lissodus*	*nodosus* (Seilacher, 1943)	Unnamed	Hybodontiformes		0.9	1.8	2.4	3.6	0.8	1.4					
559	*Lissodus*	*nodosus* (Seilacher, 1943)	Unnamed	Hybodontiformes					5							
560	*Lissodus*	*nodosus* (Seilacher, 1943)	Unnamed	Hybodontiformes	species well below 1 m in length?											
563	*Lissodus*	*minimus* (Agassiz, 1839)	Unnamed	Hybodontiformes				2	5							
595	*Lissodus*	*minimus* (Agassiz, 1839)	Unnamed	Hybodontiformes				1	7							
597	*Lissodus*	*minimus* (Agassiz, 1839)	Unnamed	Hybodontiformes		1.13	1.3	1.1	1.93	0.92						
613	*Lissodus*	sp.	Unnamed	Hybodontiformes					0.5		0.75					
614	*Lissodus*	*lepagei* Duffin, 1993	Unnamed	Hybodontiformes			0.8	0.77	>1.48		0.6					
617	*Lissodus*	*lepagei* Duffin, 1993	Unnamed	Hybodontiformes					<2							
623	*Lissodus*	sp.	Unnamed	Hybodontiformes					0.5		0.25					
627	*Lissodus*		Unnamed	Hybodontiformes				2	4							
628	*Lissodus*		Unnamed	Hybodontiformes				2	4							
629	*Lissodus*		Unnamed	Hybodontiformes				2	4							
630	*Lissodus*		Unnamed	Hybodontiformes				2	4							
631	*Lissodus*		Unnamed	Hybodontiformes				2	4							

632	*Lissodus*		Unnamed	Hybodontiformes				2	4							
633	*Lissodus*		Unnamed	Hybodontiformes				2	4							
634	*Lissodus*		Unnamed	Hybodontiformes				2	4							
635	*Lissodus*		Unnamed	Hybodontiformes				2	4							
636	*Lissodus*		Unnamed	Hybodontiformes				2	4							
637	*Lissodus*		Unnamed	Hybodontiformes				2	4							
638	cf. *Lissodus*		Unnamed	Hybodontiformes								>58 (fragm.)				
640	*Lonchidion*	*humblei* Murry, 1981	Lonchidiidae	Hybodontiformes				1	1.56							
652	*Lonchidion*	*herganensis* Fischer, Voigt, Schneider, Buchwitz & Voigt, 2011	Lonchidiidae	Hybodontiformes		0.32	0.77	0.88	2.04	0.44	0.87					
653	*Diplolonchidion*	*murryi* Heckert, 2004	Lonchidiidae	Hybodontiformes					2							
654	*Parvodus?*	sp.	Lonchidiidae	Hybodontiformes					1.5							
655	*Gansuselache*	*tungshengi* Wang, Zhang, Zhu, Zhao, 2009	Lonchidiidae?	Hybodontiformes	490 mm in length				3							
656	*Steinbachodus*	*estheriae* Reif, 1980	Steinbachodontidae	Hybodontiformes	80–100 cm in length	0.8	1.9	1.4	3							
661	*Reticulodus*	*synergus* Murry & Kirby, 2002	Distobatidae	Hybodontiformes					10							
665	gen. indet.	sp. indet.	*incertae sedis*	Hybodontiformes								15.8 (fragm.)		12.6	7.5	
666	gen. indet.	sp. indet.	*incertae sedis*	Hybodontiformes								50				
673	gen. indet.	sp. indet.	*incertae sedis*	Hybodontiformes		0.4	0.6	1.3	1.8	0.6	0.8					
675	*Homalodontus*	*apicognagus* (Mutter, De Blanger, Neuman, 2007)	Homalodontidae	Hybodontiformes?	1.2–1.5 m in length	5.1		3.3	11.9							
676	*Homalodontus*	cf. *apicognagus* (Mutter, De Blanger and Neuman, 2007)	Homalodontidae	*incertae sedis* (Hybodontiformes?)						0.4						
677	*Homalodontus*	*homalorhizo* (Mutter, De Blanger, Neuman, 2007)	Homalodontidae	Hybodontiformes?				1.2				17-20		4		
679	'Palaeozoic Genus 1'	*zideki* (Johnson, 1981)	*incertae sedis*	Hybodontiformes				0.6	2.88	0.4	1.19					
682	'Palaeozoic Genus 1'	*zideki* (Johnson, 1981)	*incertae sedis*	Hybodontiformes					< 2							
684	cf. 'Palaeozoic Genus 1'	sp.	*incertae sedis*	Hybodontiformes			1.1		0.6		0.7					
685	'Palaeozoic Genus 1'	sp.	*incertae sedis*	Hybodontiformes		1.5	3	2	4							
689	*'Lissodus'*	*sardiniensis* Fischer *et al.*, 2010	*incertae sedis*	Hybodontiformes				0.34	1.31							
692	cf. *'Lissodus'*	sp.	*incertae sedis*	Hybodontiformes								9				
704	*Omanoselache*	*contrarius* Johns, Barnes & Orchard, 1997	*incertae sedis*	Hybodontiformes					<1							
705	*Omanoselache*	*contrarius* Johns, Barnes & Orchard, 1997	*incertae sedis*	Hybodontiformes					2		0.2					
706	*Omanoselache*	*contrarius* Johns, Barnes & Orchard, 1997	*incertae sedis*	Hybodontiformes					1.3		0.5					
708	*Omanoselache*	*bucheri* Cuny, Rieppel & Sander, 2001	*incertae sedis*	Hybodontiformes					3.3		1.2					
709	*Omanoselache*	*hendersconi* Koot, Cuny, Tintori and Twitchett, 2013	*incertae sedis*	Hybodontiformes		0.6	0.8	1	4	0.6	0.9					
710	*Omanoselache*	*angiolinii* Koot, Cuny, Tintori and Twitchett, 2013	*incertae sedis*	Hybodontiformes		0.6	0.7	1.6	1.9		0.5					
711	*Omanoselache*	*angiolinii* Koot, Cuny, Tintori and Twitchett, 2013	*incertae sedis*	Hybodontiformes		0.6	0.7	1.6	1.9		0.5					
712	*Omanoselache*	sp. H	*incertae sedis*	Hybodontiformes		0.2	0.6	0.8	1.9	0.2	0.5					
713	*Omanoselache*	sp. H	*incertae sedis*	Hybodontiformes		0.2	0.6	0.8	1.9	0.2	0.5					
718	*Omanoselache*	cf. sp. H	*incertae sedis*	Hybodontiformes			0.5	1.6	2.2		0.3					
719	*Omanoselache*	cf. sp. H	*incertae sedis*	Hybodontiformes			0.5	1.5	2.2		0.3					
720	*Omanoselache*	cf. sp. H	*incertae sedis*	Hybodontiformes			0.4		1.6		0.4					
721	*Omanoselache*	cf. sp. H	*incertae sedis*	Hybodontiformes			0.4		1.6		0.4					
722	*Omanoselache*	sp. A	*incertae sedis*	Hybodontiformes			0.7				0.6					

724	*Omanoselache*	sp. A	*incertae sedis*	Hybodontiformes					1							
725	*Omanoselache*	cf. sp. A	*incertae sedis*	Hybodontiformes			0.8		1.8		0.6					
726	cf. *Omanoselache*	sp.	*incertae sedis*	Hybodontiformes			0.9		2.5		1					
727	cf. *Omanoselache*	sp.	*incertae sedis*	Hybodontiformes			0.9		2.5		1					
728	cf. *Omanoselache*	sp.	*incertae sedis*	Hybodontiformes			0.4	0.9	1	0.3	0.4					
729	*Reesodus*	*underwoodi* Koot, Cuny, Tintori and Twitchett, 2013	*incertae sedis*	Hybodontiformes		0.4	0.5	0.9	1.2	0.3	0.5					
730	*Terescodus*	*amplexus* Koot, Cuny, Tintori and Twitchett, 2013	*incertae sedis*	Hybodontiformes		0.5	0.6	1.1	2	0.3	0.4					
731	gen. indet.	sp. indet.	*incertae sedis*	Hybodontiformes			0.6	1.6			0.5					
732	*Gunnellodus*	*bellistriatus* (Gunnell, 1933)		Hybodontiformes?		1.5	3	0.4	1	0.7	1					
734	*Sphenacanthus*	*sanpaulensis* Chahud, Fairchild & Petri, 2010	Sphenacanthidae									88		7		
737	*Wodnika*	*striatula* Münster, 1843	Sphenacanthidae									85		11		
739	*Wodnika*	*striatula* Münster, 1843	Sphenacanthidae		50–80 cm in length							60-100				
741	*Wodnika*	*borealis* Maisey, 1982	Sphenacanthidae		up to 100 cm in length							>150				
747	*Khuffia*	*lenis* Koot, Cuny, Tintori and Twitchett, 2013	Sphenacanthidae	*incertae sedis* (Euselachii)		0.5	0.6	1	1.2	0.3	0.4					
748	*Khuffia*	*prolixa* Koot, Cuny, Tintori and Twitchett, 2013	Sphenacanthidae	*incertae sedis* (Euselachii)		0.7	0.8	1.3	1.6	0.3	0.5					
749	gen. indet.	sp. indet. A		*incertae sedis* (Euselachii)		0.5	1.1	1.8	2		0.5					
750	gen. indet.	sp. indet. B		*incertae sedis* (Euselachii)			1.1		1.9		0.9					
751	gen. indet.	sp. indet. C		*incertae sedis* (Euselachii)			0.5	>1.1			0.4					
752	gen. indet.	sp. indet.		*incertae sedis* (Euselachii)								21,87 (incompl.)				
754	*Coccolepella*	cf. *kordi* (Duffin and Ward, 1983)	Anachronistidae				0.5		1.1		0.6					
758	*Coccolepella*	sp. nov.	Anachronistidae						1.1							
764	*Pseudodalatias*	*barnstonensis* (Sykes, 1971)	Pseudodalatiidae					3	5							
775	*Pseudodalatias*	*henarejensis* Botella, Plasencia, Marquez-Aliaga, Cuny & Dorka, 2009	Pseudodalatiidae			0.5	2.5									
776	cf. *Palidiplospinax*	sp.	Palaeospinacidae	Synechodontiformes			1									
777	Genus S	sp. T	*incertae sedis*	Synechodontiformes		0.4	1.3	0.8	2.3	0.3	0.5					
778	Genus S	sp. T	*incertae sedis*	Synechodontiformes		0.4	1.3	0.8	2.3	0.3	0.5					
779	Genus S	sp. T	*incertae sedis*	Synechodontiformes			0.5		1.1		0.3					
780	Genus S	sp. T	*incertae sedis*	Synechodontiformes			0.5		1.1		0.3					
782	Genus S	cf. sp. T	*incertae sedis*	Synechodontiformes		0.5	0.6	1	1.7		0.3					
783	Genus S	sp. A	*incertae sedis*	Synechodontiformes		0.4	1.3	0.8	2.3	0.3	0.5					
787	cf. Genus S	sp.	*incertae sedis*	Synechodontiformes			0.7		1.2		0.5					
788	*Synechodus* (pre-Jurassic)	*antiquus* Ivanov, 2005	*incertae sedis*	Synechodontiformes					1.6							
789	*Synechodus* (pre-Jurassic)	sp.	*incertae sedis*	Synechodontiformes			0.9									
790	*Synechodus* (pre-Jurassic)	*rhaeticus* Duffin, 1982	*incertae sedis*	Synechodontiformes		2		3	8			72	9	11.5		
798	*Synechodus* (pre-Jurassic)	*incrementum* Johns, Barnes and Orchard, 1997	*incertae sedis*	Synechodontiformes					1.74							
799	*Synechodus* (pre-Jurassic)	*multinodosus* Johns, Barnes and Orchard, 1997	*incertae sedis*	Synechodontiformes				1.31	2.16							
801	*Synechodus* (pre-Jurassic)	*volaticus* Johns, Barnes and Orchard, 1997	*incertae sedis*	Synechodontiformes					<0.4							

802	*Synechodus* (pre-Jurassic)	sp. 1	*incertae sedis*	Synechodontiformes				0.5	1							
804	*Synechodus* (pre-Jurassic)	sp.	*incertae sedis*	Synechodontiformes			0.6	0.8	> 1							
806	*Synechodus* (pre-Jurassic)	sp. indet.	*incertae sedis*	Synechodontiformes			0.6	1.7			0.4					
807	*Synechodus* (pre-Jurassic)	sp. indet.	*incertae sedis*	Synechodontiformes			0.5	0.7	1.7	0.4	0.4					
810	*Nemacanthus*	sp.	*incertae sedis*	Synechodontiformes		6.3	8									
811	*Nemacanthus*	*elegans* Evans, 1904	*incertae sedis*	Synechodontiformes								163		23		
812	*Nemacanthus*	sp.	*incertae sedis*	Synechodontiformes								4.5 (fragm.)		1.5		
826	*Nemacanthus*	sp.	*incertae sedis*	Synechodontiformes								60		8		
827	gen. indet.	sp. indet.	*incertae sedis*	Synechodontiformes		1.8										
828	Genus P	sp. P	*incertae sedis*	Synechodontiformes		0.4	0.5	0.7	1.6	0.2	0.3					
829	Genus P	sp. P	*incertae sedis*	Synechodontiformes		0.4	0.5	0.7	1.6	0.2	0.3					
831	cf. Genus P	sp.	*incertae sedis*	Synechodontiformes		0.4	0.6		1.5		0.4					
846	*Rhomphaiodon*	*minor* (Agassiz, 1837)	*incertae sedis*	Synechodontiformes			<3									
849	*Rhomphaiodon*	*minor* (Agassiz, 1837)	*incertae sedis*	Synechodontiformes		0.95	3 (10)		1.9	3.6 (14)		2.1				
851	*Rhomphaiodon*	*nicolensis* Duffin, 1993	*incertae sedis*	Synechodontiformes		1	10	1	12							
853	*Griphodon*	*candaui* Cuny, Martin, Rauscher & Mazin, 1998	*incertae sedis*	Synechodontiformes			6									
854	*Mucrovenator*	*minimus* Cuny, Rieppel & Sander, 2001	*incertae sedis*	Synechodontiformes			2.5		2.5							
859	*Hoplacanthus*	*richelsdorfensis* Schaumberg, 1982	*incertae sedis*		approx. 75 cm in length		3		5							
860	*Hueneichthys*	*costatus* Reif, 1977	*incertae sedis*						< 2							
861	*Reifia*	*minuta* Duffin, 1980	*incertae sedis*				0.7		1		0.4					
863	*Vallisia*	*coppi* Duffin, 1982	*incertae sedis*				2.5		2							
864	*Vallisia*	*coppi* Duffin, 1982	*incertae sedis*				2.5		2							
868	*Dicrateodus*	*tricuspidatus* Schmid, 1861	*incertae sedis*	Hybodontiformes		<1	>2	0.2	1	0.5	1.5					
871	*Dicrateodus*	cf. *tricuspidatus* Schmid, 1861	*incertae sedis*	Hybodontiformes		<1	>2	0.2	1	0.5	1.5					
873	*Duffinselache*	*helvellensis* Duffin, 1998	*incertae sedis*	Hybodontiformes			0.7		4.1		0.6					
876	*Rhomaleodus*	*budurovi* Andreev & Cuny, 2012	*incertae sedis*			0.4	0.5	0.6	0.95							
878	*Pseudocetorhinus*	*pickfordi* Duffin, 1998		*incertae sedis* (Neoselachii)		3		4.5	10	3						
885	Hexanchidae gen. indet.	sp. indet.	*incertae sedis*				7		11							
886	*Lyphaikodus*	*gladius* Minikh, 1996	*incertae sedis*						2		3					
887	*Lyphaikodus*	*gladius* Minikh, 1996	*incertae sedis*						2		3					
888	*Amelacanthus*	cf. *sulcatus* (Agassiz, 1837)		*incertae sedis* (Neoselachii)								>30		10		
892	gen. indet.	sp. indet. A		*incertae sedis* (Neoselachii)			0.8		1.2		0.6					
893	gen. indet.	sp. indet. B		*incertae sedis* (Neoselachii)		1										
895	gen. indet. (Neoselachii?)	sp. indet.	*incertae sedis*				3.5		6							
898	*Acronemus*	*tuberculatus* (Bassani, 1886)		*incertae sedis* (Hybodontiformes! Neoselachii)	30-35 cm in length											
904	*Orodus*	*ipeunaensis* Chahud, Fairchild & Petri, 2010	Orodontidae	Orodontiformes			5.3	10.2	10.4		5.4					
908	*"Caseodus"*	*variedentis* Mutter & Neuman, 2008	Caseodontidae	Eugeneodontiformes	1–1.5 m in length			3	25							

909	*Caseodus*	cf. *validentis* Mutter and Neuman, 2008	Caseodontidae	Eugeneodontiformes			0.6		1.1		0.4							
912	*Fadenia*	*crenulata* Nielsen, 1932	Caseodontidae	Eugeneodontiformes				0.5	2.2									
915	*Fadenia*	*urroclasmata* Mutter & Neuman, 2008	Caseodontidae	Eugeneodontiformes	1 m in length				6 (8-10)									
921	*Ectobocodus*	*schaefferi* Zangerl, 1981	Eugeneodontidae	Eugeneodontiformes				3	38									
922	*Ectobocodus*	*xenesi* Hampe, Hairapetian, Dorka, Witzmann, Akbari & Korn, 2013	Eugeneodontidae	Eugeneodontiformes					2.82									
923	gen. indet.	sp. indet.	Eugeneodontidae	Eugeneodontiformes					2.67									
937	*Helicoprion*	sp.	Agassizodontidae	Eugeneodontiformes														
938	*Helicoprion*	sp.	Agassizodontidae	Eugeneodontiformes														
939	*Helicoprion*	sp.	Agassizodontidae	Eugeneodontiformes														
948	*Helicoprion*	sp.	Agassizodontidae	Eugeneodontiformes														
953	*Helicoprion*	*bessonowi* Karpinsky, 1899	Agassizodontidae	Eugeneodontiformes														
954	*Helicoprion*	*ergassaminon* Bendix-Almgreen, 1966	Agassizodontidae	Eugeneodontiformes														
955	*Helicoprion*	*ferrieri* Hay, 1907	Agassizodontidae	Eugeneodontiformes														
956	*Helicoprion*	*ferrieri* Hay, 1907	Agassizodontidae	Eugeneodontiformes														
957	*Helicoprion*	cf. *ferrieri* Hay, 1907	Agassizodontidae	Eugeneodontiformes														
958	*Helicoprion*	*ferrieri* Hay, 1907	Agassizodontidae	Eugeneodontiformes														
959	*Helicoprion*	*nevadensis* Wheeler, 1939	Agassizodontidae	Eugeneodontiformes														
960	*Helicoprion*	*sierrensis* Wheeler, 1939	Agassizodontidae	Eugeneodontiformes														
963	*Helicoprion*	sp. indet.	Agassizodontidae	Eugeneodontiformes														
964	*Helicoprion*	*jingmenense* Chen, Cheng & Yin, 2007a	Agassizodontidae	Eugeneodontiformes														
990	gen. indet.	sp. indet.	Edestidae	Eugeneodontiformes				2	3									
992	gen. indet.	sp. indet.		Eugeneodontiformes	1 m in length													
994	gen. indet.	sp. indet.		Eugeneodontiformes ?				1.8			1							
1001	*Janassa*	*bituminosa* (Schlotheim, 1820)	Janassidae	Petalodontiformes					1.25		1							
1010	*Janassa*	*kerri* (Weigelt, 1930)	Janassidae	Petalodontiformes		6	7	4	10									
1011	*Janassa*	*kerri* (Weigelt, 1930)	Janassidae	Petalodontiformes			11.5		12									
1015	*Janassa*	*unguicula* (Eastman, 1903)	Janassidae	Petalodontiformes						11	19 (25)							
1019	*Janassa*	sp.	Janassidae	Petalodontiformes			32.5		21									
1023	*Megactenopetalus*	*kaibabanus* David, 1944	Pristodontidae	Petalodontiformes			90		96	12	26							
1028	*Megactenopetalus*	*kaibabanus* David, 1944	Pristodontidae	Petalodontiformes			(55)		(110)			(200)		20	22			
1035	gen. indet.	sp. indet.		Petalodontiformes			11		10.6									
1036	*Petalodus*	sp. A	Petalodontidae	Petalodontiformes		17	20		36									
1037	*Petalodus*	sp. B	Petalodontidae	Petalodontiformes		15	16		30									
1038	*Petalodus*	sp. C	Petalodontidae	Petalodontiformes		5	9	24	34									
1039	*Petalodus*	sp. D	Petalodontidae	Petalodontiformes			21		34									
1050	*Itapyrodus*	*punctatus* Silva Santos, 1990	Petalodontidae	Petalodontiformes		5.1	16.5	6.3	20.4	3.5	10.5							
1056	gen. indet.	sp. indet.		Petalodontiformes?			1.7				1.9							
1069	*Helodus*	sp.	Helodontidae	Helodontiformes					18-22		6							
1078	*Crassidonta*	*stuckenbergi* Branson, 1916	Cochliodontidae	Cochliodontiformes					34		28							
1080	*Crassidonta*	*subcrenulata* Teichert, 1943	Cochliodontidae	Cochliodontiformes		8	16	22	37	14	26							
1085	*Deltodus*	aff. *mercurei* Newberry, 1876	Cochliodontidae	Cochliodontiformes				7		8	12							
1093	*Sandalodus*	sp.	Cochliodontidae	Cochliodontiformes					10									
1094	gen. indet.	sp. indet.	Cochliodontidae *incertae sedis*	Cochliodontiformes					9		20							
1095	*Solenodus*	cf. *crenulatus* Trautschold, 1874	*incertae sedis*	Cochliodontiformes				2.3	4.2		4							
1108	*Arctacanthus*	*exiguus* Yamagishi, 2004		Chimaeriformes?			2.9		0.9		2.8							
1110	*Arctacanthus* ?	sp.		Chimaeriformes?		1.6			1.4									

1117	*Macrodontacanthus*	*kingi* Romer, 1942		*incertae sedis*							140 (200?)					
1118	gen. indet.	sp. indet.		*incertae sedis*					11.92		12.7					
1200	*Bartholomia* Johnson, 2003				4.5-5m long (Zidek *et al.* 2004)	1	3									Ginter *et al.* 2010
1201	*Lebachacanthus* Soler-Gijón, 1997				up to 3 m long (Hampe 1988b)	6	13									Ginter *et al.* 2010
1202	*Orthacanthus* Agassiz, 1843				up to 2.5 m long (Schneider 1996)		≥20									Ginter *et al.* 2010
1203	*Xenacanthus* Beyrich, 1848				0.2-1.0 m long (Schneider 1996)											
1204	*Wurdigneria* Richter, 2005				up to 100 mm in length (Richter 2005)											
1205	*Kaihatvenator* Hodnett, Elliot, Olson & Wittke, 2012				5-6 m long (Hodnett *et al.* 2012)											
1206	*Palaeobates* Meyer, 1849								100							Cappetta 1987
1207	Unnamed Rees, 2008 (Family)				up to 25 cm long (Rees 2008; Fischer 2008)				≤ 5							Ginter *et al.* 2010
1208	*Lissodus* Brough, 1935 s.s.				20-30 cm long (Schneider 1996), 15-50 cm long (Fischer 2008)				< 4							Cappetta 1987
1209	*Gansuselache* Wang, Zhang, Zhu & Zhao, 2009				49 cm long (Wang *et al.* 2009)											
1210	*Steinbachodus* Reif, 1980								< 3							Cappetta 1987
1211	*Sphenacanthus* Agassiz, 1837				40-50 cm long (Schneider 1996)											
1212	*Wodnika* Münster, 1843				up to 100 cm in length (Maisey 1982)											
1213	*Coodeyella* Gunnell, 1933								≤ 2							Ginter *et al.* 2010
1214	Neoselachii, Order *incertae sedis*				probably small bodysize (<1m) (Cuny & Benton 1999)											
1215	*Hoplacanthus* Schaumberg, 1982				up to 75 mm long		3		5							Ginter *et al.* 2010
1216	*Reilla* Duffin, 1980								< 1							Cappetta 1987
1217	*Wallisia* Duffin, 1982						≤ 2.5									Cappetta 1987
1218	*Lovatodus* Schmid, 1861						2									Cappetta 1987
1219	*Duffinselache* Andreev & Cuny, 2012								4.1							Andreev & Cuny 2012
1220	*Acronemus* Rieppel, 1982				up to 35 cm in length (Rieppel 1982)											
1221	*Caseodus* Zangerl, 1981				up to about 1 m											
1222	*Helicoprion* Karpinsky, 1899				estimated 5-8m in length (Lebedev 2009)											Lebedev 2009
1223	*Sandalodus* Newberry & Worthen, 1866								100							Stahl 1999

A2.3. ANALYTICAL AND STATISTICAL DATA – CHAPTER 7

A2.3.1 OCCURRENCES PER COUNTRY/REGION – FIGURE 7.3 (A)

Country	Occurrences			Country	Occurrences		
	P	Tr	Tot.		P	Tr	Tot.
North America	**241**	**97**	**338**	**Europe – cont.**			
N Canada – Elles.	2	2	4	Hungary	-	1	1
N Canada – Melv.	2	-	2	Italy	7	9	16
W Canada	2	23	25	Kazakhstan	2	-	2
E Greenland	16	4	20	Luxembourg	-	25	25
Arctic USA	1	-	1	Poland	-	37	37
C USA	46	-	46	NW Russia	11	-	11
E USA	19	3	22	(S)W Russia	59	18	77
N USA	24	-	24	Spain	-	1	1
S USA	90	27	117	Spitsbergen	2	29	31
W USA	39	38	77	Switzerland	-	14	14
South America	**23**	**4**	**27**	**Asia & Middle East**	**90**	**102**	**192**
Bolivia	5	-	5	Azerbaijan	-	2	2
Brazil	15	3	18	S/E China	12	19	31
Chile	-	1	1	N China	1	-	1
Mexico	3	-	3	India	2	12	14
Africa	**1**	**5**	**6**	Iran	12	-	12
Angola	-	1	1	Israel	-	1	1
Madagascar	-	1	1	Japan	23	30	53
South Africa	1	3	4	Kyrgyzstan	-	1	1
Australia	**7**	**3**	**10**	Laos	1	-	1
E Australia	-	3	3	Malaysia	-	2	2
W Australia	7	-	7	Oman	30	12	42
Europe	**146**	**396**	**542**	Pakistan	8	4	12
Austria	1	3	4	N Russia	-	2	2
Belgium	-	16	16	NE Russia	1	1	2
Bulgaria	-	4	4	SE Russia	-	4	4
Czech Republic	7	-	7	Saudi Arabia	-	4	4
England	5	45	50	Tibet	-	2	2
France	10	65	75	Timor	-	5	5
Germany	42	129	171	Turkey	-	1	1

A2.3.2 OCCURRENCES PER HEMISPHERE – FIGURE 7.3 (B)

Age – position	Country	Occurrences	Total occ.	%
Any – global	All countries	1115	1115	100
Recent – N hemisphere	All countries, exclusive of those listed below	1070	1070	95.96
Recent – S hemisphere	Brazil	18	45	4.04
	Bolivia	5		
	Chile	1		
	Angola	1		
	South Africa	4		
	Madagascar	1		
	Timor	5		
	Australia	10		
Recent – Europe	All European countries	542	542	48.61
Recent - USA	All regions of the USA	287	287	25.74
Triassic – N hemisphere	All countries, exclusive of those listed below	607	607	88.61
Triassic – S hemisphere	All recent southern countries	17	78	11.39
	S-USA	27		
	Turkey	1		
	Israel	1		
	Saudi Arabia	4		
	Oman	12		
	Pakistan	4		
	India	12		
	Mexico, C- USA, Iran	no occurrences		
Permian – N hemisphere	All countries, exclusive of those listed below	508	508	80.76
Permian – S hemisphere	All recent southern countries	28	121	19.18
	Mexico	3		
	Italy	7		
	Laos	1		
	S/E China	12		
	Iran	12		
	Oman	30		
	Pakistan	8		
	India	2		
	Japan (C Panth.)	18		
	Tibet, Malaysia, Turkey, Israel, Saudi Arabia	no occurrences		

A2.3.3 PUBLICATION DATA – FIGURE 7.5, 7.6 AND TABLE 7.1

Publications (pub.) per country/region describing new material and year of first publication (yr.), with data ranking (rk.). This study has contributed as one publication to each total marked with an asterisk.

Country	Pub.	Rk.	Yr.	Rk.	Country	Pub.	Rk.	Yr.	Rk.
North America	**133**	**-**		**-**	**Europe – cont.**	**-**	**-**	**-**	**-**
N Canada	3*	32	1970	35	Italy	10	11.5	1886	13
W Canada	7	16.5	1968	34	Kazakhstan	1	47.5	2009	52
E Greenland	9*	13	1932	22	Luxembourg	6	19.5	1964	31
Arctic USA	1	47.5	1982	41	Poland	5	24	1836	2.5
C USA	16	8	1884	11.5	NW Russia	7	16.5	1989	44
E USA	11	10	1881	10	(S)W Russia	34	4	1871	7
N USA	4	28	1916	20	Spain	1	47.5	2009	52
S USA	52	2	1876	9	Spitsbergen	8*	14.5	1873	8
W USA	30	5.5	1904	17	Switzerland	8	14.5	1891	15
South America	**18**	**-**		**-**	**Asia & Middle East**	**76**	**-**		**-**
Bolivia	2	37.5	1981	39	Azerbaijan	3	32	1955	29
Brazil	10	11.5	1975	37	S/E China	15*	9	1950	26.5
Chile	1	47.5	1992	45	N China	1	47.5	2009	52
Mexico	5	24	1945	24	India	5*	24	1964	31
Africa	**7**	**-**		**-**	Iran	6*	19.5	1950	26.5
Angola	1	47.5	1954	28	Israel	1	47.5	1947	25
Madagascar	1	47.5	1982	41	Japan	21*	7	1903	16
South Africa	5	24	1909	18	Kyrgyzstan	1	47.5	2011	54
Australia	**9**	**-**		**-**	Laos	1	47.5	1933	23
E Australia	3	32	1890	14	Malaysia	1	47.5	2006	49
W Australia	6	19.5	1884	11.5	Oman	3*	32	1998	46
Europe	**242**	**-**		**-**	Pakistan	6	19.5	1863	6
Austria	4	28	1928	21	N Russia	2	37.5	1976	38
Belgium	5	24	1983	43	NE Russia	2	37.5	1964	31
Bulgaria	3	32	1966	33	SE Russia	2	37.5	2006	49
Czech Republic	4	28	1847	5	Saudi Arabia	1	47.5	1999	47
England	30	5.5	1836	2.5	Tibet	2	37.5	1972	36
France	41	3	1836	2.5	Timor	2*	37.5	2006	49
Germany	74	1	1836	2.5	Turkey	1	47.5	1982	41
Hungary	1	47.5	1911	19					

A2.3.4 SPECIES DATA MATRIX (STARTS NEXT PAGE)

Entries are provided in batches of two pages, providing data on numbers of known species per genus and per time interval.

	Species diversity	Carboniferous	Bound.	Cisuralian									Bound.	Guadalupian						Bound.	Lopingian				Bound.
				Asselian	Bound.	Sakmarian	Bound.	Artinskian	Bound.	Kungurian				Roadian	Bound.	Wordian	Bound.	Capitanian			Wuchiapingian	Bound.	Changxingian		
Phoebo-dontif.?	Unnamed genus																								
	Species in open nomenclature							1																	
Branso-nellif.	*Barbclabornia*			1		1		1		1															
	Bransonella					1																			
	Species in open nomenclature																								
Xenacan-thiformes	*Dicentrodus*									1						1									
	Lebachacanthus			2		1		1		1	2														
	Orthacanthus			5		3		2		2	2														
	Xenacanthus			5		2		1																	
	Triodus			7		2		1																	
	Plicatodus			1																					
	Wurdigneria									1									2						
	Mooreodontus																								
	Orthacanthus (open nomenclature)			1						1													1		
	Xenacanthus (open nomenclature)			2		1					2														
	Triodus (open nomenclature)			3				1																1	
	Wurdigneria (open nomenclature)							1																	
	Species in open nomenclature										1													2	
Symmorii-formes	*Stethacanthus*			1										1		1		1							
	"Physonemus" / Batacanthus													1		1									
	Stethacanthulus			1		1		1						1		2		1			1				
	Stethacanthus (open nomenclature)							1		1															
	Species in open nomenclature													1											
	Ctenacanthus															1		1							
	Glikmanius			1		1		1		2	1			1		3		1	1						

	Species diversity	Lower Triassic								Bound.	Middle				Bound.	Upper Triassic						Bound.	Jurassic
		Griesbachian	Bound.	Dienerian	Bound.	Smithian	Bound.	Spathian			Anisian	Bound.	Ladinian			Carnian	Bound.	Norian	Bound.	Rhaetian			
Phoebo-dontif.?	Unnamed genus																			1			
	Species in open nomenclature										1					1		1					
Branso-nellif.	*Barbclabornia*																						
	Bransonella																						
	Species in open nomenclature																						
Xenacan-thiformes	*Dicentrodus*																						
	Lebachacanthus																						
	Orthacanthus																						
	Xenacanthus																						
	Triodus																						
	Plicatodus																						
	Wurdigneria																						
	Mooreodontus										1					5		2					
	Orthacanthus (open nomenclature)										1										1		
	Xenacanthus (open nomenclature)								1		1		1			1							
	Triodus (open nomenclature)																						
	Wurdigneria (open nomenclature)																						
	Species in open nomenclature																						
Symmorii-formes	*Stethacanthus*																						
	"Physonemus" / Batacanthus																						
	Stethacanthulus																						
	Stethacanthus (open nomenclature)																						
	Species in open nomenclature																						
	Ctenacanthus																						
	Glikmanius																						

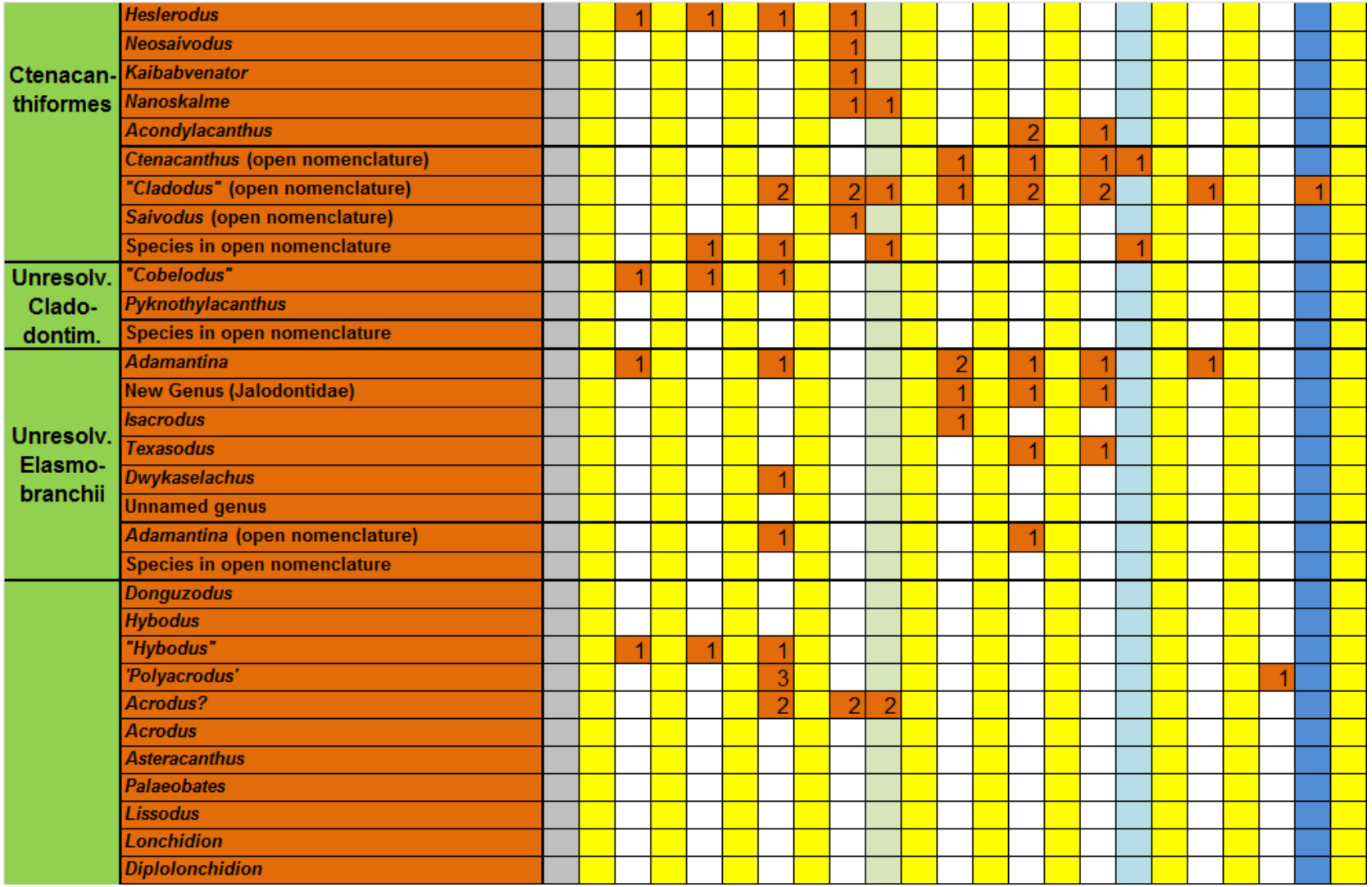
Ctenacan-thiformes
Unresolv. Clado-dontim.
Unresolv. Elasmo-branchii
Heslerodus
Neosaivodus
Kaibabvenator
Nanoskalme
Acondylacanthus
Ctenacanthus (open nomenclature)
"Cladodus" (open nomenclature)
Saivodus (open nomenclature)
Species in open nomenclature
"Cobelodus"
Pyknothylacanthus
Species in open nomenclature
Adamantina
New Genus (Jalodontidae)
Isacrodus
Texasodus
Dwykaselachus
Unnamed genus
Adamantina (open nomenclature)
Species in open nomenclature
Donguzodus
Hybodus
"Hybodus"
'Polyacrodus'
Acrodus?
Acrodus
Asteracanthus
Palaeobates
Lissodus
Lonchidion
Diplolonchidion

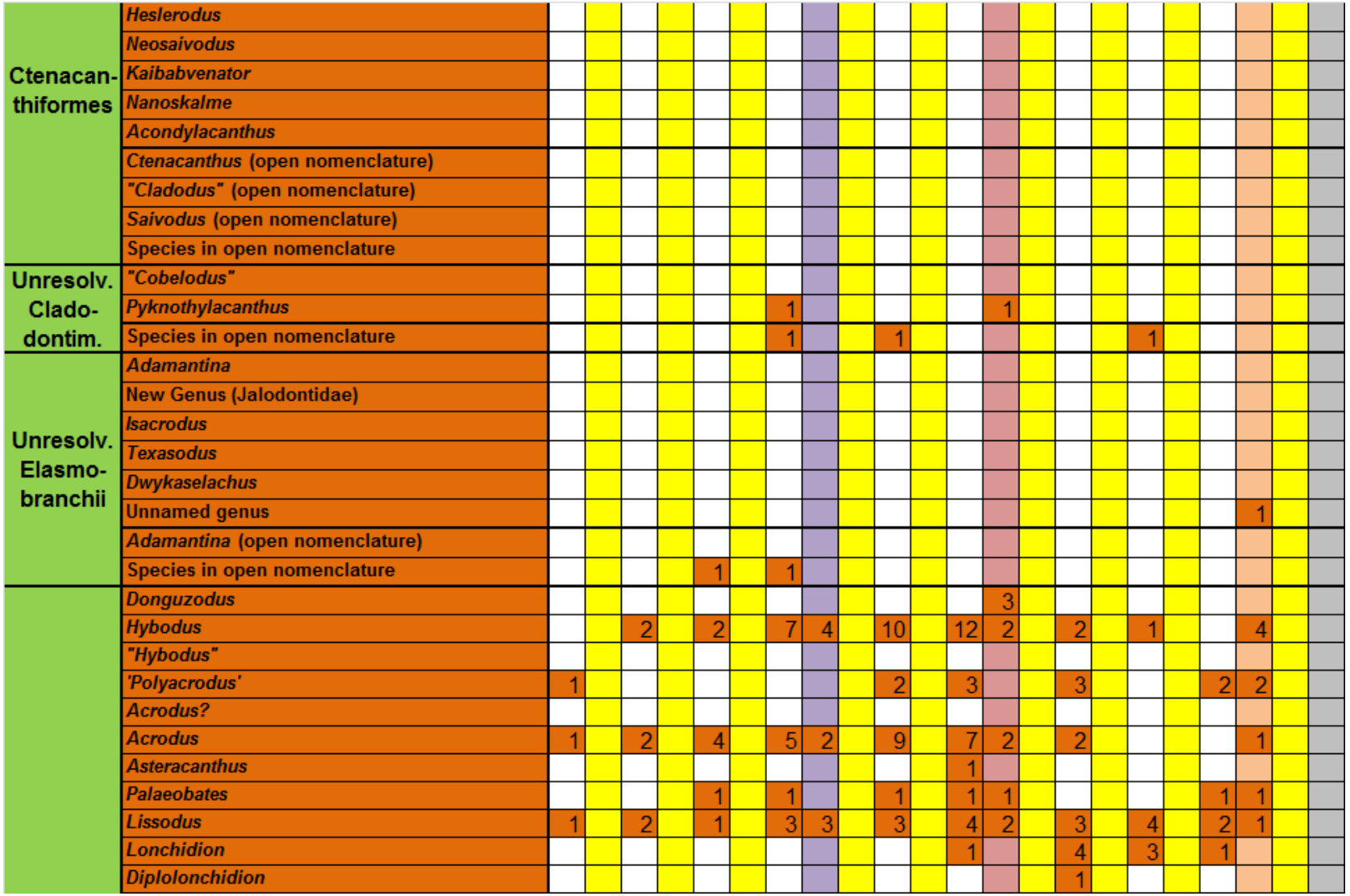
Ctenacan-thiformes
Unresolv. Clado-dontim.
Unresolv. Elasmo-branchii
Heslerodus
Neosaivodus
Kaibabvenator
Nanoskalme
Acondylacanthus
Ctenacanthus (open nomenclature)
"Cladodus" (open nomenclature)
Saivodus (open nomenclature)
Species in open nomenclature
"Cobelodus"
Pyknothylacanthus
Species in open nomenclature
Adamantina
New Genus (Jalodontidae)
Isacrodus
Texasodus
Dwykaselachus
Unnamed genus
Adamantina (open nomenclature)
Species in open nomenclature
Donguzodus
Hybodus
"Hybodus"
'Polyacrodus'
Acrodus?
Acrodus
Asteracanthus
Palaeobates
Lissodus
Lonchidion
Diplolonchidion

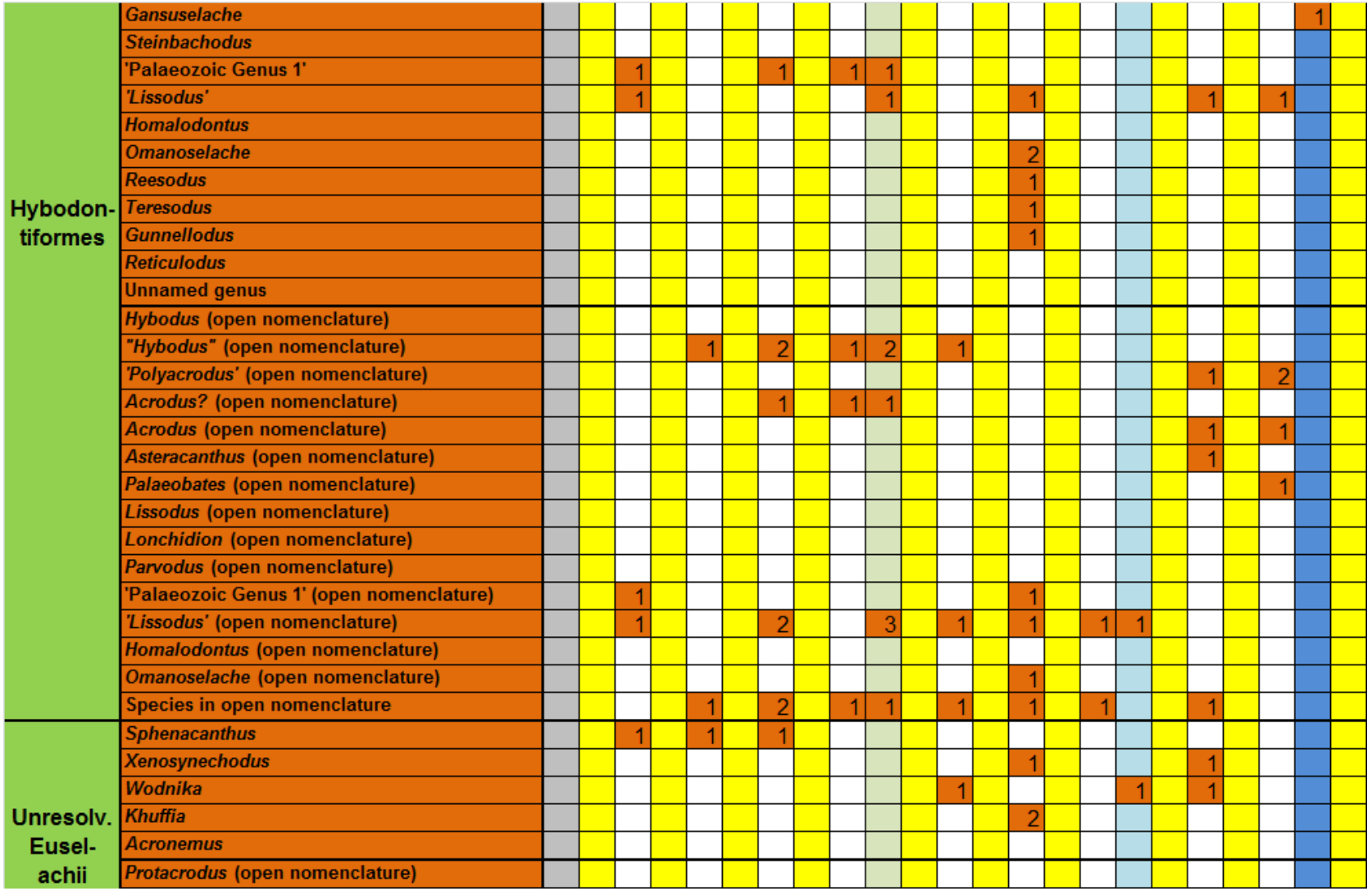
Hybodon-tiformes
Unresolv. Eusel-achii
Gansuselache
Steinbachodus
'Palaeozoic Genus 1'
'Lissodus'
Homalodontus
Omanoselache
Reesodus
Teresodus
Gunnellodus
Reticulodus
Unnamed genus
Hybodus (open nomenclature)
"Hybodus" (open nomenclature)
'Polyacrodus' (open nomenclature)
Acrodus? (open nomenclature)
Acrodus (open nomenclature)
Asteracanthus (open nomenclature)
Palaeobates (open nomenclature)
Lissodus (open nomenclature)
Lonchidion (open nomenclature)
Parvodus (open nomenclature)
'Palaeozoic Genus 1' (open nomenclature)
'Lissodus' (open nomenclature)
Homalodontus (open nomenclature)
Omanoselache (open nomenclature)
Species in open nomenclature
Sphenacanthus
Xenosynechodus
Wodnika
Khuffia
Acronemus
Protacrodus (open nomenclature)

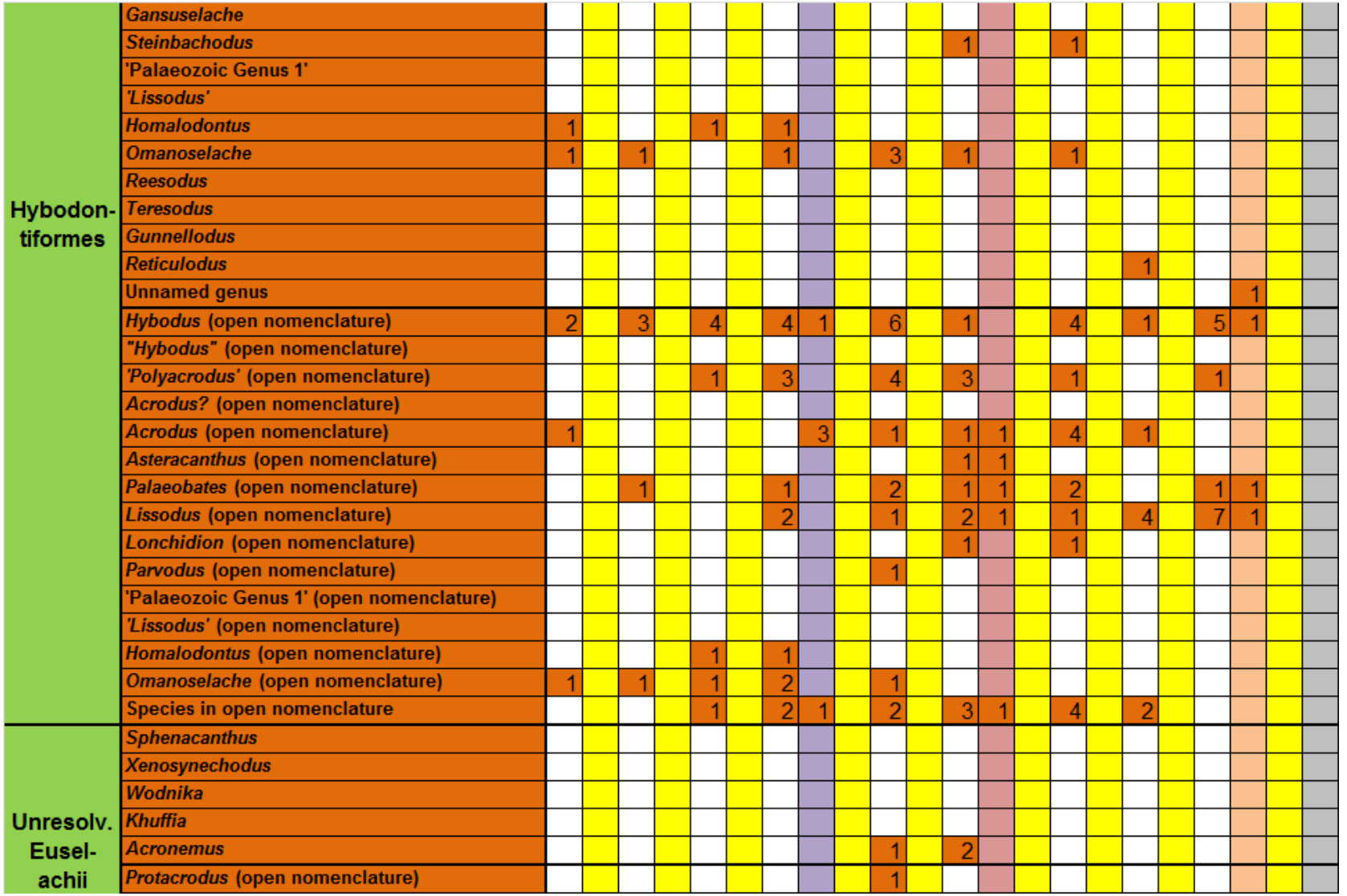
Hybodon-tiformes
Unresolv. Eusel-achii
Gansuselache
Steinbachodus
'Palaeozoic Genus 1'
'Lissodus'
Homalodontus
Omanoselache
Reesodus
Teresodus
Gunnellodus
Reticulodus
Unnamed genus
Hybodus (open nomenclature)
"Hybodus" (open nomenclature)
'Polyacrodus' (open nomenclature)
Acrodus? (open nomenclature)
Acrodus (open nomenclature)
Asteracanthus (open nomenclature)
Palaeobates (open nomenclature)
Lissodus (open nomenclature)
Lonchidion (open nomenclature)
Parvodus (open nomenclature)
'Palaeozoic Genus 1' (open nomenclature)
'Lissodus' (open nomenclature)
Homalodontus (open nomenclature)
Omanoselache (open nomenclature)
Species in open nomenclature
Sphenacanthus
Xenosynechodus
Wodnika
Khuffia
Acronemus
Protacrodus (open nomenclature)

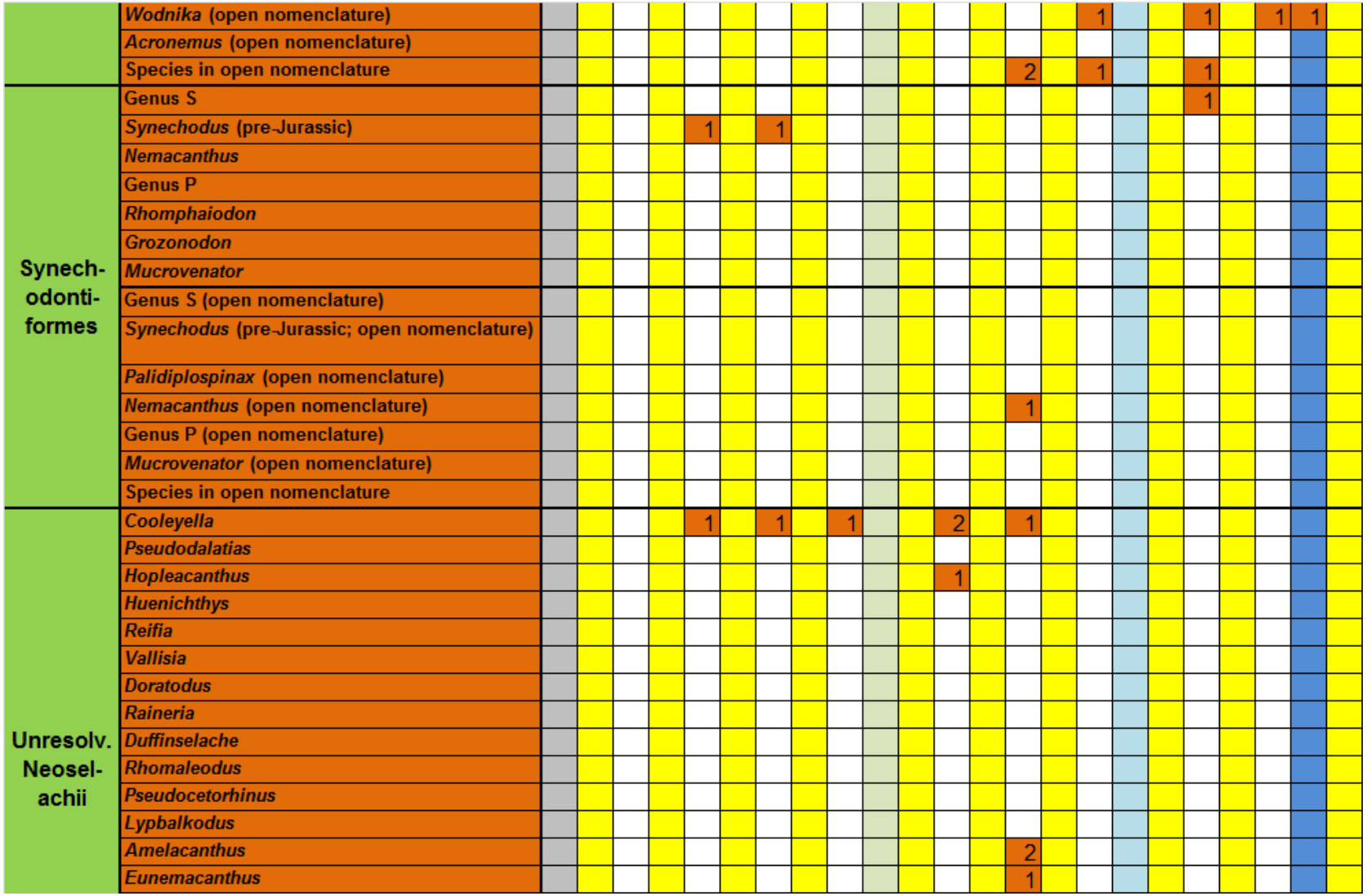
Wodnika (open nomenclature)
Acronemus (open nomenclature)
Species in open nomenclature
Synech-odonti-formes
Genus S
Synechodus (pre-Jurassic)
Nemacanthus
Genus P
Rhomphaiodon
Grozonodon
Mucrovenator
Genus S (open nomenclature)
Synechodus (pre-Jurassic; open nomenclature)
Palidiplospinax (open nomenclature)
Nemacanthus (open nomenclature)
Genus P (open nomenclature)
Mucrovenator (open nomenclature)
Species in open nomenclature
Unresolv. Neosel-achii
Cooleyella
Pseudodalatias
Hopleacanthus
Huenichthys
Reifia
Vallisia
Doratodus
Raineria
Duffinselache
Rhomaleodus
Pseudocetorhinus
Lypbalkodus
Amelacanthus
Eunemacanthus

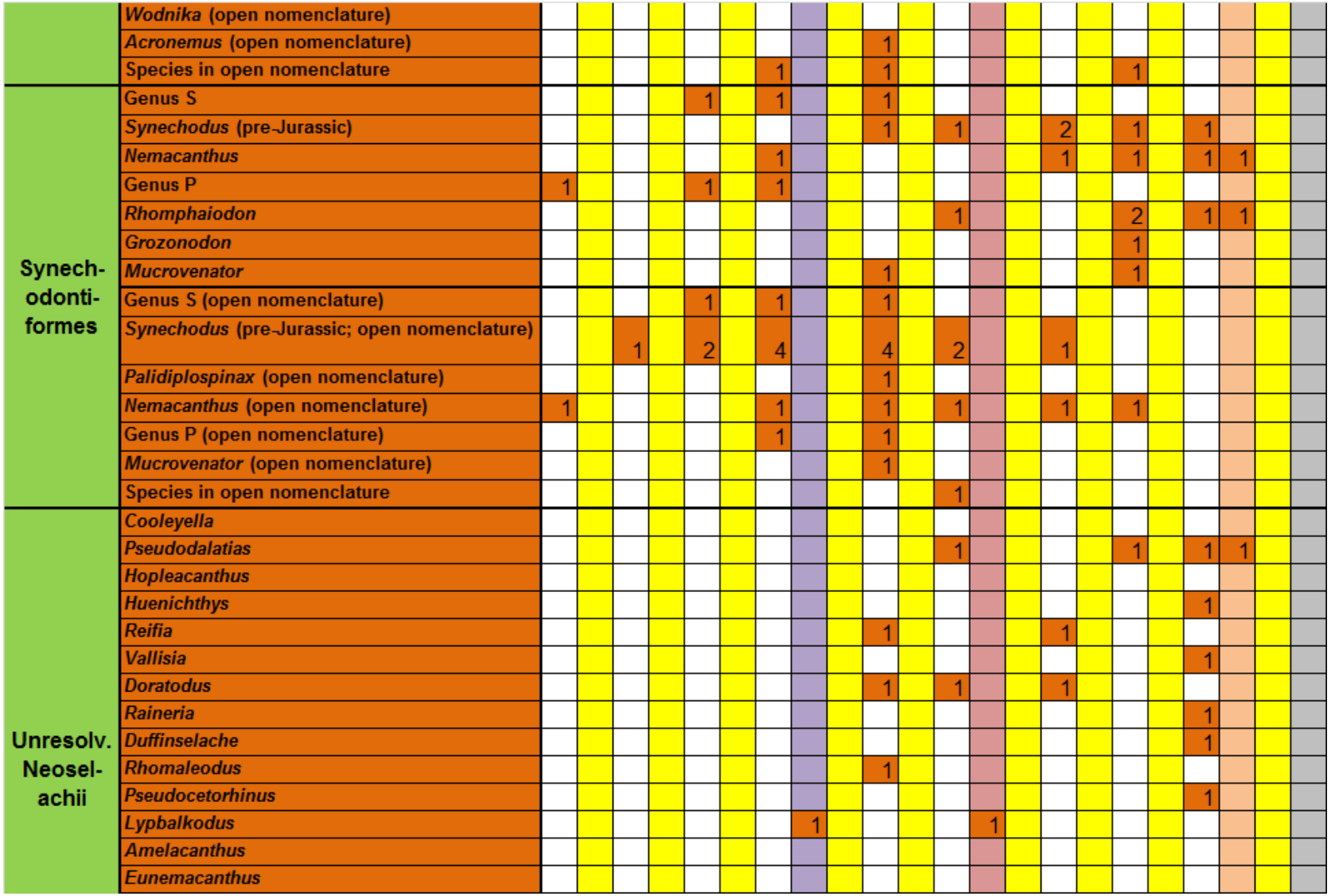
Wodnika (open nomenclature)
Acronemus (open nomenclature)
Species in open nomenclature
Synech-odonti-formes
Genus S
Synechodus (pre-Jurassic)
Nemacanthus
Genus P
Rhomphaiodon
Grozonodon
Mucrovenator
Genus S (open nomenclature)
Synechodus (pre-Jurassic; open nomenclature)
Palidiplospinax (open nomenclature)
Nemacanthus (open nomenclature)
Genus P (open nomenclature)
Mucrovenator (open nomenclature)
Species in open nomenclature
Unresolv. Neosel-achii
Cooleyella
Pseudodalatias
Hopleacanthus
Huenichthys
Reifia
Vallisia
Doratodus
Raineria
Duffinselache
Rhomaleodus
Pseudocetorhinus
Lypbalkodus
Amelacanthus
Eunemacanthus

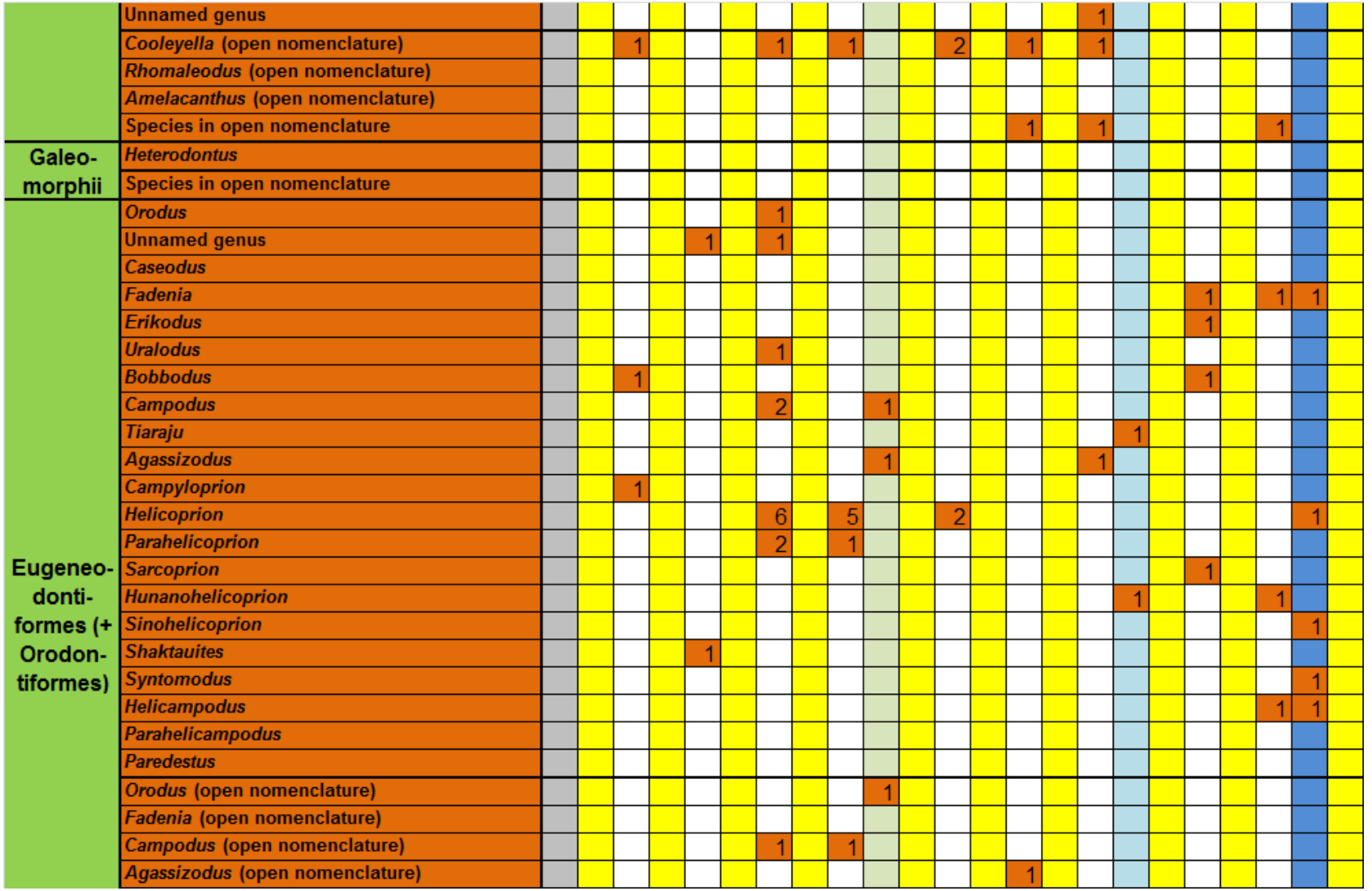
Unnamed genus
Cooleyella (open nomenclature)
Rhomaleodus (open nomenclature)
Amelacanthus (open nomenclature)
Species in open nomenclature
Galeo-morphii
Heterodontus
Species in open nomenclature
Eugeneo-donti-formes (+ Orodon-tiformes)
Orodus
Unnamed genus
Caseodus
Fadenia
Erikodus
Uralodus
Bobbodus
Campodus
Tiaraju
Agassizodus
Campyloprion
Helicoprion
Parahelicoprion
Sarcoprion
Hunanohelicoprion
Sinohelicoprion
Shaktauites
Syntomodus
Helicampodus
Parahelicampodus
Paredestus
Orodus (open nomenclature)
Fadenia (open nomenclature)
Campodus (open nomenclature)
Agassizodus (open nomenclature)

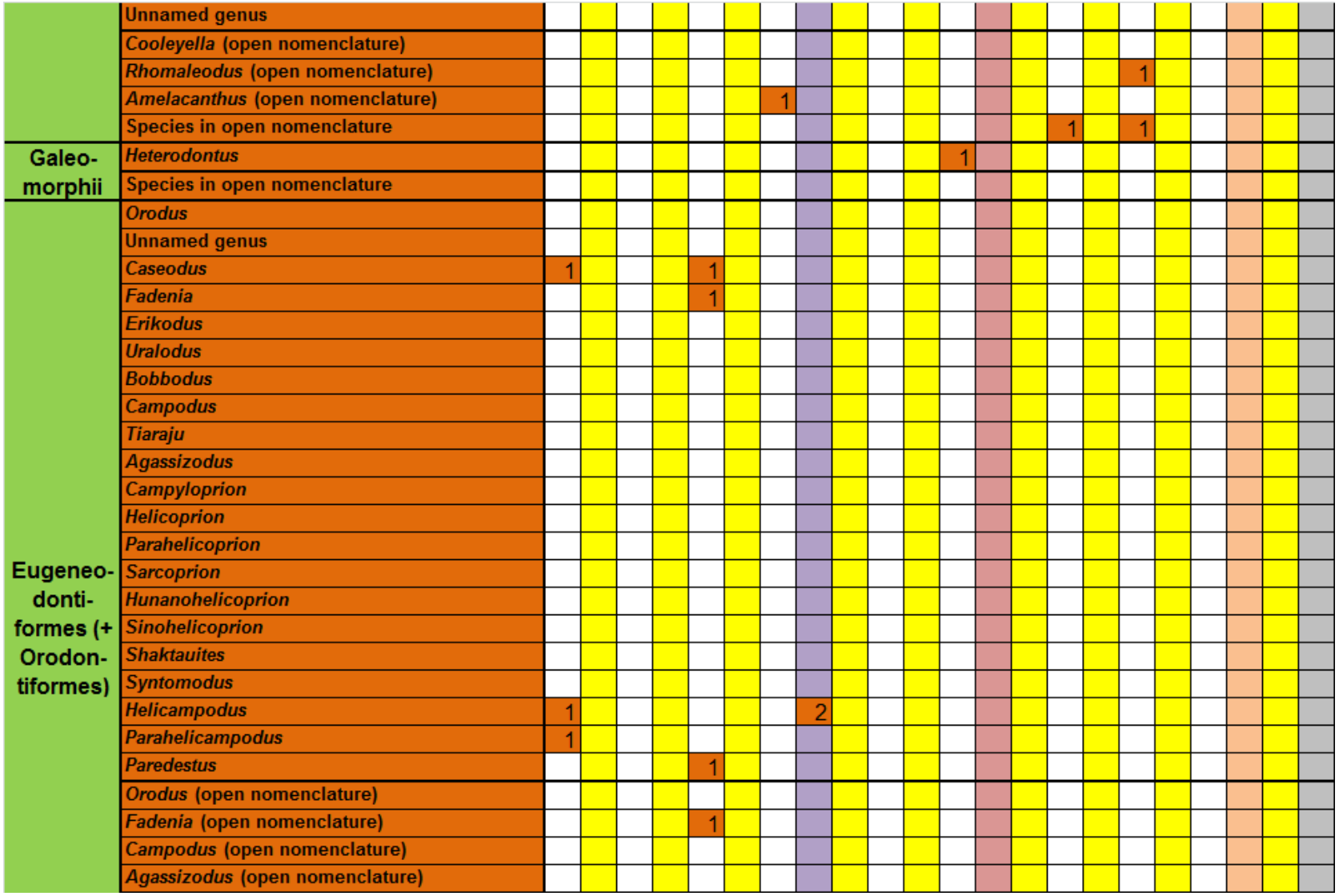
Unnamed genus
Cooleyella (open nomenclature)
Rhomaleodus (open nomenclature)
Amelacanthus (open nomenclature)
Species in open nomenclature
Galeo-morphii
Heterodontus
Species in open nomenclature
Eugeneo-donti-formes (+ Orodon-tiformes)
Orodus
Unnamed genus
Caseodus
Fadenia
Erikodus
Uralodus
Bobbodus
Campodus
Tiaraju
Agassizodus
Campyloprion
Helicoprion
Parahelicoprion
Sarcoprion
Hunanohelicoprion
Sinohelicoprion
Shaktauites
Syntomodus
Helicampodus
Parahelicampodus
Paredestus
Orodus (open nomenclature)
Fadenia (open nomenclature)
Campodus (open nomenclature)
Agassizodus (open nomenclature)

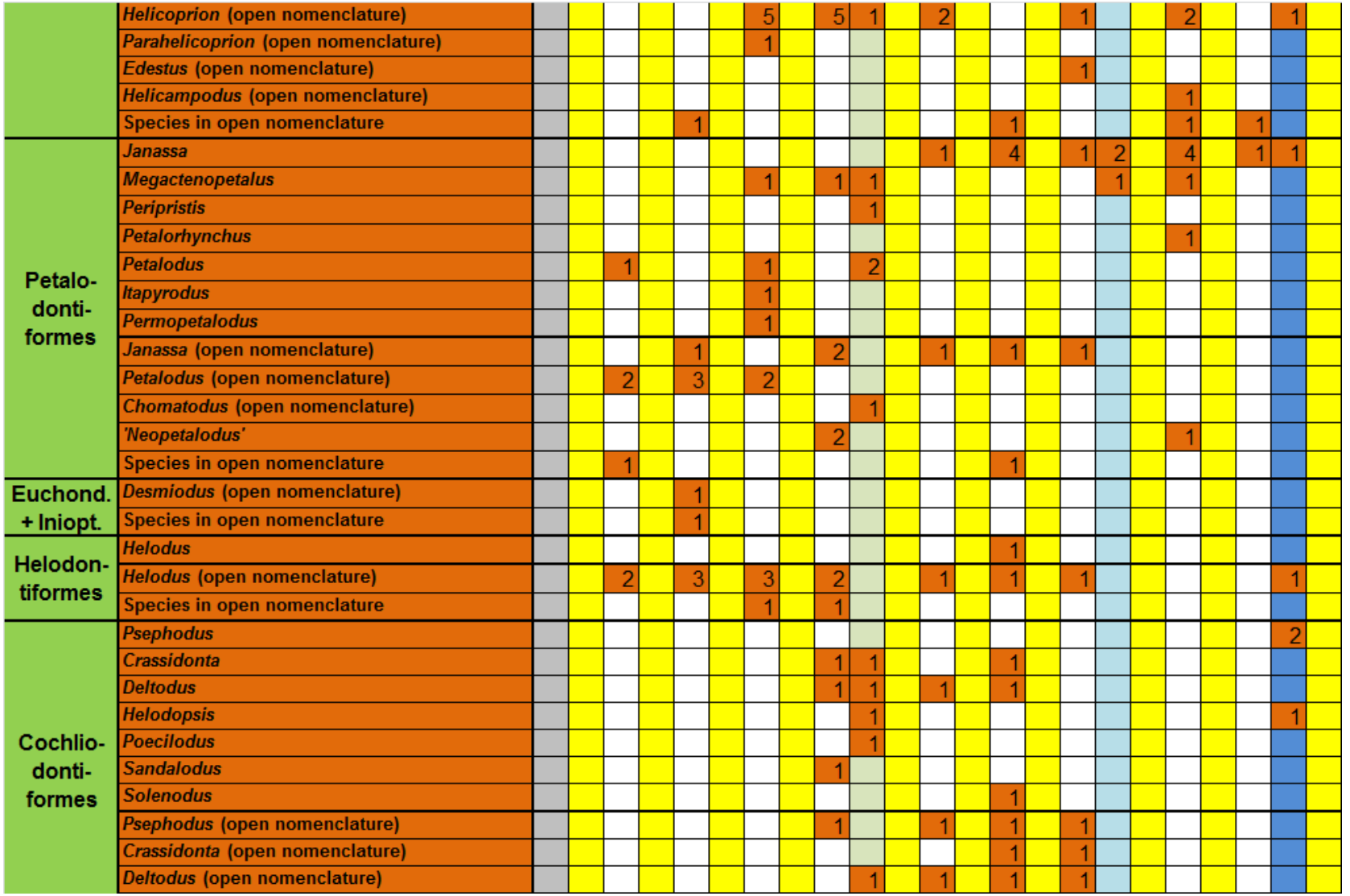
Helicoprion (open nomenclature)
Parahelicoprion (open nomenclature)
Edestus (open nomenclature)
Helicampodus (open nomenclature)
Species in open nomenclature
Petalo-donti-formes
Janassa
Megactenopetalus
Peripristis
Petalorhynchus
Petalodus
Itapyrodus
Permopetalodus
Janassa (open nomenclature)
Petalodus (open nomenclature)
Chomatodus (open nomenclature)
'Neopetalodus'
Species in open nomenclature
Euchond. + Iniopt.
Desmiodus (open nomenclature)
Species in open nomenclature
Helodon-tiformes
Helodus
Helodus (open nomenclature)
Species in open nomenclature
Cochlio-donti-formes
Psephodus
Crassidonta
Deltodus
Helodopsis
Poecilodus
Sandalodus
Solenodus
Psephodus (open nomenclature)
Crassidonta (open nomenclature)
Deltodus (open nomenclature)

	Helicoprion (open nomenclature)																							
	Parahelicoprion (open nomenclature)																							
	Edestus (open nomenclature)																							
	Helicampodus (open nomenclature)																							
	Species in open nomenclature			1		2																		
Petalo-donti-formes	*Janassa*																							
	Megactenopetalus																							
	Peripristis																							
	Petalorhynchus																							
	Petalodus																							
	Itapyrodus																							
	Permopetalodus																							
	Janassa (open nomenclature)																							
	Petalodus (open nomenclature)																							
	Chomatodus (open nomenclature)																							
	'Neopetalodus'																							
	Species in open nomenclature																							
Euchond. + Iniopt.	*Desmiodus* (open nomenclature)																							
	Species in open nomenclature																							
Helodon-tiformes	*Helodus*																							
	Helodus (open nomenclature)																							
	Species in open nomenclature																							
Cochlio-donti-formes	*Psephodus*																							
	Crassidonta																							
	Deltodus																							
	Helodopsis																							
	Poecilodus																							
	Sandalodus																							
	Solenodus																							
	Psephodus (open nomenclature)																							
	Crassidonta (open nomenclature)																							
	Deltodus (open nomenclature)																							

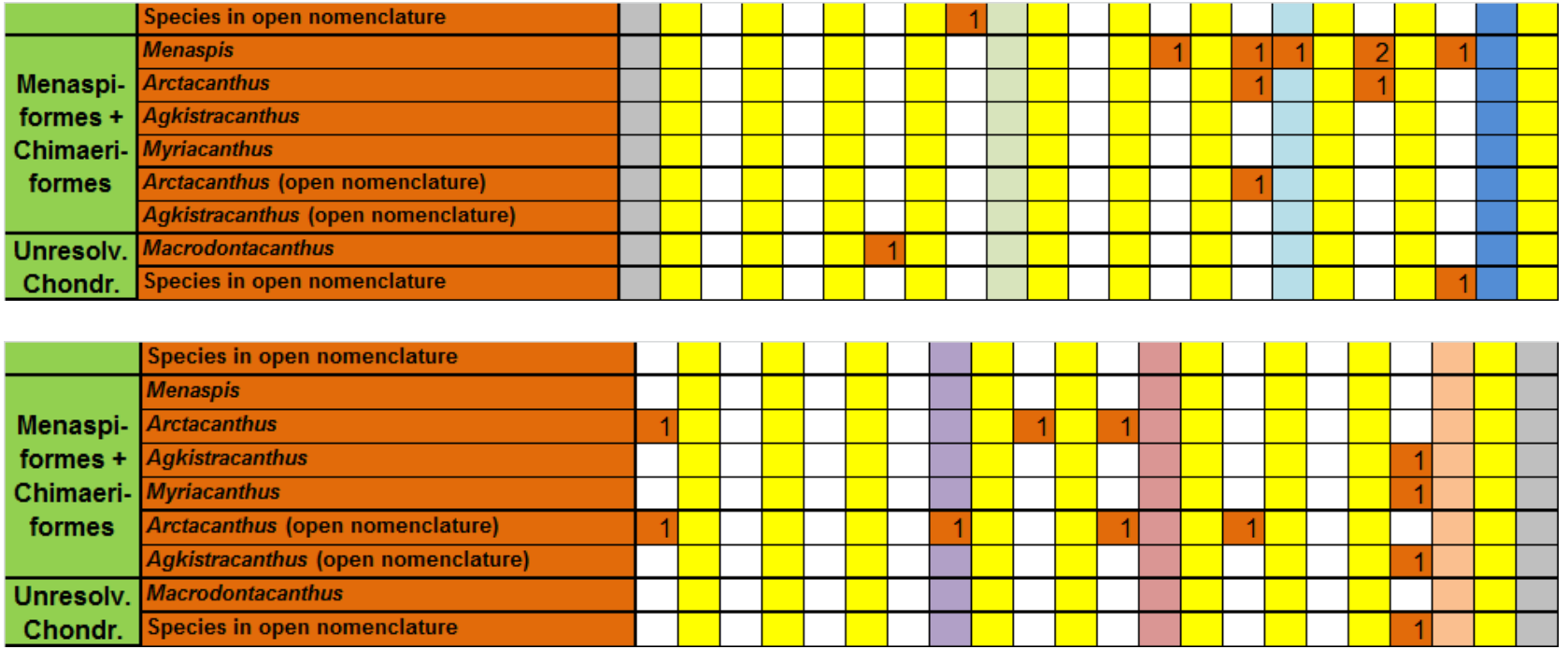
Species in open nomenclature
Menaspi-formes + Chimaeri-formes
Menaspis
Arctacanthus
Agkistracanthus
Myriacanthus
Arctacanthus (open nomenclature)
Agkistracanthus (open nomenclature)
Unresolv. Chondr.
Macrodontacanthus
Species in open nomenclature

Species in open nomenclature
Menaspi-formes + Chimaeri-formes
Menaspis
Arctacanthus
Agkistracanthus
Myriacanthus
Arctacanthus (open nomenclature)
Agkistracanthus (open nomenclature)
Unresolv. Chondr.
Macrodontacanthus
Species in open nomenclature

A2.3.5 Occurrence and species data – Figure 7.8

Refer to A2.4.2 for genus data.

(Sub)stage	Occurrences	Species richness	
		Named	Total (incl. open nomenclature)
Rhaetian	116.4	18	34
Norian	49.15	18	32
Carnian	72.65	27	50
Ladinian	105	39	58
Anisian	109.95	37	71
Spathian	58.7	22	48
Smithian	29.7	14	29
Dienerian	18.7	7	14
Griesbachian	16.7	10	16
Changhsingian	16.33	7	16
Wuchiapingian	46.33	19	31
Capitanian	28.83	13	30
Wordian	62	36	57
Roadian	37	16	30
Kungurian	64.66	26	50
Artinskian	94.16	40	69
Sakmarian	34.66	20	34
Asselian	69.99	34	48

R^2	0.0716
R	0.2676
α(2)	0.05
n	18
df	16
critical *t*	2.120
t	1.111
t < critical *t*?	yes, accept H_o: $R^2 = 0$
p-value	0.28

A2.3.6 SPEARMAN RHO DATA – FIGURE 7.9 AND TABLE 7.2

(Sub)stage	Interval duration (Myr)	Rank	Taxonomic occurrences	Rank	Named genera, fossil	Rank	Named genera, range-through	Rank	Named species, fossil	Rank
Rhaetian	7.2	3	116.4	1	16	11.5	22	12	18	11.5
Norian	19.5	1	49.2	10	13	14	20	15.5	18	11.5
Carnian	7	4.5	72.7	5	16	11.5	25	10	27	6
Ladinian	5.6	8	105	3	18	10	25	10	39	2
Anisian	6.6	6	110	2	22	5	25	10	37	3
Spathian	3.3	14	58.7	9	13	14	19	17.5	22	8
Smithian	0.7	16	29.7	14	13	14	20	15.5	14	14
Dienerian	0.5	17.5	18.7	16	6	18	19	17.5	7	17.5
Griesbachian	0.5	17.5	16.7	17	12	16	21	13.5	10	16
Changhsingian	2	15	16.3	18	11	17	21	13.5	7	17.5
Wuchiapingian	5.7	7	46.3	11	22	5	35	8	19	10
Capitanian	5.2	10	28.8	15	22	5	41	7	13	15
Wordian	3.7	11	62	8	31	2	48	4	36	4
Roadian	3.5	12	37	12	19	8.5	44	6	16	13
Kungurian	7	4.5	64.7	7	28	3	49	3	26	7
Artinskian	10.8	2	94.2	4	33	1	52	1	40	1
Sakmarian	5.4	9	34.7	13	19	8.5	47	5	20	9
Asselian	3.4	13	70	6	21	7	50	2	34	5

A2.3.7 OCCURRENCE DATA PER PALAEOBASIN – FIGURE 7.10

(Substage) / Epoch	Taxonomic occurrences					
	C-Pangaea	E-Panthalassa	Boreal	Palaeotethys	Neotethys	C/W-Panthalassa
Rhaetian	0.5	0	0.25	115.65	0	0
Norian	12	4	0.25	28.9	2	2
Carnian	19.5	6	0.25	35.9	2	9
Ladinian	0	7	0.25	89.75	0	8
Anisian	0	16	1	57.75	4.2	31
Spathian	2	14	12.5	0	12.2	18
Smithian	0	11	4.5	0	6.2	8
Dienerian	0	0	12.5	0	1.2	5
Griesbachian	0	0	6.5	1	4.2	5
Changhsingian	0	0	3	3.33	4	6
Wuchiapingian	2	1	12	17.33	10	4
Capitanian	6	14	2	5.83	0	1
Wordian	3	20	3	11	24	1
Roadian	8	15.5	6	7.5	0	0
Kungurian	20.66	24.5	4	3.5	4	8
Artinskian	50.83	6	2	29.33	4	2
Sakmarian	21.33	0	1	9.33	2	1
Asselian	22.16	0	3	43.83	0	1
Cisuralian	146.98	31.5	10	93.99	13	15
Guadalupian	21	49.5	11	30.33	24	7
Lopingian	3	3	16	24.66	20	14
Early Triassic	4	26	37	12	26.8	37
Middle Triassic	0	24	2.25	161.5	8.2	39
Late Triassic	33	15	1.75	200.45	4	12

A2.3.8 CHONDRICHTHYAN CLADOGRAM DISPLAYED USING THE CBM

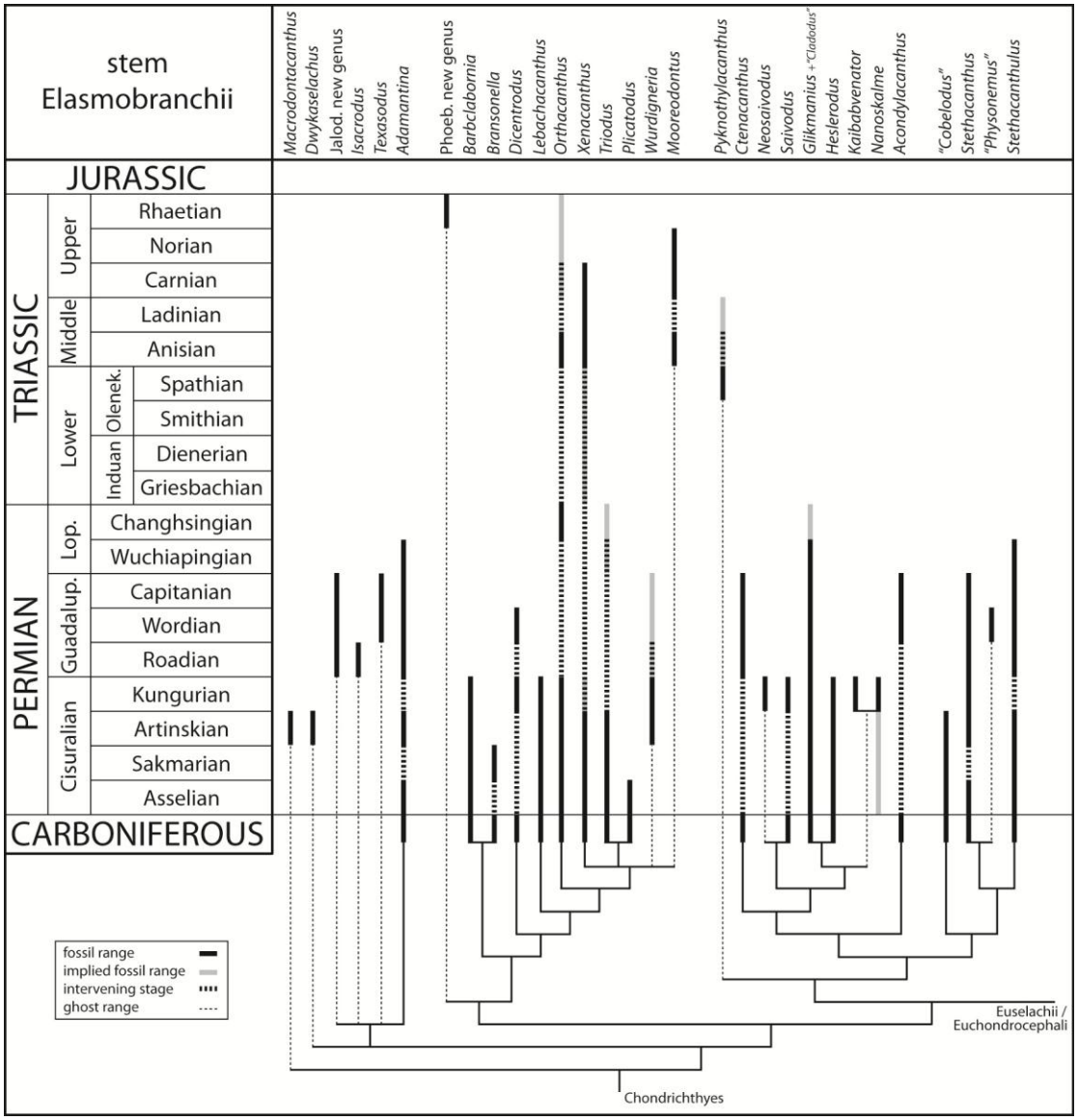

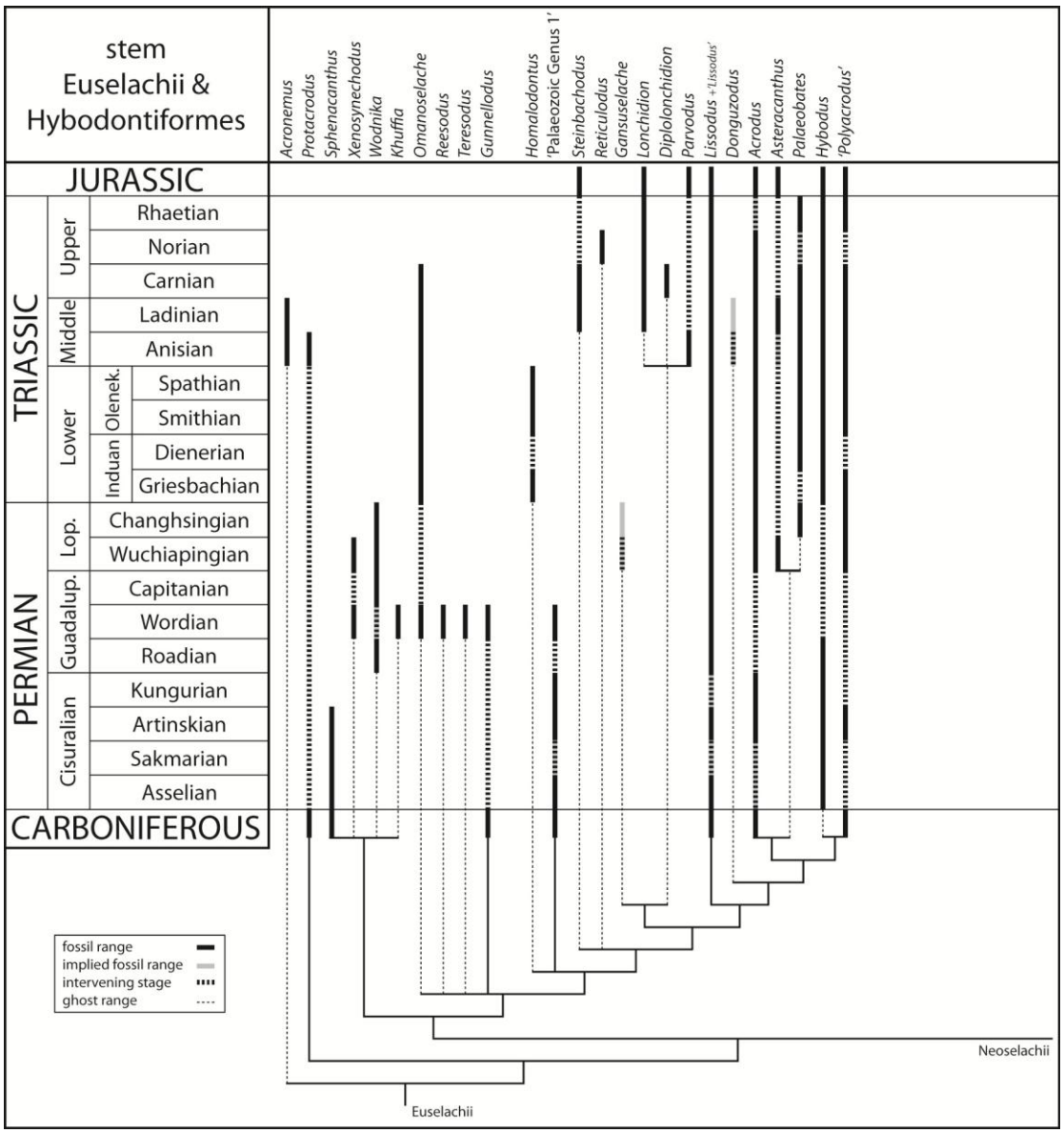
stem Euselachii & Hybodontiformes
Acronemus
Protacrodus
Sphenacanthus
Xenosynechodus
Wodnika
Khuffia
Omanoselache
Reesodus
Teresodus
Gunnellodus
Homalodontus
'Palaeozoic Genus 1'
Steinbachodus
Reticulodus
Gansuselache
Lonchidion
Diplolonchidion
Parvodus
Lissodus + 'Lissodus'
Donguzodus
Acrodus
Asteracanthus
Palaeobates
Hybodus
'Polyacrodus'
JURASSIC
TRIASSIC
Upper
Middle
Lower
Olenek.
Induan
Rhaetian
Norian
Carnian
Ladinian
Anisian
Spathian
Smithian
Dienerian
Griesbachian
PERMIAN
Lop.
Guadalup.
Cisuralian
Changhsingian
Wuchiapingian
Capitanian
Wordian
Roadian
Kungurian
Artinskian
Sakmarian
Asselian
CARBONIFEROUS
fossil range
implied fossil range
intervening stage
ghost range
Neoselachii
Euselachii

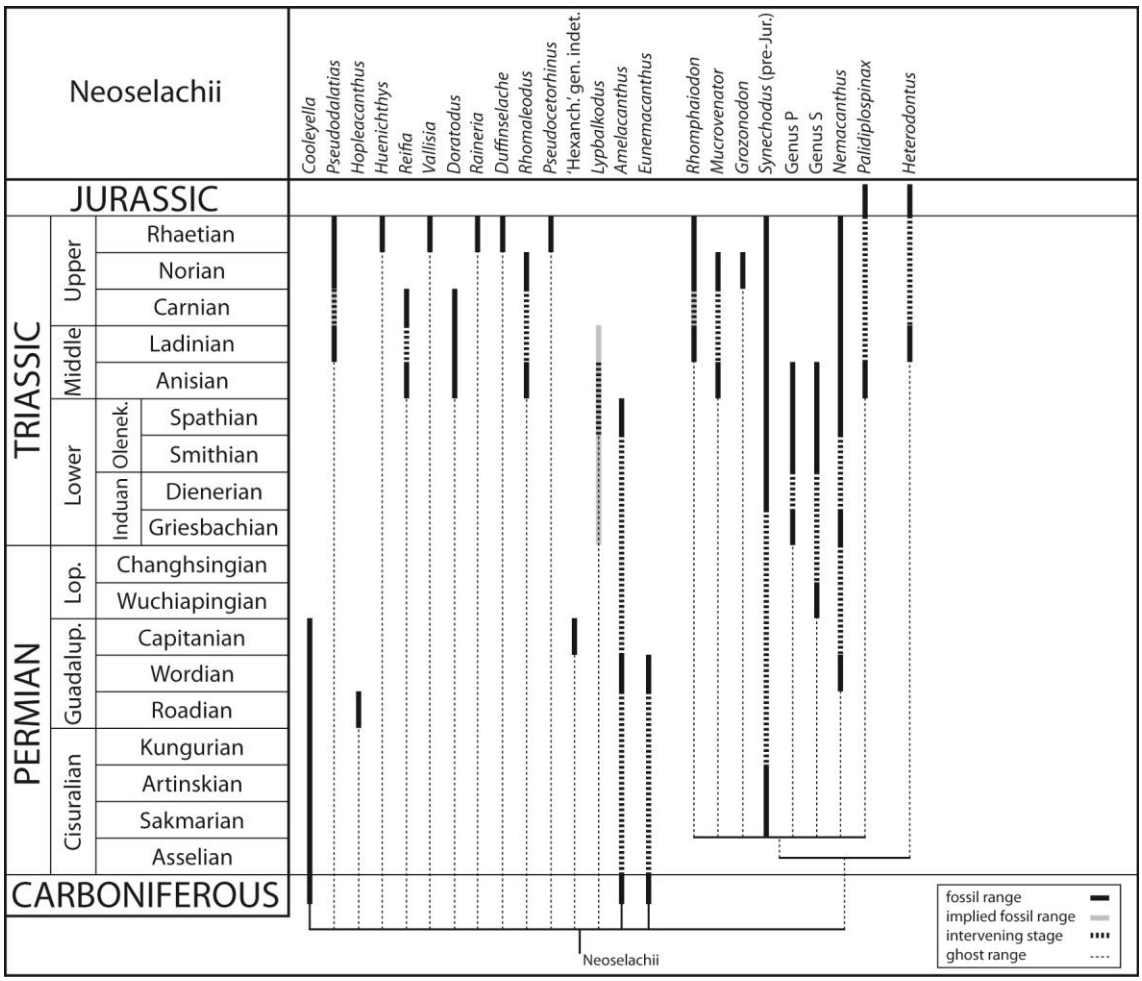
Neoselachii
Cooleyella
Pseudodalatias
Hopleacanthus
Huenichthys
Reifia
Vallisia
Doratodus
Raineria
Duffinselache
Rhomaleodus
Pseudocetorhinus
'Hexanch.' gen. indet.
Lypbalkodus
Amelacanthus
Eunemacanthus
Rhomphaiodon
Mucrovenator
Grozonodon
Synechodus (pre-Jur.)
Genus P
Genus S
Nemacanthus
Palidiplospinax
Heterodontus
JURASSIC
TRIASSIC
Upper
Middle
Lower
Olenek.
Induan
Rhaetian
Norian
Carnian
Ladinian
Anisian
Spathian
Smithian
Dienerian
Griesbachian
PERMIAN
Lop.
Guadalup.
Cisuralian
Changhsingian
Wuchiapingian
Capitanian
Wordian
Roadian
Kungurian
Artinskian
Sakmarian
Asselian
CARBONIFEROUS
Neoselachii
fossil range
implied fossil range
intervening stage
ghost range

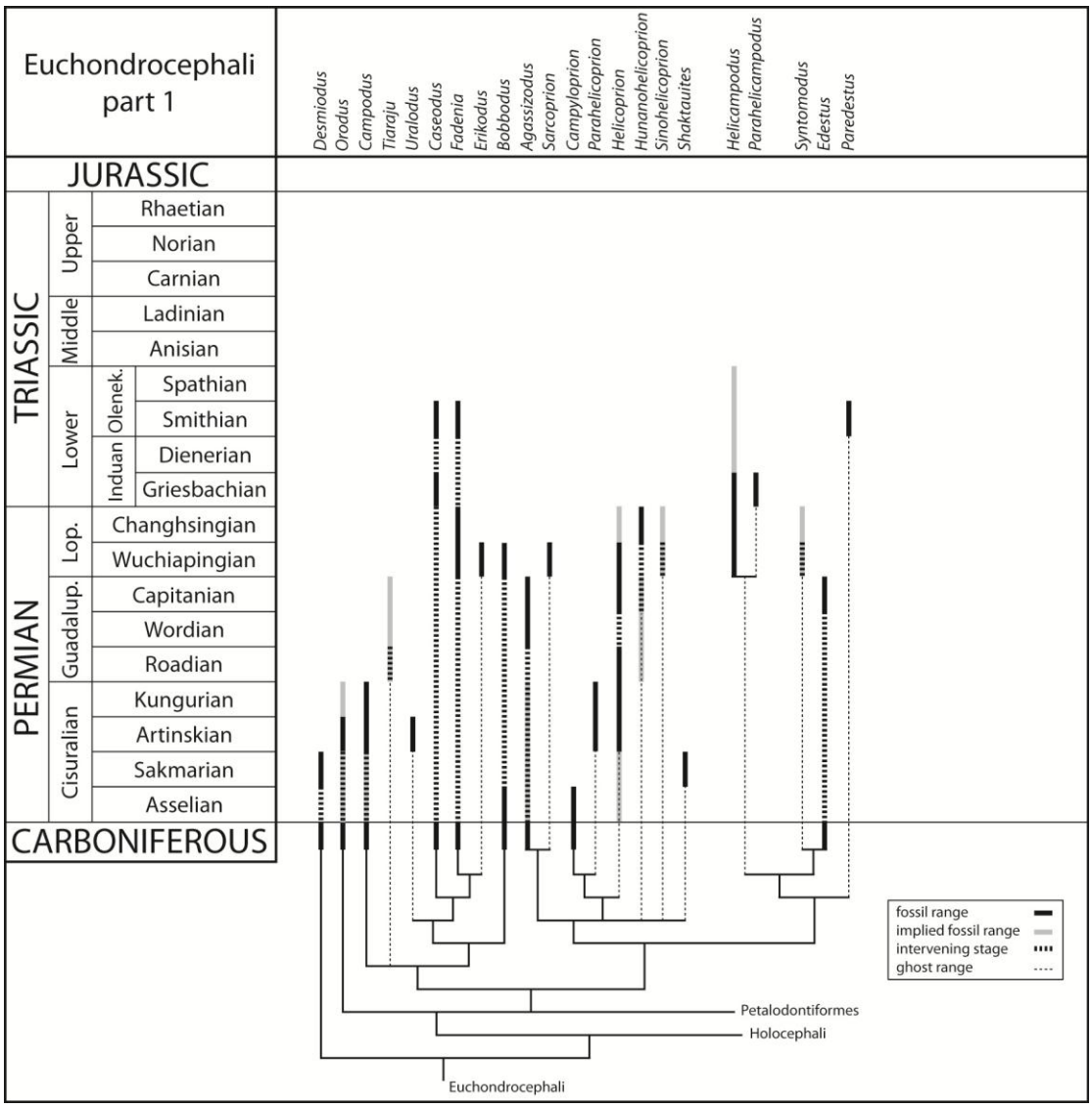
Euchondrocephali part 1
Desmiodus
Orodus
Campodus
Tiaraju
Uralodus
Caseodus
Fadenia
Erikodus
Bobbodus
Agassizodus
Sarcoprion
Campyloprion
Parahelicoprion
Helicoprion
Hunanohelicoprion
Sinohelicoprion
Shaktauites
Helicampodus
Parahelicampodus
Syntomodus
Edestus
Paredestus
JURASSIC
TRIASSIC
Upper
Middle
Lower
Olenek.
Induan
Rhaetian
Norian
Carnian
Ladinian
Anisian
Spathian
Smithian
Dienerian
Griesbachian
PERMIAN
Lop.
Guadalup.
Cisuralian
Changhsingian
Wuchiapingian
Capitanian
Wordian
Roadian
Kungurian
Artinskian
Sakmarian
Asselian
CARBONIFEROUS
fossil range
implied fossil range
intervening stage
ghost range
Petalodontiformes
Holocephali
Euchondrocephali

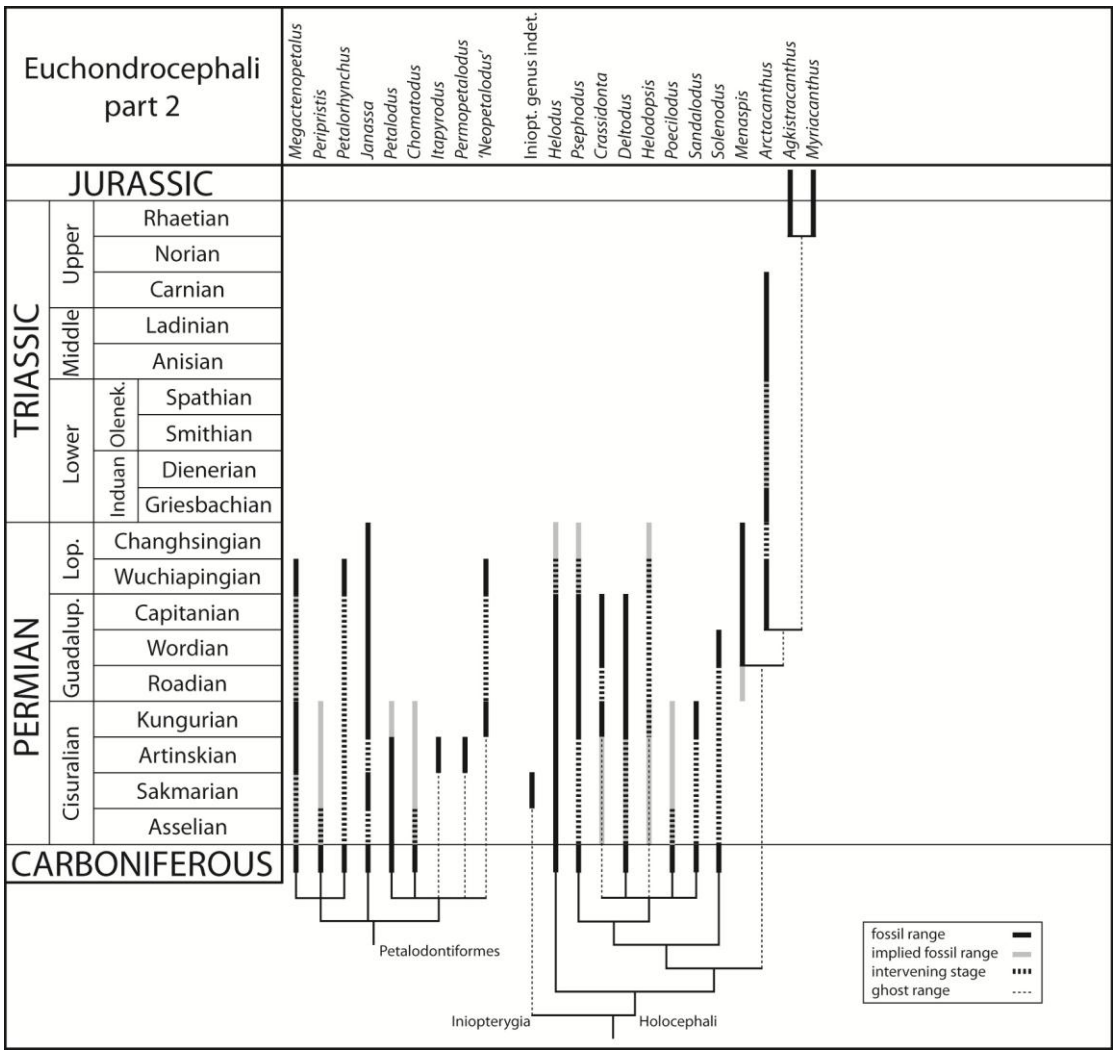
Euchondrocephali part 2
Megactenopetalus
Peripristis
Petalorhynchus
Janassa
Petalodus
Chomatodus
Itapyrodus
Permopetalodus
'Neopetalodus'
Iniopt. genus indet.
Helodus
Psephodus
Crassidonta
Deltodus
Helodopsis
Poecilodus
Sandalodus
Solenodus
Menaspis
Arctacanthus
Agkistracanthus
Myriacanthus
JURASSIC
TRIASSIC
Upper
Middle
Lower
Olenek.
Induan
Rhaetian
Norian
Carnian
Ladinian
Anisian
Spathian
Smithian
Dienerian
Griesbachian
PERMIAN
Lop.
Guadalup.
Cisuralian
Changhsingian
Wuchiapingian
Capitanian
Wordian
Roadian
Kungurian
Artinskian
Sakmarian
Asselian
CARBONIFEROUS
Petalodontiformes
Iniopterygia
Holocephali
fossil range
implied fossil range
intervening stage
ghost range

A2.3.9 CHONDRICHTHYAN CLADOGRAM DISPLAYED USING THE DDBM

Direct branching only shown in Permian–Triassic interval, whereas classic descendence is shown below for comparative purposes.

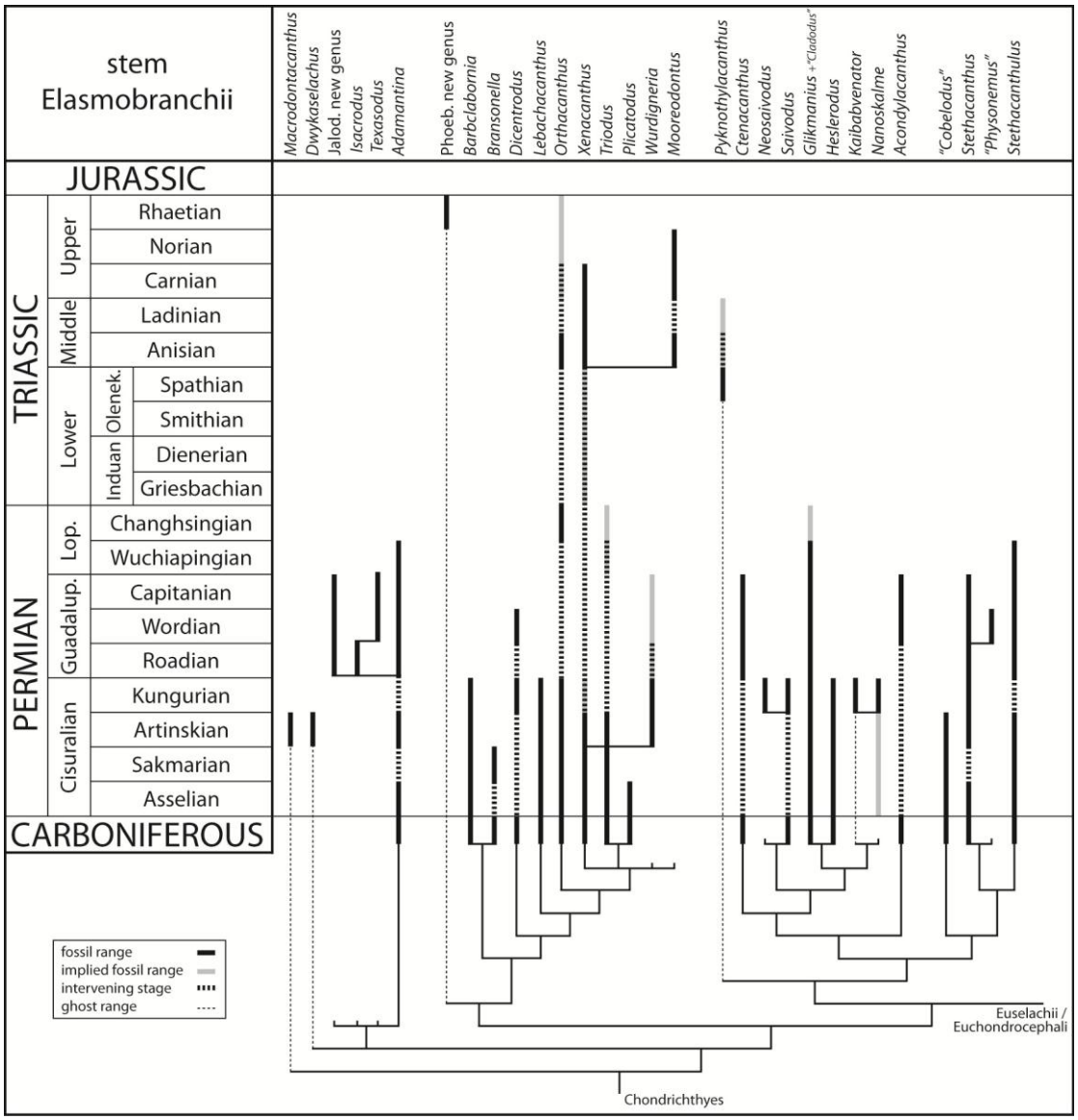

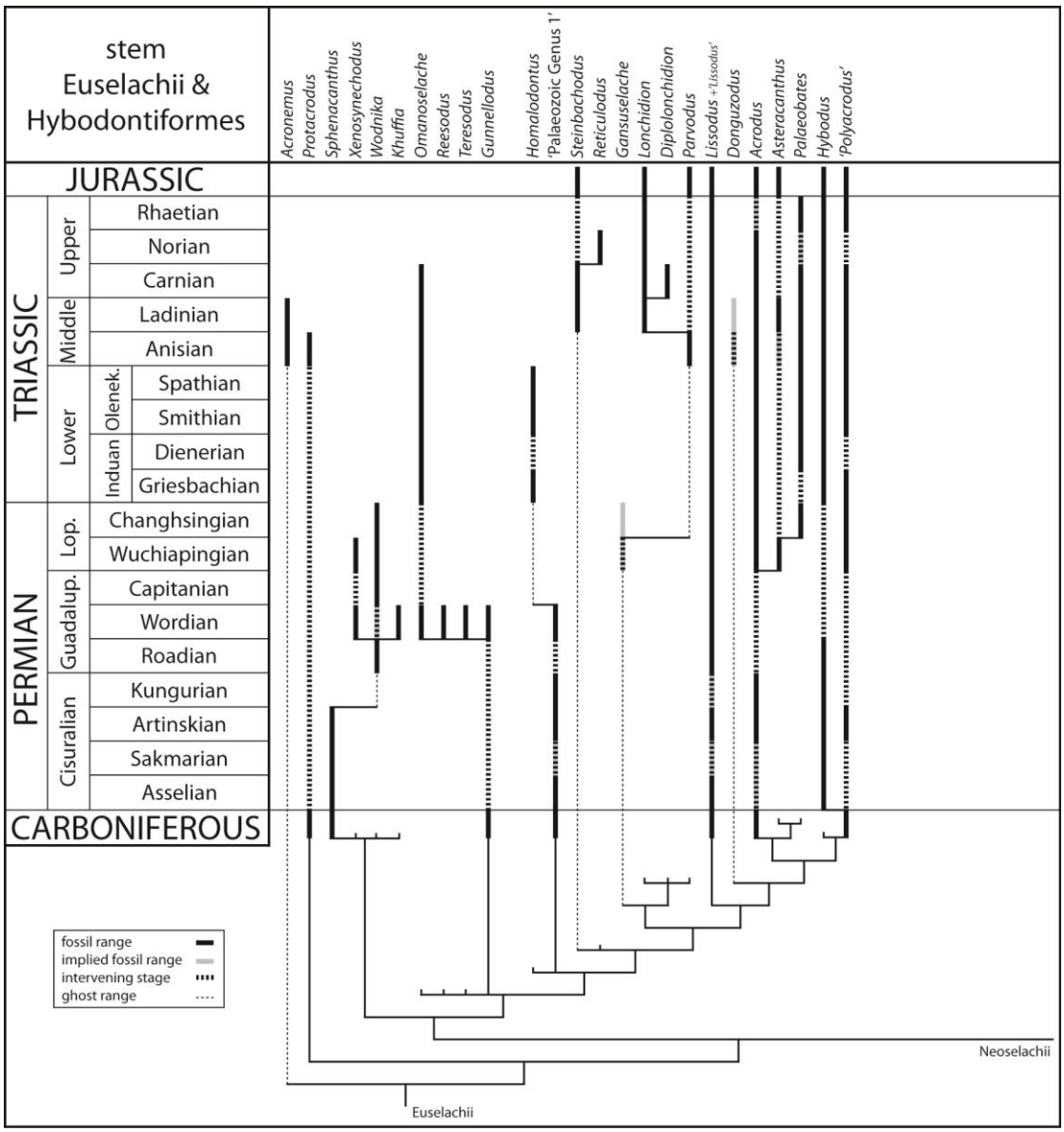
stem Euselachii & Hybodontiformes
Acronemus
Protacrodus
Sphenacanthus
Xenosynechodus
Wodnika
Khuffia
Omanoselache
Reesodus
Teresodus
Gunnellodus
Homalodontus
'Palaeozoic Genus 1'
Steinbachodus
Reticulodus
Gansuselache
Lonchidion
Diplolonchidion
Parvodus
Lissodus +'Lissodus'
Donguzodus
Acrodus
Asteracanthus
Palaeobates
Hybodus
'Polyacrodus'
JURASSIC
TRIASSIC
Upper
Rhaetian
Norian
Carnian
Middle
Ladinian
Anisian
Lower
Olenek.
Spathian
Smithian
Induan
Dienerian
Griesbachian
PERMIAN
Lop.
Changhsingian
Wuchiapingian
Guadalup.
Capitanian
Wordian
Roadian
Cisuralian
Kungurian
Artinskian
Sakmarian
Asselian
CARBONIFEROUS
fossil range
implied fossil range
intervening stage
ghost range
Neoselachii
Euselachii

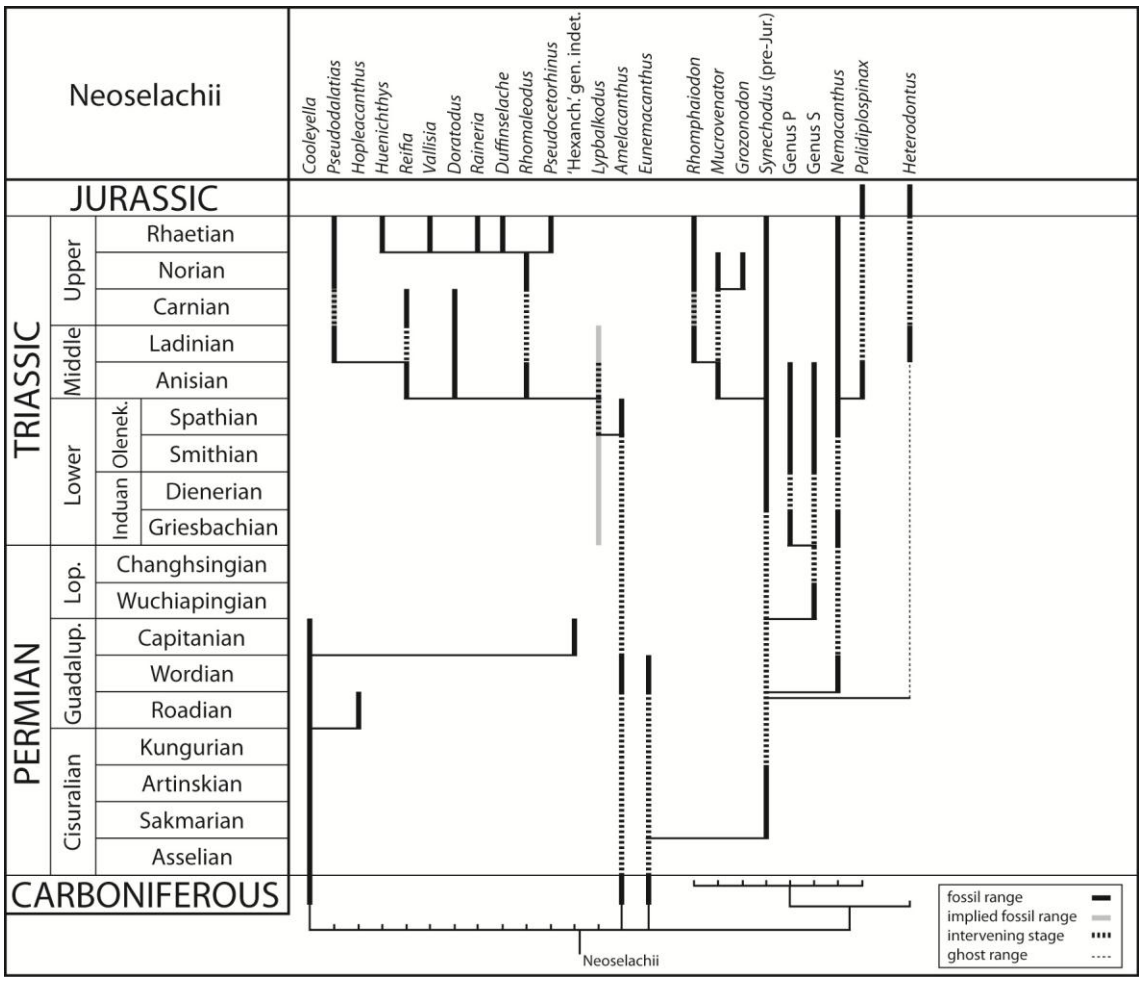
Neoselachii
Cooleyella
Pseudodalatias
Hopleacanthus
Huenichthys
Reifia
Vallisia
Doratodus
Raineria
Duffinselache
Rhomaleodus
Pseudocetorhinus
'Hexanch.' gen. indet.
Lypbalkodus
Amelacanthus
Eunemacanthus
Rhomphaiodon
Mucrovenator
Grozonodon
Synechodus (pre-Jur.)
Genus P
Genus S
Nemacanthus
Palidiplospinax
Heterodontus
JURASSIC
TRIASSIC
Upper
Middle
Lower
Olenek.
Induan
Rhaetian
Norian
Carnian
Ladinian
Anisian
Spathian
Smithian
Dienerian
Griesbachian
PERMIAN
Lop.
Guadalup.
Cisuralian
Changhsingian
Wuchiapingian
Capitanian
Wordian
Roadian
Kungurian
Artinskian
Sakmarian
Asselian
CARBONIFEROUS
Neoselachii
fossil range
implied fossil range
intervening stage
ghost range

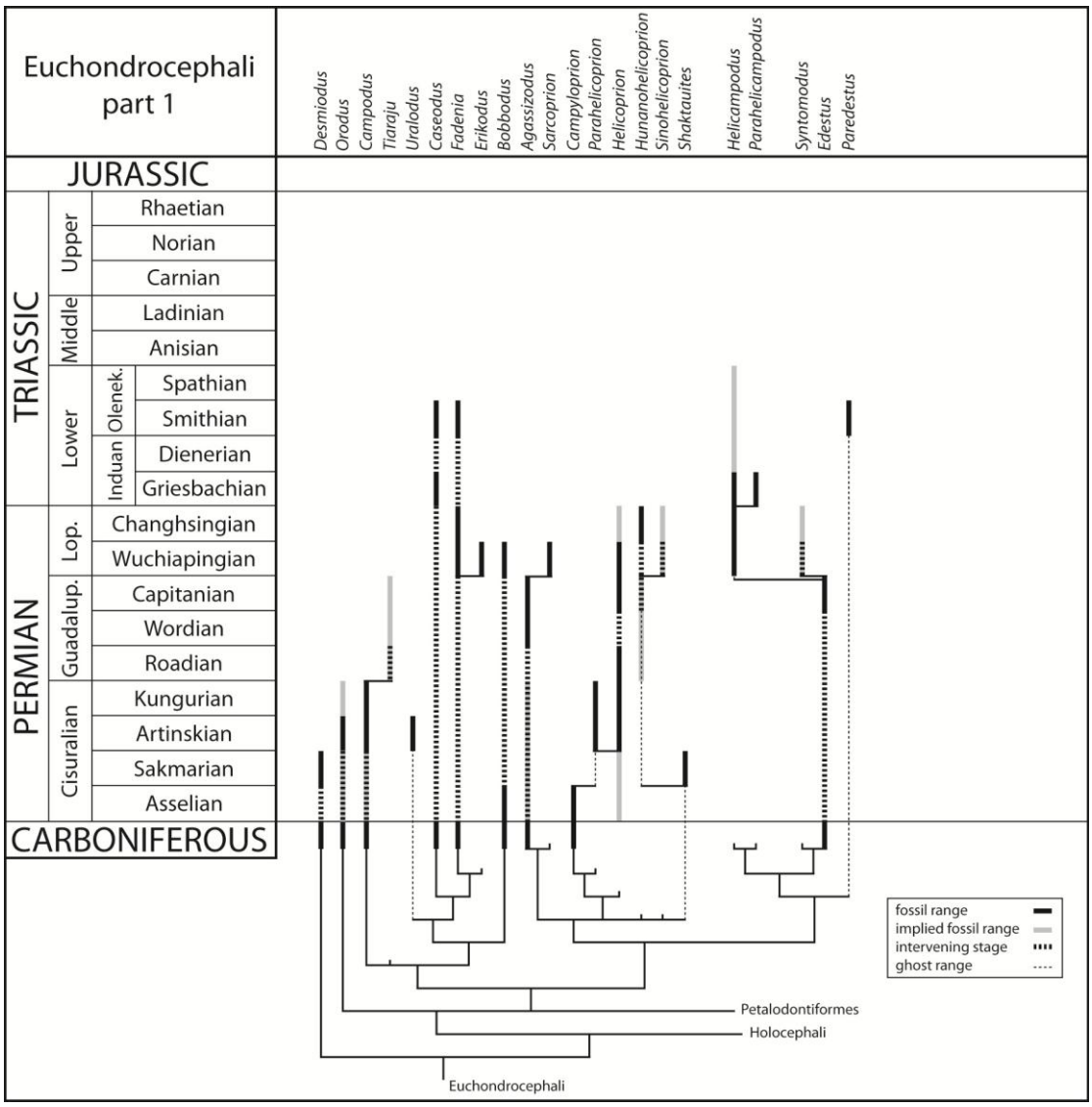
Euchondrocephali part 1
Desmiodus
Orodus
Campodus
Tiaraju
Uralodus
Caseodus
Fadenia
Erikodus
Bobbodus
Agassizodus
Sarcoprion
Campyloprion
Parahelicoprion
Helicoprion
Hunanohelicoprion
Sinohelicoprion
Shaktauites
Helicampodus
Parahelicampodus
Syntomodus
Edestus
Paredestus
JURASSIC
TRIASSIC
Upper
Middle
Lower
Olenek.
Induan
Rhaetian
Norian
Carnian
Ladinian
Anisian
Spathian
Smithian
Dienerian
Griesbachian
PERMIAN
Lop.
Guadalup.
Cisuralian
Changhsingian
Wuchiapingian
Capitanian
Wordian
Roadian
Kungurian
Artinskian
Sakmarian
Asselian
CARBONIFEROUS
fossil range
implied fossil range
intervening stage
ghost range
Petalodontiformes
Holocephali
Euchondrocephali

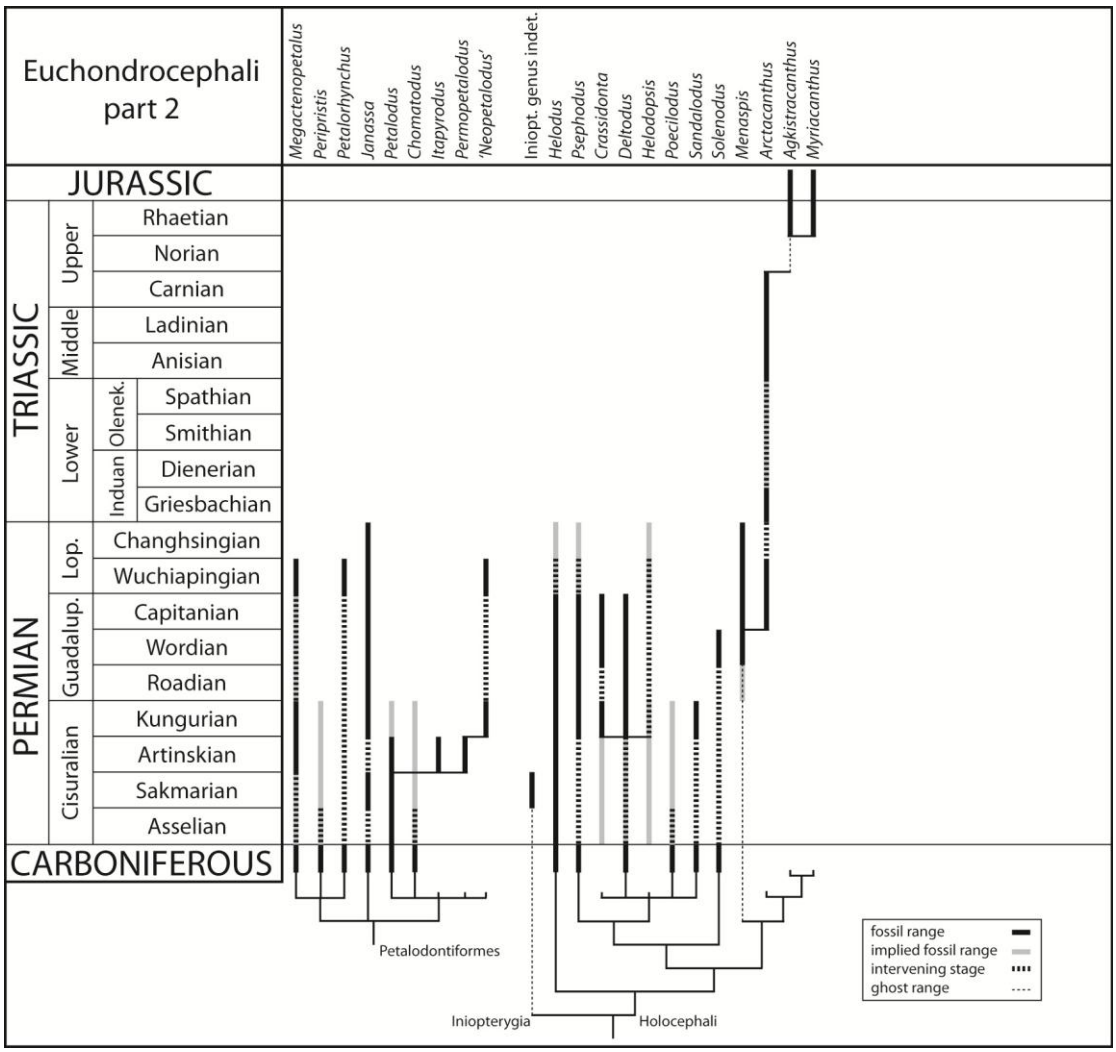
Euchondrocephali part 2
Megactenopetalus
Peripristis
Petalorhynchus
Janassa
Petalodus
Chomatodus
Itapyrodus
Permopetalodus
'Neopetalodus'
Iniopt. genus indet.
Helodus
Psephodus
Crassidonta
Deltodus
Helodopsis
Poecilodus
Sandalodus
Solenodus
Menaspis
Arctacanthus
Agkistracanthus
Myriacanthus
JURASSIC
TRIASSIC
Upper
Middle
Lower
Olenek.
Induan
Rhaetian
Norian
Carnian
Ladinian
Anisian
Spathian
Smithian
Dienerian
Griesbachian
PERMIAN
Lop.
Guadalup.
Cisuralian
Changhsingian
Wuchiapingian
Capitanian
Wordian
Roadian
Kungurian
Artinskian
Sakmarian
Asselian
CARBONIFEROUS
Petalodontiformes
Iniopterygia
Holocephali
fossil range
implied fossil range
intervening stage
ghost range

A2.3.10 PHYLOGENETIC RANGE DATA – FIGURE 7.11

(Sub)stage	Stem Elasmobranchii				Stem Elasmobranchii + Hybodontiformes				Neoselachii				Euchondrocephali part 1				Euchondrocephali part 2			
	Fossil ranges	Intervening stages	CBM ghost ranges	DDBM ghost ranges	Fossil ranges	Intervening stages	CBM ghost ranges	DDBM ghost ranges	Fossil ranges	Intervening stages	CBM ghost ranges	DDBM ghost ranges	Fossil ranges	Intervening stages	CBM ghost ranges	DDBM ghost ranges	Fossil ranges	Intervening stages	CBM ghost ranges	DDBM ghost ranges
Rhaetian	1	0	0	0	5	4	0	0	9	2	0	0	0	0	0	0	2	0	0	0
Norian	1	0	1	1	5	5	0	0	7	2	5	0	0	0	0	0	0	0	1	1
Carnian	2	1	1	1	9	2	1	0	4	6	6	0	0	0	0	0	1	0	1	0
Ladinian	1	2	1	1	10	1	2	0	6	4	6	0	0	0	0	0	1	0	1	0
Anisian	3	1	1	1	9	2	4	1	9	1	9	1	0	0	0	0	1	0	1	0
Spathian	1	2	2	1	7	2	5	4	5	1	14	1	0	0	0	0	0	1	1	0
Smithian	0	2	3	2	7	2	5	4	3	2	15	1	3	0	0	0	0	1	1	0
Dienerian	0	2	3	2	5	4	5	4	1	4	15	1	0	2	1	1	0	1	1	0
Griesbachian	0	2	3	2	6	3	5	4	2	3	15	1	3	1	1	1	1	0	1	0
Changhsingian	1	1	3	2	5	4	6	5	0	4	16	1	3	1	2	1	2	1	1	0
Wuchiapingian	3	3	3	2	6	4	7	4	1	3	16	1	6	4	2	1	6	3	1	0
Capitanian	8	3	3	2	2	6	8	5	2	3	17	1	3	4	6	1	7	4	1	0
Wordian	10	3	3	2	8	5	8	4	4	1	18	1	1	5	7	2	7	4	1	0
Roadian	7	6	5	2	3	5	13	4	2	3	19	0	1	6	7	2	4	6	1	1
Kungurian	12	6	7	2	3	4	14	5	1	3	20	0	3	5	8	2	8	3	1	1
Artinskian	14	4	9	3	6	2	14	4	2	2	20	0	5	5	8	2	5	6	4	1
Sakmarian	10	6	12	5	2	6	14	4	2	2	20	0	2	7	11	4	4	6	6	1
Asselian	12	5	12	5	4	4	14	4	1	2	13.5	0	2	7	12	3	2	10	7	2

(Sub)stage	Total				CBM			DDBM		
	Fossil ranges	Intervening stages	Raw div. FR+IS	SCM	Ghost ranges	Diversity FR+IS+GR	SCM	Ghost ranges	Diversity FR+IS+GR	SCM
Rhaetian	17	6	23	73.9	0	23	73.9	0	23	73.9
Norian	13	7	20	65	7	27	48.1	2	22	59.1
Carnian	16	9	25	64	9	34	47.1	1	26	61.5
Ladinian	18	7	25	72	10	35	51.4	1	26	69.2
Anisian	22	4	26	84.6	15	41	53.7	3	29	75.9
Spathian	13	6	19	68.4	22	41	31.7	6	25	52
Smithian	13	7	20	65	24	44	29.5	7	27	48.1
Dienerian	6	13	19	31.6	25	44	13.6	8	27	22.2
Griesbachian	12	9	21	57.1	25	46	26.1	8	29	41.4
Changhsingian	11	11	22	50	28	50	22	9	31	35.5
Wuchiapingian	22	17	39	56.4	29	68	32.4	8	47	46.8
Capitanian	22	20	42	52.4	35	77	28.6	9	51	43.1
Wordian	30	18	48	62.5	37	85	35.3	9	57	52.6
Roadian	17	26	43	39.5	45	88	19.3	9	52	32.7
Kungurian	27	21	48	56.3	50	98	27.6	10	58	46.6
Artinskian	32	19	51	62.7	55	106	30.2	10	61	52.5
Sakmarian	20	27	47	42.6	63	110	18.2	14	61	32.8
Asselian	21	28	49	42.9	58.5	107.5	19.5	14	63	33.3

R^2	0.3790	0.4341	0.5559
R	0.6156	0.6589	0.7456
α(2)	0.05	0.05	0.05
n	18	18	18
df	16	16	16
critical *t*	2.12	2.12	2.12
t	3.125	3.503	4.475
t < critical *t*?	no, reject H_o: $R^2 = 0$	no, reject H_o: $R^2 = 0$	no, reject H_o: $R^2 = 0$
p-value	0.007	0.003	0.0004

(Sub)stage	**Total duration (Myr)**	**CBM (duration in Myr)**		**DDBM (duration in Myr)**	
	Fossil ranges	Ghost ranges	RCI (%)	Ghost ranges	RCI (%)
Rhaetian	165.6	0		0	
Norian	390	136.5		39	
Carnian	175	63		7	
Ladinian	140	56		5.6	
Anisian	171.6	99		19.8	
Spathian	62.7	72.6		19.8	
Smithian	14	16.8		4.9	
Dienerian	9.5	12.5		4	
Griesbachian	10.5	12.5		4	
Changhsingian	44	56		18	
Wuchiapingian	222.3	165.3		45.6	
Capitanian	218.4	182		46.8	
Wordian	177.6	136.9		33.3	
Roadian	150.5	157.5		31.5	
Kungurian	336	350		70	
Artinskian	550.8	594		108	
Sakmarian	253.8	340.2		75.6	
Asselian	166.6	198.9		47.6	
ΣSRL / ΣMIG	3258.9	2649.7	**18.7**	580.5	**82.2**

A2.3.11 FAMILY DATA MATRIX (STARTS NEXT PAGE)

Entries are provided in batches of two pages, providing data on the presence of families in each time interval. Presence is marked by ‘1’, whereas Lazarus occurrences are marked by darker shaded boxes with ‘lz’.

	Family diversity	Carboniferous	Bound.	Cisuralian								Bound.	Guadalupian						Bound.	Lopingian				Bound.
				Asselian	Bound.	Sakmarian	Bound.	Artinskian	Bound.	Kungurian			Roadian	Bound.	Wordian	Bound.	Capitanian			Wuchiapingian	Bound.	Changxingian		
Bransonelliformes	Unnamed	1	1	1	1	1	1	1	1	1	1													
Xenacanthiformes	Diplodoselachidae	1	1	1	1	1	1	1	1	1	1	1	lz	1	1	1	lz		1	lz	1	1		1
	Xenacanthidae	1	1	1	1	1	1	1	1	1	1	1	lz	1	lz	1	lz	1	1	lz	1	lz	1	1
Symmoriiformes	Symmoriidae	1	1	1	1	lz	1	1	1	1		1	1	1	1	1	1							
	Falcatidae	1	1	1	1	1	1	1	1	lz		1	1	1	1	1	1		1	1				
Ctenacanthiformes	Ctenacanthidae	1	1	1	1	1	1	1	1	1	1	1	1	1	1	1	1	1	1	1			1	
	Heslerodidae	1	1	1	1	1	1	1	1	1														
Unresolved	Jalodontidae	1	1	1	1	lz	1	1	1	lz		1	1	1	1	1	1		1	1				
Hybodontiformes	Hybodontidae	1	1	1	1	1	1	1	1	1	1	1	1	1	lz	1	lz		1	1	1	1		
	Unnamed																							
	Lonchidiidae																							
	Steinbachodontidae																							
	Homalodontidae																							
	Distobatidae																							
Unresolved Euselachii	Protacrodontidae	1	1	lz	1	lz	1	lz	1	lz		1	lz	1	lz	1	lz		1	lz	1	lz		1
	Sphenacanthidae	1	1	1	1	1	1	1					1	1	1	1	1	1	1	1	1	1	1	
Synechodontiformes	Palaeospinacidae																							
Unresolved Neoselachii	Anachronistidae	1	1	1	1	1	1	1	1	1		1	1	1	1	1	1							
	Pseudodalatiidae																							
Galeomorphii	Heterodontidae																							
Eugeneodontiformes (+ Orodontiformes)	Orodontidae	1	1	lz	1	lz	1	1			1													
	Caseodontidae	1	1	lz	1	lz	1	1	1	lz		1	lz	1	lz	1	lz		1	1	1	1	1	1
	Eugeneodontidae	1	1	1	1	lz	1	lz	1	lz		1	lz	1	lz	1	lz		1	1				
	Agassizodontidae	1	1	1	1	1	1	1	1	1	1	1	1	1	1	1	1	1	1	1	1	1	1	
	Edestidae	1	1	lz	1	lz	1	lz	1	lz		1	lz	1	lz	1	1		1	1	1	1	1	1

	Family diversity	Lower Triassic								Bound.	Middle				Bound.	Upper Triassic						Bound.	Jurassic
		Griesbachian	Bound.	Dienerian	Bound.	Smithian	Bound.	Spathian			Anisian	Bound.	Ladinian			Carnian	Bound.	Norian	Bound.	Rhaetian			
Bransonelliformes	Unnamed																						
Xenacanthiformes	Diplodoselachidae	lz	1	lz	1	lz	1	lz		1	1	1	lz		1	lz					1		
	Xenacanthidae	lz	1	lz	1	lz	1	lz	1	1	1	1	1		1	1							
Symmoriiformes	Symmoriidae																						
	Falcatidae																						
Ctenacanthiformes	Ctenacanthidae																						
	Heslerodidae																						
Unresolved	Jalodontidae																						
Hybodontiformes	Hybodontidae	1	1	1	1	1	1	1	1	1	1	1	1	1	1	1	1	1	1	1	1	1	1
	Unnamed	1	1	1	1	1	1	1	1	1	1	1	1	1	1	1	1	1	1	1	1	1	1
	Lonchidiidae										1	1	1		1	1	1	1	1	1		1	1
	Steinbachodontidae												1		1	1	1	lz	1	lz		1	1
	Homalodontidae	1	1	lz	1	1	1	1															
	Distobatidae																	1					
Unresolved Euselachii	Protacrodontidae	lz	1	lz	1	lz	1	lz			1												
	Sphenacanthidae																						
Synechodontiformes	Palaeospinacidae										1	1	lz		1	lz	1	lz	1	lz		1	1
Unresolved Neoselachii	Anachronistidae																						
	Pseudodalatiidae												1		1	lz	1	1	1	1	1		
Galeomorphii	Heterodontidae												1		1	lz	1	lz	1	lz		1	1
Eugeneodontiformes (+ Orodontiformes)	Orodontidae																						
	Caseodontidae	1	1	lz	1	1																	
	Eugeneodontidae																						
	Agassizodontidae																						
	Edestidae	1	1	lz	1	1			1														

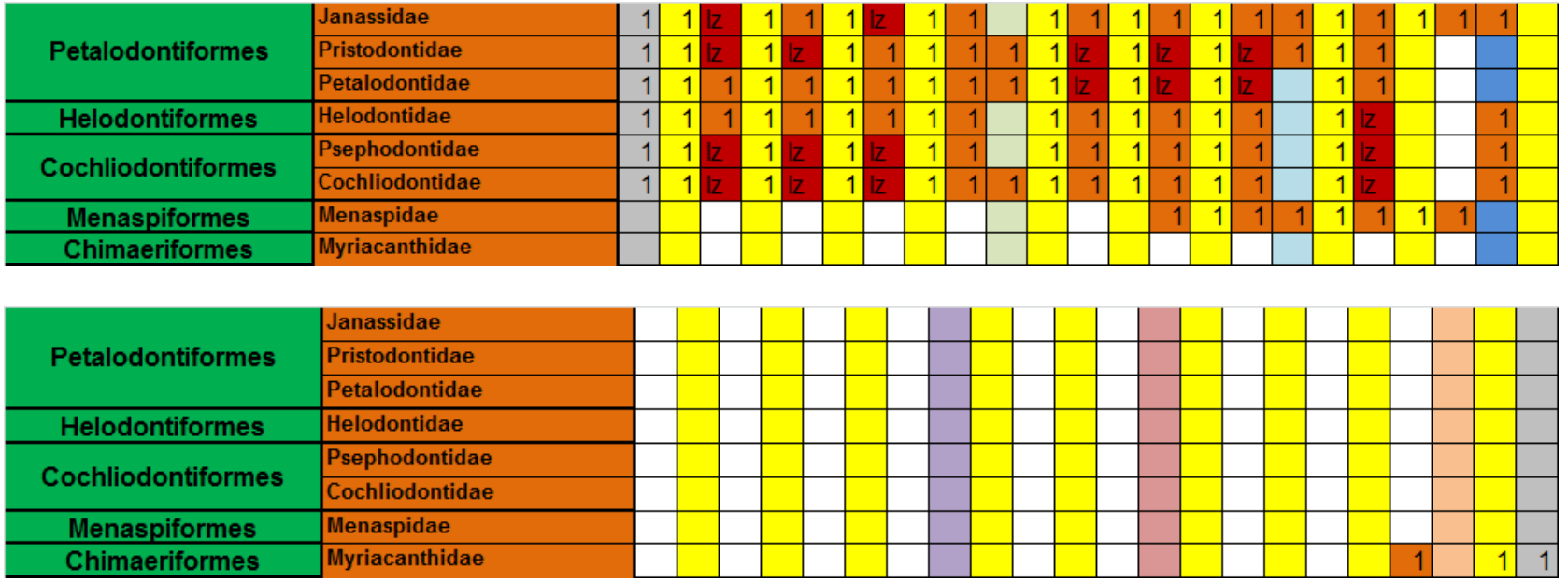
Petalodontiformes
Janassidae
Pristodontidae
Petalodontidae
Helodontiformes
Helodontidae
Cochliodontiformes
Psephodontidae
Cochliodontidae
Menaspiformes
Menaspidae
Chimaeriformes
Myriacanthidae

A2.3.12 FAMILY DATA – FIGURE 7.12

(Sub)stage	Family richness		
	Fossil	Lazarus	Total
Rhaetian	5	3	8
Norian	5	3	8
Carnian	5	4	9
Ladinian	7	2	9
Anisian	7	0	7
Spathian	3	3	6
Smithian	5	3	8
Dienerian	2	6	8
Griesbachian	5	3	8
Changhsingian	8	2	10
Wuchiapingian	13	6	19
Capitanian	13	8	21
Wordian	13	8	21
Roadian	12	8	20
Kungurian	15	6	21
Artinskian	17	6	23
Sakmarian	13	10	23
Asselian	15	8	23

A2.3.13 GDD DATA – FIGURE 7.13

(Sub)stage	Mean GDD	EMSD:Mean GDD	Raw SD:Mean GDD
Rhaetian	23	0.59	1.00
Norian	24.5	0.67	0.82
Carnian	30	0.70	0.83
Ladinian	30.5	0.72	0.82
Anisian	35	0.53	0.74
Spathian	33	0.52	0.58
Smithian	35.5	0.51	0.56
Dienerian	35.5	0.54	0.54
Griesbachian	37.5	0.47	0.56
Changhsingian	40.5	0.44	0.54
Wuchiapingian	57.5	0.43	0.68
Capitanian	64	0.54	0.66
Wordian	71	0.56	0.68
Roadian	70	0.56	0.61
Kungurian	78	0.53	0.62
Artinskian	83.5	0.52	0.61
Sakmarian	85.5	0.52	0.55
Asselian	85.25	0.55	0.57

A2.4. ANALYTICAL AND STATISTICAL DATA – CHAPTER 8

A2.4.1 GENUS DATA MATRIX (STARTS NEXT PAGE)

Entries are provided in batches of two pages, providing data on the presence of genera in each time interval. Presence is marked by ‘1’, whereas Lazarus occurrences are marked by darker shaded boxes with ‘lz’.

	Genus diversity	Carboniferous	Bound.	Cisuralian								Bound.	Guadalupian						Bound.	Lopingian				Bound.
				Asselian	Bound.	Sakmarian	Bound.	Artinskian	Bound.	Kungurian			Roadian	Bound.	Wordian	Bound.	Capitanian			Wuchiapingian	Bound.	Changxingian		
Phoebodontiformes?	No named genera																							
	Genera in open nomenclature							1																
Bransonelliformes	*Barbclabornia*	1	1	1	1	1	1	1	1	1	1													
	Bransonella	1	1	lz	1	1																		
	Genera in open nomenclature																							
Xenacanthiformes	*Dicentrodus*	1	1	lz	1	lz	1	lz	1	1		1	lz	1	1									
	Lebachacanthus	1	1	1	1	1	1	1	1	1	1													
	Orthacanthus	1	1	1	1	1	1	1	1	1	1	1	lz	1	lz	1	lz		1	lz	1	1		1
	Xenacanthus	1	1	1	1	1	1	1	1	lz	1	1	lz	1	lz	1	lz		1	lz	1	lz		1
	Triodus	1	1	1	1	1	1	1	1	lz		1	lz	1	lz	1	lz		1	lz			1	
	Plicatodus	1	1	1																				
	Wurdigneria							1	1	1		1	lz					1						
	Mooreodontus																							
	Genera in open nomenclature										1												2	
Symmoriiformes	*Stethacanthus*	1	1	1	1	lz	1	1	1	1		1	1	1	1	1	1							
	"Physonemus" / Batacanthus												1	1	1									
	Stethacanthulus	1	1	1	1	1	1	1	1	lz		1	1	1	1	1	1		1	1				
	Genera in open nomenclature												1											
Ctenacanthiformes	*Ctenacanthus*	1	1	lz	1	lz	1	lz	1	lz		1	1	1	1	1	1	1						
	Glikmanius	1	1	1	1	1	1	1	1	1	1	1	1	1	1	1	1	1						
	"Cladodus"	1	1	lz	1	lz	1	1	1	1	1	1	1	1	1	1	1		1	1			1	
	Heslerodus	1	1	1	1	1	1	1	1	1														
	Saivodus	1	1	lz	1	lz	1	lz	1	1														
	Neosaivodus									1														
	Kaibabvenator									1														

	Genus diversity	Lower Triassic								Bound.	Middle				Bound.	Upper Triassic						Bound.	Jurassic
		Griesbachian	Bound.	Dienerian	Bound.	Smithian	Bound.	Spathian			Anisian	Bound.	Ladinian			Carnian	Bound.	Norian	Bound.	Rhaetian			
Phoebodontiformes?	No named genera																						
	Genera in open nomenclature										1					1		1		1			
Bransonelliformes	*Barbclabornia*																						
	Bransonella																						
	Genera in open nomenclature																						
Xenacanthiformes	*Dicentrodus*																						
	Lebachacanthus																						
	Orthacanthus	lz	1	lz	1	lz	1	lz		1	1	1	lz		1	lz					1		
	Xenacanthus	lz	1	lz	1	lz	1	lz	1	1	1	1	1		1	1							
	Triodus																						
	Plicatodus																						
	Wurdigneria																						
	Mooreodontus										1	1	lz		1	1	1	1					
	Genera in open nomenclature																						
Symmoriiformes	*Stethacanthus*																						
	"Physonemus" / Batacanthus																						
	Stethacanthulus																						
	Genera in open nomenclature																						
Ctenacanthiformes	*Ctenacanthus*																						
	Glikmanius																						
	"Cladodus"																						
	Heslerodus																						
	Saivodus																						
	Neosaivodus																						
	Kaibabvenator																						

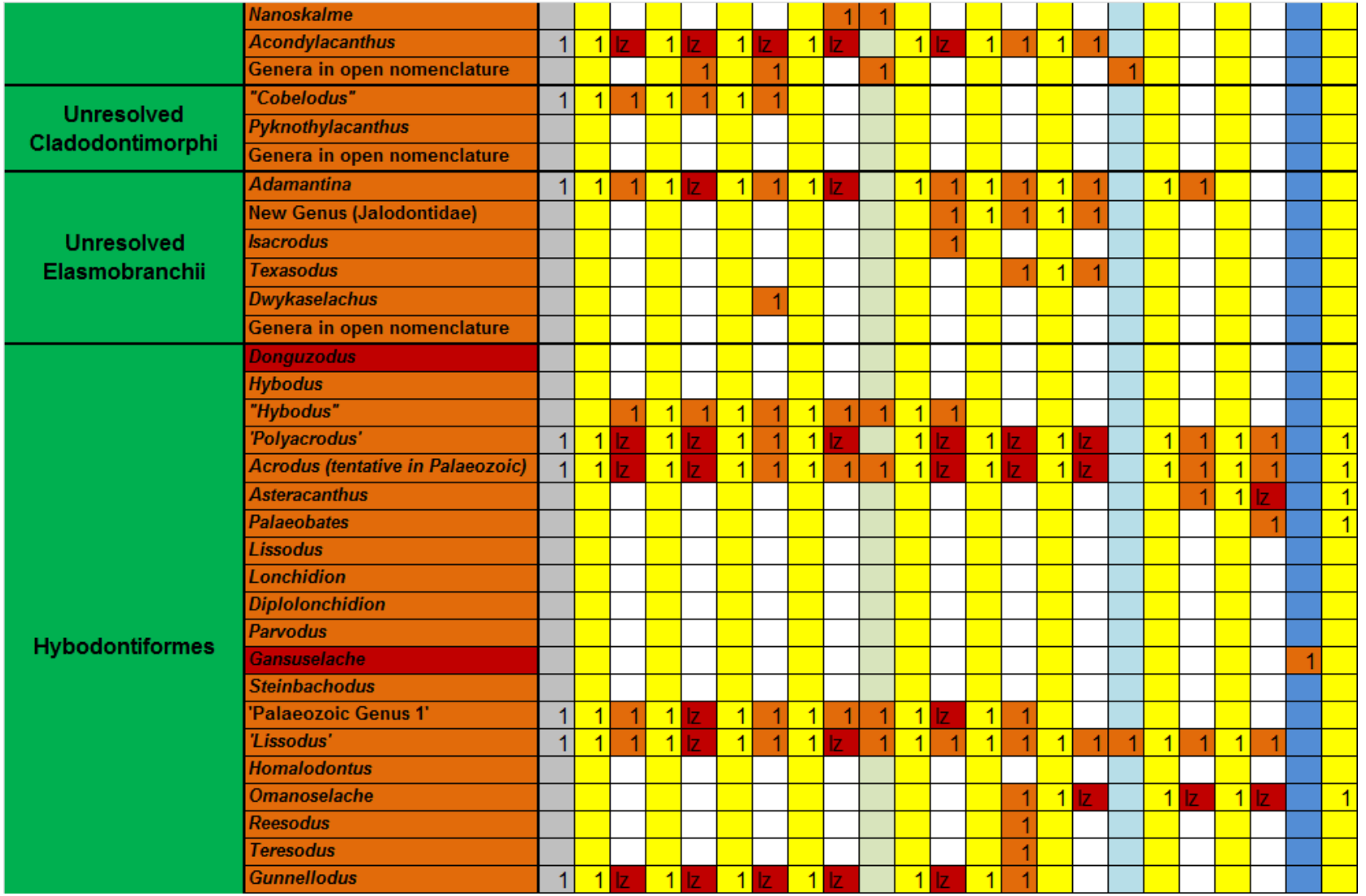
Nanoskalme
Acondylacanthus
Genera in open nomenclature
Unresolved Cladodontimorphi
"Cobelodus"
Pyknothylacanthus
Genera in open nomenclature
Unresolved Elasmobranchii
Adamantina
New Genus (Jalodontidae)
Isacrodus
Texasodus
Dwykaselachus
Genera in open nomenclature
Hybodontiformes
Donguzodus
Hybodus
"Hybodus"
'Polyacrodus'
Acrodus (tentative in Palaeozoic)
Asteracanthus
Palaeobates
Lissodus
Lonchidion
Diplolonchidion
Parvodus
Gansuselache
Steinbachodus
'Palaeozoic Genus 1'
'Lissodus'
Homalodontus
Omanoselache
Reesodus
Teresodus
Gunnellodus

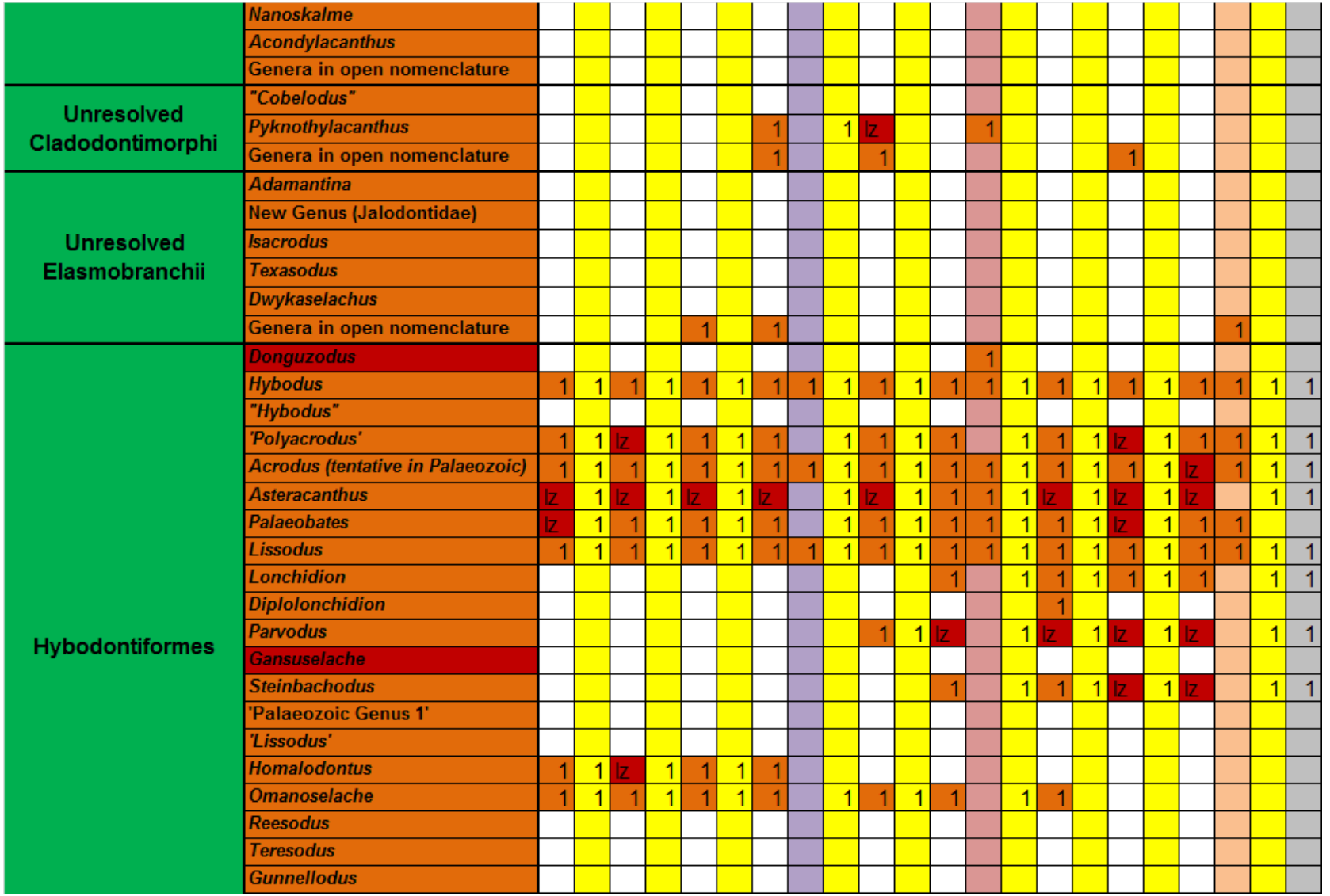
Unresolved Cladodontimorphi
Unresolved Elasmobranchii
Hybodontiformes
Nanoskalme
Acondylacanthus
Genera in open nomenclature
"Cobelodus"
Pyknothylacanthus
Genera in open nomenclature
Adamantina
New Genus (Jalodontidae)
Isacrodus
Texasodus
Dwykaselachus
Genera in open nomenclature
Donguzodus
Hybodus
"Hybodus"
'Polyacrodus'
Acrodus (tentative in Palaeozoic)
Asteracanthus
Palaeobates
Lissodus
Lonchidion
Diplolonchidion
Parvodus
Gansuselache
Steinbachodus
'Palaeozoic Genus 1'
'Lissodus'
Homalodontus
Omanoselache
Reesodus
Teresodus
Gunnellodus

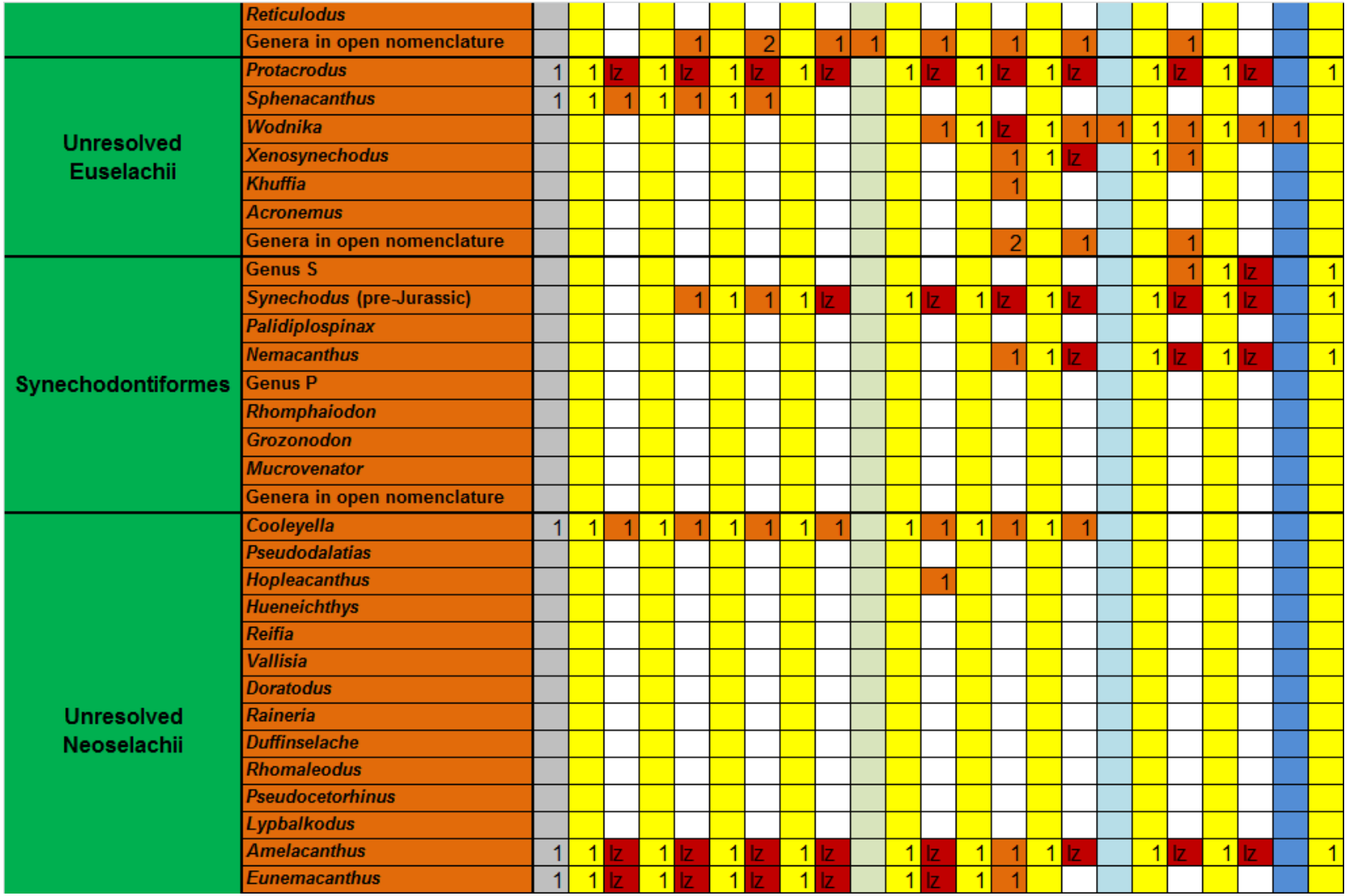
Reticulodus
Genera in open nomenclature
Unresolved Euselachii
Protacrodus
Sphenacanthus
Wodnika
Xenosynechodus
Khuffia
Acronemus
Genera in open nomenclature
Synechodontiformes
Genus S
Synechodus (pre-Jurassic)
Palidiplospinax
Nemacanthus
Genus P
Rhomphaiodon
Grozonodon
Mucrovenator
Genera in open nomenclature
Unresolved Neoselachii
Cooleyella
Pseudodalatias
Hopleacanthus
Hueneichthys
Reifia
Vallisia
Doratodus
Raineria
Duffinselache
Rhomaleodus
Pseudocetorhinus
Lypbalkodus
Amelacanthus
Eunemacanthus

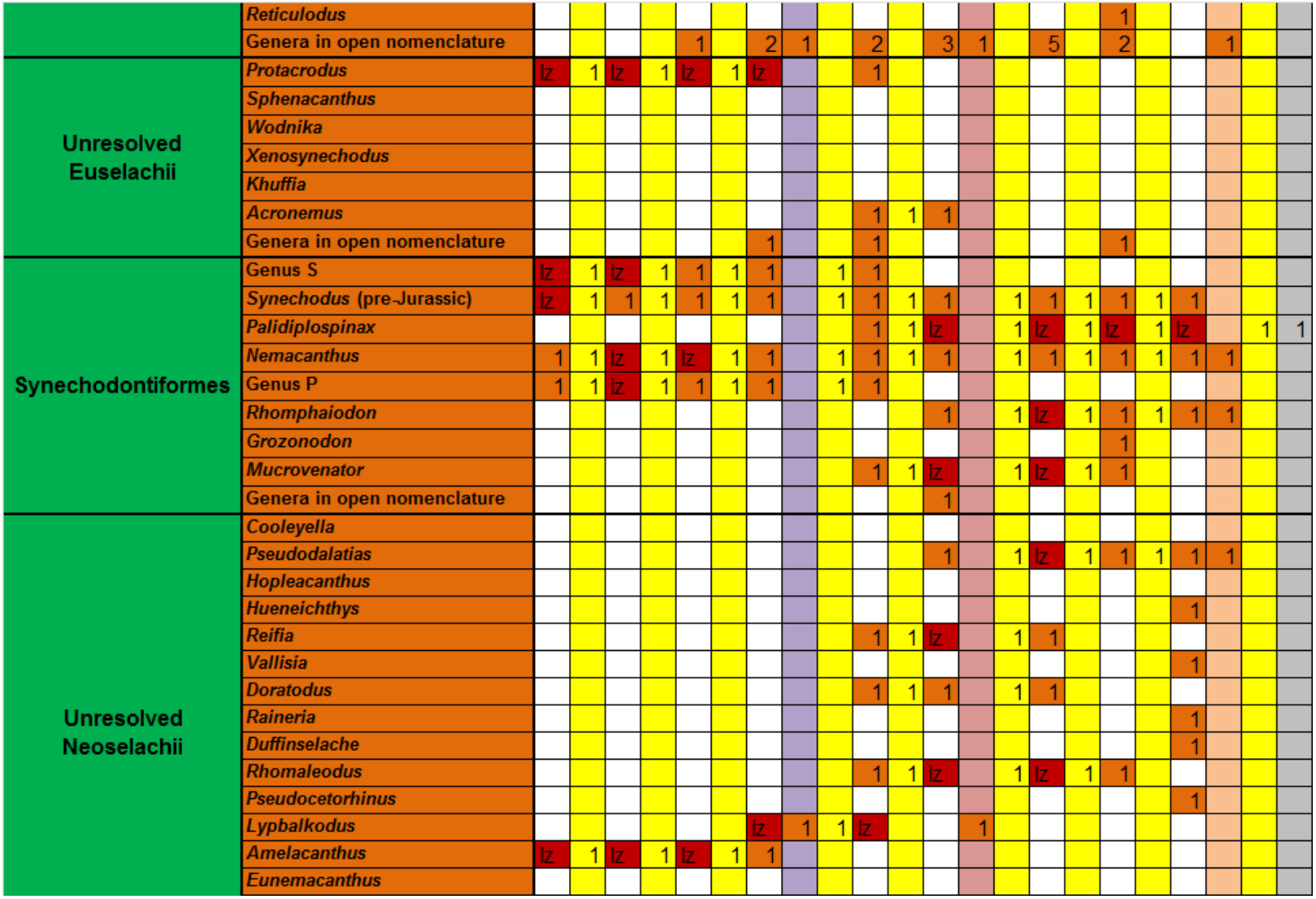
Reticulodus
Genera in open nomenclature
Unresolved Euselachii
Protacrodus
Sphenacanthus
Wodnika
Xenosynechodus
Khuffia
Acronemus
Genera in open nomenclature
Synechodontiformes
Genus S
Synechodus (pre-Jurassic)
Palidiplospinax
Nemacanthus
Genus P
Rhomphaiodon
Grozonodon
Mucrovenator
Genera in open nomenclature
Unresolved Neoselachii
Cooleyella
Pseudodalatias
Hopleacanthus
Hueneichthys
Reifia
Vallisia
Doratodus
Raineria
Duffinselache
Rhomaleodus
Pseudocetorhinus
Lypbalkodus
Amelacanthus
Eunemacanthus

	Genera in open nomenclature														1		2						1			
Galeomorphii	*Heterodontus*																									
	Genera in open nomenclature																									
Eugeneodontiformes (+ Orodontiformes)	*Orodus*	1	1	lz	1	lz	1	1			1															
	Caseodus	1	1	lz	1	lz	1	lz	1	lz		1	lz	1	lz	1	lz		1	lz	1	lz				1
	Fadenia	1	1	lz	1	lz	1	lz	1	lz		1	lz	1	lz	1	lz		1	1	1	1	1	1		
	Erikodus																			1						
	Uralodus							1																		
	Bobbodus	1	1	1	1	lz	1	lz	1	lz		1	lz	1	lz	1	lz		1	1						
	Campodus	1	1	lz	1	lz	1	1	1	1	1															
	Tiaraju																	1								
	Agassizodus	1	1	lz	1	lz	1	lz	1	lz	1	1	lz	1	1	1	1									
	Campyloprion	1	1	1																						
	Helicoprion							1	1	1	1	1	1	1	lz	1	1		1	1			1			
	Parahelicoprion							1	1	1																
	Sarcoprion																			1						
	Hunanohelicoprion																lz	1	1	lz	1	1				
	Sinohelicoprion																						1			
	Shaktauites					1																				
	Edestus	1	1	lz	1	lz	1	lz	1	lz		1	lz	1	lz	1	1									
	Syntomodus																						1			
	Helicampodus																			1	1	1	1	1		
	Parahelicampodus																									
	Paredestus																									
	Genera in open nomenclature					2		1							1					1		1				
Petalodontiformes	*Janassa*	1	1	lz	1	1	1	lz	1	1		1	1	1	1	1	1	1	1	1	1	1	1			
	Megactenopetalus	1	1	lz	1	lz	1	1	1	1	1	1	lz	1	lz	1	lz	1	1	1						
	Peripristis	1	1	lz							1															
	Petalorhynchus	1	1	lz	1	lz	1	lz	1	lz		1	lz	1	lz	1	lz		1	1						
	Petalodus	1	1	1	1	1	1	1	1		1															
	Chomatodus	1	1	lz							1															

	Genera in open nomenclature															1		1							
Galeomorphii	*Heterodontus*												1		1	lz	1	lz	1	lz		1	1		
	Genera in open nomenclature																								
Eugeneodontiformes (+ Orodontiformes)	*Orodus*																								
	Caseodus	1	1	lz	1	1																			
	Fadenia	lz	1	lz	1	1																			
	Erikodus																								
	Uralodus																								
	Bobbodus																								
	Campodus																								
	Tiaraju																								
	Agassizodus																								
	Campyloprion																								
	Helicoprion																								
	Parahelicoprion																								
	Sarcoprion																								
	Hunanohelicoprion																								
	Sinohelicoprion																								
	Shaktauites																								
	Edestus																								
	Syntomodus																								
	Helicampodus	1							1																
	Parahelicampodus	1																							
	Paredestus					1																			
	Genera in open nomenclature			1		2																			
Petalodontiformes	*Janassa*																								
	Megactenopetalus																								
	Peripristis																								
	Petalorhynchus																								
	Petalodus																								
	Chomatodus																								

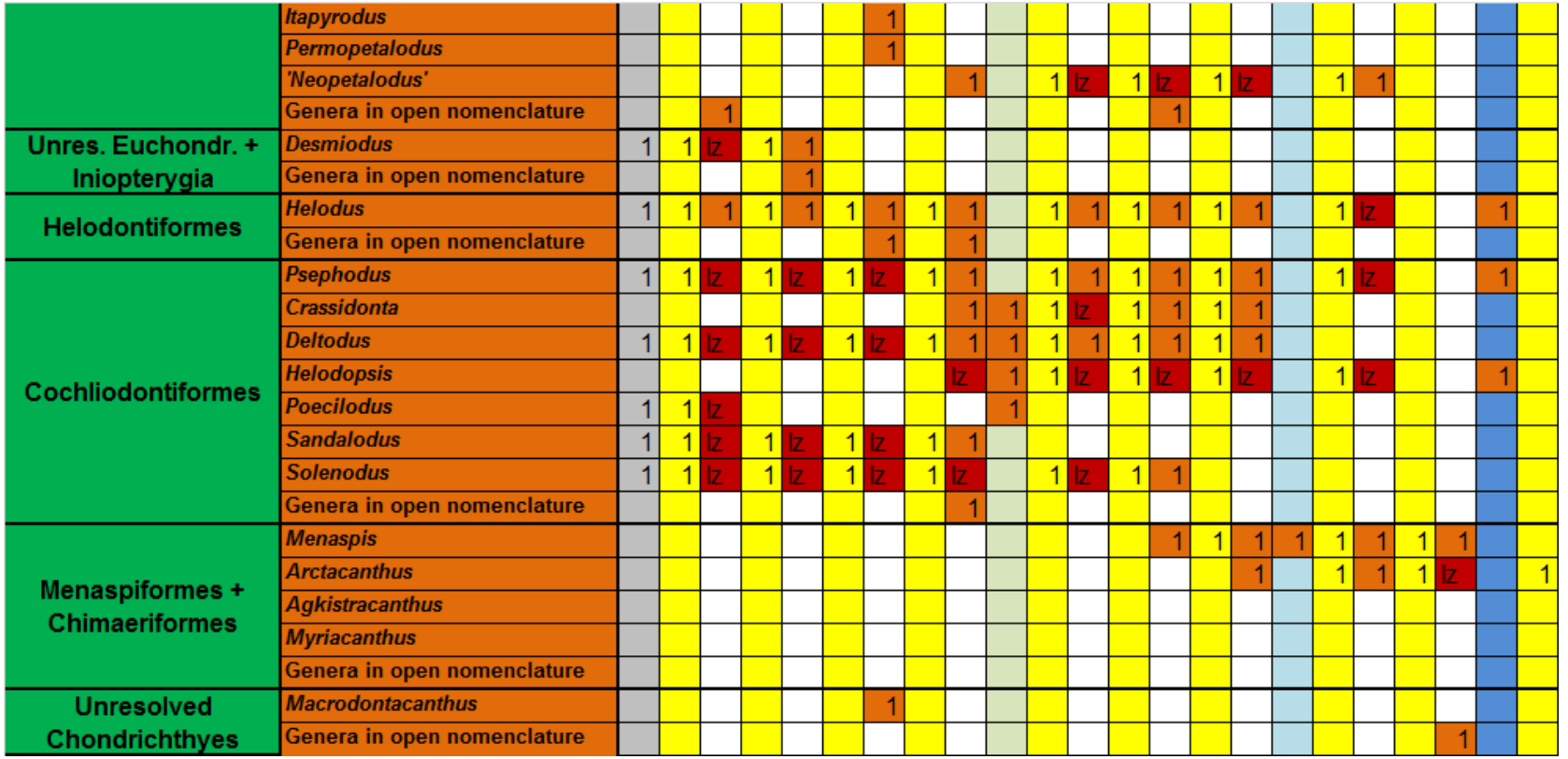
Itapyrodus
Permopetalodus
'Neopetalodus'
Genera in open nomenclature
Unres. Euchondr. + Iniopterygia
Desmiodus
Genera in open nomenclature
Helodontiformes
Helodus
Genera in open nomenclature
Cochliodontiformes
Psephodus
Crassidonta
Deltodus
Helodopsis
Poecilodus
Sandalodus
Solenodus
Genera in open nomenclature
Menaspiformes + Chimaeriformes
Menaspis
Arctacanthus
Agkistracanthus
Myriacanthus
Genera in open nomenclature
Unresolved Chondrichthyes
Macrodontacanthus
Genera in open nomenclature

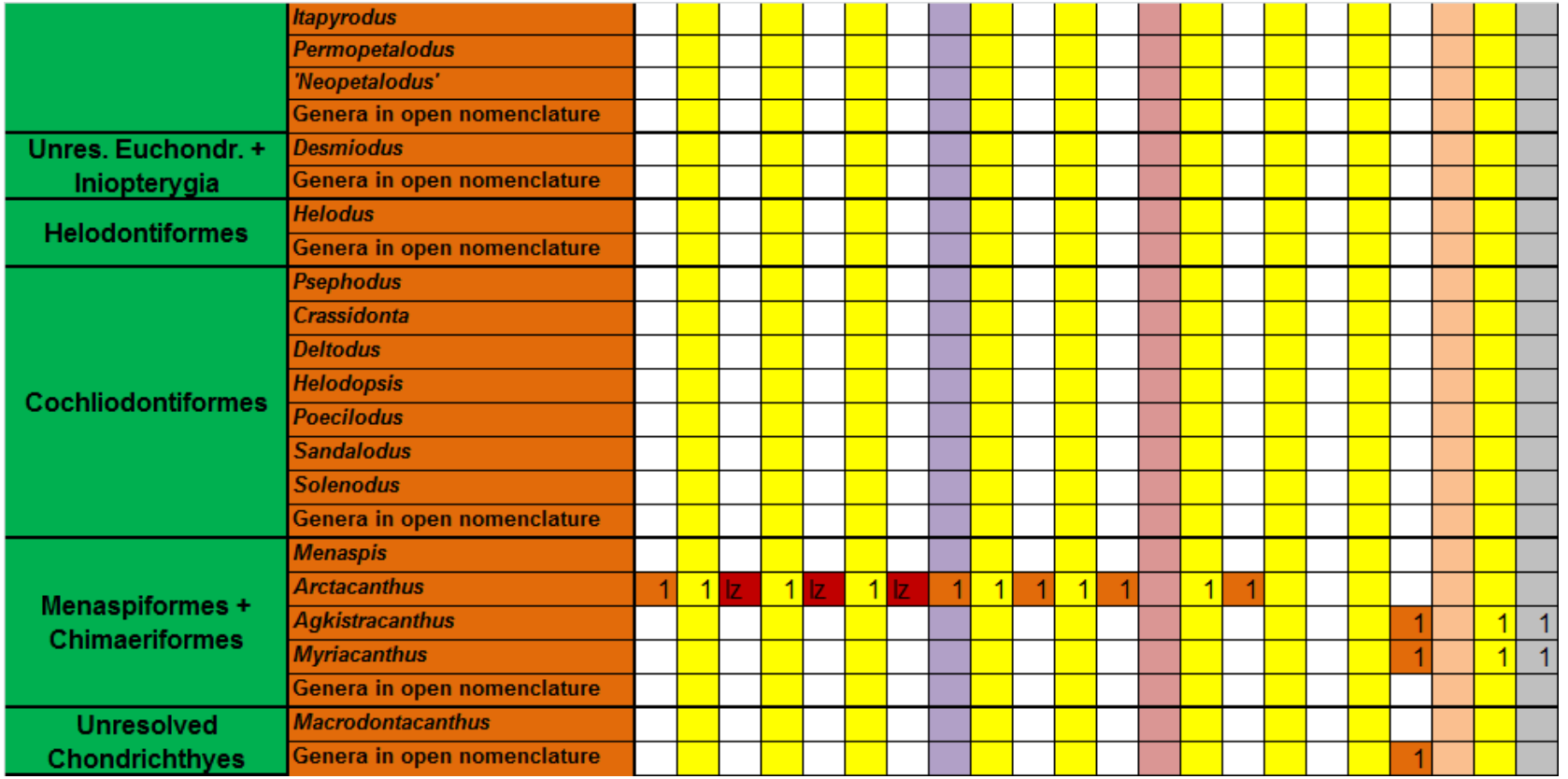
Itapyrodus
Permopetalodus
'Neopetalodus'
Genera in open nomenclature
Unres. Euchondr. + Iniopterygia
Desmiodus
Genera in open nomenclature
Helodontiformes
Helodus
Genera in open nomenclature
Cochliodontiformes
Psephodus
Crassidonta
Deltodus
Helodopsis
Poecilodus
Sandalodus
Solenodus
Genera in open nomenclature
Menaspiformes + Chimaeriformes
Menaspis
Arctacanthus
Agkistracanthus
Myriacanthus
Genera in open nomenclature
Unresolved Chondrichthyes
Macrodontacanthus
Genera in open nomenclature

A2.4.2 GENUS DATA – FIGURE 8.1

(Sub)stage	Genus richness					
	Fossil, named	Fossil, incl. open nomencl.	Lazarus, named	Total, named	Total, incl. open nomencl.	Boundary crossers
Rhaetian	16	18	6	22	24	12
Norian	13	19	7	20	26	15
Carnian	16	23	9	25	32	18
Ladinian	18	22	7	25	29	24
Anisian	22	27	3	25	30	20
Spathian	13	18	6	19	24	16
Smithian	13	17	7	20	24	17
Dienerian	6	7	13	19	20	19
Griesbachian	12	12	9	21	21	19
Changhsingian	11	14	10	21	24	16
Wuchiapingian	22	25	13	35	38	20
Capitanian	22	26	19	41	45	30
Wordian	31	37	17	48	54	39
Roadian	19	21	25	44	46	40
Kungurian	28	31	21	49	52	39
Artinskian	33	39	19	52	58	44
Sakmarian	19	24	28	47	52	44
Asselian	21	22	29	50	51	45

R^2	0.5872
R	0.7663
α(2)	0.05
n	18
df	16
critical *t*	2.120
t	4.771
t < critical *t*?	no, reject H_o: $R^2 = 0$
p-value	0.0002

A2.4.3 GENUS DATA PER ORDER – FIGURE 8.2 AND 8.3

Genus richness per order, including genera in open nomenclature.

(Sub)stage	Phoebodontiformes?	Xenacanthimorpha	Cladodontomorphi	Hybodontiformes	Neoselachii	Eugeneodontiformes (incl. Orodontiformes)	Petalodontiformes	Holocephali
Rhaetian	1	0	0	9	11	0	0	2
Norian	1	1	1	12	10	0	0	0
Carnian	1	3	0	16	11	0	0	1
Ladinian	0	3	0	13	11	0	0	1
Anisian	1	3	2	10	10	0	0	1
Spathian	0	2	2	10	6	0	0	1
Smithian	0	2	0	9	5	5	0	1
Dienerian	0	2	0	8	5	3	0	1
Griesbachian	0	2	0	8	5	4	0	1
Changhsingian	0	2	0	6	5	5	1	2
Wuchiapingian	0	3	2	6	4	9	4	5
Capitanian	0	3	6	5	6	7	4	7
Wordian	0	4	7	9	6	7	5	7
Roadian	0	5	8	7	5	6	4	6
Kungurian	0	7	11	7	4	8	4	9
Artinskian	1	7	10	8	4	11	6	6
Sakmarian	0	7	10	7	4	10	4	5
Asselian	0	8	9	6	3	8	7	6

A2.4.4 SPEARMAN RHO DATA – TABLE 8.1 AND 8.2
See A2.3.5 for interval duration ranking data.

(Sub)stage	Fossil, named genus richness	Rank	Fossil genus richness (incl. open nomenclature)	Rank	Lazarus, named genus richness	Rank	Range-through, named genus richness	Rank	Range-through genus richness (incl. open nomenclature)	Rank	EMSD	Rank
Rhaetian	16	11.5	18	13.5	6	16.5	22	12	24	14.5	13.5	18
Norian	13	14	19	12	7	14	20	15.5	26	12	16.5	17
Carnian	16	11.5	23	8	9	11.5	25	10	32	9	21	10
Ladinian	18	10	22	9.5	7	14	25	10	29	11	22	9
Anisian	22	5	27	4	3	18	25	10	30	10	18.5	12
Spathian	13	14	18	13.5	6	16.5	19	17.5	24	14.5	17	16
Smithian	13	14	17	15	7	14	20	15.5	24	14.5	18	13.5
Dienerian	6	18	7	18	13	8.5	19	17.5	20	18	19	11
Griesbachian	12	16	12	17	9	11.5	21	13.5	21	17	17.5	15
Changhsingian	11	17	14	16	10	10	21	13.5	24	14.5	18	13.5
Wuchiapingian	22	5	25	6	13	8.5	35	8	39	8	25	8
Capitanian	22	5	26	5	19	5.5	41	7	45	7	34.5	7
Wordian	31	2	37	2	17	7	48	4	54	2	39.5	5.5
Roadian	19	8.5	21	11	25	3	44	6	46	6	39.5	5.5
Kungurian	28	3	31	3	21	4	49	3	52	3.5	41	4
Artinskian	33	1	39	1	19	5.5	52	1	58	1	43.5	3
Sakmarian	19	8.5	24	7	28	2	47	5	52	3.5	44.5	2
Asselian	21	7	22	9.5	29	1	50	2	51	5	47	1

A2.4.5 CHI-TEST DATA – FIGURE 8.4

Taxonomic structure

Taxonomic group	Actual frequencies			Expected frequencies		χ^2 elements	
	extinct	survived	total	extinct	survived	extinct	survived
Xenacanthimorpha	0	3	**3**	0.771	2.229	0.771	0.267
Cladodontomorphi	4	2	**6**	1.543	4.457	3.913	1.355
Hybodontiformes	0	4	**4**	1.029	2.971	1.029	0.356
Neoselachii	1	3	**4**	1.029	2.971	0.001	0.000
Eugeneodontiformes	2	5	**7**	1.800	5.200	0.022	0.008
Petalodontiformes	0	4	**4**	1.029	2.971	1.029	0.356
Holocephali	2	5	**7**	1.800	5.200	0.022	0.008
total	**9**	**26**	**35**		**df**	χ^2	***p***
Capitanian/Wuchiapingian					**6**	**9.136**	**0.17**
Xenacanthimorpha	1	2	**3**	1.258	1.742	0.053	0.038
Cladodontomorphi	2	0	**2**	0.839	1.161	1.608	1.161
Hybodontiformes	0	5	**5**	2.097	2.903	2.097	1.514
Neoselachii	0	4	**4**	1.677	2.323	1.677	1.211
Eugeneodontiformes	4	4	**8**	3.355	4.645	0.124	0.090
Petalodontiformes	3	1	**4**	1.677	2.323	1.043	0.753
Holocephali	3	2	**5**	2.097	2.903	0.389	0.281
total	**13**	**18**	**31**		**df**	χ^2	***p***
Wuchiapingian/Changhsingian					**6**	**12.040**	**0.06**
Xenacanthimorpha	0	2	**2**	0.421	1.579	0.421	0.112
Hybodontiformes	1	5	**6**	1.263	4.737	0.055	0.015
Neoselachii	0	4	**4**	0.842	3.158	0.842	0.225
Eugeneodontiformes	1	3	**4**	0.842	3.158	0.030	0.008
Petalodontiformes	1	0	**1**	0.211	0.789	2.961	0.789
Holocephali	1	1	**2**	0.421	1.579	0.796	0.212
total	**4**	**15**	**19**		**df**	χ^2	***p***
Changhsingian/Griesbachian					**5**	**6.465**	**0.26**
Xenacanthimorpha	0	2	**2**	0.316	1.684	0.316	0.059
Hybodontiformes	0	8	**8**	1.263	6.737	1.263	0.237
Neoselachii	0	5	**5**	0.789	4.211	0.789	0.148
Eugeneodontiformes	3	0	**3**	0.474	2.526	13.474	2.526
Holocephali	0	1	**1**	0.158	0.842	0.158	0.030
total	**3**	**16**	**19**		**df**	χ^2	***p***
Smithian/Spathian					**4**	**19**	**0.0008**

A2.4.6 STANDING DIVERSITY MATRIX (STARTS NEXT PAGE)

Entries are provided in batches of two pages, providing data on the type of presence of genera in each time interval. Abbreviations indicate: ‘F’ first occurrence; ‘L’ last occurrence; ‘t’ top interval boundary crossed; ‘b’ bottom interval boundary crossed; ‘or’ origination associated with boundary; ‘ex’ extinction associated with boundary. Lazarus occurrences are marked by darker shaded boxes. Occurrences at epoch level are not included (set at ‘0’).

	Standing genus diversity	Carboniferous	Bound.	Cisuralian								Bound.	Guadalupian						Bound.	Lopingian				Bound.
				Asselian	Bound.	Sakmarian	Bound.	Artinskian	Bound.	Kungurian			Roadian	Bound.	Wordian	Bound.	Capitanian			Wuchiapingian	Bound.	Changxingian		
Phoebodontiformes?	No named genera																							
Bransonelliformes	*Barbclabornia*	1		bt		bt		bt		bL		ex												
	Bransonella	1		bt		bL	ex																	
Xenacanthiformes	*Dicentrodus*	1		bt		bt		bt		bt			bt		bL	ex								
	Lebachacanthus	1		bt		bt		bt		bL		ex												
	Orthacanthus	1		bt		bt		bt		bt			bt		bt		bt			bt		bt		
	Xenacanthus	1		bt		bt		bt		bt			bt		bt		bt			bt		bt		
	Triodus	1		bt		bt		bt		bt			bt		bt		bt			bL	ex		0	
	Plicatodus	1		bL	ex																			
	Wurdigneria							Ft	or	bt			bL	ex				0						
	Mooreodontus																							
Symmoriiformes	*Stethacanthus*	1		bt		bt		bt		bt			bt		bt		bL		ex					
	"Physonemus" / Batacanthus												Ft	or	bL	ex								
	Stethacanthulus	1		bt		bt		bt		bt			bt		bt		bt			bL	ex			
Ctenacanthiformes	*Ctenacanthus*	1		bt		bt		bt		bt			bt		bt		bL	0	ex					
	Glikmanius	1		bt		bt		bt		bt	0		bt		bt		bL	0	ex					
	"Cladodus"	1		bt		bt		bt		bt	0		bt		bt		bt			bL	ex		0	
	Heslerodus	1		bt		bt		bt		bL		ex												
	Saivodus	1		bt		bt		bt		bL		ex												
	Neosaivodus									FL														
	Kaibabvenator									FL														
	Nanoskalme									FL	0													
	Acondylacanthus	1		bt		bt		bt		bt			bt		bt		bL		ex					
Unresolved Cladodontomorphi	*"Cobelodus"*	1		bt		bt		bL	ex															
	Pyknothylacanthus																							

	Standing genus diversity	Lower Triassic								Bound.	Middle				Bound.	Upper Triassic						Bound.	Jurassic
		Griesbachian	Bound.	Dienerian	Bound.	Smithian	Bound.	Spathian			Anisian	Bound.	Ladinian			Carnian	Bound.	Norian	Bound.	Rhaetian			
Phoebodontiformes?	No named genera																						
Bransonelliformes	*Barbclabornia*																						
	Bransonella																						
Xenacanthiformes	*Dicentrodus*																						
	Lebachacanthus																						
	Orthacanthus	bt		bt		bt		bt			bt		bt			bL	ex				0		
	Xenacanthus	bt		bt		bt		bt	0		bt		bt			bL	ex						
	Triodus																						
	Plicatodus																						
	Wurdigneria																						
	Mooreodontus										Ft	or	bt			bt		bL	ex				
Symmoriiformes	*Stethacanthus*																						
	"Physonemus" / Batacanthus																						
	Stethacanthulus																						
Ctenacanthiformes	*Ctenacanthus*																						
	Glikmanius																						
	"Cladodus"																						
	Heslerodus																						
	Saivodus																						
	Neosaivodus																						
	Kaibabvenator																						
	Nanoskalme																						
	Acondylacanthus																						
Unresolved Cladodontomorphi	*"Cobelodus"*																						
	Pyknothylacanthus							Ft		or	bL	ex			0								

Unresolved Elasmobranchii	*Adamantina*	1		bt		bt		bt		bt			bt		bt		bt			bL	ex					
	New Genus (Jalodontidae)												Ft	or	bt		bL		ex							
	Isacrodus												FL													
	Texasodus														Ft	or	bL		ex							
	Dwykaselachus							FL																		
Hybodontiformes	*Donguzodus*																									
	Hybodus																									
	"Hybodus"			Ft	or	bt		bt		bt	0		bL	ex												
	'Polyacrodus'	1		bt		bt		bt		bt			bt		bt		bt			bt		bt				
	Acrodus (tentative in Palaeozoic)	1		bt		bt		bt		bt	0		bt		bt		bt			bt		bt				
	Asteracanthus																			Ft	or	bt				
	Palaeobates																					Ft		or		
	Lissodus																									
	Lonchidion																									
	Diplolonchidion																									
	Parvodus																									
	Gansuselache																								0	
	Steinbachodus																									
	'Palaeozoic Genus 1'	1		bt		bt		bt		bt	0		bt		bL	ex										
	'Lissodus'	1		bt		bt		bt		bt	0		bt		bt		bt	0		bt		bL			ex	
	Homalodontus																									
	Omanoselache														Ft	or	bt			bt		bt				
	Reesodus														FL											
	Teresodus														FL											
	Gunnellodus	1		bt		bt		bt		bt			bt		bL	ex										
	Reticulodus																									
Unresolved Euselachii	*Protacrodus*	1		bt		bt		bt		bt			bt		bt		bt			bt		bt				
	Sphenacanthus	1		bt		bt		bL	ex																	
	Wodnika												Ft	or	bt		bt	0		bt		bL		0	ex	
	Xenosynechodus														Ft	or	bt			bL	ex					

Unresolved Elasmobranchii	*Adamantina*																							
	New Genus (Jalodontidae)																							
	Isacrodus																							
	Texasodus																							
	Dwykaselachus																							
Hybodontiformes	*Donguzodus*													0										
	Hybodus	Ft	or	bt		bt		bt	0		bt		bt	0		bt		bt		bt	0		1	
	"Hybodus"																							
	'Polyacrodus'	bt		bt		bt		bt			bt		bt			bt		bt		bt	0		1	
	Acrodus (tentative in Palaeozoic)	bt		bt		bt		bt	0		bt		bt	0		bt		bt		bt	0		1	
	Asteracanthus	bt		bt		bt		bt			bt		bt	0		bt		bt		bt			1	
	Palaeobates	bt		bt		bt		bt			bt		bt	0		bt		bt		bL	0	ex		
	Lissodus	Ft	or	bt		bt		bt	0		bt		bt	0		bt		bt		bt	0		1	
	Lonchidion												Ft		or	bt		bt		bt			1	
	Diplolonchidion															FL								
	Parvodus										Ft	or	bt			bt		bt		bt			1	
	Gansuselache																							
	Steinbachodus												Ft		or	bt		bt		bt			1	
	'Palaeozoic Genus 1'																							
	'Lissodus'																							
	Homalodontus	Ft	or	bt		bt		bL		ex														
	Omanoselache	bt		bt		bt		bt			bt		bt			bL	ex							
	Reesodus																							
	Teresodus																							
	Gunnellodus																							
	Reticulodus																	FL						
Unresolved Euselachii	*Protacrodus*	bt		bt		bt		bt			bL	ex												
	Sphenacanthus																							
	Wodnika																							
	Xenosynechodus																							

	Khuffia														FL												
	Acronemus																										
Synechodontiformes	Genus S																					Ft	or	bt			
	Synechodus ('pre-Jurassic')					Ft	or	bt		bt			bt		bt		bt					bt		bt			
	Palidiplospinax																										
	Nemacanthus														Ft	or	bt					bt		bt			
	Genus P																										
	Rhomphaiodon																										
	Grozonodon																										
	Mucrovenator																										
Unresolved Neoselachii	*Cooleyella*	1		bt		bt		bt		bt			bt		bt		bL		ex								
	Pseudodalatias																										
	Hopleacanthus												FL														
	Huenichthys																										
	Reifia																										
	Vallisia																										
	Doratodus																										
	Raineria																										
	Duffinselache																										
	Rhomaleodus																										
	Pseudocetorhinus																										
	Lypbalkodus																										
	Amelacanthus	1		bt		bt		bt		bt			bt		bt		bt					bt		bt			
	Eunemacanthus	1		bt		bt		bt		bt			bt		bL	ex											
Galeomorphii	*Heterodontus*																										
	Orodus	1		bt		bt		bL	ex		0																
	Caseodus	1		bt		bt		bt		bt			bt		bt		bt					bt		bt			
	Fadenia	1		bt		bt		bt		bt			bt		bt		bt					bt		bt	0		
	Erikodus																					FL					
	Uralodus							FL																			
	Bobbodus	1		bt		bt		bt		bt			bt		bt		bt					bL	ex				

	Khuffia																						
	Acronemus										Ft	or	bL		ex								
Synechodontiformes	Genus S	bt		bt		bt		bt			bL	ex											
	Synechodus ('pre-Jurassic')	bt		bt		bt		bt			bt		bt			bt		bt			bL		ex	
	Palidiplospinax										Ft	or	bt			bt		bt			bt			1
	Nemacanthus	bt		bt		bt		bt			bt		bt			bt		bt			bL	0	ex	
	Genus P	Ft	or	bt		bt		bt			bL	ex												
	Rhomphaiodon												Ft		or	bt		bt			bL	0	ex	
	Grozonodon																	FL						
	Mucrovenator										Ft	or	bt			bt		bL	ex					
Unresolved Neoselachii	*Cooleyella*																							
	Pseudodalatias												Ft		or	bt		bt			bL	0	ex	
	Hopleacanthus																							
	Huenichthys																				FL			
	Reifia										Ft	or	bt			bL	ex							
	Vallisia																				FL			
	Doratodus										Ft	or	bt			bL	ex							
	Raineria																				FL			
	Duffinselache																				FL			
	Rhomaleodus										Ft	or	bt			bt		bL	ex					
	Pseudocetorhinus																				FL			
	Lypbalkodus							Ft	0	or	bL	ex		0										
	Amelacanthus	bt		bt		bt		bL		ex														
	Eunemacanthus																							
Galeomorphii	*Heterodontus*												Ft		or	bt		bt			bt			1
	Orodus																							
	Caseodus	bt		bt		bL	ex																	
	Fadenia	bt		bt		bL	ex																	
	Erikodus																							
	Uralodus																							
	Bobbodus																							

Eugeneodontiformes (+ Orodontiformes)	*Campodus*	1		bt		bt		bt		bL	0	ex													
	Tiaraju																	0							
	Agassizodus	1		bt		bt		bt		bt	0		bt		bt		bL		ex						
	Campyloprion	1		bL	ex																				
	Helicoprion							Ft	or	bt	0		bt		bt		bt			bL	ex		0		
	Parahelicoprion							Ft	or	bL		ex													
	Sarcoprion																			FL					
	Hunanohelicoprion																Ft	0	or	bt		bL		ex	
	Sinohelicoprion																						0		
	Shaktauites					FL																			
	Edestus	1		bt		bt		bt		bt			bt		bt		bL		ex						
	Syntomodus																						0		
	Helicampodus																			Ft	or	bt	0		
	Parahelicampodus																								
	Paredestus																								
Petalodontiformes	*Janassa*	1		bt		bt		bt		bt			bt		bt		bt	0		bt		bL	0	ex	
	Megactenopetalus	1		bt		bt		bt		bt	0		bt		bt		bt	0		bL	ex				
	Peripristis	1		bL	ex						0														
	Petalorhynchus	1		bt		bt		bt		bt			bt		bt		bt			bL	ex				
	Petalodus	1		bt		bt		bL	ex		0														
	Chomatodus	1		bL	ex						0														
	Itapyrodus							FL																	
	Permopetalodus							FL																	
	'Neopetalodus'									Ft		or	bt		bt		bt			bL	ex				
Unresolv. Euchondr.	*Desmiodus*	1		bt		bL	ex																		
Helodontiformes	*Helodus*	1		bt		bt		bt		bt			bt		bt		bt			bL	ex		0		
Cochliodontiformes	*Psephodus*	1		bt		bt		bt		bt			bt		bt		bt			bL	ex		0		
	Crassidonta									Ft	0	or	bt		bt		bL		ex						
	Deltodus	1		bt		bt		bt		bt	0		bt		bt		bL		ex						
	Helodopsis									Ft	0	or	bt		bt		bt			bL	ex		0		
	Poecilodus	1		bL	ex						0														
	Sandalodus	1		bt		bt		bt		bL		ex													

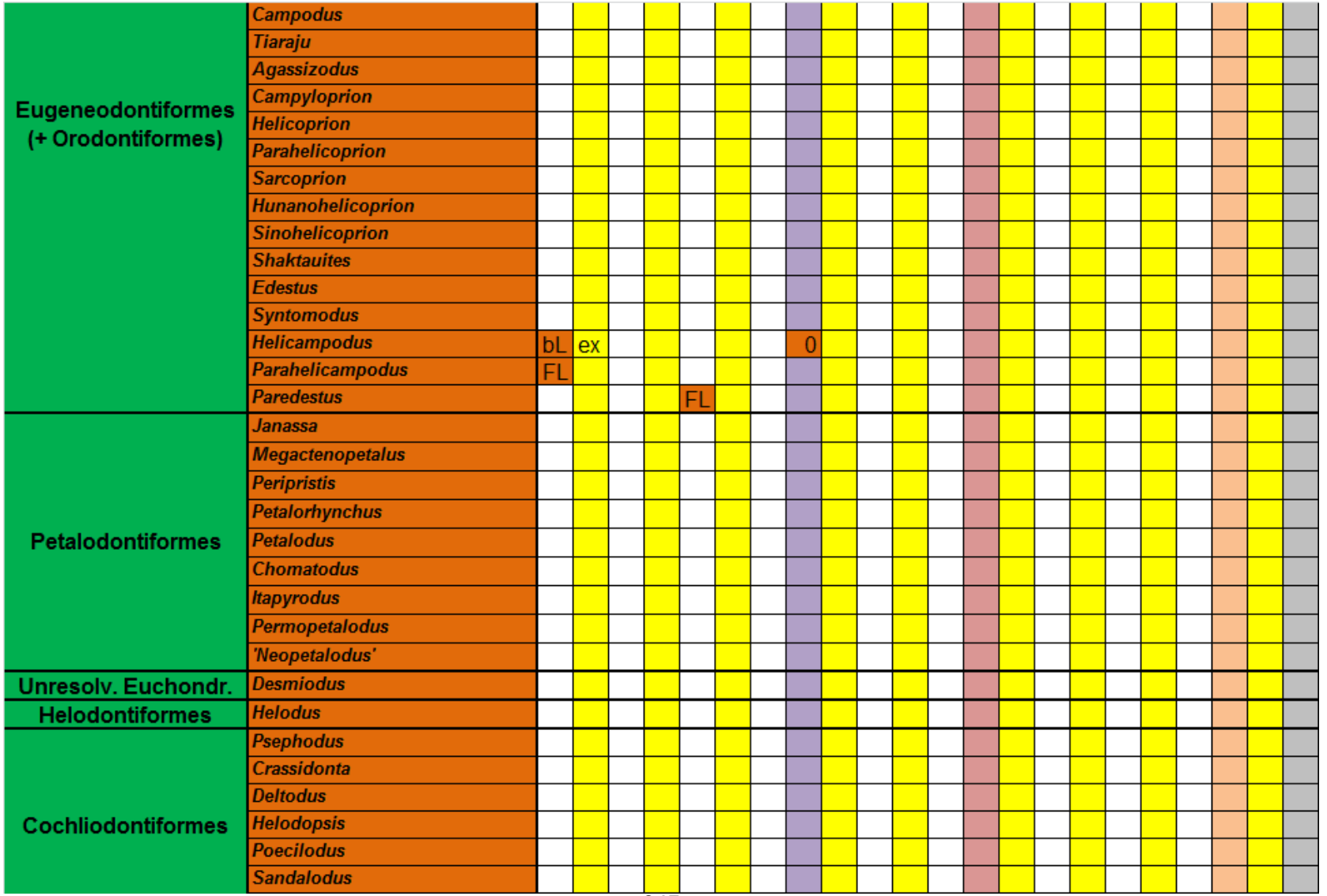
Eugeneodontiformes (+ Orodontiformes)
Campodus
Tiaraju
Agassizodus
Campyloprion
Helicoprion
Parahelicoprion
Sarcoprion
Hunanohelicoprion
Sinohelicoprion
Shaktauites
Edestus
Syntomodus
Helicampodus
Parahelicampodus
Paredestus
bL
ex
FL
0
FL
Petalodontiformes
Janassa
Megactenopetalus
Peripristis
Petalorhynchus
Petalodus
Chomatodus
Itapyrodus
Permopetalodus
'Neopetalodus'
Unresolv. Euchondr.
Desmiodus
Helodontiformes
Helodus
Cochliodontiformes
Psephodus
Crassidonta
Deltodus
Helodopsis
Poecilodus
Sandalodus

	Solenodus	1		bt		bt		bt		bt			bt		bL	ex												
Menaspiformes + Chimaeriformes	*Menaspis*														Ft	or	bt	0		bt		bL		ex				
	Arctacanthus																Ft		or	bt		bt						
	Agkistracanthus																											
	Myriacanthus																											
Unresolv. Chondr.	*Macrodontacanthus*							FL																				

	Solenodus																											
Menaspiformes + Chimaeriformes	*Menaspis*																											
	Arctacanthus	bt		bt		bt		bt	0		bt		bt				bL	ex										
	Agkistracanthus																						Ft		or	1		
	Myriacanthus																						Ft		or	1		
Unresolv. Chondr.	*Macrodontacanthus*																											

A2.4.7 STANDING DIVERSITY, ORIGINATION AND EXTINCTION DATA – FIGURE 8.5

(Sub)stage	N(FL)	N(bL)	N(Ft)	N(bt)	N(TOT)	EMSD
Rhaetian	5	5	2	10	22	13.5
Norian	2	3	0	15	20	16.5
Carnian	1	6	0	18	25	21
Ladinian	0	1	5	19	25	22
Anisian	0	5	8	12	25	18.5
Spathian	0	2	2	15	19	17
Smithian	1	2	0	17	20	18
Dienerian	0	0	0	19	19	19
Griesbachian	1	1	4	15	21	17.5
Changhsingian	0	5	1	15	21	18
Wuchiapingian	2	13	3	17	35	25
Capitanian	0	11	2	28	41	34.5
Wordian	3	6	5	34	48	39.5
Roadian	2	2	3	37	44	39.5
Kungurian	3	7	3	36	49	41
Artinskian	5	4	3	40	52	43.5
Sakmarian	1	2	1	43	47	44.5
Asselian	0	5	1	44	50	47

(Sub)stage	P(O)	P(E)	P(D)	P(T)	VV(O)	VV(E)	p	q
Rhaetian	0.04	0.06	-0.02	0.11	0.02	0.05	0.03	0.06
Norian	0.01	0.01	-0.01	0.02	0.00	0.01	0.00	0.01
Carnian	0.01	0.04	-0.03	0.05	0.00	0.04	0.00	0.04
Ladinian	0.04	0.01	0.03	0.04	0.04	0.01	0.04	0.01
Anisian	0.05	0.03	0.02	0.08	0.07	0.04	0.08	0.05
Spathian	0.03	0.03	0.00	0.06	0.04	0.04	0.04	0.04
Smithian	0.07	0.21	-0.14	0.29	0.00	0.16	0.00	0.16
Dienerian	0.00	0.00	0.00	0.00	0.00	0.00	0.00	0.00
Griesbachian	0.48	0.19	0.29	0.67	0.46	0.11	0.47	0.13
Changhsingian	0.02	0.12	-0.10	0.14	0.03	0.14	0.03	0.14
Wuchiapingian	0.03	0.08	-0.05	0.10	0.02	0.09	0.03	0.10
Capitanian	0.01	0.05	-0.04	0.06	0.01	0.06	0.01	0.06
Wordian	0.05	0.05	-0.01	0.10	0.03	0.04	0.04	0.04
Roadian	0.03	0.03	0.01	0.06	0.02	0.01	0.02	0.02
Kungurian	0.02	0.03	-0.01	0.05	0.01	0.02	0.01	0.03
Artinskian	0.01	0.02	0.00	0.03	0.01	0.01	0.01	0.01
Sakmarian	0.01	0.01	-0.00	0.02	0.00	0.01	0.00	0.01
Asselian	0.01	0.03	-0.02	0.04	0.01	0.03	0.01	0.03

A2.4.8 STANDING DIVERSITY PER ORDER – FIGURE 8.6 AND 8.7

(Sub)stage	Phoebodontiformes?	Xenacanthimorpha	Cladodontomorphi	Hybodontiformes	Neoselachii	Eugeneodontiformes (incl. Orodontiformes)	Petalodontiformes	Holocephali
Rhaetian	0	0	0	8.5	4	0	0	1
Norian	0	0.5	0	9	7	0	0	0
Carnian	0	2	0	9.5	9	0	0	0.5
Ladinian	0	3	0	9	8.5	0	0	1
Anisian	0	2.5	0.5	7.5	6	0	0	1
Spathian	0	2	0.5	7.5	5	0	0	1
Smithian	0	2	0	8	5	1	0	1
Dienerian	0	2	0	8	5	2	0	1
Griesbachian	0	2	0	6.5	4.5	2.5	0	1
Changhsingian	0	2	0	5	4	3.5	0.5	1.5
Wuchiapingian	0	2.5	1	4.5	3.5	4.5	2.5	3.5
Capitanian	0	3	4	4	3.5	5.5	4	5.5
Wordian	0	3.5	6.5	4.5	4	6	4	6
Roadian	0	4.5	6.5	5.5	4	6	4	6
Kungurian	0	6	7	6	4	7	3.5	5.5
Artinskian	0	6.5	8.5	6	4	7.5	3.5	5
Sakmarian	0	6.5	9	6	3.5	7	4	5
Asselian	0	7.5	9	5.5	3	7.5	5	5.5

A2.4.9 ORIGINATION AND EXTINCTION PER ORDER – FIGURE 8.8

(Sub)stage	Phoebodontiformes?		Xenacanthimorpha		Cladodontomorphi		Hybodontiformes		Neoselachii		Eugeneodontiformes (incl. Orodontiformes)		Petalodontiformes		Holocephali	
	P(O)	P(E)	P(O)	P(E)	P(O)	P(E)	P(O)	P(E)	P(O)	P(E)	P(O)	P(E)	P(O)	P(E)	P(O)	P(E)
Rhaetian	-	-	-	-	-	-	0.00	0.02	0.06	0.11	-	-	-	-	0.14	0.00
Norian	-	-	0.00	0.05	-	-	0.01	0.01	0.01	0.02	-	-	-	-	-	-
Carnian	-	-	0.00	0.10	-	-	0.01	0.03	0.00	0.03	-	-	-	-	0.00	0.14
Ladinian	-	-	0.00	0.00	-	-	0.04	0.00	0.05	0.00	-	-	-	-	0.00	0.00
Anisian	-	-	0.05	0.00	0.00	0.15	0.02	0.00	0.08	0.05	-	-	-	-	0.00	0.00
Spathian	-	-	0.00	0.00	0.30	0.00	0.00	0.04	0.05	0.05	-	-	-	-	0.00	0.00
Smithian	-	-	0.00	0.00	-	-	0.00	0.00	0.00	0.00	0.48	1.43	-	-	0.00	0.00
Dienerian	-	-	0.00	0.00	-	-	0.00	0.00	0.00	0.00	0.00	0.00	-	-	0.00	0.00
Griesbachian	-	-	0.00	0.00	-	-	0.75	0.00	0.40	0.00	0.50	1.00	-	-	0.00	0.00
Changhsingian	-	-	0.00	0.00	-	-	0.08	0.08	0.00	0.00	0.00	0.13	0.00	0.50	0.00	0.25
Wuchiapingian	-	-	0.00	0.06	0.00	0.18	0.04	0.00	0.04	0.00	0.07	0.09	0.00	0.13	0.00	0.11
Capitanian	-	-	0.00	0.00	0.00	0.13	0.00	0.00	0.00	0.05	0.03	0.05	0.00	0.00	0.03	0.05
Wordian	-	-	0.00	0.07	0.00	0.04	0.10	0.14	0.05	0.05	0.00	0.00	0.00	0.00	0.04	0.04
Roadian	-	-	0.00	0.06	0.04	0.00	0.00	0.05	0.06	0.06	0.00	0.00	0.00	0.00	0.00	0.00
Kungurian	-	-	0.00	0.04	0.04	0.06	0.00	0.00	0.00	0.00	0.00	0.04	0.04	0.00	0.04	0.02
Artinskian	-	-	0.01	0.00	0.00	0.01	0.00	0.00	0.00	0.00	0.03	0.02	0.03	0.05	0.00	0.00
Sakmarian	-	-	0.00	0.03	0.00	0.00	0.00	0.00	0.05	0.00	0.02	0.02	0.00	0.00	0.00	0.00
Asselian	-	-	0.00	0.04	0.00	0.00	0.05	0.00	0.00	0.00	0.00	0.04	0.00	0.10	0.00	0.05

A2.4.10 LIFE-HISTORY TRAIT ASSIGNMENTS

Genus	**Salinity**	**Feeding habit**	**Reference**	**Ecomorpho-type**	**Reference**
Phoebodontiformes (no named genera)	marine/freshwater	clutching/grasping/piercing	Ginter *et al.* 2002, 2010	Bathic	Ginter *et al.* 2002
Barbclabornia	freshwater	microphagous (clutching/grasping/piercing)	Zidek *et al.* 2004 (non clutching/grasping/piercing, Johnson 2003)	Freshwater	Johnson 2003; Zidek *et al.* 2004
Bransonella	marine (/brackish)	crushing	Schneider 1996	Littoral (marine)	Johnson & Thayer 2009
Dicentrodus	marine/freshwater	N/A		Freshwater	Zidek *et al.* 2004
Lebachacanthus	freshwater	cutting	almost indistinguishable from Orthacanthus (Ginter *et al.* 2010)	Freshwater	~Compagno 1990
Orthacanthus	freshwater (/brackish)	cutting	Schneider 1996; Johnson 1999, 2003	Freshwater	~Compagno 1990
Xenacanthus	freshwater (/brackish)	cutting	Schneider 1996	Freshwater	~Compagno 1990
Triodus	freshwater (/brackish)	clutching/grasping/piercing	Schneider 1996	Freshwater	Compagno 1990
Plicatodus	freshwater	clutching/grasping/piercing	Schneider 1996	Freshwater	~Compagno 1990
Wurdigneria	freshwater (/brackish)	cutting	Richter 2005	Freshwater	Richter 2005
Mooreodontus	freshwater	clutching/grasping/piercing	Schneider 1996	Freshwater	~Compagno 1990
Stethacanthus	marine	clutching/grasping/piercing	Ginter *et al.* 2002	Pelagic	Ginter *et al.* 2002
"Physonemus" / *Batacanthus*	marine	N/A		Pelagic	Ginter *et al.* 2002; Brett and Walker 2002
Stethacanthulus	marine	clutching/grasping/piercing	~Williams 2001; Brett and Walker 2002	Pelagic / Bathic	Williams 2001; Ginter *et al.* 2002; Brett and Walker 2002
Ctenacanthus	marine/freshwater	clutching/grasping/piercing	~Williams 2001; Brett and Walker 2002; Ginter *et al.* 2002	Littoral (marine)	~Williams 2001
Glikmanius	marine	clutching/grasping/piercing	Hodnett *et al.* 2012; ~Williams 2001; Brett and	Littoral (marine)	Hodnett *et al.* 2012; ~Williams 2001

			Walker 2002; Ginter *et al.* 2002		
"Cladodus"	marine	clutching/grasping/piercing & cutting	Hodnett *et al.* 2012; ~Williams 2001; Brett and Walker 2002; Ginter *et al.* 2002	Pelagic	~Brett and Walker 2002; Ginter *et al.* 2002
Heslerodus	marine	clutching/grasping/piercing	Hodnett *et al.* 2012; ~Williams 2001; Brett and Walker 2002; Ginter *et al.* 2002	Littoral (marine)	Hodnett *et al.* 2012; ~Brett and Walker 2002; Ginter *et al.* 2002
Saivodus	marine	clutching/grasping/piercing	~Williams 2001; Brett and Walker 2002; Ginter *et al.* 2002, 2010	Pelagic	~Brett and Walker 2002; Ginter *et al.* 2002, 2010
Neosaivodus	marine	clutching/grasping/piercing	Hodnett *et al.* 2012	Littoral (marine)	Hodnett *et al.* 2012
Kaibabvenator	marine	cutting	Hodnett *et al.* 2012	Pelagic	Hodnett *et al.* 2012
Nanoskalme	marine	clutching/grasping/piercing & cutting	Hodnett *et al.* 2012	Littoral (marine)	Hodnett *et al.* 2012
Acondylacanthus	marine	N/A		Littoral (marine)	~Williams 2001
"Cobelodus"	marine	clutching/grasping/piercing	~Williams 2001; Brett and Walker 2002; Ginter *et al.* 2002, 2010	Pelagic	Compagno 1990
Pyknothylacanthus	marine	N/A		Littoral (marine)	~Williams 2001
Adamantina	marine	crushing	~Schneider 1996	Littoral (marine)	~Bendix-Almgreen 1993
New Genus (Jalodontidae)	marine	?		?	
Isacrodus	marine	crushing		Littoral (marine)	
Texasodus	marine	crushing		Littoral (marine)	
Dwykaselachus	marine	?		?	Murray 2000
Donguzodus	marine	grinding	Minikh 2001 (close to *Acrodus*)	Benthic	
Hybodus	marine/freshwater	clutching, tearing, crushing	Cappetta 1987; Cuny and	Littoral (marine)	Compagno 1990

			Benton 1999; Brett and Walker 2002; Ginter *et al.* 2010		
"Hybodus"	marine/freshwater	? various, crushing?		Littoral (marine)	
'Polyacrodus'	marine/freshwater	crushing, clutching	Ginter *et al.* 2010	Littoral (marine)	
Acrodus	marine/freshwater	grinding (crushing)	Cappetta 1987; Cuny and Benton 1999	Benthic	~Cappetta 1987
Asteracanthus	marine	clutching, grinding	Cappetta 1987; Rees 2008 (crushing)	Benthic	
Palaeobates	marine	grinding	Cappetta 1987; Cuny and Benton 1999	Benthic	
Lissodus	marine/freshwater	crushing, clutching	Cappetta 1987; Ginter *et al.* 2002; Rees and Underwood 2002	Benthic	Cappetta 1987; Ginter *et al.* 2002
Lonchidion	freshwater	cutting, crushing	Rees and Underwood 2002	Freshwater	~Fischer 2008
Diplolonchidion	freshwater	? crushing		Freshwater	~Milner et al. 2006
Parvodus	marine	cutting, crushing	Rees and Underwood 2002	Littoral (marine)	Rees and Underwood 2008
Gansuselache	?	crushing	~Wang *et al.* 2009	Freshwater	?
Steinbachodus	freshwater (/brackish)	crushing	Reif 1980	Benthic	
'Palaeoz. Genus 1'	marine/freshwater	crushing		Benthic	
'Lissodus'	marine/freshwater	crushing		Benthic	
Homalodontus	marine	clutching, grinding	~Mutter *et al.* 2007	Benthic	~Mutter *et al.* 2007
Omanoselache	marine	crushing		Benthic	
Reesodus	marine	crushing		Benthic	
Teresodus	marine	crushing		Benthic	
Gunnellodus	marine	?		?	
Reticulodus	freshwater	grinding	~Irmis 2005; Cappetta 2012	Freshwater	~Irmis 2005; Milner *et al.* 2006
Protacrodus	marine	crushing	Ginter *et al.* 2002, 2010	Benthic	~Ginter *et al.* 2002
Sphenacanthus	freshwater (/brackish)	crushing	Ginter *et al.* 2010	Freshwater	
Wodnika	marine/freshwater	crushing	~Maisey 1982; Cappetta	Benthic	~Compagno 1990;

			1987		Diedrich *et al.* 2009b
Xenosynechodus	?	?		?	
Khuffia	marine	clutching/grasping/piercing		Littoral (marine)	
Acronemus	marine	clutching, crushing	Liszkowski 1993	Littoral (marine)	Liszkowski 1993
Genus S	marine	clutching, cutting		Pelagic	
Synechodus ('pre-Jurassic')	marine	clutching, crushing(/grinding)	Liszkowski 1993; Johns *et al.* 1997; Duffin 1998b	Littoral (marine)	~Compagno 1990; Ginter *et al.* 2010
Palidiplospinax	marine	clutching, crushing	~Liszkowski 1993	Littoral (marine)	~Compagno 1990; Ginter *et al.* 2010
Nemacanthus	marine	N/A		*?*	
Genus P	marine	clutching, crushing		Pelagic	
Rhomphaiodon	marine (/brackish)	clutching	Cuny and Benton 1999	Littoral (marine)	
Grozonodon	?	clutching	~Cuny and Benton 1999	Littoral (marine)	
Mucrovenator	marine	clutching	Cuny *et al.* 2001	Littoral (marine)	Cuny *et al.* 2001
Cooleyella	marine	clutching/grasping/piercing, crushing	~Compagno 1990	Benthic	Duffin and Ward 1983; ~Duffin 1985; Compagno 1990
Pseudodalatias	marine	clutching/cutting	Cappetta 1987	Bathic	
Hopleacanthus	marine	clutching	~Ginter *et al.* 2010	Littoral (marine)	
Huenichthys	marine (/brackish)	clutching	~Cuny and Benton 1999	Littoral (marine)	
Reifia	marine	clutching, crushing	Cappetta 1987	Littoral (marine)	
Vallisia	marine (/brackish)	clutching	Cuny and Benton 1999	Littoral (marine)	
Doratodus	freshwater (/brackish)	clutching	Cuny and Benton 1999	Littoral (marine)	
Raineria	?	?	Same as *Pseudodalatias*? Cappetta 1987	*?*	
Duffinselache	marine	crushing		Littoral (marine)	
Rhomaleodus	?	clutching, crushing		Littoral (marine)	
Pseudocetorhinus	marine (/brackish)	microphagous	Compagno 1990	Pelagic	Compagno 1990
Lypbalkodus	marine	clutching/cutting	Minikh 2001; close to *Pseudodalatias*	Bathic	
Amelacanthus	marine	?		?	
Eunemacanthus	marine	?		*?*	

Heterodontus	marine	crushing	Ginter *et al.* 2010	Benthic	Compagno 1990
Orodus	marine/freshwater	crushing	Hansen and Mapes 1990; Ginter *et al.* 2002	Pelagic	Compagno 1990
Caseodus	marine	grinding	~Compagno 1990	Pelagic	Compagno 1990
Fadenia	marine	crushing	~Compagno 1990	Pelagic	Compagno 1990
Erikodus	marine	crushing	~Compagno 1990	Pelagic	Compagno 1990
Uralodus	?	crushing	~Kozlov 2000	Pelagic	~Compagno 1990
Bobbodus	?	crushing, cutting	~Ginter *et al.* 2010	Pelagic	~Compagno 1990
Campodus	marine	grinding	~Ginter *et al.* 2010	Pelagic	~Compagno 1990
Tiaraju	freshwater	crushing, cutting	~Ginter *et al.* 2010	Pelagic	~Compagno 1990
Agassizodus	marine	grinding, cutting	Hansen and Mapes 1990; ~Ginter *et al.* 2010	Pelagic	~Compagno 1990
Campyloprion	?	cutting	~Ginter *et al.* 2010	Pelagic	~Compagno 1990
Helicoprion	marine	cutting, crushing	Ginter *et al.* 2010	Pelagic	Compagno 1990
Parahelicoprion	marine	cutting	~Ginter *et al.* 2010	Pelagic	~Compagno 1990
Sarcoprion	marine	cutting, crushing	Brett and Walker 2002; Ginter *et al.* 2010	Pelagic	~Compagno 1990
Hunanohelicoprion	?	cutting	~Lebedev 2009	Pelagic	~Compagno 1990
Sinohelicoprion	?	cutting	~Lebedev 2009	Pelagic	~Compagno 1990
Shaktauites	?	cutting	~Lebedev 2009	Pelagic	~Compagno 1990
Edestus	marine	cutting	~Ginter *et al.* 2010	Pelagic	Compagno 1990
Syntomodus	?	cutting	~Ginter *et al.* 2010	Pelagic	~Compagno 1990
Helicampodus	marine	cutting	~Ginter *et al.* 2010	Pelagic	~Compagno 1990
Parahelicampodus	marine	cutting	~Ginter *et al.* 2010	Pelagic	~Compagno 1990
Paredestus	marine	cutting	~Ginter *et al.* 2010	Pelagic	~Compagno 1990
Janassa	marine (/brackish)	crushing	Brett and Walker 2002; Ginter *et al.* 2010	Benthic	Compagno 1990
Megactenopetalus	marine (/brackish)	cutting	~Hansen and Mapes 1990	Benthic	Compagno 1990
Peripristis	freshwater (/brackish)	cutting	~Hansen and Mapes 1990	Benthic	Compagno 1990
Petalorhynchus	?	crushing	Brett and Walker 2002; Ginter *et al.* 2010	Benthic	Compagno 1990
Petalodus	marine/freshwater	cutting	Hansen and Mapes 1990	Benthic	Compagno 1990

Chomatodus	?	crushing	~Brett and Walker 2002	Benthic	Compagno 1990
Itapyrodus	marine/freshwater	crushing	Chahud *et al.* 2010	Benthic	Compagno 1990
Permopetalodus	?	cutting	~Kozlov 2000	Benthic	Compagno 1990
'Neopetalodus'	marine	cutting?		Benthic	Compagno 1990
Desmiodus	marine	crushing	~Ginter *et al.* 2010	Benthic	~Compagno 1990; Ginter *et al.* 2010
Helodus	marine/freshwater	crushing	Hansen and Mapes 1990; Brett and Walker 2002	Benthic	Compagno 1990
Psephodus	marine (/brackish)	crushing	Stahl 1999; Brett and Walker 2002	Benthic	~Compagno 1990
Crassidonta	marine	crushing	Stahl 1999; Brett and Walker 2002	Benthic	~Compagno 1990
Deltodus	marine	crushing	Hansen and Mapes 1990; Stahl 1999; Brett and Walker 2002	Benthic	~Compagno 1990
Helodopsis	marine	crushing	Stahl 1999; Brett and Walker 2002	Benthic	~Compagno 1990
Poecilodus	marine	crushing	Stahl 1999; Brett and Walker 2002	Benthic	~Compagno 1990
Sandalodus	marine	crushing	Stahl 1999; Brett and Walker 2002	Benthic	~Compagno 1990
Solenodus	marine	crushing	Stahl 1999; Brett and Walker 2002	Benthic	~Compagno 1990
Menaspis	marine	crushing	~Stahl 1999	Benthic	~Stahl 1999
Arctacanthus	marine	?		Benthic	Chen *et al.* 2007a
Agkistracanthus	marine	crushing	~Stahl 1999	Benthic	~Stahl 1999; Compagno 1990
Myriacanthus	marine/freshwater	crushing	~Stahl 1999	Benthic	~Stahl 1999; Compagno 1990
Macrodontacanthus	marine	N/A		?	

A2.4.11 SALINITY TOLERANCE DATA – FIGURE 8.9

(Sub)stage	Freshwater	Mixed/ euryhaline	Marine	Undetermined salinity
Rhaetian	2	5	14	1
Norian	4	4	10	2
Carnian	7	4	13	1
Ladinian	6	4	14	1
Anisian	4	4	16	1
Spathian	2	4	13	0
Smithian	2	4	14	0
Dienerian	2	4	13	0
Griesbachian	2	4	15	0
Changhsingian	2	4	14	1
Wuchiapingian	3	5	23	4
Capitanian	3	6	28	4
Wordian	3	8	34	3
Roadian	4	9	29	2
Kungurian	6	8	33	2
Artinskian	7	11	30	4
Sakmarian	6	10	28	3
Asselian	8	10	28	4

A2.4.12 CHI-TEST DATA – FIGURE 8.10

Salinity tolerance

Category	Actual frequencies			Expected frequencies		χ^2 elements	
	extinct	survived	total	extinct	survived	extinct	survived
freshwater	0	3	**3**	0.892	2.108	0.892	0.377
mixed/euryhaline	1	5	**6**	1.784	4.216	0.344	0.146
marine	10	18	**28**	8.324	19.676	0.337	0.143
total	**11**	**26**	**37**		**df**	χ^2	***p***
Capitanian/Wuchiapingian					**2**	**2.239**	**0.33**
freshwater	1	2	**3**	1.161	1.839	0.022	0.014
mixed/euryhaline	1	4	**5**	1.935	3.065	0.452	0.286
marine	10	13	**23**	8.903	14.097	0.135	0.085
total	**12**	**19**	**31**		**df**	χ^2	***p***
Wuchiapingian/Changhsingian					**2**	**0.995**	**0.61**
freshwater	0	2	**2**	0.400	1.600	0.400	0.100
mixed/euryhaline	2	2	**4**	0.800	3.200	1.800	0.450
marine	2	12	**14**	2.800	11.200	0.229	0.057
total	**4**	**16**	**20**		**df**	χ^2	***p***
Changhsingian/Griesbachian					**2**	**3.036**	**0.22**
freshwater	0	2	**2**	0.300	1.700	0.300	0.053
mixed/euryhaline	0	4	**4**	0.600	3.400	0.600	0.106
marine	3	11	**14**	2.100	11.900	0.386	0.068
total	**3**	**17**	**20**		**df**	χ^2	***p***
Smithian/Spathian					**2**	**1.513**	**0.47**

A2.4.13 GENERAL ECOMORPHOTYPE DATA – FIGURE 8.12

(Sub)stage	Freshwater	Pelagic	Littoral marine	Benthic	Bathic
Rhaetian	1	1	9	8	1
Norian	3	0	9	6	1
Carnian	5	0	10	8	1
Ladinian	4	0	11	8	1
Anisian	3	2	11	7	1
Spathian	2	2	4	8	1
Smithian	2	5	3	8	0
Dienerian	2	4	3	8	0
Griesbachian	2	6	3	8	0
Changhsingian	2	5	2	10	0
Wuchiapingian	3	10.5	3	15	0.5
Capitanian	3	9.5	7	17	0.5
Wordian	4	9.5	8	20	0.5
Roadian	5	9.5	9	16	0.5
Kungurian	7	12.5	10	16	0.5
Artinskian	8	14.5	8	16	0.5
Sakmarian	7	12.5	9	15	0.5
Asselian	8	12.5	8	18	0.5

A2.4.14 CHI-TEST DATA – FIGURE 8.13

General ecomorphotype

Category	Actual freq.			Expected freq.		χ^2 elements	
	extinct	survived	total	extinct	survived	extinct	survived
freshwater	0	3	**3**	0.811	2.189	0.811	0.300
pelagic	3	6.5	**9.5**	2.568	6.932	0.073	0.027
littoral marine	4	3	**7**	1.892	5.108	2.349	0.870
benthic	3	14	**17**	4.595	12.405	0.553	0.205
bathic	0	0.5	**0.5**	0.135	0.365	0.135	0.050
total	**10**	**27**	**37**		**df**	χ^2	***p***
Capitanian/Wuchiapingian					**4**	**5.374**	**0.25**
freshwater	1	2	**3**	1.313	1.688	0.074	0.058
pelagic	5.5	5	**10.5**	4.594	5.906	0.179	0.139
littoral marine	1	2	**3**	1.313	1.688	0.074	0.058
benthic	6	9	**15**	6.563	8.438	0.048	0.038
bathic	0.5	0	**0.5**	0.219	0.281	0.362	0.281
total	**14**	**18**	**32**		**df**	χ^2	***p***
Wuchiapingian/Changhsingian					**4**	**1.311**	**0.86**
freshwater	0	2	**2**	0.526	1.474	0.526	0.188
pelagic	1	4	**5**	1.316	3.684	0.076	0.027
littoral marine	0	2	**2**	0.526	1.474	0.526	0.188
benthic	4	6	**10**	2.632	7.368	0.712	0.254
total	**5**	**14**	**19**		**df**	χ^2	***p***
Changhsingian/Griesbachian					**3**	**2.497**	**0.48**
freshwater	0	2	**2**	0.333	1.667	0.333	0.067
pelagic	3	2	**5**	0.833	4.167	5.633	1.127
littoral marine	0	3	**3**	0.500	2.500	0.500	0.100
benthic	0	8	**8**	1.333	6.667	1.333	0.267
total	**3**	**15**	**18**		**df**	χ^2	***p***
Smithian/Spathian					**3**	**9.360**	**0.02**
	crossed	acquired	total	crossed	acquired	crossed	acquired
freshwater	2	0	**2**	1.765	0.235	0.031	0.235
pelagic	2	0	**2**	1.765	0.235	0.031	0.235
littoral marine	3	1	**4**	3.529	0.471	0.079	0.596
benthic	8	0	**8**	7.059	0.941	0.125	0.941
bathic	0	1	**1**	0.882	0.118	0.882	6.618
total	**15**	**2**	**17**		**df**	χ^2	***p***
Smithian/Spathian					**4**	**9.775**	**0.044**
freshwater	2	1	**3**	2.000	1.000	0.000	0.000
pelagic	2	0	**2**	1.333	0.667	0.333	0.667
littoral marine	4	7	**11**	7.333	3.667	1.515	3.030
benthic	7	0	**7**	4.667	2.333	1.167	2.333
bathic	1	0	**1**	0.667	0.333	0.167	0.333
total	**16**	**8**	**24**		**df**	χ^2	***p***
Spathian/Anisian					**4**	**9.545**	**0.049**

A2.4.15 FEEDING HABIT DATA – FIGURE 8.14

(Sub)stage	Crushing	Grinding	Micro-phagous	Clutching	Cutting	Cutting/ clutching	Tearing
Rhaetian	8.33	2.5	1	5.83	1	1	0.33
Norian	5.83	3.5	0	7.33	1	1	0.33
Carnian	8.33	2.5	0	7.83	3	1	0.33
Ladinian	7.83	2.5	0	8.33	3	1	0.33
Anisian	6.83	2.5	0	8.33	3	1	0.33
Spathian	4.33	3	0	3.83	2.5	1	0.33
Smithian	5.33	4	0	3.83	3.5	0	0.33
Dienerian	5.33	4	0	3.83	2.5	0	0.33
Griesbachian	5.33	4	0	3.83	4.5	0	0.33
Changhsingian	8	3.5	0	2	4.5	0	0
Wuchiapingian	15.5	2.5	0	4.5	8.5	0	0
Capitanian	17.5	2.5	0	7	8	0	0
Wordian	21.5	2.5	0	8	7	0	0
Roadian	18.5	2.5	0	8	8	0	0
Kungurian	17.5	3.5	1	10.5	11.5	0	0
Artinskian	19.5	3.5	1	10	11	0	0
Sakmarian	19	3.5	1	10	8.5	0	0
Asselian	20.5	3.5	1	10.5	9.5	0	0

A2.4.16 CHI-TEST DATA – FIGURE 8.15

Feeding habit

Category	Actual frequencies			Expected frequencies		χ^2 elements	
	extinct	survived	total	extinct	survived	extinct	survived
crushing	3.5	14	**17.5**	4.500	13.000	0.222	0.077
grinding	0.5	2	**2.5**	0.643	1.857	0.032	0.011
clutching	3.5	3.5	**7**	1.800	5.200	1.606	0.556
cutting	1.5	6.5	**8**	2.057	5.943	0.151	0.052
total	**9**	**26**	**35**		**df**	χ^2	***p***
Capitanian/Wuchiapingian					**3**	**2.706**	**0.44**
crushing	7.5	8	**15.5**	7.000	8.500	0.036	0.029
grinding	0	2.5	**2.5**	1.129	1.371	1.129	0.930
clutching	2.5	2	**4.5**	2.032	2.468	0.108	0.089
cutting	4	4.5	**8.5**	3.839	4.661	0.007	0.006
total	**14**	**17**	**31**		**df**	χ^2	***p***
Wuchiapingian/Changhsingian					**3**	**2.333**	**0.51**
crushing	4	4	**8**	2.222	5.778	1.422	0.547
grinding	0	3.5	**3.5**	0.972	2.528	0.972	0.374
clutching	0	2	**2**	0.556	1.444	0.556	0.214
cutting	1	3.5	**4.5**	1.250	3.250	0.050	0.019
total	**5**	**13**	**18**		**df**	χ^2	***p***
Changhsingian/Griesbachian					**3**	**4.154**	**0.25**
crushing	1	4.3	**5.3**	0.941	4.392	0.004	0.001
grinding	1	3	**4**	0.706	3.294	0.123	0.026
clutching	0	3.8	**3.8**	0.676	3.157	0.676	0.145
cutting	1	2.5	**3.5**	0.618	2.882	0.237	0.051
tearing	0	0.3	**0.3**	0.059	0.275	0.059	0.013
total	**3**	**14**	**17**		**df**	χ^2	***p***
Smithian/Spathian					**4**	**1.334**	**0.86**
crushing	4.3	2.5	**6.8**	4.348	2.485	0.000	0.000
grinding	2.5	0	**2.5**	1.591	0.909	0.519	0.909
clutching	3.3	5	**8.3**	5.303	3.030	0.732	1.280
cutting	2.5	0.5	**3**	1.909	1.091	0.183	0.320
cutting/clutching	1	0	**1**	0.636	0.364	0.208	0.364
tearing	0.3	0	**0.3**	0.212	0.121	0.069	0.121
total	**14**	**8**	**22**		**df**	χ^2	***p***
Spathian/Anisian					**5**	**4.706**	**0.45**

A2.4.17 DISTRIBUTION DATA PER ORDER – FIGURE 8.19–8.26

Phoebodonti-formes (Sub)stage	Boreal	E-Panthalassa	C-Pangaea	Palaeotethys	Neotethys	C/W-Panthalassa
Rhaetian	0	0	0	1	0	0
Norian	0	0	1	0	0	0
Carnian	0	0	1	0	0	0
Ladinian	0	0	0	0	0	0
Anisian	0	0	0	1	0	0
Spathian	0	0	0	0	0	0
Smithian	0	0	0	0	0	0
Dienerian	0	0	0	0	0	0
Griesbachian	0	0	0	0	0	0
Changhsingian	0	0	0	0	0	0
Wuchiapingian	0	0	0	0	0	0
Capitanian	0	0	0	0	0	0
Wordian	0	0	0	0	0	0
Roadian	0	0	0	0	0	0
Kungurian	0	0	0	0	0	0
Artinskian	0	0	1	0	0	0
Sakmarian	0	0	0	0	0	0
Asselian	0	0	0	0	0	0

Xenacanthi-morpha (Sub)stage	Boreal	E-Panthalassa	C-Pangaea	Palaeotethys	Neotethys	C/W-Panthalassa
Rhaetian	0	0	0	0	0	0
Norian	0	0	1	0	1	0
Carnian	0	0	2	1	1	0
Ladinian	0	0	0	1	0	0
Anisian	0	0	0	1	0	2
Spathian	0	0	0	0	0	0
Smithian	0	0	0	0	0	0
Dienerian	0	0	0	0	0	0
Griesbachian	0	0	0	0	0	0
Changhsingian	0	0	0	0	0	1
Wuchiapingian	0	0	0	0	0	0
Capitanian	0	0	0	0	0	0
Wordian	0	0	0	1	0	0
Roadian	0	0	0	0	0	0
Kungurian	0	0	5	0	0	0
Artinskian	0	0	4	1	2	0
Sakmarian	1	0	3	3	0	0
Asselian	0	0	5	5	0	0

Cladodonto-morphi (Sub)stage	Boreal	E-Panthalassa	C-Pangaea	Palaeotethys	Neotethys	C/W-Panthalassa
Rhaetian	0	0	0	0	0	0
Norian	0	0	0	0	0	1
Carnian	0	0	0	0	0	0
Ladinian	0	0	0	0	0	0
Anisian	0	0	0	0	0	1
Spathian	0	2	0	0	0	0
Smithian	0	0	0	0	0	0
Dienerian	0	0	0	0	0	0
Griesbachian	0	0	0	0	0	0
Changhsingian	0	0	0	0	0	0
Wuchiapingian	1	0	0	0	1	0
Capitanian	1	4	1	4	0	0
Wordian	1	5	2	4	2	0
Roadian	2	3	2	0	0	0
Kungurian	0	7	0	2	0	1
Artinskian	1	1	1	7	0	0
Sakmarian	0	0	1	3	1	0
Asselian	2	0	1	3	0	0

Hybodonti-formes (Sub)stage	Boreal	E-Panthalassa	C-Pangaea	Palaeotethys	Neotethys	C/W-Panthalassa
Rhaetian	0	0	1	4	0	0
Norian	0	2	5	3	2	0
Carnian	0	4	4	8	2	5
Ladinian	1	3	0	9	0	5
Anisian	0	5	0	5	2	8
Spathian	5	5	1	0	3	5
Smithian	2	3	0	0	1	4
Dienerian	4	0	0	0	0	4
Griesbachian	4	0	0	0	2	3
Changhsingian	1	0	0	1	2	2
Wuchiapingian	0	0	1	1	3	0
Capitanian	1	0	1	0	0	0
Wordian	1	0	0	1	5	1
Roadian	1	1	1	0	0	0
Kungurian	0	1	3	0	1	0
Artinskian	0	0	5	3	1	0
Sakmarian	0	0	1	1	0	0
Asselian	0	0	1	2	0	0

Neoselachii (Sub)stage	Boreal	E-Panthalassa	C-Pangaea	Palaeotethys	Neotethys	C/W-Panthalassa
Rhaetian	0	0	0	9	0	0
Norian	0	2	0	5	0	1
Carnian	0	1	0	3	0	1
Ladinian	0	1	0	6	0	1
Anisian	1	1	0	5	0	4
Spathian	2	3	0	0	3	3
Smithian	1	1	0	0	2	0
Dienerian	0	0	0	0	1	0
Griesbachian	1	0	0	0	1	0
Changhsingian	0	0	0	0	0	1
Wuchiapingian	0	0	0	0	1	0
Capitanian	0	1	1	0	0	1
Wordian	0	1	1	1	4	0
Roadian	0	1	1	2	0	0
Kungurian	0	1	0	0	0	0
Artinskian	0	0	0	2	0	0
Sakmarian	0	0	0	2	0	0
Asselian	0	0	0	1	0	0

Eugeneodonti-formes (incl. Orodontiformes (Sub)stage	Boreal	E-Panthalassa	C-Pangaea	Palaeotethys	Neotethys	C/W-Panthalassa
Rhaetian	0	0	0	0	0	0
Norian	0	0	0	0	0	0
Carnian	0	0	0	0	0	0
Ladinian	0	0	0	0	0	0
Anisian	0	0	0	0	0	0
Spathian	0	0	0	0	0	0
Smithian	0	5	0	0	0	0
Dienerian	1	0	0	0	0	0
Griesbachian	2	0	0	1	0	0
Changhsingian	2	0	0	0	1	1
Wuchiapingian	3	1	0	1	2	2
Capitanian	0	3	0	0	0	0
Wordian	0	1	0	0	1	0
Roadian	1	1	0	0	0	0
Kungurian	1	2	1	2	1	1
Artinskian	0	2	3	4	1	1
Sakmarian	0	0	1	1	1	0
Asselian	0	0	1	1	0	0

Petalodonti-formes (Sub)stage	Boreal	E-Panthalassa	C-Pangaea	Palaeotethys	Neotethys	C/W-Panthalassa
Rhaetian	0	0	0	0	0	0
Norian	0	0	0	0	0	0
Carnian	0	0	0	0	0	0
Ladinian	0	0	0	0	0	0
Anisian	0	0	0	0	0	0
Spathian	0	0	0	0	0	0
Smithian	0	0	0	0	0	0
Dienerian	0	0	0	0	0	0
Griesbachian	0	0	0	0	0	0
Changhsingian	0	0	0	1	0	0
Wuchiapingian	1	0	0	1	2	2
Capitanian	0	1	0	1	0	0
Wordian	0	1	0	1	1	0
Roadian	0	1	0	1	0	0
Kungurian	0	2	1	0	0	2
Artinskian	0	1	3	2	0	1
Sakmarian	0	0	2	0	0	1
Asselian	0	0	1	1	0	1

Holocephali (Sub)stage	Boreal	E-Panthalassa	C-Pangaea	Palaeotethys	Neotethys	C/W-Panthalassa
Rhaetian	0	0	0	2	0	0
Norian	0	0	0	0	0	0
Carnian	0	0	0	0	0	1
Ladinian	0	0	0	0	0	1
Anisian	0	0	0	0	0	1
Spathian	0	0	0	0	0	0
Smithian	0	0	0	0	0	0
Dienerian	0	0	0	0	0	0
Griesbachian	0	0	0	0	0	1
Changhsingian	0	0	0	1	0	0
Wuchiapingian	1	0	0	1	0	0
Capitanian	0	4	0	2	0	0
Wordian	0	3	0	2	2	0
Roadian	0	3	0	0	0	0
Kungurian	0	3	1	0	2	2
Artinskian	1	1	1	0	0	0
Sakmarian	0	0	1	0	0	0
Asselian	0	0	1	0	0	0

A2.4.18 DISTRIBUTION DATA PER PALAEOBASIN – FIGURE 8.27

(Sub)stage	Boreal	E-Panthalassa	C-Pangaea	Palaeotethys	Neotethys	C/W-Panthalassa
Rhaetian	0	0	1	17	0	0
Norian	0	5	7	8	3	2
Carnian	0	5	7	12	3	7
Ladinian	1	4	0	18	0	7
Anisian	1	6	0	13	2	17
Spathian	7	11	1	0	7	8
Smithian	3	10	0	0	3	4
Dienerian	5	0	0	0	1	4
Griesbachian	7	0	0	1	3	4
Changhsingian	3	0	0	4	4	5
Wuchiapingian	7	1	1	6	10	4
Capitanian	4	13	5	8	0	1
Wordian	4	11	5	11	17	1
Roadian	5	10	7	4	0	0
Kungurian	1	16	11	4	4	6
Artinskian	2	5	21	20	4	2
Sakmarian	1	0	12	10	2	1
Asselian	3	0	11	13	0	1

A2.4.19 CHI-TEST DATA – FIGURE 8.28

Palaeobasins

Category	Actual frequencies					Expected frequencies				χ^2 elements			
	Capitanian	Wuchiapingian	Changhsingian	Griesbachian	total	Capitanian	Wuchiapingian	Changhsingian	Griesbachian	Capitanian	Wuchiapingian	Changhsingian	Griesbachian
Boreal	4	7	3	7	21	7.154	6.692	3.692	3.462	1.390	0.014	0.130	3.617
E-Panthalassa	13	1	0	0	14	4.769	4.462	2.462	2.308	14.205	2.686	2.462	2.308
C-Pangaea	5	1	0	0	6	2.044	1.912	1.055	0.989	4.275	0.435	1.055	0.989
Palaeotethys	8	6	4	1	19	6.473	6.055	3.341	3.132	0.360	0.000	0.130	1.451
Neotethys	0	10	4	3	17	5.791	5.418	2.989	2.802	5.791	3.876	0.342	0.014
C/W-Panthalassa	1	4	5	4	14	4.769	4.462	2.462	2.308	2.979	0.048	2.618	1.241
total	31	29	16	15	91						**df**	**χ^2**	***p***
Capitanian–Griesbachian (incl. freshwater genera)											**15**	**52.416**	**4.8^{-06}**
	Smithian	Spathian	Anisian	total		Smithian	Spathian	Anisian		Smithian	Spathian	Anisian	
Boreal	3	7	1	11		2.366	4.022	4.613		0.170	2.206	2.830	
E-Panthalassa	10	11	6	27		5.806	9.871	11.323		3.029	0.129	2.502	
C-Pangaea	0	1	0	1		0.215	0.366	0.419		0.215	1.101	0.419	
Palaeotethys	0	0	13	13		2.796	4.753	5.452		2.796	4.753	10.452	
Neotethys	3	7	2	12		2.581	4.387	5.032		0.068	1.556	1.827	
C/W-Panthalassa	4	8	17	29		6.237	10.602	12.161		0.802	0.639	1.925	
total	20	34	39	93							**df**	**χ^2**	***p***
Smithian–Anisian (incl. freshwater genera)											**10**	**37.418**	**4.8^{-05}**

A2.4.20 DISTRIBUTION DATA PER PALAEOLATITUDINAL ZONE – FIGURE 8.29

Including freshwater genera

(Sub)stage	61–90°N	31–60°N	0–30°N	0–30°S	31–60°S	61–90°S
Rhaetian	0	1	17	1	0	0
Norian	0	1	13	7	3	0
Carnian	0	5	17	7	3	0
Ladinian	0	2	23	0	0	0
Anisian	1	3	24	1	4	0
Spathian	1	6	14	6	3	1
Smithian	1	5	12	2	1	0
Dienerian	0	6	1	1	0	0
Griesbachian	0	7	5	2	2	0
Changhsingian	0	7	1	6	1	0
Wuchiapingian	0	13	5	11	1	0
Capitanian	0	12	18	0	0	0
Wordian	0	13	15	18	0	0
Roadian	0	7	18	0	0	0
Kungurian	0	4	22	7	8	0
Artinskian	0	19	18	5	8	0
Sakmarian	0	8	15	2	1	0
Asselian	0	7	14	6	0	0

Excluding freshwater genera

(Sub)stage	61–90°N	31–60°N	0–30°N	0–30°S	31–60°S	61–90°S
Rhaetian	0	1	17	1	0	0
Norian	0	1	13	3	1	0
Carnian	0	4	15	2	1	0
Ladinian	0	1	21	0	0	0
Anisian	1	3	23	1	2	0
Spathian	1	6	14	6	3	0
Smithian	1	5	12	2	1	0
Dienerian	0	6	1	1	0	0
Griesbachian	0	7	5	2	2	0
Changhsingian	0	6	1	6	1	0
Wuchiapingian	0	13	5	11	0	0
Capitanian	0	12	18	0	0	0
Wordian	0	13	15	18	0	0
Roadian	0	7	18	0	0	0
Kungurian	0	4	17	6	7	0
Artinskian	0	19	11	2	8	0
Sakmarian	0	7	10	2	1	0
Asselian	0	7	6	3	0	0

A2.4.21 CHI-TEST DATA – FIGURE 8.30

Palaeolatitudinal zones (including and excluding freshwater genera)

Category	Actual frequencies					Expected frequencies				χ^2 elements			
	Capitanian	Wuchiapingian	Changhsingian	Griesbachian	total	Capitanian	Wuchiapingian	Changhsingian	Griesbachian	Capitanian	Wuchiapingian	Changhsingian	Griesbachian
31–60°N	12	13	7	7	**39**	12.857	12.857	6.429	6.857	0.057	0.002	0.051	0.003
0–30°N	18	5	1	5	**29**	9.560	9.560	4.780	5.099	7.450	2.175	2.989	0.002
0–30°S	0	11	6	2	**19**	6.264	6.264	3.132	3.341	6.264	3.581	2.627	0.538
31–60°S	0	1	1	2	**4**	1.319	1.319	0.659	0.703	1.319	0.077	0.176	2.391
total	**30**	**30**	**15**	**16**	**91**						**df**	χ^2	***p***
Capitanian–Griesbachian (incl. freshwater genera)											**9**	**29.701**	**0.0005**
	Smithian	Spathian	Anisian	total		Smithian	Spathian	Anisian		Smithian	Spathian	Anisian	
61–90°N	1	1	1	**3**		0.741	1.094	1.165		0.090	0.008	0.023	
31–60°N	5	6	3	**14**		3.459	5.106	5.435		0.687	0.157	1.091	
0–30°N	12	14	24	**50**		12.353	18.235	19.412		0.010	0.984	1.084	
0–30°S	2	6	1	**9**		2.224	3.282	3.494		0.022	2.250	1.780	
31–60°S	1	3	4	**8**		1.976	2.918	3.106		0.482	0.002	0.257	
61–90°S	0	1	0	**1**		0.247	0.365	0.388		0.247	1.107	0.388	
total	**21**	**31**	**33**	**85**							**df**	χ^2	***p***
Smithian–Anisian (incl. freshwater genera)											**10**	**10.671**	**0.38**

Category	Actual frequencies					Expected frequencies				χ^2 elements			
	Capitanian	Wuchiapingian	Changhsingian	Griesbachian	total	Capitanian	Wuchiapingian	Changhsingian	Griesbachian	Capitanian	Wuchiapingian	Changhsingian	Griesbachian
31–60°N	12	13	6	7	**38**	12.809	12.382	5.978	6.831	0.051	0.031	0.000	0.004
0–30°N	18	5	1	5	**29**	9.775	9.449	4.562	5.213	6.920	2.095	2.781	0.009
0–30°S	0	11	6	2	**19**	6.404	6.191	2.989	3.416	6.404	3.735	3.034	0.587
31–60°S	0	0	1	2	**3**	1.011	0.978	0.472	0.539	1.011	0.978	0.591	3.956
total	**30**	**29**	**14**	**16**	**89**						**df**	χ^2	***p***
Capitanian–Griesbachian (excl. freshwater genera)											**9**	**32.187**	**0.0002**
	Smithian	Spathian	Anisian	total		Smithian	Spathian	Anisian		Smithian	Spathian	Anisian	
61–90°N	1	1	1	**3**		0.778	1.111	1.111		0.063	0.011	0.011	
31–60°N	5	6	3	**14**		3.630	5.185	5.185		0.517	0.128	0.921	
0–30°N	12	14	23	**49**		12.704	18.148	18.148		0.039	0.948	1.297	
0–30°S	2	6	1	**9**		2.333	3.333	3.333		0.048	2.133	1.633	
31–60°S	1	3	2	**6**		1.556	2.222	2.222		0.198	0.272	0.022	
total	**21**	**30**	**30**	**81**							**df**	χ^2	***p***
Smithian–Anisian (excl. freshwater genera)											**8**	**8.243**	**0.41**

A2.4.22 DIVERSITY PER ORDER – FIGURE 8.32

(Sub)stage	Phoebodontiformes?	Bransonelliformes	Xenacanthiformes	Symmoriiformes	Ctenacanthiformes	Hybodontiformes	Synechodontiformes	Heterodontiformes	Orodontiformes	Eugeneodontiformes	Petalodontiformes	Helodontiformes	Cochliodontiformes	Menaspiformes	Chimaeriformes
Rhaetian	0	0	0	0	0	9	4	1	0	0	0	0	0	0	2
Norian	0	0	1	0	0	10	6	1	0	0	0	0	0	0	0
Carnian	0	0	3	0	0	11	5	1	0	0	0	0	0	0	1
Ladinian	0	0	3	0	0	10	5	1	0	0	0	0	0	0	1
Anisian	0	0	3	0	0	8	6	0	0	0	0	0	0	0	1
Spathian	0	0	2	0	0	8	4	0	0	0	0	0	0	0	1
Smithian	0	0	2	0	0	8	4	0	0	3	0	0	0	0	1
Dienerian	0	0	2	0	0	8	4	0	0	2	0	0	0	0	1
Griesbachian	0	0	2	0	0	8	4	0	0	4	0	0	0	0	1
Changhsingian	0	0	2	0	0	6	3	0	0	4	1	0	0	1	1
Wuchiapingian	0	0	3	1	1	5	3	0	0	8	4	1	2	1	1
Capitanian	0	0	3	2	4	4	2	0	0	7	4	1	4	1	1
Wordian	0	0	4	3	4	8	2	0	0	6	4	1	5	1	0
Roadian	0	0	5	3	4	6	1	0	0	6	4	1	5	0	0
Kungurian	0	1	6	2	9	6	1	0	0	8	4	1	6	0	0
Artinskian	0	1	6	2	6	6	1	0	1	9	6	1	4	0	0
Sakmarian	0	2	5	2	6	6	1	0	1	7	4	1	4	0	0
Asselian	0	2	6	2	6	6	0	0	1	7	6	1	5	0	0

APPENDIX 3 SYSTEMATIC PALAEONTOLOGY

A3.1. SYSTEMATIC CLASSIFICATION

Class	Subclass	Cohort	Subcohort	Superorder	Order	Suborder	Superfamily	Family	Subfamily	Genera
Chondrichthyes Huxley, 1880										
	Elasmobranchii Bonaparte, 1838									
					Phoebodontiformes Ginter, Hairapetian and Klug, 2002					
										New genus
				Xenacanthimorpha Nelson, 1976						
					Bransonelliformes Hampe and Ivanov, 2007					
								Unnamed		
										Barbclabornia Johnson, 2003
										Bransonella Harlton, 1933
					Xenacanthiformes Berg, 1937					
								Diplodoselachidae Dick, 1981		
										Dicentrodus Traquair, 1888
										Lebachacanthus Soler-Gijón, 1997b
										Orthacanthus Agassiz, 1843
								Xenacanthidae Fritsch, 1889		
										Xenacanthus Beyrich, 1848
										Triodus Jordan, 1849
										Plicatodus Hampe, 1995
										Wurdigneria Richter, 2005
										Mooreodontus Hampe and Schneider, 2010 (in Ginter, Hampe and Duffin, 2010)
				Cladodontomorphi Ginter, Hampe and Duffin, 2010						
										"*Cobelodus*" Zangerl, 1973 (= new genus)
					Symmoriiformes Zangerl, 1981					
								Symmoriidae Dean, 1909		
										Stethacanthus Newberry, 1889
										"Physonemus" McCoy, 1848 / *Batacanthus* St. John and Worthen, 1875
								Falcatidae Zangerl, 1990		
										Stethacanthulus Zangerl, 1990
					Ctenacanthiformes Glikman, 1964					
								Ctenacanthidae Dean, 1909		
										Ctenacanthus Agassiz, 1837 (in 1843)
										Glikmanius Ginter, Ivanov and Lebedev, 2005
								Heslerodidae Maisey, 2010		
										Heslerodus Ginter, 2002b
								incertae sedis		
										Saivodus Duffin and Ginter, 2006
										Neosaivodus Hodnett, Elliot, Olson and Wittke, 2012
										Kaibabvenator Hodnett, Elliot, Olson and Wittke,

										2012
										Nanoskalme Hodnett, Elliot, Olson and Wittke, 2012
										Acondylacanthus St. John and Worthen, 1875
					incertae sedis					
										Pyknothylacanthus Mutter and Rieber, 2005
				incertae sedis						
										Dwykaselachus Oelofsen, 1986
								Jalodontidae Ginter, Hairapetian and Klug, 2002		
										New genus
										Isacrodus Ivanov, Nestell and Nestell, 2012
										Texasodus Ivanov, Nestell and Nestell, 2012
										Adamantina Bendix-Almgreen, 1993
		Euselachii Hay, 1902								
							Protacrodontoidea Zangerl, 1981			
								Protacrodontidae Capetta, Duffin and Zidek, 1993		
										Protacrodus Jaekel, 1925
					Hybodontiformes Maisey, 1975					
							Hybodontoidea Owen, 1846			
								Hybodontidae Owen, 1846		
										Donguzodus Minikh, 1996b
									Hybodontinae Owen, 1846	
										Hybodus Agassiz, 1837
										'Polyacrodus' Jaekel, 1889
									Acrodontinae Casier, 1959	
										Acrodus Agassiz, 1838
										Asteracanthus Agassiz, 1837
										Palaeobates Meyer, 1849
								Unnamed Rees, 2008		
										Lissodus Brough, 1935 s.s.
								Lonchidiidae Herman, 1977 *sensu* Rees and Underwood 2002		
										Lonchidion Estes, 1964
										Diplolonchidion Heckert, 2004
										Parvodus Rees and Underwood, 2002
								?Lonchidiidae		
										Gansuselache Wang, Zhang, Zhu and Zhao, 2009
								Steinbachodontidae Reif, 1980b		
										Steinbachodus Reif, 1980b
								Distobatidae Werner, 1989		
										Reticulodus Murry and Kirby, 2002
							Hybodontoidea?			
								Homalodontidae Mutter, Neuman and De Blanger, 2008		
										Homalodontus Mutter, Neuman and De Blanger, 2008
								incertae sedis		
										'Palaeozoic Genus 1' Rees and Underwood, 2002
							incertae sedis			
										Omanoselache Koot, Cuny, Tintori and Twitchett, 2013
										Reesodus Koot, Cuny, Tintori and Twitchett, 2013
										Teresodus Koot, Cuny, Tintori and Twitchett, 2013
										Gunnellodus Wilimovsky, 1954
					incertae sedis					
								Sphenacanthidae Maisey, 1982a		

										Sphenacanthus Agassiz, 1837
										Wodnika Von Münster, 1843
										Xenosynechodus Glikman, 1980
										Khuffia Koot, Cuny, Tintori and Twitchett, 2013
			Neoselachii Compagno, 1977							
								Anachronistidae Duffin and Ward, 1983		
										Cooleyella Gunnell, 1933
								Pseudodalatiidae Reif, 1978b		
										Pseudodalatias Reif, 1978b
					Synechodontiformes Duffin and Ward, 1993					
								Palaeospinacidae Regan, 1906		
										Palidiplospinax Klug and Kriwet, 2008
								incertae sedis		
										Genus S
										'Synechodus' (pre-Jurassic) Woodward, 1888
										Nemacanthus Agassiz, 1837
										Genus P
										Rhomphaiodon Duffin, 1993a
										Grozonodon Cuny, Martin, Rauscher and Mazin, 1998
										Mucrovenator Cuny, Rieppel and Sander, 2001
					incertae sedis					
										Hopleacanthus Schaumberg, 1982
										Hueneichthys Reif, 1977
										Reifia Duffin, 1980
										Vallisia Duffin, 1982b
										Doratodus Schmid, 1861
										Raineria Osswald, 1928
										Duffinselache Andreev and Cuny, 2012
										Rhomaleodus Andreev and Cuny, 2012
										Pseudocetorhinus Duffin, 1998b
										'Hexanchidae gen. et sp. indet.'
										Lypbalkodus Minikh, 1996b
										Amelacanthus Maisey, 1982a
										Eunemacanthus St. John and Worthen, 1883
				Galeomorphii Compagno, 1973						
					Heterodontiformes Berg, 1937					
								Heterodontidae Gray, 1851		
										Heterodontus De Blainville, 1816
			incertae sedis							
										Acronemus Rieppel, 1982
	Euchondrocephali Lund and Grogan, 1997									
					Orodontiformes Zangerl, 1981					
								Orodontidae De Koninck, 1878		
										Orodus Agassiz, 1838
					Eugeneodontiformes Zangerl, 1981					
							Caseodontoidea Zangerl, 1981			
								Caseodontidae Zangerl, 1981		
										Caseodus Zangerl, 1981
										Fadenia Nielsen, 1932
										Erikodus Nielsen, 1952
										Uralodus Kozlov, 2000
								Eugeneodontidae Zangerl, 1981		
										Bobbodus Zangerl, 1981
								incertae sedis		

										Campodus De Koninck, 1844
										Tiaraju Richter, 2007
							Edestoidea Hay, 1929			
								Agassizodontidae St. John and Worthen, 1875		
										Agassizodus St. John and Worthen, 1875
										Campyloprion Eastman, 1902
										Helicoprion Karpinsky, 1899
										Parahelicoprion Karpinsky, 1924
										Sarcoprion Nielsen, 1952
										Hunanohelicoprion Liu, 1994
										Sinohelicoprion Liu and Chang, 1963
										Shaktauites Chuvashov, 2001
								Edestidae Jaekel, 1899		
										Edestus Leidy, 1855
										Syntomodus Obruchev, 1964
										Helicampodus Branson, 1935
										Parahelicampodus Nielsen, 1952
										Paredestus Mutter and Neuman, 2008
					Petalodontiformes Zangerl, 1981					
								Janassidae Jaekel, 1899		
										Janassa Münster, 1839
								Pristodontidae Woodward, 1889a		
										Megactenopetalus David, 1944
										Peripristis St. John, 1870
										Petalorhynchus Newberry and Worthen, 1866
								Petalodontidae Newberry and Worthen, 1866		
										Petalodus Owen, 1840 (in 1845)
										Chomatodus Agassiz, 1838
										Itapyrodus Silva Santos, 1990
										Permopetalodus Kozlov, 2000
										'Neopetalodus'
	Euchondrocephali? *incertae sedis*									
										Desmiodus St. John and Worthen, 1875
				Iniopterygia Zangerl and Case, 1973						
										gen. indet.
				Holocephali Bonaparte, 1832–1941						
					Helodontiformes Patterson, 1965					
								Helodontidae Patterson, 1965		
										Helodus Agassiz, 1838
					Cochliodontiformes Obruchev, 1953					
								Psephodontidae Zangerl, 1981		
										Psephodus Morris and Roberts, 1862 (ex. Agassiz, 1859)
								Cochliodontidae Owen, 1867		
										Crassidonta Branson, 1916
										Deltodus Morris and Roberts, 1862 (ex. Agassiz, 1859)
										Helodopsis Waagen, 1879
										Poecilodus Agassiz, 1838
										Sandalodus Newberry and Worthen, 1866
								incertae sedis		
										Solenodus Trautschold, 1874
					Menaspiformes Obruchev, 1953					
								Menaspidae Woodward, 1891		
										Menaspis Ewald, 1848

					Chimaeriformes Obruchev, 1953					
										Arctacanthus Nielsen, 1932
						Myriacanthoidei Patterson, 1965				
								Myriacanthidae Woodward, 1889b		
										Agkistracanthus Duffin and Furrer, 1981
										Myriacanthus Agassiz, 1836
	incertae sedis									
										Macrodontacanthus Romer, 1942

A3.2. SYSTEMATIC PALAEONTOLOGY AND MORPHOLOGICAL DESCRIPTION

Class CHONDRICHTHYES Huxley, 1880

Subclass ELASMOBRANCHII Bonaparte, 1838

Superorder CLADODONTOMORPHI Ginter, Hampe and Duffin, 2010

Order SYMMORIIFORMES Zangerl, 1981

Family FALCATIDAE Zangerl, 1990

Genus STETHACANTHULUS Zangerl, 1990

Stethacanthulus sp. cf. *S. decorus* (Ivanov, 1999)

Figure A3.1, A–H

1999 *Denaea*? *decora* Ivanov, pp. 273–276, text-fig. 2; pl. 7, fig. 12; pl. 8.

Material. Sample 100302-F, Batain Melange at Qarari, yielded three broken specimens, comprising one base and two cusps. Specimens used for light microscopy imaging: OM98, OM100; remaining specimen: OM99.

Samples 100302-H, 110223-A, Batain Melange at the “Bridge”, yielded 12 isolated cusp fragments. Specimens used for light microscopy imaging: OM102, OM105; remaining specimens: OM91–95, OM101, OM103–104, OM106–107.

Sample 100227-C, Maqam Formation, yielded one isolated cusp. Specimen: OM89.

Description. Symmetrical teeth of small size (2.8 mm mesio-distally, 2.4 mm labio-lingually and up to 2.5 mm high). The crown is multicuspid comprising a main cusp and three pairs of lateral cusplets, which may be divergent, but this is difficult to assess due to the fact that the cusps are missing from the only recovered base. The main cusp is the highest and is slightly sigmoidal. The diameter of the cusplet bases suggests that the intermediate of the three cusplets is larger than the mesial or distalmost cusplets. All cusps are slender and high, rounded to oblong in cross-section, and distinctly inclined lingually. They are finely but densely striated vertically along their entire length. The cristae are non-anastomosing and reach the cusp apices, but they may terminate a little distance from the apex lingually, and on the labial face, they converge in the central part of the cusp near the apex, approaching a lanceolate ornamentation pattern. The enameloid is yellowish-white and often translucent. It does not form a histological connection between cusps, which remain separate entities, although a bridge-like structure appears on at least one side of the main cusp, resulting from a slight widening of the cusp at the base and an associated raised lateral crista.

The base is very shallow and trapezoidal to irregularly hexagonal in apical outline. All cusps are placed along the labial edge, creating a large lingual torus of which the central part is expanded with a rounded edge, and depressed on the oral side. This means that the basal edge also dips in lingual view and it further causes the basal face to bulge in this area, whereas it shows a paired lateral depression. The basolabial edge is straight, but the labial outline is somewhat undulating in apical view. The base is devoid of any articulation devices. Three medium-sized foramina open on the oral side of the lingual torus, positioned in a horizontal row near the main cusp. Each is accompanied by a labio-lingual groove that approach but do not reach the lingual basal edge. Two small foramina occur in a similar position at each of the mesialmost lateral cusplets. Three foramina open on the labial face of the base, positioned in a row underneath the main cusp, which are assumed to link up with those on the oral side. No foramina are observed on the basal face.

Remarks. This material is very limited, but as a result of a recovered tooth base, sufficient morphological characteristics can be observed to make a reliable identification. Its symmoriiform affinity is indicated by the lack of a histological connection between cusps, as was first noted by Seqeira and Coates (2000). Similar bridge-like features as described here can also occasionally be observed in teeth shown in Ginter *et al.* (2010, fig. 63). The material further conforms to the description of a cladodont dentition with very small teeth, as was deemed diagnostic of the Falcatidae by Zangerl (1990), a characteristic that was not modified by Maisey's (2009) slight adjustments to the family description. The teeth described here are most similar to teeth of *Denaea* Pruvost, 1922 and *Stethacanthulus* Zangerl, 1990, but the first can be disregarded based most importantly on the absence of any articulation devices in the material described here. This characteristic instead corroborates the identification as *Stethacanthulus*, the teeth of which possess a central oral depression and lateral aboral depressions that provide surface area for attachment of connective tissue (Ginter *et al.* 2010). Further diagnostic features of *Stethacanthulus* that are recognised in the teeth from Oman include the approximately irregular hexagonal apical outline of the base, grooves associated with foramina on the oral side, and the sigmoidal lateral outline of the main cusp (Ginter *et al.* 2010), the latter of which, together with the ornamentation pattern, forms the main basis for inclusion of the specimen from Wadi Maqam in this taxon. Maisey (2007, 2008) reorganised the named species within this genus (see also Ginter *et al.* 2010), considering *S. longipeniculus* Zangerl, 1990 as the male morph and therefore the junior synonym of *S. meccaensis* (Williams, 1985), both of which originate from the Pennsylvanian (Carboniferous) of Indiana and Oklahoma, USA (see Maisey 2009 for further discussion). *Stethacanthulus decorus* (Ivanov, 1999) from the Cisuralian (Permian) of the southern Urals, Russia, has so far been left out of this discussion because it is solely based on teeth. The material from the Guadalupian (e.g., Wordian) and Lopingian (Wuchiapingian) of Oman described here differs from *S. meccaensis* in that it possesses three medium-sized foramina instead of a single large foramen on the oral surface, and three small foramina on the labial face rather than a

single prominent foramen positioned underneath the main cusp on the aboral surface (Ginter *et al.* 2010). It also lacks any evidence of a weak bridge-like connection over any groove associated with a foramen, which may occur in *S. meccaensis* (Ginter *et al.* 2010). It closely resembles the diagnosis of *S. decorus*, especially with the described shapes observed in the base (see Ivanov 1999). However, the lanceolate ornamentation is not as strongly expressed here, lacking the distinct and raised ridges ("overlapping chevrons"). Also, still only two foramina are present on the oral surface as well as on the basolabial edge in *S. decorus*. Although the Oman material is considered closer to *S. decorus* based on the described basal features, it cannot be referred to the species until more material can be recovered and the full range of variation assessed.

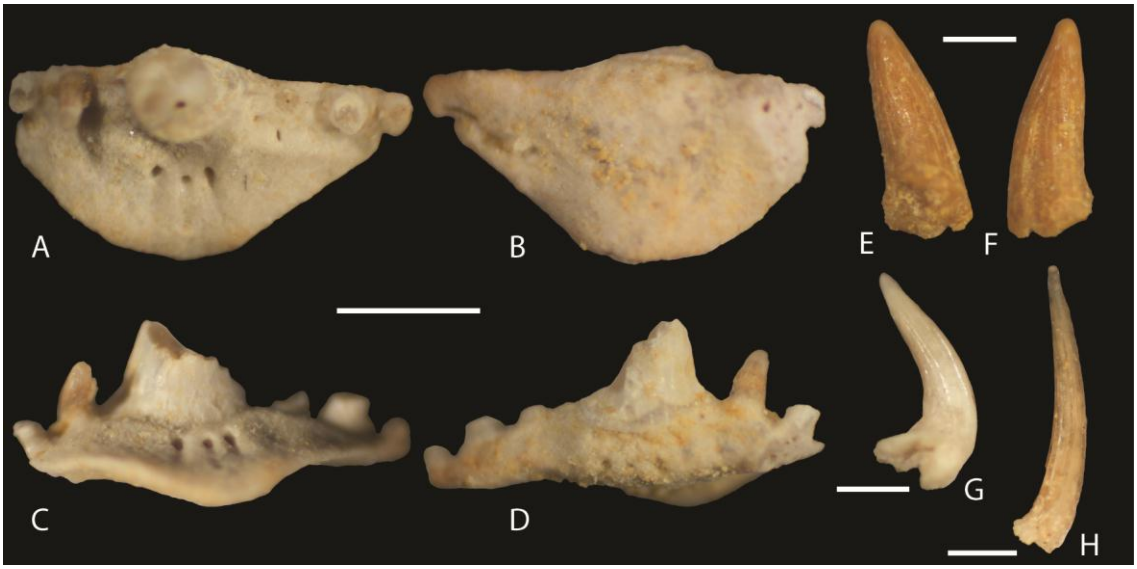

Figure A3.1 – Falcatid teeth from the Batain Melange, Qarari and the "Bridge", Batain Plain, northeastern Oman. Figs A–H. *Stethacanthulus* sp. cf. *S. decorus* (Ivanov, 1999). A–D, OM98, Qarari, sample 100302-F; tooth base. A, apical, B, basal, C, lingual, and D, labial views; scale bar 1 mm. E–F, OM100, Qarari, sample 100302-F; tooth cusp. E, lingual, and F, labial views; scale bar 400 µm. G, OM102, the "Bridge", sample 110223-A; tooth cusp. Lateral view; scale bar 600 µm. H, OM105, the "Bridge", sample 110223-A; tooth cusp. Lateral view; scale bar 600 µm.

Order CTENACANTHIFORMES Glikman, 1964

Family CTENACANTHIDAE Dean, 1909

Genus GLIKMANIUS Ginter, Ivanov and Lebedev, 2005

Type species. *Cladodus occidentalis* Leidy, 1859; from the Pennsylvanian upper Coal Measures of Manhattan, Kansas, USA.

Diagnosis (emended from Ginter, Ivanov and Lebedev 2005) and *Remarks* published in Koot *et al.* (2013).

Glikmanius cf. *myachkovensis* (Lebedev, 2001)

Figure A3.2, A–H; Figure A3.3, C

2001 *Symmorium*? *myachkovensis* Lebedev, pp. 196–197, pl. 41, fig. 4.

2005 *Glikmanius myachkovensis* Ginter, Ivanov and Lebedev, pp. 627–629, figs 2C, 3A–F.

Material. Samples AO40, AO55, AO47bis, AO50, Khuff Formation, yielded 649 specimens of variable completeness and with some indications of wear. Specimens used for SEM imaging: MPUM10926, MPUM10927; remaining specimens: MPUM10893 (65), MPUM10914 (420), MPUM10933 (54), MPUM10946 (108).

Samples 965-2, 965-3, 965-8, 965-9, Khuff Formation, yielded 13 specimens in varying degrees of completeness and with some indications of wear. Specimen used for SEM imaging: UC20366; specimens used for SEM microstructure study: UC20305, UC20369; remaining specimens: UC20239, UC20303, UC20323, UC20338, UC20361 (tentative: UC20304, UC20350, UC20368, UC20381, UC20382).

Samples 110219-J, 110219-L, 110219-M, Saiq Formation, yielded four specimens, isolated cusps. Specimens: OM45, OM48–49, OM69.

Description published in Koot *et al.* (2013).

Enameloid microstructure. The enameloid is made up of a compact and homogeneous layer of single crystallites (SCE), which covers the entire surface and increases in thickness in the longitudinal ridges and cutting edges, but the structure remains unchanged. The crystallites are rod-shaped, short (0.5 µm or less) and randomly orientated, but at the surface they tend to be perpendicular to the surface.

Remarks published in Koot *et al.* (2013).

Glikmanius culmenis Koot, Cuny, Tintori and Twitchett, 2013

Figure A3.2, I–T

Derivation of name and *Type* information published in Koot *et al.* (2013).

Material. Samples AO40, AO55, AO47bis, AO50, Khuff Formation, yielded 137 specimens of variable completeness and with some indications of wear. Specimens used for SEM imaging: MPUM10909, MPUM10910, MPUM10928; remaining specimens: MPUM10894 (25), MPUM10915 (101), MPUM10934 (3), MPUM10947 (5).

Diagnosis, *Description* and *Remarks* published in Koot *et al.* (2013).

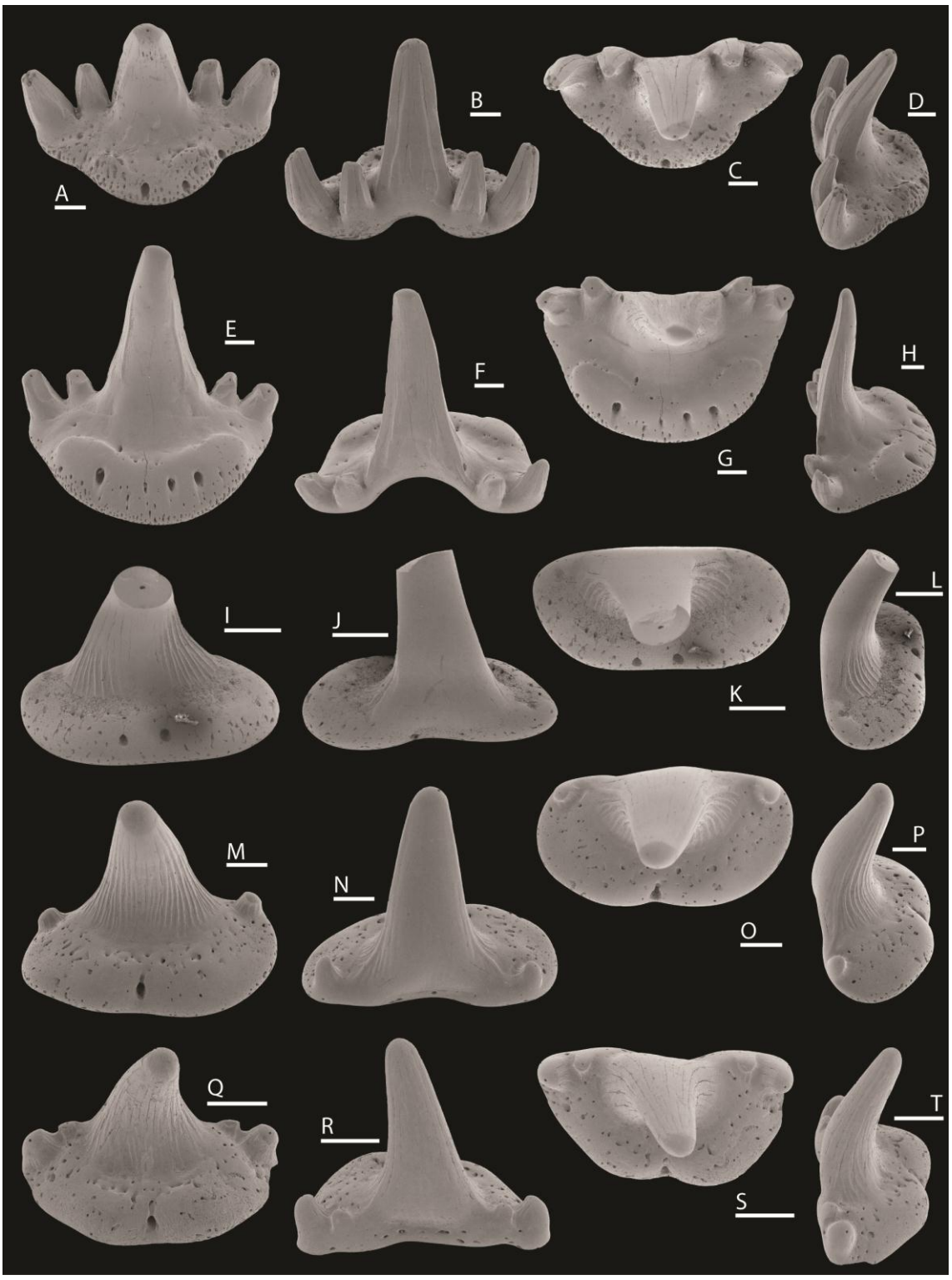

Figure A3.2 – Ctenacanth teeth from the Khuff Formation, Haushi Cliff, Haushi-Huqf area, central eastern Oman. Figs A–H. *Glikmanius* cf. *myachkovensis* (Lebedev, 2001). A–D, MPUM10926, loc K4, sample AO47bis; tooth. A, lingual, B, labial, C, apical, and D, lateral views; scale bars 500 µm. E–H, MPUM10927, loc K4, sample AO47bis; tooth. E, lingual, F, labial, G, apical, and H, lateral views; scale bars 500 µm. Figs I–T. *Glikmanius culmenis* Koot, Cuny, Tintori and Twitchett, 2013. I–L, MPUM10909, loc K4, sample AO55; tooth, paratype. I, lingual, J, labial, K, apical, and L, lateral views; scale bars 500 µm. M–P, MPUM10910,

loc K4, sample AO55; tooth, paratype. M, lingual, N, labial, O, apical, and P, lateral views; scale bars 500 µm. Q–T, MPUM10928, loc K4, sample AO47bis; tooth, holotype. Q, lingual, R, labial, S, apical, and T, lateral views; scale bars 500 µm.

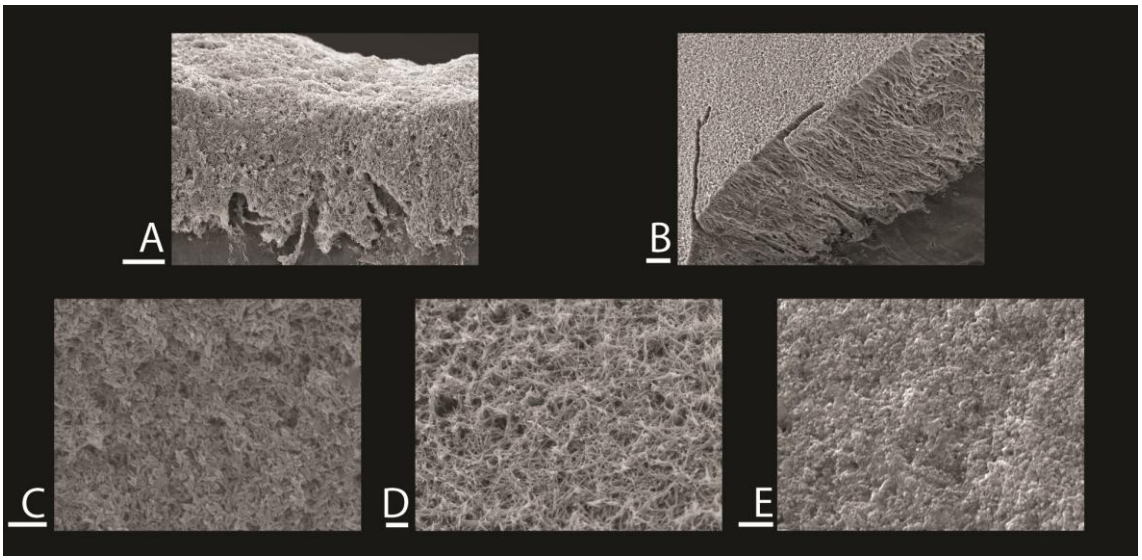

Figure A3.3 – Enameloid microstructure of teeth from the Khuff Formation, Haushi-Huqf area, central eastern Oman. Figs A–B. *Omanoselache hendersoni* Koot, Cuny, Tintori and Twitchett, 2013. A, UC20285, loc 6-7, sample 965-2, Haushi Cliff; tooth. M, detail of enameloid fracture surface; scale bar 5 µm. B, UC20298, loc 6-7, sample 965-2, Haushi Cliff; tooth. N, detail of enameloid fracture surface; scale bar 10 µm. Fig C. *Glikmanius* cf. *myachkovensis* (Lebedev, 2001). UC20305, loc 6-7, sample 965-2, Haushi Cliff; tooth. C, detail of enameloid fracture surface; scale bar 1 µm. Fig D. *Teresodus amplexus* Koot, Cuny, Tintori and Twitchett, 2013. UC20367, loc 6-2, sample 965-9, Saiwan; tooth. D, detail of enameloid surface; scale bar 1 µm. Fig E. *Gunnellodus bellistriatus* (Gunnell, 1933). UC20242, loc 6-7, sample 965-2, Haushi Cliff; tooth. E, detail of enameloid surface; scale bar 0.5 µm.

Superorder CLADODONTOMORPHI? Ginter, Hampe and Duffin, 2010

Gen. et sp. indet.

Figure A3.4, A–B

Material. Samples 300311-I, 300311-J, 300311-O, Kamura Formation, yielded seven broken specimens. Specimens used for light microscopy imaging: JP60, JP62; remaining specimens: JP61, JP95; tentatively assigned specimens: JP33–35.

Description. The main cusp is rounded in transverse section near the apex versus more labio-lingually compressed towards the base, as well as wider mesio-distally. The crown surface is ornamented with strong vertical cristae running along the length of the cusp. The cristae are not positioned entirely parallel to each other and some cristae may terminate when approaching another. The cristae do not anastomose.

Remarks. The nature of this material is very fragmentary and besides the general features of the main cusp, no observations could be made. The tentative assignment to the Cladodontomorphi is made based on a general resemblance to teeth from taxa that belong to this group, in the knowledge that cladodont teeth have previously been recovered from Japanese deposits (e.g., Goto 2000; Yamagishi 2006, 2011).

Figure A3.4 – Chondrichthyan tooth fragments Kamura Formation, Miyazaki Prefecture, southwestern Japan. Figs A–B. Cladodontomorphi? gen. et sp. indet. A, JP62, Shioinouso east, sample 300311-J; tooth fragment, labial/lingual view; scale bar 400 µm. B, JP60, Shioinouso east, sample 300311-J; crown fragment, surficial view; scale bar 300 µm.

Order *INCERTAE SEDIS*

Family JALODONTIDAE Ginter, Hairapetian and Klug, 2002

Genus ADAMANTINA Bendix-Almgreen, 1993

Type species. *Adamantina benedictae* Bendix-Almgreen, 1993; from the Wuchiapingian Ravnefjeld Formation at Kap Stosch, East Greenland.

Adamantina sp.

Figure A3.5, A–D

Material. Sample CH-F136-79, Trold Fiord Formation, yielded three broken specimens. Specimen used for SEM imaging: 462; remaining specimens: 461, 463 (tentative, single cusp fragment).

Description. Largest crown fragment (462) measuring minimally 1.7 mm apico-basally and 1.3 mm mesio-distally, possessing a thick enameloid covering. The crown is somewhat labio-lingually compressed but still distinctly convex labially. One broad, leaf-like cusp is completely preserved, which curves lingually. It is ornamented on the labial face with strong spiral cristae, which follow a lanceolate pattern. The lingual cusp surface is largely smooth. No basal features can be assessed.

Remarks. Assignment of this material to *Adamantina* Bendix-Almgreen, 1993 is based on the very characteristic crown sculpture, combined with the shape of the cusp. The genus was first described from the Wuchiapingian of East Greenland (Bendix-Almgreen 1993) and is also known from the Lower Mississippian and Cisuralian (Asselian–Artinskian) of northern Russia (Ivanov 1999). In addition, tentative assignments include Upper Pennsylvanian specimens from Brazil (Duffin *et al.* 1996) and from the mid-continental region of the USA (Tway and Zidek 1983; see Ivanov

1999). The specimen described here, therefore, represents the first known occurrence of *Adamantina* in the Guadalupian (Wordian) and also the first record from the Canadian Arctic. Its morphology is believed to be closer to the type species, *A. benedictae* Bendix-Almgreen, 1993, rather than *A. foliacae* Ivanov, 1999, because of the spirally curved cristae and the low position of the adjacent cusp. Although it must remain highly speculative until further material can be recovered, the large angle between the lateral cusp and the adjacent (missing) cusp, and the erect orientation of the cristae on the adjacent cusp, suggest that this crown may have been discuspid and therefore that the smaller central cusp would have been absent. This would signify the presence of a new species, because *A. benedictae* possesses three cusps (Bendix-Almgreen 1993), and *A. foliacae* three to five (Ivanov 1999).

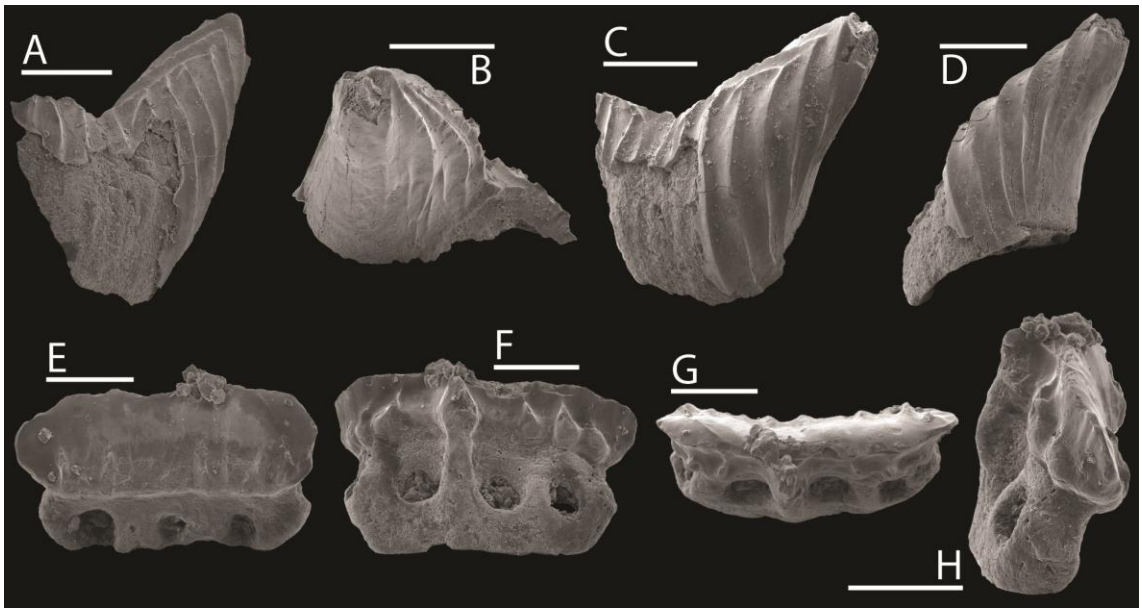

Figure A3.5 – Chondrichthyan teeth from the Trold Fiord and Blind Fiord formations, Ellesmere Island, Canadian Arctic. Figs A–D. *Adamantina* sp. 462, sample CH-F136-79 HN, Trold Fiord Formation; tooth. A, labial, B, apico-lingual, C, apico-labial, and D, lateral views; scale bars 500 µm. Figs E–H. *Caseodus* sp. cf. *C. varidentis* Mutter and Neuman, 2008. 446, sample 93 OF TE-5 1663 62-TE 325A, Blind Fiord Formation; tooth. E, lingual, F, labial, G, apico-labial, and H, lateral views; scale bars 300 µm.

Cohort EUSELACHII Hay, 1902

Order HYBODONTIFORMES Maisey, 1975

Remarks. The Permian material from Oman described in this study displays characteristics typical for hybodont crown morphology, including a prominent main cusp that is always higher than the lateral cusplets, with cusplet height decreasing away from the centre of the tooth, and a very gradual heterodonty pattern (Ginter *et al.* 2010). However, the base morphology is unusual compared to typical hybodonts known from the Mesozoic. “Palaeozoic small-toothed hybodonts are extremely poorly known” (Rees and Underwood 2002, p. 471), and in particular the base structure, which is due to a lack of isolated teeth and poor visibility in preserved body fossils. The material from the Khuff Formation provides an exceptional opportunity for comparison due to the abundance of isolated teeth preserved with the base still attached to the crown in virtually every instant. This in itself is a noteworthy feature of Palaeozoic hybodont teeth, substantiated by figured material in previous publications (e.g., Johnson 1981), because it is a widely recognised characteristic of Mesozoic hybodonts that the base has a weak attachment to the crown and is almost never recovered with the crown. This phenomenon has, however, as far as the author is aware, been mentioned only once before in literature by Underwood and Cumbaa (2010), who note resorption of the crown-base junction during tooth dehiscence in post-Triassic hybodonts, and no difference with Permian hybodonts has previously been observed. The base in the Permian material from Oman is also observed to possess more right angles and larger foramina than in Mesozoic hybodont teeth, but this may fall within the expected variation among taxa within the order.

Superfamily HYBODONTOIDEA Owen, 1846

Family HYBODONTIDAE Owen, 1846

Subfamily HYBODONTINAE Owen, 1846

Genus HYBODUS Agassiz, 1837

Type species. *Hybodus reticulatus* Agassiz, 1837; from the Lower Jurassic of Lyme Regis, England.

cf. *Hybodus* sp. (Japan)

Figure A3.6, A–B

Material. Samples 05.7.14.ak, 05.7.15.q, Kamura Formation, yielded three broken specimens. Specimen used for light microscopy imaging: JP117; remaining specimens: JP97, JP118.

Description. Small, elongate teeth (around 1.4 mm mesio-distally, 0.2 mm labio-lingually, and 0.5–0.6 mm high). The crown is multicuspid with a main cusp that is always higher than the lateral cusplets. Up to two lateral cusplets may be present on either side of the main cusp, which are well-defined. An asymmetrical distribution can occur with one and two cusplets on each respective lateral extremity. An acute longitudinal crest is developed. The crown is ornamented with vertical cristae on all cusps extending from the crown shoulder upwards, which are strongly developed on the lower half of the crown but may actually reach the cusp apices. The cristae are most pronounced lingually. True nodes are absent, but the cristae may be significantly raised on the crown shoulder at the base of a cusp or cusplet. The base is not preserved, preventing its features to be assessed.

Remarks. According to Ginter *et al.* (2010), the genus *Hybodus* Agassiz, 1837 is in need of extensive revision and the same is true for the entire family of the Hybodontidae. However, they list the following features of the type species, *H.*

reticulatus Agassiz, 1837, which should be considered characteristic for the genus: slender main cusp that may be distally inclined, up to three lateral cusplet pairs, and vertical ridges on the lower half of the crown. The material described generally conforms to the typical morphology of *Hybodus*, although the ornamentation pattern reaches higher up the crown, which is why it is here assigned to the genus with some reservation. The material further matches the features described for *Hybodus* sp. 2 of Yamagishi (2006), observed in samples from Taho and Kamura in Japan (the material from Taho was erroneously referred to *Synechodus* in Yamagishi 2004), although the lingual inclination is not well expressed in the material described here and the basal features cannot be observed.

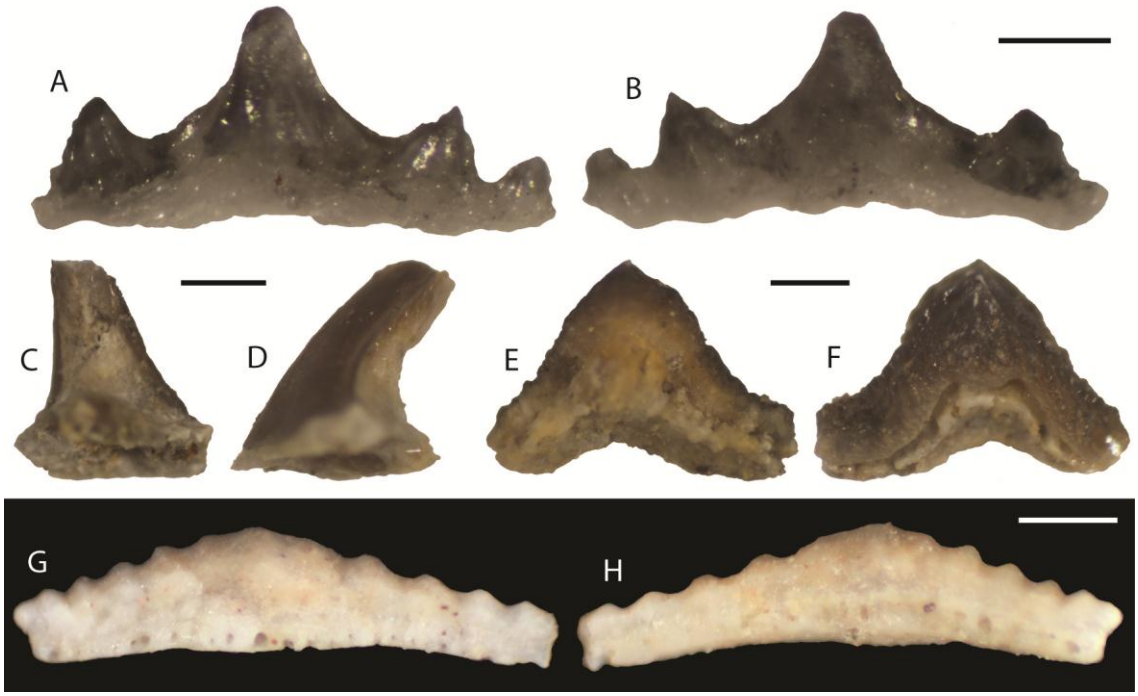

Figure A3.6 – Chondrichthyan teeth and spines? from the Kamura Formation Miyazaki Prefecture, southwestern Japan. Figs A–B. cf. *Hybodus* sp. A, JP117, sample 05.7.15.q, Kamura Formation; tooth fragment. A, lingual view, B, labial view; scale bar 300 µm. Figs C–D. aff. *Arctacanthus*? sp. C, JP110, sample 05.7.15.h, Kamura Formation; tooth fragment. C, posterior view, D, lateral view; scale bar 600 µm. Figs E–F. *Acrodus spitzbergensis* Hulke, 1873. E, JP114, sample 05.7.15.k, Kamura Formation; tooth. E, lingual view, F, labial view; scale bar 500 µm. Figs G–H. *Omanoselache* sp. cf. *O.* sp. H. G, JP96, sample 05.7.14.ak, Kamura Formation; tooth. G, lingual view, H, labial view; scale bar 400 µm.

cf. *Hybodus* sp. (southwestern USA)

Figure A3.7, A–B

Material. Sample 92-OF DC10, Union Wash Formation, yielded five broken specimens. Specimens used for light microscopy imaging: 300, 302; remaining specimens: 301, 303–304.

Description. Small teeth (1.0–1.5 mm mesio-distally, 0.3 mm labio-lingually, and approximately 0.5 mm high). The crown is multicuspid with a high and slender main cusp, which is always higher than the lateral cusplets and may be distally slanted. Any pegs are lacking. At least two lateral cusplets may be present on either side of the main cusp, which are high and well-defined. The crown is ornamented with vertical cristae on all cusps extending from the crown shoulder to the apices. The base is not preserved.

Remarks. The same remarks as for the Japanese material apply to the material described here, except for the comparison to other material.

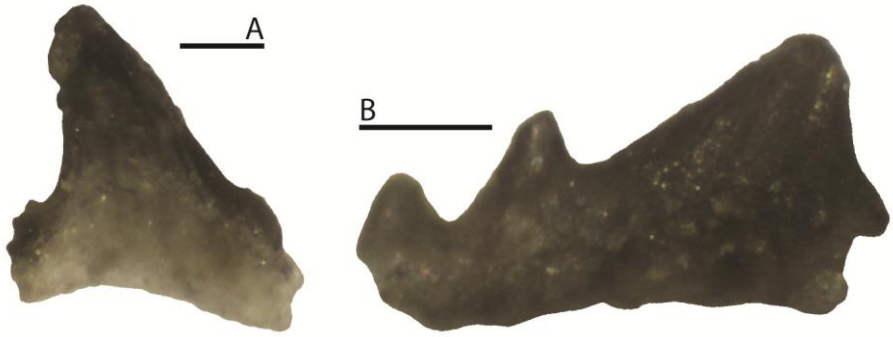

Figure A3.7 – Chondrichthyan teeth from the Union Wash Formation at Darwin Canyon, California, southwestern USA. Figs A–B. cf. *Hybodus* sp. A, 300, sample 92-OF DC10, Union Wash Formation; tooth fragment, lingual/labial view; scale bar 200 µm. B, 302, sample 92-OF DC10, Union Wash Formation; tooth fragment, lingual/labial view; scale bar 200 µm.

Subfamily ACRODONTINAE Casier, 1959

Genus ACRODUS Agassiz, 1838

Type species. *Acrodus nobilis* Woodward, 1916; from the Lower Jurassic of Lyme Regis, southern England.

Acrodus spitzbergensis Hulke, 1873

Figure A3.6, E–F; Figure A3.8, M–O

1873 *Acrodus spitzbergensis* Hulke, p. 10 (*fide* Stensiö 1921).

1889a *Acrodus spitzbergensis* Woodward, p. 299.

1918 *Acrodus spitzbergensis*? Stensiö, pp. 76–77.

1921 *Acrodus spitzbergensis* Stensiö, pp. 10–18, pl. 2, figs 1–19; text-fig. 4.

1928 *Acrodus spitzbergensis* Corroy, p. 14 (94).

1979 *Acrodus spitzbergensis* Birkenmajer and Jerzmańska, pp. 23–25, fig. 13; pl. 2, figs 3, 7–8.

1996 *Acrodus spitzbergensis* Rieppel, Kindlimann and Bucher, pp. 502–504, fig. 2e–f.

2001 *Acrodus spitzbergensis* Cuny, Rieppel and Sander, pp. 286–287, figs 3A–C, 4A–D.

2004 *Acrodus spitzbergensis* Błażejowski, pp. 160–162, fig. 8.

2004 *Acrodus* sp. e.g. *spitzbergensis* Yamagishi, p. 568, fig. 3.4.

2006 *Acrodus* cf. *spitzbergensis* Yamagishi, pp. 65–67, pl. 1, figs C–F.

Material. Samples 300311-I, 300311-J, 300311-K, 05.7.15.k, Kamura Formation, yielded 13 complete and broken specimens. Specimen used for SEM imaging: JP51;

specimen used for light microscopy imaging: JP114; remaining specimens: JP36–37 (tentative), JP52–59, JP72.

Description. One complete anterior tooth is preserved (2.0 mm mesio-distally, 1.3 mm labio-lingually, and 1.4 mm high). Otherwise, only small tooth fragments remain, which measure from 0.5 mm up to approximately 2 mm in maximal labio-lingual dimension. The main cusp is low and almost pyramidal. The lingual crown face shows a bulge at the main cusp, which is of significant size in the anterior tooth, surmounted by a relatively strong crista terminating in the cusp apex. The crown of the anterior tooth is monocuspid and strongly arched, with one extremity falling away from the centre at an angle of roughly 45° and the other starting off the same, but curving back towards a horizontal plane near the base, which is the cause of some asymmetry in the tooth. In addition, the lateral extremities are projected labially, causing the apical outline of the tooth to be concave labially and distinctly convex lingually, although the curved extremity aligns with the central axis of the tooth near the very tip. The extremities also appear to be slightly tapering and rounded at the end. The crown surface ornamentation consists of well-developed anastomosing cristae, which are especially strongly developed on the main cusp, creating a very rough texture on the crown surface. The cristae generally follow a transverse orientation, although they may be oriented away from the main cusp to a variable degree. A longitudinal crest is developed, which may be either single (anterior teeth) or double (lateral teeth). In the latter case, the two crests are separated by a longitudinal groove, and the transverse cristae terminate in an undulating ridge positioned low on the labial face and in a series of two undulating ridges positioned high on the lingual face. The crown/base junction is significantly incised, causing a shelf-like underside of the protruding crown. If the base is placed on a horizontal plane, the crown is angled downwards labially, causing the crown/base junction on that side to be largely obscured from view, whereas it is well-exposed on the lingual side.

The base is shallow and arched to the same degree as the crown. It is perforated by randomly located foramina, of which a few larger ones appear on both the lingual and labial face. The basal face is flat to slightly concave.

Remarks. The material recovered in addition to the anterior tooth is of a very fragmentary nature, which means that the main feature that could be observed in these specimens is the crown surface ornamentation. As a result of this, it could be established that some of the fragments originally belonged to lateral teeth. In these tooth fragments, the tentative interpretation of the labial and lingual faces is based on comparison with Rieppel *et al.* (1996, fig. 2e–f).

The material described here is assigned to *Acrodus spitzbergensis* Hulke, 1873 based on the recognition of a general morphological resemblance to and characteristics known to be typical of the taxon. These include the arching of the anterior teeth, the presence of a longitudinal crest and distinct transverse crest, as well as the shallow nature and similar arching of the base (Stensiö 1921). Gradual heterodonty in this species was remarked by Stensiö (1921) and its presence in the Japanese material can be determined upon comparing the anterior tooth described here with the anterolateral tooth imaged by Yamagishi (2004, fig. 3.4a, b), in which the arching is less, but a similar lateral outline can be seen.

The crown ornamentation pattern differs somewhat from the material described by Stensiö (1921), in that the upper half of the crown was often smooth in the material he described. However, the assignment of this material to *Acrodus spitzbergensis* Hulke, 1873 is confirmed by the observation of a double longitudinal crest. This feature was first described on a specimen from the Triassic of Spitsbergen (Hulke 1873) and interpreted by Stensiö (1921), based on further Triassic material from Spitsbergen, as diagnostic of lateral teeth, whereas anterior teeth possessed the usual single longitudinal crest (see also Rieppel *et al.* 1996). The same feature was subsequently observed in Anisian material from northwestern Nevada, USA (Rieppel *et al.* 1996; Cuny *et al.* 2001). *A. spitzbergensis* was tentatively recognised in Lower–Upper

Triassic Japanese deposits (Kyoto and Ehime prefectures) by Yamagishi (2004, 2006), based on material without a double longitudinal crest. The material described from the Kamura Formation in this study therefore confirms the presence of *A. spitzbergensis* in Japan.

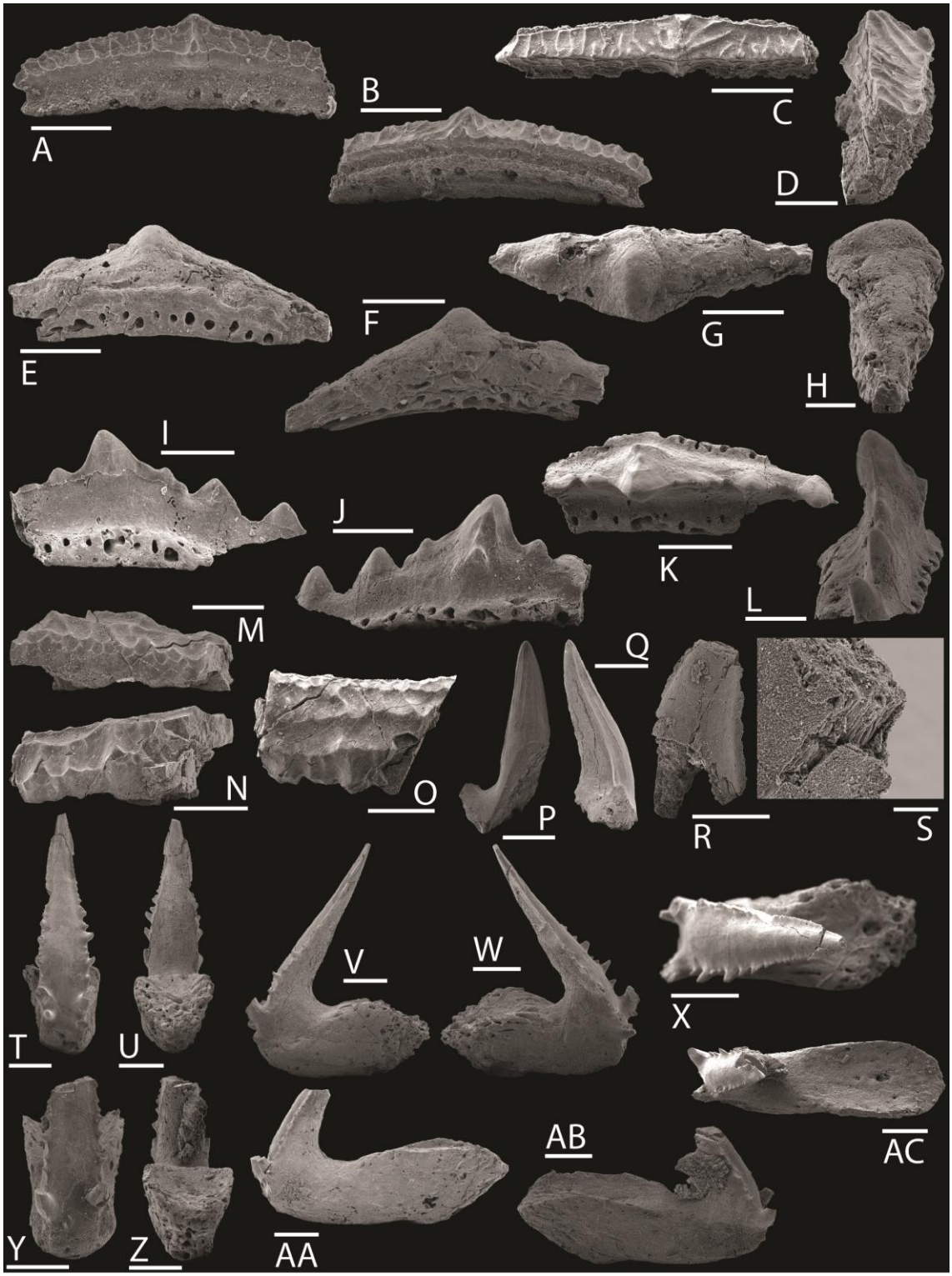

Figure A3.8 – ▲ Chondrichthyan teeth and spines from the Kamura Formation, Miyazaki Prefecture, southwestern Japan. Figs A–D. *Omanoselache* sp. cf. *O.* sp. H. JP2, Shioinouso east, sample 290311-R; tooth. A, lingual, B, labial, and C, apical views; scale bars 400 µm, D, lateral view; scale bar 200 µm. Figs E–H. Hybodontiformes gen. et sp. indet. JP49, Shioinouso east, sample 300311-J; tooth. E, lingual, F, labial, and G, apical views; scale bars 400 µm, H, lateral view; scale bar 200 µm. Figs I–L. Neoselachii gen. et sp. indet. A. JP50, Shioinouso east, sample 300311-J; tooth. I, lingual, J, labial, and K, apical views; scale bars 300 µm, L, lateral view; scale bar 200 µm. Figs M–O. *Acrodus spitzbergensis* Hulke, 1873. JP51, Shioinouso east, sample 300311-J; tooth fragment. M, lingual, N, labial, and O, apical views; scale bars 300 µm. Figs P–Q. Synechodontiformes gen. et sp. indet. JP74, Shioinouso east, sample 300311-K; tooth fragment. P, labial, and Q, lateral views; scale bars 500 µm. Figs R–S. Neoselachii gen. et sp. indet. B. JP84, Shioinouso east, sample 300311-M; tooth fragment. R, lingual/labial view; scale bar 400 µm, and S, detail of enameloid fracture surface; scale bar 50 µm. Figs T–AC. aff. *Arctacanthus exiguus* Yamagishi, 2004. T–X, JP39, Shioinouso east, sample 300311-J; spine. T, anterior, U, posterior, V, lateral, W, lateral, and X, apical views; scale bars 500 µm. Y–AC, JP42, Shioinouso east, sample 300311-J; spine. Y, anterior, Z, posterior, AA, lateral, AB, lateral, and AC, apical views; scale bars 500 µm.

Genus PALAEOBATES Meyer, 1849

Type species. *Strophodus angustissimus* Agassiz, 1838; from an unspecified Triassic locality.

Palaeobates sp.

Material. Sample SV-2, Vikinghøgda Formation, yielded numerous tooth fragments: SV01 (lot number).

Description. The tooth fragments indicate teeth of a mesio-distally elongated oval shape in apical outline of small to medium size (0.4–1.2 mm mesio-distally, 0.1–0.4 mm labio-lingually, and 0.2–0.3 mm high, but larger dimensions may have occurred). The crown is moderately arched, whereas the base is straight to slightly arched. The apical surface is flat, without evidence of cusps or cusplets, and the lateral extremities

are rounded in the outermost part. Labially, the crown shoulder follows the same outline as the base, but on the lingual side, The crown shoulder overhangs the crown/base junction and base slightly on the labial side, yet prominently on the lingual side. Although the apical outline of the crown is generally smooth, one central protuberance was observed on the lingual face in the fragment of a small tooth. The crown ornamentation consists of a single longitudinal crest that runs mesio-distally along the centre of the crown and extends virtually along the entire length, but fades on the mesial/distalmost parts of the extremities. Cristae run from the crest towards the crown shoulder, running vertically in the central part and fanning out to an oblique position towards the extremities. Furthermore, the cristae are well-raised, undulating and frequently anastomose in the region along the central axis of the crown (reticulate pattern), but straighten out towards and subsequently fade near the crown shoulder. The labial and lingual crown faces are, therefore, generally smooth, but in some fragments, small vertical lobes or folds were observed, but the lateral extent and exact position of these could not be determined. Some fragments solely consist of the upper crown layer, revealing the thin nature of the enameloid layer.

The base is high (up to three fourths of the total tooth height) and often remains narrow. The lingual face is distinctly concave, whereas the labial face is straight to slightly convex. A clearly defined basal face is present, which may transition into the labial and lingual faces in an acutely angular manner. The base is porous (sometimes trabecular), perforated by numerous foramina on all aspects, but a row of larger openings occur underneath the crown/base junction on both the lingual and labial faces. The vascularisation type is anaulacorhize.

Remarks. The tooth fragments described here bear great resemblance to both *Acrodus* and *Palaeobates*, two closely related genera with a largely overlapping palaeogeographical distribution. Both genera have also been recorded from the Induan (Dienerian) and Olenekian of Spitsbergen (Stensiö 1921; Birkenmajer and Jerzmańska 1979; Błażejowski 2004; Romano and Brinkmann 2010). The identification as

Palaeobates is preferred for the described material, based on characteristics described by Stensiö (1921) that correspond to features observed here: large, elongate teeth that may become very small posteriorly; flattened crown without lateral cusplets but sometimes with main cusp, and often with longitudinal crest; crown ornamented with fine, very ramified cristae that anastomose and form a reticulate pattern; thin enameloid layer and trabecular dentine in the base. Additional remarks mention a well-defined basal face perpendicular to the height axis and the potential occurrence of round protuberances on one crown face (Stensiö 1921). Romano and Brinkmann (2010) further mentioned the crown overhanging the base sometimes to a considerable extent, and that the ornamentation usually only occurs on the apical crown surface, leaving the lingual and labial faces smooth. Teeth of *Acrodus*, however, usually display an ornamentation with more vertical cristae that follow a less complex pattern and a transverse crest, which continues onto the basal part of the crown, and possess a more obliquely positioned basal surface that may not be distinctly developed (Stensiö 1921; Błażejowski 2004). Although sufficient characteristics could be observed to make a generic identification, as a result of the fragmentary nature of the studied material, no identification at species level is attempted.

Superfamily *INCERTAE SEDIS*

Genus OMANOSELACHE Koot, Cuny, Tintori and Twitchett, 2013

Derivation of name published in Koot *et al.* (2013).

Type species. *Omanoselache hendersoni* Koot, Cuny, Tintori and Twitchett, 2013; from the Wordian (Guadalupian) Khuff Formation in the Haushi-Huqf area, central eastern Oman.

Referred species. 'Polyacrodus' contrarius Johns, Barnes and Orchard, 1997, pp. 31–33, pl. 2, figs 1–14; pl. 3, figs 1–15; *'Polyacrodus' bucheri* Cuny, Rieppel and Sander, 2001, pp. 291–292, figs 3H–J, 4G–H, 5A–C.

Diagnosis (emended from Koot, Cuny, Tintori and Twitchett, 2013). Gradual monognathic heterodont dentition consisting of elongate teeth, which are basally arched and symmetrical anteriorly and asymmetrical (antero)laterally. Moderate main cusp with rounded to bluntly tipped apex. Up to four pairs of well-developed lateral cusplets may be present with additional small cusplets distally in asymmetrical teeth. Longitudinal crest always present, sometimes with crenulations. Strong lingual peg with pronounced surmounting vertical crista. Small labial peg, often indented. Crown surface smooth or with a small number of cristae. Base with lingual protrusion. Anaulacorhize vascularisation with randomly located foramina, which may be enlarged lingually. Labially, a row of small foramina occurs near the crown-base junction in addition to larger foramina opening in the basolabial sulcus.

Distribution. Oman Mountains, northern Oman (this study); central eastern Oman (this study); Bouwn, Timor (Yamagishi 2006); Spiti, India (this study); Kedah, Malaysia (tentative; Yamagishi 2006); Kyushu, Japan (this study); South Primorye, Russia (Yamagishi 2006, 2009); Guizhou Province, China (Chen *et al.* 2007a; this study); BC, Canada (Johns *et al.* 1997); Nevada, California, and Idaho?, USA (Cuny *et al.* 2001; this study).

Stratigraphical range. Wordian, Guadalupian, middle Permian–Carnian, Upper Triassic.

Omanoselache hendersoni Koot, Cuny, Tintori and Twitchett, 2013

Figure A3.3, A–B; Figure A3.9, A–L

Derivation of name and *Type* information published in Koot *et al.* (2013).

Material. Samples AO40, AO55, AO47bis, Khuff Formation, yielded 717 complete and broken specimens. Specimens used for SEM imaging: MPUM10883 (anterior), MPUM10884 (anterolateral) MPUM10885 (lateral); remaining specimens: MPUM10896 (576), MPUM10917 (104), MPUM10936 (34).

Samples 965-2, 965-8, Khuff Formation, yielded 25 complete and broken specimens. Specimens used for SEM imaging: UC20257 (anterior), UC20259, UC20262 (lateral); specimens used for SEM microstructure study: UC20278, UC20285 (anterior), UC20298 (lateral); remaining specimens: UC20255, UC20265, UC20271, UC20275, UC20282, UC20294, UC20299, UC20336, UC20337, UC20356 (anterior), UC20233, UC20264, UC20267, UC20301 (lateral) (tentative anteriors: UC20256, UC20291, UC20311, UC20357).

Diagnosis and *Description* published in Koot *et al.* (2013).

Enameloid microstructure. The enameloid is made up of a homogeneous layer of single crystallites (SCE), which covers the entire surface. The crystallites are rod-shaped, long (1 µm or more) and randomly orientated. Fracture surfaces may show bundling perpendicular to the surface (“pillars”), which is a typical hybodont feature designed to counteract compressive force (Cuny *et al*. 2001).

Remarks published in Koot *et al.* (2013).

Omanoselache angiolinii Koot, Cuny, Tintori and Twitchett, 2013

Figure A3.9, M–X

Derivation of name and *Type* information published in Koot *et al.* (2013).

Material. Samples AO40, AO55, AO47bis, AO50, Khuff Formation, yielded 86 complete and broken specimens. Specimens used for SEM imaging: MPUM10929 (anterior), MPUM10887 (anterolateral) MPUM10930 (lateral); remaining specimens: MPUM10898 (34), MPUM10919 (25), MPUM10938 (19), MPUM10949 (5).

Sample 965-2, Khuff Formation, yielded one specimen: UC20273.

Samples 969-5, 969-6, Saiq Formation, yielded three broken specimens: UC20391, UC20400, UC20401.

Samples 110219-E, 110219-M, Saiq Formation, yielded three complete and broken specimens: OM28–29, OM67.

Diagnosis, *Description* and *Remarks* published in Koot *et al.* (2013).

Omanoselache sp. H

Figure A3.10, A–AB; Figure A3.11, O–Q

Preliminary holotype. One complete tooth (GSC135704, Figure A3.10, A–D).

Preliminary paratypes. Two complete teeth (GSC135650, Figure A3.10, E–H; GSC135628, Figure A3.10, Y–AB).

Preliminary type locality. Jabel Safra, Oman Mountains, Sultanate of Oman.

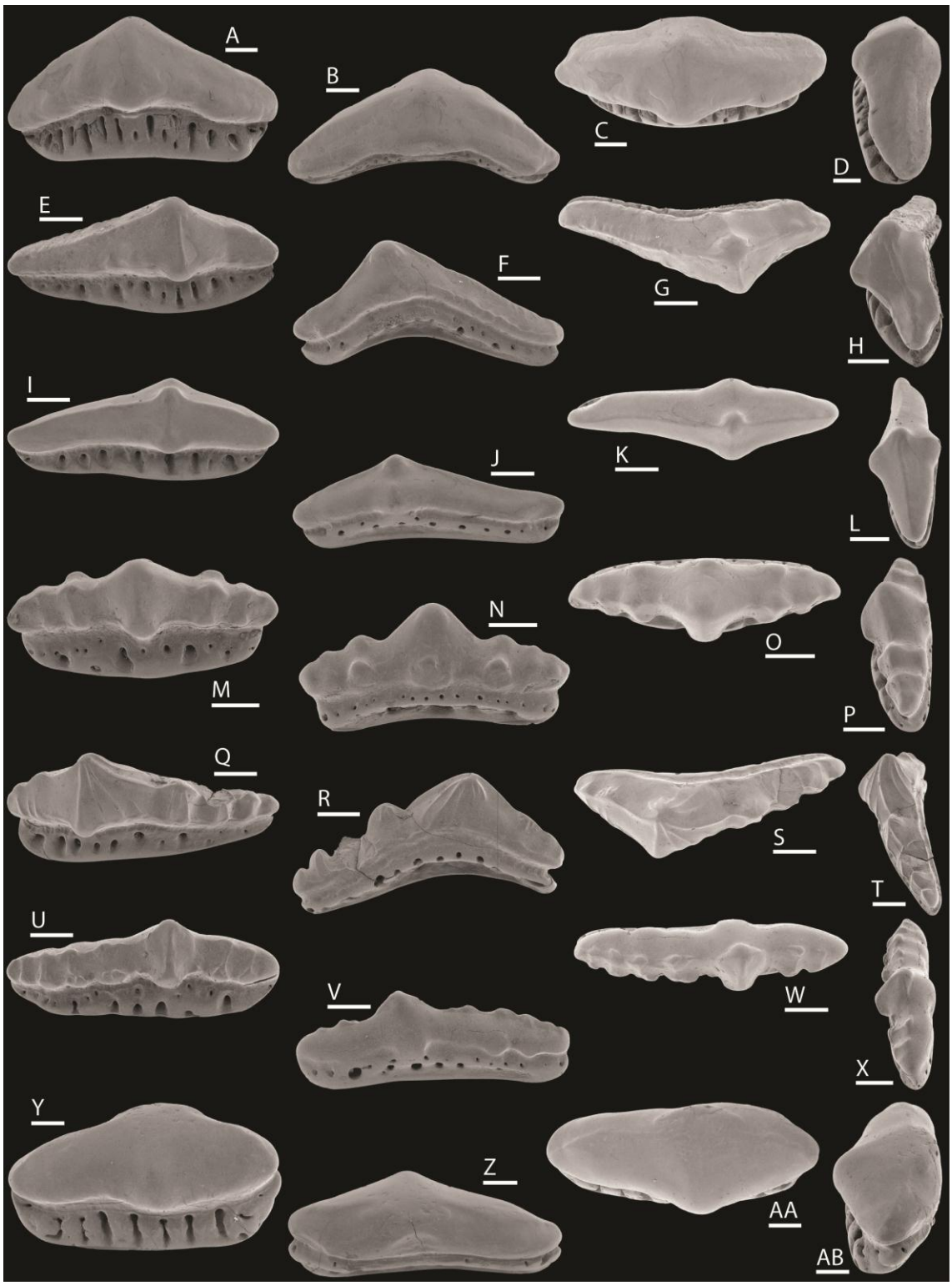

Figure A3.9 – Hybodont teeth from the Khuff Formation, Haushi Cliff, Haushi-Huqf area, central eastern Oman. Figs A–L. *Omanoselache hendersoni* Koot, Cuny, Tintori and Twitchett, 2013. A–D, MPUM10883, loc K1, sample AO40; tooth, paratype. A, lingual, B, labial, C, apical, and D, lateral views; scale bars 300 µm. E–H, MPUM10884, loc K1, sample AO40; tooth, holotype. E, lingual, F, labial, G, apical, and H, lateral views; scale bars 300 µm. I–L, MPUM10885, loc K1, sample AO40; tooth, paratype. I, lingual, J, labial, K, apical, and L, lateral views; scale bars 300 µm. Figs M–X. *Omanoselache angiolinii* Koot, Cuny, Tintori and Twitchett, 2013. M–P, MPUM10929, loc K4, sample AO47bis; tooth, paratype. M, lingual, N, labial, O,

apical, and P, lateral views; scale bars 300 µm. Q–T, MPUM10887, loc K1, sample AO40; tooth, holotype. Q, lingual, R, labial, S, apical, and T, lateral views; scale bars 300 µm. U–X, MPUM10930, loc K4, sample AO47bis; tooth, paratype. U, lingual, V, labial, W, apical, and X, lateral views; scale bars 300 µm. Figs Y–AB. cf. *Omanoselache* sp. MPUM10886, loc K1, sample AO40; tooth. Y, lingual, Z, labial, AA, apical, and AB, lateral views; scale bars 300 µm.

Preliminary type stratum. Red limestone (Hallstatt-type) olistolith, Block 3, Oman Exotics, Kawr Group?, Hawasina Allochthonous, Spathian (upper Olenekian, Lower Triassic).

Material. Samples 103A, 103C, 104A, C85314, 118B, Hallstatt-type limestone olistoliths and Alwa Formation, yielded 15 complete and broken specimens. Specimens used for SEM imaging: GSC135704 (anterior), GSC135650, GSC135770 (anterolateral), GSC135865 (lateral), GSC135628, GSC135727, GSC135869 (posterior); specimens used for SEM microstructure study: GSC135655, GSC135793; remaining specimens: GSC135691, GSC135722, GSC135729, GSC135815, GSC135870, GSC135880.

Referred material. Lissodus sp.1; Yamagishi 2006: p. 79, pl. 5 B–D; *Polyacrodus* sp.2; Yamagishi 2006: p. 81, pl. 6 A–C; *Synechodus* sp.1; Yamagishi 2006 (in part): pp. 90–92, pl. 9 E–F.

Preliminary diagnosis. Pyramidal main cusp with bluntly tipped apex, which may be slanted distally, and cuspidate crown. Lateral cusplets much reduced in posterior teeth. One extremity may be turned labially or lingually. Strong and apico-basally extensive lingual peg. Numerous nodes on the crown shoulder, joined by a circumferential rim. Well-developed cristae. Vascularisation anaulacorhize but may resemble the pseudopolyaulacorhize type.

Description. Small and elongate teeth (0.8–1.9 mm mesio-distally, 0.2–0.5 mm labio-lingually and 0.2–0.6 mm high) with a fusiform apical outline and one extremity being more rounded. The opposite extremity may be turned labially or lingually, which is often clearly observed in posterior teeth. In apical view, both the labial and lingual basal edge are generally straight, but may be convex lingually. The base is variable in height, but normally constitues 30–50% of the total tooth height. Gradient monognathic heterodonty is recognised with symmetrical anterior teeth and asymmetrical (antero)lateral and posterior teeth. The crown in (antero)lateral teeth is distinctly arched and also the base is moderately arched in anterolaterals. Anterolateral teeth have the greatest mesio-distal dimension, but the teeth generally become smaller in all dimensions from the anterior towards the posterior. The main cusp is pyramidal in shape with a bluntly tipped to rounded apex, may be distally slanted and is always higher than the lateral cusplets. Three to five pairs of cusplets (or unequal in number) are usually clearly distinguishable in anterior to anterolateral teeth, but up to nine may be present in very reduced form. The lateral cusplets remain low and are not well separated at the base. They are oriented vertically or slightly directed lingually. All cusps are considerably reduced in posterior teeth. An acute longitudinal crest traverses the cusp apices along the entire mesio-distal dimension of the teeth. A very well-developed peg is present lingually on the main cusp, which is apico-basally extensive. It is surmounted by a strong vertical crista connecting it to the cusp apex, which may bifurcate near the base, especially in anterior teeth. Labially, a node to small peg is developed, which, in anterolaterals, is off-set from the centre and the cusp face is slightly concave. Numerous nodes are present on the lingual and labial crown shoulders, although better developed lingually and generally in association with the lateral cusplets. The nodes are connected by longitudinal ridges, which make up an entire and well-raised circumferential rim. In anterolateral teeth, this rim is U-shaped on the labial face of the main cusp. All pegs and nodes are reduced in posterior teeth. The ornamentation consists of 1–2 straight or oblique vertical cristae per cusp on both lingual and labial faces connecting the nodes and cusp apices. In rare occurrences, the

cristae anastomose just below the apex. The crown surface is otherwise smooth. The crown/base junction is slightly incised.

The base protrudes beyond the crown lingually. Randomly located foramina of varying size occur lingually. Small foramina are randomly located labially, but larger foramina terminate near or on the labio-basal edge, sometimes causing the basal edge to appear corrugated. The vascularisation is anaulacorhize but may in cases resemble the pseudopolyaulacorhize type with parallel canals that are open on the labialmost part of the basal face.

Enameloid microstructure. The enameloid is made up of a homogeneous layer of single crystallites (SCE), which covers the entire surface. The crystallites are rod-shaped, 0.5–1 µm in length and randomly orientated. Exposure of deeper enameloid layers and examination of fracture surfaces showed that the SCE persists throughout.

Remarks. The material in this taxon is assigned to *Omanoselache* because it matches the following diagnosed characters for the genus: gradual monognathic heterodont dentition; symmetrical anteriorly and asymmetrical (antero)laterally; basal arching; well-developed longitudinal crest; strong lingual peg; small labial peg that may be indented; ornamentation pattern, lingually protruding base; and anaulacorhize vascularisation. It further matches the hypothesised interlocking tooth arrangement for teeth of *Omanoselache* with an off-set labial node in anterolaterals, combined with a U-shaped rim and slightly concave face of the main cusp, creating accommodation space for the lingual peg of the succeeding tooth. This material has been assigned to a new species, because it differs from both the named species in this genus, *O. hendersoni* Koot, Cuny, Tintori and Twitchett, 2013 and *O. angiolinii* Koot, Cuny, Tintori and Twitchett, 2013, with regard to the larger number of lateral cusplets, the stronger ornamentation, and the presence of numerous nodes joined by a raised circumferential rim at the crown shoulder.

The hybodontiform affinity of *Omanoselache* is here again illustrated by the presence of anaulacorhize vascularisation, gradient monognathic heterodonty and a layer of single crystallite enameloid. A missing base in some cases also supports this assignment, although it is not consistent with the general pattern in Mesozoic hybodonts. The resemblance to pseudopolyaulacorhize vascularisation in some teeth may be explained by the fact that the Hybodontiformes and Neoselachii are believed to be sister groups (Klug 2010). Their split has tentatively been placed in the Late Devonian, based on skeletal characteristics (Coates and Gess 2007), but their tooth morphologies did not start to diverge significantly until the Middle Triassic (Andreev and Cuny 2012). Anaulacorhize vascularisation has been recognised among Triassic neoselachians (Andreev and Cuny 2012) and some of their dentitions possessed transitional morphologies (see Johns *et al.* 1997).

Johns *et al.* (1997) described *'Polyacrodus' contrarius* Johns, Barnes and Orchard, 1997, which was grouped with '*P.*' *bucheri* Cuny, Rieppel and Sander, 2001 and placed in the family Homalodontidae by Mutter *et al.* (2007a; 2008a) without official generic assignment while awaiting further taxonomic revision of '*Polyacrodus*'. These species require assignment to a new genus to reflect their new systematic position and to underline their separation from the poorly defined genus '*Polyacrodus*'. Diagnostic characteristics for this new genus would include: heterodont dentition with low, pyramidal main cusp but higher than the reduced lateral cusplets, which may also be absent; well-developed lingual peg in anterior and lateral teeth, but weaker to absent in posterior teeth; crown sparsely ornamented with vertical ridges, connecting the longitudinal crest with the crown shoulder, which may possess many reduced nodes joined by a circumferential rim; and basal vascularisation anaulacorhize. All these characteristics fit with *Omanoselache*, which is why both species are here referred to this genus. They consitute later representatives of the group, because *'P.' contrarius*' oldest record to date was from the Ladinian (Middle Triassic; Johns *et al.* 1997) and *'P.' bucheri* is known from the Anisian (Middle Triassic; Cuny *et al.* 2001). The characteristic of blunt posterior teeth is also present in the Homalodontidae (Mutter *et*

al. 2007a), but the monocuspid mesial teeth of homalodontid dentitions does not fit with *Omanoselache*. Further revision of comparable Mesozoic taxa may provide the necessary insight to establish the relationships between these taxa.

There are a number of similarities between *'P.' contrarius* and *O.* sp. H, especially with regard to posterior teeth because of the reduced lateral cusplets and consequently their blunt appearance. Both dentitions further characteristically share a raised rim and numerous nodes at the crown shoulder, above a slightly incised crown shoulder. The teeth are at least moderately arched and display lateral cusplets that may be vertically oriented or somewhat inclined lingually. The ornamentation also compares well with regard to vertical cristae associated with the nodes and the basally bifurcated crista surmounting the lingual peg. Despite these similarities, confirming once more their rightful place in the same genus, both sets of material cannot be assigned to one single species. Differences of *'P.' contrarius* from *O.* sp. H warranting this separation include: smaller tooth dimensions; crown height equal to or smaller than base; lateral cusplets always more reduced, also in anterior teeth; longitudinal crest lingually off-set, causing the labial face to be enlarged and gradually sloping, whereas the lingual face is reduced and steeply inclined; and concavities in the crown surface in between vertical cristae. The off-set longitudinal crest and depressed crown surface is observed, however, in other occurrences of *Omanoselache* globally (e.g., *O.* sp. cf. *O.* sp. H, *Omanoselache* sp. A; this study).

Examination of five complete and fragmented teeth from Wadi Wasit, originally studied by Yamagishi (2006) and referred to *Lissodus* sp.1, has shown that the material should be re-assigned to *O.* sp. H. The bases of the teeth are mostly lacking, but the crown morphology is identical to the posterior teeth of *O.* sp. H and the size of the specimens ($\leq$1.2 mm) also corresponds to the smaller end of the spectrum observed in *O.* sp. H. Yamagishi's (2006) interpretation of the peg on the main cusp as labial is believed to be inaccurate and is interpreted as lingual instead. Having been recovered from late Griesbachian deposits (*Clarkina carinata* conodont Zone), these teeth represent the oldest occurrence of the species.

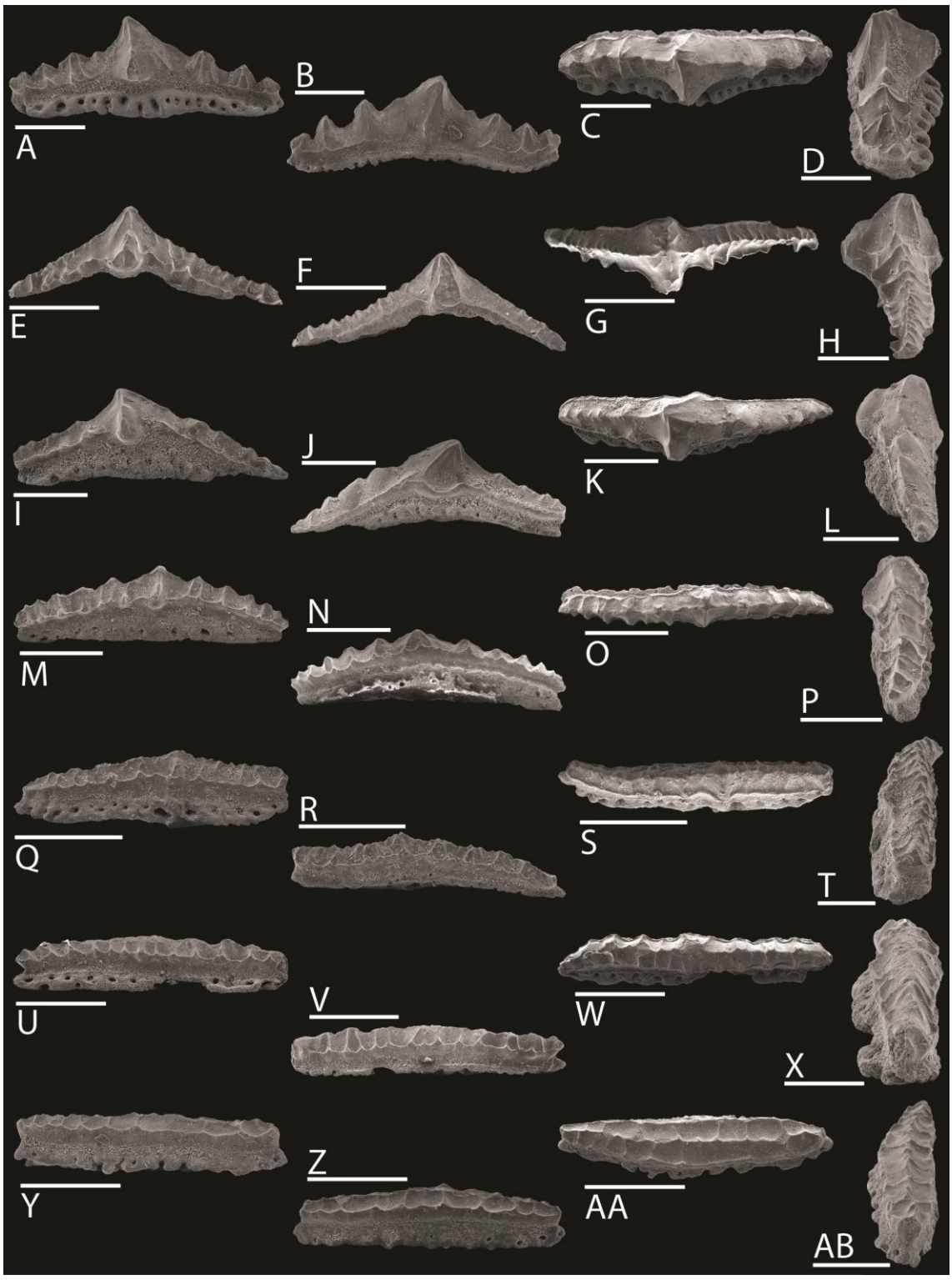

Figure A3.10 – Hybodont teeth from the Hallstatt-type limestone olistoliths at Jabel Safra and Alwa Formation at Wadi Alwa, Oman Mountains, northern Oman. Figs A–AB. *Omanoselache* sp. H. A–D, GSC135704, sample 103C, Jabel Safra; tooth, holotype. A, lingual, B, labial, C, apical views; scale bars 500 µm, and D, lateral view; scale bar 400 µm. E–H, GSC135650, sample 103A, Jabel Safra; tooth, paratype. E, lingual, F, labial, G, apical views; scale bars 500 µm, and H, lateral view; scale bar 300 µm. I–L, GSC135770, sample 104A, Jabel Safra; tooth. I, lingual, J, labial, K, apical views; scale bars 500 µm, and L, lateral view; scale bar 400 µm. M–P, GSC135865, sample C85314, Wadi Alwa; tooth. M, lingual, N,

labial, O, apical views; scale bars 500 µm, and P, lateral view; scale bar 300 µm. Q–T, GSC135727, sample 103C, Jabel Safra; tooth. Q, lingual, R, labial, S, apical views; scale bars 500 µm, and T, lateral view; scale bar 200 µm. U–X, GSC135869, sample C85314, Wadi Alwa; tooth. U, lingual, V, labial, W, apical views; scale bars 400 µm, and X, lateral view; scale bar 200 µm. Y–AB, GSC135628, sample 103A, Jabel Safra; tooth, paratype. Y, lingual, Z, labial, AA, apical views; scale bars 300 µm, and AB, lateral view; scale bar 200 µm.

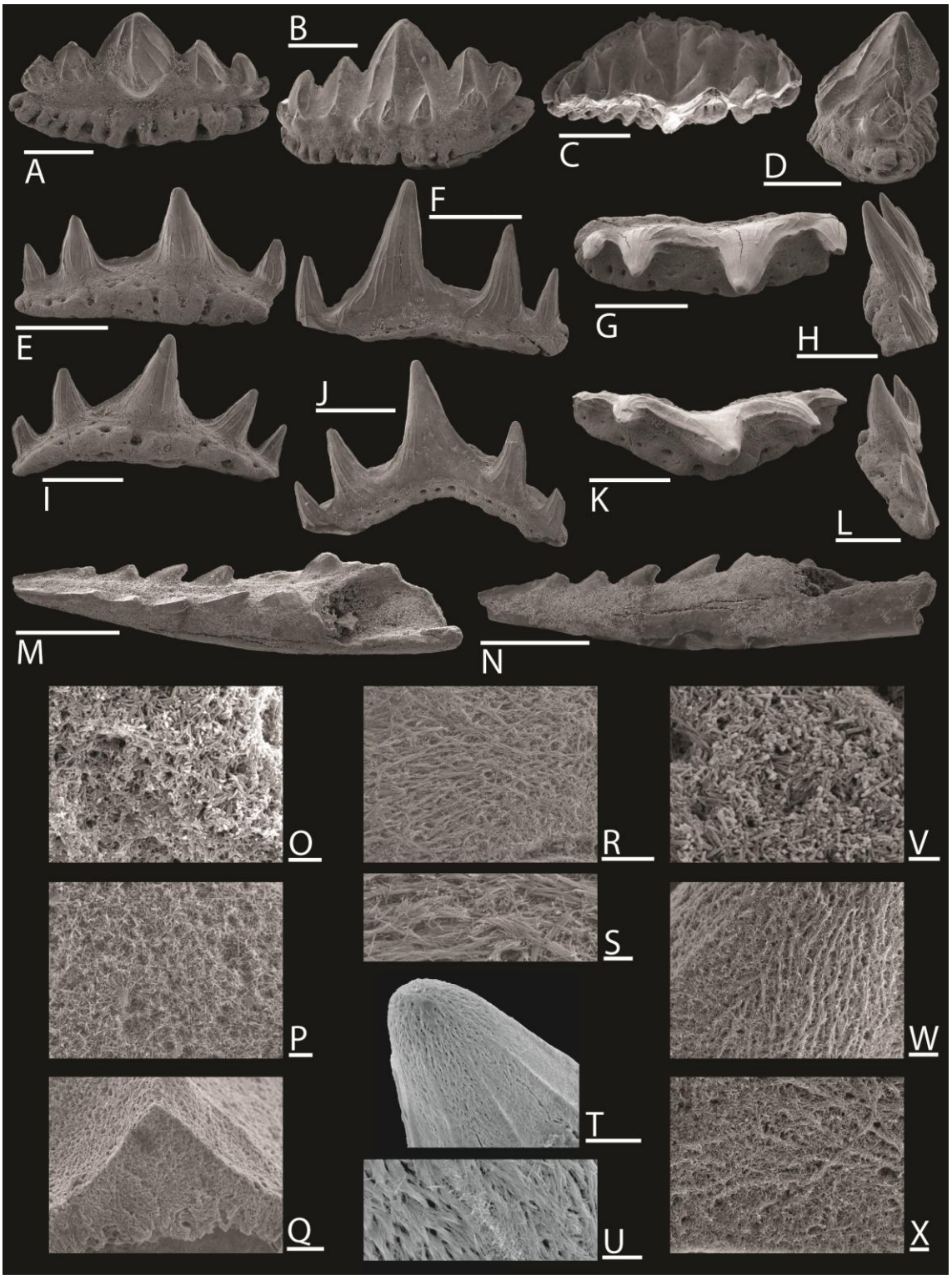

Figure A3.11 – ◄ Euselachian and synechodontiform teeth and a neoselachian fin spine from the Hallstatt-type limestone olistoliths at Jabel Safra and Alwa Formation at Wadi Alwa, Oman Mountains, northern Oman. Figs A–D. Euselachii gen. et sp. indet. B, GSC135659, sample 103B, Jabel Safra; tooth. A, lingual, B, labial, C, apical, and D, lateral views; scale bars 500 µm. Figs E–L. Genus S sp. A. E–H, GSC135709, sample 103C, Jabel Safra; tooth. E, lingual, F, labial, G, apical, and H, lateral views; scale bars 500 µm. I–L, GSC135724, sample 103C, Jabel Safra; tooth. I, lingual, J, labial, K, apical, and L, lateral views; scale bars 500 µm. Figs M–N. cf. *Amelacanthus* sp., GSC135736, sample 103C, Jabel Safra; fin spine. M, lateral, and N, anterior views; scale bars 500 µm. Figs O–Q. *Omanoselache* sp. H. O, GSC135655, sample 103A, Jabel Safra; tooth, single crystallite enameloid in surface detail near longitudinal crest; scale bar 1 µm. P–Q, GSC135793, sample 104A, Jabel Safra; tooth. P, single crystallite enameloid in surface detail on main cusp; scale bar 2 µm, and Q, homogeneous single crystallite enameloid in fracture surface through longitudinal crest; scale bar 10 µm. Figs R–U. Genus S sp. T. R–S, GSC135740, sample 103C, Jabel Safra; tooth. R, primitive bundled enameloid in surface detail of labial face of apical main cusp; scale bar 10 µm, and S, detail of R; scale bar 2 µm. T–U, GSC135866, sample C85314, Wadi Alwa; tooth. T, parallel-bundled enameloid and cristae of single crystallite enameloid in first lateral cusplet from main cusp; scale bar 30 µm, and U, detail of T; scale bar 5 µm. Figs V–X. *G*enus P sp. P. V, GSC135820, sample 104A, Jabel Safra; tooth, single crystallite enameloid in surface detail of labial face of apical main cusp; scale bar 1 µm. W–X, GSC135630, sample 103A, Jabel Safra; tooth. W, primitive bundled enameloid in surface detail of labial face of main cusp apex; scale bar 5 µm, and X, detail of dissolving crystallite bundle in surface detail of labial face of apical main cusp; scale bar 2 µm.

Omanoselache sp. cf. *O.* sp. H (Japan)

Figure A3.8, A–D

Material. Samples 290311-R, 05.7.14.ak, Kamura Formation, yielded two complete and broken specimens. Specimen used for SEM imaging: JP2; specimen used for light microscopy imaging: JP96.

Description. Small and mesio-distally elongated teeth (1.6–2.2 mm mesio-distally, minimum dimension incomplete; 0.3 mm labio-lingually; and 0.5 mm high), with slight apico-basal arching. The incomplete specimen appears symmetrical, whereas the complete specimen shows slight asymmetry. The crown is of roughly equal height as

the base and the crown-base junction is slightly incised. The crown is multicuspid with a pyramidal main cusp, which is blunt and remains low, and with minimally four well-defined or numerous, but much reduced, lateral cusplets. The main cusp bears a strong peg basally on its lingual face, with a pronounced surmounting crista, which terminates in the cusp apex. On the labial face, there is evidence of a small labial peg. The longitudinal crest is acute and may be somewhat lingually off-set, causing the lingual face of the crown to be steeply inclined, whereas the labial face is gradually sloping. Numerous well-developed cristae ornament the crown surface, which is otherwise smooth. The crown surface of the complete specimen is smooth, but appears generally worn down. The cristae generally connect the longitudinal crest with the crown shoulder, following a slightly wavy pattern, but often terminate prematurely on the labial face. Also, on the labial face of the main cusp, the cristae are directed away from the vertical and are oriented towards the cusp apex. Small nodes are associated with the cristae along the crown shoulder, which are linked by U-shaped ridges, essentially creating a circumferential rim. Labially, this rim is strongly developed and somewhat raised apically.

The base shows a distinct lingual protrusion and a large basolabial sulcus. Few large foramina randomly penetrate the lingual face. Labially, a single row of large foramina opens on the baso-labial edge of the sulcus, in addition to a discontinuous row of small foramina near the crown-base junction. The vascularisation is anaulacorhize.

Remarks. These teeth fit all the diagnosed characters of *Omanoselache*. Most markedly with regard to the apico-basal arching and the low, pyramidal main cusp with a strong lingual peg at its base, which is why the specimens are assigned to this genus. Of the species assigned to *Omanoselache*, the teeth bear the closest affinity with *O.* sp. H, based on the large number of reduced lateral cusplets. However, some doubt is introduced by the particularly strong development of the vertical cristae in one of the teeth described here and also the strong inclination of the lingual crown face, which is why the material is listed as *Omanoselache* sp. cf. *O.* sp. H.

Omanoselache sp. cf. *O.* sp. H (China)

Material. Samples O-10, Luolou Formation, O-27, GQC-173, GQC-182, Xinyuan Formation, yielded eight complete and broken specimens: 368, 401, 425–426, 428, 430–432.

Description. Small and elongate teeth (1.5–2.2 mm mesio-distally, 0.3 mm labio-lingually and 0.5 mm high) with moderate basal arching and some heterodonty, most clearly observed in the symmetry versus slight asymmetry in the material. The teeth are polycuspid, with a low and blunt, pyramidal main cusp and up to four pairs of low to reduced lateral cusplets. In asymmetrical teeth, the number of lateral cusplets is unequal on both extremities (e.g., two mesially and three distally). A well-developed and apico-basally extensive lingual peg is present on the main cusp, surmounted by a strong vertical crista terminating in the cusp apex. A small peg is present labially, also surmounted by a vertical crista. An acute longitudinal crest traverses the entire mesio-distal dimension of the teeth and small to moderate nodes are developed at the crown shoulder both labially and lingually, which are joined by a raised circumferential rim that can be relatively straight or form small U-shapes in between nodes in lateral view. Vertical cristae are present, few in number but very pronounced, to the extent that the remainder of the smooth crown surface appears depressed. They are mainly associated with the cusps, connecting the apices with the crown shoulder, and can be single or split into two, diverging from the cusp apex. The crown/base junction is moderately incised.

The base protrudes beyond the crown lingually and possesses a large baso-labial sulcus. It is penetrated by multiple randomly located foramina, which are larger lingually than labially and also open in the sulcus. The vascularisation is of the anaulacorhize type.

Remarks. All the diagnostic characteristics of *Omanoselache* are recognised in this material. The described material bears most affinity to *O.* sp. H, including the cuspidate crown with potentially reduced lateral cusplets and numerous nodes at the crown shoulder. The lateral cusplets appear, however, to be more individually defined (wider spaced) and the cristae are stronger developed, to the extent that the intermediate crown surface appears retracted. The limited nature of the material prevents adequate assessment of the importance of these features, which is why this material remains listed as *Omanoselache* sp. cf. *O.* sp. H. In comparison with the Japanese tooth, the Chinese material differs in the sense that the lateral cusplets are more pronounced and there are fewer vertical cristae. The teeth further possess somewhat larger nodes and a more protruding circumferential rim, especially lingually. With that, the lingual crown face is less steeply inclined, but shows recesses in between the cristae. Based on these differences, the Japanese and Chinese material cannot be considered the same.

Omanoselache sp. cf. *O.* sp. H (southwestern USA)

Figure A3.12, A–D

Material. Samples 92-OF DC10, Union Wash Formation, 89 OF HB236, Prida Formation, yielded three broken specimens. Specimen used for SEM imaging: 298; remaining specimens: 299, 330 (tentative).

Description. Small and elongate teeth (1.6 mm mesio-distally, 0.4 mm labio-lingually, and 0.4 mm high) with a fusiform apical outline. In apical view, one extremity is curved lingually, causing asymmetry in the teeth. The crown is distinctly arched. The main cusp is pyramidal in shape with a bluntly tipped to rounded apex, which shows minor signs of distal slanting, and is higher than the lateral cusplets, of which three are positioned mesially and at least two distally (extremity damaged). The lateral cusplets remain low and are not well separated at the base. They are oriented vertically or

slightly directed lingually. An acute longitudinal crest traverses the cusp apices along the entire mesio-distal dimension of the teeth. A very well-developed peg is present lingually on the main cusp, which is apico-basally extensive and surmounted by a strong vertical crista connecting it to the cusp apex, and labially, a small node is developed. Both the peg and node are off-set from the centre, but to opposite sides. Numerous nodes are present on the lingual and labial crown shoulders, which are connected by well-raised (especially laterally) longitudinal ridges that make up an entire circumferential rim. The ornamentation consists of 1–2 straight or oblique vertical cristae per cusp on both lingual and labial faces connecting the nodes and cusp apices. Additional cristae are present on the main cusp labially, but these often terminate prematurely. The crown surface is otherwise smooth. The base is not preserved.

Remarks. A hybodont affinity for the material described here is suggested by the missing base. It is assigned to *Omanoselache*, because it records the following diagnosed characters for the genus: possible asymmetry; basal (and crown) arching; well-developed longitudinal crest; strong lingual peg; and small labial peg or node. It further matches the diagnostic characters specific to *O.* sp. H, including a cuspidate crown with blunt, pyramidal main cusp, which may be slanted distally; one extremity turned labially or lingually; strongly developed lingual peg; numerous nodes on the crown shoulder, joined by a circumferential rim; and well-developed cristae. The assignment remains tentative only because of the additional cristae on the labial face of the main cusp, which are reminiscent of the pattern commonly observed in palaeospinacids. Study of the enameloid microstructure would allow the distinction to be made with certainty if more and better preserved material can be recovered.

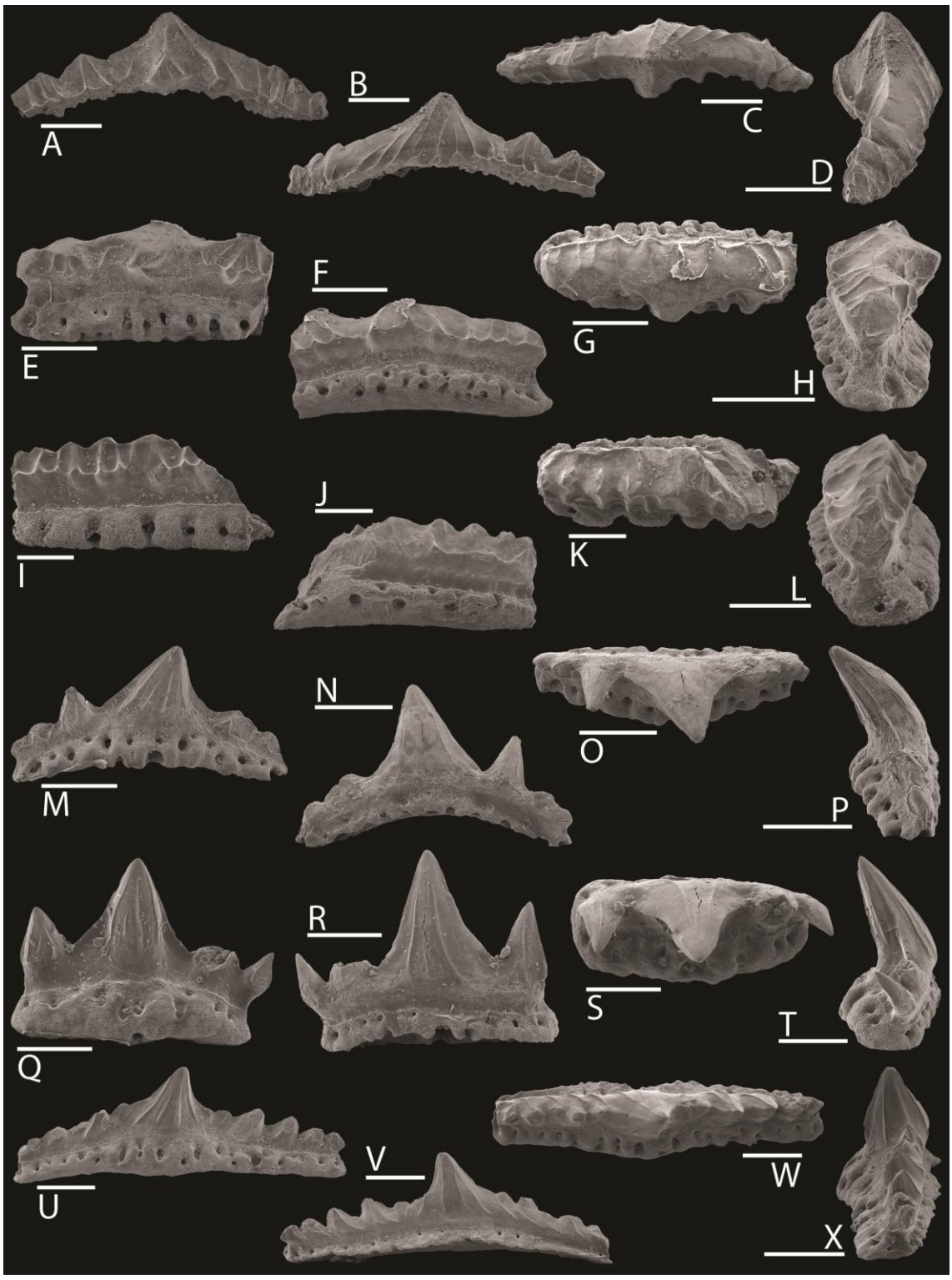

Figure A3.12 – Chondrichthyan teeth from the Union Wash Formation at Darwin Canyon, California, and the Thaynes Formation at Bear Lake, Idaho, southwestern USA. Figs A–D. *Omanoselache* sp. cf. *O.* sp. H. 298, sample 92-OF DC10, Darwin Canyon; tooth. A, lingual, B, labial, C, apical, and D, lateral views; scale bars 300 µm. Figs E–L. cf. *Omanoselache* sp. indet. E–H, 326, sample o-64671 91-OF, Bear Lake; tooth. E, lingual, F, labial, G, apical, and H, lateral views; scale bars 300 µm. I–L, 327, sample o-64671 91-OF, Bear Lake; tooth. I, lingual, J, labial, K, apical, and L, lateral views; scale bars 200 µm. Figs M–P. Genus S sp. T. 292, sample 93 OF W-11, Bear Lake; tooth. M, lingual, N, labial, O, apical, and P, lateral views;

scale bars 300 µm. Figs Q–X. *'Synechodus'* sp. (pre-Jurassic). Q–T, 297, sample 93 OF W-13, Bear Lake; tooth. Q, lingual, R, labial, S, apical, and T, lateral views; scale bars 200 µm. U–X, 293, sample 93 OF W-11, Bear Lake; tooth. U, lingual, V, labial, W, apical, and X, lateral views; scale bars 300 µm.

Omanoselache sp. A (India)

Figure A3.13, A–D

Material. Sample 95-OF GU-1, Tamba Kurkur Formation, yielded one broken specimen. Specimen used for SEM imaging: 450.

Referred material. Polyacrodus sp.3 Yamagishi 2006, p. 83, pl. 6, figs D–G; *Polyacrodus* indet. Yamagishi 2009, p. 202, fig. 158.3–158.6.

Description. The general diagnostic characteristics of the genus are present in the Indian tooth, including mesio-distal elongation and a moderate pyramidal main cusp with a strong lingual peg and surmounting crista. However, this tooth does not show apico-basal arching. The longitudinal crest is very well developed, with a steep lingual face and a more gradually sloping labial face. The crown is multicuspid, but the lateral cusplets are very much reduced. It is ornamented with strong vertical cristae, which are relatively numerous and regular. In the central part of the extremities, the cristae on the lingual and labial faces meet in the longitudinal crest and therefore seemingly traverse the entire labio-lingual width of the tooth. On the main cusp, the cristae are oriented towards the cusp apex on the labial face and towards the strong crista surmounting the peg on the lingual face. Small nodes are associated with the cristae along the crown shoulder, which are linked by weak U-shaped ridges.

The base shows a distinct lingual protrusion and a large basolabial sulcus. The vascularisation is anaulacorhize.

Remarks. All main diagnostic characteristics of *Omanoselache* are observed in the morphology of this material, which therefore warrants inclusion in the genus. Of all the

species assigned to *Omanoselache*, this material bears the closest affinity with *O.* sp. H, based on the large number of reduced lateral cusplets. However, a number of features prevent this tooth to be assigned to the species. This includes the numerous, well-developed and regular nature of the vertical cristae. Also, the fact that the lingual face of the main cusp bears pronounced cristae that meet in the vertical crista surmounting the lingual peg is believed to be a characteristic feature. The importance of the weak development of the circumferential rim and the lack of arching in the tooth cannot be assessed due to the limited nature of the material. This material is believed to belong to a new species, but its designation must await further evidence.

Omanoselache sp. A (China)

Material. Samples O-15, GQC183B, Xinyuan Formation, yielded two broken specimens: 380, 433.

Description. The lateral cusplets are much reduced. The longitudinal crest is lingually off-set, causing the lingual crown face to be steeper than the labial face. In lateral teeth, the cusplets are most significantly reduced and the crown faces approach the horizontal plane. A distinct and slightly raised circumferential rim is present. Numerous and regular vertical cristae appear lingually, leaving the labial face largely smooth, but causing the longitudinal crest to be crenulated.

Remarks. The nature of the material described here is very limited and poorly preserved. Nevertheless, sufficient similarities can be observed to warrant inclusion with *Omanoselache*. It is further attributed to *Omanoselache* sp. A, based on the steepness of the lingual crown face and the large number of regular vertical cristae. Insufficient material is currently available to assess the full range of variation in this taxon and therefore to make an official diagnosis.

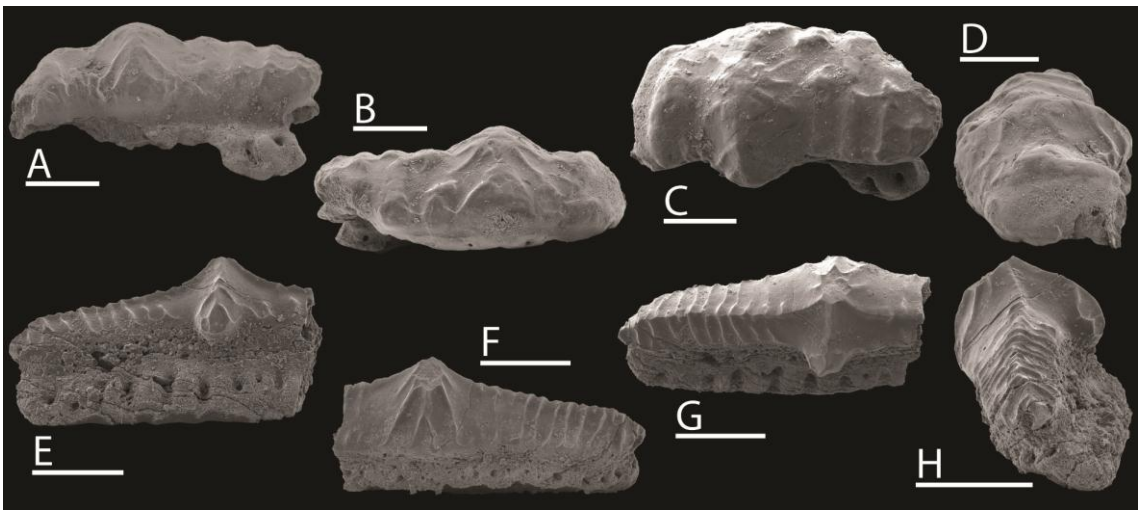

Figure A3.13 – Hybodont teeth from the Saiq Formation at the Saiq Plateau, Oman Mountains, northern Oman and from the Tamba Kurkur Formation at Guling, Spiti, India. Figs A–D. cf. *Omanoselache* sp., OM66, sample 110219-M, Saiq Plateau; tooth. A, lingual, B, labial, C, apical, and D, lateral views; scale bars 500 µm. Figs E–H. *Omanoselache* sp. A, 450, sample 95-OF GU-1, Spiti; tooth. E, lingual, F, labial, G, apical, and H, lateral views; scale bars 500 µm.

Omanoselache sp. cf. *O.* sp. A

Figure A3.14, A–D

Material. Samples O-13, Luolou Formation, O-16, O-18, O-21, O-40, Xinyuan Formation, yielded eight broken specimens. Specimens used for SEM imaging: 387; remaining specimens: 374, 385–386, 389–390, 419, 423.

Description. Elongate teeth of massive appearance (1.8 mm mesio-distally, incomplete dimension; 0.6 mm labio-lingually; and 0.8 mm high) with some asymmetry and very slight basal arching. The base is approximately half the full height of the teeth and exceeds that laterally. The crown is multicuspid with a low main cusp, which is generally pyramidal in shape, although this can be somewhat obscured by the ornamentation, and with at least two pairs of lateral cusplets of decreasing height away from the centre of the tooth. The cusplets are also low, but can be pointed, and although they are not well-separated at the base, they are set apart by depressions in the apical and labial/lingual crown surfaces. The main cusp bears a strong lingual peg

with a well-developed surmounting crista. A labial bulge may also be present, which is followed to a lesser extent in the base, or the labial outline in apical view may be straight. A low and blunt longitudinal crest traverses the entire mesio-distal length of the teeth and is positioned slightly lingually off-centre, causing the lingual crown face to be somewhat steeper than the labial. The ornamentation consists of strong, well-spaced vertical cristae, which radiate from the cusp apices and either terminate early or connect to a weak circumferential rim at the crown shoulder. Two cristae further originate from the crista surmounting the lingual peg and one occasionally originates at the longitudinal crest near the main cusp. The crown/base junction is moderately incised, especially lingually.

The base bears a slight lingual protrusion. There is only very slight evidence of a baso-labial sulcus. Foramina of varying size are randomly located both lingually and labially, as is typical of anaulacorhize vascularisation.

Remarks. The morphological characteristics described here, including the decreasing cusplet height and the anaulacorhize vascularisation, are indicative of a hybodont affinity. Most are also similar to characteristics diagnostic of *Omanoselache*, including the pyramidal main cusp and strong lingual peg. The cristae originating from the strong crista surmounting the lingual peg and the steeper lingual crown face further suggest a potential similarity to *Omanoselache* sp. A. However, because of a lesser regularity in the vertical cristae, which are more oblique here, the assignment of this material remains uncertain.

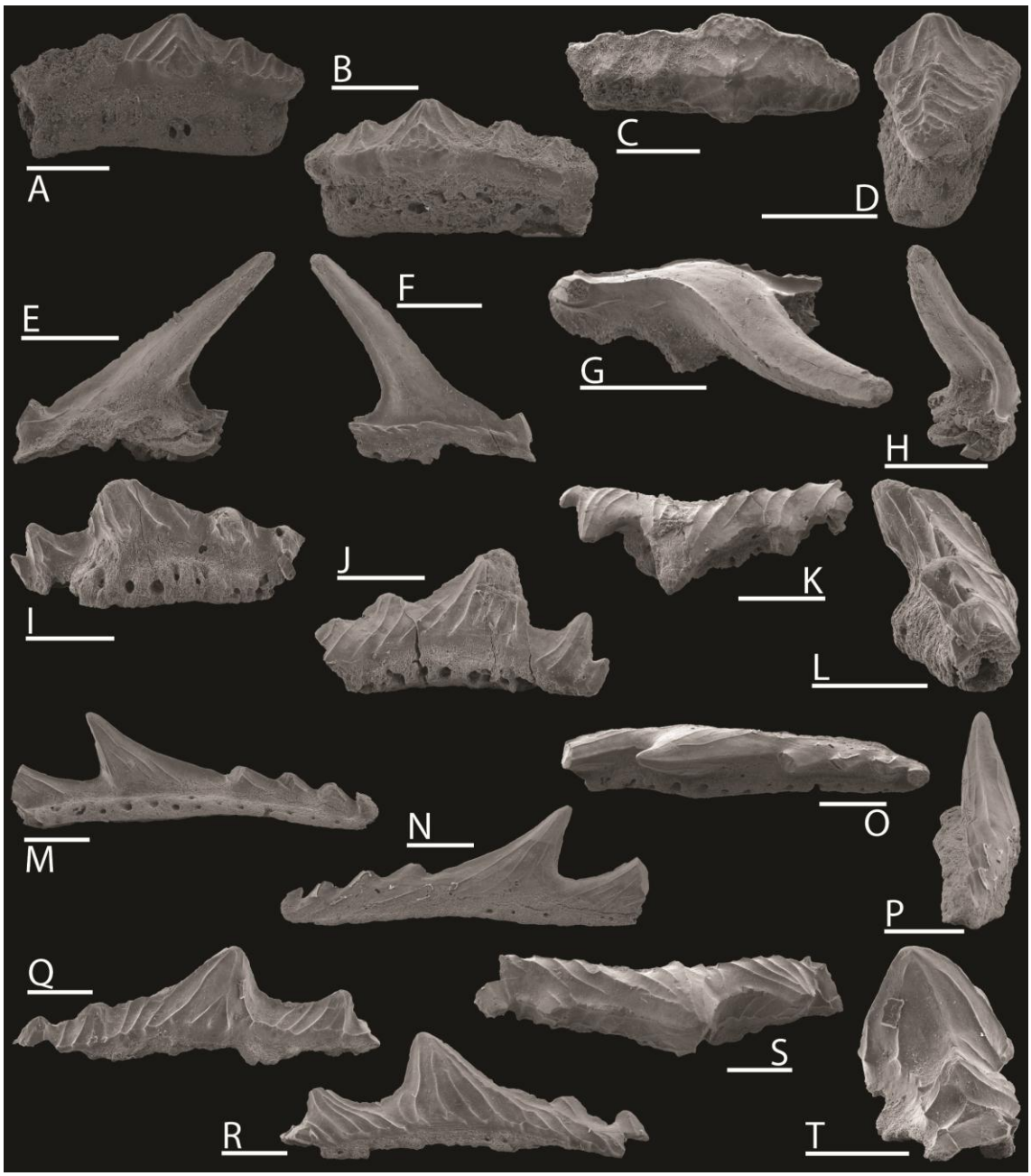

Figure A3.14 – Chondrichthyan teeth from the Xinyuan Formation, Lower Guandao section, Guizhou Province, southern China. Figs A–D. *Omanoselache* sp. cf. *O.* sp. A. 387, sample O-18; tooth. A, lingual, B, labial, C, apical, and D, lateral views; scale bars 500 µm. Figs E–H. cf. *Palidiplospinax* sp. 383, sample O-15; tooth fragment. E, lingual, F, labial, G, apical, and H, lateral views; scale bars 400 µm. Figs I–P. Genus S sp. T. I–L, 406, sample O-29; tooth. I, lingual, J, labial, K, apical, and L, lateral views; scale bars 300 µm. M–P, 412, sample O-34; tooth. M, lingual, N, labial, O, apical, and P, lateral views; scale bars 300 µm. Figs Q–T. *'Synechodus'* sp. (pre-Jurassic). 405, sample O-29; tooth. Q, lingual, R, labial, S, apical, and T, lateral views; scale bars 300 µm.

cf. *Omanoselache* sp. (Oman)

Figure A3.9, Y–AB; Figure A3.13, A–D

Material. Samples AO40, AO55, AO47bis, Khuff Formation, yielded 14 complete and broken specimens. Specimen used for SEM imaging: MPUM10886; remaining specimens: MPUM10897 (4), MPUM10918 (4), MPUM10937 (5).

Sample 110219-M, Saiq Formation, yielded two broken specimens. Specimen used for SEM imaging: OM66; remaining specimen: OM70.

Description and *Remarks* published in Koot *et al.* (2013).

cf. *Omanoselache* sp. (southwestern USA)

Figure A3.12, E–L

Material. Sample o-64671 91-OF, Thaynes Formation, yielded two broken specimens. Specimens used for SEM imaging: 326, 327.

Description. Two damaged tooth fragments (0.9–1.0 mm mesio-distally, incomplete dimension, 0.3–0.4 mm labio-lingually, and 0.4 mm high) from originally elongated and low-crowned teeth. The crown is polycuspid with two to four lateral cusplets and shows evidence of a lingual peg. A blunt longitudinal crest traverses the cusps, which is somewhat off-set lingually, causing the lingual crown face to be more steeply sloping than the labial. Vertical cristae connect to the crest, reaching up from the crown shoulder. The cristae may also be obliquely oriented towards the cusp apices. The crown shoulder is ornamented with a distinct and raised circumferential rim. Nodes are also developed, especially lingually.

The base protrudes beyond the crown lingually and also displays a smaller protrusion labially. Foramina of variable size open randomly on the lingual face.

Labially, a slight baso-labial sulcus appears with foramina appearing just inside it and smaller foramina positioned above, near the crown/base junction. The vascularisation is anaulacorhize.

Remarks. The fragmented nature of this material makes any reliable identification difficult. Nevertheless, a hybodont affinity is suggested by the anaulacorhize basal vascularisation. In light of the identifications made on western North American material in this study and in previous work on later Triassic material (e.g., Sosson and Martin 1985; Rieppel *et al.* 1996; and Cuny *et al.* 2001), it is suggested that the teeth described here are closest in morphology to '*Polyacrodus*', i.e., *Omanoselache*. This is corroborated by the polycuspid crown, the potentially large lingual peg, and the presence of a well-developed circumferential rim. This identification must remain tentative, however, until better preserved material can be recovered.

Genus REESODUS Koot, Cuny, Tintori and Twitchett, 2013

Derivation of name published in Koot *et al.* (2013).

Type species. *Reesodus underwoodi* Koot, Cuny, Tintori and Twitchett, 2013.; from the Wordian (Guadalupian) Khuff Formation of the Haushi-Huqf area, central eastern Oman.

Referred species. '*Lissodus*' *wirksworthensis* Duffin, 1985; '*Lissodus*' *pectinatus* Lebedev, 1996; '*Lissodus*' sp. in Ivanov (1996).

Diagnosis and *Remarks* published in Koot *et al.* (2013).

Distribution. Derbyshire, central England (Duffin 1985); western and central Russia (Lebedev 1996; Ivanov 1996); central eastern Oman (this study).

Stratigraphical range. Tournaisian, Mississippian, early Carboniferous–Wordian, Guadalupian, middle Permian.

Reesodus underwoodi Koot, Cuny, Tintori and Twitchett, 2013

Figure A3.15, A–D

Derivation of name and *Type* information published in Koot *et al.* (2013).

Material. Sample AO40, Khuff Formation, yielded six complete specimens. Specimen used for SEM imaging: MPUM10891; remaining specimens: MPUM10899 (5).

Samples 965-1, 965-2, Khuff Formation, yielded six complete and broken specimens. Specimens used for SEM imaging: UC20231, UC20269, UC20290; remaining specimens: UC20234, UC20235, UC20324.

Diagnosis, *Description* and *Remarks* published in Koot *et al.* (2013).

Genus TERESODUS Koot, Cuny, Tintori and Twitchett, 2013

Derivation of name published in Koot *et al.* (2013).

Type species. *Teresodus amplexus* Koot, Cuny, Tintori and Twitchett, 2013; from the Wordian (Guadalupian) Khuff Formation of the Haushi-Huqf area, central eastern Oman.

Diagnosis published in Koot *et al.* (2013).

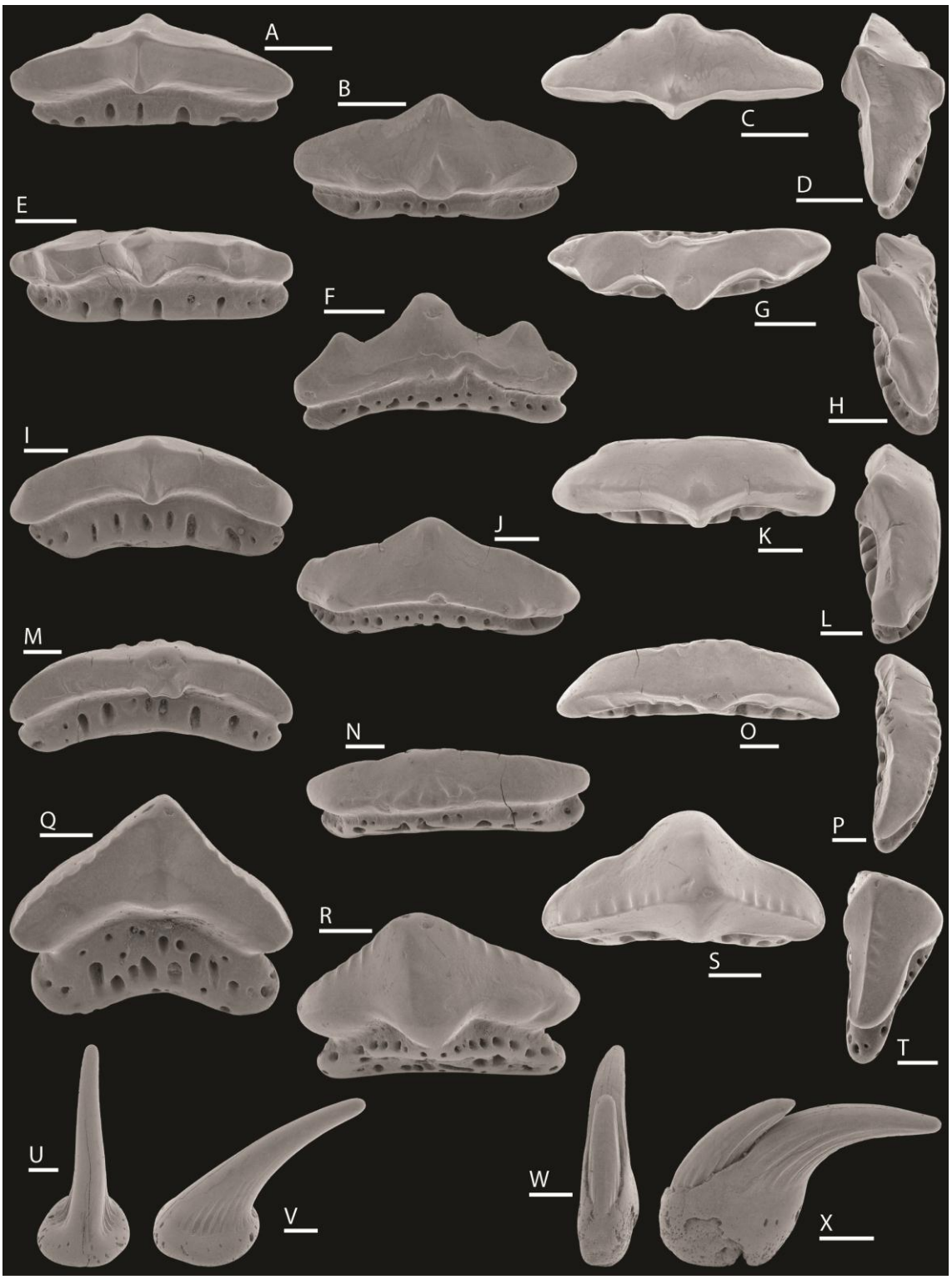

Figure A3.15 – Hybodont teeth from the Khuff Formation, Haushi Cliff, Haushi-Huqf area, central eastern Oman. Figs A–D. *Reesodus underwoodi* Koot, Cuny, Tintori and Twitchett, 2013. MPUM10891, loc K1, sample AO40; tooth, holotype. A, lingual, B, labial, C, apical, and D, lateral views; scale bars 300 µm. Figs E–P. *Teresodus amplexus* Koot, Cuny, Tintori and Twitchett, 2013. E–H, MPUM10888, loc K1, sample AO40; tooth, paratype. E, lingual, F, labial, G, apical, and H, lateral views; scale bars 300 µm. I–L, MPUM10889, loc K1, sample AO40; tooth, holotype. I, lingual, J, labial, K, apical, and L, lateral views;

scale bars 300 µm. M–P, MPUM10890, loc K1, sample AO40; tooth, paratype. M, lingual, N, labial, O, apical, and P, lateral views; scale bars 300 µm. Figs Q–T. cf. ‘Palaeozoic Genus 1’ sp. MPUM10932, loc K4, sample AO47bis; tooth. Q, lingual, R, labial, S, apical, and T, lateral views; scale bars 300 µm. Figs U–X. *Gunnellodus bellistriatus* (Gunnell, 1933). U–V, MPUM10911, loc K4, sample AO55; tooth. U, anterior, and V, lateral views; scale bars 300 µm. W–X, MPUM10880, loc K1, sample AO40; tooth. W, anterior, and X, lateral views; scale bars 300 µm.

Distribution. Central eastern Oman (this study).

Stratigraphical range. Wordian, Guadalupian, middle Permian.

Teresodus amplexus Koot, Cuny, Tintori and Twitchett, 2013

Figure A3.3, D; Figure A3.15, E–P

Derivation of name and *Type* information published in Koot *et al.* (2013).

Material. Samples AO40, AO55, AO47bis, AO50, Khuff Formation, yielded 103 complete and broken specimens. Specimens used for SEM imaging: MPUM10888 (anterior), MPUM10889 (anterolateral), MPUM10890 (lateral); remaining specimens: MPUM10900 (69), MPUM10920 (14), MPUM10939 (14), MPUM10950 (3).

Samples 965-2, 965-9, Khuff Formation, yielded 12 complete and broken specimens. Specimens used for SEM imaging: UC20258, UC20261 (anterior), UC20358 (posterior); specimen used for SEM microstructure study: UC20367; remaining specimens: UC20279 (anterior), UC20266, UC20274, UC20286, UC20297, UC20306 (lateral), UC20260, UC20263 (posterior).

Diagnosis and *Description* published in Koot *et al.* (2013).

Enameloid microstructure. The enameloid is made up of a homogeneous layer of single crystallites (SCE), which covers the entire surface. The crystallites are rod-shaped, long (1 µm or more) and randomly orientated.

Remarks published in Koot *et al.* (2013).

Genus cf. ‘PALAEOZOIC GENUS 1’ Rees and Underwood, 2002

cf. ‘Palaeozoic Genus 1’ sp.

Figure A3.15, Q–T

Material. Sample AO47bis, Khuff Formation, yielded one complete specimen. Specimen used for SEM imaging: MPUM10932.

Description and *Remarks* published in Koot *et al.* (2013).

Gen. et sp. indet.

Figure A3.8, E–H

Material. Sample 300311-J, Kamura Formation, yielded one broken specimen. Specimen used for SEM imaging: JP49.

Description. Small and elongate tooth (1.6 mm mesio-distally, incomplete dimension; 0.5 mm labio-lingually; and 0.6 mm high), with slight apico-basal arching. The crown is of almost equal height as the base, but no enameloid covering remains. The main cusp is large, but blunt, and remains low. It bears a strong lingual peg and there is some evidence of a small labial peg.

The base is perforated by randomly located foramina of varying size, although general large. Lingually, they approach a row-like organisation. The vascularisation appears anaulacorhize.

Remarks. Due to the absence of the enameloid covering, the crown ornamentation cannot be assessed. Also, the extent of the wear that at least removed the superficial layer is unknown, which means that less pronounced features such as crests and cristae may have been entirely removed. This specimen has been classed as hybodontiform based on the anaulacorhize vascularisation. As far as can be observed, there are a small number of similarities with *Omanoselache*. These include the large, but low main cusp with its well-developed lingual peg, as well as the slight apico-basal arching of the entire tooth. A distinct difference, however, is the lack of lingual protrusion of the base. The general poor preservation of this specimen prevents any further identification and it therefore must remain listed as Hybodontiformes indet.

Order HYBODONTIFORMES?

Genus GUNNELLODUS Wilimovsky, 1954

Type species. *Idiacanthus bellistriatus* Gunnell, 1933; from the Pennsylvanian Kansas City Group of Missouri, USA.

Diagnosis (emended from Gunnell, 1933) and *Remarks* published in Koot *et al.* (2013).

Gunnellodus bellistriatus (Gunnell, 1933)

Figure A3.3, E; Figure A3.15, U–X; Figure A3.22, K

1933 *Idiacanthus bellistriatus* Gunnell, pp. 293–294, pl. 31, fig. 60.

1933 *Idiacanthus cameratus* Gunnell, p. 294, pl. 32, fig. 29.

1933 *Idiacanthus* sp. Gunnell, p. 294, pl. 33, figs 39, 41.

1933 *Idiacanthus trispinosus* Gunnell, p. 294, pl. 33, fig. 46.

1954 *Gunnellodus* Wilimovsky, p. 693.

Material. Samples AO40, AO55, AO47bis, AO50, Khuff Formation, yielded 254 singular and articulated tooth specimens, both complete and broken. Specimens used for SEM imaging: MPUM10911 (singular), MPUM10880 (articulated); remaining specimens: MPUM10895 (75), MPUM10916 (111), MPUM10935 (53), MPUM10948 (13). MPUM11051 from AO214 was imaged with light microscopy for additional observations.

Samples 965-2, 965-3, 965-5, 965-8, 965-9, Khuff Formation, yielded 12 singular and articulated tooth specimens, both complete and broken. Specimens used for SEM imaging: UC20321, UC20341; specimen used for SEM microstructure study: UC20242; remaining specimens: UC20240, UC20241, UC20287, UC20288, UC20320, UC20348, UC20351, UC20380, UC20384.

Referred species. *Gunnellodus cameratus* (Gunnell, 1933); *Gunnellodus* sp. (Gunnell, 1933); *Gunnellodus trispinosus* (Gunnell, 1933).

Diagnosis (emended from Gunnell, 1933) and *Description* published in Koot *et al.* (2013).

Enameloid microstructure. The enameloid is made up of a homogeneous layer of single crystallites (SCE), which covers the entire surface. The crystallites are very short, rounded and randomly orientated. Little organisation is present.

Remarks published in Koot *et al.* (2013).

Order *INCERTAE SEDIS*

Family SPHENACANTHIDAE Maisey, 1982a

Genus KHUFFIA Koot, Cuny, Tintori and Twitchett, 2013

Derivation of name published in Koot *et al.* (2013).

Type species. *Khuffia lenis* Koot, Cuny, Tintori and Twitchett, 2013; from the Wordian (Guadalupian) Khuff Formation of the Haushi-Huqf area, central eastern Oman.

Diagnosis published in Koot *et al.* (2013).

Distribution. Central eastern Oman (this study).

Stratigraphical range. Wordian, Guadalupian, middle Permian.

Khuffia lenis Koot, Cuny, Tintori and Twitchett, 2013

Figure A3.16, A–H

Derivation of name and *Type* information published in Koot *et al.* (2013).

Material. Samples AO40, AO55, AO47bis, Khuff Formation, yielded 79 complete and broken specimens. Specimens used for SEM imaging: MPUM10881, MPUM10882; remaining specimens: MPUM10901 (74), MPUM10921 (2), MPUM10940 (1).

Sample 965-2, Khuff Formation, yielded five complete and broken specimens. Specimen used for SEM imaging: UC20270; remaining specimens: UC20281, UC20289, UC20325, UC20332.

Diagnosis, *Description* and *Remarks* published in Koot *et al.* (2013).

Khuffia prolixa Koot, Cuny, Tintori and Twitchett, 2013

Figure A3.16, I–L

Derivation of name and *Type* information published in Koot *et al.* (2013).

Material. Sample AO40, Khuff Formation, yielded 27 complete and broken specimens. Specimen used for SEM imaging: MPUM10892; remaining specimens: MPUM10902 (26).

Sample: 965-2, Khuff Formation, yielded one complete specimen. Specimen used for SEM imaging: UC20232.

Diagnosis, *Description* and *Remarks* published in Koot *et al.* (2013).

Superfamily HYBODONTOIDEA? Owen, 1846

Family HOMALODONTIDAE Mutter, Neuman and De Blanger, 2008

Genus HOMALODONTUS Mutter, Neuman and De Blanger, 2008

Type species. *Homalodontus aplopagus* (Mutter, De Blanger and Neuman, 2007; from the Olenekian of Wapiti Lake, British Columbia, Canada.

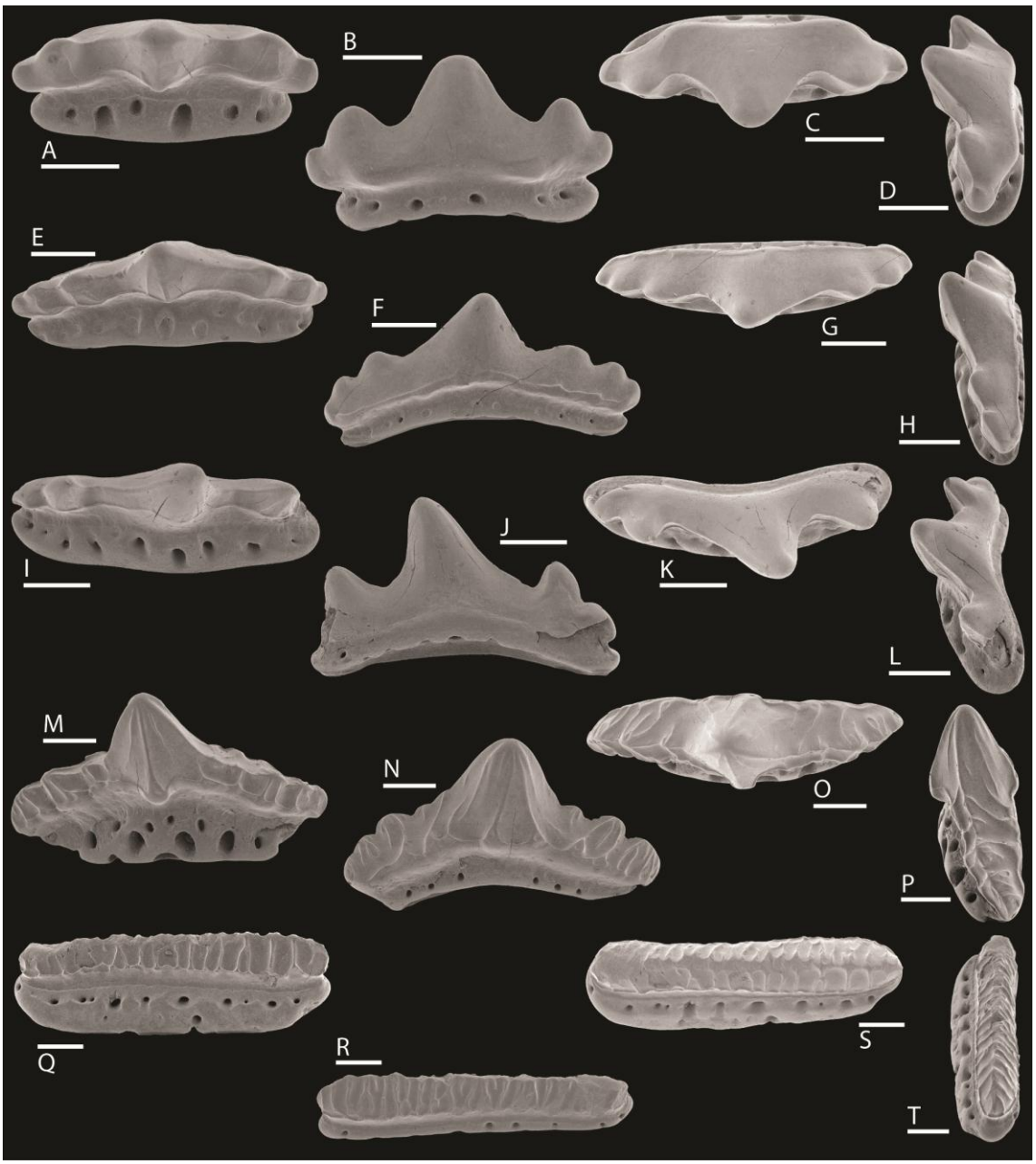

Figure A3.16 – Euselachian teeth from the Khuff Formation, Haushi Cliff and Saiwan, Haushi-Huqf area, central eastern Oman. Figs A–H. *Khuffia lenis* Koot, Cuny, Tintori and Twitchett, 2013. A–D, MPUM10881, loc K1, sample AO40; tooth, paratype. A, lingual, B, labial, X, apical, and D, lateral views; scale bars 300 µm. E–H, MPUM10882, loc K1, sample AO40; tooth, holotype. E, lingual, F, labial, G, apical, and H, lateral views; scale bars 300 µm. Figs I–L. *Khuffia prolixa* Koot, Cuny, Tintori and Twitchett, 2013. MPUM10892, loc K1, sample AO40; tooth, holotype. I, lingual, J, labial, K, apical, and L, lateral views; scale bars 300 µm. Figs M–T. Euselachii gen. et sp. indet. A. M–P, MPUM10931, loc K4, sample AO47bis; tooth. M, lingual, N, labial, O, apical, and P, lateral views; scale bars 300 µm. Q–T, MPUM11045, loc Saiwan, sample AO123; tooth. Q, lingual, R, labial, S, apical, and T, lateral views; scale bars 300 µm.

Homalodontus sp. cf. *H. aplopagus* (Mutter, De Blanger and Neuman, 2007)

Figure A3.17, A–D

Material. Sample 93 OF TE-5 1663 62-TE 325A, Blind Fiord Formation, yielded one broken specimen. Specimen used for light microscopy imaging: 447.

Description. This tooth fragment measures approximately 0.8 mm mesio-distally and 0.4 mm labio-lingually. It represents a rounded lateral extremity of an elongated tooth. No lateral cusplets are visible. The crown overhangs the base on all sides and possesses a flattened apical surface, which is smooth in the central part, but is otherwise adorned with coarse transverse cristae. These cristae originate apically, where they are equally flattened, but become stronger on the lingual and labial faces, where they bifurcate and continue towards the base. The cristae are not positioned entirely perpendicular to the central midline of the tooth, but at a slight angle. A slight circumferential rim occurs at the undulating crown shoulder, connecting the cristae.

The base is of roughly equal depth as the crown and has a generally rectangular, but slightly undulating outline. The basal face is moderately concave and shows a small number of randomly located small foramina. The same is true for the lateral faces of the base, but on one (lingual?) face, a large number of vertically flattened foramina are positioned relatively close together.

Remarks. The transversely crenulated ornamentation of this tooth fragment from Ellesmere Island is reminiscent of that observed in *Acrodus* Agassiz, 1838, which is a common genus in boreal areas (e.g., Stensiö 1921; Birkenmajer and Jerzmańska, 1979; Błażejowski, 2004). However, the specimen described here is assigned to a hybodont of uncertain affinities, *Homalodontus* Mutter, Neuman and De Blanger, 2008, based on a number of distinct similarities with features observed in this genus, and specifically in the species *H. aplopagus* (Mutter, De Blanger and Neuman, 2007). The most striking similarity is the transverse cristae, which bifurcate and are basally

pronounced, but leave a largely unornamented area in the central part of the crown. Posterior teeth of *H. aplopagus* are elongate and blunt, and cusps or cusplets may be entirely absent (Mutter *et al.* 2007a), which is also in agreement with the specimen described here. Further similarities are observed in the equal height of the base and the crown, the irregular and scattered nature of the foramina, and specifically also the distinct concavity of the basal face. The circumferential rim at the crown shoulder is a typical feature of '*Polyacrodus*' *contrarius* Johns, Barnes and Orchard, 1997 and '*Polyacrodus*' *bucheri* Cuny, Rieppel and Sander, 2001, which have been assigned tentatively to the Homalodontidae (Mutter *et al.* 2007a, 2008a), but it is not included in the diagnosis of the Homalodontidae or of *Homalodontus*. It is possible that it was not observed in the material from Wapiti Lake as a result of its preservation or the thin nature of the rim, but based on the available imagery, it is considered here that it is indeed a characteristic present in all taxa assigned to the Homalodontidae. Both the generic and specific assignment are strongly supported based on the observed characteristics, especially also due to the absence of a basal concavity in *H. homalorhizo*, which is the only other species assigned to *Homalodontus*. However, because the full range of variation cannot be assessed due to the very limited nature of the available material, and because of the inability to directly compare basal characteristics due to the absence of tooth base imagery of the type material, a tentative identification at species level is deemed appropriate.

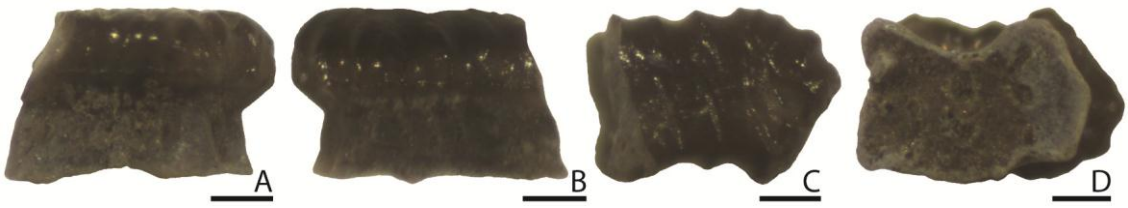

Figure A3.17 – Chondrichthyan tooth from the Blind Fiord Formation, Ellesmere Island, Canadian Arctic. Figs A–D. *Homalodontus* sp. cf. *H. aplopagus* (Mutter, De Blanger and Neuman, 2007). 447, sample 93 OF TE-5 1663 62-TE 325A, Blind Fiord Formation; tooth fragment. A, lingual?, B, labial?, C, apical, and D, basal views; scale bars 200 µm.

Family *INCERTAE SEDIS*

Gen. et sp. indet. A

Figure A3.16, M–T

Material. Samples AO55, AO47bis, AO50, AO123, Khuff Formation, yielded ten complete and broken specimens. Specimens used for SEM imaging: MPUM10931 (anterior), MPUM11045 (posterior); remaining specimens: MPUM10922 (4), MPUM10941 (3), MPUM10951 (1).

Description and *Remarks* published in Koot *et al.* (2013).

Gen. et sp. indet. B

Figure A3.11, A–D

Material. Samples 103B, 103C, 104A, Hallstatt-type limestone olistoliths, yielded three complete and broken specimens. Specimen used for SEM imaging: GSC135659; remaining specimens: GSC135687, GSC135819.

Description. The teeth are elongate but massive (1.9 mm mesio-distally, 0.9 mm labio-lingually, 1.1 mm high). The apical outline of the tooth is slightly convex lingually and distinctly convex labially and the basal face is straight to slightly convex. The teeth are polycuspid with a low, robust main cusp and equally compact lateral cusplets of laterally decreasing height. Two distinct pairs of lateral cusplets are developed, but slight asymmetry with up to three cusplets on one extremity may occur. All cusps are slightly lingually directed and a blunt longitudinal crest is developed across the entire mesio-distal length of the tooth. A strong lingual peg is present on the main cusp and nodes are present labially at the height of the crown shoulder. The nodes are situated

at the base of every cusp and two accessory nodes are present on the main cusp. Strong vertical cristae surmount each peg or node, terminating in the cusp apex. Additional cristae ascend the cusps at an angle, but are more numerous lingually. A longitudinal rim is present lingually at the crown shoulder, but absent labially.

The base makes up about one third of the total height of the tooth and is shallower labially than lingually. It protrudes lingually beyond the crown and is randomly perforated by foramina of varying size. The vascularisation is anaulacorhize, but may approach the pseudopolyaulacorhize type with parallel canals that are open on the labialmost part of the basal face.

Remarks. The affinity of these teeth is unclear. There are some similarities between this material and *Omanoselache*, including a polycuspid crown with low cusps and both symmetrical and asymmetrical teeth, as well as a strong lingual peg, nodes and a rim at the crown shoulder, vertical cristae, a lingual protrusion and anaulacorhize vascularisation of the base. However, the teeth are much more massive and the base is inflated with a convex basal face. The robust base is reminiscent of *Rhomphaiodon* Duffin, 1993a, a primitive synechodontiform from the Upper Triassic, which also possesses anaulacorhize vascularisation with parallel open canals (ancestral to typical pseudopolyaulacorhizy), and there are further similarities in basal and also crown morphology. Nevertheless, the crown differs significantly in having lower cusps and a much stronger developed lingual peg. The crown ornamentation also follows a different pattern.

Gen. et sp. indet. C

Figure A3.8, I–L

Material. Sample 300311-J, Kamura Formation, yielded one broken specimen. Specimen used for SEM imaging: JP50.

Description. Small and elongate tooth (1.1 mm mesio-distally, incomplete dimension; 0.4 mm labio-lingually; and 0.5 mm high) with a labio-lingually slender crown, on which the enameloid covering only remains in the apical part. The crown is multicuspid with a high, yet blunt main cusp, which is slightly distally(?) inclined. There is evidence of a labial peg at the base of the main cusp, but this area appears damaged or worn. A lingual peg is absent. At least two pairs of lateral cusplets can be observed, with a minimum of three cusplets on one extremity. The lateral cusplets are of increasing size away from the main cusp. A poorly defined longitudinal crest traverses the main cusp and at least the medialmost two cusplet pairs. One vertical crista is present on the lingual face of the main cusp and three somewhat wavy cristae appear labially, oriented towards the cusp apex. No further ornamentation is observed on the remaining enameloid.

The base is significantly projected lingually and also protrudes somewhat labially. Randomly located foramina of varying size open on the projected parts of the base. The vascularisation appears anaulacorhize.

Remarks. This specimen is of unknown affinity. The increasing lateral cusplet size away from the main cusp prevents assignment to the Hybodontiformes, because teeth of that order are characterised by decreasing cusplet height away from the main cusp (Ginter *et al.* 2010). Divergent patterns have been observed in the Cladodontomorphi, where the largest lateral cusplets are never the most proximal pair but rather the distalmost or penultimate pair from the main cusp (Ginter *et al.* 2010), as well as in other euselachians (e.g., second lateral cusplet pair from main cusp larger than the first in *Protacrodus*; Ginter *et al.* 2010). Neoselachians are derived euselachians (see Ginter *et al.* 2010) and although they are the most age appropriate group, increasing cusplet height away from the central part of the tooth is unusual for this group as well. There are a number of suggestive characteristics, including the overall crown morphology with a relatively labio-lingually compressed crown, no distinct pegs on the

main cusp, and the first mesial lateral cusplet somewhat resembling a blade, but this is deemed insufficient evidence to warrant assignment to the Neoselachii.

Subcohort NEOSELACHII Compagno, 1977

Family ANACHRONISTIDAE Duffin and Ward, 1983

Genus COOLEYELLA Gunnell, 1933

Type species. *Cooleyella peculiaris* Gunnell, 1933; from the Pennsylvanian (upper Carboniferous) Kansas City Group in Missouri, USA.

Cooleyella sp. cf. *C. fordi* (Duffin and Ward, 1983)

Figure A3.18, A–D

1983 *Anachronistes fordi* Duffin and Ward, pp. 95–98, pl. 13, figs 1–10; pl. 14, figs 1–7, 9; text-figs 2A, 3D.

1996 *Cooleyella fordi* Duffin *et al.*, p. 239.

Material. Samples AO50, AO214, Khuff Formation, yielded two complete specimens. Specimen used for SEM imaging: MPUM10945; remaining specimen: MPUM11055.

Description and *Remarks* published in Koot *et al.* (2013).

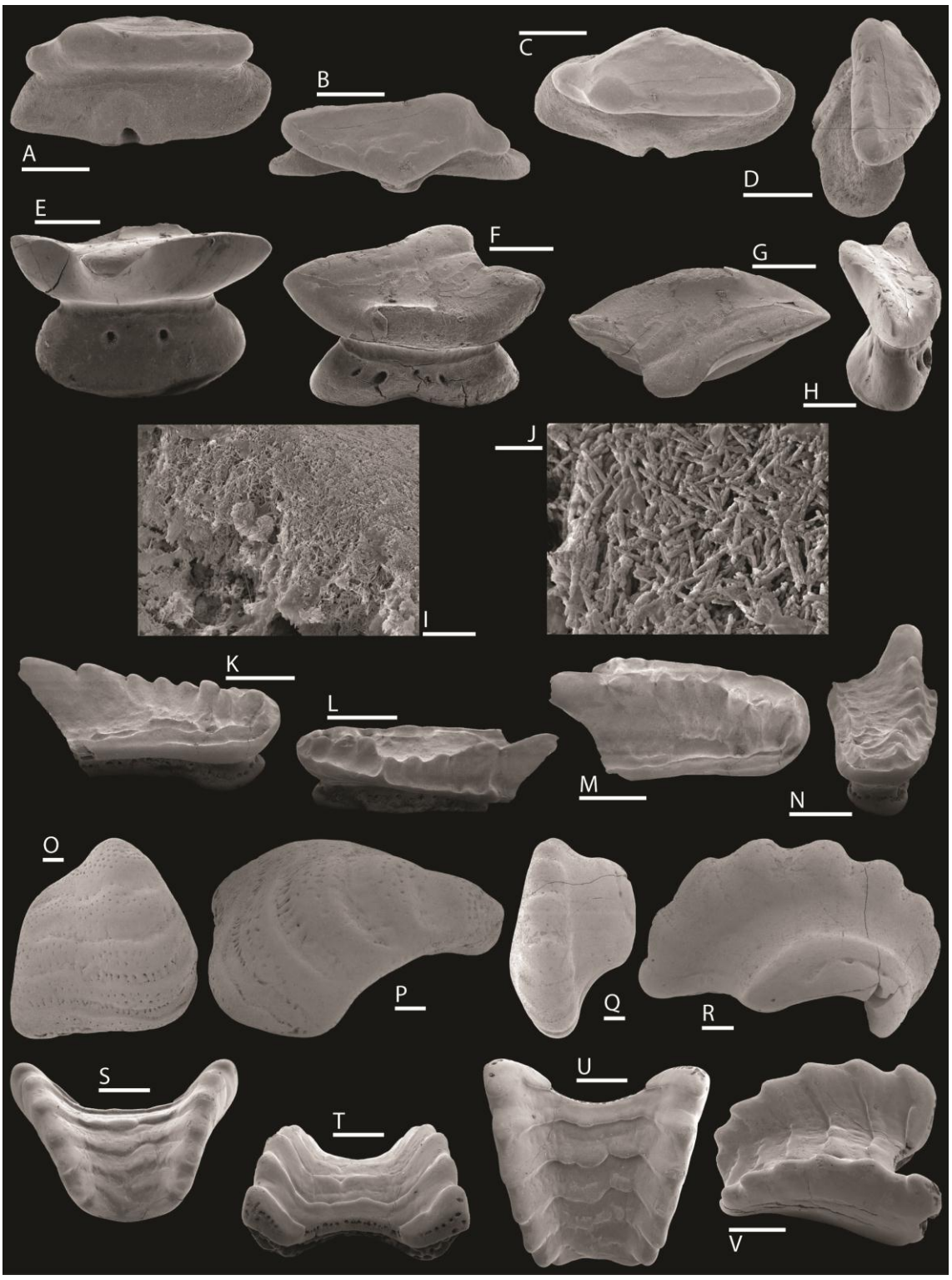

Figure A3.18 – Neoselachian teeth and euchondrocephalian tooth plates from the Khuff Formation, Haushi Cliff and Saiwan, Haushi-Huqf area, central eastern Oman. Figs A–D. *Cooleyella* sp. cf. *C. fordi* (Duffin and Ward, 1983). MPUM10945, loc K4, sample AO50; tooth. A, lingual, B, labial, C, apical, and D, lateral views; scale bars 300 µm. Figs E–J. Neoselachii gen. et sp. indet. A. MPUM11024, loc unknown, sample AO38; tooth. E, lingual, F, labial, G, apical, and H, lateral views; scale bars 300 µm; I, enameloid fracture surface; scale bar 5 µm; J, detail enameloid layer; scale bar 1 µm. Figs K–N. Petalodontiformes? gen. et sp. indet. MPUM11053, loc Saiwan, sample AO214; tooth fragment. K, lingual, L, labial, M, apical,

and N, lateral views; scale bars 1 mm. Figs O–R. *Deltodus* sp. aff. *D. mercurei* Newberry, 1876. O–P, MPUM10912, loc K4, sample AO55; tooth plate. O, apical, and P, lateral views; scale bars 500 µm. Q–R, MPUM10913, loc K4, sample AO55; tooth plate. Q, apical, and R, lateral views; scale bars 500 µm. Figs S–V. *Solenodus* sp. cf. *S. crenulatus* Trautschold, 1874. MPUM11052, loc Saiwan, sample AO214; tooth plate. S, lingual, T, labial, U, apical, and V, lateral views; scale bars 1 mm.

Order SYNECHODONTIFORMES Duffin and Ward, 1993

Remarks. The Synechodontiformes are currently no longer classified with the Galeomorphii, as listed in Cappetta (1987, 2012), nor with the Squalomorphii, as listed in Ginter *et al.* (2010). Klug (2010) showed that the neoselachian order is sister to both these groups (despite erroneously listing the order with the Galeomorphii in the Supporting Information, Appendix S9).

Preliminary diagnosis (emended from Duffin and Ward 1993). Neoselachian sharks in which the calcified vertebrae are cyclospondylous or asterospondylous. The dentition shows linear gradient monognathic heterodonty. The anterior teeth have a crown bearing a central cusp flanked by lateral cusplets or blade-like ridges. The base of the cusp and cusplets is striated to a greater or lesser extent. The root has a relatively shallow, flat labial face. The basal face of the root is flat to concave. The lingual face of the root is convex and lingually displaced. The root vascularization is of modified anaulacorhizoid type (pseudopolyaulacorhizoid). The basal face of the root has a series of open vascular canals originating labially and shallowing (until covered) and terminating lingually. These canals may be horizontal, or short and steeply inclined. The tooth is osteodont with at least parallel-bundled enameloid.

Family PALAEOSPINACIDAE Regan, 1906

Diagnosis. See Duffin and Ward, 1993, p. 58.

Genus cf. PALIDIPLOSPINAX Klug and Kriwet, 2008

Type species. *Synechodus enniskilleni* Duffin and Ward, 1993; from the Sinemurian of Lyme Regis, England.

cf. *Palidiplospinax* sp.

Figure A3.14, E–H

Material. Samples O-15, O-24, Xinyuan Formation, yielded two broken specimens. Specimen used for SEM imaging: 383, remaining specimen: 396 (tentative).

Description. Slender and small, elongate tooth (0.9 mm mesio-distally, incomplete dimension; 0.4 mm labio-lingually, incomplete dimension; and 1.0 mm high). The crown is multicuspid, possessing a high main cusp, which is distally slanted (approximately 35°), and one incipient lateral cusplet mesially. In lateral view, the main cusp has a sigmoid profile, because it is curved lingually at the base and returns to a more erect position about halfway up the cusp. A well-developed longitudinal crest is traverses the tooth in a mesio-distal direction, but is labially off-set and becomes a distinctly raised ridge (approaching a blade) towards the base of the main cusp. The crown surface is smooth, save for a complex ridge at the labial crown shoulder, consisting of short, distally raised, imbricated ridges. The base is perforated by foramina and may have protruded lingually.

Remarks. Despite the limited nature and poor preservation of the material, the best preserved tooth fragment shows a general resemblance to teeth of *Palidiplospinax* Klug and Kriwet, 2008. Specific features in common with this genus include lingual curvature of the main cusp (although this character is also commonly observed in other taxa) and likely also the presence of horizontally extended heels with incipient cusplets

at the lateral edges. The number of lateral cusplets distal to the main cusp and true shape and vacularisation of the base could not be determined, but the ornamentation is much more smooth than generally observed in *Palidiplospinax* (see Klug and Kriwet 2008). This would suggest an affinity with *P. occultidens* (Duffin and Ward, 1993), which possesses teeth with laterally extended heels, bearing a single, very incipient pair of cusplets on the lateral edges in all but the symphyseal teeth (i.e., distally inclined teeth), as well as very reduced crown ornamentation (Duffin and Ward 1993; Klug and Kriwet 2008). Parasymphyseal teeth of *P. occultidens* are highly crowned with a slender main cusp that can be distally inclined and possess a labially off-set longitudinal crest (Duffin and Ward 1993). Most importantly, they are of a sigmoid outline in lateral view, being lingually curved at the base and then returning to an upright position (Duffin and Ward 1993). A significant difference is the type of ornamentation, which is described as short, fine vertical ridges at the base of the crown, whereas the apical part is smooth, and which are figured to originate from an occasionally anastomosing ridge at the crown shoulder (Duffin and Ward 1993, see also text-fig. 10). This does not correspond with the Chinese fragment described here. Any similarity with *Synechodus politus* (Thies, 1992), a closely related taxon that is also distinguished by teeth with a largely smooth crown, can be dismissed based on the fact that the numerous small vertical folds appearing near the base on the labial face of posterior teeth, only occur on the lateral heels and not underneath the main cusp. Hence, the material described here remains listed as cf. *Palidiplospinax* and definite conclusions must await the recovery of further material. These fragments currently are the only evidence of a dental morphology reminiscent of *Palidiplospinax* from the Triassic (Anisian) and may represent an ancestral form to the Early Jurassic genus.

Family *INCERTAE SEDIS*

Genus GENUS S

Preliminary type species. Genus S sp. T; from Olenekian (Lower Triassic) Hallstatt-type limestone olistoliths at Jabel Safra, Oman Mountains, Sultanate of Oman.

Preliminary diagnosis. Gradient monognathic heterodont teeth with high main cusp in anteriors; lateral cusplets of laterally decreasing size; lingually inclined cusps, often also slanted distally, causing the main cusp to be asymmetrical; two to three cusplet pairs in symmetrical anteriors; three to four cusplets mesially and two to three cusplets distally in asymmetrical laterals; distinctly arched base in anteriors to moderately so in laterals; continuous longitudinal crest; crown surface ornamented with few straight, well-developed, rarely anastomosing vertical cristae; crown shoulder smooth, labial overhang absent; pseudopolyaulacorhize vascularisation; enameloid microstructure comprising parallel-bundled enameloid, restricted to the cusp apex, and a superficial layer of single crystallite enameloid, which is continued in the vertical cristae and the longitudinal crest.

Distribution. Oman Mountains, Sultanate of Oman (this study); Bouwn, Timor (Yamagishi 2006; this study); Dzjulfa, Iran (this study); Guizhou Province, China (this study); Idaho and Utah, USA (this study).

Stratigraphical range. Wuchiapingian, Lopingian, Permian–Anisian, Middle Triassic.

Genus S sp. T (Oman)

Figure A3.11, R–U; Figure A3.19, A–X

Preliminary holotype. One complete tooth (GSC135697, Figure A3.19, E–H).

Preliminary paratypes. Two complete teeth (GSC135708, Figure A3.19, M–P; GSC135614, Figure A3.19, Q–T).

Preliminary type locality. Jabel Safra, Oman Mountains, Sultanate of Oman.

Preliminary type stratum. Red limestone (Hallstatt-type) olistolith, Block 3, Oman Exotics, Kawr Group?, Hawasina Allochthonous, Spathian (upper Olenekian, Lower Triassic).

Material. Samples 103A, 103B, 103C, 104A, 104B/C, C85314, 117A, Hallstatt-type limestone olistoliths and Alwa Formation, yielded 140 complete and broken specimens. Specimens used for SEM imaging: GSC135685, GSC135697 (anterior), GSC135703 (anterolateral), GSC135614, GSC135708 (lateral), GSC135754 (posterolateral); specimens used for SEM microstructure study: GSC135642, GSC135739, GSC135740, GSC135862, GSC135866; remaining specimens: GSC135615–GSC135627, GSC135633, GSC135640, GSC135643, GSC135644, GSC135647, GSC135651–GSC135654, GSC135656, GSC135660–GSC135664, GSC135666, GSC135674–GSC135683, GSC135686, GSC135688–GSC135690, GSC135692, GSC135694–GSC135696, GSC135698–GSC135702, GSC135706, GSC135707, GSC135711–GSC135713, GSC135715, GSC135717, GSC135721, GSC135725, GSC135738, GSC135742, GSC135749, GSC135750, GSC135755–GSC135762, GSC135764, GSC135765, GSC135767–GSC135769, GSC135771–GSC135778, GSC135780–GSC135788, GSC135790–GSC135792, GSC135796, GSC135800–GSC135808, GSC135810, GSC135812, GSC135814, GSC135828–GSC135830, GSC135834, GSC135835, GSC135841–GSC135843, GSC135845–GSC135848, GSC135856, GSC135863, GSC135864, GSC135867, GSC135868, GSC135887.

Preliminary diagnosis. Lateral cusplets not well-separated; all cusps sub-rounded and longitudinal crest pronounced through labio-lingual crown compression.

Description. The teeth are slender and elongate. They are variable in size but generally small (0.8–2.3 mm mesio-distally, 0.3–0.5 mm labio-lingually, 0.4–1.3 mm high). In apical view, the labial outline of the teeth is near-straight or distinctly concave, whereas the lingual outline is convex. Gradient monognathic heterodonty can be recognised in the material: anteriors are shorter mesio-distally, highly cusped, symmetrical and possess a distinctly to moderately arched base, whereas laterals are longer mesio-distally, lower cusped, asymmetrical and possess a moderately to weakly arched base. The teeth are polycuspid with a robust main cusp and well-developed lateral cusplets that all incline lingually. Both main and lateral cusps may be slanted distally to an increasing degree posteriorly, causing the main cusp to be distinctly asymmetrical in lateral and posterior teeth, and the lateral cusplets are connected at the base and decrease in size towards the extremities. The number of lateral cusplets varies with tooth position: two pairs in anteriors and three pairs in anterolaterals, whereas laterals possess three to four cusplets mesially and two to three cusplets distally. All cusps tend to be translucent towards the apex and are sub-rounded in shape due to slight labio-lingual compression of the crown. This creates an acute longitudinal crest that runs along the entire length of the teeth, but is best developed on the main cusp. The entire crown is ornamented by a low number of straight and well-developed vertical cristae that start at the crown shoulder and only occasionally anastomose near the cusp apices. The ornamentation is often best developed on the lingual face and may be completely absent in places. The crown shoulder is completely devoid of any pegs or nodes.

The base generally comprises 20–25% of the entire tooth height and the labial face, especially, is shallow and flat. Lingually, the base distinctly protrudes beyond the crown, but particularly in anterior teeth, the lingual face may be thickened and raised in the

central part of the tooth. Foramina penetrate the base labio-lingually in a horizontal plane and the canals are exposed on the labial half of the basal face, creating a jagged appearance of the labial basal edge. Lingually, the foramina are randomly located but may approach a row-like organisation. The vascularisation is characteristic of pseudopolyaulacorhizy.

Juvenile teeth are generally much smaller but all characteristic features are developed. They are less ornamented, more translucent and perforated by smaller foramina.

Enameloid microstructure. Initial etching treatment showed that the outer layer is made up of homogeneous single crystallite enameloid (SCE). The crystallites are rod-shaped, long (1 µm or more) and randomly orientated, but appear to be organised in a plane parallel to the surface, indicative of shiny layer enameloid (SLE). It covers the entire crown surface, also near the cusp apices, where the enameloid layer is thicker and microstructural features are usually best developed (Cuny and Risnes 2005). Exposure of deeper enameloid layers showed primitive bundling of the crystallites parallel to the crown surface. The bundles follow a subparallel interweaving pattern, are roughly 1 µm thick and individual crystallites can often still be recognised. Near cusp apices, the bundles run longitudinally along the length axis of the cusp, but nearer the base, there is a decrease in their organisation. Although primitive, the fabric is characteristic of parallel-bundled enameloid (PBE). The longitudinal crest and vertical cristae show no bundling and consist entirely of SCE. Radial bundles have not been observed, but are known to be few in number and poorly developed in Triassic taxa (Cuny and Risnes 2005).

Remarks. Histological study of the enameloid layer revealed a primitive microstructural pattern. Parallel-bundled enameloid is considered an apomorphic feature of Neoselachii (excluding batoids; see references in Maisey *et al.* 2004), confirming the neoselachian affinities of the material described here. Inclusion within the

Synechodontiformes can be argued based on the following diagnostic characteristics: gradient monognathic heterodonty, anterior teeth bearing a central cusp flanked by lateral cusplets, cristae on all cusps, shallow and flat labial basal face, convex and protruding lingual basal face, as well as pseudopolyaulacorhize vascularisation (Duffin and Ward 1993). The material further shares characteristics with the Palaeospinacidae, including: moderately high central cusp, deep vascular canals in basal face and basolabial margin prominently corrugated. Assignment to *Palidiplospinax* is rejected because of the much more extensive lingual curvature of the main cusp in teeth belonging to this genus, as well as a smaller number of lateral cusplets, much weaker development of the vertical cristae and pronounced U-shape of the base in basal view (Klug and Kriwet 2008). Instead, there is great morphological similarity to *Synechodus* Woodward, 1888, based on the characteristics diagnosed by Klug (2009): symmetrical anterior teeth and asymmetrical lateral teeth due to variable number of lateral cusplets; central cusp more than twice the height of the first cusplet pair and exponential lateral decrease of cusp height; crown height decreasing posteriorly; cusps not well-separated from each other; as well as the fact that the main cusp is increasingly distally slanted posteriorly and may be slightly lingually inclined, as stated by Ginter *et al.* (2010). Regardless of these similarities, however, the material is separated and assigned to a new genus because of three major discrepancies with typical *Synechodus* morphology. These comprise extensive basal arching (throughout the dentition) in the Oman material, the absence of a labial crown overhang, and the absence of fully developed triple-layered enameloid (TLE). The genus is placed within the Synechodontiformes based on the presence of pseudopolyaulacorhize vascularisation, which is unique to this order (Klug 2010). Modifications to the ordinal diagnosis are proposed to accommodate the differences. It is further considered that the genus may be positioned within the Palaeospinacidae as a sister genus to *Synechodus* based on the morphological similarities, but this is not applied here due to the controversial affinities of many synechodontiform genera based on the scarcity of skeletal remains (Klug 2010).

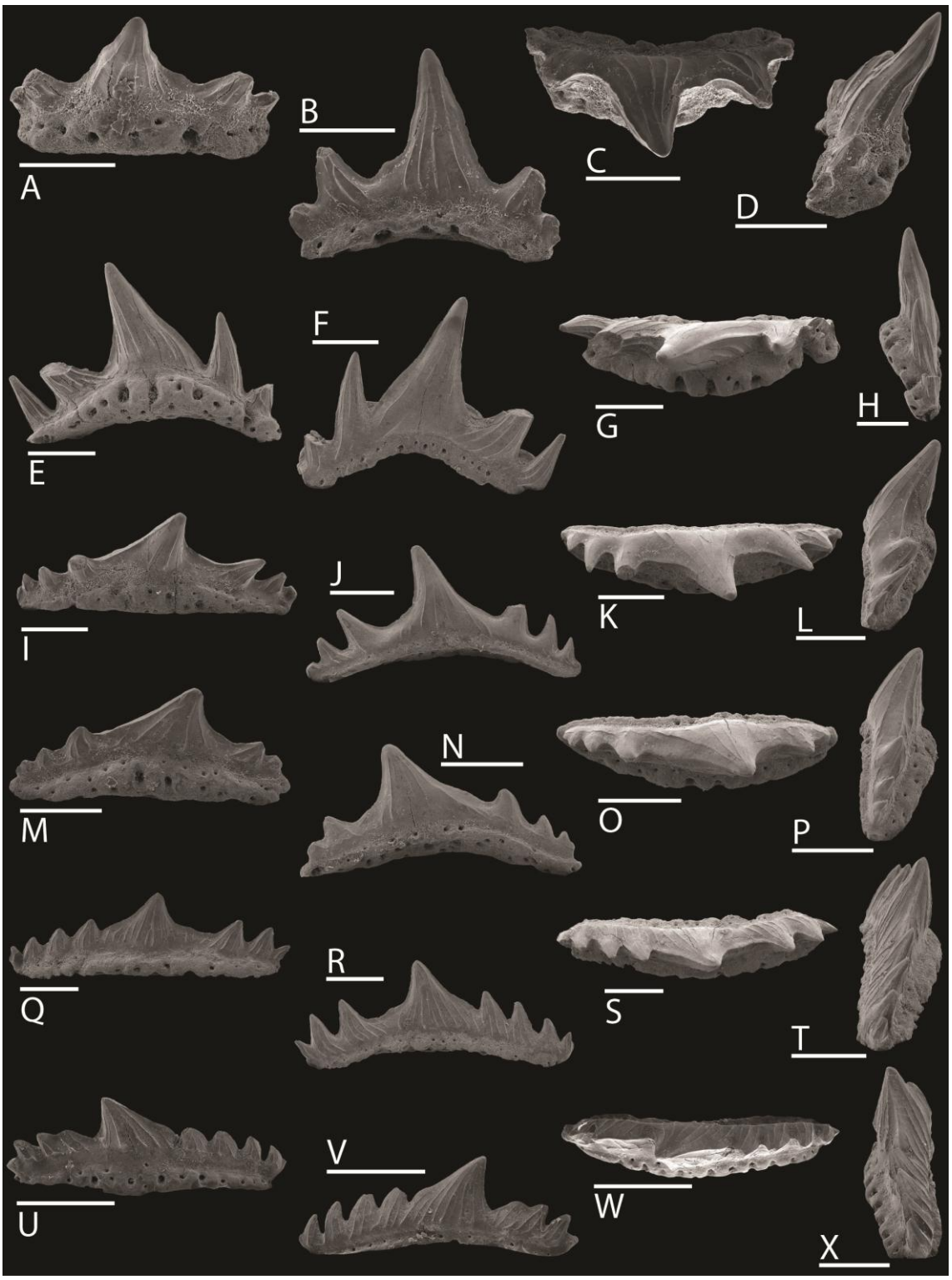

Figure A3.19 – Synechodontiform teeth from the Hallstatt-type limestone olistoliths at Jabel Safra, Oman Mountains, northern Oman. Figs A–X. Genus S sp. T. A–D, GSC135685, sample 103C; tooth. A, lingual, B, labial, C, apical, and D, lateral views; scale bars 300 µm. E–H, GSC135697, sample 103C; tooth, holotype. E, lingual, F, labial, G, apical, and H, lateral views; scale bars 500 µm. I–L, GSC135703, sample 103C; tooth. I, lingual, J, labial, K, apical, and L, lateral views; scale bars 500 µm. M–P, GSC135708, sample 103C; tooth, paratype. M, lingual, N, labial, O, apical, and P, lateral views; scale bars 500 µm. Q–T,

GSC135614, sample 103A; tooth, paratype. Q, lingual, R, labial, S, apical, and T, lateral views; scale bars 500 µm. U–X, GSC135754, sample 104A; tooth. U, lingual, V, labial, W, apical views; scale bars 500 µm, and X, lateral view; scale bar 300 µm.

Genus S sp. T (Iran)

Figure A3.20, A–D

Material. Sample 02 OF KZK 10, Ali Bashi Formation(?), yielded three broken specimens. Specimen used for SEM imaging: 275; remaining specimens: 276–277.

Description. Elongate teeth of small size (1.1 mm mesio-distally, 0.3 mm labio-lingually and 0.5 mm high) with significant basal arching and slight asymmetry. The crown is labio-lingually compressed and highly cusped. The main cusp may be distally slanted and up to two pairs of lateral cusplets are present that decrease in size away from the centre of the tooth. All cusps are lingually inclined. An acute and raised longitudinal crest traverses all cusps in a mesio-distal direction. The crown/base junction is not incised and smooth. Sparse and wavy vertical cristae ornament the crown both lingually and labially, but only in the central part of the cusps, whereas they fade towards the cusp apices and the crown base.

The height of the base is restricted, both lingually, where it protrudes beyond the crown, and labially. It is perforated by few large and randomly located foramina, which are retracted underneath the baso-labial edge on the labial face. The vascularisation is of the pseudopolyaulacorhize type.

Remarks. This material is of Synechodontontiform affinity and deemed to represent anterior teeth of Genus S sp. T, based on the following shared characteristics: highly cusped; lingually inclined cusps; generally two cusplet pairs in symmetrical anteriors; distinctly arched base in anteriors; labio-lingual crown compression; continuous

longitudinal crest; few vertical cristae; crown shoulder smooth; and pseudopolyaulacorhize vascularisation.

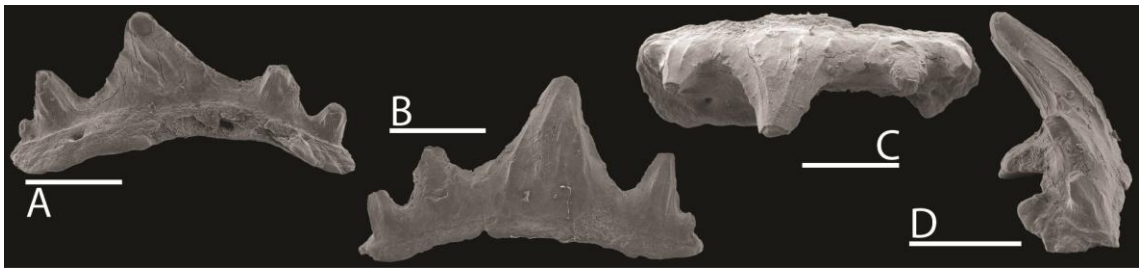

Figure A3.20 – Chondrichthyan teeth from the Ali Bashi Formation?, Transcaucasian region, northwestern Iran. Figs A–D. Genus S sp. T. 275, sample O2 OF KZK 10; tooth. A, lingual, B, labial, C, apical, and D, lateral views; scale bars 300 µm.

Genus S sp. T (southwestern USA)

Figure A3.12, M–P

Material. Samples 93 OF W-11, 99-IG CNA-HS 4, 93 OF W-14, Thaynes Formation, yielded five complete and broken specimens. Specimen used for SEM imaging: 292; remaining specimens: 294 (tentative), 343, 345, 350.

Description. Slender and elongate teeth (1.1 mm mesio-distally, 0.3 mm labio-lingually, 0.5 mm high) that are symmetrical and possess a distinctly arched base. In apical view, the labial outline of the teeth is near-straight, whereas the lingual outline is convex. The teeth are polycuspid and highly cusped with a robust main cusp and well-developed lateral cusplets that all incline lingually. The main cusp may be slanted distally, causing it to be asymmetrical in lingual or labial view. At least two and potentially three pairs of lateral cusplets are present, which appear to be poorly separated and decrease in size towards the extremities. The crown is labio-lingually compressed, creating an acute longitudinal crest that runs along the entire mesio-distal length of the teeth, but is best developed on the main cusp, where blade-like features appear near the base. The

crown is ornamented by few straight and well-developed vertical cristae that start at or just above the crown shoulder, but often terminate before they reach the cusp apices. The ornamentation is best developed on the lingual face and the crown shoulder is otherwise completely smooth. The crown/base junction is not incised.

The base remains low and especially the labial face is shallow and flat. Lingually, the base protrudes beyond the crown and is thickened in the central part. Foramina penetrate the base labio-lingually in a horizontal plane and the canals are exposed on the labial half of the basal face, creating a jagged appearance of the labial basal edge. Lingually, the foramina are of variable size and randomly located. The vascularisation is characteristic of pseudopolyaulacorhizy.

Remarks. These teeth are assigned to the new synechodontiform genus recognised from the Olenekian of Oman, Genus S, based on the presence of all the diagnostic characteristics that could be assessed. These include: high main cusp and cusplets of laterally decreasing size; lingually inclined cusps; asymmetrical main cusp if slanted distally; two to three cusplet pairs in symmetrical teeth; distinctly arched base; continuous longitudinal crest; crown surface ornamented with few straight, well-developed vertical cristae; crown shoulder smooth, labial overhang absent; and pseudopolyaulacorhize vascularisation. The presence of some labio-lingual crown compression, an acute longitudinal crest, and poorly separated lateral cusplets indicate assignment to Genus S sp. T. This expands the geographical range of the genus and species from the Tethyan/western Panthalassic realm to the eastern Panthalassic realm.

Genus S sp. cf. Genus S sp. T

Figure A3.14, I–P

Material. Samples O-3, O-11, O-13, O-14, Luolou Formation, O-15, O-22, O-24?, O-27, O-28, O-29, O-31, O-34, O-36, O-40, O-41, GDL-55, GDL-57, Xinyuan Formation, yielded 24 broken specimens. Specimens used for SEM imaging: 406, 412; remaining specimens: 371, 373, 376, 378–379, 391–392, 402–403, 407, 411, 414–415, 417, 421–422, 424, 443–444; tentatively assigned specimens: 363, 369, 408.

Description. Slender and elongate teeth (1.0–1.7 mm mesio-distally, incomplete maximal dimension; 0.3 mm labio-lingually; and 0.5–0.6 mm high), which form part of a gradient heterodont dentition. In apical view, the labial outline of the teeth is near-straight in lateral teeth or distinctly concave in teeth positioned more towards the anterior, in which case the lingual outline is convex. Heterodonty is further expressed in anteriors being shorter mesio-distally and near-symmetrical, whereas laterals are longer mesio-distally and distinctly asymmetrical. Basal arching is pronounced in anteriormost teeth, but only slight to absent in anterolateral and more posterior teeth. The polycuspid teeth bear a robust main cusp and well-developed lateral cusplets that are connected at the base and decrease in size towards the extremities. All cusps incline lingually and may be slanted distally to an increasing degree posteriorly, causing asymmetry in the main cusp. Anterior teeth possess two pairs of lateral cusplets, whereas laterals possess up to four cusplets mesially and at least two cusplets distally. The crown is slightly labio-lingually compressed, causing the cusps to be sub-rounded in shape, and further resulting in a moderately acute longitudinal crest traversing the entire mesio-distal length of the teeth. The ornamentation of the crown consists of well-spaced and well-developed vertical cristae that may be slightly wavy and curved, starting at the smooth crown shoulder and oriented towards the cusp apices. They may terminate prematurely or rarely anastomose near the apex.

The base is shallow, especially labially. It protrudes beyond the crown lingually, and in anteriors the central part may be thickened and raised. Foramina penetrate the base and the canals are exposed on the labial half of the basal face. On the lingual face, foramina are randomly located but may approach a row-like organisation. The vascularisation is characteristically pseudopolyaulacorhize.

Remarks. The tooth morphology and heterodonty pattern observed in this material are identical to Genus S sp. T in all aspects of crown and base, except for some variation in one characteristic feature. In Genus S sp. T, there is a gradual decrease in the extent of basal arching towards the posterior, but arching is distinctly present in all teeth. In this material, basal arching is only very pronounced in the anteriormost teeth and only weakly developed or entirely absent in teeth in a more lateral position. This is deemed insufficient grounds to fully distinguish the material described here, but some caution is applied by listing it as Genus S sp. cf. Genus S sp. T.

Genus S sp. A

Figure A3.11, E–L

Material. Samples 103C, 104A, Hallstatt-type limestone olistoliths, yielded six complete and broken specimens. Specimens used for SEM imaging: GSC135709, GSC135724; remaining specimens: GSC135705, GSC135710, GSC135726, GSC135753.

Sample 30/09/2003, Hallstatt-type limestone, yielded one broken specimen: 451.

Samples O-11, Luolou Formation, O-28, O-36, Xinyuan Formation, yielded three broken specimens: 370, 404, 413.

Referred material. Synechodus sp.1 Yamagishi 2006 (in part), p. 90–92, pl. 9A–D; pl. 9G–H.

Description. The teeth display the same morphological characteristics as Genus S sp. T in most aspects of crown and base. However, the lateral cusplets are distinctly isolated from each other due to the absence of a raised connecting ridge, causing the crown to be extremely low in between the cusplets. Furthermore, the lateral compression of the crown is reduced, which causes the cusps to be rounded.

Remarks. In comparison with Genus S sp. T, a relatively limited number of specimens display these deviating characteristics, which means that they could be the result of natural variation. In that case, these specimens should be assigned to Genus S sp. T, but no evidence can currently be presented towards this interpretation. Because the unique characteristics are pronounced, the material remains separate until further study can clarify its true relationship.

cf. Genus S sp.

Figure A3.21, A–D

Material. Sample 110222-B, Alwa Formation, yielded one complete specimen. Specimen used for SEM imaging: OM21.

Remarks. The general morphology of this specimen is typical of Genus S, but uncertainty is caused by unusual features such as the high degree of distal slanting of the main cusp and the low number of lateral cusplets in an asymmetrical tooth (one distally and two mesially), whereas a minimum of two lateral cusplets distally is normally observed in Genus S. These features may be pathological (G. Cuny, pers. comm. 2012).

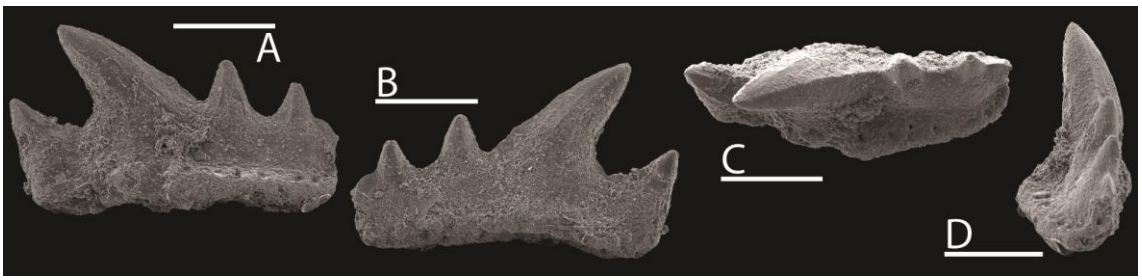

Figure A3.21 – Synechodontiform tooth from the Alwa Formation at Wadi Alwa, Ba'id area, Oman Mountains, northern Oman. Figs A–D. cf. Genus S sp. OM21, sample 110222-B; tooth. A, lingual, B, labial, C, apical, and D, lateral views; scale bars 400 µm.

Genus 'SYNECHODUS' Woodward, 1888 (pre-Jurassic)

Type species. *Synechodus dubrisiensis* Mackie, 1863; from the Cenomanian (Upper Cretaceous) Lower Chalk of Dover, Kent, England.

Remarks. In previous years, a variety of taxa based on Triassic material have been attributed to *Synechodus* Woodward, 1888, comprising: *'S.' rhaeticus* (Duffin, 1982a) from the Rhaetian (uppermost Triassic) of southern England (Duffin 1982a, 1998a); *'S.' triangulus* Yamagishi, 2004 from the lower Anisian (Middle Triassic) of southern Japan (Yamagishi 2004); *'Synechodus'* sp. and a new *'Synechodus'* species from the Olenekian and Anisian (Lower–Middle Triassic) of northern Siberia, Russia (Ivanov and Klets 2007, loc. 1–3 in fig. 1); and *'S.' incrementum* Johns, Barnes and Orchard, 1997 (Norian), *'S.' multinodosus* Johns, Barnes and Orchard, 1997 (Carnian), *'S.' volaticus* Johns, Barnes and Orchard, 1997 (Ladinian–Carnian), *'Synechodus'* sp. 1 (Ladinian), and *'Synechodus'* sp. 2 (Ladinian–Carnian) from the Middle–Upper Triassic of northeastern British Columbia, Canada (Johns *et al.* 1997). However, Klug (2010) removed these taxa from the genus and placed them in open nomenclature, for the reason that they had been assigned to *Synechodus* based on insufficient knowledge. Following her practice, the taxa are now unofficially referred to as 'pre-Jurassic *Synechodus*', a group that represents all Permian and Triassic occurrences of similar morphology but uncertain affinity and one that may not represent a single genus. Full

revision of *Synechodus* and ‘pre-Jurassic *Synechodus*’ is required to settle their respective systematic placement.

‘Synechodus’ sp. (pre-Jurassic; China)

Figure A3.14, Q–T

Material. Samples O-10, Luolou Formation, O-29, O-31, Xinyuan Formation, yielded three broken specimens. Specimen used for SEM imaging: 405; remaining specimens: 366, 410.

Description. Elongate teeth of small size (1.7 mm mesio-distally, incomplete dimension; 0.4 mm labio-lingually; and 0.6 mm high) with slight basal arching. Polycuspid crown with moderately high main cusp, and minimally two lateral cusplets mesially and one distally. The lateral cusplets are low and undistinguished, of decreasing height away from the main cusp, and all cusps may be distally slanted. The crown is not labio-lingually compressed, causing the main cusp to appear somewhat massive in lateral view. A longitudinal crest traverses the entire mesio-distal dimension of the teeth and is particularly raised on the main cusp and towards the first cusplet pair. The crown is ornamented with well-developed vertical cristae, which originate at the crown shoulder and are oriented towards the cusp apices labially or more vertical lingually. Labially, they may either terminate in the apex, or fade lower on a cusp, or rarely anastomose near the apex. At the crown shoulder, sporadic evidence of a reticulate pattern is present, although very weakly developed. Instead, a circumferential rim is more generally developed, but remains low. The crown/base junction is moderately incised and the crown overhangs it significantly labially.

The base shows some evidence of a lingual protrusion and possesses a baso-labial sulcus. The vascularisation type is intermediate between anaulacorhizy and pseudopolyaulacorhizy with small foramina opening close to the crown/base junction

on the shallow labial basal face and larger foramina located in the sulcus with the vascular canals partly exposed.

Remarks. A close relationship with the Synechodontiformes is indicated by the striation of the crown and identical basal morphological characteristics (Duffin and Ward 1993). Furthermore, a potential palaeospinacid affinity is suggested by the moderately high main cusp and the absence of blades flanking the main cusp (Duffin and Ward 1993). The material described here can be differentiated from Genus S based on the more bulky appearance in lateral view due to the absence of labio-lingual compression, the development of a weak circumferential rim, and some reticulate ornamentation. Most important, however, is the significant labial overhang. This is a feature first observed by Cappetta (1973) in *Synechodus* Woodward, 1888 of Cretaceous–Eocene age, which is also characterised by low and not well-separated cusps. This was formalised by Duffin and Ward (1993), who deemed it diagnostic of the genus, and followed in the emended diagnosis by Klug (2009). The material cannot be officially referred to *Synechodus*, however, for reasons detailed in the generic remarks, which means that this material should be referred to as *'Synechodus'* (pre-Jurassic). Of the species relevant to this group, the closest morphological relationship is believed to be with *'S.' incrementum*, based on the ornamentation pattern, but it appears less well developed and Johns *et al.* (1997) further describe a lingual crown overhang in addition to a labial overhang, which is absent in the Chinese material. A specific identification must therefore await the recovery of further material.

'Synechodus' sp. (pre-Jurassic; southwestern USA)

Figure A3.12, Q–X

Material. Samples 93 OF W-11, 93 OF W-13, o-64671 91-OF, 02 OF CP-C1-BASE, Thaynes Formation, yielded five complete and broken specimens. Specimens used for

SEM imaging: 297 (anterior), 293 (lateral); remaining specimens: 325, 360 (tentative), 648, 649.

Description. Small teeth that are elongated to a variable ratio (0.7–1.7 mm mesio-distally, 0.3–0.4 mm labio-lingually, and 0.5 mm high), caused by gradient heterodonty observed in the material. Anterior teeth are highly cusped, mesio-distally restricted, with a flat basal face, whereas (antero)lateral teeth become increasingly more mesio-distally elongated, with a lower crown and slight basal arching. The crown is polycuspid with a main cusp that is at least twice the height of the flanking lateral cusplet pair. The number of lateral cusplets range in number from 1–2 in anterior teeth to five in laterals, and may be unequal on opposite extremities, even in anteriors, causing asymmetry in the teeth. The lateral cusplets are of decreasing height away from the main cusp, and all cusps are erect in anteriors and distally slanted in (antero)lateral teeth. Labio-lingual compression of the crown is significant in anteriors, but more moderate in lateral teeth, which may cause the main cusp to appear somewhat massive in lateral view. A longitudinal crest traverses all cusps along the midline of the teeth and is particularly raised on the main cusp and towards the first cusplet pair, creating a blade-like appearance. The crown is ornamented with well-spaced and well-developed vertical cristae, which originate at the crown shoulder and are generally oriented towards the cusp apices, but may be obliquely inclined in a distal direction in lateral teeth. The cristae either terminate in the cusp apex, or a short distance from it. Labially, they rarely anastomose near the apex. The crown/base junction is smooth lingually, but labially the crown significantly overhangs the base.

The base protrudes beyond the crown lingually and also shows some evidence of a slight labial protrusion. The labial face of the base remains shallow. It possesses a baso-labial sulcus with jagged margin, caused by exposed vascular canals on the basal face labially. Small foramina open on the labial face near the crown/base junction, whereas lingually, foramina of varying size are positioned randomly. The vascularisation type is pseudopolyaulacorhize.

Remarks. The synechodontiform affinity of this material is indicated by the crown ornamentation, often typically observed in this order, and morphological characteristics of the base (Duffin and Ward 1993). Any similarity in tooth shape and crown ornamentation to *Rhomphaiodon* Duffin, 1993a, a neoselachian of uncertain affinities, is rejected as a basis for assignment of the American material to this genus, because of distinct differences, including the much larger size (10x) of *Rhomphaiodon* teeth, the fact that lateral cusplet pairs are limited to a maximum number of three and that they attain a much larger height, the absence of a labial crown overhang, and anaulacorhize vascularisation. The significant labial overhang of the crown over the crown/base junction suggests that these teeth should be assigned to *Synechodus* Woodward, 1888, because it is considered diagnostic of the genus (Duffin and Ward 1993; Klug 2009). For reasons detailed in the generic remarks, however, the material cannot be officially referred to *Synechodus*, which means that this material should be referred to as *'Synechodus'* (pre-Jurassic). Of the species relevant to this group, the closest morphological relationship is believed to be with *'Synechodus'* sp. and a new *'S.'* species from the Olenekian and Anisian of northern Siberia, Russia (Ivanov and Klets 2007), but is not considered identical (based on visual comparison only, because an adequate description of the Russian specimens is lacking). The American material may belong to a new species, mainly based on the distinct appearance of the anterior teeth.

Genus NEMACANTHUS Agassiz, 1837

Type species. *Nemacanthus monilifer* Agassiz, 1837; from the Rhaetian at Aust Cliff, England.

Nemacanthus sp.

Figure A3.22, A–E

Material. Sample AO40, Khuff Formation, yielded two fragments. Specimen used for imaging: MPUM10905; remaining specimen: MPUM10906 (1). MPUM11057 from another level of the Khuff Formation in the Haushi-Huqf area was imaged for additional observations.

Description and *Remarks* published in Koot *et al.* (2013).

Gen. et sp. indet.

Figure A3.8, P–Q

Material. Sample 300311-K, Kamura Formation, yielded four broken specimens. Specimen used for SEM imaging: JP74; tentatively assigned specimens: JP73, JP75–JP76.

Description. These cusp fragments are slender and high (measuring minimally 0.9 mm mesio-distally and 1.8 mm high). The cusp apex is pointed, but bluntly tipped. A low longitudinal crest (cutting edge) ascends the cusp on both lateral faces and few equally fine cristae ornament at least the labial face. The cusp possesses a sigmoid profile.

Remarks. This material is assigned to the Synechodontiformes based on the height and sigmoid curvature of the (main) cusp. Similar morphology is present in *Sphenodus* Agassiz, 1843 (Duffin and Ward 1993) and a sigmoid profile is also known to occur in Early Jurassic specimens of *Palidiplospinax occultidens* (Duffin and Ward, 1993).

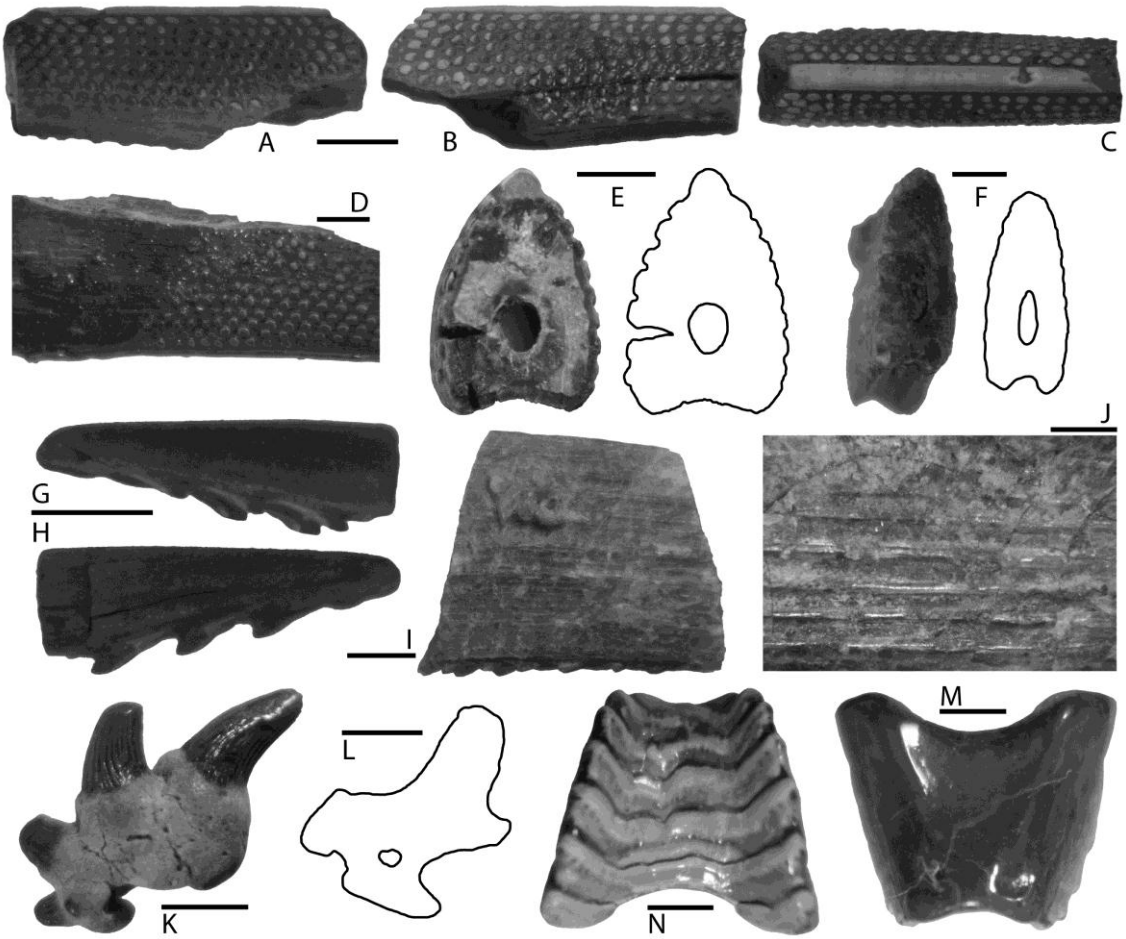

Figure A3.22 – Neoselachian fin spines, hybodont teeth and euchondrocephalian tooth plates from the Khuff Formation, Haushi Cliff and Saiwan, Haushi-Huqf area, central eastern Oman. Figs A–E. *Nemacanthus* sp. A–C, E, MPUM10905, loc K1, sample AO40; dorsal fin spine fragment. A, lateral, B, lateral, and C, anterior views; scale bar 2 mm, and E, cross-section; scale bar 1 mm. D, MPUM11057; dorsal fin spine fragment. Lateral view, detail; scale bar 2 mm. Figs F–J. *Amelacanthus* sp. cf. *A. sulcatus* (Agassiz, 1837). G–H, MPUM10907, loc K1, sample AO40; dorsal fin spine fragment. G, lateral, and H, lateral views; scale bar 1 mm. F, I–J, MPUM11058; dorsal fin spine fragments. F, cross-section; scale bar 2 mm, I, lateral view; scale bar 2 mm, and J, lateral view, detail; scale bar 1 mm. Fig K. *Gunnellodus bellistriatus* (Gunnell, 1933). MPUM11051, loc Saiwan, sample AO214; articulated teeth. Lateral view; scale bar 1 mm. Fig L. Petalodontiformes? gen. et sp. indet. MPUM11054, loc Saiwan, sample AO214; tooth fragment. Section outline; scale bar 0.5 mm. Figs M–N. *Solenodus* sp. cf. *S. crenulatus* Trautschold, 1874. MPUM11052, loc Saiwan, sample AO214; tooth plate. M, apical, and N, basal views; scale bars 1 mm.

Genus GENUS P

Preliminary type species. Genus P sp. P; from Olenekian (Lower Triassic) Hallstatt-type limestone olistoliths at Jabel Safra, Oman Mountains, Sultanate of Oman.

Preliminary diagnosis. Gradient monognathic heterodont dentition; symmetrical anterior teeth and asymmetrical lateral teeth; slight basal arching anteriorly; anteriormost teeth with a U-shaped base and base of the crown in apical view; 1–3 well-developed lateral cusplet pairs and additional cusplets in asymmetrical teeth; pointed cusps, recurved or directed lingually; crown labio-lingually compressed; acute longitudinal crest; small to moderate lingual peg, which may also be absent; no labial peg; small nodes and weak circumferential rim at the crown shoulder; oblique and straight vertical cristae; lingually protruding base; anaulacorhize to polyaulacorhize vascularisation.

Distribution. Oman Mountains, Sultanate of Oman (this study); Guizhou Province, China (this study).

Stratigraphical range. Griesbachian, Induan, Lower Triassic–Anisian, Middle Triassic.

Genus P sp. P

Figure A3.11, V–X; Figure A3.23, A–AB

Preliminary holotype. One complete tooth (GSC135735, Figure A3.23, E–H).

Preliminary paratypes. Two complete teeth (GSC135693, Figure A3.23, Q–T; GSC135855, Figure A3.23, Y–AB).

Preliminary type locality. Jabel Safra, Oman Mountains, Sultanate of Oman.

Preliminary type stratum. Red limestone (Hallstatt-type) olistolith, Block 3, Oman Exotics, Kawr Group?, Hawasina Allochthonous, Spathian (upper Olenekian, Lower Triassic).

Material. Samples 103A, 103C, 104A, 104B/C, 117A, WA 22, Hallstatt-type limestone olistoliths and Alwa Formation, yielded 22 complete and broken specimens. Specimens used for SEM imaging: GSC135735, GSC135886 (anterior), GSC135752, GSC135861 (anterolateral), GSC135649, GSC135693 (lateral), GSC135855 (posterior); specimens used for SEM microstructure study: GSC135630, GSC135766, GSC135820; remaining specimens: GSC135629, GSC135631, GSC135634, GSC135638, GSC135641, GSC135723, GSC135751, GSC135789, GSC135794, GSC135799, GSC135840, GSC135849.

Sample 100224-G, Al Jil Formation, yielded one fragmented specimen: OM85. This tooth fragment is a partial hollow crown, but shows the labial face of the main cusp and one entire extremity with two lateral cusplets. Vertical cristae are present, as well as a clear circumferential rim and longitudinal crest. A small peg is present at the base of the main cusp labially and the cusps are slightly recurved lingually. The assignment is made with some uncertainty and must remain as cf. Genus P sp. P because of the limited and fragmented nature of the material. If confirmed, having been recovered from the Griesbachian (basal *Clarkina carinata* conodont Zone), it would represent the oldest record of this genus and species.

Preliminary diagnosis. As for genus.

Description. Gracile teeth that gradually become more elongated in lateral and posterior teeth (0.7–1.6 mm mesio-distally, 0.2–0.3 mm labio-lingually and maximally 0.4–0.5 mm high). Gradient heterodont dentition in which anterior and anterolateral

teeth are symmetrical and may be slightly arched apico-basally, but posterior teeth are straight and distinctly asymmetrical. In apical view, the outline of the teeth is characterised by straight to slightly convex lingual and labial margins. Only one specimen (GSC135886) possesses a distinctly U-shaped base and base of the crown with a concave labial and convex lingual margin. The main cusp comprises about half the tooth height and is always higher than the 1–3 well-developed lateral cusplet pairs, which are of decreasing height away from the central part of the teeth. All cusps are somewhat pointed, as well as recurved or directed lingually, but this is most extreme in anterior teeth and the cusps adopt a more erect position in more posterior teeth. The crown is labio-lingually flattened, creating an acute longitudinal crest. A small to moderate lingual peg may be developed at the base of the main cusp, but can also be entirely absent. The labial side of the main cusp may show a slight rounded bulge, but a peg is never present. Small nodes at the crown shoulder are usually present, joined by a weak circumferential rim, but these are best developed labially. The ornamentation pattern consists of oblique and straight vertical cristae on both lingual and labial faces, originating from the rim at the crown shoulder and either connecting it with or otherwise oriented towards the cusp apices. They occasionally anastomose near the cusp apices.

The base is characterised by a lingual protrusion beyond the crown. Small foramina of varying size are positioned in a row-like fashion on the lingual face. Few foramina open randomly on the labial face, but more numerous and larger foramina are located near the baso-labial margin and in some cases the canals are open for some length, creating a corrugated appearance of the baso-labial margin. This pattern indicates an anaulacorhize to polyaulacorhize vascularisation.

Enameloid microstructure. The pattern described here is the result of combined observations from a number of teeth, because no teeth were available of which the entire crown surface could be examined. Typical and homogeneous single crystallite enameloid (SCE) was observed over the entire crown, consisting of rod-shaped

crystallites that are randomly orientated and on average 1 µm in length. However, weak organisation of the crystallites—which remained individually discernible—into bundles of roughly 1 µm thick was observed near the apex of the main cusp. They follow a subparallel interweaving pattern, but are generally oriented along the height axis of the main cusp and parallel to the crown surface. It was not possible to determine beyond doubt whether the bundles continue towards the base of the crown and then become covered by thickening SCE, or whether the bundles are discontinued. Nevertheless, support for the latter comes from the observation that the organisation of the crystallites making up bundles seems to become weaker towards lower parts of the cusp and they then disperse. Although primitive, the fabric is characteristic of parallel-bundled enameloid (PBE). Remnants of SCE were observed covering the PBE, which would indicate the presence of a shiny layer enameloid (SLE).

Remarks. The neoselachian affinities of this taxon are suggested by the anaulacorhize to pseudopolyaulacorhize vascularisation of the base of the teeth (Duffin and Ward 1993), and confirmed by the presence of PBE (see references in Maisey *et al.* 2004). Taphonomic recrystallisation of the enameloid layer towards the base of the crown in many teeth, where the layer is thinnest (Cuny and Risnes 2005), hindered interpretation of the microstructural pattern in this dentition. Combined observations nevertheless indicated that the observed pattern is primitive. The characteristics of this taxon further show similarity to synechodontiform morphology, including: heterodont dentition; main cusp flanked by lateral cusplets, cristae at the base of all cusps; and lingually protruding base with flat to slightly concave basal face. There is some resemblance between the crown morphology of anterior teeth of Genus P and *'Synechodus' incrementum* Johns, Barnes and Orchard, 1997 Type A, but the crown morphology of lateral and posterior teeth of Genus P as well as the general basal morphology is more similar to *'S.' multinodosus* Johns, Barnes and Orchard, 1997 Type B. The presence of a lingual peg in most teeth, although small, prevents inclusion

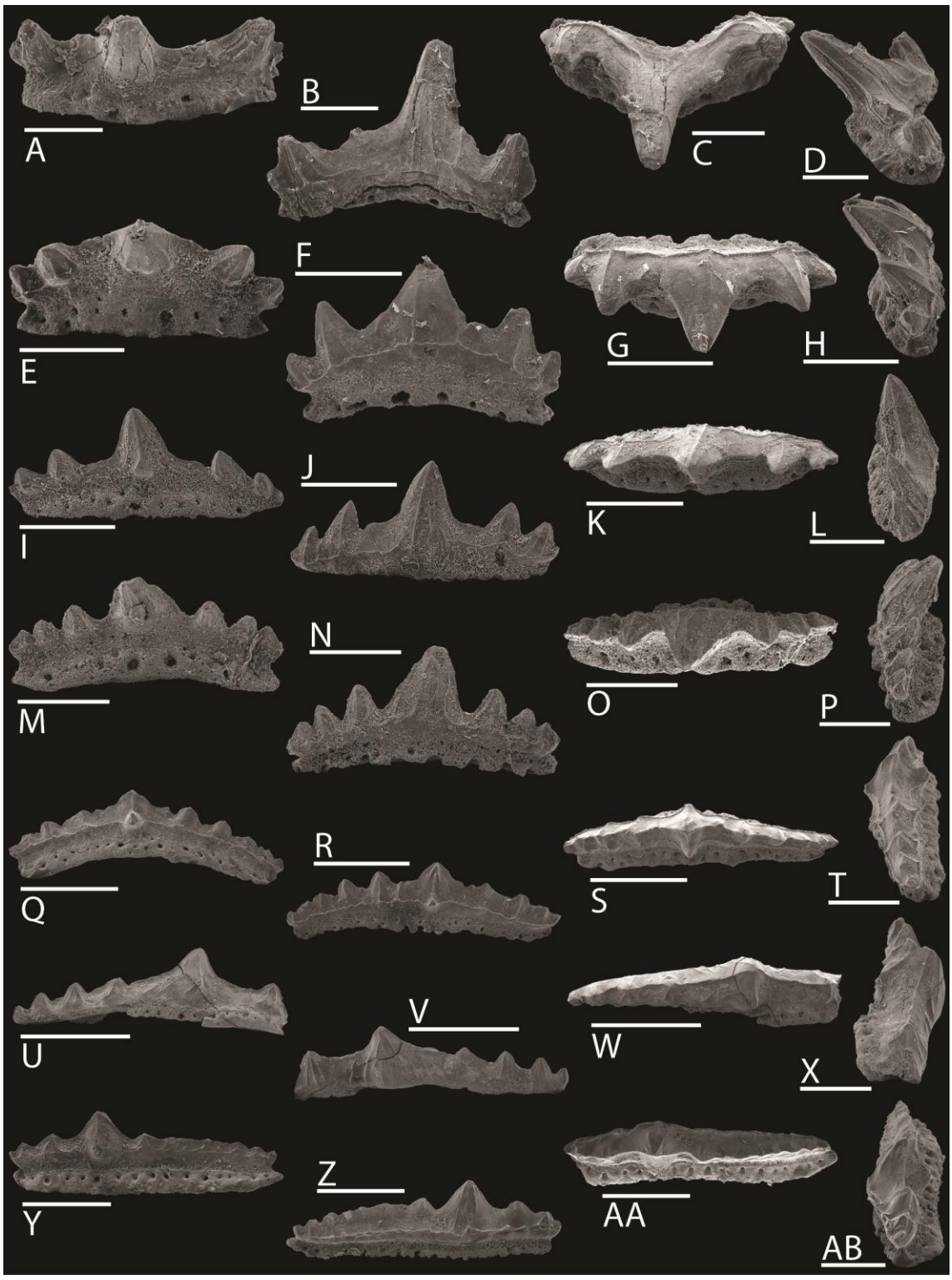

Figure A3.23 – Synechodontiform teeth from the Hallstatt-type limestone olistoliths at Jabel Safra and Alwa Formation at Wadi Alwa, Oman Mountains, northern Oman. Figs A–AB. Genus P sp. P. A–D, GSC135886, sample WA 22, Wadi Alwa; tooth. A, lingual, B, labial, C, apical, and D, lateral views; scale bars 200 µm. E–H, GSC135735, sample 103C, Jabel Safra; tooth, holotype. E, lingual, F, labial, G, apical, and H, lateral views; scale bars 300 µm. I–L, GSC135752, sample 104A, Jabel Safra; tooth. I, lingual, J, labial, K, apical views; scale bars 400 µm, and L, lateral view; scale bar 300 µm. M–P, GSC135861, sample 117A, Wadi Alwa; tooth. M, lingual, N, labial, O, apical views; scale bars 400 µm, and P, lateral

view; scale bar 300 µm. Q–T, GSC135693, sample 103C, Jabel Safra; tooth, paratype. Q, lingual, R, labial, S, apical views; scale bars 500 µm, and T, lateral view; scale bar 300 µm. U–X, GSC135649, sample 103A, Jabel Safra; tooth. U, lingual, V, labial, W, apical views; scale bars 1 mm, and X, lateral view; scale bar 500 µm. Y–AB, GSC135855, sample 117A, Wadi Alwa; tooth, paratype. Y, lingual, Z, labial, AA, apical views; scale bars 500 µm, and AB, lateral view; scale bar 300 µm.

in the Palaeospinacidae, which leaves the systematic position of this taxon unclear at present, but the primitive nature of the enameloid microstructure indicates that this taxon belongs among the stem group neoselachians.

cf. Genus P sp.

Figure A3.24, A–H

Material. Samples O-14, Luolou Formation, O-23, O-31, O-40, GQC182, Xinyuan Formation, yielded five complete and broken specimens. Specimens used for SEM imaging: 420, 427; remaining specimens: 375 (tentative due to damage), 394, 409.

Description. Small and elongate teeth (1.5 mm mesio-distally, 0.4 mm labio-lingually and 0.4–0.6 mm high), which display some heterodonty. Teeth in an anterior position are symmetrical and significantly basally arched, whereas lateral teeth are distinctly asymmetrical and only slightly arched. The multicuspid crown consists of a moderate and bluntly pointed main cusp, as well as lateral cusplets of decreasing size away from the centre of the tooth. Anterior teeth possess maximally three pairs of cusplets, but lateral teeth display one cusplet mesially and two distally. The main cusp can be very slightly distally slanted, but is generally asymmetrical, with a steep distal face and more gradually sloping mesial face. The main cusp further possesses a lingual peg and also a labial bulge that is positioned lower on the cusp, which can be observed in lateral view. These projections are better developed in lateral teeth, whereas anterior teeth have a more sleek appearance. A moderately acute longitudinal crest traverses the full

mesio-distal dimension of the teeth, including the cusp apices. The ornamentation consists of sparse, but well-developed cristae that run either vertically or are somewhat oblique. They are generally oriented towards the cusp apices and may anastomose below the apex. They originate from an irregular circumferential rim at the crown shoulder with small nodes, below which the crown/base junction is moderately incised. The crown surface is otherwise smooth.

The base possesses a distinct but restricted and thin lingual protrusion, as well as a shallow baso-labial sulcus. It is perforated by foramina of varying size, which approach a row-like organisation lingually, but are randomly positioned labially, some of which open on the baso-labial edge, resulting in a slightly corrugated appearance. This is typical of anaulacorhize vascularisation, approaching the pseudopolyaulacorhize type.

Remarks. The affinity of these teeth is difficult to determine. The anaulacorhize vascularisation suggests a hybodont relationship, but there are a number of features which are similar to those diagnostic of Genus P. This includes heterodonty involving symmetrical anterior teeth and asymmetrical lateral teeth with some basal arching, as well as 1–3 lateral cusplets on either side of the main cusp. The material is too limited

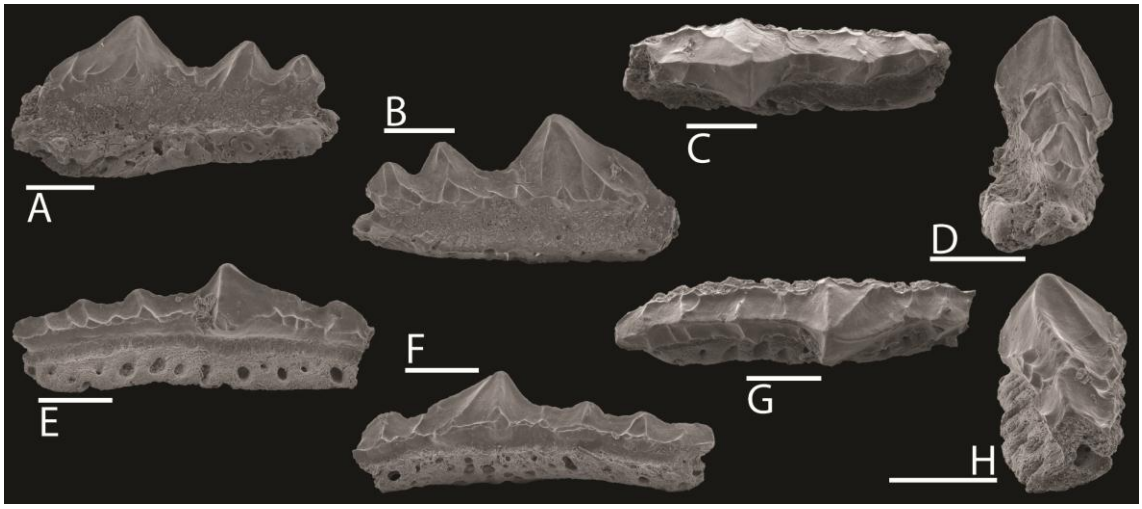

Figure A3.24 – Chondrichthyan teeth from the Xinyuan Formation, Lower Guandao section, Guizhou Province, southern China. Figs A–H. cf. Genus P. A–D, 420, sample O-40; tooth. A, lingual, B, labial, C,

apical, and D, lateral views; scale bars 300 µm. E–H, 427, sample GQC-182; tooth. E, lingual, F, labial, G, apical, and H, lateral views; scale bars 300 µm.

to assess the presence of anteriors with one or two cusplet pairs and multiple additional cusplets in posterior teeth. Further corresponding features are a small lingual peg and labial bulge, the ornamentation pattern, and the basal morphology, although the pseudopolyaulacorhize pattern is somewhat better expressed in Genus P. This material differs in the lack of labio-lingual compression of the crown and the cusps being erect rather than directed lingually. This is the reason why the material is assigned only tentatively to Genus P.

Order *INCERTAE SEDIS*

Gen. et sp. indet. A

Figure A3.18, E–J

Material. Samples AO38, AO214, Khuff Formation, yielded two complete specimens. Specimen used for SEM imaging: MPUM11024; remaining specimen: MPUM11050.

Description, *Enameloid microstructure* and *Remarks* published in Koot *et al.* (2013).

Gen. et sp. indet. B

Figure A3.8, R–S

Material. Sample 300311-M, Kamura Formation, yielded 11 isolated cusp fragments. Specimen used for SEM imaging: JP84; remaining specimens: JP82–83; tentatively assigned specimens: JP85–92.

Description. These isolated cusp fragments are small (approximately 0.5 mm in mesio-distal dimension and minimally 1.0 mm high). In apical view, their outline is rounded to slightly labio-lingually compressed. The cusps possess a thin, raised longitudinal crest (cutting edge).

Enameloid microstructure. The enameloid appears to be made up of (at least) a layer of parallel bundled enameloid (PBE). The bundles are 0.8–1 µm thick.

Remarks. This material is assigned to the Neoselachii based on the strong development of a well-raised and thin cutting edge. This feature has also been recognised in hybodonts but only in taxa of younger age, such as *Egertonodus* Maisey, 1987 from the Middle Jurassic of England (Rees and Underwood 2008). Furthermore, it appears that a layer of PBE is present, although it cannot be entirely ruled out that the observed features are the result of recrystallisation due to the poor preservation of the material.

Genus AMELACANTHUS Maisey, 1982a

Type species. *Onchus sulcatus* Agassiz, 1837; from the lower Carboniferous Limestone of Gloucestershire and Shropshire, England and Armagh, Northern Ireland.

Amelacanthus sp. cf. *A. sulcatus* (Agassiz, 1837)

Figure A3.22, F–J

1837 *Onchus sulcatus* Agassiz, vol. 3, p. 8, pl. 1, fig. 6.

1883 *Ctenacanthus sulcatus* Davis, p. 343.

1891 *Ctenacanthus sulcatus* Woodward, p. 101.

1982a *Amelacanthus sulcatus* Maisey, pp. 8–10, fig. 5A–E.

Material. Samples AO40, AO55, AO47bis, AO50, Khuff Formation, yielded 25 fragments. Specimen used for imaging: MPUM10907; remaining specimens: MPUM10908 (11), MPUM10925 (3), MPUM10943 (9), MPUM10953 (1). MPUM11058 from another level of the Khuff Formation in the Haushi-Huqf area was imaged for additional observations.

Description and *Remarks* published in Koot *et al.* (2013).

Genus cf. AMELACANTHUS Maisey, 1982a

Type species. *Onchus sulcatus* Agassiz, 1837; from the lower Carboniferous of Gloucestershire and Shropshire, England and Armagh, Northern Ireland.

cf. *Amelacanthus* sp.

Figure A3.11, M–N

Material. Sample 103C, Hallstatt-type limestone olistolith, yielded two fragmented specimens. Specimen used for SEM imaging: GSC135736; remaining specimen: GSC135737.

Description. Apex fragments belonging to slightly posteriorly recurved spines (largest fragment approximately 1.3 mm in length, and 0.3–0.4 mm in width and anteroposterior dimension) with pointed apex. The anterior and lateral margins are smooth and rounded. The posterior wall is concave with flattened centre and potentially a low rise mesially, as well as well-developed downward pointing denticles (‘hooks’) at about equal height on both margins, which appear 0.3 mm below the apex and gradually increase in size. An acute crest runs from the apex along both margins of the posterior wall, traversing all denticles.

Remarks. The affinities of the spine fragments described here are difficult to ascertain, because of the limited nature of the material. However, there are many similarities with the apex fragment of *Amelacanthus* sp. cf. *A. sulcatus* (Agassiz, 1837) from the Wordian of Oman. Shared characteristics with *Amelacanthus* Maisey, 1982a include: spines slender and slightly recurved; anterior margin acute but rounded; posterior wall concave or flat, sometimes with a low rise mesially; distinct anterior rib absent; posterolateral margins ornamented apically by small, usually downcurved and rounded or pointed denticles (Maisey 1982a). The concave posterior wall suggests a neoselachian relationship for the taxon, but a definitive association with any of the teeth described in this fauna is not possible.

Subclass EUCHONDROCEPHALI Lund and Grogan, 1997

Order EUGENEODONTIFORMES Zangerl, 1981

Superfamily CASEODONTOIDEA Zangerl, 1981

Family CASEODONTIDAE Zangerl, 1981

Genus CASEODUS Zangerl, 1981

Type species. *Orodus basalis* Cope, 1894; from the Pennsylvanian (upper Carboniferous) of the Mecca Quarry Shale in Illinois, USA.

Diagnosis. *Sensu* Mutter and Neuman, 2008, p. 12.

Caseodus sp. cf. *C. varidentis* Mutter and Neuman, 2008

Figure A3.5, E–H; Figure A3.25, A

Material. Sample 93 OF TE-5 1663 62-TE 325A, Blind Fiord Formation, yielded two nearly complete specimens. Specimen used for SEM imaging: 446; specimen used for light microscopy imaging: 445.

Description. The teeth are of variable morphology. The imaged tooth is elongate, oblong in outline in labial and lingual view, largely symmetrical, and distinctly labio-lingually compressed (1.1 mm mesio-distally, 0.4 mm labio-lingually, and 0.6 mm high). Labially, the base is two thirds of the total tooth height, whereas lingually, it is one third of the height. In labio-apical view, the outline of the crown and base is concave lingually, and convex labially. The crown is apparently devoid of cusps, but may have borne a blunt and low main cusp (area damaged). A distinct longitudinal crest is developed, which is labially directed, due to the subvertical labial face and the first gradually and then more steeply sloping lingual face. A transverse crest is absent. Few large and vertically elongated nodes are developed at the crown shoulder and extending across the lower half of the crown. They resemble coarse and short cristae and are stronger developed labially. The crown surface is otherwise smooth. Labially, a peg-like structure is present in the central part of the tooth, which is supported by a basal buttress. The crown overhangs the base somewhat on the lingual face and the lateral extremities.

The base is simple and does not protrude beyond the crown, although if the crown shoulder is aligned on a horizontal plane, the base is directed lingually. Few very large foramina perforate the base and penetrate it entirely.

The remaining specimen is elongate, not as labio-lingually compressed, and of similar dimensions. It is shallowly U-shaped in apical outline, with the strongest curve asymmetrically placed. The lingual outline is convex and the labial outline concave. It possesses three irregular labial buttresses, the largest of which (positioned in the

middle) is supported by the base. The longitudinal crest is particularly prominent, as is the rest of the ornamentation, consisting of very well-raised (especially lingually) and occasionally anastomosing vertical cristae that originate at the crown shoulder and terminate in the longitudinal crest. They also adorn the labial crown buttresses. The base is damaged, but displays simple vascularisation, consisting of few large foramina positioned randomly.

Remarks. The eugeneodont affinity of these teeth is suggested by the strong development of the vertical cristae and the buttresses on the labial face. Mutter and Neuman (2008) have indicated that major problems exist with regard to eugeneodontid systematics, which is why the identification made here must remain tentative based on the limited nature of the material. Nevertheless, the specimens resemble most a lateral pavement tooth and a distal tooth of *Caseodus* Zangerl, 1981.

A study performed on Early Triassic eugeneodontid sharks from the Wapiti Lake area in western Canada, which is of the same age and in the same palaeogeographical area as Ellesmere Island, identified the occurrence of *C. varidentis* Mutter and Neuman, 2008, the youngest representative species of a genus that was previously only known from the Carboniferous. Ginter *et al.* (2010) describe teeth of this genus as elongate and low-crowned, spaced by strong buttress projections on the labial face. The lack of strong crenulations on the lingual face of the teeth is a diagnostic characteristic of upper teeth of *Caseodus* (Mutter and Neuman 2008) that is recognised in the material studied here. The diagnosis of *C. varidentis* describes blunt or pavement teeth with a variable degree of ornamentation, and the conspicuous development of a labial buttress. Mutter and Neuman (2008) further mention that the majority of teeth are small (3 mm) and lack a main cusp, and that distal teeth possess a distinct longitudinal crest and are slender in apical and lateral view. This agrees with the material described here, except for the even smaller size. The distal tooth morphology shown in Mutter and Neuman (2008, fig. 6f) is similar to the ornamentation observed in the material from Ellesmere Island. Additional similarities exist with regard to basal features described

from the Wapiti Lake dentitions, including a base that is as deep or deeper than the crown and large vascular cavities (Mutter and Neuman 2008). The material described here is assigned to *C. varidentis* with some reservations appropriate for its limited nature and because of the lack of isolated type material from this species, which precludes visual comparison of all crown and basal characteristics.

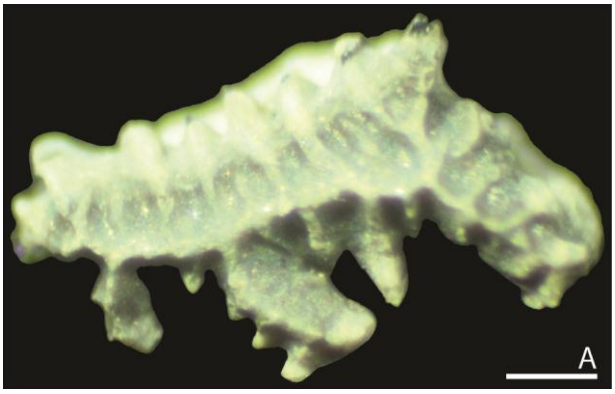

Figure A3.25 – Chondrichthyan tooth from the Blind Fiord Formation, Ellesmere Island, Canadian Arctic. Fig A. *Homalodontus* sp. cf. *H. aplopagus* (Mutter, De Blanger and Neuman, 2007). 445, sample 93 OF TE-5 1663 62-TE 325A, Blind Fiord Formation; tooth, apical view; scale bar 200 µm.

Genus FADENIA Nielsen, 1932

Type species. *Fadenia crenulata* Nielsen, 1932; from the Wuchiapingian (Lopingian) *Posidonia* Shale Member of the Foldvik Creek Formation in East Greenland.

Diagnosis. *Sensu* Mutter and Neuman, 2008, p. 18.

Fadenia crenulata Nielsen, 1932

Figure A3.26, A–G

1932 *Fadenia crenulata* Nielsen, pp. 43–49, text-figs 3B, D, 7b; pl. 2, fig. 1; pl. 3, figs 1–4; pl. 4, figs 1–12; pl. 5, figs1–12; pl. 6, figs 1–18; pl. 9, figs 1–2; pl. 12, figs 1–2; pl. 15, figs 8–10; pl. 16, fig. 6.

1952 *Fadenia crenulata* Nielsen, pp. 41–43, text-fig. 17A–C; pl. 12, figs 1–2; pl. 13, fig. 2.

1988 *Fadenia crenulata* Bendix-Almgreen *et al.*, p. 101.

Material. Samples 090816-F, 090816-G, Ravnefjeld Formation, 090816-A, 090816-B, 090818-A, Schuchert Dal/Wordie Creek Formation, yielded numerous specimens, partly encased in matrix. Specimens used for imaging: GR3–7, GR10; remaining specimens: GR2, GR11 (lot).

Description. Tooth fragments varying from 0.5 to 2.2 cm in mesio-distal dimension, displaying tubular dentine on a sectioned or worn surface. At least one symphysial tooth can be recognised, displaying acutely angled lateral extremities with a blunt median ridge, whereas lateral and posterior specimens may be curved (with the crest dividing the crown into two different-sized portions) or entirely flat. The crowns are tumid and the surface is either smooth or ornamented with fine, anastomosing cristae, especially on lateral surfaces. The lower margin of the crown may also be strongly folded. The base is perforated by randomly located foramina of variable size.

Remarks. The described features are characteristic of *Fadenia crenulata* Nielsen, 1932, which has previously been recovered from the Guadalupian and Lopingian of East Greenland (Nielsen 1932; Bendix-Almgreen *et al.* 1988) and the material is therefore identified as such. *Erikodus groenlandicus* Nielsen, 1932 shares some of the described features, but generally possesses flatter teeth that lack a median ridge and instead show a weak crest transverse to the sagittal plane in symphyseal teeth, which does not match the material described here. Its presence among the material can therefore be excluded.

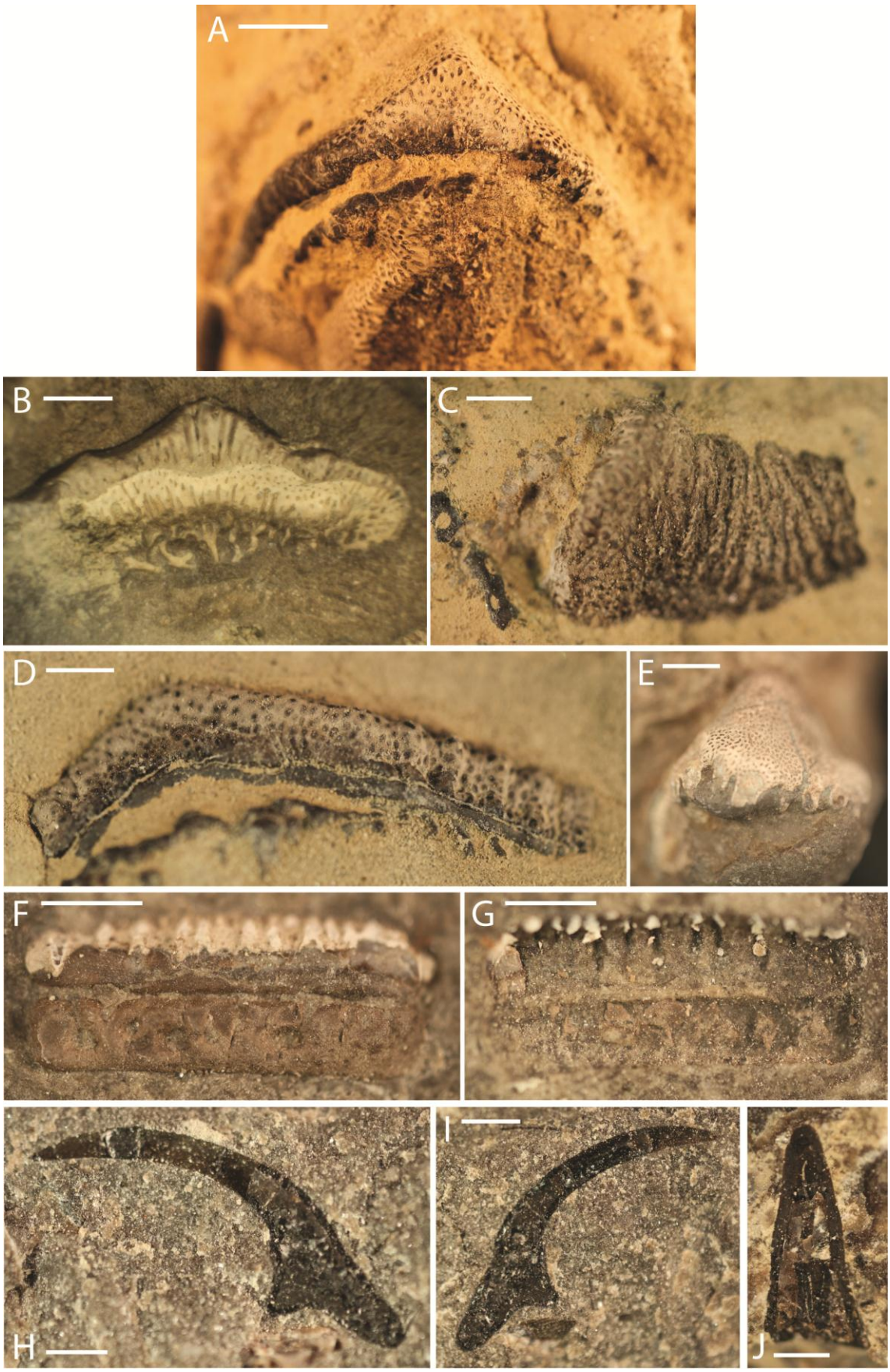

Figure A3.26 – Chondrichthyan teeth and spines from the Schuchert Dal and Ravnefjeld? formations at Kap Stosch, East Greenland. Figs A–G. *Fadenia crenulata* Nielsen, 1932. A, GR10, sample 090816-G; symphysial tooth. Fracture surface, anterior view; scale bar 4 mm. B, GR7, sample 090818-A; tooth.

Fracture surface, lateral view; scale bar 3 mm. C, GR4, sample 090816-G; tooth. Apical view of crown surface; scale bar 2 mm. D, GR5, sample 090816-G; tooth. Cross-section; scale bar 2 mm. E, GR6, sample 090818-A; symphyseal? tooth. Lingual view; scale bar 3 mm. F–G, GR3a, b, sample 090816-F; tooth. Opposing fracture surfaces, lateral view; scale bars 2 mm. Figs H–J. gen. et sp. indet. H–I, GR9a, b, sample 090820-D; cephalic spine?. Opposing fracture surfaces; scale bars 2 mm. J, GR8, sample 090816-H; cephalic spine?. Fracture surface of apical part; scale bar 1 mm.

Order EUGENEODONTIFORMES? Zangerl, 1981

Gen. et sp. indet. (East Greenland)

Figure A3.27, A–B

Material. Sample 09.08.22.c, Schuchert Dal/Wordie Creek Formation, yielded one specimen, partly encased in matrix. Specimen used for (light microscopy) imaging: GR1.

Description. Tooth that partly protrudes from encasing matrix (1.8 mm mesio-distally, maximal observable dimension, and 1.0 mm labio-lingually) with a tumid central part. One lateral extremity is completely exposed, whereas the opposite extremity may be completely exposed but could be presumed to still be partly covered by the matrix. The tooth is, therefore, potentially mesio-distally symmetrical. It possesses a low, tumid crown and pyramidal main cusp. There are two very low apices on the complete extremity and at least one on the potentially incomplete extremity. The crown possesses a labial buttress at the base of the main cusp and two flanking buttresses at the height of the first cusplet pair, which are somewhat curved centrally. The outermost cusplet also possesses a labial buttress that protrudes labially in a straight manner. The lingual outline of the tooth in apical view is undulating and shows bulges directly opposite the buttresses, of which the one at the main cusp is the largest. A longitudinal crest is present, which is well-developed and moderately acute on the main cusp, in addition to a transverse crest, which is gently creased lingually. Labially, the transverse

crest fades to a low and thin ridge on the buttress, and a row of low, rounded tubercles appears on either side, with the tubercles arranged in an alternate manner. The same feature is present on at least one of the flanking buttresses. Few vertical cristae radiate out from the outermost cusplet apex and may reach the crown/base junction. The crown surface is otherwise smooth. Wear facets occur near the apex of the main cusp, revealing the internal tubular dentine. No basal features can be observed due to its encasement in matrix.

Remarks. The specimen was mechanically prepared in an attempt to expose the crown and basal features of the tooth or even to extract it fully. Indeed, a large portion of the crown was uncovered, but the brittle nature of the tooth prevented any further action at this stage without risking significant and irreparable damage to the specimen. It is therefore documented here in its current state. The application of a suitably safe preparation method may be a possibility in future.

An eugeneodontiform affinity for this tooth is based on the presence of tubular dentine, which is normally distinctive for petalodontiforms, but also occurs in orodontiforms and eugeneodontiforms (Ginter *et al.* 2010), combined with typical crown morphological characteristics. These include the strong buttress projections on the labial face, which have been observed in lateral teeth of a number of eugeneodont genera, including *Caseodus* Zangerl, 1981, *Bobbodus* Zangerl, 1981, *Agassizodus* St. John and Worthen, 1875, as well as *Arpagodus* Trautschold, 1879. The general morphology of the tooth described here is reminiscent of this, but it is more mesio-distally restricted. Based on descriptions and comparison with figured material, the closest similarity is observed with either a mesio-lateral tooth of the the caseodontoid species *Caseodus varidentis* Mutter and Neuman, 2008 (fig.6b), or with a large lateral pavement tooth of the edestoid species *Agassizodus variabilis* Zangerl, 1981 (fig.85F). Both chronologically and geographically, *C. varidentis* is closer to the specimen from the Changhsingian of East Greenland described here, having been recovered from the Olenekian of western Canada, whereas *A. variabilis* is known from the Pennsylvanian

of the USA (e.g., Illinois and Nebraska; Ginter *et al.* 2010), although this cannot be used to draw a more definitive conclusion. No distinct features in crown surface ornamentation allow a more specific identification, especially because the occurrence of tubercles flanking cristae and crests has not previously been mentioned in the literature and the inward curvature of the buttresses is equally unusual. If further careful preparation of the specimen can reveal the full range of morphological characteristics or at least basal features, this will aid in better establishing its systematic assignment, which may require the creation of a new taxon.

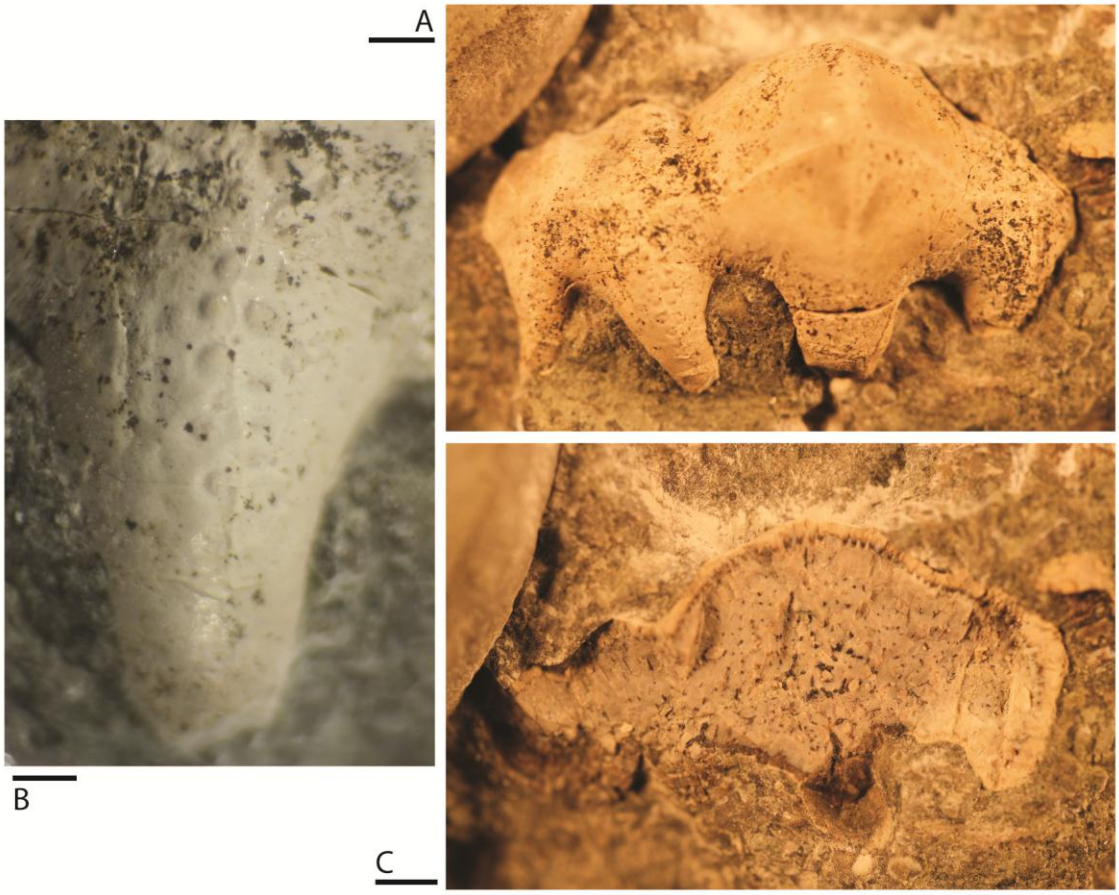

Figure A3.27 – Chondrichthyan tooth from the Schuchert Dal Formation at Kap Stosch, East Greenland. Figs A–C. Eugeneodontiformes? gen. et sp. indet. GR1, sample 09.08.22.c; tooth. A, apical view of exposed part of the tooth; scale bar 2 mm, B, detail of centralmost labial buttress on sinistral lateral extremity; scale bar 0.5 mm, C, apical view of fracture surface after removal of the crown; scale bar 2 mm.

Gen. et sp. indet. (Oman)

Figure A3.28, A–D

Material. Sample 965-2, Khuff Formation, yielded two broken specimens. Specimen used for SEM imaging: UC20272; remaining specimen: UC20310.

Description and *Remarks* published in Koot *et al.* (2013).

Order PETALODONTIFORMES? Zangerl, 1981

Gen. et sp. indet.

Figure A3.18, K–N; Figure A3.22, L

Material. Sample AO214, Khuff Formation, yielded two broken specimens. Specimen used for SEM imaging: MPUM11053; remaining specimen: MPUM11054.

Description and *Remarks* published in Koot *et al.* (2013).

Superorder HOLOCEPHALI Bonaparte, 1832-1841

Order COCHLIODONTIFORMES Obruchev, 1953

Family COCHLIODONTIDAE Owen, 1867

Genus DELTODUS Morris and Roberts, 1862

Type species. *Poecilodus sublaevis* Agassiz, 1838; from the Viséan (lower Carboniferous) of Armagh, Northern Ireland.

Deltodus sp. aff. *D. mercurei* Newberry, 1876

Figure A3.18, O–R

1876 *Deltodus mercurei* Newberry, p. 137, pl. 3, figs 1, 1a.

1883 *Deltodus mercurii* St. John and Worthen, pl. 10, fig. 2a–d.

1883 *Deltodus powelli* St. John and Worthen, pp. 154–156, pl. 9, fig. 1a–f.

1883 *Deltodus propinquus* St. John and Worthen, pp. 156–158, pl. 10, fig. 4a–e (not fig. 3a–e).

1916 *Deltodus mercurii* Branson, pp. 648–652, pl. 5, figs 1–11; pl. 2, figs 27–28; pl. 6, figs 1–6.

1943 *Deltodus mercurii* Hussakof, p. 1834.

1982 *Deltodus mercurii* McKee, pp. 121–122

1982 *Deltodus* sp. McKee, p. 488.

Material. Samples AO40, AO55, Khuff Formation, yielded 24 complete and broken specimens. Specimens used for SEM imaging: MPUM10912, MPUM10913; remaining specimens: MPUM10903 (1), MPUM10923 (21).

Description and *Remarks* published in Koot *et al.* (2013).

Family *INCERTAE SEDIS*

Genus SOLENODUS Trautschold, 1874

Type species. *Solenodus crenulatus* Trautschold, 1874; from the Pennsylvanian at Mjatschkowa in the Moscow region, Russia.

Solenodus sp. cf. *S. crenulatus* Trautschold, 1874

Figure A3.18, S–V; Figure A3.22, M–N

1874 *Solenodus crenulatus* Trautschold, p. 293, pl. 28, fig. 11.

Material. Samples AO55, AO214, Khuff Formation, yielded four complete and broken specimens. Specimen used for light microscope and SEM imaging: MPUM11052; remaining specimens: MPUM11032 (3).

Description and *Remarks* published in Koot *et al.* (2013).

Subclass EUCHONDROCEPHALI? Lund and Grogan, 1997

Superorder HOLOCEPHALI? Bonaparte, 1832–1841

Order CHIMAERIFORMES? Obruchev, 1953

Genus ARCTACANTHUS Nielsen, 1932

Type species. *Arctacanthus uncinatus* Nielsen, 1932; from the Wuchiapingian *Martinia* limestone of Clavering Ø and Kap Stosch, East Greenland.

aff. *Arctacanthus exiguus* Yamagishi, 2004

Figure A3.8, T–AC

2004 *Arctacanthus exiguus* Yamagishi, pp. 567–568, fig. 3.1–3.3.

Material. Samples 300311-I, 300311-J, 300311-K, 05.7.14.ak, 05.7.14.aw, Kamura Formation, yielded 23 complete and broken specimens. Specimens used for SEM

imaging: JP39, JP42; remaining specimens: JP9–16, JP40–41, JP43–48, JP76, JP98–100, JP106.

Description. These remains are spines of small size (0.9 mm mesio-distally, 2.8 mm antero-posteriorly and 2.9 mm apico-basally) and almost entirely bilaterally symmetrical. The crown consists of a high main cusp, which gradually tapers toward an acute apex. Its anterior and posterior faces are convex. The main cusp is straight along most of its length, but recurved posteriorly at the base (25–30°). Two acute and well-raised cristae run laterally from the apex along the entire length of the main cusp, but curve slightly anteriorly from halfway down the cusp in lateral view. They are adorned with numerous pointed denticles, which generally increase in size basally and are arranged symmetrically, although not consistently. The denticles gradually change orientation from being directed laterally in the upper half of the main cusp to anteriorly in the lower half of the main cusp. The position of either the basalmost or the penultimate denticle on both cristae is occupied by an accessory cusplet. These are much enlarged compared to the denticles and posteriorly recurved. The anterior face of the crown is largely smooth, except for very fine vertical striae along the entire length of the main cusp and on the accessory cusplets. The posterior enameloid covering has worn off in the best preserved specimens, preventing any observations on ornamentation. A medial anterior ridge is lacking.

The crown is positioned on the anteriormost part of the base. The base is largely oriented perpendicular to the crown (at its base) and elongated posteriorly. In lateral view, the height of the base is least near the crown and increases posteriorly. The apical part is also larger in width than the basal part, as best observed in posterior view. The basal face is flat, whereas the apical face is concave. One large foramen, in some cases accompanied by a smaller foramen, penetrates the posterior part of the apical face.

Remarks. The morphology of *Arctacanthus* Nielsen, 1932 is very characteristic, yet the affinity of these types of remains is still unclear. Most recently, Chen *et al.* (2007a) concluded that they most likely represent dermal denticles from the frontal claspers of Chimaeriformes, in accordance with Nielsen's (1932) initial view, which was based on Permian remains of *A. uncinatus* Nielsen, 1932 from Clavering Ø and Kap Stosch, East Greenland. *Arctacanthus wyomingensis* Branson, 1934 was erected to differentiate the specimens from the Permian Phosphoria Beds of Wyoming, USA from the East Greenland specimens, but no distinct morphological differences were identified (see Branson 1933, 1934; Nielsen 1935). *Arctacanthus exiguus* Yamagishi, 2004 from the Anisian of Japan was differentiated from *A. uncinatus* based on the lack of strong striae at the base of the crown and the much smaller size (the height of *A. exiguus* is approximately 10% of that of *A. uncinatus*), which is also true for the material described here, which is why it is attributed to *A. exiguus*. Minor differences with the material described by Yamagishi (2004) include a straight main cusp rather than a sigmoid lateral outline, and bilateral symmetry versus asymmetry introduced by slight twisting of the main cusp. These differences may be explained by their relative position on the clasper cartilage (Chen *et al.* 2007a), because stronger asymmetry has been linked to an increasingly lateral position (Duffin and Reynders 1995). The generic assignment is provided as aff. *Arctacanthus*, following the discussion by Chen *et al.* (2007a) based on aff. *Arctacanthus* specimens from the Ladinian/Carnian of China, which also exhibit these smaller proportions. They proposed that the smaller specimens potentially originated from a chimaeriform genus of smaller body size, which would be the Triassic representative of a lineage that suvived the late Permian mass extinction. The absence of any chimaeriform teeth in the Kamura fauna contrasts with the relative abundance of aff. *Arctacanthus* specimens and is explained by Chen *et al.* (2007a), who noted that chimaeriform taxa produce a very limited number of tooth plates during their lifespan.

aff. *Arctacanthus*? sp.

Figure A3.6, C–D

Material. Sample 05.7.15.h, Kamura Formation, yielded two broken specimens. Specimen used for light microscopy imaging: JP110; remaining specimen: JP111 (tentative).

Description. These remains resemble spines of small size (1.4 mm mesio-distally and minimally 1.6 mm apico-basally) and appear bilaterally symmetrical. The crown consists of a high main cusp, which gradually tapers towards an apex. Its anterior and posterior faces are convex and it is recurved posteriorly at the base. Two acute and well-raised cristae run laterally from the apex along the entire length of the main cusp. They are smooth. The anterior face of the crown is largely smooth, except for very fine vertical striae along the entire length of the main cusp. The posterior enameloid covering has worn off, preventing any observations on ornamentation. A medial anterior ridge is lacking. The crown is positioned on the anteriormost part of the base, which is not preserved.

Remarks. This material differs from the typical morphology of *Arctacanthus* Nielsen, 1932 in that the lateral cristae are entirely smooth and completely devoid of any denticles. This does not appear to be the result of wear. The material therefore compares best to the aff. *Arctacanthus* material described by Chen *et al.* (2007a) from the Ladinian/Carnian of China. These also possess fewer denticles, predominantly positioned near the base, and the remainder of the lateral edges of the cusp are smooth. The recovery of better preserved material is required to confirm these interpretations, and until that time, the material is listed as aff. *Arctacanthus*? sp.

ADDITIONAL ELASMOBRANCH MATERIAL

Dermal denticles – Haushi-Huqf area, Oman

Figure A3.28, E–W

A large number of dermal denticles (also referred to as menaspoid scales in Angiolini *et al.* 2003a) have been recovered from both the MPUM and UC collections. In the MPUM collection, the relevant lot numbers are: MPUM10904, MPUM10924, MPUM10942, MPUM10952. Establishing their precise affinity with particular taxa is problematic, because they were never found in direct association with teeth, but always as isolated elements. However, both ctenacanth and hybodont teeth have been recovered in the fauna and this is reflected in the dermal denticle assemblage. Nine morphotypes are recognised (Table 3.1). Ctenacanth denticles are of compound morphology (Reif 1978; see also e.g., Williams 1998; Ginter 2002a), whereas hybodontid denticles have a generally rounded base with a flat or convex basal face and a weakly developed neck (Reif 1978; Thies 1995). Morphotype 7 is identified tentatively as a symmoriiform dental element, based on similarities observed with a median(?) symmetric element of *Stethacanthus altonensis* (St. John and Worthen, 1875) from the Mississippian, described and figured in Lebedev (1996; fig.5A).

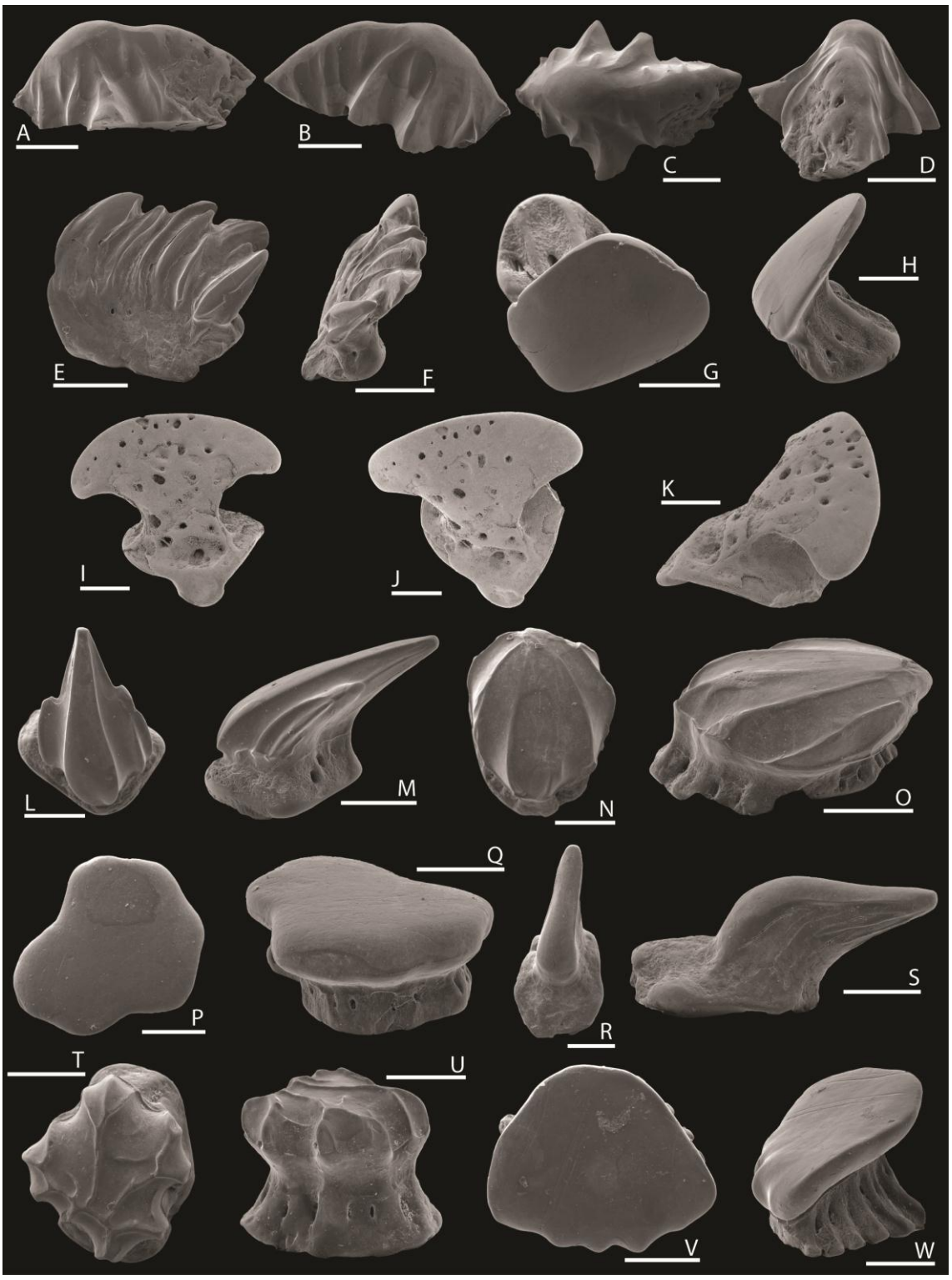

Figure A3.28 – Eugeneodontiform? tooth fragments and dermal denticles from the Khuff Formation, Haushi-Huqf area, central eastern Oman. Figs A–D. Eugeneodontiformes? gen. et sp. indet. UC20272, loc 6-7, sample 965-2, Haushi Cliff; tooth fragment. A, lingual/labial, B, lingual/labial, C, apical, and D, lateral views; scale bars 500 µm. Figs E–W. Gen. et sp. indet., dermal denticles. E–F, morphotype 1, loc 6-7, sample 965-4, Haushi Cliff. E, lateral, and F, posterior views; scale bars 300 µm. G–H, morphotype 2, loc 6-7, sample 965-4, Haushi Cliff. G, apical, and H, lateral views; scale bars 200 µm. I–K, morphotype 3, MPUM10944, loc K4, sample AO50, Haushi Cliff. I, anterior, J, apical, and K, lateral views; scale bars 300

µm. L–M, morphotype 4, loc 6-7, sample 965-4, Haushi Cliff. L, apical, and M, lateral views; scale bars 200 µm. N–O, morphotype 5, loc 6-7, sample 965-2, Haushi Cliff. N, apical, and O, lateral views; scale bars 200 µm. P–Q, morphotype 6, loc 6-7, sample 965-2, Haushi Cliff. P, apical, and Q, lateral views; scale bars 200 µm. R–S, morphotype 7, loc 6-7, sample 965-2, Haushi Cliff. R, apical, and S, lateral views; scale bars 200 µm. T–U, morphotype 8, loc 6-7, sample 965-2, Haushi Cliff. T, apical, and U, lateral views; scale bars 200 µm. V–W, morphotype 9, UC20377, loc 6-2, sample 965-9, Saiwan. V, apical, and W, lateral views; scale bars 300 µm.

Dermal denticles – Jabel Safra and Wadi Alwa, Oman

Figure A3.29, A–X

Dermal denticles have been recovered from the GSC collection. The relevant lot numbers are GSC135741 and GSC135818. Establishing their affinity with particular taxa in this fauna is not possible, because the denticles were not recovered in association with any teeth. The difficulty of identifying denticles was highlighted by Johns *et al.* (1997), who attributed it to the disarticulated state of the material in most collections and the heterogeneous nature of the squamation in many chondrichthyans. However, the hybodont and neoselachian composition of the fauna is reflected in the dermal denticle assemblage. There are 12 morphotypes, which are classified according to pedicle type and interpreted as shown in Table 3.3. The classification is based on the pedicle types of Johns *et al.* (1997), and the interpretation on the synechodontiform denticles figured in Duffin and Ward (1993), which typically possess a tetrahedroid pedicle, and on the hybodont denticles figured in Thies (1995), shown to typically possess a fluted truncate pedicle.

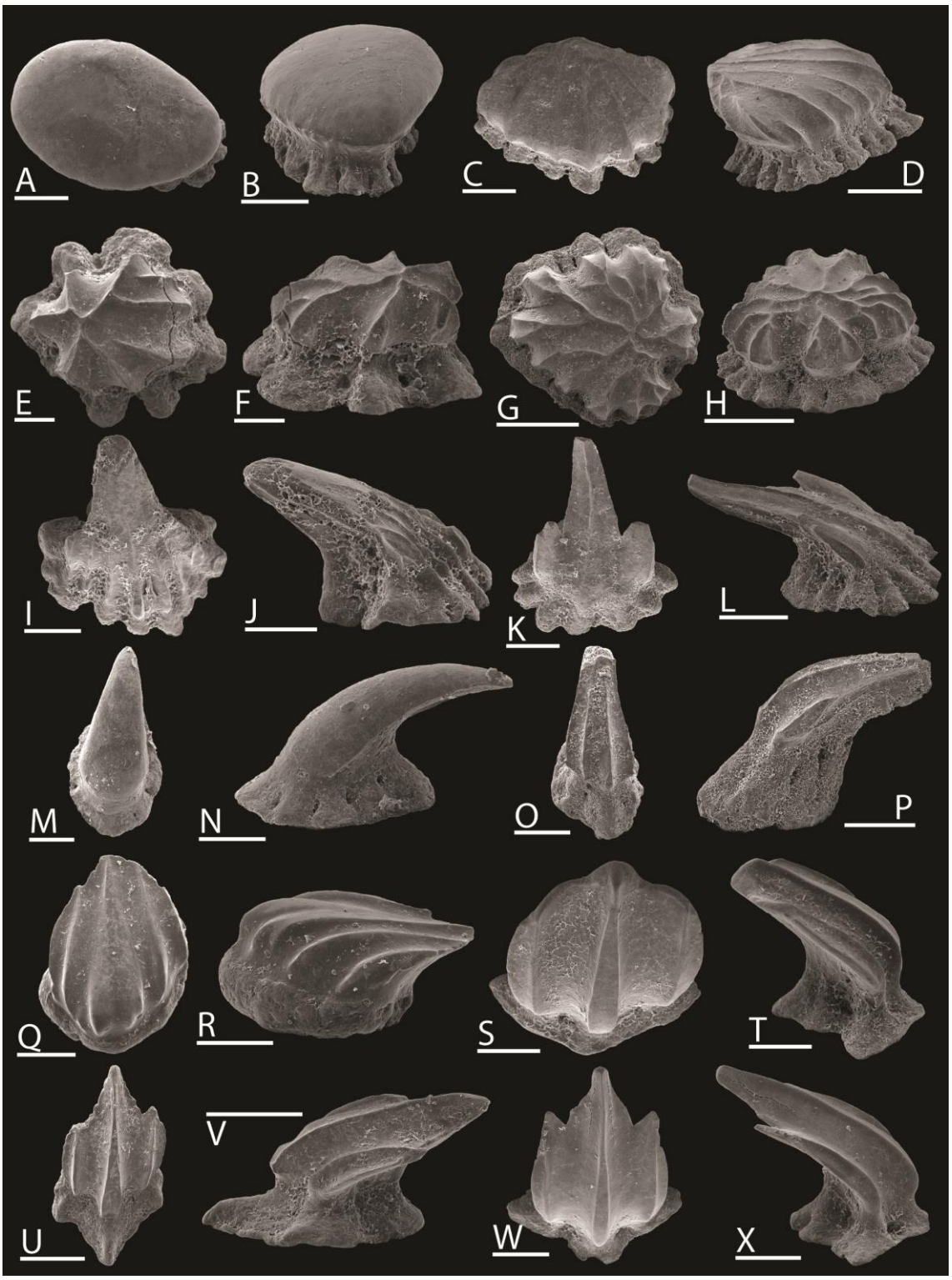

Figure A3.29 – Dermal denticles from the Hallstatt-type limestone olistoliths at Jabel Safra, Oman Mountains, northern Oman. Figs A–X. Gen. et sp. indet., dermal denticles. A–B, morphotype 10, sample 103C. A, apical, and B, lateral views; scale bars 100 µm. C–D, morphotype 11, sample 103C. C, apical, and D, lateral views; scale bars 100 µm. E–F, morphotype 12, sample 103C. E, apical, and F, lateral views; scale bars 50 µm. G–H, morphotype 13, sample 104A. G, apical, and H, lateral views; scale bars 300 µm. I–J, morphotype 14, sample 104A. I, apical, and J, lateral views; scale bars 100 µm. K–L, morphotype 15, sample 103C. K, apical, and L, lateral views; scale bars 100 µm. M–N, morphotype 16, sample 103C. M,

apical, and N, lateral views; scale bars 100 µm. O–P, morphotype 17, sample 104A. O, apical, and P, lateral views; scale bars 200 µm. Q–R, morphotype 18, sample 104A. Q, apical, and R, lateral views; scale bars 100 µm. S–T, morphotype 19, sample 103C. S, apical, and T, lateral views; scale bars 100 µm. U–V, morphotype 20, sample 104A. U, apical, and V, lateral views; scale bars 200 µm. W–X, morphotype 21, sample 103C. W, apical, and X, lateral views; scale bars 100 µm.

Dermal denticles – Canadian Arctic

Figure A3.30, A–C

Morphotype 22. Sample CH-F78-79, Assistance Formation, yielded one broken specimen. Specimen used for light microscopy imaging: 456. The pedicle is damaged, but appears to have been tetrapetaloid with a narrow crown/pedicle junction. The crown is erect near the base and gently curves posteriorly towards the apex. It is distinctly antero-posteriorly compressed and its outline is near-circular. The anterior crown surface is even and smooth, whereas the subcrown shows a mesial ridge, flanked by two vertically elongate depressions. The presence of a principal cusp cannot be assessed due to damage to the crown, but it is similar to *Fragilicorona brevirostrum* Johns, Barnes and Orchard, 1997 (pl. 25, fig. 1–2, 12–13) from northeastern British Columbia.

Morphotype 23. Sample CH-F79-79, Assistance Formation, yielded one complete specimen. Specimen used for light microscopy imaging: 457. The pedicle is posteriorly expanded and lobed. The crown/pedicle junction is very distinct, because the crown swells rapidly, especially on the lateral faces. The crown is inflated, but remains laterally restricted and spine-like, tapering towards the apex. It is also slanted laterally in the upper half. The crown surface is smooth on all faces.

Morphotype 24. Sample CH-F136-79, Trold Fiord Formation, yielded five specimens. Specimen used for light microscopy imaging: 466; remaining specimens: 464–465,

467–468. Variable in size. Pedicle appears rounded, with downwards sloping anterior part. The crown is spine-like with tapering apical part and curves moderately to distinctly posteriorly. The lower half is coarsely striated, whereas the upper half is smooth.

Figure A3.30 – Chondrichthyan dermal denticles from the Assistance and Trold Fiord formations, Ellesmere Island, Canadian Arctic and the Prida Formation at Coyote Canyon, Nevada, southwestern USA. Figs A–D. Gen. et sp. indet., dermal denticles. A, morphotype 22, 456, sample CH-F78-79, Assistance Formation; baso-posterior view; scale bar 200 µm. B, morphotype 23, 457, sample CH-F79-79, Assistance Formation; lateral view; scale bar 200 µm. C, morphotype 24, 466, sample CH-F136-79, Trold Fiord Formation; lateral view; scale bar 200 µm. D, morphotype 25, 353, sample 92 OF COY 4, Prida Formation; lateral view; scale bar 200 µm.

Dermal denticles – southwestern USA

Figure A3.30, D

Morphotype 25. Samples 91 OF HB110, 92 OF COY 4, Prida Formation, yielded four specimens. Specimen used for light microscopy imaging: 353; remaining specimens: 336, 352, 356. The pedicle is fluted truncate, and the lobes are continued into the strong striations, which run along the entire posteriorly directed crown. The crown is rounded in cross-section in the upper half, with a prominent mesial keel, but possesses antero-posterior, blade-like features near the base, which are developed to variable degree. There is great similarity between these specimens and *Parvidiabolus acutus* Johns, Barnes and Orchard, 1997 (pl. 18, figs 11–15) from northeastern British Columbia, but the crown is lower in the material described here.

ADDITIONAL EUCHONDROCEPHALAN? MATERIAL

Indeterminate spines – East Greenland

Figure A3.26, H–J

Samples 090816-H, 090820-D, Ravnefjeld Formation, and 090816-J, Schuchert Dal/Wordie Creek Formation, yielded several specimens. Specimens imaged with light microscopy: GR8–9 (lots); remaining specimens: GR12 (lot). Strongly posteriorly recurved spine with apparently smooth crown surface. Base with concave basal face and enlarged anterior lobe pointing downward. The base is atypical of a dorsal fin spine and the specimen is reminiscent of *Arctacanthus* Nielsen, 1932, a taxon that has previously been recorded from East Greenland (Nielsen 1932) and has most recently been interpreted as potentially representing chimaeriform frontal clasper denticles (Chen *et al.* 2007a). They were initially thought to be cephalic spines, which are better known from hybodonts (e.g., Wang *et al.* 2009), but these show a more complex crown morphology than the material described here. Hence, the specimens must remain unidentified.

REFERENCES

AGASSIZ, L. 1833–1843. *Recherches sur les poissons fossiles, 5 vols.*, Imprimerie de Petitpierre, Neuchâtel, 1420 pp.

AGASSIZ, L. 1859. *Notes on the collections of Lord Enniskillen and Sir Philip Egerton & London notes*, A. Ms. (unsigned), 14 sheets, MCZ archives, Harvard University, Cambridge, Massachusetts, U.S.A.

AHLBERG, P. E. 2009. Birth of the jawed vertebrates. *Nature,* **457**, 1094–1095.

ALBERTI, F., v. 1864. *Überblick über die Trias, mit Berücksichtigung ihres Vorkommens in den Alpen,* Stuttgart, Cotta, 353 pp.

ALESSANDRI, G. 1910. Studii sui pesci triasici della Lombardia. *Memorie della Societá Italiana di Scienze Naturali, Milano,* **7**, 1–145.

ALLISON, P. A. and BRIGGS, D. E. G. 1993. Paleolatitudinal sampling bias, Phanerozoic species-diversity, and the end-Permian extinction. *Geology,* **21**, 65–68.

ALROY, J. 2008. Dynamics of origination and extinction in the marine fossil record. *Proceedings of the National Academy of Sciences,* **105**, 11536–11542.

ALROY, J. 2010a. The shifting balance of diversity among major marine animal groups. *Science,* **329**, 1191–1194.

ALROY, J. 2010b. Geographical, environmental and intrinsic biotic controls on Phanerozoic marine diversification. *Palaeontology,* **53**, 1211–1235.

ALROY, J. 2010c. Fair sampling of taxonomic richness and unbiased estimation of origination and extinction rates. *In:* ALROY, J. and HUNT, G. (eds) *Quantitative Methods in Paleobiology.* Paleontological Society, Papers, **16**, 55–80.

ALVAREZ, W. and O'CONNOR, D. 2002. Permian-Triassic boundary in the Southwestern United States: Hiatus or continuity? *Geological Society of America, Special Papers,* **356**, 385–393.

AMTHOR, R. 1907. Das Bonebed im Rhät des Apfelstadtgrundes südöstlich von Gotha. *Zeitschrift für Naturwissenschaften,* **80**, 91–96.

ANDREEV, P. and CUNY, G. 2012. New Triassic stem selachimorphs (Chondrichthyes, Elasmobranchii) and their bearing on the evolution of dental enameloid in Neoselachii. *Journal of Vertebrate Paleontology,* **32**, 255–266.

ANGIOLINI, L. and BUCHER, H. 1999. Taxonomy and quantitative biochronology of Guadalupian brachiopods from the Khuff Formation, Southeastern Oman. *Geobios,* **32**, 665–699.

ANGIOLINI, L., NICORA, A., BUCHER, H., VACHARD, D., PILLEVUIT, A., PLATEL, J. P., BAUD, A., BROUTIN, J., MARCOUX, J. and AL HASHMI, H. 1998. Late Permian fauna from the Khuff Formation, southeastern Oman: preliminary report. *Rivista Italiana di Paleontologia e Stratigrafia,* **104**, 329–340.

ANGIOLINI, L., BALINI, M., GARZANTI, E., NICORA, A., TINTORI, A., CRASQUIN, S. and MUTTONI, G. 2003a. Permian climatic and paleogeographic changes in Northern Gondwana: the Khuff Formation of Interior Oman. *Palaeogeography, Palaeoclimatology, Palaeoecology,* **191**, 269–300.

ANGIOLINI, L., BALINI, M., GARZANTI, E., NICORA, A. and TINTORI, A. 2003b. Gondwanan deglaciation and opening of Neotethys: the Al Khlata and Saiwan Formations of Interior Oman. *Palaeogeography, Palaeoclimatology, Palaeoecology,* **196**, 99–123.

ANTUNES, M. T., MAISEY, J. G., MARQUES, M. M., SCHAEFFER, B. and THOMSON, K. S. 1990. Triassic fishes from the Cassange Depression (R. P. de Angola). *Ciencias da Terra (UNL),* **Numero Especial**, 1–64.

APPLEGATE, S. P. 1965. Tooth terminology and variation in sharks with special reference to the sand shark, *Carcharias taurus* Rafinesque. *Contributions in Science, Natural History Museum of Los Angeles,* **86**, 3–17.

APPLEGATE, S. P. 1989. Pisces. *In:* CARREÑO, A. L., PERRILLIAT, M. C., GONZALEZ-ARREOLA, C., APPLEGATE, S. P., CARRANZA-CASTAÑEDA, O. and MARTÍNEZ-HERNANDEZ, E. (eds) *Fósiles tipo mexicanos.* Universidad Nacional Autónoma de México, Instituto de Geología, Centenario Instituto de Geología (1886–1986), 417–419.

ARAKI, H. 1980. Discovery of *Helicoprion*, a chondrichthyes from the Kesennuma City, Miyagi Prefecture, Japan. *Journal of the Geological Society of Japan,* **86**, 135–137 (in Japanese).

ATUDOREI, N.-V. 1998. *Constraints on the Upper Permian to Upper Triassic marine carbon isotope curve - Case studies from the Tethys.* PhD thesis, University of Lausanne, 155 pp.

AUERBACH, I. B. 1871. Mount Bogda. *Notes of the Russian Geographical Society,* **4**, 82.

BALME, B. E. 1979. Palynology of Permian-Triassic boundary beds of Kap Stosch, East Greenland. *Meddelelser om Grønland,* **200**, 1–35.

BAMBER, E. W., TAYLOR, G. C. and PROCTER, R. M. 1968/1969. Carboniferous and Permian stratigraphy of northeastern British Columbia. *Geological Survey of Canada, Paper,* **68-15**.

BARNES, G. L. 2003. Origins of the Japanese Islands: The New “Big Picture”. *Japan Review,* **15**, 3–50.

BARRERA, E. and KELLER, G. 1994. Productivity across the Cretaceous-Tertiary boundary in high latitudes. *Geological Society of America, Bulletin,* **106**, 1254–1266.

BASSANI, F. 1886. Sui fossili e sull'età degli schisti bituminosi triasici di Besano in Lombardia. *Atti della Societá Italiana di Scienze Naturali, Milano,* **29**, 15–72.

BAUD, A., RICHOZ, S., BEAUCHAMP, B., CORDEY, F., GRASBY, S., HENDERSON, C. M., KRYSTYN, L. and NICORA, A. 2012. The Buday’ah Formation, Sultanate of Oman: A Middle Permian to Early Triassic oceanic record of the Neotethys and the late Induan microsphere bloom. *Journal of Asian Earth Sciences,* **43**, 130–144.

BEAUCHAMP, B., HARRISON, J. C., UTTING, J., BRENT, T. A. and PINARD, S. 2001. Carboniferous and Permian subsurface stratigraphy, Prince Patrick Island, Northwest Territories, Canadian Arctic. *Geological Survey of Canada, Bulletin,* **565**, 1–93.

BELL, J., HOLDEN, J., PETTIGREW, T. H. and SEDMAN, K. W. 1979. The Marl Slate and basal Permian breccia at Middridge, Co. Durham. *Proceedings of the Yorkshire Geological and Polytechnic Society,* **42**, 439–460.

BENDER, P. A. and HANCOX, P. J. 2003. *Fossil fishes of the Lystrosaurus and Cynognathus assemblage zones, Beaufort Group, South Africa: correlative implications*, Council for Geoscience, South Africa, Bulletin **136**.

BENDER, P. A. and HANCOX, P. J. 2004. Newly discovered fish faunas from the Early Triassic, Karoo Basin, South Africa, and their correlative implications. *Gondwana Research,* **7**, 185–192.

BENDIX-ALMGREEN, S. E. 1966. New investigations on *Helicoprion* from the Phosphoria Formation of south-east Idaho, U.S.A. *Biologiske Skrifter,* **14**, 1–54.
BENDIX-ALMGREEN, S. E. 1975. Fossil fishes from the marine late Palaeozoic of Holm Land - Amdrup Land, North-East Greenland. *Meddelelser om Grønland,* **195**, 38.
BENDIX-ALMGREEN, S. E. 1976. Palaeovertebrate faunas of Greenland. *In:* ESCHER, A. and WATT, W. S. (eds) *Geology of Greenland.* The Geological Survey of Greenland, Copenhagen, 536–573.
BENDIX-ALMGREEN, S. E. 1993. *Adamantina benedictae* n.g. et sp. – en nyhed fra Østgrønlands marine Øvre Perm. *In:* JOHNSEN, O. (ed.) *Geologisk Museum – 100 år på Øster Vold.* Rhodos, Copenhagen, 48–58.
BENDIX-ALMGREEN, S. E. 1994. *Adamantina benedictae* n.g. et sp. - a new elasmobranch from the marine Upper Permian of East Greenland. *Ichthyolith Issues,* **14**, 21–22.
BENDIX-ALMGREEN, S. E. and MALZAHN, E. 1969. Über neue oder wenig bekannte Elasmobranchier aus dem deutschen Kupferschiefer. *Notizblatt des Hessischen Landesamtes für Bodenforschung,* **97**, 44–45.
BENDIX-ALMGREEN, S. E., CLACK, J. A. and OLSEN, H. 1988. Upper Devonian and Upper Permian vertebrates collected in 1987 around Kejser Franz Joseph Fjord, central East Greenland. *Rapport Grønlands Geologiske Undersøgelse,* **140**, 95–102.
BENGTSON, P. 1988. Open nomenclature. *Palaeontology,* **31**, 223–227.
BENTON, M. J. 1987. Mass extinctions among families of non-marine tetrapods: the data. *Mémoires de la Société Géologique de France, Numéro Spécial,* **150**, 21–32.
BENTON, M. J. (ed.) 1993. *The Fossil Record 2,* Chapman and Hall, London, 841 pp.
BENTON, M. J. 1995. Diversification and extinction in the history of life. *Science,* **268**, 52–58.
BENTON, M. J. 1998. The quality of the fossil record of vertebrates. *In:* DONOVAN, S. K. and PAUL, C. R. C. (eds) *The adequacy of the fossil record.* Wiley, New York, 269–303.
BENTON, M. J. 2001. Fossil Record: Quality. *Encyclopedia of Life Sciences (eLS).* John Wiley & Sons, Ltd., 1–8 [www.els.net].
BENTON, M. J. 2005. *Vertebrate Palaeontology, 3rd ed.,* Blackwell Publishing, Oxford, 472 pp.
BENTON, M. J. 2009. The Red Queen and the Court Jester: species diversity and the role of biotic and abiotic factors through time. *Science,* **323**, 728–732.
BENTON, M. J. 2012. No gap in the Middle Permian record of terrestrial vertebrates. *Geology,* **40**, 339–342.
BENTON, M. J. and STORRS, G. W. 1994. Testing the quality of the fossil record: Paleontological knowledge is improving. *Geology,* **22**, 111–114.
BENTON, M. J. and TWITCHETT, R. J. 2003. How to kill (almost) all life: the end-Permian extinction event. *Trends in Ecology & Evolution,* **18**, 358–365.
BENTON, M. J., HITCHIN, R. and WILLS, M. A. 1999. Assessing congruence between cladistic and stratigraphic data. *Systematic Biology,* **48**, 581–596.
BENTON, M. J., WILLS, M. A. and HITCHIN, R. 2000. Quality of the fossil record through time. *Nature,* **403**, 534–537.

BERG, L. S. 1937. A classification of fish-like vertebrates. *Bulletin of the Academy of Sciences of the USSR - Class of Sciences, Mathematics and Nature,* **1937**, 1277–1280.

BERMAN, D. S. 1970. Vertebrate fossils from the Lueders Formation, Lower Permian of north-central Texas. *University of California Publications, Geological Sciences,* **86**, 1–39.

BERNARDI, M., AVANZINI, M. and BIZZARINI, F. 2011. Vertebrate fauna from the San Cassiano Formation (early Carnian) of the Dolomites region. *Geo.Alp,* **8**, 122–127.

BEYRICH, E. 1848. Über *Xenacanthus decheni* und *Holacanthus gracilis*, zwei Fische aus der Formation des Rothliegenden in Norddeutschland. *Monatsberichte der Königlich-Preußische Akademie der Wissenschaften,* **1848**, 24–33.

BIBLIOGRAPHY OF FOSSIL VERTEBRATES ONLINE. The Society of Vertebrate Paleontology. Website: http://vertpaleo.org/Publications/Bibliography-of-Fossil-Vertebrates.aspx

BININDA-EMONDS, O. R. P. 2004. The evolution of supertrees. *Trends in Ecology & Evolution,* **19**, 315–322.

BIRKELUND, T. and PERCH-NIELSEN, K. 1976. Late Palaeozoic – Mesozoic evolution of central East Greenland. *In:* ESCHER, A. and WATT, W. S. (eds) *Geology of Greenland.* The Geological Survey of Greenland, Copenhagen, 304–339.

BIRKENMAJER, K. and JERZMAŃSKA, A. 1979. Lower Triassic shark and other fish teeth from Hornsund, South Spitsbergen. *Studia Geologica Polonica,* **60**, 7–37.

BIZZARINI, F., PROSSER, F., PROSSER, G. and PROSSER, I. 2001. Osservazioni preliminari sui resti di vertebrati della formazione di S. Cassiano del Bosco di Stuores (Dolomiti nord-orientali). *Annali del Museo civico di Rovereto,* **17**, 137–148.

BJERAGER, M., SEIDLER, L., STEMMERIK, L. and SURLYK, F. 2006. Ammonoid stratigraphy and sedimentary evolution across the Permian-Triassic boundary in East Greenland. *Geological Magazine,* **143**, 635–656.

BLAINVILLE, H. M. D., DE 1816. Prodrome d'une nouvelle distribution systématique du règne animal. *Bulletin de la Société Philomathique de Paris,* **8**, 105–112 + 121–124.

BLAINVILLE, H. M. D., DE 1818. Sur les ichthyolithes ou les poissons fossiles. *Nouveau Dictionnaire d'Histoire Naturelle, Deterville, Paris,* **27**, 310–395.

BLAKEY, R. 2012. *Colorado Plateau Geosystems - Reconstructing the ancient Earth*. Website: http://cpgeosystems.com/index.html

BŁAŻEJOWSKI, B. 2004. Shark teeth from the Lower Triassic of Spitsbergen and their histology. *Polish Polar Research,* **25**, 153–167.

BLENDINGER, W. 1988. Permian to Jurassic deep water sediments of the eastern Oman Mountains: Their significance for the evolution of the Arabian margin of the South Tethys. *Facies,* **19**, 1–31.

BLENDINGER, W., FURNISH, W. M. and GLENISTER, B. F. 1992. Permian cephalopod limestones, Oman Mountains: evidence for a Permian seaway along the northern margin of Gondwana. *Palaeogeography, Palaeoclimatology, Palaeoecology,* **93**, 13–20.

BLIECK, A. 2011. From adaptive radiations to biotic crises in Palaeozoic vertebrates: a geobiological approach. *Geologica Belgica,* **14**, 203–227.

BLIECK, A., TURNER, S., BURROW, C. J., SCHULTZE, H. P., REXROAD, C. B., BULTYNCK, P. and NOWLAN, G. S. 2010. Fossils, histology, and phylogeny: Why conodonts are not vertebrates. *Episodes,* **33**, 234–241.

BLIECK, A., CONTI, M. A., FLÜGEL, H. W., GAND, G., HUBMANN, S., LELIÈVRE, H., MARIOTTI, N., NICOSIA, U., POPLIN, C., SCHNEIDER, J. W. and WERNEBURG, R. 1995. The Alps, a quasi-desert in Palaeozoic vertebrate database, and the Gondwana-Laureuropa palaeogeographic relationships. *Ichthyolith Issues,* **15**, 8–13.

BLIECK, A., CONTI, M. A., DALLA VECCHIA, F. M., FLÜGEL, H. W., GAND, G., HUBMANN, B., LELIÈVRE, H., MARIOTTI, N., NICOSIA, U., POPLIN, C., SCHNEIDER, J. W. and WERNEBURG, R. 1997. Palaeozoic vertebrates of the Alps: a review. *Bulletin de la Société Géologique de France,* **168**, 343–350.

BROILI, F. 1904. Über *Diacranodus texensis* Cope (= *Didymodus? compressus* Cope). *Neues Jahrbuch für Mineralogie, Geologie und Paläontologie,* **29**, 467–484.

BROTZEN, F. 1955. Occurrence of Vertebrates in the Triassic of Israel. *Nature,* **176**, 404–405.

BROTZEN, F. 1956. Stratigraphical studies on the Triassic vertebrate fossils from Wadi Raman, Israel. *Arkiv for Mineralogi och Geologi Kungliga Svenska Vetenskapsakademien,* **2**, 191–217.

BONAPARTE, C. L. J. 1832–1841. *Iconografia della Fauna Italica, per le quattro classi degli animali vertebrati, 3 vols.*, Dalla Tipografia Salviucci, Rome.

BONAPARTE, C. L. J. 1838. Selachorum tabula analytica. *Nuovi Annali delle Scienze Naturali Bologna,* **1**, 195–214.

BÖTTCHER, R. 2010. Description of the shark egg capsule *Palaeoxyris friessi* n. sp. from the Ladinian (Middle Triassic) of SW Germany and discussion of all known egg capsules from the Triassic of the Germanic Basin. *Palaeodiversity,* **3**, 123–139.

BOTELLA, H. 2006. The oldest fossil evidence of a dental lamina in sharks. *Journal of Vertebrate Paleontology,* **26**, 1002–1003.

BOTELLA, H., DONOGHUE, P. C. J. and MARTÍNEZ-PÉREZ, C. 2009a. Enameloid microstructure in the oldest known chondrichthyan teeth. *Acta Zoologica,* **90**, 103–108.

BOTELLA, H., PLASENCIA, P., MARQUEZ-ALIAGA, A., CUNY, G. and DORKA, M. 2009b. *Pseudodalatias henarejensis* nov. sp. a new pseudodalatiid (Elasmobranchii) from the Middle Triassic of Spain. *Journal of Vertebrate Paleontology,* **29**, 1006–1012.

BOTTJER, D. J. 2012. Life in the Early Triassic Ocean. *Science,* **338**, 336–337.

BOY, J. A. 1976. Überblick über die Fauna des saarpfälzischen Rotliegenden (Unter-Perm). *Mainzer Geowissenschaftliche Mitteilungen,* **5**, 13–85.

BOY, J. A. and SCHINDLER, T. 2000. Ökostratigraphische Bioevents im Grenzbereich Stephanium/Autunium (höchstes Karbon) des Saar-Nahe-Beckens (SW-Deutschland) und benachbarter Gebiete. *Neues Jahrbuch für Geologie und Paläontologie, Abhandlungen,* **216**, 89–152.

BRANDT, S. 1996. *Janassa korni* (Weigelt) — Neubeschreibung eines petalodonten Elasmobranchiers aus dem Kupferschiefer und Zechsteinkalk (Perm) von Eisleben (Sachsen-Anhalt). *Paläontologische Zeitschrift,* **70**, 505–520.

BRANDT, S. 1997. Die Fossilien des Mansfelder und Sangerhäuser Kupferschiefers. *Schriftenreihe des Mansfeld-Museums (N. F.),* **2**, 1–68.

BRANSON, E. B. 1916. The Lower Embar of Wyoming and its fauna. *Journal of Geology,* **24**, 639–664.
BRANSON, C. C. 1933. Fish fauna of the Middle Phosphoria Formation. *Journal of Geology,* **41**, 174–183.
BRANSON, C. C. 1934. Permian sharks of Wyoming and of East Greenland. *Science, New Series,* **79**, 431.
BRANSON, C. C. 1935. A labyrinthodont from the Lower Gondwana of Kashmir and a new edestid from the Permian of the Salt Range. *Memoirs of the Connecticut Academy of Arts and Sciences,* **9**, 19–26.
BRAYARD, A., ESCARGUEL, G., BUCHER, H., MONNET, C., BRÜHWILER, T., GOUDEMAND, N., GALFETTI, T. and GUEX, J. 2009a. Good genes and good luck: Ammonoid diversity and the end-Permian mass extinction. *Science,* **325**, 1118–1121.
BRAYARD, A., BRÜHWILER, T., BUCHER, H. and JENKS, J. I. M. 2009b. *Guodunites*, a low-palaeolatitude and trans-Panthalassic Smithian (Early Triassic) ammonoid genus. *Palaeontology,* **52**, 471–481.
BRETT, C. E. and WALKER, S., E. 2002. Predators and predation in Paleozoic marine environments. *Paleontological Society, Papers,* **8**, 93–118.
BRIDGES, L. V. and DE FORD, R. K. 1962. Pre-Carboniferous Paleozoic rocks in central Chihuahua, Mexico. *American Association of Petroleum Geologists, Bulletin,* **45**, 98–104.
BRINKMANN, W., ROMANO, C., BUCHER, H., WARE, D. and JENKS, J. 2010. Palaeobiogeography and stratigraphy of advanced gnathostomian fishes (Chondrichthyes and Osteichthyes) in the Early Triassic and from selected Anisian localities (Report 1863-2009). *Zentralblatt für Geologie und Paläontologie, part II,* **5/6**, 765–812.
BROGLIO LORIGA, C. 1967. Elenco dei fossili degli strati di S. Cassiano. *In:* LEONARDI, P. (ed.) *Le Dolomiti - Geologia dei monti tra l'Isarco e il Piave*, **1**, 298–310.
BROOKFIELD, M. E., TWITCHETT, R. J. and GOODINGS, C. 2003. Palaeoenvironments of the Permian-Triassic transition sections in Kashmir, India. *Palaeogeography, Palaeoclimatology, Palaeoecology,* **198**, 353–371.
BROOM, R. 1909. The fossil fishes of the upper Karoo beds of South Africa. *Annals of the South African Museum,* **7**, 251–269.
BROUGH, J. 1931. On fossil fishes from the Karoo system and some general consideration on the bony fishes of the Triassic period. *Proceedings of the Zoological Society of London,* **Part 1**, 235–296.
BROUGH, J. 1935. On the structure and relationships of the Hybodont sharks. *Memoirs & Proceedings of the Manchester Literary and Philosophical Society,* **79**, 35–50.
BROWN, J. C. 1905. Note on *Janassa bituminosa*, Schlot., from the marl slate, Thickley, Durham. *The Naturalist,* July **1905**, 1–3.
BRYANT, H. C. 1914. Teeth of a cestraciont shark from the Upper Triassic of Northern California. *University of California Publications, Bulletin of the Department of Geology,* **8**, 27–30.
BRYANT, W. L. 1934. New fishes from the Triassic of Pennsylvania. *Proceedings of the American Philosophical Society,* **73**, 319–326.

BUCHER, H. 1992. Ammonoids of the *Hyatti* Zone (Middle Anisian, Middle Triassic) and the Anisian transgression in the Star Peak Group (northwestern Nevada). *Palaeontographica Abteilung A,* **223**, 137–166.

BUCHER, H., NASSICHUK, W. W. and SPINOSA, C. 1997. Upper Permian *Stacheoceras* from the Himalayas. *Eclogae Geologicae Helvetiae,* **90**, 599–604.

BURROW, C. J., HOVESTADT, D. C., HOVESTADT-EULER, M., TURNER, S. and YOUNG, G. C. 2008. New information on the Devonian shark *Mcmurdodus*, based on material from western Queensland, Australia. *Acta Geologica Polonica,* **58**, 155–163.

CAPPETTA, H. 1973. Selachians from the Carlile Shale (Turonian) of South Dakota. *Journal of Paleontology,* **47**, 504–514.

CAPPETTA, H. 1987. *Chondrichthyes II Mesozoic and Cenozoic Elasmobranchii, Handbook of Paleoichthyology, vol. 3B,* Gustav Fischer Verlag, Stuttgart, 193 pp.

CAPPETTA, H. 2012. *Chondrichthyes (Mesozoic and Cenozoic Elasmobranchii: Teeth), Handbook of Paleoichthyology, Vol. 3E,* Verlag Dr. Friedrich Pfeil, München, 512 pp.

CAPPETTA, H., DUFFIN, C. and ZIDEK, J. 1993. Chondrichthyes. *In:* BENTON, M. J. (ed.) *The Fossil Record 2,* Chapman and Hall, London, 593–609.

CARR, T. R. 1981. *Paleogeography, depositional history and conodont paleoecology of the lower Triassic Thaynes Formation in the Cordilleran miogeosyncline.* PhD Thesis, University of Wisconsin.

CARR, T. R. and PAULL, R. K. 1983. Early Triassic stratigraphy and paleogeography of the Cordillera miogeocline. *In:* DOLLY, E. D., REYNOLDS, M. W. and SPEARING, D. R. (eds) *Mesozoic Paleogeography of the West-central United States, Rocky Mountain Paleogeography Symposium, 2. SEPM Rocky Mountain Section.*

CASE, G. R. 1973. *Fossil sharks: a pictorial review,* Pioneer Litho Co., New York, 165 pp.

CASIER, E. 1947a. Constitution et évolution de la racine dentaire des Euselachii. I. Note préliminaire. *Bulletin du Musée royal d'histoire naturelle de Belgique,* **23**, 1–15.

CASIER, E. 1947b. Constitution et évolution de la racine dentaire des Euselachii. II. Étude comparative des types. *Bulletin du Musée royal d'histoire naturelle de Belgique,* **23**, 1–32.

CASIER, E. 1947c. Constitution et évolution de la racine dentaire des Euselachii. III. Évolution des principaux caractères morphologiques et conclusions. *Bulletin du Musée royal d'histoire naturelle de Belgique,* **23**, 1–45.

CASIER, E. 1959. Contribution à l'étude des poissons fossiles de la Belgique - XII. Sélaciens et Holocéphales sinémuriens de la province de Luxembourg. *Bulletin de l'Institut Royal des Sciences Naturelles de Belgique*, **35**, 1–27.

CHABAKOV, A. 1927. Synopsis of the ichthyofauna of the Permian deposits of Russia. *Verhandlungen der Königlichen Russischen Mineralogischen Gesellschaft zu St. Petersburg, series II (Zapiski, Rossiskoe Mineralogicheskoe obshchestro),* **56**, 199–213 (in English).

CHABAKOV, A. W. 1928. *Anodontacanthus ruthenorum* sp. n., a new ichthyodorulite from the Permian of European part of USSR. *Annuaire de la Société Paléontologique de Russie,* **7**, 127–132.

CHAHUD, A., FAIRCHILD, T. R. and PETRI, S. 2010. Chondrichthyans from the base of the Irati Formation (Early Permian, Paraná Basin), São Paulo, Brazil. *Gondwana Research,* **18**, 528–537.

CHANG, M. and MIAO, D. 2004. An overview of Mesozoic fishes in Asia. *In:* ARRATIA, G. and TINTORI, A. (eds) *Mesozoic Fishes 3 - Systematics, Paleoenvironments and Biodiversity.* Verlag Dr. Friedrich Pfeil, München, 535–563.

CHEN, Z.-Q. and BENTON, M. J. 2012. The timing and pattern of biotic recovery following the end-Permian mass extinction. *Nature Geoscience,* **5**, 375–383.

CHEN, L., CUNY, G. and WANG, X. 2007a. The chondrichthyan fauna from the Middle-Late Triassic of Guanling (Guizhou province, SW China). *Historical Biology,* **19**, 291–300.

CHEN, X., CHENG, L. and YIN, K. 2007b. The first record of *Helicoprion* Karpinsky (Helicoprionidae) from China. *Chinese Science Bulletin,* **52**, 2246–2251.

CHENG, G., MU, S., YIN, G. and LIU, G. 2004. The helicoprionid fossil from Lower Permian Maokou stage in Weining, Guizhou Province. *Acta Geoscientica Sinica,* **25**, 443–445.

CHORN, J. 1978. *Helicoprion* (Elasmobranchii, Edestidae) from the Bone Spring Formation (Lower Permian) of West Texas. *University of Kansas, Paleontological Contributions,* **89**, 2–4.

CHRZĄSTEK, A. and NIEDŹWIEDSKI, R. 2004. Kręgowce Retu i dolnego wapienia Muszlowego na Śląsku (Vertebrates of the Rhetian and Lower Musselkalk in Silesia). *Prac Geologiczno-Mineralogiczne LXIV.* Wrocław, 1998. Acta Universitatis Wratislavensis, 69–81.

CHUVASHOV, B. I. 1989. On finding of *Helicoprion* sp. in the Lower Permian of the Kozhim River (Nearpolar Urals). *Ezhegodnik Instituta Geologii i Geokhimii Ural'skogo Otdeleniya Akademii Nauk SSSR, Sverdlovsk*, 18–21 [in Russian].

CHUVASHOV, B. I. 2001. Permian sharks of the family Helicoprionidae – stratigraphic and geographic distribution, ecology, a new member. *Materialy po stratigrafii i palaeontologii Urala,* **6**, 12–27 (in Russian).

CIAMPAGLIO, C. N., CLAYTON, A. A. and MEEHAN, C. 2009. Analysis of chondrichthyan generic richness, morphological diversification, and ecospace diversity across the Permian–Triassic boundary. *Geological Society of America, Abstracts with Programs.* **41**(4), 58.

CLAPHAM, M. E. and PAYNE, J. L. 2011. Acidification, anoxia, and extinction: A multiple logistic regression analysis of extinction selectivity during the Middle and Late Permian. *Geology,* **39**, 1059–1062.

CLAPHAM, M. E., SHEN, S. and BOTTJER, D. J. 2009. The double mass extinction revisited: reassessing the severity, selectivity, and causes of the end-Guadalupian biotic crisis (Late Permian). *Paleobiology,* **35**, 32–50.

CLAYTON, A. A. and CIAMPAGLIO, C. N. 2011. End Permian anomaly: how did chondrichthyans escape history's largest devastation? *Geological Society of America, Abstracts with Programs.* **43**(1), 98.

CLAYTON, A. A., CIAMPAGLIO, C. N. and CARNEY, C. K. 2008. Analysis of patterns and processes of Chondrichthyes across the Permian–Triassic boundary. *Geological Society of America, Abstracts with Programs.* **40**(5), 85.

COATES, M. I. and SEQUEIRA, S. E. K. 2001. Early sharks and primitive gnathostome interrelationships. *In:* AHLBERG, P. E. (ed.) *Major Events in Early Vertebrate Evolution: Palaeontology, phylogeny, genetics and development.* Systematics Association, 241–262.

COATES, M. I. and GESS, R. W. 2007. A new reconstruction of *Onychoselache traquairi*, comments on early chondrichthyan pectoral girdles and hybodontiform phylogeny. *Palaeontology,* **50**, 1421–1446.
COATES, M. I., JEFFERY, J. E. and RUTA, M. 2002. Fins to limbs: what the fossils say. *Evolution & Development,* **4**, 390–401.
COCKS, L. R. M. and TORSVIK, T. H. 2011. The Palaeozoic geography of Laurentia and western Laurussia: A stable craton with mobile margins. *Earth-Science Reviews,* **106**, 1–51.
COMPAGNO, L. J. V. 1970. Systematics of the genus *Hemitriakis* (Selachii: Carcharhinidae, and related genera). *Proceedings of the California Academy of Science, ser.4,* **48**, 63–98.
COMPAGNO, L. J. V. 1973. Interrelationships of living elasmobranchs. *In:* GREENWOOD, P. H., MILES, R. S. and PATTERSON, C. (eds) *Interrelationships of Fishes.* Zoological Journal of the Linnean Society, **53** (Supplement 1), 15–61.
COMPAGNO, L. J. V. 1977. Phyletic relationships of living sharks and rays. *American Zoologist,* **17**, 303–322.
COMPAGNO, L. J. V. 1990. Alternative life-history styles of cartilaginous fishes in time and space. *Environmental Biology of Fishes,* **28**, 33–75.
COPE, E. D. 1881. Catalogue of Vertebrata of the Permian formation of the United States. *American Naturalist,* **15**, 162–164.
COPE, E. D. 1883. On some Vertebrata from the Permian of Illinois. *Proceedings of the Academy of Natural Sciences of Philadelphia,* **35**, 108–110.
COPE, E. D. 1884. On the structure of the skull in the elasmobranch genus *Didymodus*. *Proceedings of the American Philosophical Society,* **21**, 572–590.
COPE, E. D. 1888. Systematic catalogue of the species of Vertebrata found in the beds of the Permian epoch in North America, with notes and descriptions. *Transactions of the American Philosophical Society,* **16**, 285–297.
COPE, E. D. 1891. On the characters of some Paleozoic fishes. I-VII. *Proceedings of the United States National Museum,* **14**, 447–463.
COPE, E. D. 1894. New and little known Paleozoic and Mesozoic fishes. *Journal of the Academy of Natural Sciences Philadelphia (Series 2),* **9**, 427–448.
COX, C. B. and SMITH, D. G. 1973. A review of the Triassic vertebrate faunas of Svalbard. *Geological Magazine,* **110**, 405–418.
CUNY, G. 1993. Evolution des faunes Vertébrés à la limite Trias-Jurassique en France et au Luxembourg: implications à l'Europe occidentale. *Mémoires des Sciences de la Terre, Académie des Sciences, Université Pierre et Marie Curie***,** 235 pp.
CUNY, G. 1995a. French vertebrate faunas and the Triassic-Jurassic boundary. *Palaeogeography, Palaeoclimatology, Palaeoecology,* **119**, 343–358.
CUNY, G. 1995b. Révision des faunes de vertébrés du site de Provenchères-sur-Meuse (Trias Terminal, Nord-Est de la France). *Palaeovertebrata,* **24**, 101–134.
CUNY, G. 1998. Primitive neoselachian sharks: A survey. *Oryctos,* **1**, 3–21.
CUNY, G. 2002. *Les requins sont-ils des fossiles vivants? L'evolution des poissons cartilagineux,* EDP Sciences, Les Ulis Cedex A, 205 pp.
CUNY, G. and RAMBOER, G. 1991. Nouvelles données sur la faune et l'âge de Saint-Nicolas-de-Port. *Revue de Paléobiologie,* **10**, 69–78.
CUNY, G. and BENTON, M. J. 1999. Early radiation of the Neoselachian sharks in Western Europe. *Geobios,* **32**, 193–204.

CUNY, G. and RISNES, S. 2005. The enameloid microstructure of the teeth of synechodontiform sharks (Chondrichthyes: *Neoselachii*). *PalArch,* **3**, 8–19.
CUNY, G., MAZIN, J.-M. and RAUSCHER, R. 1994. Saint-Germain-Ies-Arlay: Un nouveau site Rhétien date par la palynologie et l'étude des vertébrés dans Ie Departement du Jura (France). *Revue de Paléobiologie,* **14**, 35–48.
CUNY, G., RIEPPEL, O. and SANDER, P. M. 2001. The shark fauna from the Middle Triassic (Anisian) of North-Western Nevada. *Zoological Journal of the Linnean Society,* **133**, 285–301.
CUNY, G., MARTIN, M., RAUSCHER, R. and MAZIN, J.-M. 1998. A new neoselachian shark from the Upper Triassic of Grozon (Jura, France). *Geological Magazine,* **135**, 657–668.
CUNY, G., HUNT, A., MAZIN, J.-M. and RAUSCHER, R. 2000. Teeth of enigmatic neoselachian sharks and an ornithischian dinosaur from the uppermost Triassic of Lons-le-Saunier (Jura, France). *Paläontologische Zeitschrift,* **74**, 171–185.
CORROY, G. 1928. Les vertébrés du trias de Lorraine et le trias Lorrain. *Annales de Paléontologie,* **17**, 83–136.
DALLA VECCHIA, F. M. 2000. A new petalodont tooth (Chondrichthyes, Petalodontiformes) from the Lower Permian of the Carnic Alps (Friuli, NE Italy). *Bollettino della Società Paleontologica Italiana,* **39**, 225–228.
DATTILO, B. F., BRETT, C. E., TSUJITA, C. J. and FAIRHURST, R. 2008. Sediment supply versus storm winnowing in the development of muddy and shelly interbeds from the Upper Ordovician of the Cincinnati region, USA. *Canadian Journal of Earth Sciences,* **45**, 243–265.
DAVID, L. R. 1944. A Permian shark from the Grand Canyon. *Journal of Paleontology,* **18**, 90–93.
DAVIDSON, P. 1919. A cestraciont spine from the Middle Triassic of Nevada. *Bulletin of the Department of Geology,* **11**, 433–435.
DAVIS, J. W. 1883. On the fossil fishes of the Carboniferous Limestone Series of Great Britain. *Transactions of the Royal Society of Dublin,* **1**, 327–548.
DAYMOND, S. 1993. Stethacanthid shark teeth from the Permian Holmwood Shale Formation (Fossil Cliff Member), Irwin River district, Western Australia. *Fossil Collector,* **40**, 23–28.
DEAN, B. 1909. Studies on fossil fishes (sharks, chimaeroids, and arthrodires). *Memoirs of the American Museum of Natural History,* **9**, 211–287.
DEECKE, W. 1926. Pisces Triadici. *In:* POMPECKJ, F. J. (ed.) *Fossilium Catalogus I: Animalia, pars 33.* W. Junk, Berlin, 201 pp.
DELSATE, D. 1992. Chondrichthyens mésozoiques du Luxembourg. Note préliminaire. *Bulletin de la Société des naturalistes luxembourgeois,* **93**, 181–193.
DELSATE, D. 1993. Synthèse des faunes d'Elasmobranches du Trias et du Jurassique de Lorraine. *Cossmanniana,* Hors-série **2**, 52–55.
DELSATE, D. 1995. Chondrichthyens mésozoïques du Grand Duché de Luxembourg. *In:* HERMAN, J. and VAN WAES, H. (eds) *Elasmobranches et Stratigraphie.* Belgian Geological Survey, Professional Paper, **278**, 11–21.
DELSATE, D. 1997. Chondrichthyens mésozoïques du Grand Duché de Luxembourg: compléments. *Travaux scientifiques du Musée National d'Histoire Naturelle de Luxembourg,* **27**, 53–79.
DELSATE, D. 1998. Mammifères, thérapsides, Archosaures et Poissons du Rhétien de Syren. *Lithorama,* **25**, 18–40.

DELSATE, D. and DUFFIN, C. J. 1999. A new fish fauna from the Middle Triassic (Upper Muschelkalk) of Moersdorf (Grand Duchy of Luxembourg). *Travaux scientifiques du Musée national d'histoire naturelle, Luxembourg,* **32**, 5–53.

DELSATE, D. and LEPAGE, J. C. 1991. Requins et Raies en Lorraine. *Geolor Magazine,* **3**, 6–9.

DELSATE, D. and LEPAGE, J. C. 1993. Selaciens du Trias et du Jurassique de Lorraine. *Centre de Recherches Lorraines a.s.b.l.,* Cahier **1993**, 25–35.

DERYCKE-KHATIR, C. 2005. Microrestes de vertébré du Paléozöique Superieur dela manche au Rhin. *Société Géologique du Nord,* **33**, 71–72.

DERYCKE-KHATIR, C., VACHARD, D., DÉGARDIN, J.-M., FLORES DE DIOS, A., BUITRÓN, B. and HANSEN, M. 2005. Late Pennsylvanian and Early Permian chondrichthyan microremains from San Salvador Patlanoaya (Puebla, Mexico). *Geobios,* **38**, 43–55.

DICK, J. R. F. 1978. On the Carboniferous shark *Tristychius arcuatus* Agassiz from Scotland. *Transactions of the Royal Society of Edinburgh,* **70**, 63–109.

DICK, J. R. F. 1981. *Diplodoselache woodi* gen. et sp. nov., an early Carboniferous shark from the Midland Valley of Scotland. *Transactions of the Royal Society of Edinburgh, Earth Sciences,* **72**, 99–113.

DIEDRICH, C. 2009a. A coelacanthid-rich site at Hasbergen (NW Germany): taphonomy and palaeoenvironment of a first systematic excavation in the Kupferschiefer (Upper Permian, Lopingian). *Palaeobiodiversity and Palaeoenvironments,* **89**, 67–94.

DIEDRICH, C. 2009b. The vertebrates of the Anisian/Ladinian boundary (Middle Triassic) from Bissendorf (NW Germany) and their contribution to the anatomy, palaeoecology, and palaeobiogeography of the Germanic Basin reptiles. *Palaeogeography, Palaeoclimatology, Palaeoecology,* **273**, 1–16.

DINELEY, D. L. and METCALF, S. J. 1999. British Triassic fossil fishes sites. *In:* DINELEY, D. L. and METCALF, S. J. (eds) *Fossil Fishes of Great Britain.* Joint Nature Conservation Committee, Peterborough. Geological Conservation Review Series, **16**, 325–352.

DONELAN, C. and JOHNSON, G. D. 1997. *Orthacanthus platypternus* (Chondrichthyes: Xenacanthida) occipital spines from the Lower Permian Craddok Bonebed, Baylor County, Texas. *Abstract of Papers. Fifty-Seventh Annual Meeting, Society of Vertebrate Paleontology. Journal of Vertebrate Paleontology,* **17** (Supplement to No. 3), 43A.

DONG, Z. 1972. An ichthyosaur fossil from the Qomolangma Feng region. *Memoirs of the Institute of Vertebrate Paleontology and Paleoanthropology, Academia Sinica,* **9**, 7–10 (in Chinese).

DORKA, M. 2001. Shark remains from the Triassic of Schöningen, Lower Saxony, Germany. *Neues Jahrbuch für Geologie und Paläontologie, Abhandlungen,* **221**, 219–247.

DORKA, M. 2003. Teeth of *Polyacrodus* Jaekel, 1889 from the Triassic of the Germanic Basin. *Mitteilungen aus dem Museum für Naturkunde in Berlin. Geowissenschaftliche Reihe,* **6**, 147–155.

DOUGLAS, J. A. 1950. The Carboniferous and Permian faunas of south Iran and Iranian Baluchistan. *Memoirs of the Geological Survey of India, Palaeontologia Indica, New Series, 22, Memoir,* **7**, 1–57.

DREYER, D. 1962. Zur Entstehung und Paläontologie der Bonebedlagen im Unteren Rät Thüringens. *Freiberger Forschungshefte,* **125**, 129–143.

DROSER, M. L., BOTTJER, D. J., SHEEHAN, P. M. and MCGHEE, G. R. 2000. Decoupling of taxonomic and ecologic severity of Phanerozoic mass extinctions. *Geology,* **28**, 675–678.

DUFFIN, C. J. 1978. The Bath Geological Collections. f. The importance of certain vertebrate fossils collected by CHARLES MOORE: an attempt at scientific perspective. *Geological Curators Group Newsletter,* **2**, 59–67.

DUFFIN, C. J. 1980a. A new euselachian shark from the Upper Triassic of Germany. *Neues Jahrbuch für Geologie und Paläontologie, Monatshefte,* **1980**, 1–16.

DUFFIN, C. 1980b. The Upper Triassic section at Chilcompton, Somerset, with notes on the Rhaetic of the Mendips in general. *Mercian Geology,* **7**, 251–268.

DUFFIN, C. J. 1981. Comments on the selachian genus *Doratodus* Schmid (1861) (Upper Triassic, Germany). *Neues Jahrbuch für Geologie und Paläontologie, Monatshefte,* **1981**, 289–302.

DUFFIN, C. J. 1982a. A palaeospinacid shark from the Upper Triassic of south-west England. *Zoological Journal of the Linnean Society,* **74**, 1–7.

DUFFIN, C. J. 1982b. Teeth of a new selachian from the Upper Triassic of England. *Neues Jahrbuch für Geologie und Paläontologie, Monatshefte,* **1982**, 156–166.

DUFFIN, C. J. 1985. Revision of the hybodont selachian genus *Lissodus* Brough (1935). *Palaeontographica Abteilung A,* **188**, 105–152.

DUFFIN, C. J. 1989. Comments on the Mesozoic record of *Lissodus* (Selachii, Hybodontidae). *Mesozoic Research,* **2**, 83–90.

DUFFIN, C. J. 1993a. Late Triassic sharks teeth (Chondrichthyes, Elasmobranchii) from Saint-Nicolas-de-Port (north-east France). *In:* HERMAN, J. and VAN WAES, H. (eds) *Elasmobranches et Stratigraphie.* Belgian Geological Survey, Professional Paper, **264**, 7–32.

DUFFIN, C. J. 1993b. Mesozoic chondrichthyan faunas. 1. Middle Norian (Upper Triassic) of Luxembourg. *Palaeontographica,* **A229**, 15–36.

DUFFIN, C. 1994. Myriacanthid holocephalans (Chondrichthyes) from the British Late Triassic. *Neues Jahrbuch für Geologie und Paläontologie, Abhandlungen,* **192**, 1–16.

DUFFIN, C. J. 1998a. New shark remains from the British Rhaetian (latest Triassic) - 2. Hybodonts and palaeospinacids. *Neues Jahrbuch für Geologie und Paläontologie, Monatshefte,* **1998**, 240–256.

DUFFIN, C. J. 1998b. New shark remains from the British Rhaetian (latest Triassic) - 1. The earliest Basking shark. *Neues Jahrbuch für Geologie und Paläontologie, Monatshefte,* **1998**, 157–181.

DUFFIN, C. J. 1999. Chapter 14. Fish. *In:* SWIFT, A. and MARTILL, D. M. (eds) *Fossils of the Rhaetian Penarth Group.* London: Palaeontological Association, 191–222.

DUFFIN, C. J. 2001. Synopsis of the selachian genus *Lissodus* Brough, 1935. *Neues Jahrbuch für Geologie und Paläontologie, Abhandlungen,* **221**, 145–218.

DUFFIN, C. J. and DELSATE, D. 1993. The age of the Upper Triassic vertebrate fauna from Attert (Province of Luxembourg, Belgium). *In:* HERMAN, J. and VAN WAES, H. (eds) *Elasmobranches et Stratigraphie.* Belgian Geological Survey, Professional Paper, **264**, 33–44.

DUFFIN, C. and FURRER, H. 1981. Myriacanthid holocephalan remains from the Rhaetian (Upper Triassic) and Hettangian (Lower Jurassic) of Graubünden (Switzerland). *Eclogae Geologicae Helvetiae,* **74**, 803–829.

DUFFIN, C. J. and GAŹDZICKI, A. 1977. Rhaetian fish remains from the Tatra Mountains. *Acta Geologica Polonica,* **27**, 333–348.

DUFFIN, C. J. and GINTER, M. 2006. Comments on the selachian genus *Cladodus* Agassiz, 1843. *Journal of Vertebrate Paleontology,* **26**, 253–266.
DUFFIN, C. J. and IVANOV, A. 2008. New chondrichthyan teeth from the Carboniferous of Britain and Russia. *Acta Geologica Polonica,* **58**, 191–197.
DUFFIN, C. J. and REYNDERS, J. P. H. 1995. A fossil chimaeroid from the Gronsweld Member (Late Maastrichtian, Late Cretaceous) of northeast Belgium. *In:* HERMAN, J. and VAN WAES, H. (eds) *Elasmobranches et Stratigraphie.* Belgian Geological Survey, Professional Paper, 278, 111–156.
DUFFIN, C. J. and WARD, D. J. 1983. Neoselachian sharks' teeth from the Lower Carboniferous of Britain and the Lower Permian of the U.S.A. *Palaeontology,* **26**, 93–110.
DUFFIN, C. J. and WARD, D. J. 1993. The Early Jurassic palaeospinacid sharks of Lyme Regis, southern England. *In:* HERMAN, J. and VAN WAES, H. (eds) *Elasmobranches et Stratigraphie.* Belgian Geological Survey, Professional Paper, **264**, 53–102.
DUFFIN, C. J., RICHTER, M. and NEIS, P. A. 1996. Shark remains from the Late Carboniferous of the Amazon Basin, Brazil. *Neues Jahrbuch für Geologie und Paläontologie, Monatshefte,* **1996(4)**, 232–256.
DUFFIN, C. J., COUPATEZ, P., LEPAGE, J. C. and WOUTERS, G. 1983. Rhaetian (Upper Triassic) marine faunas from «Le Golfe du Luxembourg» in Belgium (preliminary note). *Bulletin de la Société belge de Géologie,* **92**, 311–315.
DUNKLE, D. H. and VAN SICKLE, D. H. 1968. Distribution and preliminary identification of fish remains in Wyoming, Table 5. *In:* YOCHELSON, E. L. (ed.) *Biostratigraphy of Phosphoria, Park City and Shedham formations.* U. S. Geological Survey, Professional Paper, **313-D**, 629–630.
DUNKLE, D. H. and WILLIAMS, J. S. 1948. *Helicoprion*-like fossils in the Phosphoria formation (abstract). *Geological Society of America, Bulletin,* **59**, 1362.
DURAND, J. F. 2005. Major African contributions to Palaeozoic and Mesozoic vertebrate palaeontology. *Journal of African Earth Sciences,* **43**, 53–82.
EASTMAN, C. R. 1902. On *Campyloprion*, a new form of *Edestus*-like dentition. *Geological Magazine,* **9**, 148–152.
EASTMAN, C. R. 1903. Carboniferous fishes from the central western States. *Bulletin of the Museum of Comparative Zoology,* **39**, 163–226.
ECK, H. 1865. *Über die Formationen des bunten Sandsteins und des Muschelkalks in Oberschlesien und ihre Versteinerungen.* Thesis, Berlin.
EGERTON, P. G. 1847. On the nomenclature of the fossil chimaeroid fishes. *Quarterly Journal of the Geological Society of London,* **3**, 350–353.
EGERTON, P. G. 1872. On *Prognathus guentheri* Egerton, a new genus of fossil fish from the Lias of Lyme Regis. *Quarterly Journal of the Geological Society of London,* **28**, 233–237.
EICHWALD, E. 1860. *Lethaea Rossica ou Paléontologie de la Russie. Tome I, Anciènne période*, 1057 pp.
ENDLICH, F. M. 1870. *Das Bonebed Württembergs.* Thesis, Tübingen, 30 pp.
ENGEL, T. 1908. *Geognosticher Wegweiser durch Württemberg,* Schweizerbart, Stuttgart.
ERWIN, D. H. 1993. *The Great Paleozoic Crisis: Life and Death in the Permian,* Columbia University Press, New York, 327 pp.
ERWIN, D. H. 1994. The Permo-Triassic extinction. *Nature,* **367**, 231–236.

ERWIN, D. H. 1998. The end and the beginning: recoveries from mass extinctions. *Trends in Ecology & Evolution,* **13**, 344–349.

ERWIN, D. H. 2001. Lessons from the past: biotic recoveries from mass extinctions. *Proceedings of the National Academy of Sciences of the United States of America,* **98**, 5399–5403.

ERWIN, D. H. 2006a. *Extinction: How Life on Earth Nearly Ended 250 Million Years Ago,* Princeton University Press, Oxford, 296 pp.

ERWIN, D. H. 2006b. *The Mother of Mass Extinctions* [seminar, 12th July 2006 at the Santa Fe Institute, USA]. Website: http://fora.tv/2006/07/12/Mother_of_Mass_Extinctions.

ERWIN, D. H. and DROSER, M. L. 1993. Elvis taxa. *Palaios,* **8**, 623–624.

ERWIN, D. H., VALENTINE, J. W. and SEPKOSKI, J. J. 1987. A comparative-study of diversification events – the early Paleozoic versus the Mesozoic. *Evolution,* **41**, 1177–1186.

ERWIN, D. H., BOWRING, S. A. and YUGAN, J. 2002. End-permian mass extinctions: a review. *Geological Society of America, Special Papers,* **356**, 363–383.

ESTES, R. 1964. Fossil vertebrates from the Late Cretaceous Lance Formation Eastern Wyoming. *University of California Publications in Geological Sciences,* **49**, 1–187.

ETHERIDGE 1871. On the physical structure and organic remains of the Penarth (Rhaetic) beds of Penarth and Lavernock; also with description of the Westbury-on-Severn section. *Transactions of the Cardiff Naturalists' Society,* **3**, 39–62.

EVANS, H. M. 1904. A new cestraciont spine from the lower Triassic of Idaho. *Bulletin of the Department of Geology, University of California,* **3**, 397–402.

EWALD, J. 1848. Über *Menaspis*, eine neue fossile Fischgattung. *Berichte der Akademie der Wissenchaften zur Berlin,* **1848**, 33–35.

EWELL, K. and EVERHART, M. J. 2005. A Paleozoic shark fauna from the Council Grove Group (Lower Permian). *Abstracts of the annual meeting of the Kansas Academy of Science, April 17, 2004. Transactions of the Kansas Academy of Science,* **108**, 71–72.

FENTON, S., GRICE, K., TWITCHETT, R. J., BÖTTCHER, M. E., LOOY, C. V. and NABBEFELD, B. 2007. Changes in biomarker abundances and sulfur isotopes of pyrite across the Permian–Triassic (P/Tr) Schuchert Dal section (East Greenland). *Earth and Planetary Science Letters,* **262**, 230–239.

FERNANDINO, D. 1992. Faunal variations within parasequences from the type section of the Fossil Cliff Member of the Holmwood Shale (Sakmarian, Early Permian), northern Perth Basin, Western Australia. *Association of Australasian Palaeontology, Conference.* Perth, Western Australia. Abstracts and Program, p.10.

FISCHER, J. 2005. *Tektonik, Beckenentwicklung und Entwässerungssysteme im Variscikum − Bezüge zur Paläobiogeographie hybodonter Haie.* Unpublished Master thesis, TU Bergakademie Freiberg, 103 pp.

FISCHER, J. 2008. Brief synopsis of the hybodont form taxon *Lissodus* Brough, 1935, with remarks on the environment and associated fauna. *Paläontologie, Stratigraphie, Fazies (16), Freiberger Forschungshefte,* **C528**, 1–23.

FISCHER, J., SCHNEIDER, J. W. and RONCHI, A. 2010. New hybondontoid shark from the Permocarboniferous (Gzhelian–Asselian) of Guardia Pisano (Sardinia, Italy). *Acta Palaeontologica Polonica,* **55**, 241–264.

FISCHER, J., VOIGT, S., SCHNEIDER, J. W., BUCHWITZ, M. and VOIGT, S. 2011. A selachian freshwater fauna from the Triassic of Kyrgyzstan and its implication for Mesozoic shark nurseries. *Journal of Vertebrate Paleontology,* **31**, 937–953.

FISCHER, J., VOIGT, S., FRANZ, M., SCHNEIDER, J. W., JOACHIMSKI, M. M., TICHOMIROWA, M., GÖTZE, J. and FURRER, H. 2012. Palaeoenvironments of the late Triassic Rhaetian Sea: Implications from oxygen and strontium isotopes of hybodont shark teeth. *Palaeogeography, Palaeoclimatology, Palaeoecology,* **353–355**, 60–72.

FITZGERALD, P. C. and CARLSON, S. J. 2006. Examining the latitudinal diversity gradient in Paleozoic terebratulide brachiopods: should singleton data be removed? *Paleobiology,* **32**, 367–386.

FOOTE, M. 2000. Origination and extinction components of taxonomic diversity: general problems. *Paleobiology,* **26**, 74–102.

FOOTE, M. 2007. Extinction and quiescence in marine animal genera. *Paleobiology,* **33**, 261–272.

FOOTE, M. and SEPKOSKI, J. J. 1999. Absolute measures of the completeness of the fossil record. *Nature,* **398**, 415–417.

FOOTE, M. and MILLER, A. I. 2007. *Principles of Paleontology (3rd ed.)*, W.H. Freeman & Co Ltd, New York, 480 pp.

FOSSE, G., RISNES, S. and HOLMBAKKEN, N. 1974. Mineral distribution and mineralization pattern in enameloid of certain elasmobranchs. *Archives of Oral Biology,* **19**, 771–780.

FRAISER, M. L. and BOTTJER, D. J. 2004. The non-actualistic Early Triassic gastropod fauna: a case study of the Lower Triassic Sinbad Limestone Member. *Palaios,* **19**, 259–275.

FRAISER, M. L. and BOTTJER, D. J. 2005. Restructuring in benthic level-bottom shallow marine communities due to prolonged environmental stress following the end-Permian mass extinction. *Comptes Rendus Palevol,* **4**, 583–591.

FRAISER, M. L. and BOTTJER, D. J. 2007. Elevated atmospheric CO_2 and the delayed biotic recovery from the end-Permian mass extinction. *Palaeogeography, Palaeoclimatology, Palaeoecology,* **252**, 164–175.

FRAISER, M. L., TWITCHETT, R. J. and BOTTJER, D. J. 2005. Unique microgastropod biofacies in the Early Triassic: Indicator of long-term biotic stress and the pattern of biotic recovery after the end-Permian mass extinction. *Comptes Rendus Palevol,* **4**, 543–552.

FRASER, N. C. 1994. Assemblages of small tetrapods from Brithish LateTriassic fissure deposits. *In:* FRASER, N. C. and SUES, H.-D. (eds) *In the shadow of the dinosaurs. Early Mesozoic tetrapods.* Cambridge University Press, 214–226.

FREDERICKS, G. 1915. La faune paléozoique supérieure des environs de la ville de Krasnoufimsk. *Mémoires du Comité Géologique. Nouvelle Série,* Livre **109**, 98 pp.

FREYTET, P., GALTIER, J., RONCHI, A., SCHNEIDER, J. W., TINTORI, A. and WERNEBURG, R. 2002. Early Permian continental biota from Southeastern Sardinia (Ogliastra and Gerrei). *Rendiconti della Società Paleontologica Italiana,* **1**, 169–176.

FRIEDMAN, M. and SALLAN, L. C. 2012. Five hundred million years of extinction and recovery: a Phanerozoic survey of large-scale diversity patterns in fishes. *Palaeontology,* **55**, 707–742.

FRITSCH, A. 1889. *Fauna der Gaskohle und der Kalksteine der Permformation Böhmens. Vol. 2,* Řivnáč, Prague, 114 pp.
FRITSCH, A. 1890, 1895. *Fauna der Gaskohle und der Kalksteine der Permformation Böhmens. Vol. 3,* Prague, Řivnáč, 48 pp.
FRÖBISCH, J. 2008. Global taxonomic diversity of anomodonts (Tetrapoda, Therapsida) and the terrestrial rock record across the Permian–Triassic boundary. *PLoS ONE,* **3**, e3733 (14 pp.).
GAILLARDOT, C.-A. 1835. Observations sur les fossiles du calcaire conchylien de la Lorraine. *Annales des Sciences Naturelles. Ser. 2. Zoologie et biologie animale,* **3**, 46–50.
GAITZSCH, B. 1995. Grüneberg-Formation. *In:* PLEIN, E. (ed.) *Stratigraphie von Deutschland I. Norddeutsches Rotliegendbecken. Rotliegend-Monographie Teil II.* Courier Forschungsinstitut Senckenberg,**183**, 102–106.
GALFETTI, T., BUCHER, H., OVTCHAROVA, M., SCHALTEGGER, U., BRAYARD, A., BRÜHWILER, T., GOUDEMAND, N., WEISSERT, H., HOCHULI, P. A., CORDEY, F. and GUODUN, K. 2007. Timing of the Early Triassic carbon cycle perturbations inferred from new U–Pb ages and ammonoid biochronozones. *Earth and Planetary Science Letters,* **258**, 593–604.
GANS, T. 1983. Obituary GEORG HAAS, 1905-1981. *American Zoologist,* **23**, 343–346.
GARCÍA, V. B., LUCIFORA, L. O. and MYERS, R. A. 2008. The importance of habitat and life history to extinction risk in sharks, skates, rays and chimaeras. *Proceedings of the Royal Society B: Biological Sciences,* **275**, 83–89.
GAUDRY, A. 1883. *Les enchaînements du monde animal dans les temps géologiques. Fossiles Primaires,* Libraire F. Savy, Paris, 319 pp.
GEBHARDT, U. 1988. Taxonomie und Palökologie von *Lissodus lacustris* n. sp. (Hybodontoidea) aus dem Stefan C (Oberkarbon) der Saalesenke. *Freiberger Forschungshefte,* **C419**, 38–41.
GEINITZ, H. B. 1837. *Beitrag zur Kenntnis des thüringer Muschelkalkgebirges,* Jena, 38 pp.
GEINITZ, H. B. 1861/1862. *Dyas oder die Zechsteinformation und das Rothliegende (Permische Formation zum Theil). Heft I. Die animalischen Ueberreste der Dyas,* Engelmann, Leipzig, 130 pp.
GIEBEL, C. G. 1848. *Fauna der Vorwelt mit steter Berucksichtigung der lebenden Thiere. Bd. I: Wirbelthiere, Abt. 3,* Leipzig, FU. Brodhaus, 467 pp.
GIEBEL, C. G. 1856. Rätselhafter Fisch aus dem Mansfelder Kupferschiefer. *Zeitschrift fur Naturwissenschaften,* **7**, 367–372.
GILLIS, J. A. and DONOGHUE, P. C. J. 2007. The homology and phylogeny of chondrichthyan tooth enameloid. *Journal of Morphology,* **268**, 33–49.
GINTER, M. 2002a. Chondrichthyan fauna of the Frasnian–Famennian boundary beds in Poland. *Acta Palaeontologica Polonica,* **47**, 329–338.
GINTER, M. 2002b. Taxonomic notes on "*Phoebodus heslerorum*" and *Symmorium reniforme* (Chondrichthyes, Elasmobranchii). *Acta Palaeontologica Polonica,* **47**, 547–555.
GINTER, M. 2004. Devonian sharks and the origin of Xenacanthiformes. *In:* ARRATIA, G., WILSON, M. V. H. and CLOUTIER, R. (eds) *Recent Advances in the Origin and Early Radiation of Vertebrates.* Verlag Dr. Friedrich Pfeil, München, 473–486.

GINTER, M., HAIRAPETIAN, V. and KLUG, S. 2002. Famennian chondrichthyans from the shelves of North Gondwana. *Acta Geologica Polonica,* **52**, 169–215.

GINTER, M., IVANOV, A. and LEBEDEV, O. 2005. The revision of "*Cladodus*" *occidentalis*, a late Palaeozoic ctenacanthiform shark. *Acta Palaeontologica Polonica,* **50**, 623–631.

GINTER, M., HAMPE, O. and DUFFIN, C. 2010. *Chondrichthyes (Paleozoic Elasmobranchii: teeth), Handbook of Paleoichthyology, vol. 3D,* Verlag Dr. Friedrich Pfeil, München, 165 pp.

GLENNIE, K. W. 2005. *The Geology of the Oman Mountains - An outline of their origin*. Second edition, Scientific Press Ltd, Beaconsfield, 110 pp.

GLENNIE, K. W., BOEUF, M. G. A., HUGHES CLARKE, M. W., MOODY-STUART, M., PILAAR, W. F. H. and REINHARDT, B. M. 1974. Geology of the Oman Mountains, parts 1–3. *Verhandelingen van het Koninklijk Nederlands geologisch mijnbouwkundig Genootschap,* **31**, 1–423.

GLIKMAN, L. S. 1964. *Sharks of the Palaeogene and their stratigraphic significance*, Doklady Akademii Nauk Soyuza Sovetskikh Sotsialisticheskikh Respublik, Moscow, 228 pp. (in Russian).

GLIKMAN, L. S. 1980. *Evolution of Cretaceous and Cenozoic lamnoid sharks,* Nauka, Moscow, 248 pp. (in Russian).

Global Land Cover Facility [Online]. University of Maryland. Available: http://www.landcover.org/ [Accessed 2009].

GODEFROIT, P., CUNY, G., DELSATE, D. and ROCHE, M. 1998. Late Triassic vertebrates from Syren (Luxembourg). *Neues Jahrbuch für Geologie und Paläontologie, Abhandlungen,* **210**, 305–343.

GOLDFUSS, G. A. 1847. *Beiträge zur vorweltlichen Fauna des Steinkohlengebirges,* Henry & Cohen, Bonn, 28 pp.

GOLSHANI, F. and JANVIER, P. 1974. Tooth fragment of a petalodontid fish (Elasmobranchii, Bradyodonti) from the Permian of central Iran. *Geological Survey of Iran, Report,* **31**, 55–61.

GOMEZ PALLEROLA, J. E. 1992. Nota sobre los tiburones hybodontos de las calizas litográficas del Cretácico Inferior del Montsec (Lérida). *Boletin Geológico y Minero,* **103**, 3–33.

GOTO, M. 1972. Fossil Chondrichthyes of Japan. *Journal of the Geological Society of Japan,* **78**, 585–600 (in Japanese with English abstract).

GOTO, M. 1975. New find of the Permian and Triassic fish fossils in Japan - On the dermal denticles and teeth of fishes discovered from Karasawa Area, southeast Asio Mountains. *Earth Science (Chikyu Kagaku),* **29**, 72–74 (in Japanese with English abstract).

GOTO, M. 1984. Discovery of a petalodont tooth from the Nabeyama Formation (Middle Permian) in Kuzuu, Tochigi Prefecture, Central Japan. *Earth Science (Chikyu Kagaku),* **38**, 140–142 (in Japanese).

GOTO, M. 1985. Evolution and adaptation of tooth in elasmobranchs. *Monograph of the Association for the Geological Collaboration in Japan,* **30**, 19–35.

GOTO, M. 1991. Evolutionary trends of the tooth structure in Chondrichthyes. *In:* SUGA, S. and NAKAHARA, H. (eds) *Mechanisms and Phylogeny of Mineralization in Biological Systems.* Springer Verlag, Tokyo, 447–451.

GOTO, M. 1994a. Palaeozoic and early Mesozoic fish faunas of the Japanese Islands. *The Island Arc,* **3**, 247–254.

GOTO, M. 1994b. On the Palaeozoic and Mesozoic fish remains from the Japanese Islands. *Monograph of the Association for the Geological Collaboration in Japan,* **43**, 1–16.
GOTO, M. 1996a. Palaeozoic fish remains from Japan (IGCP-328). *Japan contribution to the IGCP*, 51–60.
GOTO, M. 1996b. On the Palaeozoic and Mesozoic chondrichthyan fish remains from Japan. *Kaiyo Monthly,* **28**, 330–337.
GOTO, M. 1996c. Palaeozoic fish remains from Japan and its palaeobiogeographical significance. *Chikyu Monthly,* **18**, 381–386.
GOTO, M. 1999a. Restoration of the Palaeozoic fish remains of Japan. *Kaiyo Monthly Special Issues,* **16**, 45–53.
GOTO, M. 1999b. Fish remains from the Akasaka Limestone (Permian) - On the fish remains from the Palaeozoic of Japan. *Kanagawa Prefectural Museum of Natural History*, Special Note **3**, 72–77.
GOTO, M. 2000. Restoration of the Palaeozoic fish remains from Japan (IGCP-406). *Japan contribution to the IGCP*, 31–38.
GOTO, M. 2002. Studies on the Palaeozoic shark remains from Japan. The Sharks: Evolution and Adaptation of Sharks. *Catalogue of the chondrichthyan specimens in Gerard Ramon Case Collection.* Kanagawa Prefectural Museum of Natural History, Naka-ku, Yokohama, **2**, 90–96.
GOTO, M. and KUGA, N. 1982. A review on the fossil Chondrichthyes of Mesozoic and Palaeozoic of Japan. *Fossil Club Bulletin,* **14**, 47–53 (in Japanese with English abstract).
GOTO, M. and OKURA, M. 2004. The chondrichthyan tooth remains from the Carboniferous and Permian of Fukuji, Gifu Prefecture, central Japan. *Earth Science (Chikyu Kagaku),* **58**, 215–228 (in Japanese).
GOTO, M., OKURA, M. and OGAWA, H. 1988. On teeth and dermal teeth of Chondrichthyes from the Akasaka Limestone (Middle Permian), Central Japan. *Earth Science (Chikyu Kagaku),* **42**, 290–297 (in Japanese with English abstract).
GOTO, M., KUGA, N. and HACHIYA, K. 1991. On the hybodont elasmobranch teeth of three genera from the Mesozoic of Japan. *Journal of the Geological Society of Japan,* **97**, 743–750 (in Japanese with English abstract).
GOTO, M., UYENO, T. and YABUMOTO, Y. 1996a. Summary of Mesozoic elasmobranch remains from Japan. *In:* ARRATIA, G. and VIOHL, G. (eds) *Mesozoic Fishes – Systematics and Paleoecology.* Verlag Dr. Friedrich Pfeil, München, 73–82.
GOTO, M., TANAKA, T. and UTSUNOMIYA, S. 2010. On a tooth remain of *Lissodus* (Elasmobranchii) from the Taho Limestone (Lower Triassic) in Seiyo City, Ehime Prefecture, Southwest Japan. *Earth Science (Chikyu Kagaku),* **64**, 111–116 (in Japanese with English abstract).
GOTO, M., OKURA, M., KANEKO, N. and SUZUKI, Y. 1996b. On the elasmobranchian tooth remains from the Carboniferous of Fukuji, Gifu Prefecture, central Japan, and from the Permian of Motoyoshi, Miyagi Prefecture, northeast Japan. *Abstracts of the 1996 Annual Meeting of the Palaeontological Society of Japan,* 90 (in Japanese).
GOTO, M., KANEKO, N., SUZUKI, Y. and OKURA, M. 2000. First record of a *Xenacanthus* shark tooth from the Paleozoic of Japan. *Journal of the Geological Society of Japan,* **106**, 737–742 (in Japanese with English abstract).

GOUDEMAND, N., ORCHARD, M. J., BUCHER, H. and JENKS, J. 2012. The elusive origin of *Chiosella timorensis* (Conodont Triassic). *Geobios,* **45**, 199–207.

GOULD, S. J. and VRBA, E. S. 1982. Exaptation - A missing term in the science of form. *Paleobiology,* **8**, 4–15.

GRADSTEIN, F. M., OGG, J. G., SCHMITZ, M. and OGG, G. M. (eds) 2012. *The Geologic Time Scale 2012*. Elsevier, Amsterdam, 1176 pp.

GRASBY, S. E. and BEAUCHAMP, B. 2008. Intrabasin variability of the carbon-isotope record across the Permian–Triassic transition, Sverdrup Basin, Arctic Canada. *Chemical Geology,* **253**, 141–150.

GRAY, J. E. 1851. *List of the specimens of fish in the collection of the British Museum. Part I. Chondropterygii,* British Museum (Natural History), London, X + 160 pp.

GRICE, K., CAO, C. Q., LOVE, G. D., BOTTCHER, M. E., TWITCHETT, R. J., GROSJEAN, E., SUMMONS, R. E., TURGEON, S. C., DUNNING, W. and JIN, Y. G. 2005. Photic zone euxinia during the Permian-Triassic superanoxic event. *Science,* **307**, 706–709.

GROGAN, E. D. and LUND, R. 2008. A basal elasmobranch, *Thrinacoselache gracia* n. gen & sp., (Thrinacodontidae, New Family) from the Bear Gulch Limestone, Serpukhovian of Montana, USA. *Journal of Vertebrate Paleontology,* **28**, 970–988.

GROGAN, E. D., LUND, R. and GREENFEST-ALLEN, E. 2012. The origin and relationships of early chondrichthyans. *In:* CARRIER, J. C., MUSICK, J. A. and HEITHAUS, M. R. (eds) *Biology of Sharks and Their Relatives, 2nd ed.* CRC Press, Boca Raton, 633 pp.

GUEX, J., HUNGERBÜHLER, A., JENKS, J. F., O'DOGHERTY, L., ATUDOREI, N.-V., TAYLOR, D. G., BUCHER, H. and BARTOLINI, A. 2010. Spathian (Lower Triassic) ammonoids from western USA (Idaho, California, Utah and Nevada). *Mémoires de Géologie (Lausanne),* **49**, 1–82.

GUINOT, G. and CAPPETTA, H. 2011. Enameloid microstructure of some Cretaceous Hexanchiformes and Synechodontiformes (Chondrichthyes, Neoselachii): New structures and systematic implications. *Microscopy Research and Technique,* **74**, 196–205.

GUINOT, G., ADNET, S. and CAPPETTA, H. 2012. An analytical approach for estimating fossil record and diversification events in sharks, skates and rays. *PLoS ONE,* **7**, e44632.

GUNNELL, F. H. 1933. Conodonts and Fish Remains from the Cherokee, Kansas City, and Wabaunsee Groups of Missouri and Kansas. *Journal of Paleontology,* **7**, 261–297.

HAGDORN, H. and REIF, W.-E. 1988. „Die Knochenbreccie von Crailsheim“ und weitere Mitteltrias-Bonebeds in Nordost-Württemberg – Alte und neue Deutungen. *In:* HAGDORN, H. (ed.) *Neue Forschungen zur Erdgeschichte von Crailsheim. Zur Erinnerung an Hofrat Richard Blezinger.* Goldschneck, Stuttgart, 116–143.

HALLAM, A. 2002. How catastrophic was the end-Triassic mass extinction? *Lethaia,* **35**, 147–157.

HALLAM, A. and WIGNALL, P. B. 1997. *Mass Extinctions and Their Aftermath*. Oxford University Press, New York, 320 pp.

HALLAM, A. and WIGNALL, P. B. 1999. Mass extinctions and sea-level changes. *Earth-Science Reviews,* **48**, 217–250.

HAMADA, T. and ITOIGAWA, J. 1983. *Fossils of Japan,* Shogaku-Kan, Tokyo, 168 pp. (in Japanese).

HAMPE, O. 1988a. Über die Bezahnung des *Xenacanthus* (Chondrichthyes: Xenacanthida; Unterperm, SW-Deutschland). *Neues Jahrbuch für Geologie und Paläontologie, Monatshefte,* **1988**, 743–756.

HAMPE, O. 1988b. Über die Bezahnung des *Orthacanthus* (Chondrichthyes: Xenacanthida; Oberkarbon–Unterperm). *Paläontologische Zeitschrift,* **62**, 285–296.

HAMPE, O. 1989. Revision der *Triodus*-arten (Chondrichthyes: Xenacanthida) aus dem saarpfälzischen Rotliegenden (Oberkarbon — Perm, SW-Deutschland) aufgrund ihrer bezahnung. *Paläontologische Zeitschrift,* **63**, 79–101.

HAMPE, O. 1994. Neue Erkenntnisse zur permokarbonischen Xenacanthiden-Fauna (Chondrichthyes: Elasmobranchii) und deren Verbreitung im südwestdeutschen Saar-Nahe-Becken. *Neues Jahrbuch für Geologie und Paläontologie, Abhandlungen,* **192**, 53–87.

HAMPE, O. 1995. *Plicatodus jordani* n. g., sp., a new xanacanthid shark from the Lower Permian of Europe (Saar-Nahe Basin, Germany). *Bulletin du Muséum national d'Histoire naturelle. Section C, Sciences de la terre, paléontologie, géologie, minéralogie,* **17**, 209–226.

HAMPE, O. 1996. Dermale Skelettelemente von *Lissodus* (Chondrichthyes: Hybodontoidea) aus dem Unterperm des Saar-Nahe-Beckens. *Paläontologische Zeitschrift,* **70**, 225–243.

HAMPE, O. 1997. Dental growth anomalies and morphological changes in teeth of the Xenacanthida (Lower Permian; Saar-Nahe Basin, SW-Germany). *Modern Geology,* **21**, 121–135.

HAMPE, O. 2003. Revision of the Xenacanthida (Chondrichthyes: Elasmobranchii) from the Carboniferous of the British Isles. *Earth and Environmental Science Transactions of the Royal Society of Edinburgh,* **93**, 191–237 [for 2002].

HAMPE, O. 2012. Addendum to Handbook of Paleoichthyology, vol. 3D – The Permian euselachian *Wodnika*. *In:* CAPPETTA, H. (ed.) *Handbook of Paleoichthyology - Chondrichthyes (Mesozoic and Cenozoic Elasmobranchii: Teeth), Vol. 3E.* München: Verlag Dr. Friedrich Pfeil, p. 467.

HAMPE, O. and IVANOV, A. 2007. Bransonelliformes - a new order of the Xenacanthimorpha (Chondrichthyes, Elasmobranchii). *Fossil Record - Mitteilungen aus dem Museum für Naturkunde,* **10**, 190–194.

HAMPE, O., HAIRAPETIAN, V., WITZMANN, F., DORKA, M. and AKBARI, A. 2011. A first fish fauna from the late Permian of Baghuk Mountain, Iran. *Ichthyolith Issues, Special Publication,* **12**, 21–22.

HAMPE, O., HAIRAPETIAN, V., DORKA, M., WITZMANN, F., AKBARI, A. M. and KORN, D. 2013. A first Late Permian fish fauna from Baghuk Mountain (Neo-Tethyan shelf, central Iran). *Bulletin of Geosciences,* **88**, 1–20.

HANCOCK, A. and HOWSE, R. 1870. On *Janassa bituminosa* SCHLOTHEIM from the Marl-slate of Midderidge, Durham. *Annals and Magazine of Natural History, Series 4,* **5**, 47–62.

HANSEN, M. C. 1978. A presumed lower dentition and a spine of a Permian petalodontiform chondrichthyan, *Megactenopetalus kaibabanus*. *Journal of Paleontology,* **52**, 55–60.

HANSEN, M. C. 1985. Systematic relationship of petalodontiform chondrichthyans. *C.R. 9ème Cong. Internat. Strat. Géol. Carbonifère, Washington, D.C. and*

Champaign-Urbana, Illinois 1979. Paleontology, Paleoecology, Paleogeography, **5**, 523–541.

HANSEN, M. C. and MAPES, R. H. 1990. A predator - prey relationship between sharks and cephalopods in the Late Palaeozoic. *In:* BOUCOT, A. J. (ed.) *Evolutionary Paleobiology of Behavior and Coevolution.* Elsevier, Amsterdam, Oxford, New York, Tokyo, 189–195.

HARDMANN, E. T. 1884. *Report on the geology of the Kimberley District, Western Australia,* By Authority, Perth, 22 pp.

HARLAND, W. B., HOLLAND, C. H., M.R., H., HUGHES, N. F., REYNOLDS, A. B., RUDWICK, M. J. S., SATTERTHWAITE, G. E., TARLO, L. B. H. and WILLEY, E. C. (eds) 1967. *The Fossil Record.* Geological Society, London, Special Publication, **2**, 828 pp.

HARLTON, B. H. 1933. Micropaleontology of the Pennsylvanian Johns Valley Shale of the Ouachita Mountains, Oklahoma, and its relationship to the Mississippian Caney Shale. *Journal of Paleontology,* **7**, 3–29.

HARRISON, J. C. 1995. Melville Island's salt based fold belt (Arctic Canada). *Geological Survey of Canada, Bulletin,* **472**, 1–331.

HAUBOLD, H. and SCHAUMBERG, G. 1985. Die Fossilien des Kupferschiefers. *Die Neue Brehm-Bücherei,* **333**, 223 pp.

HAUSER, M., VACHARD, D., MARTINI, R., MATTER, A., PETERS, T. and ZANINETTI, L. 2000. The Permian sequence reconstructed from reworked carbonate clasts in the Batain Plain (northeastern Oman). *Comptes Rendus de l'Académie des Sciences - Series IIA - Earth and Planetary Science,* **330**, 273–279.

HAUSER, M., MARTINI, R., MATTER, A., KRYSTYN, L., PETERS, T., STAMPFLI, G. and ZANINETTI, L. 2002. The break-up of East Gondwana along the northeast coast of Oman: evidence from the Batain basin. *Geological Magazine,* **139**, 145–157.

HAUTMANN, M. 2001. Extinction: End-Triassic Mass Extinction. *Encyclopedia of Life Sciences (eLS).* John Wiley & Sons, Ltd. [www.els.net].

HAY, O. P. 1899. On some changes in the names, generic and specific, of certain fossil fishes. *American Naturalist,* **33**, 783–792.

HAY, O. P. 1900. Descriptions of some vertebrates of the Carboniferous age. *Proceedings of the American Philosophical Society,* **39**, 96–123.

HAY, O. P. 1902. Bibliography and catalogue of the fossil vertebrata of North America. *United States Geological Survey, Bulletin,* **179**, 1–868.

HAY, O. P. 1907. A new genus and species of fossil shark related to *Edestus* Leidy. *Science,* **26**, 22–24.

HAY, O. P. 1909. On the nature of *Edestus* and related genera, with descriptions of one new genus and three new species. *Proceedings of the United States National Museum,* **37**, 43–61.

HAY, O. P. 1929/1930. Second bibliography and catalogue of the fossil vertebrata of North America. *Carnegie Institution of Washington Publication,* **390**, 1–1074.

HAYASHI, I. 1968. The permian conodonts in chert of the Adoyama Formation. Ashio Mountains, Central Japan. *Earth Science (Chikyu Kagaku),* **22**, 69–77 (in Japanese, with English abstract).

HAYASHI, I. 1971. Conodonts from the Nabeyama Formation, Kuzuu District, Tochigi Prefecture, Japan. *Earth Science (Chikyu Kagaku),* **25**, 251–257 (in Japanese, with English abstract).

HE, B., XU, Y.-G., HUANG, X.-L., LUO, Z.-Y., SHI, Y.-R., YANG, Q.-J. and YU, S.-Y. 2007. Age and duration of the Emeishan flood volcanism, SW China: Geochemistry and SHRIMP zircon U-Pb dating of silicic ignimbrites, post-volcanic Xuanwei Formation and clay tuff at the Chaotian section. *Earth and Planetary Science Letters,* **255**, 306–323.

HECKERT, A. B. 2004. Late Triassic microvertebrates from the lower Chinle Group (Otischalkian–Adamanian: Carnian), southwestern U.S.A. *New Mexico Museum of Natural History and Science Bulletin,* **27**, 1–170.

HECKERT, A. B. and JENKINS, H. S. 2005. The microvertebrate fauna of the Upper Triassic (Revueltian) Snyder Quarry, North-Central New Mexico. *56th Field Conference Guidebook, Geology of the Chama Basin*, 319–334.

HECKERT, A. B., IVANOV, A. and LUCAS, S. G. 2007. Dental morphology of the Hybodontoid shark *Lonchidion humblei* Murry from the Upper Triassic Chinle Group, USA. *In:* LUCAS, S. G. and SPIELMANN, J. A. (eds) *The Global Triassic.* New Mexico Museum of Natural History and Science Bulletin, **41**, 45–48.

HECKERT, A. B., JENKINS, H. S., LUCAS, S. G. and MUTTER, R. J. 2004. The Microvertebrate Fauna of the Upper Triassic Snyder Quarry, from the Painted Desert Member of the Petrified Forest Formation (Revueltian), North-Central New Mexico. *New Mexico Geology,* **26**, 75.

HEIDTKE, U. 1982. Der Xenacanthide *Orthacanthus senckenbergianus* aus dem pfälzischen Rotliegenden (Unter-Perm). *Mitteilungen der Pollichia,* **70**, 65–86.

HEIDTKE, U. 1998. Revision der Gattung *Orthacanthus* Agassiz 1843 (Chondrichthyes: Xenacanthida). *Paläontologische Zeitschrift,* **72**, 135–147.

HEIDTKE, U. H. J. 2007. Räuber in Flüssen und Seen - Haie im Süßwasser. *In:* SCHINDLER, T. and HEIDTKE, U. H. J. (eds) *Kohlesümpfe, Seen und Halbwüsten. Dokumente einer rund 300 Millionen Jahre alten Lebewelt zwischen Saarbrücken und Mainz.* Pollichia Sonderveröffentlichung, **10**, 206–229.

HENDERSON, C. M. 1988. *Conodont paleontology and biostratigraphy of the Upper Carboniferous to Lower Permian Canyon Fiord, Belcher Channel, Nansen, and Van Hauen formations and an unnamed formation, southwestern Ellesmere Island, Canadian Arctic Archipelago.* PhD thesis, University of Calgary, 287 pp.

HENDERSON, C. M. 2005. International correlation of the marine Permian time scale. *Permophiles. Newsletter of the Subcommission on Permian Stratigraphy,* **46**, 6–9.

HENDERSON, C. M. and MEI, S. 2000. Preliminary cool water Permian conodont zonation in North Pangea: a review. *Permophiles. Newsletter of the Subcommission on Permian Stratigraphy,* **36**, 16–23.

HENDERSON, C. M. and MEI, S. 2003. Stratigraphic versus environmental significance of Permian serrated conodonts around the Cisuralian–Guadalupian boundary: new evidence from Oman. *Palaeogeography, Palaeoclimatology, Palaeoecology,* **191**, 301–328.

HENRIKSEN, N. 2008. *Geological History of Greenland - Four billion years of Earth evolution*. Geological Survey of Denmark and Greenland (GEUS), Copenhagen, 272 pp.

HENRIKSEN, N., HIGGINS, A. K., KALSBEEK, F. and PULVERTAFT, T. C. R. 2009. Greenland from Archaean to Quaternary. Descriptive text to the 1995

Geological map of Greenland, 1:2 500 000. 2nd edition. *Geological Survey of Denmark and Greenland Bulletin,* **18**, 1–126.

HENRY, J. 1875. Étude stratigraphique et paléontologique de L'Infralias dans la Franche-Comté. *Mémoires de la Société d'Émulation du Doubs, 4e série,* **10**, 285–476.

HERMAN, J. 1977. Les Sélaciens des terrains Néocrétacés & paléocenes de Belgique & des contrées limitrophes. *Mémoires pour servir à l'explication des Cartes géologiques et Miniéres de la Belgique,* **15**, 1–450.

HEYLER, D. 1969. Vertebrés de l'Autunien de France. *Cahiers de Paléontologie***,** 1–259.

HEYLER, D. 1987. Vertébrés des bassins stéphaniens et autuniens du Massif Central Français; paléobiogéographie et paléoenvironnements. *Annales de la Société Géologique du Nord,* **151**, 123–130.

HEYLER, D. and POPLIN, C. 1982. Sur quelques neurocrânes d'Elasmobranches du Permien du Bassin d'Autun (Saône et Loire, France). *Annales de Paléontologie,* **68**, 15–32.

HEYLER, D. and DEBRIETTE, P. 1986. Sur les Xénacanthiformes (Poissons, Élasmobranches) à la lumière de découvertes récentes dans le Permo-Carbonifère de France. *Actes du 111e Congrès national des Sociétés savantes.* Comité des Traveaux Historiques et Scientifiques, Poitiers, **1**, 89–109.

HEYLER, D. and POPLIN, C. 1989. Systematics and relationships among the Xenacanthiformes (Pisces, Chondrichthyes) in the light of Carboniferous and Permian French material. *Acta Musei Reginaehradecensis,* **A22**, 69–78.

HEYLER, D. and POPLIN, C. 1990. Les Vertébrés autuniens de Buxières-les-Mines (Allier, France). *Bulletin du Muséum national d'Histoire naturelle. Section C, Sciences de la terre, paléontologie, géologie, minéralogie,* **12**, 225–239.

HODNETT, J.-P. M., ELLIOTT, D. K., OLSON, T. J. and WITTKE, J. H. 2012. Ctenacanthiform sharks from the Permian Kaibab Formation, northern Arizona. *Historical Biology,* **24**, 381–395.

HOFFET, J. H. 1933. Ètude géologique sur le centre de l’Indochine entre Tourane et le Mekong. *Bulletin de la Service géologique du Indochine,* **20**, 3–154.

HOFFMAN, B. L. and HAGEMAN, S. A. 2011. Shark "teeth" of the form genus *Gunnellodus* Wilimovsky (*Idiacanthus* Gunnell) represent stethacanthid denticles. *Abstracts of the 143rd annual meeting of the Kansas Academy of Science, Baker University, Baldwin City, Kansas, April 8–9, 2011. Transactions of the Kansas Academy of Science,* **114**, 161.

HOFMANN, R., GOUDEMAND, N., WASMER, M., BUCHER, H. and HAUTMANN, M. 2011. New trace fossil evidence for an early recovery signal in the aftermath of the end-Permian mass extinction. *Palaeogeography, Palaeoclimatology, Palaeoecology,* **310**, 216–226.

HOLLAND, S. M. 1995. The stratigraphic distribution of fossils. *Paleobiology,* **21**, 92–109.

HOLSER, W. T., SCHÖNLAUB, H.-P., ATTREP, M., BOECKELMANN, K., KLEIN, P., MAGARITZ, M., ORTH, C. J., FENNINGER, A., JENNY, C., KRALIK, M., MAURITSCH, H., PAK, E., SCHRAMM, J.-M., STATTEGGER, K. and SCHMOLLER, R. 1989. A unique geochemical record at the Permian/Triassic boundary. *Nature,* **337**, 39–44.

HOLSER, W. T., SCHÖNLAUB, H.-P., BOECKELMANN, K., MAGARITZ, M. and ORTH, C. J. 1991. The Permian-Triassic of the Gartnerkofel-1 core (Carnic

Alps, Austria): synthesis and conclusions. *Abhandlungen der Geologischen Bundesanstalt,* **45**, 213–232.
HORACEK, M., KOIKE, T. and RICHOZ, S. 2009. Lower Triassic $\delta^{13}C$ isotope curve from shallow-marine carbonates in Japan, Panthalassa realm: confirmation of the Tethys $\delta^{13}C$ curve. *Journal of Asian Earth Sciences,* **36**, 481–490.
HOTINSKI, R. M., BICE, K. L., KUMP, L. R., NAJJAR, R. G. and ARTHUR, M. A. 2001. Ocean stagnation and end-Permian anoxia. *Geology,* **29**, 7–10.
HOTTON III, N. 1952. Jaws and teeth of american xenacanth sharks. *Journal of Paleontology,* **26**, 489–500.
HOUNSLOW, M. W., HU, M., MØRK, A., VIGRAN, J. O., WEITSCHAT, W. and ORCHARD, M. J. 2007. Magneto-biostratigraphy of the Middle to Upper Triassic transition, central Spitsbergen, arctic Norway. *Journal of the Geological Society, London,* **164**, 581–597.
HOUNSLOW, M. W., PETERS, C., MØRK, A., WEITSCHAT, W. and VIGRAN, J. O. 2008. Biomagnetostratigraphy of the Vikinghøgda Formation, Svalbard (Arctic Norway), and the geomagnetic polarity timescale for the Lower Triassic. *Geological Society of America, Bulletin,* **120**, 1305–1325.
HROUDA, F. and BRANDT, S. 2005. Friedrich Eduard Mackroth (1807–1866) - Pionier der Zechtsteinforschung in Gera. *Veröffentlichungen Museum für Naturkunde der Stadt Gera, Naturwissenschaftlichen Reihe,* **32**, 138–144.
HUBER, P., LUCAS, S. G. and HUNT, A. P. 1993. Chapter 4. Late Triassic fish assemblages of the North American western interior. *In:* MORALES, M. (ed.) *Aspects of Mesozoic Geology and Paleontology of the Colorado Plateau.* Museum of Northern Arizona Bulletin, **59**, 51–66.
HUELSENBECK, J. P. and RANNALA, B. 2000. Using stratigraphic information in phylogenetics. *In:* WIENS, J. J. (ed.) *Phylogenetic Analysis of Morphological Data.* Smithsonian Institution Press, Washington, D.C., 165–191.
HULKE, J. W. 1873. Memorandum on some fossil vertebrate remains collected by the Swedish expeditions to Spitzbergen in 1864 and 1868. *Bihang Svenska Vetenskaps-Akademiens Handlingar,* **1**, 1–11.
HUNT, A. P. and LUCAS, S. G. 1989. Late Triassic Vertebrate Localities in New Mexico. *In:* LUCAS, S. G. and HUNT, A. P. (eds) *Dawn of the Age of Dinosaurs in the American Southwest.* New Mexico Museum of Natural History, 72–101.
HUNT, A. P. and LUCAS, S. G. 1993. Late Triassic microvertebrate localities in New Mexico (USA): Implications for paleoecology. *New Mexico Museum of Natural History and Science Bulletin,* **3**, 187–191.
HUNT, A. P., LUCAS, S. G., SANTUCCI, V. L. and ELLIOTT, D. K. 2005. Permian vertebrates of Arizona. *In:* HECKERT, A. B. and LUCAS, S. G. (eds) *Vertebrate Paleontology in Arizona.* New Mexico Museum of Natural History and Science Bulletin, **29**, 10–15.
HUSSAKOF, L. 1911. The Permian fishes of North America. *Carnegie Institution of Washington Publications,* **146**, 155–178.
HUSSAKOF, L. 1943. Permian fishes from the Kaibab Formation of Arizona. *Geological Society of America, Bulletin,* **54**, 1834.
HUXLEY, T.H. 1880. On the application of the laws of evolution to the arrangement of the Vertebrata, and more particularly of the Mammalia. *Proceedings of the Zoological Society of London,* **1880**, 649–662.

IMMENHAUSER, A., SCHREURS, G., GNOS, E., OTERDOOM, H. W. and HARTMANN, B. 2000. Late Palaeozoic to Neogene geodynamic evolution of the northeastern Oman margin. *Geological Magazine,* **137**, 1–18.

INGAVAT, R. and JANVIER, P. 1981. Bradyodont (Chondrichthyes) teeth from the Permian and Carboniferous of northern Thailand. *Geobios,* **14**, 651–653.

INTERNATIONAL COMMISSION ON STRATIGRAPHY. Website: http://www.stratigraphy.org/

IRMIS, R. B. 2005. The vertebrate fauna of the Upper Triassic Chinle Formation in Northern Arizona. *Mesa Southwest Museum Bulletin,* **9**, 63–88.

ISOZAKI, Y. 2006. Guadalupian (Middle Permian) giant bivalve Alatoconchidae from a mid-Panthalassan paleo-atoll complex in Kyushu, Japan: A unique community associated with Tethyan fusulines and corals. *Proceedings of the Japan Academy, Series B,* **82**, 25–32.

ISOZAKI, Y. 2009. Integrated "plume winter" scenario for the double-phased extinction during the Paleozoic-Mesozoic transition: The G-LB and P-TB events from a Panthalassan perspective. *Journal of Asian Earth Sciences,* **36**, 459–480.

ISOZAKI, Y. and OTA, A. 2001. Middle-Upper Permian (Maokouan-Wuchiapingian) boundary in mid-oceanic paleo-atoll limestone of Kamura and Akasaka, Japan. *Proceedings of the Japan Academy, Series B,* **77**, 104–109.

ISOZAKI, Y., MARUYAMA, S. and FURUOKA, F. 1990. Accreted oceanic materials in Japan. *Tectonophysics,* **181**, 179–205.

ISOZAKI, Y., KAWAHATA, H. and OTA, A. 2007a. A unique carbon isotope record across the Guadalupian-Lopingian (Middle-Upper Permian) boundary in mid-oceanic paleo-atoll carbonates: The high-productivity "Kamura event" and its collapse in Panthalassa. *Global and Planetary Change,* **55**, 21–38.

ISOZAKI, Y., KAWAHATA, H. and MINOSHIMA, K. 2007b. The Capitanian (Permian) Kamura cooling event: The beginning of the Paleozoic-Mesozoic transition. *Palaeoworld,* **16**, 16–30.

ISOZAKI, Y., ALJINOVIĆ, D. and KAWAHATA, H. 2010. The Guadalupian (Permian) Kamura event in european Tethys. *GSA Annual Meeting, Denver. Geological Society of America, Abstracts with Programs*, **42**, 70.

ISOZAKI, Y., ALJINOVIĆ, D. and KAWAHATA, H. 2011. The Guadalupian (Permian) Kamura event in European Tethys. *Palaeogeography, Palaeoclimatology, Palaeoecology,* **308**, 12–21.

ISOZAKI, Y., YAO, J., MATSUDA, T., SAKAI, H., JI, Z., SHIMIZU, N., KOBAYASHI, N., KAWAHATA, H., NISHI, H., TAKANO, M. and KUBO, T. 2004. Stratigraphy of the Middle-Upper Permian and Lowermost Triassic at Chaotian, Sichuan, China: Record of Late Permian double mass extinction event. *Proceedings of the Japan Academy, Series B,* **80**, 10–16.

ITANO, W. M., HOUCK, K. J. and LOCKLEY, M. G. 2012. Systematics and occurrences of Edestus (Chondrichthyes) worldwide and new occurrences from Colorado and Texas. *Historical Biology,* **24**, 397–410.

IVANOV, A. 1996. The Early Carboniferous chondrichthyans of the South Urals, Russia. *In* STROGEN, P., SOMERVILLE, I. D. and JONES, G. L. (eds) *Recent Advances in Lower Carboniferous Geology.* Geological Society, London, Special Publications, **107**, 417–425.

IVANOV, A. 1999. Late Devonian – Early Permian chondrichthyans of the Russian Arctic. *Acta Geologica Polonica,* **49**, 267–285.

IVANOV, A. 2000. Permian elasmobranchs (Chondrichthyes) of Russia. *Ichthyolith Issues, Special Publication,* **6**, 39–42.
IVANOV, A. 2005. Early Permian Chondrichthyans of the Middle and South Urals. *Revista Brasileira de Paleontologia,* **8**, 127–138.
IVANOV, A. 2007. Early Permian cartilaginous fishes from the Urals. *Upper Paleozoic Russia: Stratigraphy and Paleogeography. All-Russian conference dedicated to the memory of Professor Vyacheslav IG Halymbadzhi, 25–27 September 2007.* Kazan: Kazan State University, 122–123 (in Russian).
IVANOV, A. O. 2010. Late Paleozoic anachronistid sharks: morphology and distribution of teeth. *Evolution of organic-canonical peace and biotic crises: Proceedings of the UPR session LVI.* St. Petersburg: 127–128.
IVANOV, A. 2011. Permian anachronistid sharks of the East European Platform and Urals. *Palaeozoic and Mesozoic vertebrates of Eurasia: evolution, community change, taphonomy and palaeobiogeography. Proceedings of the conference dedicated to the 80th birthday of Vitaly IG Ochev (1931-2004), 6 December, 2011.* Paleontological Institute, Russian Academy of Sciences, Moscow, 17–19 [in Russian].
IVANOV, A. and CUNY, G. 2000. The dental histology of the Late Palaeozoic shark *Cooleyella*. *Abstracts of the 9th International Symposium on Early Vertebrates/Lower Vertebrates.* Flagstaff, Arizona, USA: 11.
IVANOV, A. and DERYCKE, C. 2005. Viséan elasmobranchs of Belgium. *Ichthyolith Issues, Special Publication,* **9**, 13–17.
IVANOV, A. and KLETS, T. 2007. Triassic marine fishes from Siberia, Russia. *New Mexico Museum of Natural History and Science, Bulletin,* **41**, 108–109.
IVANOV, A. and LEBEDEV, O. 2007. Permian chondrichthyans of the Kanin Peninsula, Arctic Russia. *XVI International Congress on the Carboniferous and Permian.* Nanjing, China: Journal of Stratigraphy, **21** (Supp. I), 57.
IVANOV, A., NESTELL, M. and NESTELL, G. 2007a. Middle Permian chondrichthyans from West Texas and relationships of the Jalodontidae. *Ichthyolith Issues, Special Publication,* **10**, 48.
IVANOV, A., LUCAS, S. G., RINEHART, L. F. and SPIELMANN, J. A. 2007b. Pennsylvanian-Permian petalodont Chondrichthyan from the Big Hatchet Mountains, southern New Mexico. *New Mexico Geological Society Spring Meeting, April 13, 2007.* Socorro, New Mexico, 23.
IVANOV, A. O., NESTELL, M. and NESTELL, G. 2011. Middle Permian fish assemblages from West Texas. *Ichthyolith Issues, Special Publication,* **12**, 27.
IVANOV, A., NESTELL, M. and NESTELL, G. 2012. New jalodontid chondrichthyans from the Middle Permian of West Texas, USA. *Historical Biology,* **24**, 359–368.
JABLONSKI, D., ROY, K. and VALENTINE, J. W. 2006. Out of the tropics: evolutionary dynamics of the latitudinal diversity gradient. *Science,* **314**, 102–106.
JACOBS, L. L. and MURRY, P. A. 1980. The vertebrate community of the Triassic Chinle Formation near St. Johns, Arizona. *In:* JACOBS, L. L. (ed.) *Aspects of Vertebrate History.* Museum of Northern Arizona, Flagstaff, 55–73.
JACOBSEN, N. D., TWITCHETT, R. J. and KRYSTYN, L. 2011. Palaeoecological methods for assessing marine ecosystem recovery following the Late Permian mass extinction event. *Palaeogeography, Palaeoclimatology, Palaeoecology,* **308**, 200–212.
JAEKEL, O. 1889. Die Selachier aus dem oberen Muschelkalk Lothringens. *Abhandlungen der Geologischen Specialkarte Elsass-Lothringen,* **3**, 273–332.

JAEKEL, O. 1891. Über *Menaspis armata* Ewald. *Sitzungsberichten der Gesellschaft Naturforschender Freunde zu Berlin,* **7**, 115–131.
JAEKEL, O. 1898. Über *Hybodus*. *Sitzungsberichten der Gesellschaft Naturforschender Freunde zu Berlin,* **1898**, 135–143.
JAEKEL, O. 1899. Über die Organisation der Petalodonten. *Zeitschrift der Deutschen Geologischen Gesellschaft,* **51**, 258–298.
JAEKEL, O. 1911. Wirbeltierreste aus der Trias des Bakonyerwaldes. *Resultate der wissenschaftlichen Erforschung des Balatonsees,* **1**, Anhang: Palaeontologie, 3.
JAEKEL, O. 1914. Über die Wirbelthierfunde in oberen Trias von Halberstadt. *Paläontologische Zeitschrift,* **1**, 155–215.
JAEKEL, O. 1925. Das Mundskelett der Wirbeltiere. *Gegenbaurs Morphologisches Jahrbuch,* **55**, 402–409.
JAIN, S. L. 1980. Freshwater xenacanthid (= pleuracanth) shark fossils from the Upper Triassic Maleri Formation, India. *Journal of the Geological Society of India,* **21**, 39–47.
JAIN, S. L., ROBINSON, P. L. and ROY CHOWDHURY, T. K. 1964. A new vertebrate fauna from the Triassic of the Deccan, India. *Quarterly Journal of the Geological Society of London,* **120**, 115–124.
JAMNICZKY, H. A., BRINKMAN, D. B. and RUSSELL, A. P. 2008. How much is enough? A repeatable, efficient and controlled sampling protocol for assessing taxonomic diversity and abundance in vertebrate microfossil assemblages. *In:* SANKEY, J. T. and BASZIO, S. (eds) *Vertebrate Microfossil Assemblages - Their Role in Paleoecology and Paleobiogeography.* Indiana University Press, Bloomington & Indianapolis, 9–16.
JAN, I. U., STEPHENSON, M. H. and KHAN, F. R. 2009. Palynostratigraphic correlation of the Sardhai Formation (Permian) of Pakistan. *Review of Palaeobotany and Palynology,* **158**, 72–82.
JANVIER, P. 1981. On some fish remains from the Permian of North-Eastern Thailand. *Journal of the Geological Society of Thailand, Bangkok,* **4**, 23–28.
JANVIER, P. 1996. *Early Vertebrates,* Oxford Monographs on Geology and Geophysics, no. 33. Oxford University (Clarendon) Press, Oxford, 364 pp.
JEFFERY, C. H. 2001. Heart urchins at the Cretaceous/Tertiary boundary: a tale of two clades. *Paleobiology,* **27**, 140–158.
JENKINS, H. S. and HECKERT, A. B. 2004. Revueltian (Early-Mid Norian) microvertebrates from the Upper Triassic Snyder Quarry, Painted Desert Member, Petrified Forest Formation, North-Central New Mexico. *Journal of Vertebrate Paleontology – abstracts,* **24**, 75A.
JEPPSSON, L. and ANEHUS, R. 1995. A buffered formic acid technique for conodont extraction. *Journal of Paleontology,* **69**, 790–794.
JEPPSSON, L., FREDHOLM, D. and MATTIASSON, B. 1985. Acetic acid and phosphatic fossils - a warning. *Journal of Paleontology,* **59**, 952–956.
JEPPSSON, L., ANEHUS, R. and FREDHOLM, D. 1999. The optimal acetate buffered acetic acid technique for extracting phosphatic fossils. *Journal of Paleontology,* **73**, 964–972.
JIN, F. 2006. An overview of Triassic fishes from China. *Vertebrata Palasiatica,* **44**, 28–42.
JIN, Y. G., ZHANG, J. and SHANG, Q. H. 1994. Two phases of the end-Permian mass extinction. *Canadian Society of Petroleum Geologists, Memoir,* **17**, 813–822.

JIN, Y. G., WANG, Y., WANG, W., SHANG, Q. H., CAO, C. Q. and ERWIN, D. H. 2000. Pattern of marine mass extinction near the Permian-Triassic boundary in South China. *Science,* **289**, 432–436.

JIN, Y., SHEN, S., HENDERSON, C. M., WANG, X., WANG, W., WANG, Y., CAO, C. and SHANG, Q. 2006. The Global Stratotype Section and Point (GSSP) for the boundary between the Capitanian and Wuchiapingian Stage (Permian). *Episodes,* **29**, 253–262.

JOHANSON, Z. and SMITH, M. M. 2003. Placoderm fishes, pharyngeal denticles, and the vertebrate dentition. *Journal of Morphology,* **257**, 289–307.

JOHANSSON, A. K. 1992. The hybodont shark *Lissodus* from the Richmond Basin of Virginia (Late Triassic, Newark Supergroup). *Journal of Vertebrate Paleontology,* **12** (3, Suppl.), 35A.

JOHNS, M. J. 1996. Diagnostic pedicle features of Middle and Late Triassic elasmobranch scales from Northeastern British Columbia, Canada. *Micropaleontology,* **42**, 335–350.

JOHNS, M. J., BARNES, C. R. and ORCHARD, M. J. 1997. Taxonomy and biostratigraphy of Middle and Late Triassic elasmobranch ichthyoliths from Northeastern British Columbia. *Geological Survey of Canada, Bulletin,* **502**, 1–235.

JOHNS, M. J., BARNES, C. R. and ORCHARD, M. 1999. Progress on Triassic ichthyolith biostratigraphy and regional thermal-maturation studies, Trutch and Halfway map areas, northeastern British Columbia. *Current Research, Part A, Geological Survey of Canada,* **1999**, 51–59.

JOHNSON, G. D. 1979. *Early Permian vertebrates from Texas: Actinopterygii (Schaefferichthys), Chondrichthyes (including North American Pennsylvanian and Triassic Xenacanthodii), and Acanthodii.* PhD thesis, Southern Methodist University, 653 pp.

JOHNSON, G. D. 1980. Xenacanthodii (Chondrichthyes) from the Tecovas Formation (Late Triassic) of West Texas. *Journal of Paleontology,* **54**, 923–932.

JOHNSON, G. D. 1981. Hybodontoidei (Chondrichthyes) from the Wichita-Albany Group (Early Permian) of Texas. *Journal of Vertebrate Paleontology,* **1**, 1–41.

JOHNSON, G. D. 1984. A new species of Xenacanthodii (Chondrichthyes, Elasmobranchii) from the Late Pennsylvanian of Nebraska. *Special Publication Carnegie Museum of Natural History,* **9**, 178–186.

JOHNSON, G. D. 1992. Chondrichthyan biostratigraphy of the North American Permian System. *In:* NAIRN, A. E. M. and KOROTEEV, V. (eds) *Contributions to Eurasian Geology. Papers Presented at the International Congress on the Permian System of the World, Perm, Russia, 1991—Part 1. Occasional Publications.* ESRI, New Series, **8B**, 41–50.

JOHNSON, G. D. 1996. Vertebrate microfossils from the Lueders Formation, Albany Group, and the faunal transition from the Wichita Group into the Clear Fork Group, Lower Permian of Texas. *Modern Geology,* **20**, 371–382.

JOHNSON, G. D. 1999. Dentitions of Late Palaeozoic *Orthacanthus* species and new species of ?*Xenacanthus* (Chondrichthyes: Xenacanthiformes) from North America. *Acta Geologica Polonica,* **49**, 215–266.

JOHNSON, G. D. 2003. Dentitions of *Barbclabornia* (new genus, Chondrichthyes: Xenacanthiformes) from the Upper Palaeozoic of North America. *Mitteilungen aus dem Museum für Naturkunde in Berlin, Geowissenschaftliche Reihe,* **6**, 125–146.

JOHNSON, G. D. 2005a. An unusual tricuspid chondrichthyan tooth from the Lower Permian of Texas, U.S.A. *Revista Brasileira de Paleontologia,* **8**, 159–164.

JOHNSON, G. D. 2005b. Underdeveloped and unusual Xenacanth shark teeth from the Lower Permian of Texas. *Proceedings of the South Dakota Academy of Science,* **84**, 215–223.

JOHNSON, G. D. 2006. Iniopterygian tooth whorls from the Lower Permian of Texas, U.S.A. *In:* YANG, Q., WANG, Y. and WELDON, E. A. (eds) *Ancient Life and Modern Approaches - Abstracts of the Second International Palaeontological Congress.* University of Science and Technology of China Press, Hefei, 143–144.

JOHNSON, G. D. 2008. Ctenacanthiform cladodont teeth from the Lower Permian Wichita Group, Texas, U.S.A. *Acta Geologica Polonica,* **58**, 205–209.

JOHNSON, G. D. 2011. Origin of *Orthacanthus texensis* and *O. platypternus* from *O. ?compressus* (Chondrichthyes, Xenacanthiformes) in the Lower Permian of Texas, USA. *In:* JOHNSON, G. D. (ed.) *12th International Symposium on Early Vertebrates/Lower Vertebrates.* Ichthyolith Issues, Special Publication, **12**, 29–31.

JOHNSON, G. D. 2012. Possible origin of the xenacanth sharks *Orthacanthus texensis* and *Orthacanthus platypternus* in the Lower Permian of Texas, USA. *Historical Biology,* **24**, 369–379.

JOHNSON, G. D. and THAYER, D. W. 2009. Early Pennsylvanian xenacanth chondrichthyans from the Swisshelm Mountains, Arizona, USA. *Acta Palaeontologica Polonica,* **54**, 649–668.

JOHNSON, G. D., RICHTER, M. and RAGOGNA, E. W. 2002. Global distribution of Permo−Triassic genera of xenacanthiform chondrichthyans. *Journal of Vertebrate Paleontology,* **22** (Supplement to No 3), 72A.

JORDAN, H. 1849. *Triodus sessilis*, ein neuer Fisch der Kohlenformation von Lebach. *Neues Jahrbuch für Mineralogie, Geologie und Paläontologie,* **1849**, 843.

JORDAN, D. S. 1907. The fossil fishes of California, with supplementary notes on other species of extinct fishes. *University of California Publications, Bulletin of the Department of Geology,* **5**, 95–14.

JUBB, R. A. and GARDINER, B. G. 1975. A preliminary catalogue of identifiable fossil fish material from Southern Africa. *Annals of the South African Museum,* **67**, 381–440.

KAMBE, N. 1963. On the boundary between the Permian and Triassic systems in Japan: With the description of the Permo-Triassic formations at Takachiho-cho, Miyazaki Prefecture in Kyushu and the Skytic fossils contained. Geological Survey of Japan, Kawasaki-shi, **198**, 4–13.

KANMERA, K. and NAKAZAWA, K. 1973. Permian-Triassic relationships and faunal changes in the eastern Tethys. *In:* LOGAN, A. and HILLS, L. V. (eds) *The Permian and Triassic Systems and their Mutual Boundary.* Canadian Society of Petroleum Geologists, Memoir, **2**, 100–119.

KARPINSKY, A. P. 1899. Über die Reste von Edestiden und die neue Gattung *Helicoprion*. *Verhandlungen Russisches Kaiserliches Mineralogisches Gesellschaft zu St. Petersburg, series II,* **36**, 361–475.

Also as: On edestid remains and on the new genus *Helicoprion*. *Zapiski Imperatorskoj Akademii Nauk,* **7**, 1–67 (in Russian).

KARPINSKY, A. P. 1903/1904. Occurrence of remains of genus *Campodus* de Kon. in the Artinskian deposits of Russia. *Zapiski St.-Peterburgskogo Mineralogicheskogo obschestva,* **41**, 32–37 (in Russian).

KARPINSKY, A. P. 1911. Notes on *Helicoprion* and other edestids. *Izvestiya Imperatorskoy Akademii Nauk,* **5**, 1105–1122 (in Russian).

KARPINSKY, A. P. 1916. On new species of *Helicoprion* (*Helicoprion clerci*, n. sp.). Preliminary report. *Izvestiya Imperatorskoj Akademii Nauk,* **6**, 701–708 (in Russian).

KARPINSKY, A. P. 1922. *Helicoprion ivanovi* n. sp. *Bulletin de l'Académie des Sciences de Russie. VI série,* **16**, 369–378.

KARPINSKY, A. P. 1924. *"Helicoprion"* (*Parahelicoprion*) *clerci*. *Zapiski Ural'skogo Obschestva Ljubitelej Estestvoznanija v gorode Sverdlovske,* **39**, 1–10 (in Russian).

KATO, T., HASEGAWA, K. and ISHIBASHI, T. 1995. Discovery of Early Triassic hybodontoid shark tooth from the southern Kitakami Massif. *The Journal of the Geological Society of Japan,* **101**, 466–469 (in Japanese).

KAUFFMAN, E. G. and HARRIES, P. J. 1996. The importance of crisis progenitors in recovery from mass extinction. *In:* HART, M. B. (ed.) *Biotic Recovery From Mass Extinction Events.* Geological Society, London, Special Publications, **102**, 15–39.

KAULFUß, U. 2004. *Lithofazies, Genese und Stratigraphie des Permokarbon im Becken von Bourbon−l'Archambault (Massif central) – Fallstudie Buxières−les−Mines.* Unpublished Master thesis, TU Bergakademie Freiberg, 82 pp.

KAYE, F. T. and PADIAN, K. 1994. Microvertebrates from the *Placerias* Quarry: a window on Late Triassic vertebrate diversity in the American Southwest. *In:* FRASER, N. C. and SUES, H.-D. (eds) *In the Shadow of the Dinosaurs: Early Mesozoic Tetrapods.* Cambridge University Press, 171–196.

KEARSEY, T., TWITCHETT, R. J., PRICE, G. D. and GRIMES, S. T. 2009. Isotope excursions and palaeotemperature estimates from the Permian/Triassic boundary in the Southern Alps (Italy). *Palaeogeography, Palaeoclimatology, Palaeoecology,* **279**, 29–40.

KELLY, M. A. and ZANGERL, R. 1976. *Helicoprion* (Edestidae) in the Permian of West Texas. *Journal of Paleontology,* **50**, 992–994.

KEMP, T. S. 1975. Vertebrate localities in the Karoo System of the Luangwa Valley, Zambia. *Nature,* **254**, 415–416.

KHABAKOV, A. V. 1926–27. On facies distribution of fish fauna in the Upper Permian deposits of European Russia. *Geologicheskij Vestnik,* **5**, 36–39 (in Russian).

KHABAKOV, A. V. 1939. Class Pisces. Fishes. *In:* LICHAREW, B. (ed.) *Atlas Rukovodyaschikh Form Iskopaemykh Faun SSSR.* GONTI NKTP SSSR, 206–216 (in Russian).

KIDDER, D. L. and WORSLEY, T. R. 2004. Causes and consequences of extreme Permo-Triassic warming to globally equable climate and relation to the Permo-Triassic extinction and recovery. *Palaeogeography, Palaeoclimatology, Palaeoecology,* **203**, 207–237.

KIESSLING, W. and DANELIAN, T. 2011. Trajectories of Late Permian–Jurassic radiolarian extinction rates: no evidence for an end-Triassic mass extinction. *Fossil Record,* **14**, 95–101.

KIMURA, T., HAYAMI, I. and YOSHIDA, S. 1991. *Geology of Japan,* Tokyo, University of Tokyo Press, 287 pp.

KIRBY, R. E. 1989. Late Triassic Vertebrate Localities of the Owl Rock Member (Chinle Formation) in the Ward Terrace Area of Northern Arizona. *In:* LUCAS, S. G. and HUNT, A. P. (eds) *Dawn of the Age of Dinosaurs in the American Southwest.* New Mexico Museum of Natural History, 12–28.

KIRBY, R. E. 1993. Relationships of Late Triassic basin evolution and faunal replacement events in the southwestern United States: perspectives from the upper part of the Chinle Formation in northern Arizona. *New Mexico Museum of Natural History and Science Bulletin,* **3**, 233–242.

KIRSCHVINK, J. L. and ISOZAKI, Y. 2007. Extending the sensitivity of paleomagnetic techniques: magnetostratigraphy of weakly-magnetized, organic-rich black limestone from the Permian of Japan. *American Geophysical Union, Fall Meeting.* Abstract GP43B-1223.

KLAUSEWITZ, W. 1986. Redescription of *Orthacanthus senckenbergianus* Fritsch. *In:* UYENO, T., ARAI, R., TANIUCHI, T. and MATSUURA, K. (eds) *Indo-Pacific Fish Biology: Proceedings of the Second International Conference on Indo-Pacific Fishes.* Ichthyological Society of Japan, Tokyo, 125–132.

KLAUSEWITZ, W. 1987. Der "senckenbergische Urdornhai" *Orthacanthus senckenbergianus*. *Natur und Museum,* **117**, 135–142.

KLUG, S. 2009. A new palaeospinacid shark (Chondrichthyes, Neoselachii) from the Upper Jurassic of southern Germany. *Journal of Vertebrate Paleontology,* **29**, 326–335.

KLUG, S. 2010. Monophyly, phylogeny and systematic position of the †Synechodontiformes (Chondrichthyes, Neoselachii). *Zoologica Scripta,* **39**, 37–49.

KLUG, S. and KRIWET, J. 2008. A new basal galeomorph shark (Synechodontiformes, Neoselachii) from the Early Jurassic of Europe. *Naturwissenschaften,* **95**, 443–448.

KLUG, S., KRIWET, J., BÖTTCHER, R., SCHWEIGERT, G. and DIETL, G. 2009. Skeletal anatomy of the extinct shark *Paraorthacodus jurensis* (Chondrichthyes, Palaeospinacidae), with comments on synechodontiform and palaeospinacid monophyly. *Zoological Journal of the Linnean Society,* **157**, 107–134.

KNER, R. 1867. Über *Orthacanthus dechenii* Goldf. oder *Xenacanthus dechenii* Beyr. *Sitzungsberichte der Kaiserlichen Akademie der Wissenschaften, Mathematisch-Naturwissenschaftliche Klasse,* **55**, 540–584.

KNOLL, A. H., BAMBACH, R. K., CANFIELD, D. E. and GROTZINGER, J. P. 1996. Comparative Earth history and Late Permian mass extinction. *Science,* **273**, 452–457.

KNOLL, A. H., BAMBACH, R. K., PAYNE, J. L., PRUSS, S. and FISCHER, W. W. 2007. Paleophysiology and end-Permian mass extinction. *Earth and Planetary Science Letters,* **256**, 295–313.

KOEHRER, B., ZELLER, M., AIGNER, T., POEPPELREITER, M., MILROY, P., FORKE, H. and AL-KIND, S. 2010. Facies and stratigraphic framework of a Khuff outcrop equivalent: Saiq and Mahil formations, Al Jabal al-Akhdar, Sultanate of Oman. *GeoArabia,* **15**, 91–156.

KOIKE, T. 1996. The first occurrence of Griesbachian conodonts in Japan. *Transactions and Proceedings of the Palaeontological Society of Japan, new series,* **181**, 337–346.

KOKEN, E. 1901. *Helicoprion* im Productus-Kalk der Salt-Range. *Centralblatt für Mineralogie, Geologie und Paläontologie*, **1901**, 225–227.
KONINCK, L. G., DE 1844. *Description des animaux fossiles qui se trouvent dans le terrain Carbonifère de Belgique,* Dessain, Liège, IV + 716 pp.
KONINCK, L. G., DE 1863. Descriptions of some fossils from India. *Quarterly Journal of the Geological Society of London,* **19**, 1–19.
KONINCK, L. G., DE 1878. Faune du calcaire carbonifière de la Belgique. Première partie, poissons et genre nautile. *Annales du Musee Royal d'Histoire Naturelle de Belgique,* **2**, 9–76.
KOOT, M. B., CUNY, G., TINTORI, A. and TWITCHETT, R. J. 2013. A new diverse shark fauna from the Wordian (Middle Permian) Khuff Formation in the interior Haushi-Huqf area, Sultanate of Oman. *Palaeontology,* **56**, 303–343.
KORTE, C., JASPER, T., KOZUR, H. W. and VEIZER, J. 2005. $\delta^{18}O$ and $\delta^{13}C$ of Permian brachiopods: A record of seawater evolution and continental glaciation. *Palaeogeography, Palaeoclimatology, Palaeoecology,* **224**, 333–351.
KOTLYAR, G. V. and PRONINA, G. P. 1995. Murgabian and Midian stages of the Tethyan realm. *Permophiles. Newsletter of the Subcommission on Permian Stratigraphy,* **27**, 23–26.
KOWALEWSKI, M. 2002. The fossil record of predation: an overview of analytical methods. *Paleontological Society, Papers,* **8**, 3–42.
KOZLOV, V. A. 2000. On the new finds of shark teeth in the Artinskian deposits of the Cisuralian Region. *Materials on the Stratigraphy and Palaeontology of the Urals,* **4**, 148–153 [in Russian with English abstract].
KOZUR, H. W. 2003. Integrated ammonoid, conodont and radiolarian zonation of the Triassic. *Hellesches Jahrbuch Geowissenschaften,* **25**, 49–79.
KRAINER, K., LUCAS, S. G. and STRASSER, M. 2011. Vertebrate fossils from the Northalpine Raibl Beds, western Northern Calcareous Alps, Tyrol (Austria). *Austrian Journal of Earth Sciences,* **104**, 97–106.
KRASNOPOLSKY, A. 1889. Allgemeine geologische Karte von Russland. Blatt 126. Perm-Solikamsk. Geologische Untersuchungen am Westabhange des Urals. *Trudy Geologicheskiĭ Komitet (U.S.S.R.),* **XI**, 1–522 (in Russian with German summary).
KRÄTSCHMER, K. and FORST, M. H. 2005. Ein Neufund von assoziierten Skelettelementen von *Sphenacanthus* cf. *carbonarius* (GIEBEL 1848) aus dem Top Oberkarbon (Breitenbach-Fm., Stefan C) des Saar-Nahe Beckens (SW-Deutschland) mit Anmerkungen zur Paläoökologie der Vertebraten-Lokalitäten von Altkirchen. *Geowissenschaftliche Beiträge zum Saarpflälzischen Rotliegenden,* **3**, 29–37.
KRIWET, J., KIESSLING, W. and KLUG, S. 2009. Diversification trajectories and evolutionary life-history traits in early sharks and batoids. *Proceedings of the Royal Society B: Biological Sciences,* **276**, 945–951.
KROTOV, B. 1903/1904. Fische der Permischen Ablagerungen Russlands. *Memoirs of the Society of Naturalists of the University of Kazan,* **28**. Also: *Transactions of the Naturalists' Society of the Imperial University of Kazan*, **38**, 1–40 (in russian).
KRYSTYN, L., RICHOZ, S., BAUD, A. and TWITCHETT, R. J. 2003. A unique Permian-Triassic boundary section from the Neotethyan Hawasina Basin, Central Oman Mountains. *Palaeogeography, Palaeoclimatology, Palaeoecology,* **191**, 329–344.

KUHN, E. 1945. Über *Acrodus*-Funde aus dem Grenzbitumenhorizont der anisischen Stufe der Trias des Monte San Giorgio (Kt. Tessin). *Eclogae Geologicae Helvetiae,* **38**, 662–673.

KUMMEL, B. and TEICHERT, C. 1966. Relations between the Permian and Triassic formations in the Salt Range and Trans-Indus ranges, West Pakistan. *Neues Jahrbuch für Geologie und Paläontologie, Abhandlungen,* **125**, 297–333.

KUMMEL, B. and TEICHERT, C. 1970. Stratigraphy and paleontology of the Permian-Triassic boundary beds, Salt Range and Trans-Indus ranges, West Pakistan. *In:* KUMMEL, B. and TEICHERT, C. (eds) *Stratigraphic boundary problems: Permian and Triassic of West Pakistan.* University of Kansas, Department of Geology, Special Publications, Lawrence, Kansas, **4**, 1–110.

KUMP, L. R., PAVLOV, A. and ARTHUR, M. A. 2005. Massive release of hydrogen sulfide to the surface ocean and atmosphere during intervals of oceanic anoxia. *Geology,* **33**, 397–400.

LANE, J. A. 2010. Morphology of the braincase in the Cretaceous hybodont shark *Tribodus limae* (Chondrichthyes: Elasmobranchii), based on CT scanning. *American Museum Novitates,* **3681**, 1–70.

LANG, R. 1910. Der mittlere Keuper im südlichen Württemberg. *Jahreshefte des Vereins für vaterländische Naturkunde in Württemberg,* **65**, 77–131; **66**, 1–54.

LARSON, E. R. and SCOTT, J. 1951. On *Helicoprion* from Elko County, Nevada [abstract]. *Geological Society of America Program, Annual Meeting, Cordilleran Section,* 35.

LASKER, H. R. 1978. Measurement of taxonomic evolution – preservational consequences. *Paleobiology,* **4**, 135–149.

LEBEDEV, O. A. 1996. Fish assemblages in the Tournaisian–Visean environments of the East European Platform. *In* STROGEN, P., SOMERVILLE, I. D. and JONES, G. L. (eds) *Recent Advances in Lower Carboniferous Geology.* Geological Society, London, Special Publications, **107**, 387–415.

LEBEDEV, O. A. 2001. Vertebrates. *In:* MAHLINA, M. H., ALEKSEEV, A. S., GOREVA, N. V., GORÛNOVA, R. V., ISAKOVA, T. N., KOSSOVAÂ, O. L., LAZAREV, S. S., LEBEDEV, O. A. and ŠKOLIN, A. A. (eds) *Srednij karbon Moskovskoj sineklizy (ûžnaâ čast'). Tom 2. Paleontologičeskaâ harakteristika.* Naučnyj mir, Moscow, 196–201 (328 pp., in Russian).

LEBEDEV, O. A. 2009. A new specimen of *Helicoprion* Karpinsky, 1899 from Kazakhstanian Cisurals and a new reconstruction of its tooth whorl position and function. *Acta Zoologica,* **90**, 171–182.

LEHRMANN, D. J. 1999. Early Triassic calcimicrobial mounds and biostromes of the Nanpanjiang basin, south China. *Geology,* **27**, 359–362.

LEHRMANN, D. J., PAYNE, J. L., ENOS, P., MONTGOMERY, P., WEI, J., YU, Y., XIAO, J. and ORCHARD, M. J. 2005. Field excursion 2: Permian-Triassic boundary and a Lower-Middle Triassic boundary sequence on the Great Bank of Guizhou, Nanpanjiang Basin, southern Guizhou Province. *Albertiana,* **33**, 169–186.

LEHRMANN, D. J., RAMEZANI, J., BOWRING, S. A., MARTIN, M. W., MONTGOMERY, P., ENOS, P., PAYNE, J. L., ORCHARD, M. J., HONGMEI, W. and JIAYONG, W. 2006. Timing of recovery from the end-Permian extinction: Geochronologic and biostratigraphic constraints from south China. *Geology,* **34**, 1053–1056.

LEI, Y. 1983. A new *Sinohelicoprion* (Helicoprionid, shark) from Later Permian of Hunan, South China. *Vertebrata Palasiatica,* **21**, 347–351.
LEIDY, J. 1855. Indications of five species, with two new genera, of extinct fishes. *Proceedings of the Academy of Natural Sciences of Philadelphia,* **7**, 414.
LEIDY, J. 1856. Descriptions of some remains of fishes from the Carboniferous and Devonian formations of the United States. *Journal of the Academy of Natural Sciences Philadelphia (Series 2),* **3**, 159–165.
LEIDY, J. 1859. Descriptions of *Xystracanthus arcuatus* and *Cladodus occidentalis*. *Proceedings of the Academy of Natural Sciences of Philadelphia* **[unnumbered volume]**, 3.
LI, J. L. and JIN, F. 2003. Recent advances in research in *Keichousaurus* vertebrate fauna. *Progress in Natural Science,* **13**, 796–800 (in Chinese).
LISZKOWSKI, J. 1993. Die Selachierfauna des Muschelkalks in Polen: Zusammensetzung, Stratigraphie und Paläoökologie. *In:* HAGDORN, H. and SEILACHER, A. (eds) *Muschelkalk. Schöntaler Symposium 1991.* Sonderbände der Gesellschaft für Naturkunde in Württemberg, **2**, 177–185.
LIU, H.-T. 1962. Two new *Hybodus* from North Shensi (Shaanxi), China. *Vertebrata Palasiatica,* **6**, 150–152.
LIU, Z. 1994. New material of helicoprionid shark from Lianyuan of Hunan. *Vertebrata Palasiatica,* **32**, 127–133.
LIU, H.-T. and CHANG, M. M. 1963. First discovery of helicoprionid in China. *Vertebrata Palasiatica,* **7**, 123–129.
LIU, H. T. and HSIEH, H. H. 1965. The discovery of bradyodont from Yangsin Series, the Lower Permian of Liangshan, Shensi. *Vertebrata PalAsiatica,* **9**, 280–283.
LIU, G. and WANG, Q. 1994. New material of *Sinohelicoprion* from Changxing, Zhejiang Province. *Vertebrata Palasiatica,* **32**, 244–248.
LLOYD, G. T. and FRIEDMAN, M. 2013. A survey of palaeontological sampling biases in fishes based on the Phanerozoic record of Great Britain. *Palaeogeography, Palaeoclimatology, Palaeoecology,* **372**, 5–17.
LOGAN, A. and MCGUGAN, A. 1968. Biostratigraphy and faunas of the Permian Ishbel Group, Canadian Rocky Mountains. *Journal of Paleontology,* **42**, 1123–1139.
LONG, J. A. 1995. *The Rise of Fishes: 500 Million Years of Evolution,* Johns Hopkins University Press, Baltimore and London, 223 pp.
LONG, J. A. 2010. *The Rise of Fishes: 500 Million Years of Evolution,* 2nd ed., Johns Hopkins University Press, Baltimore and London, 304 pp.
LONG, J. A. and YOUNG, G. C. 1995. Sharks from the Middle–Late Devonian Aztec Siltstone, southern Victoria Land, Antarctica. *Records of the Western Australian Museum,* **17**, 287–308.
LÓPEZ-ARBARELLO, A. 2004. The record of Mesozoic fishes from Gondwana (excluding India and Madagascar). *In:* ARRATIA, G. and TINTORI, A. (eds) *Mesozoic Fishes 3 - Systematics, Paleoenvironments and Biodiversity.* Verlag Dr. Friedrich Pfeil, München, 597–624.
LOZOVSKY, V., MINIKH, M., GRUNT, T., KUKHTINOV, D., PONOMARENKO, A. and SUKACHEVA, I. 2009. The Ufimian stage of the East European scale: status, validity, and correlation potential. *Stratigraphy and Geological Correlation,* **17**, 602–614.
LU, P. J., YOGO, M. and MARSHALL, C. R. 2006. Phanerozoic marine biodiversity dynamics in light of the incompleteness of the fossil record. *Proceedings of the*

National Academy of Sciences of the United States of America, **103**, 2736–2739.

LUND, R. 1985. The morphology of *Falcatus falcatus* (St. John and Worthen), a Mississippian stethacanthid chondrichthyan from the Bear Gulch Limestone of Montana. *Journal of Vertebrate Paleontology,* **5**, 1–19.

LUND, R. 1986. On *Damocles serratus*, nov. gen. et sp. (Elasmobranchii: Cladodontida) from the Upper Mississippian Bear Gulch Limestone of Montana. *Journal of Vertebrate Paleontology,* **6**, 12–19.

LUND, R. and GROGAN, E. D. 1997. Relationships of the Chimaeriformes and the basal radiation of the Chondrichthyes. *Reviews in Fish Biology and Fisheries,* **7**, 65–123.

LUND, R. and GROGAN, E. D. 2004. Five new euchondrocephalan Chondrichthyes from the Bear Gulch Limestone (Serpukhovian, Namurian E2b) of Montana, USA. *In:* ARRATIA, G., WILSON, M. V. H. and CLOUTIER, R. (eds) *Recent Advances in the Origin and Early Radiation of Vertebrates.* Verlag Dr. Friedrich Pfeil, München, 505–531.

MCCOY, F. 1848. On some new fossil fish of the Carboniferous period. *Annals and Magazine of Natural History,* **2**, 1–10; 115–133.

MCCOY, F. 1855. *A systematic description of the British Palaeozoic fossils in the Geological Museum of the University of Cambridge,* Cambridge, 1–661.

MCGHEE, G. R., SHEEHAN, P. M., BOTTJER, D. J. and DROSER, M. L. 2004. Ecological ranking of Phanerozoic biodiversity crises: ecological and taxonomic severities are decoupled. *Palaeogeography, Palaeoclimatology, Palaeoecology,* **211**, 289–297.

MCGHEE, G. R., CLAPHAM, M. E., SHEEHAN, P. M., BOTTJER, D. J. and DROSER, M. L. 2013. A new ecological-severity ranking of major Phanerozoic biodiversity crises. *Palaeogeography, Palaeoclimatology, Palaeoecology,* **370**, 260–270.

MCGOWAN, A. J. 2004. Ammonoid taxonomic and morphologic recovery patterns after the Permian–Triassic. *Geology,* **32**, 665–668.

MCGOWAN, A. J. 2005. Ammonoid recovery from the Late Permian mass extinction event. *Comptes Rendus Palevol,* **4**, 517–530.

MCGOWAN, A. J. and SMITH, A. B. 2007. Ammonoids across the Permian/Triassic boundary: A cladistic perspective. *Palaeontology,* **50**, 573–590.

MCGOWAN, A. J., SMITH, A. B. and TAYLOR, P. D. 2009. Faunal diversity, heterogeneity and body size in the Early Triassic: testing post-extinction paradigms in the Virgin Limestone of Utah, USA. *Australian Journal of Earth Sciences,* **56**, 859–872.

MCKEE, E. D. 1982. The Supai Group of Grand Canyon. *U. S. Geological Survey, Professional Paper,* **1173**, 1–504.

MACKIE, S. J. 1863. On a new species of *Hybodus* from the lower chalk. *The Geologist,* **6**, 241–246.

MCKINNEY, M. L. 1985. Mass extinction patterns of marine invertebrate groups and some implications for a causal phenomenon. *Paleobiology,* **11**, 227–233.

MADER, H. 1986. Schuppen und Zähne von Acanthodiern und Elasmobranchiern aus dem Unter-Devon Spaniens (Pisces). *Göttinger Arbeiten zur Geologie und Paläontologie,* **28**, 1–59.

MAISEY, J. G. 1975. The interrelationships of phalacanthous selachians. *Neues Jahrbuch für Geologie und Paläontologie, Monatshefte,* **1975**, 553–567.

MAISEY, J. G. 1977. The fossil selachian fishes *Palaeospinax* Egerton, 1872 and *Nemacanthus* Agassiz, 1837. *Zoological Journal of the Linnean Society,* **60**, 259–273.
MAISEY, J. G. 1978. Growth and form of finspines in hybodont sharks. *Palaeontology,* **21**, 657–666.
MAISEY, J. G. 1980. An evaluation of jaw suspension in sharks. *American Museum Novitates,* **2706**, 1–17.
MAISEY, J. G. 1982a. Studies on the Paleozoic selachian genus *Ctenacanthus* Agassiz. No. 2. *Bythiacanthus* St. John and Worthen, *Amelacanthus*, new genus, *Eunemacanthus* St. John and Worthen, *Sphenacanthus* Agassiz, and *Wodnika* Münster. *American Museum Novitates,* **2722**, 1–24.
MAISEY, J. G. 1982b. The anatomy and interrelationships of mesozoic hybodont sharks. *American Museum Novitates,* **2724**, 1–48.
MAISEY, J. G. 1983. Some Pennsylvanian chondrichthyan spines from Nebraska. *Transactions of the Nebraska Academy of Sciences,* **11**, 81–84.
MAISEY, J. G. 1984a. Chondrichthyan phylogeny: a look at the evidence. *Journal of Vertebrate Paleontology,* **4**, 359–371.
MAISEY, J. G. 1984b. Studies on the Paleozoic selachian genus *Ctenacanthus* Agassiz. No. 3. Nominal species referred to *Ctenacanthus*. *American Museum Novitates,* **2774**, 1–20.
MAISEY, J. G. 1987. Cranial anatomy of the Lower Jurassic shark *Hybodus reticulatus* (Chondrichthyes, Elasmobranchii) : with comments on hybodontid systematics. *American Museum Novitates,* **2878**, 1–39.
MAISEY, J. G. 1989. *Hamiltonichthys mapesi*, g. & sp. nov. (Chondrichthyes; Elasmobranchii), from the Upper Pennsylvanian of Kansas. *American Museum Novitates,* **2931**, 1–42.
MAISEY, J. G. 1990. Selachii. *In:* ANTUNES, M. T., MAISEY, J. G., MARQUES, M. M., SCHAEFFER, B. and THOMSON, K. S. (eds) *Triassic fishes from the Cassange Depression (R. P de Angola).* Ciencias da Terra (UNL), Numero Especial, 1–64.
MAISEY, J. G. 2007. The braincase in Paleozoic symmoriiform and cladoselachian sharks. *Bulletin of the American Museum of Natural History,* **307**, 1–122.
MAISEY, J. G. 2008. Some observations on *Denaea fournieri* (Chondrichthyes, Symmoriiformes) from the Lower Carboniferous of Belgium. *Acta Geologica Polonica,* **58**, 185–190.
MAISEY, J. G. 2009. The spine-brush complex in symmoriiform sharks (Chondrichthyes; Symmoriiformes), with comments on dorsal fin modularity. *Journal of Vertebrate Paleontology,* **29**, 14–24.
MAISEY, J. G. 2010. Heslerodidae (Chondrichthyes, Elasmobranchii), a new family of Paleozoic phalacanthous sharks. *Kirtlandia,* **57**, 13–21.
MAISEY, J. G. 2011. The braincase of the Middle Triassic shark *Acronemus tuberculatus* (Bassani, 1886). *Palaeontology,* **54**, 417–428.
MAISEY, J. G. 2012. What is an ‘elasmobranch’? The impact of palaeontology in understanding elasmobranch phylogeny and evolution. *Journal of Fish Biology,* **80**, 918–951.
MAISEY, J. G. in prep. *Chondrichthyes (Elasmobranchii: skeletal anatomy),* Verlag Dr. Friedrich Pfeil, München.
MAISEY, J. G., NAYLOR, G. J. P. and WARD, D. J. 2004. Mesozoic elasmobranchs, neoselachian phylogeny and the rise of modern elasmobranch diversity. *In:*

ARRATIA, G. and TINTORI, A. (eds) *Mesozoic Fishes 3 - Systematics, Paleoenvironments and Biodiversity.* Verlag Dr. Friedrich Pfeil, München, 17–56.
MALABARBA, M. C., ABDALA, F., WEISS, F. E. and PEREZ, P. A. 2003. New data on the Late Permian vertebrate fauna of Posto Queimado, Rio do Rasto Formation, southern Brazil. *Revista Brasileira de Paleontologia,* **6**, 49–54.
MALYSHEVA, E. O., IVANOV, A., BEZNOSOV, P. A., BELYAEV, A. A. and MITYAKOV, S. N. 2000. Facies and ichthyofauna of the Kazanian from the Vym' River (Komi Republic, Russia). *Ichthyolith Issues, Special Publication,* **6**, 59–63.
MALZAHN, E. 1968. Über neue Funde von *Janassa bituminosa* (Schloth.) im niederrheinischen Zechstein - Ein Beitrag zur Histologie der Zähne, Haut und Lebensweise. *Geologisches Jahrbuch,* **85**, 67–96.
MALZAHN, E. 1972. Zur Kenntnis des Kopfskeletts von *Janassa bituminosa* (Schloth.) aus dem hessischen Kupferschiefer. *Geologisches Jahrbuch,* **90**, 431–440.
MARTIN, I. 1863. De la Zone à *Avicula contorta* de la Côte-d'Or. *Mémoires de l'Académie des Sciences, Arts et Belles-Lettres de Dijon,* **11**.
MARZOLF, J. E. 1993. Palinspastic reconstruction of Early Mesozoic sedimentary basins near the latitude of Las Vegas; implications for the Early Mesozoic Cordilleran cratonal margin. *In:* DUNNE, G. C. and MCDOUGALL, K. A. (eds) *Mesozoic Paleogeography of the Western United States II.* Pacific Section, Society of Economic Paleontologists, **71**, 433–462.
MAURY, P., MONGIN, D., MARTIN, M. and LANDEMAINE, O. 1984. Découverte d'une faune du Norien supérieur à la base stratigraphique de la Klippe de la Grande Séolane (Alpes-de-Haut-Provence). *Bulletin de la Société Géologique de France,* **26**, 955–960.
MAY, W. J. and HALL, J. D. 2002. Geology and vertebrate fauna of a new site in the Wellington Formation (Lower Permian) of Northern Oklahoma. *Oklahoma Geology Notes,* **62**, 63–66.
MEI, S. and HENDERSON, C. M. 2001. Evolution of Permian conodont provincialism and its significance in global correlation and paleoclimate implication. *Palaeogeography, Palaeoclimatology, Palaeoecology,* **170**, 237–260.
MERINO-RODO, D. and JANVIER, P. 1986. Chondrichthyan and actinopterygian remains from the Lower Permian Copacabana Formation of Bolivia. *Geobios,* **19**, 479–493.
METCALFE, I. and ISOZAKI, Y. 2009. Current perspectives on the Permian-Triassic boundary and end-Permian mass extinction: Preface. *Journal of Asian Earth Sciences,* **36**, 407–412.
METCALFE, I., NICOLL, R. S., MUNDIL, R., FOSTER, C., GLEN, J., LYONS, J., XIAOFENG, W., CHENG-YUAN, W., RENNE, P. R., BLACK, L., XUN, Q. and XIAODONG, M. 2001. The Permian-Triassic Boundary and Mass Extinction in China. *Episodes,* **24**, 239–244.
MEYER, H. VON 1849. Fische, etc. aus dem Muschelkalk Oberschlesiens. *Palaeontographica,* **1**, 233–234.
MEYER, H., VON 1851. Fische, Crustaceen, Echinodermen und andere Versteinerungen aus dem Muschelkalk Oberschlesiens. *Palaeontographica,* **1**, 216–242.
MEYER, H., VON and PLIENINGER, T. 1844. *Beiträge zur Paläontologie Württembergs, enthaltend die fossile Wirbelthierreste aus dem Triasgebilden*

mit besonderer Rücksicht auf die Labyrinthodonten des Keupers, E. Schweizerbart'sche Verlagsbuchhandlung, Stuttgart, 132 pp.
MEYER, K. M. and KUMP, L. R. 2008. Oceanic euxinia in Earth history: causes and consequences. *Annual Review of Earth and Planetary Sciences,* **36**, 251–288.
MILLER, H. W. and MANN, R. J. 1958. *Petalodus* (bradyodont) from the Permian of Kansas and Oklahoma. *Transactions of the Kansas Academy of Science,* **61**, 97–103.
MILNER, A. R. C., KIRKLAND, J. I. and BIRTHISEL, T. A. 2006. The geographic distribution and biostratigraphy of Late Triassic-Early Jurassic freshwater fish faunas of the southwestern United States. *New Mexico Museum of Natural History and Science Bulletin,* **37**, 522–529.
MINIKH, A. V. 1975. Ichthyorodulites and their importance to Tatarian and Triassic stratigraphy East of the European part of the USSR. *Problems of Stratigraphy and Paleontology, Saratov University,* **1**, 29–32.
MINIKH, A. V. 1985. New representatives of sharks of the genus *Hybodus* from the Triassic of the Eastern European part of the USSR. *Paleontological Journal (Paleontologicheskii zhurnal),* **3**, 66–70.
MINIKH, A. V. 1996a. Head spines of sharks (Hybodontiformes) from the Middle Triassic of European Russia. *Paleontological Journal (Paleontologicheskii Zhurnal),* **30**, 112–113.
MINIKH, A. V. 1996b. New taxa of squaloid fish from the Triassic of southern European Russia. Saratov, 09-04-1996: VINITI, 1127–B96.
MINIKH, A. V. 1999. New shark species of the *Ctenacanthus Ag.* genus from the Kazanian stage of the Upper Permian; the basin of the Pinega river. *Transactions of the Scientific Research Geological Institute of the N.G. Chernyshevskii Saratov State University, New Series,* **1**, 133–138 [in Russian with English abstract].
MINIKH, A. V. 2001. Sharks from the Triassic of European Russia. *Transactions of the Scientific Research Geological Institute of the N.G. Chernyshevskii Saratov State University, New Series,* **8**, 46–54.
MINIKH, A. V. 2004. New elasmobranchians from the Ufimian and Kazanian stages of the Permian in the northern regions of European Russia. *Transactions of the Scientific Research Geological Institute of the N.G. Chernyshevskii Saratov State University, New Series,* **41**, 128–132 [in Russian with English abstract].
MINIKH, A. V. 2006. Class Chondrichthyes. *In:* CLAY, T. A. (ed.) *Upper Perm Kanin Peninsula.* Moscow: "Science", 180–183.
MINIKH, A. V. and MINIKH, M. G. 1981. Fishes. *In:* OCHEV, V. G. (ed.) *Opomyy Razrez Tatarskogo Yarusa Reki Sukhony.* Saratov: Izdatelstvo Saralovskogo Universiteta, 55–64 (in Russian).
MINIKH, A. V. and MINIKH, M. G. 1996. Fishes. *In:* ESAULOVA, N. K. and LOZOVSKIY, V. R. (eds) *Stratotypes and Reference Sections of the Upper Permian in the Regions of the Volga and Kama Rivers.* Kazan, 258–266 [in Russian].
MINIKH, A. V. and MINIKH, M. G. 1998. Fishes. *In:* ESAULOVA, N. K., LOZOVSKY, V. R. and ROZANOV, A. Y. (eds) *Stratotypes and Reference Sections of the Upper Permian in the Regions of the Volga and Kama Rivers.* GEOS, Moscow, 173–176.
MINIKH, A. V., MINIKH, M. G. and YANKEVICH, D. I. 2003. Fishes at the Lower–Upper Permian Boundary in the Reference Section along the Kozhim River of

the Pechora Cisuralia Region. *Izvestiya Vuzov, Geologiya I Razvedka (Jurnal),* **6**, 46–49.
MORALES, M. 1987. Terrestrial fauna and flora from the Triassic Moenkopi Formation of the southwestern United States. *Journal of the Arizona-Nevada Academy of Science,* **22**, 1–19.
MØRK, A., ELVEBAKK, G., FORSBERG, A. W., HOUNSLOW, M. W., NAKREM, H. A., VIGRAN, J. O. and WEITSCHAT, W. 1999. The type section of the Vikinghøgda Formation: a new Lower Triassic unit in central and eastern Svalbard. *Polar Research,* **18**, 51–82.
MORRIS, J. and ROBERTS, G. E. 1862. On the Carboniferous limestone of Oreton and Farlow, Clee Hills, Shropshire. *Quarterly Journal of the Geological Society of London,* **18**, 94–106.
MÜLLER, A. 1964. Untersuchungen über das Rät in Luxemburg. *Publications du Service Geologique du Luxembourg,* **14**, 255–282.
MÜLLERIED, F. K. G. 1945. El edestido *Helicoprion* encontrado por primera vez en Mexico, en al estado de Coahuilo. *Ciencia. Revista Hispano-Americana de Ciencias Puras y Aplicadas,* **6**, 208–212.
MUNDIL, R., METCALFE, I., LUDWIG, K. R., RENNE, P. R., OBERLI, F. and NICOLL, R. S. 2001. Timing of the Permian-Triassic biotic crisis: implications from new zircon U/Pb age data (and their limitations). *Earth and Planetary Science Letters,* **187**, 131–145.
MUNDIL, R., LUDWIG, K. R., METCALFE, I. and RENNE, P. R. 2004. Age and timing of the Permian mass extinctions: U/Pb dating of closed-system zircons. *Science,* **305**, 1760–1763.
MUNDIL, R., PÁLFY, J., RENNE, P. R. and BRACK, P. 2010. The Triassic timescale: new constraints and a review of geochronological data. *In:* LUCAS, S. G. (ed) *The Triassic Timescale.* Geological Society, Special Publications, London, **334**, 41–60.
MÜNSTER, G., VON 1839. Beschreibung einiger seltenen Verteinerungen des Zechsteins. *Beiträge zur Petrefactenkunde,* **1**, 44–47.
MÜNSTER, G., VON 1840. Über einige Placoiden im Kupferschiefer zu Richelsdorf. *Beiträge zur Petrefactenkunde,* **3**, 122–126.
MÜNSTER, G., VON 1843. Nachtrag zu der Beschreibung einiger merkwürdiger Fische aus den Kupferschiefern. *Beiträge zur Petrefactenkunde,* **6**, 47–52.
MURATA, M. 1981. Chondrichthyes. *Kinshozan - Its Culture and Nature.* Kinshozan Fossil Research Club, Gifu, 231–233 (in Japanese).
MURCHISON, R. I. and STRICKLAND, H. E. 1840. On the Upper Formations of the New Red Sandstone System in Gloucestershire, Worcestershire, and Warwickshire; showing that the Red or Saliferous Marls, including a peculiar Zone of Sandstone, represent the “Keuper” or “ Marnes Irisées;” with some account of the underlying Sandstone of Ombersley, Bromsgrove, and Warwick, proving that it is the “Bunter Sandstein” or “Grès Bigarré” of Foreign Geologists. *Transactions of the Geological Society,* **5**, 331–348.
MURRAY, A. M. 2000. The Palaeozoic, Mesozoic and Early Cenozoic fishes of Africa. *Fish & Fisheries,* **1**, 111–145.
MURRY, P. A. 1981. A new species of freshwater hybodont from the Dockum Group (Triassic) of Texas. *Journal of Paleontology,* **55**, 603–607.
MURRY, P. A. 1982. *Biostratigraphy and Paleoecology of the Dockum Group, Triassic of Texas.* Ph. D. dissertation, Southern Methodist University, 459 pp.

MURRY, P. A. 1986. Vertebrate Paleontology of the Dockum Group, Western Texas and Eastern New Mexico. *In:* PADIAN, K. (ed.) *The Beginning of the Age of Dinosaurs.* Cambridge University Press, 109–137.

MURRY, P. A. 1989. Geology and Paleontology of the Dockum Formation (Upper Triassic), West Texas and Eastern New Mexico. *In:* LUCAS, S. G. and HUNT, A. P. (eds) *Dawn of the Age of Dinosaurs in the American Southwest.* New Mexico Museum of Natural History, 102–144.

MURRY, P. A. and LONG, R. A. 1989. Geology and Paleontology of the Chinle Formation, Petrified Forest National Park and Vicinity, Arizona and a Discussion of Vertebrate Fossils of the Southwestern Upper Triassic. *In:* LUCAS, S. G. and HUNT, A. P. (eds) *Dawn of the Age of Dinosaurs in the American Southwest.* New Mexico Museum of Natural History, 29–64.

MURRY, P. A. and KIRBY, R. E. 2002. A new hybodont shark from the Chinle and Bull Canyon Formations, Arizona, Utah and New Mexico. *New Mexico Museum of Natural History and Science Bulletin,* **21**, 87–106.

MUSASHI, M., ISOZAKI, Y., KOIKE, T. and KREULEN, R. 2001. Stable carbon isotope signature in mid-Panthalassa shallow-water carbonates across the Permo-Triassic boundary: evidence for ^{13}C-depleted superocean. *Earth and Planetary Science Letters,* **191**, 9–20.

MUSASHI, M., ISOZAKI, Y., KOIKE, T. and KREULEN, R. 2006. Carbon isotope study on mid-Panthalassa shallow-water limestone across the Permo-Triassic boundary: Reassessment. *In:* WONG, T. E. (ed.) *Proceedings of the XVth International Congress on Carboniferous and Permian Stratigraphy.* Utrecht, The Netherlands, 10–16 August 2003: Royal Netherlands Academy of Arts and Sciences, 131–138.

MUSASHI, M., ISOZAKI, Y. and KAWAHATA, H. 2010. An Early-Middle Guadalupian (Permian) isotopic record from a mid-oceanic carbonate buildup: Akiyoshi Limestone, Japan. *Global and Planetary Change,* **73**, 114–122.

MUTTER, R. J. 1998a. Tooth variability and reconstruction of dentition in *Acrodus* sp. (Chondrichthyes, Selachii, Hybodontoidea) from the *Grenzbitumenzone* (Middle Triassic) of Monte San Giorgio (Ticino, Switzerland). *Geologica Insubrica,* **3**, 23–31.

MUTTER, R. J. 1998b. Zur systematischen Stellung einiger Bezahnungsreste von *Acrodus georgii* sp. nov. (Selachii, Hybodontoidea) aus der Grenzbitumenzone (Mittlere Trias) des Monte San Giorgio (Kanton Tessin, Schweiz). *Eclogae Geologicae Helvetiae,* **91**, 513–519.

MUTTER, R. J. and RIEBER, H. 2005. *Pyknotylacanthus spathianus* gen. et sp. nov., a new ctenacanthoid from the Early Triassic of Bear Lake (Idaho, USA). *Revista Brasileira de Paleontologia,* **8**, 139–148.

MUTTER, R. J. and NEUMAN, A. G. 2006. An enigmatic chondrichthyan with Paleozoic affinities from the Lower Triassic of western Canada. *Acta Palaeontologica Polonica,* **51**, 271–282.

MUTTER, R. J. and NEUMAN, A. G. 2008a. New eugeneodontid sharks from the Lower Triassic Sulphur Mountain Formation of Western Canada. *In* CAVIN, L., LONGBOTTOM, A. and RICHTER, M. (eds) *Fishes and the Break-up of Pangaea.* Geological Society, London, Special Publications, **295**, 9–41.

MUTTER, R. J. and NEUMAN, A. G. 2008b. Jaws and dentition in an Early Triassic, 3-dimensionally preserved eugeneodontid skull (Chondrichthyes). *Acta Geologica Polonica,* **58**, 223–227.

MUTTER, R. J. and NEUMAN, A. G. 2009. Recovery from the end-Permian extinction event: evidence from "Lilliput *Listracanthus*". *Palaeogeography, Palaeoclimatology, Palaeoecology,* **284**, 22–28.

MUTTER, R. J., DE BLANGER, K. and NEUMAN, A. G. 2007a. Elasmobranchs from the Lower Triassic Sulphur Mountain Formation near Wapiti Lake (BC, Canada). *Zoological Journal of the Linnean Society,* **149**, 309–337.

MUTTER, R. J., RICHTER, M. and TOLEDO, C. E. V. 2007b. In pursuit of causes for the greatest mass extinction: The Permo-Triassic Boundary in the Southern Hemisphere - part I: Fishing for fossils in 260 million years old sedimentary rocks of a former epicontinental sea in southern Brazil. *Vierteljahrsschrift der Naturforschenden Gesellschaft in Zürich,* **152**, 71–78.

MUTTER, R. J., NEUMAN, A. G. and DE BLANGER, K. 2008a. *Homalodontus* nom. nov., a replacement name for *Wapitiodus* Mutter, de Blanger and Neuman, 2007 (Homalodontidae nom nov., ?Hybodontoidea), preoccupied by *Wapitiodus* Orchard, 2005. *Zoological Journal of the Linnean Society,* **154**, 419–420.

MUTTER, R. J., TOMASSI, H. Z. and DO CARMO, D. A. 2008b. In pursuit of causes for the greatest mass extinction: the Permo-Triassic Boundary in the Southern Hemisphere – part II: Investigating 260 million years old, meteorite-impacted sedimentary rocks in central-west Brazil. *Vierteljahrsschrift der Naturforschenden Gesellschaft in Zürich,* **153**, 81–91.

NABBEFELD, B., GRICE, K., TWITCHETT, R. J., SUMMONS, R. E., HAYS, L., BÖTTCHER, M. E. and ASIF, M. 2010. An integrated biomarker, isotopic and palaeoenvironmental study through the Late Permian event at Lusitaniadalen, Spitsbergen. *Earth and Planetary Science Letters,* **291**, 84–96.

NAKAMURA, K., KIMURA, G. and WINSNES, T. S. 1987. Brachiopod zonation and age of the Permian Kapp Starostin Formation (Central Spitsbergen). *Polar Research,* **5**, 207–219.

NASSICHUK, W. W. 1971. *Helicoprion* and *Physonemus*, Permian vertebrates from the Assistance Formation, Canadian Arctic archipelago. *Canada Geological Survey Bulletin,* **192**, 83–93.

NASSICHUK, W. W. and SPINOSA, C. 1970. *Helicoprion* sp., a Permian elasmobranch from Ellesmere Island, Canadian Arctic. *Journal of Paleontology,* **44**, 1130–1132.

NELSON, J. S. 1976. *Fishes of the World,* Wiley & Sons, New York, XV + 416 pp.

NEWBERRY, J. S. 1856. Description of several new genera and species of fossil fishes, from the Carboniferous strata of Ohio. *Proceedings of the Academy of Natural Sciences of Philadelphia,* **8**, 96–100.

NEWBERRY, J. S. 1876. Geological Report. *In: Report of the exploring expedition from Santa Fe, New Mexico, to the junction of the Grand and Green Rivers of the Great Colorado of the West in 1859, under the command of Capt. J. N. Macomb, Corps of Topographical Engineers.* Government Printing Office, Washington, D. C., 9–118.

NEWBERRY, J. S. 1889. The Paleozoic fishes of North America. *U.S. Geological Survey Monographs,* **16**, 1–340.

NEWBERRY, J. S. and WORTHEN, A. H. 1866. Descriptions of new species of vertebrates, mainly from the sub-Carboniferous limestone and Coal Measures of Illinois. *Geological Survey of Illinois,* **2**, 9–141.

NEWBERRY, J. S. and WORTHEN, A. H. 1870. Descriptions of fossil vertebrates. *Geological Survey of Illinois,* **4**, 343–374.

NEWMAN, D. H. 1974. Paleoenvironments of the Lower Triassic Thaynes Formation near Cascade Springs, Wasatch County, Utah. *Brigham Young University Geology Studies,* **21**, 63–96.
NICOLL, R. S., METCALFE, I. and CHENG-YUAN, W. 2002. New species of the conodont genus *Hindeodus* and the conodont biostratigraphy of the Permian-Triassic boundary interval. *Journal of Asian Earth Sciences,* **20**, 609–631.
NIELSEN, E. 1932. Permo–Carboniferous fishes from East Greenland. *Meddelelser om Grønland,* **86**, 63.
NIELSEN, E. 1935. The Permian and Eotriassic vertebrate-bearing beds at Godthaab Gulf (East Greenland). *Meddelelser om Grønland,* **98**, 1–111.
NIELSEN, E. 1936. Some few preliminary remarks on Triassic fishes from East Greenland. *Meddelelser om Grønland,* **112**, 1–55.
NIELSEN, E. 1952. On new or little known *Edestidae* from the Permian and Triassic of East Greenland. *Meddelelser om Grønland,* **144**, 55 pp.
NIELSEN, J. K. and SHEN, Y. 2004. Evidence for sulfidic deep water during the Late Permian in the East Greenland Basin. *Geology,* **32**, 1037–1040.
NIELSEN, J. K., SHEN, Y., PIASECKI, S. and STEMMERIK, L. 2010. No abrupt change in redox condition caused the end-Permian marine ecosystem collapse in the East Greenland Basin. *Earth and Planetary Science Letters,* **291**, 32–38.
OBRUCHEV, D. V. 1953. Studies on edestids and the works of A. P. Karpinsky. *U.S.S.R. Academy of Sciences, works of the Palaeontological Institute, Publications,* **45**, 1–86.
OBRUCHEV, D. V. 1964. Subclass Holocephali. *In:* ORLOV, Y. A. (ed.) *Fundamentals of Palaeontology. Agnathans, Fishes.* Nauka Publishers, Moscow, 238–266 (in Russian).
OBRUCHEV, D. V. 1965. Otrad Bradyodonti. *Razvitie i smena morskikh organizmov na rubezhe Paleozoya i Mesozoya.* Trudy Paleontologicheskii Institut Akademii Nauk SSSR, pp. 266-267 [in Russian].
OBRUCHEV, D. V. 1967. Agnatha, Pisces. *In:* ORLOV, Y. A. (ed.) *Fundamentals of Paleontology. Vol. 11.* Israel Program for Scientific Translations, Jerusalem, 825 pp. (Russian version: Osnovy Paleontologii, Moskau 1964).
OELOFSEN, B. W. 1981. The fossil record of the class Chondrichthyes in southern Africa. *Palaeontologia Africana,* **24**, 11–13.
OELOFSEN, B. W. 1986. A fossil shark neurocranium from the Permo-Carboniferous (lowermost Ecca Formation) of South Africa. *In:* UYENO, T., ARAI, R., TANIUCHI, T. and MATSUURA, K. (eds) *Indo-Pacific Fish Biology: Proceedings of the Second International Conference on Indo-Pacific Fishes.* Ichthyological Society of Japan, Tokyo, 107–124.
OERTLE, G. 1928. Das Vorkommen von Fischen In der Trias Württembergs. *Neues Jahrbuch für Mineralogie, Geologie und Paläontologie, Beilage-Band, Abteilung B,* **60**, 325–472.
OKURA, M. 1984. Discovery of a petalodont tooth from Fukuji, Kamitakara-mura, Gifu Prefecture, central Japan. *Newsletter of Gifu Natural Research Club,* **3**, 3–4 (in Japanese).
OLSON, E. C. 1962. Late Permian terrestrial vertebrates, U.S.A. and U.S.S.R. *Transactions of the American Philosophical Society, New Series,* **52**, 1–224.
OLSON, E. C. 1965. New Permian vertebrates from the Chickasha Formation in Oklahoma. *Oklahoma Geological Survey Circular,* **70**, 1–70.

OLSON, E. C. 1967. Early Permian vertebrates of Oklahoma. *Oklahoma Geological Survey Circular,* **74**, 1–111.

ONO, T. 1980. *'Neopetalodus'* occured from Kinshozan. *Friends of Fossils (Kaseki no Tamo),* **20**, 1 (in Japanese).

ORCHARD, M. J. 1994. Conodont biochronology around the Early–Middle Triassic boundary: new data from North America, Oman and Timor. *In:* GUEX, J. and BAUD, A. (eds) *Proceedings of the Triassic Symposium, Lausanne, 20–25 October 1991*. Mémoires de Géologie, Université de Lausanne, Helvetia, **22**, 105–114.

ORCHARD, M. J. 1995. Taxonomy and correlation of Lower Triassic (Spathian) segminate conodonts from Oman and revision of some species of *Neospathodus*. *Journal of Paleontology,* **69**, 110–122.

ORCHARD, M. J. 2007. Conodont diversity and evolution through the latest Permian and Early Triassic upheavals. *Palaeogeography, Palaeoclimatology, Palaeoecology,* **252**, 93–117.

ORCHARD, M. J. 2008. Lower Triassic conodonts from the Canadian Arctic, their intercalibration with ammonoid-based stages and a comparison with other North American Olenekian faunas. *Polar Research,* **27**, 393–412.

ORCHARD, M. J. 2010. Triassic conodonts and their role in stage boundary definition. *In:* LUCAS, S. G. (ed.) *The Triassic Timescale.* Geological Society, Special Publications, London, **334**, 139–161.

ORCHARD, M. and IRWIN, S. 1994 [Unpublished]. Procedure for acetic acid digestion of carbonate samples. Vancouver: Geological Survey of Canada, 1–4.

ORCHARD, M. J. and KRYSTYN, L. 1998. Conodonts of the lowermost Triassic of Spiti, and new zonation based on *Neogondolella* successions. *Revista Italiana di Paleontologia Stratigraphia,* **104**, 341–368.

ORCHARD, M. J. and TOZER, E. T. 1997. Triassic conodont biochronology, its calibration with the ammonoid standard, and a biostratigraphic summary for the Western Canada sedimentary basin. *Bulletin of Canadian Petroleum Geology,* **45**, 675–692.

ORCHARD, M. J. and ZONNEVELD, J.-P. 2009. The Lower Triassic Sulphur Mountain Formation in the Wapiti Lake area: lithostratigraphy, conodont biostratigraphy, and a new biozonation for the lower Olenekian (Smithian). *Canadian Journal of Earth Sciences,* **46**, 757–790.

ORCHARD, M. J., NASSICHUK, W. W. and LIN, R. 1994. Conodonts from the Lower Griesbachian *Otoceras latilobatum* bed of Selong, Tibet and the position of the Permian-Triassic boundary. *Proceedings of the Pangea Conference, Canadian Society of Petroleum Geologists, Memoir,* **17**, 823–843.

ORCHARD, M. J., LEHRMANN, D., WEI, J., WANG, H. and TAYLOR, H. 2007. Conodonts from the Olenekian-Anisian boundary beds, Guandao, Guizhou Province, China. *New Mexico Museum of Natural History and Science, Bulletin,* **41**, 347–354.

OSSIAN, C. R. 1974. *Paleontology, Paleobotany and Facies Characteristics of a Pennsylvanian Delta in Southeastern Nebraska.* PhD thesis, University of Texas, 393 pp.

OSSIAN, C. R. 1976. Redescription of *Megactenopetalus kaibabanus* David 1944 (Chondrichthyes: Petalodontidae) with comments on its geographic and stratigraphic distribution. *Journal of Paleontology,* **50**, 392–397.

OSSWALD, K. 1928. *Raineria* nov. gen. - Ein Selachier-Rostrum aus dem Alpinen Rhät. *Zeitschrift der Deutschen Geologischen Gesellschaft,* **80**, 496–510.
OTA, A. and ISOZAKI, Y. 2000. Stratigraphy of the Upper Permian seamount-top limestone in Southwest Japan: Ancient cap reef on a mid-oceanic paleo-seamount. *Eos, Transactions, American Geophysical Union,* **81**, 218.
OTA, A. and ISOZAKI, Y. 2006. Fusuline biotic turnover across the Guadalupian-Lopingian (Middle-Upper Permian) boundary in mid-oceanic carbonate buildups: Biostratigraphy of accreted limestone in Japan. *Journal of Asian Earth Sciences,* **26**, 353–368.
OTA, A., ISOZAKI, Y. and KAWAHATA, H. 2002. Secular change in stable carbon isotope ratio across the Middle/Upper Permian boundary in paleo-atoll limestone in Kyushu, Japan. *Journal of Geography,* **111**, 684–694.
OVTCHAROVA, M., BUCHER, H., SCHALTEGGER, U., GALFETTI, T., BRAYARD, A. and GUEX, J. 2006. New Early to Middle Triassic U–Pb ages from South China: Calibration with ammonoid biochronozones and implications for the timing of the Triassic biotic recovery. *Earth and Planetary Science Letters,* **243**, 463–475.
OWEN, R. 1840–1845. *Odontography; or, a treatise on the comparative anatomy of the teeth; their physiological relations, mode of development and microscopic structure, in the vertebrate animals,* Bailliere, London, LXXIV + 655 pp.
OWEN, R. 1846. *Lectures on the comparative anatomy and physiology of the vertebrate animals, delivered at the Royal College of Surgeons of England in 1844 and 1846, Part 1 - Fishes*. London, 308 pp.
OWEN, R. 1867. On the mandible and mandibular teeth of cochliodonts. *Geological Magazine,* **4**, 59–63.
PALEOBIOLOGY DATABASE. Website: http://www.paleodb.org/
PARKER, W. G. 2005. Faunal review of the Upper Triassic Chinle Formation of Arizona. *In:* MCCORD, R. D. (ed.) *Vertebrate Paleontology of Arizona.* Mesa Southwest Museum Bulletin, **11**, 34–54.
PARKER, S. 2008. *The Encyclopedia of Sharks,* A & C Black, London, 224 pp.
PATTERSON, C. 1965. The phylogeny of the chimaeroids. *Philosophical Transactions of the Royal Society of London B: Biological Sciences,* **249**, 101–219.
PATTERSON, C. 1966. British Wealden sharks. *Bulletin of the British Museum (Natural History) Geology,* **11**, 281–350.
PATTERSON, C. 1968. *Menaspis* and the bradyodonts. *In:* ØRVIG, T. (ed.) *Current Problems of Lower Vertebrate Phylogeny, Proceedings of the 4th Nobel Symposium.* Alquist and Wiksell, Stockholm, 171–205.
PATTERSON, C. and SMITH, A. B. 1987. Is the periodicity of extinctions a taxonomic artefact? *Nature,* **330**, 248–251.
PAYNE, J. L. 2005. Evolutionary dynamics of gastropod size across the end-Permian extinction and through the Triassic recovery interval. *Paleobiology,* **31**, 269–290.
PAYNE, J. L. and CLAPHAM, M. E. 2012. End-Permian mass extinction in the oceans: An ancient analog for the twenty-first century? *Annual Review of Earth and Planetary Sciences,* **40**, 89–111.
PAYNE, J. L. and FINNEGAN, S. 2007. The effect of geographic range on extinction risk during background and mass extinction. *Proceedings of the National Academy of Sciences,* **104**, 10506–10511.
PAYNE, J. L., LEHRMANN, D. J., WEI, J. Y., ORCHARD, M. J., SCHRAG, D. P. and KNOLL, A. H. 2004. Large perturbations of the carbon cycle during recovery from the end-Permian extinction. *Science,* **305**, 506–509.

PAYNE, J. L., LEHRMANN, D. J., CHRISTENSEN, S., WEI, J. and KNOLL, A. H. 2006a. Environmental and biological controls on the initiation and growth of a Middle Triassic (Anisian) reef complex on the Great Bank of Guizhou, Guizhou Province, China. *Palaios,* **21**, 325–343.

PAYNE, J. L., LEHRMANN, D. J., WEI, J. and KNOLL, A. H. 2006b. The pattern and timing of biotic recovery from the end-Permian extinction on the Great Bank of Guizhou, Guizhou Province, China. *Palaios,* **21**, 63–85.

PAYNE, J. L., LEHRMANN, D. J., FOLLETT, D., SEIBEL, M., KUMP, L. R., RICCARDI, A., ALTINER, D., SANO, H. and WEI, J. 2007. Erosional truncation of uppermost Permian shallow-marine carbonates and implications for Permian-Triassic boundary events. *Geological Society of America, Bulletin,* **119**, 771–784.

PERCH-NIELSEN, K., BROMLEY, R. G., BIRKENMAJER, K. and AELLEN, M. 1972. Field observations in Palaeozoic and Mesozoic sediments of Scoresby Land and northern Jameson Land. *Rapport Grønlands Geologiske Undersøgelse,* **48**, 39–59.

PIASECKI, S. 1984. Preliminary palynostratigraphy of the Permian-Lower Triassic sediments in Jameson Land and Scoresby Land, East Greenland. *Bulletin of the Geological Society of Denmark,* **32**, 139–144.

PIASECKI, S. and STEMMERIK, L. 1991. Late Permian anoxia in central East Greenland. *In:* TYSON, R. V. and PEARSON, T. H. (eds) *Modern and Ancient Continental Shelf Anoxia.* Geological Society of London, Special Publications, **58**, 275–290.

PILLEVUIT, A., MARCOUX, J., STAMPFLI, G. and BAUD, A. 1997. The Oman exotics: A key to the understanding of the Neotethyan geodynamic evolution. *Geodinamica Acta,* **10**, 209–238.

PITRAT, C. W. 1973. Vertebrates and the Permo-Triassic extinction. *Palaeogeography, Palaeoclimatology, Palaeoecology,* **14**, 249–264.

POLCYN, M. J., WINKLER, D. A., JACOBS, L. L. and NEWMAN, K. 2002. Fossil occurrences and structural disturbance in the Triassic Chinle Formation at North Stinking Springs Mountain near St. Johns, Arizona. *New Mexico Museum of Natural History and Science Bulletin,* **21**, 43–49.

POPLIN, C. and HEYLER, D. 1989. Évolution et phylogénie des Xenacanthiformes (= Pleuracanthiformes) (Pisces, Chondrichthyes). *Annales de Paléontologie,* **75**, 187–222.

PORTLOCK, J. E. 1843. *Report on the geology of the county of Londonderry, and parts of Tyrone and Fermanagh,* Dublin, XXXI + 784 pp.

PRADEL, A., TAFFOREAU, P. and JANVIER, P. 2010. Study of the pectoral girdle and fins of the Late Carboniferous sibyrhynchid iniopterygians (Vertebrata, Chondrichthyes, Iniopterygia) from Kansas and Oklahoma (USA) by means of microtomography, with comments on iniopterygian relationships. *Comptes Rendus Palevol,* **9**, 377–387.

PRADEL, A., TAFFOREAU, P., MAISEY, J. G. and JANVIER, P. 2011. A new Paleozoic Symmoriiformes (Chondrichthyes) from the Late Carboniferous of Kansas (USA) and cladistic analysis of early chondrichthyans. *PLoS ONE,* **6**, e24938.

PRASAD, G. V. R., SINGH, K., PARMAR, V., GOSWAMI, A. and SUDAN, C. S. 2008. Hybodont shark teeth from the continental Upper Triassic deposits of India. *In:* ARRATIA, G., SCHULTZE, H. P. and WILSON, M. V. H. (eds) *Mesozoic Fishes*

4 - Homology and Phylogeny. Proceedings of the International Meeting Miraflores de la Sierra, 2005. Verlag Dr. Friedrich Pfeil, München, 413–432.
PRETO, N., KUSTATSCHER, E. and WIGNALL, P. B. 2010. Triassic climates — State of the art and perspectives. *Palaeogeography, Palaeoclimatology, Palaeoecology,* **290**, 1–10.
PREUSCHOFT, H., REIF, W. E. and MÜLLER, W. H. 1974. Funktionsanpassungen in Form und Struktur an Haifischzähnen. *Zeitschrift für Anatomie und Entwicklungsgeschichte,* **143**, 315–344.
PRIEM, F. 1908. Etude des Poissons Fossiles du Bassin Parisien. *Annales de Paléontologie*, **6**, 1–144.
PRUSS, S. B., CORSETTI, F. A. and BOTTJER, D. J. 2005. The unusual sedimentary rock record of the Early Triassic: A case study from the southwestern United States. *Palaeogeography, Palaeoclimatology, Palaeoecology,* **222**, 33–52.
PRUVOST, P. 1922. Description de *Denaea fournieri*, sélacien nouveau du Marbre noir de Denée. Part 2 of FOURNIER, G. and PRUVOST, P. Découverte d'un poisson nouveau dans le marbre noir de Denée. *Bulletins de l'Académie royale des Sciences et Belles-Lettres de Bruxelles, Série 5,* **8**, 213–218.
QUENSTEDT, F. A. 1852. *Handbuch der Petrefaktenkunde,* Tübingen, 792 pp.
QUENSTEDT, F. A. 1856. *Der Jura. Part 1,* Laupp, Tübingen, 1–208.
QUENSTEDT, F. A. 1858. *Der Jura,* Tübingen, VI + 842 pp.
QUENSTEDT, F. A. 1885. *Handbuch der Petrefaktenkunde,* Tübingen, 1239 pp.
RABU, D., LE METOUR, J., BECHENNEC, F., BEURRIER, M., VILLEY, M. and BOURDILLON-JEUDY DE GRISSAC, C. 1990. Sedimentary aspects of the Eo-Alpine cycle on the northeast edge of the Arabian Platform (Oman Mountains). *In* ROBERTSON, A. H. F., SEARLE, M. P. and RIES, A. C. (eds) *The Geology and Tectonics of the Oman Region.* Geological Society, London, Special Publications, **49**, 49–68.
RAGONHA, E. W. 1984. Taxionomia de dentes e espinhos isolados de Xenacanthodii (Chondrichthyes Elasmobranchii) da formação Corumbataí. Considerações cronológicas e paleográficas. *Revista Brasileira de Geociências,* **14**, 179 (abstract).
RAMPINO, M. R. and ADLER, A. C. 1998. Evidence for abrupt latest Permian mass extinction of foraminifera: results of tests for the Signor-Lipps effect. *Geology,* **26**, 415–418.
RASCHI, W. and ELSOM, J. 1986. Comments on the structure and development of the drag reduction-type placoid scale. *In:* UYENO, T., ARAI, R., TANIUCHI, T. and MATSUURA, K. (eds) *Indo-Pacific Fish Biology. Proceedings of the Second International Conference on Indo-Pacific Fishes.* Ichthyological Society of Japan, Tokyo, 408–424.
RASMUSSEN, J. A., PIASECKI, S., STEMMERIK, L. and STOUGE, S. 1990. Late Permian conodonts from central East Greenland. *Neues Jahrbuch für Geologie und Paläontologie, Abhandlungen,* **178**, 309–324.
REES, J. 2008. Interrelationships of Mesozoic hybodont sharks as indicated by dental morphology – preliminary results. *Acta Geologica Polonica,* **58**, 217–221.
REES, J. and UNDERWOOD, C. J. 2002. The status of the shark genus *Lissodus* Brough, 1935, and the position of nominal *Lissodus* species within the Hybodontoidea (Selachii). *Journal of Vertebrate Paleontology,* **22**, 471–479.
REES, J. and CUNY, G. 2007. On the enigmatic neoselachian *Agaleus dorsetensis* from the European Early Jurassic. *GFF,* **129**, 1–6.

REES, J. and UNDERWOOD, C. J. 2008. Hybodont sharks of the English Bathonian and Callovian (Middle Jurassic). *Palaeontology,* **51**, 117–147.
REGAN, C. T. 1906. A classification of the selachian fishes. *Proceedings of the Zoological Society of London,* **1906**, 722–758.
REIF, W.-E. 1973a. Morphologie und Ultrastruktur des Hai-"Schmelzes". *Zoologica Scripta,* **2**, 231–250.
REIF, W.-E. 1973b. Ontogenese des Hautskelettes von *Heterodontus falcifer* (Selachii) aus dem Untertithon. *Stuttgarter Beitrage zur Naturkunde B,* **7**, 1–16.
REIF, W.-E. 1977. Tooth enameloid as a taxonomic criterion: 1. A new euselachian shark from the Rhaetic-Liassic boundary. *Neues Jahrbuch für Geologie und Paläontologie, Monatshefte*, **9**, 565–576.
REIF, W.-E. 1978a. Types of morphogenesis of the dermal skeleton in fossil sharks. *Paläontologische Zeitschrift,* **52**, 110–128.
REIF, W.-E. 1978b. Tooth enameloid as a taxonomic criterion: 2. Is "*Dalatias*" *barnstonensis* Sykes, 1971 (Triassic, England) a squalomorphic shark? *Neues Jahrbuch für Geologie und Paläontologie, Monatshefte,* **1**, 42–58.
REIF, W.-E. 1980a. Development of dentition and dermal skeleton in embryonic *Scyliorhinus canicula*. *Journal of Morphology,* **166**, 275–288.
REIF, W.-E. 1980b. Tooth enameloid as a taxonomic criterion: 3. A new primitive shark family from the lower Keuper. *Neues Jahrbuch für Geologie und Paläontologie, Monatshefte,* **160**, 61–72.
REIF, W.-E. 1982a. Evolution of dermal skeleton and dentition in vertebrates – the odontode regulation theory. *Evolutionary Biology,* **15**, 287–368.
REIF, W.-E. 1982b. Morphogenesis and function of the squamation in sharks. *Neues Jahrbuch für Geologie und Paläontologie,* **164**, 172–183.
REIF, W.-E. 1985. *Squamation and Ecology of Sharks,* Senckenbergischen Naturforschenden Gesellschaft, Frankfurt am Main, **78**, 1–101.
REIF, W.-E. and GOTO, M. 1979. Placoid scales from the Permian of Japan. *Neues Jahrbuch für Geologie und Paläontologie, Monatshefte,* **1979**, 201–207.
REIF, W. E. and DINKELACKER, A. 1982. Hydrodynamics of the squamation in fast swimming sharks. *Neues Jahrbuch für Geologie und Paläontologie,* **164**, 184–187.
REIFF, W. 1938. Obere bunte Estherienschichten, Schilfsandstein und Dunkle Mergel im mittleren Württemberg. *Tübinger Geographische und Geologische Abhandlungen,* **1**, 26.
RICHOZ, S. 2006. Stratigraphie et variations isotopiques du carbone dans le Permien supérieur et le Trias inférieur de quelques localités de la Néotéthys (Turquie, Oman et Iran). *Mémoires de Géologie (Lausanne),* **45**, 1–275.
RICHOZ, S., BAUD, A., BÉCHENNEC, F., CORDEY, F., MAURY, R., KRYSTYN, L., TWITCHETT, R. J. and MARCOUX, J. 2005. Permo–Triassic deposits of the Oman Mountains: from basin and slope to the shallow platform - Post-conference excursion no. A13 in the Oman Mountains, January 14–17, 2005. *International Association of Sedimentology, 24th Regional Meeting, January 10–13, 2005.* Muscat, Oman.
RICHOZ, S., KRYSTYN, L., WEIDLICH, O., BAUD, A., BEAUCHAMP, B., BERNECKER, M., CORDEY, F., GRASBY, S., HENDERSON, C. M., MARCOUX, J., NICORA, A. and TWITCHETT, R. 2010. The Permian-Triassic transition in the Oman Mountains - transect of the Tethyan margin from shallow to deep-water deposits. IGCP 572 Field Guide Book 2, GUtech Geoscience

Workshop Publication 1. *IGCP 572 Annual Meeting & Field Workshop, 20–26 February 2010.* Muscat, Oman.

RICHTER, M. 2005. A new xenacanthid shark (Chondrichthyes) from the Teresina Formation, Permian of the Paraná Basin, southern Brazil. *Revista Brasileira de Paleontologia,* **8**, 149–158.

RICHTER, M. 2007. First record of Eugeneodontiformes (Chondrichthyes: Elasmobranchii) from the Paraná Basin, Late Permian of Brazil. *In:* DE SOUZA CARVALHO, I., DE CASSIA TARDIN CASSAB, R., SCHWANKE, C., DE ARAUJO CARVALHO, M., SEQUEIRA FERNANDES, A. C., DA CONCEIÇÃO RODRIGUES, M. A., SARDENBERG SALGADO DE CARVALHO, M., ARAI, M. and QUEIROZ OLIVEIRA, M. E. (eds) *Paleontologia: cenários de vida.* Interciéncía Ltda., Rio de Janeiro, **1**, 149–156.

RICHTER, M. and LANGER, M. C. 1998. Fish remains from the Upper Permian Rio do Rasto Formation (Paraná Basin) of southern Brazil. *Journal of African Earth Sciences,* **27**, 158–159.

RIEPPEL, O. 1981. The hybodontiform sharks from the Middle Triassic of Mte. San Giorgio, Switzerland. *Neues Jahrbuch für Geologie und Paläontologie, Abhandlungen,* **161**, 324–353.

RIEPPEL, O. 1982. A new genus of shark from the Middle Triassic of Monte San Giorgio, Switzerland. *Palaeontology,* **25**, 399–412.

RIEPPEL, O., KINDLIMANN, R. and BUCHER, H. 1996. A new fossil fish fauna from the Middle Triassic (Anisian) of North-Western Nevada. *In:* ARRATIA, G. and VIOHL, G. (eds) *Mesozoic Fishes – Systematics and Paleoecology.* Verlag Dr. Friedrich Pfeil, München, 501–512.

ROHDE, R. A. 2005. *GeoWhen Database*. Website: http://www.stratigraphy.org/bak/geowhen/index.html.

ROLLE, F. 1858. Über einige an der Grenze von Keuper und Lias in Schwaben auftretende Versteinerungen. *Sitzungsberichte der Kaiserlichen Akademie der Wissenschaften in Wien,* **26**, 13–32.

ROMANO, C. and BRINKMANN, W. 2010. A new specimen of the hybodont shark *Palaeobates polaris* with three-dimensionally preserved Meckel's cartilage from the Smithian (Early Triassic) of Spitsbergen. *Journal of Vertebrate Paleontology,* **30**, 1673–1683.

ROMER, A. S. 1942. Notes on certain American Paleozoic fishes. *American Journal of Science,* **240**, 216–228.

ROMER, A. S. 1945. *Vertebrate Paleontology,* Chicago University Press, Chicago, Illinois, 587 pp.

ROMER, A. S. 1966. *Vertebrate Paleontology,* University of Chicago Press, Chicago, Illinois, 468 pp.

RONCHI, A., SARRIA, E. and BROUTIN, J. 2008. The "Autuniano Sardo": basic features for a correlation through the Western Mediterranean and Paleoeurope. *Bolletino della Società Geologica Italiana,* **127**, 655–681.

RUBIDGE, B. S. 2005. Re-uniting lost continents - Fossil reptiles from the ancient Karoo and their wanderlust. *South African Journal of Geology,* **108**, 135–172.

RUZHENTSEV, V. E. and SARYCHEVA, T. G. 1955. Razvitie semena morskikh organismov na rubezhe paleoja i mesozoja. *Trudy Paleontologicheskogo Instituta,* **108** (Parts I and II in English translation – The development and change of marine organisms at the Palaeozoic-Mesozoic boundary, Parts I and

II: Translated by D.A. Brown, Australian National University, Canberra, A.C.T. 1968, 1969).
SAFFORD, J. M. 1853. Tooth of *Getalodus ohioensis*. *American Journal of Science and Arts,* **16**, 142.
SAHNEY, S. and BENTON, M. J. 2008. Recovery from the most profound mass extinction of all time. *Proceedings of the Royal Society B: Biological Sciences,* **275**, 759–765.
SAHNI, A. and CHHABRA, N. L. 1976. Microfish remains from certain Triassic sections in the Kashmir and Kumaun Himalayas. *Proceedings of the VI Indian Colloquium on Micropaleontology and Stratigraphy*, 218–224.
ST. JOHN, O. 1870. Descriptions of fossil fishes from the upper Coal-Measures of Nebraska. *Proceedings of the American Philosophical Society,* **11**, 431–437.
ST. JOHN, O. and WORTHEN, A. H. 1875. Description of fossil fishes. *Geological Survey of Illinois,* **6**, part II, section I, 245–488.
ST. JOHN, O. and WORTHEN, A. H. 1883. Descriptions of fossil fishes. A partial revision of the Cochliodonts and Psammodonts, including notices of miscellaneous materials acquired from the Carboniferous formations of the United States. *Geological Survey of Illinois,* **7**, 55–264.
SALAMON, M. A., EAGLE, M. K. and NIEDŹWIEDZKI, R. 2003. A new ceratite record from Upper Silesia (Poland). *Geological Quarterly,* **47**, 281–288.
SALLAN, L. C. and FRIEDMAN, M. 2012. Heads or tails: staged diversification in vertebrate evolutionary radiations. *Proceedings of the Royal Society B: Biological Sciences,* **279**, 2025–2032.
SALLAN, L. C., KAMMER, T. W., AUSICH, W. I. and COOK, L. A. 2011. Persistent predator–prey dynamics revealed by mass extinction. *Proceedings of the National Academy of Sciences,* **108**, 8335–8338.
SANDER, P. M. 1990. Keuper und Lias der Tongrube Frick. *In:* WEIDERT, W. K. (ed.) *Klassische Fundstellen.* Korb: Goldschneck, **2**, 89–96.
SANDER, P. M. 1992. The Norian Plateosaurus Bonebeds of central Europe and their taphonomy. *Palaeogeography, Palaeoclimatology, Palaeoecology,* **93**, 255–299.
SANDER, P. M. and GEE, C. T. 1989. Earthwatch - Freiwillige graben Fricker Dinosaurier aus. *Universität Zürich,* **1989**, 33–34.
SANDER, P. M. and GEE, C. T. 1989. Mit Earthwatch auf Dinosaurierjagd. *Fossilien,* **4**, 157–165.
SANDER, P. M. and KRAHL, A. 2007. Stop 5—Conner Ranch/Cottonwood Creek of Romer. 5. *In:* SANDER, P. M. (ed.) *The Lower Permian of North Texas.* Austin: Society of Vertebrate Paleontology 67th Annual Meeting, field trip guidebook, 1–53.
SANDER, P. M., RIEPPEL, O. and BUCHER, H. 1994. New marine vertebrate fauna from the Middle Triassic of Nevada. *Journal of Paleontology,* **68**, 676–680.
SANDERSON, M. J., PURVIS, A. and HENZE, C. 1998. Phylogenetic supertrees: Assembling the trees of life. *Trends in Ecology & Evolution,* **13**, 105–109.
SANO, H. and NAKASHIMA, K. 1997. Lowermost Triassic (Griesbachian) microbial bindstone-cementstone facies, southwest Japan. *Facies,* **36**, 1–24.
SANO, H., WADA, T. and NARAOKA, H. 2012. Late Permian to Early Triassic environmental changes in the Panthalassic Ocean: Record from the seamount-associated deep-marine siliceous rocks, central Japan. *Palaeogeography, Palaeoclimatology, Palaeoecology,* **363–364**, 1–10.

SANSOM, I. J. 2000. Late Triassic (Rhaetian) conodonts and ichthyoliths from Chile. *Geological Magazine,* **137**, 129–135.
SANSOM, I. J., SMITH, M. M. and SMITH, M. P. 1996. Scales of thelodont and shark-like fishes from the Ordovician of Colorado. *Nature,* **379**, 628–630.
SANSOM, I. J., ALDRIDGE, R. J. and SMITH, M. M. 2000. A microvertebrate fauna from the Llandovery of South China. *Transactions of the Royal Society of Edinburgh: Earth Sciences,* **90**, 255–272.
SANSOM, I. J., DAVIES, N. S., COATES, M. I., NICOLL, R. S. and RITCHIE, A. 2012. Chondrichthyan-like scales from the Middle Ordovician of Australia. *Palaeontology,* **55**, 243–247.
SASAGAWA, I. 2002. Mineralization patterns in elasmobranch fish. *Microscopy Research and Technique,* **59**, 396–407.
SASAKI, M. 2003. Early Cretaceous sinistral shearing and associated folding in the South Kitakami Belt, northeast Japan. *Island Arc,* **12**, 92–109.
SAUVAGE, H. E. 1883. Note sur les poissons du Muschelkalk de Pontpierre (Lorraine). *Bulletin de la Societé géologique de France,* **3**, 492–496.
SCHAEFFER, B. 1967. Comments on elasmobranch evolution. *In:* GILBERT, P. W., MATHEWSON, R. F. and RALL, D. P. (eds) *Sharks, skates and rays.* Johns Hopkins Press, Baltimore, 3-35.
SCHAEFFER, B. 1973. Fishes and the Permian-Triassic boundary. *In:* LOGAN, A. and HILLS, L. V. (eds) *The Permian and Triassic systems and their mutual boundary.* Canadian Society of Petroleum Geologists, Memoir, **2**, 493–497.
SCHAEFFER, B. 1981. The xenacanth shark neurocranium, with comments on elasmobranch monophyly. *Bulletin of the American Museum of Natural History,* **169**, 1–66.
SCHAEFFER, B. and MANGUS, M. 1970. *Synorichthys* sp. (Palaeonisciformes) and the Chinle-Dockum and Newark (Upper Triassic) Fish Faunas. *Journal of Paleontology,* **44**, 17–22.
SCHAEFFER, B. and MANGUS, M. 1976. An Early Triassic fish assemblage from British Columbia. *Bulletin of the American Museum of Natural History,* **156**, 519–563.
SCHAUMBERG, G. 1977. Der Richelsdorfer Kupferschiefer und seine Fossilien. III. Die tierischen Fossilien des Kupferschiefers. 2. Vertebraten. *Aufschluss,* **28**, 297–352.
SCHAUMBERG, G. 1982. *Hopleacanthus richelsdorfensis* n. g. n. sp., ein euselachier aus dem permischen Kupferschiefer von Hessen (W-Deutschland). *Paläontologische Zeitschrift,* **56**, 235–257.
SCHAUMBERG, G. 1992. Neue Informationen zu *Menaspis armata* Ewald. *Paläontologische Zeitschrift,* **66**, 311–329.
SCHAUMBERG, G. 1999. Ergänzungen zur Revision des Euselachiers *Wodnika striatula* Münster 1843 aus dem oberpermischen Kupferschiefer und Marl-Slate. *Geologica et Palaeontologica,* **33**, 203–217.
SHAW, S. H. 1947. *Southern Palestine, geological map on a scale of 1/250,000 with explanatory notes,* Government of Palestine, Public Works Department, Geological Section, Jerusalem, 42 pp.
SCHEINPFLUG, R. 1984. Wirbeltierfunde in mainfränkischen Hauptmuschelkalk. *Aufschluß,* **35**, 21–36.
SCHINDLER, T. and POSCHMANN, M. 2001. Das Profil einer Pipeline-Trasse bei Odenbach und seine lithostratigraphischen Leithorizonte (Lauterecken-

Formation, Unterperm; Saar-Nahe-Gebiet, SWDeutschland). *Mainzer Geowissenschaftliche Mitteilungen,* **30**, 91–104.
SCHLOTHEIM, E. F., VON 1820. *Die Petrefactenkunde auf ihrem jetzigen Standpunkte,* Becker, Gotha.
SCHMID, E. E. 1861. Die Fischzähne der Trias bei Jena. *Nova Acta Academia Leopoldiana-Carolinensis,* **29**, 1–42.
SCHMIDT, M. 1928. *Die Lebewelt unsere Trias*, Hohenlohe'sche buchhandlung Ferdinand Rau, Öringen, 461 pp.
SCHNEIDER, J. W. 1985. Elasmobranchier-Zahntypen (Pisces, Chondrichthyes) und ihre stratigraphische Verbreitung im Karbon und Perm der Saale-Senke (DDR). *Freiberger Forschungshefte,* **C400**, 90–100.
SCHNEIDER, J. W. 1988. Grundlagen der Morphogenie, Taxonomie und Biostratigraphie isolierter Xenacanthodier-Zähne (Elasmobranchii). *Freiberger Forschungshefte,* **C419**, 71–80.
SCHNEIDER, J. W. 1996. Xenacanth teeth—a key for taxonomy and biostratigraphy. *Modern Geology,* **20**, 321–340.
SCHNEIDER, J. W. and ZAJÍC, J. 1994. Xenacanthiden (Pisces, Chondrichthyes) des mitteleuropäischen Oberkarbon und Perm – Revision der Originale zu Goldfuss 1847, Beyrich 1848, Kner 1867 und Fritsch 1879–1890. *Freiberger Forschungshefte,* **C452**, 101–151.
SCHOLLE, P. A., STEMMERIK, L., ULMER-SCHOLLE, D., DI LIEGRO, G. and HENK, F. G. 1993. Palaeokarst-influenced depositional and diagenetic patterns in Upper Permian carbonates and evaporites, Karstryggen area, central East Greenland. *Sedimentology,* **40**, 895–918.
SCHUBERT, J. K. and BOTTJER, D. J. 1995. Aftermath of the Permian-Triassic mass extinction event: paleoecology of Lower Triassic carbonates in the western U.S.A. *Palaeogeography, Palaeoclimatology, Palaeoecology,* **116**, 1–39.
SCHULTZE, H.-P. 1985. Marine to onshore vertebrates in the lower Permian of Kansas and their paleoenvironmental implications. *The University of Kansas Paleontological Contributions, Paper,* **113**, 1–12.
SCHULTZE, H.-P. 1986. Permian Vertebrates from Germany. *Journal of Vertebrate Paleontology,* **6**, 206–208.
SCHULTZE, H.-P. 2009. Interpretation of marine and freshwater paleoenvironments in Permo-Carboniferous deposits. *Palaeogeography, Palaeoclimatology, Palaeoecology,* **281**, 126–136.
SCHULTZE, H. P. and KRIWET, J. 1999. Die Fische der Germanischen Trias. *In:* HAUSCHKE, N. and WILDE, V. (eds) *Trias, eine ganz andere Welt. Mitteleuropa im frühen Erdmittelalter.* Verlag Dr. Friedrich Pfeil, München, 239–250.
SCHULTZE, H.-P. and WEST, R. R. 1996. An eugeneodontid elasmobranch from the Late Paleozoic of Kansas. *Journal of Paleontology,* **70**, 162–165.
SCHULTZE, H.-P. and SOLER-GIJÓN, R. 2004. A xenacanth clasper from the ?uppermost Carboniferous - Lower Permian of Buxières-les-Mines (Massif Central, France) and the palaeoecology of the European Permo-Carboniferous basins. *Neues Jahrbuch für Geologie und Paläontologie, Abhandlungen,* **232**, 325–363.
SCHULTZE, H.-P., SOLER−GIJÓN, R., HAMPE, O. and HEWARD, A. 2008. Vertebrates from the Gharif Formation, Lower Permian of Oman. *In:* ŠTAMBERG, S. and ZAJÍC, J. (eds) *Faunas and palaeoenvironments of the*

Late Palaeozoic - Special Publication for the 5th Symposium on Permo−Carboniferous Faunas, 7–11 July 2008. Museum of Eastern Bohemia, Hradec Králové, 41–42 (abstract).

SCOTESE, C. R. 2003. *PALEOMAP Project*. Website: http://www.scotese.com

SCOTESE, C. R. 2008. Permian and Triassic plate tectonic, paleogeographic and paleoclimatic reconstructions and animation. *Geological Society of America, Abstracts with Programs,* **40**, 535.

SEEGIS, D. 2005. Fische. *In:* BEUTLER, G., HAUSCHKE, N., NITSCH, E. and VATH, U. (eds) *Stratigraphie von Deutschland IV - Keuper.* Courier Forschungsinstitut Senckenberg, **253**, 55–57.

SEIDLER, L. 2000. Incised submarine canyons governing new evidence of Early Triassic rifting in East Greenland. *Palaeogeography, Palaeoclimatology, Palaeoecology,* **161**, 267–293.

SEILACHER, A. 1943. Elasmobranchier-reste aus dem oberen Muschelkalk und dem Keuper Württemburgs. *Neues Jahrbuch für Mineralogie, Geologie und Paläontologie, Monatshefte B,* **1943**, 256–271.

SEILACHER, A. 1948. Ein weiterer altertümlicher Elasmobranchier (*Phoebodus keuperinus* n. sp.) aus dem württembergischen Gipskeuper. *Neues Jahrbuch für Geologie und Paläontologie, Monatshefte, Abteilung B,* **1948**, 24–27.

SENNIKOV, A. and GOLUBEV, V. 2006. Vyazniki biotic assemblage of the terminal Permian. *Paleontological Journal,* **40**, S475–S481.

SEPKOSKI, J. J. 1978. A kinetic-model of Phanerozoic taxonomic diversity. I. Analysis of marine orders. *Paleobiology,* **4**, 223–251.

SEPKOSKI, J. J. 1982. A compendium of fossil marine families. *Milwaukee Public Museum Contributions in Biology and Geology,* **51**, 1–125.

SEPKOSKI, J. J. 1984. A kinetic model of Phanerozoic taxonomic diversity. III. Post-Paleozoic families and mass extinctions. *Paleobiology,* **10**, 246–267.

SEPKOSKI, J. J. 1992. A compendium of fossil marine animal families, 2nd ed. *Milwaukee Public Museum Contributions in Biology and Geology,* **83**, 1–156.

SEPKOSKI, J. J. 2002. A compendium of fossil marine animal genera. *Bulletins of American Paleontology,* **363**, 1–560.

SEQUEIRA, S. E. K. and COATES, M. I. 2000. Reassessment of '*Cladodus*' *neilsoni* Traquair: a primitive shark from the Lower Carboniferous of East Kilbridge, Scotland. *Palaeontology,* **43**, 153–172.

SHACKLETON, R. M., RIES, A. C., BIRD, P. R., FILBRANDT, J. B., LEE, C. W. and CUNNINGHAM, G. C. 1990. The Batain Melange of NE Oman. *In* ROBERTSON, A. H. F., SEARLE, M. P. and RIES, A. C. (eds) *The Geology and Tectonics of the Oman Region.* Geological Society, London, Special Publications, **49**, 673–696.

SHARK-REFERENCES. Website: http://shark-references.com/

SHEN, S.-Z., XIE, J.-F., ZHANG, H. and SHI, G. R. 2009. Roadian–Wordian (Guadalupian, Middle Permian) global palaeobiogeography of brachiopods. *Global and Planetary Change,* **65**, 166–181.

SHEN, S.-Z., CROWLEY, J. L., WANG, Y., BOWRING, S. A., ERWIN, D. H., SADLER, P. M., CAO, C.-Q., ROTHMAN, D. H., HENDERSON, C. M., RAMEZANI, J., ZHANG, H., SHEN, Y., WANG, X.-D., WANG, W., MU, L., LI, W.-Z., TANG, Y.-G., LIU, X.-L., LIU, L.-J., ZENG, Y., JIANG, Y.-F. and JIN, Y.-G. 2011. Calibrating the end-Permian mass extinction. *Science,* **334**, 1367–1372.

SHIGETA, Y., ZAKHAROV, Y. D., MAEDA, H. and POPOV, A. M. (eds) 2009. *The Lower Triassic system in the Abrek Bay area, South Primorye, Russia,* Tokyo: National Museum of Nature and Science, **38**, 1–218.

SHIRAI, S. 1996. Chapter 2 - Phylogenetic Interrelationships of neoselachians (Chondrichthyes: Euselachii). *In:* STIASSNY, M. L. J., PARENTI, L. R. and JOHNSON, G. D. (eds) *Interrelationships of Fishes.* Academic Press, Burlington, 9–34.

SIEDLECKI, S. 1970. A *Helicoprion* from the Permian of Spitsbergen. *Norsk Polarinstitutt Årbok,* **1968**, 36–54.

SIGOGNEAU-RUSSELL, D. and HAHN, G. 1994. Late Triassic microvertebrates from central Europe. *In:* FRASER, N. C. and SUES, H.-D. (eds) *In the shadow of the dinosaurs. Early Mesozoic tetrapods.* Cambridge University Press, 197–213.

SILVA SANTOS, R. 1990. Paleoictiofáunula da Formação Pedra do Fogo, Nordeste do Brasil: Holocephali — Petalodontidae. *Anais da Academia Brasileira de Ciências,* **62**, 347–355.

SIMPSON, L. C. 1974. *Acanthodes* and *Hybodus* in the Permian of Texas and Oklahoma. *Journal of Paleontology,* **48**, 1291–1293.

SIMPSON, L. C. 1976. *Paleontology of the Garber Formation (Lower Permian), Tillman County, Oklahoma.* University of Oklahoma, unpublished M.S. thesis, 216 pp.

SIMPSON, L. C. 1979. Upper Gearyan and lower Leonardian terrestrial vertebrate faunas of Oklahoma. *Oklahoma Geology Notes,* **39**, 3–21.

SMITH, A. B. 1994. *Systematics and the Fossil Record: documenting evolutionary patterns,* Blackwell Scientific Publications, Oxford, 223 pp.

SMITH, A. B. and JEFFERY, C. H. 1998. Selectivity of extinction among sea urchins at the end of the Cretaceous period. *Nature,* **392**, 69–71.

SMITH, M. M. 1992. Microstructure and evolution of enamel amongst osteichthyan fishes and early tetrapods. *In:* SMITH, P. and TCHERNOV, E. (eds) *Structure, function and evolution of teeth. Proceedings of the 8th International Symposium on Dental Morphology, Tel Aviv.* Freund Publishing House, London, 73–101.

SMITH, M. M. 1995. Heterochrony in the evolution of enamel in vertebrates. *In:* MCNAMARA, K. J. (ed.) *Evolutionary change and heterochrony.* John Wiley & Sons, Chichester, 125–150.

SOLER-GIJÓN, R. 1995. Evidence of predator-prey relationship in xenacanth sharks of the Upper Carboniferous (Stephanian C) from Puertollano, Spain. *Geobios,* **28**, 151–156.

SOLER-GIJÓN, R. 1997a. Euselachian sharks from the Late Carboniferous of the Puertollano Basin, Spain: Biostratigraphic and palaeoenvironmental implications. *Modern Geology,* **21**, 137–169.

SOLER-GIJÓN, R. 1997b. New discoveries of xenacanth sharks from the Late Carboniferous of Spain (Puertollano Basin) and Early Permian of Germany (Saar-Nahe Basin): Implications for the phylogeny of xenacanthiform and anacanthous sharks. *Neues Jahrbuch für Geologie und Paläontologie, Abhandlungen,* **205**, 1–31.

SOLER-GIJÓN, R. 2000. Phylogenetic relationships of *Lebachacanthidae* Soler-Gijón 1997 (Xenacanthiformes; Elasmobranchii). *Paläontologische Zeitschrift,* **74**, 363–377.

SOLER-GIJÓN, R. and HAMPE, O. 1998. Evidence of *Triodus* Jordan 1849 (Elasmobranchii: Xenacanthidae) in the Lower Permian of the Autun basin

(Muse, France). *Neues Jahrbuch für Geologie und Paläontologie, Monatshefte,* **1998**, 335–348.

SONG, H., WIGNALL, P. B., CHEN, Z.-Q., TONG, J., BOND, D. P. G., LAI, X., ZHAO, X., JIANG, H., YAN, C., NIU, Z., CHEN, J., YANG, H. and WANG, Y. 2011. Recovery tempo and pattern of marine ecosystems after the end-Permian mass extinction. *Geology,* **39**, 739–742.

SOSSON, M. and MARTIN, M. 1985. Découverte d'une faune de vertébrés marins du Trias supérieur dans le Hot Springs Range (nord-ouest du Nevada, U.S.A.): implications paléogéographiques. *Comptes-rendus des séances de l'Académie des sciences. Série 2, Mécanique-physique, chimie, sciences de l'univers, sciences de la terre,* **300**, 177–180.

SOUR-TOVAR, F., QUIROZ-BARROSO, S. A. and APPLEGATE, S. P. 2000. Presence of *Helicoprion* (Chondrichthyes, Elasmobranchii) in the Permian Patlanoaya Formation, Puebla, Mexico. *Journal of Paleontology,* **74**, 363–366.

SOUR-TOVAR, F. S., APPLEGATE, S. P., QUIROZ-BARROSO, S. A. and MORALES-SOTO, S. 1991. Presencia de *Helicoprion* sp. en rocas pérmicas de la Formación Patlanoaya, estado de Puebla, México. *Tercer Congreso Nacional de Paleontología*, 130 pp.

STAHL, B. J. 1999. *Chondrichthyes III Holocephali, Handbook of Paleoichthyology, vol. 4,* Verlag Dr. Friedrich Pfeil, München, 164 pp.

STANLEY, S. M. 2009. Evidence from ammonoids and conodonts for multiple Early Triassic mass extinctions. *Proceedings of the National Academy of Sciences,* **106**, 15264–15267.

STANLEY, S. M. and YANG, X. 1994. A double mass extinction at the end of the Paleozoic era. *Science,* **266**, 1340–1344.

STEFANOV, S. A. 1966. Fischreste aus der Trias Bulgariens. *Travaux sur la Géologie de Bulgarie - série Paléontologie,* **8**, 123–129.

STEFANOV, S. A. 1977. Biostratigraphy of the Balkanide carbonate Triassic on the basis of conodonts and fish remains. *Geologica Balcanica,* **7**, 65–84.

STEMMERIK, L. 2000. Late Palaeozoic evolution of the North Atlantic margin of Pangaea. *Palaeogeography, Palaeoclimatology, Palaeoecology,* **161**, 95–126.

STEMMERIK, L., BENDIX-ALMGREEN, S. E. and PIASECKI, S. 2001. The Permian-Triassic boundary in central East Greenland: past and present views. *Bulletin of the Geological Society of Denmark,* **48**, 159–167.

STENSIÖ, E. A. 1918. Notes on some fish remains collected at Hornsund by the Norwegian Spitzbergen Expedition in 1917. *Norsk Geologisk Tidsskrift,* **5**, 75–78.

STENSIÖ, E. A. 1921. *Triassic fishes from Spitsbergen, Part I*, Adolf Holzhausen, Vienna, 307 pp.

STENSIÖ, E. A. 1925. Triassic fishes from Spitsbergen, Part 2. *Kungliga Svenska Vetenskapsakademiens Handlingar,* **2**, 6 + 261 pp.

STENSIÖ, E. A. 1932. Triassic Fishes from East Greenland. *Meddelelser om Grønland,* **83**, 1–305.

STENSIÖ, E. A. 1961. Permian vertebrates. *In:* RAASCH, G. O. (ed.) *Geology of the Arctic - Proceedings of the first international symposium on Arctic geology, vol. 1.* University of Toronto Press, Toronto, 231–247.

STEPHENSON, R. A., EMBRY, A. F., NAKIBOGLU, S. M. and HASTAOGLU, M. A. 1987. Rift-initiated Permian to Early Cretaceous subsidence of the Sverdrup Basin. *In:* BEAUMONT, C. and TANKARD, A. (eds) *Sedimentary Basins and*

Basin-Forming Mechanisms. Atlantic Geoscience Society Special Publication, 213–231.

STEYER, J.-S. and ESCUILLIE, F. 1997. Le chantier de fouilles paléontologiques dans le permien inférieur de Buxières-les-Mines (Allier, France) en août 1996: Compte rendu préliminaire et perspectives. *Revue Scientifique du Bourbonnais,* **95**, 11–18.

STEYER, J. S., ESCUILLIE, F., POUILLON, J.-M., BROUTIN, J., DEBRIETTE, P., FREYTET, P., GAND, G., POPLIN, C., RAGE, J.-C., RIVAL, J., SCHNEIDER, J. W., STAMBERG, S., WERNEBURG, R. and CUNY, G. 2000. New data on the flora and fauna from the ?uppermost Carboniferous-Lower Permian of Buxieres-les-Mines, Bourbon l'Archambault Basin (Allier, France); a preliminary report. *Bulletin de la Société Géologique de France,* **171**, 239–249.

STONE, P., STEVENS, C. H. and ORCHARD, M. J. 1991. Stratigraphy of the Lower and Middle Triassic Union Wash Formation, East-Central California. *U.S. Geological Survey Bulletin,* **1928**, 1–26.

STORRS, G. W. 1994. Fossil vertebrate faunas of the British Rhaetian (latest Triassic). *Zoological Journal of the Linnean Society,* **112**, 217–259.

STREELMAN, J. T. and DANLEY, P. D. 2003. The stages of vertebrate evolutionary radiation. *Trends in Ecology & Evolution,* **18**, 126–131.

STRUCKMANN, C. 1871. Notiz über die fisch- und Saurier-Reste aus dem oberen Muschelkalke von Warberg am Elm im Herzogthum Braunschweig. *Zeitschrift der Deutschen Geologischen Gesellschaft,* **23**, 412–416.

STUCKENBERG, A. 1905. Die fauna der oberkarbonischen Suite des Wolgadurchbruches bei Samara. *Mémoires du Comité Géologique de St. Pétersbourg. Nouvelle Série,* Livre **23**, 144 pp.

SUAREZ, M. and BELL, C. M. 1992. Triassic rift-related sedimentary basins in northern Chile (24°–29°S). *Journal of South American Earth Sciences,* **6**, 109–121.

SUES, H.-D., OLSEN, P. E., CARTER, J. G. and PEYER, K. 2001. A remarkable Triassic tetrapod assemblage from the Deep River basin of North Carolina. *Geological Society of America, Abstract with Programs,* **33**, 27.

SULEJ, T., BRONOWICZ, R., TAŁANDA, M. and NIEDŹWIEDZKI, G. 2010. A new dicynodont–archosaur assemblage from the Late Triassic (Carnian) of Poland. *Earth and Environmental Science Transactions of the Royal Society of Edinburgh,* **101**, 261–269.

SULEJ, T., NIEDŹWIEDZKI, G. and BRONOWICZ, R. 2012. A new Late Triassic vertebrate fauna from Poland with turtles, aetosaurs, and coelophysoid dinosaurs. *Journal of Vertebrate Paleontology,* **32**, 1033–1041.

SUMIDA, S. S., ALBRIGHT, G. M. and REGA, E. A. 1999. Late Paleozoic fishes of Utah. *In:* GILLETTE, D. D. (ed.) *Vertebrate paleontology of Utah.* Geological Survey of Utah Miscellaneous Publication, **99-1**, 13–20.

SUN, Y., JOACHIMSKI, M. M., WIGNALL, P. B., YAN, C., CHEN, Y., JIANG, H., WANG, L. and LAI, X. 2012. Lethally Hot Temperatures During the Early Triassic Greenhouse. *Science,* **338**, 366–370.

SURLYK, F., HURST, J. M., PIASECKI, S., ROLLE, F., SCHOLLE, P. A., STEMMERIK, L. and THOMSEN, E. 1986. The Permian of the Western Margin of the Greenland Sea - A Future Exploration Target. *In:* HALBOUTY, M. T. (ed.) *Future Petroleum Provinces of the World.* American Association of Petroleum Geologists, Memoirs, **40**, 629–659.

SWEET, W. C. 1976. Conodonts from the Permian–Triassic boundary beds at Kap Stosch, East Greenland. *Meddelelser om Grønland,* **197**, 51–54.
SYKES, J. H. 1971. A new dalatiid fish from the Rhaetic bone-bed at Barnstone, Nottinghamshire. *Mercian Geologist,* **4**, 13–22.
SYKES, J. H. 1974. Teeth of *Dalatias barstonensis* in the British Rhaetic. *Mercian Geologist,* **5**, 39–48.
SYKES, J. H., CARGILL, J. S. and FRYER, H. G. 1970. The stratigraphy and palaeontology of the Rhaetic Beds (Rhaetian: Upper Triassic) of Barnstone, Nottinghamshire. *Mercian Geology,* **3**, 233–264.
TANNENBAUM, F. 1983. *The microvertebrate fauna of the Placerias and Downs Quarries, Chinle Formation (Upper Triassic) near St. Jolms, Arizona.* Unpublished M. S. thesis, Department of Paleontology, University of California at Berkeley, 111 pp.
TARVER, J. E., BRADDY, S. J. and BENTON, M. J. 2007. The effects of sampling bias on Palaeozoic faunas and implications for macroevolutionary studies. *Palaeontology,* **50**, 177–184.
TEICHERT, C. 1940. *Helicoprion* in the Permian of Western Australia. *Journal of Paleontology,* **14**, 140–149.
TEICHERT, C. 1943. Bradyodont sharks in the Permian of Western Australia. *American Journal of Science,* **241**, 543–552.
TEIXEIRA, C. 1954. Sur un Hybodontoidé du Karroo de l'Angola. *Revista de Junta das Missões Geogràficas e de Investigações do Ultramar,* **2**, 205–207.
TEIXEIRA, C. 1956. Sur un Hybodontoidé du Karroo de l'Angola. *Revista da faculdade de Ciencias, Lisboa, series C, Ciencias Naturais,* **5**, 135–136.
TEIXEIRA, C. 1979. Les Poissons fossiles du Karroo du Lutoa et de Iongo en Angola. *Reconhecimento Científico de Angola/ Estudos de Geologia, de Paleontologia e de Micologia.* Publicações do II Centenário da Academia das Ciências de Lisboa, 275–300.
THIES, D. 1982. A neoselachian shark tooth from the Lower Triassic of the Kocaeli (= Bithynian) Peninsula, W Turkey. *Neues Jahrbuch für Geologie und Paläontologie, Monatshefte,* **1982**, 272–278.
THIES, D. 1992. A new species of *Palaeospinax* (Chondrichthyes, Neoselachii) from the Lower Jurassic *Posidonia* Shale of Southern Germany. *Paläontologische Zeitschrift,* **66**, 137–146.
THIES, D. 1995. Placoid Scales (Chondrichthyes: Elasmobranchii) from the Late Jurassic (Kimmeridgian) of Northern Germany. *Journal of Vertebrate Paleontology,* **15**, 463–481.
THIES, D. and REIF, W. E. 1985. Phylogeny and evolutionary ecology of Mesozoic Neoselachii. *Neues Jahrbuch für Geologie und Paläontologie, Abhandlungen,* **169**, 333–361.
THOMPSON, K. L. 1995. *Paleoecology and biostratigraphy of the Fossil Mountain Member, Kaibab Formation, in north-western Arizona.* unpublished MSc thesis, Northern Arizona University, Flagstaff, 160 pp.
THOMSON, K. S. 1977. Chapter 12 - The Pattern of Diversification among Fishes. *In:* HALLAM, A. (ed.) *Patterns of evolution as Illustrated by the Fossil Record.* Developments in Palaeontology and Stratigraphy, **5**, 377–404.
THOMSON, K. S. 1982. An Early Triassic hybodont shark from northern Madagascar. *Postilla,* **186**, 1–16.

THÜRACH, H. 1888. Obersicht über die Gliederung des Keupers im nördlichen Franken. *Geognostische Jahreshefte,* **1**, 75–102.
TINTORI, A. 1980. Teeth of the selachian genus *Pseudodalatias* (SYKES, 1971) from the Norian (Upper Triassic) of Lombardy. *Rivista Italiana di Paleontologia e Stratigrafia,* **86**, 19–30.
TINTORI, A. 1998. New chondrichthyan fauna from the Guadalupian (middle Permian) of the Sultanate of Oman. *In:* GINTER, M. and WILSON, M. V. H. (eds) *Ichthyolith Issues Special Publication*, **4**, 48–49.
TOLEDO, C. E. V., BRITO, P. M. and BERTINI, R. J. 1997. Chronological meaning about the presence of petalodonts (Holocephali incertae sedis) in the Corumbataí Formation of São Paulo State (Brazil). *Boletim de Resumos de XV Congresso Brasileiro de Paleontologia, São Pedro,* **15**, 103.
TOMMASI, A. 1890. Rivista della fauna raibliana del Friuli. *Annali del Regio Istituto Tecnico Antonio Zanon di Udine,* **2**, 1–77.
TOZER, E. T. and CALON, T. J. 1990. Triassic ammonoids from Jabal Safra and Wadi Alwa, Oman, and their significance. *In* ROBERTSON, A. H. F., SEARLE, M. P. and RIES, A. C. (eds) *The Geology and Tectonics of the Oman Region.* Geological Society, London, Special Publications, **49**, 203–211.
TRAQUAIR, R. H. 1888. Notes on Carboniferous Selachii. *Proceedings of the Royal Physical Society of Edinburgh,* **9**, 412–426.
TRAUTSCHOLD, H. 1874. Die Kalkbrüche von Mjatschkowa. Eine Monographie des oberen Bergkalks. Erste Hälfte. *Nouveau Mémoires de la Société Impériale des Naturalistes de Moscou,* **13**, 277–326.
TRAUTSCHOLD, H. 1879. Die Kalkbrüche von Mjatschkowa. Eine Monographie des oberen Bergkalks. Schluss. *Nouveau Mémoires de la Société Impériale des Naturalistes de Moscou,* **14**, 3–82.
TURNER, S. 1993. Fish, a contribution to IGCP 328: Palaezoic microvertebrates. *In:* SKWARKO, S. K. (ed.) *Palaeontology of the Permian of Western Australia.* Geological Survey of Western Australia, **136**, 83–86.
TURNER, S. and YOUNG, G. C. 1987. Shark teeth from the early Middle Devonian Cravens Peak Beds, Georgina Basin, Queensland. *Alcheringa,* **11**, 233–244.
TURNER, S. and MILLER, R. F. 2005. New ideas about old sharks. *American Scientist,* **93**, 244–252.
TWAY, L. E. and ZIDEK, J. 1982. Catalog of Late Pennsylvanian ichthyoliths, Part I. *Journal of Vertebrate Paleontology,* **2**, 328–361.
TWAY, L. E. and ZIDEK, J. 1983. Catalog of Late Pennsylvanian ichthyoliths, Part II. *Journal of Vertebrate Paleontology,* **2**, 414–438.
TWAY, L. E., HARRISON, W. E. and ZIDEK, J. 1986. Thermal alteration of microscopic fish remains; an initial study. *Palaios,* **1**, 75–79.
TWITCHETT, R. J. 1999. Palaeoenvironments and faunal recovery after the end-Permian mass extinction. *Palaeogeography, Palaeoclimatology, Palaeoecology,* **154**, 27–37.
TWITCHETT, R. J. 2001a. Incompleteness of the Permian-Triassic fossil record: a consequence of productivity decline? *Geological Journal,* **36**, 341–353.
TWITCHETT, R. J. 2001b. Post-Permian Radiation. *Encyclopedia of Life Sciences (eLS)*. Nature Publishing Group, London, 1–4 [www.els.net].
TWITCHETT, R. J. 2006. The palaeoclimatology, palaeoecology and palaeoenvironmental analysis of mass extinction events. *Palaeogeography, Palaeoclimatology, Palaeoecology,* **232**, 190–213.

TWITCHETT, R. J. 2007a. The Lilliput effect in the aftermath of the end-Permian extinction event. *Palaeogeography, Palaeoclimatology, Palaeoecology,* **252**, 132–144.

TWITCHETT, R. 2007b. The Late Permian mass extinction event and recovery: biological catastrophe in a greenhouse world. *In:* SAMMONDS, P. R. and THOMPSON, J. M. T. (eds) *Advances in earth science: from earthquakes to global warming.* Imperial College Press, London, 69–90.

TWITCHETT, R. 2007c. Climate change across the Permian/Triassic boundary. *In:* WILLIAMS, M., HAYWOOD, A. M., GREGORY, F. J. and SCHMIDT, D. N. (eds). *Deep-Time Perspectives on Climate Change: Marrying the Signal from Computer Models and Biological Proxies.* The Micropalaeontological Society, Special Publications. The Geological Society of London, 191–200.

TWITCHETT, R. J. and BARRAS, C. G. 2004. Trace fossils in the aftermath of mass extinction events. *In:* MCILROY, D. (ed.) *The Application of Ichnology to Palaeoenvironmental and Stratigraphic Analysis.* Geological Society of London, Special Publications, **228**, 397–418.

TWITCHETT, R. J. and OJI, T. 2005. Early Triassic recovery of echinoderms. *Comptes Rendus Palevol,* **4**, 531–542.

TWITCHETT, R. J., LOOY, C. V., MORANTE, R., VISSCHER, H. and WIGNALL, P. B. 2001. Rapid and synchronous collapse of marine and terrestrial ecosystems during the end-Permian biotic crisis. *Geology,* **29**, 351–354.

TWITCHETT, R. J., KRYSTYN, L., BAUD, A., WHEELEY, J. R. and RICHOZ, S. 2004. Rapid marine recovery after the end-Permian mass-extinction event in the absence of marine anoxia. *Geology,* **32**, 805–808.

UNDERWOOD, C. J. 2002. Sharks, rays and a chimaeroid from the Kimmeridgian (Late Jurassic) of Ringstead, Southern England. *Palaeontology,* **45**, 297–325.

UNDERWOOD, C. J. 2006. Diversification of the Neoselachii (Chondrichthyes) during the Jurassic and Cretaceous. *Paleobiology,* **32**, 215–235.

UNDERWOOD, C. J. and CUMBAA, S. L. 2010. Chondrichthyans from a Cenomanian (Late Cretaceous) bonebed, Saskatchewan, Canada. *Palaeontology,* **53**, 903–944.

URBANEK, A. 1993. Biotic crises in the history of Upper Silurian graptoloids: A palaeobiological model. *Historical Biology: An International Journal of Paleobiology,* **7**, 29–50.

VAN VALEN, L. M. 1984. A resetting of Phanerozoic community evolution. *Nature,* **307**, 50–52.

VICKERS-RICH, P., RICH, T. H., RIEPPEL, O., THULBORN, R. A. and MCLURE, H. A. 1999. A Middle Triassic vertebrate fauna from the Jilh Formation, Saudi Arabia. *Neues Jahrbuch für Geologie und Paläontologie, Abhandlungen,* **213**, 210–232.

WAAGEN, W. 1879. Salt-Range fossils. *Productus* Limestone fossils; Pisces. *Palaeontologia Indica,* **1**, 9–20; Suppl. **1880**, 73–81.

WAAGEN, W. 1895. Salt-Range fossils 2. Fossils from the Ceratite Formation, Part I: Pisces-Ammonoidea. *Palaeontologia Indica,* **2**, 1–323.

WADE, R. T. 1942. The Triassic fishes of New South Wales. *Proceedings of the Royal Society of New South Wales,* **75**, 144–147.

WANG, N.-Z., YANG, S. R., JIN, F. and WANG, W. 2001. Early Triassic Hybodontoidea from Tiandong of Guangxi, China. *Vertebrata Palasiatica,* **39**, 251–265.

WANG, N.-Z., ZHU, X. S., JIN, F. and WANG, W. 2007a. Chondrichthyan microremains under Permian-Triassic boundary both in Zhejiang and Jiangxi provinces, China - Fifth report on the fish sequence study near the Permian-Triassic boundary in South China. *Vertebrata Palasiatica,* **45**, 13–36.

WANG, N. Z., JIN, F., WANG, W. and ZHU, X. S. 2007b. Actinopterygian fishes from the Permian-Triassic boundary beds in Zhejian and Jiangxi provinces, South China and fish mass extinction, recovery and radiation. *Vertebrata Palasiatica,* **45**, 307–329.

WANG, N.-Z., ZHANG, X., ZHU, M. and ZHAO, W.-J. 2009. A new articulated hybodontoid from Late Permian of northwestern China. *Acta Zoologica,* **90**, 159–170.

WARRINGTON, G. and WHITTAKER, A. 1984. The Blue Anchor Formation (Late Triassic) in Somerset. *Proceedings of the Ussher Society,* **6**, 100–107.

WATANABE, K., KANMERA, K. and NAKASHIMA, K. 1979. Conodont biostratigraphy in the Kamura limestone (Triassic), Takachiho-cho, Nishiusukigun, Miyazaki Prefecture [in Japanese]. *In:* KOIKE, T. and IGO, H. (eds) *Biostratigraphy of Permian and Triassic Conodonts and Holothurian Sclerites in Japan.* Commemorative Volume of the Retirement of Professor Mosaburo Kanuma, Tokyo, 127–137.

WEIDLICH, O. 2002. Permian reefs re-examined: extrinsic control mechanisms of gradual and abrupt changes during 40 my of reef evolution. *Geobios,* **35**, 287–294.

WEIDLICH, O. and BERNECKER, M. 2003. Supersequence and composite sequence carbonate platform growth: Permian and Triassic outcrop data of the Arabian platform and Neo-Tethys. *Sedimentary Geology,* **158**, 87–116.

WEIDLICH, O. and BERNECKER, M. 2007. Differential severity of Permian-Triassic environmental changes on Tethyan shallow-water carbonate platforms. *Global and Planetary Change,* **55**, 209–235.

WEIDLICH, O. and BERNECKER, M. 2011. Biotic carbonate precipitation inhibited during the Early Triassic at the rim of the Arabian Platform (Oman). *Palaeogeography, Palaeoclimatology, Palaeoecology,* **308**, 129–150.

WEIGELT, J. 1930. Wichtige Fischreste aus dem Mansfelder Kupferschiefer. *Leopoldina,* **6**, 601–624.

WELLES, S. P. 1947. Vertebrates from the Upper Moenkopi Formation of northern Arizona. *University of California Publications in Geological Sciences,* **27**, 241–294.

WEMPLE, E. M. 1906. New cestraciont teeth from the West-American Triassic. *University of California Publications, Bulletin of the Department of Geology,* **5**, 71–73.

WERNEBURG, R. 1994. Der Lettenkohlensandstein von Bedheim (Südthüringen) und seine Wirbeltierfauna (Unter-Keuper). *Beiträge zur Geologie von Thüringen,* **1**, 53–63.

WERNEBURG, R., RONCHI, A. and SCHNEIDER, J. W. 2007. The Early Branchiosaurids (Amphibia) of Sardinia (Italy): Systematic Palaeontology, Palaeoecology, Biostratigraphy and Palaeobiogeographic Problems. *Palaeogeography, Palaeoclimatology, Palaeoecology,* **252**, 383–404.

WERNER, Y. L. 1982. Obituary GEORG HAAS, 1905-1981. *Copeia,* **1982**, 491–493.

WERNER, C. 1989. Die Elasmobranchier-Fauna des Gebel Dist Member der Bahariya Formation (Obercenoman) der Oase Bahariya, Ägypten. *Palaeo Ichthyologica,* **5**, 1–112.

WESTOLL, T. S. 1941. The age of certain Permian fish-bearing strata. *Geological Magazine,* **78**, 37–44.

WHEELER, H. E. 1939. *Helicoprion* in the Anthracolithic (Late Paleozoic) of Nevada and California, and its stratigraphic significance. *Journal of Paleontology,* **13**, 103–114.

WHEELEY, J. R. and TWITCHETT, R. 2005. Palaeoecological significance of a new Griesbachian (Early Triassic) gastropod assemblage from Oman. *Lethaia,* **38**, 37–45.

WHITE, E. I. 1968. Devonian fishes of the Mawson-Mulock area, Victoria Land, Antarctica – Trans-Antarctic Expedition 1955–1958, Scientific Reports no. 16. *Geology,* **5**, 1–26.

WHITENACK, L. B. and GOTTFRIED, M. D. 2010. A morphometric approach for addressing tooth-based species delimitation in fossil mako sharks, *Isurus* (Elasmobranchii: Lamniformes). *Journal of Vertebrate Paleontology,* **30**, 17–25.

WHITENACK, L. B. and MOTTA, P. J. 2010. Performance of shark teeth during puncture and draw: implications for the mechanics of cutting. *Biological Journal of the Linnean Society,* **100**, 271–286.

WHITENACK, L. B., SIMKINS, D. C. and MOTTA, P. J. 2011. Biology meets engineering: the structural mechanics of fossil and extant shark teeth. *Journal of Morphology,* **272**, 169–179.

WIGNALL, P. B. and HALLAM, A. 1993. Griesbachian (Earliest Triassic) palaeoenvironmental changes in the Salt Range, Pakistan and southeast China and their bearing on the Permo-Triassic mass extinction. *Palaeogeography, Palaeoclimatology, Palaeoecology,* **102**, 215–237.

WIGNALL, P. B. and TWITCHETT, R. J. 2002a. Extent, duration and nature of the Permian-Triassic superanoxic event. *In:* KOEBERL, C. and MACLEOD, K. G. (eds) *Catastrophic Events and Mass Extinctions: Impacts and Beyond.* Geological Society of America, Special Papers, **356**, 395–413.

WIGNALL, P. B. and TWITCHETT, R. J. 2002b. Permian-Triassic sedimentology of Jameson Land, East Greenland: incised submarine channels in an anoxic basin. *Journal of the Geological Society, London,* **159**, 691–703.

WIGNALL, P. B., BOND, D. P. G., HAAS, J., WANG, W., JIANG, H. S., LAI, X. L., ALTINER, D., VÉDRINE, S., HIPS, K., ZAJZON, N., SUN, Y. and NEWTON, R. J. 2012. Capitanian (Middle Permian) mass extinction and recovery in western Tethys: A fossil, facies, and $\delta^{13}C$ study from Hungary and Hydra Island (Greece). *Palaios,* **27**, 78–89.

WILCZEWSKI, N. 1967. *Mikropaläontologische Untersuchungen im Muschelkalk Unterfrankens.* Dissertation, Würzburg, 111 + XVI.

WILGA, C. A. D., MOTTA, P. J. and SANFORD, C. P. 2007. Evolution and ecology of feeding in elasmobranchs. *Integrative and Comparative Biology,* **47**, 55–69.

WILIMOVSKY, N. J. 1954. *Gunnellodus*, a new name for *Idiacanthus* Gunnell. *Journal of Paleontology,* **28**, 693.

WILLIAMS, M. E. 1985. The "Cladodont level" sharks of the Pennsylvanian black shales of central North America. *Palaeontographica Abteilung A,* **190**, 83–158.

WILLIAMS, M. E. 1998. A new specimen of *Tamiobatis vetustus* (Chondrichthyes, Ctenacanthoidea) from the Late Devonian Cleveland Shale of Ohio. *Journal of Vertebrate Paleontology,* **18**, 251–260.

WILLIAMS, M. E. 2001. Tooth retention in cladodont sharks: with a comparison between primitive grasping and swallowing, and modern cutting and gouging feeding mechanisms. *Journal of Vertebrate Paleontology,* **21**, 214–226.

WILSON, M. V. H. and BRUNER, J. C. 2004. Mesozoic fish assemblages of North America. *In:* ARRATIA, G. and TINTORI, A. (eds) *Mesozoic Fishes 3 - Systematics, Paleoenvironments and Biodiversity.* Verlag Dr. Friedrich Pfeil, München, 575–595.

WINKLER, T. C. 1880. Description de quelques restes de poissons fossiles des terrains triasiques des environs de Wurzbourg. *Archives du Musée Teyler,* **5**, 109–149.

WOODS, A. D. 1998. *Paleoenvironmental analysis of the Union Wash Formation, east-central California: Evidence for unique Early Triassic paleoceanographic conditions.* PhD Thesis, University of Southern California.

WOODS, A. D. and BAUD, A. 2008. Anachronistic facies from a drowned Lower Triassic carbonate platform: Lower member of the Alwa Formation (Ba'id Exotic), Oman Mountains. *Sedimentary Geology,* **209**, 1–14.

WOODS, A. D., BOTTJER, D. J. and CORSETTI, F. A. 2007. Calcium carbonate seafloor precipitates from the outer shelf to slope facies of the Lower Triassic (Smithian-Spathian) Union Wash Formation, California, USA: Sedimentology and palaeobiologic significance. *Palaeogeography, Palaeoclimatology, Palaeoecology,* **252**, 281–290.

WOODWARD, A. S. 1885. Chapters on fossil sharks and rays. IV. Cestraciontidae. *Science Gossip,* **May 1886**, 106–109.

WOODWARD, A. S. 1886. On a remarkable ichthyodorulite from the Carboniferous series, Gascoyne, Western Australia. *Geological Magazine,* **3**, 1–7.

WOODWARD, A. S. 1888. A synopsis of the vertebrate fossils of the English chalk. *Proceedings of the Geologists' Association, London,* **10**, 273–338.

WOODWARD, A. S. 1889a. *Catalogue of the fossil fishes in the British Museum, vol. 1,* London, British Museum (Natural History), pp. i–xlvii and 1–474.

WOODWARD, A. S. 1889b. On the Myriacanthidae, an extinct family of chimaeroid fishes. *Annals and Magazine of Natural History,* **4**, 275–280.

WOODWARD, A. S. 1889c. Palaeichthyological notes. 2. On *Diplodus Moorei*, sp. nov., from the Keuper of Somersetshire. *Annals and Magazine of Natural History,* **3**, 299–300.

WOODWARD, A. S. 1890. The fossil fishes of the Hawkesbury series at Gosford. *Memoirs of the Geological Survey of New South Wales, Palaeontology,* **4**, 1–55.

WOODWARD, A. S. 1891. *Catalogue of the fossil fishes in the British Museum, vol. 2,* London, British Museum (Natural History), pp. i–xliv and 1–567.

WOODWARD, A. S. 1893. Palaeoichthyological notes. *Annals and Magazine of Natural History,* Ser. 6, **12**, 281–287.

WOODWARD, A. S. 1908. The fossil fishes of the Hawkesbury series at St. Peters. *Memoirs of the Geological Survey of New South Wales, Palaeontology,* **10**, 1–32.

WOODWARD, A. S. 1916. On a new species of *Edestus* from the Upper Carboniferous of Yorkshire. *Quarterly Journal of the Geological Society of London,* **72**, 1–6.

WÜRDIG-MACIEL, N. L. 1975. Ichtiodontes e ichtiodorulitos (Pisces) da Formação Estrada Nova e sua aplicação na estratigrafia do Grupo Passa Dois. *Pesquisas, Instituto de Geociências, Universidade Federal do Rio Grande do Sul,* **5**, 7–165.

YABE, H. 1902. Notes on some shark's teeth from the Mesozoic formation of Japan. *The Journal of the Geological Society of Japan,* **9**, 399–404.

YABE, H. 1903. On the fusulina-limestone with *Helicoprion* in Japan. *The Journal of the Geological Society of Japan,* **10**, 1–13.

YABUMOTO, Y. and UYENO, T. 2001. Triassic fishes from the Mine Group in Yamaguchi, Japan. *In:* TINTORI, A. (ed.) *Mesozoic Fishes, Systematics, Paleoenvironments and Biodiversity.* Serpiano, Switzerland: Abstracts, 71.

YAMAGISHI, H. 2004. Elasmobranch remains from the Taho Limestone (Lower–Middle Triassic) of Ehime Prefecture, Southwest Japan. *In:* ARRATIA, G. and TINTORI, A. (eds) *Mesozoic Fishes 3 - Systematics, Paleoenvironments and Biodiversity.* Verlag Dr. Friedrich Pfeil, München, 565–574.

YAMAGISHI, H. 2006. *Permo-Triassic elasmobranch fauna: diversity, paleobiogeography and recovery after the mass extinction.* PhD, University of Tokyo, 128 pp.

YAMAGISHI, H. 2009. Chondrichthyans. *In:* SHIGETA, Y., ZAKHAROV, Y. D., MAEDA, H. and POPOV, A. M. (eds) *The Lower Triassic system in the Abrek Bay area, South Primorye, Russia.* Tokyo: National Museum of Nature and Science Monographs, **38**, 196–202.

YAMAGISHI, H. and FUJIMOTO, T. 2011. Chondrichthyan remains from the Akasaka Limestone Formation (Middle Permian) of Gifu Prefecture, Central Japan. *Bulletin of the Kanagawa Prefectural Museum. Natural Science,* **40**, 1–6.

YANG, S. R., WANG, X. P. and HAO, W. C. 1984. New knowledge of the Lower Triassic of Zoudeng, Tiandong County of Guangxi Province, China. *In:* HUANG, T. K. (ed.) *Selected Papers in Honor of Prof . Yoh, S.S. on the Sixty Years for his Geological Study and Education.* Geological Publishing House, Beijing, 105–117 (in Chinese with English summary).

YANKEVICH, D. I. and MINIKH, M. G. 1998. lchthyofauna. *In:* GRUNT, T. A., ESAULOVA, N. K. and KANEV, G. P. (eds) *Biota Vostoka Evropeyskoj Rossii na Rubezhe Rannej i Pozdnej Permi.* Geos, Moscow, 220–229 (in Russian).

YIN, H., ZHANG, K., TONG, J., YANG, Z. and WU, S. 2001. The Global Stratotype Section and Point (GSSP) of the Permian-Triassic Boundary. *Episodes,* **24**, 102–114.

YOCHELSON, E. L. and VAN SICKLE, D. H. 1968. Biostratigraphy of the Phosphoria, Park City, and Shedhorn Formations, with a section on fish. *United States Geological Survey Professional Paper,* **313-D**, 571–660.

YOKOI, T. 1994. On teeth and dermal teeth of shark and fish teeth from Akasaka Limestone (Middle Permian) Kinsyouzan, Gifu Pref., central Japan [in Japanese]. *Earth Science (Chikyu Kagaku),* **48**, 203–210.

YOKOI, T. 2000. On teeth and dermal teeth of shark and fish teeth from Akasaka Limestone (Middle Permian) Kinshozan, Gifu Pref., Central Japan. *Chigaku Kenkyu,* **48**, 203–210.

YOUNG, G. C. 1950. Notes on the first occurrence of the order Bradyodonti in China. *Science Record,* **3**, 243–246.

YOUNG, G. C. 1982. Devonian sharks from south-eastern Australia and Antarctica. *Palaeontology,* **25**, 817–843.

YOUNGQUIST, W. 1952. Triassic conodonts from southeastern Idaho. *Journal of Paleontology,* **26**, 650–655.

ZHANG, M. 1976. A new helicoprionid shark from Xizang. *Scientia Geologica Sinica,* **10**, 332–336.

ZHANG, N.-S. 1979. On a new species of *Sinohelicoprion qomolangma* sp. nov. from Tibet. *Mount Jolmo Lungma Scientific Unit (A report of a scientific expedition in the Mount Jolmo Lungma Region, 1975).* Science Press, Beijing, 117–122 (in Chinese).

ZANGERL, R. 1973. Interrelationships of early chondrichthyans. *In:* GREENWOOD, P. H., MILES, R. S. and PATTERSON, C. (eds) *Interrelationships of fishes.* Zoological Journal of the Linnean Society, **53** (Supplement 1), 1–14.

ZANGERL, R. 1979. New Chondrichthyes from the Mazon Creek fauna (Pennsylvanian) of Illinois. *In* NITECKI, M. N. (ed.) *Mazon Creek Fossils.* Academic Press, New York, 449–500.

ZANGERL, R. 1981. *Chondrichthyes I Paleozoic Elasmobranchii, Handbook of Paleoichthyology, vol. 3A,* Gustav Fischer Verlag, Stuttgart, 115 pp.

ZANGERL, R. 1990. Two new stethacanthid sharks (Stethacanthidae, Symmoriida) from the Pennsylvanian of Indiana, U.S.A. *Palaeontographica Abteilung A,* **213**, 115–141.

ZANGERL, R. and CASE, G. R. 1973. Iniopterygia, a new order of chondrichthyan fishes from the Pennsylvanian of North America. *Fieldiana Geology Memoirs,* **6**, 1–67.

ZIDEK, J. 1973. Oklahoma Paleoichthyology Part II: Elasmobranchii (*Cladodus*, minute elements of cladoselachian derivation, *Dittodus*, and *Petrodus*). *Oklahoma Geology Notes,* **33**, 87–103.

ZIDEK, J. 1976. Oklahoma paleoichthyology, Part V: Chondrichthyes. *Oklahoma Geology Notes,* **36**, 175–192.

ZIDEK, J. 1978. New chondrichthyan spines from the late Paleozoic of Oklahoma. *Journal of Paleontology,* **52**, 1070–1078.

ZIDEK, J., JOHNSON, G. D., MAY, W. and CLABORN, A. 2004. New specimens of xenacanth and hybodont sharks (Elasmobranchii: Xenacanthida and Hybodontoidea) from the Lower Permian of southwestern Oklahoma. *Oklahoma Geology Notes,* **63**, 136–147.

ZITTEL, K. A. 1887–1890. Handbuch der Paläontologie. 1. Abtheilung Paläozoologie, 3: Vertebrata (Pisces, Amphibia, Reptilia, Aves). München & Leipzig, Oldenbourg, XII + 900 pp.

ZONNEVELD, J. P. 2011. Suspending the rules: unraveling the ichnological signature of the Lower Triassic post-extinction recovery interval. *Palaios,* **26**, 677–681.

ZONNEVELD, J.-P., GINGRAS, M. K. and BEATTY, T. W. 2010. Diverse ichnofossil assemblages following the P–T mass extinction, Lower Triassic, Alberta and British Columbia, Canada: Evidence for shallow marine refugia on the northwestern coast of Pangaea. *Palaios,* **25**, 368–392.